

Reliability: Theory and Applications

ELECTRONIC JOURNAL OF INTERNATIONAL GROUP ON RELIABILITY
JOURNAL IS REGISTERED IN THE LIBRARY OF THE U.S. CONGRESS

THE FIFTH EURASIAN RISK-2023 CONFERENCE



ISSN 1932-2321

SPECIAL ISSUE 5 (75)

Volume 18

GNEDENKO FORUM
INTERNATIONAL GROUP ON RELIABILITY



November 2023

Guest Editors

This special issue of the journal "Reliability: Theory and Applications" contains quality articles on innovative approaches to risk minimization. We would like to express our gratitude to all the participants of the RISK-2023 Conference for the submitted articles and the reviewers for their effective work in evaluating the submitted materials. We sincerely appreciate their excellent timely responses. The invited editors are also very grateful to the secretary, Doctor of Sci., Alexander Bochkov, for his constant support and constructiveness in the process of reviewing and drafting the proposal of the special issue. We hope that this special issue will make a significant contribution to improving the scientific field of assessment, analysis and management of natural and man-made risks.

Prof. Dr. Sviatoslav TIMASHEV

Ural Federal University, Russia

Old Dominion University, USA

e-mail: timashevs@gmail.com

Prof. Dr. Vugar ALIYEV

CEO & Founder

International Event Organizer Company

AMIR Technical Services LLC,

e-mail: prof.vugar.aliyev@gmail.com

ISSN 1932-2321

© "Reliability: Theory & Applications", 2006, 2007, 2009-2023

© " Reliability & Risk Analysis: Theory & Applications", 2008

© I.A. Ushakov

© A.V. Bochkov, 2006-2023

<http://www.gnedenko.net/Journal/index.htm>

All rights are reserved

**The reference to the magazine "Reliability: Theory & Applications"
at partial use of materials is obligator**



The Fifth Eurasian Conference

dedicated to the 100th anniversary of Heydar Aliyev

Innovations in Minimization of Natural and Technological Risks

www.eurasianrisk2023.com

ORGANIZERS

- Event Organizer Company AMIR Technical Services;
- “Azerbaijan Caspian Shipping” CJSC, Azerbaijan State Marine Academy;
- Mines Paris – PSL, France;
- Politecnico di Milano, Italy;
- City University of Hong Kong;
- International Group on Reliability - Gnedenko Forum, the USA;
- European Safety and Reliability Association (ESRA);
- Qingdao University, China

OBJECTIVES

- Identification and transfer of "know-how" knowledge and technologies on innovative approaches to minimize risks;
- Support of the UN Sendai Framework for Action on Disaster Risk Reduction 2015-2030.

Table of Contents

THE FINAL DECISION FIFTH EURASIAN CONFERENCE RISK-2023	30
---	-----------

Prof. Sviatoslav Timashev, Prof. Vugar Aliyev

RANDOMNESS, UNCERTAINTY, INCOMPLETENESS, RISK AND ITS MEASUREMENTS	31
---	-----------

Vladimir Rykov, Boyan Dimitrov, Alexander Bochkov, Elvira Zaripova, Olga Kochueva

In this work we analyze different aspects regarding the terminology, understanding concepts and approaches in modeling and measuring components and variables related to safety and risk. This discussion conversation is open for further interpretations and suggestions. We study it with the help of models (images) artificial, descriptions, scientific approaches, discussions, etc., and using the help of poly-semantic languages. Various kinds of risks arise precisely because of the uncertainty of the situation. Mathematical models use uncertainties in several ways: randomness, which is explained and measured by objective probability and estimated using statistical methods. Uncertainty, measured by subjective probabilities, is estimated by expert methods, or by fuzzy uncertainty methods. Each of these approaches has its advantages and disadvantages. Despite the difference in approaches to measuring uncertainties, the development of a risk situation are described in an appropriate way using an event tree. We show the construction of an event tree, that allows us to see details and specify in the development of a risk situation. We also discuss how this approach can be used to evaluate the sensitivity of the output characteristics of the process to the parameters of the initial information.

REFLECTIONS ON DUAL NATURE OF RISK. TOWARD A FORMALISM	44
---	-----------

Alexander Bochkov

We seem to know almost everything about risk and, at the same time, nothing. By focusing on the etymology of the word "risk", researchers have neglected its nature, causes and characteristics. At the same time, risk manifests itself differently in different situations and can be both a characteristic of a random event and a characteristic and measure of the quality of a process carried out over time. In the latter case, risk is inherent in the properties of a wave process, which requires the search for measures other than probabilistic ones to measure and assess it. This paper attempts to summaries the most characteristic different manifestations of risk and to propose a way of assessing risk that takes account of these differences. The paper

can be seen as an invitation to debate the nature of risk and how its formalism should be constructed.

**RELIABILITY BASED DESIGN OF CIVIL AND INDUSTRIAL
ENGINEERING STRUCTURES USING THE LIFE QUALITY
INDEX CRITERION 75**

Anna Bushinskaya, Sviatoslav Timashev

The paper considers and analyses the current world practice of assigning acceptable values for the probability of failure of civil and industrial engineering structures based on monetary optimization using the life quality index. The analysis is illustrated by calculating the approximate target values of the threshold probability of failure for multi-storey residential buildings in the Sverdlovsk region of the Russian Federation using the LQI criterion and the social willingness to pay concept assessment of the effectiveness of the costs of safety measures.

MULTIFACTORIAL EMERGENCY FORECASTING METHODS 89

Vugar Aliyev, Zurab Gasitashvili, Merab Pkhovelishvili, Natela Archvadze,
Lia Shetsiruli

Recently, great tragedies have occurred, which are caused by the coincidence of various factors in time and in locations. Failure to take into account the fact that different events will coincide in time and location is an error in the forecasting method, since such situations require the use of parallel data, which we will discuss here. The article gives a specific example of the coincidence of 5 natural geological and hydrometeorological events and shows how a natural disaster could have been avoided using a new forecasting method.

**POSSIBILITIES OF LINEAMENT ANALYSIS OF DEM SRTM
DURING GEODYNAMIC ZONING OF SEISMIC HAZARDOUS
TERRITORIES (on the example of the North-Tien-Shan region) 96**

Aleksandr Fremd, Arailim Gaipova, Dinara Talgarbaeva

Lineament analysis of space images can be successfully used for the purposes of formalized analysis and development of maps of geodynamic zoning with the ranking of the study area into areas that differ in the degree of relative geodynamic activity. As calculated indicators of geodynamic (neotectonic) activity, the density of faults, megacracks and other lineaments, expressed by their total length per unit area, was used. Therefore, the parameter "density of strokes" is taken as the basis for the taxonomic division of the study area into regions according to the degree of tectonic disturbance of the earth's crust. All constructions are implemented on the basis of lineament analysis included in the CATALIST software package (Canada) On the example of two seismically hazardous regions of the Northern Tien Shan (Almaty and Zhambyl), the distribution features and properties of lineament density parameters are illustrated, followed by the construction of maps of geodynamic activity.

TERRITORIAL RISKS ASSESSMENT OF NATURAL HAZARDS 111

Ulyana Postnikova, Olga Taseiko, Maksim Anikin

The presence of an unstructured data array predetermines the need to create an interconnected system of risk factors. The purpose of the study is to analyze the vulnerability of the Krasnoyarsk region territories to hazardous natural phenomena. This paper analyzes floods and forest fires, which are the most typical natural hazards for the areas under consideration. To identify areas most prone to natural hazards, a ranking was carried out according to the level of risk using GIS technologies.

THE KURA ACTIVE FAULT – POTENTIAL SOURCE OF SIGNIFICANT HAZARD 118

Alexander Strom

An active fault stretching for more than 100 km along the Kura River between the tailing part of the Mingçevoir Reservoir in the east and the Azerbaijan-Georgia border in the west – the so-called Kura fault – is described in brief based on the analysis of space images. This active reverse fault with distinct evidence of Late Quaternary movements crosses the waterfronts of the Shamkir and the Enikend reservoirs.

MANAGING THE RISK OF EMERGENCIES CAUSED BY GROUNDWATER FLOODING OF THE HISTORICAL BUILT-UP AREAS 125

Elena Arefyeva

The article presents an approach to managing the risk of groundwater flooding emergencies, including those in historical built-up areas. The approach is based on the application of a set of methods, including the method of forecasting, the method of developing an optimal control action, and developing a compromise solution. The peculiarity of historical built-up areas is that there is a significant cultural layer that does not allow drainage, because watered soil preserves the cultural layer. At the same time, architectural monuments need to drain the foundations and not water the soils of the foundations of structures.

PERSPECTIVE OF USING GROUNDWATER IN THE GANIKH-AYRICHAY FOOTHILLS 136

Esmira Mustafayeva, Allahverdi Tagiyev

Most of the qualitative groundwater resources of Azerbaijan are concentrated in the Ganikh-Ayrichay foothills. As a result of research conducted in this area, it was revealed that the Ganikh-Ayrichay foothills has great prospects for water supply in Baku. According to earlier hydrogeological studies in Ganikh-Ayrichay foothills, widespread sources on the plains are asso-

ciated with rocks of the fourth period, with gravel and various old rocks. Sources associated with the cliffs of the fourth period, are associated with groundwater rivers.

PROCESSING OF DATA BASED ON FUZZY RULES 142

Kifayat Mammadova, Yegana Aliyeva, Matanat Hasanquliyeva

After establishing a fuzzy rule base using the interpolation result mechanism, arranging a fuzzy inference system is performed. The established system will infer about the level of risk using a fuzzy rule base and input statistics. In this work, the construction of the inference system has been determined using fuzzy rules interpolation.

MORPHOMETRICAL CHARACTERISTICS OF AVALANCHES WITH THE USE OF A UAV (on the example of Ile Alatau) 148

Aidana Kamalbekova, Victor Blagoveshchensky, Sandugash Ranova, Uldzhan Aldabergen

The article deals with the experience of using an unmanned aerial vehicle (DJI Matrice 300 RTK) and Agisoft Metashape software to obtain the characteristics of avalanches that descended in late March in the Shukur and Kotyrbulak tracts (Pioneer avalanche) in the Ile Alatau mountains. UAVs can perform observations in remote and dangerous areas, quickly reach the scene, and capture high-quality images and video.

ESTIMATION OF THE PROBABILITY OF ELIMINATING CRITICAL FAILURES OF DISTANTLY CONTROLLED OBJECTS 153

Alexander Dokukin, Mikhail Lomakin

The problem of determining the probability of timely elimination of critical failures under conditions of incomplete data represented by small samples of hardware dwell time in failure state and critical hardware time is considered. This probability is the probability of stochastic dominance of the critical time of the hardware over the time of the hardware in the state of failure, i.e. the probability that the random time of the hardware in the state of failure is less than the critical time of the hardware. Critical time is the time during which the elimination of the occurred failures does not lead to the occurrence of an unrecoverable failure of the object or to a significant reduction in the efficiency of its functioning.

THE ESSENCE OF THE DELPHI METHOD AND ITS MAIN ADVANTAGES AND DISADVANTAGES 158

Albina Berkaeva, Sergey Yablochnikov, Andrey Butyrin, Irina Tararyshkina, Tofiq Mansurov

This article is devoted to the study of the essence and main meaning of the Delphi method, developed in the 50s of the 20th century in the United States. In those years, this method was used to identify the impact of scientific and technological progress in matters of a military nature. Now, the Delphi method is universal and can be applied in any branch of activity, which increases its relevance. In addition, we have studied the main advantages and disadvantages of using this method at the level of world experience. We also considered the problems of using the Delphi method at the level of the Russian economy.

CLIMATE AND ENVIRONMENTAL MONITORING OF THE BALTIC SEA: GENERAL PRINCIPLES AND APPROACHES 164

Leyla Bashirova, Vadim Sivkov, Marina Ulyanova, Aleksander Gavrikov,
Arseniy Artamonov

The environment of the Baltic Sea is heavily influenced by human activities. In addition, the region is undergoing significant changes in the face of global climate change. Therefore, it is necessary to assess the state of the environment and greenhouse gas emissions in the region. In 2022, the Programme for the development of the system of climate and environmental monitoring of the Russian seas was launched. For the Baltic Sea, the spatial and temporal scheme of the regional monitoring module has been designed to carry out long-term, regular, and large-scale surveys. The satellite monitoring is based on the analysis of radiometer data and includes analyses of the spatial and temporal variability of suspended particulate matter and chlorophyll a concentrations, as well as sea surface temperature. The shipboard monitoring consists of seasonal and monthly surveys. The coastal monitoring is based on data from sensors installed on a 57-m met tower as a permanent climate and environmental monitoring station located on the coast of the south-eastern part of the Baltic Sea (Kaliningrad Oblast, Russia).

INTERNATIONAL MODELS OF RISK MANAGEMENT: FERMA, COSO AND ISO 172

Valentina Dzobelova, Sergey Yablochnikov, Maxim Makhboroda,
Lyubov Manukhina, Anna Vedyashova

This article discusses the most important risk management standards that play a very significant role in the activity of any enterprise, both at the micro- and macro level, in order to reduce negative factors that have an impact on the financial activities of the enterprise. During the analysis, we considered the main models of risk management known as FERMA, COSO and ISO, the origin of which is European, American and international, respectively. The scientific work reveals the essence of each risk management model, highlighting their features and characteristics.

BIOMORPHOLOGICAL ANALYSIS AND OCCURANCE OF ENDEMIC AND RELICT SPECIES OF THE CHECHEN REPUBLIC 178

Zazu Iriskhanova, Khava Khanaeva, Birlant Khasueva

This article provides a biomorphological analysis and occurrence of endemic and relict species of the Chechen Republic. Endemic species (taxa unique to a particular geographical area) are characteristic elements of local biodiversity. Narrow endemics occupy isolated habitats, often associated with limited ranges of ecological conditions or small common geographic ranges. The analysis is based on the processing of herbarium materials and field observations of the authors.

ENGINEERING ESTIMATION OF AIR REGIME OF BUILDING FACADE SYSTEMS WITH FIRE CUT OFFS 186

Samira Akbarova, Reyhan Akbarli

The facade is one of the most important elements of the building in terms of its fire safety, as a fire leads to serious building damage and human casualties. The article considers the influence of fire cut-offs on the parameters of the airflow in the ventilated gap of the hinged facade system. An engineering estimation of solid and perforated horizontal fire cut-offs used in Azerbaijan is presented.

PROSPECTS FOR AZERBAIJAN'S PARTICIPATION IN THE DIVERSIFICATION OF ENERGY SOURCES AND REDUCING THE RISKS OF ENERGY SUPPLY FAILURE TO EUROPE 195

Eldar Gasumov, Ramiz Gasumov, Gazanfar Suleymanov, Khalig Kurbanov

The article considers the prospects for Azerbaijan's participation in the diversification of energy supplies to the European market, in the conditions of the energy crisis due to the difficult geopolitical situation in the world. Possible ways to reduce the serious risks of failures in the supply of energy resources while ensuring the energy security of the countries of the European continent are given. The negative impact of the crisis that has arisen in the energy market on the global energy supply chain to the EU countries and on the state of the world economy is analyzed. Steps taken by the EU to radically increase supply via traditional EU import routes as well as completely new sources of energy are examined. Various measures implemented by European countries to ensure their own energy security, including the diversification of the supply of energy resources used to generate energy, including through non-renewable mineral substances, renewable organic resources and a number of natural processes, are considered.

ECOLOGY OF USED ENGINE OIL ADDINOL 206

Elvira Guseinova, Gahraman Hasanov, Elman Akhyadov

Comprehensive spectroscopic studies of used and regenerated with chloric acid samples of ADDINOL engine oil were carried out. It was revealed that during the operation of engine oil, structural changes in hydrocarbon components, the formation of oxygen-containing compounds, and the accumulation of products of thermal destruction and friction occur. An assessment was made of the qualitative changes in used motor oil under the influence of chloric acid.

**GEOHAZARDS AND ENVIRONMENTAL RISK ASSESSMENT
PRACTICES OF PETROLEUM AND GAS PIPELINES USING
MICROWAVE REMOTE SENSING 212**

Emil Bayramov, Manfred Buchroithner, Martin Kada, Saida Aliyeva

These studies focused on the quantitative assessment of the surface displacement velocities and rates and their natural and man-made controlling factors as the potential risks along the seismically active 70 km section of buried oil and gas pipeline in Azerbaijan using Persistent Scatterer Interferometric Synthetic Aperture Radar (PS-InSAR) and Small Baseline Subset (SBAS-InSAR) remote sensing analysis. The diverse spatial distribution and variation of ground movement processes along pipelines demonstrated that general geological and geotechnical understanding of the study area is not sufficient to find and mitigate all the critical sites of subsidence and uplifts for the pipeline operators. This means that both techniques outlined in this paper provide a significant improvement for ground deformation monitoring or can significantly contribute to the assessment of geohazards and preventative countermeasures along petroleum and gas pipelines.

CREATING FOREST CARBON LANDFILLS: FOREST CARBON 222

Rustam Gakaev, Magomed-Sadyk Bahaev, Islam Gumaev

Currently, significant attention is paid to environmental issues at all levels of management. Over the long history of human civilization, significant environmental damage has been accumulated, because not only large-scale industrial production, but also ordinary human life leads to the formation of a significant amount of harmful products that pollute the atmosphere, soil, and water spaces. The huge scale of the accumulated damage makes it necessary to resolve environmental issues at the highest level - the level of international organizations and the leadership of individual states.

**EVALUATING MEASURES TO SUPPORT DRYLAND RURAL
POPULATIONS UNDER HIGH CLIMATIC UNCERTAINTY AND
RISK: THE EXAMPLE OF THE ARAL SEA REGION 231**

Georgy Fomenko, Marina A. Fomenko

Evaluating international technical assistance projects usually calls for assessing the efficiency and effectiveness of planned indicators. As climatic uncertainty and risk increase, there is a need to improve approaches to assessing the activities of such projects. Using the example of a project to adapt dryland dehqan households, cooperatives, and farms in the Aral Sea region (the Republic of Karakarpakistan in Uzbekistan) to climate change, this research methodically substantiates a set of indicators to assess the long-term effectiveness of adaptation measures. With regard to humanitarian support measures (which are strengthening the hydrometeorological monitoring network, creating early warning systems, raising public awareness about various climate threats and possibilities to reduce their negative consequences, and reclaiming

the dried-up Aral Sea bottom to reduce dustiness) that pursue noneconomic goals, an assessment was made against previously established project performance indicators.

RISK ASSESSMENT OF USING ARTIFICIAL INTELLIGENCE SYSTEMS IN CREATIVE HUMAN ACTIVITIES 238

Elshad Aliyev

Developing at an incredible pace, high technologies occupy almost all areas of human activity. Today, one of the most striking examples of high technology is undoubtedly systems classified as artificial intelligence (AI). AI and robots are widely used in manufacturing, heavy industry, agriculture, and many other industries, as well as in the arts. The development of artificial intelligence is of interest to many philosophers, sociologists and other scientists and raises many questions. A. Turing, S. McCarthy, A. Barr, M. A. Boden, M. Kokkelberg, A. Elgammal, S. Awdry and other scientists have conducted detailed studies of artificial intelligence systems, philosophical aspects, and creativity. However, despite numerous scientific studies, the questions raised are still relevant. Do Robotic Artworks Prove the Creative Power of Artificial Intelligence? Can AI Be Creative in General? Most of these questions have different answers and lead to conflicting opinions. The article analyzes the creative potential of various modern AI systems and qualitatively assesses the risk of their uncontrolled use in creative areas of human activity.

INHALED NON-CARCINOGENIC RISKS BASED ON EVOLUTIONARY MODELS FROM DISEASES OF THE DIGESTIVE SYSTEM OF THE POPULATION OF KRASNOYARSK 251

Liubov Kalimanova, Olga Taseiko

The assessment methodology for epidemiological non-carcinogenic risks makes it possible to evaluate the potential consequences for human health of different variants of previous and predicted exposures to pollutants. The article considers the influence of pollution in the atmospheric air of Krasnoyarsk on the formation of mortality risks from diseases of the digestive system.

CLASSIFICATION OF ACCIDENTAL OIL SPILLS IN OIL EXTRACTION AND ASSESSMENT OF ENVIRONMENTAL RISKS 258

Hajar Ismayilova, Ulviyya Huseynova, Hikmat Babirov

The distribution and characteristics of the results of accidents in oil pumping and hydrocarbon transportation systems by degrees of severity are given in separate categories. A new methodical approach was proposed for the evaluation of the ecological and economic risk factor.

RESEARCH OF REDUCING THE RISKS THAT MAY ARISE DURING THE PREPARATION OF GAS TRANSPORTATION 262

Fikrat Seyfiyev, Sahib Abdurahimov, Irada Hajiyeva, Meherrem Harbizadeh, Vagif Rustamov, Ulfet Tagi-zade

In order to prevent risks that may occur due to hydrates and other reasons in the system during gas collection and preparation for transport, detailed information is provided due to the study results of methanol prepared on the basis of local chemical products and diethylene glycol, used as an absorbent in the gas-methanol-water system, in laboratory conditions. According to the results of the research conducted on the basis of samples taken from the fields, surfactants, i.e., methanol, used to prevent the hydrate formation in production facilities, pipelines for the purpose of preventing accidents, failures, and the risk of environmental pollution there are many possibilities to optimize the amount of reagents required. In the next stage, methanol can be captured and reused through the diethylene glycol regeneration unit. By capturing methanol from the gas phase and regenerating both methanol itself and the diethylene glycol inhibitor, it is possible to protect the environment and minimize the risks that may occur in technological processes.

ANALYSIS AND DAMAGE ASSESSMENT OF HAIL PROCESSES IN GEORGIA AND AZERBAIJAN USING RADAR DATA (ON THE EXAMPLE OF MAY 28 AND JULY 13, 2019) 267

Mikheil Pipia, Avtandil Amiranashvili, Nazibrola Beglarashvili, Elizbar Elizbarashvili, Otar Varazanashvili

The results of the analysis of radar studies of hail processes over the territories of Georgia and Azerbaijan on May 28 and July 13, 2019 are presented. Based on the values of the maximum size of hailstones in clouds, using the Zimenkov-Ivanov model, the expected sizes of hailstones falling on the earth's surface are calculated. The degree of damage to vineyards, wheat and corn, depending on the size of the hail, was determined by summarizing the known data on damage to these crops at different kinetic energy of hail and data on the average kinetic energy of hail of different magnitudes. Based on this compilation, regression equations were obtained for the relationship between the degree of damage to these crops and the size of hailstones, which have the form of a sixth degree of a polynomial. According to this equation, calculations were made of the degree of maximum damage to vineyards, wheat and corn along the trajectories of hail clouds over the territories of Georgia and Azerbaijan.

UP-TO-DATE DETAILED SEISMIC ZONING OF REGIONS IN KAZAKHSTAN (PGA CASE) 275

Natalya Silacheva

The results of the first project in Kazakhstan on the Detailed Seismic Zoning of regions on a new methodological basis are presented. The Probabilistic Seismic Hazard Assessment is carried out for the territories of East Kazakhstan (since 2022 EKO and Abay), Almaty (since

2022 Almaty and Zhetysay) and Zhambyl regions using a methodology consistent with the main provisions of Eurocode 8 and updated compared to that used in maps of the recent General Seismic Zoning of Kazakhstan territory. Modern methods and tools of analysis were used, as well as the most complete and up-to-date information available for the territories under consideration. The seismic source model included areal sources and active faults. The developed maps are discussed and hazard curves and uniform hazard spectra for the main cities in the considered regions are presented. The obtained results are generally consistent with the General Seismic Zoning but display some differences in PGA distribution due to including active faults and a comprehensively revised catalogue. Zoning maps will be the basis for the development of new state building regulations of the Republic of Kazakhstan.

DIAGNOSTICS OF RISKY MULTIPHASE FLOW ZONES IN OIL PIPELINES 283

Gulnara Zeynalova, Gafar Ismayilov

This article examines the properties and formation of free-flow areas in the compressed profile of indicative oil pipelines. The risks of the formation of multiphase flow zones in oil pipelines were investigated and a method for diagnosis was developed. Additionally, this article studies the issues related to the presence of free-flow zones formed within the stationary regimes of oil pipelines, as well as the identification of their coordinates. Case studies are drawn based on the hydraulic slope and the pressure balance and contingent upon the lay, which aim to account for

EQUATION OF STATE OF HYDROCARBONS FOR THE LIQUID PHASE 288

Vagif Hasanov, Nurmammad Mammadov, Jeyhun Naziyev,
Malahat Mammadova, Adila Zeynalova

It is necessary to construct equations of state that qualitatively and quantitatively accurately reflect the behavior of the thermodynamic surface in the considered range of parameters, in order to compile tables of the thermodynamic properties of liquids. A sufficient amount of high-precision experimental data on the P-V-T dependence is necessary to constructing such equations. Most of the equations are not suitable for extrapolation, they are valid in limited areas of state parameters. An equation of state with three coefficients is proposed to describe the P-ρ-T dependence of liquid hydrocarbons of various molecular structures (benzene, n-octane, isooctane, octene-1).

GEODYNAMIC REGIME OF FORMATION OF THE MESO-CENOZOIC SEDIMENTARY COVER OF THE ABSHERON ARCHIPELAGO 296

Yelena Pogorelova, Murad Abdulla-zada, Allahverdi Tagiyev

The main goal of geodynamic analysis is to learn to perceive sedimentary basins as integral natural objects, to determine their genesis, structure and stages of evolution, classification of sedimentary basins and forecast of their oil and gas potential. It is well known that the chang-

es that occur in the earth's crust are mainly the result of subcrustal processes and adjacent plate interaction. The type of the Earth's crust underlying the sedimentary basin determines the physical basis, stability, tectonic restructuring and sedimentation conditions throughout the evolution of the basin. Geodynamic conditions of sedimentary cover formation in the region under consideration were studied on the basis of the principles of tectonic formation of the Caspian basin and the adjacent area, developed by Azerbaijani and foreign scientists.

**DETERMINATION OF THE ENVIRONMENTAL TEMPERATURE
DEGREE ON MAGNETIC LEVITATION CORE INDUCTION 304**

Orkhan Afandiyev, Aynura Allahverdiyeva

The issues on determining the degree of influence of temperature changes caused by climatic features of the area, internal heat generation during the operation of an electronic circuit and other reasons on the value of the magnetic induction of the levitating magnetic core are analyzed in the article. Based on the results of preliminary studies, the model of the Magnetic Levitation System (MLS), the dependence on the temperature of the magnetic induction on the levitating core was obtained. The preliminary investigation results of the MLS show that the magnetic induction of the levitating core is a linear monotonically decreasing function of temperature. The aim of this issue is to study the effect of temperature on the nature of the power characteristics of the MLS, the temperature in the measuring chamber of which has a significant effect, which indicates the violation of the levitation current stability caused by temperature changes in the magnetic induction of the levitating magnetic core (which indicates the violation of the levitation current stability).

**RISK ASSESSMENT STUDY OF KEY COMPONENTS OF THE
DIGITAL ECONOMY 308**

Laila Gazieva, Timur Aygumov, Alexander Natalson

This study provides a comprehensive risk assessment of key components of the digital economy to ensure sustainable growth and mitigate potential adverse impacts. The research methodology included a literature review, analysis of academic sources, data and economic indicators, case studies, and development of risk assessment models. The results of the analysis confirm that the digital economy provides significant opportunities for development and progress in modern society. However, it also carries certain risks and challenges, such as cybersecurity, data privacy, ethical issues, artificial intelligence, and misinformation. These insights enable business leaders, governments and the public to prioritize risk management and develop strategies that advance the sustainable and responsible development of the digital economy. Based on this study, measures can be taken to improve cybersecurity, ensure data privacy, ethical use of artificial intelligence and counter disinformation, in order to provide a favorable and sustainable environment for the further development of the digital economy.

**OIL AND GAS PROSPECTS OF TECTONIC CRASHING ZONES OF
THE KURA INTERMOUNTAIN DEPRESSION 313**

Gultar Nasibova, Emil Ismayilzadeh, Shura Ganbarova, Mehriban Ismayilova

The article considers lithofacies and structural-tectonic conditions of oil and gas formation in the Kura depression. In addition, the formation of oil and gas accumulation zones in the crushing nodes in the Mesozoic deposits was determined and the role of faults in their formation was studied, tectonic crushing zones were found using seismically active zones in these deposits, the issues of prospects analysis were studied and the issues of prospecting and exploration were considered.

Taking into consideration that the tectonic crushing zones are formed in Mesozoic deposits composed mainly of competence rocks, it can be predicted that oil and gas fields in these zones are associated mainly with Mesozoic age rocks. In the Middle Kura depression, the surface of the Mesozoic deposits lies at a depth of up to 4-5 km, therefore it is considered favorable for exploration. Due to this, the oil and gas prospects of the tectonic crushing zones was studied in the Mesozoic deposits as a prospecting object of the Middle Kura depression.

THE IMPACT AND PROSPECTS OF USING ARTIFICIAL INTELLIGENCE IN THE ECONOMY 323

Larisa Aguzarova, Fatima Aguzarova, Kamilla Tsallaeva

This paper discusses issues related to the development of technologies and the relationship of this process with economic processes. Due to the rapid digitalization, the importance and role of artificial intelligence are growing. At the same time there are many problems and they are considered in this paper: unemployment of technical workers, a security problem that is associated with the confidentiality, the existing neural networks cannot be suitable for use in all industries etc. When using the generalization method, the authors have made relevant conclusions and recommendations for using Artificial Intellect: to solve the following universal tasks: automatic translation; getting business intelligence; recognition of visual signs; character recognition; information extraction; understanding and analyzing texts; image analysis; ensuring information security and protection against cyber-attacks; speech recognition; robotic tools for the implementation of tasks at different levels and in different fields.

THE ROLE OF THE HUMAN FACTOR IN THE MARKET ECONOMY 330

Albina Berkaeva, Irina Yablochnikova, Georgi Kutsuri, Tengiz Tinikashvili, Ekaterina Stativa

One of the basic resources of economic growth is the human factor, the relevance of which in the modern economic system is actively increasing. This is primarily because every day many companies are becoming more and more aware of the importance of the considered category in any business for efficient and successful operation. Indeed, in the current realities, it is the human factor that is responsible for the well-being and success of enterprises due to the competence and professionalism of employees. In this regard, in our opinion, the main task of any management team is to find ways to manage the company's employees as efficiently as possible by creating favorable mutually beneficial conditions for both the labor power and the entire business as a whole.

THE MAIN TRENDS IN THE LABOUR MARKET DEVELOPMENT

IN THE CONTEXT OF THE ECONOMY DIGITALIZATION 336

Valentina Dzobelova, Sergey Bakunin, Vitaly Lukinov, Viktoria Erofeeva

The article considers the influence of the digital economy development on the labour market, identifying its main advantages and disadvantages. The increase in the unemployment rate due to the disappearance of a number of obsolete professions, that have lost their relevance in the context of modern developing relations, can be attributed to the fundamental negative factors of the labour market digitalization. In addition, after analyzing the opinions of various domestic and foreign experts, it is concluded that it is impossible until 2030 to completely replace human labour with robotics, despite the rapid development of information and communication technologies.

OPTIMIZATION OF THE COMPOSITION OF SPARE PARTS FOR THE AGING TYPE OBJECTS 342

Aleksandr Antonov, Aleksandr Murkin

The paper solves the problem of optimizing the composition of spare parts for objects of aging type. A model for calculating the profit from the operation of equipment with spare elements is proposed. The Kijima-Sumita model is used as a model to describe the process of exhaustion of the object's operability. The developed model is investigated on simulation data.

TECHNOLOGIES OF INFORMATION SUPPORT OF TERRITORIAL SAFETY MANAGEMENT 349

Valeriy Nicheporchuk, Ulyana Postnikova

The paper presents approaches aimed at solving the problems of territorial administration related to: limited availability of integrated monitoring data, the impossibility of reproducing risk calculations by independent groups of researchers; the general nature of recommendations on the composition and scope of preventive measures, formed based on the results of risk calculations and not taking into account the specifics of S-N-T systems; lack of indicators for assessing the impact on safety of the implemented preventive measures; lack of scientific substantiation of management processes, the absence of generally accepted models for forecasting the security of territories for a long-term period, which allow more systematic planning of strategic

EVALUATION OF THE INFLUENCE OF LONGITUDINAL OSCILLATIONS ON DYNAMIC RESISTANCE OF NON-UNIFORM CORES 356

Asim Imamaliyev

The relevance of the problem of calculating the vibrations of complex rod systems is due to the practical need to improve the technical characteristics of the designed machines and mechanisms and ensure their functioning under ever wider ranges of operational impacts, as well as to reduce the material consumption of machines and structures. To fully determine the strains and stresses that occur at any point in the system during vibrations, it is necessary to know the displacements at these points. This leads to the need to consider systems with an infinite number of degrees of freedom.

**ESG - CRITERIA AT THE PRESENT STAGE OF SOCIETY
DEVELOPMENT 369**

Alisa Olisaeva, Marina Galazova, Leyla Magomayeva, Anastasia Ledovskaya

The current challenge facing society and business is to study the ESG agenda, implement it into operations and develop appropriate recommendations to promote ESG principles to improve the environment and well-being of the global community. In order to address inequality and stimulate economic growth, the UN adopted the 2030 Agenda for Sustainable Development in 2015 and launched a plan to ensure sustainability for present and future generations, reduce poverty and improve the lives of people around the world.

**THEORETICAL AND CONCEPTUAL APPROACHES TO STUDYING
THE NATURE OF ECONOMIC GROWTH 369**

Alina Gudieva, Tatyana Sitokhova, Marianna Kelekhsaeva,
Magomed Suleymanov, Kantemir Khachirov

The subject of this article is the study of the theoretical foundations of the phenomenon of economic growth. During the study, the authors chose a general retrospective methodology and predominantly historical analysis.

**DEVELOPMENT OF MOLECULAR GENETIC APPROACHES TO
PREDICT THE OCCURANCE OF FOCI OF BACTERIAL DISEASES
IN FOREST ECOSYSTEMS 381**

Lyubov Ivashchenko, Stanislav Panteleev, Oleg Baranov

In the course of the study, specific primers were developed to identify 20 species of phytopathogenic bacteria from 12 genera associated with the occurrence of infectious diseases in seven forest-forming species of Belarus. The results showed that the developed oligonucleotides are specific for the 16S (mtDNA and cpDNA) and 23S rRNA genes of the studied phytopathogenic bacteria.

**MAIN TRENDS IN CLIMATE CHANGE IN THE HOLOCENE EPOCH
OF THE ANTROPOGENIC PERIOD IN THE WORLD AND IN THE**

CAUCASUS 387

Arun Daukaev, Rustam Gakaev, Tumisha Bachaeva

The article is devoted to the problem of climate change on Earth, and in particular in the Caucasus. The main trends in climate change are traced during the Holocene epoch of the Quaternary period. Attention is focused on the most noticeable periods of cooling and warming - the medieval warming period, the Little Ice Age, the newest warming period, which began at the end of the 19th century. The issue of global warming is also touched upon.

THE ESTIMATED REASON FOR THE LOW EFFICIENCY OF HYDROCYCLONES IN PETROLEUM INDUSTRY 391

Gafar Ismayilov, Amrah Gulubayli, Samir Musayev, Shafa Musayeva

In the paper, according to the multiphase technology, the reason for the low efficiency of hydrocyclones for multiphase disperse systems was analyzed. The condition of equality of the shear and centrifugal forces during the operation of the hydrocyclone is shown. It has been established that, based on the correct choice of technological parameters, it is possible to avoid the negative effect of the shear force in cylindrical flows on the operation of hydrocyclones.

THE PROBLEM OF POVERTY IN THE MODERN WORLD IN THE CONTEXT OF SUSTAINABLE DEVELOPMENT 396

Ayna Salamova, Saleh Khodjaliev, Sergey Dokholyan

Described figures from official statistics: towards the present time, approximately 40% of us live below this poverty line. It created the choice of topic and its relevance. To study this problem in detail, it is necessary to conduct an in-depth scientific study, a thorough theoretical analysis and the development of practical guidelines based on the presented basis. These guidelines could be used to develop and implement an effective economic and social policy that would undoubtedly be aimed at reducing poverty to the lowest level.

ASSESSMENT OF THE IMPACT OF CLIMATE CHANGE ON THE PRECIPITATION REGIME IN THE SOUTHERN SLOPE OF THE GREATER CAUCASIAN PROVINCE 404

Sevinj Rzaeva, Jamal Guseynov, Allahverdi Tagiyev

The impact of global climate changes on the perennial precipitation regime in the southern part of the Greater Caucasus region was studied. In the analysis, the precipitation observation data of 8 meteorological stations during the years 1991-2020 were used. Multi-year (1991-2020) various indicators of precipitation were compared with the base quantities. In the study, the multi-year period was considered for 2 periods (1991-2005, 2006-2020) and the monthly, seasonal and annual trends of precipitation were compared. The study found that the multi-

year average temperature in the province for the last 30 years was 11-14°C in the lowlands and 6-7°C in the mid-mountains.

FORECASTING OF THE PROBABILITY OF UNNATURAL DESTRUCTIVE EVENTS OCCURRENCE AT REFINERY COMPLEXES 411

Oksana Morozova, Stanislav Butuzov, Valery Artyukhin

The paper proposes some approaches to building a model for predicting the probability of emergency situations at the enterprises of the oil refining complex in modern conditions. The approach is based on modeling using the binomial distribution. The initial data of the model are open data on the occurrence of emergencies on the territory of the Russian Federation for the period 2022–2023.

SUSTAINABLE DEVELOPMENT: ECONOMIC EFFICIENCY OF ECOSYSTEMS 417

Magomed Suleymanov, Evgeniya Atamas, Aliheydar Shahmarov

Attempts to undermine the significance of the UN 2030 Agenda for Sustainable Development adopted in 2015 under the influence of the COVID-19 pandemic quickly gave way to the importance of uniting efforts aimed at achieving the 17 Goals that are the basis of governance (SDGs). Efforts at many levels - from states and their regional entities to municipalities, corporations, or ultimately the level of specific people in society by and large. Attention to sustainable development issues is also growing against the backdrop of an obvious deterioration in the climate situation and the need to create energy security.

RISK ASSESSMENT IN SUBSEA PIPELINES FOR THE CASPIAN SEA CONDITIONS 422

Ramiz Ismayilov, Rugiya Asgerova, Ismayil Ismayilov, Turkan Guliyeva

The article presents the results of studies conducted on the analysis of risks in the underwater pipelines of the Azerbaijan sector of the Caspian Sea. For the study, the results of long-term observations of the state of the state of underwater pipelines and the opinions of experts in this field were collected. Based on the analysis of these data, the most characteristic situations were identified that, to one degree or another, led to the loss of pipeline performance and the need for repair and restoration work. It was found that the main hazards for subsea pipelines in the Caspian Sea are external and internal corrosion. Pipelines floating, damage at pipe junctions, vibrations, damage from falling foreign objects, and wave impacts in the coastal strip.

THE LABOR CONTRIBUTION OF THE DEPORTED PEOPLES TO THE DEVELOPMENT OF THE ECONOMY OF CENTRAL

ASIA IN 1940-1950 428

Sapiyat Tsutsulaeva

The deportation of Chechens and Ingush were a repression with social and economic consequences for the deportees themselves. This forced displacement of Kazakhstanis and living in difficult conditions in new settlements caused great problems and difficulties for them, as well as for the economy of Kazakhstan. Their forced displacement and living in difficult conditions made it possible to solve many problems with economic development at all.

ECONOMIC SECURITY IN EUROPEAN COUNTRIES: CHALLENGES, SOLUTIONS, AND RECOMMENDATIONS 434

Rizvan Aliev, Tamerlan Magomaev, Aпти Mentsiev

Addressing the risk of the European population trap demands responsible population control and sustainable resource management. The research emphasizes the interconnectedness of economic and national security, advocating for a holistic approach that integrates policies to foster economic resilience, promote social inclusion, and safeguard national interests. Policymakers must consider these multifaceted dimensions to ensure sustainable economic security and prosperity in the face of global challenges.

DEVELOPMENT OF ACHIMOV DEPOSITS SEDIMENTATION MODEL OF ONE OF THE WEST SIBERIAN OIL AND GAS PROVINCE FIELDS 441

Yury Nefedov, Danila Griбанov, Emil Gasimov, Dmitry Peskov, Gao Han, Nikita Vostrikov, Shafagat Pashayeva

The results obtained characterize the expected sediment geometry, lithology distribution due to sea level changes, paleogeography, paleoclimate, tectonics and sediment input rates. The results allow the evaluation of different options and enable us to predict the distribution of prospective oil and gas bearing sediments in areas where no wells have been drilled. As a result, a sedimentation model was obtained, which reflects the formation of the elements of the sedimentation system of the study area. According to the sedimentation model, the main facies zones of the turbidite sediments under consideration are identified.

DIAGNOSIS OF THE RISK OF OIL LEAKS FROM PIPELINES 449

Hajar Ismayilova, Fidan Ismayilova, Mansur Shahlarly

The research paper studies the issue of detecting the location and amount of hydrocarbon losses in cases of accident-damage (spill), which occur during the transportation of oil and oil products via the technological and main pipes. The grapho-analytical method has been introduced and tested in order to determine a location and degree of the leakage following the change in working parameters.

**NPP MAINTENANCE AND REPAIR RISK MANAGEMENT:
THE CASE OF RUSSIA 456**

Mariia Volos, Evgenii Polev

The process efficiency indicators as indicators of risk tolerance are considered. An effectiveness assessment of the risk management system of the maintenance and repair process is presented. The key shortcomings are identified. The line of further research on shortcomings exclusion is formulated.

**MODERN TEACHING TRENDS IN MARITIME ENGLISH AS A GLOBAL
INSTRUMENT IN SPREADING OF INDIVISIBLE BUSINESS
ENVIRONMENT IN MARITIME INDUSTRY 465**

Gulchohra Aliyeva

The obvious conclusion by examining the proceedings of the Sub-Committee on the International Maritime English Conference (IMEC) is that the English language is rapidly gaining ground on effective delivering of lectures within the maritime establishments because its composition, flexibility, vocabulary and pragmatics completely makes it to become the “Lingua Franca” of Maritime English.

**SPECIAL TAX REGIMES AS A TOOL FOR ENSURING ECONOMIC
SECURITY 472**

Larisa Aguzarova and Fatima Aguzarova

The subject of this article is the study of special tax regimes as a tool for ensuring economic security. In the course of scientific research, the authors used general scientific methods. Among them: improvement of tax legislation in terms of certain elements of the regimes under consideration and conditions for their application; exemption from tax payments of newly created business entities until they receive profits; creation of comfortable conditions with counterparties. The authors emphasize that the main purpose of applying the regimes is the strengthening and further development of business entities, as well as ensuring economic security.

**USE OF SECONDARY ENERGY RESOURCES OF MODULAR POWER
PLANTS WITH A GAS ENGINE AND REDUCTION OF HARMFUL
EMISSIONS 479**

Jamala Mamedova

The paper considers the use of exhaust gas heat in modular power plants. In this regard, fuel consumption at power plants will decrease, efficiency of power plant will increase the emission of harmful gases into the atmosphere and environmental burden will reduce.

**AEROSPACE MONITORING OF SEA OIL POLLUTION
BASED ON TECHNOLOGIES OF COGNITIVE AND EXPERT
SYSTEMS 483**

Nazif Sattarov

The development of new technologies and methodologies that provide information support for ecological observations (in particular, environmental audit and risk analysis), is of decisive importance. In this regard, remote sensing from orbiters exemplifies a powerful method of planetary exploration. Onboard sensors provide unique views of the Earth's surface combined with a large range. On the base of the above-mentioned facts, this paper is aimed at discussing several important features of aerospace monitoring of the oil pollution of the Caspian Sea surface using technologies of cognitive and expert systems.

**MONITORING OF INDIVIDUAL SEISMIC RISK AT ALL STAGES OF
DEVELOPMENT OF A POSSIBLE EARTHQUAKE SOURCE 489**

Gennady Nigmatov, Andrei Savinov, Temir Nigmatov

The effectiveness of measures on seismic safety of the population will depend on how correctly the possible earthquake source and seismic hazard zones, in which destructive seismic impact is expected, seismic resistance of buildings in these hazard zones, the number of population falling into the seismic zone, possible consequences have been determined. Knowing the possible consequences, it is easy to determine the necessary forces and means to prevent risks and rescue the population.

**ASSESSMENT OF THE WATER BALANCE OF THE TERRITORY AND
RIVERS WATER RESOURCES USING A NEW OPERATIONAL-
INTERACTIVE METHOD 500**

Rza Makhmudov, Vugar Aliyev, Movlud Teymurov, Emil Gafarov

A new method (CWBM) is proposed for calculating the water balance of the territory and water resources of rivers. CWBM was developed on the basis of reliable scientific sources (satellite images, GIS-technologies, modern scientific approaches, advanced hydrological models). Comparison of the actual and calculated with CWBM method flow for 113 river basins of Azerbaijan shows that the error between them was up to 10% for 92 and 10-15% for 21 rivers.

**CONSTRUCTION OF A MULTI-CONNECTED CONTROL SYSTEM
FOR SAFE COKE PRODUCTION 510**

Aygun Safarova, Elchin Melikov, Tamella Magerramova

The risks that may arise from all waste types in production objects are identified and controlled. According to the oil company's policy, reducing the impact of waste on the environment determines its recycling. In the technological processes course, environmental protection and safety personnel constantly monitor installation for gas safety, inspect the air and toxic environment, and ensure gas safety at work. When the raw material is heated to the required temperature in the furnace, the gas fuel supplied to the furnace creates a fire hazard. Technically, oil products coking makes it possible to cost-effectively and expediently increase and improve oil refining.

**DETERMINATION OF DRINKING WATER RESOURCES IN THE
KARABAKH PLAIN (AGHDAM REGION): THE ROLE OF
EXPLORATION AND RESEARCH 518**

Vagif Karimov, Mehriban Ismailova, Jafar Sharifov, Yuri Nefedov

The article uses data obtained during exploratory drilling. By conducting comprehensive studies and analyzing available literary sources, the characteristics of the hydrogeological situation associated with the occurrence of groundwater and water strikes were clarified. Also, the hydrological conditions in the area where the research was conducted were studied and analyzed. The conditions of groundwater formation, chemical composition, mineralization and other indicators of groundwater are studied, the areas of their distribution are determined, and recommendations are given for their rational use for irrigation and other purposes in agriculture and to provide the need for fresh water in the liberated Aghdam region.

**DATA-DRIVEN DIGITAL TRANSFORMATION: CHALLENGES AND
STRATEGIES FOR EFFECTIVE BIG DATA MANAGEMENT 526**

Adam Mentsiev, Timur Aygumov, Elmira Amirova

The study is devoted to the study and analysis of the risks associated with managing big data during the period of digital transformation of organizations. The purpose of the work is to identify the problems and risks that organizations face when integrating and using big data in an effort to remain competitive and successful in today's economic realities. The study uses a mixed approach to data analysis, which allows a comprehensive study of the issues of data management in the process of digital transformation. In the course of the work, the main problems and risks that organizations face when working with big data are identified. These risks include data governance and privacy, data security, data integration and interoperability, scalability and infrastructure, data quality and integrity, and employee skill and experience issues. The study proposes strategies to address these challenges, including developing a comprehensive data governance framework, investing in data security, and using advanced analytics and artificial intelligence.

**PORTABLE PROPERTIES OF THE RESERVOIR WATERS USED IN
POWER SYSTEM 532**

Vagif Hasanov, Jeyhun Naziyev, Leyla Hasanova, Aqil Omarov, İrada Aliyeva, Gulshan Akhundova

In comparison with the sea shipping, systematic pollution of the sea by oil seems insignificant under oil-and-gas field engineering. Measurements of the viscosity of reservoir waters by remote capillary in the temperature interval of (298.15 to 598.15) °K and the pressure of (0.1 to 40) MPa are reported. The relative uncertainty in the viscosity does not exceed ± 1.8 %. An equation describing viscosity of the studied reservoir waters and the dependence with the mineralization, pressure and temperatures is given.

SIMULATION MODELING AND MAPPING OF CATASTROPHIC FLOODS IN POORLY STUDIED AREAS FOR EMERGENCY RISK MANAGEMENT 539

Irina Oltyan, Elena Arefyeva, Mikhail Bolgov, Nikita Oltyan

Method presented in the article for modeling parameters of catastrophic floods, such as the water level of the given probability of exceedance and depth of corresponding probability of exceedance, as well as the flooding area for unexplored territories, is based on the use of the digital relief model approach, construction of hydrographic network in the form of oriented graph characterizing the direction of water flow, invoking generalized regime hydrological information in the form of estimated parameters maps of the maximum flow, and the use of virtual gauging stations, as information reference points for calculations.

FIBER-OPTIC SENSOR FOR FUNCTIONAL SECURITY OF THE OBJECT PERIMETER PROTECTION SYSTEM 552

Tofiq Mansurov, Elnur Mansurov, Irina Yablochnikova, Gulnar Gurbanova, Rahman Mammadov

Experimental studies have been carried out to determine the susceptibility of various types of optical fiber to macrobending, the dependence of the attenuation of the optical radiation signal on the macrobending radius, the length of the macrobending arc, and the mass of the unauthorized access object.

HIGH-PRECISION GROUND-BASED PHOTOMETRIC MONITORING METHOD FOR VALIDATING SATELLITE MONITORING OF ASSOCIATED HYDROCARBON GAS BURNING 560

Yegana Aliyeva, Kifayat Mammadova, Matanat Hasanguliyeva

The conducted research allowed to identify redundancy in correction procedures in known three-wave solar photometers. Two new methods for constructing compensated photometers are proposed. In the proposed constructions, the correction procedure is limited to the calculation and installation of one correction factor.

SOME ASPECTS OF OPERATIONAL RISK MANAGEMENT IN OIL AND GAS FIELD PIPELINES 565

Gafar Ismayilov, Elman Iskandarov, Zivar Farzalizade, Rabiya Abishova

Field technological pipelines - capital engineering structures designed for long-term operation and intended for the uninterrupted transport of well products (oil, gas, condensates, water and their mixtures) to the treatment complex. Negative risk events accompanying the operation of field process pipelines, including failure, total or partial loss of serviceability may occur during operation and are related to several factors. This paper outlines the risk factors, the main adverse impacts and threats to oil and gas field pipelines, and the rules for operational risk mitigation for oil and gas field pipelines.

GLOBAL RISKS OF BIOLOGICAL INVASIONS OF PHYTOPATHOGENIC ORGANISMS AND IMPROVEMENT OF THE QUARANTINE MONITORING SYSTEM USING COMPUTER MODELING 569

Vyacheslav Zviagintsev, Anna Prokhorova, Tatiana Surina,
Daria Belomesyeva

As a result of assessing the distribution of adventitious species of phytopathogens on the territory of Belarus, a trend of increasing the number of recorded invasions was identified. Every year, an average of 3-4 new pathogens of infectious diseases of woody plants are identified in forests and gardens, and over the past 25 years, at least 57 new types of phytopathogens have been recorded. Many of the newly identified species have already passed the stage of acclimatization, and some have a significant impact on the sanitary condition of forests and parks, causing significant damage.

THE USE OF NATURAL FILTRATION SORBENTS TO SOLVE THE SAFETY PROBLEMS OF INDUSTRIAL POLLUTION FACILITIES 582

Peter Belousov, Anastasia Rumyantseva, Ksenia Kim, Boris Pokidko, Vitaliy Milyutin,
Yulia Izosimova, Ekaterina Tyupina

This work is devoted to the review of mineral and organic natural sorbents for the purpose of purification of polluted waters of industrial enterprises. Structural features, differences in the composition and properties of the most common natural sorbents, features of their application and sorption mechanisms of pollutants are shown.

ENVIRONMENTAL RISKS ASSESSMENT OF COASTAL AREA IN THE SOUTH-EASTERN BALTIC SEA TO OIL POLLUTION 588

Elena Krek, Alexander Krek, Vadim Sivkov, Zhanna Stont

A low probability of oil pollution of coasts from two main potential sources located in the waters of Kaliningrad Region (Russian Federation) in the Baltic Sea is shown based on the results of modelling using Seatrack Web (SMHI, HELCOM). The most threatened areas of the coastal zone and coast, in the middle part of the Curonian Spit – UNESCO World Heritage site, as well as the distal part of the Vistula Spit and on the entire western coast of the Sambia Peninsula, were identified.

APPLICATION OF A RANK FUZZY REGRESSION MODEL TO PREDICT THE TECHNICAL CONDITION OF WELL PIPES 592

Ibrahim Habibov, Oleg Dyshin, Gulnara Feyziyeva, Irada Ahmadova, Zohra Garayeva

The paper proposes a method for predicting the maximum loss of pipe thickness based on the results of electromagnetic inspection by the step values of the depth of immersion of the lower part of the pipe into the well. Based on the use of fuzzy regression with fuzzy input/fuzzy output, a method for assessing the level of impact of the main formation parameters on the technical condition of well pipes is proposed.

GEOCHEMICAL SOUNDING OF TECTONIC FAULTS MEASUREMENT-BASED EXHALATION OF SOIL RADON 602

Yelizaveta Yessenzhigitova, Abdulaziz Abdullaev, Maksim Markin, Vladimir Borisov, Aset Muhamadiev

The scientific and methodological issues of geochemical sounding and localization of tectonic fault activity based on profile measurements of exhalation (volumetric activity) of soil radon (Rn 222), as well as emanation surveys on the territory of Ust-Kamenogorsk, carried out here in 2021-2023 in connection with seismic micro zoning (SMR) are outlined. It has been established that those geochemical methods of deep sounding of tectonic faults allow to reliably clarify the location and determine the activity of tectonic faults in the study area and provide new materials for seismic zoning of critical objects and determining seismic risk factors.

INVESTIGATION OF PARTICLES EMISSIONS WHEN USING VARIOUS ELECTRODES FOR UNDERWATER WELDING 612

Konstantin Kirichenko, Vladimir Chernousov, Anton Pogodaev, Alexander Gridasov, Yuri Kalinin, Igor Vakhniuk, Alexey Kholodov, Sergei Parshin, Kirill Golokhvast

The article is devoted to the study of the mass and quantitative concentration of suspended particles during underwater welding for sea water from the Ajax Bay (Sea of Japan) using two technological modes with special electrodes for welding and cutting metal. The mass concentration of PM10 particles does not exceed the threshold MPC values established in the Russian Federation, Belarus and the USA.

**EXAMINATION OF THE PRESCRIPTION OF A DOCUMENT AS
A WAY TO IDENTIFY MALFEASANCE 619**

Dmitriy Mokhorov, Dmitriy Anisimov, Vladimir Kochemirovsky

The article discusses the signs of artificial and natural aging of documents under the influence of temperature and humidity changes. It is shown that the use of technologies for artificial aging of documents can create risks of concealing malfeasance, leading to economic, technological damage and health. Methods for detecting signs of artificial aging and the possibility of using physicochemical methods of analysis to detect falsification are discussed.

**DESIGN AND APPLICATION OF NANOCOMPOSITE BASED ON CLAY
MINERAL (GLAUCONITE) AS ECO-FRIENDLY FERTILISER FOR
AGRICULTURE 632**

Maxim Rudmin, Boris Makarov, Prokopi Maximov, Evan Dasi

This study explores constructing and using nanocomposite fertilisers from glauconite amalgamated with a carbamide solution-gel. The ensuing nanocomposite exhibits enhanced intercalation between ammonium and glauconite, as substantiated by extensive analyses using techniques such as XRD, TEM, FTIR, TG-DSC, SEM-EDS, Brunauer–Emmett–Teller (BET) analysis, soil leaching experiments, lab and field agricultural tests.

**METHODOLOGY OF RISK ASSESSMENT OF FORENSIC TECHNICAL EX-
PERTISE IN RECOGNIZING THE AUTHENTICITY OF AN ELECTRONIC
DIGITAL SIGNATURE 645**

Pavel Menshikov, Alex Tsirdava

The article discusses the issues of using an electronic digital signature as enhanced authentication of the signature owner, as well as preserving the integrity of the document content. Particular attention is paid to the issues of differences in the types of electronic signatures (ES). ES has long been part of the usual electronic document flow, it is used in the banking sector.

**NATURAL RESOURCE POTENTIAL OF MOUNTAIN LANDSCAPES OF
THE CHECHEN REPUBLIC FOR THE DEVELOPMENT OF REGENERATIVE
ANIMAL HUSBANDRY 648**

Zagir Ataev, Rashiya Bekmurzaeva

The article discusses the regional features of the natural components and landscape structure of the Makazhoy basin as a natural resource potential for the potential development of regenerative animal husbandry in the mountainous part of the Chechen Republic.

APPLICATION OF UNMANNED AERIAL VEHICLES TO OBTAIN MORPHOMETRIC CHARACTERISTICS OF LANDSLIDES 656

Ulzhan Aldabergen, Victor Blagoveshchensky, Sandugash Ranova,
Aidana Kamalbekova

On the basis of the obtained aerial photographs, were built a 3D digital elevation model, an orthophoto of the terrain, longitudinal and transverse profiles of the landslide area and the adjacent slope using special software Agisoft Metashape Professional.

RISK ASSESSMENT OF THE NEGATIVE IMPACT ON HUMAN HEALTH OF ELEMENTAL CONTAMINANTS IN BROWN ALGAE (Laminariaceae) AND PRODUCTS BASED ON THEM 663

Viktor Shchukin, Elena Khorolskaya, Nataliya Kuz'mina

The content of elements Al, As (inorganic form), Cd, Cr, Co, Cu, Fe, Hg, I, Mn, Mo, Ni, Se, Pb, Sr, V, Zn in Laminariae thalli was measured by inductively coupled plasma mass spectrometry. Based on obtained data, the non-carcinogenic risks of the analyzed elements on human health where assessed when they enter the body together with a therapeutic dose of medicinal native products based on Laminariae thalli. It was found that the total hazard index at the 95th percentile concentrations level is 1.44. The maximum contribution to the hazard index is made attributed to iodine ($HQ_{95\%}=1.37$).

ON THE INFLUENCE OF SEISMIC INTENSITY IN A ROCK MASS IN THE DESIGN OF TRANSPORT TUNNELS 670

Mikhail Lebedev, Yuriy Isaev, Kirill Dorokhin, Alexey Malovichko,
Ruslan Dyagilev, Mikhail Pyatunin

The results of experiments on simultaneous recording of seismic signals from various sources on the Earth surface and at a depth of up to 250 m are stated. The peculiarities of change with depth of the spectral composition of teleseismic earthquake and microseismic oscillations have been studied, which testify in favour of a significant decrease in the level of seismic effects on underground structures in a wide range of frequencies in relation to buildings and structures on the daylight surface.

STATISTICAL ANALYSIS OF SUSTAINABLE DEVELOPMENT OF MODERN ECONOMY 678

Alisa Olisaeva, Marina Galazova, Leyla Baysultanova

The importance of solving the problem of food security and healthy nutrition is emphasized. In the course of scientific research, general and special methods of scientific knowledge were ap-

plied: analysis, synthesis and comparison, as well as statistical data analysis and visualization.

**INFLUENCE OF THE ENVIRONMENT ON THE DEPORTED
(BY THE EXAMPLE OF THE CHECHEN PEOPLE) 687**

Sapiyat Tsutsulaeva

When Chechens were forced to abandon the land and move into unfamiliar regions, they faced changes in climate conditions, natural resources and habitats. The situation was similar for people who left them from their homeland as well as for agriculture and livestock.

**ENVIRONMENTAL ECONOMICS AND SUSTAINABLE
DEVELOPMENT 695**

Magomed Suleymanov, Aminat Huazheva, Elman Akhyadov

In the presented paper it has been determined that the main problem with the use of these tools is their lack of consistency: the start of their work is scheduled for almost the same time, while their effectiveness depends on the results of each other's work.

**ANALYSIS OF THE USE OF COATED PIPES IN MARINE
VESSELS 703**

Vagif Gasanov, Elvin Ibragimli

Based on the information obtained through Arduino microcontroller, the coordinate of the crack is found. So, since we obtain the information about the instantaneous displacement of the electrode with the encoder, we determine the coordinate of the crack according to the maximum value of the current leakage based on the diagram obtained.

**NEWEST TRENDS IN INTERDISCIPLINARY RISK-BASED RESEARCH
AND GOVERNANCE OF CRITICAL AND STRATEGIC INFRASTRUC-
TURES 708**

Sviatoslav Timashev

This paper is a condensed version of the keynote lecture presented at the opening of the fifth Eurasian conference on Risk in Baku, Azerbaijan, October 17 2023. It is mostly based on results of the content analysis of 1500+ peer reviewed papers related to reliability, resilience, risk and safety of infrastructure systems published over the last 25 years, provided by renowned international specialists in these topics.

THE FINAL DECISION
Fifth Eurasian Conference RISK-2023
“Innovations in Minimization of Natural and Technological Risks”
October 17 – 19, 2023, Baku, AZERBAIJAN

We are the participants of the 5th Eurasian Conference "Innovations in Minimization of Natural and Technological Risks" having discussion and summary international experience of traditional and innovative approaches to the assessment, analysis and management of natural and man-made risks, declare that the main goals of the RISK-2023 conference have been achieved:

- bringing together scientists and specialists in the field of analysis, assessment and management of natural and man-made risks and providing them with the opportunity to exchange information, ideas and innovative solutions;
- promoting the transfer of innovative and advanced knowledge about natural and man-made risks, and technologies for their minimization;
- promoting mutual understanding and professional interaction of scientists, specialists and organizations in order to develop the theory and improve the best practices for minimizing natural and man-made risks;
- deepening cooperation and mutual understanding between industry actors, scientific and academic institutions in the analysis, assessment and management of natural and man-made risks;
- supporting the Sendai (Japan) UN Framework for Action on Disaster Risk Reduction 2015–2030. As a guiding baseline document, reflecting strategic objectives and priority areas for action, as well as expected results on a better understanding of disaster risk in all its aspects;
- identification of the innovative approaches to identify various types of natural and anthropogenic hazards, methods of analyzing and assessing them and methods of making managerial decisions that ensure the safety of the population and sustainable socio-economic development of various regions of the Eurasian continent.

We are the participants of the 5th Eurasian conference “Innovations in Minimization Natural and Technological Risks” confirming our commitment to an active position in the formation of national and interstate mechanisms for ensuring the safety of the population and territories. We consider that it is important to involve all stakeholders in the risk analysis, risk assessment and risk management.

We call for uniting efforts of scientists and specialists from Eurasian countries to increase the efficiency and responsibility of solutions to minimize the risks of natural and anthropogenic emergencies which is expressing the concerning about the scale of losses from accidents and disasters caused by natural and man-made disasters,

We consider the existing of an organic relationship between minimizing the risk of emergencies and sustainable development of the country are important which involve all stakeholders in the analysis, risk assessment and risk management.

Considering the consensus of the conference participants, we express our support for the proposal of the chairman of the conference to hold the next Eurasian conference in Baku, Azerbaijan, in 2024.

On behalf of the Organizing Committee of RISK-2023 Conference,

Prof. Sviatoslav TIMASHEV
Prof. Vugar ALIYEV

RANDOMNESS, UNCERTAINTY, INCOMPLETENESS, RISK AND ITS MEASUREMENTS

Vladimir Rykov^{1,2}, Boyan Dimitrov³, Alexander Bochkov⁴,
Elvira Zaripova⁵, Olga Kochueva¹

¹Gubkin Oil & Gas Russian State University, Russia,

²Peoples Friendship University of Russia (RUDN University), Russia,

³Kettering University, Flint, USA,

⁴JSC NIIAS, Moscow, Russia

⁵Moscow University of the Ministry of Internal Affairs of the RF named after V.J.Kikot, Russia

vladimir_rykov@mail.ru

bdimitro@kettering.edu

a.bochkov@vniias.ru

ezarip@gmail.com

olgakoch@mail.ru

Abstract

In this work we analyze different aspects regarding the terminology, understanding concepts and approaches in modeling and measuring components and variables related to safety and risk. This discussion conversation is open for further interpretations and suggestions. We study it with the help of models (images) artificial, descriptions, scientific approaches, discussions, etc., and using the help of poly-semantic languages. Various kinds of risks arise precisely because of the uncertainty of the situation. Mathematical models use uncertainties in several ways: randomness, which is explained and measured by objective probability and estimated using statistical methods. Uncertainty, measured by subjective probabilities, is estimated by expert methods, or by fuzzy uncertainty methods. Each of these approaches has its advantages and disadvantages. Despite the difference in approaches to measuring uncertainties, the development of a risk situation are described in an appropriate way using an event tree. We show the construction of an event tree, that allows us to see details and specify in the development of a risk situation. We also discuss how this approach can be used to evaluate the sensitivity of the output characteristics of the process to the parameters of the initial information.

Keywords: risk, relative risk, uncertainty, certainty, risk tree, incompleteness, modeling, measurements, probability measures, randomness

I. Introduction

We live in a complex world full of indefinite uncertain situations, and incompleteness. In the XVII - XVIII centuries, when there was a discussion about the possibility of studying random phenomena, the main difference between DETERMINISTIC and RANDOM phenomena was formulated:

Deterministic phenomena UNIVERSALLY respond to the repetition of the experiment in the same HOMOGENEOUS conditions, and random ones - MULTIPLE. At the same time, random phenomena suggest the possibility of their MULTIPLE (ideally, infinite) repetition in the same (homogeneous) conditions.

However, we note that not all uncertain phenomena allow a probabilistic interpretation, which requires the possibility of their repeated observation under homogeneous conditions. This

led to the need to build other models for the study of uncertain (except random) phenomena.

Since risks are associated with the uncertainty of the situation in which they occur, a significant part of this article is devoted to clarifying concepts and terminology in the field of uncertainty, randomness and risks. Numerous studies are devoted to risks in modern literature. However, a sufficiently definite understanding of this concept among specialists has not yet been achieved. The works [1] – [3] offer a fairly consistent analysis of the interpretation of the concept of risk at the time of their publication.

The concept of risk in the mathematical literature appeared for the first time in connection with the “ruin” problem in insurance and financial models in mathematics, and was the subject of so-called “collective” risk models. These models have brought to life a large stream of deep GENERAL mathematical research [4], [5].

Features of the models of “individual risks”, which include risks in oil and gas industries their specificity, and the need for an individual approach to the study of various types of risks. The article [6] gives a detailed study of the origin and development of the concept of risk, which, however, does not help much in formalizing this concept for a clear study of the phenomena associated with it.

In many studies related to the concept of risks, probabilistic terminology is used unreasonably from our point of view. In this sense, it is categorically impossible to agree with the concept of chance reasoning about the chance or “biological determinism” of the emergence of life on Earth [7]. By themselves, studies of the conditions, causes, and development of living matter on Earth are, of course, interesting, and useful and deserve every encouragement. Still, the concept of “INCIDENCE” should not be involved in their description, because in science it is already ENGAGED and strictly defined. The fact that the word chance in “everyday language” occurs in different contexts should not replace it in scientific research. In this regard, when studying such phenomena as reliability, risk, security, etc., it is necessary, first of all, to understand how it is possible to use such concepts as randomness, probability, etc. for their study.

In this regard, a significant part of this article is devoted to clarifying the concepts and terminology in the field of risks. At the same time, we note that not all uncertain phenomena allow a probabilistic interpretation, which requires the possibility of their repeated observation under homogeneous conditions. This led to the need to build other models for the study of uncertain (except random) phenomena.

First of all, we note that the language itself, due to its ambiguity, introduces its share of uncertainty into the interpretation of various concepts and we will try to give an unambiguous interpretation of various terms in their strictly scientific sense.

II. Polysemous of language. Various concept of uncertainty and their mathematical models

According to the complexity of the World and the languages and technology, all languages are poly-semantic. There are at least three different areas of language use: every day, literary and artistic (including poetic), scientific, etc. What is acceptable in ordinary language (different interpretation of words), is good in literature, is absolutely unacceptable in science, where an unambiguous understanding of words and terms is assumed and required. In this regard, we will try to give exact meanings (unambiguous language designations) to various concepts of uncertainties.

Various risks arise precisely because of the uncertainty of the situation. In everyday life, we are constantly confronted with various types of phenomena, in addition to *deterministic* and *unique* phenomena to deal with different types of uncertain phenomena. Various risks arise precisely because of the uncertainty of the situation. In the study of such phenomena as “reliability”, “risk”, “security”, etc., it is necessary, first of all, to understand how it is possible to use such concepts as randomness, probability, etc. for their study.

Mathematicians model uncertainties in several ways:

- randomness, which is measured by objective probability and estimated using statistical methods due to Kolmogorov [8];
- virtual uncertainty, which is measured by subjective probabilities according to DeFinetti and Savage [9];
- uncertainty that can be estimated by expert methods [10];
- uncertainty that is considered in the framework of fuzzy theory according to Zadeh [11];
- and may be some other types of uncertainties.

In this regard, bearing in mind the ambiguity of the language, it is proposed to clarify the above concepts. Below a classification of various types of phenomena is presented in the diagram in Fig.1.

It is proposed not to call all uncertain phenomena and events random, but, for example, unique, uncertain, possible, and fuzzy, and measure not by probabilities, but by chances, possibilities, belongings, etc.

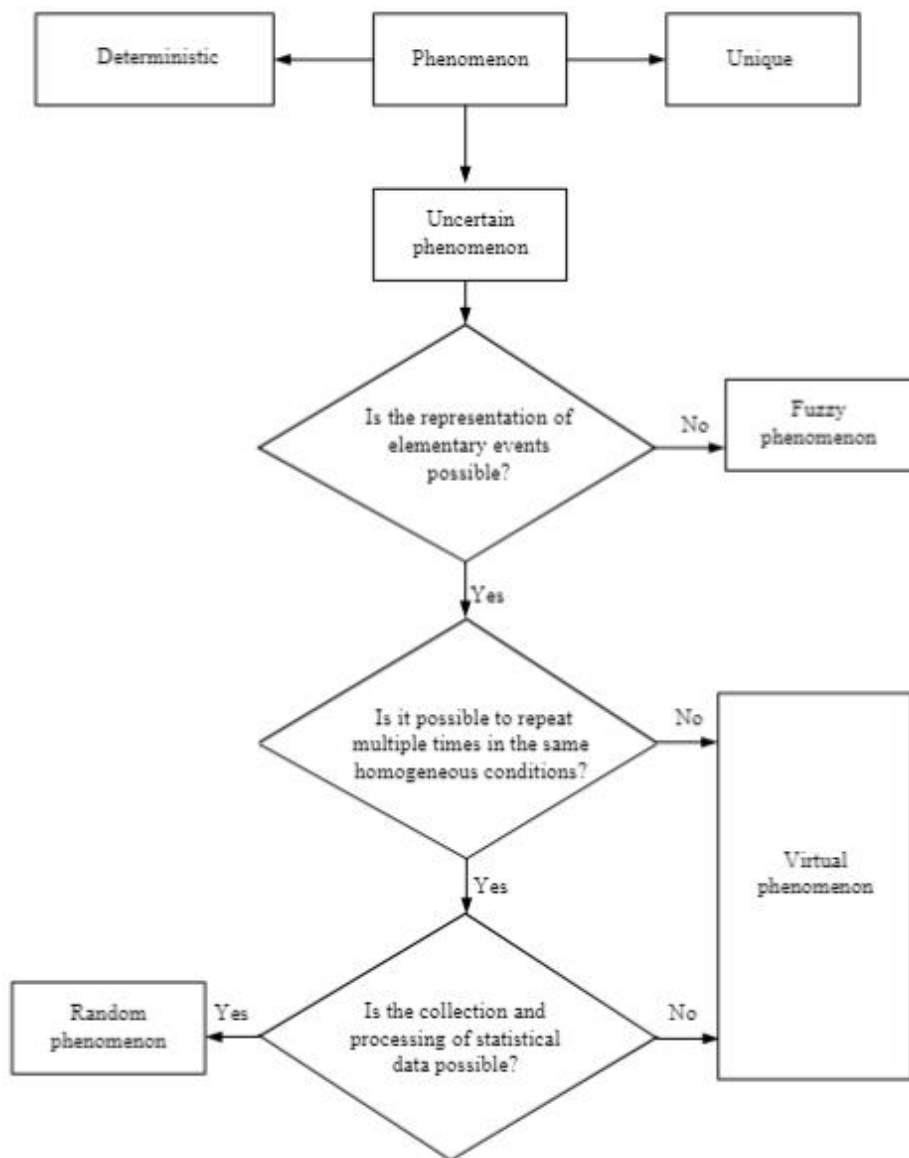


Fig. 1: Classification of phenomena

Their features described below:

- *Deterministic* phenomenon is a phenomenon that uniquely responds to the creation of the

same (homogeneous) conditions, including when it is repeatedly observed.

- *Unique* An event is an *event* that has only been observed once in the past and for the foreseeable future.

- By a *random* phenomenon we mean a phenomenon that can be observed many times under the same conditions and *reacts* to them with a multi-valued set of possible events, among which the minimal ones can be unambiguously identified. In this case, the measure of randomness is the objective probability, measured by frequency.

- A *virtual* phenomenon is understood as a phenomenon that reacts to the creation of identical conditions with a *multi-valued* set of possible events, among which it is possible to single out the minimal ones, but the possibilities of repeated observation of such phenomena under the same conditions are impossible or severely limited. We will call the measure of a virtual event a chance or a subjective probability, which is set by an expert in compliance with certain rules.

- *Fuzzy* is a phenomenon that reacts to the creation of the same conditions with ambiguous (vague, fuzzy) events, among which elementary (minimal) events are not singled out, and their belonging to one or another (possible) event is characterized by a membership function specified by an expert.

The above concepts are fundamental and not subject to strict definition. To understand what we mean, here are a few examples of various phenomena:

- deterministic: sunrise and sunset, pendulum swing;
- unique: "Big Bang" - the birth of the Universe, the birth of living matter on Earth;
- random: life expectancy of residents of various countries, up-time of incandescent lamps of a fixed manufacturer;
- virtual: the presence of an oil (coal, gold) deposit in some fixed area;
- fuzzy: train speed is rather fast, weather is rather overcast, teenager is rather tall.

All of the above is illustrated by the following Fig.2.

Each of these approaches has its advantages and disadvantages:

1. The advantage of the randomness model is the objectivity of estimates, the disadvantage is the difficulty (and sometimes impossibility) of obtaining the necessary initial information;
2. The disadvantage of the second and third approaches is the subjectivity of the estimates of the initial information, and as a result, the subjectivity of the conclusions;
3. In fuzzy logic models, the construction of the membership function is also at the mercy of the researcher, which leads to the subjectivity of the conclusions.

Regardless of which concept to follow when describing and studying risk, it develops over time and is associated with some costs. Therefore, the time of occurrence of a risk event and the costs it brings are its main characteristics. However, depending on the accepted concept of risk analysis, these characteristics can be measured and evaluated objective, subjective probabilities (and distribution functions built on their basis) or studied within fuzzy sets.

III. Understandings and measures of the risks

3.1. Understanding the risk

Risk is inherent in human activity. Activity is a conscious active interaction of the subject with the object, during which the subject purposefully influences the object, satisfying any of his needs, achieving the goal. Only a person who is able to realize possible losses or gains as a result of some action is at risk. Only a person is able to determine the purpose of his activity. Technique does not have subjectivity - it is only a means to achieve goals. Which should be efficient, reliable and safe.

Any activity is a random process aimed at achieving a certain goal, which is a change of states. States can be stable and unstable. Completion of the process - achievement of the final target state. Depending on external and internal factors, the trajectory of achieving the final target state may be different. To control a random process, a functional should be defined, for which an optimization problem should be set (search for the optimal control strategy), taking into account the existing

external and internal constraints (Kashtanov).

The change of states is preceded by a decision made by a person (refusal of a decision is also a decision), taking into account the state of the external environment and the control object. Since the decision maker does not, as a rule, have all the information about the external and internal environment, the decision is made under conditions of partial or complete uncertainty.

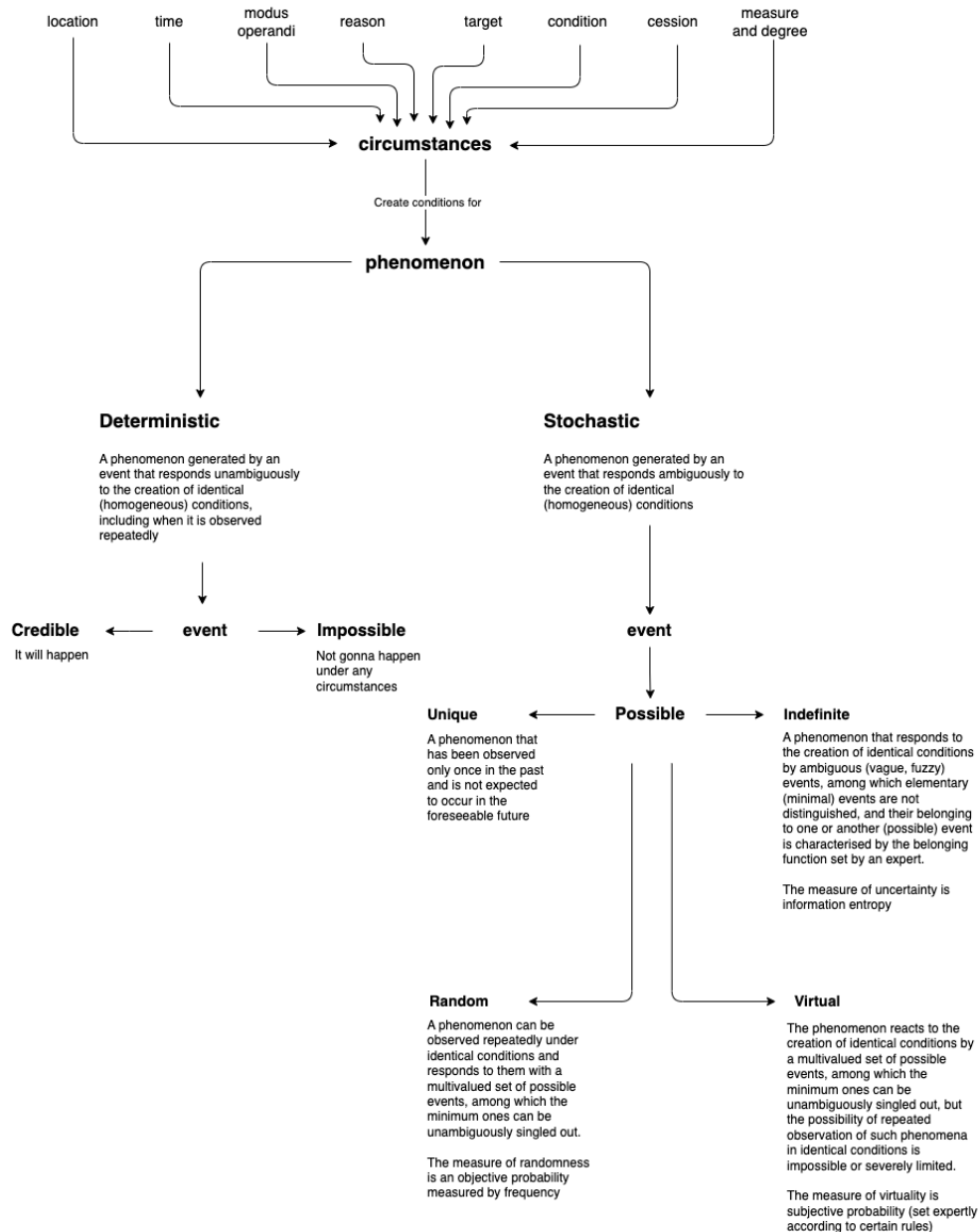


Fig. 2: Event-occurrence diagram

States have properties. For example, reliability is the property of an object to function continuously without fail with a 100 efficiency level. Only cancellations are considered. The failure criterion divides everything by yes/no. Functioning efficiency is the property of a system to function continuously, although, possibly, with a reduced level of output parameters. Stability - the property of the system to return (within a reasonable time) to the previous 100 percents level of functioning after the failure of individual components. Survivability is the property of an object to continue functioning within acceptable limits after the failure of individual components. Risk is a generalized property of the states of a real or model controlled random

process, on the trajectories of which a functional is specified that determines the goal of control and an optimization problem is set (search for an optimal control strategy, effective control) under constraints. Particular properties of states - circumstances (place, time, mode of action, causes, goals, conditions, concessions, measures and degrees, and opportunities), expected loss, probability of an undesirable event, objective and subjective uncertainty, possibility of loss, combination of probability and severity of consequences, consequences, the severity of consequences and their uncertainty, the impact of uncertainty on goals, etc.

3.2. On measuring the risks

Every measure uses numbers. but numbers are met everywhere. Important is to know the meaning of these numbers and what do they measure. In risks measures there is no exception.

Each particular property has its own measure (according to Riemann or Lebesgue). Numerous risk measures have been proposed in the literature. The choice of an appropriate risk measure is critical for the next decision step:

- Risk as a relative value (comparison with a control group, defined as the ratio of the probability of an outcome in the exposed group to the probability of an outcome in the unexposed group). Relative risk is often used in statistical analysis of paired outcomes when the outcome of interest has a relatively low probability [12]. Interesting measure of the risks is the so called relative risk used in bio-statistics and in medical statistics let us explain it in simple way. Assume, B is a risky event, like having a serious disease. and let A be a result of some test. Relative risk of B with respect of the event A is called the ratio called the ratio of the conditional probabilities $P(B|A)P(B|notA)$. This measure may take arbitrary positive values, while most of the risk measures are probabilities - numbers between 0 and 1.

- p-value as measure of risk. any statistical program after finishing the work on some dates gives at the end many numeric results, and there one will see a lots of numbers indicated p-values. This is actually a measure of the risk to admit the null hypothesis is not true, when actually it is. Therefore, it is important to know what is the hypothesis tested behind these p-values.

- Risk as a posterior error estimate (in mathematical statistics and decision theory, Bayesian estimate is a statistical estimate that minimizes the a posterior expectation of a loss function (a posterior loss expectation); ordinary (non-Bayesian) risk is the mathematical expectation of the variance of the posterior distribution) [13].

- Risk as a probability of loss (a consequence of the occurrence of some random event from a possible family of all events or the totality of possible damage in some stochastic situation and its probability (this concept covers the so-called frequency, statistical approach, most often applied to queuing systems, in insurance, theory reliability, etc.)) [14], [15].

- Risk in decision games with nature (payment for a decision in case of uncertainty of the response to the chosen decision (this includes the so-called Wald's maximum utility (guaranteed result, minimum gain) or Savage's mini-max regret (maximum loss), Hurwitz criterion (optimism coefficient))) [16].

- Risk as the difficulty of achieving the goal (geometric anti-risk, defined through a functional that describes the evolution of the system on a set of given trajectories, being a measure of assessing the quality of the system in relation to the quality required to achieve the goal) [17].

- Risk as a measure of the difference between states (semi-Hamming measure - a measure of the assessment of the degree of discrepancy between the real and the reference process, a measure of quality) [18].

- Risk as a measure of the stability of the center of the quasi-attract or in the phase space of states (for example, the product of variation ranges (in the sense of Stewart)) [19].

- Risk as an anti-potential for development (risks act as lowers of the rate of reproduction of the entire system) [20].

- Risk as a violation of the sequence of significant factors (violation of the lexicographic order, is estimated as a minimum of the total inconsistency of expert assessments (based on the equality of all participants in the examination) of the options for the development of the system,

measured in inversions of the transitions necessary to restore the lexicographic order of the compared options) [21] and etc.

If an activity leads to uncertain outcomes, then different decisions lead to different stochastic outcome variables. Probabilistic functionals are used to compare the results obtained with different solutions. Such functionals relate a quality value to a stochastic outcome variable or measure the degree of risk. In the latter case, these functionals are also called risk functionals or risk measures. When speaking about risk measurement in this article, we prefer to use the name "risk functional", and we reserve the term "measure" for probability measures.

In our paper, we consider the basic non-atomic probability space (Ω, F, P) and the linear space of real random variables defined on it. This space can be either the space Y of all measurable real functions on (Ω, F) , or some subspace of integrable functions.

The probability functional R is an extended real function defined on Y or on some of its subsets, i.e. we assume that R can take the values $+\infty$ or $-\infty$, but not both.

Risk, as a generalized property, is evaluated in two ways:

a) according to Kolmogorov - Borell - Riemann - when the integration is carried out over the damage (we add up the damages from all risks);

b) according to Lebesgue - the damage should be, as it were, fixed, but everything happens with different probability depending on the behavior of the person (we determine what we can lose).

The Risk trees discussed further also contain an interesting approach in measuring the risks.

IV. About the risk tree

Despite the different approaches to the measurement of uncertainty and the specificity of the evolution of risk situations, its development can be described in the same way using an event tree. The idea of the event tree dates back to the 1960s when in Bell-Lab it was used to study the reliability of complex objects and systems. Review of earliest studies in this direction one can find in [22]. Later it was used in other applications, including risk research. The information about the novel investigations in this direction one can find in Internet.

The construction of the event tree makes it possible to detail and specify the evolution of a risk situation. Therefore, in the paper, the technique of creating a complex program of construction and analysis of an event tree is offered, which is applicable to various types of risks and hazards. Regardless of the quality of the source information, event tree analysis allows us to assess the sensitivity of the output characteristics of the considered situation to the type and parameters of the initial information.

In the works [23, 24], a technique for constructing, equipping and analyzing a risk tree was developed. In our previous reports at the conferences Risk-21, Risk-22 [25, 26], as well in [27, 28], where the methodology was applied to analyze the risks of monitoring the subsea pipeline. Formally, the methodology is divided into three parts: building a risk tree, equipping it with information, and analyzing the risk tree.

Building a risk tree is the same for all types of uncertainties. The structure of the tree, the arrangement of elements, gateways for all types of uncertainties are the same. Equipping the risk tree with data for each type of uncertainty is different. For random events, the estimate will be represented by an objective probability, for a virtual phenomenon, expert estimates can be applied, and fuzzy events can be measured by a membership function. Using probability, chances and membership functions, one can obtain an estimate of the considered risk event.

This presentation methodology is detailed in [23, 24].

The risk tree is independent of the chosen concept of risk analysis. However, its equipping with initial information essentially relies on the chosen concept. Finally, the last stage, with the first two correctly performed, is implemented automatically.

Complex risk phenomena have a hierarchical (tree-like) structure descending from the main (root) risk event through intermediate events to the minimum (leaf) events that initiate the

development of the risk phenomenon. To describe such a structure, it is convenient to use the vector notation. Each minimal (elementary) event is associated with the vector $\vec{i} = (i_1, i_2, \dots, i_r)$, where i_0 means the main risk event, i_1 is the number of the first possible risk event under consideration. events of the first level, i_2 is the number of the event of the second level, leading to the event i_1 , etc. up to the leaf event i_r , leading along this path to the main risk event $(i_1, i_2, \dots, i_{r-1})$, where r is the hierarchy level of the considered minimum event, and different minimum events can have different hierarchy levels.

To work with the risk tree, we also need truncated vectors $\vec{i}_k = (i_1, i_2, \dots, i_k)$ to denote an intermediate event of the k -th level, and denote the j -th subevent of this event via $j(\vec{i}_k)$. So, each minimal event of the considered risk phenomenon is completely identified by the vector $\vec{i} = (i_1, i_2, \dots, i_r)$, and various intermediate events are truncated vectors $\vec{i}_k = (i_1, i_2, \dots, i_k)$.

To work with the risk tree, each event will be characterized by the structural variable $x_{\vec{i}_k}$. The structure variable is set to 1, $x_{\vec{i}_k} = 1$, when the event \vec{i}_k occurs, otherwise $x_{\vec{i}_k} = 0$. For each event, using structural variables, it is possible to calculate structural functions in accordance with the rules of reliability theory [23, 24].

When constructing a risk tree, it is convenient to use the notation taken from the monograph by Heinley and Kumamoto [22]. Rectangles in the risk tree denote events that can be divided into sub-events, circles denote final <<leaf>> events, event labels in the risk tree are shown in the table 0. The corresponding connections between events in the form of gates, together with the structural functions corresponding to them, are given in the table 1.

Table 1: Symbol table in the risk tree





Event Symbols	Description
	Basic event
	Event represented by a gate

Table 2: Table of gateways in the risk tree

Gate Symbols	Name	Description
	$\prod_{i=1}^n x_i$ AND gate	Output event occurs if all input events occur simultaneously
	$1 - \prod_{i=1}^n (1 - x_i)$ OR gate	Output event occurs if any one of input event occur

It is possible to calculate the most dangerous risky path of development, risky by the criterion of maximum risk probability, by highlighting for all components of the event \vec{i}_k the number of its component $j_{i_k}^*$, on which this maximum is reached.

Let the event \vec{i}_k contain $n(\vec{i}_k)$ components, then the maximum probability is $q_{i_k}^*$ its implementation \vec{i}_k due to the component $j_{i_k}^*$ is found by the formula 1:

$$q_{i_k}^* = \max_{1 \leq j \leq n(i_k)} q_{(i_k, j)}; \quad j_{i_k}^* = \arg \max_{1 \leq j \leq n(i_k)} q_{(i_k, j)}. \quad (1)$$

Starting from the lower level, you can find the most dangerous path to the \vec{i}_k subsystem, starting from leaf events, according to the criterion of the maximum risk probability, including for the entire system using the formula 2:

$$\vec{i}_k(q) = (j_{i_k}^*, j_{i_{k+1}}^*, \dots, j_{i_{r-1}}^*); \quad \vec{i}_{k+l+1} = (\vec{i}_{k+l}, j_{i_{k+l}}^*), \quad l \geq 0. \quad (2)$$

Building a dangerous path according to the criteria of the maximum risk probability, the largest penalties, can serve as an additional focus for decision makers.

In the next section, we will use this technique to build, equip, and analyze a geological risk tree based on expert research from [29, 30, 31, 32, 33, 34]. The methodology for assessing risk events is proposed in the articles [25, 26, 27, 28].

V. Risk tree for assessing the success of geological exploration

As an example, let's consider the construction of a tree of success (failure) of geological exploration for one promising object. The papers [29, 30, 31, 32, 33, 34] propose a system of events affecting exploration, statistical data and expert assessments of negative events.

The key event, let's denote it (0), for which the risk tree is built, is the failure to receive economic profit in the development of a promising facility for oil and gas production. The tree will be built from top to bottom (left to right), implying two scales at once: by time (unsuccessful events that occur first) and by development stages (from the top layer of the earth inward to the discovery of hydrocarbons):

- the presence or absence of a successful natural reservoir;
- the presence or absence of an effective trap;
- presence or absence of hydrocarbons in the trap;
- safety / absence of hydrocarbons in the trap, as well as full financial support / failure of the project.

(0) – Exploration at site is not successful.

This key event in the first stage of geological exploration associated with an effective natural reservoir can be broken down into 4 possible sub-events for which the geological project may not be successful. Firstly, the failure of the project will be revealed immediately if an effective natural reservoir is not found. Two indicators are responsible for this: the presence of facies (rocks) for which the formation of reservoirs is favorable, and sufficient porosity of these rocks. Porosity reflects the percentage of pore space in relation to the total rock volume. Through the communicating pores, a sufficient amount of hydrocarbons enters the well, an example of a porous rock with non-communicating pores can be pumice. The following non-overlapping combinations of these options arise.

- (1) – lack of favorable faces in the presence of acceptable porosity in the rock;
- (2) – the presence of favorable faces with unacceptable porosity, eg shale;
- (3) – lack of favorable rock and porosity not acceptable;
- (4) – The failure of the project arose as a result of a deeper geological analysis, which we will reveal later, now the event can be described as <<another reason for the failure of the project>>.

Thus, three events (1), (2) and (3) end immediately and are leaf events, and event (4) can be represented through sub-events, due to which the failure of the project is possible during the subsequent (deeper) geological analysis.

Event (4) is divided into four sub-events. This stage of the geological analysis establishes the presence of suitable rock and acceptable porosity, and then an effective hydrocarbon trap is required for the success of the project. A trap is a part of the reservoir bounded from above and from the sides by impermeable rocks (the so-called impermeable seal, tire), in which oil and gas can theoretically collect. Seals have low permeability and are capable of retaining hydrocarbons at very

high pressures. There are false seals without oil deposits, in which there are only minor oil shows. Here and below, commas in the vector representation of elements will be omitted. Consider the events:

(41) – no trap, although seal quality is acceptable;

(42) – there is an oil show, but the seal is of poor quality and does not retain hydrocarbon, it does not accumulate;

(43) – no trap and no seal;

(44) – the trap is effective, but the failure of the project is due to other reasons, you can call this event <<failure of the project for other reasons>>.

Events (41), (42), (43) are final and are leaf events in the risk tree. Event (44) occurs at the stage when both the reservoir and the impermeable trap are effective, but the causes of failure are in the underlying geological layers. Let's consider the third stage of the exploration study, which is called "the presence of hydrocarbons in the trap". This requires two conditions: the presence of mature oil and gas source strata, which, under the influence of time, temperature and pressure, generate hydrocarbons, and the presence of favorable conditions for the migration of hydrocarbons into traps. Thus, we distinguish four sub-events of event (44):

(441) – there are no mature oil and gas source strata, but there are pores and cracks along which hydrocarbons can theoretically move into traps;

(442) – there are mature oil and gas source strata, but unfavorable conditions for the movement of hydrocarbons into traps;

(443) – no mature oil and gas source strata and unfavorable conditions for the movement of hydrocarbons into traps;

(444) – there are mature suitable oil and gas source sequences and favorable conditions for moving hydrocarbons into traps, but the event is not successful for reasons that will be revealed in the next level.

Let's consider the fourth stage of development of the geological project. At this stage of development, project development is looking at "holding/preservation of hydrocarbons in the trap", and we will add here <<other reasons, for example, the economic nature of the legal entity>> that the development of the facility is not economically viable. Event (444) is divided into two sub-events:

(4441) – Hydrocarbon is not stored in the trap, migrates;

(4442) – financial problems of a legal entity.

In the current example, exploration is not successful if at least one risk event occurs.

Let's equip the events of the risk tree in the figure 2 with an expert assessment of practicing geologists [29, 30, 33, 34], fix the probabilities of phased failure in the Table 2 .

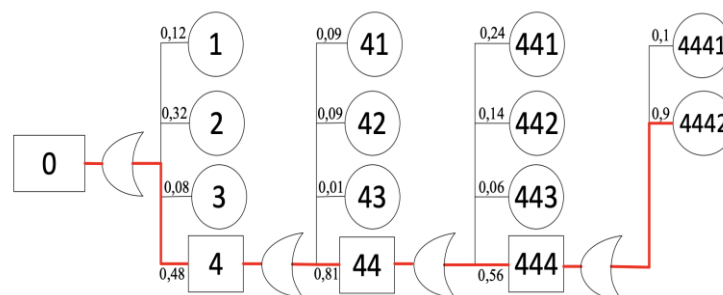


Fig. 3: A dangerous path according to the criterion of the maximum probability of failure

Table 3: Probabilities of failure by events

Events	q_i	Events	q_i
(1)	0.12	(44)	0.81
(2)	0.32	(441)	0.24
(3)	0.08	(442)	0.14

(4)	0.48	(443)	0.06
(41)	0.09	(444)	0.56
(42)	0.09	(4441)	0.1
(43)	0.01	(4442)	0.9

In the example under study, the probabilities $q_{(4441)} = 0.1$ and $q_{(4442)} = 0.9$ are given, thus, using the formulas (1) and (2) we get: $q_{(444)}^* = \max_{1 \leq j \leq 2} q_{(444j)} = 0.9$, and $j_{(444)}^* = \operatorname{argmax}_{1 \leq j \leq 2} q_{(444j)} = 2$. At the level above $q_{(441)} = 0.24, q_{(442)} = 0.14, q_{(443)} = 0.06$ and $q_{(444)} = 0.56$ i.e. probability $q_{(44)}^* = \max_{1 \leq j \leq 4} q_{(44j)} = 0.56$ and $j_{(44)}^* = \operatorname{argmax}_{1 \leq j \leq 4} q_{(44j)} = 4$. At the next level $q_{(41)} = 0.09, q_{(42)} = 0.09, q_{(43)} = 0.01$ and $q_{(44)} = 0.81$ i.e. probability $q_{(4)}^* = \max_{1 \leq j \leq 4} q_{(4j)} = 0.81$ and $j_{(4)}^* = \operatorname{argmax}_{1 \leq j \leq 4} q_{(4j)} = 4$. At the upper level $q_{(1)} = 0.12, q_{(2)} = 0.32, q_{(3)} = 0.08$ and $q_{(4)} = 0.48$ i.e. probability $q_{(0)}^* = \max_{1 \leq j \leq 4} q_{(j)} = 0.48$ and $j_{(0)}^* = \operatorname{argmax}_{1 \leq j \leq 4} q_{(j)} = 4$. The dangerous path according to the criterion of the maximum probability of failure leads through the elements (4),(44),(444),(4442), in the figure 2 the found dangerous path in the risk tree is highlighted in red.

The dangerous path according to the criterion of the events The next Diagram of events explains the ways of analyzing a process to achieve the risk target.

VI. Conclusion

The current work shows the features of random phenomena. The concepts of random, virtual and fuzzy phenomena are classified. Depending on the classification of phenomena, one can end up with an assessment that can be both objective for random phenomena and subjective due to the subjectivity of the initial information. To assess the risk events of the described phenomena, a risk tree is built and, using the mathematical apparatus, an assessment for the situation can be obtained.

In the current work, an example with expert assessments from practicing geologists is given. A technique for choosing a dangerous path is described. For other risk events of complex engineering structures with average service life of elements, by changing, for example, the coefficients of variation, it is possible to change the direction of the dangerous path. This toolkit can serve as additional advice for decision makers.

The authors invite to further joint work experts with real data and requests related to the assessment of risk events of complex engineering systems and structures to calculate the main and alternative dangerous routes, fines.

This collective work is a result of long discussion between members of the board of the Gnedenko Forum. Authors thank all of these members.

References

- [1] Rykov, V. and Yastrebenetsky, M. (1999) Risk: notion and measurement. Proceedings of the International Conference <<Probabilistic analysis of rare events: Theory and problems of safety, insurance and ruin>>. Riga, Latvia, Riga Avian University, 63–70.
- [2] Rykov, V. and Yastrebenetsky, M. (2007) Back to the definition of Risk notion. Abstract to MMR- Conference, Glasgow.
- [3] Rykov, V. (2011) Reliability, Safety, Risk: Control and Management. Proceedings of the 7-th International Conference <<Mathematical Methods in Reliability >> Beijing, China. Ed. by Lirong C., Xian Z. Beijing: Institute of Technology Press.
- [4] Cramer, H. (1930) On the mathematical theory of risk. Forsakringsaktiebolaget Skandias Festschrift; Centraltryckeriet: Stockholm, Sweden, pp. 7–84.
- [5] Cramér, H. (1955) Collective Risk Theory: A Survey of the Theory from the Point of View of the Theory of Stochastic Processes; Ab Nordiska Bokhandeln: Stockholm, Sweden.

https://doi.org/10.1007/978-3-642-40607-2_17.

- [6] Aven, T. (2012) The risk concept – historical and recent development trends. *Reliability Engineering & System Safety*. 99. 33–44. [10.1016/j.ress.2011.11.006](https://doi.org/10.1016/j.ress.2011.11.006).
- [7] Brooks M. (ed) (2015) *Chance. The science and secrets of luck, randomness and probability*. New Scientist, 2915
- [8] Kolmogorov, A.N. (1974) *Basic concepts of the theory of probabilities. Grundbegriffe der Wahrscheinlichkeitsrechnung*, 2nd ed.; Translated from A.N. Kolmogoroff; Fizmatgiz: Moscow, Russia, (In Russian) .
- [9] Savage, L.J. (1954) *The Foundations of Statistics*. John Wiley: New York, NY, USA, .
- [10] Cooke, R.M. (1991) *Experts in Uncertainty: Opinion and Subjective Probability in Science*. Oxford University Press: Oxford, UK. 336p.
- [11] Zadeh, L.A. (1965) Fuzzy sets. *Information and Control*; ; Volume 8, pp. 338-353. [https://doi.org/10.1016/S0019-9958\(65\)90241-X](https://doi.org/10.1016/S0019-9958(65)90241-X).
- [12] Siström CL, Garvan CW (2004). "Proportions, odds, and risk". *Radiology*. 230 (1): 12–19. [doi:10.1148/radiol.2301031028](https://doi.org/10.1148/radiol.2301031028). PMID 14695382
- [13] Nozer D. Singpurwalla (2006) *Reliability and Risk: A Bayesian Perspective // Wiley Series Probability and Statistics*, ISBN: 978-0-470-06033-9, 2006.- 400B p.
- [14] Rykov V. V., Itkin V. (2017) *Reliability of technical systems and technogenic risk: textbook*. - Moscow: INFRA-M, 2017. - 192 p. - (Higher education).
- [15] Korolev V.Yu., Bening V.E., Shorgin S.Ya. *Mathematical foundations of risk theory*. - Moscow: Fizmatlit, 2011. - 620 С. ISBN: 978-5-9221-1267-3
- [16] Zhukovsky V.I., Zhukovskaya L.V. (2010) *Risk in multicriteria and conflict systems under uncertainty / ed. Ed. 2nd ed. Moscow: Publishing House LKI, 2010. - 272 p.*
- [17] Russman, I., A. Kaplinsky, and V. Umyvakin (1991). *Modeling and algorithmization of poorly formalized problems of choosing the best system options / Voronezh: Voronezh State University, 1991.- 168 p. (in Russian)*.
- [18] Bochkov, A.V. (2019) *Methodology of ensuring safe functioning and sustainability of the Unified system of gas supply in emergency situations: dissertation ... Doctor of Technical Sciences: 05.26.02 / Bochkov Alexander Vladimirovich; [Place of protection: LLC "Research Institute of natural gases and gas technologies - Gazprom VNIIGAZ"]*, 2019. - 385 p.
- [19] Bochkov, A.V. (2023), *Applied issues of chaotic dynamics in the management of unique evolutionary systems*, Editor(s): Mangey Ram, Liudong Xing, In *Advances in Reliability Science, Reliability Modeling in Industry 4.0*, Elsevier, 2023, Pages 45-81, ISBN 9780323992046, <https://doi.org/10.1016/B978-0-323-99204-6.00014-5>.
- [20] Zhigirev, N.; Bochkov, A.; Kuzmina, N.; Ridley, A. (2022) *Introducing a Novel Method for Smart Expansive Systems' Operation Risk Synthesis*. *Mathematics* 2022, 10, 427. <https://doi.org/10.3390/math10030427>
- [21] Bochkov A., Zhigirev N., Kuzminova A. (2022) *Inversion Method of Consistency Measurement Estimation Expert Opinions // Reliability: Theory & Applications*, vol. 17, no. 3 (69), 2022, pp. 242-252. [doi:10.24412/1932-2321-2022-369-242-252](https://doi.org/10.24412/1932-2321-2022-369-242-252).
- [22] Henley, E.G. and Kumamoto, H. (1981) *Reliability Engineering and Risk Assessment*. Prentice-Hall: New Jersey, NJ, USA. p. 07632. ISBN-0-13-772251-6.
- [23] Rykov, V. V. and Itkin, V.Yu (2016) *Reliability of technical systems and technogenic risk. Textbook*. INFRA-M, 214 p.
- [24] Rykov V.V. *Reliability of Engineering Systems and Technological Risks*. ISTE. WILEY, 2016, 212p.
- [25] Rykov, V., Ivanova, N. and Farhadov, M. (2022) *On principles of risk analysis with a practical example*. RT&A, Special Issue 3 (66), Volume 17, pp. 38–41.
- [26] Rykov, V., Farkhadov, M., Kochueva, O. and Zaripova, E. (2022) *Sensitivity analysis of risk characteristics to the type of initial information based on a pipeline monitoring system*. *Reliability: Theory and Applications*. Special Issue B,,– 4 (70) Volume 17.
- [27] Rykov, V., Ivanova, N. and Kozyrev, D. (2021) *Risk tree as an assistant tool for the*

decision-maker. 13th International Congress on Ultra Modern Telecommunications and Control Systems and Workshops (ICUMT) pp. 109-114. DOI: 10.1109/ICUMT54235.2021.9631604

[28] Rykov, V., Kochueva, O., Farkhadov, M., Zaripova, E. and Zhaglova, A. (2023) Sensitivity Analysis of Risk Characteristics of Complex Engineering Systems: An Application to a Subsea Pipeline Monitoring System. *J. Mar. Sci. Eng.* 11, 352. <https://doi.org/10.3390/jmse11020352>

[29] Pÿhe CCOP guidelines for risk assessment of petroleum prospects. (2000).

[30] Polyakov, A. A. and Murzin Sh. M. (2012) International experience in geological risk analysis. *NeftegasovaĬ geologiĬ. TeoriĬ i praktika*, 7 (4).

[31] Hope, S., Bjordal, E.N., Diack, H.M., Eddershaw, B.W., Joanny, L., Ortone, G., Payne, F.G., Searson, A.H., Sedlacek, K.W. and van Strien, W. (1982) Methodologies for hazard analysis and risk assessment in the petroleum refining and storage industry.

[32] Hope, S., Eddershaw, B. W., Joanny, L., Bjordal, E. N., Diack, H. M., van Strien, W. (1984). Methodologies for hazard analysis and risk assessment in the petroleum refining and storage industry" Part I. *Fire Technology*, 20(3), 23-38.

[33] Emelyanova, N.M., Poroskun, V.I. (2018) Geological-economical evaluation and analysis of plays risks. *NeftegasovaĬ geologiĬ. TeoriĬ i praktika*. 13(2).

[34] Kerimov, V. Yu., Bondarev, A. V., Mustaev, R. N., Khoshtaria, V. N. (2017) Estimation of geological risks in searching and exploration of hydrocarbon deposits. *Neftyanoje hozyajstvo*. 8, pp.36-43.

REFLECTIONS ON DUAL NATURE OF RISK. TOWARD A FORMALISM

Alexander Bochkov



JSC NIIAS, Moscow, Russia
a.bochkov@gmail.com

Abstract

We seem to know almost everything about risk and, at the same time, nothing. By focusing on the etymology of the word "risk", researchers have neglected its nature, causes and characteristics. At the same time, risk manifests itself differently in different situations and can be both a characteristic of a random event and a characteristic and measure of the quality of a process carried out over time. In the latter case, risk is inherent in the properties of a wave process, which requires the search for measures other than probabilistic ones to measure and assess it. This paper attempts to summarize the most characteristic different manifestations of risk and to propose a way of assessing risk that takes account of these differences. The paper can be seen as an invitation to debate the nature of risk and how its formalism should be constructed.

Keywords: risk, random, Bayesian estimates, quality, anti-potential, difficulty of achieving, measure of disorderliness

I. Introduction

Corpuscular-wave dualism (or quantum-wave dualism) is a property of nature consisting in the fact that material microscopic objects may under some conditions exhibit properties of classical waves and under other conditions - properties of classical particles. Typical examples of objects exhibiting dual corpuscular-wave behavior are electrons and light; the principle is also valid for larger objects, but, as a rule, the more massive the object, the less its wave properties are manifested (we are not talking here about the collective wave behavior of many particles, such as waves on the liquid surface). The idea of corpuscular-wave dualism was used during development of quantum mechanics to interpret phenomena observed in microcosm in terms of classical concepts. Quantum objects are neither classical waves, nor classical particles, exhibiting properties of the former or the latter only depending on conditions of experiments that are conducted on them. Corpuscular-wave dualism is unexplainable within classical physics and may be interpreted only in quantum mechanics.

Similarly, risk is understood by different researchers as either an event or a process. This difference in perception is partly dictated by the basic theoretical background of the researcher.

For example, specialists in the field of mathematical statistics and probability theory prefer to perceive risk as an event, because in this approach it is possible to apply the rich tools developed in this field of knowledge to describe this event in some space of states and to obtain a quantitative measure for subsequent comparison of different assessments. In this approach, risk is considered in terms of the probability of the event itself, and the expected damage from this event for the risk taker. Essentially, the expected damage (that is, what the subject is willing to risk) is reduced by a fraction proportional to the probability of the risk event. The most obvious example of this approach is insurance against frequent accidents (for example, traffic accidents, common diseases, failures of technical devices and mechanisms, etc.). In this case, the researcher has representative

statistics that he can process (analyze) and obtain the necessary distributions and analytical dependences for estimating. This also includes attempts to relate risk to uncertainty. This again introduces the concept of uncertainty, the rules for modeling it, and ways of determining the probability associated with risk. In this way, a probabilistic space is defined, in which risk is dealt with. At the same time, it is often argued that both concepts, uncertainty and probability, are basic and, therefore, no definitions can be given to them. Any such axiomatic attitude is based on set theory. It uses the basic concept of a set. There is no definition of a set (like any other basic concept in any theory). A set can be informally described as a set of objects having some common features (i.e., the concept of "set" here is expressed through the concept of "set").

Specialists, if I may say so, with basic engineering training, gravitating towards applied mathematical knowledge, consider risk as a process (in the limit - a wave process), which has points of maximum and minimum impact, at which, respectively, the phenomena of resonance (mutual strengthening or weakening) of different risk factors are possible. Under this approach, risk is seen as a measure of failure to achieve the goal set by the risk-taking subject, that is, it is an assessment of the quality of organization of a purposeful process of some activity. For a risk event to occur, a certain moment in time. As an example, we can take the task of removing a large vessel which happened to be on a shoal at low tide. It is extremely expensive to get it out at high tide, but it costs almost nothing if you know about tidal cycles and just wait for the right moment. Similar events occur infrequently, and to react to them adequately, one needs not analysis (because there is often almost nothing to analyze), but risk synthesis. That is, it is necessary to analyze all information known about the place of the expected occurrence of a risk event, as well as about the object that can be exposed to risk, and then perform risk synthesis and assess the possibility to achieve the goal (which will be the maximum risk avoidance). That is, risk, depending on the totality of factors and characteristics of the risk object (and risky subject) itself, manifests itself in two ways. And its analysis and assessment, respectively, should be carried out with this duality (wave-event duality of risk assessment), without substituting one assessment apparatus for another. The blind transfer of probability analysis to the field of risk synthesis leads to disastrous consequences (although, on a close planning horizon, it can provide estimates that are acceptable to the risk-taker).

The dual nature of risk leads to eight basic concepts that encompass the modern view of risk as an event assessment and a process assessment.

The first group is the concepts in which risk characterizes the event:

- **Risk as a relative value** (risk is defined as the ratio of the probability of an outcome in an exposed group to the probability of an outcome in an unexposed group).
- **Risk as a consequence of the occurrence of some random event** from a possible family of all events, or a set of possible damages in some stochastic situation and its probability (this concept covers the so-called frequency, statistical approach, most often applied to mass service systems, in insurance, reliability theory, etc.).
- **Risk as a criterion for choosing a decision in "games with nature"** when the response to the chosen decision is uncertain (this includes the so-called Wald's maximal utility (guaranteed result, minimal gain) or Savage's minimal regret (maximal loss), the Hurwitz criterion (coefficient of optimism)).
- **Risk as a Bayesian estimate** (here the probability is considered as the degree of confidence in the event, which can change when new information is collected, the risk in this case is the mathematical expectation of the variance of the posterior distribution).

The second group are concepts that describe risk as a characteristic of the process:

- **Risk, as the difficulty of achieving** the goal (risk is defined through a functional that describes the evolution of the system on a set of given trajectories, being a measure of the quality of the system in relation to the quality required to achieve the goal).
- **Risk as a measure of process quality assessment** (risk is a measure of the degree of mismatch between the real process and the reference process).

- **Risk as an anti-potential for development** (risks act as slower of the speed of reproduction of the entire system).
- **Risk as a measure of disorderliness** (risk is estimated as a minimum of the total inconsistency of expert evaluations (based on the equality of all participants of the examination) of the variants of system development, measured in the inversions of transitions, necessary to restore the lexicographic order of compared variants).

Let's look at each concept in more detail.

II. Risk as a relative value

Risk in this concept is an objective-subjective feeling that under certain conditions something undesirable, dangerous event can happen [1]. Relative risk (RR) in medical statistics and epidemiology is the ratio of the risk of an event occurring in individuals exposed to a risk factor (p-exposed) to a control group (P non-exposed). Relative risk is often used in statistical analyses of paired outcomes when the outcome of interest has a relatively low probability. For example, in medical research to compare the risk of disease in patients receiving a treatment (or placebo) with patients receiving the treatment under study or to compare the risk of complications in patients receiving a drug with patients not receiving or receiving a placebo. A particular appeal of relative risk is the ease of calculation for uncomplicated cases.

Assuming a causal relationship between exposure and outcome, relative risk values can be interpreted as follows:

- $RR = 1$ means that the impact does not affect the result.
- $RR < 1$ means that the risk of the outcome is reduced by the exposure, which is a "protective factor."
- $RR > 1$ means that the risk of the outcome is increased by the exposure, which is a "risk factor."

As always, correlation does not mean causation; causation can be inverse, or they can both be caused by a common mixed variable. In regression models, risk is usually included as an indicator variable along with other factors that may affect risk. Relative risk is usually reported as the average of sample values of independent variables. In statistical modeling, approaches such as Poisson regression (for counting events per unit exposure) have an interpretation of relative risk: the estimated effect of the explanatory variable is multiplicative for rate and thus leads to relative risk. Logistic regression (for binary outcomes or counting successes in several trials) should be interpreted in terms of odds ratio: the effect of the explanatory variable is multiplicative of the odds and thus leads to an odds ratio. Relative risk can be interpreted in Bayesian terms as an a posteriori exposure relation (i.e., after observation of the disease) normalized by an a priori exposure relation.

III. Risk as a consequence of a random event

One of the main, basic problems of mathematical statistics is the problem of restoring the unknown law of distribution of a random variable over a finite number of its realizations. In more detail, we consider a random variable ξ for which a set of its random realizations is known (from experiments) X_1, \dots, X_n . It is required to determine the distribution law as accurately as possible ξ , e.g., probability density $p_\xi(x)$.

A *random event* is a subset of the set of outcomes of a random experiment; when a random experiment is repeated many times, the frequency of occurrence of the event serves as an estimate of its probability. A random event that is never realized as a result of a random experiment is called impossible. A random event that is always realized by a random experiment is called credible. "...in homogeneous *mass operations*, the percentage of one or another kind of *event* important to us under given conditions is almost always about the same, only rarely deviating any

significant amount from some average figure. We can say that this average figure is a characteristic indicator of a given mass operation (under given, strictly defined conditions) ... So, what do we call the probability of events in each mass operation? A mass operation always consists of the repetition of many similar single operations. We are interested in a certain result of a single operation and, above all, in the number of such results in this or that mass operation. The percentage (or generally the proportion) of such "successful" results in each mass operation we call the probability of this result, which is important for us. We must always keep in mind that the question about the probability of this or that event (result) makes sense only in exactly defined conditions of our mass operation. Any essential change of these conditions entails, as a rule, change of the probability we are interested in". [2].

A set of random realizations X_1, \dots, X_n is called a sample, the number of realizations n - the volume of the sample. If the random realizations considered as random variables are independent, then the sample is called repeated, otherwise it is called unrepeated. For repeated sampling, and only for it, the joint probability density function of a population of random variables X_1, \dots, X_n (if it exists) has the form $\prod_{i=1}^n p_{\xi}(x)$. Further on, unless otherwise stated, it is assumed that X_1, \dots, X_n - repeated sampling. In mathematical statistics, any measurable function (scalar or vector) of sample terms X_1, \dots, X_n is usually called a statistic.

3.1. Risk in insurance

In insurance, we will call the risk the totality of the value of possible damage in some stochastic situation and its probability. The magnitude of the possible damage in a stochastic situation is obviously unknown before the implementation of this situation and therefore random. Thus, the theoretical and probabilistic analogue of the concept of damage, obviously, is the concept of a random variable. The totality of values of a random variable and their probabilities in the theory of probability is set by the distribution of a random variable. Thus, we would like to understand risk as a random variable. However, if risks are identified with random variables set on different probability spaces, the task of comparing such risks is fundamentally unsolvable and even meaningless, since their corresponding random variables as functions of elementary outcomes depend on arguments with different meaning. Therefore, in such situations, we must identify risks with distribution functions.

The mathematical theory of risk should be formally understood as a set of models and methods of probability theory applied to the analysis of random variables and their distributions. This interpretation is rather broad and is reduced to the fact that so interpreted risk theory should be identified with the discipline, which is assigned the name "applied probability theory" and which includes such an important and rich in results field as reliability theory.

Probability theory studies properties of mathematical models of random phenomena or processes. By randomness we will understand uncertainty that cannot be eliminated in principle. With the help of probability theory concepts and statements we can describe the very mechanisms of uncertainty manifestation, reveal regularities in manifestations of randomness. Here we will deal with the probability theory based on the system of axioms, which was proposed in 20-30s of XX century by Andrey Nikolayevich Kolmogorov.

Let us call a stochastic situation characterized by the following properties or conditions:

- *Unpredictability*: the outcome of the situation cannot be predicted in advance with absolute certainty.
- *Reproducibility*: it is at least theoretically possible to reproduce the situation in question as many times as desired under unchanged conditions.
- *Stability of frequencies*: whatever the event of interest related to the situation in question is, when this situation is repeatedly reproduced, the frequency of the event (i.e., the ratio of the number of cases in which the event in question was observed to the total number of reproductions

of the situation) fluctuates around a certain number, getting closer and closer to it as the number of reproductions of the situation increases.

The property of unpredictability is obvious. If the outcome of a situation is predictable unambiguously, then there is no need to involve the apparatus of probability theory at all.

The property of the reproducibility of a situation is key to be sure of the success of applying the apparatus of probability theory to its description. It is this property that is meant when they say that probability theory and mathematical statistics are aimed at studying mass phenomena. In connection with the condition of reproducibility, one should be very careful about attempts to apply probability theory to the analysis of unique phenomena or systems. For example, there have been numerous attempts to give a quantitative answer to the question of how likely it is that other planets inhabited by intelligent beings exist in the universe. However, so far there is insufficient evidence to believe that the existence of other planets and, even more so, the existence of intelligent life on them is a mass phenomenon. Therefore, the existing predictions are very controversial and therefore inadequate.

Finally, the property of frequency stability allows us to connect the mathematical definition of event probability with the intuitive notion of it as a certain understood limit on the frequency of an event in the unrestricted reproduction of the corresponding situation.

The individual claim (or insurance claim) equal to the total amount of funds paid by the insurer under some insurance contract, i.e. a random value taking a zero value if the insurer's payments under this insurance contract did not take place (no insurance event), and a non-zero value equal to the sum of all insurance payments under the contract if at least one insurance event took place, is usually considered an elementary risk component of the insurer. The conditional value of the claim value, provided that the claim is different from zero, is called the loss.

The existing literature on risk theory provides the following classification of risk models:

- *Individual risk model* (according to the terminology [3, 4, 5]) or dynamic insurance model (according to the terminology [6]) describes the situation in which a set of insurance objects (insurance portfolio) is considered, formed at one time, insurance premiums are collected at the moment of the portfolio formation, the term of all insurance contracts is the same, and during this period insurance events occur, leading to insurance payments – claims.

- *Collective risk model* (in the terminology of [3, 4, 5]) or dynamic insurance model (in the terminology of [6]), in which it is assumed that insurance contracts are concluded by the insurer at moments of time, forming some random process, each contract has its own duration, and during the time of this contract the insurance events may occur, leading to losses of the insurance company (insurer). Such a model can be considered both on a finite and infinite time interval. When considering a dynamic model, it is always assumed that there is some initial capital allocated by the insurer for a given insurance portfolio.

3.2. Risk in technology

Risk in engineering is associated with the occurrence of some random event \mathcal{A} which we will call a risk event from the possible family \mathcal{F} of all events describing the risk situation under consideration [7]. These events are usually distributed in some way over time and are accompanied by certain material or other costs - generally speaking, also incidental in magnitude.

Thus, risk is characterized by two quantities - the time T the time of occurrence of a risk event and the value X bringing them damage therefore under the risk we will understand a probabilistic model $(\Omega, \mathcal{F}, \mathbf{P})$ on which a two-component random variable (T, X) the first component of which T - time of risk event occurrence \mathcal{A} counted from some fixed point in time, and the second X specifies the damage caused by this risk event. It should be kept in mind that the quantity T may depend on the moment t_0 of the beginning of the counting. Therefore, when measuring the time to the occurrence of a sharp event, it should be measured from some natural starting point. In the theory of reliability such moment is the moment when the equipment is put into operation, in the models

of life insurance - the moment when a person is born, in the models of ecological risks the time is measured between successive moments of the relevant hazardous risk events, etc.

Note also that if the risk is investigated on a fixed time interval, the risk event may not occur during the time interval in question. As it has already been noted, we often must deal with a sequence of risk events. Such situations are studied as part of risk processes:

$$\{(S_n, X_n): n = 0, 1, \dots\},$$

where S_n - the non-decreasing sequence of moments of risk events, and X_n - the sequence of damages associated with them.

For any random variable, its basic measure is its bivariate distribution:

$$F(t, x) = \mathbf{P}\{T \leq t, X \leq x\},$$

concentrated, naturally, due to the nature of the phenomenon in the first quadrant of the plane $\{t \geq 0, x \geq 0\}$. In most real cases, however, information about the joint distribution of the time of occurrence of the sharp event and the amount of damage is rarely available and one has to be limited to the corresponding marginal distributions of the time of occurrence of the risk event:

$$F_T(t) = \mathbf{P}\{T \leq t\}$$

and the amount of damage

$$F_X(x) = \mathbf{P}\{X \leq x\}.$$

If the risk is considered on a fixed time interval, then instead of the time of T of risk event occurrence \mathcal{A} it is natural to consider its indicator $1_{\{\mathcal{A}\}}$ and the damage is measured by its conditional distribution if the risk event occurs:

$$G(x; \mathcal{A}) = \mathbf{P}\{X \leq x | \mathcal{A}\}.$$

In this case, the unconditional value of the damage is represented by a distribution that is joint with the occurrence of a risk event, having a jump of zero (since, naturally, in the absence of a risk event, the value of the damage is zero):

$$F_X(x) = 1 - \mathbf{P}(\mathcal{A})(1 - G(x; \mathcal{A})).$$

In general, it is natural to measure risk by the distribution of the moment of the occurrence of a risk event $F_T(t) = F(t) = F(t, \infty)$ and the conditional distribution of damage when it occurs:

$$G(x; t) = \mathbf{P}\{X \leq x | T = t\}.$$

Their joint distribution is expressed by the formula:

$$F(x, t) = \int_0^t G(x; u) f_T(u) du.$$

The simplest case is to assume the independence of these quantities. In this case the relations take place:

$$G(x; u) = G(x) = F_X(x) = F(\infty, x); \quad F(x, t) = G(x)F(t).$$

In many real-world situations, this assumption is perfectly acceptable, with the only note being that the value of future damage now is estimated by means of present damage, which is measured by the value:

$$\hat{X} = e^{-sT} X,$$

where s - is the inflation rate of the bank interest.

Indeed, to compensate for the damage X in time, it is enough to put in the bank the amount of \hat{X} at s interest. In this case the actual dependence of the future damage on time is just expressed in the form of the present value of the damage. Further on we will stick to the assumption of independence of the time of the risk event and the amount of the damage brought by it.

This approach allows a lot of analytical analysis of some specific characteristics and cases and is used in many other new research projects. It is done only within a theoretical framework and assumptions. Practical applications require sufficient statistical data to estimate the function $F(x, t)$.

IV. Risk as a criterion of choice in games with nature

In terms of "playing with nature," the decision-making problem can be formulated as follows: The decision-maker (DM) can choose one of m of possible variants of his decisions:

X_1, X_2, \dots, X_M , and with respect to the conditions under which the possible choices will be realized, one can make n assumptions: Y_1, Y_2, \dots, Y_N . The estimates of each decision option under each condition are (X_m, Y_n) are known and are given in the form of a matrix of benefits of the DM: $A = A(X_m, Y_n) = |A_{mn}|$. It is assumed that there is no a priori information about the probabilities of this or that situation occurring Y_n is not available.

According to the methodology of game theory, alternatives are factors controlled by the DM, i.e., chosen by him at his discretion [8]. In addition to alternatives, there are non-controllable factors, which affect the outcome of the problem and which the DM cannot control (e.g., natural phenomena). To fully analyze and decide, the DM must have some information about the values of the uncontrollable factors.

The theory of operations research, based on the information of the DM divides [9] uncontrollable factors into three groups:

- *Fixed* - these are factoring whose values are known precisely, so, for example, the sale of shares occurs only when buyers know exactly the quotation of monetary units against the dollar and euro (in this case, the quotation and is an uncontrollable fixed factor).
- *Random* factors are random variables whose distribution functions are known precisely.
- *Uncertain* factors are deterministic or random variables for which only the range of possible values or the class of possible distribution laws is known.

Of the above, the groups of random and uncertain factors are of fundamental importance. The fixed factors inherently do not differ from all other parameters of the mathematical model, because their values are known and cannot be changed at will of the DM. Random and indeterminate factors also cannot be changed at will of the DM, but in addition, they take unknown values. With respect to random factors, the probability density function is known, which means that if, for example, a random factor takes some finite number of values y_1, \dots, y_k then the decision maker knows the probabilities p_1, \dots, p_k with which these values are taken. If a random factor is a continuous random value, the probability density is known. In both cases the criteria are replaced by their mathematical expectations $p(x)$. Even less is known about uncertainties. If the uncertainty is a deterministic quantity, then the range of its possible values is known Y i.e., it is only necessary to consider the inclusion of $y \in Y$. If the uncertainty is a random value, then we do not know the probability density, but a possible class of such densities.

Uncertainties can be roughly divided into the following five groups:

1. Uncertainties that have arisen due to actions on the part of persons who have their own goals, but who are not DMs. Uncertainties of this type are called [9] strategic uncertainties.
2. Uncertainties reflecting the vagueness of the DM's knowledge of their goals. This uncertainty is not an uncontrollable factor (in the strict sense), because the choice of the goal is at the disposal of the DM.
3. Uncertainties arising from insufficient knowledge of processes or values. Decision-making based on incomplete data can be understood as a conflict with nature.
4. Uncertainties arising in the process of collecting, processing and transmitting information. Approximated information can appear because of many reasons, which include, in particular: computational errors, errors in data transmission, limited accuracy of representation and processing of numbers, limitations on the accuracy of measurements. Already in manual calculations [10] one must deal with the rounding effect arising since only a finite number of decimal places are retained in the process of calculations. Direct application of interval methods [11] to computational processes makes it possible to enclose in intervals solutions of problems whose input data are known only that they lie in certain intervals. Rounding errors encountered in the process of calculations are also included in the resulting intervals. So-called interval arithmetic [12] was introduced to obtain two-sided approximations in which intervals rather than numbers are used and both input data and intermediate and, naturally, results are situated within certain intervals.
5. Special types of uncertainties arising in the control of mechanical systems. A special role here is assigned to control of motion of systems and observation processes under conditions

of incomplete information (in other words, under conditions of uncertainty). These problems represent a natural generalization of control problems with complete information and arise in many applied problems. Incompleteness of information in these problems is a consequence of several real factors.

It should be noted that when modeling most socio-economic, technical, organizational situations, as a rule, it is not possible to build a single scalar criterion describing the interests (and thus determining the behavior) of the parties involved in the simulated process. For example, the desire to increase output and improve its quality is supplemented by the requirement to reduce production costs and minimize environmental damage, that is, the quality of functioning of most socio-economic (and not only) systems is usually assessed by a set of criteria. The corresponding models are investigated within the framework of the theory of multicriteria problems - an actively developing direction of the theory of decision-making. In them, a single value of each criterion corresponds to each decision (alternative) to be taken. However, in real conditions this requirement is often not met. A typical situation is when with respect to some parameters of the system or external influences it is known only that they can change within certain limits, within which they can take any value, unpredictable in advance.

For the DM the problem is reduced to the following: a rectangular matrix is given $m \times n$ matrix $A = (a_{ij})$ and DM needs to choose a row $i \in \{i_1, \dots, i_m\}$, which is optimal according to some optimality criterion. In this case, DM does not know which of the possible "states of nature" (uncertainties, weakly formalizable threats) $j \in \{j_1, \dots, j_n\}$ can be realized, i.e., when choosing a solution, DM must consider the possibility of any of these states. The DM does not have any probabilistic characteristics of the manifestation of outcomes a_{i_1}, \dots, a_{i_n} because he has no experience in solving such problems. Nevertheless, since he must decide, the question arises about the criteria for choosing a decision under the conditions of weakly formalizable factors. This criterion must prescribe a precise algorithm that, for any decision problem under uncertainty, unambiguously specifies the action that can be characterized as "optimal, according to the selected criterion".

In the general case we consider a single-criteria problem with uncertainty

$$\langle X, Y, f_1(x, y) \rangle \#(1)$$

where the choice of solution (alternatives) x from the set $X \subset \mathbb{R}^n$ is at the disposal of the DM. The goal of the DM is the choice $x \in X$ for which the scalar criterion $f_1(x, y)$ reaches the greatest possible value. At the same time, the decision maker must consider the effect of interferences, errors and other kinds of uncertainty y , of which we only know that they take a value from the given set $Y \subset \mathbb{R}^m$.

Criteria are chosen in such a way that they are well coordinated with the intuitive perceptions of the DM about the optimality (reasonableness).

Such criteria include:

- *Maximin criterion* (or Wald's maximin utility criterion [13]) - in each row of the matrix choose a minimum score. The optimal solution corresponds to such a solution, which corresponds to the maximum of this minimum, i.e., $\bar{F} = F(\bar{X}, Y) = \max_{1 \leq m \leq M} (\min_{1 \leq n \leq N} (A_{mn}))$. This criterion is very cautious and focuses on worst-case conditions, only among which the best and now guaranteed result is found. The generally accepted approach to deciding in problem (1) is based on the maxim (guaranteed result or Wald's maximized utility) principle. As the unimproved solution $x^* \in X$ here is chosen the maximal strategy defined by the first equality

$$\max_{x \in X} \min_{y \in Y} f_1(x, y) = \min_{y \in Y} f_1(x^*, y) = f_1^* \#(2)$$

The "substantive" meaning of the maxim's principle is that if the DM has chosen and used any arbitrary solution $x \in X$, then he "guarantees himself" the value of the criterion $\min_{y \in Y} f_1(x, y) = f_1[x]$ при of any uncertainty $y \in Y$. This fact follows from the inequalities $f_1[x] = \min_{y \in Y} f_1(x, y) \leq f_1(x, y), \forall y \in Y$. It is natural for the decision maker to strive for the greatest such guarantee. It is realized on the solution $x^* \in X$ of (2), since, according to (2), firstly, $f_1(x^*, y) \geq f_1^*, \forall y \in Y$, and second, $f_1[x] = \min_{y \in Y} f_1(x, y) \leq f_1^* = \min_{y \in Y} f_1(x^*, y), \forall x \in X$. Thus, the application of the principle of makismine leads to f_1^* - the largest (maximum) of all possible guarantees $f_1[x]$. The

meaning of this solution: by choosing and using x^* , the DM "guarantees" a criterion (outcome) value $f_1(x^*, y)$ which, given the realization of any uncertainty $y \in Y$ cannot become less than the guaranteed value f_1^* . Maximin guides the DM to a "catastrophe" - to the realization of the "worst" uncertainty for the DM. Usually such a realization is unlikely. That is why Savage suggested in 1951 the principle of minimax risk (minimax regret) as an improvement of the maximin criterion.

- *Minimax criterion* (or Savage's minimax regret criterion [14]). In each column of the matrix, the maximum score $\bar{A}_n = \max_{1 \leq m \leq M} (A_{mn})$ and a new matrix is compiled, the elements of which are defined by the relation $R_{mn} = \bar{A}_n - A_{mn}$. This is the size of the regret that the strategy Y_n a non-optimal choice is made X_m . The value R_{mn} is called risk, which is understood as the difference between the maximum gain that would take place if it were reliably known that the most advantageous situation would occur \bar{Y}_n for the decision-maker, and the real gain in the choice of decision X_m under the conditions of Y_n . This new matrix is called the risk matrix. From the risk matrix, one chooses the decision in which the value of risk takes the smallest value in the most unfavorable situation, i.e. $\bar{F} = F(\bar{X}, Y) = \min_{1 \leq m \leq M} (\max_{1 \leq n \leq N} (R_{mn}))$. That is, the essence of this criterion is to minimize risk. Like the Wald criterion, Savage's criterion is very cautious. They differ in their different understanding of the worst situation: in the first case it is the minimum gain, in the second it is the maximum loss of gain compared to what could have been achieved under given conditions. To each uncertainty $y^* \in Y$ let us assign a number $\max_{x \in X} f_1(x, y^*)$. Thus, DM defines for itself the maximal value of criterion under each possible uncertainty $y^* \in Y$. Then the decision-maker makes a difference between indicated maximal value of criterion $f_1(x, y^*)$ and value of the same criterion at any solution $x \in X$ that is

$$\max_{z \in X} f_1(z, y^*) - f_1(x, y^*) \quad \#(3)$$

where y^* - is a fixed uncertainty.

By doing so, the DM numerically assesses his "regret" that he is using x instead of $\bar{x} = \arg \max_{x \in X} f_1(x, y^*)$. Obviously, the "regret" will be zero if the solution chosen is \bar{x} under uncertainty y^* . The difference (3) characterizes the risk of the decision maker. The risk arises because the decision maker does not know exactly what uncertainty $y^* \in Y$ may materialize. The DM then seeks to choose a solution $x \in X$ in which the risk ("regret") would be as low as possible. To do this, we apply the maximization principle described above to the following problem $\langle X, Y, -[\max_{z \in X} f_1(z, y) - f_1(x, y)] \rangle$, which is reduced to $\min_{x \in X} \max_{y \in Y} \Phi_1(x, y) = \max_{y \in Y} \Phi_1(x^0, y)$, where the risk (regret) function $\Phi_1(x, y) = \max_{z \in X} f_1(z, y) - f_1(x, y)$. The value of the risk function on the concrete pair $(x, y) \in X \in Y$ we further call the risk of the DM when he uses the alternative $x \in X$ and the realization of uncertainty $y \in Y$. The DM evaluates its risk-the difference between the "best" (maximum) value of the criterion f_1 and the value realized. It is natural for the DM to strive to minimize this risk. According to the above definition, the decision-maker, adhering to x^0 , "secures for himself" the risk $\Phi_1(x^0, y)$ which, given any uncertainty $y \in Y$ cannot become greater than its guaranteed value. Φ_1^0 .

- *Pessimism-optimism index criterion* (Hurwitz criterion¹ [15]). We introduce a certain coefficient α called the "optimism coefficient", $0 < \alpha < 1$. In each row of the winnings matrix we find the largest score $\max_{1 \leq n \leq N} (A_{mn})$ and the smallest $\min_{1 \leq n \leq N} (A_{mn})$. They are multiplied by α and $(1 - \alpha)$ and then their sum is calculated. The optimal solution is the solution to which the maximum of this sum corresponds, i.e.

$$\bar{F} = F(\bar{X}, Y) = \max_{1 \leq m \leq M} \left(\alpha \times \max_{1 \leq n \leq N} (A_{mn}) + (1 - \alpha) \times \min_{1 \leq n \leq N} (A_{mn}) \right).$$

At $(\alpha = 0)$ the Hurwitz criterion is transformed into the Wald criterion. This is a case of extreme "pessimism. At $(\alpha = 1)$ (a case of extreme "optimism"), the person making the decision expects the most favorable situation to accompany it. The "optimism factor" α is assigned subjectively, based on experience, intuition, etc. The more dangerous the situation, the more

¹ The Gurwitz criterion has nothing to do with risk analysis. Except for the subjective perception of "random" and "voluntary" risks.

cautious the approach to the choice of decision should be, and the lower value is assigned to the coefficient α .

- *Laplace criterion.* Since the probabilities of occurrence of a given situation Y_n are unknown, they are equally probable. Then for each row of the winnings matrix the arithmetic mean of the evaluations is calculated. The optimal solution will correspond to such a solution to which the maximum value of this arithmetic mean corresponds, i.e.

$$\bar{F} = F(\bar{X}, Y) = \max_{1 \leq m \leq M} \left(\frac{1}{N} \sum_{n=1}^N A_{mn} \right)$$

A few remarks about uncertainties. According to Knight [16], the distinction between risk and uncertainty is a matter of knowledge about the future. Risk describes situations that are available to be "measured" in terms of probability, while uncertainty refers to situations in which the information is too imprecise to be generalized by means of probability. Uncertainty, then, is a consequence of a lack of knowledge about reality. Over time, what is currently considered uncertainty can turn into risks (e.g., long-term weather forecasts are currently characterized by great uncertainty, but medium-term forecasts can already characterize the risks of certain events). But, the harm and benefit of an action are determined by the totality of the circumstances. And often only the boundaries of changes are known about the uncertainties, and any statistical characteristics are either absent or unprofitable to obtain. Uncertainties in (1) are denoted by y , and their set by Y ; we may assume that the set Y is known to the DM a priori.

In the problem (1) the outcome for the DM is estimated by the value of the function $f_1(x, y)$ defined on the product $X \times Y$ and called the criterion for DM (it can be income for the seller, for the buyer - the amount of money saved, the amount of purchased goods, the time of goal achievement and other factors evaluating the outcome for DM). Although "non (ne) bis in idem" (you cannot do the same thing twice, that is, it should not be repeated, in Latin), once again describe the process of decision-making in the problem (1). It occurs as follows. The decision maker chooses and uses his solution $x \in X$. At the same time and independently of this choice some uncertainty is realized $y \in Y$. On the resulting pair of $(x, y) \in X \times Y$ criterion $f_1(x, y)$ takes a particular value $f_1(x, y)$, called the outcome for the DM. For certainty, let us assume that the DM seeks the greatest possible outcome (if, for example, the criterion $f(x, y)$ evaluates the sum of losses or the cost of production, then in the problem (1.1.1) we should put $f_1(x, y) = f(x, y)$, for $\max_{x \in X} | -f(x, y) | = - \min_{x \in X} f(x, y)$).

It follows from the above that risk assessment is only possible if there are alternative choices. If there is only a single choice, then the risk is automatically zero and the spread of payments is only a characteristic of the uncontrollable natural environment. However, the alternative is always present in the form of a refusal to decide. In some cases, the refusal to decide may give an optimum on the columns, and then there will be non-zero risks in the options at the expense of choosing the wrong decision. For example, it is better not to play in a casino than to play by sticking to a strategy. In chess, on the other hand, it makes sense to play even in the case of a single (forced) move. For example, if my opponent declares "check", there is nothing to close, and retreat is only possible for the only chess cell. The risk is also zero, since refusing to play is an automatic defeat.

Availability of probability estimates $\sum_{n=1}^N p_n = 1$ to describe the state of the natural environment $p_1 = p(Y_1), p_2 = p(Y_2), \dots, p_N = p(Y_N)$ allows to refuse from choosing the most unfavorable case when using the Savage criterion, and to write down the desired solution in the form:

$$\bar{F} = F(\bar{X}, Y) = \min_{1 \leq m \leq M} \left(\sum_{n=1}^N p_n \times \left(\max_{1 \leq n \leq N} A_{mn} - A_{mn} \right) \right)$$

This is the more correct formula. Only when, for any pair (X_m, Y_n) the payment is determined only by the size of the loss $A_{mn} = B - C_{mn}$

$$\bar{F} = F(\bar{X}, Y) = \min_{1 \leq m \leq M} \left(\sum_{n=1}^M p_n \times (B - C_{mn}) \right) = B + \min_{1 \leq m \leq M} \left(\sum_{n=1}^M p_n \times C_{mn} \right).$$

And only when the level of loss at the optimum for the conditions Y_1, Y_2, \dots, Y_N does not depend on n and is equal to \bar{C} , then:

$$\bar{F} = F(\bar{X}, Y) = \min_{1 \leq m \leq M} \left(\sum_{n=1}^M p_n \times (B - C_{mn}) \right) = B - \bar{C} + \min_{1 \leq m \leq M} \left(\sum_{n=1}^M p_n \times C_{mn} \right).$$

Only in this case is the solution really determined by the value of the mathematical expectation of the loss. But adjusted for B и \bar{C} . The science of these corrections is contained in many papers. Usually, we take B и \bar{C} equal to zero. For example, in ecology, it costs nothing to improve "air" (no profit), and if no one gets sick, the optimal damage is taken as 0.

V. Risk as a Bayesian evaluation

The Bayesian paradigm of statistical inference and non-competitive decision making is simple to state. It is essentially a probabilistic view of the world, which states that all uncertainty should be described only in terms of probability and its calculation, and that probability is personal or subjective. Why is the Bayesian paradigm relevant to reliability, risk and survivability analysis? From a philosophical point of view, the answer is obvious: the Bayesian paradigm is based on the logical structure of the calculus of probability. From a pragmatic point of view, we can say that in risk analysis we often deal with unique situations, so the notion of relative frequency is not always appropriate. Another argument is that in many cases there is no direct prior data, so any uncertainty estimates can only be based on raw information; the Bayesian paradigm allows for this. Finally, risk, reliability and survivability analyses are most reliable when experts play a key role; the Bayesian paradigm allows expert experience to be formally incorporated into the analysis by considering a priori probabilities.

In mathematical statistics and decision theory, a Bayesian decision estimate is a statistical estimate that minimizes the posterior expectation of the loss function (that is, the posterior expectation of the loss). In other words, it maximizes the posterior expectation of the utility function. In statistical decision theory it is shown that a detection system with a decision selection rule by the maximum posterior probability criterion minimizes the number of erroneous decisions. The sum of the number of false alarms and omissions in a sufficiently long sequence of decisions, that is, the probability of error of any kind, is minimal compared to a system using a rule with any other criterion. However, the rule does not establish any correlation between the number of false alarms and signal misses, so it should be applied when false alarms and signal misses are undesirable to the same extent. The effectiveness of the detection system is evaluated by their total number on some time interval. It is known that this criterion is used, for example, in communication systems.

When reconstructing the values of the parameters sought, the researcher usually has additional (a priori) information about the parameters, in addition to the information "inherent" in the sample X_1, \dots, X_n . So far, parameter estimates have been based only on the sample X_1, \dots, X_n and did not consider additional information about the parameters. Taking additional information into account will improve the reliability and accuracy of the estimation.

At present, there are two main methods of accounting for auxiliary information depending on its nature - Bayesian and minimax. Below, in addition to these two methods of accounting for a priori information, another method is outlined - a generalized maximum likelihood method [17].

In the framework of Bayesian theory, this estimate can be defined as a posteriori maximum estimate. A Bayesian estimate will be such an estimate, which minimizes the Bayesian risk among all other estimates. The risk (not Bayesian, but ordinary) will be equal to the mathematical expectation of the variance of the posterior distribution. Application of the Bayesian approach implies treating the sought parameter u as a random variable. Then the a priori information is

given in the form of a priori distribution $p_{\text{app}}(u)$ of random variable u . In most applied problems, the sought parameter is a deterministic quantity, and therefore the artificially imposed Bayesian approach of treating deterministic quantities as random quantities causes numerous criticisms of the Bayesian method. It should be noted, however, that in many cases the Bayesian method successfully accounts for a priori information and produces reasonable estimates.

So, in the Bayesian approach u - is a random variable. Let us denote by $p(x_1, \dots, x_n, u)$ the joint probability density of a set of random variables X_1, \dots, X_n, u .

We have $p(x_1, \dots, x_n, u) = p(x_1, \dots, x_n | u)p_{\text{app}}(u) = p(u | x_1, \dots, x_n)p(x_1, \dots, x_n)$, where $p(u | x_1, \dots, x_n)$ - is the conditional probability density of a random variable u at fixed values x_1, \dots, x_n , $p(x_1, \dots, x_n)$ - is the marginal joint probability density of a set of random variables X_1, \dots, X_n which can be found by formula

$$p(x_1, \dots, x_n) = \int_U p(x_1, \dots, x_n, u) du = \int_U p(x_1, \dots, x_n | u) p_{\text{app}}(u) du.$$

From the above it follows the formula

$$p(u | x_1, \dots, x_n) = \frac{p(x_1, \dots, x_n | u) p_{\text{app}}(u)}{\int_U p(x_1, \dots, x_n | u) p_{\text{app}}(u) du}.$$

Since there is one realization of a set of random variables X_1, \dots, X_n given by sample (1.1), then finally we obtain Bayes formula:

$$p(u | X_1, \dots, X_n) = L_n(u | X_1, \dots, X_n; u) p_{\text{app}}(u) / C,$$

where the normalization factor:

$$C = \int_U p(X_1, \dots, X_n | u) p_{\text{app}}(u) du.$$

does not depend on u .

The function $p(u | x_1, \dots, x_n)$ is called the posterior probability density function.

The point Bayesian estimate (B-estimate) \hat{u}_B choose one of the characteristics of the posterior probability density function, such as the mode, the expectation, or the median of the posterior distribution. Clearly, in the general case, all three estimates will be different.

There is another way of obtaining a point Bayesian estimate, in which a positive loss function is specified $W(|\hat{u} - u|)$ where \hat{u} - parameter estimate u . Based on the chosen loss function $W(t)$ and the resulting posterior density $p(u; x_1, \dots, x_n)$ we construct the functional

$$R(\hat{u}; X_1, \dots, X_n) = \int_U W(|\hat{u} - u|) p(u | X_1, \dots, X_n) du,$$

which is commonly referred to as *the posterior risk* of estimation and for a given sample X_1, \dots, X_n . Then the B-estimate is defined as a solution to an extreme problem:

$$\hat{u}_B = \arg \min_{\hat{u}} R(\hat{u}; X_1, \dots, X_n)$$

i.e., the B-estimate minimizes the posterior risk.

In determining the B-estimate according to the formula for \hat{u}_B there also remains the ambiguity of the Bayesian point estimate because of the possibility of choosing different loss functions $W(t)$. The first method usually takes as its B-estimate the mode of the posterior distribution (the most likely value of the posterior random variable u). In the second method, the quadratic loss function is most often chosen $W(t) = t^2$. De Groot and Rao studied the type of B-estimates for different loss functions. They found that for $W(t) = |t|$, $W(t) = t^2$ и $W(t) = \eta(t + \delta) - \eta(t - \delta)$, $\delta > 0$ (rectangular window), the B-estimate coincides respectively with the median, expectation, and mode (for unimodal and symmetric with respect to the mode of the posterior density) of the posterior distribution. If posterior distribution is unimodal and symmetric about mode, then all B-estimates for any symmetrical convex loss function coincide. The theoretical foundations of the Bayes method are presented in the monographs by De Groot [18] and Zacks [19].

In mathematical statistics and decision theory, a Bayesian decision estimate is a statistical

estimate that minimises the posterior expectation of the loss function (that is, the posterior expectation of the loss). In other words, it maximises the posterior expectation of the utility function. In statistical decision theory, it is shown that a detection system with a decision selection rule using the maximum posterior probability criterion minimises the number of false alarms. The sum of the number of false alarms and omissions in a sufficiently long sequence of decisions, i.e. the probability of any type of error, is minimal compared to a system using a rule with any other criterion. However, the rule does not establish any correlation between the number of false alarms and the number of missed signals, so it should be used when false alarms and missed signals are equally undesirable. The effectiveness of the detection system is evaluated by their total number over a given time interval. It is well known that this criterion is used, for example, in communication systems. In the framework of Bayesian theory, this estimate can be defined as an a posteriori maximum estimate. A Bayesian estimate will be one that minimises the Bayesian risk among all other estimates. The (non-Bayesian, but ordinary) risk will be equal to the mathematical expectation of the variance of the posterior distribution.

VI. Risk as a Difficulty of Achieving a Goal

This concept was formed and developed by the school of Russian mathematician Isaak Russman [20, 21]. Risk assesses the difficulty of obtaining a declared result d_k under the existing estimates of resource quality (μ_k) and the requirements for this quality (ε_k) [22]. The notion of the difficulty of achieving a goal for a given quality and quality requirements of the resource and result derives from the considerations that it is more difficult to obtain a result of a certain quality the lower the quality of the resource (μ_k) or the higher the requirements for its quality (ε_k).

The functioning of a reliable system is characterized by the preservation of its main characteristics within the established limits. The peculiarity of management in socio-economic systems is that in most cases it is focused not on the complete extinguishing of deviations (the performance of this task in modern conditions is extremely difficult), and to maintain fluctuations of output parameters within limits that do not threaten the system with loss of stability and destruction. In other words, this means that the actions of such a system are aimed at minimizing the deviations of its current state from some given ideal - the goal, which is a key aspect in the study of the properties and mechanisms of the behavior of control systems. In relation to the system the goal can be considered as a desired state of its outputs, i.e., some value of its target functions.

The system is considered in the process of achieving the goal, in the movement from its current state to some future result, the quantitative expression of which is A_{pl} . Suppose the time is given to achieve the goal t_{pl} . Let us also assume that there is a minimal speed V_{min} of moving to the goal in time and the maximal speed of V_{max} . It is most convenient to measure the result and the time needed to reach it in dimensionless values, for this purpose let us assume that A_{pl} и t_{pl} equal to one or 100%.

From general considerations, the difficulty d_k of the result must have the following basic properties:

- at $\mu_k = \varepsilon_k$ be maximal, i.e., equal to one (indeed, the difficulty of obtaining a result is maximal at the lowest admissible value of quality);
- at $\mu_k = 1$ и $\mu_k > \varepsilon_k$ be minimal, i.e., equal to zero (at the highest possible value of quality regardless of the requirements (at $\varepsilon_k < 1$) the difficulty should be minimal);
- at $\mu_k > 0$ и $\varepsilon_k = 0$ be minimal, i.e., equal to zero (obviously, if there are no requirements to the quality of a resource component, a μ_k is greater than zero, then the difficulty of obtaining a result for this component must be minimal).

For these three conditions at $\varepsilon_k < \mu_k$ a function of the form is valid:

$$d_k = \frac{\varepsilon_k(1 - \mu_k)}{\mu_k(1 - \varepsilon_k)}$$

We also believe that $d_k = 0$ at $\mu_k = \varepsilon_k = 0$ и $d_k = 1$ at $\mu_k = \varepsilon_k = 1$.

Note, the resulting formula has a well-founded probabilistic interpretation.

In Fig. 1, the lines OD and OB correspond to the trajectories of the system with minimum and maximum velocities.

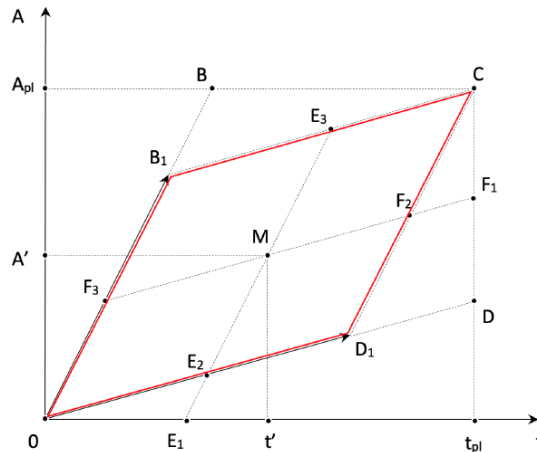


Fig. 1: Geometric interpretation of the system movement to the target

The broken line OD_1C is the boundary of the forbidden zone, and for any point M with coordinates (t', A') , describing the position of the system on an arbitrary trajectory of motion to the target within the limits of the parallelogram OB_1CD_1 , the distance is taken as the value of the risk of not reaching the target:

$$r(M) = \max \left\{ \ln \frac{1}{1 - d_1}, \ln \frac{1}{1 - d_2} \right\},$$

$$\text{где } d_1 = \frac{\varepsilon_1(1 - \mu_1)}{\mu_1(1 - \varepsilon_1)}, d_2 = \frac{\varepsilon_2(1 - \mu_2)}{\mu_2(1 - \varepsilon_2)}, \varepsilon_1 = \frac{|E_1E_2|}{|E_1E_3|}, \mu_1 = \frac{|E_1M|}{|E_1E_3|}, \varepsilon_2 = \frac{|F_1F_2|}{|F_1F_3|}, \mu_2 = \frac{|F_1M|}{|F_1F_3|}$$

The Russman criterion contains *the idea of an optimal modification of a system* (a growing system - a reproducing growth system). This is the optimization of development by redistributing energies (resources).

VII. Risk as a measure of process quality

If a certain quality standard of the object (process) is set, the risk of the object (process) is defined as a value proportional to the deviation of its current state from this quality standard. In fact, risk in this case is a measure of the quality of the object (process). The measure of risk itself is the threat of changes in the composition or properties of the object (process) or its environment, or the appearance of changes associated with the emergence of undesirable processes due to arbitrary influences [23, 24]. The measure of the threat of failure to achieve the goal is considered in this case as a variable, which is a function of the current state of the object (process): it increases when the assessed situation approaches a certain acceptable boundary, after which the object (process) cannot achieve the corresponding goals. The described approach assumes the availability of retrospective information on the realization of risks.

Mathematical formulation of the problem. The set of attributes 2X (risk factors), a set of admissible realizations of situations $O = \{o_1, \dots, o_D\}$ (for example, the risk is realized or not realized), and there exists a target function $o^*: X \rightarrow O$, the values of which $o_i = o^*(x_i)$ are known only on the finite subset of attributes $\{x_1, \dots, x_\rho\} \subset X$. The "sign-answer" pairs (x_i, y_i) will be called precedents. The set of pairs $X_\rho = (x_i, o_i)_{i=1}^\rho = 1$ will constitute the training sample. You want to

² Traits can be binary (1/0, red/green), nominal (set of values), ordinal (set of ordered values) or quantitative.

use the sample X_ℓ to restore the dependence o^* that is, we must construct the separating function $\pi(o): X \rightarrow 0$, which would approximate the target function $o^*(x)$, not only on the objects of the training sample, but also on the entire set of X . The separating function $\pi(o)$ is called the choice logic function $\pi: \pi(o) \rightarrow \{0,1\}$, indicating that the situation o is selected into some subset $\pi(o)$ ($\pi(o) = 1$) or not ($\pi(o) = 0$).

In the general case the choice functions may be arbitrary, but to use them correctly to describe the acts of choice, it is necessary to $\pi(o)$ to impose several restrictions (the so-called axioms of choice).

Axiom 1 (inheritance): if $O' \subseteq O$, then $\pi(O') \supseteq (\pi(O) \cap O')$, that is, if the choice is bounded, then both the "best of the best" objects belonging to $(\pi(O) \cap O')$, and those objects that are the best among those available in the restricted sample $O' \subseteq O$, but which would not be chosen if choice were available on all alternatives O .

Axiom 2 (agreement): $\prod_i \pi(O_i) \subseteq \pi(\cup_i O_i)$, that is, if some object O has been chosen as the best in each of the sets O_i , then it should be chosen also when considering the whole set of sets $\cup_i O_i$.

Axiom 3 (rejection): $(\pi(O) \subseteq O' \subseteq O) \Rightarrow (\pi(O') = \pi(O))$ that is, if we discard any part of the "rejected" objects, then on the remaining subset of objects the result of selection will not change. The set of objects $O = \{o_1, \dots, o_D\}$ which obeys all three listed axioms (inheritance, agreement, rejection) is called Pareto-optimal set.

Axiom 4 (path-independent): $\pi(X_1 \cup X_2) = \pi(\pi(X_1) \cup \pi(X_2))$. This axiom is identical to the joint fulfillment of the axioms of inheritance and agreement. This axiom reflects the requirement to preserve the result of choice when implementing multi-step selection procedures. For example, the most systematically significant object is determined among the most systematically significant objects of the same type. Therefore, a set obeying the discard axiom and the Plott axiom is naturally a Pareto-optimal set.

So, we have two matrices of evaluated attributes $p(l, k)$ и $q(n, k)$ for situations with positive dynamics and situations with negative dynamics ($k = 1, \dots, K$ - number of the attribute; the values $l = 1, \dots, L$ - of the row of the situations with positive dynamics, and the values $n = 1, \dots, N$ - of the row of the situations with negative dynamics). The axioms mentioned above are sufficient to adequately describe the structure of optimal solutions of choice problems. The accepted axiomatics shows that the constructed separating rule must be a monotone function with respect to the set of situations identified as regular (with positive dynamics). As a result, the resulting classifier of situations monotonically turns into a product of rules. This important property can be used in order not to retrain the classifier when new situations are received.

To set a partial order, you need the number of features at least $\lceil \log_2 N \rceil + 1$ where N - is the number of situations. If there are fewer signs, there will necessarily be the same descriptions for at least a couple of situations.

General view of the separating rule: $y = \sum_{v=1}^V x_{v,1} \cdot \dots \cdot x_{v,D_v}$, where y - description score ($y = 1$ for situations with "positive" dynamics for the DM, $y = 0$ for situations with "negative" dynamics for DM); v - number of the group of variables; D_v - dimensionality (number of features in the group); $x_{v,1}$ - value of the first characteristic in the group; x_{v,D_v} - value of the last trait in the group.

To identify the features that must be considered in the separating rule, a method for their analysis has been developed [24], using the Hamming metric³:

$$\rho(O_i, O_j) = \sum_{k=1}^K [O_{ik}(1 - O_{jk}) + (1 - O_{ik})O_{jk}]$$

The value of this metric - the distance between one-dimensional objects of the same type (rows, columns) is measured by the number of their non-matching pairs. The unit is added by the "exclusive OR" condition (addition modulo 2). Mismatching is interpreted as an error, and the

³ Originally, the metric was formulated by Richard Hamming during his work at Bell Labs to determine the measure of difference between code combinations (binary vectors) in the vector space of code sequences, in which case the Hamming distance between two binary sequences (vectors) of length n . This is the formulation of Hamming distance in the NIST Dictionary of Algorithms and Data Structures.

closeness of objects is thus evaluated by the minimum number of "corrections" that one or the other, or both objects need to make for the objects to become identical, indistinguishable. Naturally, the equality is fulfilled: $\rho(O_i, O_j) = \rho(O_j, O_i)$. Since in the problem of risk identification we can limit ourselves to the natural class of monotone functions, we are not interested in all mismatches in a pair, but only in "ordered" ones, i.e., we can use the semi-Hemming metric:

$$\mu(O_i, O_j) = \sum_{k=1}^K O_{ik}(1 - O_{jk})$$

which reflects only the number of "successful" for the DM attributes μ for which in the description of the first of the compared situations the value is "correct" (equal to 1), and in the second situation it is "wrong" (equal to 0). By combinations of "good" characteristics the situations "positive" for DM are separated from "negative", and by the metric μ the size of the transition zone is specified. The semi-Hemming metric allows to eliminate inconsistent pairs of situations, which knowingly do not satisfy the conditions of strict inequalities, defining partial order.

Graphically, the solution algorithm is illustrated by the diagram in Fig. 2.

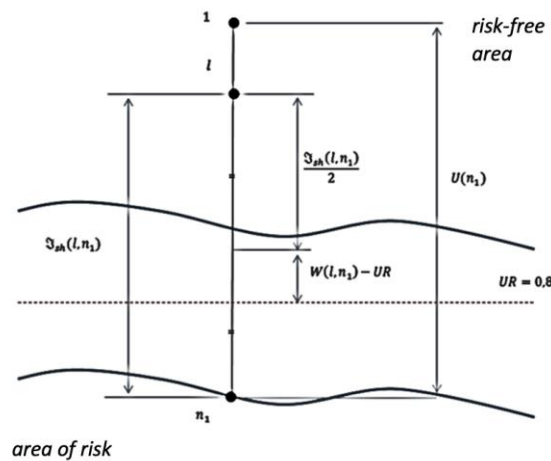


Fig. 2: Determining the measure of threat of non-achievement by an object (process) target state for situations with "positive" dynamics for the DM

Semi-Hemming matrix \mathfrak{S}_{sh} dimensions (L, N) :

$$\mathfrak{S}_{sh}(l, n) = \sum_k (p(l, k) - q(n, k)) \cdot b(p(l, k), q(n, k))$$

The penalty function $b(p(l, k), q(n, k))$ Equals:

$$b(p(l, k), q(n, k)) = \begin{cases} 0, & \text{при } p(l, k) \leq q(n, k); \\ 1, & \text{при } p(l, k) > q(n, k). \end{cases}$$

In those cases where all penalties ($k = 1, \dots, K$) are equal 0, we speak of the complete dominance of the situation with negative dynamics n . An unsolvable contradiction arises. Define "reserves" for situations with positive dynamics and situations with negative dynamics. For $l = 1, \dots, L$ the value of the stockpile, respectively, is equal to:

$$Z(l) = \min_n \mathfrak{S}_{sh}(l, n).$$

The lowest of all $Z(l)$ value $ZZ = \min_l Z(l)$ determines the "separability threshold" of all situations with positive dynamics from all situations with negative dynamics. In principle, the "separability threshold" can be reached for more than one pair (l_1, n_1) .

For situations with "positive" for the DM dynamics for all n_1 we calculate $U(n_1) = \sum_k (1 - q(n_1, k))$. These values account for the half-sum of the distance $\mathfrak{S}_{sh}(l, n_1)$, hence:

$$W(l, n_1) = UR + (1 - UR) \cdot \left(\frac{\mathfrak{S}_{sh}(l, n_1)}{2 \cdot (U(n_1) - \frac{\mathfrak{S}_{sh}(l, n_1)}{2})} \right) = UR + (1 - UR) \cdot \left(\frac{\mathfrak{S}_{sh}(l, n_1)}{2 \cdot (U(n_1) - \mathfrak{S}_{sh}(l, n_1))} \right).$$

The bottom line is a measure of risk: $W(l) = \min_{n_1} W(l, n_1)$.

Here UR - is the level of the acceptable risk boundary.

For situations with "negative" dynamics for the DM, similarly: for all l_1 calculate $V(l_1) = \sum_k(1 - p(l_1, k))$. These values account for the half-sum of the distance $\mathfrak{S}_{sh}(l_1, n)$, therefore:

$$S(l_1, n) = UR - UR \left(\frac{\mathfrak{S}_{sh}(l_1, n)}{2 \cdot (V(l_1) - \frac{\mathfrak{S}_{sh}(l_1, n)}{2})} \right) = UR - UR \cdot \left(\frac{\mathfrak{S}_{sh}(l_1, n)}{2 \cdot (V(l_1) - \mathfrak{S}_{sh}(l_1, n))} \right).$$

As a result, the measure of risk, respectively: $S(n) = \max_{l_1} S(l_1, n)$.

VIII. Risk as an Anti-Development Potential

The interpretation of risk as an anti-potential for development implies that it is considered in the context of some developing purposeful system [25]. Against the background of the global transformation processes that have begun in recent years, the relevance of solving the problems of effective management of structurally complex socio-technical systems has significantly increased. The notion of the value of objects (assets) included in such systems "presses" cost estimates of the significance of decisions made and becomes defining, but the definition of this "value" remains more of an art than a scientifically grounded methodology. Intuitively it is clear that with limited resources (of all kinds) it is necessary to strive to use these resources in the most rational way. However, to develop a rational solution, one must learn to evaluate the results of the system's purposeful activity, to compare them with the tasks set and the costs associated with this or that solution. To compare, respectively, one must learn to measure, that is, to have some quantitative measure that characterizes the result of the functioning of an individual object and the entire complex socio-technical system, as well as a "tool" that makes it possible to evaluate the result obtained.

Since the problem is to choose the best of the compared options for the growth and development of the system, we must first learn to measure the quality of the decisions made. The quality of any decision is fully manifested only in the process of its implementation (in the process of target functioning of the controlled object or system). Therefore, the most objective is to evaluate the quality of a decision by the effectiveness of its application. Thus, for a reasonable choice of the preferred solution it is necessary to measure the effectiveness of the target functioning of the managed object or system from its compared options [26] in conditions of existing uncertainty and risk. Comparison of development options and decision making directly depends on the competence of decision makers (DM), on their ability to comprehensively assess the risks associated with the functioning and development of the system. DM usually use analytical tools based on mathematical methods (from Kantorovich's "simplex method" [27] to modern methods of machine learning, neural networks [28,29,30], methods of support vectors [31], genetic algorithms [32], etc.) to provide a reasonable choice of DM.

There are several classes of decision-making tasks:

- Deterministic, which is characterized by an unambiguous connection between the decision and its outcome and is aimed at constructing a function of "progress", and the definition of stable parameters in which the optimum is achieved.
- Stochastic, in which each decision made can lead to one of a set of outcomes occurring with a certain probability, and using methods of simulation programming [33], game theory [34] and other methods of adaptive stochastic control [35] to choose the optimal strategy in the calculation on the average, statistical characteristics of random factors.
- In conditions of uncertainty, when the optimality criterion depends not only on the strategies of the operating party and fixed risk factors but also on uncertain factors of non-stochastic nature, and interval mathematics [36] or approximations in the form of fuzzy (fuzzy) sets [37, 38] are used for decision-making.

In the latter case, as a rule, methods of processing the opinions of independent experts are involved [39, 40]. Despite the widespread use of expert systems in practice for many DMs remains

unclear the fairness of using certain methods of analysis, especially when the results contradict "common sense" (in their understanding) [41], so developers must formulate and adhere to some principles, without which the automation of methods adopted in expert systems, becomes unacceptable.

Often expert evaluation procedures are based on the method of processing matrices of pairwise comparisons of different alternatives, known as the Saaty algorithm (or hierarchy analysis method) [42], which is quite widely used despite criticisms [43, 44, 45] and the lack of unambiguous solutions to several research questions.

First, if the dimensionality of the matrix of pairwise comparisons is large, the number of comparisons for each expert increases to $N \times (N - 1) / 2$ where N - the number of alternatives under consideration. There are problems of "poor" filling of the matrix of comparisons by the experts and "insufficiency" of the qualitative scale used in the method.

Second, not all experts can compare in pairs all the proposed alternatives, so some matrices of pairwise comparisons will remain unevaluated (*NA*). This problem is partially solved by Saaty's development of the hierarchy analysis method to the analytic network method, but the latter contains several strong assumptions that impose restrictions on its application [46, 47].

Third, as a rule, there is no "benchmark" alternative, through which the remaining estimates are obtained by transformation $A_{i,j} = A_{i,1} \times A_{j,1}^{-1}$, which is used, for example, in combinatorial methods of missing data recovery.

Fourth, when generalizing the experts' opinions and moving to a general matrix of pairwise comparisons, values with a significant variation appear in the same cells, which leads to the need to work with the estimates given in the interval scale [48].

Finally, when the alternative for comparison is not the object itself, but some scalar way of determining the risks, then the problem of selecting objects is reduced to the assessment of the weights of the factors affecting the integral risk. As a result, there is a complex problem of analyzing the risks of objects, solved through the value of minimizing the integral risk [49].

The theory of complex systems (synergetic) uses nonlinear modeling and fractal analysis for forecasting. In the last decade such innovative directions as theoretical history, mathematical modeling of history based on a synergetic, holistic description of society as a non-linear developing system are actively developing.

Modern complex socio-technical systems are characterized by a distributed in space, a great variety of their constituent objects and the interaction of their various types, the heterogeneous structure of transport and technological chains, unique conditions of impact on individual objects and on the system of risks of different nature. If the stability of operation of such complex systems is understood as their fulfillment of the plan of their development with permissible deviations in the volume and time of task performance, their management is reduced to the minimization of unplanned losses in the event of abnormal situations and carrying out measures to prevent them, i.e., to the analysis, assessment and management of associated risks. The concept of management of such systems is to achieve an optimal balance between the value of the object, associated risks and performance indicators, on the basis of which economic goals are formed and the use of the object is ensured in such a way that it creates added value. In general, the optimal profit-oriented management consists in the ability to find a balance in the redistribution of available resources (material, human and informational) between "production activity" and "maintenance of the development potential".

The closest to the above is described by the models of interaction between the developing object and its environment – the model of self-improving developing systems by V. Glushkov. He introduced a new class of dynamic models based on nonlinear integrodifferential equations with prehistory [50]. He also developed approaches to modeling so-called "self-improving systems" and proved theorems on the existence and uniqueness of solutions describing their systems of equations [51]. However, it should be noted that the name "evolving" applied to the class of systems under consideration is not quite correct and contains some ambiguous ambiguity. The growth of the system may not be accompanied by its development (for example, improvement of

the science of creation and design, instructions of manufacturing or use of a product) and vice versa (for example, expectations of a quick practical return from basic science). Usually, growth and development combine with each other, there is a smooth or jumping change of proportions between them, and some "equilibrium" state with the external environment comes (or does not come).

Parallel to V. Glushkov's work, sectoral research also began on the scientific and technological revolution (STR) [52, 53], which laid the foundations for potential systems theory, and work based on biophysical and economic models [54], which proposed a model involving integrodifferential equations describing the production, adoption and forgetting of knowledge in production cycles due to the transition to a different scientific and technological basis. It shows the cyclical nature of capacity accumulation and the need to develop complex systems (health, education, industrial safety systems, ecology and other infrastructure projects by generations).

Understanding and development of the mentioned models led N. Zhigirev and A. Bochkov to the need to introduce a class of so-called "smart expansive systems". [55], which consists of three subsystems (Fig. 3).

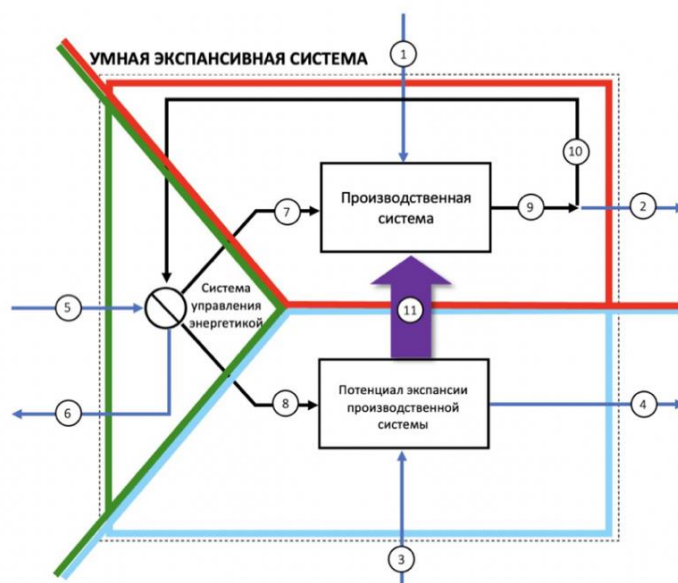


Fig. 3: Schematic diagram of a Smart Expansion System

Smart Expansive System (SES) is an open system, which can be growing or developing, or simultaneously both growing and developing (when, for example, objects of different "generations" are included in it). Sometimes the growth of a system is accompanied by so-called "flattening" (alignment at one level of development) and degradation in its development. SES openness is caused by the fact that it needs to effectively allocate the necessary resources from the external environment, possibly "cleaning them before using (including human resources), and to remove waste of vital activity.

The production subsystem is evaluated by the reproduction rate multiplier at a conditional minimum of development potential. Below this minimum (the critical mass of potential) the growth and development of the SES is impossible in principle. The potential catalytic function describing this multiplier is, in the limit, an asymptotic curve with saturation (like a logistic curve), although potential inhibition is also possible since the production subsystem occupies the space of the general SES. This behavior is analogous to the flow system of a "brusselator" (an intensively running conveyor belt), when the initial substrates flow out of it without time to react with the catalyst, not mot row for enough of it [56].

The production subsystem serves to measure the success of expansion, defined, for example, by the volume of useful products produced by the system.

The expansion potential subsystem of the production subsystem is designed to catalyze the management of forms produced and resources (sometimes measured by money, which has a dual structure - the cost of renewing matter and the cost of maintaining information in the broad sense of the word) produced in the production subsystem.

The energy management subsystem is a two-loop resource management system (financial and temporal) between production and contribution to infrastructure projects.

In Fig. 3, the externally directed flow of energies (5) is distributed by the regulating subsystem to the production subsystem (7) and is directed to the expansion potential subsystem to produce knowledge and improvement of technologies, "recipes" for the preparation of products (the so-called flow to the development of "infrastructure"). From the external environment the expansion potential subsystem also receives additional information about new knowledge, inventions and technologies (3) and has a catalytic effect on the production subsystem (11). The production subsystem, in turn, receives from the external environment a flow of "purified" semi-finished products (1) for further expansion. In the process of expansion inevitably there is a partial forgetting of information caused by various reasons, including physical death of carriers of original thought-forms (4), which causes weakening of expansion potential of the whole system.

From the production subsystem to the external environment there is an outflow (2) of products, unused semi-finished products, waste product assembly, etc. Cleared from (2), the energy flow coming by the results of labor into the production subsystem and the results of the sale of products on the market supports the functioning of the regulatory subsystem. In the latter, over time, dissipation of energies (6), not yet distributed across subsystems, is possible, capable of causing, under certain conditions, the collapse of the control system.

Let us dwell a little more on the peculiarities of the deterministic and stochastic approach to SES modeling.

For the deterministic case, the SES is described by a two-parameter model in terms of time (1) and in terms of energy distribution proportions (3).

The first equation describing the system is in some sense autonomous:

$$\frac{dX(t)}{dt} = \left(g \times \frac{\varphi(\beta)}{1 + \beta} - a \right) \times X(t) - b \times X^2(t), \quad (1)$$

where $X(t)$ - the volume of the "production subsystem", measured by the number of products; $a \times X(t)$ - the summand of the linear part - the maintenance of the production technology requires linear costs, in economics, for example, it is the cost of depreciation; $g \times \frac{\varphi(\beta)}{1 + \beta} \times X(t)$ - the linear production function of the useful subsystem with the parameter β ; $s = \frac{1}{1 + \beta}$ ($0 \leq \beta \leq \infty$) - The proportion of the distribution of energy from the newly created forms s ($s \in [0,1]$; $(1 - s) = \frac{\beta}{1 + \beta}$ ($0 \leq \beta \leq \infty$); g - the scale factor of production losses, usually fulfilled by $0 \leq g \leq 1$; $\varphi(\beta)$ - a preset amplifier of mold production by reading "correct information" (assembly instructions) (information as a catalytic function); $b \times X^2(t)$ - a quadratic term taking into account the limitedness of "semi-finished products" and the competition of finished "products" in the surrounding world.

The function $\varphi(\beta)$ has the form of a logistic curve (Fig. 4), which in the general case is not necessary if the requirements of positive bounded monotonicity are met. This function can have discontinuities of the first kind. The final form of the function $\varphi(\beta)$ with argument β is also determined by the degree of detail required in the calculation.

The segments on the abscissa axis $[\beta_1; \beta_2]$, $[\beta_2; \beta_L]$ и $[\beta_R; \beta_5]$ at $X_k(\beta) < 0$ are the degradation regions of the smart expansive system. Accordingly, the segments $[0; \beta_1]$, $[\beta_L; \beta^*]$ и $[\beta^*; \beta_R]$ at $X_k(\beta) > 0$ - the regions of its growth (development). And only from β_2 the expansion of the system begins (on the segment $[\beta_2; \beta^*]$ grows $X_k(\beta)$ and on the other segments it only decreases). It does not make sense to search for a solution above the limit value $\beta = \beta_5$ it does not make sense to search for a solution, although at the point β_R the system begins to actively degrade.

The type of the logistic curve is chosen in such a way that on the segment $[0; \beta_1]$ the efficiency of the productive subsystem is extremely low (this is the area of low-skilled labor and some

potentially breakthrough ideas in science). The segment $[\beta_L; \beta_R]$ corresponds to mass production with the use of available knowledge and skills. The optimum $X_k(\beta^*)$ is located inside $[\beta_L; \beta_R]$, while at the same time there is an underdeveloped and under-demanded $[\beta_L; \beta^*]$ science is insufficiently developed and demanded, and on $[\beta^*; \beta_R]$ - science is "too much" and the results of scientific research simply do not have time to be implemented and mastered in the production subsystem.

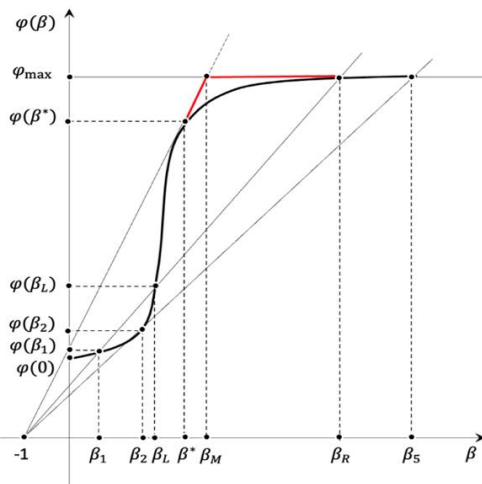


Fig. 4: Dependence of "development potential" on funds spent

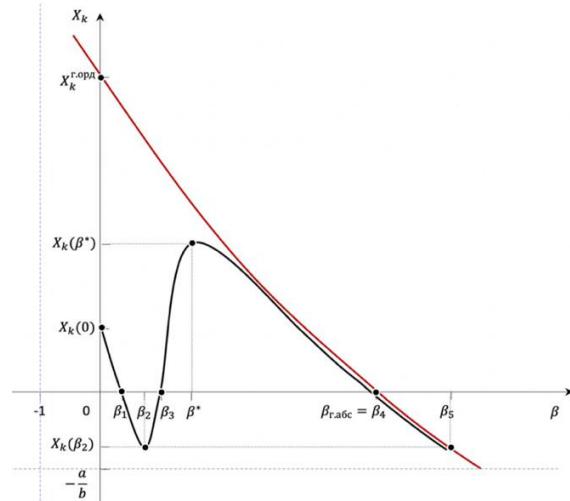


Fig. 5: Dependence graph $X_k(\beta)$

Point $\beta = 0$ in Fig. 4 corresponds to a situation where all resources are spent exclusively on the growth of the production subsystem. The potential of such a system is low because of constant losses, which can be avoided if there is the capacity to anticipate and deal with emerging risks.

Plot $(0, \beta_1)$ shows that if the resources allocated to study and counteract threats and risks are low, the return on such research and activities is less than the resources allocated to them. Gathering information, research on internal and external threats at a low level does not allow to obtain an adequate assessment to improve the quality of decision-making in most cases of one way or another.

At the site (β_1, β^*) the contribution to the development potential begins to give a positive return, but only at the point β_L the so-called level of "self-repayment" of costs for the development of the "potential" of the system will be reached $\varphi(\beta_L)$. Therefore, it is reasonable to consider this point as a point of "critical" position. Decrease of potential $\varphi(\beta)$ to the level of $\varphi(\beta_L)$ is a threat that "by virtue of circumstances" it will be economically viable to implement a "survival strategy" - a strategy of complete rejection of expenditures to solve problems of anticipating and preempting threats and risks and ensuring reproduction only by building up low-efficient capacities in the production subsystem. $\beta \rightarrow 0$.

The optimum is reached at some point β^* . This point has a very definite meaning. Thus, if resources for capacity development are allocated "too much". $(\beta > \beta^*)$ then the resources $(\beta - \beta^*)$ are incorrectly withdrawn from the current reproduction, and a situation occurs, when disproportionate efforts are spent on studying and counteracting numerous risks, which the developing system may never face. The optimum does not depend on the values of g, a, b . There may be cases where a is so large that even with an optimal solution the system does not develop but degrades. The condition of nondegeneracy of the solution is the presence of positive ordinates $y X_k$ (Fig. 4).

In the general case on the segment $[0, \beta_L]$ over-regulation and excessive formalization of the system control can only be harmful, and on the interval $[\beta^*, \infty)$ there is a situation in which the cost of searching for an existing solution is so high that it is preferable to get it from scratch. The

final graph $X_k(\beta)$ considering the graph compression $\varphi(\beta)$ by g and shifting by the value a down vertically, and then dividing by the value of b is shown in Fig. 5.

The second equation describes the dynamics of the laws of the system's functioning, by which the $X(t)$:

$$\frac{dY(t)}{dt} = f \times (Y_0 - Y(t)) + h \times \frac{\beta \times \varphi(\beta)}{1 + \beta} \times X(t), \quad (2)$$

where Y_0 - is some initial state. The regulator f describes the loss of knowledge, while the $\left(h \times \frac{\beta \times \varphi(\beta)}{1 + \beta}\right) \times X(t)$ corresponds to the complexity of laws for new unknown control functions ("emergence") that are not available in subsystems.

The final solution is as follows:

$$Y_K = Y_0 + \frac{ha^2}{4 \times gbf} \times C, \quad (3)$$

where the parameter $C = \left[\left(\frac{2}{A} \times \frac{\varphi(\beta)}{(1+\beta)} - 1\right)^2 - 1\right] \times \beta$ is searched as the maximum value from the above range. The maximum C is reached either at the edges of the segment or at one of the local minima. Thus, in Fig. 4, on the asymptote $\beta \in [\beta_M, \beta_R]$ is satisfied by $\varphi(\beta) = \varphi_{max}$.

There are, however, unique systems whose value depends solely on the capacity of the producer. When the potential is high, and its value is not underestimated in relation to the "fair," i.e. $g \gg 0$ - the second bracket is satisfied, even when $x_{max} = 1$ and there is no competition from other producers $b \cong 0$.

The presence of two optimal solutions β^* (in terms of production quantity) and β^{opt} (intelligently) defined through the constant C_{opt} , suggests that the optimal one would be $\beta^{opt} > \beta^*$ rejection of the shaft in favor of the maximum use of the expansion potential, that is - production with the "optimal" reserve of the "possible use" of the products produced (multifunctionality). Despite the schematic nature of the described model, it gives an idea that threats and risks can be considered as "anti-potentials" of development (i.e. they are retarders of the reproduction rate of the whole system). To model a real system, it is necessary to analyze the "raw" process data, and then synthesize them into a meaningful structure that explains the process under study.

The model of system growth considering the influence of random perturbations of system productivity on the rate of its reproduction considers that in the "quasi-linear section" of system expansion, not only the rate of expansion, but also the dispersion of the process is important. In this case "volatility" of the process itself plays a greater role than profitability of the "production subsystem". Despite the increase "on average" of the amount of product from each element of the system, nevertheless, each of the elements separately is characterized by a limited time of effective functioning. At the same time, the index of "population on mortality" under natural restrictions on the mathematical expectation is mainly influenced by the value of dispersion. That is why, for example, in economics, where processes with mathematical expectation values of the order of several percent are studied, it is the dispersion values that appear in the definitions of "risks."

Here it is extremely important to note that to estimate the values of mathematical expectation and dispersion, their quantitative calculation for the initial moment of time based on group estimates is made. Further, it is hypothesized that these estimates obtained for the group can be used to predict the motion trajectories of each element of the group individually. This is a very strong assumption, since it asserts, first, that the obtained estimates will remain constants for the whole prediction time, and second, it asserts that each element at any time behaves like some element at zero time. Such assumptions are valid only for ergodic processes.

But not all processes described by the model under consideration are ergodic. In systems consisting of elements of more than one type, the need to consider such "risks" increases significantly. And these "risks" themselves are much higher.

The described models can be complemented by the model of the influence of capital fluctuations on the growth of the system, which is connected not with the properties of the system

itself, but with the level of fluctuations in the parameters (influencing factors) of the external environment (fluctuations in the level of corruption, changes in tax legislation, etc.). The most probable values of the number of elements in such a model are always less than its average value. Some value is introduced as a threshold of criticality of the state. If the current value is lower than the critical value, the probability of bankruptcy increases sharply. It is important to note that as time increases, the critical values also increase. Moreover, if the amplitude of fluctuations of the distribution variance estimate is large and the mathematical expectation and the initial value are small enough, the probability of system degradation tends to unity.

Thus, on average, external fluctuations accelerate the growth of the system, but the price for such accelerated growth is an increased probability of its degeneration (decrease of mathematical expectation of its degeneration time). And since the expansion process is multifactorial, and the "prehistory" of behavior of such system (as it takes place, for example, in mass service systems), as a rule, there is no analysis based on statistics of past observation periods, but synthesis of risk of functioning of "smart expansion system" is necessary. For SES, it is more correct to speak of risk synthesis rather than analysis. Although the concept of "synthesis" is almost never used in relation to risk as opposed to "analysis", risk analysis is specific to systems where risk events are frequent enough to allow the well-developed apparatus of probability theory and mathematical statistics to be applied. This approach works in insurance, for example, in reliability theory, when we are dealing with flows of insured events, accidents or failures. But when it comes to safety in an era whose main characteristic is constant variability and variability, it can only be done through risk synthesis, by developing increasingly sophisticated automated advising systems - professional cues (PAFs) - or by replacing professionals with highly intelligent robotic systems. Risk becomes "synthetic" from "analytical" in this case.

As the analysis of integral assessments of the state of complex objects and systems used in systems research shows, generalized criteria (indices) of risks are widely used: additive (weighted arithmetic average) and multiplicative (weighted geometric average) forms:

- arithmetic (smoothing out the "outliers" of individual risk indicators) $R_{ar} = \sum_{i=1}^M (\alpha_i \times r_i)$;
- geometric (reinforcing the negative "emissions" of NPR) $R_{ge} = \prod_{i=1}^M r_i^{\alpha_i}$;
- geometric anti-risk $1 - R_{\emptyset} = U_{\emptyset} = \prod_{i=1}^M (u_i)^{\alpha_i} = \prod_{i=1}^M (1 - r_i)^{\alpha_i}$.

Weighting coefficients α_i of partial evaluations r_i satisfy the condition:

$$\sum_{i=1}^M \alpha_i = 1; \alpha_i > 0 (i = 1, \dots, M). \quad (4)$$

Actual numbers r_i (partial risks) take values from the interval $[0, 1]$.

For UES, the most acceptable form of risk representation is geometric anti-risk, which satisfies the basic a priori requirements underlying the risk approach to constructing a nonlinear integral estimate R_{\emptyset} , namely:

1. *smoothness* - continuous dependence of the integral R and its derivatives from partial estimates: $R(r_1, \dots, r_M)$;
2. *boundedness* - the boundaries of the interval of variation of the partial r_i and integral R estimates:

$$0 < R(r_1, \dots, r_M) < 1; \text{ при } 0 < r_1, r_2, \dots, r_M < 1. \quad (5)$$

3. *equivalence* - the same importance of private assessments r_i и r_j ;
4. *hierarchical unilevel* - only partial assessments are aggregated r_i which belong to the same level of the hierarchical structure;
5. *neutrality* - the integral assessment coincides with the private assessment, when the other takes the minimum value:

$$R(r_1, 0) = r_1; R(0, r_2) = r_2; R(0, 0) = 0; R(1, 1) = 1. \quad (6)$$

6. *uniformity* $R(r_1 = r, \dots, r_M = r) = r$.

Geometric anti-risk derives from the notion of "difficulty of reaching the goal" proposed by Isaak Russman (see above) and is a "top estimate" for the weighted average arithmetic and weighted average geometric risk. The geometric anti-risk satisfies, moreover, the so-called "fragility of good" theorem in the catastrophe theory, according to which "...for a system belonging to a particular part of the stability boundary, at small changes in parameters it is more likely to fall into the region of instability than into the region of stability. This is a manifestation of the general principle that all good (e.g., stability) is more fragile than bad" [57]. Risk analysis uses a similar principle of the limiting risk factor. Any system can be considered "good" if it satisfies a certain set of requirements but must be considered "bad" if at least one of them is not met. At the same time, all "good", such as the environmental safety of territories, is more fragile - it is easy to lose it, and difficult to restore.

A continuous function $R(r_1, \dots, r_i, \dots, r_n)$, satisfying the above conditions, has the following general form:

$$R(r_1, \dots, r_i, \dots, r_n) = 1 - \left\{ \prod_{i=1}^n (1 - r_i) \right\} \times g(r_1, \dots, r_i, \dots, r_n), \quad (7)$$

If in the special case $g(r_1, \dots, r_i, \dots, r_n) \equiv 1$, then, respectively:

$$R(r_1, \dots, r_i, \dots, r_n) = 1 - \left\{ \prod_{i=1}^n (1 - r_i) \right\}, \quad (8)$$

which gives an underestimation of the integral risk from the calculation that the flow of abnormal situations for the objects of the system is a mixture of ordinary events taken from homogeneous, but differing values of r_i ($i = 1, \dots, n$) samples.

Since risks for real systems are usually dependent, we get

$$g(r_1, \dots, r_i, \dots, r_n) = 1 - \sum_{i=1}^{n-1} \sum_{j=i+1}^n C_{ij} \times [r_i]^{\alpha_{ij}} \times [r_j]^{\beta_{ij}}, \quad (9)$$

$$\sum_{i=1}^{n-1} \sum_{j=i+1}^n C_{ij} \leq 1, C_{ij} \geq 0, \alpha_{ij} > 0, \beta_{ij} > 0, \quad (10)$$

where C_{ij} - coefficients of risk coherence of the i -th and j -th abnormal situation for the system objects; α_{ij} и β_{ij} - positive coefficients of elasticity of substitution of the corresponding risks, which allow taking into account the facts of "substitution" of risks, mainly due to the fact that simultaneously the measures to reduce all risks cannot be carried out due to the limited time and resources of the DM.

The current values of partial risks r_i ($i = 1, \dots, n$) included in (7) are values that change over time at different rates (for example, depending on the seasonal factor, the priorities of technological problems in some systems of the fuel and energy complex change significantly). Private risks r_i are built, as a rule, through the convolutions of the corresponding resource indicators - influencing factors, which have a natural or cost expression. These influence factors are measured in some own synthetic scales (e.g., the Saaty multiplicative scale of pairwise comparisons [46]), the mutual influence of which should also be studied, since they are generally non-linear and piecewise continuous. To obtain estimates of the influence factors, it is necessary to construct weighted scales. To solve this problem the so-called "vector compression method" was developed [58, 59, 60, 61].

IX. Risk as a measure of disorderliness

It is obvious that when talking about risk, we cannot avoid talking about many accompanying circumstances during the development of a situation from less risky to riskier, up to the occurrence of the risky event itself. All these circumstances, as defined by the International Organization for Standardization (ISO), are combined in the concept of uncertainties affecting the achievement of the goal of any activity.

First, we are talking about the point in time when a risky event will happen, the place where it will happen, the time during which this event will last, the intensity of the impact of risk factors, the possibility (probability) of such an event in principle and the expected consequences after its realization. Since we are talking about activities, the results of which are affected by uncertainty, to assess a rare event, we must somehow estimate all the above circumstances and only after that, and only with a certain margin of error, speak about the coming risk event. If the circumstances of the activity periodically repeat, it is possible to determine the probability of the event by statistical methods based on the analysis of the frequency of this repeat, and the consequences (damage) can be estimated based on the mathematical expectation of losses from experience.

Both in the case of a statistically certain event and in the case of a rare event, it is important not only to know all the circumstances of the risk event, but also the order in which they occur and follow. Knowledge of this order can help assess the proximity of a risk event even without having actual information about the circumstances themselves. Here the apparatus of group theory and methods of group permutations come to the rescue. As an estimation of an order of circumstances (factors) of a risk event, as a rule, is made with attraction of expert opinions, the problem of collective choice inevitably arises - a problem of reduction of several individual expert opinions on an order of preference of compared objects (alternatives) in a uniform "group" preference. The complexity of collective choice consists in the necessity of processing the ratings of compared alternatives, set by different experts in private own scales.

Below is the author's original algorithm [61] for processing expert preferences in the collective choice problem, based on the notion of the total "error" of experts and measuring their contribution to the collective measure of their consistency.

In practice, the efficiency of decision-making requires the development and application of specialized algorithmic and methodological support. If a group of experts participates in the decision support process, the so-called collective (group) choice problem arises. The existing algorithms for solving collective choice problems [62, 63, 64] can be roughly divided into three classes. A representative of the first class is the Schulze method [65] (based on the proof of the Arrow theorem) with the selection of Pareto-optimal solutions (Schwartz exception) from the first ranking to the last, with the selection recalculating the criteria for the next step. The disadvantage of the method is a rather complicated algorithm of constant recalculation, which significantly complicates the practical use of the method.

A typical representative of the second class is the skating system [66], which has proven itself in the ballroom dance competitions. It is simple in computational calculations and is based on the so-called understandable majority principle. Unfortunately, in many ways, it is this simplicity that can lead to unstable decisions, and, therefore, the inability to distribute the final places among contestants in one round, or to recognize a draw between competitors [67, 68].

The third class consists of regression models, the type of nonlinear factor analysis and other methods of information compression [69, 70], in which the desired solution is constructed in the form of the problem of minimizing the accumulated errors. The difference between the methods of the third class is that they are not focused on the choice of the leader in the ratings, but are determined by the optimum, which is influenced by the entire volume of data.

The mentioned methods of solving the problems of collective choice in general are inherent to the problem of coordinating the experts' evaluations when comparing the evaluated objects.

In 1951 C. Arrow formulated [71] the theorem "On the impossibility of collective choice within the framework of the ordinality method", mathematically generalizing the Condorcet paradox [72]. The theorem asserts that within the framework of this approach there is no method for combining individual preferences for three or more alternatives that would satisfy some quite fair conditions (the axioms of choice) and would always give a logically consistent result.

When the uncertainty of the objects themselves is superimposed on the ambiguous opinions of the experts, some hierarchy is assumed in solving the choice problem. This is the case, for example, in the method of hierarchy analysis [46], when each of M of the experts has his/her own opinion, different from the others, concerning the weights of the objects in question N objects

through the coefficients of the preference matrix ($S_{ij}^m = \frac{w_j^m}{w_i^m}$ ($i = 1, \dots, N; j = 1, \dots, N; i \neq j; m = 1, \dots, M$)). Usually, the weights are averaged and work with a generalized matrix S_{ij} which leads, as a rule, to a violation of the basic axioms of "right" choice (universality, completeness, monotone, lack of dictator, independence), proposed by W. Pareto [73, 74], R. Koch [75], C. Plott [76] and others. The rejection of one or another averaging procedure complicates the task of selection and leads, for example, to the need to solve the problem of "merging multidimensional scales" [59]. Experts need to reach consensus [55], at least with the accuracy of determining private ratings in the full order of objects, and then seek agreement in the weighting coefficients between neighboring nearest objects, setting a single scale, to obtain consistent solutions.

In the general case [61] we consider N comparison objects $O_1, \dots, O_k, \dots, O_N$ whose indices are the first N members of the natural series $E_{PIO} = \langle 1, \dots, k, \dots, N \rangle$ - correspond to the order in which the objects are presented for examination. In the examination of objects, the following people take part M experts $E_1, \dots, E_m, \dots, E_M$. Each of the experts E_m has his own idea of the order of objects $g_m = \langle g_{m,1}, \dots, g_{m,n}, \dots, g_{m,N} \rangle$ which indexes increase with decreasing of some quality of objects from the expert's point of view. The value $g_{m,1}$ corresponds to the index of object O_{k_1} , taking part in examination with maximal quality according to expert's opinion $\exists_{m,}$ a $g_{m,N}$ - the worst-quality object with the index O_{k_N} :

$$G = (g_{m,n})_{\substack{m=\overline{1,M} \\ n=\overline{1,N}}} = \begin{pmatrix} g_{1,1} & \dots & g_{1,N} \\ \dots & \ddots & \dots \\ g_{M,1} & \dots & g_{M,N} \end{pmatrix}.$$

Thereby g_m - it is a permutation of object ratings (PORs), the argument of which is the order of $E_{POR} = \langle 1, \dots, n, \dots, N \rangle$.

Places $p_m = \langle p_{m,1}, \dots, p_{m,k}, \dots, p_{m,N} \rangle$ by values inverse to ABM g_m ($p_m = g_m^{-1}$) are permutations of object indices (PIO) with argument E_{PIO} :

$$P = (p_{m,n})_{\substack{m=\overline{1,M} \\ n=\overline{1,N}}} = \begin{pmatrix} p_{1,1} = g_{1,1}^{-1} & \dots & p_{1,N} = g_{1,N}^{-1} \\ \dots & \ddots & \dots \\ p_{M,1} = g_{M,1}^{-1} & \dots & p_{M,N} = g_{M,N}^{-1} \end{pmatrix}.$$

It is necessary to find an optimum of the consistency measure and to restore the full collective order in preferences on the basis of private expert ratings, i.e., to compress all private POR rankings g_m ($m = 1, \dots, M$) in the form of a POR $g_m^* = \langle g_1^*, \dots, g_N^* \rangle$ which would reduce the total inconsistency of expert evaluations $g_{m,n} \rightarrow g_m^*$ (based on the equality of all expert participants), measured in the inversions of the transitions from $g_{m,n} \kappa g_m^*$, that is

$$K^* = \min K(g) = \min_{g_m} \left(\sum_{m=1}^M K_m(\langle g_1, \dots, g_N \rangle) \right),$$

where $K_m(\langle g_1, \dots, g_N \rangle)$ - is the sum of inversions in the evaluations of m of the -one expert, K^* - is the marginal measure of inconsistency of the experts' opinions.

Finding an optimum in permutations of object ratings is equivalent to finding a permutation of the object index p^* : $p^* = \langle p_1^*, \dots, p_N^* \rangle$, since $K(g_m^*) = K(p_m^*)$ where $p^* = (g^*)^{-1}$ (the lengths of the inverse paths ($E \rightarrow g$) are the same as the forward paths ($p = g^{-1} \rightarrow E$) at any g). This problem belongs to the class of integer programming problems (on the structure graph $V(G, G \times G)$ of the POR graph arranged by levels of errors). Methods for solving such problems are sufficiently well developed [77,78], but none of them guarantees the uniqueness of the global minimum. A complete enumeration of all ABMs can provide some guarantee. Such a variant is possible for $N \leq 10$. For each g is considered $K(P_m, g)$ is the sum of $K(g)$, and the current state of the set of global minima is "memorized". The subset $g \in G$ for which $K(g) = K^*$, we call the set of global minima - G^K . Since M is odd, it, like the set of local minima, consists of isolated solutions (permutations) obeying the following rules.

Rule 1. If $P_m g_l(E) < P_m g_{l+1}(E)$, then the sum of inversions $K(g_m)$ is increased by 1, and if $P_m g_l(E) > P_m g_{l+1}(E)$, the sum of inversions decreases by 1.

Rule 2. The decrease and increase of the sum depend on the number of rows in which the second condition M^2 (Rule 1) dominates the first condition M^1 . The ratio is

$M^1 + M^2 = M$. Then the sum $K(g)$ from the influence of s_i will decrease by exactly $M^2 - M^1$ units (при $M^2 > M/2$) or increase by $M^1 - M^2$ units (при $M^2 < M/2$).

Rule 3. "Cutoff condition. The POR g belongs to the set of local minima G^P if for all $j = 1, \dots, N - 1$ the sum of errors only increases with rotation of neighboring columns by the symbol s_j . That is $g \in G^P$ has neighboring vertices of the graph V , exceeding by sum the found local optimum g by at least one.

The search G^P makes sense at large N , but at small N it is also effective, because the decrease (increase) of some selected pair does not depend on the place where the pair stands, but only on the contents of the obtained inversions. Depending on the number of compared objects (N) 2 variants of further actions are possible: either direct calculation, or consecutive iterations.

The questions concerning the comparison of the proposed method with other methods of information compression (for example, with the factor analysis, with the averaging method or with the Schulze method) are left out of the present discussion. The further development of this method implies its application in ranking determinations that allow equality of estimates of compared objects when determining weight coefficients of compared objects (like pairwise comparisons in the method of hierarchy analysis and solving problems of heterogeneous scales fusion).

X. Conclusions

Risk is always a consequence of our ignorance, which generates uncertainties of various kinds in the decision-making process. Previously, uncertainty was assumed to be due only to the subject's lack of knowledge, while nature itself is dominated by a universal causal relationship of phenomena and events. However, many causal relationships remain unresolved due to the incompleteness of our knowledge. Science seeks to compensate for this deficiency through probabilistic laws, predicting the results of future events with the help of past events. If man had perfect knowledge of all causes and effects of natural phenomena, then everything would be precisely defined for him. So thought Laplace. But in human relations, as John von Neumann rightly believed, uncertainty arises from the ignorance of some people of the intentions, behavior, and actions of others. So, while the natural sciences have made remarkable progress in uncovering uncertainty in nature through laws based on the repeatability of the phenomena under study, the social and economic sciences have been much less successful. This is largely since the analysis of social processes must consider, along with objective conditions, such subjective factors as goals, interests and motives of people's activities, which are difficult to describe by probabilistic laws. The logic of circumstances is often stronger than the logic of intentions.

Based on previous research, science has developed a rational model of decision-making under uncertainty that describes the rational behavior of an individual or group, which often results in the successful achievement of a goal. In everyday life, we also make different decisions all the time, often without thinking about why some of them are successful and others are not. Experience shows that in the case of successful decisions, the goal is usually set and justified correctly, the possibility of achieving it is assessed intuitively correctly, and all reasoning is based on the logic of common sense. There is no doubt that intuition and life experience are quite sufficient for solving the simplest practical tasks of everyday and even managerial activity, which do not require precise calculations. However, personal experience, intuition, and common sense are insufficient for solving complex management problems in economics, social life, as well as in contemporary politics and other types of public activity. Careful analysis of the problem, precise calculations, and construction of mathematical models, including risk models, are necessary.

The most important requirement, which any rational decision must also satisfy, is that all alternatives for choosing a decision must be ordered by an appropriate preference relation, which has the properties of certainty, comparability, and transitivity. Although the methods of modern science make it possible to make increasingly accurate predictions and thus to overcome risks,

uncertainty remains an inevitable companion of human activity. Under these conditions, the problem of risk assessment and forecasting acquires relevance. Therefore, its solution should involve not only traditional probabilistic-statistical methods, but also new research methods that have emerged in the framework of synergetic, nonlinear dynamics and the theory of nonequilibrium systems, as well as expert methods.

It is important to consider that the risk depends on the target function of the object.

It can be forced (a farmer living next to a nuclear power plant, riding a bus as a passenger), it can be professional (working at a nuclear power plant, being a bus driver), it can be off system (nuclear power plants for the country, buses as part of transport). The farmer needs to be compensated for possible damage from the accident - for example, in the form of cheap electricity. A professional need to compensate for damage to health, but here the risk is voluntary - he can work in another safer place. With transport it is more complicated - under capitalism in firms a quality specialist is appointed whose main task is to ensure that within the allocated amounts (profit and profitability), for example, the bus is safe, but only within the "warranty" period. That is, it is important to him that everything "falls apart", but after this period. And then the responsibility lies with the professional.

It is the "risk synthesis" within the framework of the concepts presented above that is designed to solve such problems effectively.

References

- [1] Dimitrov, B. The Axioms in My Understanding from Many Years of Experience. *Axioms* 2021, 10, 176. <https://doi.org/10.3390/axioms10030176>
- [2] Gnedenko B.V., Hinchin A.Y. Elementary Introduction to Probability Theory. Main Editorial Office of Physical and Mathematical Literature of "Nauka" Publisher, 1970. – 168 p.
- [3] Cramer H. Collective Risk Theory. - Stockholm: Skandia Jubilee Volume, 1955.
- [4] Bowers N.L., Gerber H.U., Hickman J.C., Jones D.A., Nesbitt C.J. Actuarial Mathematics. - Itasca, Illinois: The Society of Actuaries, 1986. Russian translation available: Bowers N., Gerber X., Jones D. Nesbitt S., Hickman J. Actuarial mathematics. - Moscow: Janus-K, 2001. – 644 p.
- [5] Panjer H. H., Willmot G. E. Insurance Risk Models. - Schaumburg, IL: The Society of Actuaries, 1992.
- [6] Rotar V. I., Beninet V. E. Introduction to the Mathematical Theory of Insurance // Review of Applied and Industrial Mathematics. Series: Financial and Insurance Mathematics. - 1994. - Ò.I. vol.5 pp.698-779.
- [7] Rykov V. V., Itkin V. Reliability of technical systems and technogenic risk: textbook. - MOSCOW: INFRA-M, 2017. - 192 p. - (Higher education).
- [8] Zhukovskiy V.I., Zhukovskaya L.V. Risk in multicriteria and conflict systems under uncertainty / ed. Ed. 2nd ed. Moscow: Publishing House LKI, 2010. - 272 p.
- [9] Germeyer Y.B. Games with non-opposite interests. Moscow: Nauka, 1976. 327 p.
- [10] Hemming R.W. Numerical methods. Moscow: Nauka, 1972. - 472 p.
- [11] Moore R.E. Interval Analysis. N.Y.: Prentice-Hall, 1966.
- [12] Shokin Y.I. Interval Analysis. Novosibirsk: Siberian Branch of Russian Academy of Sci., 1981 – 112 p.
- [13] Wald A. Statistical Decision Functions. N.Y.: Wiley, 1950.
- [14] Savage L.Y. The theory of statistical decision // J.American Statistic Association. 1951. № 46. pp.55-67.
- [15] Hurwicz L. Optimality criteria for decision making under ignorance, in Cowles Commission Discussion Paper, Statistics. 1951. № 370.
- [16] Frank H. Knight. The Meaning of Risk and Uncertainty. In: F.Knight. Risk, Uncertainty, and Profit. Boston: Houghton Mifflin Co. Translation by S. A. Afontsev.
- [17] Kryanev A. V., Lukin G. Mathematical Methods of Processing of Uncertain Data. -

MOSCOW: FIZMATLIT, 2003. - 216 p. - ISBN 5-9221-0412-8.

- [18] De Groot. M. Optimal statistical solutions. - Moscow: Mir, 1974. - 492 p.
- [19] Sachs S. Theory of Statistical Inference. - M.: The World, 1975. - 776 p.
- [20] Russman I. B., Bermant M. A. On the Problem of Quality Estimation. Journal of Economics and Mathematical Methods, No. 4, 1978, pp. 691-699.
- [21] Russman I. B., Gaidai A. A. Continuous control of goal attainment process. "Management of large systems". Collected works of the Institute of management problems of RAS, Issue 7, Moscow, 2004, pp. 106-113.
- [22] Memorial site of I.Russman. https://www.adeptis.ru/russman/scientific_heritage.html
- [23] Bochkov, A.V. Hazard and Risk Assessment and Mitigation for Objects of Critical Infrastructure, pp. 57-135. In: Ram M., Davim J. (eds) Diagnostic Techniques in Industrial Engineering. Management and Industrial Engineering. Springer, Cham, DOI https://doi.org/10.1007/978-3-319-65497-3_3, Publisher Name: Springer, Cham. - 2017. ISBN 978-3-319-65496-6. - 247 p.
- [24] Bochkov Alexander Vladimirovich. Methodology of ensuring safe functioning and sustainability of the Unified system of gas supply in emergency situations: dissertation ... Doctor of Technical Sciences: 05.26.02 / Bochkov Alexander Vladimirovich; [Place of protection: LLC "Research Institute of natural gases and gas technologies - Gazprom VNIIGAZ"], 2019. - 385 p.
- [25] Zhigirev, N.; Bochkov, A.; Kuzmina, N.; Ridley, A. Introducing a Novel Method for Smart Expansive Systems' Operation Risk Synthesis. Mathematics 2022, 10, 427. <https://doi.org/10.3390/math10030427>
- [26] Petukhov G.B. Fundamentals of the theory of efficiency of purposeful processes. Part 1. Methodology, Methods, and Models. Moscow: Publishing house of the Ministry of Defense of the USSR, 1989. - 647 p.
- [27] Kantorovich L. V. Mathematical and Economic Works. Selected works. Moscow, Nauka, 2011. - 760 p.
- [28] Wasserman F. Neurocomputer Technique: Theory and Practice / Translated from English - Moscow: Mir, 1992. - 240 p.
- [29] Kohonen T. Self-Organizing Maps. Springer-Verlag, 1995.
- [30] Specht D. Probabilistic Neural Networks. Neural Networks, 1990, №1.
- [31] Vyugin V. Mathematical foundations of the theory of machine learning and prediction. - ICMNO, 2013. - 390 p.
- [32] Gladkov L. A., Kureichik V. V., Kureichik V. M. Genetic algorithms: Tutorial. - 2nd ed. - Moscow: Fizmatlit, 2006. - 320 p.
- [33] Taha Khemdi A. Operations research. Williams, 2016. - 912 p.
- [34] Germeyer Y. B. Introduction to the theory of operations research. Moscow - Nauka, 1971. - 383 p.
- [35] Saridis J. Self-organizing stochastic control systems. Moscow: Nauka, 1980. - 397 p.
- [36] Kalmykov S.A., Shokin Y.I., Yuldashev Z.H. Methods of interval analysis. Novosibirsk: Nauka, 1986.
- [37] Zadeh L. A. Fuzzy sets and their application in pattern recognition and cluster analysis // Classification and Cluster / Edited by J. Van Raisen. - M. Mir, 1980. - pp. 208-247.
- [38] Fuzzy sets and possibility theory. Recent advances. Ed. by R.R. Yager. - Moscow: Radio and Communications, 1986. - 408 p.
- [39] Larichev O. I. Theory and Methods of Decision-Making, and Chronicle of Events in Magic Countries. - 3rd ed. - M.: Logos, 2006. - 392 p.
- [40] Fodor J., Roubens M.: Fuzzy preference modelling and multicriteria decision support. (Kluwer Academic Publishers, Dordrecht, 1994).
- [41] Larichev O. I., Petrovsky A. B. Decision support systems. The current state and prospects for their development. //Progress of science and technology. Ser. of Technical Cybernetics. - Vol.21. Moscow: VINITI, 1987, pp. 131-164, http://www.raai.org/library/papers/Larichev/Larichev_Petrovsky_1987.pdf

- [42] Saati T. Decision Making. Method of hierarchy analysis // Translated from English by R.G. Vachnadze. Moscow: Radio and communications, 1993. - 278 p.
- [43] Nogin V. D. The simplified version of the method of hierarchy analysis based on nonlinear convolution of criteria // Zhurnal Vychisl. Vol. 44. No.7. pp. 1261-1270.
- [44] Podinovskiy V. V., Podinovskaya O. V. V. On the incorrectness of the method of hierarchy analysis // Problems of Control, 2011, № 1. - pp. 8-13.
- [45] Gusev S. S. Analysis of methods and approaches for solving the problems of multicriteria choice in conditions of uncertainty // Interactive Science. 2018. №1 (23). - pp. 69-75.
- [46] Saati T.L. Decision Making under Dependencies and Feedbacks: Analytical Networks / T.L. Saati. - M.: Librocom Book House, 2009. - 360 p.
- [47] Seredkin K.A. On the limits of applicability of the method of analytical networks in the problems of decision making in natural sciences / K.A. Seredkin // Artificial Intelligence and Decision Making. - 2018. - №2. - pp. 95-102.
- [48] Bochkov A. V., Zhigirev N. N., Ridley A. N. Method for Recovery of Priority Vector of Alternatives in Conditions of Uncertainty or Incompleteness of Expert Evaluations. Reliability. 2017. T. 17. № 3 (62). pp. 41-48.
- [49] Ridley A. N. Methodology of risk synthesis in systems management. In the book: Gagarin readings - 2019 Collection of abstracts of XLV International Youth Scientific Conference. Moscow Aviation Institute (National Research University), 2019.
- [50] Glushkov V.M., Ivanov V.V., Yanenko V.M. Modeling of developing systems. M.: Nauka, 1983. - 350p.
- [51] Glushkov V.M. Introduction to the Theory of Self-Enhancing Systems. Ed. 2, stereotypical. - MOSCOW. LENAND, 2022. - 112 p. (From the heritage of academician V.M. Glushkov; Science of the Artificial. No. 42). 52.
- [52] Automated control system for the scientific-production association (ACS "Ekstremum"): Technical Project / manuscript B.N. Onykiy, manuscript Yu.A. Erivanskiy, responsible executor. L.L. Semyonov, responsible executor. D. V. Mikhailov; the 17th Main Directorate. - M. Book 4: The Subsystem of Technical and Economic Production Planning. - 1974. - 113 p.
- [53] Automated control system of scientific-production association (ACS "Extremum"): Technical Project / hand in hand: B.N. Onykiy, Yu.A. Erivanskiy, responsible executor. A. Erivanskiy Yu. executor; 17 Main Department. - M. Kn. 2: Research and Development Control Subsystem. - 1974. - 124 p.
- [54] Zhigirev N.N. Human-machine procedures for resource allocation in developing systems [Text]: (05.13.06-automated control systems): Dissertation of Candidate of Technical Sciences / N.N. Zhigirev; Sci. Dissertation of doctoral candidate of engineering sciences / supervised by B.N. Onykiy - MIFI, 1987. - 134 p.
- [55] Zhigirev, N.; Bochkov, A.; Kuzmina, N.; Ridley, A. Introducing a Novel Method for Smart Expansive Systems' Operation Risk Synthesis. Mathematics 2022, 10, 427. <https://doi.org/10.3390/math10030427>
- [56] Prigogine I., Lefever R. Symmetry Breaking Instabilities in Dissipative Systems II, Journal of Chemical Physics, 48, 1968. pp. 1695-1700.
- [57] Arnold V. I. Theory of Catastrophes, Moscow: Nauka, 1990. -128 p. ISBN 5-02-014271-9
- [58] Bochkov, A. V., Zhigirev N. N., Ridley A. N. Method for restoring the vector of priorities of alternatives in conditions of uncertainty or incompleteness of expert evaluations. Reliability. 2017. T. 17. № 3 (62). pp.41-48.
- [59] Bochkov, A.V., Lesnykh, V.V., Zhigirev, N.N., Lavrukhin, Yu.N. Some methodical aspects of critical infrastructure protection // Safety Science, Volume 79, November 2015, pp. 229-242. <https://doi.org/10.1016/j.ssci.2015.06.008>
- [60] Bochkov, A.; Niias, J.; Ridley, A.; Kuzmina, N.; Zhigirev, N. Vector compression method to convert the incomplete matrix of pairwise comparisons in the analytic hierarchy process. In Proceedings of the International Symposium on the Analytic Hierarchy Process, Web Conference, December 3-6, 2020; <https://doi.org/10.13033/isahp.y2020.070>.

- [61] Bochkov A., Zhigirev N., Kuzminova A. "Inversion Method of Consistency Measurement Estimation Expert Opinions" // *Reliability: Theory & Applications*, vol. 17, no. 3 (69), 2022, pp. 242-252. doi:10.24412/1932-2321-2022-369-242-252
- [62] Kemeney J., Snell J. *Cybernetic modeling. Some applications*. Moscow: Soviet Radio, 1972. - 192 p.
- [63] Larichev O.I. *Theory and Methods of Decision-Making and Chronicle of Events in the Enchanted Lands*. 2nd edition revised and enlarged. Moscow: Logos, 2002. - 382 p. - ISBN 5-94010-180-1.
- [64] Kaplinsky A.I., Russman I.B., Umyvakin V.M. *Modeling and algorithmization of weakly formalized problems of the best system choice*. Voronezh: Publishing house of the All-Russian State University of Civil Engineering, 1991. - 168 p.
- [65] Markus Schulze, *The Schulze Method of Voting*. Computer Science and Game Theory. Cornell University, 2018. URL: <https://doi.org/10.48550/arXiv.1804.02973>.
- [66] Ralf Pickelmann, 1999. *Das Skating system*. URL: <http://www.tbw.de/rpcs/skating>.
- [67] Ferran Rovira, 1997. *Porqu e ganamos, porqu e perdemos?* TopDance, 15, 16. URL: <http://inicia.es/de/ballrun/skating.htm>.
- [68] Xavier Mora, *The Skating System*. 2nd edition. July 2001. URL: <https://mat.uab.cat/~xmora/escrutini/skating2en.pdf>.
- [69] Lisitsin D.V. *Methods of constructing regression models*. Novosibirsk: NSTU, 2011. - 77 p.
- [70] Kim O. J., Mueller C.W., Klecka W.R., et al. *Factor, discriminant and cluster analysis*. Ed. by I. S. Enyukov. - Moscow: Finances and Statistics, 1989. - 215 p.
- [71] Kenneth J. Arrow, 1951, 2nd ed. *Social Choice and Individual Values*, Yale University Press. ISBN 0-300-01364-7.
- [72] Condorcet J. *Esquisse d'un tableau historique des progres de l'esprit humain*. - Librocom, 2011. - 280 p. - (From the Heritage of World Philosophical Thought. Social Philosophy). ISBN 978-5-397-01568-4.
- [73] Nogin V. 73. D. *Multitude and the Pareto Principle* - SPb: Publishing and Printing Association of Higher Education Institutions, 2022, 2nd edition, revised and supplemented - 111 p.
- [74] Pareto V. *Textbook of political economy*. RIOR, 2018. - 592 p.
- [75] Koch R. *The 80/20 principle*. Exmo, 2012. - 443 p.
- [76] Ross M. Miller, Charles R. Plott, and Vernon L. Smith. *Intertemporal Competitive Equilibrium: An Empirical Study of Speculation*. *Economics. Quarterly Journal of Economics*. Volume 91. Issue 4, November 1977. pp. 599-624. URL: <https://doi.org/10.2307/1885884>
- [77] Coffman A., Henri-Laborder A. *Methods and models of operations research. Integer programming*. Textbook. - Moscow: Mir, 1977. - 432 p.
- [78] Schraever A. *Theory of linear and integer programming*. Monograph in two volumes. Translated from English: Mir, 1991. (360 p.) - 344 p.

RELIABILITY BASED DESIGN OF CIVIL AND INDUSTRIAL ENGINEERING STRUCTURES USING THE LIFE QUALITY INDEX CRITERION

Anna Bushinskaya^{1,2}, Sviatoslav Timashev^{1,2}

¹Science and Engineering Center "Reliability and Safety of Large Systems and Machines",
Ural Branch, RAS, Russia

²Ural Federal University, Russia

bushinskaya@gmail.com

timashevs@gmail.com

Abstract

The paper considers and analyses the current world practice of assigning acceptable values for the probability of failure of civil and industrial engineering structures based on monetary optimization using the life quality index. The analysis is illustrated by calculating the approximate target values of the threshold probability of failure for multi-storey residential buildings in the Sverdlovsk region of the Russian Federation using the LQI criterion and the social willingness to pay concept assessment of the effectiveness of the costs of safety measures.

Keywords: reliability, probability of failure, civil and industrial engineering structures, life quality index, social willingness to pay, monetary optimization

I. Introduction

The failure of a structure entails a risk to life, so the economically viable level of safety of the structure to which it is designed and operated must also include a social assessment (**by** evaluating the cost **effectiveness** of safety measures). This circumstance is not regulated **yet** in any way by the regulatory and technical documentation of the Russian Federation. The reliability assessment of civil and industrial engineering structures within the framework of the world standards in force (based on the limit states design method) is carried out by comparing some conditional reliability measures (failure probability P_f and associated reliability index β_f) with their allowable (target) values:

$$P_f \leq P_t, \beta_f \geq \beta_t, \quad (1)$$

where P_t, β_t are the target values of the probability of failure (POF) and the reliability index (RI), respectively.

To estimate the POF P_f , a simple limit state function (LFS) is used:

$$g = R - S, \quad (2)$$

where S is the external load (effect of impacts) and R is the bearing capacity (resistance) of the structure, considered as random variables (RV).

As a measure of reliability, RI β is used, which is associated with the probability of failure P_f by the Laplace function, that is, under the assumption that the *load and resistance obey a normal or lognormal distribution laws*.

When the load and resistance are independent and normally distributed, the structure POF can be estimated by the formula:

$$P_f = P[g < 0] = \frac{1}{\sigma_g \sqrt{2\pi}} \int_{-\infty}^0 \exp\left[-\frac{(t - \mu_g)^2}{2\sigma_g^2}\right] dt = \Phi\left(\frac{0 - \mu_g}{\sigma_g}\right), \quad (3)$$

where μ_g, σ_g^2 are the mathematical expectation and variance of RV g , respectively; $\Phi(x)$ is a function of the standard normal distribution law.

The RI (with independent R and S) is defined as the ratio of the mathematical expectation μ_g to the standard deviation σ_g :

$$\beta = \frac{\mu_g}{\sigma_g}. \quad (4)$$

From (4) it follows that

$$P_f = P(g < 0) = \Phi(-\beta) = 1 - \Phi(\beta). \quad (5)$$

Equation (5) relates the probability of failure to the reliability index, from which it is possible to determine the reliability index corresponding to the given POF:

$$\beta = -\Phi^{-1}(P_f). \quad (6)$$

For the case when R and S are lognormally distributed, the RI is calculated by the formula:

$$\beta = \frac{\mu_Y}{\sigma_Y} = \frac{\ln\left(\frac{E[R]}{E[S]} \sqrt{\frac{1+V_S^2}{1+V_R^2}}\right)}{\sqrt{\ln\left(\frac{[1+V_R^2]}{[1+V_S^2]}\right)}}, \quad (7)$$

where $E[R], E[S]$ are, respectively, the mathematical expectations of resistance and load; V_R, V_S are, respectively, the coefficients of variation of resistance and load.

The obvious logical step in assigning acceptable/permisible values for the POF of civil and industrial engineering structures should be based on monetary optimization using a benefit-cost assessment of the effectiveness of safety measures, with considering the economic value of a statistical life.

In the current national standard GOST R ISO 2394-2016 of the Russian Federation the permisible level of structural reliability is related to the consequences of failure and the cost of safety measures formalistically and in a simple form. This GOST is based on the international standard ISO 2394:1998 *General principles on reliability for structures*, which has been replaced by ISO 2394:2015 [1].

The generally accepted approach to the assignment of permisible target reliability measures is discussed below, based on the ISO standard [1] and the standard developed by the Joint Committee for Structural Safety (JCSS)[2].

II. Monetary optimization (based on economic costs) of construction projects

ISO 2394:2015 [1] and PMC JCSS [2] are based on Rudiger Rackwitz' seminal works [3, 4]. These papers posit that design codes should be optimized in terms of costs, benefits, and failure effects. The objective function is based on the approach proposed by Rosenblueth and Mendoza (1971) [6] for optimizing the reliability of isostatic structures, using the Cox renewal theory (1967) [5].

For optimization based on the economic costs of civil and industrial engineering objects the following objective function is proposed [3, 4]:

$$\max_p \{Z(p) = B - C(p) - A(p) - D(p) - U(p) - M(p) - I(p)\}, \quad (8)$$

where p is the decision parameter, the so-called *global safety factor*, GSF (described below);
 B is the benefit derived from the useful existence (revenue producing time) of the object;
 $C(p)$ are the construction costs;
 $A(p)$ are the obsolescence costs;
 $D(p)$ are the damage costs due to a failure of the structure's bearing capacity (corresponding to its limit states);
 $U(p)$ are the costs associated with operability failures (maintaining the serviceability of the structure (corresponding to its operability/serviceability limit states);
 $M(p)$ are the costs associated with fatigue and other failures due to aging;
 $I(p)$ are the diagnostics and maintenance costs.

Here it is appropriate to define the scope of this paper more precisely. In general, there are three types of hazards for a civil or an industrial engineering system: Structural (Geo- and industrial, man-made hazards); Operational and Black-Swan-type hazards. There is also a hazard, that is the system itself, as it produces its own carbon footprint that damages the environment. In this paper only the bearing capacity limit state type of failures and associated with it damages are considered.

The last two components of the objective function (8), costs $M(p)$ and $I(p)$ are not considered in the optimization scheme (see [4]). It is also assumed that the cost of failures during operation $U(p)$ can be neglected (see Appendix B in [4]) and the benefit B does not depend on the parameter p . Then the objective function (8) takes the simplified form:

$$\min_p \{Z(p) = C(p) + A(p) + D(p)\}. \quad (9)$$

The approach described in [4] posits that under a few simplifying assumptions, all cost components in (9) can be estimated as a function of construction costs $C(p)$. To achieve this, it is assumed that: (1) the construction is periodically rebuilt (renewed) after each failure or obsolescence, (2) obsolescence and failure are independent events and occur at random times [this is needed for estimating the $A(p)$ and $D(p)$]; (3) the times between failure (renewal) events have *the same distribution and are independent* (i.e., the loads and resistances are independent during successive renewal periods, and there are no changes in the design rules after the first and all subsequent failures); (4) even if the structure changes during renewal, the failure time distribution must remain the same; (5) the renewal (reconstruction) time is negligible compared to the average service life of the structure [4].

A structure that will eventually fail after some time must be optimized at the time of decision (design), that is, at time $t = 0$. Hence, it is necessary to discount all costs of the objective function (9).

In design optimization of structures, renewal theory is used to estimate the total costs associated with a series of structures to be built in the future. A renewal strategy, referring to structural design codes, is a systematic renewal (or repair) after a structure becomes obsolete or fails, as the need for structures persists beyond the life of individual objects, and even if the structure is not restored as an exact copy on the same location, new structures will always be based on the same or similar design standards. Hence, the time horizon T_u for making decisions based on design codes is usually very long and can be assumed to approach infinity ($T_u \rightarrow \infty$). Thus, the objective function is not limited to a single structure; it relates to several similar ones that should be built in the future [10].

Return to the objective function (9). The expected present value of obsolescence costs (with systematic renewal) is estimated as:

$$A(p) = (C(p) + A) \sum_{n=1}^{\infty} E[\exp(-\gamma T_n)] = (C(p) + A) \sum_{n=1}^{\infty} \int_0^{\infty} \exp(-\gamma \tau_n) f_n(\tau_n) d\tau_n. \quad (10)$$

where $C(p)$ denotes the expected (re)construction costs, A are the demolition costs (do not depend on the decision parameter); T_n is the time to the n -th reconstruction (obsolescence) event.

The mathematical expectation in equation (10) is, by definition, the Laplace transform of the function $f_n(t)$ (PDF of the RV T_n), hence:

$$\sum_{n=1}^{\infty} E[\exp(-\gamma T_n)] = \sum_{n=1}^{\infty} [f^*(\gamma)]^n. \quad (11)$$

The sum on the right in this expression is equal to the Laplace transform of the renewal density. Assuming a uniform Poisson process of obsolescence events occurring (resulting in an exponentially distributed time between renewals), then the expected present value of obsolescence costs will be a function of the obsolescence rate $\omega = 1/E[T]$, i.e.

$$A(p) = (C(p) + A) \frac{\omega}{\gamma}. \quad (12)$$

Usually, when calculating, $\omega = 0.02$ (2%) is used. The obsolescence rate can be considered as the average time interval between the object reconstructions, and the average interval between reconstructions, in turn, as the expected service life of the structure ($\omega = 0.01$ implies a reconstruction once every 100 years [4]).

Although the Poisson flow for obsolescence events is probably not very realistic, Equation (12) is used to study the effect of (average) service life on optimization results; the behavior will be, at least qualitatively, similar for other probabilistic models [10].

Ignoring the cost of obsolescence is unacceptable, since it is tantamount to assuming an infinite service life (until failure occurs), which is also unrealistic. Further, only the demolition costs A are neglected, since in any case they are assumed to be independent of the decision parameter p .

A similar approach is used to estimate the expected present value of $D(p)$ resulting from a failure. For simplicity, it is assumed that failure can only occur during random disturbances (e.g., earthquakes, hurricanes, fires) that follow a Poisson process with intensity λ . Randomness in the intensity and occurrence of an external impact can be modeled as a marked Poisson process [7–9]. In this case, the cost associated with the failure of the structure is defined as:

$$D(p) = (C(p) + H) \frac{\lambda P_{f,ULS}(p)}{\gamma}, \quad (13)$$

where H are the costs that accrue in case of failure in addition to the costs of reconstruction (or construction of a new building); λ is the intensity of the process of random disturbances, which can lead to the bearing capacity type of failure with annual (unconditional frequency)/probability $P_{f,ULS}(p)$.

Construction costs $C(p)$ are modeled as a function of the global safety factor p :

$$C(p) = C_0 + C_1(p), \quad (14)$$

where C_0 refers to that part of the construction costs that does not depend on the decision parameter (some “fixed” construction cost); $C_1(p)$ are the marginal safety costs.

Global safety factor p as a decision parameter, is defined [3,4] as the ratio of the mathematical expectations of resistance R and load S :

$$p = \frac{E[R]}{E[S]}. \quad (15)$$

According to [3, 4], the dependence of the POF on the decision-making parameter p is determined under the assumption of a log-normal distribution of resistance and impact effects. Then, from formula (7), it follows that the RI

$$\beta(p) = \frac{\ln \left(p \sqrt{\frac{1+V_S^2}{1+V_R^2}} \right)}{\sqrt{\ln \left([1+V_R^2][1+V_S^2] \right)}}. \quad (16)$$

In this case, the failure probability is modeled as:

$$P_f(p) = P\{g = p \cdot R - S \leq 0\}, \quad (17)$$

where resistance R and load S are modeled as VRs with coefficients of variation V_R and V_S respectively. Equation (17) assumes that both RVs are normalized with respect to their mathematical expectations, so that $E[R] = E[S] = 1$. In this case, the bearing capacity is:

$$g_{ULS} = R(p) - S, \quad (18)$$

where RV $R(p) = p \cdot R$ is modeled with an average equal to p , and the load S is modeled with an average equal to one.

Ultimately, the objective function (9) takes the form:

$$\min_p \left\{ Z(p) = C(p) + C(p) \frac{\omega}{\gamma} + (C(p) + H) \frac{\lambda P_{f,ULS}(p)}{\gamma} \right\}. \quad (19)$$

By relating all cost components to a fixed construction cost C_0 , the optimal level of reliability can be determined as a function of safety and failure damage cost.

If the failure of the structure is not caused by random perturbations, then for failures due to time-varying loads, Eq. (19) is simplified (see [4] for details). In this case, to study the parameters, it is assumed that $\lambda = 1$. For simplicity, from now on the notation λ is omitted since the focus is on the normal/standard design case.

III. Monetary optimization and life safety criterion

The purpose of the analysis when setting the target values of reliability measures is to establish both some optimal value p^* of the decision-making parameter (the level of ensuring the safety of the structure) based on monetary optimization, and the minimum (threshold) value of this parameter p_{acc} from the condition of ensuring life safety (saving people's lives) using LQI criterion that determines the boundary of the admissible area for p , within which monetary optimization should be performed. Fig. 1 shows the interaction between the safety parameter p^* set on the basis of monetary optimization and the boundary (threshold) value p_{acc} set according to the criterion of ensuring human safety (acceptable risk to life).

The permissible limit (threshold) value p_{acc} is determined according to [1] based on the Marginal Life Saving Costs Principle, according to which the decisions made that affect life safety are considered acceptable if the costs associated with possible measures to save one additional (anonymous) life, are balanced with the costs that society is economically capable of, or willing to bear for the sake of saving one statistical individual.

The estimate of the marginal safety costs is based on the Life Quality Index (LQI). This is a complex indicator is equal to (USD·year) [12-14]:

$$LQI = G^q e(0), \quad (20)$$

where G (USD) is the gross domestic product (GDP) per capita; $e(0)$ (years) is the average life expectancy (ALE) at birth; q is a complex coefficient depending on the duration of the active phase of life and the measure of compromise between the resources available for consumption and the value of healthy life time [14]:

$$q = \frac{w}{\beta(1-w)}, \quad (21)$$

where β is the ratio of income S (in USD per capita per month) to GDP:

$$\beta = \frac{S \cdot 12}{g}, \quad (22)$$

w is the duration of the phase of active life (the ratio of the duration of profitable work and leisure, including hobbies):

$$w = h \cdot M/P, \quad (23)$$

h is the ratio of the number of worked hours to the total hours, taking into account a 40-hour working week $h = 0.24$; M (in thousands of people) is the number of people employed in the economy; P (in thousands of people) is the total population.

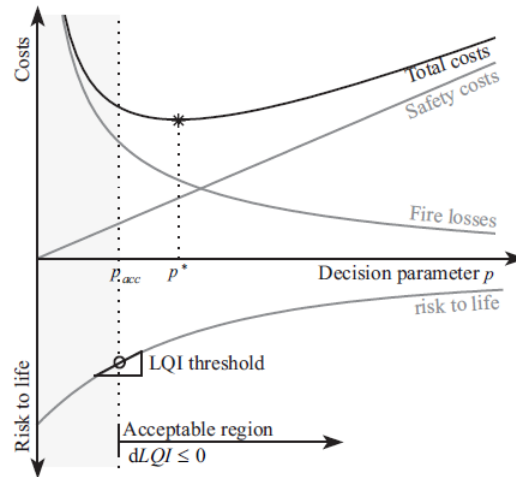


Fig. 1: Interaction of the monetary optimization criteria p^* and the social criterion p_{acc} related to society's investment in life safety [11]

Using this concept, ISO 2394 [1] defines a basic requirement according to which a target POF can be set based on monetary optimization only when the risk of loss of human life because of failure is minimized (which is equivalent to defining the limit or threshold value of the reliability measure). Otherwise, the LQI-criterion is used to determine the limit target values of POF.

Costs H , which are charged in case of failure in addition to the costs of reconstruction, include the costs of dismantling, as well as human losses, expressed in monetary units:

$$H = C_d + N_F \cdot H_c, \quad (24)$$

where C_d is the demolition cost; N_F is the estimated number of human casualties and injuries; H_c is the compensation payment in case of human death or permanent injury (loss of limb or cognition).

Failure costs $D(p)$ are not included in the acceptance criteria, since the reduction in these cost components can be seen as a monetary benefit from improved safety. Thus, the following rule can be formulated:

When establishing a criterion based on LQI, it is sufficient to quantify the marginal increase in construction and obsolescence costs with a corresponding change (decrease) in risk to life (see Fig. 1) as a function of the decision parameter:

$$\frac{d[C(p) + A(p)]}{dp} \geq -\frac{1}{\gamma_s} \frac{dN_F(p)}{dp} \cdot SWTP. \quad (25)$$

In criterion (25), the risk to human life is determined by: (1) the expected number of victims $N_F(p)$, (2) the social discount rate γ_s , and (3) the social willingness to pay (SWTP). The latter is the amount of money a society is willing to pay to reduce mortality by one unit. The concept of SWTP is based on the assumption that investments in life saving measures will lead to a change in the level (intensity) of mortality. From the change in mortality intensity $d\mu(a)$ the change in the

remaining life expectancy $de(a)$ for each age group can be calculated.

In general, SWTP for saving one additional life of a statistically average individual is defined as follows [10, 20-23]:

$$SWTP = -dG = \frac{G}{q} E_A \left[\frac{de_d(a)}{e_d(a)} \right], \quad (26)$$

where dG is the loss of disposable income (reduction in GDP per capita) due to investment in life saving measures (hence, dG is negative), $E_A \left[\frac{de_d(a)}{e_d(a)} \right]$ is the age-averaged relative change of discounted life expectancy $e_d(a)$.

Age-averaging is introduced to account for the fact that different life saving strategies may have different effects on different age groups. Discounting is introduced to take into account the effect that lives saved are saved in the future [1].

Discounted life expectancy for age a is determined by the formula [10, 23]

$$e_d(a) = \int_a^{a_u} \exp \left[-\int_a^t [\mu(\tau) + \gamma] d\tau \right] dt, \quad (27)$$

where $\mu(a)$ is the intensity of mortality at the age a (determined from mortality tables), γ is the discount rate, a_u is the maximum age to which people live in the country, region, industry, company, or the cohort under consideration.

For a small reduction in mortality, the SWTP for saving one life can be obtained using the demographic constant C_x for a certain mortality regimen x [1, 20-23]:

$$SWTP \approx \frac{G}{q} C_x, \quad (28)$$

There are three main mortality regimens (see details in [21, 23]). Here we consider the so-called Δ -regimen when the change of mortality intensity is the same for all ages: $\mu_\Delta(a) = \mu(a) + \Delta$. This regimen is suitable for most cases related to structural safety, since the risk reduction measures usually have the same effect on all people, regardless of their age [1].

According to [20-23], for the Δ -regimen:

$$C_x = \int_0^{a_u} \frac{\int_a^{a_u} (t-a) \exp \left[-\int_a^t [\mu(\tau) + \gamma] d\tau \right] dt}{\int_a^{a_u} \exp \left[-\int_a^t [\mu(\tau) + \gamma] d\tau \right] dt} h(a) da, \quad (29)$$

where $h(a)$ is the PDF of the age distribution of the considered population.

Along with SWTP (corresponds to the amount that society can afford to invest to save one life), there is also the concept of Social Value of a Statistical Life (SVSL), which corresponds to the amount that a society can pay for each death (compensation payment) [1]:

$$SVSL \approx \frac{G}{q} E_A [e_d(a)], \quad (30)$$

where $E_A [e_d(a)]$ is the age-averaged discounted life expectancy:

$$\bar{e}_d = E_A [e_d(a)] = \int_0^{a_u} e_d(a) h(a) da. \quad (31)$$

According to [23], the age-averaged life expectancy without discounting $\bar{e}_d \approx \frac{e(0)}{2} = 40$ years for industrialized countries. Using a typical average discount rate (3%-4%) one gets

$$\bar{e}_d \approx \frac{e(0)}{4} = 20 \text{ years.}$$

Using the results of section II, criterion (26) can be transformed to the form:

$$C_1 \left(1 + \frac{\omega}{\gamma_s} \right) \geq \frac{1}{\gamma_s} SWTP \cdot N_F \frac{dP_f(p)}{dp}. \quad (32)$$

In criterion (32), the risk to life is expressed in terms of the probability of failure $P_f(p)$ and the estimated (expected) number of victims N_F . Since the LQI-criterion is a society determined /established boundary condition, the social discount rate γ_s is used in criterion (32).

For a combination of an LQI-criterion with functions used in monetary optimization, Rackwitz and Streicher [16] relate the LQI-criterion to the relative cost of safety measures C_1 / C_0 , assuming a fixed value of construction costs C_0 . As a result of applying this assumption, the criterion becomes dependent on the scale of C_1 / C_0 .

The transformation of inequality (32) leads to the following criterion:

$$-\frac{dP_f(p)}{dp} \leq \frac{C_1(\gamma_s + \omega)}{SWTP \cdot N_F} = k_1. \quad (33)$$

The numerator $C_1(\gamma_s + \omega)$ on the right side of the inequality shows how much the annual costs associated with ensuring safety measures unit increase with an increase in the value of the decision parameter p (global safety factor). In the denominator of the right side of inequality (33), the consequences of the loss of human lives N_F because of the failure are given in monetary units. Thus, the coefficient k_1 is the ratio of the costs of ensuring the safety measures to the costs associated with the marginal cost of saving N_F human lives (SWTP). Reliability targets according to LQI can now be obtained as a function of the constant k_1 .

Table 1 according to ISO 2394 [1] presents the tentative minimum target reliability measures obtained using the LQI criterion and monetary optimization, for various classes of relative life saving costs. These classes are defined in terms of the range of the constant k_1 (second column of Table 1). The values in Table 1 are derived from log-normal distributions of load and resistance effects with coefficients of variation $0.1 \leq V \leq 0.3$.

Table 1: Tentative minimum target reliability measures (ULS, $T_{ref} = 1 \text{ year}$) based on the LQI-criterion and monetary optimization according to ISO 2394 [1]

Relative life saving costs	$k_1 = \frac{C_1(\gamma + \omega)}{SWTP \cdot N_F}$	LQI-objective measure of reliability
Large	$10^{-2} \dots 10^{-3}$	$\beta = 3.1 (P_f = 10^{-3})$
Medium	$10^{-3} \dots 10^{-4}$	$\beta = 3.7 (P_f = 10^{-4})$
Small	$10^{-4} \dots 10^{-5}$	$\beta = 4.2 (P_f = 10^{-5})$

Note: the values in the table were obtained with $0.1 \leq V \leq 0.3$. The target probability of failure may be increased by a factor of 5 for higher coefficients of variation of the basic RVs. For low variability, on the other hand, it should be reduced by a factor of 2, $\gamma_s = 0.04$, $\omega = 0.02$.

It was shown in [17] that combinations of different distributions for load and resistance with their values of coefficients of variation $V \leq 0.3$ have little effect on optimization results. The distribution of resistance is important only when $V_R \geq 0.3$. At the same time, it is noted [17] that this is an extremely rare case for resistance (a Black Swan event). At the same time, these estimates are given without an in-depth analysis that takes into account the uncertainties of the calculation

models of resistances and loads.

For the case of small variation coefficients of resistance and load effects, ($0.1 \leq V \leq 0.3$) it is proposed to determine the target value of the threshold probability of failure p_{acc} as a measure of reliability based on the LQI criterion using the following simplified formula [17]:

$$p_{acc} \cong \frac{1}{5} k_1 = \frac{1}{5} \frac{C_1(\gamma + \omega)}{SWTP \cdot N_F}. \quad (34)$$

At the same time, it is noted that if the consequences associated with the loss of human life in case of failure are very high (constant $k_1 > 10^{-2}$), criterion (34) should not be applied. The threshold (boundary) value p_{acc} , set using the LQI -criterion, determines a certain range of acceptable values within which monetary optimization should be performed.

The optimal solution p^* is determined when the first derivative of the objective function (19) at point p^* is equal to zero

$$\frac{dZ(p)}{dp} = \frac{dC(p^*)}{dp} \left(1 + \frac{\omega}{\gamma}\right) + \frac{dC(p^*)}{dp} \frac{P_f(p^*)}{\gamma} + \frac{dP_f(p^*)}{dp} \frac{C(p^*) + H}{\gamma} = 0. \quad (35)$$

Considering that $P_f(p^*) \ll \gamma$, the second term in (36) can be neglected, then

$$\frac{dC(p^*)}{dp} = \frac{C(p^*) + H}{(\gamma + \omega)} \cdot \frac{dP_f(p^*)}{dp}. \quad (36)$$

Substituting (36) into criterion (33) and considering that $\frac{dP_f(p)}{dp} < 0$ for all p , we obtain:

$$\frac{SWTP \cdot N_F}{(C(p^*) + H)} \leq \frac{\gamma_s + \omega}{\gamma + \omega}. \quad (37)$$

Criterion (37), considering compensation payments $H_c N_F$ can be rewritten as follows:

$$\frac{N_F \cdot H_c}{C(p^*) + H} \leq \frac{(\gamma_s + \omega)}{(\gamma + \omega)} \cdot \frac{H_c}{SWTP}. \quad (38)$$

Criterion (38) includes three components: (1) the ratio of death compensation payments $H_c N_F$ resulting from a failure to the full costs associated with the failure $C(p^*) + H$. Obviously, this ratio is always less than unity; (2) the ratio of the social discount rate γ_s to the discount rate γ set by a private decision maker and performing monetary optimization. In the case of applying the LQI-criterion from a social point of view $\gamma_s = \gamma$ and then $\frac{\gamma_s + \omega}{\gamma + \omega} = 1$. In monetary optimization, when the decision is made by an individual, usually $\gamma > \gamma_s$; (3) the ratio of how the loss of life translates into monetary optimization (compensation payments H_c) and a LQI criterion for the threshold value of SWTP, respectively.

The amount of compensation payments H_c depends on several different factors. For a private decision maker, most likely it is impossible to accept one fixed value of H_c regardless of the specific situation. Hence, in the general case, the ratio $H_c / SWTP$ should be considered as some variable.

As shown in [17], for many computational cases it can be assumed that $\gamma_s / \gamma = \frac{\gamma_s + \omega}{\gamma + \omega}$. Hence, it suffices to check whether the ratio of the discount rates is γ_s / γ greater than the ratio of the cost of SWTP for saving N_F human life to the total damage cost from structure failure $C(p^*) + H$. For a social decision maker, $\gamma_s / \gamma = 1$ and criterion (39) is simplified to checking whether $SWTP \cdot N_F$ is

greater than $C(p^*) + H$.

Target reliability measures associated with the consequences of failure and based on monetary optimization according to ISO 2394 [1] are given in Table. 2. Consequence classes should be taken according to Table F.1 of ISO 2394 [1], which contains not only a description of the expected consequences of failure, but also the predicted number of victims (for example, for Class 2 - no more than 5; Class 3 - no more than 50; a Class 4 - no more than 500).

Table 2: Tentative target reliabilities (ULS, $T_{ref} = 1$ year), based on monetary optimization according to ISO 2394 [1]

Relative cost of safety measures	Failure consequences (classes according to Table F.1 [15])		
	Class 2	Class 3	Class 4
Large	$3.1(P_f \approx 10^{-3})$	$3.3(P_f \approx 5 \cdot 10^{-4})$	$3.7(P_f \approx 10^{-4})$
Medium	$3.7(P_f \approx 10^{-4})$	$4.2(P_f \approx 10^{-5})$	$4.4(P_f \approx 5 \cdot 10^{-6})$
Small	$4.2(P_f \approx 10^{-5})$	$4.4(P_f \approx 5 \cdot 10^{-5})$	$4.7(P_f \approx 10^{-6})$

It should be noted that the same values of failure probabilities and reliability indexes (see Table 3) are presented in the PMC JCSS code [2], which is also based on [3]. The target values of POF depend not only on the failure consequences, but also on the relative cost of the safety measures.

Table 3: Target values of reliability index β_{tag} (failure probabilities) for $T_{ref} = 1$ year and ULS according to [2]

Relative cost of security measures C_1/C_0	Small	Medium	Large (significant)
	Consequences $\rho < 2$	Consequences $2 \leq \rho < 5$	consequences $5 \leq \rho < 10$
Large (A)	$3.1(P_{tag} \approx 10^{-3})$	$3.3(P_{tag} \approx 5 \cdot 10^{-4})$	$3.7(P_{tag} \approx 10^{-4})$
Medium (B)	$3.7(P_{tag} \approx 10^{-4})$	$4.2(P_{tag} \approx 10^{-5})$	$4.4(P_{tag} \approx 5 \cdot 10^{-6})$
Small (C)	$4.2(P_{tag} \approx 10^{-5})$	$4.4(P_{tag} \approx 5 \cdot 10^{-5})$	$4.7(P_{tag} \approx 10^{-6})$

At the same time, PMC JCSS [2] proposes to consider following additional aspects when differentiating reliability and classifying structural designs:

a) qualify the failure consequences using the coefficient ρ , which is the ratio of the total cost of damage $C_0 + C_1(p) + H$ associated with the same structure failure, to the cost $C_0 + C_1(p)$ of its (re) construction:

$$\rho = \frac{C_0 + C_1(p) + H}{C_0 + C_1(p)} = 1 + \frac{H}{C_0 + C_1(p)} \approx 1 + \frac{H}{C_0}. \quad (39)$$

The construction cost includes a fixed part C_0 and a cost $C_1(p)$ depending on the decision parameter. The cost H denotes the direct damage associated with the failure, including the actual cost of damage and subsequent total or partial dismantling of the structural system as a whole or part of it, environmental consequences (carbon footprint), damage to infrastructure, communications, etc., as well as human casualties expressed in monetary units. When $\rho > 10$ the target values of the probability of failure and the reliability index should be set, based on the

results of a systematic risk analysis for the design object;

b) Reliability target values given in Table 3 refer to the structural system or, with some allowance, for the dominant form of system failure. The same values apply to a key structural element (that dominates the failure of the system). Based on this, it is assumed that structural systems with several equally significant forms (modes) of failure should be designed with a higher level of reliability.

The values given are, of course, tentative. At the same time, the methods of their determination contain quite significant uncertainties. This refers, in the first place, to the division into appropriate classes of the relative cost of safety measures (C_1 / C_0), mainly adopted from [17, 18], in which the following relative cost intervals are established:

- large cost (A): $10^{-2} \leq C_1 / C_0 \leq 10^{-1}$;
- normal/medium (B): $10^{-3} \leq C_1 / C_0 \leq 10^{-2}$;
- small (C): $10^{-4} \leq C_1 / C_0 \leq 10^{-3}$.

These cost classes were derived in [17] from dependencies $[(C_1 / C_0) - (H / C_0)]$ when compared with the optimal values of target reliability measures according to PMC JCSS [2]. They are derived following [3] at a discount rate $\gamma = 0,03$, coefficient $\omega = 0,02$, variation coefficients $V_R = V_S = 0,3$ for a log-normal distributions of resistance and load effects.

In general, ISO 2394:2015 [1] and PMC JCSS [2], which are based on [3, 4], provide a more appropriate reliability differentiation for existing designs than Eurocodes [19, 20], as they consider the cost of safety measures.

IV. Determination of acceptable reliability targets for residential buildings in the Sverdlovsk region of the Russian Federation based on the LQI criterion

To assess the threshold probability of failure p_{acc} , as a measure of reliability based on the LQI criterion, for residential multi-storey buildings in the Sverdlovsk region, the initial data for 2021 were used, presented in Table. 4. All monetary components were converted into USD at the average exchange rate in 2021: 1 USD = 73.65 rubles.

Table 4: Initial data for assessing the threshold probability of failure of residential multi-storey buildings in the Sverdlovsk region (for 2021)

Parameter	Meaning
GDP per capita, G	710.381 thousand rubles/person 9645.36 USD/person
Life expectancy at birth, e_0	68.79 years
Cash income per capita/mo, S	40.275 thousand roubles \$ 546.84 USD
Population, P	4277.203 thousand people
Number of people employed in the economy, M	2034.600 thousand people
The average cost of construction of 1m ² of residential multi-storey buildings, C_0	44.800 thousand rubles/m ² 608.28 USD/m ²
Average key rate of the Central Bank of Russia	6%

For further analysis, when estimating the (discounted) life expectancy and the demographic constant C_v , it is necessary to know the type of mortality intensity function $\mu(a)$ and, therefore, the

law of mortality. Assume that the mathematical model of mortality is the Gompertz-Makham law (G–M), according to which:

$$\mu(a) = M + \alpha e^{\beta a},$$

where M is the Makeham coefficient characterizing the contribution to accidental mortality of impacts (the effect of which does not depend on age), α is the level of initial mortality, β is the rate of increase in mortality. The G–M law is most suitable for studying the process of human mortality [24], since it contains both the exponentially growing component of mortality due to aging, and the age-independent component associated with extreme situations.

The G–M law parameters are calculated according to the mortality (survival) tables. Mortality tables (MT) are built using age-specific mortality rates (MR). The Russian database on fertility and mortality in Russian regions is located on the website of the Center for Demographic Research of the Russian Economic School [25]. A MT was built based on the MR of the Sverdlovsk region for 2021, according to the methodology of the Federal State Statistics Service [26]. The G–M model parameters are calculated according to the method [24] on the basis of the obtained MT:

$$M = 7.4 \cdot 10^{-4}, \alpha = 2.1 \cdot 10^{-4}, \beta = 7.6 \cdot 10^{-2}.$$

The mean absolute percentage error between the life expectancy calculated according to the G–M law and the life expectancy from the mortality table is 6.5%. Fig.2 shows the values of the ALE obtained on the basis of the G–M law and their discounted values.

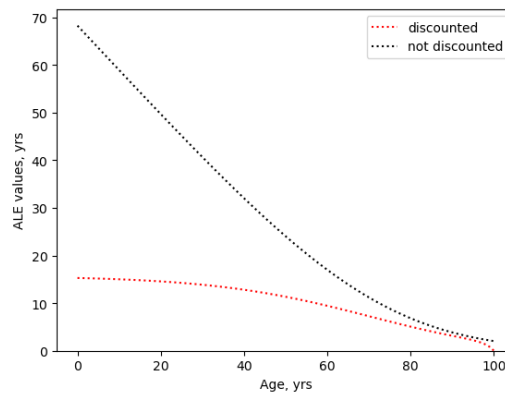


Fig. 2: ALE obtained on the basis of the G–M law and their discounted values

The demographic constant calculated by formula (29), at the discount rate $\gamma = 0.06$, is equal to $C_x = 10.4$ (years). For comparison, according to [23], $\gamma = 0.03$ for industrialized countries, C_x ranges from 13.9 to 16.9. In our case, when $\gamma = 0.03$, the constant $C_x = 14.2$, which fits into the overall picture. Using formulas (21)-(23) and Table 4, $w = 0.11$, $\beta = 0.68$, $q = 0.19$. Then for the Sverdlovsk region LQI = 383 USD·year and at $\gamma = 0.06$ SWTP = 535,748 USD per year. At $\gamma = 0.03$ SWTP = 732,298 USD

To estimate SVSL, it is necessary to have the density $h(a)$ of the age distribution of the Sverdlovsk region population. Since at the time of writing this paper, these statistics were not available in the public domain, the age distribution for the whole of Russia was used, shown in Fig. 3.

Thus, we got that compensation payments for the death of one person SVSL = 609,941 USD, i.e. costs that are economically feasible to invest in saving lives. Using dependencies (33) and (34), the target values of POF of residential multi-storey buildings in the Sverdlovsk region of Russia were calculated and presented in Table 5. To obtain the threshold (limit) values of POF p_{acc} it is necessary to divide the data of Table 5 by 5 (see formula (34)).

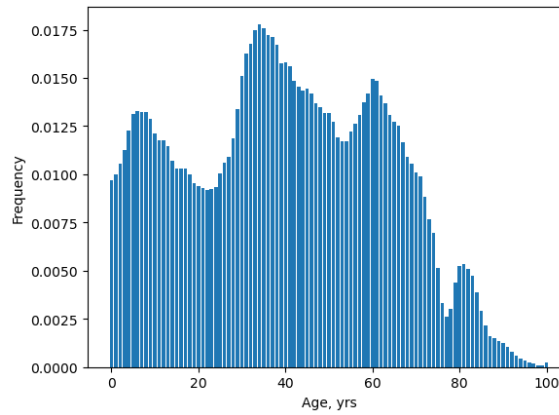


Fig. 3: Age distribution of the Russian population

Table 5: k_1 values for residential multi-storey buildings in the Sverdlovsk region depending on the relative cost of safety measures and human losses in case of structural failure

N_f/m^2	Residential multi-storey buildings construction cost $C_0 = 608.28$ USD/m ²		
	Relative cost of safety measures C_0/C_1		
	0.001 (small)	0.01 (normal)	0.1 (large)
0.0001	$9 \cdot 10^{-4}$	$9 \cdot 10^{-3}$	$9 \cdot 10^{-2}$
0.001	$9 \cdot 10^{-5}$	$9 \cdot 10^{-4}$	$9 \cdot 10^{-3}$
0.01	$9 \cdot 10^{-6}$	$9 \cdot 10^{-5}$	$9 \cdot 10^{-4}$
0.1	$9 \cdot 10^{-7}$	$9 \cdot 10^{-6}$	$9 \cdot 10^{-5}$

The residential norm in Russia is 10 m² per person, hence, $N_f / m^2 = 0.1$ and K_1 changes from $9 \cdot 10^{-7}$ to $9 \cdot 10^{-5}$ (depending on the relative cost of safety measures). Based on the obtained values, for the normal relative cost of safety measures, a tentative target value of the threshold POF can be taken as $p_{acc} \approx \frac{1}{5} k_1 = 2 \cdot 10^{-6}$, set using the LQI -criterion, which determines a certain range of acceptable values within which monetary optimization should be performed.

V. Conclusion

The generally accepted approaches to the assignment of acceptable target reliability measures [1,2] are considered and analyzed. These standards reflect the main results of [3,4], but have several important uncertainties left unresolved. Future research should consider the effect of different diagnostic, monitoring, maintenance strategies and the sub/supra resilience effect [27, 28] on the target values of reliability of civil and industrial engineering infrastructures and systems.

References

- [1]. International Organization for Standardization, ISO 2394:2015 General principles on reliability for structures, 2015.
- [2]. Joint Committee for Structural Safety (JCSS) / Probabilistic Model Code, 2001.
- [3]. Rackwitz, R. Optimization and risk acceptability based on the life quality index // Structural Safety, 2002. 24. p. 297-331.
- [4]. Rackwitz, R., Optimization - the basis of code-making and reliability verification// Structural Safety, 2000. 22(1). p. 27-60.
- [5]. D. Cox and W. Smith. "Renewal Theory", Soviet Radio, Moscow, 1967

- [6]. Rosenblueth, E. and Mendoza, E. (1971). Reliability optimization in isostatic structures. *Journal of the Engineering Mechanics Division*, 97(6):1625-1648
- [7]. Rosenblueth, E., Optimum Design for Infrequent Disturbances, *Journ, Struct. Div., ASCE*, 102, ST9, 1976, pp. 1807-1825
- [8]. Hasofer, AM, Design for Infrequent Overloads, *Earthquake Eng. and Struct. Dynamics*, 2, 4, 1974, pp. 387-388
- [9]. Taylor HM, Karlin S. An introduction to stochastic modeling. 3rd ed. San Diego, CA: Academic Press; 1998.
- [10]. Fischer, K., Societal decision-making for optimal fire safety. Doctoral Dissertation, ETH Zurich, Switzerland, 2014
- [11]. K. Fisher, MH Faber. The LQI acceptance criterion and human compensation costs for monetary optimization - a discussion note // *LQI Symposium*, 2012.
- [12]. Lind NC Target reliabilities from social indicators. *Proc ICOSSAR93 Balkema* 1994; 93: 1897-904.
- [13]. Nathwani, JS Affordable safety by choice : the life quality method / JS Nathwani, NC Lind, DM Pandey. – Waterloo: University of Waterloo, 1997.
- [14]. Pandey, M.D.; Nathwani, J.S.; Lind, N.C. (2006). The derivation and calibration of the Life-Quality Index (LQI) from economic principles. *Structural Safety*, 28(4):341-360.
- [15]. R. Skjong, K. Ronold. Social Indicator for Risk Acceptance // *Proc. OMAE*. – Lisbon, Portugal, 1998.
- [16]. Rackwitz, R. and Streicher, H. (2002). Optimization and target reliabilities. In *JCSS Workshop on Reliability Based Code Calibration*, Zurich, Switzerland.
- [17]. K. Fisher, C. Viljoen, J. Köhler, MH Faber Optimal and acceptable reliabilities for structural design // *Structural Safety*, doi.org/10.1016/j.strusafe. 2018.09.002.
- [18]. Virguez, E. Supporting Decisions on Global Health and Life Safety Investments / E. Virguez, MH Faber.
- [19]. Eurocode - Basis of structural design: EVS-EN 1990:2002/A1:2006/AC:2010. Eurocode European Committee for Standardization, 2002.
- [20]. Basis of Structural Design : Project EN 1990 Eurocode.
- [21]. Rackwitz, R. (2006). The effect of discounting, different mortality reduction schemes and predictive cohort life tables on risk acceptability criteria. *Reliability Engineering and System Safety*, 91(4):469-484.
- [22]. Rackwitz, R. (2008). The philosophy behind the Life Quality Index and empirical verifications. *JCSS Basic Documents on Risk Assessment in Engineering*, www.jcss.byg.dtu.dk.
- [23]. Lentz, A. (2007). Acceptability of civil engineering decisions involving human consequences. Dissertation, Technische Universität München, München, Germany.
- [24]. Gavrilov L.A., Gavrilova N.S. The biology of longevity. Rep. ed. V. P. Skulachev. 2nd ed., revised. and additional M.: Nauka, 1991. 280 p (In Russian).
- [25]. Russian database on fertility and mortality: http://www.demogr.nes.ru/index.php/en/demogr_indicat/data
- [26]. <https://www.gks.ru/storage/mediabank/Prez-251219.pdf>
- [27]. Timashev S.A. Infrastructures. Part I. Reliability and Longevity, Ural Branch Russian academy of sciences. Yekaterinburg, 2015 (In Russian).
- [28]. Timashev S.A. Infrastructures. Part II. Diagnostics. Monitoring. Maintenance. Human Factor. Resilience. Ural Branch Russian academy of sciences. Yekaterinburg, 2020 (In Russian).

MULTIFACTORIAL EMERGENCY FORECASTING METHODS

Vugar Aliyev¹, Zurab Gasitashvili², Merab Pkhovelishvili², Natela Archvadze³,
Lia Shetsiruli⁴

•

¹ AMIR Technical Services Company, Azerbaijan

² Georgian Technical University

³ Ivane Javakhishvili Tbilisi State University, Georgia

⁴ Grigor Robakidze University, Batumi, Georgia

prof.vugar.aliyev@gmail.com

zur_gas@gtu.ge

merab5@list.ru

natela.archvadze@tsu.ge

lia.shetsiruli02@gruni.edu.ge

Abstract

Recently, great tragedies have occurred, which are caused by the coincidence of various factors in time and in locations. Failure to take into account the fact that different events will coincide in time and location is an error in the forecasting method, since such situations require the use of parallel data, which we will discuss here. The article gives a specific example of the coincidence of 5 natural geological and hydrometeorological events and shows how a natural disaster could have been avoided using a new forecasting method.

Keywords: forecasting, risk analysis, emergency situation, forecasting methods, expert assessment

I. Introduction

The relevance of the problem is determined by the fact that the modern period is characterized by the development of global problems, potentially leading to emergency situations, both in the natural, man-made, and social spheres. These include global climate change, the permanent growth of the technogenic sphere, the problems of terrorism, the negative phenomena caused by globalization, and others. It is necessary to pay considerable attention to the issues of life safety, technosphere safety, ecology, environmental protection and, in this regard, forecasting of crisis and emergency situations of a natural and man-made nature and their consequences. Planning and making adequate management decisions in the field of ensuring safety, preventing and reducing the consequences of emergency situations is impossible without solving forecasting problems [1].

We consider a new system for predicting the risks of natural processes, which is based, on the one hand, on parallel data [2], and on the other hand, on models for predicting events belonging to different areas, but coinciding with each other in time and locations. In addition, it should be noted that if there are no models of different areas, then experts are used for forecasting, who estimate the risk of certain events in%. When using parallel data, a fairly high reliability of the forecast is obtained, which makes it possible to reduce risks or avoid them altogether.

II. New approach to risk forecasting

The result of predicting the risk of a certain event is to determine when, where and with what (what) characteristics the event will occur. In general, non-parametric methods are often used in risk forecasting, such as the least squares method, which evaluates the accuracy of the forecast. Adaptive methods, autoregressive methods and many other methods are also used. It is also important to use expert forecasting methods, including those based on non-numerical data. Particularly relevant is the development of forecasting methods under risk, based on the use of joint combined economic-mathematical and econometric (both statistical and expert) methods in forecasting models.

Precursors in risk forecasting are those that precede the forecasted event and on the basis of which the forecasting model of this event is built.

When considering the actual task of predicting the risk of a natural event, it should be noted that the precursor is mainly a certain geophysical phenomenon that precedes the occurrence of a natural event. Geophysical precursors (phenomena) include, for example, seismic, hydrogeodynamic, deformational, geochemical, thermal, gravitational, and electromagnetic events. As well as the results of observations obtained by remote monitoring of recently developed satellite technologies, etc.

Forecasting a specific natural phenomenon means determining a sequence of actions aimed at detecting the characteristic features of an event or anomalous changes in various geological and geophysical fields, their joint consideration and analysis in order to determine, for example, in the case of an earthquake forecast, location, time and power. That is, the results of forecasting during an earthquake are the place of the earthquake, the time of the event and its power.

[3, 4] discusses a prediction model specifically for risks. In this case, this means that for the same events, different models are created based on different predecessors, which calculate the risks of an event according to certain indicators for this event. These indicators are: the number of justified and unjustified forecasts and the probability of justification. The probability of justification is calculated for each model and determines how many times the event was predicted and how many times the event actually happened. After that, by calculating the risk coefficients, the justification probabilities of all possible pairs of models are considered, then triples, and the best one is selected [5].

When discussing the hybrid risk prediction model, we proceeded from the fact that there is one predicted event and several models for it. Now consider another situation where there is a risk zone and it is necessary to estimate the risk for a given time interval. Suppose there are models based on different predecessors: A_1, A_2, \dots, A_n . Some of these models can predict the same event, but you need to have a model that belongs to a different area. For example, be geological (models for predicting landslides, floods, determining the danger of natural disasters) or, for example, models for forecasting hydrometeorological phenomena that can be attributed to natural hydrometeorological events. river basins, models for studying current processes on glaciers, and others. If there are no models of different fields, then the expert is engaged in forecasting. We will discuss this process in the next paragraph.

Parallel data (or datasets) are different types of data that influence (or predict) a particular event. For example, parallel data during a particular disaster is a collection of the following data: geological, meteorological and hydrological parameters, historical and current data, including decoded information from satellite, radar and aerial photographs, as well as data obtained as a result of field hydrometeorological / geological surveys. The probability of the appearance of each pattern may be small, but under certain conditions, when there is a coincidence in time and locations, this is already a sign of tragedy.

It is possible to formulate a new algorithm for predicting risk: to assess a specific risk (i.e., a specific place and period of time is determined), models A_1, A_2, \dots, A_n are considered. Prognostic models of the same event are separated from them and their probability of occurrence is calculated. After the model risk percentages for each forecast are obtained for different types of events, the sum of these risks is calculated. That is, a separate risk is calculated for one type of event, separately for another type of event, separately for a third type of event, etc., but the calculation is made in the same place at the same time, and the final result is the sum of these risks.

Quisque ullamcorper placerat ipsum. Cras nibh. Morbi vel justo vitae lacus tincidunt ultrices. Lorem ipsum dolor sit amet, consectetur adipiscing elit. In hac habitasse platea dictumst. Integer tempus convallis augue. Etiam facilisis. Nunc elementum fermentum wisi. Aenean placerat. Ut imperdiet, enim sed gravida sollicitudin, felis odio placerat quam, ac pulvinar elit purus eget enim. Nunc vitae tortor. Proin tempus nibh sit amet nisl. Vivamus quis tortor vitae risus porta vehicula.

III. Engage experts

The new approach to forecasting assumes that there are at least two industry models that are different from event forecasting models, but if this is not the case, then we use experts. In general, the role of experts in predicting such events is very large, since the information obtained by automatic measurement sensors requires a great deal of knowledge and experience from the event specialist.

If several experts participate in the process, then we calculate the sum of the experts' ratings, divide by the number of experts and calculate the average value.

Systematic research and analysis of problem solving takes on an important role in the evaluation of public relations. There is a need to include expert groups and their knowledge in assessments and analysis, whose subjective data in building models create a new type of uncertainty. In parallel with the classical directions of modeling, the assumption of mixed, phase-probabilistic uncertainty becomes important. In this case, it is necessary to use phase methods of expert knowledge engineering and phase logic along with statistical data analysis, which ensures the construction of appropriate full-fledged automated systems and intelligent assistive technologies.

IV. Example

On August 3 this year, in the municipality of Oni, Georgia, a natural disaster unfolded in the Shovi resort, people died, and several million dollars in damage was received. As a result of a natural disaster, the Shov sanatorium was destroyed - it was covered with several meters of lava. The natural disaster triggered geological and hydrological events at the same time. In particular, in the upper reaches of the river there are 2 glaciers that are melting intensively. There was a lot of rain. All these things went on a rampage and the result was a catastrophe. The data given in the example is taken from the official page of the Environmental Protection Agency [6].

It would be possible to predict the event in question if we used a new risk prediction algorithm. The parallel data on which the models are built are as follows:

1. Average annual air temperature anomalies (see Fig.1).
2. Anomalies in the average annual precipitation (see Fig.2).

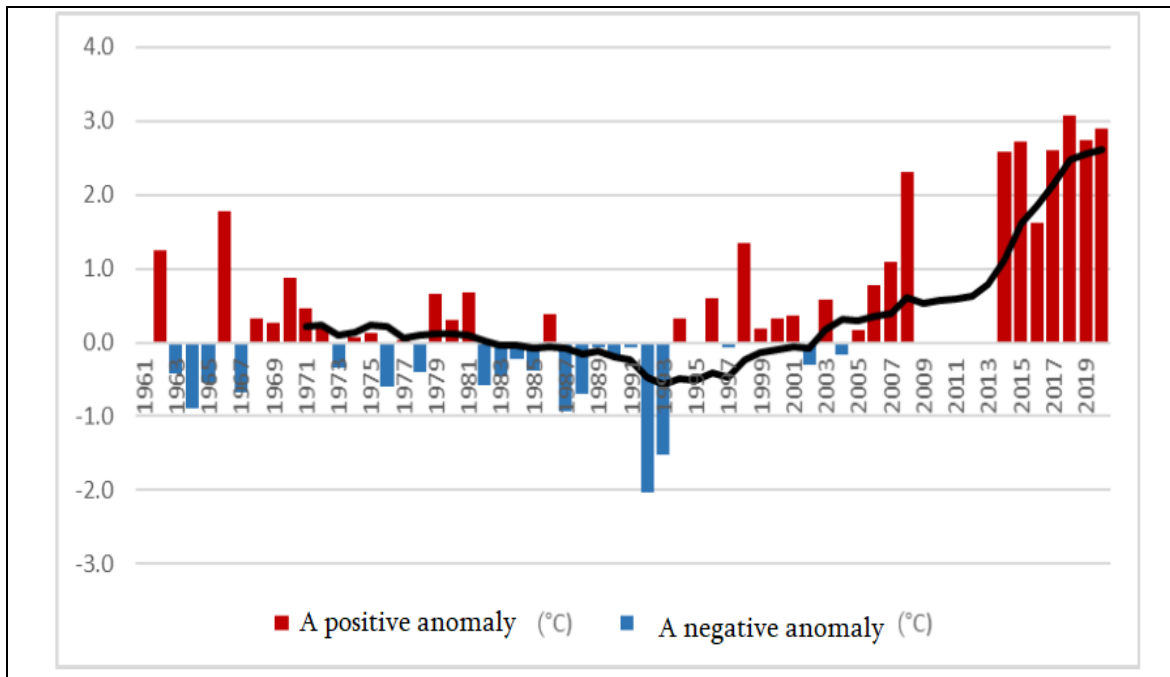


Fig. 1: Average annual air temperature anomalies (in relation to the period 1961-1990) 1961-2020 for the period and the 11-year moving average

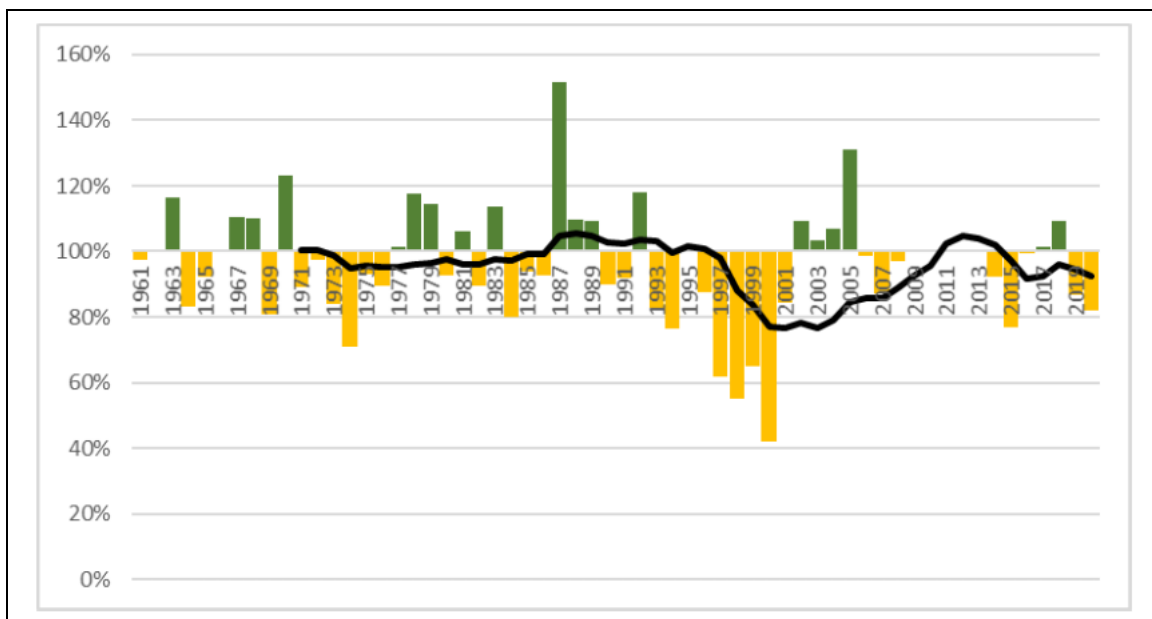


Fig. 2: Anomalies in the average annual amounts of atmospheric precipitation (in relation to the period 1961-1990) 1961-2017 for the period and the 11-year moving average

3. Sunshine duration anomalies (see Fig.3):

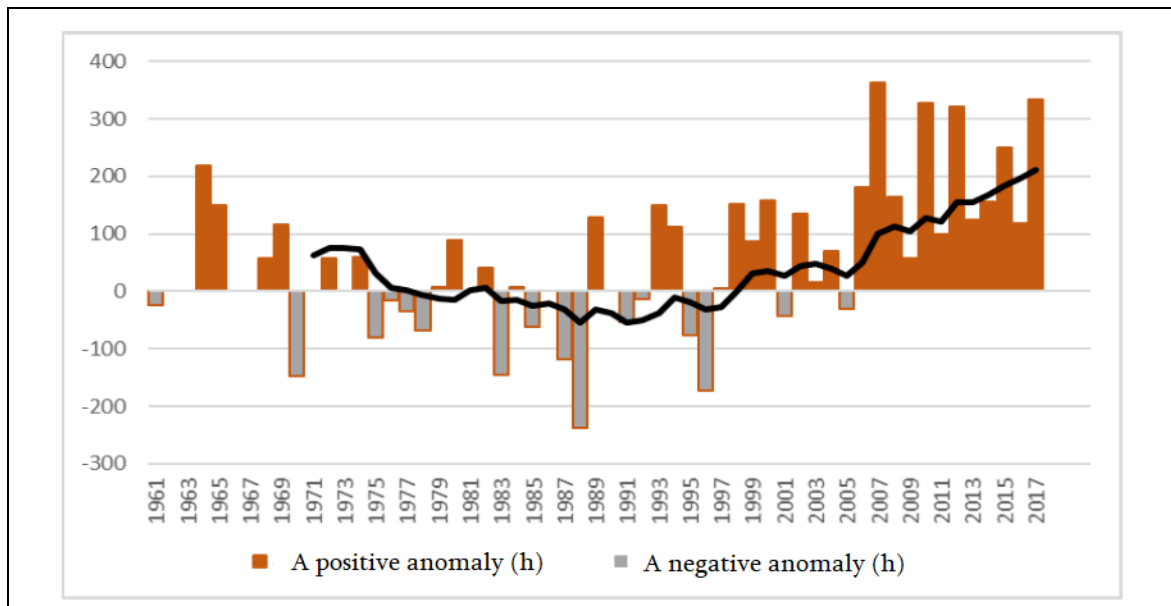


Fig. 3: Sunshine duration anomalies (relative to the period 1961-1990) 1961-2017 for the period and the 11-year moving average

The complex geological structure of the valley, seismotectonic conditions, high energy potential of the area (morphological conditions) and climatic changes create a favorable environment for the creation and activation of natural processes in the valley. However, it should be emphasized that until August 3, 2023, b. During the last 100 years, there has been no significant alluvial runoff in the Bubiscali reservoir.

Suppose that there are 5 models of natural geological and hydrometeorological phenomena. Each model estimates the risk of a particular event in %. In particular, such phenomena include: intensive melting of the glacier, precipitation in the form of rain, stone avalanches in the upper reaches, landslide-erosion processes and the passage of mudflows. Let's denote the risk assessment models for these events as A_1, A_2, A_3, A_4, A_5 respectively.

For each model, risk probability values should be calculated. These values are given in Table 1. These values are in the interval [20÷40].

Table 1: A_1, A_2, A_3, A_4, A_5 model risk probabilities

Models	Probability of success in %
A_1	38.9
A_2	30.2
A_3	20.5
A_4	27.8
A_5	23.6

The expert involved in the forecasting process analyzed the information obtained from the results of the observation (see Fig.4):

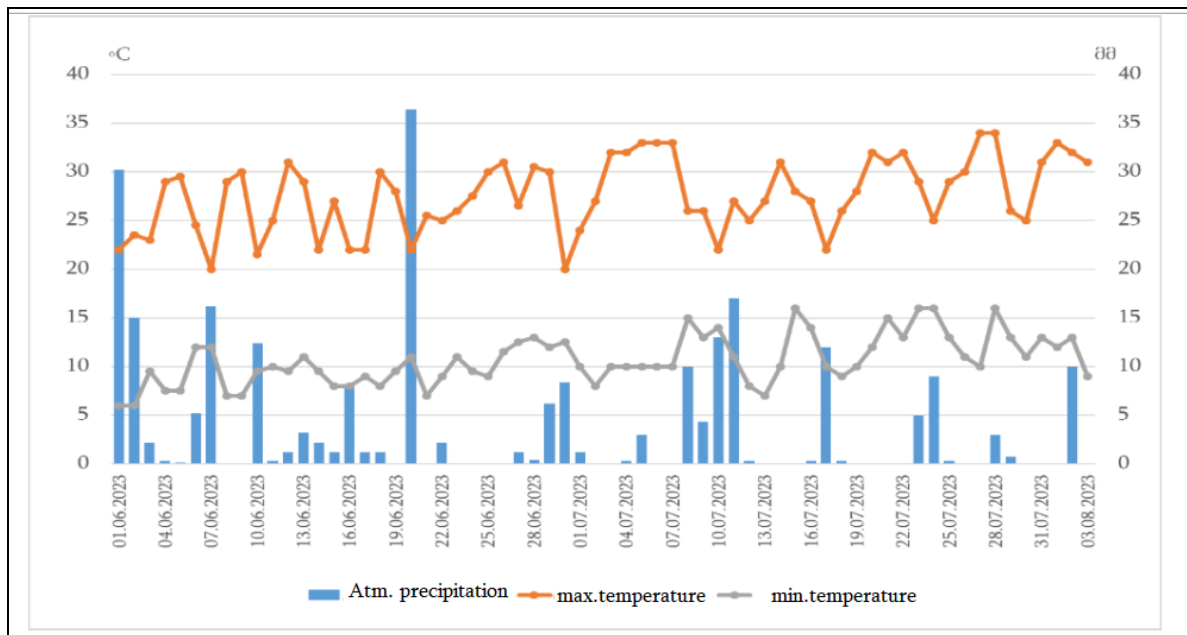


Fig. 4: Maximum and minimum air temperatures and precipitation for the period 01.06-03.08 2023, Shovi

It is worth noting the fact that, based on the analysis of data from a hydrological station (an automatic water flow meter) on the Chanchakh River, the river. There was no prolonged water stagnation in the Bubisskali valley either before the disaster or during the development of the disaster (see Fig.5):

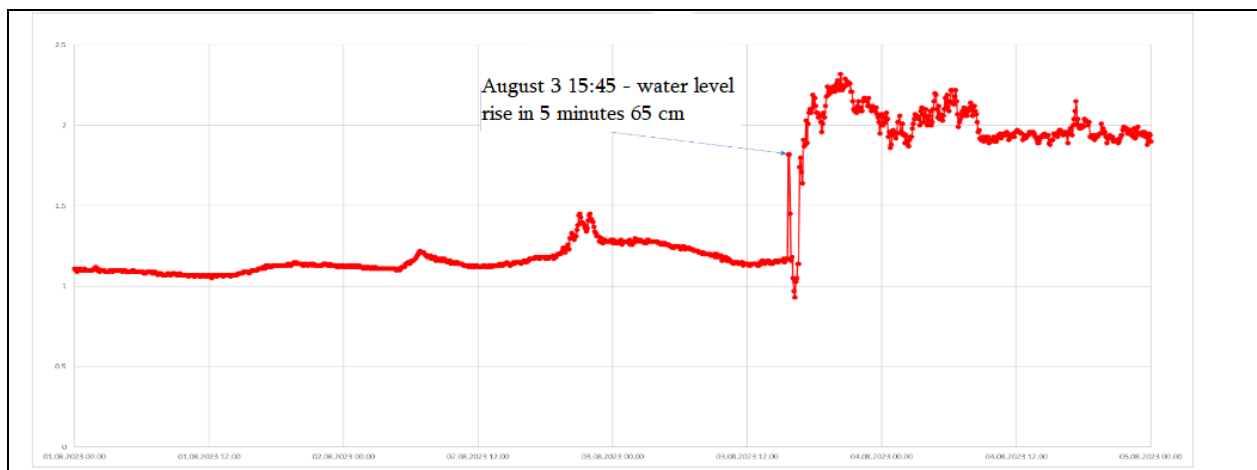


Fig. 5: Maximum water level (at the mouth of the Chanchakhi River, Rion River) and atmospheric precipitation (given) in the period 01.06-03.08.2023

The expert's conclusion about a sufficiently high hazard risk is based on the fact that all geological and hydrometeorological events coincide in time and occur in the same area, although each forecast gave a relatively low percentage of risk (from 20% to 40%) even under these conditions (combination in time and space) already necessitates a risk - a tragedy is expected. The sum of risks

of various events already exceeds 100%

V. Conclusion

We need a new approach to risk measurement because the existing models are outdated and do not serve the purpose for which they are intended.

The article considers a new model for predicting the risks of natural phenomena based on parallel data. He is in the same place and at the same time, and all these factors increase the risk of a natural disaster.

References

- [1]. Zhu X., Zhang G., Sun B. A comprehensive literature review of the demand forecasting methods of emergency resources from the perspective of artificial intelligence - *Natural Hazards*, 2019 – Springer.
- [2]. Gasitashvili, Z., Pkhovelishvili, M., Archvadze, N. Prediction of events means of data parallelism. *Proceedings - Mathematics and Computers in Science and Engineering, MACISE 2019*, 2019, pp. 32–35, 8944725. <https://ieeexplore.ieee.org/abstract/document/8944725>
- [3]. Aliyev, V., Gasitashvili, Z., Pkhovelishvili, M., Archvadze, N. Algorithm for Building a Hybrid Model of the Existing Risk model. *Reliability: Theory and Applications*, 2022, 17, pp. 106–110. http://www.gnedenko.net/Journal/2022_4%20SI.htm
- [4]. Aliyev V.A., Gasitashvili Z.A., Pkhovelishvili M.G., Archvadze N.N. Predictive Models: Necessary and Sufficient. // *Informatics and Control Problems*, 2023, v.43, issue 2, pp.30-34. www.icp.az
- [5]. Gasitashvili, Z., Pkhovelishvili, M., Archvadze, N. Reducing Risks through Improvement of Prediction Models. *Reliability: Theory and Applications*, 2022, 17, pp. 197–202.
- [6]. National Environmental Agency. Initial assessment of natural phenomena that occurred on August 3, 2023 in the gorge of Bubisskali (basin of the river Chanchakha). <https://nea.gov.ge/Ge/News/1178>

POSSIBILITIES OF LINEAMENT ANALYSIS OF DEM SRTM DURING GEODYNAMIC ZONING OF SEISMIC HAZARDOUS TERRITORIES

(on the example of the North-Tien-Shan region)

Aleksandr Fremd, Arailim Gaipova, Dinara Talgarbaeva



Institute of Seismology of the Ministry of Emergency Situations of the Republic of Kazakhstan
afremd@list.ru

Abstract

Lineament analysis of space images can be successfully used for the purposes of formalized analysis and development of maps of geodynamic zoning with the ranking of the study area into areas that differ in the degree of relative geodynamic activity.

As calculated indicators of geodynamic (neotectonic) activity, the density of faults, megacracks and other lineaments, expressed by their total length per unit area, was used. Therefore, the parameter "density of strokes" is taken as the basis for the taxonomic division of the study area into regions according to the degree of tectonic disturbance of the earth's crust. All constructions are implemented on the basis of lineament analysis included in the CATALIST software package (Canada)

On the example of two seismically hazardous regions of the Northern Tien Shan (Almaty and Zhambyl), the distribution features and properties of lineament density parameters are illustrated, followed by the construction of maps of geodynamic activity.

The lineament analysis of the DEM SRTM of the regional level of generalization made it possible to establish the main features of the geodynamics of the regions - Zhambyl and Almaty regions at the present stage.

The results obtained have proven their effectiveness and the ability to conduct an objective assessment of the seismicity of the territories, the reliability of which is confirmed by seismological and other ground-based observation data.

Keywords: geodynamics, seismicity, lineament analysis, zoning, seismic risk

I. Introduction

Lineament analysis of space images, which became widely known thanks to the work of Zlatopolsky A.A. [4], Bondura V.G. [1], Kopylova I.S. [5], etc., can be successfully used for the purposes of formalized analysis and development of maps of geodynamic zoning with the ranking of the study area into areas that differ in the degree of relative geodynamic activity.

It was found [5] that one of the most important calculated indicators of geodynamic (neotectonic) activity is the density of faults, megacracks and other lineaments, expressed as their total length per unit area. Therefore, the parameter "density of strokes" is taken as the basis for the taxonomic division of the study area into regions according to the degree of tectonic disturbance of the earth's crust.

But the network of lineaments reflects not only the structural block divisibility of the lithosphere, but also its integral and modern stress state, which manifests itself in different orientations of fault systems that characterize modern geodynamic activity of various scales, from

planetary to local. Maps that make it possible to judge the distribution of possible areas of increased geodynamic risk are maps of the density of the intersection nodes of differently directed lineaments.

Thus, the use of lineament analysis of space images provides complexity and consistency as necessary components of solving the problems of identifying zones of geodynamic activation and, in particular, on the territory of the Tien Shan seismically active region.

II. Methodology

Characteristics of the fault tectonics of the North-Tien-Shan region

The territory of the North Tien Shan region is a vast area of modern geodynamic processes, located within the boundaries [(67-75) o in longitude and (39-43) o N], which by the time of formation belongs to the Paleozoic.

It is believed that the Late Cenozoic orogeny of the Tien Shan was caused by the collision of the Hindustan continent with Eurasia. The kinematics of active faults and GPS data indicate that the direction of horizontal compression of the Tien Shan region at that time was close to meridional [12].

The main conclusion of the author [9] is that “during the Late Cenozoic deformation of the Tien Shan, in most cases, new faults did not arise, but movements along the Paleozoic faults occurred.” That is, the Late Paleozoic faults “revived” in the regional deformation fields that arose during earthquakes [9,10].

The fault tectonics of the Zhambyl and Almaty areas of study are characterized by rose-direction diagrams (Figure 1-A, B), built according to the DEM SRTM and [7].

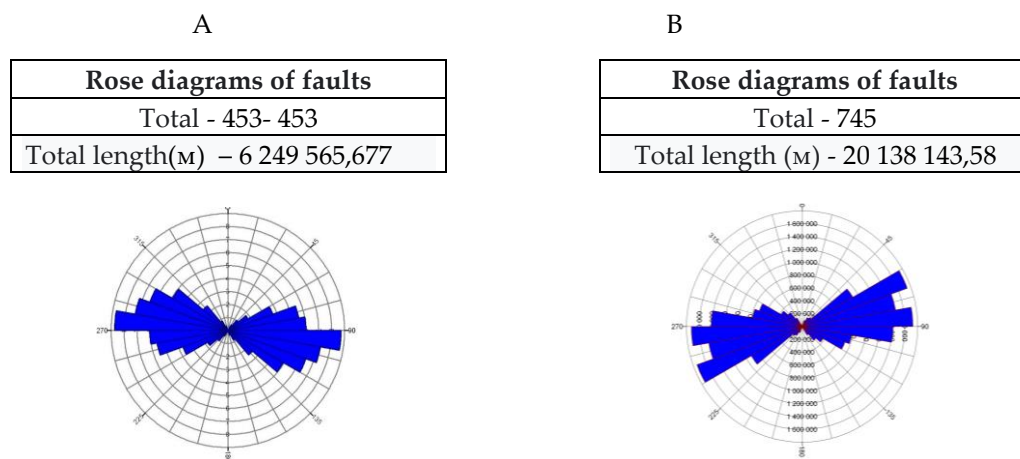


Fig. 1: Rose diagrams of faults in Zhambyl (A) and Almaty (B) regions North-Tien-Shan region according to the DEM SRTM

Comparison of the radiation pattern (Figure 1-A) constructed for 453 faults identified by the SRTM DEM in the Zhambyl sector of the North Tien Shan region with the patterns given in [9] suggests that most of them can be attributed into the category of active ones, i.e., those in which progress occurred in the recent past and, therefore, is possible in the near future [13].

An analysis of the distribution of all faults identified by the DEM SRTM (745 faults) for the Almaty sector showed that the sublatitudinal strike direction of about 75o is dominant and statistically significant (Figure 1-B). It is with this direction that most of the distinguished elements

of fault tectonics are associated, which coincides with the strike of modern geodynamically active faults and corresponds to the main strike of mountain ranges in this region

I would like to emphasize that, according to the authors of [15], the Northern Tien Shan is undergoing intense compression in the north-north-west direction, which corresponds to the sublatitudinal strike of ridges, depressions, faults, and other structural elements. But at the same time, it "is in conditions of vertical expansion, which manifests itself as an uplift of the earth's surface"[15]. Such a ratio of forces of external influence inevitably generates inhomogeneities of the deformation field and movements of the earth's crust, leading to the conclusion about the existence of blocks of the earth's crust moving at different speeds, which "interacting with each other, change their position and deform" [15].

The characteristics of such blocks are considered in detail in [11].

To complete the characterization of the nature of the seismicity of the region, we note that, according to the results of complex geophysical studies in the structure of the earth's crust of the Tien Shan, a feature was revealed - "the existence in its composition of two parts: the upper - brittle, 16-25 km thick and the lower - plastic thickness of 30-35 km " [14].

Observations of the hypocentricity of the sources showed that the sources of earthquakes with $M \sim (2.5 - 4.5)$ occurred at depths of 5–25 km; Almost all earthquakes are recorded in the fragile layer of the Earth's crust [14].

And the very nature of seismicity is explained by the structure of the upper mantle - the existence of areas of deconsolidation on a cut, 67 km deep (crust / mantle boundary zone), which became the main reason for the intensive uplift of these mountain systems. According to the authors of [13], plumes and associated intramantle flows are the source of left-handed displacements along sublatitudinal faults.

Methodology for processing and building maps

The advantage of DEM over optical images is that only relief elements are involved in the analysis and brightness anomalies caused by other sources (vegetation, technogenic objects) are excluded, which means that there are no errors in assessing the presence of structures of a different direction [5].

In order to select a variant that emphasizes the systems of the known fault-block divisibility of the North Tien Shan region in the most contrast, known fault lines were superimposed on the maps.

For their processing and construction, a standard set of software for lineament analysis of the PC "CATALIST" ("GEOMATICA"), ArcGIS, as well as author's programs were used. The processing parameters were selected empirically, i.e. subjectively. These are the search radius - 5 km and the minimum length of the stroke (fault) - 2 km.

To build maps of geodynamic activity, the lineament density parameter was used, which in the context is identified with the density of faults, megafractures, expressed in their total length per unit area and can be used as one of the indicators of geodynamic activity [5].

III. Results

Characteristics of directionality and density of lineaments in the territories of regions

The purpose of this study is the development and verification of maps of regional geodynamic activity based on the lineament analysis of the DEM SRTM of the average spatial resolution of the territories of the Zhambyl and Almaty regions of the North Tien Shan region.

Zhambyl region

As already noted, as the initial data, materials of the first level (Level-1) radar topographic survey (Shuttle radar topographic mission (SRTM)) with a resolution of 30 meters were used, which approximately corresponds to the topographic base at a scale of 1: 100,000

As a result of processing the SRTM DTM, maps of the distribution of lineaments were built, which were subsequently converted into density maps, followed by the construction of a rose pattern (Fig. 2).

It is obvious that the distribution of lineaments over the area can be called multidirectional and does not unambiguously characterize unconditionally and in detail the fragmentation of the earth's crust. One can rather assert about the different spatial organization and mapping of the structural features of the relief. But at the same time, the integral component of their distribution and the strike of fault lines, of course, correlate with each other (Fig.2, A). This fact shows itself well on the lineament density map (Fig.2, B).

In essence, areas of high density values can indicate the presence of a regional fault or its elements, as well as contribute to the identification of ring structures and the formation of an estimate of the block divisibility of the lithosphere and even a number of its other properties related to kinematics and SSS. Therefore, the distribution of lineaments should be considered as a set of systems that reflect the internal patterns of the tectonophysical structure and state of the object of study [6].

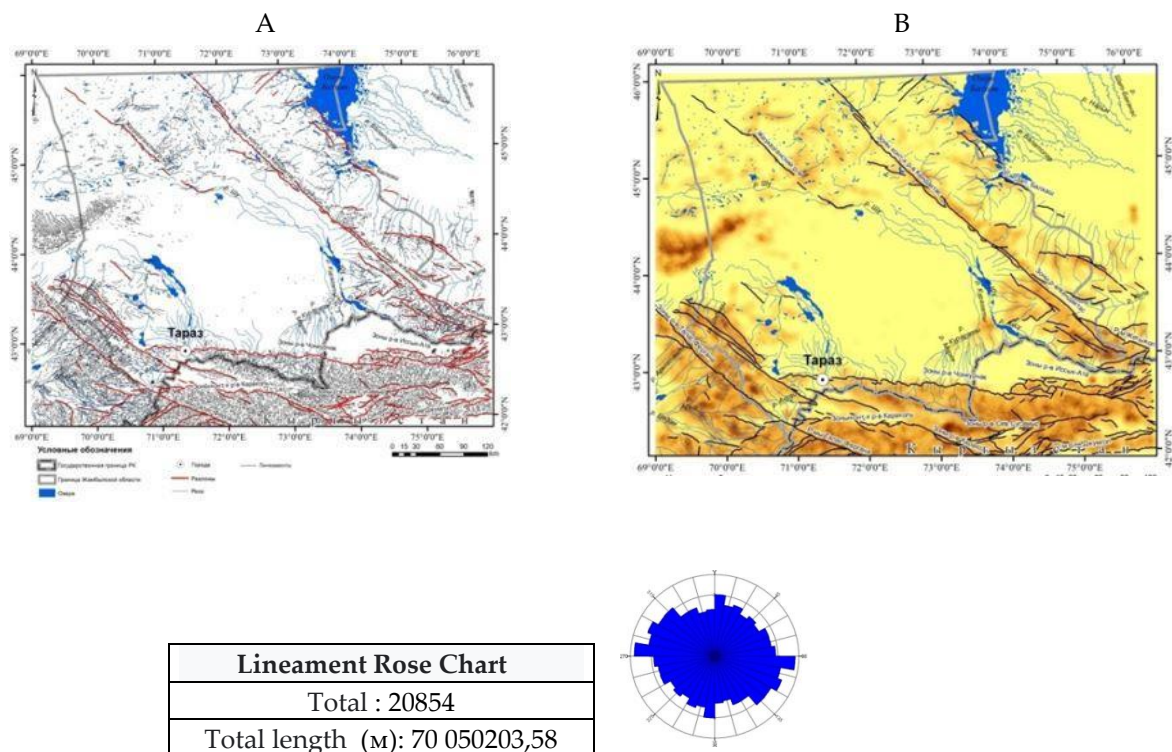


Fig. 2: Maps of the distribution of lineaments (A) and their density (B) on the territory of the Zhambyl region.

The directivity diagram shows (Fig.2) that although the identified lineaments reflect the dominant direction of the known faults (Fig.3), at the same time, it contains a meridian maximum and statistically representative multidirectional elements, which together can characterize the fragmentation of the region's crust.

And here it is useful to consider the distribution of lineaments, or rather their density index in connection with seismicity, as well as their role in revealing hidden faults that are not mapped on the earth's surface.

The relationship between the density of faults, their activation, and the location of earthquake sources was previously considered in a number of works for various regions [2, 8, etc.]. It is shown that manifestations of seismicity are most likely where there is a high fracture density. And even, moreover, a direct correlation between the density of faults and magnitude has been established.

But at the same time, it is noted that a fragmented medium is not able to accumulate significant stresses necessary for the occurrence of strong earthquakes and is characterized mainly by weak, but frequent manifestations of seismic activity [2].

The territory of the region is characterized by numerous low-magnitude epicenters of the order $M= 4.0-6.0$, which cover the entire area, but to a greater extent gravitate towards zones of increased density of lineaments and associated faults.

Such energy of seismicity may indicate a high fragmentation of the region's crust and the possible existence of hidden small blocks that experience multidirectional movements with subsequent discharge of low stresses. Strong earthquakes occur at the boundaries of large-block structures and are confined to zones of medium increased density [2].

Structurization (correlation) of zones of high density of lineaments and known manifestations of seismicity can be more obvious if we consider a map of the density of nodes of their intersection and the distribution of epicenters.

As shown in Fig.3-A, the high-intensity lineament intersections generally correlate well with known fault lines. But in some cases this is not obvious and can be explained by the fragmentation and multidirectionality of block displacements.

The distribution of epicenters does not contradict this conclusion, but it is difficult to visually illustrate the direct dependence due to their mass character and crowding (Fig.3-B). Although in general, it can be argued that the ratio of epicenters and lineament intersection nodes shown in Figure 7 indicates that seismic manifestations are to a certain extent associated with areas of moderate and relatively high density of intersection nodes. This indicator can be considered a conditionally necessary sign of the geodynamic activity of both faults and those structural elements that fall into the zone of their geodynamic influence.

From the comments made on the density maps, it follows that the lines of regional faults are in good qualitative agreement with the strike of the values of the anomalous density of the lineaments and, in the first approximation, they can be used as an indicator of the detection of faults, taking into account the known geological and geophysical data.

The length of lineaments, their density and connection with earthquakes.

If we talk about lineaments as breaks in the continuity of the crust, then it should be taken into account that the magnitude of an earthquake is affected precisely by the length of the lineament [3].

That is, the relative strength of earthquakes depends on the degree of fragmentation of the crust (fault length) and, therefore, it seems necessary to consider the correspondence of this indicator to the North Tien Shan region. Indeed, in essence, this is a mapping of lineaments of different ranks, as projections of deep faults on the earth's surface in their connection with seismicity.

As a result of the constructions, it turned out that there is no differentiation of lineaments of different lengths over the area. but in general, lineaments 1–3 km long predominate. Their density significantly exceeds the density of other groups and especially the 5-20 km group. Although the latter, in fact, are represented everywhere. And, consequently, earthquake epicenters and density anomalies retain their spatial similarity.

This implies the conclusion that large and ubiquitous, but less representative in number, faults can play a significant role in the manifestations of the geodynamic activity of the region.

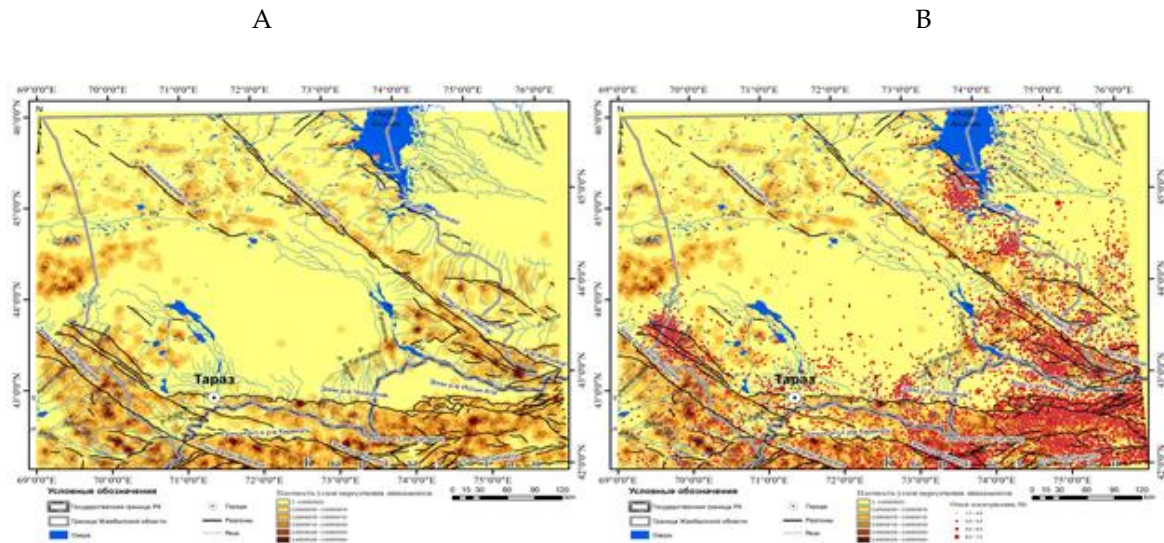


Fig. 3: Density map of lineament intersection nodes (A) and their relationship with earthquake epicenters (B) of the Zhambyl region

Characteristics of lineament density maps by directional sectors

The construction of density maps for lineaments of different lengths made it possible to identify directions that are of interest from the point of view of assessing the territorial zonality of a possible manifestation of seismic activity.

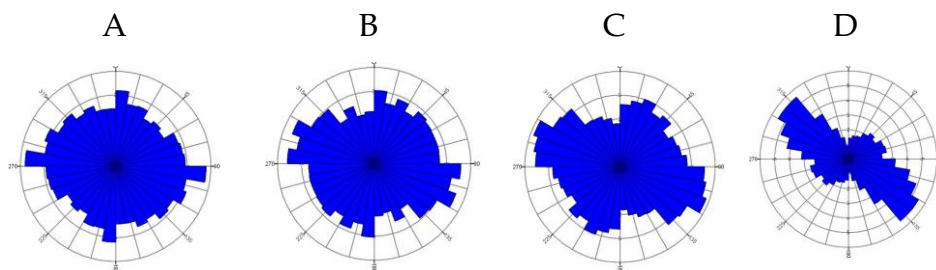


Fig. 4: Rose diagrams for lineaments with length: A - (1-2) km; B - (2-3) km; C - (3-5) km; D - (5-20) km

Taking into account the dominant directions shown in the diagrams (Fig.4), the sectors were determined and the corresponding density maps were built based on the base maps of the density and the density of intersection nodes for lineaments with a length of 2 km.

For the diagram (Figure 4, A), two sectors were chosen: (0-10)° - submeridional and (90-100)° - sublatitudinal.

The distributions of lineament density values obtained for these two directions (Fig.5) showed that the main contribution to the distribution of lineaments over the area with a lineament length of 2 km is associated with submeridional orientation.

Sublatitudinal lineaments dominate in the southern part of the Northern Tien Shan (Fig.5, C). If we turn again to the length, it should be noted that sublatitudinal lineaments with a length of 3 km or more do not make a significant (quantitative) contribution to the overall pattern of lineament distribution density and thereby reduce the seismogenic potential of strong earthquakes in the region. Although, of course, they cannot be ignored.

This implies that seismic activity in the region is mainly due to lineaments up to 3 km long, which form the main and, as mentioned above, a small fault-block structure (Fig.5).

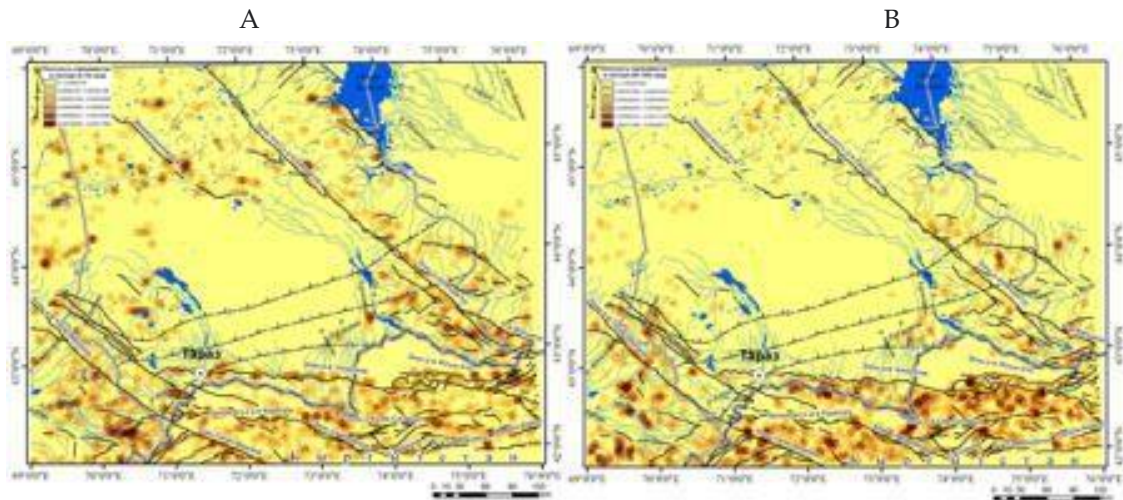


Fig. 5: Lineament density distributions for sectors: (0-10)^o - A and (90-100)^o - B in the territory of the Zhambyl region

Lineament Rose Chart
Total: 3 418
Total length (m): 29 144 304,39

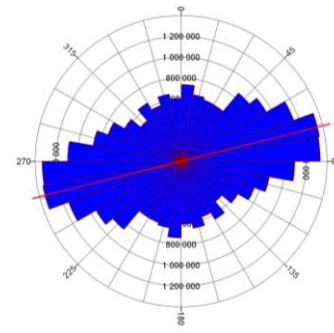


Fig. 6: Rose-diagram of lineaments of all directions of the Almaty region

Almaty region

The SRTM DEM of the Almaty region was processed to extract lineaments and build density and node density maps.

An analysis of the distribution of all lineaments identified by the DEM SRTM (3418 pieces) showed that the sublatitudinal strike direction of about 75° is dominant and statistically significant (Fig.6). It is with this direction that most of the distinguished elements of fault tectonics are associated, which coincides with the dominant direction of the faults (Fig.1, C). But, at the same time, a fairly large number of lineaments are associated with others, including submeridional strike (Fig.6).

As well as for the Zhambyl region, the calculation of the lineament density map was carried out for strokes exceeding 2 km in length (Fig.7). The results of the performed calculations are shown in Fig.7 (A, B). It is obvious that the zones of geodynamic activation are associated with areas of the highest density. This is confirmed by the position of the epicenters of all the largest earthquakes (Fig.7, B). As is known [2], the high density of lineaments is associated with fault crossing zones, which, in turn, reflect the geodynamic activity of fault areas.

It has been established that the manifestations of seismicity in the region are to a certain extent associated with areas of moderate and relatively high density of intersection nodes. This

the general situation, which, of course, may have its own specific features in the manifestation of seismicity.

The density map of lineament intersection nodes shown in Figure 9 reflects the main manifestations of seismicity in the North Tien Shan region for the foreseeable period of time.

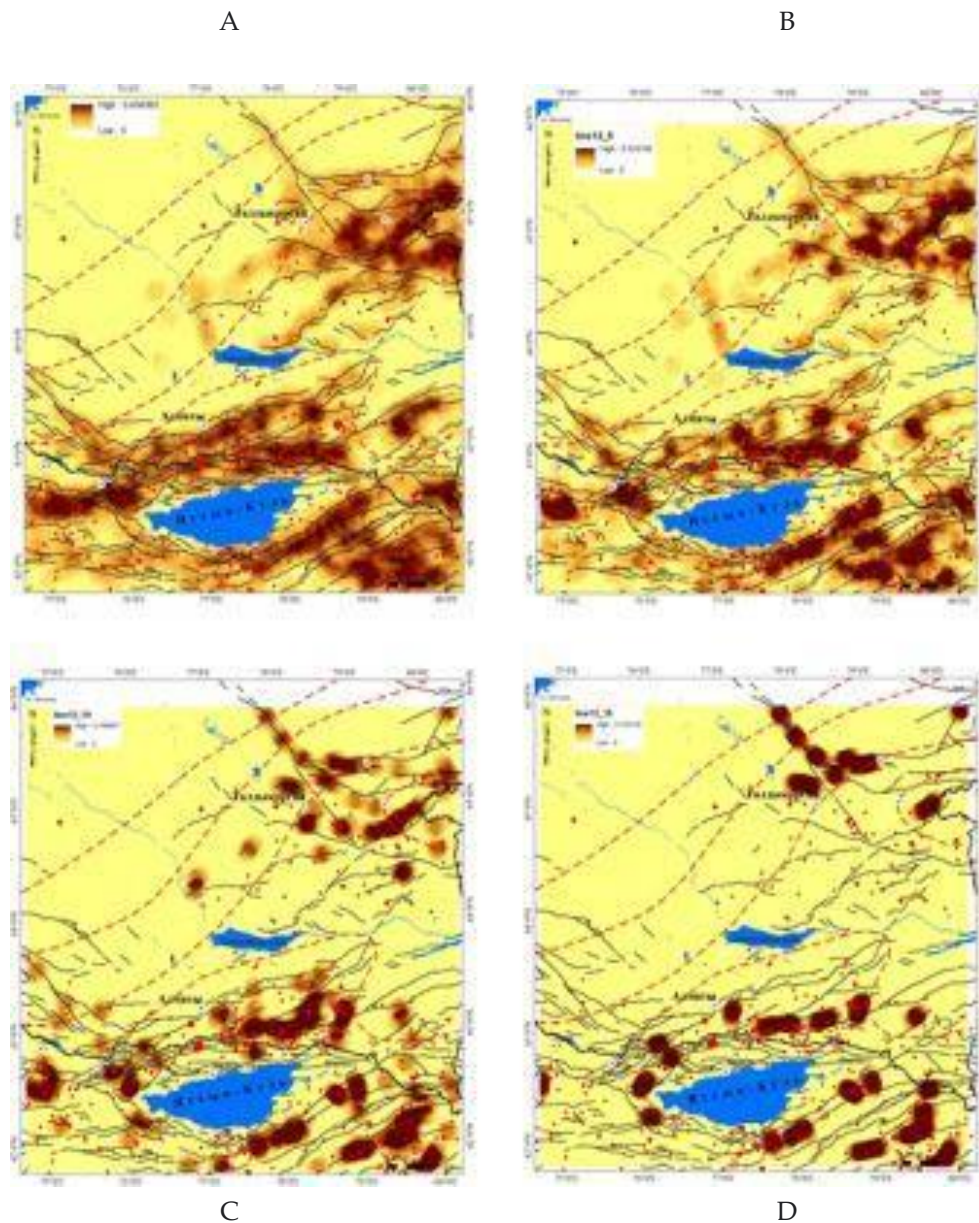


Fig. 8: Distribution maps of lineament density values for conditional lengths of faults (in km):
2-A; 5-B; 10-C; 15-D.

Obviously, with a conditional fault length of 5 km, one can see both the main sources of earthquakes and the background against which they occur. In particular, the sources of strong earthquakes described above manifested themselves in lineaments (faults) with a length of 5 km.

Characteristics of lineament density maps by sectors

The purpose of this section is to show the possibility of zoning according to directions in connection with seismicity - a preliminary assessment of zones of geodynamic activation.

Preliminary zoning of the territory of the Almaty region of the North Tien Shan region according to the degree of geodynamic activation was carried out on the basis of the distribution of lineament intersection nodes, which essentially fix not only the areas of the highest density of

differently directed faults, but also their connection with the directions of the main tectonic faults prevailing in a particular sector and epicenters of known earthquakes.

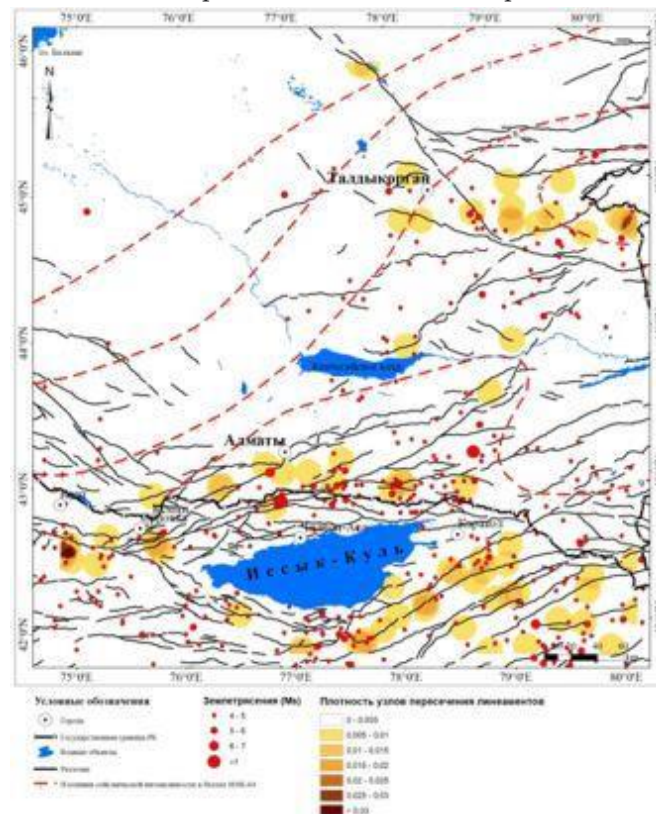


Fig. 9: Density map of lineament intersection nodes for conditional the length of the fault is 5 km.

Taking into account the rose diagram shown in Fig.6, a set of maps of the distribution of intersection nodes by sectors was formed, giving a visual representation of the location of zones of geodynamic activation and associated active faults of one direction or another.

Thus, in the sector $(0-37)^{\circ}$, the intersection nodes form a curvilinearly elongated area, passing in close proximity to the city of Almaty, but characterized by earthquakes of relatively small magnitude (4-5). And the epicenters of strong earthquakes are, as it were, in the area of "seismic calm". At the same time, it can be seen that the epicenters of strong earthquakes close to Almaty are associated with faults located in the $(140-180)^{\circ}$ sector. There is also an area elongated in the sublatitudinal direction that controls low-magnitude earthquakes in the southeastern sector. At the same time, the epicenter of a strong, but relatively remote from Almaty earthquake is located in the sector $(0-37)^{\circ}$.

The above example testifies not only to the connection of earthquake sources with zones of high density of lineament intersection nodes, which in turn characterize seismically active faults, but also, most importantly, retrospectively shows the degree of geodynamic hazard of differently directed faults. This circumstance must be taken into account when calculating the degree of seismic hazard associated with the direction of external forces on certain parts of the earth's crust.

Maps of regional geodynamic activity of the territory of the North-Tien- Shan region

In accordance with the methodology for zoning the territory according to the degree of geodynamic activity proposed by A.S. Kopylov [5], an analysis of the SRTM DEM was performed with the construction of lineament maps for the North Tien Shan region and their subsequent ranking in terms of density, expressed in their total length by area unit.

Zhambyl region

Fig.10 shows a map of regional geodynamic activity for the territory of the Zhambyl region.

According to the proposed methodology, relief and lineaments act as a form of displaying a geodynamic activity model that can be ranked and then converted into appropriate maps, from stable to highly active (Fig.10).

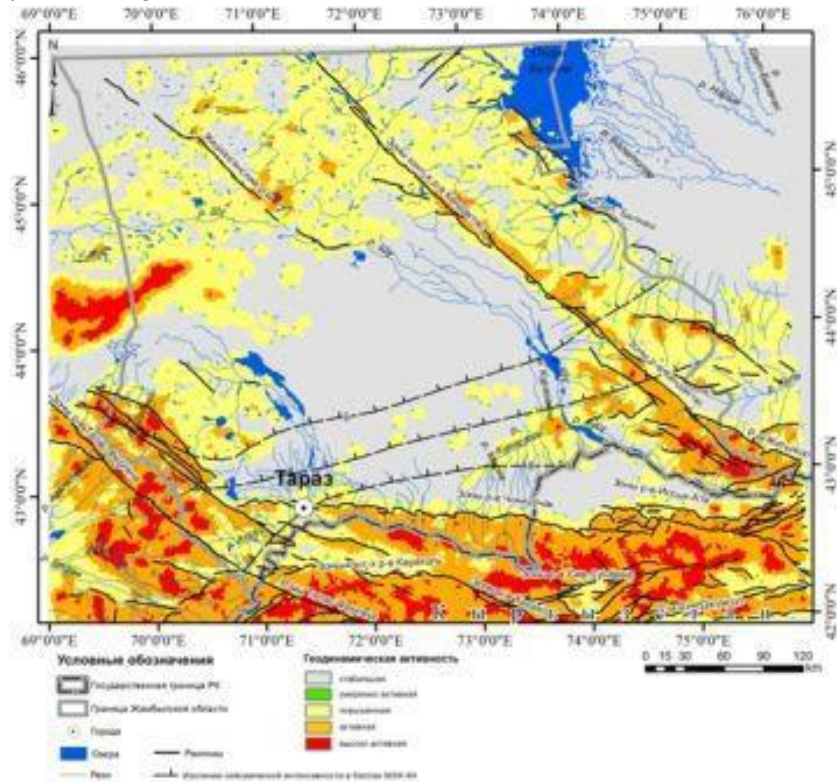


Fig. 10: Map of regional geodynamic activity of the Zhambyl region

Upon closer examination of the completed constructions, it can be noted that all highly active areas are located in the zones of geodynamic influence of regional faults. First of all, the Talas-Fergana fault and its continuations in the form of separate fragments located in the southern part of the Tien Shan region stand out.

As a rule, all highly active and active zones are confirmed by the location of the epicenters of weak earthquakes. For example, the Kendyktas fault, located in the active zone, is also marked by a large number of epicenters.

The city of Taraz itself is located in a zone of moderate activity at the junction of two active zones, and an isoseist of 8 points passes through it. But a significant part of the territory is characterized by the degree of geodynamic activity as "stable" and "increased".

At the same time, the entire southern and flank zones of the region are areas characterized as "active" and "highly active", which are crossed by numerous faults of varying degrees of activation.

Based on the opinion of the authors of [9] and the distribution map of epicenters, it can be assumed that all recent movements are associated with small-block slips without the formation of new large modern ruptures.

That is, the geodynamic activity of the region as a whole can be called moderate with some manifestations of activity in the zones of hidden faults.

Verification of the constructed maps with the map "Typification of the Zhambyl region according to the morphological conditions for the formation of geodynamic processes" showed that fragments of high activity zones correspond to areas of active contrasting recent movements and recent uplifts.

Thus, if we consider lineaments as an indicator of fragmentation of the crust, then, as was established earlier [3, 19], earthquake epicenters gravitate towards zones of increased fault density. Moreover, the higher the density, the higher the magnitude.

But on the other hand, it is known that a fragmented medium is not able to accumulate large stresses and their discharge is accompanied by weak, but frequent earthquakes.

In the region under consideration, by definition [9], all geodynamic processes are inactive and are associated with known regional faults. But at the same time, numerous epicenters of small magnitude indicate that the seismicity of the region is due to small blocks and movements along hidden faults separating them.

To assess the degree of reliability of the results obtained, verification was carried out, which confirmed the main conclusions about the distribution of GAS in the Zhambyl region.

Almaty region

Upon closer examination of the completed constructions (Fig.11), it can be noted that all highly active areas near the city of Almaty are in the zone of geodynamic influence of the Chilik-Kendyktas fault. There are other objects that also require a close study of the manifestations of seismicity.

To increase the reliability of the constructions made and the conclusions that follow from them about regional seismicity, a map of "engineering-geological zoning of Kazakhstan under the conditions of the formation of dangerous geodynamic processes" was used (V.P. Bochkarev, S.A. Novitsky, etc., 2004, M 1:2 000 000) - see inset in Fig.11.

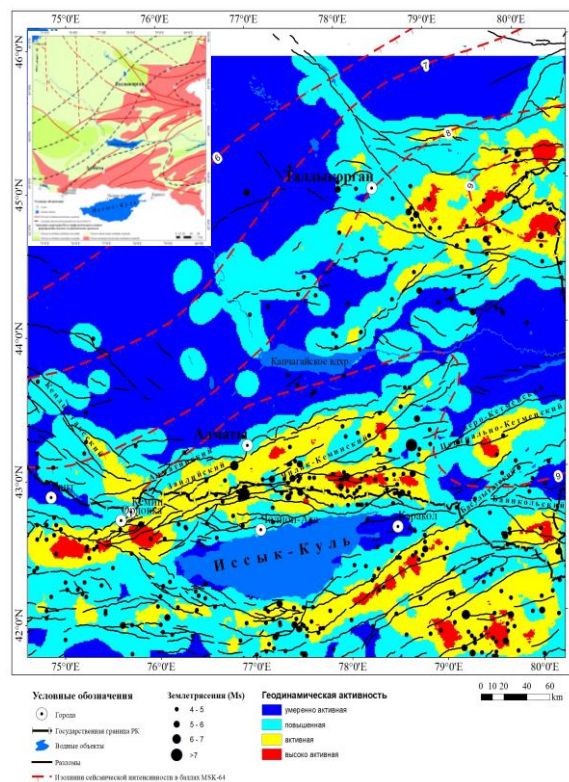


Fig. 11: Map of regional geodynamic activity of the Almaty region

Comparing it with maps of geodynamic activity, we can conclude that the areas identified as "active" and "highly active" correspond to areas of significant recent uplifts. There are also areas of the highest geodynamic activity (Fig.11).

It follows from the foregoing that the lineament analysis of the regional level of generalization makes it possible to establish the main features of the distribution of epicenters in their connection with the distribution of the values of the density parameter of the elements of fault-block divisibility in the Almaty region.

The performed zoning made it possible to establish the location of both the seismic calm zone and the zones of increased seismic background.

Thus, the geodynamic analysis of the lineament density made it possible to zoning the territory of the region according to the degree of geodynamic activity. The resulting maps provide a visual representation of the distribution of geodynamically active zones (GAZ), which include areas with high fracturing, characterized by high contrast relative to the background. Large GAS have a complex mosaic structure.

In general, all this gives grounds to believe that the lineament analysis of the SRTM DTM allows for an objective assessment of the seismicity of the territory, the reliability of which is confirmed by seismological and other ground-based observation data.

IV. Conclusion

The lineament analysis of the regional level of generalization made it possible to establish the main features of the geodynamics of the regions - Zhambyl and Almaty regions at the present stage.

The performed ranking and construction of maps of geodynamic activity of the regional level of generalization can be considered indicative in two positions.

In the methodological plan, a technology was tested for using satellite data to solve the problems of regional geodynamic zoning of the territories of seismically hazardous regions.

Moreover, the proposed calculation options generally give an idea of other methodological possibilities of using satellite images in solving seismological problems.

On the other hand, results have been obtained that give an independent idea of the geodynamics of the geological environment with the construction of appropriate maps for ranking territories according to the degree of potential geodynamic activity.

The proposed zoning options and their characteristics cannot and should not be limited to the presented maps. They are the basis for a detailed tectonophysical analysis of the geodynamic situation, including the use of SSS.

In particular, they can be used to establish a correlation between the density of lineaments and earthquake energy, to identify patterns in the spatial distribution of epicenters of strong earthquakes with a degree of fragmentation of the crust, to identify the spatial relationship of earthquakes with fault intersection nodes, to identify the sizes of zones of geodynamic influence of large extended faults, a retrospective analysis of the geodynamic fault activity in the areas of deposits, etc. That is, the solution of those problems that can contribute to the discovery of regular relationships between the manifestation of seismic activation and the geotectonic structure of a particular region, and without which an objective assessment of the seismic potential of seismically active territories is impossible.

Ideally, all these studies should be accompanied by monitoring of displacements of points on the earth's surface of the areas under study with the construction of appropriate maps based on the interpretation of satellite radar data and seismological observations.

Summarizing the above, one can quote Sherman S.I. et al. [2]: "the fault density parameter should be considered more broadly as a very informative indicator of the tectonophysical properties of the fragile lithosphere", which, in combination with SSS and other parameters, contributes to "the identification of patterns of fault activation and modern fault formation in the lithosphere."

Acknowledgements. The work was carried out within the framework of the Program "Improvement of scientific and methodological technology for forecasting strong earthquakes in earthquake-prone territories of the Republic of Kazakhstan according to the data of integrated ground-space monitoring" for 2021-2023.

References

- [1] Bondur V.G., Kuznetsova L. Space monitoring of the geodynamics of seismically hazardous territories using the method of lineament analysis. Proceed. of 31st Int. Symp. on Remote Sensing of Environment, St. Petersburg, 2005
- [2] Sherman S.I., Zlogodukhova O.G., Demyanovich V.M., Density of faults, its influence on seismic process and fluid permeability of the lithosphere. Proceedings of the Siberian Branch of the Section of Earth Sciences of the Russian Academy of Natural Sciences. No. 5 (31), 2000 - S. 68-77.
- [3] Goldin S.V. Macro- and mesostructures of the source area of the earthquake. Physical mesomechanics 8 1, 2005, pp. 8-14
- [4] Zlatopolsky A.A. WinLESSA Version 3.3.2: user manual. - 2011. - 30 p.
- [5] Kopylov I.S. Scientific and methodological foundations of geocological research oil and gas regions and assessment of the geological safety of cities and facilities using remote methods: dis. ... doc. geological and mineralogical sciences: 25.00.36 / Perm State National Research University - Perm, 2014. - 351 p.
- [6] Tvertinova T.Yu. Lineaments as a reflection of the structural framework of the lithosphere (Lineaments - faults or phantoms?) Electronic scientific publication Almanac Space and Time. T. 4. Issue. 1, 2013, Special issue SYSTEM PLANET EARTH
- [7] Geological Institute of the Russian Academy of Sciences. Laboratory of tectonics and modern geodynamics. Description of the database of active faults in Eurasia http://neotec.ginras.ru/index/database/database_04.html
- [8] Vashchilov Yu.Ya. Kalinina L.Yu. Deep faults and lineaments and location of earthquake epicenters on land in the northeast of Russia. and. "Volcanology and seismology", 2008, No. 3, 19-31.
- [9] Burtman V.S. Fault systems in the upper crust of the Central Asian Fold Belt Izv.
- [10] Burtman V.S. Disjunctive dislocations in the upper crust of the Tien Shan. REPORTS OF THE ACADEMY OF SCIENCES, 2019, volume 484, no. 3, p. 316-319
- [11] Abdrakhmatov K.E., Dzhanabilova S.O. The latest fault-block structure of the northern Tien Shan and seismicity. Bulletin of the Institute of Seismology of the National Academy of Sciences of the Kyrgyz Republic No. 1(7), 2016. P.8-16.

[12] Burtman V.S. Tien Shan and High Asia: geodynamics in the Cenozoic. Moscow: Geos, 2012. 187 p.

[13] Trifonov V.G., Zelenin E.A., et al., Active Tectonics of Central Asia. GEOTECTONICS, 2021, no. 3, p. 1–18.

[14] Tychkov S.A., Kuchai O.A. et al., The nature of contemporary deformations of the northern Tien-Shan. (geodetic and seismological data). Geology and Geophysics, 2008, v. 49, no. 4, p. 367-381

[15] Kostyuk A.D., Sycheva N.A. et al. Deformation of the earth's crust of the Northern Tien Shan data of earthquake sources and space geodesy. PHYSICS OF THE EARTH, 2010, no. 3, With. 52–65.

TERRITORIAL RISKS ASSESSMENT OF NATURAL HAZARDS

Ulyana Postnikova^{1,2}, Olga Taseiko^{1,3}, Maksim Anikin³

¹Federal Research Center for Information and Computational Technologies, Russia

²Siberian Federal University, Russia

³Reshetnev Siberian State University of Science and Technology, Russia

ulyana-ivanova@inbox.ru

Abstract

The socio-economic development of the territories is determined by the solution of state policy tasks, the effectiveness of the application of organizational and managerial practices, the prediction of possible dangerous events and the adoption of measures to reduce the risk of accidents and natural disasters. Modern trends in territorial administration are associated with the use of a risk-based approach. Information on the frequency of occurrence of adverse events can serve as a basis for identifying sources of various risks levels. The presence of an unstructured data array predetermines the need to create an interconnected system of risk factors. The purpose of the study is to analyze the vulnerability of the Krasnoyarsk region territories to hazardous natural phenomena. This paper analyzes floods and forest fires, which are the most typical natural hazards for the areas under consideration. To identify areas most prone to natural hazards, a ranking was carried out according to the level of risk using GIS technologies.

Keywords: risk-based approach, natural hazards, territorial management

I. Introduction

Improving the security of the territory (country, region, municipality) in the face of the possible implementation of natural and man-made disasters is one of the key tasks in the framework of sustainable development. Technogenic and natural emergencies are significant sources of danger and risk to the life of the population. Recently, the risk-based approach has been widely used in various fields of research. A significant number of works [1-8] are devoted to the issues of risk analysis. However, the currently existing regulatory and methodological base for the quantitative assessment of hazards requires significant additions, which is complicated by the difficulty of analyzing natural disasters. Effective territorial management should be based on determining the level of threats to life, the range of risk factors and their significance.

Floods are one of the most dangerous natural phenomena that occur as a result of changing weather conditions. Heavy rains, a large amount of snowfall are prerequisites for floods. The main cause of destruction is the impact on buildings and structures of hydraulic shocks of water masses, ice floes floating at high speed, various debris, watercraft, etc. [9]. In the region, floods are mainly caused by spring floods, high summer-autumn rain floods, high water levels during jam events, as well as flooding of the area due to the destruction of reservoir dams, rupture of dams [10]. According to the data of the Yenisei Basin Water Administration and the materials of state reports, more than 1,000 floods occurred on the territory of the Krasnoyarsk Territory from 1967 to 2021, in which more than 50 thousand people suffered.

In the Krasnoyarsk region, the problem associated with an intensive decrease in the area of the forest fund is especially acute. The reduction of the forest fund is one of the global environmental problems, which leads to additional threats associated with a decrease in biodiversity, weakening of water regulation and protective functions. The Krasnoyarsk region as one of the largest reserves of forest resources among the regions of Russia. The areas of weakened and dead stands increase annually under the influence of unfavorable factors. The main reason for the decrease in the stability of forest plantations of the region are fires and insect pests. According to official data, more than 280 thousand hectares of forest plantations have died in the Krasnoyarsk region over the past ten years [11].

In the work, an assessment was made of the risks of natural hazards, the most typical for all territorial entities of the Krasnoyarsk region - floods and the reduction of the forest fund (forest fires, insect pests and forest diseases).

II. Methods

Based on statistical data on the implementation of natural hazards (reduction of the forest fund or floods), a risk calculation was performed. The level of risk $R_i^{fo/fl}$ for the i -th ($i = \overline{1, \dots, 41}$) region depends on the value of damage $U_i^{fo/fl}$ [mln. rub] and the probability of occurrence of a hazardous event $P_i^{fo/fl}$ (1):

$$R_i^{fo/fl} = P_i^{fo/fl} \times U_i^{fo/fl} \quad (1)$$

The probability of reducing the forest P_{ij}^{fo} and was estimated as the ratio of the area damaged due to cause j on the i -th site to the total area of the forest fund on the territory of the region, taking into account the forest cover indicator::

$$P_{ij}^{fo} = \frac{S_{ij}}{S} \times L_i \quad (2)$$

where S_{ij} – the damaged area of the forest fund due to cause j in region i , S – the total area of the forest fund, L_i – the forest cover in the i -th region, $j=1$ – forest fires, $j=2$ – insect pests, $j=3$ – forest diseases.

To assess the likelihood of hydrological hazards P_{ik}^{fl} y cause of each event was taken into account:

$$P_{ik}^{fl} = \frac{n_{ik}}{N} \quad (3)$$

where n_{ik} – is the number of events of type k in region i , N – is the total number of events in the entire territory for the entire period under consideration, $k=1$ are snow floods, $k=2$ are rain floods, $k=3$ are jam floods.

Determination of damages from the consequences of natural hazards is one of the tasks that have not yet had an unambiguous solution. Thus, when assessing damage from floods, only the cost of destruction of buildings and structures is taken into account [12]:

$$U_{ik}^{fl} = C_{r,n} \times H_{ik} \times K_m \quad (4)$$

where $C_{r,ii}$ - is the average cost of the housing stock per 1 rural resident, H_{ij} - is the number of residents affected by destruction in the i -th district from the occurrence of a hazardous hydrological phenomenon due to k , K_m - is the degree of destruction / loss of the residual book value by zones: ($K_1= 0,8$ - destruction; $K_2=0,4$ - zone of medium destruction; $K_3=0,1$ - zone of weak destruction).

Forest fire damage assessment should take into account many factors, such as the value of burned objects and finished products in the forest, the cost of extinguishing fires, damage from air pollution. Due to limited initial data, when assessing damage U_{ij}^{fo} the costs of reforestation were taken into account in accordance with [13]:

$$U_{ij}^{fo} = C \times k_i / 100 \times F \quad (5)$$

where C - is the standard cost of growing plantings up to the age of crown closing, equal to 800 rubles/ha; k_{ij} - the percentage damage to the forest in the i -th plot due to j , F - the area of the forest fund in the entire territory under consideration that died or was damaged due to j .

To assess the complex natural risk, the following ratio is used:

$$R_c^{nr} = \sum_{j=1}^J R_j^{fo} + \sum_{k=1}^K R_k^{fl} \quad (6)$$

where R_j^{fo} - is the risk of reducing the forest fund from the causes of damage j , R_k^{fl} - the risk of dangerous hydrological phenomena by the factors of origin k .

III. Results

Despite the variety of reasons for the occurrence of hydrological hazards in the Krasnoyarsk region, the largest number of them are due to snow, jam and rain events (Table 1).

Table 1: Probability of floods by cause

Cause of occurrence:	Probability of an event:
Rain floods	0,076
Jamming floods	0,27
Snow floods	0,44
Mixed floods	0,05
Slope drain	0,017
Freezing of the stream	0,007
Dam break	0,003

Fig.1 presents risk maps of hazardous hydrological phenomena for the territories of the Krasnoyarsk region for the most common causes of their occurrence.

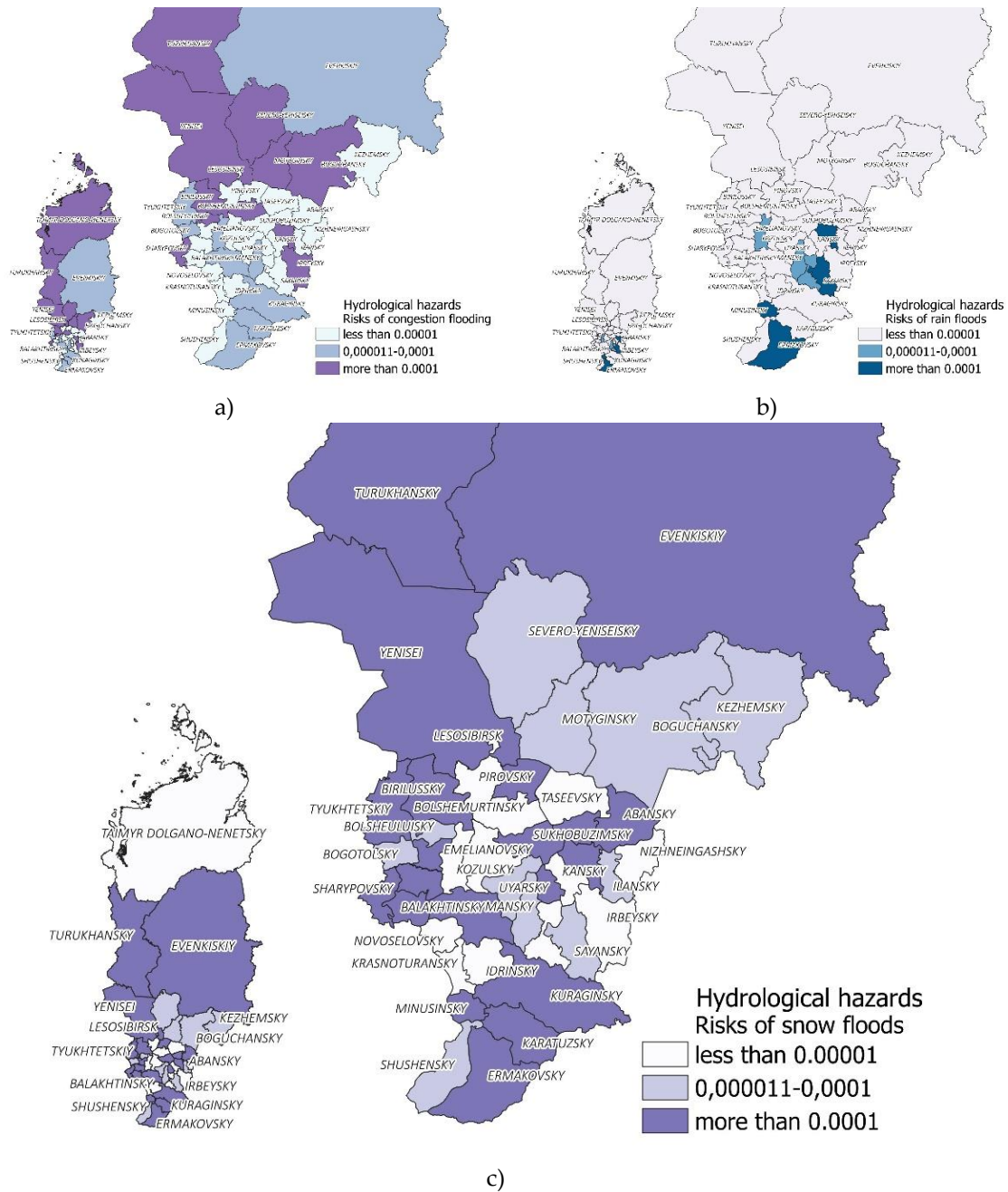


Fig. 1: Hydrological hazard risk maps (a - jamming floods, b - rain floods, c - snow floods)

Drawing up risk maps makes it possible to quantify the possible loss of life and material damage caused by the development of one or more hazardous processes. The greatest risk from hazardous hydrological phenomena, formed by jamming floods, was identified in Turukhansky, Taimyrsky Dolgano-Nenetsky and Yenisei regions, the greatest danger associated with rain floods is concentrated in Yermakovskiy, Minusinsk, Sayansky and Kansk regions, and the greatest risk of snow floods is in Nazarovskiy, Kuraginskiy and Karatuz municipal districts (Fig. 1).

The paper presents an analysis of the reduction of the forest fund on the territory of the Krasnoyarsk Territory according to various factors (Table 2). Forest fires, insect pests, forest diseases have the greatest impact on the state of plantations and are one of the leading factors in the annual weakening and drying of forests.

Table 2: Probability of forest fund reduction by factors

Factors of reduction of the forest fund	Probability of an event
Forest fires	0,002
Damage by insect pests	0,003
Adverse weather conditions and soil-climatic factors	$9,8 \cdot 10^{-5}$
Diseases of the forest	0,0003
Anthropogenic factors	$8,7 \cdot 10^{-5}$
Non-pathogenic factors	0,00025

The territories of the Evenk, Yenisei, and Turukhansk regions are at the highest risk of forest fires (Fig. 2). The highest forest fire risk values were obtained for the territories of the Kezhemsky, Motyginsky, Severo-Yeniseisky and Boguchansky regions. The forests of the Balakhtinsky, Motyginsky, Ermakovsky and Kezhemsky districts are most prone to diseases forest The greatest danger associated with pests is concentrated in the Bolshemurtinsky, Balakhtinsky, Pirovsky and Irbeysky districts..

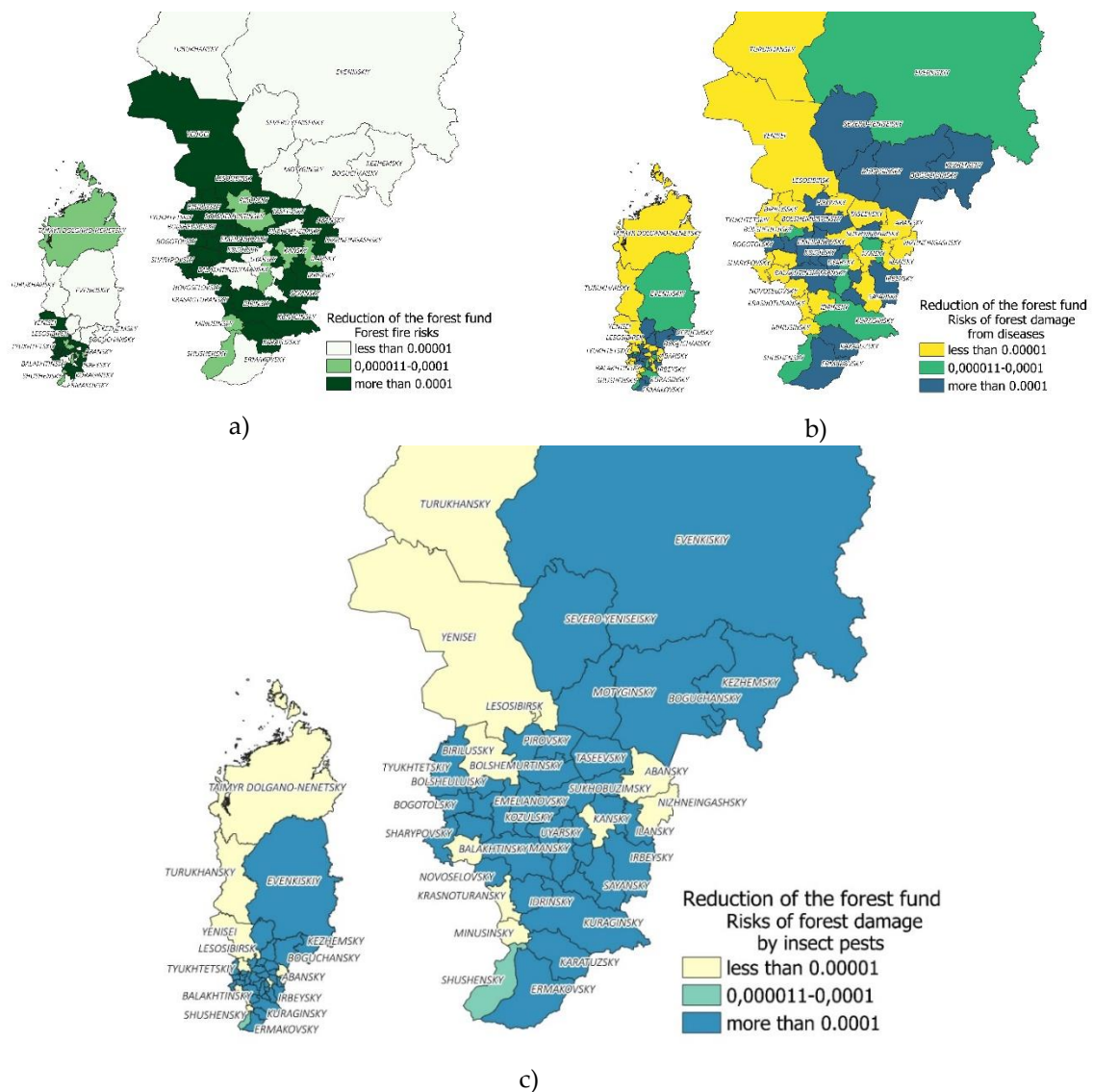


Fig. 2: Risk maps of forest fund reduction (a - forest fires, b - forest diseases, c - insect pests)

Based on the proposed model for assessing the complex natural risk (formula 6), territorial formations with a high level of danger were identified (Fig. 3).

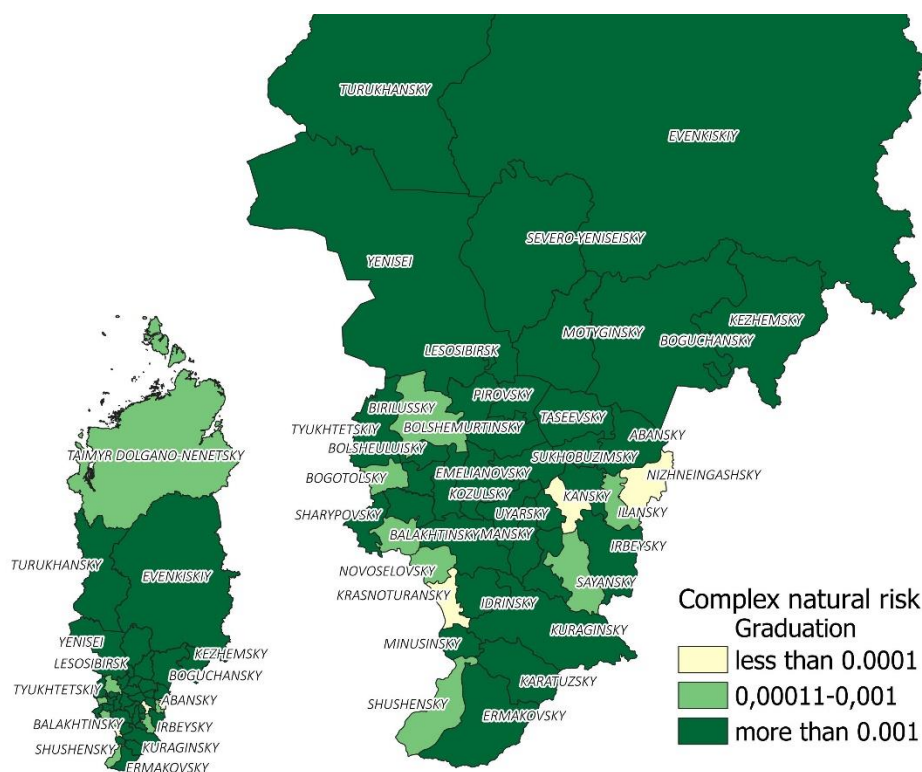


Fig. 3: Complex natural risk map

Probabilistic assessments of the risks of hazardous natural phenomena make it possible to predict the occurrence of such phenomena in the future, which can be the basis for an economically feasible increase in the protection of territories. Although a reduction, if not in the number, then at least in the extent of flooding, can be achieved to some extent by reforestation efforts.

IV. Discussion

The analysis of natural hazards is an important component in the prevention and reduction of possible negative consequences for the population, economy and infrastructure. The assessment of natural risks is important for the protection of the population, the conservation of natural resources, the development of infrastructure and the economy. The social and economic security of the Krasnoyarsk region as a whole directly depends on effective management based on risk assessment.

References

- [1] Assessment and management of natural risks // Materials of the All-Russian conference "Risk-2000". – M.: Ankil, 2000. – 478 p.
- [2] Makhutov N.A., Petrov V.P., Akhmetkhanov R.S. Natural-technogenic-social systems and risks // Problems of safety and emergency situations. 2004. No. 3. pp. 3-28.
- [3] Akimov V.A., Oltyan I.Yu., Ivanova E.O. Methodology for ranking emergency situations of natural, man-made and biological-social nature according to the degree of their catastrophism // Technologies of civil security. 2021. Vol. 18. No. 1 (67). pp. 4-7.

[4] Faleev M.I., Oltyan I.Yu., Arefyeva E.V., Bolgov M.V. Methodology and technology of remote risk assessment // Problems of risk analysis. 2018. Vol. 15. No. 4. pp. 6-19.

[5] Oltyan I.Yu., Arefyeva E.V., Krapukhin V.V., Vereskun A.V., Kotosonova M.N., Baler M.A. Re-implementation of the Sendai Framework Program for Disaster Risk Reduction in the Russian Federation // Publishing House: All-Russian Research Institute on Civil Defense and Emergency Situations of the Ministry of Emergency Situations of Russia. Results of the fifth year (Moscow). Moscow, 2021. 344 p.

[6] Artyukhin V.V., Arefyeva E.V., Vereskun A.V., Morozova O.A., Posokhov N.N., Sosunov I.V., Oltyan I.Yu., Chyasnavicius Yu.K., Gutarev S.V., Leonova E.M., Leonova A.N., Bryk D.I., Zhukova L.A. Risk management of man-made disasters and natural disasters (manual for heads of organizations) // Under the general editorship of M.I. Faleev. Moscow, 2016. 270 p.

[7] Anisimova T.B. Plotnikova T.V. Atlas of natural and man-made hazards and risks of emergency situations in the Russian Federation (ed. Shoigu S.K.), M. 2004. – 272 p.

[8] Postnikova U., Taseiko O., Efremova I. Assessment of territorial man-caused risks in the Arctic territories using probabilistic-graphic models. Reliability: Theory and Applications. Special Issue № 4 (70). 2022. Vol. 17. P 207–211.

[9] The scale and danger of floods in the Siberian regions // Cyberleninka URL: <https://cyberleninka.ru/article/n/masshtaby-i-opasnost-navodneniy-v-sibirskom-regione-rossii/viewer> (accessed: 04/01/2023).

[10] Floods in the history of the Krasnoyarsk Territory // Website of the Yenisei district URL: [https://enadm.ru/uploads/prevention/public_safety / FloodshistoryKrasnoyarsk.pdf](https://enadm.ru/uploads/prevention/public_safety/FloodshistoryKrasnoyarsk.pdf) (date of issue: 15.06.2023).

[11] Overview of the sanitary and forest pathology state of the forests of the Krasnoyarsk Territory for 2019 and forecast for 2020: Branch of the Federal State Institution "Roslesozashchita" "Forest Protection Center of the Krasnoyarsk Territory" : 355 p.

[12] RD 153-34.2-002-01, TEMPORARY METHODOLOGY FOR ASSESSING DAMAGE POSSIBLE AS A RESULT OF AN ACCIDENT OF A HYDRAULIC ENGINEERING STRUCTURE // Federal Service for Environmental, Technical and Nuclear Supervision URL: <http://enis.gosnadzor.ru/activity/control/hydro/Временная%20методика%20оценки%20ущерба,%20возможного%20вследствие%20аварии%20гидротехнического%20сооружения.pdf> (accessed: 15.06.2023).

[13] Rosleskhoz Order No. 53 dated 03.04.1998 "On approval of Instructions for determining damage caused by forest fires". URL: http://www.consultant.ru/document/cons_doc_LAW_31959/5f4bed452dc0105baf6db594cad944092e1e0587/ (accessed: 15.06.2023).

THE KURA ACTIVE FAULT – POTENTIAL SOURCE OF SIGNIFICANT HAZARD

Alexander Strom

•

JSC "Hydroproject Institute", Russia
strom.alexandr@yandex.ru

Abstract

An active fault stretching for more than 100 km along the Kura River between the tailing part of the Mingəçevir Reservoir in the east and the Azerbaijan-Georgia border in the west – the so-called Kura fault – is described in brief based on the analysis of space images. This active reverse fault with distinct evidence of Late Quaternary movements crosses the waterfronts of the Shamkir and the Enikend reservoirs. Considering its expressiveness and location just at the foundations of the hydraulic structures it seems that hazard posed by this active fault could be underestimated and that more efforts should be undertaken to reveal its recent history.

Keywords: Kura fault, surface rupture, earthquake magnitude, single-event displacement

I. Introduction

Active faults pose a significant threat to communities and infrastructure. They produced dual hazard, being considered as main causative tectonic structures responsible for large earthquakes, and, besides that, being able to destroy or damage any artificial structure if surface rupture would occur directly at structure foundation. Such phenomenon occurred, for example, during the 1999 Chi-Chi earthquake in Taiwan when concrete dam was ruptured by a fault stretching along the river [1, 2].

An active fault more than 100 km long stretches along the Kura River in the Western Azerbaijan between the tailing part of the Mingəçevir Reservoir in the east and the Azerbaijan-Georgia border in the west (Fig. 1), crossing waterfronts of the Şəmkir and the Yenikend reservoirs (Fig. 2). This fault named the Kura fault, has been known as an active tectonic structure since 90th, when it was identified by M.L. Kopp (unpublished data). It is included in the Eurasia Database of Active Faults (EDAF) [3, 4] with confidence level "C" that means that "*few pieces of evidence of activity are known as well as the lack of seismicity, the lack of surface deformations, or both*" [4].

Indeed, no one large earthquake has been reported here in the historical times. However, statement of "*the lack of surface deformations*" along this tectonic structure is wrong, as it will be demonstrated hereafter based on the analysis of the remote sensing data. These findings specified the exact location of the Kura active fault at some sections and demonstrate that hazard posed by this fault seems to be underestimated significantly, both for the hydraulic schemes directly crossed by it, and for the entire region that might be affected if large earthquakes could originate along the Kura fault considered as a causative structure capable for such events.

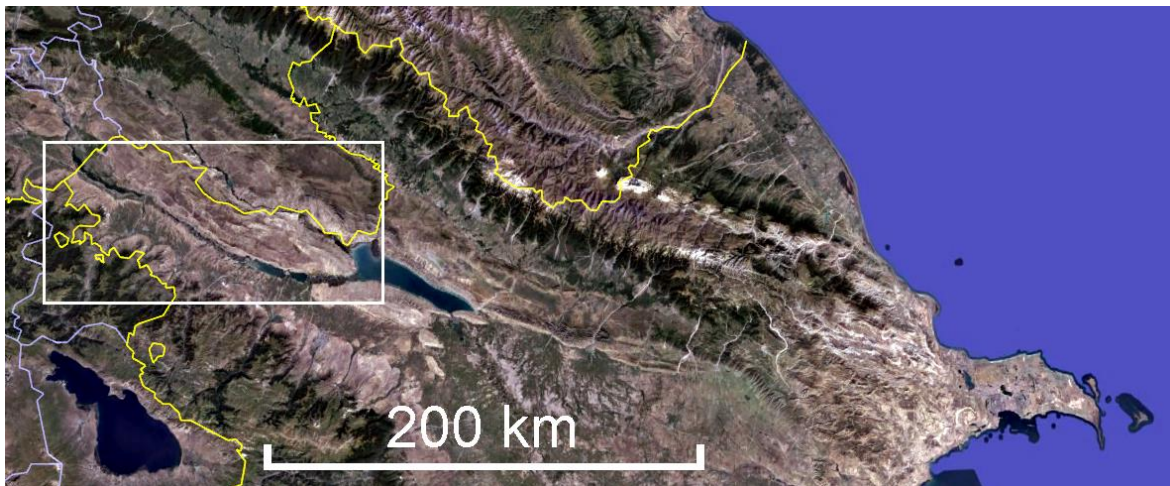


Fig. 1: Position of the study area in Northern Azerbaijan (marked by white rectangle)

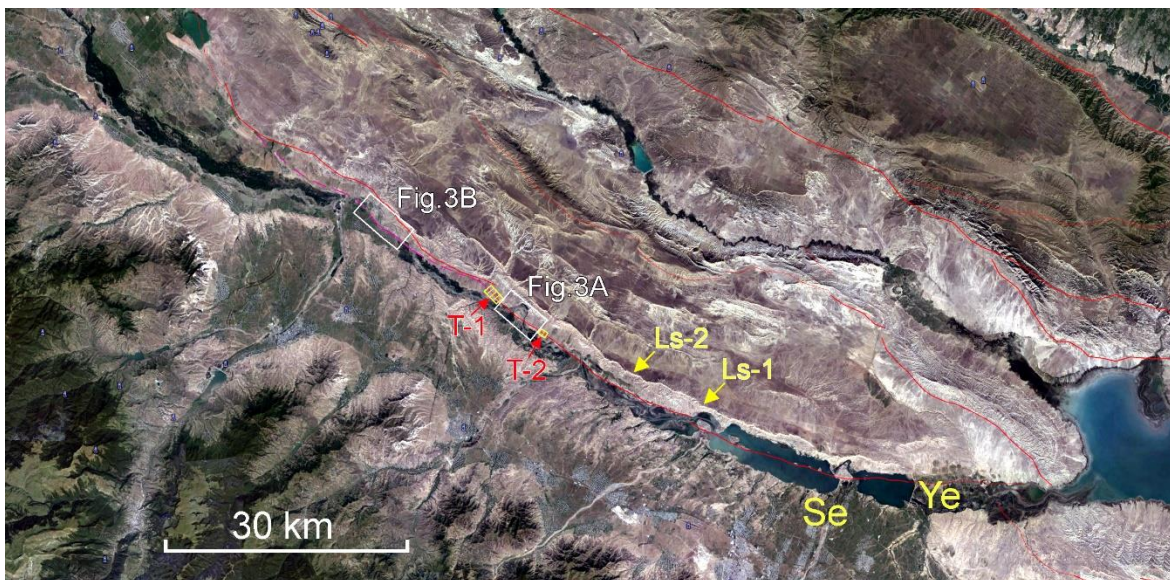


Fig. 2: Space image of the area marked in Fig. 1. Red lines – active faults according to the EDAF. Pink lines specified position of the Kura active faults. Ye – the Yenikend HPP, S – the Şamkir HPP, white rectangles – fault sections shown in Fig. 3A and B; T-1 and T-2 – sites most suitable for trenching shown in Figs 4 and 5; arrows marked by Ls-1 and Ls-2 indicate sites with deep seated gravirational slope deformations shown in Figs. 6 and 7

II. Geomorphic evidence of recent faulting

Distinct evidence of recent activity can be found along the entire length of the Kura fault. The most impressive are remnants of the uplifted north-eastern side visible on the right bank of the river where they are cut by the meandering stream (Fig. 3). Steep south-western slopes of these remnants, 15 to 40 m high, coincide with the reverse fault along which the hanging wall was thrust over the flat plains of the footwall. Such cumulative displacement accumulated during last stage of the Kura fault long-term evolution. The fact that the Kura River meanders have been incised locally through uplifting hanging wall indicates that there should be some period of the stabilization when meandering stream had crossed the fault line migrating from the footwall to hanging wall and back. When fault movements had activated, the stream could not leave its circuitous course and, due to intensive bottom erosion separated these remnants from the main ridge bounded by the Kura River valley at the south-east and the Yori River valley in the north-

west that forms the uplifted hanging wall of the Kura reverse fault.

At some sections the frontal edge of the hanging wall is even slightly higher than its part passing closer to the main ridge that might be caused by some flattening of the deeper part of the fault plane. Such structural peculiarities were described in several mountain systems characterized by intensive transverse shortening and reverse or thrust faulting, in Central Tien Shan near the Naryn town in particular [5].

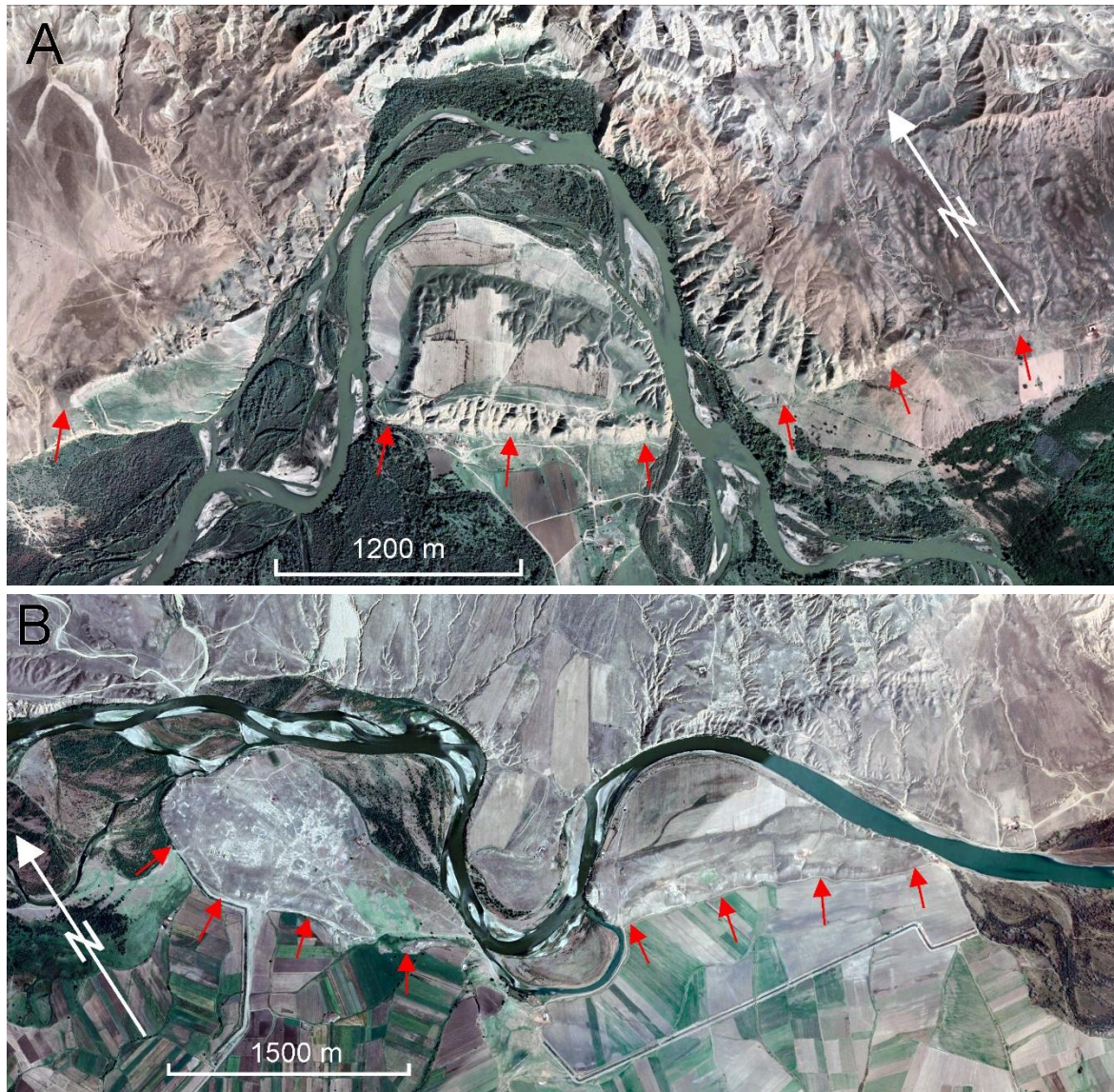


Fig. 3: Remnants of the Kura fault hanging wall on the right bank of the River, separated from the main uplifted block by the meandering stream. A - 8 km upstream from the Kirzan village; B - 2 km east from the Qiraq Kesamen village

III. Sites suitable for detail investigations

Despite impressiveness of landforms shown in Fig. 3 and reflecting recent activity of the Kura fault, detail paleoseismological studies should be carried out to restore most recent history of its evolution. They will require extensive trenching that is the main technique to derive information critically important for seismic hazard assessment: 1) mode of fault displacement – was it the permanent tectonic creep or periodic rupturing events associated with earthquakes and what is the long-term sleep rate of the Kura fault; 2) ages of the recurrent rupturing events and, therefore, their

recurrence interval; 3) amount of single-event offsets that allows estimating magnitudes of past earthquakes [6]. One more aim of trenching is to select fault section(s) affected by single-event rupturing episodes. Such information is also very important to derive magnitudes of such seismotectonic events since rupture length is correlated with earthquake magnitude [7 - 9]. Such study, however, requires extensive trenching at numerous sites distributed along the entire fault length. It should be also noticed that, since no significant permanent deformations of the Şəmkir and the Yenikend HPP waterfronts have been reported yet, most likely the Kura fault evolves in the periodic rupturing events mode with minimal or zero deformations between these episodes.

Planning such studies, one should consider that trenching at the sites with significant – up to 40 m cumulative vertical offset where active fault crosses the river meanders will be too laborious. Besides, in the footwall, where the colluvial wedges could be accumulated and, thus, where trenching should be most informative, trenching could face difficulties caused by groundwater inflow, that will require trench draining that would be quite problematic.

The most appropriate sites for trenching are those where fault scarp height does not exceed several meters, located at some distance from the river floodplain and above its level where watertable should be at the significant depth. Two fault sections with such conditions were selected on space images. One is located at 41.142° N, 45.662° E (Fig. 4); another one – about 8.5 km from the first one, at 41.096° N, 45.74° E. (Fig. 5).

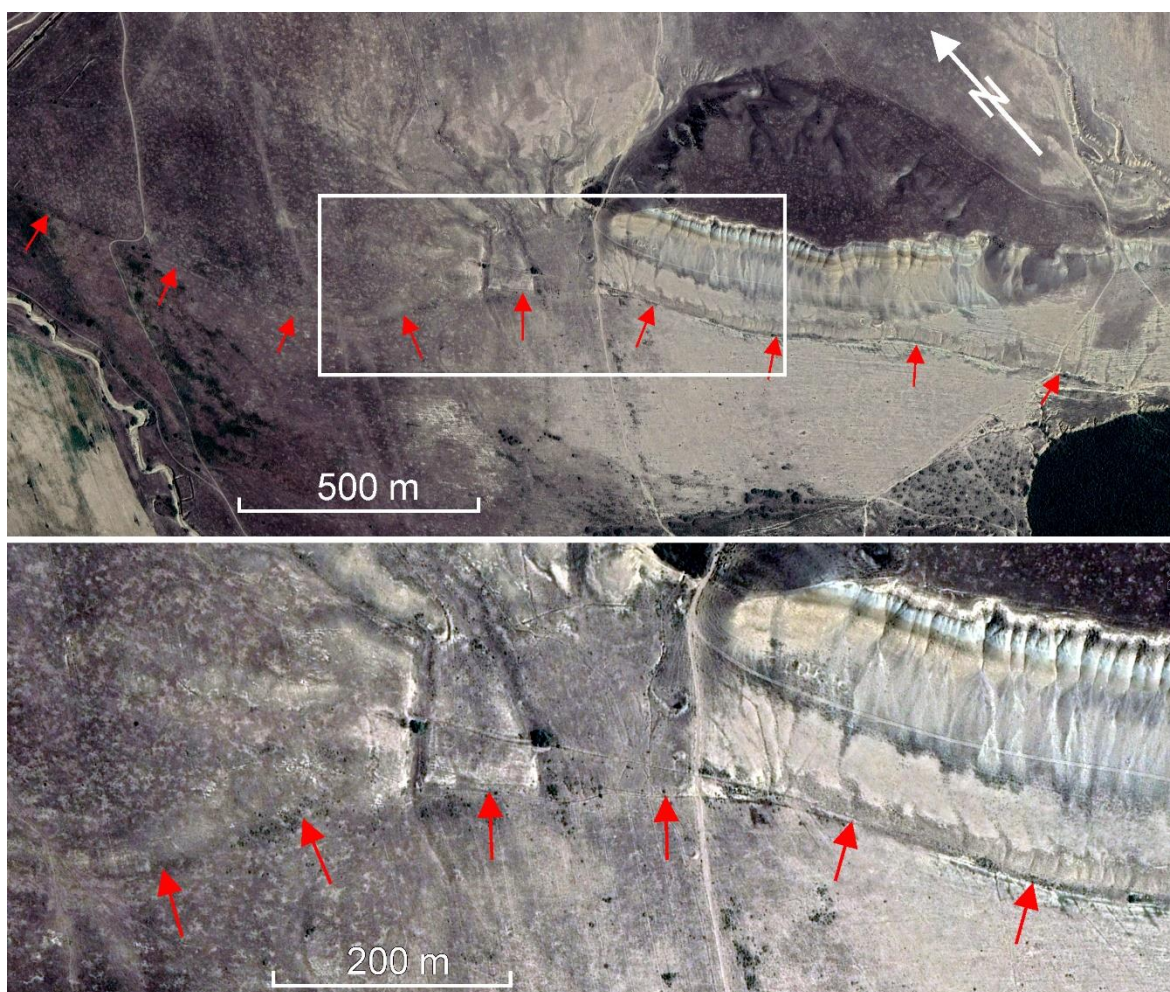


Fig. 4: The Kura fault sections at 41.14° N, 45.66° E with 3-5 m high fault scarp marked by red arrows, optimal for trenching (T-1 in Fig. 2). The lower image is the zoomed fragment outlined above.

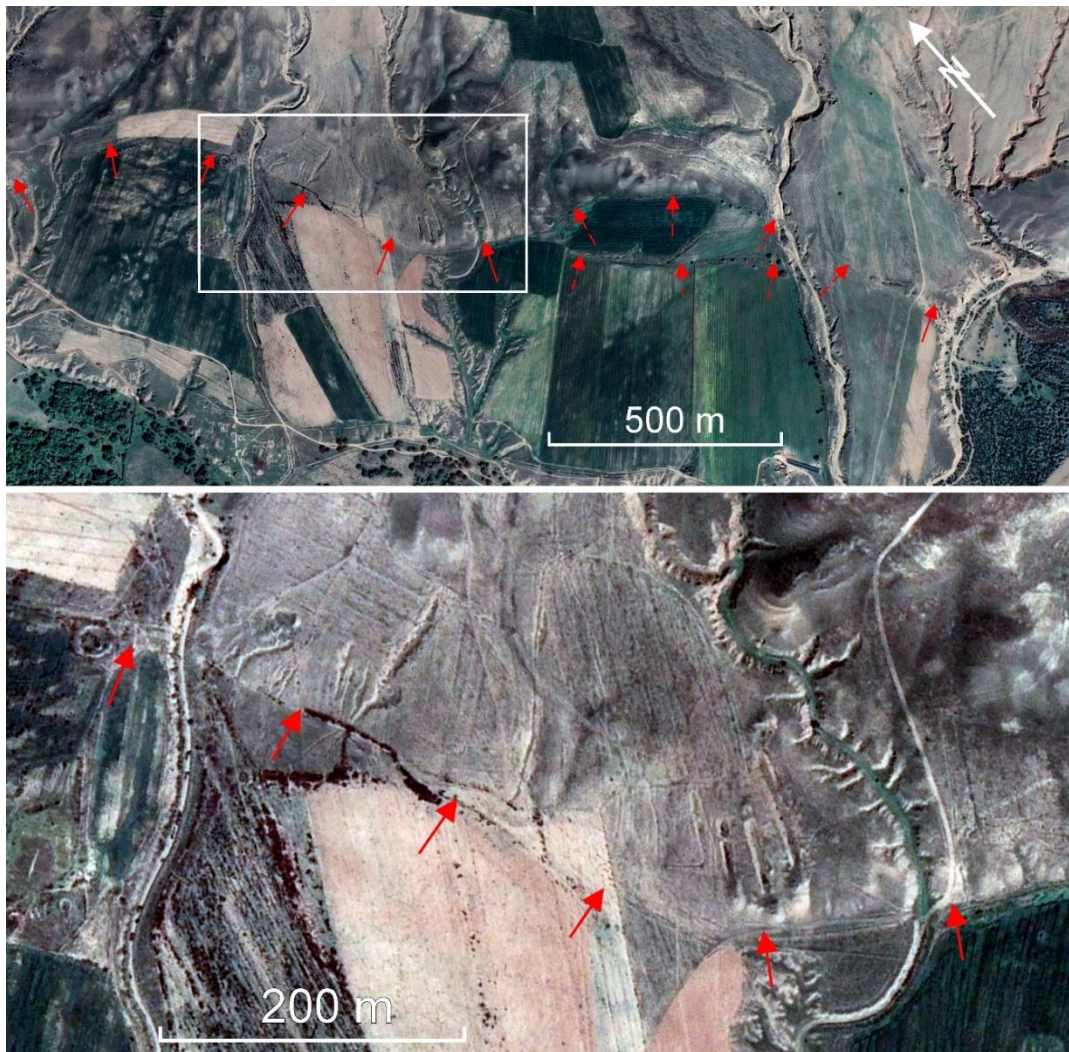


Fig. 5: The Kura fault sections at 41.097° N, 45.74° E with 4-5 m high scarp marked by red arrows, optimal for trenching (T-2 in Fig. 2). The lower image is the zoomed fragment outlined above. The indubitable fault scarp is marked by solid arrows, the assumed section – by dashed arrows

At both sites hanging wall of the up to 5 m high fault scarp is incised by several young dry gullies that almost disappear at the footwall, indicating recent activity of the Kura fault. Trenching at these sites should provide information on the most recent rupturing events. According to the space images available, local areas at both sites are not used for cropping, thus such earthwork will not disturb local farmers. Of course, more sites should be selected for trenching to trace single-event ruptures, but those described above looks most promising to start trenching campaign.

IV. Slope deformations of the hanging wall

Besides distinct evidence of recent faulting described in brief above, evidence of large-scale slope deformations can be seen at several sections along the crest of the ridge that forms the hanging wall of the Kura fault. The most evident deformations (Fig. 6) are at 41.02° N, 45.98° E. One more, less impressive site where, nevertheless, fractures on top of the ridge stretch for about 1200 m passing up to 300 m behind the watershed was found at 41.057° N, 45.87° E (Fig. 7). It should be pointed out that fractures at the latter site are well visible on space images made in April 2014 and available at Google Earth. Later the top of the ridge underwent intensive agricultural development that masked these fractures.

Such fractures bounding large blocks and extending far behind the watershed, thus, affecting the ridge crest and upper part of the opposite slope, indicate formation of the deep-seated gravitational slope deformations (DSGSD) [10, 11]. DSGSDs are typical of hanging walls of active reverse faults and can be triggered by earthquakes associated with such faults.

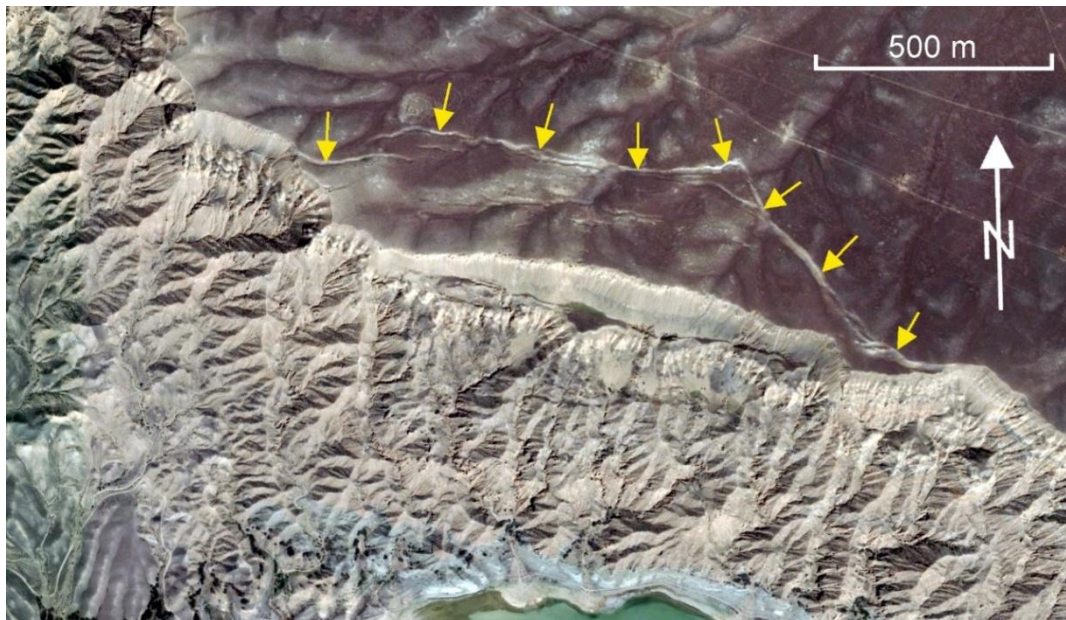


Fig. 6: Deep seated gravitational slope deformation on top of the ridge above the tail part of the Şəmkir reservoir (Ls-1 in Fig. 2). Scarps are marked by orange arrows

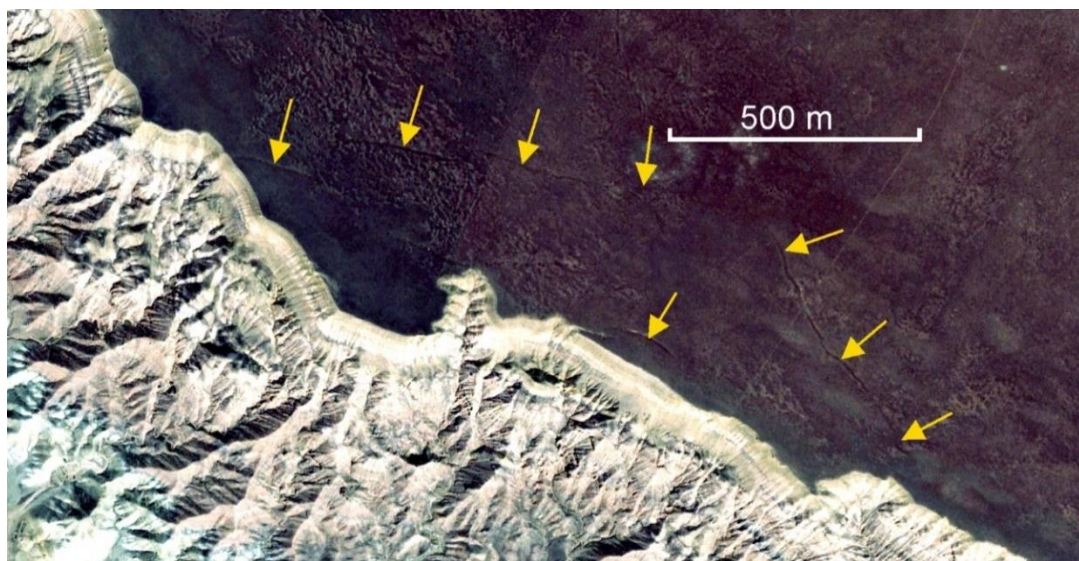


Fig. 7: Fissured indicating the initial stage of the deep seated gravitational slope deformation on top of the ridge (Ls-2 in Fig. 2). Fractures are marked by orange arrows. Image made on April 5, 2014

V. Discussion and conclusions

The aim of this paper is to attract attention of researchers studying active tectonics and seismic hazard of Transcaucasian region to this, potentially quite hazardous active fault. According to the data presented herein, the confidence level of the Kura fault should be changed to “CONF B” (denotes unambiguous surface deformations, although no recent slips have been described yet, and the

attribution of earthquakes is questionable [4]). Results of more detailed studies could even change it to “CONF A”, if structural and sedimentological evidence of past earthquakes will be identified by trenching [6]. Much higher confidence level should be considered for assessing hazard that this active fault poses to Western Azerbaijan and neighboring parts of Georgia and Armenia, and, in particular, to hydraulic schemes along the Kura River that might be affected by surface faulting associated with this tectonic structure directly.

If periodic rupturing mode of the Kura fault evolution will be proved, magnitude of the past and, correspondingly, of possible future earthquakes could be derived based on the empirical relationships between single-event displacement and surface rupture length on the one hand and earthquake magnitude, either M_w [7, 8] or M_s [9], on the other hand. Considering significant overall length of the Kura fault and assumed multimeter single-event offsets, magnitude of earthquakes that might be associated with this fault could be quite high. Depending on the ages of past events and on the duration of their return period assumed seismic effects could exceed those provided by the previous estimates and considered in construction codes [12].

References

- [1] Lee, J. C., Chu H.-T., Angelier J., et al. (2002). Geometry and structure of northern surface ruptures of the 1999 $M_w = 7.6$ Chi-Chi Taiwan earthquake: Influence from inherited fold belt structures. *Journal of Structural Geology* 24, 173–192.
- [2] Lin A., Oichi T., Chen A. and Maruyama T. (2001). Co-seismic displacements, folding and shortening structures along the Chelungpu surface rupture zone occurred during the 1999 Chi-Chi (Taiwan) earthquake. *Tectonophysics* 330, 225–244.
- [3] Bachmanov, D. M., Trifonov V. G., Kozhurin, A.I., Zelenin, E. A. (2022). Active Faults of Eurasia Database AFEAD version 2022. DOI: 10.13140/RG.2.2.25509.58084
- [4] Zelenin E. A, Bachmanov D. M., Garipova S. T., Trifonov V. G., Kozhurin A. I. (2022). The Active Faults of Eurasia Database (AFEAD): the ontology and design behind the continental-scale dataset. *Earth System Science Data*. vol. 14. p. 4489-4503.
- [5] Abdrakhmatov, K.E., Thompson, S., Weldon, R.. Active tectonics of the Tien Shan. Bishkek, Ilim Publishers, 2007. (in Russian).
- [6] McCalpin, J.P. Paleoseismology, 2nd Edition. International Geophysics Series, Vol. 95. Elsevier, 2009.
- [7] Wells, D.L., and Coppersmith, K.J. (1994). New empirical relationships among magnitude, rupture length, rupture width, rupture area, and surface displacement. *Bulletin of the Seismological Society of America*. 1994. V. 4. 974–1002.
- [8] Leonard, M. (2010). Earthquake fault scaling: self-consistent relating of rupture length,width, average displacement, and moment release. *Bulletin of the Seismological Society of America*, V. 100, No. 5A, 1971–1988,
- [9] Strom, A.L. and Nikonov, A.A. (1997). Relationships between seismic faults parameters and earthquakes' magnitude. *Izvestia, Physics of the Earth*. 33(12): 1011-1022.
- [10] Jomard, H., Lebourg, Th., and Guglielmi, Y. (2014). Morphological analysis of deep-seated gravitational slope deformation (DSGSD) in the western part of the Argentera massif. A morpho-tectonic control? *Landslides*, 11, 107-117.
- [11] Pánek, T., and Klimeš, J. (2016). Temporal behavior of deep-seated gravitational slope deformations: A review, *Earth Science Reviews*. 156, 14-38.
- [12] Akhundov, A., Mammadli, T., Garaveliyev, E., Yethirmishli, Q., and Tanircan G. (2010) Seismic hazard assessment for Azerbaijan. The NATO Science for Peace and Security Programme.

MANAGING THE RISK OF EMERGENCIES CAUSED BY GROUNDWATER FLOODING OF THE HISTORICAL BUILT-UP AREAS

Elena Arefyeva

All-Russian Research Institute for Civil Defense and Emergencies of the EMERCOM of Russia
elaref@mail.ru

Abstract

The article presents an approach to managing the risk of groundwater flooding emergencies, including those in historical built-up areas. The approach is based on the application of a set of methods, including the method of forecasting, the method of developing an optimal control action, and developing a compromise solution. The peculiarity of historical built-up areas is that there is a significant cultural layer that does not allow drainage, because watered soil preserves the cultural layer. At the same time, architectural monuments need to drain the foundations and not water the soils of the foundations of structures.

Keywords: groundwater flooding, optimization approach, Boussinesq equation, historical territories, architectural monuments

I. Introduction

Urbanized territories are a complex of interconnected systems of natural and man-made character. Their joint functioning determines the degree of quality of the urban infrastructure function. Unbalanced economic activity can initiate hidden and activate existing dangerous natural processes. Their timely tracking, forecasting and decision-making aimed at their prevention is the task of municipal structures and structures responsible for security.

It has been established that the hazards caused by geological and hydrological processes in cities are of a synergistic nature [1]. One realized danger causes a chain of subsequent dangerous processes. The damage from the total emergencies caused by synergistic chains exceeds the sum of individual damages in the separate development of such processes. And the measures taken are not adequate to the development of a sequence of negative events. The action of synergetic processes - consequences continues after the action of the initiating factor. Such initiating factors for the emergence of synergistic chains include flooding.

Flooding initiates dangerous natural processes, such as karst, landslides, suffosions, loess subsidence, soil swelling, and at the same time, the bearing capacity of soils decreases, the seismic intensity of the territory increases, etc. [2, 3]. Particularly affected by the negative impact of the underground hydrosphere are historical cities and architectural monuments that are not adapted to modern man-made impacts [2]. Almost half of Russian cities (425) are historical cities (79% in the European part, 11% in the Urals, 10% in Siberia and the Far East). 25,000 monuments of federal significance. This is a huge cultural historical heritage, which is being destroyed before our eyes when measures are not taken to protect against dangerous processes. The most defenseless from dangerous natural impacts were such cities as St. Petersburg, Novgorod, Pskov, Smolensk, Rostov the Great, Yaroslavl [4].

These processes can lead and lead to emergency situations. The negative impacts of groundwater on buildings and structures cause from 50 to 80% of all accidents and collapses [5, 6].

The operational reliability of buildings and structures is reduced by 30%. The damage from emergencies during flooding is up to 5.5 billion dollars annually [7].

Emergencies can potentially arise if the following conditions exist [1]:

the presence of a hydrogeological or engineering-geological hazard in a given area and the location of the object of protection within this hazard;

absence or unsatisfactory operation of the engineering protection system;

unsatisfactory state of structures of buildings.

The usual protective and preventive measures against undergroundwater flooding are various types of drainage, waterproofing systems, and surface runoff control systems [8]. Since emergency situations during flooding are usually caused by man-made causes, this allows us to conclude that the process of preventing these emergencies is manageable [1, 8]. A feature of historical cities is the presence of a cultural layer - a valuable archaeological material. Groundwater for the cultural layer is a preservative. The foundation of buildings in Russian northern cities was traditionally located on a wooden base. Soil moisture ensures the safety of the wooden base, and its drying leads to rotting and deformation and destruction of buildings. At the same time, basements and foundations of buildings must be drained. Therefore, in built-up areas, it is necessary to perform a soft regulation of the groundwater regime, without sharp fluctuations in the groundwater level, in order to prevent additional negative effects. Thus, drainage can cause suffusion, subsidence of the surface, overdrying of the soil, and further deformation of buildings [1, 8].

An important solution for soft regulation is the use of a criterion - the threshold of hydrogeological hazard, the critical level of groundwater, determined for each object and plot of a built-up area [5].

To determine the critical and limiting levels of groundwater for various buildings, a typology of objects was obtained depending on the properties of the foundation foundations. In historical territories, 4 main classes of objects were identified according to drainage requirements; these are objects that allow and do not allow a moist state of buried structures and basements, and among these groups are objects located on a stone or wooden base [1].

II. Methods

To develop solutions for flexible optimal regulation of the groundwater regime, including the regulation of groundwater regime in the historical built-up areas, a software-computer complex has been developed; mathematical modeling is carried out.

Calculation of the estimated groundwater level (geofiltration equation) is performed using the Boussinesq equation (it is a parabolic partial differential equation) with appropriate boundary and initial conditions). Coefficients of equations characterizing the properties of soils and additional infiltration nutrition [9].

The initial data for modeling are distributed fields of numerical values of the coefficients of equations (water conductivity, water loss, infiltration, etc.). With the help of monitoring, by interpolation and extrapolation, calculated geofiltration schemes are compiled - the parameters of the geological environment [1, 5].

The control parameters are the water levels in the drains, the volume of pumped water. Optimality criterion: the volume of the drained prism of the cultural layer, the drained area of the buried premises.

Regulating parameters are set in the form of boundary conditions of the geofiltration equation or source function [1, 5].

The optimization criteria are formulated as a functional. Minimization of the functional determines the degree of closeness of the calculated reduced values of the groundwater level with the help of control actions to a given value [1, 5]. At the same time, taking into account the

presence of an acceptable lower limit, it is ensured that the groundwater level does not go beyond its limits.

The gradient of the functional is determined through the solution of the adjoint problem to the direct problem [10, 11, 12]. The definition of the gradient of the optimizing functionality (and the construction of a sequence minimizing it is carried out according to the gradient projection method, which is included in the main mathematical method [5,10]. The result of calculations in the iterative process is the optimal solution that provides a minimum of optimizing functionality [10, 11] and is the desired optimal control parameter, which physically corresponds to the selected real drain position or the volume of water pumped out from drain [1, 5].

The process of groundwater flooding in general form will be described by a parabolic equation with a source function $f(x, t)$ [5, 9]:

$$\frac{\partial y(u)}{\partial t} + A(t) * y(u) = f(x, t) + u(t) \tag{1}$$

$$(x, t) \in Q; y(u) = 0, (x, t) \in \partial Q; y(x, 0) = y_0(0), x \in D, \partial Q = \partial D * (0, T);$$

Where is $A(t) * y(u) = -\sum_{i=1}^n \sum_{j=1}^n \frac{\partial}{\partial x_i} a_{ij}(x, t) \frac{\partial y}{\partial x_j}$; - a differential operator;

$u \in U = L_2(Q); u = (u_1, u_2, \dots, u_k)$; -- control vector; $y(t) = (y_1(t), y_2(t), \dots, y_k(t))$ - phase trajectory; $Y = \{y\}$ --phase space; $z(u) = C * y(u)$ - the observed state of the object; $C : L_2(0, T; V) \rightarrow H_1$ - linear operator; H_1 - Hilbert space.

The quality of control in general terms is described by a criterion - an optimizing functional:

$$J(u) = \|Cy(u) - z_0\|_{H_1}^2 + (Nu, u)_U; \quad (Nu, u) \geq c \|u\|_U^2, \tag{2}$$

$c > 0, \forall u \in U$, u - and is the control vector,

Taking into account the accepted notation, the optimal control problem is formulated as follow.

Let the set of admissible controls be U , it is required to find such a control u from U , so that the solution of the original Boussinesq equation (1) with the initial and boundary conditions [9], the control would deliver a minimum to the functional $J(u)$ [5]:

$$\begin{aligned} u &\in U_D, \\ J(u) &= \inf J(u), \\ u(t), &0 \leq t \leq T \end{aligned} \tag{3}$$

From the point of view of solving a specific control optimization problem, the statement is formulated as follows: by controlling the water level in the drains (the depth of the drains) or the water flow in them, achieve the necessary drainage of the object with minimal drainage of the nearby territory (for example, the cultural layer, park zone) and maintain the specified range of GWL changes with the help of water discharges in drains. For the two-dimensional case (plane-parallel filtration flow), the following Boussinesq equation is considered, which is non-linear and can only be solved numerically using stable convergent difference schemes, for example, implicit Crank-Nicolson schemes.

Non-stationary filtration of groundwater in an area of arbitrary shape D , contoured by a curvilinear boundary Γ with a single-layer non-pressure-pressure planned flow, is described by a

system of two differential equations of parabolic type. In a non-pressure subdomain (D_1)-piecewise-heterogeneous in terms of porosity-capacitance, a single-layer planned flow on a non-horizontal aquiclude (in the presence of a hydraulic connection with a neighboring aquifer and the amount of infiltration supply entering the free surface of groundwater) is described by a nonlinear differential equation of the form [9]:

$$\mu \frac{\partial h}{\partial t} = \frac{\partial}{\partial x} \left[k(h - H^B) \frac{\partial h}{\partial x} \right] + \frac{\partial}{\partial y} \left[k(h - H^B) \frac{\partial h}{\partial y} \right] \pm \frac{k_0}{m_0} (\bar{H} - h) + w(x, y, t) \quad (4)$$

where $k(x, y)$ and $h(x, y, t)$ are functions that determine, respectively, the filtration coefficient and the absolute elevation of the groundwater level of the main aquifer; H^B is the absolute elevation of the base of the aquifer; $k_0(x, y)$ and $m_0(x, y)$ -functions, which determine, respectively, the filtration coefficient and the thickness of the weakly permeable interlayer separating aquifers; $\bar{H}(x, y)$ - absolute mark of the groundwater level of the underlying aquifer; $w(x, y, t)$ - intensity of infiltration nutrition; $\mu(x, y)$ is the coefficient of water loss when the free surface is lowered ($\frac{\partial h}{\partial t} < 0$) or the coefficient of undersaturation when the free surface is raised ($\frac{\partial h}{\partial t} > 0$).

For a unique solution to (4) and (5), boundary conditions are set: boundary and initial. Let the outer contour be denoted by Γ , and the inner one, corresponding to the assignment of boundary conditions for wells, drains, canals, springs, denoted by p . Therefore, by boundary conditions we mean both "external" and "internal" boundary conditions (BC) [9].

Boundary conditions of the 1st kind:

$$\begin{aligned} h(x, y, t) \Big|_{\Gamma+p} &= h(s, t), \\ s &\in \Gamma + p \end{aligned} \quad (6)$$

Boundary conditions of the second kind have the form:

$$\begin{aligned} -T \frac{\partial h}{\partial n} \Big|_{\Gamma+p} &= q(s, t), \\ s &\in \Gamma + p \end{aligned} \quad (7)$$

where p is the normal to the contour ($\Gamma + p$); in the case of an impenetrable boundary, we have $q(s, t) = 0$.

The initial conditions look like:

$$\begin{aligned} h(x, y, 0) &= h_0(x, y); x, y \in D_1; \\ H(x, y, 0) &= H_0(x, y); x, y \in D_2. \end{aligned} \quad (8)$$

The initial conditions have the form: Boundary conditions of the first kind set the groundwater level at the boundary. In the case of laying drains (internal boundary conditions) - the area is divided into sub-areas bounded by drains, and the water level in them - are the boundary conditions of the first kind. Boundary conditions of the second kind, when the water flow in drains (both horizontal and vertical drainage) is set on the inner boundary. In the boundary conditions of the third kind, the relationship between surface and ground waters is specified. Equations (4) and (5) with boundary conditions (6-8) form the basis for solving the optimization problem of managing the groundwater regime in order to prevent the development of emergencies, which is generally given in formulas (1-3).

Thus, the problem of optimal management of the prevention of hydrogeological emergencies at facilities is a sequence of tasks [5, 9, 14-18]:

- solution of a direct predictive problem, including simulation of the filtration process (modeling of the geological and hydrogeological environment using schematization - drawing up a geofiltration model of the environment, modeling the process of flooding - the filtration process using equations of mathematical physics with the assignment of boundary and initial conditions) [5, 9, 14];
- construction of an optimization model for regulating the groundwater regime in order to prevent emergencies at facilities based on the formation of optimization criteria, methods for solving extreme problems (conjugate gradient method) [5, 14];
- development of an optimization modeling algorithm for generating a control action, based on the numerical implementation of the constructed algorithms.

Consider a one-dimensional case, it is applicable to a large number of flood protection objects that have a shape close to a square with a uniform aquiclude profile. Using the superposition principle, a two-dimensional problem can be approximated by one-dimensional problems [17].

Mathematically, the problem is formulated for hydrogeological sections in a one-dimensional region on the interval $x_l < x < x_r$.

In the difficult conditions of a built-up area, in the presence of simultaneously different requirements for drainage standards (objects, buildings with different bases of foundations, and other requirements from soils vulnerable to a sharp decrease in soils or the presence of a wooden base of structures on frozen and heaving soils), the functional was chosen as an optimization criterion (1) to be minimized [5, 17, 22]:

$$J^l(h, u) = J^l_n + J^l_k, \quad l=1, 2, \dots; \quad (9)$$

where $J^l_n = A^h \int_Q (h(x, T, u) - h_n(x))^2 dx$, the functional-criterion of control responsible for the unsinkability of the object; where A^h -- some weight;

$h(x, T, u)$ - the level obtained as a result of the calculated control actions;

T – the time by which it is required to carry out water reduction works;

u - control vector (control parameters of the drain – depth of laying, water flow, etc.;

$h_n(x)$ - function of limiting groundwater level for an object;

$Q=(x_1, x_2)$, region of integration, (x_1, x_2 - drain location).

J^l_k - the functional-criterion "responsible" for the requirement that the water level "arrange" the adjacent soil, in other words, при $J^l_k = 0$ cultural layer or park zone, soil unstable in terms of suffusion in some vicinity of the protected object is not strongly overdried.

The form of this term-functional (10) is as follows (for two filtration areas separated by the protection object):

$$J^l_k = A_{k1} \int_{Q1} (h(x, T, u) - h_k(x))^2 dx + A_{k2} \int_{Q2} (h(x, T, u) - h_k(x))^2 dx, \quad (10)$$

Where are A_{k1}, A_{k2} -- some weights;

$h_k(x)$ - limit level function for the adjacent cultural layer, soil.

Limiting and critical levels for objects and other structures are given in the work [5].

Let us now formulate the control optimization problem:

it is required during the iterative process to minimize the functional $J^l(h, u)$ provided that the groundwater profile $h(x, T, u)$ - satisfies the Boussinesq equations (4) or (5) with boundary conditions (6, 7), in general, the parabolic equation is given in expression (1). For many practical problems, a two-dimensional equation can be reduced to a series of one-dimensional equation and, using the principle of superposition, combine the resulting solutions. Levels in the vicinity of drains h_1 and h_2 are control actions, $u = (h_1, h_2)$ -control vector, equation in the first region $x_l < x < x_1$:

$$\frac{\partial h}{\partial t} = a \frac{\partial^2 h}{\partial x^2} + f(x, t), \quad 0 < t < T \quad ; \quad (11)$$

$$\frac{\partial h}{\partial x} = 0, x = x_l$$

$$h = h_1, x = x_1$$

Where is h_1 - level in the first drain, control parameter.

Equation in the second - central region $x_1 < x < x_2$:

$$\frac{\partial h}{\partial t} = a^2 \frac{\partial^2 h}{\partial x^2} + f(x, t), \quad 0 < t < T; \quad (12)$$

$$h = h_1, x = x_1$$

$$h = h_2, x = x_2$$

Where is h_2 - level in the first drain, control parameter.

Equation in the third region $x_2 < x < x_r$:

$$\frac{\partial h}{\partial t} = a^2 \frac{\partial^2 h}{\partial x^2} + f(x, t), \quad 0 < t < T: \quad (13)$$

$$\frac{\partial h}{\partial x} = 0, x = x_r$$

$$h = h_2, x = x_2.$$

Initial distribution $h(x, 0) = h_0(x)$, $f(x, t)$ is a function of additional infiltration (precipitation, pipe leaks, pumping water from the ground).

To minimize the functional $J(u)$ - goal criterion, it is required to calculate its gradient, for which the conjugate gradient method is used.

Let us write the adjoint equations for the region $x_1 < x < x_1$ for formula (11):

$$\psi_t = -a^2 \psi_{xx} - 2A_l^{h_k} \max(\underline{h_k} - h(x, t, u), 0)$$

$$\psi_x = 0, x = x_l$$

$$\psi = 0, x = x_1$$

$$\psi(x, t = T) = 2A^{h_k(x)} (h(x, T, u) - h_0(x)); \quad (14)$$

For the domain $x_1 < x < x_2$, for formula (12), and for formula (13), similar equations are written.

Adjoint equations are solved similarly to the main ones. The formal replacement of the direction of time from "+" to "-" leads to the fact that the value of the function is set not at the final, but at the initial moment of time. The variables are changed $t = T - t$. Finally, the gradient of the functional is determined by the formula:

$$J' = (a^2(\psi'(x_2^+, t) - \psi'(x_2^-, t)), a^2(\psi'(x_1^-, t) - \psi'(x_1^+, t))),$$

ecnu.

$$h_1 = h_1(t), h_2 = h_2(t), \tag{15}$$

u

$$J' = (a^2 \int_0^T (\psi'(x_2^+) - \psi'(x_2^-)) dt, a^2 \int_0^T (\psi'(x_1^+) - \psi'(x_1^-)) dt,$$

The last expression is given for the gradient if groundwater levels are assumed to be time independent.

The derivatives Ψ' of the solution of adjoint problems in the neighborhoods of the points x_1 and x_2 are denoted by the derivatives $\psi'(x_{1,2}^{\pm})$, while "+" means the right neighborhood, and "-" corresponds to the left neighborhood.

Hence $\psi'(x_1^+, t)$ и $\psi'(x_2^-, t)$ -- solution of the adjoint problem in the domain $x_1 < x < x_2$.

Accordingly -- $\psi'(x_1^-, t)$ - solution of the adjoint problem in the domain $x_1 < x < x_1$.

And $-\psi'(x_2^+, t)$ - solution of the adjoint problem in the domain $x_2 < x < x_k$.

Finally, to determine the optimal control-control action, one can use the iterative gradient projection method

$$u_{l+1} = P_U (u_l - \alpha_l J'(u_l)), l = 1, 2, 3... \tag{16}$$

for some initial u_0 . The operator P_U is the projection operator on the space of admissible controls.

The desired control provides a minimum for the functional $J(u)$.

III. Results

As an example of calculations in Fig.1. the drainage of the protection facility of the Faceted Chamber on the territory of the Novgorod Kremlin is given - the optimal position of the drains was obtained with complete drainage of the basement [17]. Variants of calculations for the recommended optimal drainage to ensure protection from the negative impact of groundwater protection objects. The results obtained are the basis for the expert to make the final control decision on the prevention of emergencies at protected objects and allow making recommendations on engineering measures (Fig. 1) [17- 20].

The flooding process is described by a mathematical model representing the geofiltration equation for describing non-stationary planned filtration (the Boussinesq equation) with the corresponding boundary conditions [5]. Such equations do not have an analytical solution, so numerical simulation is used [10, 11, 12]. Explicit or implicit difference schemes are used, such as the Dufort-Frankel scheme and the method of alternating directions. A grid is superimposed on the filtration area, and the initial data necessary for the calculations are "entered" into each grid cell. For the first time, the original input of initial information was implemented in the model, which allows taking into account all archival, stock information about the engineering-geological and hydrogeological conditions of the built-up area, given on paper [22].

Data input includes a layer-by-layer graphical setting of the calculated parameters (in the form of maps of the corresponding isolines), boundary conditions, critical and initial levels of groundwater, terrain, which allows them to be converted into a monochromatic format in which the numerical values of the parameters correspond to shades of the selected color, which allows

the software the complex to perceive this format as numerical data continuously distributed in the study area.

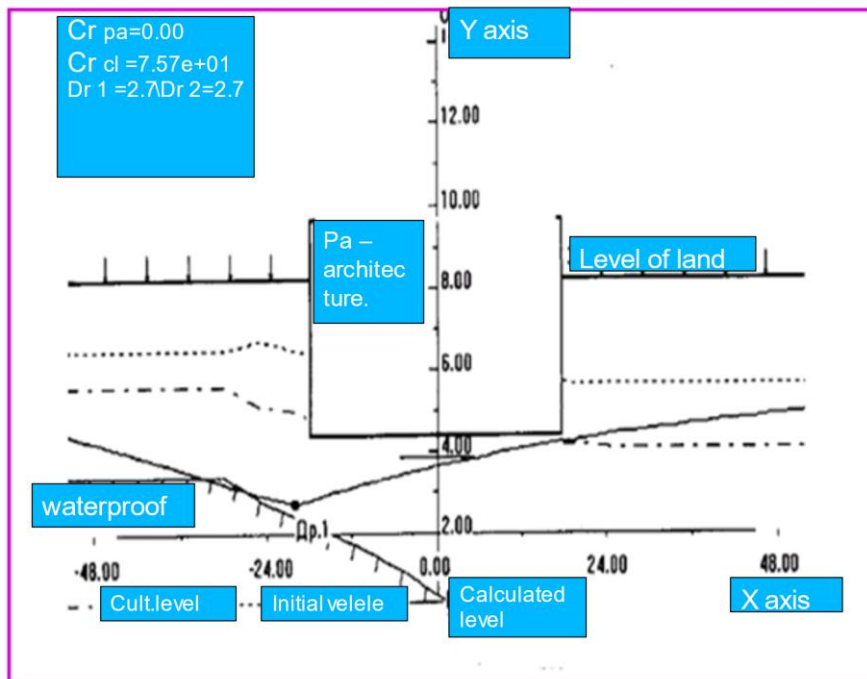


Fig. 1: The result of the calculation of the drain for the object of protection - the Faceted Chamber (Novgorod Kremlin).

The change in the intensity of the hue of the selected color corresponds to the change in the numerical values of the parameters of the source data. The input data can be simultaneously presented in three formats: in a tabular, numerical task (in each cell); in a graphic in a monochrome image (Fig. 2) [22]. The use of such data input makes it possible to divide the filtering area into any number of cells, limited by the computer memory, greatly simplifying and reducing the time of data entry, increasing the accuracy of calculations (Fig. 3) [22].

The parameters entered for calculations are shown in Figure 3b) (column on the left). The parameters must be set in the entire computational domain: groundwater level, water permeability, infiltration, water loss parameters, water level in the reservoir, critical level for the entire domain and individual objects. Parameters can be set both using maps and tables, while dividing the area into cells, the size of which is adjusted depending on the accuracy of the required forecast. The division of the computational domain into cells is specified for the main parameter (H), for all other parameters this division is preserved. All other parameters are “attached” to each cell of the grid, i.e. each cell of the grid contains all the specified layer-by-layer information (Fig. 3). Layers (calculation parameters) can be added by defining a new layer [22].

Unlike existing models of flooding, the developed software and computing system implemented in a common software shell allows, in a single iterative process, to determine the excess of the critical level of groundwater for various objects, evaluate the effectiveness of control actions, take into account and enter all archival and stock information, evaluate the impact rivers and reservoirs, accidents at hydraulic structures, graphically present the results of calculations in three formats (graphical: two-dimensional, three-dimensional, and also numerical). The original algorithm for entering initial information significantly improves the quality and speed of entering initial data, allows you to enter data on the same topographic basis layer by layer, impose additional restrictions and conditions for predictive calculations [21, 22].

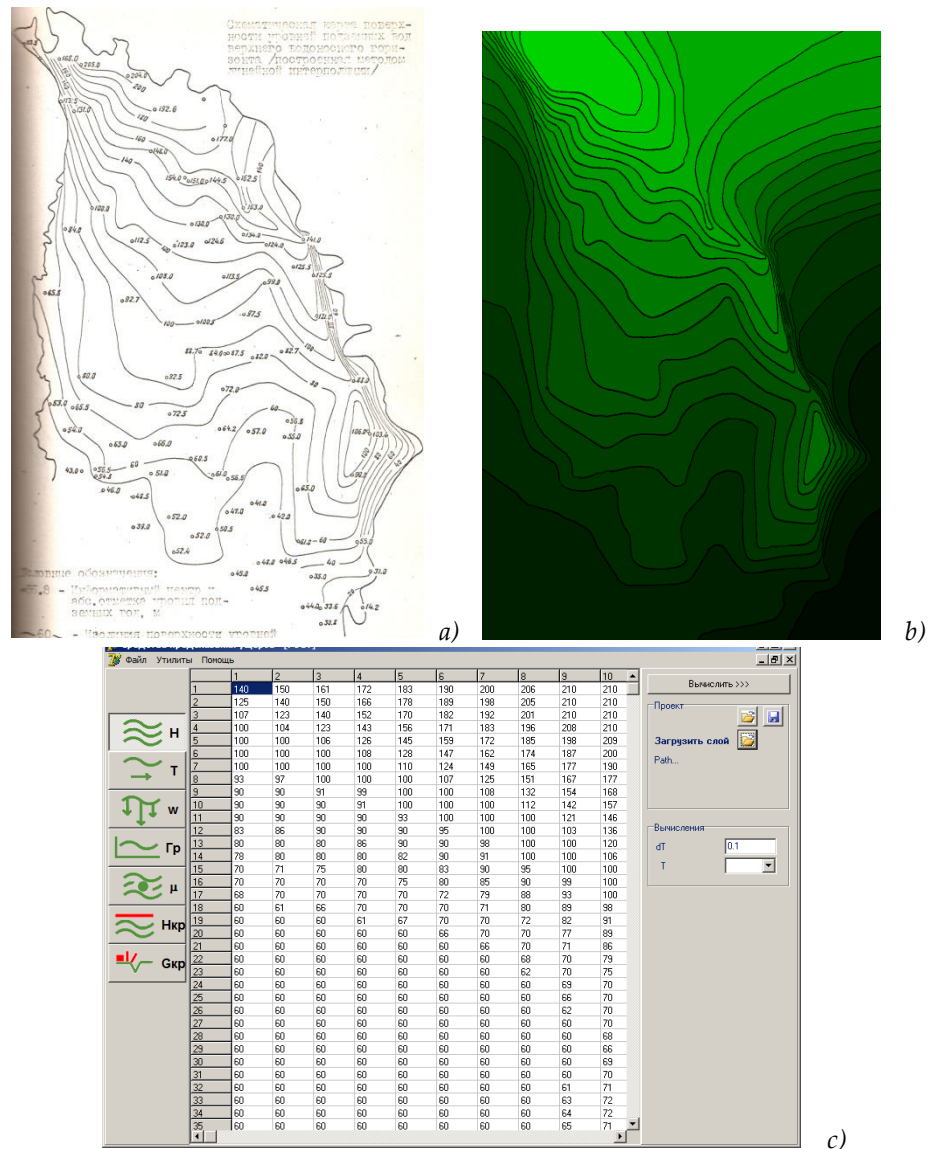


Fig. 2: An example of transferring data from archival maps (a) to the electronic color range (b) and their numerical values in the area under consideration (c)

IV. Discussion

The developed set of methods and models served as the basis for creating a situational model - a special software-computer complex. The model represents elements of local GIS and a block of mathematical modeling of geofiltration. It was performed for local objects where there was no need to use expensive software products and there was a requirement for the openness of program codes to correct predictive models. The software-computer complex allows solving the following tasks in the simulation mode:

- predict and evaluate the potential and actual flooding of technosphere objects (by exceeding their critical levels);
- predict and evaluate the achievement and excess of the critical level of groundwater during the development of flooding throughout the territory under consideration;
- predict and evaluate the possibility of development of hazardous processes induced by flooding;
- to carry out the forecast of flooding of the territory in case of flooding of rivers, breakthrough of dams, dams;
- develop and evaluate in a simulation mode options for the operation of drainage systems;

assessment of the degree of groundwater level reduction as a result of the operation of drainage systems;
 assessment the impact of control actions on the natural and man-made environment.

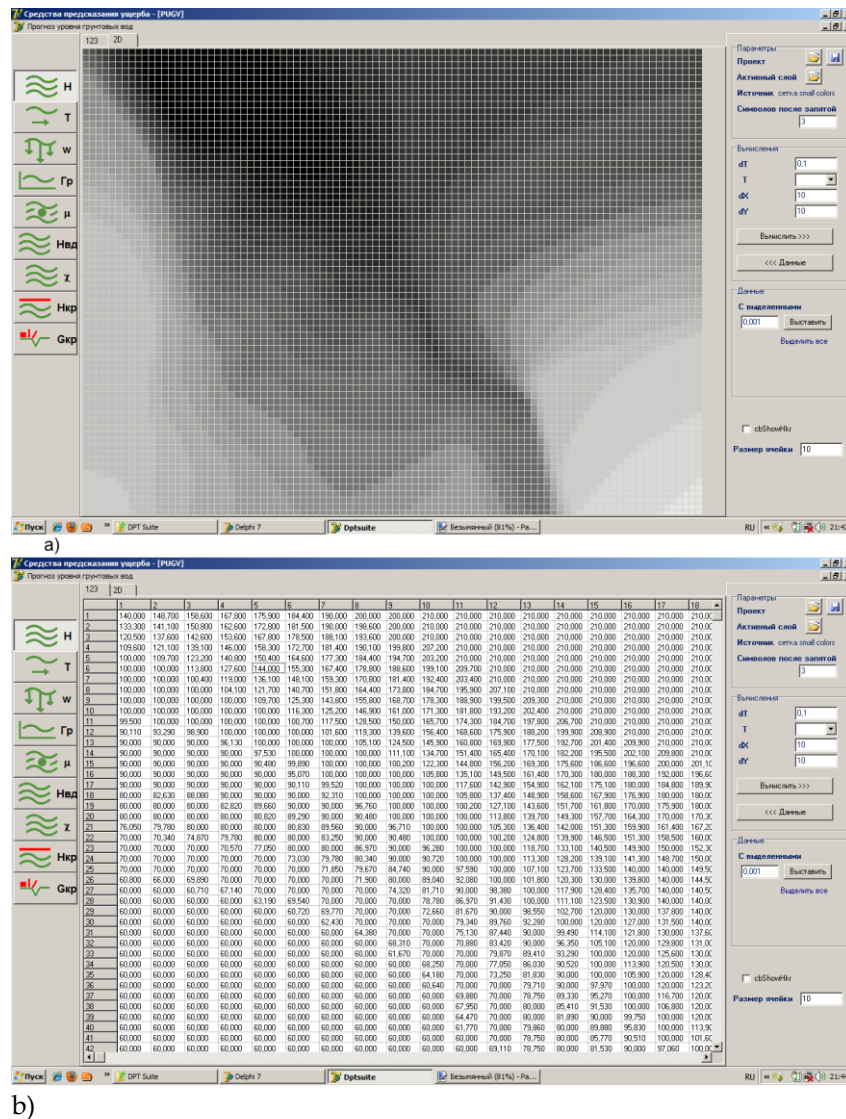


Fig. 3: Formation of initial data (on the example of groundwater levels): a) conversion of the map into a graphical monochromatic format; b) digital format for setting the initial data, corresponding to the graphic one.

Managing the risk of emergencies in case of flooding of built-up areas using the developed methods and technologies can reduce the risk of collapses and accidents of buildings and structures. The approaches have been tested in some built-up historical areas [23].

References

[1] Arefyeva E.V., Mukhin V.I. Assessment of territorial security in case of flooding. - M., APGS EMERCOM of Russia, 2008. – 101p.
 [2] Dzekter E.S. Patterns of formation of flooding of built-up areas, principles of forecasting and engineering protection.-M.: 1987.- 77 p.
 [3] Khomenko V.P. Suffosion processes in the territories of cities.// Problems of engineering geology and engineering seismology of cities and urbanized territories. Materials of scientific-practical. Sem. 1990-T.1.- M., 1990.- S.118-124.

- [4] Arefyeva E. V., Considering emergency hazards in construction and operation of infrastructures. IOP Conf. Ser.: Mater. Sci. Eng. 687 066023/ E V Arefyeva, E V Muraveva, T Yu Frose. International Conference on Construction, Architecture and Technosphere Safety (2019) 066023 IOP Publishing doi:10.1088/1757-899X/687/6/066023 c.
- [5] Arefyeva E.V. Regulation of the groundwater regime during flooding of objects and built-up areas // Industrial and civil construction. - 2007. - No. 11. - S. 47-48.
- [6] Arefyeva, E.V.; The issues of sustainability of historical and cultural areas associated with their periodic underflooding and solutions. / E. V. Arefyeva, Muraveva, E.V., Alekseeva, E.I. 2019 IOP Conf. Ser.: Mater. sci. Eng. 687 066031./ International Conference on Construction, Architecture and Technosphere Safety IOP Conf. Series: Materials Science and Engineering 687 (2019) 066031 IOP Publishing doi:10.1088/1757-899X/687/6/066031
- [7] Roitman A.G. Deformations and damage to buildings. - M.: Stroyizdat, 1987. - 159 p.
- [8] Dzektsler E.S. Engineering protection of built-up areas from flooding // Design and engineering surveys. - 1986. - №5. - P.27-29.
- [9] Gavich I.K. Theory and practice of modeling in hydrogeology. - M.: Nedra, 1980.-358 p.
- [10] Vasiliev F.P. Methods for solving extreme problems. - M.: Nauka, 1987. - 397 p.
- [11] Yevtushenko Yu.G. Methods for solving extreme problems and their application in optimization systems. - M.: Nauka, 1982. - 432 p.
- [12] Lavrentiev M.M., Incorrect problems of mathematical physics and analysis./ Lavrentiev M.M., Romanov V.G. - M.: Nauka, 1980. - 285 p.
- [13] Lyons J.-L. Optimal control of systems described by partial differential equations. - M.: Mir, 1972. - 293 p.
- [14] Galeati G. Optimal dewatering schemes in the foundation design of an electronuclear plant // Galeati G., Gambolatti G. Water Resour. Res, 1988. - Vol. 24. - No. 4. - P. 541-552.
- [15] Ahlfeld D., Combining physical containment with optimal withdrawal for contaminated groundwater remediation // Ahlfeld D., Mulvey J., Pinder G. Proc. of the VI Intl. Conf. on Finite Elem. in Water resources. - Lisboa: Portugal, 1986. - R. 205-214.
- [16] Willis R., Water resources manager. In North China plain // Willis R., Finney B., Zhang Daosual /J. of Water res. Plann. and Manag. - 1989. - Vol.115. - No. 5. - 3. - R. 598-615.
- [17] Arefyeva E.V. Flooding of objects and built-up territories as a potential source of emergency situations // Industrial and civil construction. - 2007. - No. 10. - S. 33-34.
- [18] Arefyeva E., Assessment of the vulnerability of architectural monuments to dangerous natural process./ Arefyeva E., Alekseeva E., Gorina L.. Lecture Notes in Civil Engineering, 2022.T.180.p.159-170.
- [19] Muravyeva, E.V. Improving the sustainability of cultural heritage sites using the UNIFORM.// Muravyeva, E.V., Arefyeva, E.V., Danilina, N.E. IOP Conference Series: Materials Science and Engineering 2020 | Conference paper DOI: 10.1088/1757-899X/962/4/042018 EID: 2-s2.0-85097056033 Part of ISBN: 1757899X 17578981
- [20] Arefyeva E.V. On some issues related to forecasting emergency situations caused by hydrological hazards and their consequences // Arefyeva E.V. , Bolgov M.V. Scientific and educational problems of civil protection. AGZ EMERCOM of Russia, No. 2017'4 (35), p. 102-110.
- [21] Arefyeva E.V. Information support in the problems of modeling and forecasting emergency situations related to the underground hydrosphere of a built-up area. // Civil security technologies. -. Civil Security Technologies, No. 1, 2016, pp. 28-34.
- [22] Arefyeva E.V. Situational-optimization model for determining hazards for built-up areas / Arefyeva E.V. , Ziganshin A.I., Rybakov A.V. Scientific and educational problems of civil protection, scientific journal, - No. 1, 2012. P. 31-37.
- [23] Alekseeva E.I., Arefyeva E.V. Assessment of exposure of objects of cultural heritage of the Republic of Tatarstan to hazardous exogenous geological processes // Vestnik NTSBDZhD. 2021. No. 3 (49) S. 73-80/.

PERSPECTIVE OF USING GROUNDWATER IN THE GANIKH-AYRICHAY FOOTHILLS

Esmira Mustafayeva¹, Allahverdi Tagiyev²

¹ Azerbaijan State University of Economics

² Azerbaijan State Oil and Industry University

m_esmira@unec.edu.az

allahverdi.taghiyev@gmail.com

Abstract

Most of the qualitative groundwater resources of Azerbaijan are concentrated in the Ganikh-Ayrichay foothills. As a result of research conducted in this area, it was revealed that the Ganikh-Ayrichay foothills has great prospects for water supply in Baku. According to earlier hydrogeological studies in Ganikh-Ayrichay foothills, widespread sources on the plains are associated with rocks of the fourth period, with gravel and various old rocks. Sources associated with the cliffs of the fourth period, are associated with groundwater rivers.

Groundwater areas in the plains are mainly formed under the influence of natural and artificial factors. The role of natural factors in the plain is one of the main factors. Their area of great influence is surrounded by the foothills. The role of river cones and natural hydrological factors near them in the formation of the hydrodynamic regime of underground water should be emphasized. Drinking groundwater in the study area is widespread.

Keywords: Greater Caucasus Mountains, water supply, hydrodynamic regime, aquifer, percent of mineralization, Ganikh-Ayrichay foothills, natural hazards, climate change

I. Introduction

In recent times, the demand for drinking water has increased due to global climate change. Climate change is causing problems in many areas, one of which is the reduction of drinking water. The risks of a decrease in water resources due to warming in the Greater Caucasus Mountains in Azerbaijan are also increasing (Fig. 1). The risk of a sharp decrease in drinking water is considered one of the biggest problems in the current period. In order to create a sustainable system, there is a need for integrated management of water resources.

In the eastern part of the Ganikh-Ayrichay foothill plain, it is surrounded by Dashakhilchay from the west, Bumchay, Zaglichay from the east, the southern slopes of the Greater Caucasus Mountains from the north, the Acinohur heights from the south and in the north-west of the South Caspian basin. The length of the working area is 40 km, the width is 15 km, and the area is 600 km².

The Ganikh-Ayrichay foothills is very rich in underground water due to the accumulation of thick water-permeable sediments, the presence of numerous rivers and the fall of large amounts of atmospheric sediments. Groundwater is collected here in undecomposed continental sediments. They are formed due to infiltration of atmospheric sediments and surface water (rivers, irrigation canals) and condensation of water vapors in the aeration zone. The waters of the underground water streams of the Great Caucasus's bedrock and river valleys are also of great importance in this respect. The presence of a graben-like structure is characteristic for the flow cones of rivers. As a result, a single aqueous complex consisting of coarse-grained rocks is divided into soil and

several pressure-aqueous horizons with a clay and clay layer that increases in thickness towards the south [1,2].

The groundwater horizon is found everywhere in the area. The depth of the soil mirror is 0.5-1.0 m in the wedge zone, 70-90 m in the south of the valley. The direction of groundwater flow is from northeast to southwest. The inclination of the ground water table corresponds to the inclination of the relief and varies from 0.05 to 0.003. The thickness of the horizon is 4.6-328.5 m. The maximum value is marked at the top of the cones. The groundwater horizon is partially drained by springs. Their consumption is 0.4-20.0 l/s. In the borders of the Ganikh-Ayrichay foothills, springs are mainly found in the wedge zones, on the border of the bearing cones and inter-cone depressions, in the valleys of Ganikh and Ayrichay [3].

Consumption of wells crossing the groundwater horizon is 0.1-33.5 l/s, specific consumption is 0.1-13.6 l/s.m. The percolation coefficient of the desiccating rocks varies from 0.2 to 35.5 m/day, the permeability varies from 8.64 to 3900 m²/day. The permeability of the horizon is 3.32x10³-8.5x10⁴ m²/day. Groundwater in all areas is sweet, mineralization is 0.6 g/l. The chemical composition of the water is mainly calcium carbonate [4,5].

The average annual variation amplitude of groundwater level in Zagatala region is 2.98 m, and the average monthly variation amplitude is 3.07 m.

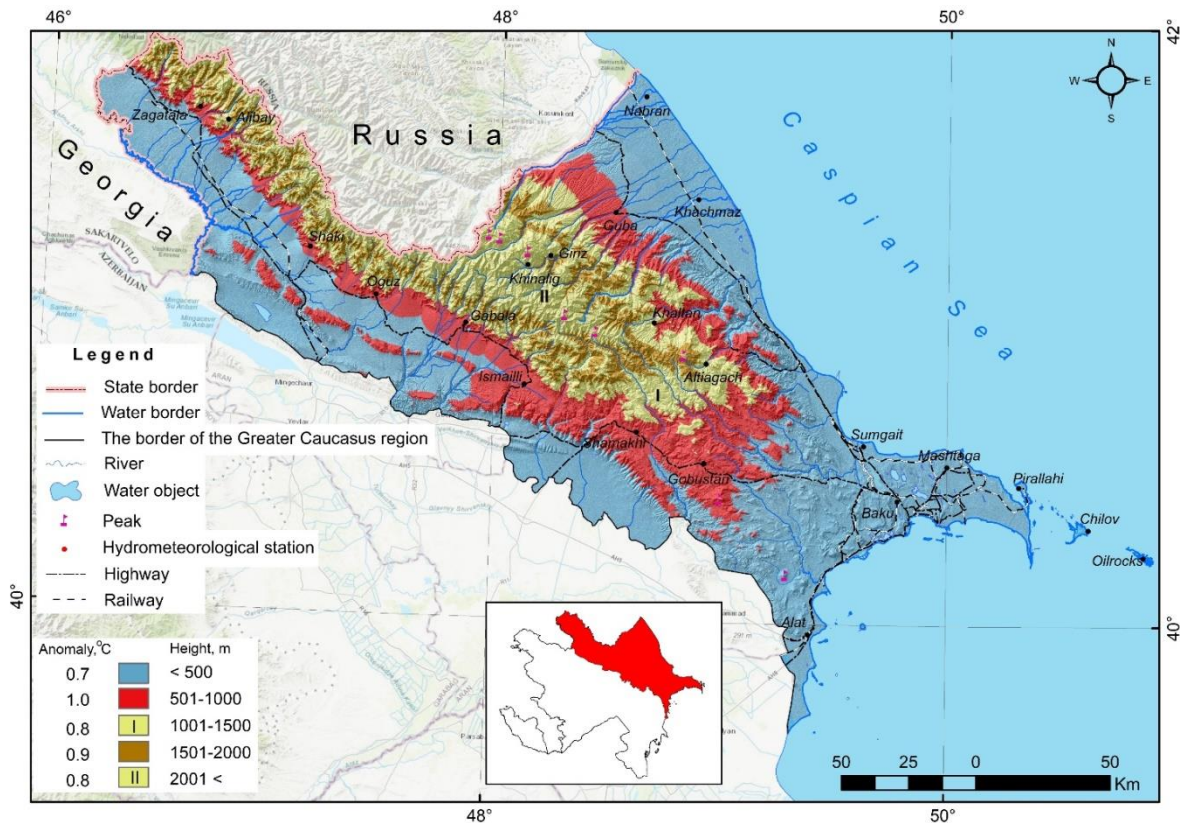


Fig. 1: Air Temperature anomaly by altitude zones (1991-2020)

A pressurized water horizon consisting of several water layers up to 350 m depth was registered in the area. A pressurized aquifer is found everywhere below the wedge zone. The sedimentary rocks consist of gravels and gravels with sand and sand-silt filler [6].

The ceiling of the pressurized water horizon was opened at depths of 4.0-177 m through wells. In most parts of the territory, the horizon lies at a depth of 30-40 m. The piezometric level is 71.0 m below the ground surface and at a height of (+35 m). The inclination of the piezometric level is 0.05-0.0025 m according to the terrain. The truncated thickness of the horizon varies from

9.5 to 319 m. The layer separating the soil and pressure water horizons consists of clays and gravelly sediments with clay filler. Their thickness is 5-30 m, sometimes 45 m [7].

Consumption of wells cutting the pressurized water horizon is 0.2-40 l/s, specific consumption is 0.1-10.5 l/s.m. varies between The seepage coefficient of desiccating rocks is 0.1-45.1 m/day, the permeability coefficient is 6-17, sometimes 55 m²/day. The piezoconductivity coefficient varies from 3.9x10⁴ to 1.35x10⁷ m²/day. Pressurized waters are sweet, mineralization is 0.1-0.6 g/l, chemical composition is calcium carbonate, sometimes calcium carbonate-chlorine [8,9,10].

The regime of changes in the level of the pressurized water horizon is closely related to the regime of changes in the level of groundwater. The average monthly change amplitude of the piezometric level is 0.84-0.86 m, the average annual change amplitude is 0.53-1.32 m, the average monthly change amplitude of well consumption is 0.71-1.06 l/s, and the average annual change amplitude is It is 0.44-0.49 l/s.

The amount of microelements found in underground water is within the limit of allowable norms.

II. Methods

The physico-chemical composition of water samples taken from existing water wells and springs in the Ganikh-Ayrichay valley was studied. Based on the obtained results, the chemical composition of underground water was expressed by the Kurlov formula and interpreted. So, ground and pressure waters of the plain have practically similar chemical composition. The total mineralization rate of pressurized water does not exceed 0.5-0.7 g/l. These waters are mainly hydrocarbonate and mixed cation content (Fig. 2.).

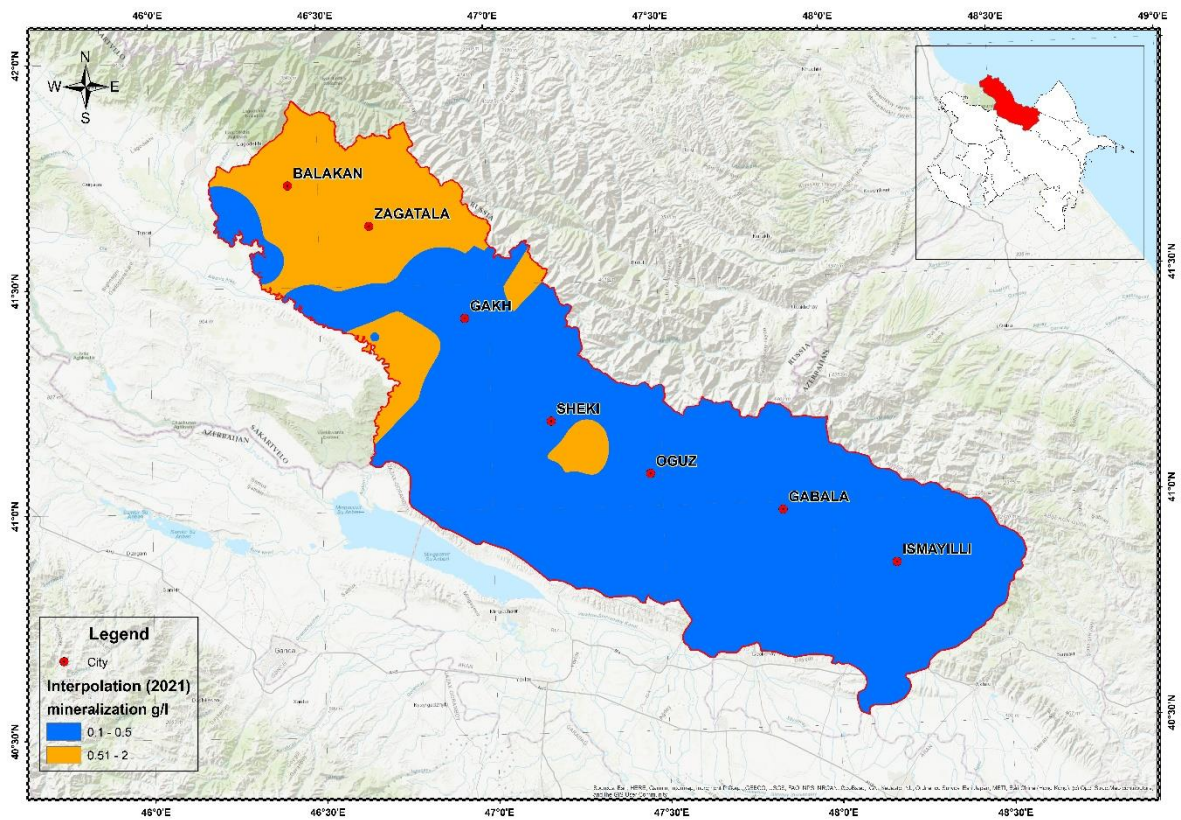


Fig. 2: Map of the degree of mineralization of groundwater in the Ganikh-Ayrichay valley

Hydro-chemical regimes of pressurized waters in the region are distinguished by their stability over many years. The temperature of pressurized water varies between 11.0-16.5 °C. The

annual amplitude is 3.5-4.5 °C. The minimum temperature is recorded in March-April, and the maximum temperature is recorded in September-October. The temperature of groundwater varies from 10-12 °C to 15-16 °C, depending on their depth. The annual amplitude of groundwater temperature is 4-5 °C in areas located in irrigated areas with a depth of 1.0-3.0 m, and in areas with a depth of 30-40 meters, the annual amplitude of groundwater temperature varies around 0.5-1.5 °C (table 1).

The role of atmospheric sediments in the formation of their annual and multi-year regimes is more pronounced in the observation points located directly in the groundwater feeding zone in the territory of Oguz region. In recent years, the depth of groundwater level in these observation points varies between 15.0-20.0 m, 35.0-40.0 m. In the annual section, their closer lying on the ground surface was recorded in April-May, when the snow melts and spring rains increase, and their deeper lying in August-September.

Table 1: Some well data on groundwater in the Ganikh-Ayrichay valley

No	Research stations, No.	Location of research stations	Depth of wells, m	Groundwater level (m)	Groundwater consumption (l/s)	Groundwater temperature, (° C)	Chemical composition of water (by Kurlov's formula)
1	2	3	5	7	8	9	
1	113	Ititala village, Balakan district, opposite Goshabulag	20,0	$\frac{0,55}{x}$		15.0	$M_{0,3} \frac{HCO_3 52,1 SO_4 43,7}{(Na + K) 82,7 Ca 11,2}$
2	114	Lahic village, Zagatala region, garden yard	120,0	$\frac{x}{0,32}$		15.0	$M_{0,5} \frac{HCO_3 63,3 SO_4 32,4}{(Na + K) 77,0 Ca 12,7 Mg 10,3}$
3	114a	The center of Layj village, Zagatala region	12,0	$\frac{2,63}{x}$		15.5	$M_{0,6} \frac{HCO_3 63,8 SO_4 27,7}{Mg 55,3 Ca 28,7 (Na + K) 16,3}$
4	B-262	Naib spring, southeast of Danachi village, Zagatala region	-	$\frac{x}{0,43}$		14.0	$M_{0,4} \frac{HCO_3 52,4 SO_4 46,4}{Ca 50,8 (Na + K) 41,6}$
5	7/1	Kharabtala village, Gakh region, entrance of the forest	200,0	$\frac{x}{0,50}$		16.0	$M_{0,4} \frac{HCO_3 65,3 SO_4 31,5}{(Na + K) 87,0}$
6	18/18	Gulluk village, Gakh district	20,0	$\frac{16,26}{x}$		15.5	$M_{0,5} \frac{HCO_3 71,4 SO_4 25,7}{Ca 52,3 (Na + K) 42,1}$
7	29	Gulluk village, Gakh district	40,0	$\frac{x}{0,30}$		15.5	$M_{0,6} \frac{HCO_3 66,2 SO_4 30,0}{(Na + K) 83,0 Ca 12,6}$
8	52	Gulluk village, Gakh district	120,0	$\frac{17,17}{x}$		16.0	$M_{0,6} \frac{HCO_3 68,9 SO_4 28,3}{Ca 55,3 (Na + K) 26,6 Mg 18,1}$
9	55	Gulluk village, Gakh district	70,0	$\frac{0,04}{x}$		16.0	$M_{0,5} \frac{HCO_3 67,5 SO_4 26,9}{(Na + K) 41,1 Ca 37,6 Mg 21,3}$
10	116	Gakh region, Kipchak village, hospital yard	120,0	$\frac{+0,27}{x}$		15.0	$M_{0,5} \frac{HCO_3 60,3 SO_4 37,9}{(Na + K) 60,6 Ca 31,3}$
11	B-401	Gakh district, Ilisu road, Amin spring	-	$\frac{x}{1,25}$		16.0	$M_{0,4} \frac{HCO_3 59,9 SO_4 38,3}{(Na + K) 56,4 Ca 34,0}$

In the foothill region, observation points located directly in the upper parts of the flow cones of the Alijan and Damiraparan rivers are in the zone of influence of the hydrological regimes of

the rivers. In the reporting years, the depth of the groundwater level in these observation points varied from 69.0 to 92.0 meters, and the annual amplitudes were from 0.38 to 2.11 m in these wells.

Irrigation agriculture has developed in the central and southwestern regions of the plain. Surface and underground water are widely used for irrigation. In the reporting years, the average annual depth of the groundwater level in observation points 10^A and 114^A located in these areas was in the range of 0.07-0.79 m. The annual amplitude of the level is 0.47-0.60 m, the minimum depth of groundwater is 0.07-0.19 m, even some years it is above the surface of the earth, in spring months in April-June, the maximum depth is 0.65- 1.48 m was recorded in late summer and early autumn, when irrigation works were completed, in August-October.

In the plain, the pressure water horizons and water complexes of the Quaternary period were opened in full thickness by means of hydrogeological exploration wells. In general, pressurized water is widespread throughout the plain.

The depths of the wells studying the regime of pressurized water horizons included in the observation network do not exceed 250-300 meters. Hydrodynamic regimes of pressurized waters are characterized by their relative stability compared to ground waters throughout the plain. The annual change of the amplitude of pressurized water, close to the amplitude of the ground water level, indicates that the source of nutrition and conditions of the soil and pressurized water horizons are the same.

Although there is no noticeable difference in the annual changes in the consumption of pressurized water, in general, the increase in consumption is recorded in the spring-summer season, and the minimum limits are observed at the end of the year. Although the observation points are located in different areas of the plain, a general regularity is observed in the change of their costs. In the reporting years, the average annual consumption of water in wells at these observation points is 0.50-3.00 l/sec, and the annual amplitude change is 0.60-3.50 l/sec. Thus, the average annual consumption in well No. 29 is 1.80-2.20 l/sec, and the annual amplitude change is 1.50-2.00 l/sec.

In the studied areas and in the parts connected with the foothills of the Greater Caucasus, the waters of the groundwater horizon come to the surface in the form of springs. The consumption of springs varies from 0.4 l/s to 300 l/s. The largest springs are located 2.5-3.0 km north of Mollali village of Oguz region. Here, the consumption of springs varies between 285-305 l/s. The most common consumption of springs varies between 10-40 l/s. The groundwater of the Ganikh-Ayrichay foothills spreads along horizons with an absolute height of 380-400 m, coming out in the form of a spring at the foot of the cones of the rivers and in the depressions between the cones. The consumption of springs in these areas varies from 0.1-0.2 l/s to 20-30 l/s.

The spring of ground water to the surface of the earth is spread along horizons with an absolute height of 380-390 m in the areas where the southern edges of the Ganikh-Ayrichay foothills meet with Acinohur. The consumption of the largest springs in these areas reaches 155 l/s. Among such springs, the "Girkhbulag" spring can be mentioned. This spring is located 3 km south of the village of Nich in the area where the northern foot of Acinohur elevation and the valley meet. The area of the spring is 1, 1.5 ha and it consists of many springs. The total consumption of those springs is up to 150 l/s. The consumption of other springs spread here varies from 15-20 l/s to 1-6 l/s. These springs combine to form the Karasu and Sarisu rivers.

Rocks in which groundwater is distributed have great water content. Consumption of wells detecting groundwater varies between 10÷15-45÷50 l/s. The specific consumption in wells varies between 0.6-6.7 l/s.m. The seepage coefficient of water retaining rocks varies between 1.4-31.51 m/day. The permeability of the groundwater horizon varies between 138-7620 m²/day. The coefficient of level transfer in groundwater varies between 3.33×10^3 - 8.5×10^4 m²/day.

The degree of mineralization of groundwater in the territory of the Ganikh-Ayrichay foothills varies between 0.2-0.5 g/l and reaches 0.7 g/l in the southern parts of the valley. The type of chemical composition of groundwater is mainly hydrocarbonate-calcium.

The exact description of the chemical composition of groundwater and the degree of mineralization is given in the title "Characteristics of the quality of groundwater". Pressurized

underground water is distributed in the area of the Ganikh-Ayrichay foothills, starting from the zone where the groundwater comes to the surface in the form of a spring, and some areas to the north of it. In this zone, as mentioned above, groundwater and pressurized water create an aquifer that forms a single hydraulic system.

In the areas explored up to a depth of 350 m in the Ganikh-Ayrichay foothills, water retaining layers consisting of several floors were discovered.

III. Results

Based on the results of the studies, it is known that the hydro-chemical regimes of the groundwater of the plain are characterized by their relative stability. Indicators of general mineralization do not exceed 0.5-0.7 g/l throughout the plain, with the exception of discharge zones. In discharge zones, the total mineralization of groundwater often rises to 1.0-1.3 g/l. According to the hydro-chemical composition, they belong to the hydro-carbonate, sulfate-hydro-carbonate, calcium-magnesium-sodium type.

Groundwater regimes on the plain are formed under the influence of natural and artificial factors. The role of natural factors is the main one on the plain. Their large sphere of influence covers the foothills. Along with the foothill areas, special attention should be paid to the runoff cones of rivers widely developed on the plains, and the role of natural hydrological factors near them in the formation of the hydrodynamic regimes of groundwater.

Conducted studies show that underground water in the Ganikh-Ayrichay foothills is suitable for drinking. Also, there are waters of therapeutic importance in this area.

References

- [1] Bondarenko, L.V., Maslova, O.V., Belkina, A.V., Sukhareva, K.V. 2018. Global climate change and its aftermath. Herald of the Russian Economic University named after B. Plekhanova. 2, 84-93. <https://doi.org/10.21686/2413-2829-2018-2-84-93>
- [2] Geology of Azerbaijan. 2008. Vol. VIII. Hydrogeology. Baku, Nafta-Press. 380 p.
- [3] Israfilov, Yu.H, Israfilov, R.H., Guliyev, H.H., Efendiyev, G.M. 2016. Risk assessment of the water resources losses of the Azerbaijan republic due to climate changes. news of ANAS, Earth Sciences, № 3-4. 37-47.
- [4] Taghiyev A.Sh. Climate change and water resources management. International Scientific Conference on Sustainable Development. Baku, 24-25 november, 2017. 55-61.
- [5] Taghiyev A.Sh. Hydrogeological conditions of the Ganykh-Ayrichay basin and prospects for the use of groundwater. Proceedings of the conference, PART II, pp.201-203.
- [6] Tagiev, I.I., Babaev, N.I. 2017. Some geochemical and hydrogeological, regularities of formation and distribution of mineralwaters of Azerbaijan. XXXIX International scientific-practical conference, Actual problems in modern science and ways of their solutions, Moscow, 15-19.
- [7] Tagiev I.I. 2001. Status and problems of protection of the environment and nature use in the Republic of Azerbaijan, Ministry of Science and Technology of the USSR, Moscow.
- [8] Tagiev, I.I., Kerimov, V.M. 2021. Prospects for the development of alternative energy and the use of thermal waters in Azerbaijan. Ural Geolog. Journal. 3 (141). 51-57.
- [9] Tagiyev I.I., Ismailova M.M., Karimov V.M., Sharifov J.J. Groundwater of Ganikh-Ayrichay foothills on the prospects of use Reliability: Theory and Applications, Special Issue № 3 (66) Volume 17, 2022, 113-118. DOI: <https://doi.org/10.24412/1932-2321-2022-366-76-81>
- [10] Rzaeva, S.M., Tagiyev A.Sh. and Zeynalova S.A. "Impact of climate change on the groundwater of the Ganikh-Ayrichay foothills." Reliability: Theory & Applications 17.SI 4 (70) (2022): 180-187. DOI: <https://doi.org/10.24412/1932-2321-2022-470-180-187>

PROCESSING OF DATA BASED ON FUZZY RULES

Kifayat Mammadova, Yegana Aliyeva, Matanat Hasanquliyeva

•

Azerbaijan State Oil and Industry University

kifayat.mammadova.adnsu@gmail.com

yegane.aliyeva.1969@mail.ru

metahasanquliyeva@rambler.ru

Abstract

After establishing a fuzzy rule base using the interpolation result mechanism, arranging a fuzzy inference system is performed. The established system will infer about the level of risk using a fuzzy rule base and input statistics. In this work, the construction of the inference system has been determined using fuzzy rules interpolation. The construction determines the distances between input signals and relation functions based on if-then rules. The cross section α used here reduces the distance between input variables. In this work, interpolation is used to measure the distance between α -section fuzzy sets.

Such economics issues as forecasting, planning, calculation of expected income are considered in uncertainty conditions, incomplete information conditions using interpolation.

Keywords: fuzzy sets, Z numbers, fuzzy rules, judgments, interpolation, difference of fuzzy sets, forecasting, expected income

I. Introduction

The presentation and processing of data is a class of mathematical problems having an obvious practical direction, primarily in the field of information science, radio engineering, control and communication theory, radar and navigation equipment. In most cases, in solving mathematical problems, the initial data is represented by a number of points of arbitrary dependence of form $y(x)$. In the free state, this dependence may be unknown. The interpolation apparatus is used to calculate the intermediate values of a function.

Non-fuzzy interpolation methods allowing to solve specific problems of approximate calculations and obtain stable solutions are used to illustrate the uncertainties and unmanageable errors occurring in the development of various models used in technical applications, to reduce the impact of uncertainties. The application of fuzzy set theory methods in the above-mentioned problems provides simple and effective algorithms. One way to filter data with uncontrollable distortions is fuzzy interpolation, which is a natural generalization of the corresponding distinct analog. Distinct and fuzzy interpolation algorithms are based on the use of Newton and Lagrange polynomials. Spline interpolation is widely used in computational mathematics with the further development of variation methods to solve difference problems.

Significant advancement has also been achieved in solving various problems using fuzzy linear systems in computational mathematics, control theory, and other fields. In this paper, based on fuzzy calculations and the theory of fuzzy linear systems, Newton's interpolation problem for fuzzy data is solved and conditions are provided for the presence or absence of strong, weak interpolation [1].

In the paper, the model of fuzzy data interpolation in the production process is developed. A polynomial with a fuzzy coefficient is constructed as a model function. Moreover, the concept of gravity point used to determine the distances between data is presented. The optimization

problem is solved by the minimum of the squares sum of the distances between the initial and model data and the equality of fuzzy functions.

II. Inclusion of fuzzy interpolation

Being a part of classical sets, fuzzy sets are always perceived as an extension of classical sets. The elements of these sets have a degree of relation. Let us give definitions of fuzzy sets and fuzzy triangle relation functions used in this paper.

Defintion 1. Suppose, $U = \{x_1, x_2, \dots, x_n\}$ is a space of judgments, universe. The fuzzy set A taken from the set U is a relation function of $(A \subset U) \mu_A: U \rightarrow [0,1]$ A set and indicates the relation function of $\mu_A(x) \in [0,1]$ x - to $A[0,1]$.

Defintion 2. R is a fuzzy subset A defined by the elements of a set of real numbers (a_1, a_2, a_3) . The triangular fuzzy relation function of the set A means the following function:

$$\mu_A(x) = \begin{cases} 0, & -\infty \leq x \leq a_1 \\ \frac{x-a_1}{a_2-a_1}, & a_1 \leq x \leq a_2 \\ \frac{a_2-x}{a_3-a_2}, & a_2 \leq x \leq a_3 \\ 0, & -\infty \leq x \leq \infty \end{cases} \quad (1)$$

The fuzzy triangular relation function is often used to represent linguistic terms numerically. Here, triangular relation functions were used to represent the constraints and reliability of Z-number. Systems based on fuzzy regulations cover the fuzzy sets in the previous and subsequent parts of the rules, as well as determine the relationship between the input and output of the system. In addition, using fuzzy rules base and inputs, fuzzy inference is performed to make decision. Various fuzzy information mechanisms are proposed for the development of fuzzy data. These mechanisms are mainly based on analogy, similarity, composition, interpolation and distance approach. In these approaches, the performance, speed and complexity of the inference mechanisms are considered to be important issues [2-4].

This paper discusses an inference mechanism based on fuzzy interpolation considerations proposed by Cauchy and Hirota. Fuzzy interpolation can be used effectively to develop a database of rules in conditions of uncertainty. In this case, some conditions are required to be carried out. The fuzzy sets used under such conditions must be continuous, convex, and limited normal. Interpolation is based on measuring the distance between two fuzzy sets. In this work, interpolation is used to measure the distance between α -section fuzzy sets. Consider two fuzzy sets A_1 and A_2 . α -section of fuzzy sets A_1 and A_2 will be marked with A_1^α and A_2^α . Suppose, fuzzy set A_1 is smaller than A_2 , i.e. $A_1 < A_2$, if

$$\inf\{A_1^\alpha\} < \inf\{A_2^\alpha\} \vee \sup\{A_1^\alpha\} < \sup\{A_2^\alpha\}. \quad (2)$$

Where $\inf\{A_1^\alpha\}$ and $\inf\{A_2^\alpha\}$ are lower boundries for $A_1 \vee A_2$, $\sup\{A_1^\alpha\}$ and $\sup\{A_2^\alpha\}$ are upper boundries for $A_1 \vee A_2$ (1). Consider the mechanism of interpolation justification. Let's consider a fuzzy controller based on a fuzzy rule base with one input and one output. Suppose that the current input variable X is taken equal to A^* as a result of the observation. Let's determine the value of output Y of the system based on the corresponding rules database A^* . Suppose, A^* is smaller than fuzzy set A_1 and greater than fuzzy set A_2 i.e., $A_1 < A^* < A_2$ and at the same time $B_1 < B_2$. Let's define a system output for A^* input. The problem can be expressed as follows [1]:

It is provided:

X is taken equal to A^* , and Y equal to B^* .

if X is A_1 , then Y is B_1 ,

if X is A_2 , then Y is B_2 ,

(3)

Where,

$$\frac{d(A^*, A_1)}{d(A^*, A_2)} = \frac{d(B^*, B_1)}{d(B^*, B_2)} \quad (4)$$

Where, $d(\cdot)$ is the distance between two fuzzy sets. Using α -sections based metrics, Cauchy and Hirota finally determined fuzzy sets. The distance between the two fuzzy sets intersected by d^L at the bottom and d^U at the top can be calculated as follows by using α [2,3]:

$$\begin{aligned} d_{ij}^L &= d^L(A_{ij}^\alpha, X_j^\alpha) = d(\inf\{A_{ij}^\alpha\}, \inf\{X_j^\alpha\}) = \inf\{A_{ij}^\alpha\} - \inf\{X_j^\alpha\}, \\ d_{ij}^U &= d^U(A_{ij}^\alpha, X_j^\alpha) = d(\sup\{A_{ij}^\alpha\}, \sup\{X_j^\alpha\}) = \sup\{A_{ij}^\alpha\} - \sup\{X_j^\alpha\} \\ &= d^L(B_j^\alpha, Y_j^\alpha) = d(\inf\{B_j^\alpha\}, \inf\{Y_j^\alpha\}) = \inf\{B_j^\alpha\} - \inf\{Y_j^\alpha\} \\ &= d^U(B_j^\alpha, Y_j^\alpha) = d(\sup\{B_j^\alpha\}, \sup\{Y_j^\alpha\}) = \sup\{B_j^\alpha\} - \sup\{Y_j^\alpha\} \end{aligned} \quad (5)$$

Homming or Euclidean formula can be used to measure distances in (5). Using the distance, Cauchy and Hirota put forward a proposal based an interpolation for the rule of $2k$.

$$\begin{aligned} \inf\{B_j^{*\alpha}\} &= \frac{\sum_{i=1}^{2k} (1/d^L(A_{ij}^\alpha, A_i^{*\alpha})) \inf\{B_j^\alpha\}}{\sum_{i=1}^{2k} 1/d^L(A_{ij}^\alpha, A_i^{*\alpha})}, \\ \sup\{B_j^{*\alpha}\} &= \frac{\sum_{i=1}^{2k} (1/d^U(A_{ij}^\alpha, A_i^{*\alpha})) \sup\{B_j^\alpha\}}{\sum_{i=1}^{2k} 1/d^U(A_{ij}^\alpha, A_i^{*\alpha})} \end{aligned} \quad (6)$$

Where, $B_j^{*\alpha} = [\inf\{B_j^{*\alpha}\}, \sup\{B_j^{*\alpha}\}]$. In order to find the result of the fuzzy system Z, consider the justification using interpolation.

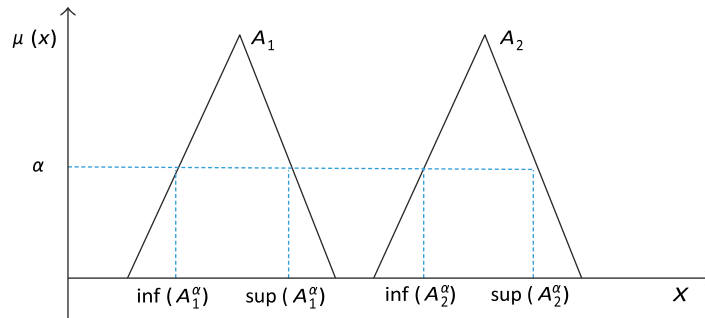


Fig. 1: α is the cross section of the relation function: infimum and supremum.

III. Fuzzy inference system based on Z-numbers

Defintion 1. Number Z is an ordered pair of fuzzy numbers denoted by $Z(A, B)$, where the first component A is a constraint for the values of fuzzy variable X, and the second component B is a measure of reliability for A components.

Figure 1 uses the triangular relation functions to illustrate the components of number Z. Where, A will express the fuzzy value of variable X, and B will express the accuracy degree or reliability measure, or accuracy probability of A; for example, X is A with possible constraints, i.e.

$$B(X) : X \subset A \rightarrow Poss(X = u) = \mu_A(x) \quad (7)$$

Where, $\mu_A(x)$ is the relation function of fuzzy set A constrained by $B(X)$. u is the total value of X. $\mu_A(x)$ is a relation degree that provides u . One of the most effective ways to present fuzzy data is to use number Z. For example, let's consider the forecast of grain harvest in our country. As you know, this parameter depends on a number of factors. "If we say that the grain harvest will be

higher this year, it is considered an event that can happen 100%. More precisely, this event can be expressed as follows: "This year the grain harvest will be higher" [5-7].

As it is shown, the event can be illustrated by a number Z , i.e., " $X = Z(A, B)$ ". Where, fuzzy variable X is the "grain harvest". The values of variable X are described using the pair (A, B) . A is "higher" constraint and B is the reliability of A , which is illustrated as "most probable".

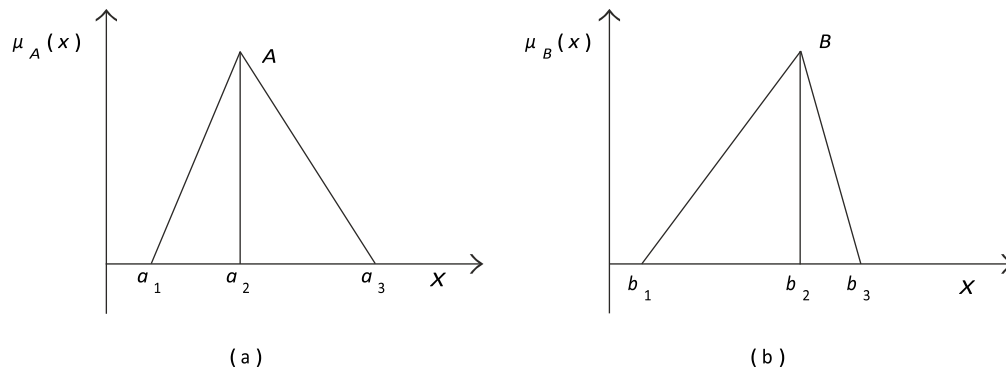


Fig. 2: $Z, Z(A, B)$: a) constraint; b) reliability

Definition 2. Suppose, $Z_1(A_1, R_1)$ and $Z_2(A_2, R_2)$ are two Z numbers. The α -cross-sectional distance between numbers Z_1 and Z_2 is defined as follows:

$$D(Z_1^\alpha, Z_2^\alpha) = |a_1^{L\alpha} - a_2^{L\alpha}| + |a_1^{R\alpha} - a_2^{R\alpha}| + |r_1^{L\alpha} - r_2^{L\alpha}| + |r_1^{R\alpha} - r_2^{R\alpha}| \quad (8)$$

where, $a_1^{L\alpha}, a_2^{L\alpha}, r_1^{L\alpha}, r_2^{L\alpha}, a_1^{R\alpha}, a_2^{R\alpha}, r_1^{R\alpha}, r_2^{R\alpha}$ are respectively α -cross-sectional fuzzy triangular numbers of fuzzy sets A_1, R_1, A_2, R_2 from right and left sides.

Consider the development of Z -number based interpolation mechanism. Suppose that *if-then* fuzzy rules with multiple inputs and one output, have the following form:

$$\begin{aligned} &\text{if } x_1 = (A_{11}, R_{11}) \dots, v \exists x_m = (A_{1m}, R_{1m}), \text{ then } y = (B_1, R_1), \\ &\text{if } x_1 = (A_{21}, R_{21}) \dots, v \exists x_m = (A_{2m}, R_{2m}), \text{ then } y = (B_2, R_2), \end{aligned} \quad (9)$$

...

$$\text{if } x_1 = (A_{n1}, R_{n1}) \dots, v \exists x_m = (A_{nm}, R_{nm}), \text{ then } y = (B_n, R_n),$$

where A_{ij} and R_{ij} are fuzzy limiting and reliability parameters, respectively, and x_i and y are system inputs and outputs. Here $j = 1, \dots, m$, m are the number of input signals; $i = 1, \dots, n$, n are the number of rules. Let's use the fuzzy interpolation given above for fuzzy rules based on Z numbers in Fig.2. Suppose that these input signals are included in a fuzzy system. In the first iteration, the distance between the input signal included and the fuzzy values of the variables according to the rules used in the previous section will be calculated. The distance is calculated using the α -section using Hamming or Euclidean distances.

In the next section, the metrics will be calculated separately for each constraint and reliability variable [1-4].

Formula (5) is used in the previous part of the rules to find the metrics of the relation function at the bottom and top. α sections of A are used to determine the lower and upper distances [8]:

$$d_{ij}(A_{ij}^\alpha, X_j^\alpha) = d_{ij}^\alpha = |A_{ij}^\alpha - X_j^\alpha|, \quad (10)$$

$$d_i^\alpha = \sum_j^m d_{ij}(A_{ij}^\alpha, X_j^\alpha),$$

here, $d_j(A_{ij}^\alpha, X_j^\alpha)$ is the metrics between two fuzzy sets defined for rule i ; $j=1, \dots, m$ and m are the number of input signals; $i=1, \dots, n$ and n are the number of the rules. Distances are described as lower and upper metrics:

$$d_{ij}^{\alpha}(A_{ij}^{\alpha}, X_i^{\alpha}) = \{d_{ij}^L(A_{ij}^{\alpha}, X_i^{\alpha}), d_{ij}^U(A_{ij}^{\alpha}, X_i^{\alpha})\} \text{ and } d_i^{\alpha}(d_i^L, d_i^U).$$

In the special case, equation $\alpha = \{0,1\}$.(2.10) is applied to the constraint A and reliability R . The total distance will form the sum of the two distances:

$$d_i^{\alpha} = dc_i^{\alpha} + dr_i^{\alpha}, \quad (11)$$

where, dc_i^{α} and dr_i^{α} are the distances calculated sequentially with (8) for the constraint and reliability parameters. d_i^{α} is the calculated distance for this rule. Each of the calculated distances is characterized by two left and right values [9]:

$$\begin{aligned} dc_i^{\alpha} &= (dc_i^L, dc_i^U) \\ dr_i^{\alpha} &= (dr_i^L, dr_i^U) \\ d_i^{\alpha} &= d_i^{\alpha L} + d_i^{\alpha R} \end{aligned} \quad (12)$$

Output data for output fuzzy set is calculated as:

$$\begin{aligned} Y^{\alpha} &= \frac{\sum_{i=1}^n (1/d_i^{\alpha}) B_{Y_i}^{\alpha}}{1/\sum_{i=1}^n 1/d_i^{\alpha}} \\ R_Y^{\alpha} &= \frac{\sum_{i=1}^n (1/d_i^{\alpha}) B_{Y_i}^{\alpha}}{1/\sum_{i=1}^n 1/d_i^{\alpha}} \end{aligned} \quad (13)$$

Formula (13) is used to find the values of constraints and reliability of fuzzy sets. If we combine (10) and (13), the following equations can be obtained:

$$\begin{aligned} Y^{\alpha} &= \frac{\sum_{i=1}^n (1/\sum_j^m d_L(A_{X_{i,j}^{\alpha}}, X_j^{\alpha})) B_{Y_i}^{\alpha}}{1/(\sum_{i=1}^n (1/(\sum_j^m d_L(A_{X_{i,j}^{\alpha}}, X_j^{\alpha}))))} \\ R_Y^{\alpha} &= \frac{\sum_{i=1}^n (1/\sum_j^m d_L(A_{X_{i,j}^{\alpha}}, X_j^{\alpha})) B_{Y_i}^{\alpha}}{1/(\sum_{i=1}^n (1/(\sum_j^m d_L(A_{X_{i,j}^{\alpha}}, X_j^{\alpha}))))} \end{aligned} \quad (14)$$

The fuzzy signal Z of the system can be obtained using (10) - (13).

It should be noted that B_{Y_i} is used to find the output signal, and variables R_{Y_i} are used to find reliability on the right of formula (13) or (14). After obtaining the output signals, the number Z is converted into a non-fuzzy number. To do this, a formula is used to calculate the middle of two fuzzy numbers.

$$Y = ((Y_1 + 4 * Y_m + Y_r)/6) * ((R_{Y_1} + 4 * R_{Y_m} + R_{Y_r})/6) \quad (15)$$

Formula (15) is used to obtain the exact value of the output signal. Here Y is the fuzzy output value and R_Y is the reliability. It should be noted that in the previous and next parts of the rules base we use triangular fuzzy sets for input and output parameters. Given the levels $\alpha = 0$ and $\alpha = 1$, we can obtain the left value of the output signal Y_l , the average Y_m and the right Y_r . Left (Y_l, R_{Y_l}) and right (Y_r, R_{Y_r}) values correspond to the level $\alpha = 0$, the average value (Y_m, R_{Y_m}) corresponds to the level $\alpha = 1$. First, the left and right values are determined according to the level $\alpha = 0$, then the highest value of the triangle corresponding to the level $\alpha = 1$ is determined. These values are applied to find the output triangle relation function.

IV. Conclusions

In this work, the construction of the result system was determined using interpolation of fuzzy rules. The distances between the input signals and relation functions based on *if-then* rules are determined in the construction. The cross section α used here reduces the distance between the input variables. In this work, interpolation is used to measure the distance between α -section fuzzy sets.

References

- [1] Lütfi Z., Aliyev R.A. "Fuzzy Logic Theory and Applications", World Scientific, 2018.
- [2] Aliyev R.A., Aliyev R.R. Soft Computing. Bakı, Chashıoglu, 2004, 484 s.
- [3] Oscar Castillo, Patricia Melin. Type-2 Fuzzy Logic: Theory and Applications. Springer Berlin, Heidelberg. Published: 21 October 2010, 244p. <https://doi.org/10.1007/978-3-540-76284-3>.
- [4] George Klir and Bo Yuan. Fuzzy sets and fuzzy logic: Theory and Applications". Prentice Hall PTR, Upper Saddle River, New Jersey, 1995, XV + 574 pages. ISBN 0-13-101171-5.
- [5] İhsan Kaya, Murat Çolak, Fulya Terzi. A comprehensive review of fuzzy multi criteria decision making methodologies for energy policy making. Energy Strategy Reviews. Energy Strategy Reviews 24 (2019), pp.207–228.
- [6] Xiuxia Du, and Pingkang Li. Fuzzy Logic Control Optimal Realization Using GA for Multi-Area AGC Systems. International Journal of Information Technology Vol.12 No.7 2006, pp. 63-72.
- [7] Kamari M. L., Isvand H., Nazari M. A. Applications of Multi-Criteria Decision-Making (MCDM) Methods in Renewable Energy Development: A Review. Renewable Energy Research and Application, Vol 1, No 1, 2020, 47-54.
- [8] Bayram G. Ibrahimov, Faxri I. Huseynov. Research and analysis mathematical model for evaluating noise immunity in telecommunication system// SYNCHROINFO JOURNAL, IEEE Austria Section, No.1, 2020. – pp. 2-6. DOI: 10.36724/2664-066X-2020-6-1-2-6.
- [9] Mammadova K.A. Construction of fuzzy power generation model of thermal power plants. Scientific collection «interconf». No1, 2021, pp.1065-1075.

MORPHOMETRICAL CHARACTERISTICS OF AVALANCHES WITH THE USE OF A UAV (ON THE EXAMPLE OF ILE ALATAU)

Aidana Kamalbekova, Victor Blagoveshchensky, Sandugash Ranova,
Uldzhan Aldabergen

Institute of Geography and Water Security JSC, Almaty, Kazakhstan

aidana.kamalbekova@gmail.com

ingeo_2009@mail.ru

sandu2004@mail.ru

aldabergen_u@mail.ru

Abstracts

The article deals with the experience of using an unmanned aerial vehicle (DJI Matrice 300 RTK) and Agisoft Metashape software to obtain the characteristics of avalanches that descended in late March in the Shukur and Kotyrbulak tracts (Pioneer avalanche) in the Ile Alatau mountains. UAVs can perform observations in remote and dangerous areas, quickly reach the scene, and capture high-quality images and video. In Agisoft Metashape, data processing is performed to create digital elevation maps, 3D models and obtain various geometric data. The resulting data can be used to analyze and predict avalanche processes, as well as to develop measures to reduce the risk of such processes in the future.

Keywords: unmanned aerial vehicles, digital elevation model, orthophoto, 3D surface models, Agisoft Metashape, snow avalanches

I. Introduction

Avalanches are widespread in the mountainous regions of Kazakhstan, with hundreds of avalanches being recorded in the Ile Alatau. Since the middle of the last century, 95 people have died under avalanches in Kazakhstan and 80% of the incidents occurred in the Ile Alatau mountains. The use of unmanned aerial vehicles (UAVs) to study avalanches is a relatively new but very promising direction [1,2]. Drones nowadays are developing at an amazing speed, it is reasonable to use drones in almost all spheres of activity. Drones make it possible to carry out observations in remote and dangerous areas, as well as to obtain high-quality images and accurate data, which makes them a valuable tool for monitoring hazardous processes.

Unmanned aerial vehicles offer significant advantages for research [3]. Some of the major advantages include:

1. Safety: their use can greatly enhance the safety of researchers.
2. Efficiency: they can be brought to the scene quickly, allowing rapid damage assessment, assurance that the area is safe, and decisions to evacuate or secure the scene.
3. High accuracy: they can capture high quality images and video that can be used for analysis. This provides more accurate and detailed information than a ground based survey.
4. Low cost: their use can be more cost effective than using pilot-operated aircraft or ground-based means. This can reduce the cost of surveys and provide better access to data.
5. Large coverage: they can move quickly over large areas, allowing large areas to be studied quickly.

6. Automatic control: they can be controlled automatically, which reduces the need for a pilot, and may also allow operation in areas that are difficult to access or in poor weather conditions.

To obtain avalanche characteristics using a UAV, the following steps should be carried out:

1. Equipment preparation: for data collection, it is necessary to use a UAV with a camera capable of recording high-resolution images. In our study, we used a DJI Matrice 300 RTK drone. It is equipped with many sensors and features that allow it to perform different tasks, two cameras that allow it to capture high quality video and photos, a LiDAR sensor that allows it to create accurate 3D models of the terrain. To improve its positioning accuracy, the DJI Matrice 300 RTK uses the RTK (Real Time Kinematic) system, which provides positioning accuracy to within a centimeter. It also has the ability to utilize the PPK (Post Processing Kinematic) system, which allows for increased positioning accuracy with post flight processing.

2. Location selection: it is necessary to select a location where avalanches are observed.

3. UAV flight: after preparing the equipment and selecting the location, the UAV should be launched and fly over the study area. To obtain the most accurate data, it is recommended to fly at different altitudes and camera angles.

4. Data processing: after obtaining the photos it is necessary to process them using Agisoft Metashape program. The program can be used to create digital elevation maps, 3D surface models based on photographs, and various geometric data, including longitudinal profiles, digital elevation maps (DEM) and digital terrain models (DTM). In order to build a 3D model, a set of photographs including high-resolution images of objects must be taken. Once the set of photos is loaded into the program, Agisoft Metashape will align and merge the photos to create a 3D model of the object. Additional steps are required to produce a digital elevation map and digital terrain model. First, the program determines the position of each point on the object's surface and uses this data to create a point cloud. Then it creates DEM and DEM using the point cloud data. To obtain a longitudinal profile, it is necessary to select the line along which the profile is to be drawn. This can be done, for example, by selecting a line on a digital elevation map. The program then automatically builds the longitudinal profile by displaying the zone elevations along this line. Agisoft Metashape can also be used to analyze the size and shape of objects, obtain volumes and areas. The program can provide valuable information about the structure and geometry of the areas under study, as well as predict possible future hazards.

5. Data analysis: the obtained data can be used to analyze and predict avalanche processes, as well as to develop measures to reduce the risk of such processes in the future.

Using this method, we determined the parameters of avalanches that descended in late March 2022 in the Shukur and Kotirbulak tracts (Pioneer avalanche) in the Ile Alatau Range.

To determine the avalanche parameters, we used the method of differential aerial photography. Its essence consists in comparing two digital elevation models obtained by aerial photography: one digital elevation model is obtained immediately after avalanches, when the avalanche snowpack has not yet had time to melt; the other digital elevation model is obtained after full melting of the snowpack in summer.

By subtracting the second digital elevation model from the first, a digital avalanche snowpack model is obtained, which makes it possible to determine the avalanche volume. This method is one of the most accurate and reliable ways to determine the volume of avalanche snow slopes, as it allows taking into account the changes in the territory after the avalanche.

According to the survey results, the following parameters of the avalanche in Shukur were determined: avalanche stopping point - 2353 m, length - 140 m, average width - 29 m, area - 4117 m², average thickness - 2.4 m, maximum thickness - 6 m, volume - 9865 m³.

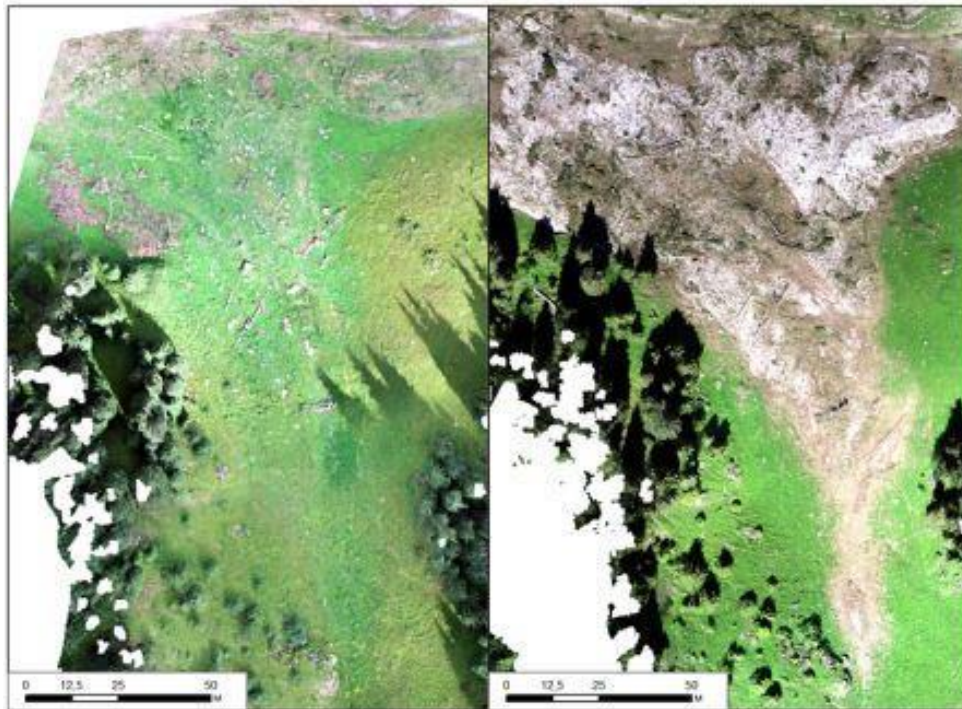


Fig. 1: Orthophoto of the avalanche rollout area in Shukur with (right) and without (left) avalanche snowpack



Fig. 2: 3D model of avalanche rollout area with avalanche snowpack

Pioneer avalanche data: stop point - 1845 m, length - 265 m, average width - 32 m, area - 8480 m², average thickness - 3.6 m, maximum thickness - 7.2 m, volume - 30528 m³.

In the 21st century, technology does not stand still. Older equipment is being replaced by digital and laser devices. The use of various new technologies is replacing traditional methods. Avalanche researchers, in order to accurately determine the limits of avalanche spread and avalanche volumes, use a very labor-intensive method in which the contours of the avalanche snowpack are measured with geodetic instruments and its thickness is measured with avalanche probes. The limit of avalanche thickness measured in this way is 3 meters. Only a small number of avalanches can be measured with this method. The remaining majority of avalanches are mapped

visually, and their volumes are also estimated visually with a very large error [4, 5]. In this paper, we demonstrate how this problem can be solved by using aerial photography of avalanche stopping zones from unmanned aerial vehicles (UAVs).



Fig. 3: Orthophotomaps of the area with and without avalanche snowpack near the "Pioneer" campground

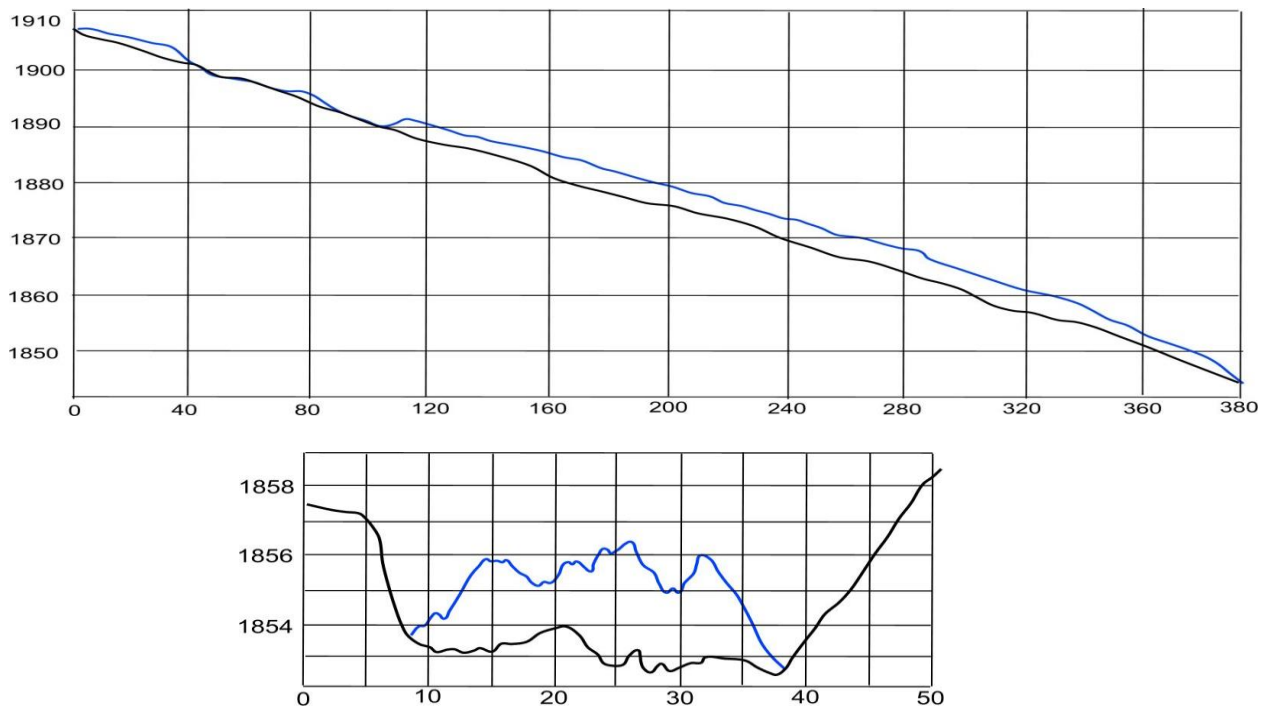


Fig. 4: Longitudinal and transverse profiles of avalanche snowpack

Acknowledgements. The article was written based on the results of research under the project "Development of a method for forecasting snow avalanches in Ile Alatau using artificial intelligence methods", funded by the Committee of Science of the MNVO RK (grant No. AP09260155).

References

- [1] Low cost surveying using an unmanned aerial vehicle // ISPRS - International Archives of the Photogrammetry Remote Sensing and Spatial Information Sciences 40(1):311-315, August 2013, <https://doi.org/10.5194/isprsarchives-XL-1-W2-311-2013>.
- [2] Yawar Hussain, Romy Schlögel, Agnese Innocenti, Omar Hamza, Roberto Iannucci, Salvatore Martino, Hans-Balder Havenith, Review on the Geophysical and UAV-Based Methods Applied to Landslides// Remote Sens. 2022, 14(18), 4564 <https://doi.org/10.3390/rs14184564>
- [3] Use of unmanned aerial vehicles in monitoring application and management of natural hazards// Geomatics, Natural Hazards and Risk Volume 8, 2017 - Issue 1, pages 1-4 <https://doi.org/10.1080/19475705.2017.1315619>
- [4] Ystykul K.A., Seredovich V.A. Investigation of snow avalanches using the technology of terrestrial laser scanning // Vestnik KazNU, Geographical Series. - №1 (40). - 2015. - C. 372-380. EDN: YWRNYL
- [5] Ystykul K.A., Seredovich V.A., Baigurin J.D. Mapping of avalanche danger zones in the high-mountain recreational zone of Ile Alatau using laser scanning data // Interexpo Geo-Siberia. - 2016. - T. 1. - № 2. - C. 101-107. EDN: ROXVAD

ESTIMATION OF THE PROBABILITY OF ELIMINATING CRITICAL FAILURES OF DISTANTLY CONTROLLED OBJECTS

Alexander Dokukin, Mikhail Lomakin

•

All-Russian Research Institute for Civil Defense and Emergency Situations of the Ministry of
Emergency Situations of Russia, Moscow, Russia

vniigoshs@vniigoshs.ru

aldokukin@yandex.ru

Abstract

The problem of determining the probability of timely elimination of critical failures under conditions of incomplete data represented by small samples of hardware dwell time in failure state and critical hardware time is considered. This probability is the probability of stochastic dominance of the critical time of the hardware over the time of the hardware in the state of failure, i.e. the probability that the random time of the hardware in the state of failure is less than the critical time of the hardware. Critical time is the time during which the elimination of the occurred failures does not lead to the occurrence of an unrecoverable failure of the object or to a significant reduction in the efficiency of its functioning. The problem of determining the probability of timely elimination of critical failures is formulated as a problem of finding guaranteed (lower and upper) probability estimates on the set of available initial data, represented by small samples of the time of stay of the equipment in the state of failure and critical time of the equipment. The guaranteed estimates of the probability of timely elimination of critical failures are found using the results of solving the problem of Markov moments.

Keywords: probability, critical failures, distantly controlled objects

I. Introduction

Remotely Operated Controlled Objects (ROOs) are complex and expensive objects designed to solve important national economic, scientific and applied tasks. RCEs include artificial satellites, spacecraft, probes, pipelines and oil pipelines. In the process of their target functioning they are exposed to a large number of external factors. [1] This impact in most cases is the cause of failures of their hardware. Hardware failures lead to different consequences for DKO. In the case of some hardware failures, the recovery of its performance is automatic with the built-in system of control, diagnostics and recovery, in the case of other failures for their detection, diagnosis and recovery requires the involvement of ground control complex facilities, including ground control and management facilities [1]. Among the failures of the second group there are such failures, the untimely elimination of which leads (may lead) to the occurrence of unrecoverable hardware failure, and further to the failure of RSC or to a significant reduction in the efficiency of its operation. Let us call such hardware failures critical failures; they include failures of the power

supply system, failures of the satellite navigation system, failures of the orientation and stabilization system, etc.

Let at a random moment of time there is a hardware failure, which after some random time ξ manifests itself, as a rule, is detected during the telemetry control session following the failure. The detected failure is diagnosed and eliminated within the period of time γ .

Currently, only the task of technical condition monitoring is solved on board some ROVs. The task of diagnostics and technical condition management in most cases is realized remotely. [2].

The random dwell time of the hardware in a failure state σ will consist of the time of failure occurrence ξ and the time of diagnostics and restoration of the equipment operability γ . The value of time σ will be determined by the ratio:

$$\sigma = \xi + \gamma, \quad (1)$$

where σ - is the random dwell time of the equipment in the state of failure,

ξ - random time of hardware failure manifestation,

γ - random time of diagnostics and restoration of equipment operability.

Let η - a random time during which the elimination of critical failures does not lead to an unrecoverable hardware failure or to a significant reduction in the efficiency of its operation. Let us call this time the critical time.

The task is to determine the probability of timely elimination of DKO equipment failures - the probability that the random dwell time of the equipment in the state of failure will be less than the critical time, i.e. to determine the probability of $P = P(\sigma < \eta)$, the probability of stochastic dominance of the critical time of the hardware over the time of the hardware stay in the state of failure.

At known functions of distribution of time of stay of the equipment in a state of failure and critical time this problem is solved. Ratios for determining the probability $P = P(\sigma < \eta)$ with respect to the basic distribution functions of random variables σ, η are given, for example, in [3]. In a real situation, the distribution functions of the time of the equipment stay in the state of failure and the critical time are not known. The present paper is devoted to the consideration of this case.

II. Main results

Let $\sigma v = (\sigma v_1, \sigma v_2, \dots, \sigma v_{n\sigma})R^{n\sigma}$ - a sample of values of the time of the equipment staying in the failure state, $\eta v = (\eta v_1, \eta v_2, \dots, \eta v_{n\eta})R^{n\eta}$ - sample of values of critical time of the equipment. The components of the sample $\sigma v_i > 0$ are independent equally distributed values from some unknown distribution $H(t)$, $\eta v_i > 0$ are independent equally distributed values from some unknown distribution $G(t)$. The samples $\sigma v, \eta v$ are finite samples of small volume, for which it is impossible to recover the original distributions $F(t)$ and $G(t)$.

Let us transform the expression for the probability of timely elimination of critical failures. We have

$$P = P(\sigma < \eta) = P\left(\frac{\sigma}{\eta} < 1\right) = P(\sigma\lambda < 1) = P(\beta < 1). \quad (2)$$

where $\lambda = \frac{1}{\eta}$; $\beta = \sigma\lambda$.

Let's find on the basis of samples $\sigma v, \eta v$ sample initial moments (hereinafter - moments) of random variables σ, λ, β :

$$\mu_{j\sigma} = \frac{1}{n\sigma} \sum_{i=1}^{n\sigma} \sigma v_i^j; \mu_{j\lambda} = \frac{1}{n\eta} \sum_{i=1}^{n\eta} \left(\frac{1}{\eta v_i}\right)^j; j = \overline{1, k}; k > 0. \quad (3)$$

Random variables σ, λ are independent quantities, therefore, the random variables σ^j, λ^j are also independent. The mathematical expectation of the product of random variables σ^j, λ^j is equal to the product of mathematical expectations of these quantities

$$M(\sigma^j \lambda^j) = M(\sigma^j) M(\lambda^j); j = \overline{1, k}; k > 0. \quad (4)$$

Then the moments of the random variable β will be defined by the expression:

$$\mu_{j\beta} = \mu_{j\sigma} \mu_{j\lambda}; j = \overline{1, k}; k > 0. \quad (5)$$

Let us define the set F_0 - the set of distribution functions $F(t)$ of the random variable β with moments equal to the moments defined by the relation (8)

$$F_0 = \{F(t): \int_0^\infty t^j dF(t) = \mu_{j\beta}; j = \overline{1, k}; k > 0\}. \quad (6)$$

The problem of determining the probability of timely elimination of critical failures of DKO equipment due to incompleteness of initial data represented by small samples of the time of equipment stay in the state of failure and critical time of the equipment should be formulated as a problem of determining the guaranteed (lower and upper) estimates. It is necessary to determine the lower and upper (guaranteed) estimates of probability $P = P(\beta < 1)$ on the set of distributions F_0 , i.e. to find

$$P_n = \min_{F(t) \in F_0} P(\beta < 1); P_v = \max_{F(t) \in F_0} P(\beta < 1). \quad (7)$$

Ratio $P = P(\beta < 1)$ can be written in the form:

$$P = P(\beta < 1) = \int_0^1 dF(t). \quad (8)$$

The solution of the latter problem, defined by relation (10), is obtained in [5-10] and it is summarized as follows.

Highest (lowest) value of the integral

$$J(F) = \int_0^\tau c(t) dF(t). \quad (9)$$

at $F(t) \in F_0$ is achieved on the only stepwise distribution $F(t)$ which among the growth points t_1, t_2, \dots, t_v has a point;

at odd k the number of growth points v of the distribution function $F(t)$ is determined by the relation $v = (k + 3) / 2$ and $t_0 = 0 < t < t_{12} < \dots < t < t_v$

at even k the number of growth points v of the distribution function $F(t)$ is determined by the relation $v = k / 2 + 1$ with $0 < t_1 < t_2 < \dots < t < t_v$

numbers $p_j, t_j, j = \overline{1, v}$ satisfy the system of equations:

$$\mu_{j\beta} = \sum_{i=1}^v t_i^j p_i; j = \overline{1, k}; k > 0. \quad (10)$$

The function $c(t)$ must have a non-negative $k+1$ th derivative.

Let us consider for certainty the problem of determining the lower estimate of probability $P = P(\beta < 1)$ on the set of distribution functions F_0 .

Let two moments of a random variable be defined $\beta - \mu_1, \mu_2$, (further, where it does not cause discrepancies, the index β is omitted) then using the above result we find the lower estimate of probability $P = P(\beta < 1)$ which is defined by the following expression [6]:

$$P_n = \frac{(\mu_1 - 1)^2}{(\mu_1 - 1)^2 + \mu_2 - \mu_1^2}, 1 > \mu_1. \quad (11)$$

In the case when three moments of a random variable are defined $\beta - \mu_1, \mu_2, \mu_3$, we find the lower estimate of the probability $P = P(\beta < 1)$ which is determined by the following expression [6]:

$$P_n = \frac{\mu_1^3 + \mu_3 - 2\mu_2^2 - \mu_3\mu_1 + \mu_2^2}{\mu_1^3 + \mu_3 - 2\mu_2^2}, 1 > \mu_1. \quad (12)$$

In the last ratio, the symbol "1" ($\tau=1$ - growth point of the distribution function $F(t)$) is used to confirm that the numerator and denominator dimensions are the same.

In the case when more than three moments of a random variable are defined β the estimate of the probability $P = P(\beta < 1)$ should be calculated numerically.

Let us consider the case when four moments of the random variable are defined $\beta - \mu_1, \mu_2, \mu_3, \mu_4$. In this case, the number of growth points of the distribution function $F(t)$ is equal to three, the system of equations (10) will have the form:

$$\begin{cases} p_1 + p_2 + p_3 = 1, \\ p_1 t_1 + p_2 t_2 + p_3 t_3 = \mu_1, \\ p_1 t_1^2 + p_2 t_2^2 + p_3 t_3^2 = \mu_2, \\ p_1 t_1^3 + p_2 t_2^3 + p_3 t_3^3 = \mu_3, \\ p_1 t_1^4 + p_2 t_2^4 + p_3 t_3^4 = \mu_4. \end{cases} \quad (13)$$

Since the distribution function $F(t)$ is a left continuous function, the growth point $\tau=1$ can be either t_2 or t_3 then we should consider two systems of equations

$$\begin{cases} p_1 + p_2 + p_3 = 1, \\ p_1 t_1 + p_2 \tau + p_3 t_3 = \mu_1, \\ p_1 t_1^2 + p_2 \tau^2 + p_3 t_3^2 = \mu_2, \\ p_1 t_1^3 + p_2 \tau^3 + p_3 t_3^3 = \mu_3, \\ p_1 t_1^4 + p_2 \tau^4 + p_3 t_3^4 = \mu_4, \end{cases} \quad (14)$$

$$\begin{cases} p_1 + p_2 + p_3 = 1, \\ p_1 t_1 + p_2 t_2 + p_3 \tau = \mu_1, \\ p_1 t_1^2 + p_2 t_2^2 + p_3 \tau^2 = \mu_2, \\ p_1 t_1^3 + p_2 t_2^3 + p_3 \tau^3 = \mu_3, \\ p_1 t_1^4 + p_2 t_2^4 + p_3 \tau^4 = \mu_4. \end{cases} \quad (15)$$

To solve the systems of equations (14), (15) we used Microsoft Excel package (item) "Solution Search" sub-item "Search for the solution of nonlinear problems by OPG method¹". In this case, the first equation of the systems of equations (17), (18) was considered as a target function of the following form

$$CF = p_1 + p_2 + p_3 - 1,$$

the value of which should be equal to zero, the other equations were considered as constraints in the optimization problem.

The results of numerical solution of the problem of determining the lower estimate of the probability of $P = P(\beta < 1)$ - of the probability of timely elimination of failures of DKO equipment on the set of distribution functions F_0 at different values of the first four moments are given in Table 1.

Table 1: Lower estimate of the probability of timely elimination of failures space craft hardware

μ_1	μ_2	μ_3	μ_4	P_n
0,200	0,080	0,048	0,038	0,959
0,300	0,180	0,162	0,194	0,832
0,400	0,320	0,384	0,614	0,648
0,500	0,500	0,750	1,500	0,579
0,600	0,720	1,296	3,110	0,488
0,700	0,980	2,058	5,762	0,429
0,800	1,280	3,072	9,830	0,330

¹ The OPG method is the generalized reduced gradient method.

III. Conclusion

The problem of determining the probability of timely elimination of critical failures of DKO equipment in the conditions of incomplete data represented by small samples of the time of equipment stay in the state of failure and critical time of the equipment is considered. This problem is formulated as the problem of determining guaranteed (lower and upper) estimates of the probability that the random dwell time of the equipment in the failure state is less than the random critical time of the equipment, i.e., the probability of stochastic dominance of the critical time of the equipment over the dwell time of the equipment in the failure state. To determine the probability of timely elimination of critical failures of DKO equipment, the results of solving the problem of Markov moments are used, with their help we obtained relations for determining the lower estimate of this probability at two and three moments of a random variable equal to the ratio of the time of stay of the equipment in the state of failure to the critical time of the equipment. At four moments of the last random variable, the lower estimates of the probability of timely elimination of critical failures of DKO equipment were determined numerically using Microsoft Excel.

References

- [1] Novikov L.S. Radiation Effects on Spacecraft Materials. - M.: Universitetskaya kniga, 2010. -192 c.
- [2] Baranovsky, A.M.; Privalov, A.E. System of control and diagnostics of the onboard equipment of a small spacecraft (in Russian) // Izv. VUZov. Instrument engineering. 2009. T.52, № 4. C.51-56.
- [3] Ostreikovskiy V.A. Multifactor reliability tests. - M.: Energia, 1978. -152 c.
- [4] Gnedenko B.V. Probability Theory Course. - Moscow: Fizmatgiz, 1988. - 406 c.
- [5] Lomakin M. And Guaranteed estimates of probability of failure-free operation in the class of distributions with fixed moments // Izvestia AS USSR. Automatics and Telemechanics. 1991. NO. 1 FROM 154-161
- [6] Lomakin M., Buryi A., Dokukin A., Niyazova J. Strekha A., Balvanovich A.. Estimation of quality indicators based on sequential measurements analysis // International Journal for Quality Research. 2020. No. 1. pp. 823-834.
- [7] Lomakin, M.I.; Sukhov, A.V.; Dokukin, A.V.; Niyazova, Yu.M. Estimation of the spacecraft reliability indicators in the conditions of incomplete data // Space Research. 2021. T. 59. № 3. C. 235-239.
- [8] Lomakin M.I., Niyazova Y.M., Dokukin A.V., Zlydnev M.I., Garin A.V. Quality assessment of business processes in the conditions of incomplete data // Welding production. 2022. № 4. C. 52 - 58.
- [9] Crane M.G., Nudelman A.A. The problem of Markov moments and extremal problems (Ideas and problems of P.L. Chebyshev and A.A. Markov and their further development). - Moscow: Nauka, 1973. - 551 c.
- [10] Akhiezer N.I. Classical problem of moments. - Moscow: Fizmatgiz, 1961. - 310 c.

THE ESSENCE OF THE DELPHI METHOD AND ITS MAIN ADVANTAGES AND DISADVANTAGES

Albina Berkaeva¹, Sergey Yablochnikov², Andrey Butyrin³, Irina Tararyshkina⁴,
Tofig Mansurov⁵

•

¹North-Ossetian State University named after Kosta Levanovich Khetagurov, Russia

²Moscow technical University of communications and Informatics, Russia

³National Research Moscow State University of Civil Engineering, Russia

⁴Ryazan State University named after S.A. Yesenin, Russia

⁵Azerbaijan Technical University

d-albina@yandex.ru

vvkfek@mail.ru

stoisud@mail.ru

irina.28995@gmail.com

Abstract

This article is devoted to the study of the essence and main meaning of the Delphi method, developed in the 50s of the 20th century in the United States. In those years, this method was used to identify the impact of scientific and technological progress in matters of a military nature. Now, the Delphi method is universal and can be applied in any branch of activity, which increases its relevance. In addition, we have studied the main advantages and disadvantages of using this method at the level of world experience. We also considered the problems of using the Delphi method at the level of the Russian economy.

Keywords: the Delphi method, managerial decisions, brainstorming, questionnaire method, interview, expert assessment, statistics

I. Introduction

In the modern world, almost all companies during their activity are faced with certain problematic issues that require timely intervention and prompt decision. Accordingly, the main task of any management team is to search for solutions to this problem in order to plan their further management functions. In our opinion, the stage of decision-making, which is a rather labor-intensive and responsible process, certainly plays an important role in management.

The importance of competent managerial decisions, in turn, increases due to the fact that the decision-maker is responsible not only for personal interests, but, firstly, for the interests of the entire enterprise.

Undoubtedly, in the current realities, there are a number of ways to facilitate the choice of effective solutions, but many companies pay great attention to the Delphi method as the most effective one.

II. Methods

Thus, the main aim of this article is to reveal the essence of the Delphi method, which consists in the development of certain recommendations for the most effective management decision-making, based on the results of an anonymous questionnaire between a group of experts, as well as the consideration of the advantages and disadvantages of the Delphi method use at the current level of the economy development.

In addition, we'd like to note that the Delphi method pursues the ultimate objective to obtain the most accurate and reliable information due to the correct analysis of the proposals of the expert group on a particular problem.

The object of our study is the Delphi method. And the subject is the assessment of the advantages and disadvantages of the Delphi method based on world experience. Also, we'd like to add that during writing this article, various research methods were used, in particular, comparison, synthesis, analysis, and others [1]. The works of both foreign and domestic scientists, economists, as well as various articles, textbooks, Internet resources dedicated to the research topic, served as the theoretical basis.

Thus, based on the above, we can conclude that the topic of our study is quite relevant at the current level of economic development and is widespread mostly in Western countries.

Initially, the Delphi method was developed to assess the impact of various developments on the military sphere, but over time, this method began to be used for any research, thereby becoming universal.

III. Results

So, let's try to reveal the essence of this method, and we would like to start with studying some historical information. Note that this method has an ancient Greek origin and was named after the city of Delphi, inhabited by oracle-soothsayers at the temple of God Apollo.

The mathematician N. Dalkey, the philosopher N. Rescher, the American psychologist T. Gordon and the futurologist O. Helmer were the founders of this method in the 50s of the 20th century.[2]

At the same time, we'd like to note that this method has gained great popularity, serving as an assistant in identifying the most important directions of scientific and technological progress, as well as determining the advisability of investing in certain programs.

That is, the use of the Delphi method gives us the opportunity to assess the state of the industry under consideration also in the long term.

As foreign practice shows, for most of the countries this method is associated, first of all, with its applicability in various government programs, and not separately in the activity of enterprises.

As an example, we can also mention Japan, which applied the Delphi method not at the level of specific enterprises, but, on the contrary, at the level of the entire state to predict national-industrial development in the 70s of the 20th century.

So, what is the essence of this method?

The main message of the Delphi method is to obtain the most reliable expert assessment on a particular issue on which this analysis was carried out with the obligatory observance of the principles of anonymity, remote form of participation, as well as the principle of multilevelness.

Let's note that the questionnaire method, interviews and brainstorming serve as auxiliary tools.

In other words, as a basic requirement, it is possible to include the observance of the most important principle, which is that the experts should be independent and unfamiliar with each other.

This, in turn, gives us the opportunity to obtain the most reliable result due to the fact that experts will not be able to influence the opinions of other experts, thanks to the observance of the

principle of anonymity and remote form of participation.

That is, in other words, the main purpose of the Delphi method is to identify the most optimal way to solve the problem through a competent analysis of the results obtained according to the objective opinions of the expert group.

Accordingly, as we see it, two groups of participants are required to carry out this method of analysis.

The first group is needed in the role of experts who have the status of "independent" in order to assess the problem, while the second is necessary so that, based on expert assessments, they can obtain a generalized conclusion by analyzing the ratio of answers, thereby performing an analytical function.

IV. Discussion

At the same time, the entire methodology consists of several stages, the results of which are calculated using various statistical methods. Regarding the main stages of such an analysis, we'd like to single out the main ones: preparatory, main and final. What is the essence of each stage, and what are their main components? Let's try to answer these questions.

As we see it, the analysis begins with a preparatory stage, during which, foremost, the search for a group of experts to conduct this investigation takes place.

As a rule, it is recommended to form such group of 20 people for a more accurate analysis. But, of course, it is possible to recruit fewer experts. It is also very important to have unambiguously formulated questions that require an exact answer.

The second stage is the main stage, which is characterized, first of all, by determining the problematics by analysts, with further splitting of this problematic into several questions by experts. After collecting these questions, analysts develop a questionnaire based on the most frequently asked questions.

Accordingly, after the questionnaire is ready, the analysts send it to the experts, and they, in turn, scrutinize it and, if necessary, ask to improve the questionnaire if there is not enough information for an expert assessment of the problem under consideration.

After all the improvements, the task of the experts is to apply their knowledge for a thorough explanation of each issue according to the questionnaire. In other words, the expert is required to offer the best option on this issue, by considering all the risks and predicting further development stages.

As for analysts, they must also collect all the material and sort similar answers into one. If there are conflicting points, a generalization of such issues between a group of experts is required, which may lead to a change in the opinion of one or another expert.

And finally, the last stage is devoted to summing up.

Thus, these actions are repeated as long as the respondents do not find a common denominator. In case of some inconsistencies, this indicates that the topic has not yet been fully studied and requires more analysis.

Besides, an important place in the Delphi method is given to the determination of the consistency level of expert opinions, which are calculated using the concordance coefficient, which is mathematically denoted by the letter W and has the formula:

$$W = 12 \left[\sum_{i=1}^n \sum_{j=1}^m x_{ij} - \frac{1}{2} m(n+1) \right] / m^2(n^3 - n)$$

where

m is the number of experts;

n is the number of ranking objects;

x_{ij} is the rank assigned to the i -th factor by the j -th expert.

In this case, we should note that the concordance coefficient has a value from 0 to 1.

If the opinions of experts do not correspond to each other, the value of $W=0$; in case of complete agreement, it is equal to 1. In addition, the normal value of this index ranges from 0.5 and more at a confidence level of 0.995.

Thus, having considered the essence and the main stages of the expert assessment realization of the considered method, we would like to go into the question of the positive and negative aspects of using the Delphi method in practice.

First of all, the processing of statistical information for each individual can be considered as the main advantage, which, in turn, significantly reduces the degree of deviation both for each answer and among the interviewed people.

It is a common fact that a person by nature is an individual, dependent on other people's opinion. And it is always easier to manage such people in the sense that they do not defend their views and interests, and are ready to join the opinion of the majority.

Also, sometimes there is such situation that a person lives according to someone else's opinion, while not even realizing it.

Surely each of us noticed that in large companies the opinion of a more qualified employee is more valued, and even if there is an opposite opinion of the majority, there is some kind of moral pressure in the group assessment during the decision-making process.

That is why, in order to reduce the prerequisites for group influence, the Delphi method goes to the rescue.

From the above, follows the fact that each isolated employee alone can assess a particular situation and predict further development more correctly and objectively, compared to a team of people.

Such division of persons into groups greatly reduces the disagreement between employees, since each of them makes a decision separately. Accordingly, the collective pressure that affects the decision is also excluded.

In other words, according to the Delphi method, a kind of anonymous brainstorming is carried out, where independent of each other experts "team up" and analysts, based on the proposed answers, make a group decision according to special regulations.

At first glance, the considered method seems to be "ideal" with a number of advantages, but, as with any category, this method also has disadvantages, which we will discuss further.

Let's start with the fact that already from the moment of this method appearance, the first criticisms and dissatisfaction occurred, which consisted of several factors.

Firstly, one of the disadvantages of this model is the uneven distribution of authorities between analysts and experts, which is observed in the sense that analysts can exert some influence on a group of experts.

Secondly, it is necessary to understand that not in all cases the opinion of the majority is reliable.

Thirdly, for analysts' part, there is often a failure to use the ideas of minorities that differ from standard opinions, which is incorrect, since often the truth can be hidden precisely in the opinion of a minority, which, unfortunately, will not be applied and considered in the analysis of a particular situation.

Fourthly, the disadvantage of using the Delphi method is also the inability to conduct a fast analysis, since this is a rather labor-intensive and slow process that can take quite a long time.

Fifthly, on the part of analysts it can be observed a situation of being in a comfort zone, which is accompanied by inefficient decision-making, simply focusing on the opinion of the majority, without delving into the issue.

Thus, having considered the main disadvantages of the Delphi method, in our opinion, we can propose the following measures that will be aimed at eliminating these negative aspects of the method.

First of all, we propose during analysts' group formation to select persons with different areas of scientific and social character and preparedness.

Also, we recommend giving the same problem to several expert groups for a deeper analysis.

And an important role is played by the professionalism of analysts in terms of taking all possible answers into account by analyzing those options that do not really seem right at first glance and do not correspond to the opinion of the majority. After all, as we said earlier, the most effective solution to a particular problem can be hidden in such creative answers.

After analyzing all of the above, we can conclude that the Delphi method is quite common in the West.

The widespread implementation of this method is mainly used in such industries as business, strategic planning, futurology, as well as technological developments and other areas.

So, as we see it, the essence of the Delphi method is to effectively assess and resolve certain management issues using the remote and anonymous participation of experts.

Accordingly, the main goal of the method under consideration is the collection of the necessary information by conducting step-by-step surveys to obtain the most optimal solution in the considered situation.

Thus, let's note that at the present level of societal development in Western countries, the Delphi method does not lose its relevance and is in great demand.

In the case of the economy of our country, in Russia, this method, unfortunately, is practically not used, since we do not have the necessary tools for proper control of its application compared to other countries.

The problem of this issue is based on the fact that there are no non-centralized analytical structural units on the territory of the Russian Federation.

That is, in other words, this phenomenon is also connected with the fact that since the historical period of the development of the economy of our country, such analyzes have not been carried out to implement the Delphi method, and there were also no specialized analytical groups that would have a non-centralized existence, which would allow to be independent from the opinion of the majority.

At the same time, we should note that after all there were attempts to introduce this method in the USSR in the 70s during the period of forecasting the scientific and technological development of the country and the whole world.

During this period, the emphasis was mainly put on the circulating sector and the state apparatus. But the result as such was not obtained.

Undoubtedly, during the 21st century, the situation for the application of this method has become much simpler, but there are still the same difficulties in terms of the lack of a proper regulatory framework.

Therefore, for our country an important role is played by the ability to use the experience of other countries in which this method is actively used and is in great demand in order to promote the Delphi method in Russia.

So, we can conclude that the Delphi method serves as a useful tool in making certain decisions on the management of enterprises and the state. In particular, the use of this method is more relevant for large companies.

Thus, we have considered the main essence of the Delphi method and identified the main advantages and disadvantages of its application.

As we see it, despite the implementation of any method of risk analysis, it is necessary to always be prepared for the fact that in today's unstable developing relations the situation can change at any moment and have deviations from the foreseen.

But, in general, despite these disadvantages, it would be advisable not to forget about the main advantages of this method with proper use of it.

References

[1] Ableev S.R. History of world philosophy: a textbook for universities / S.R. Ableev. – M.: Yurayt Publishing House, 2018. – 318 p.

[2] Baryshev A.V. Fundamentals of the development of managerial decisions: a study guide /

A.V. Baryshev. – Moscow: FORUM: INFRA-M, 2021. – 164 p.

[3] Vorontsovsky A.V. Risk assessment: textbook and practical course for Bachelor's and Master's programmes / A.V. Vorontsovsky. – M.: Yurayt Publishing House, 2019. – 179 p.

[4] Genkin B.M. Motivation and organization of effective work (theory and practice): monograph / B.M. Genkin. – 2nd ed., revised. – Moscow: Norma: INFRA-M, 2020. – 352 p.

[5] Egorshin A.P. Effective management of the organization: study guide / A.P. Egorshin. Moscow: INFRA-M, 2021 (2018). – 388 p.

[6] Zhukovsky V.I. Risk assessment and multi-step positional conflicts: study guide for universities / V.I. Zhukovsky, M.E. Salukvadze. – 2nd, revised and enlarged edition – M.: Yurayt Publishing House, 2019. - 305 p.

[7] Kislyakov G.V. Management: basic terms and concepts: vocabulary / G.V. Kislyakov, N.A. Kislyakova. – 2nd ed. – Moscow: INFRA-M, 2019. – 176 p.

[8] Makhovikova G.A. Analysis and risks assessment in business. Textbook / G.A. Makhovikova, T.G. Kasyanenko. – M.: Yurayt Publishing House, 2019. – 464 p.

[9] Titov V.N. Theory and history of management: textbook and practical course for universities / V.N. Titov, G.N. Sukhanova. – Moscow: Yurayt Publishing House, 2021. – 487 p.

[10] Kuptsov, M.I., Yablochnikova, I.O., Yablochnikov, S.L., Dzobelova, V.B. & Mineev, V.I. (2020). Modeling Internet Business Optimization Processes, 2020 International Conference on Engineering Management of Communication and Technology (EMCTECH), Vienna, Austria, 2020, pp. 1-5, doi: 10.1109/EMCTECH49634.2020.9261507.

CLIMATE AND ENVIRONMENTAL MONITORING OF THE BALTIC SEA: GENERAL PRINCIPLES AND APPROACHES

Leyla Bashirova, Vadim Sivkov, Marina Ulyanova, Aleksander Gavrikov, Arseniy
Artamonov

•

Immanuel Kant Baltic Federal University, Russia

bas_leila@mail.ru

vadim.sivkov@atlantic.ocean.ru

Abstract

The environment of the Baltic Sea is heavily influenced by human activities. In addition, the region is undergoing significant changes in the face of global climate change. Therefore, it is necessary to assess the state of the environment and greenhouse gas emissions in the region. In 2022, the Programme for the development of the system of climate and environmental monitoring of the Russian seas was launched. For the Baltic Sea, the spatial and temporal scheme of the regional monitoring module has been designed to carry out long-term, regular, and large-scale surveys. The satellite monitoring is based on the analysis of radiometer data and includes analyses of the spatial and temporal variability of suspended particulate matter and chlorophyll a concentrations, as well as sea surface temperature. The shipboard monitoring consists of seasonal and monthly surveys. The coastal monitoring is based on data from sensors installed on a 57-met tower as a permanent climate and environmental monitoring station located on the coast of the south-eastern part of the Baltic Sea (Kaliningrad Oblast, Russia).

Keywords: shipboard monitoring, satellite monitoring, permanent monitoring station, meteorological tower, carbon dioxide and methane fluxes, primary productivity, oceanographic properties

I. Introduction

The imbalance of the global climate system, the inability to accurately predict the climate changes and the following feedbacks, as well as a great influence of those changes on the social and economic spheres determine the global climate agenda for the next decades. To bind an international treaty on climate change, the Paris Agreement was adopted by 196 Parties at the UN Climate Change Conference (COP21) in Paris, France, on December 12, 2015 [15]. Since Russia signed the Paris Agreement, it has committed to take action to reduce greenhouse gas (GHG) emission and develop a long-term low GHG emission strategy. From this time, a low-carbon transformation of Russia started and several legislative documents have been approved in order to achieve carbon neutrality by 2060.

According to the Decree of the Government of the Russian Federation No. 3183-r [4], the National Action Plan for the First Phase of Adaptation to Climate Change was approved on December 25, 2019 for the period up to 2022. The main aim of the first Stage of the Plan was to develop a regulatory and guidance documentation, as well as a legal framework for carrying out adaptation measures at the national, regional, and sectoral levels. This will help reduce the vulnerability of society and the economy to the negative effects of climate change, and take advantage of the opportunities that climate change presents.

In 2020, the Decree of the President of the Russian Federation No. 666 “On the reduction of greenhouse gas emissions” was approved [6]. The Decree mandates: a) to ensure that greenhouse gas emissions are reduced to 70 percent of the 1990 level by 2030, taking into account the maximum possible absorption capacity of forests and other ecosystems and subject to the sustainable and balanced socio-economic development of the Russian Federation; b) to develop and adopt a strategy for the socio-economic development of the Russian Federation with a low level of greenhouse gas emissions by 2050, taking into account the specificities of economic sectors; c) to ensure the creation of conditions for the implementation of measures to reduce and prevent greenhouse gas emissions and to increase the absorption of such gases.

Since 2021, several regulatory instruments were developed and approved. After approval of the Order of the Ministry of Science and Higher Education of the Russian Federation No. 74 “About supersites for the development and testing the carbon balance control technologies” [14], the Carbon Supersites Programme was launched. The Programme implies designation of the reference sites (the carbon supersites) for comprehensive GHG studies within the National Action Plan for Adaptation to Climate Change. On February 8, the Decree of the President of the Russian Federation No. 76 “On Measures to Implement the State Scientific and Technical Policy in the Field of Environmental Development of the Russian Federation and Climate Change” [7] was approved. The document committed to develop the Federal Science and Technology Programme of the Russian Federation in the areas of environmental improvement and climate change for 2021–2030 within six months.

The Federal Law No. 296-FZ “On Limiting Greenhouse Gas Emissions” (2021, July, [9]) and the Decree of the Government of the Russian Federation No. 3052-r “On approval of the Strategy for the socio-economic development of the Russian Federation with low greenhouse gas emissions until 2050” (2021, October, [3]) define measures to ensure the reduction of GHG emissions, taking into account the maximum possible absorption capacity of forests and other ecosystems and subject to the sustainable and balanced socio-economic development of the Russian Federation.

In 2022, the Decree of the Government of the Russian Federation No. 133 “On approval of the Federal Science and Technology Programme of the Russian Federation in the areas of environmental improvement and climate change for 2021–2030 [2] and the Decree of the Government of the Russian Federation No. 3240-r “On approval of the Most Important Innovative Project of National Importance for development of the Unified System for Monitoring Climate-active Substances and an Action Plan (“Road Map”) for the implementation of the first stage (2022–2024) of the Project [5] were approved. Several research centers have been established in Russia to address this issue. In order to develop the climate and environmental monitoring systems for the Russian seas, the Consortium No. 2 “Center for Climate and Environmental Monitoring of the World Ocean and Russian Seas (OCEAN: MONITORING AND ADAPTATION)” was founded. As a member of the consortium, Immanuel Kant Baltic Federal University (IKBFU) has launched the two programmes of climate and environmental monitoring of the Baltic Sea in 2022.

The Baltic Sea is a semi-enclosed marginal sea that is undergoing significant transformation in the face of increasing anthropogenic pressures and global climate change [1600]. As a unique basin, it serves as a natural laboratory, so-called ocean in miniature. Here, the response to global processes and their consequences can be traced on a regional scale. The Baltic Sea represents a pronounced maximum of CO₂ sequestration due to extremely high level of water eutrophication and, consequently, high rate of primary bioproduction (photosynthesis). In addition, the largest hydrocarbon fields in the Baltic Sea are being explored off the coast of the Kaliningrad Oblast. Therefore, the assessment of GHG emission to the hydrosphere and atmosphere is also necessary for the region.

Natural changes in ecosystem parameters, in the form of sustained deviations from mean values, can only be observed, and sometimes even predicted, by long-term, regular, and large-scale surveys. This should be taken into account when develop the spatial and temporal scheme of the regional monitoring module. Short-term (episodic) observations can only capture random ecosystem responses, which are extremely difficult to assess and predict. In this context,

continuous long-term integrated monitoring of the Baltic Sea ecosystem is of great importance.

II. Current state of monitoring system in the Baltic Sea region

Legislations and commitments regulate the Baltic Sea status assessments [12]. According to ISO 4225:2020, monitoring is repeated measurement to follow changes over a period of time [1]. In Russia, Federal Law No. 7-FZ "On environmental protection" defines environmental monitoring as comprehensive observations of the state of the environment [10]. A unified system of state environmental monitoring shall be established to ensure environmental protection.

The tasks of the unified system of environmental monitoring are: (1) regular monitoring of the state of the environment, including processes, phenomena, and changes in the state of the environment occurring in natural ecological systems; (2) storing, processing (generalization, systematization) information on the state of the environment; (3) analysis of the obtained information for the purpose of early detection of changes in the state of the environment under the influence of natural and (or) anthropogenic factors, assessment and forecasting of these changes; (4) providing state authorities, local government bodies, legal entities, individual entrepreneurs, and citizens with information on the state of the environment. The unified system of environmental monitoring includes the following subsystems: (1) monitoring of the state and pollution of the environment; (2) air quality monitoring; (3) monitoring of the internal sea waters and territorial sea of the Russian Federation; (4) monitoring of the exclusive economic zone of the Russian Federation.

At the international level, current monitoring of the Baltic Sea and assessment activities are guided by the HELCOM Monitoring and Assessment Strategy adopted in 2013. Today there are 12 agreed HELCOM monitoring programmes covering sources and inputs of human pressures and various variables reflecting the state of the environment. HELCOM monitoring programmes are compiled in the HELCOM Monitoring Manual. The latter refers to the existing HELCOM guidelines where more detailed information can be found (<https://helcom.fi/action-areas/monitoring-and-assessment/monitoring-guidelines/>).

Reckermann et al. [1600] have suggested several state variables of the Earth system of the Baltic Sea region. Environmental state variables include coastal processes, hypoxia, submarine groundwater discharge, marine ecosystems, land use and land cover, non-indigenous species, indirect parameters such as carbon and nutrient cycles, biota and ecosystems. Whereas, climate state variables include climate change, acidification, and direct parameters of the climate system.

As for climate monitoring in the Baltic Sea region, observational records are too heterogeneous for statistical studies of extremes due to many data gaps. Moreover, a model for the entire Baltic Sea coastal zone is still missing, and the effect of climate change on the coastal filter capacity is still unknown [1300]. The main gaps in the current environmental monitoring of the Baltic Sea are: insufficient monitoring effort, missing/inadequate indicator, missing thematic category, problems with data storage/handling, indicator under development, insufficient monitoring coordination, monitoring costs too high, no specific information on gap type [12].

III. Development of the monitoring system for the Russian sectors of the Baltic Sea

In order to develop a system of climate and environmental monitoring for the Russian sectors of the Baltic Sea, an international approach (HELCOM) and the main principles of the industrial environmental monitoring system of LUKOIL-KLM Ltd. (Kravtsovskoye oilfield – D6) [170], as well as the best practices of long-term research of leading Russian scientific organizations have been applied. The system includes three types of monitoring: satellite, shipboard, and coastal. The monitoring area includes the Russian sectors of the Gulf of Finland and the south-eastern part of the Baltic Sea, as well as the Curonian and Vistula lagoons. The coastal zone is also a subject of monitoring.

3.1. Satellite monitoring

Satellite monitoring is based on the analysis of radiometer data and includes spatial and temporal variability of suspended particulate matter and chlorophyll *a* concentrations, and sea surface temperature. Sea surface temperature is obtained at a spatial resolution of 1 km from the Moderate Resolution Imaging Spectroradiometer (MODIS) infrared radiometers aboard the Aqua and Terra satellites (<https://oceancolor.gsfc.nasa.gov>). Chlorophyll *a* and suspended particulate matter concentrations are calculated from the Sentinel-3A Ocean and Land Colour Instrument (OLCI) data using a neural network algorithm [11] at a spatial resolution of 300 m (<https://codas.eumetsat.int>). Satellite images are processed with SeaDAS 8.2.0.

3.2. Shipboard monitoring

Starting in 2022, the following parameters are set for monitoring (Table 1). To cover the diversity of conditions in the monitoring area, monitoring points are located in the open sea and adjacent lagoons (Figures 1 and 2). In the open sea, the seasonal surveys are carried out on board the research vessels of the Ministry of Science and Higher Education of the Russian Federation. In the coastal zone of the south-eastern part of the Baltic Sea and in the shallow lagoons, the monthly surveys are conducted on board small vessels.

Table 1: *The main parameters of the climate and environmental monitoring in the Russian sectors of the Baltic Sea, including the adjacent shallow lagoons*

Climate monitoring	Environmental monitoring
Fluxes of CO ₂ at the air/water interface	Elements of the carbonate system (alkalinity and pH values)
Fluxes of CH ₄ at the air/water interface	Spatial distribution of chlorophyll <i>a</i> in the water column
Fluxes of suspended particulate matter and particulate organic carbon (POC)	Spatial distribution of suspended particulate matter in the water column
Primary productivity of phytoplankton and fixation of carbon and CO ₂ from the atmosphere	Planktic and benthic communities
	Bacterial production and degradation of organic matter
	Spatial distribution of total organic and inorganic carbon in the water column
Oceanographic properties	Oceanographic properties
Hydrometeorological factors	Hydrometeorological factors

3.3. Coastal monitoring

The inclusion of regular surveys of key areas of the coastal zone as part of the regional monitoring module is based on the fact that this is where the most active energy and mass exchange takes place. This explains the richness and diversity of shallow marine landscapes [8]. Therefore, the zone of maximum ecological sensitivity is adjacent to the coastline.

In addition to shipboard monitoring, a permanent climate and environmental monitoring station has been launched. The 57 meters high met tower Carl C. A/S has been installed on the coast of the Baltic Sea at Scientific and Practical Base of the IKBFU (Kaliningrad Oblast, city of Pionersky, Rybnoe Settlement) (Figure 3).

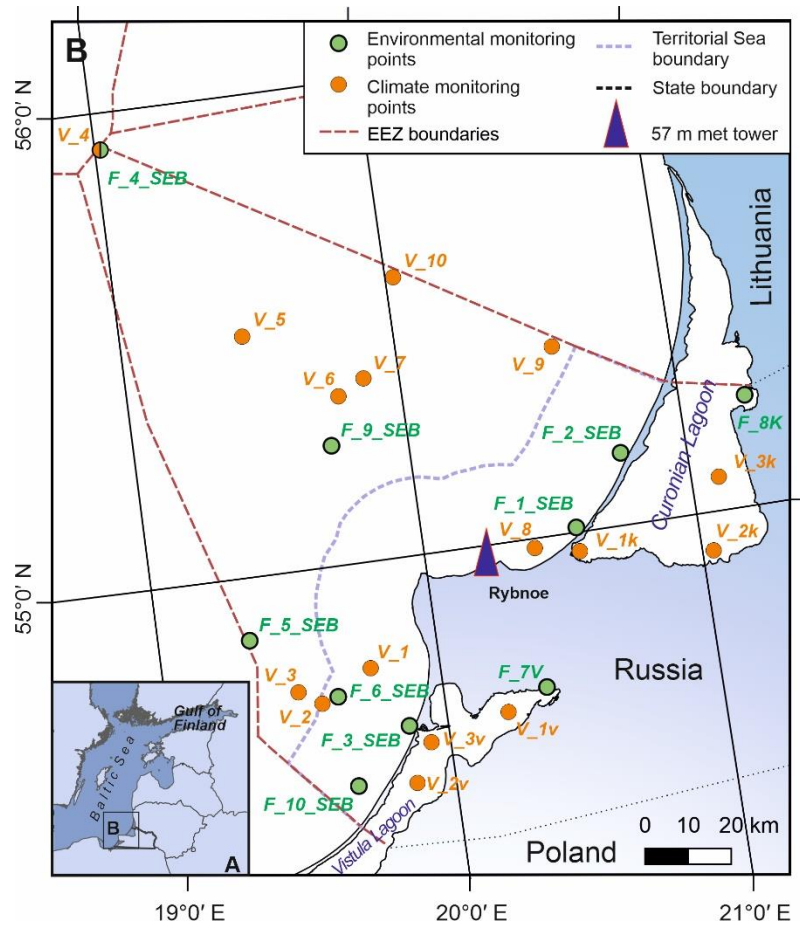


Fig. 1: Location of climate and environmental monitoring points in the Russian sector of the south-eastern part of the Baltic Sea, including the Curonian and Vistula lagoons

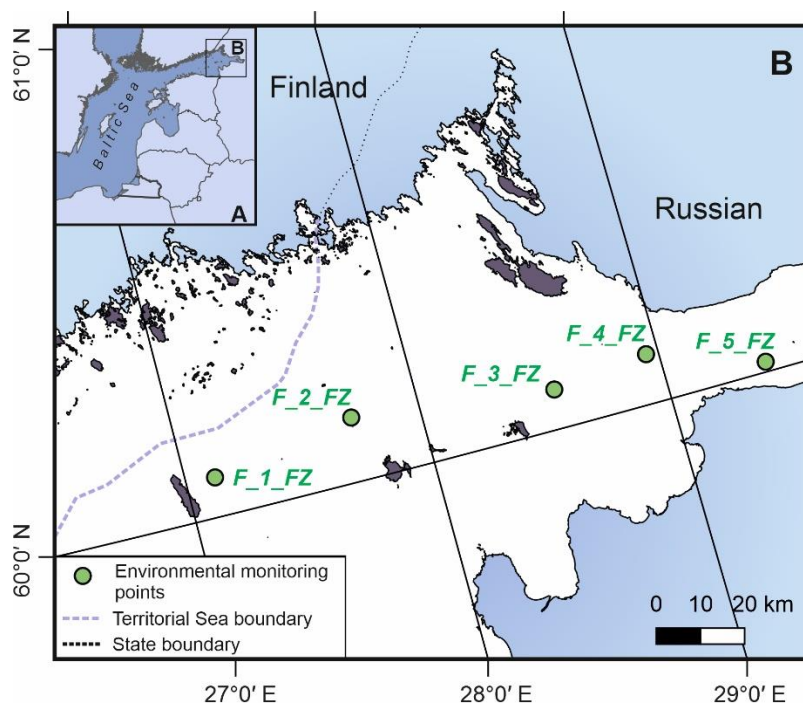


Fig. 2: Location of environmental monitoring points in the Russian sector of the Gulf of Finland of the Baltic Sea

The following meteorological equipment is currently installed on the tower:
 Level 54.0 m: humidity and temperature probe, acoustic anemometer 2D

Level 36.0 m: acoustic anemometer 3D

Level 30.0 m: Davis VANTAGE Pro2 weather station

Level 10.0 m: humidity and temperature probe, air quality (AQT400 Vaisala: NO₂, SO₂, CO, H₂S)

Level 7.1 m: radiometer

Level 5.0 m: humidity and temperature probe

Level 2.0 m: pressure, datalogger, Vaisala BAROCAP

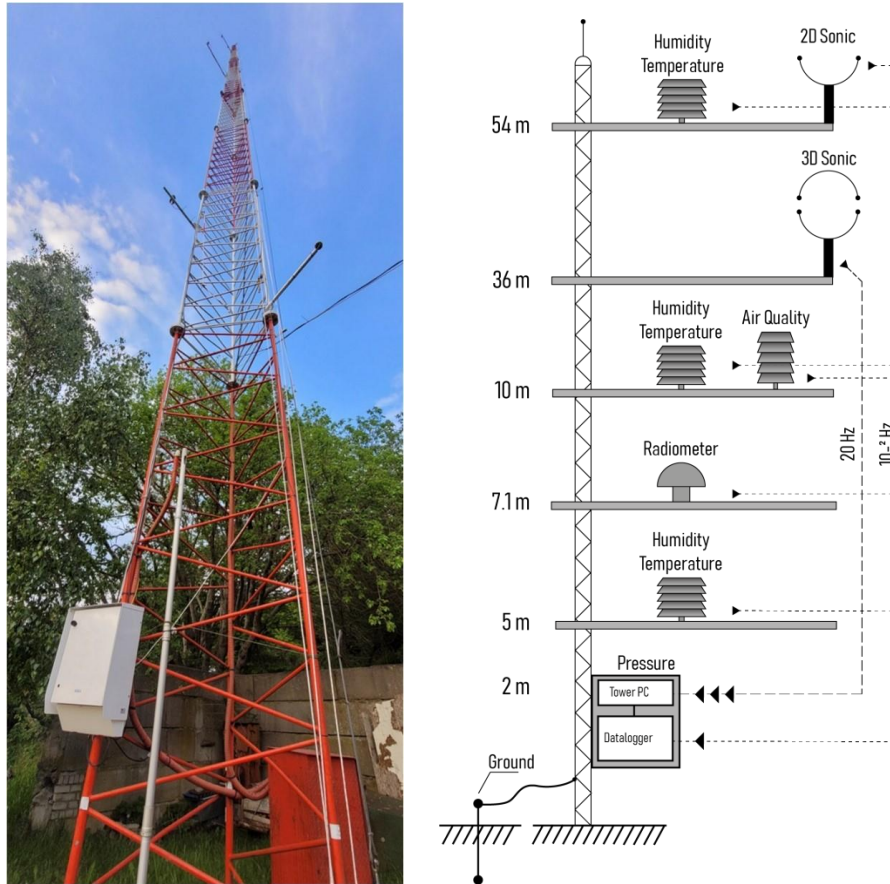


Fig. 3: Met tower (A) and a general scheme showing the location of equipment installed on the tower (B)

The ASUS TinkerBoard minicomputer is responsible for collecting, packaging, and sending data. Moreover, it is responsible for reading data from the MOXA switch via Ethernet protocol. Every 10 minutes, it stacks the read data in .npz format and sends it to the data collection server every 30 minutes. Figure 4 shows a general scheme of operation. The source code of the scripts of the data packaging and sending system is available on the portal: https://github.com/alexavr/tower_parse.

The data storage server is also responsible for displaying primary information: actual data from all sensors and several parameters of the minicomputer status (CPU temperature, free memory and Internet channel load). This information is available at the open platform: www.tower.ocean.ru. The graphical information is updated every 30 minutes. The data received is converted into the carefully described NetCDF format (once a day). The source code of the data collection and storage system scripts is written in Python Programming Language and is available on the portal: https://github.com/alexavr/tower_collect.

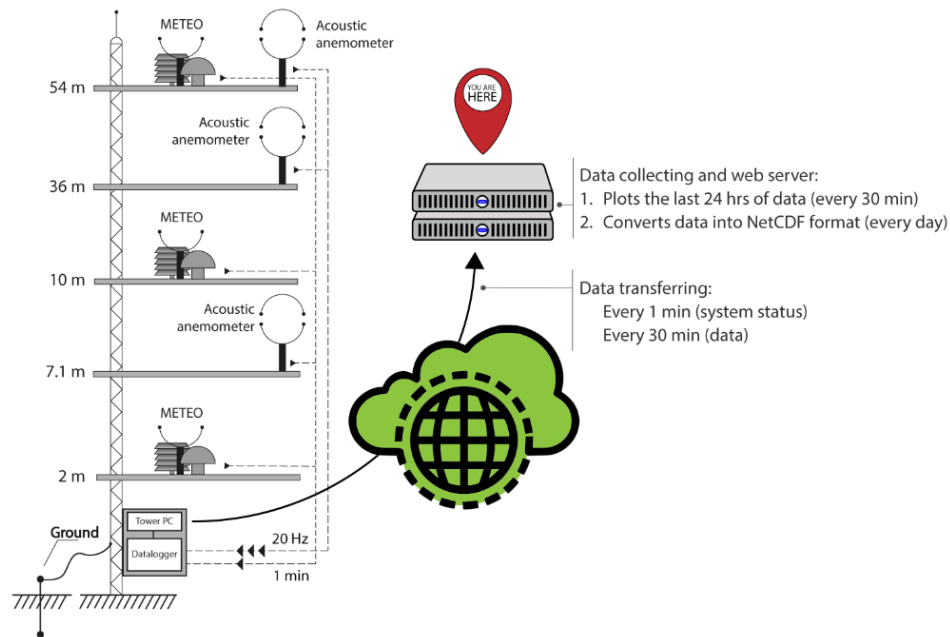


Fig. 4: General scheme of operation of the data collection and storage system at the met tower

3.4. Data availability

All data obtained as a result of the implementation of the monitoring will be transferred to the Unified Data Collection and Monitoring Management Center, which will ensure the collection, accumulation and archiving of information, information retrieval and operational analysis of the current environmental situation. Such a database will serve as a basis for the development of a specialized geographic information system. The main forms of information support will be annual bulletins with monitoring results.

IV. Conclusions

In order to contribute to a low-carbon transformation of Russia, a system of climate and environmental monitoring for the Russian sectors of the Baltic Sea has been developed based on the best practices of international and Russian experts. The system includes three types of monitoring as follows: satellite, shipboard, and coastal. The main parameters of the monitoring system have been defined and the spatial and temporal scheme of the regional monitoring module has been designed in order to carry out the long-term, regular, and large-scale surveys at the regional level. The monitoring area includes the Russian sectors of the Gulf of Finland and the south-eastern part of the Baltic Sea, as well as the Curonian and Vistula lagoons and the coastal zone. A high met tower (57 m) has been installed on the coast of the Baltic Sea and a permanent climate and environmental monitoring station has been set up.

All the data will be transmitted to the Unified Data Collection and Monitoring Management Center.

Acknowledgments. The study is supported by the state assignment of the IKBFU (Themes No. FZWM-2023-0002 and FZWM-2023-0004).

References

- [1] Air quality – General aspects – Vocabulary (ISO 4225:2020) (2020). 3rd Edition. 19 pp.
- [2] Decree of the Government of the Russian Federation No. 133 (2022, February). On approval of the Federal Science and Technology Programme of the Russian Federation in the areas of environmental improvement and climate change for 2021-2030. Available from:

<http://static.government.ru/media/files/Ekv7TcPAJBv4n3oUn6ofUdAR5cu5W1PM.pdf>

[3] Decree of the Government of the Russian Federation No. 3052-r (2021, October). On approval of the Strategy for the socio-economic development of the Russian Federation with low greenhouse gas emissions until 2050. Available from: <http://static.government.ru/media/files/ADKkCzp3fWO32e2yA0BhtIpyzWfHaiUa.pdf>

[4] Decree of the Government of the Russian Federation No. 3183-r (2019, December). On approval of the National Action Plan for the First Phase of Adaptation to Climate Change. Available from: <http://publication.pravo.gov.ru/Document/View/0001202001040016>

[5] Decree of the Government of the Russian Federation No. 3240-r (2022, October). On approval of the Most Important Innovative Project of National Importance for development of the Unified System for Monitoring Climate-active Substances and an Action Plan ("Road Map") for the implementation of the first stage (2022–2024) of the project. Available from: <https://www.garant.ru/products/ipo/prime/doc/405491263/>

[6] Decree of the President of the Russian Federation No. 666 (2020, November). On the reduction of greenhouse gas emissions. Available from: <https://www.garant.ru/products/ipo/prime/doc/74756623/>

[7] Decree of the President of the Russian Federation No. 76 (2021, February). On Measures to Implement the State Scientific and Technical Policy in the Field of Environmental Development of the Russian Federation and Climate Change. Available from: https://www.consultant.ru/document/cons_doc_LAW_376296/

[8] Dorokhov, D., Dorokhova, E., Sivkov, V. (2017). Marine landscape mapping of the south-eastern part of the Baltic Sea (Russian sector). *Baltica*, 30 (1): 15–22.

[9] Federal Law No. 296-FZ (2021, July). On Limiting Greenhouse Gas Emissions (last edition). Available from: http://www.consultant.ru/document/cons_doc_LAW_388992/

[10] Federal Law No. 7-FZ (2002, January). On environmental protection. Available from: https://www.consultant.ru/document/cons_doc_LAW_34823/

[11] Hu, C., Lee, Z., Franz, B. (2012). Chlorophyll *a* algorithms for oligotrophic oceans: A novel approach based on three-band reflectance difference. *J. Geophys. Res.*, 117: C01011.

[12] Kahlert, M., Eilola, K., Mack, L., Meissner, K., Sandin, L., Strömberg, H., Uusitalo, L., Viktorsson, L., Liess, A. (2020). Gaps in current Baltic Sea environmental monitoring – Science versus management perspectives. *Mar. Pollut. Bull.*, 160: 111669.

[13] Meier, H. E. M., Reckermann, M., Langner, J., Smith, B., and Didenkulova, I. (2023). Overview: The Baltic Earth Assessment Reports (BEAR). *Earth Syst. Dynam.*, 14: 519–531.

[14] Order of the Ministry of Science and Higher Education of the Russian Federation No. 74 (2021, February). About supersites for the development and testing the carbon balance control technologies. Available from: <https://www.consultant.ru/cons/cgi/online.cgi?req=doc&base=EXP&n=767464#eeld4rT61nKvDfJq>

[15] Paris Agreement (2015, December). In Report of the Conference of the Parties to the United Nations framework convention on climate change (21st session, 2015: Paris). Available from:

<https://heionline.org/HOL/LandingPage?handle=hein.journals/intlm55&div=46&id=&page=>

[15] [16] Reckermann, M., Omstedt, A., Soomere, T., Aigars, J., et al. (2022). Human impacts and their interactions in the Baltic Sea region. *Earth Syst. Dynam.*, 13: 1–80.

[17] Oil and environment of the Kaliningrad Region. Vol. II: Sea (2012). / ed. by V. V. Sivkov (editor-in-chief), Yu. S. Kadzhoyan, O. E. Pichuzhkina, V. N. Feldman. Kaliningrad: Terra Baltica. 576 p.

INTERNATIONAL MODELS OF RISK MANAGEMENT: FERMA, COSO AND ISO

Valentina Dzobelova¹, Sergey Yablochnikov², Maxim Makhboroda³,
Lyubov Manukhina⁴, Anna Vedyashova⁵

¹North-Ossetian State University named after Kosta Khetagurov, Russia

²Moscow Technical University of communications and Informatics, Russia

³North International Innovation University, Sochi, Russia

⁴Moscow State University of Civil Engineering (National Research University), Russia

⁵National Research Mordovia State University, Saransk, Russia

dzobelova@mail.ru

vykfe@mail.ru

maks-net@yandex.ru

4804107@mail.ru

fishann7@mail.ru

Abstract

This article discusses the most important risk management standards that play a very significant role in the activity of any enterprise, both at the micro- and macro level, in order to reduce negative factors that have an impact on the financial activities of the enterprise. During the analysis, we considered the main models of risk management known as FERMA, COSO and ISO, the origin of which is European, American and international, respectively. The scientific work reveals the essence of each risk management model, highlighting their features and characteristics.

Keywords: risk management, uncertainty, auditing, European model FERMA, American model COSO, International model ISO

I. Introduction

An important role in the development of any enterprise is played by the company's risk management methodology, which contributes to the timely analysis and search for solutions to reduce factors that are negative for the activities of the considered subjects [1]. As a rule, the risk management process covers such a range of areas as risk management, monitoring the internal environment and auditing the company's activities, as well as the compliance with certain requirements. Accordingly, the result of all the above-mentioned steps is the creation of certain standards for risk management. At the same time, each of these standards differs in its methodology and approach to responding to these risks.

Under the conditions of a contemporarily developing society, a very significant place is occupied by risk management models that have worldwide application and which are known as COSO, FERMA and ISO models.

II. Methods

So, the main aim of this article is to review and study international models of risk management through a comparative analysis between them.

The objects of our study are the international models COSO, FERMA and ISO.

The subject is the assessment of the advantages and disadvantages of each model with the highlighting of their distinctive features.

As applied research methods used in this article, we would like to highlight the method of comparative analysis between various models of risk management.

The works of various economists, who made a great contribution to science on the considered topic, as well as articles in periodicals and Internet resources were used in the course of writing this scientific work.

III. Results

What is the essence of these models? What methods are used to manage risks considering these economic categories? How do they differ from each other and are there similarities between them? What are the main advantages and disadvantages of these models? Let's try to answer these questions.

As expected, each of these models, both FERMA and COSO, propose some kind of ideal model in their opinion, necessary to manage risks that differ from each other [2].

If we consider the COSO model, we can note that the main contribution to the formation of this model was made by the auditors of PricewaterhouseCoopers.

It should be added that this information, as a rule, required professional knowledge and was not designed for the general public. Exactly the auditors mostly acted as the main users.

At the same time, in this case, much attention was paid to the compliance with the basic requirement regarding the reliability and accuracy of the financial statements of companies.

Note that the compliance with the reliability of information in the reports in the United States of America is a mandatory requirement for public enterprises [3].

Concerning the FERMA model, it should be noted that its developers are a small group of European organizations with a highly specialized focus, which in terms of risk management increases the scope of persons for whom this information can be understood, compared to the COSO model.

As the experience of world practice shows, the FERMA model is in great demand due to its easiness and accessibility for a wider scope of persons and has a recommendatory nature [4].

At the same time, the main information, presented in this model, is taken from ISO 31000, which is decoded as the international standard for risk management.

Thus, as we see it, risk management plays a rather important role for any organization.

After all, thanks to risk management, we get the opportunity for timely analyzing certain vulnerabilities of enterprises to quickly respond by making the most effective management decisions and reducing the level of risk.

In our opinion, the main direction of risk management is the organization of such working conditions that will be aimed at reducing risks with a corresponding increase in profits under conditions of uncertainty.

As we see it, in order to apply risk management, first of all, it is necessary to ensure that the staff has a certain competence and understands the essence of risk management with the disclosure of its significance for the prosperity of the company.

Thus, summarizing all the above, we can conclude that at this stage of economic development, the humankind actively applies the following risk management models in the course of its activities:

- American model, known as COSO
- European model FERMA
- International model ISO.

It is worth to mention that the first standard in this area was already developed in 1995 in Australia and was designated as AS/NZS 4360:2004.

Accordingly, over time, other standards of other states also began to be applied.

As for the international standard ISO 31000, it was developed and put into practice since 2009.

Undoubtedly, considering all three models, one can notice the differences between them, which, first of all, consist in the style of presentation, the volume of documentation used and the method of research.

As an example, we can compare an international standard, which is characterized by a small content (about twenty pages) and the American model, which is presented in two hundred pages.

But, in our opinion, the main similarity of all three models, first of all, is the presence of risk, which contributes to the search for solution for the way out of an uncertain situation.

For clarity and a better understanding of the significance of these models, we would like to analyze each of them separately.

Let's start with the risk management model known as FERMA.

As noted above, this European model was developed by the Federal Association of Risk Management Professionals.

An important feature of this standard is universality in terms of its application in the present time, both for short-term and long-term purposes.[5]

In practice, the FERMA model is implemented in seven stages.

First of all, the whole analysis begins with the determination of the main goals and objectives of the company.

Further, the next step is to identify and assess all the risks of the enterprise. That is, specialists collect all the information about the company's activities, studying the competitive environment and market conditions.

Accordingly, on the basis of the collected data, all risks are calculated and considered, creating a kind of a risk map that displays all the weaknesses of the enterprise, to which the attention should be paid.

Thus, with the help of a competent and effective analysis, we get the opportunity, thanks to quantitative and qualitative indicators, to identify and eliminate all risks by developing certain measures that will be aimed at maximum reduction or complete elimination of risks.

The next, third step, is the compilation of a report on all the risks that the enterprise faces in the course of its operation.

Further, on the basis of this report, some decisions are applied that are aimed at the risk management process, including such stages as calculating the effectiveness of certain decisions, the level of costs for risk reduction measures, etc.

Of course, it is almost practically impossible to completely insure oneself against all risks.

In this case, the functioning of the company is considered, based on the legislative framework.

At the sixth stage, a repeated report is carried out, which includes two components: internal and external.

Thus, in our opinion, an internal report is necessary for use and application within the enterprise, and mostly this document is given to the manager in order for him to assess the situation.

As for the external report, it is aimed at external users who, for one reason or another, are interested in this information. In this case, the report is mainly compiled according to the risk management methodology.

And the final stage of risk management according to the FERMA model is the implementation of control measures for continuous monitoring of the situation for the most rational managerial decision-making.

Summarizing all the above, we can conclude that the essence of FERMA as a European association is to work out and apply a specific plan of actions for risk management.

As a rule, this method is used to ensure the continuity of the workflow.

At the same time, FERMA focuses on the following risks in its standard: strategic, security, financial and production risks.

The chronology of the stages outlined above can be summarized as follows:

- Identification of the factors of risk management;
- Evaluation activities of the existing risks;
- Determination of methodology and technology for risk monitoring;
- Making recommendations on risk management;
- Basic requirements for a risk manager.

In our opinion, the universality of this standard in terms of its use in any organization can be attributed as an advantage.

Thus, we have considered the European risk management model FERMA.

Now, we would like to consider the next important model known as COSO.

So, COSO ERM is an American model, the founder of which is the Committee of Sponsoring Organizations.

At the same time, let's note that ERM, which is decoded as Enterprise Risk Management, served as the first document in 2004.

And the second document, published in 2017, is Enterprise Risk Management Integration with Strategy and Performance.

If we compare these two documents, then in terms of interpreting the essence of risks there are practically no differences as such, but the difference consists mainly in the methodology.

The COSO 2004 model defines risk management as a kind of work to be performed by the management and employees of the company in order to improve the financial status of the organization.

For clarity, this model can be represented in the form of a matrix having a cubic shape.

Note that the upper zone of this matrix contains information regarding both strategic and operational goals, as well as reporting and compliance with the legal requirement of the state.

The front zone includes eight stages, the necessity of which is associated with the goal of solving problems. Let's consider each of these stages.

So, the first stage begins with such an analysis, which studies the internal state of the company business and the whole staff, focusing on their reaction and response to the risk system.

The second stage is the definition of tasks. Moreover, this stage should be carried out even before the risk occurrence. The execution of this point will sufficiently protect the company from certain difficulties, enabling the enterprise to identify the main goals depending on the mission.

The next stage is the search for factors that have a negative impact on the activities of the enterprise. It is very important in this case to consider both internal and external factors.

Next, it is necessary to carry out evaluation activities to identify the level of risks in the activities of enterprises.

The fifth stage is the reaction of the risk manager to the resulting situation. As the main reactions, one can single out the acceptance or denial of these risks, a decrease or increase in its significance, etc.

Accordingly, the task of the risk manager is an elaboration of measures for reducing the risk level to a certain acceptable value.

The sixth stage is devoted to the control measures, the essence of which consists in the timely response to emerging risks.

According to the COSO model the seventh stage is the importance of communication links.

After all, it is very important for the employees to be competent and have information about the risks that threaten the company.

For this reason, it is necessary to be guided by mutual exchange processes among employees as well as between management and employees.

And, finally, the last stage is risk monitoring, which must be carried out either on a permanent basis or in regular intervals.

Moreover, we'd also like to note that the COSO 2004 model contains about 128 methods aimed at risk management, which are designed to minimize them and stabilize the normal functioning of the enterprise.

Speaking for the COSO model according to the standard published in 2017, we can note that in the new edition much attention is paid to the trends of modern society with a deep analysis of risk management.

In this context, the term "risk" is considered from the point of view of the control element, due to which the analysis and forecasting of the expected factors, that have a negative impact on the activities of the enterprise, are carried out.

We'd like to note that COSO 2017, compared to COSO 2004, includes five stages and twenty different processes required for the entire cycle. [8]

At the same time, this technique can be applied to any enterprise, regardless of the type of activity and location.

Speaking about the main stages of the COSO 2017 model, we would like to start with its first component, which characterizes the culture and methodology of management.

In this context, culture means, first of all, the competence of employees in terms of the qualitative fulfillment of their obligations.

Respectively, the management process exercises control function and is responsible for supervisory activities.

The second stage is a goal-oriented planning, with the help of which certain risks are clarified based on the goals.

The third point is effectiveness, the essence of which is the timely identification and elimination of risks that have a negative nature.

In addition, risk division by hazard level plays an important role, as it enables the organization to understand which risk needs to be focused first.

The fourth stage is to determine the efficiency of risk management based on the analysis of risks.

And, the final stage is the compliance with communication links between various departments in order to exchange data for risk management.

Thus, we have also considered the essence of the COSO risk management model.

We'd also like to give a brief description of the ISO 31000 model mentioned above.

Let's start with the fact that ISO 31000 acts as an international universal standard, which includes various regulations for risk management. According to this document, such requirements include:

- Internal environment of the organization;
- Strategic goals;
- A group of persons responsible for their actions;
- Analysis of risks and force majeure circumstances and prompt response to them;
- Carrying out monitoring;
- Data collection and analysis;
- Links between individuals having an identical interest in a particular issue.

Besides, we would like to add that today ISO 31000 serves as a unique international model for risk management.

At the same time, ISO 37000 appeared in 1946 in London; it is decoded and translated as the International Organization for Standardization.

IV. Discussion

So, we have considered the main risk management standards known as COSO, FERMA and ISO. Considering all the above-mentioned, we can conclude that the main consumer of the standard according to the American COSO model is the auditors of the company; according to the European FERMA model – competent risk managers of the enterprise; and according to the international ISO model – any organization, regardless of the form of ownership.

At the same time, an important role is played by the fact that only the American COSO model is characterized by the obligatory compliance with this standard by organizations whose securities

are quoted on the stock exchange located in New York.

In conclusion, we'd like to note the interpretation of the term "risk" that each model of risk management offers.

So, by the word "risk" the American COSO model implies the negative factors that have an impact on the company's activities, reducing the company's income.

The European FERMA model, on the other hand, interprets risks from some probable events with their further outcomes.

As for the international ISO model, the word "risk" is denoted in the context of an uncertainty factor that interferes with the implementation of the company's strategic goals. In other words, as a discrepancy between the expected indicators and those actually received and having both a positive and a negative nature. Thus, as we see it, the risk management process is not a copy of already existing methods, but, on the contrary, it serves as an addition, primarily in matters of internal audit. The considered risk management models can be easily applied in the practice of various organizations. Indeed, due to the presence of an effective risk management system, enterprises can significantly reduce the level of certain risks to achieve the most reliable and rational development and expansion without negative consequences.

Thus, we have revealed the topic of our study and identified the essence of each risk management standard.

References

- [1] Aven T. A unified framework for risk and vulnerability analysis and management covering both safety and security // *Reliability Engineering and System Safety*. 2007. N 92. P. 745–754.
- [2] Committee of Sponsoring Organizations of the Treadway Commission (COSO). 2004.
- [3] Crowe T.J., Fong P.M., Bauman T.A., Zayas-Castro J.L. Quantitative risk level estimation of business process reengineering efforts // *Business Process Management Journal*. 2002. N 8 (5). P. 490–512.
- [4] FERMA a risk management standard. Federation of European risk management association. 2002.
- [5] Graham J.D., Weiner J.B. Risk versus risk: Tradeoffs in protecting health and the environment. Cambridge: Harvard University Press, 1995.
- [6] ISO 31000:2009 – Principles and Guidelines on Implementation. 2009
- [7] Andreeva L.V., Zubareva E.V., Bodrova T.V. Accounting, analysis and audit of indicators that ensure the economic security of business entities. – M.: ITK Dashkov & K 2019. – 102 p.
- [8] Belov P.G. Risk management, system analysis and modeling in 3 vol. Volume 2: textbook and practical course for Bachelor's and Master's programmes / P.G. Belov. – M.: Publishing URAIT, 2019. – 250 p.
- [9] Vyatkin V.N. Risk management: textbook / V.N. Vyatkin, V.A. Gamza, F.V. Maevsky. – 2nd, revised and enlarged edition. – M.: Publishing URAIT, 2019. – 365 p.
- [10] Kuptsov, M.I., Yablochnikova, I.O., Yablochnikov, S.L., Dzobelova, V.B. & Mineev, V.I. (2020). Modeling Internet Business Optimization Processes, 2020 International Conference on Engineering Management of Communication and Technology (EMCTECH), Vienna, Austria, 2020, pp. 1-5, doi: 10.1109/EMCTECH49634.2020.9261507.

BIOMORPHOLOGICAL ANALYSIS AND OCCURANCE OF ENDEMIC AND RELICT SPECIES OF THE CHECHEN REPUBLIC

Zazu Iriskhanova¹, Khava Khanaeva¹, Birlant Khasueva²

•

¹Kadyrov Chechen State University, Russia

²Chechen State Pedagogical University. Russia

zazuiris@mail.ru

xeda.xanaeva@bk.ru

khasueva_013@mail.ru

Abstract

This article provides a biomorphological analysis and occurrence of endemic and relict species of the Chechen Republic. Endemic species (taxa unique to a particular geographical area) are characteristic elements of local biodiversity. Narrow endemics occupy isolated habitats, often associated with limited ranges of ecological conditions or small common geographic ranges. The analysis is based on the processing of herbarium materials and field observations of the authors.

Keywords: species, genus, family, flora, life form, biomorph, endemics, relicts, Chechen Republic

I. Introduction

Species displaying a convergent subset of potential trait values are suited to local environmental conditions. The result is a general functional convergence within a community, a functional divergence between endemic species and non-endemic sympatric species, and relatively limited trait differences for endemics.

II. Methods

The basis of the work is the material collected by the authors in 2020-2023, as well as data obtained from the study of herbarium collections of the Department of Botany, Zoology and Bioecology of the Chechen State University. A.A. Kadyrov.

III. Results

According to the information obtained during the study, 180 species of plants grow in the wild in the study area, united in 65 families.

The leading position in the spectrum belongs to the family Fabaceae Lintll. - Legumes, numbering 18 species (10.0%). The second place is occupied by the Asteraceae Dumort family. (Compositae) - Asteraceae (Asteraceae) (13 species, 7.22%). The third place is occupied by the Campanulaceae Juss family. – Bellflowers (11 species, 6.11%). In total, 65 leading families include 180 species, which is 156.67%.

The life form is the result of a long-term adaptation of a plant to local conditions of existence, expressed in its external appearance [1]. The most acceptable for biomorphological analysis is the system of "biological types" by K. Raunkier [7].

The biomorphological spectrum of the vicinity of relict and endemic species of the Chechen Republic is presented in Table 1.

Table 1: *Biomorphological spectrum of relict and endemic species of the Chechen Republic*

BIOMORPHA	Hk	T	K	Phn	Phms	Ch	Phmg	Phm
	hemicryptophytes	Terophytes	cryptophytes	nanofanerophyte	mesophanerophyte	chamephite	megaphanerophyte	microfanerophyte
Number of species 179	112	14	16	9	4	20	2	2
% of total	62,6	7,8	8,9	5,0	2,2	11,2	1,1	1,1

There are 2 species of megaphanerophytes (1.1%): *Pinus sosnowskyi* Nakai (*P. hamata* (Stev.) Sosn.; *P. kochiana* Klotzsch) - Sosnowsky's Pine, *Ostrya carpinifolia* Scop. - Common hop.

There are 4 species of mesophanerophytes (2.2%): *Taxus baccata* L. - Berry yew, *Acer laetum* C.A. May. - Light maple, *Betula raddeana* Trautv. - Birch Radde, *Carpinus caucasica* Grossh. (*Carpinus betulus* L.) - Caucasian hornbeam.

There are 2 species of microfanerophytes (1.1%): *Cornus mas* L. - Common dogwood, *Juniperus hemisphaerica* J. et C. Presl (*J. depressa* Stev.) - Hemispherical juniper.

There are 9 species of nanofanerophytes (5.0%): *Juniperus oblonga* Bieb. (*J. communis* L.) - Oblong juniper, *J. sabina* L. - M. Cossack, *Cotinus coggygria* Scop. - Leather mackerel, *Corylus aveliana* L. - Common hazel, *Rhododendron caucasicum* Pall. - Caucasian rhododendron, *Asrtagalus brachylobus* Fisch. - Short-lobed Astracanthus, *Colutea orientalis* Mill - Oriental Bubblegum, *Rosa tschatyrdagi* Chrshan. - Rosehip Chatyrdag, *Viscum album* L. - White mistletoe.

There are 20 species of hamefites (11.2%): *Huperzia selago* (L.) Bernh. ex Schrank et C. Mart. (*H. petrovii* Sipl.) - Common ram, *Lycopodium annotinum* L. - Yearly club moss, *Selaginella helvetica* (L.) Spring - Swiss club moss, *Ephedra distachya* L. - Two-eared ephedra, *E. procrea* Fisch. et C.A. May. - E. tall, *Hedera pastuchovii* Woronow - Pastukhov's ivy, *Fumana procumbens* (Dun.) Gren. et Godr. - Recumbent Fuman, *Arctostaphylos caucasica* Lipsch. (*A. iiva-nrsi* (L.) Spreng.) - Caucasian bearberry, *Asrtagalus cornutus* Pall. - Horn-bearing Astracanthus, *A. karakugensis* Bunge - A. Karakuginskaya, *A. lehmannianus* Bunge - A. Lehmann, *A. varius* S.G. Gmel. (*A. virgatus* Pall.) - A. diverse, *Caragana mollis* (Bieb.) Bess. - Soft caragana, *Ononis pusilla* L. - Small steelhead, *Scutellaria andina* Charadze - Andean skullcap, *S. leptostegia* Juz. - Sh. finely scaly, *S. raddeana* Juz. - S. Radde, *Nitraria schoberi* L. (*N. caspia* Willd.) - Schober's salt peter, *Asperula dasyantha* Klok. - Pubescent woodruff, *A. diminuta* Klok. - I. reduced, *Rhodococcum vitis-idaea* (L.) Avror. (*Vaccinium vitis-idaea* L.) - Common lingonberry.

There are 112 species of hemicryptophytes (62.6%): *Polystichum aculeatum* (L.) Roth (*P. lobatum* (Huds.) Bast.) - Small-spined multi-row, *P. braunii* (Sperm.) Fee - M. Brown, *Asplenium ruta-muraria* L. - A. septentrionale (L.) Hoffm. - K. northern, *A. trichomanes* L. - K. hairy, *A. vtride* Huds. - K. green, *Ceterach officinarum* Willd. - Pharmacy scraper, *Phyllitis scolopendrium* (L.) Newm. - Centipede, *Polypodium vulgare* L. - Common centipede, *Cypripedium calceolus* L. - True slipper, *Calamagrostis caucasica* Trin - Caucasian reed grass, *Elymus prokudinii* (Seredin) Tzvel. (*R. prokudinii* Serediri) - Prokudin's wheatgrass, *Festuca primae* E. Alexeev - Prima's fescue, *F. daghestanica* (Tzvel.) E. Alexeev - Dagestan O., *Imperata cylindrical* (L.) Raeusch. - Imperata Cylindrical, *Poa primae* Tzvel. - Prima bluegrass, *Stipa daghestanica* Grossh. - Dagestan feather grass, *Mandenovia komarovii* (Manden.) Alava - Mandenovia Komarov, *Symphyloloma*

graveolens C.A. May. - Odorous joint fruit, *Asarum ibericum* Stev. ex Ledeb. (*Asarum intermedium* (C.A. Mey.) Grossh.) - Georgian hoof, *Arctium nemorosum* Lej. - Oak burdock, *Bellis perennis* L. - Perennial daisy, *Centaurea pseudotanaitica* Galushko nomen nudum - Lozhnodon cornflower, *Crepis hydrophiloides* Charadze - Swampy skerda, *Hieracium gudergomiense* Juxip - Gudergomis hawkweed, *Jurinea annae* Sosn. - Anna's head, *J. filicifolia* Boiss. - *Psephellus andinus* Galushko et Alieva (*C. Andina* (Galushko et Alieva) Czer.) - Andean *Psephellus*, *P. prokhanovii* Galushko (*C. prokhanovii* (Galushko) Czer.) - P. Prokhanova, *P. kemulariae* Charadze (*C. kemulariae* (Charadze) Czer.) - P. *Kemulariae*, *Pulicaria dolomiticum* Galushko - Dolomitic flea beetle, *Brunnera macrophylla* (Bieb.) Johnst. - Brunner large-leaved, *Omphalodes rupestris* Rupr. ex Boiss. - Rocky umbilical, *Rindera tetraspis* Pall. - *Rindera* four-shield, *Alyssum andinum* Rupr. - Andean beetroot, *Draba ossetica* (Rupr.) Somm. et Levier - Ossetian grits, *Erucastrum subnivale* Prima - Snowy jaundice, *Isatis pseudoararatia* Galushko nomennudum - False-Araratian woad, *Matthiola daghestanica* (Conti) N. Busch - Dagestan Levkoy, *Campanula andina* Rupr. - Andean bluebell, *C. annae* Kolak. - K. Anna, *C. argunensis* Rupr. - K. argunsky, *C. collina* Bieb. - K. kholmvoi, *C. daghestanica* Fomin - Dagestan bluebell, *C. darialica* Charadze - K. dariesky, *C. fedorovii* Charadze - K. Fedorova, *C. meyeriana* Rupr. - K. Meyer, *C. petrophila* Rupr. - K. Skalny, *Symphyantra galushkoi* Taisumov et Teimurov (*Campanula galushkoi* Taisumov et Teimurov.) - *Zymphiandra* Galushko, *S. pendula* (Bieb.) A.DC. (*Campanula pendula* Bieb.) - drooping Z., *Cerastium kasbek* Parrot Meu. - Multiflorous chickweed, *Dianthus arenarius* L. - Sand carnation, *D. daghestanicus* Charadze - G. Dagestan, *D. imereticus* (Rupr.) Schischk. - G. Imeretinskaya, *Oberna multifida* (Adams) Ikonn. (*S. multifida* (Adams) Rohrh.) - Multi-cut Auburn, *Petrocoma hoefftiana* (Fisch.) Rupr. - Göfft's *Petrocoma*, *Silene chlorifolia* Smith - Green-leaved tar, *S. compacta* Fisch. ex Hornem. - Clustered flower smoly, *Sedum stoloniferum* S.G. Gmel. - Stonecrop, *Scabiosa rotata* Bieb. - Wheel scabiosa, *Drosera rotundifolia* L. - Round-leaved sundew, *Tithymalus astrachanicus* (C.A. Mey.) Prokh. (*E. astrachanica* C.A. Mey. ex Prokh., *E. praecox* (Fisch. ex Boiss.) B. Fedtsch. et Fler.) - *Euphorbia Astrakhan*, *T. glareosus* (Pall. ex Bieb.) Prokh. (*E. glaeosa* Pall, ex Bieb., *E. maleevii* Tamamsch.) - *M. cartilaginosa*, *Amoria elisabethae* (Grossh.) Roskov (*T. elisabethae* Grossh.) daghestanica Rupr. - Dagestan alfalfa, *Onobrychis dielsii* (Sirj.) Vass. - Diels sainfoin, *Onobrychis inermis* Stev. - Unarmed sainfoin, *Onobrychis novopokrovskii* Vass. - Novopokrovsky's sainfoin, *Vavilovia formosa* (Stev.) Fed. - Beautiful *Vavilovia*, *Xanthobrychis majorovii* (Grossh.) Galushko Majorovii (Grossh.) - *Xanthobrychis Mayorova*, *Gentiana grossheimii* Doluch. - *Gentian Grossheim*, *Geranium kemulariae* Charadze - *Geranium Cumularia*, *Hypericum asperuloides* Czern. ex Turkish. - St. John's wort, *Marrubium plumosum* C.A. May. - Pinnate chandra, *Nepeta biebersteiniana* (Trautv.) Pojark. - Bieberstein's catnip, *N. cyanea* Stev. - K. blue, *N. czegemensis* Pojark. - K. Chegemsky, *Satureja pachyphylla* C.Koch - Thick-leaved savory, *Stachys fugax* Pobed. - Falling cleaner, *Goniolimon besserianum* (Schult.) Kusn. - *Goniolimon Besser*, *Paeonia biebersteiniana* Rupr. - Peony of Bieberstein, *Rapaver bracteatum* Lindl. - Common poppy, *Lysimachia nummularia* L. - Coin loosestrife, *Primula darialica* Rupr. - Darial primrose, *P. luteola* Rupr. - P. yellow, *P. zeylamica* Charadze et Kapell. - P. Tseylamsky, *Pyrola rotundifolia* L. - Wintergreen, *Actaea spicata* L. - Spike cohosh, *Helleborus caucasicus* A.Br. - Caucasian hellebore, *Pulsatilla andina* (Rupr.) Woronow - Andean dream, *Ranunculus auricomus* L. - Golden buttercup, *R. tebulosica* Prima - *Tebulos buttercup*, *Alchemilla elisabethae* Juz. - Elizabeth's cuff, *A. chlorosericea* (Buuser) Juz. - M. green silk, *Potentilla alexeenkoi* Lipsky - *Potentilla Alekseenko*, *P. ghalgana* Juz. (*P. oweriniana* Boiss.) - Ingush L., *P. orientalis* Juz. - Eastern L., *P. sterilis* (L.) Garcke - Barren L., *Galium mollugo* L. - Soft bedstraw, *Haplophyllum villosum* (Bieb.) G. Don fil. - Soft-haired whole leaf, *Saxifraga charadzae* Otsch. - Saxifrage Kharadze, *Scrophularia charadzae* Kem.-Nath. - Norichnik Kharadze, *S. minima* Bieb. - N. small, *Veronica bogosensis* Tumad. - *Veronica Bogoskaya*, *V. charadzae* Kem.-Nath. - V. Kharadze, *V. daghestanica* Rupr. ex Boiss. - V.

Dagestanskaya.

There are 16 species of cryptophytes (8.9%): *E. fluviatile* L. (*E. heleocharis* Ehrh.) - marshwort, *Ophioglossum vulgatum* L. - common grasswort, *Botrychium lunaria* (L.) Sw. - Moonflower, *Marsilea quadrifolia* L. - Four-leaved Marsilia, *Allium gunibicum* Miscz. ex Grossh. (*A. mirzoevii* Tscholokaschvili) - Gunib onion, *A. paradoxum* (Bieb.) G. Don fil. - Strange L., *A. ursinum* L. - Bear L. (Cheremsha), *Sternbergia colchiciflora* Waldst. et Kit. - Sternberg Colchicum, *Merendera ghalgana* Otsch. - Merender Ingush, *Muscari armeniacum* Leichtlin (*Mszo vitsianum* Baker) - Armenian mouse hyacinth, *Iris Notha* Bieb. - Iris (Iris) fake, *Gagea daghestanica* Levichev et Murtazaliev - Dagestan goose onion, *Corydalis bayerniana* Rupr. - X. Bayern, *C. roseo-purpurea* (Rupr.) Galushko - X. pink-purple, *Nymphaea alba* L. - White water lily, *Anemonoides blanda* (Schottet Kotschy) Holub (*A. blanda* Schottet Kotschy) - Pleasant anemonoides.

Teriphites 14 species (7.8%): *Salvinia natans* (L.) All. - *Salvinia* floating, *Alyssum parviflorum* Fisch. ex Bieb. (*A. rothmaleri* Galushko.; *A. campestre* auct.) - Small-flowered beetroot, *Lepidium pinnatifidum* Ledeb. - Pinnate cress, *Microthlaspi pertoliatum* (L.) F.K. May. (*Thlaspi perfoliatum* L.) - Pierced twig, *Sameraria cardiocarpa* Trautv. - Heart-fruited *Sameraria*, *Sedum argunense* Galushko - Argun stonecrop, *Scabiosa Micrantha* Desf. - Small-flowered scabiosa, *Tithymalus szovitsii* (Fisch. et C.A. Mey.) Klotzch et Garcke ex Klotzch (*E. szovitsii* Fasch. et C.A. Mev.) - Schowitz's spurge, *Melilotus wolgicus* Poir. - Volga elecampane, *Trigonella coerulescens* (Bieb.) Halacsy - bluish fenugreek, *Centaurium spicatum* (L.) Fritsch - spike-shaped centaury, *Papaver ocellatum* Woronow - Ocellated poppy, *Trapa hyrcana* Woronow - Hyrcanian chilim, *Pseudobetkea caucasica* (Boiss.) Lincz. - Pseudo-Betkea Caucasian.

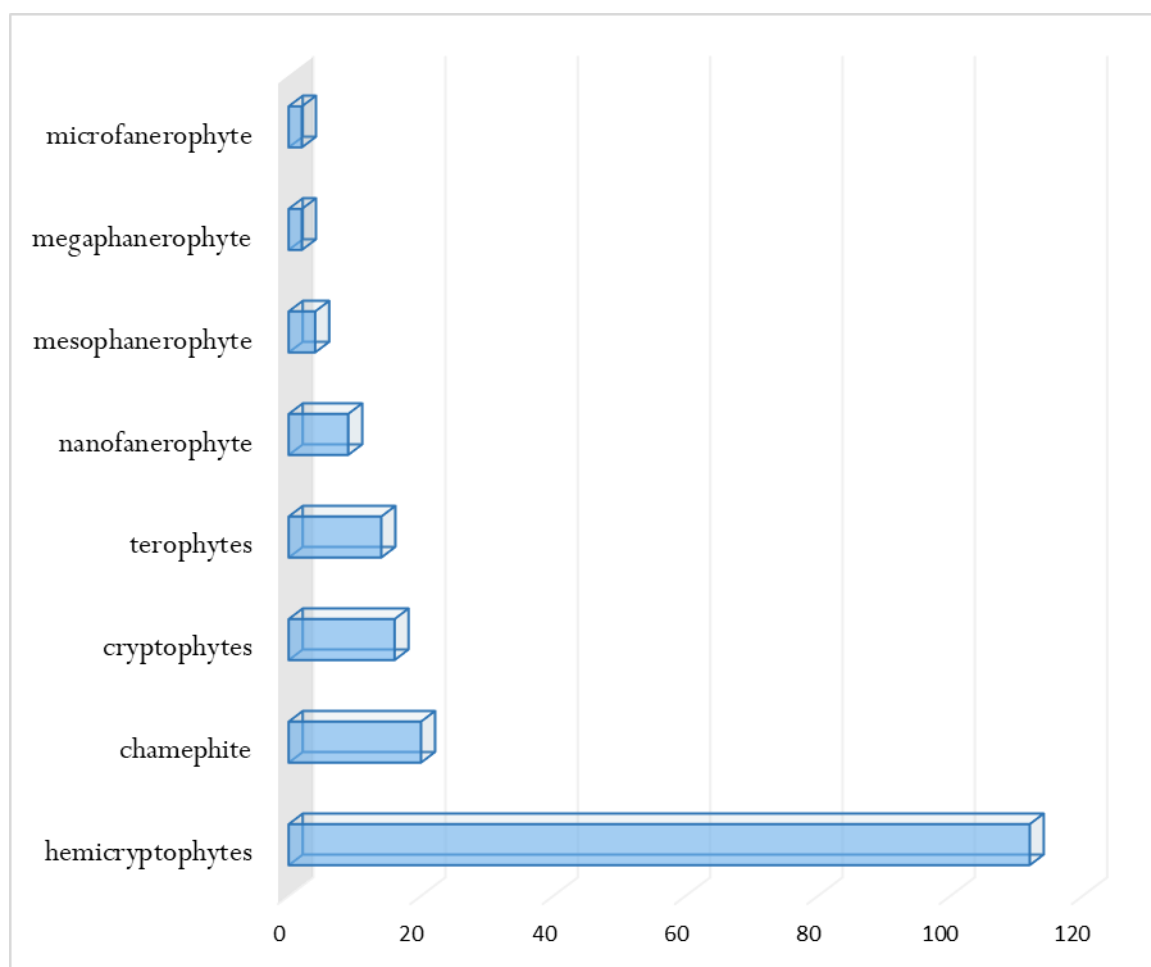


Fig. 1: Biomorphological analysis of relict and endemic species of the Chechen Republic

IV. Discussion

The relationship between environmental parameters and traits that affect survival suggests that endemics are rare due to adaptive specialization and selection in favor of limited ranges and performance of traits. In practice, an understanding of functional variability, survival mechanisms, and associated ecological conditions is necessary to inform conservation measures for such species.

In addition, species coexist in communities, and relative productivity and competition between species is a key aspect of plant survival. The variation in functional trait values for endemic species may differ from that in sympatric species, which are often more geographically distributed and may show greater functional diversity. Being a phylogenetic and geographic relic at the same time is a common occurrence, and this raises even more conservation concerns. In this case, the relict species is not only evolutionarily unique, but also especially vulnerable to local disturbance due to its limitation to a reduced area. If this relic is found in a small area that is not rich in species, it is even more endangered as conservation measures will not be taken for other reasons.

Recently, there has been a tendency to designate certain narrowly distributed or isolated populations as relics when the species distribution is fragmented, even if the evolutionary status or phylogenetic position of these populations is either unknown or presumably not "deeply branched", and even if there is no evidence that this isolation was caused by the extinction of some related populations

The dominant species is *Carpinus caucasica* Grossh. (*Carpinus betulus* L.) - Caucasian hornbeam.

Usually (26 species) there are such species as *Lycopodium annotinum* L. - annual moss, *Polystichum braunii* (Sperm.) Fee - Brown's multi-row, *Asplenium ruta-muraria* L. - *Asplenium septentrionale* (L.) Hoffm. - Northern Kostenets, *A. trichomanes* L. - K. hairy, *A. vtride* Huds. - K. green, *Pinus sosnowskyi* Nakai (*P. hamata* (Stev.) Sosn.; *P. kochiana* Klotzsch) - Sosnowsky's pine, *Juniperus hemisphaerica* J. et C. Presl (*J. depressa* Stev.) *aquatica* L. - Plantain chastuha, *Allium ursinum* L. - Bear onion (Wild leek), *Calamagrostis caucasica* Trin - Caucasian reed grass, *Jurinea absinthifolius* Galushko - *Artemisia* sagebrush, *Alyssum andinum* Rupr. - Andean beetroot, *Lepidium pinnatifidum* Ledeb. - Pinnate cress, *Campanula collina* Bieb. - Hill bell, *Symphyandra galushkoi* Taisumov et Teimurov. (*Campanula galushkoi* Taisumov et Teimurov.) - *Zimfiandra Galushko*, *S. pendula* (Bieb.) A.DC. (*Campanula pendula* Bieb.) - drooping zebra, *Cerastium kasbek* Parrot - Kazbek sapling, *Oberna multifida* (Adams) Ikonn. (*S. multifida* (Adams) Rohrh.) - Auburn multidissected, *Cornus mas* L. - Common dogwood, *Corylus aveliana* L. - Common hazel, *Rhododendron caucasicum* Pall. - Caucasian rhododendron, *Amoria elisabethae* (Grossh.) Roskov (*T. elisabethae* Grossh.) - *Amoria* (Clover) Elizabeth, *Nepeta cyanea* Stev. - Blue catnip, *Alchemilla elisabethae* Juz. - Elizabeth's cuff, *Rhodococcum vitis-idaea* (L.) Avror. (*Vaccinium vitis-idaea* L.) - Common lingonberry.

Scattered 66 species occur: *Huperzia selago* (L.) Bernh. ex Schrank et C. Mart. (*H. petrovii* Sipl.) - Common ram, *Selaginella helvetica* (L.) Spring - Swiss club moss, *Phyllitis scolopendrium* (L.) Newm. - Centipede, *Polypodium vulgare* L. - Common centipede, *Salvinia natans* (L.) All. - *Salvinia* floating, *Ephedra distachya* L. - Two-eared ephedra, *E. procrea* Fisch. et C.A. May. - E. tall, *Juniperus oblonga* Bieb. (*J. communis* L.) - Oblong juniper, *Allium gunibicum* Miscz. ex Grossh. (*A. mirzoevii* Tscholokaschvili) - Gunib onion, *Merendera ghalgana* Otsch. - Merender Ingush, *Acer laetum* C.A. May. - Light maple, *Cotinus coggygria* Scop. - Leather mackerel, *Mandenovia komarovii* (Manden.) Alava - *Mandenovia* Komarova, *Symphyoloma graveolens*

C.A. May. - Odorous spice, *Arctium nemorosum* Lej. – Oak burdock, *Bellis perennis* L. – Perennial daisy, *Centaurea pseudotanaitica* Galushko nomen nudum - Lozhnodonsky cornflower, *Crepis hydrophiloides* Charadze - swampy skerda, *Hieracium gudergomiense* Juxip - Gudergomis hawkweed, *Jurinea filicifolia* Boiss. – *Psephellus andinus* Galushko et Alieva (*C. Andina* (Galushko et Alieva) Czer.) – Andean *Psephellus*, *P. prokhanovii* Galushko (*C. prokhanovii* (Galushko) Czer.) – *P. Prokhanova*, *Pulicaria dolomiticum* Galushko, *Betula raddeana* Trautv. – Radde birch, *Brunnera macrophylla* (Bieb.) Johnst. - Brunner large-leaved, *Omphalodes rupestris* Rupr. ex Boiss. – Rocky umbilical, *Alyssum parviflorum* Fisch. ex Bieb. (*A. rothmaleri* Galushko.; *A. campestre* auct.) – small-flowered beetroot, *Draba ossetica* (Rupr.) Somm. Et Levier - Ossetian Krupka, *Campanula andina* Rupr. – Andean bluebell, *C. Annae* Kolak. – *K. Anna*, *C. argunensis* Rupr. – *K. argunsky*, *C. daghestanica* Fomin – *K. Dagestansky*, *C. darialica* Charadze – *K. darialsky*, *C. petrophila* Rupr. – *K. rocky*, *Dianthus daghestanicus* Charadze – Dagestan carnation, *D.imereticus* (Rupr.) Schischk. – Imeretian carnation, *Petrocoma hoefftiana* (Fisch.) Rupr. – *Petrokoma* Gefft, *Silene chlorifolia* Smith – Green-leaved tar, *S.compacta* Fisch. ex Hornem. – *C. Clustered*, *Tithymalus glareosus* (Pall, ex Bieb.) Prokh. (*E. glaeosa* Pall, ex Bieb., *E. maleevii* Tamamsch.) - Cartilaginous spurge, *Asrtagalus brachylobus* Fisch. – Short-lobed *Astracanthus*, *A. supinus* Bunge – *A. adjoining*, *Caragana mollis* (Bieb.) Bess. – Soft caragana, *Colutea orientalis* Mill – Oriental bladderwort, *Medicago daghestanica* Rupr. – Dagestan alfalfa, *Onobrychis inermis* Stev. – Sainfoin unarmed, *O. novopokrovskii* Vass. – *E. Novopokrovsky*, *Vavilovia formosa* (Stev.) Fed. – Beautiful *Babylovia*, *Xanthobrychis majorovii* (Grossh.) Galushko. *Majorovii* Grossh.) - *Xanthobrychis* Mayorova, *Corydalis bayerniana* Rupr. – Bayern's *Corydalis*, *C. roseo-purpurea* (Rupr.) Galushko – Pink-purple X., *Gentiana grossheimii* Doluch. – Grossheim's gentian, *Geranium kemulariae* Charadze – *Cumularia's* geranium, *Nepeta biebersteiniana* (Trautv.) Pojark. – *Bieberstein's* catnip, *N.czegemensis* Pojark. – *K. Chegemsky*, *Scutellaria raddeana* Juz. – *Radde's* skullcap, *Paeonia biebersteiniana* Rupr. – Peony of *Bieberstein*, *Primula darialica* Rupr. – *Darial* primrose, *P. luteola* Rupr. - *P. yellow*, *P.zeylamica* Charadze et Kapell. – *P. Tseylamsky*, *Actaea spicata* L. – Spike crow, *Asperula diminuta* Klok. – Reduced woodruff, *Scrophularia minima* Bieb. – Small boletus, *Veronica bogosensis* Tumad. - *Veronica Bogoskaya*, *Pseudobetckea caucasica* (Boiss.) Lincz. - *Pseudo-Betkea* Caucasian, *Viscum album* L. - White mistletoe.

57 species are rare: *E. fluviatile* L. (*E. heleocharis* Ehrh.) – marshwort, *Botrychium lunaria* (L.) Sw. – Semilunar vine, *Polystichum aculeatum* (L.) Roth (*P. lobatum* (Huds.) Bast.) – Pharmacy scraper, *Marsilea quadrifolia* L. – Four-leaved marsilia, *Juniperus sabina* L. – Cossack juniper, *Allium paradoxum* (Bieb.) G.Don fil. – Strange onion, *Iris Notha* Bieb. – *Iris* (*Iris*) fake, *Gagea daghestanica* Levichev et Murtazaliev – Dagestan goose onion, *Elymus prokudinii* (Seredin) Tzvel. (*R. prokudinii* Serediri) - *Prokudin's* wheatgrass, *Festuca primae* E. Alexeev - *Prima's* fescue, *Stipa daghestanica* Grossh. - Dagestan feather grass, *Hedera pastuchovii* Woronow - *Pastukhov's* ivy, *Asarum ibericum* Stev. ex Ledeb. (*Asarum intermedium* (C.A. Mey.) Grossh.) - Georgian hoof, *Jurinea annae* Sosn. - *Anna's* headwort, *Psephellus kemulariae* Charadze (*C. kemulariae* (Charadze) Czer.) *eraria cardiocarpa* Trautv. – Heart-fruited *Sameraria*, *Campanula fedorovii* Charadze – *Fedorov's* bellflower, *Cerastium multiflorum* C.A. Meu. – Multiflorous sapling, *Ostrya carpinifolia* Scop. – Common hop hornbeam, *Sedum argunense* Galushko – *Argun* stonecrop, *Sedum stoloniferum* S.G. Gmel. – Stonecrop, *Scabiosa micrantha* Desf. – Small-flowered scabiosa, *Drosera rotundifolia* L. – Round-leaved sundew, *Arctostaphylos caucasica* Lipsch. (*A. iiva-nrsi* (L.) Spreng.) - *Caucasian* bearberry, *Tithymalus astrachanicus* (C.A. Mey.) Prokh. (*E. astrachanica* C.A. Mey. ex Prokh., *E. praecox* (Fisch. ex Boiss.) B. Fedtsch. et Fler.) - *Astrakhan* *Euphorbia*, *Asrtagalus cornutus* Pall. – Horn-bearing *Astracanthus*, *A. varius* S.G. Gmel. (*A. virgatus* Pall.) - *A. diverse*, *Onobrychis dielsii* (Sirj.) Vass. – *Diels* sainfoin, *Trigonella coerulescens* (Bieb.) Halacsy – Blue fenugreek, *Centaureum spicatum* (L.) Fritsch – Spike centaury, *Hypericum asperuloides* Czern. Ex Turkish. – *St. John's* wort, *Marrubium plumosum* C.A. May. – *Shandra* pinnate, *Satureja*

pachyphylla C.Koch – Thick-leaved savory, Scutellaria andina Charadze – Andean skullcap, S. leptostegia Juz. – Sh. small-scaled, Stachys fugax Pobed. – Falling chistet, Nitraria schoberi L. (N. caspia Willd.) – Schober’s saltpeter, Rapaver ocellatum Woronow – Eyed poppy, Lysimachia nummularia L. – Coined loosestrife, Anemonoides blanda (Schottet Kotschy) Holub (A. blanda Schottet Kotschy) – Pleasant anemonoides, Pulsatilla. andina (Rupr.) Woronow - Andean dream, Ranunculus tebulosica Prima - Tebulos buttercup, Alchemilla chlorosericea (Buuser) Juz. – Green silk cuff, Potentilla sterilis (L.) Garcke – Barren cinquefoil, Rosa tschatyrdagi Chrshan. – Chatyrdag wild rose, Asperula dasyantha Klok. – Pubescent woodruff, Galium mollugo L. – Soft bedstraw, Haplophyllum villosum (Bieb.) G. Don fil. – Soft-haired whole leaf, Saxifraga charadzae Otsch. – Saxifrage Kharadze, Scrophularia charadzae Kem.-Nath. – Norichnik Kharadze, Veronica charadzae Kem.-Nath. – Veronika Kharadze, Trapa hyrcana Woronow – Hyrcanian chilim

Very rare 23 species: Taxus baccata L. - Berry yew, Sternbergia colchiciflora Waldst. et Kit. – Colchicum sternbergia, Muscari armeniacum Leichtlin (Mszo vitsianum Baker) – Armenian mouse hyacinth, Cypripedium calceolus L. – Real slipper, Jurinea ingushetica Galushko – Ingush headwort, Rindera tetraspis Pall. – Rindera four-shielded, Dianthus arenarius L. – Sand carnation, Fumana procumbens (Dun.) Gren. et Godr. – Foumana recumbent, Scabiosa rotate Bieb. – Tithymalus szovitsii (Fisch. et C.A. Mey.) Klotzch et Garcke ex Klotzch (E. szovitsii Fasch. et C.A. Mev.) Melilotus wolgicus Poir. – Volga elecampane, Ononis pusilla L. – Little steelwort, Goniolimon besserianum (Schult.) Kusn. – Goniolimon Besser, Nymphaea alba L. – White water lily, Rapaver bracteatum Lindl. – Common poppy, Pyrola rotundifolia L. – Round-leaved wintergreen, Helleborus caucasicus A.Br. – Caucasian hellebore, Ranunculus auricomus L. – Golden buttercup, Potentilla alexeenkoi Lipsky – Alekseenko's Potentilla, P. ghalgana Juz. (P. oweriniana Boiss.) - Ingush L., P. orienthalis Juz. - L. eastern.

Table 2: Occurrence of relict and endemic species of the Chechen Republic

No	Occurrence	Number of species	% of total number of species
1.	Soc - dominates	1	0,58
2.	PL - usually	26	15,03
3.	Sp.- absently	66	38,15
4.	Raro - rare	57	32,95
5.	Rs. -very rarely	23	13,29

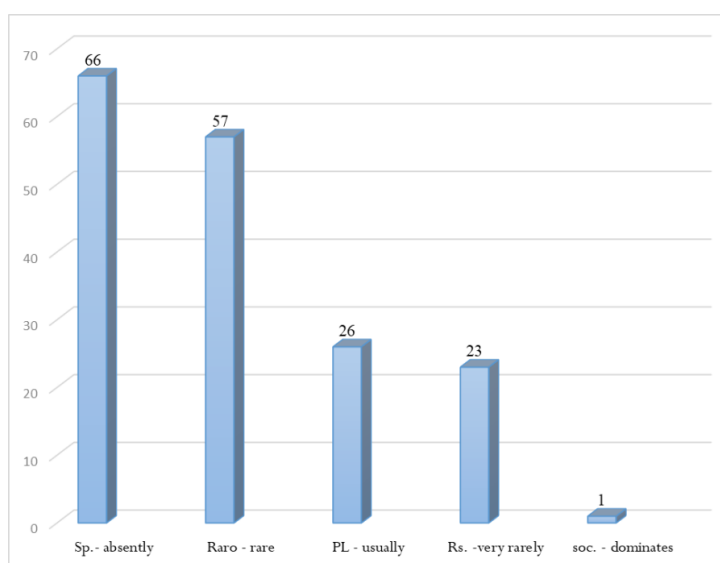


Fig. 2: Percentage distribution of species occurrence

Hemicryptophytes are represented by 112 (62.6%) species, cryptophytes - by 16 species (8.9%), terophytes by 14 species (7.8%), nanophanerophytes by 9 species (5.0%), mesophanerophytes by 4 species (2.2%), chamephytes are represented by 20 species (11.2%), megaphanerophytes and microphanerophytes by 2 species (1.1%). The largest number of species occurs scattered (66 species), 57 species are rare, 26 species are usually found, 23 species are very rare, 1 species dominates.

References

- [1] Alekhin V.V., Kudryashov L.V., Govorukhin V.S. Geography of plants with the basics of botany, 1944, p. 532
- [2] Ivanov A.L. Flora of Ciscaucasia and its genesis. Stavropol: SSU Publishing House, 1998, p. 204
- [3] Iriskhanova Z.I., Molochaeva L.G., Bakasheva Sh.M. Ecological and cenotic analysis and distribution of endemic and relict species of the Chechen Republic by floristic regions. Annual All-Russian Scientific and Practical Conference "Fundamental and Applied Problems of Biology and Chemistry" 2022. p.46-55
- [4] Iriskhanova Z.I., Molochaeva L.G. Systematic analysis, protection and occurrence of endemic and relict species of the Chechen Republic// Final scientific and practical conference of the faculty of FSBEI HE Chechen State University. A.A. Kadyrov". Grozny. 2023 . p.83-93
- [5] Umarov M.U., Taysumov M.A. Synopsis of the flora of the Chechen Republic. Grozny, 2011, p. 152
- [6] Yurtsev B.A., Kamelin R.V. Basic concepts and terms of floristry. Perm, 1991, p. 80
- [7] Raunkiaer C. The life forms of plants and statistical plant geography. - Oxford: Clarendon Press, 1934, p. 632

ENGINEERING ESTIMATION OF AIR REGIME OF BUILDING FACADE SYSTEMS WITH FIRE CUT OFFS

Samira Akbarova, Reyhan Akbarli

Azerbaijan University of Architecture and Construction

samira.akbarova@azmiu.edu.az

reyhan.akbarli@azmiu.edu.az

Abstract

The facade is one of the most important elements of the building in terms of its fire safety, as a fire leads to serious building damage and human casualties. The article considers the influence of fire cut-offs on the parameters of the airflow in the ventilated gap of the hinged facade system. An engineering estimation of solid and perforated horizontal fire cut-offs used in Azerbaijan is presented. As air exchange in the ventilated gap occurs in the thermo-gravitational mode, the features of the airflow movement in the gap are analyzed using the aerodynamic estimation method with the assumption that the gap is a single vertical air duct. Engineering estimation of the impact of cut-offs on the facade air regime is performed by the dependence on the coefficient of airflow velocity. It has been established that when using even a cut-off with a significant percentage of perforation it prevents necessary air exchange in the gap. A motivated justification is given for the need to use modernized cut-offs, which, during normal operation of the facade, do not interfere with the required air exchange in the gap, but in case of fire, cut-offs block the air movement in the gap and the ingress of burning drops of molten thermal insulation into the lower zones. The results of the engineering assessment can be used to further improve the regulatory framework for the design, installation, and reliable operation of facade systems with a ventilated air gap.

Keywords: hinged facade system, ventilated air gap, fire cut-off, coefficient of airflow velocity, engineering estimation, fire safety

I. Introduction

Every year, many natural disasters occur in various parts of the world, including earthquakes, causing significant social, economic, and energy damage to people. One of the potential and greatest dangers of earthquake consequences is the fire threat. In addition to earthquakes, the cause of fires in buildings and structures can be a violation of construction safety, the use of combustible building materials, and faulty structures [1].

Currently, hinged facade systems (HFS) with a ventilated air gap (VAG) are becoming increasingly popular in the construction of new and reconstruction of old buildings, which significantly increases the energy efficiency of the building [2]. In the modern construction industry, this facade system is also in demand due to its versatility and multi-functionality. In addition, these facades give the building an expressive exterior, they have improved thermal-shielding properties and normalize the heat and humidity regime of the building, which is achieved due to their design features [3]. Along with all the advantages, the main and most significant drawback of HFSs with VAG is their fire hazard [4], which was proved by resonant fires in Baku: 12-story residential building, near the Azadlig metro station, 2015 (Fig.1), and 9-story residential building on the Zykh highway in the Khatai district, 2017. Both buildings had HFS with VAG. The gap acted as an open chimney and allowed the fire quickly spread both vertically and

horizontally across the building's facade. It proves that the problem of preventing fire spread in the air gaps of the facade systems is relevant and it is of decisive importance for ensuring the safety of life and people activities.



Fig. 1: Facade system with a ventilated air gap of a residential building after a fire, Baku, next to Azadlig metro station, 2015

This study is devoted to the study of structural and technological solutions for fire prevention in buildings with VAG in HFS. The article discusses the influence of various types of horizontal fire cut-offs (FC) used in the facades on the parameters of the airflow in the gap. The negative impact of both solid and perforated cut-offs on the speed of air movement in the gap is evaluated and proved, as a result of which the heat and humidity characteristics of the facade deteriorate during normal operation and the expediency of using cut-offs as a fire protection measure is called into question [5]. Alternative design solutions are considered and proposed, in which the cut-off in the normal operation mode of the facade does not interfere with the movement of air in the gap, and in emergency situations blocks the movement of air in the gap, which helps to stop the fire.

II. Methods

Many researchers studied HFSs with VAG in terms of their fire safety [6]. Gagarin V.G. in their research works studied the thermo-physical properties and problems of HFSs from the point of view of the flow of aerodynamic processes in a ventilated gap in the event of a fire [7], studied the speed of air movement in the gap. The method for calculating wind loads on the facade of a building in emergency situations was given in [8,9]. Sparrow E.M. studied the phenomena of heat transfer, natural convection, and mass transfer in a gap, and conducted experiments to study the gap as a vertical air duct [10]. Gagarin et.al. substantiated the need to use fire cut-offs to comply with fire safety requirements, as well as to prevent the spread of combustion products in the event of fire [7]. Jensen G. in his work considered various European and American standards for testing HFSs for exposure to fire [11]. He also compared perforated and solid cut-offs based on the European test standard E2912-13. Pakhomov A.A. considered how the perforation degree of cut-off affects the thermo-gravitational flow during a fire and analyzed various variations of the facade design itself [12]. The full-scale tests of facades with realistic imitation of fire attacks and evaluated the fire resistance of cut-offs are shown in the article of [13].

Despite a significant number of studies on this topic, there is still no research containing an objective assessment of the effect of fire cut-offs on the air movement in the HFSs with VAG and the corresponding engineering assessment [14]. There is also great potential for the development of structural and engineering proposals to improve the design of fire cut-offs in order to minimize their negative impact on the airflow parameters during normal operation and reliable operation in the case of a fire.

III. Design features of the HFSs

The fire safety of HFSs is largely determined both by the properties of materials of construction structures, their combustibility, and the fire resistance and by the corresponding engineering and design solutions in accordance with the requirements of construction codes [15]. Engineering and design solutions include the installation of fire-prevention vertical and horizontal cut-offs, fire arresters, installation of fire-prevention windows and door protective boxes, etc. Design of HFSs (Figure 2a). includes a layer of thermal insulation with a hydro-windproof membrane and facing material, which are attached to the main masonry of the enclosing wall using special substructure elements: brackets and guides (Fig.2a). There is an air gap between the cladding panel and the thermal insulation [16]. In order to ensure the fire safety of the facade, horizontal fire cut-offs are attached in the gap (Fig.2b, 7).

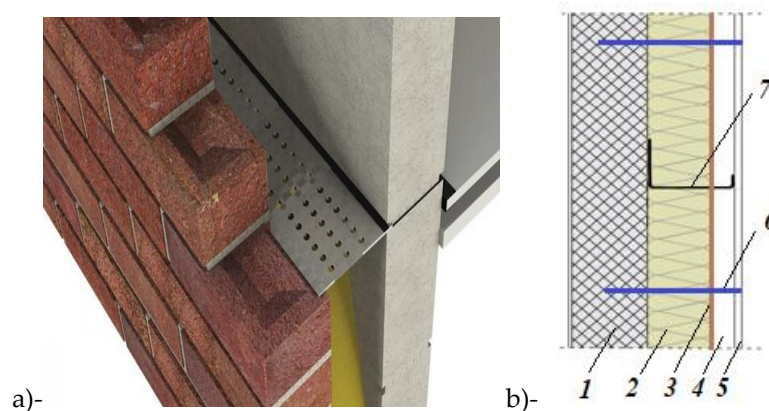


Fig. 2: a - General view of the HFS with a fire cut-off.

b - scheme of the vertical cross-section of the HFS structure with a cut-off:

1 - main masonry, 2 - heat-insulating layer, 3 - hydro-windproof membrane, 4 - air gap, 5 - cladding panel, 6 - fastening bracket, 7 - fire cut-off

The cut-off is a metal plate made of thin sheet steel with a thickness of at least 0.6 mm and a length of at least 6 m. The cut-off is set with a given specific step along the building height and it divides the wall into zones. According to the current fire safety requirements for buildings, the distance between the cut-offs should not exceed 6 meters. The cut-offs are mounted directly to the wall around the entire perimeter of the building. In the event of a fire, cut-offs on the façade prevent the spread of flames inside the gap and the ingress of burning drops of molten thermal insulation into the lower zones. Cut-offs may be perforated or without perforation- solid. The perforation of the cut-offs should provide the necessary air circulation inside the gap and meet the requirements for the heat and humidity state of the HFS. When designing and applying a fire cut-off, it is necessary to take into account the fact that the cut-off cannot completely block the movement of air in the gap, therefore, it is necessary to leave a gap between the facing material and the cut-off, or the cut-off must be perforated. But even taking into account perforation, the cutoff significantly affects the parameters of air exchange in the gap, and therefore its presence must be taken into account when calculating the fire protection of the HFSs.

IV. Estimation of effect of cut-off on airflow velocity in a ventilated gap

The object of field research is the HSF of the educational building of the Azerbaijan University of Architecture and Construction (Figure 3) located in the most weathered part of Baku, i.e. the building is operated in conditions of significant and prolonged wind effects. The average annual

wind speed is 11-16 m/s in the building's location. The building facade has 55 m high, is lined with smooth composite panels measuring 1800x700mm, there is also a steel frame substructure for fixing the facing panels and a ventilated gap with a wide of approximately 120mm. The facing panels has entry and exit slots with almost equal sizes at the base and top of the facade for ventilation of the air gap, the seal between the plates is tight and hermetic. Only the northern facade of the building has perforated cut-offs in the gap at the level of the ceilings on even-numbered floors [17].



Fig. 3: Northern facade of the educational building of the Azerbaijan University of Architecture and Construction

As the air in the gap of the facade has a non-uniform temperature and density, here the process of thermo-gravitational convection takes place. In this case, it is suitable to use aerodynamic calculation methods for an engineering assessment of the air flow parameters in the gap. Engineering assessment of the effect of cut-offs on the HFS's air regime is performed according to the main dependence [18] where the average speed of thermo-gravitational air movement in the vertical air gap is determined by the formula:

$$v = \varphi \cdot \sqrt{2 \cdot g \cdot L \cdot \left(1 - \frac{T_c}{T_h}\right)} \quad (1)$$

g - acceleration of gravity;

L - height of the ventilated gap;

T_c - temperature of the inner surface of the facing panels;

T_h - temperature of the outer surface of the windproof membrane or heat-insulating layer;

φ – coefficient of airflow velocity in the gap:

$$\varphi = \frac{1}{\sqrt{\xi + \lambda \frac{L}{h} + 1}} \quad (2)$$

λ - friction coefficient in the gap;

h - initial width of the gap;

ξ - coefficient of local pressure losses resulting from the use of cut-offs;

$$\xi \approx \left(\frac{h}{\delta}\right)^4 \quad (3)$$

δ - width of the flow constriction (Fig.4).

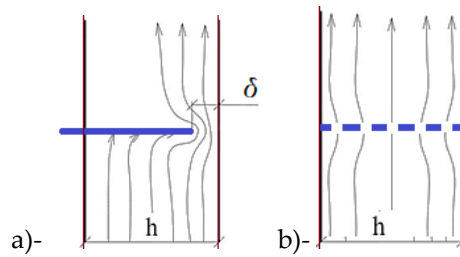


Fig. 4: Diagram of the airflow movement in the gap with: a) - solid cut-off, b) - perforated cut-off

Three different cases of HFS with VAG are considered:

1. there is no cut-off in the gap;
2. the cutoff is solid;
3. the cutoff is perforated.

Case 1 - there is no cut-off in the gap. According to formula (2), coefficient of the airflow velocity is:

$$\varphi_1 = \frac{1}{\sqrt{\xi + \lambda \frac{L}{h} + 1}} = \frac{1}{\sqrt{1 + 0.035 \frac{55}{0.12} + 1}} = 0.24 \quad (4)$$

h – width of the gap, $h = 0.12$ m;

L – height of the gap, $L = 55$ m;

λ – friction coefficient in the gap, $\lambda = 0.035$.

When there is no the cut-off in the gap coefficient of local pressure losses is:

$$\xi \approx \left(\frac{h}{\delta}\right)^4 = \left(\frac{120}{120}\right)^4 = 1 \quad (5)$$

Case 2 - the cutoff is solid and does not reach the edge of the vertical cladding panel by 24 mm (Figure 4a). Then the coefficient of local pressure losses is (Fig.4a):

$$\xi \approx \left(\frac{h}{\delta}\right)^4 = \left(\frac{120}{24}\right)^4 = 625 \quad (6)$$

δ - width of the flow constriction, $\delta = 24$ mm.

For this case, according to formula (2), the coefficient of airflow velocity in the gap is:

$$\varphi_2 = \frac{1}{\sqrt{625 + 0.035 \frac{55}{0.12} + 1}} = 0.04 \quad (7)$$

$$\frac{\varphi_1}{\varphi_2} = 7 \quad (8)$$

When there is a solid cut-off, the coefficient of airflow velocity is decreased by seven times.

Case 3 - there is perforated cut-off in the gap (Fig.4b), δ - flow constriction width, $\delta = 30$ mm.

Coefficient of local pressure losses is:

$$\xi \approx \left(\frac{120}{30}\right)^4 = 256 \quad (9)$$

$$\varphi_3 = \frac{1}{\sqrt{256 + 0.035 \frac{55}{0.12} + 1}} = 0.06 \quad (10)$$

$$\frac{\varphi_1}{\varphi_3} = 4 \quad (11)$$

In this case, the coefficient of airflow velocity is decreased by four times

V. Results

The above engineering calculation shows that setting any cut-off sharply reduces the airflow velocity in the gap:

- without any cut-off, the coefficient of airflow velocity is 0.24;
- with a solid cut-off, coefficient of airflow velocity is decreased by 7 times;
- with a perforated cut-off, coefficient of airflow velocity is decreased by 4 times.

All values are shown in Table 1.

As a result of the engineering calculation, it was found that when using even a perforated cut-off with a significant percentage of perforation, the role of the air gap is reduced to zero, because the facade stops working as ventilated. When using a continuous cut-off, even with a relatively small width of the flow constriction $\delta = 30\text{-}50$ mm, the air flow velocity drops to almost zero, air movement in the gap occurs. On the one hand, this means that the cut-off really works as a means of preventing the spread of flame along the facade during a fire, but, on the other hand, it interferes with the normal air convection inside the facade during operation. It can be concluded that the necessary solution to the problem is the use of such a cut-off design that would work only during an emergency- a fire, and the rest of the time would not interfere with the required air exchange of the gap.

VI. Discussion

Protecting the HFS from the fire spread in the gap is a complex problem since today in Azerbaijan there are no strictly standardized structural and engineering measures to prevent and minimize the impact of fires, and there are no test standards for selecting appropriate fire protection measures for building facade systems. Protection is achieved through the installation of fire cut-offs that limit the fire spread through the ventilated air gap by reducing the free cross-section or completely blocking the gap. In the world practice of ensuring the fire safety of buildings with HFS, only stationary cut-offs are used. However, as the practice of their use shows, cut-offs interfere with the operation of the facade under normal operating conditions. Ways to improve the cut-off's design involve the free flow of air under operating conditions and the prevention of air movement due to cut-off during an emergency- a fire. The designs of these types of cut-offs are shown in Fig.5.

According to the cut-off design in Figure 5a, during a fire the polyamide plastic thread 6 burns out, and the spring 4 pushes the cut-off 90°, bringing it to a horizontal position and stopping the movement of the airflow, i.e. the access of the fire to other zones is blocked, which leads to its non-distribution and subsequent termination.

Figure 5b,c show a schematic representation of the modernized cut-off made of intumescent material that expands at high temperatures and closes the cross-section of the ventilated gap, providing fire resistance up to 120 minutes [19]: 1- before expanding, 2- after expanding, 3- steel mesh with an intumescent fire barrier.

As can be seen from the scheme, the new cut-off design works only during an emergency- in case of fire. In the normal operation time, the cut-off is in a vertical position and creates only negligible losses in the airflow velocity at local resistances and does not interfere with the movement of air in the gap. This improved design differs from the analogs by the vertical location of the cut-off [20, 21].

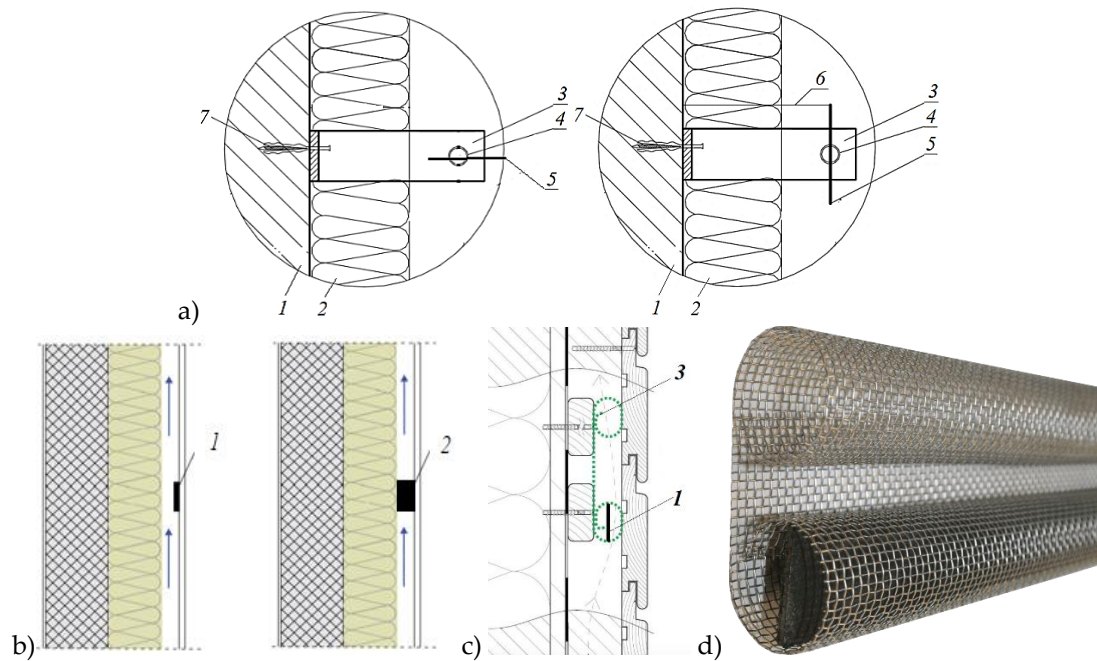


Fig. 5: Schemes of HFS with an improved fire cut-offs:

a- with polyamide thread:

1-wall; 2- insulation; 3 - fastening, 4 - torsion spring, 5 - fire cut-off,

6- polyamide plastic thread, 7- dowel-anchor

b,c - with intumescent material:

1- intumescent strip before expanding, 2- intumescent strip after expanding, 3-steel mesh

d- photo of steel mesh with intumescent strip

The coefficient of the airflow velocity in the gap for improved designs of cut-offs is shown in Table 1.

Table 1: Dependence of the coefficient of airflow velocity φ on the design solution of the ventilated facade

Constructive decisions of the HFS	coefficient of airflow velocity φ
Without cut-off	0.24
Without perforation a continuous cut-off	0.04
With a perforated cut-off	0.06
With modernized cut-off in normal operation regime	0.24
With modernized cut-off in case of fire	0

VII. Conclusions

The facade is one of the most important elements of a building in terms of its fire safety, especially when, in the event of a fire, its inadequate fire protection leads to the spread of fire, serious damage to the building, and loss of life. Examples of fires in residential buildings with hinged facade systems in Baku demonstrated how vulnerable modern facades could be to fires, which directly affected people's safety.

The article considers the influence of the horizontal fire cut-off on the parameters of the airflow in the HFS with a ventilated air gap. An engineering assessment of the applied types of cut-offs is given. Since the movement of air in the gap occurs in the thermo-gravitational mode, to analyze the features of the movement of the airflow, the coefficient of airflow velocity is used, which has different values for different types of cut-offs. Quantification of the airflow movement in the gap shows the negative impact of fire cut-offs on the required air exchange in the gap and a

decrease in the coefficient of airflow velocity by four times (equation 11) and seven times (equation 8), depending on the cut-off configuration. The requirement for natural ventilation of the facade and the requirement for its fire protection contradict each other. Improved designs of cut-offs are considered, which act as intended only during the onset of a fire, and during normal operation do not interfere with the necessary air exchange of the structure. The introduction of an improved design cut-off is a solution to the problem of ensuring air exchange of the gap and shutting off the air supply to the place of ignition in case of fire, as evidenced by the coefficients of airflow velocity, which are given in Table. 1. Assessments of the coefficient of airflow velocity in the gap of the HFS and analysis of the studied works allow us to substantiate the need for a new design solution in relation to fire safety in the structures of the HFS with VAG.

The practice has shown that the only reliable way to prove the effectiveness of cut-offs in preventing the fire spread in such complicated systems is to conduct extensive tests of facades [22]. Unfortunately, it is not recognized by current local legislation. The results of the engineering assessment can be used to further improve the regulatory framework for the design, installation, and long-term operation of HFS with VAG, for computational-experimental control during an energy audit of a building.

References

- [1] Sparrow, E.M., Ruiz, R., Azevedo, L.F. (2008), "Experimental and numerical investigation of natural convection in convergent vertical channels". *International Journal of Heat and Mass Transfer*. No. 31. pp. 907-915.
- [2] Samar, E.Y., Onokhov, O.V., Holupova A.P. (2013), Fire safety study of buildings shed-governmental facades. *Far East: Problems Of Architectural Complex*, No. 1, pp. 357-362.
- [3] Lamkin, O.B., Gravit, M.V., Nedryshkin O.V. (2015), "Experimental and theoretical studies of fire hazard indicators", *Tekhnokom facade system*, No. 11 (38), pp. 49-65.
- [4] Meshalkin, E.A. (2011), Fire safety of hinged ventilated facades, *Fire safety in construction*, No. 3, pp. 40-47.
- [5] Molchadsky, I.S., Siegern-Korn, V.N. (2018), Facade thermal insulation systems. Features of the fire hazard of hinged systems with an air gap, *Fire safety*, No. 2, pp. 56-60.
- [6] Khasanov, I.R., Molchadsky, I.S., Goltskov, K.N., Pestritsky, A.V. (2016), "Fire danger of hinged facade systems", *Fire safety*, No. 5, p. 36-47.
- [7] Gagarin, V.G., Kozlov, V.V., Guvernyuk, S.V., Ledenev, P.V., Tsykanovskiy, E.Y. (2010), "Aerothermal physics of permeable bodies in low-velocity air flows". *Academia. Architecture and construction*. 2010. No. 3, pp. 261-278.
- [8] Gagarin, V.G., Kozlov, V.V., Lushin, K.I., Pastushkov, P.P. (2013), "On the use of wind and hydroprotective membranes in hinged facade systems with a ventilated air layer", *Scientific and technical bulletin*, No. 3, p. 120-122.
- [9] Gagarin, V.G., Kozlov, V.V. (2015), "Velocity of air movement in the interlayer of the hinged facade system with natural ventilation", *Dwelling construction MGSU*, No. 10, P. 14-17.
- [10] Sparrow, E.M., Ruiz, R., Azevedo, L.F. (2008), "Experimental and numerical investigation of natural convection in convergent vertical channels". *International Journal of Heat and Mass Transfer*. No. 31. pp. 907-915.
- [11] Jensen, G. (2013), "Fire spread modes and performance of fire stops in vented facade constructions – overview and standardization of test methods", *Matec web of conference*, pp. 1-11.
- [12] Pakhomov, A.A. (2023), Influence of fire cut-offs on air exchange in a ventilated façade. [Electronic resource]. URL: <http://vfasade.blogspot.ru/2014/01/otsechki-v-ventfasade.html> (date of access: 04/01/2023).
- [13] Ostman, B., Mikkola, E. (2018), Guidance on Fire Safety of Bio-Based Facades, *COST Action FP1404*, p.41.
- [14] Vatin, N.I., Petrichenko, M.R., Nemova, D.V. (2014), "Hydraulic methods for calculating

- the system of ventilated facades”, *Applied Mechanics and Materials*, No. 633-644, pp. 1007-1012.
- [15] Kosachev, A.A. (2012), “Analysis of the fire hazard of hinged facade systems in reconstructed buildings”, *Fire and explosion safety*, No. 11 (21), pp. 77-80.
- [16] Kosachev, A.A., Korolchenko, A.Ya. (2011), “Fire danger of hinged facade systems”, *Fire safety in construction*, No. 4, p. 30-32.
- [17] Smirnov, I.A., Shesterova E. V., Nemova D. V., Petrichenko M. R. (2015), Objective estimation of the use of windproof and weatherproof membranes in double skin facades. *Applied Mechanics and Materials*. No. 725-726, pp. 130-137.
- [18] Mammadova, G.H., Akbarova, S.M. (2021). “Experimental study of air cavity thermal performance of opaque ventilated facades under extreme wind conditions: case study Baku”, *Informes De La Construcción*, 73(561), e376.
- [19] “Recommendations for the design of hinged facade systems with a ventilated air gap for new construction and renovation of buildings”, (2012), 159p.
- [20] Sapegina, E.A. (2019), “Energy efficiency of a hinged facade system with an air ventilated gap”. *Technology, organization and economics of construction*, No 177, pp.136-145.
- [21] Nemova, D.V. (2012), “Energy efficient technologies in enclosing structures”, *Construction of unique buildings and structures*, No 3, pp. 77-82.
- [22] Didem, G.Y. (2022), “Fire safety of tall buildings: approach in design and prevention”, 5th International Conference of Contemporary Affairs in Architecture and Urbanism (ICCAUA, Turkey), pp. 206-216.

PROSPECTS FOR AZERBAIJAN'S PARTICIPATION IN THE DIVERSIFICATION OF ENERGY SOURCES AND REDUCING THE RISKS OF ENERGY SUPPLY FAILURE TO EUROPE

Eldar Gasumov¹, Ramiz Gasumov², Gazanfar Suleymanov³, Khalig Kurbanov³

¹Azerbaijan State University of Oil and Industry, Azerbaijan

²North Caucasus Federal University, Russia

³Azerbaijan Technical University

E.gasumov@gmail.com

r.gasumov@yandex.ru

suleymanov.q.s@gmail.com

Abstract

The article considers the prospects for Azerbaijan's participation in the diversification of energy supplies to the European market, in the conditions of the energy crisis due to the difficult geopolitical situation in the world. Possible ways to reduce the serious risks of failures in the supply of energy resources while ensuring the energy security of the countries of the European continent are given. The negative impact of the crisis that has arisen in the energy market on the global energy supply chain to the EU countries and on the state of the world economy is analyzed. Steps taken by the EU to radically increase supply via traditional EU import routes as well as completely new sources of energy are examined. Various measures implemented by European countries to ensure their own energy security, including the diversification of the supply of energy resources used to generate energy, including through non-renewable mineral substances, renewable organic resources and a number of natural processes, are considered. The ongoing measures in connection with the energy crisis have been considered in order to reduce the negative consequences for the economies of the EU countries. The high potential of Azerbaijan is noted as a country rich in energy resources, and having all the necessary opportunities to influence the state of the gas market in Europe and diversify energy resources in the EU countries by expanding the export of Azerbaijani gas.

Keywords: diversification, export, pipeline, energy resources, RES, natural gas, risks, energy carriers

I. Introduction

Due to the difficult geopolitical situation in the world, the logistics of energy supplies, including natural gas supplies to the European continent, have changed dramatically, and the issue of diversifying energy resources to European markets has become of particular importance. The energy security of the countries of the European continent depends on the reliability of energy supplies on a sustainable and timely basis. Under the conditions of the energy crisis, there are serious risks of disruptions in the supply of energy resources, and effective steps are required to reduce them. Exchange prices for energy resources in the world are not stable with an upward trend, and the price of electricity has increased because of an increase in the cost of energy carriers – against the backdrop of an accelerated recovery of the global economy after the pandemic and due to the geopolitical crisis.

The energy crisis has disrupted global energy supply chains and weakened the global economy. For the European continent, which is heavily dependent on Russian energy resources, gas in particular, there is an urgent need to look for alternative suppliers of “blue fuel” and develop other sources of energy resources. At the same time, European markets have considerable flexibility, and market regulators are making significant efforts to prevent unreasonable price increases and reduce price pressure on end consumers. Due to the possible shortage of energy resources, even the EU countries are planning to conduct one-day anti-crisis exercises (stress test) in the field of gas supply in order to test the energy sustainability of industrial enterprises and sectors of the economy. An important goal of which is to develop internal processes for the distribution of energy load, as well as detailed planning, including the compilation of a list of potential participants.

Among the measures taken by the EU, the priorities are: refusal of long-term contracts for the supply of natural gas and its replacement with fuel from “alternative suppliers”; accelerated filling of underground storage facilities; promoting the development of renewable energy sources (RES); increasing the energy efficiency of production, including reducing the heating temperature of buildings by 1°C. However, the implementation of these measures requires a lot of time and investments, which are not always economically feasible and technologically realizable. Despite all this, Europe remains an important part of the emerging global gas market, but at the same time, its role as a significant buyer of energy resources is gradually decreasing [1, 2].

European states are considering various countries to ensure their energy security, including the Republic of Azerbaijan as a reliable supplier of energy carriers. Azerbaijan confirmed the status of a reliable partner during the peak of the energy crisis in the EU countries in 2022. In this connection, the study of the issue of Azerbaijan's participation in the diversification of energy sources and reducing the risks of failures in the supply of energy resources to ensure the energy security of the continent is an urgent task [3].

II. Methods

In the course of the study, the analytical method and comparison method were used. Methods for collecting, processing and analyzing information were determined by the specific objectives of the study based on a systematic approach.

III. Results and Discussion

World energy consumption is increasing by more than 2% annually, which accelerates the growth of oil, gas, coal and nuclear energy production. Emerging market countries accounted for 80% of the global increase in energy consumption, even though the growth in these countries was below average. The countries of the European continent are taking various measures to ensure their own energy security (ES), including the diversification of the supply of energy resources used primarily for generating electricity and in the fuel industry (Fig. 1).

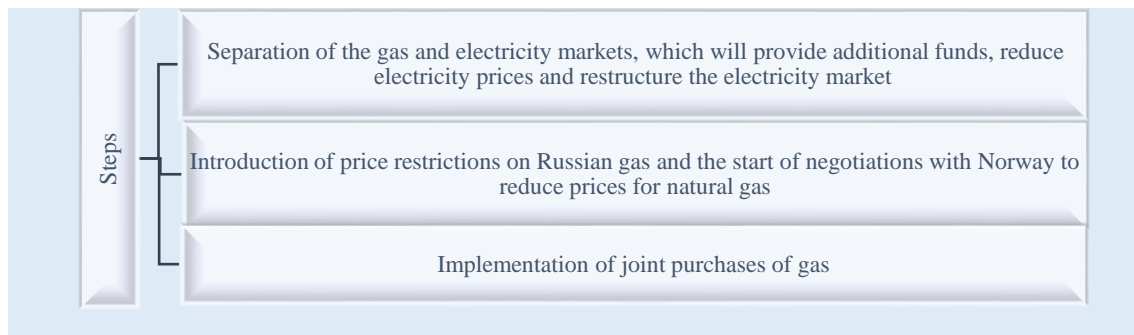


Fig. 1: EU steps to mitigate the effects of the energy crisis

Energy security for a country is defined as a way to ensure a guaranteed supply of energy resources on a sustainable and timely basis that does not negatively affect economic performance, an important aspect of which is the ability to insure against potential risks and provide adequate access to energy sources to maintain an acceptable level of social and economic well-being of states. To reduce the risks of disruptions in the supply of energy resources in Europe, taking into account the current crisis in the energy market, it is necessary to diversify the structure of energy consumption, which is a strategic task, and is aimed at strengthening both the economic and political security of the countries of the continent. When providing ES, serious risks are possible, which should be taken into account when planning (Fig. 2) [3, 4].

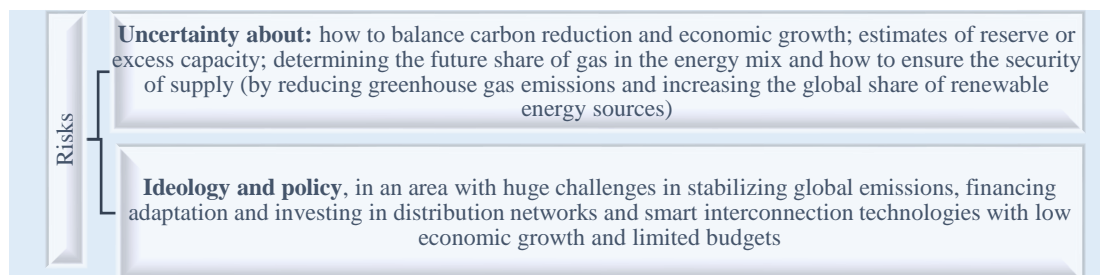


Fig. 2: Energy security risks

The European Union is considering all possible directions for obtaining energy from various sources, including non-renewable minerals, renewable organic resources and a number of natural processes (the energy of flowing water, wind, tides, etc.) (Fig. 3).

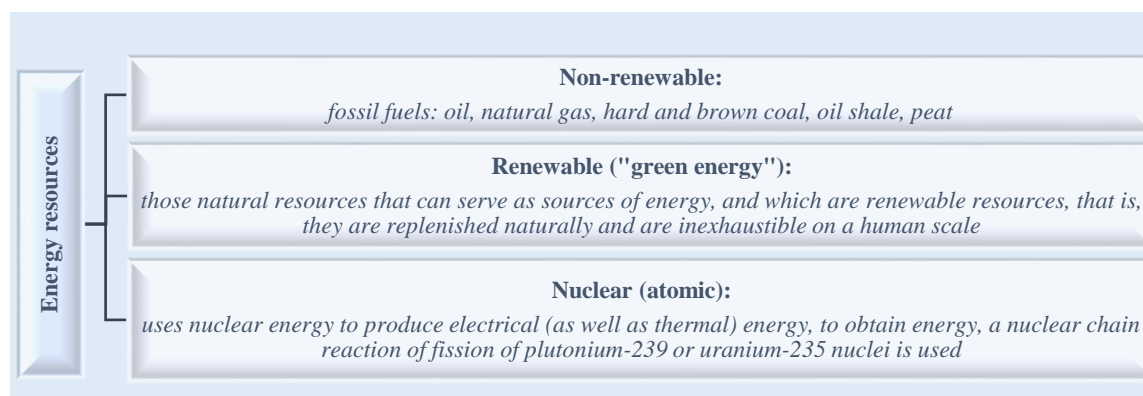


Fig. 3: Types of energy resources

Non-renewable energy resources include all types of fossil fuels, the world's proven and final (estimated) reserves in terms of standard fuel are coal up to 60%, oil and gas – 27%, the rest others. According to the forecasts of the American agency "Energy Information Administration", the share of fossil fuels by 2040 will decrease to only 78%, while energy consumption will increase by 56%. This is due to such global problems of modern civilization as the depletion of non-renewable energy resources, environmental pollution and global warming [8, 9]. Before the energy crisis, the main share of energy imports to Europe was Russian exports (Table 1).

The events of the last few years have seriously worsened the state of the world energy market. There were serious risks associated with a failure in the supply of energy resources to the European market, which created a threat to the energy security of the countries of the continent. This was facilitated by the geopolitical crisis and the EU policy in the field of energy use. The widespread development of renewable energy sources (RES) to the detriment of traditional energy sources has led to the fact that the underinvestment of the global oil and gas industry has reached 200-300 billion dollars. However, many companies have already begun to realize the fallacy of the chosen strategy. Recently, Shell announced its intention to increase investment in oil production,

as there are profits in this business: prices are high, reserves are depleted and, despite the prospect of an economic crisis, demand remains growing. However, this does not mean that the development of "green" energy is removed from the agenda, on the contrary, the issue of reducing the impact on nature and climate is still relevant.

Table 1: Main energy importers in the EU (2021)

No	Energy carriers, importers	Share, %
1	<u>Natural gas</u>	
	Russia	45
	Norway	23
	Algeria	12
	USA	6
	Qatar	5
2	<u>Raw oil</u>	
	Russia	27
	Norway	8
	Kazakhstan	8
	USA	8
3	<u>Coal</u>	
	Russia	46
	USA	15
	Australia	13

Due to the reduction in the export of Russian energy resources, countries of the European continent are looking for new suppliers to meet their needs. In the coming years, the EU expects to find a replacement for almost 100 billion cubic meters of natural gas to replace the Russian gas. Europe is attempting to drastically increase supplies via traditional European Union (EU) import routes as well as entirely new energy sources. Currently, pipeline gas is supplied to the EU from Russia, Norway, Azerbaijan, through Turkey via the Trans-Adriatic Gas Pipeline (TAP), as well as from Algeria and Libya via the Maghreb-Europe Gas Pipeline (MEG). The export of Russian gas to Europe is rapidly declining, and the main volume of Russian gas in 2022 was supplied to Europe via two routes: through Ukraine in the amount of about 42.0 million cubic meters per day and through the Nord Stream-1 Gas Pipeline in the amount of 67.0 million cubic meters per day (at the moment, supplies have been stopped), and the rest of the routes – gas pipelines – are not in operation for various reasons [10-12].

The share of Russian gas in European imports in 2022 fell to 32.7%, while its share in total consumption fell to 21%. In addition, gas exports to Europe via pipelines have almost halved to 85.4 billion cubic meters and at the same time liquefied natural gas (LNG) supplies increased by 12% to 19.5 billion cubic meters. At the same time, gas consumption in European countries decreased in 2022 by 12.7% compared to 2021 to 498.8 billion cubic meters.

Europe is seeking to diversify its energy supplies, and evidence suggests that the UK is an import hub for LNG, which then transports natural gas through pipelines to European countries. Britain's fuel exports increased by £500 million a month on gas and crude oil supplies to the Netherlands and Ireland. This indicates an increased demand on the continent to fill gas storage facilities (UGS) in anticipation of winter [1, 13].

Research shows that in 2023 the volume of capacities newly introduced to the LNG market is one of the lowest on record. At the same time, according to the Forum of Gas Exporting Countries, the volume of LNG imports to European countries (the EU and the UK) this year for the first time in history exceeded the volume of pipeline gas supplies. On the other hand, the crisis in the energy market forced the Europeans to improve energy efficiency. The International Energy Agency (IEA) estimates that in 2022 the world economy was using energy 2% more efficiently than in 2021: the rate of improvement is almost 4 times faster than in the last two years, and almost twice as fast as

over the past five years. At the same time, in order to achieve carbon neutrality by 2050, the increase in energy efficiency should average about 4% per year for a decade.

Since the beginning of 2022, there has been a reduction in gas generation in Europe, in favor of renewable and nuclear energy, and the generation of electricity from gas has decreased. A more important role in these processes was played by the implementation of the plan of the European Commission (EC), according to which the EU countries in the period from 08/01/2022 to 03/31/2023 reduced gas consumption by 15% compared to the average level of the previous five years. At the same time, gas reserves in underground storage facilities are at a relatively high level of more than 78%, while a year earlier – only by 38%.

There is also a reduction in coal generation, electricity generation from coal in the EU decreased by more than 2%, which was affected by the conscious saving of solid fuel, due to the restoration of nuclear generation, which tends to grow compared to last year.

According to the International Renewable Energy Agency (IRENA), in 2022-2027, the volume of renewable energy in the world will grow by 75%, or by 2,400 gigawatts (GW). IRENA has raised its global renewable energy growth forecast by 30% compared to 2021, and over the next five years, wind and solar power will be the main sources (more than 90%) of renewable energy generation. According to the EC plans, by the beginning of 2025, RES will overtake coal-fired thermal power plants (TPPs) and become the largest source of electricity in the world. By 2027, the installed capacity of wind power plants (WPP) will almost double (electricity generation by 570 GW), and solar power plants (SPP) will triple (by 1500 GW) [9-11].

In 2020, electricity production from renewable energy in Europe overtook fossil fuels for the first time, and green generation provided 38.2% of all electricity generation in the EU, against 37% generated by coal and gas stations. RES are gradually replacing coal and nuclear power plants (NPPs) from European generation. In particular, in Germany in 2022, RES will account for 49% of the energy consumed in the country, which is 6% more than last year [10, 14-16].

Recovery of generation is also typical for hydroelectric power plants (HPPs). The dynamics of wind and solar generation was multidirectional. At the same time, for the year as a whole, both generation segments will show an increase due to the loading of new capacities: according to Wind Europe, the EU countries put into operation 15 GW of wind generators in 2022, that is, a third more than a year earlier; in turn, the commissioning of solar power plants has accelerated according to the estimates of Solar Power Europe (Table 2).

Table 2: *Energy generation from different segments*

No	Working out	Dynamics	Indicators, %
1	Biomass production	increased	for 1
2	Fuel oil and diesel fuel	decreased	for 12
3	Share of the segment in the generation structure		
	- natural gas	decreased	from 21.2 to 15.3
	- nuclear power plants (NPP)	decreased	from 24.9 to 24.2
	- solar power plants (SPP)	increased	from 2.4 to 2.6
	- wind power plants (WPP)	increased	from 18.3 to 21.6
	- coal-fired thermal power plants (TPP)	increased	from 16.1 to 17.0
	- hydroelectric power plants (HPP)	increased	from 9.9 to 11.9

Globally, electricity generation from all fuels, excluding oil, gas, nuclear and renewables, has grown at below-average rates, with the exception of North America.

According to the forecast of British Petroleum (BP), global demand for energy resources will grow by 30% by 2035; the increase will be caused primarily by the growth of prosperity in developing countries, but at the same time will be significantly less than the growth of world GDP due to improved energy efficiency. According to forecasts, energy consumption in the world until 2035 will be multidirectional, and will primarily depend on China's transition to cleaner fuels (Table 3). As a result, the share of gas in the global energy sector will overtake the share of coal [9, 17, 18].

In recent decades, the EU has pursued a policy of expanding the number of alternative sources, despite the negative impact of high-energy prices, has not changed its position in the energy sector, including natural gas. In connection with the latest developments in the energy market, the EU supported new routes for gas supplies to its market. Azerbaijan has become one of the reliable suppliers of energy resources to European markets. The demand for energy resources in the European market is still high, which stimulates many producing countries to increase their exports to the EU countries. The Azerbaijan Republic became an active participant in these global processes, according to the results of 2021, the export of electricity from Azerbaijan increased by 522.7 million kWh, or 45.4% compared to 2020, and amounted to 1673.4 million kWh. At the same time, the share of RES in the country's power generation structure is continuously increasing.

The Azerbaijan Republic implements energy export projects in the following areas: crude oil; natural gas; electricity and RES. The export of energy resources from the AR in 2022 had an upward trend (Table 4).

Table 3: Forecast of energy consumption in the world until 2035

No No	Energy resources	Growth "+", decline "-", %
1	Oil	+ 0,7
2	Natural gas	+ 1,6
3	Coal	- 2,0

Table 4: Export of energy resources from the Azerbaijan (2022)

No No	Energy resources	Production (%)	Export
1	Oil, million tons	32,6 (80,7)	26,3
2	Natural gas, billion cubic meters including	46,7 (47,7)	22,3
	- Europe		11,4
	- Turkey		8,4
	- Georgia		2,5
3	Electricity, billion kWh		3,0

In 2020, the SGC project was implemented to transport Azerbaijani gas to Italy and Greece. Azerbaijan began supplying gas to Europe via SGC on December 31, 2020, and already in 2021, 10 billion cubic meters of natural gas were supplied to the European market, with a future achievement (including Turkey) of up to 30.0 billion cubic meters. cubic meters per year. The capacity of the gas pipeline is 10 billion cubic meters with the possibility of expanding to 20 billion cubic meters. In July 2022, Azerbaijan and the EU signed a memorandum of understanding that provides for doubling the capacity of the Southern Gas Corridor by 2027.

In 2022, gas exports from the Republic of Azerbaijan increased by 18%; production by 6.5%, and through the Trans-Anatolian Gas Pipeline (TANAP) from the Republic of Azerbaijan to Turkey, the supply amounted to 5.6 billion cubic meters of gas. Oil produced in the "Azəri-Çıraq-Günəşli" (AÇG) group of fields, as well as from Turkmenistan and Kazakhstan, condensate produced in the "Şahdəniz" field are transported through the Baku-Tbilisi-Ceyhan pipeline (South Caucasus pipeline, SCP).

Since the start of commercial operation, the Trans Adriatic Pipeline (TAP) has safely transported 25 billion cubic meters of natural gas to Greece, Bulgaria and Italy. The TAP project is a reliable energy carrier with a capacity of 12 billion cubic meters of gas per year and can be expanded in stages to further improve the energy security of Europe. Gas exports to Europe via TAP began at the end of 2020 and are designed for 25 years, and the volume will exceed 10 billion cubic meters per year. In accordance with the agreement signed between Azerbaijan and the European Union, gas transportation to Europe will be increased to 20 billion cubic meters in the next 5 years.

At present, the capacity of the Trans Adriatic Gas Pipeline (TAP), the European part of the "Southern Gas Corridor" ("SGC", the continuation of the TANAP pipeline to Europe), is 12 billion cubic meters of gas per year. The total length of the TAP pipeline is 878 km, of which 550 km run through northern Greece, 215 km through Albania, 105 km under the Adriatic Sea and 8 km through Italy. The consumers of Azeri gas through TAP are Italy, Greece and Bulgaria, as well as Hungary and Romania in the near future.

In general, Azerbaijani gas may have an impact on the state of the gas market in Europe and on the diversification of energy carriers in the EU countries. The European Union expects that potentially Azerbaijani gas can play an important role in ensuring energy security of supplies and diversifying energy sources in the region of Central and Eastern Europe.

There are potential opportunities to expand gas exports under the SGC project by increasing the capacity of the gas pipeline. In addition to the diversification of energy sources, the EU has proposed a set of measures aimed at creating a trans-border gas supply infrastructure. These measures and the support of new sources of gas production expanded the geography of imports, made it possible to put pressure on the Russian side, but did not lead to a fundamentally different alignment of forces in the European gas market. The countries of the Caspian region, the Middle East and North Africa are also planning to take advantage of EU diversification plans, some of which are already gas suppliers to the EU and Turkey. Azerbaijan has the potential to increase energy exports to the EU through existing pipelines and expand new capacities [11, 19, 20].

The Azerbaijani state company SOCAR, together with four operators of the EU natural gas transportation system from Central-Eastern and South-Eastern Europe, presented the Ring of Solidarity project. Work is underway to attract various investments in infrastructure, which are included in the fifth list of EU projects of common interest. This is because energy cooperation between the EU and the AR was defined in the new plan for a strategic partnership in the field of energy, adopted in 2022. The cooperation is related to the important role that Azerbaijan plays and will play in the diversification of Europe from Russian fuel, in particular through the expansion of "SGC", on the other hand, is based on a common program of transition to "clean energy" with actions in the field energy efficiency, renewable energy, renewable hydrogen, and in the field of prevention of fugitive methane emissions, the obligation to achieve a clean economy with zero emissions by 2050 [20-22].

In 2022, the Azerbaijan Republic had income from the sale of profitable oil, gas and condensate, mainly from the Azəri-Çıraq-Günəşli and Şahdəniz fields (Table 5).

Azerbaijan has large natural gas resources and is working on several sources of expanding gas production through the implementation of the development of new fields such as "Abşeron", "Qarabağ", "Ümid", "Babək", "Azəri-Çıraq-Günəşli" in in the short and medium term for the extraction of additional volumes of gas and its export to partners (Table 6).

Table 5: Azerbaijan's income from HC sales in 2022

No	Hydrocarbons	Revenue, billion dollars
1	Oil and gas	11 587.6
2	Condensate from the "AÇG" group of fields	9 888.8
3	Condensate from the "Shahdəniz" field	328.6
3	Gas from the "Shahdəniz" field	1 114.4
4	Gas from other oil and gas fields	164.4

Table 6: Gas resources of Azerbaijan

No	Stocks	Volume
1	Recoverable, billion cubic meters	933
2	Proven, trillion cubic meters	1,7
3	Projected, trillion cubic meters	4 - 7

An increase in natural gas production due to new gas production centers on the Caspian shelf allows increasing the export of "blue fuel". The AR is expanding cooperation with the countries of the European continent (with the participation of Turkey) in the field of gas business. The creation of a gas hub in Turkey, with the participation of Russia, with the involvement of the Caspian gas producing countries, can have a serious positive impact on the diversification of the supply of energy resources to European markets. The Turkish gas hub can become a platform for deliveries to other countries, primarily to Europe, as well as for determining the price of gas.

Economic cooperation in the development of energy resources between the UK and the AR is expanding, the documents signed by the parties create favorable conditions for the active participation of British investors in various sectors of the Azerbaijan economy, and the UK is the leader in terms of investment in the AR. British companies are actively involved, also in renewable energy projects implemented in the territories liberated from occupation. The creation of a Turkish gas hub has become more relevant in 2022, after the explosion of the Northern Streams gas pipeline.

Being a reliable supplier of energy resources to Europe, Azerbaijan sets itself the following priority tasks: the sustainable growth of a competitive economy and the "green growth" of the country with a clean environment. The AR can provide stability, which is essential for investors. The EU, through the Global Gateway project (the EU strategy for investing in infrastructure projects and establishing economic partnerships based on certain principles), intends to develop partnerships with Azerbaijan in the field of energy development.

In addition to the wide opportunities for the use of solar and wind energy, the AR has a great potential for the production of environmentally "clean" hydrogen, which is necessary for the decarbonization of heavy industry.

Azerbaijan, as an energy country with experience in diversification, is a competitive country, especially in terms of wind energy and green hydrogen. Increasing the production of electricity from traditional sources, Azerbaijan intends to increase the generation from renewable energy sources. Currently, foreign investors are engaged in the construction of three solar and wind power plants with a capacity of 710 megawatts in the Republic of Azerbaijan. The Masdar Company cooperates with Azerbaijan in the field of production of environmentally friendly hydrogen and its further export to the European market. RES energy, including large hydroelectric power plants, can produce 1.304.5 megawatts of energy, which is 17.3% of the total capacity. The goal was set to increase the production of electricity from renewable sources to 30% of the country's total energy balance by 2030 [20-22].

At the end of 2021, the total installed RES capacity in Azerbaijan amounted to 1.308 MW compared to 1.026 MW in 2012, according to a report by the International Renewable Energy Agency (IRENA). In the coming years, in order to achieve its goals, it is planned to commission 1.500 MW of renewable energy capacities. The potential for offshore wind power in the Caspian Sea is huge and is estimated at 157 GW, while on land the potential is 23 GW of solar energy. In the future, the export of electricity to Europe by cable through Georgia and the Black Sea is being considered.

Azerbaijan is the most important transport and logistics hub in the "Middle Corridor" between Asia and Europe – a route designed not only to transport energy resources, but also vital raw materials and finished products. The European Union is actively working with the states of Central Asia, Azerbaijan's participation in these projects is also being considered. As President of Azerbaijan Ilham Aliyev noted: "Demand for natural gas from new sources is growing in Europe. In this regard, we expect to double the capacity of the TANAP and TAP pipelines - from 16 to 32 and from 10 to 20 billion cubic meters per year, respectively. We do everything to meet the needs of our partners..." "...The Trans-Caspian gas pipeline is not our project. In the Trans-Caspian pipeline project, we are considered a transit country. And we have already publicly stated many times, including myself, that we are ready to provide the necessary transit for our friends and partners in the Caspian, if they decide to build a pipeline..." [18].

During the peak of the energy crisis in 2022, the "SGC" project confirmed that it is the most important source of pipeline gas supplies to the EU, where the volume of gas delivered to the EU via the pipeline increased from 8 billion cubic meters to 11.4 billion cubic meters (total exports amounted to 22.6 billion cubic meters), that is, more than 40% compared to 2021 (total exports amounted to 19 billion cubic meters), and in 2023 it will amount to 24.5 billion cubic meters .

The increase in the income of the Azerbaijan Republic from the export of energy resources was the result of new geopolitical realities. In connection with the transition to "green energy", some international financial institutions have stopped investing in projects related to fossil fuels. However, today it is obvious that the energy security of Europe cannot be achieved at the desired level without the supply of natural gas.

As the President of the Republic of Azerbaijan Ilham Aliyev noted, "... The launch of projects aimed at the development of "green" energy in the country is an important opportunity for creating a "green energy corridor", which is considered an analogue of such a large project as the "Southern Gas Corridor". In particular, the implementation of large-scale projects in the territories liberated from occupation, including the creation of a "green" energy zone in Karabakh and East Zangezur, will turn the country into a producer and exporter of alternative energy. Given the further increase in the strategic importance of the Southern Gas Corridor project in the energy transition, the expansion of the TANAP and TAP projects has already become a hot topic for Azerbaijan. The expansion of the Southern Gas Corridor until 2027 and other prospects related to the transportation of energy resources will serve to further strengthen the strategic role of our country in the diversified energy supply and energy security of our partners" [18].

Almost completely meeting the national demand for electricity through domestic generation, Azerbaijan also plans to supply electricity not only to neighboring countries, but also to the EU. According to analysts' calculations, the country will be able to export 700 MW of electricity to Europe annually via the Azerbaijan-Georgia-Turkey energy bridge in the future. Such forecasts are based on the country's export capacity, which is estimated at the level of several billion kilowatts per hour.

It is planned that electricity from the Azerbaijan Republic will be supplied to Bulgaria via power transmission lines available in Turkey. Such deliveries have already been made to Bulgaria and Greece. In 2019, the Azerbaijan Republic began supplying electricity through the territory of Georgia and Turkey to Greece, Bulgaria, and further to Romania and Hungary, it is planned to establish exports to Austria and Italy. Laying of a submarine fiber-optic cable of a high-voltage submarine 500-kilovolt DC electric cable, should have a capacity of up to 1000 MGv and will pass through Azerbaijan, Georgia along the bottom of the Black Sea to Romania.

The ongoing projects in the field of renewable energy and plans to realize the potential of offshore wind energy in the future can make Azerbaijan an important partner for Europe in the field of exporting electricity and hydrogen generated from green energy sources.

The results of the research give grounds to say with confidence that Azerbaijan's participation in the diversification of energy supplies to the European market, despite the energy crisis in the world and the difficult geopolitical situation, is being implemented successfully, has serious prospects and is confirmed by the growth dynamics of the export potential.

Conclusion

Potentially, Azerbaijan plays and in the future will play an important role in ensuring the energy security of Europe by participating in the diversification of energy sources and reducing the risks of disruption in the supply of energy resources. Azerbaijan, as an energy country with experience in diversification, is a competitive supplier of energy resources, especially in terms of wind energy, solar energy and green hydrogen. Increasing the production of electricity from traditional sources, Azerbaijan intends to increase the generation from renewable energy sources, to expand the export of energy carriers to the European continent. The sustainable development of energy production technologies in recent years, as well as global climate goals, are accelerating the transition to "green energy", which is one of the main directions of the energy policy of the Republic of Azerbaijan.

Using its rich natural resources, the AR makes a significant contribution to the global agenda, such as increasing the production of alternative and renewable energy, decarbonization and diversification of energy sources. In the medium term, Azerbaijan seeks to become an exporter of electricity obtained from alternative sources and hydrogen – "green energy".

References

- [1] Makarov, A., Mitrova, T., Kulagin, V., Mel'nikova, S., Galkina, A. (2016). Miroviye gazoviye gorizonty do 2040 goda. *Gazoviy biznes*, 3: 21–28.
- [2] Itogi goda v elektroenergetike Yevrosoyuza (2022). [Url: https://ria.ru/20221220/energetika-1839903928.html](https://ria.ru/20221220/energetika-1839903928.html).
- [3] U.S. Energy Information Administration (2018). International Energy Outlook Presentation, 312.
- [4] Mirlin, G. A. (1991). Energeticheskiye resursy. *Gornaya entsiklopediya* (pod red. Kozlovskiy Ye.A.). *Sovetskaya entsiklopediya*, 5: 472–473.
- [5] Gasumov, E.R. (2023). Overview of the situation of the European gas market. *UNEC Scientific News*, 11: 27-45.
- [6] Gasumov, E.R. (2021). Caspian region may become one of the main gas suppliers to Europe. *Scientific journal*, 18 (1): 5–9.
- [7] Gasumov, E.R. (2021). Azerbaijan's participation in the diversification of gas transport infrastructure of the continent. *UNEC Scientific News*, 9: 60-71.

- [8] Gasumov, E.R. (2021). Perspektivy sotrudnichestvo prikaspiyskikh stran pri osvoyeniye neftegazovykh mestorozhdeniy. *Yevraziyskiy soyuz uchonykh*, 2(83): 15–19.
- [9] Gasumov, E.R. (2021). Perspektivy proizvodstva i transportirovki (eksporta) vodoroda v Azerbaydzhane. *Yestestvennyye i tekhnicheskiye nauki*, 12: 228–232.
- [10] Gasumov, E.R. (2022). Perspektivy razvitiya, vozobnovlyayemoy istochnikov energii v Azerbaydzhane. V sbornike: *Tekhnicheskiye i tekhnologicheskiye sistemy. Materialy trinadtsatoy Mezhdunarodnoy nauchnoy konferentsii*. Krasnodar: 89–193.
- [11] Gasumov, E.R. (2022). Po voprosu razvitiya vodorodnoy energetiki. V sbornike: *Innovatsionnyye tekhnologii v neftegazovoy otrasli. Problemy ustoychivogo razvitiya territoriy. Sbornik trudov III Mezhdunarodnoy nauchno-prakticheskoy konferentsii*. Stavropol': 218–224.
- [12] International Energy Agency (2012). Key World Energy Statistics: 80.
- [13] British Petroleum (2014). *BP Statistical Review of World Energy*, 80.
- [14] Gasumov, E.R. (2021). Azerbaydzhan stanovit'sya gazovoy stranoy i eksportorom gaza v Yevropu. *Yestestvennyye i tekhnicheskiye nauki*, 3: 104–111.
- [15] Gasumov, E.R. (2021). Efficiency of expert supplies of Azerbaijan natural gas. *Polish journal of science*, 42–1: 28–30.
- [16] Gasumov, E.R. (2021). Azerbaijan becomes a regional energy hub. *Deutsche Internationale Zeitschrift fur Zeitgenossische Wissenschaft*, 6–2: 17–20.
- [17] Gasumov, E.R., Gasumov, R.A. (2021). Caspian region may become one of the main gas suppliers to Europe. *Science. Education. Practice: proceedings of the International University Science Forum (Canada, Toronto)*, 1: 16–23.
- [18] Gasumov, E., Gasumov, R., Suleymanov, G., Gurbanov, K. (2022). Risk management in the production and transportation of natural gas under the conditions of the economic crisis in the energy market. *RT&A, Special Issue*, 4(70). 502–508. DOI: <https://doi.org/10.24412/1932-2321-2022-470-502-508>.
- [19] Benashvili, K.A. (2020). Rol' proyekta "Yuzhnyy gazovyy koridor" v realizatsii energeticheskoy strategii Yevropeyskogo soyuza. *Kreativnaya ekonomika*, 9-14: 2181-2193.
- [20] Karpenko, V.M., Yuan', K.H. (2022). Diversifikatsiya struktury energopotrebleniya kak instrument obespecheniya natsional'noy energobezopasnosti. *Trudy BGTU*, 5(1): 145–151.
- [21] The Organization of the Petroleum Exporting Countries (2021). URL: http://www.opec.org/opec_web/en/about_us/23.htm .
- [22] Derevyago, I.P. (2020). Usloviya i vozmozhnosti perekhoda ekonomiki k zelenomu rostu // *Belorusskiy ekonomicheskiy zhurnal*, 4: 20–35.

ECOLOGY OF USED ENGINE OIL ADDINOL

Elvira Guseinova¹, Gahraman Hasanov¹, Elman Akhyadov²

•

¹Azerbaijan State Oil and Industry University, Baku, Azerbaijan

²Chechen State University named after Akhmat Kadyrov, Russia

elvira_huseynova@mail.ru

gaman51@mail.ru

akhyadov1990@mail.ru

Abstract

Comprehensive spectroscopic studies of used and regenerated with chloric acid samples of ADDINOL engine oil were carried out. It was revealed that during the operation of engine oil, structural changes in hydrocarbon components, the formation of oxygen-containing compounds, and the accumulation of products of thermal destruction and friction occur. An assessment was made of the qualitative changes in used motor oil under the influence of chloric acid. Restoration of the structure of basic hydrocarbon components was established, complete removal of succinimide additives while retaining detergent-dispersant and extreme pressure additives, as well as removal of compounds containing hydroxyl groups and a highly dispersed carbon phase. It has been established that the precipitate is a carbon-containing agglomerate, which contains components of succinimide additives.

Keywords: used engine oil, chloric acid, carbon-containing agglomerate, IR spectroscopic, morphology, succinimide additives

I. Introduction

As is known, the determination of the chemical composition of the aging products of lubricating motor oils (mechanical impurities, additives, heavy metals, solvents, fuels, acids, oxidation, polymerization, degradation products, water, etc.) is the main task in studying the possibilities of their regeneration – recycling. The effectiveness of the recycling method used should also be confirmed by the results of a comprehensive analysis of regeneration products [1–3]. This problem can be solved only if several analytical methods are used simultaneously.

In this paper, based on the results of a comparative study of the spectroscopic features of the original, spent and subjected to acid regeneration with chloric acid, engine oil ADDINOL Super Light 0546, SAE 5W-40, the sources of contamination of the lubricant and the effectiveness of the re-generation are discussed.

II. Methods

Processed synthetic engine oil ADDINOL Super Light 0546, SAE 5W-40 was chosen as the object of research. The duration of its operation was 5 thousand km.

The method of regeneration of used oil ADDINOL Super Light 0546, SAE 5W-40 consisted of treatment with chloric acid and described in detail in [4,5]. The infrared spectra of motor oil were recorded on a Nicolet IS 10 spectrometers («Thermo Scientific») in the wavenumber range from 400 to 4000 cm⁻¹. The registered samples in the form of a drop were compressed between two

transparent silicon windows until a thin film (capillary layer) was formed.

The surface morphology, as well as the elemental composition of the solid deposit sample, were studied by transmission electron microscopy (TEM) on a JEM-2100 microscope with a grating resolution of 0.14 nm (with a built-in EDX analyzer (EDS, Genesis 4000, using a Si (Li) detector).) at an accelerating voltage of 100 kV. The TEM sample was fixated on carbon substrates mounted on copper grids.

III. Results

Lubricating oils are known to be multicomponent dispersed systems. In [4], based on the results of a comprehensive study of the physicochemical parameters and dielectric characteristics of used engine oil (UMO) ADDINOL Super Light 0540, SAE 5W-40, it was found that the main products of "aging" are fine soot particles. It was also found that UEO retains surfactant additives in its composition, the molecules of which envelop finely dispersed solid particles, preventing their coagulation and sedimentation even during prolonged settling (40 hours at temperatures up to 80°C), centrifugation and vacuum filtration. Efficient settling of fine particles became possible due to the ease of interaction between the used chloric acid, which is one of the strongest oxidizing agents, and the components that make up engine oil additives [5]. The resulting breakage of chemical bonds leads to degradation and loss of the functional properties of the additives, which leads to the ease of sedimentation of oil contaminants.

To confirm or refute this mechanism, studies were carried out on 4 samples of ADDINOL Super Light 0546 engine oil: sample 1 - original engine oil (before operation), sample 2 - used engine oil (after operation), sample 3 - regenerated engine oil, sample 4 - solid residue obtained during oil regeneration.

Let's consider some spectral features of the original, used, regenerated oil (Fig. 1; a, b and c, respectively). The spectra show that the nature of the oils is similar, but there are also fundamental differences. IR spectroscopic data of sample 1 (Fig. 1, a) suggest that the original motor oil has a complex composition and includes aliphatic hydrocarbons with long chain branching, polyorganosiloxanes, and esters of dicarboxylic acids. So, based on the data obtained, it can be argued that the basis of motor oil is polyolefins. There are two characteristic bands at 2853.03 and 2923.17 cm^{-1} , corresponding to the antisymmetric and symmetric stretching vibrations of C-H of the CH₂ group. In addition, the intensity of these bands, which makes it easy to identify them, indicates that these compounds have a polar group at the end of the chain. Scissor vibrations of the CH₂ group were noted for the medium strength band at 1459.37 cm^{-1} . An absorption band was also found at 966.76 cm^{-1} related to out-of-plane bending vibrations of hydrogen atoms bonded to carbon in the trans position in unsaturated olefin derivatives (disubstituted ethylene).

The presence of polyorganosiloxanes was also noted in the composition of the original motor oil: intense bands in the region of 100-1100 cm^{-1} indicate the presence of Si-O, out-of-plane deformation vibrations of unsymmetrical disabled ethylene at 889.35 cm^{-1} can correspond to both $\text{R}^1\text{R}^2\text{C}=\text{CH}_2$ and $\text{R}^1\text{R}^2\text{C}=\text{CHR}^3$, however, the weak intensity of this band indicates the second type, since it is known that when the double bond moves from the end of the chain to the center of the molecule (the bond is in the chain), the intensity of the band will decrease. In addition, the band 1736.59 cm^{-1} in the region 1800-1750 cm^{-1} in the case of vinyl compounds is an overtone of the frequency 890 cm^{-1} and is a valuable confirmation of the presence of an unsymmetrical ethylene bond.

Absorption in the range of 3400 and 3200 cm^{-1} refers to intermolecular hydrogen bonds -OH of macromolecular compounds. In this case, the appearance of an absorption band of the bound OH group at 3388.42 cm^{-1} refers to the concentrated solution with a polymer association dissolved in a non-polar solvent (probably water in oil).

The bound group –OH is marked on the basis of a wide band of low intensity in the region of 3300-2500 cm^{-1} overlapped in places by stretching vibrations of C–H. The interval 3388.42 -3714.69 cm^{-1} falls on the absorption of the unbound group –OH. Esters of dicarboxylic acids are presented in the range 1180-1080 cm^{-1} in which there are 4 bands of different intensity, one of which contains a doublet (1150 cm^{-1}). These bands indicate antisymmetric and symmetric stretching vibrations of the C-O-C-O-C group in saturated polyesters.

In the region of about 680-610 cm^{-1} , bands which attributed to sulfates were noted. Considering the absence of the second very strong bands around is 1130-1080 cm^{-1} , which in most cases accompany sulfates and their weak character, as well as the duplicity of the bands at 608.72, 664.43, 673.10 cm^{-1} , we can conclude that these are alkaline bisulfates metals. A group of bands in the frequency range 2280-2730 cm^{-1} to the absorption of PO^+ stretching vibrations. These components are the most common additive components.

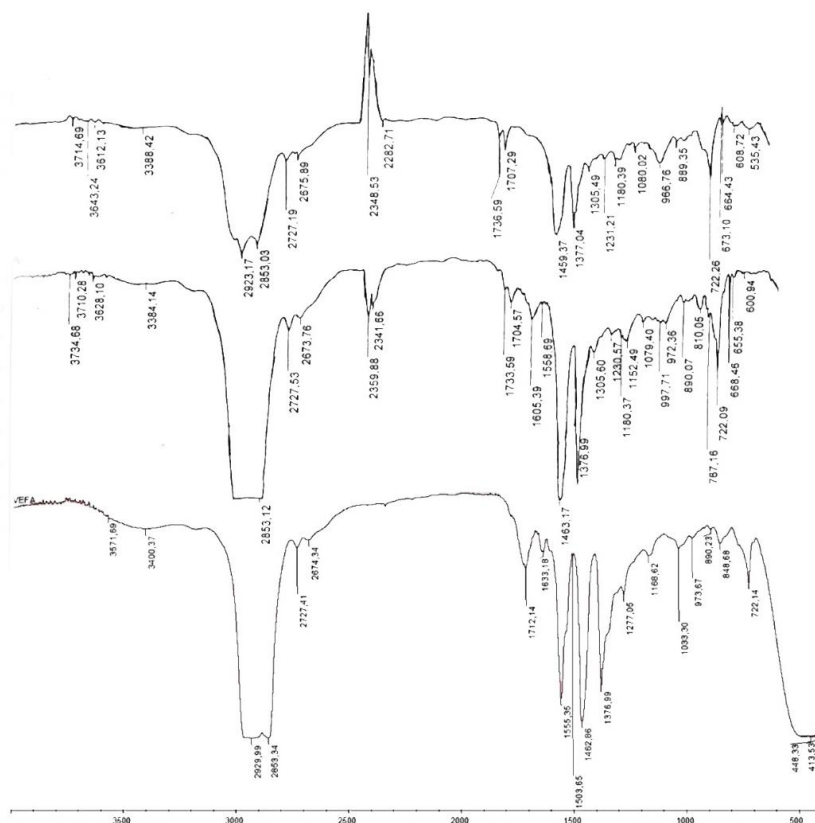


Fig. 1: IR spectra of engine oil ADDINOL Super Light 0546 (a - original; b - used; c - after regeneration)

On fig. 1, b shows the spectrum of sample 2 - engine oil after operation. An increase in the number of bands from 22 for the original motor oil to 28 for the used one makes it possible to judge the complication of the chemical composition of the used oil.

The structural changes that have taken place are especially clearly seen in the example of polyolefins: despite the fact that the general position of the absorption regions associated with the stretching and bending vibrations of the C–H bond of the CH_2 group is preserved, however, the absorption structure (number of bands, their intensity) changes. The region 2923-1450 cm^{-1} undergoes major changes, which is associated with deformation vibrations of α -olefin macromolecules, which consist of more complex monomeric units with lower symmetry. If the initial oil had absorption bands of medium strength (absorption intensity = $22 \div 26$), then in the used oil the absorption of these bands could be identified with difficulty (absorption intensity = $0.121 \div 0.828$), which may be caused by the removal of terminal polar groups that were noted in original.

It cannot be said that the absorption at 722 cm^{-1} , due to the pendulum vibrations of CH_2 groups, remained unchanged - a splitting of the band is noted (it is absent in the spectrum of the original oil), which is caused by significant changes occurring in the immediate environment of the oscillating groups. Such changes can include both external and internal influences (the appearance or absence of a hydrogen bond, mechanical and steric hindrances, the effects of inductive and dipole interactions, etc.). It can also be assumed that such a multilateral impact can be exerted by the previously discovered finely dispersed carbon particles of fuel combustion, which are formed during operation and are dispersed in the volume of used oil [4].

The occurrence of absorption bands of medium strength at 1558.69 cm^{-1} and weak at 1605.39 cm^{-1} corresponds to $\text{C}=\text{C}$ stretching vibrations conjugated with the neighboring oxygen atom or carbonyl group at the double bond. The formation of this type of compounds may be a consequence of oxidative processes accompanied by the formation of vinyl oxygen-containing compounds. This is confirmed by the appearance of a band at 997.71 cm^{-1} , which is related to outside planar bending vibrations of $\text{CH}=\text{CH}_2$ in vinyl compounds.

For heteroatom-containing compounds, it was noted that of the 2 bands assigned to bisulfates in sample 1, the 673.10 cm^{-1} band disappeared, and the 608.72 cm^{-1} band shifted to a lower frequency region up to 600.94 cm^{-1} and its characteristic doublet disappeared. In addition, a new medium-strength band appeared at 655.38 cm^{-1} . The absorption bands of phosphorus-containing stretching vibrations in the region of $2280\text{--}2730\text{ cm}^{-1}$ are shifted and less intense than in the spectrum of the original oil.

The study of the IR spectrum of sample 2 (Fig. 1, b) shows that the intensity of the absorption bands in the region of $3380\text{--}3735\text{ cm}^{-1}$, related to the stretching vibrations of the unbound OH group, remained practically unchanged, but there was a shift by $10\text{--}60\text{ cm}^{-1}$ of all bands without exception. According to the literature data, this effect is observed with an increase in the polarity of the solvent (accumulation of water and acid-type compounds).

Analyzing the IR spectrum of sample 3 - used oil subjected to acid cleaning with chloric acid (Fig. 1, c), one can see that the intense absorption peaks characteristic of bisulfates, phosphorus-containing compounds have completely disappeared (their disappearance indicates the occurrence of a chemical interaction between the components of succinimide additives and acid). But, along with this, there are also evidences of chlorine addition to the hydrocarbon chain - in the region of $750\text{--}800\text{ cm}^{-1}$, as well as two very weak new absorption bands of $\text{C}\text{--}\text{Cl}$ stretching vibrations at 413.53 and 448.33 cm^{-1} . This assumption is supported by the appearance of a new absorption band in the region of 1503.65 cm^{-1} , which is an overtone of the above bands.

But the most valuable result, in our opinion, is the nature of the band corresponding to pendulum oscillations $\text{--}(\text{CH}_2)_n\text{--}$: its splitting got disappeared and it has shifted to a higher frequency region. This result is in good agreement with the statement made above that it is the finely dispersed carbon particles of fuel combustion that are the factor responsible for the change in the oscillation frequency $\text{--}(\text{CH}_2)_n\text{--}$, and data on the high degree of coagulation of fine soot particles during regeneration.

And no less important is the disappearance of the bands related to the stretching vibrations of the OH group (after regeneration, the oil does not contain traces of polar hydroxyl groups) and the appearance of one of the most intense bands at 1555 cm^{-1} , which is probably associated with the appearance of the carboxylate anion. And the appearance of a new very weak absorption band at 3571.69 cm^{-1} is the result of the dipole interaction of halogen-substituted compounds containing a carbonyl group and a negatively charged chlorine atom [6].

After exposure to chloric acid, a precipitate formed in the oil, which, according to TEM data, has a dense, chaotic structure, consisting of crystallites combined into large agglomerates, the size of which is $70\text{--}90\text{ }\mu\text{m}$ (Fig. 2). The elemental composition of crystallites (table) of spectra 1, 3, 4, 6, 7, and 8 in Fig. 2 indicates a predominant carbon content ($82.9\text{--}88.4\%$), as well as a relatively high

oxygen content (4.5–11.6%), and an insignificant the content of other elements: sulfur (1.9-3.5%), calcium (1.2-3.5%), zinc (0.4-1.5%), phosphorus (0.2-0.3%), sodium (0.1%), iron (0.1%), magnesium (0.1%), aluminum (0.1%) and chlorine (0.1%). In addition, the EDX spectra assigned to the solid phase indicate an uneven distribution of some of them.

Table: *Elemental composition of crystallites (Fig. 2)*

Specters	Contain of elements, % weight										
	C	O	S	Ca	Zn	P	Na	Fe	Mg	Al	Cl
1	84.0	11.6	2.1	1.5	0.4	0.2	0.1	-	0.1	-	-
2	87.2	5.3	3.3	2.9	1.1	0.2	-	-	-	-	-
3	86.9	4.6	3.1	3.1	0.8	0.2	-	-	0.1	0.1	0.1
4	84.4	11.1	1.9	1.6	0.6	0.2	-	0.1	0.1	-	-
5	90.2	6.6	1.5	1.1	0.5	0.1	-	-	-	-	-
6	86.7	4.5	3.5	3.5	1.5	0.3	-	0.1	0.1	-	0.1
7	86.3	7.8	2.6	2.4	0.6	0.2	0.1	-	-	-	-
8	85.9	10.7	1.4	1.2	0.5	0.2	-	-	-	-	0.1

So, for example, in spectrum 1 relative to spectrum 6, the oxygen content is 2.6 times higher, while sulfur is 1.7 times higher, calcium is 2.3 times higher, zinc is 3.8 times lower, and phosphorus is 1.5 times lower. According to TEM data, the size of the agglomerate from which spectrum 6 was taken is more than 8 times larger than the size of the agglomerate to which spectrum 3 belongs. This indicates that spectrum 1 contains a less condensed, intermediate form. According to this principle, the EDX spectra of all agglomerates can be divided into 2 phases: less condensed (spectra 1, 4, and 8) and more condensed (spectra 3, 6, and 7). But, considering the close elemental composition of these phases, it becomes obvious that the precipitate formed during regeneration is formed both due to the condensation of polymerization products of high-molecular compounds and fragments of ash additives, and compaction of a finely dispersed graphite-like structure.

At the same time, the presence of sodium, iron, magnesium, aluminum and chlorine was not detected in the EDX spectra 2, 5 (transparent areas representing the oil phase) (Fig. 2). This indicates that the separated phase of the oil has a qualitative composition different from the sediment, and the fact that the latter includes components of the main ash additives allows us to conclude that the conclusion about the mechanism of coagulation of highly dispersed particles, which was noted earlier in is correct [4,5].

During the analysis of the results obtained, it was noted that molybdenum and barium are absent in the composition of the oil and sediment, which, according to the data of [7], are included in the composition of the additives of the original engine oil, but along with this, carbon and aluminum appeared, and a high oxygen content was noted, and both of these facts are probably related to the exploitation of the operating conditions of engine oil: partial production of additives in the first case and the appearance of products of thermal and oxidative destruction of hydrocarbons, as well as wear on the surfaces of metal engine parts.

At the same time, sulfur, calcium, zinc and phosphorus are retained in the oil, and this speaks in favor of the preservation of alkylphenol additives [8, 9].

IV. Discussion

In the course of the spectroscopic studies of ADDINOL Super Light 0546 engine oil, it was found that the composition of ADDINOL Super Light 0546 engine oil includes aliphatic

hydrocarbons with long chain branching, polyorganosiloxanes, and esters of dicarboxylic acids. The results of the research indicate that changes occur during the operation of ADDINOL Super Light 0546 engine oil: vinyl oxygen-containing compounds are formed, the structure of polyolefins changes, and acid-type compounds appear. It was found that the oil obtained during the regeneration of the spent ADDINOL Super Light 0546 sample with chloric acid was characterized by the restoration of the structure of polyolefins, the complete removal of succinimide additives while maintaining detergent-dispersant and extreme pressure additives, and the resulting precipitate is carbon-containing agglomerates, which contain components of succinimide additives.

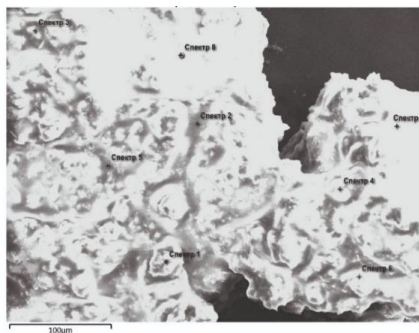


Fig. 2: Micrograph of a solid precipitate

The data obtained confirm the promise of the method of regeneration of used motor oils using chloric acid, which makes it possible to obtain a purified environmentally friendly product that is close in chemical composition to the original oil. Taking this into account, as well as the fact that the process is accompanied by the formation of not hard-to-recycle acid tar, but mineral sediment, the results obtained can become the basis for creating a waste-free technology for recycling used motor oil, solving environmental problems associated with the rational use of secondary resources.

References

- [1] Osman, D.I., Attia, S.K., Taman, A.R. Recycling of used engine oil by different solvent. *Egyptian Journal of Petroleum*, 2018, Volume 27, Issue 2, pp. 221-225.
- [2] Sarkar, S., Datta, D., Das B. Advance recovery approach for efficient recovery of waste lubricating oil by different material formulations. *Materials Today Proceedings*, 2022, Volume 49, Part 5, pp. 1891-1898.
- [3] Nour, A.H., Elamin, E.O., Nour, A.H., Alar, O.R. Dataset on the recycling of used engine oil through solvent extraction, *Chemical Data Collections*, 2021, Volume 31, 100598.
- [4] Adjamov, K.Yu., Imanova, N.I., Guseinova, E.A. Assessment of physical and chemical properties of the used motor oil. *Azerbaijan Chemical Journal*, 2017, №1, P.80-84.
- [5] Ramazanova, E.E., Adzhamov, K.Yu., Guseinova, E.A. A method for regenerating used engine oil. Eurasian patent №032029.
- [6] Bellamy, L. J. Infrared Spectra of Complex Molecules. Moscow: Foreign Literature Press, 1963, 592 p.
- [7] Speranskaya, T.A., Tarutina, L.I. Optical properties of polymers. Leningrad: Chemistry, Leningrad branch, 1976, 135 p.
- [8] Folders, K.K. Dictionary of fuels, oils, lubricants, additives and special fluids. Moscow: Chemistry, 1975, 392 p.
- [9] Kuliev A.M., Chemistry and technology of additives to oils and fuels. L.: Chemistry, 1985, 312 p.

GEOHAZARDS AND ENVIRONMENTAL RISK ASSESSMENT PRACTICES OF PETROLEUM AND GAS PIPELINES USING MICROWAVE REMOTE SENSING

Emil Bayramov^{1,2}, Manfred Buchroithner², Martin Kada³, Saida Aliyeva⁴

•

¹Nazarbayev University, Kazakhstan

²TU Dresden, Germany

³Technical University of Berlin, Germany

⁴ADA University, Azerbaijan

emil.bayramov@nu.edu.kz

manfred.buchroithner@tu-dresden.de

martin.kada@tu-berlin.de

saaliyeva@ada.edu.az

Abstract

These studies focused on the quantitative assessment of the surface displacement velocities and rates and their natural and man-made controlling factors as the potential risks along the seismically active 70 km section of buried oil and gas pipeline in Azerbaijan using Persistent Scatterer Interferometric Synthetic Aperture Radar (PS-InSAR) and Small Baseline Subset (SBAS-InSAR) remote sensing analysis. The diverse spatial distribution and variation of ground movement processes along pipelines demonstrated that general geological and geotechnical understanding of the study area is not sufficient to find and mitigate all the critical sites of subsidence and uplifts for the pipeline operators. This means that both techniques outlined in this paper provide a significant improvement for ground deformation monitoring or can significantly contribute to the assessment of geohazards and preventative countermeasures along petroleum and gas pipelines.

Keywords: PS-InSAR, SBAS-InSAR, remote sensing, geospatial, pipelines, oil and gas, radar, interferometry

I. Introduction

This research focused on the quantitative assessment of the ground deformations, their natural and man-made controlling factors as the potential risks along a 70 km long seismically active section of buried Baku–Tbilisi–Ceyhan Oil (BTC), South Caucasus Gas (SCP), Western Route Oil (WREP) and South Caucasus Pipeline Expansion Gas (SCPX) pipelines in Azerbaijan. In the frame of this research, the primary goal was to measure and map ground deformation velocities and rates along buried oil and gas pipelines over the period of 2017-2019 using PS-InSAR and SBAS-InSAR remote sensing techniques and cross-correlate the results.

The present studies hold the practical scientific value and advantage for the petroleum and gas industry with the focus on pipeline operators, since the prediction, relevant justified investment and mitigation of risks require the combined quantitative and qualitative assessment of actual ground movements and evaluation of potential consequences. Another practical value is the ability to remotely monitor ground movements, reducing the number of expensive, time-

consuming and dangerous field studies (Hole *et al.* 2011).

II. Methods

SBAS-InSAR and PS-InSAR analysis along petroleum and gas pipelines were applied to identify the spatial patterns of ground surface deformations with respect to the location of active seismic faults (Fig.1a-d). The workflow shown in Fig.2 was used for PS-InSAR and SBAS-InSAR techniques, geospatial interpolations and spatial statistical analysis.

The monitoring and characterization of ground deformation processes along the 70 km section of oil and gas pipelines have been carried out by using a stack of total of 59 Sentinel-1 satellite images using PS-InSAR and SBAS-InSAR techniques. Sentinel-1 satellite images were acquired in C-band (wavelength 5.55 cm) with a revisiting time of 6 days considering both satellites (Sentinel-1A and Sentinel-1B) and an achievable ground resolution of 5 m × 20 m (range × azimuth) for the Single Look Complex (SLC) product. The radar images cover the period January 2018 - December 2019 and have been acquired in descending orbit with VV + VH polarizations, IW beam mode, Path-6 and Absolute Orbit-29828. Sentinel-1 VV polarization bands were used since co-polarized bands provide higher coherency (Imamoglu *et al.* 2019). As it is possible to observe in Figure 3a-d, all images are well connected in time for the interferometric analysis.

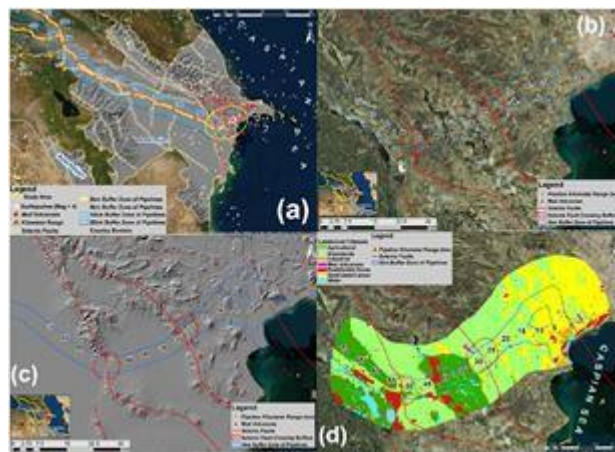


Fig. 1: (a) Map of Corridors of Oil and Gas Pipelines with the Indication of Seismic Faults, Earthquakes, Mud Volcanoes; (b) Detailed Map of Study Area with the Worldview-2 Satellite Imagery Background; (c) Detailed Map of Study Areas with the Hillshaded Terrain Background; (d) Landcover Types along the Corridor of Oil and Gas Pipelines.

PS-InSAR is a proven differential interferometric technique which involves processing of multi-temporal Synthetic Aperture Radar (SAR) data to identify persistently scattering ground features and their motion rates with millimetre precision (Ferretti *et al.* 2011).

The SBAS interferometric technique is based on the generation of interferograms through the processing of small spatial and temporal baseline interferometric pairs in order to reduce decorrelation and topographic effects (Berardino *et al.* 2003).

The main processing steps of PS-InSAR consist of interferogram generation, multi-temporal persistent scatterers (PS-InSAR) processing and removal of atmospheric phase screen (Osmanoglu *et al.* 2016). The main processing steps of SBAS consist of differential interferogram generation from selected SAR image pairs with a small orbital separation (baseline) to reduce the spatial decorrelation and topographic effects, filtering of atmospheric artifacts based on the availability of both spatial and temporal information and removal of topographic phase contribution (Lauknes *et al.* 2005).

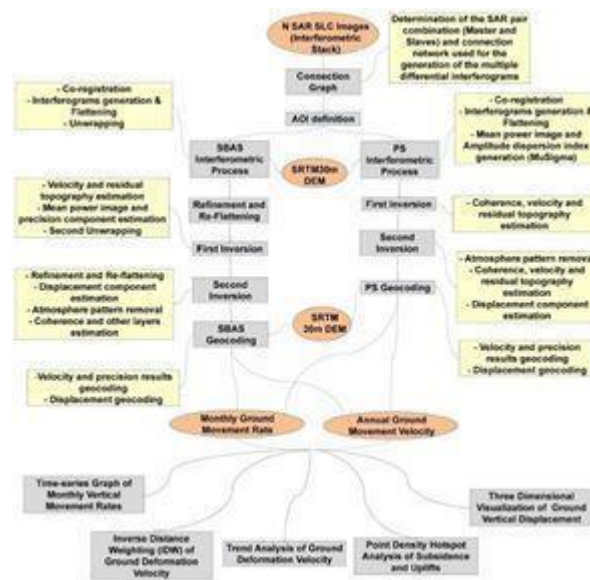


Fig. 2: Workflow for PS-InSAR, SBAS-InSAR and Spatial Statistics

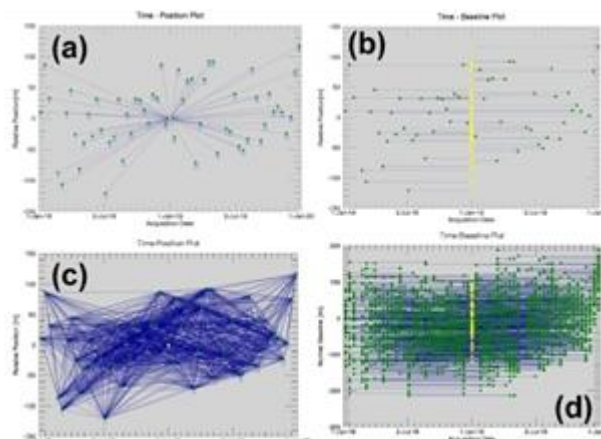


Fig. 3: Connection Graphs: (a) Time-Position Plot for PS-InSAR; (b) Time-Baseline Plot for PS-InSAR; (c) Time-Position for SBAS-InSAR; (d) Time-Baseline Plot for SBAS-InSAR;

III. Results and Discussions

As a primary factor of ground deformations, the influence of tectonic movements was observed in the wide scale analysis along 70 km long and 10 km wide section of petroleum and gas pipelines with the prevailing and continuous subsidence in the KP13–70 range of pipelines crossing two active seismic faults (Fig.4a-f; Fig.5a-d; Fig.6a-d). However, the largest subsidence rates were observed in the areas of croplands, where agricultural activities, such as overuse of groundwater, irrigation and ploughing etc. accelerate the surface deformation rates caused by the tectonic processes. The ground uplift deformations were observed in the pipeline range of KP0-KP13.

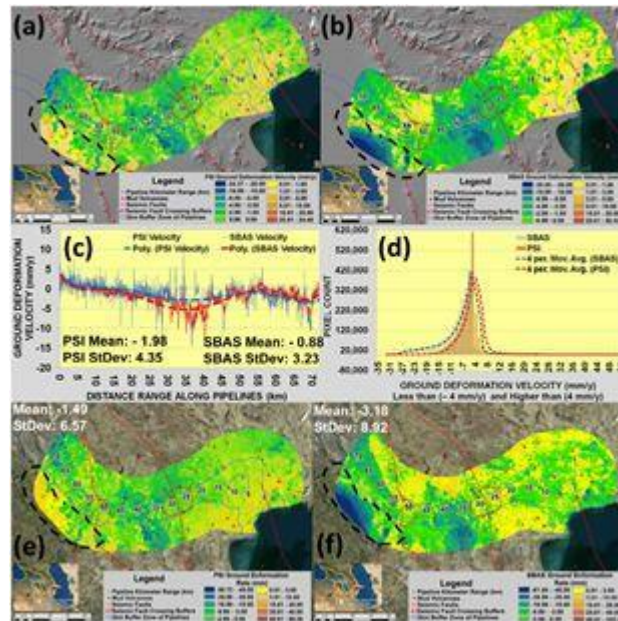


Fig. 4: (a) Map of PS-InSAR Ground Deformation Velocity along Petroleum and Gas Pipelines; (b) Map of SBAS-InSAR Ground Deformation Velocity along Petroleum and Gas Pipelines; (c) PS-InSAR and SBAS-InSAR 5km Interval Profile View of Ground Deformation Velocity; (d) Histogram of PS-InSAR and SBAS-InSAR Pixel Distribution; (e) PS-InSAR Map of Ground Movement Rates (on 27 December 2019 with the Baseline of 6 January 2018); (f) SBAS-InSAR Map of Ground Movement Rates (on 27 December 2019 with the Baseline of 6 January 2018).

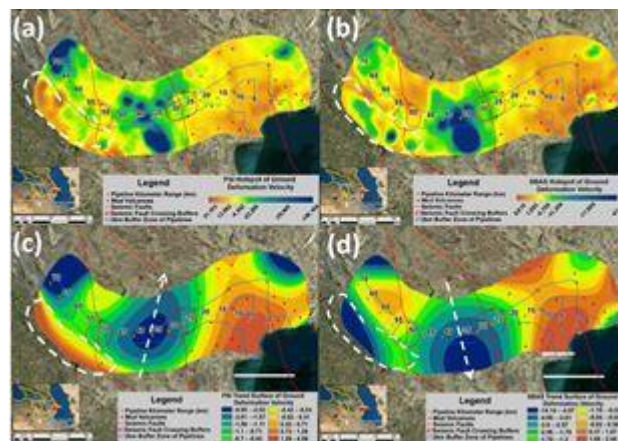


Fig. 5: (a) Map of PS-InSAR Hotspots of Ground Deformation Velocities; (b) Map of SBAS-InSAR Hotspots of Ground Deformation Velocities; (c) Map of PS-InSAR Trends of Ground Deformation Velocities; (d) Map of SBAS-InSAR Trends of Ground Deformation Velocities.

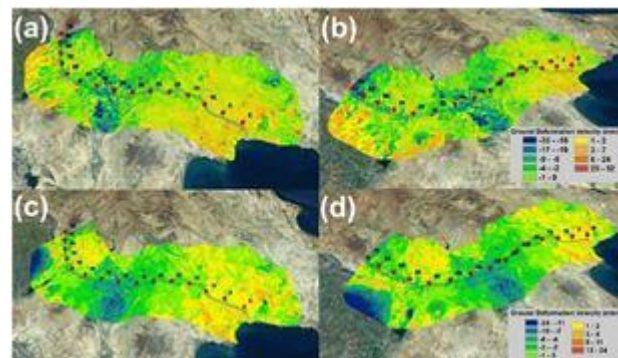


Fig. 6: Three-Dimensional Representation of PS-InSAR and SBAS-InSAR Ground Deformation Velocities (Visual Exaggeration: 3 times): (a) PS-InSAR South-West View; (b) PS-InSAR South-East View; (c) SBAS-InSAR South-West View; (d) SBAS-InSAR South-East View.

SBAS-InSAR performed better than PS-InSAR along buried petroleum and gas pipelines in the following aspects: the complete coverage of the measured points (Fig.7a-b), significantly lower dispersion of the results, continuous and realistic measurements and higher accuracy of ground deformation rates against the GPS historical measurements.

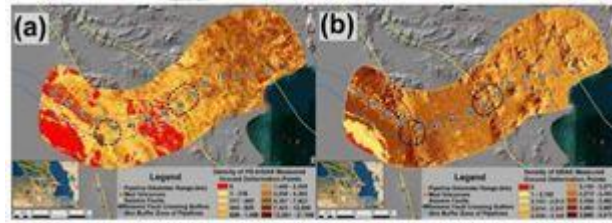


Fig. 7: (a) Density of PS-InSAR Measured Ground Deformation Points; (b) Density of SBAS-InSAR Measured Ground Deformation

The validation of ground deformation rates at KP28 + 300 using high-precision GPS measurements revealed the encouraging level of agreement with the regression coefficients equal to 0.94 for SBAS-InSAR and 0.74 for PS-InSAR (Fig. 8a-d). The validation of ground deformation rates at KP52 + 500 using high-precision GPS measurements revealed the encouraging level of agreement with the regression coefficients equal to 0.9 for SBAS-InSAR and 0.89 for PS-InSAR (Fig.8a-d). This means that the SBAS-based approach outlined in this paper is a significant improvement over current ground-based monitoring practices along pipelines. However, it is necessary to emphasize that PS-InSAR could perform better for the terminals, pump stations and aboveground pipelines since the PS-InSAR technique relies on the intensity of the backscattered radar waves to measure permanent scatterers as man-made structures with strongest returns.

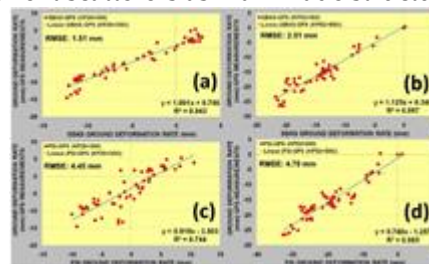


Fig. 8: (a) Validation of SBAS-InSAR Ground Deformation Rates using High-precision GPS Measurements at KP28 + 300; (b) Validation of SBAS-InSAR Ground Deformation Rates using High-precision GPS Measurements at KP52 + 500; (c) Validation of PS-InSAR Ground Deformation Rates using High-precision GPS Measurements at KP28 + 300; (d) Validation of PS-InSAR Ground Deformation Rates using High-precision GPS Measurements at KP52 + 500.

Local scale analyses were performed along 70 km section of pipelines with 250 m buffer zone for the detailed quantitative ground movement assessment of two seismic faults. Although both PS-InSAR and SBAS-InSAR measurements were highly consistent in deformation patterns and trends along pipelines, they showed differences in the spatial distribution of ground deformation classes and noisiness of produced results.

High dispersion of PS-InSAR measurements caused low regression coefficients with SBAS-InSAR for the pipeline profile range of 70 km and seismic faults at KP21–31 and KP46–54.

The minimum and maximum vertical ground deformation velocities were observed to be -21.3 and 14.1 mm/y for PS-InSAR and -15.9 and 4.5 mm/y for SBAS-InSAR measurements, respectively, along a 70 km range of pipelines with the buffer zone of 250m (Fig.9a-d).

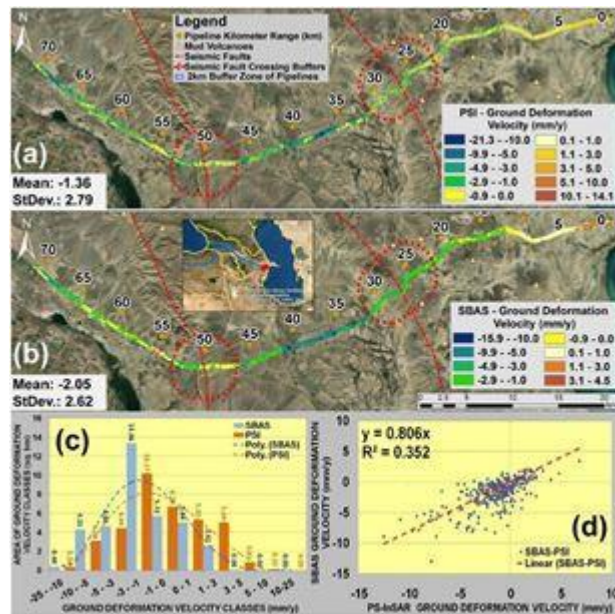


Fig. 9: Map of Ground Deformation Velocity along 70 km Petroleum and Gas Pipelines Corridor within 250 m Buffer Zone; (a) for PS-InSAR; (b) for SBAS-InSAR; (c) Area of Ground Deformation Velocity Classes; (d) Regression Analysis between PS-InSAR and SBAS-InSAR Ground Deformation Velocity for 250 m Interval Points along Pipelines.

The minimum and maximum vertical ground deformation rates were observed to be -41.3 and 32.6 mm for PS-InSAR and -28.2 and 8.2 mm for SBAS-InSAR measurements, respectively, along a 70 km range of pipelines with the buffer zone of 250m (Fig.10a-d).

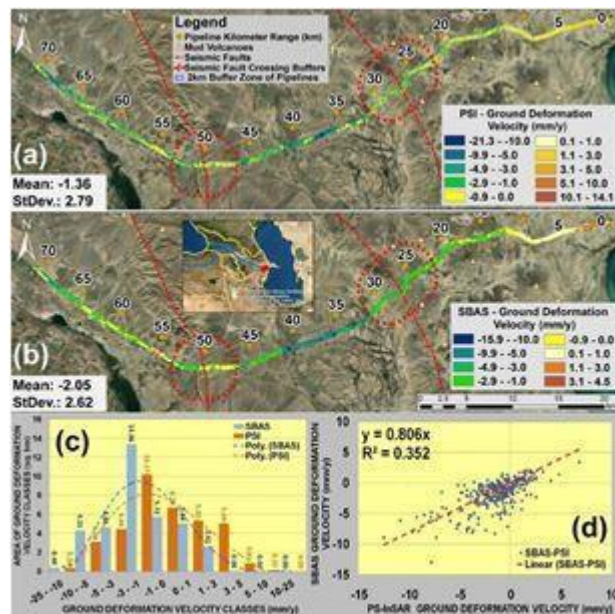


Fig. 10: Map of Ground Deformation Rates along 70 km Petroleum and Gas Pipelines Corridor within 250 m Buffer Zone; (a) for PS-InSAR; (b) for SBAS-InSAR; (c) Area of Ground Deformation Rate Classes; (d) Regression Analysis between PS-InSAR and SBAS-InSAR Ground Deformation Rates for 250 m Interval Points along Pipelines.

The ground deformation velocities within the range of Seismic Fault KP21–31 revealed the minimum and maximum values of -9.03 and 1.45 mm/y for SBAS-InSAR and -22.65 and 14.01 mm/y for PS-InSAR, respectively (Fig.11a-d).

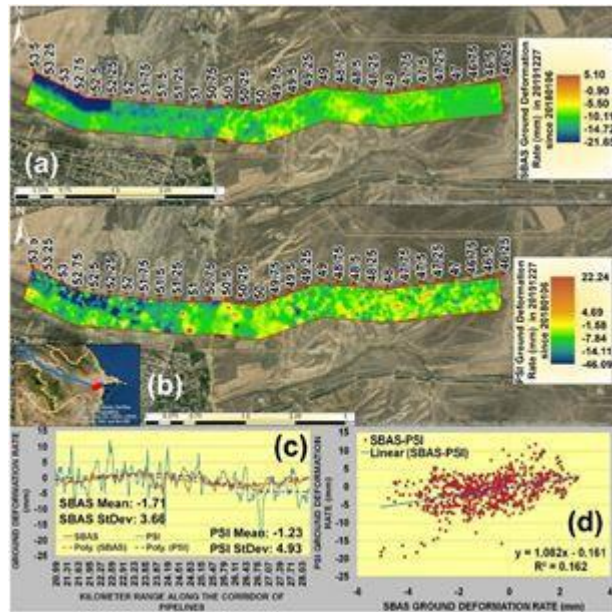


Fig. 11: Detailed Map of the Ground Deformation Velocity for 250 m Buffer Zone of Pipeline Corridor Crossing the Seismic Faults at KP21–31 range: (a) for SBAS-InSAR; (b) for PS-InSAR; (c) Profile View of PS-InSAR and SBAS-InSAR Ground Deformation Velocity for the Seismic Fault at KP21–31 range; (d) Regression Analysis between PS-InSAR and SBAS-InSAR Ground Deformation Velocity for 10m Interval Points along Pipelines within KP21–31 range.

The ground deformation rates within the range of Seismic Fault KP21–31 revealed the minimum and maximum values of -12.24 and 8.23 mm for SBAS-InSAR and -46.07 and 33.46 mm for PS-InSAR, respectively (Fig.12a-d).

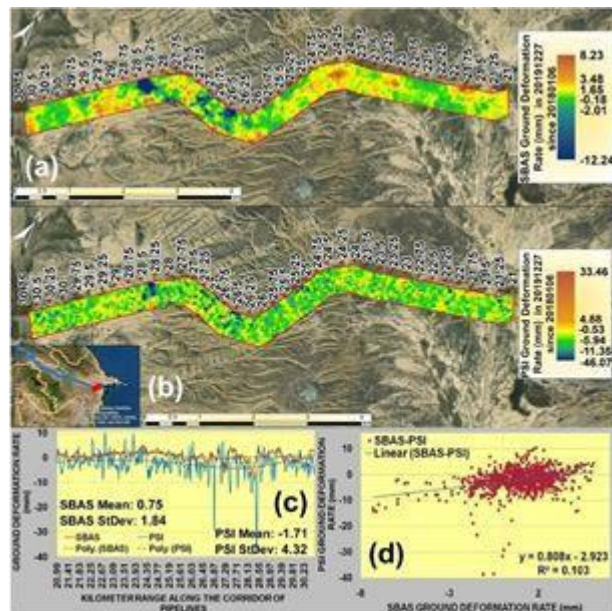


Fig. 12: Detailed Map of the Ground Deformation Rates for 250 m Buffer Zone of Pipeline Corridor Crossing the Seismic Faults at KP21–31 Range: (a) for SBAS-InSAR; (b) for PS-InSAR; (c) Profile View of PS-InSAR and SBAS-InSAR Ground Deformation Rates for the Seismic Fault at KP21–31 Range; (d) Regression Analysis between PS-InSAR and SBAS-InSAR Ground Deformation Rates for 10m Interval Points along Pipelines within KP21–31 Range.

The ground deformation velocities within the range of Seismic Fault KP46–54 revealed the minimum and maximum values of -8.31 and 2.05 mm/y for SBAS-InSAR and -19.14 and 9.41 mm/y for PS-InSAR, respectively (Fig.13a-d).

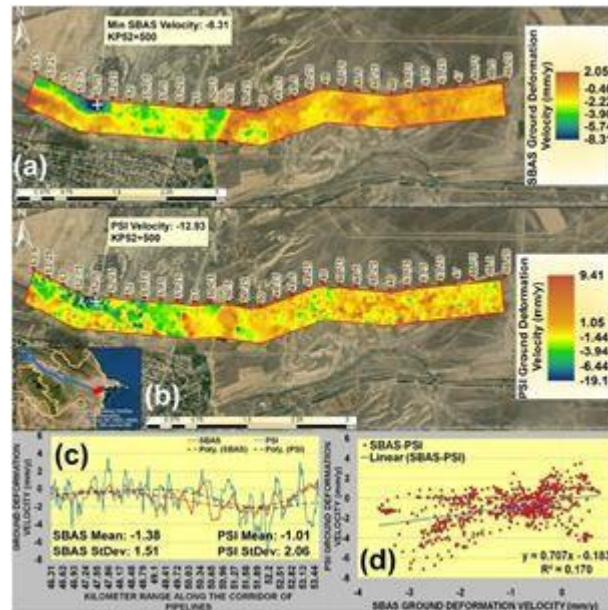


Fig. 13: Detailed Map of the Ground Deformation Velocity for 250 m Buffer Zone of Pipeline Corridor Crossing the Seismic Faults at KP46–54 range: (a) for SBAS-InSAR; (b) for PS-InSAR; (c) Profile View of PS-InSAR and SBAS-InSAR Ground Deformation Velocity for the Seismic Fault at KP46–54 range; (d) Regression Analysis between PS-InSAR and SBAS-InSAR Ground Deformation Velocity for 10m Interval Points along Pipelines within KP46–54 Range.

The ground deformation rates within the range of Seismic Fault KP46–54 revealed the minimum and maximum values of –21.65 and 5.1 mm for SBAS-InSAR and –46.09 and 22.24 mm for PS-InSAR, respectively (Fig.14a-d).

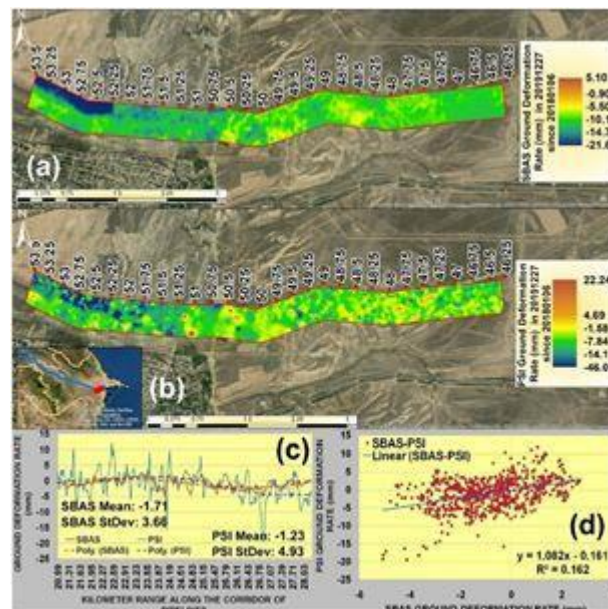


Fig. 14: Detailed Map of the Ground Deformation Rates for 250 m Buffer Zone of Pipeline Corridor Crossing the Seismic Faults at KP46–54 Range: (a) for SBAS-InSAR; (b) for PS-InSAR; (c) Profile View of PS-InSAR and SBAS-InSAR Ground Deformation Rates for the Seismic Fault at KP46–54 range; (d) Regression Analysis between PS-InSAR and SBAS-InSAR Ground Deformation Rates for 10m Interval Points along Pipelines within KP46–54 range.

The wider range of PS-InSAR values was directly related to the produced dispersion results, which makes it more complicated for the pipeline operators to prioritize vulnerable areas to ground deformation processes along pipelines.

The regression analysis and RMSE evaluations between SBAS-InSAR and PS-InSAR ground

deformation measurements revealed the correlation coefficient equal to 0.79 and RMSE equal to 4.9 mm for KP28 + 300 and the correlation coefficient equal to 0.92 and RMSE equal to 6 mm for KP52 + 500. This allows us to assume that SBAS-InSAR and PS-InSAR measurements are subject to approximate variations in the range of 4.9–6 mm, which should be considered as a limitation by pipeline operators in terms of the existing compliance standards for acceptance (Fig.15a-d).

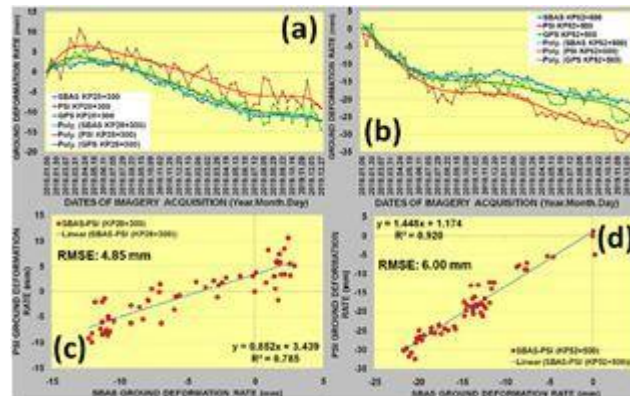


Fig. 15: (a) Graph of Ground Deformation Rates for SBAS, PS-InSAR and GPS Measurements at KP28 + 300; (b) Graph of Ground Deformation Rates for SBAS-InSAR, PS-InSAR and GPS Measurements at KP52 + 500; (c) Regression Analyses between SBAS-InSAR and PS-InSAR Ground Deformation Rates at KP28 + 300; (d) Regression Analyses between SBAS-InSAR and PS-InSAR Ground Deformation Rates at KP52 + 500.

The spatial distribution and variation of ground movement processes along pipelines demonstrated that general geological and geotechnical understanding of the study area is not sufficient to find and mitigate all the critical areas of subsidence and uplifts for the pipeline operators. The prediction of the potential subsidence or uplift locations based on the field visual verifications holds a lot of uncertainties without wide and detailed scale airborne and satellite space observation technologies. The justification of the budget for the geotechnical maintenance activities along long-range oil and gas pipelines requires sophisticated prioritization and planning of the remediation sites and clear quantitative and qualitative risk assessment proving the activeness of these sites and effectiveness of the remediation measures.

Even though SBAS-InSAR demonstrated a reliable approach for the detection of ground deformation processes along petroleum and gas pipelines, it is highly recommended to advance these studies with the integration of other geological, geotechnical, thermal and climatic information to better understand controlling natural and man-made factors.

IV. Conclusions

Both SBAS-InSAR and PS-InSAR techniques showed that the continuous subsidence was prevailing in the kilometer range of 13-70 of oil and gas pipelines crossing two seismic faults. The ground uplift deformations were observed in the pipeline kilometer range of 0-13. Although both PS-InSAR and SBAS-InSAR measurements were highly consistent in deformation patterns and trends along pipelines, they showed differences in the spatial distribution of ground deformation classes and noisiness of produced results. High dispersion of PS-InSAR measurements caused low regression coefficients with SBAS-InSAR for the entire pipeline kilometer range of 0-70. SBAS-InSAR showed better performance than PS-InSAR along buried petroleum and gas pipelines in the following aspects: the complete coverage of the measured points, significantly lower dispersion of the results, continuous and realistic measurements and higher accuracy of ground deformation rates against the GPS historical measurements. As a primary factor of ground deformations, the influence of tectonic movements was observed in the wide scale analysis along 70 km long and 10 km wide section of petroleum and gas pipelines; however, the largest subsidence rates were observed in the areas of agricultural activities which accelerate the deformation rates caused by

the tectonic processes. The diverse spatial distribution and variation of ground movement processes along pipelines demonstrated that general geological and geotechnical understanding of the study area is not sufficient to find and mitigate all the critical sites of subsidence and uplifts for the pipeline operators. This means that both techniques outlined in this paper provide a significant improvement for ground deformation monitoring or can significantly contribute to the assessment of geohazards and preventative countermeasures along petroleum and gas pipelines.

Acknowledgements and Funding. The authors would like to thank Nazarbayev University. This research was funded by the Nazarbayev University through the Social Policy Grant and the Faculty-development Competitive Research Grant (FDCRGP) - Funder Project Reference: 080420FD1917.

References

- [1] Berardino, P., Costantini, M., Franceschetti, G., Iodice, A., Pietranera, L., Rizzo, V. (2003). Use of differential SAR interferometry in monitoring and modelling large slope instability at Maratea (Basilicata, Italy). *Eng. Geol.* 2003, 68, 31–51.
- [2] Hole, J., Holley, R., Giunta, G., Lorenzo, G., Thomas, A. InSAR assessment of pipeline stability using compact active transponders. In *Proceedings of the Fringe 2011, Frascati, Italy, 19–23 September 2011*; p. 53.
- [3] Imamoglu, M., Kahraman, F., Çakir, Z., Sanli, F.B. 2019. Ground Deformation Analysis of Bolvadin (W. Turkey) by Means of Multi-Temporal InSAR Techniques and Sentinel-1 Data. *Remote Sens.*, 11, 1069.
- [4] Lauknes, T.R., Dehls, J., Larsen, Y., Høgda, K.A., Weydahl, D.J. (2005). A comparison of SBAS and PS ERS InSAR for subsidence monitoring in Oslo, Norway. In *Proceedings of the Fringe 2005 Workshop, ESA ESRIN, Frascati, Italy, 28 November–2 December 2005*.
- [5] Ferretti, A., Fumagalli, A., Novali, F., Prati, C.; Rocca, F., Rucci, A. (2011). A New Algorithm for Processing Interferometric Data-Stacks: SqueeSAR. *IEEE Trans. Geosci. Remote Sens.* 49, 3460–3470.
- [6] Osmanoglu, B.; Sunar, F.; Wdowinski, S.; Cabral-Cano, E. (2016). Time series analysis of InSAR data: Methods and trends. *ISPRS J. Photogramm. Remote Sens.*, 115, 90–102.

CREATING FOREST CARBON LANDFILLS: FOREST CARBON

Rustam Gakaev, Magomed-Sadyk Bahaev, Islam Gumaev

•

Kadyrov Chechen State University, Russia
rustam.geofak@yandex.ru

Abstract

Currently, significant attention is paid to environmental issues at all levels of management. Over the long history of human civilization, significant environmental damage has been accumulated, because not only large-scale industrial production, but also ordinary human life leads to the formation of a significant amount of harmful products that pollute the atmosphere, soil, and water spaces. The huge scale of the accumulated damage makes it necessary to resolve environmental issues at the highest level - the level of international organizations and the leadership of individual states. At the same time, interest in the environmental agenda is connected both with the health of the population and with economic aspects, because in the near future in Europe, and then, possibly, in Russia, much more significant taxes and fines for non-environmentally friendly production and products will be introduced. Among a significant number of important environmental issues of our time, one of the most acute is the issue related to emissions of the so-called greenhouse gases (primarily carbon dioxide CO₂ and methane, but also other gases) and the environmental damage resulting from this phenomenon.

Keywords: gas emissions, forest carbon, climate change, carbon landfills, environmental protection, Forest Carbon.

I. Introduction

Carbon landfills play a key role in the study of greenhouse gas emissions (Fig.1) and their impact on climate change, as well as in the development of strategies to combat this phenomenon. To estimate annual changes in carbon stocks, it is necessary to have a sufficient number of carbon landfills to cover a significant part of the territory of Russia. To assess the annual changes in carbon stocks in the forests of Russia, it is necessary to have carbon polygons for all types of forests in various climatic zones. There are more than 70 types of forests and more than 10 climatic zones in Russia, so several thousand carbon polygons need to be created to cover the territory sufficiently. In addition to forests, it is also necessary to estimate carbon stocks in soils, water ecosystems and other natural objects. This also requires the creation of carbon landfills in the respective territories. There are currently 17 carbon landfills operating in Russia, many of which are collaborating with leading Russian universities dealing with climate change issues.

Forests, in turn, are the main natural sink of greenhouse gases in terrestrial ecosystems in the world. As the world's leading forest power, Russia has natural natural capital in the form of forests accumulating 625 million tons of greenhouse gases annually. This gives Russia a significant competitive advantage, since the absorption of greenhouse gas emissions by forests occurs without significant costs from the state, the cost of measures to reduce emissions - for example, to extinguish forest fires - is moderate (3 billion rubles per year) compared to other types of measures, for example, to increase energy efficiency in industry. In general, in Russia there is a

huge and still not used reserve for reducing the carbon footprint of products due to the existing protective and other categories of forests on agricultural lands. Forests located on agricultural land are of great importance for the absorption of greenhouse gases [1]. If 1 hectare of forests on the lands of the forest fund absorbs on average about 1 ton of greenhouse gases per year, then 1 ha of protective and anti-erosion forests on agricultural lands - about 7 tons per year, i.e. 7 times more. At the same time, according to various estimates, from 40 to 90 million hectares of agricultural land in Russia are overgrown with forests, which are not yet taken into account in the national statistics of greenhouse gas absorption due to the fact that they do not belong to managed forests.



Fig. 1: CO₂ Emissions by Country 2023

Forest breeding should be aimed at obtaining varieties and species with high growth rates and high potential for carbon sequestration in the climatic conditions of Russia [7]. In recent years, along with the active spread of state regulation systems for greenhouse gas emissions, as well as various sectoral emission regulation systems, voluntary carbon offsetting schemes have been rapidly developing based on the implementation of investment projects. Voluntary carbon markets are platforms for the implementation of transactions for the sale and purchase of greenhouse gas emission reduction units.

II. Methods

Carbon farming by creating carbon farms is an innovative way of agriculture/forestry to sequester carbon in the soil (Fig.2). A carbon farm can be located on forest fund lands and on lands of other categories, for example, agricultural purposes (old arable land). In the first case, the carbon farm will be forest plantations - forest plantations, in the second case, the farm will be represented by both forest plantations and agricultural land. When creating forest plantations used as carbon farms, it is important to take into account the period of their operation, the main tree species, and the technology of creation. In the present study, we limited ourselves to a carbon farm, represented by a forest plantation with monocultures of poplar and pine.

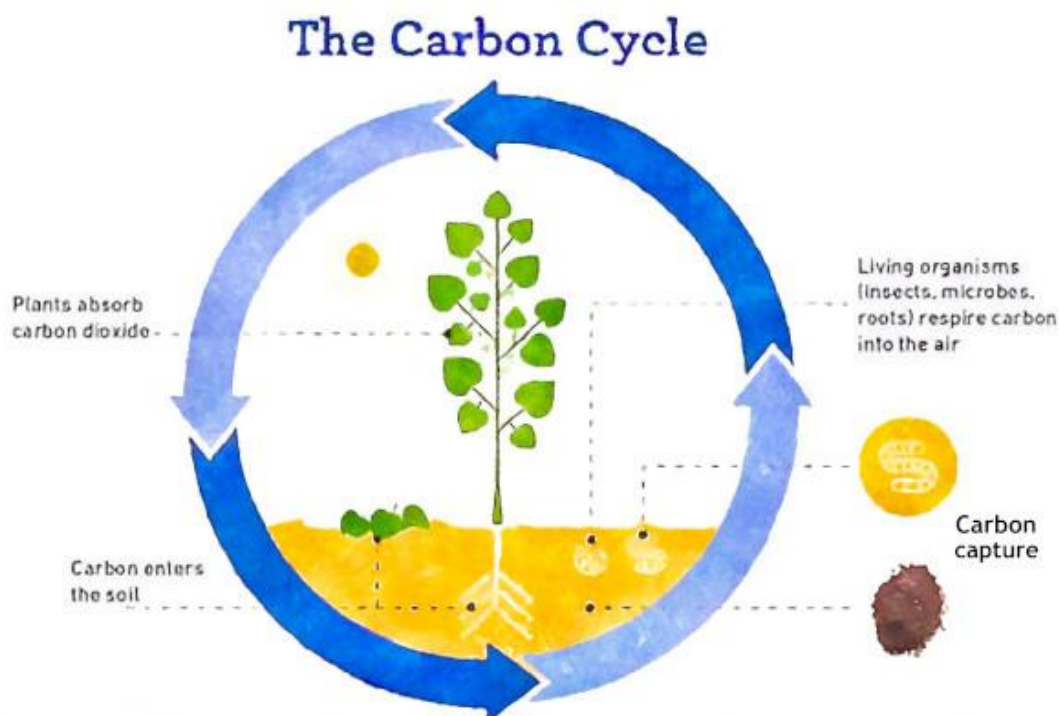


Fig. 2: Carbon farming

Seedlings with a closed root system were used to create forest plantations. At the first stage, the organization of the carbon farm included the preparation of a forestry area for the creation of a plantation (clearing the territory), the second stage included plowing, disking and cultivating the soil, fertilizing [3]. The third stage, the actual planting of seedlings with a closed root system, was characterized by the greatest labor and material intensity of work. The cost of creating one hectare of a carbon plantation is presented in Table 1 and amounts to 239.89 thousand rubles. In subsequent years, it is necessary to spend 64.0 thousand rubles on the organization of care work and maintenance of the plantation. Thus, the cost of creating and maintaining 1 hectare of poplar plantations, with a density of 2.5 thousand per piece. ha, felling age of 50 years is 303.9 thousand rubles.

The creation of carbon polygons is possible on the basis of public-private partnership, with the combined efforts of science, business and government. The reason for this lies in the presence of significant risks, determined by the long-term nature of the project to create carbon farms, the presence of uncontrollable climatic factors, as well as the possibility of forest fires and diseases of forest plantations. The risks of creating carbon farms can also lie in the economic plane and be associated with technological and market changes, which requires a balanced approach when launching carbon projects. In order to minimize the consequences of risky events, we consider it necessary at the first stage to organize a network of carbon test sites. To implement this actual practice-oriented task, there are the following prerequisites [2]:

- The Chechen Republic, geographically located on the border of the forest and steppe zones, is the most vulnerable to climate change and, therefore, needs measures to adapt ecosystems, including through the conservation and cultivation of forests;

- the key measure to reduce the greenhouse effect is the creation of artificial green spaces in non-forest areas and on forest lands, where, due to a number of circumstances, natural reforestation does not occur;

- a high concentration of specialized scientific organizations with a scientific background and competent personnel in the field of monitoring forest ecosystems and assessing ecosystem services;

- university researchers have already obtained promising tree species for the purposes of afforestation and the creation of carbon landfills, which are distinguished by stress resistance, high growth rate and productivity;

Table 1: *Cost of creation, maintenance (standard costs) of 1 hectare of poplar forest plantations, density 2.5 thousand pieces/ha, felling turnover 50 years, rub.*

Enlarged types of work included in the technology	Required number of people o-days	Costs for the maintenance and operation of equipment	General payroll	Payroll accruals 30.9%	Cost of basic materials	Total production cost
Preparatory work	7,02	617,99	5997,13	1853,1	27812,18	36280,40
Site arrangement	3,44	296,48	2963,98	915,86	17311,79	21488,11
Establishing a plantation by planting seedlings	4,77	426,2	4354,0	1345,38	176003,3	182128,76
Care and maintenance of plantations	32,64	5182,74	26498,94	8188,17	24131,50	64001,35
Total cost						303898,62

III. Results

As of January 1, 1991, the forested area within the Chechen-Ingush Republic was 285 thousand hectares, of which 7.8 thousand hectares were coniferous. The total stock of forest plantations at that time was estimated at 41.5 million cubic meters, and the stock of mature and over nature timber at 8.6 million cubic meters. The estimated cutting area for the main use was 88 thousand cubic meters. Occupying one fifth of the territory of the republic, forests consist of high-quality species, where valuable hard species predominate - beech, hornbeam, ash. In orchards and forests there are significant reserves of the most valuable furniture and ornamental wood - apple, pear, cherry and other fruit trees. All this can serve as a basis for the development of the furniture industry in the republic, capable of producing high-quality furniture from solid wood and fine veneer. The role of forest resources in the national economy of Chechnya did not remain constant. In the pre-revolutionary past, wood served as the main building material, and firewood made up the vast majority of the fuel balance. During the formative years of the logging industry, woodworking served as the basis for its industrial development. As the economic complex of the republic developed on the basis of the accelerated growth of the fuel and energy, petrochemical and machine-building groups of production, the share of the forest industry in the industry of the republic gradually decreased [3]. By the beginning of the crisis, the timber and woodworking industry was a complex of industries that ensured the cultivation and exploitation of timber, its processing into lumber and the production of furniture.

Agroforestry combines trees with other agricultural land uses such as field crops and livestock. In addition to saving production, agroforestry can remove carbon dioxide (CO₂) from the atmosphere because trees themselves capture and store carbon and increase carbon in the soil around them. Agroforestry comes in many varieties (Fig.3). Examples include forest pastures where animals graze under trees; inter-row and alley crops, in which other crops are planted

under trees or between trees; hedgerows and windbreaks in which rows of trees or woody shrubs separate areas of agricultural land; as well as pasture gardens in which animals graze under fruit trees.

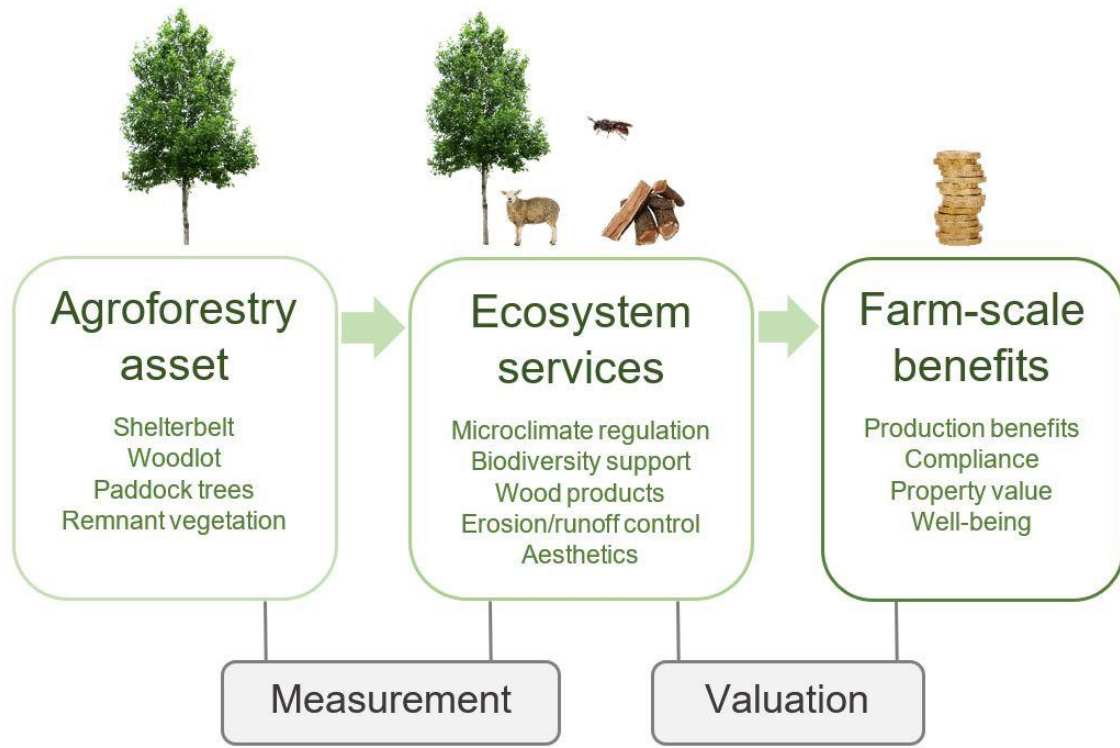


Fig. 3: *Agroforestry Decision-Making at the Farm Scale*

Co-benefits and challenges: - Food security: instead of competing with arable land, agroforestry coexists with food production; diversifies crop production and, in some cases, increases yields (for example, by improving soil quality or crop shading). - Commercial products: Agroforestry can diversify income sources by providing commercial products such as timber and non-commercial inputs such as firewood. - Ecological benefits: Trees and shrubs can contribute to the conservation of biodiversity by providing habitat; reduce erosion and improve air, water and soil quality. - Possibility of reduced yields: In some cases, agroforestry systems will produce less yield per hectare than field crops, potentially reducing farm income, especially in the short term. - Saturation: Trees can only hold a finite amount of carbon; they will eventually stop removing additional CO₂. - Reversible [4]: Carbon captured by trees can be released if trees burn, die, or are destroyed by land-use change. - Difficult to measure: Monitoring and verifying carbon removal through agroforestry is difficult and expensive. Possible scale and cost. Different approaches to agroforestry can be applied at different scales and sequester CO₂ at different rates. For example, installing windbreaks can capture 20 tons of CO₂ per square kilometer per year, while growing alley crops can capture 120 tons of CO₂ per square kilometer per year. Carbon sequestration rates also vary by region, ranging from 954 tons of CO₂ per square kilometer per year in semi-arid areas to 3,670 tons of CO₂ per square kilometer per year in humid regions. Costs also vary by practice and region. Many approaches offer very high ROI but may include high upfront costs [5]. Technological readiness. Agroforestry is an ancient, established practice that is ready for further development. As of 2010, agroforestry occupied approximately 43% of the world's agricultural land, including any agricultural land with at least 10% tree cover. This is about one billion hectares of land, which is equivalent to the land area of Canada. Current barriers to agroforestry expansion tend to be social, financial and infrastructural rather than technical: Governance and development

issues. Robust incentives, agricultural extension services, financing, input subsidies and other policies can help overcome barriers. In addition, processes, standards and technologies need to be developed to reliably measure carbon sequestration in biomass and soil under forests.

To overcome the negative consequences and ensure the rational use of the forest fund, the following is required:

1. Carrying out forest management.
2. Construction (rehabilitation) of administrative buildings (offices of forestries and forestries).
3. Restoration of the nursery.
4. Restoration of the production base.
5. Acquisition of means of communication.
6. Acquisition of a motor and tractor fleet.
7. Construction of roads for forestry purposes.
8. Construction (restoration) of cordons.

Restoration of the timber industry complex of the republic is possible if the industrial processing of wood is put under strict control and the balanced consumption of renewable resources. The development of forest areas should be entrusted to a limited circle of specialized enterprises. Which, in turn, should, along with the harvesting and processing of wood, be engaged in the systematic planting of young animals. Enterprises that have received licenses to conduct logging activities must also have targeted funding. In terms of commercial timber harvesting - targeted lending, in terms of planting young trees - budget financing with a fixed amount of work. Targeted loans allocated to operating specialized enterprises should be used to purchase new technological equipment, which should increase the level of integrated use of wood raw materials. The new equipment should include machines and units that make it possible to produce medicines, food and feed additives, sorbents, biologically active substances and other products from wood waste that meet the needs of the region. However, in the short term, the republic needs to restore and develop the timber and woodworking industries. It is economically efficient to single out three woodworking enterprises to be restored, which will have to organize a network of raw material logging organizations [6]:

- State Unitary Enterprise "Alkhan-Kalinsky woodworking plant". The company previously specialized in the production of chipboard, sliced veneer, synthetic resin, wood harvesting and processing. The restoration program provides for the development of additional nomenclature (parquet, CMP, furniture and joinery production) with an annual output of marketable products worth 30.0 million rubles, the number of employees is up to 220 people.

- State Unitary Enterprise "Grozny Experimental Furniture Factory". Specialized in the production of office and upholstered furniture. The restoration program provides for the development of additional nomenclature (office furniture, kitchen furniture, for medical and medical institutions, carpentry) with an annual volume of up to 40 million rubles, the number of employees is up to 180 people.

- State Unitary Enterprise Grozny Furniture and Woodworking Plant. Specialized in the production of upholstered furniture. The restoration program provides for the development of additional nomenclature (the production of chairs, the production of highly artistic furniture from hardwood, the production of armchairs and kitchen furniture. At present, investments are already being made to restore the Grozny furniture and woodworking plant, the Alkhan-Kalinsky DOK, the Fagus State Unitary Enterprise and the Druzhba cardboard factory. The cardboard factory is able to meet local demand for the simplest products - stationery, school supplies, writing materials, cardboard packaging and containers, labels, advertising booklets [5]. In the opinion of experts, it is advisable to consider the construction of a small enterprise for processing waste paper into sanitary and hygienic products. In view of the fact that the modern furniture market in Russia is highly monopolized, and equipment for furniture production is expensive and scarce, an external investor is needed who will bear the costs of purchasing equipment, training personnel and the risks of selling finished products in exchange for production facilities and tax benefits

from the government of the republic. Currently, the leading furniture manufacturer in the North Caucasus is the Kavkaz company, it is possible to attract its investments, another option is to look for a foreign investor. This, for example, can be the German company Schieder Mobel Holding, which has begun to actively intervene in the Russian upholstered furniture market and is looking for a territory for building a factory in the North Caucasus, as well as the Swedish trading company IKEA [6]. Among the range of finished products possible for the production, we can especially recommend the manufacture of medical furniture. This production in Russia is poorly developed, and the demand for these products is huge. It is possible to organize the production of school furniture, cabinet furniture and wardrobes in the republic on the basis of the restoration of production teams and production facilities of the Terek furniture association and the Grozny furniture factory.

IV. Discussion

The forests of the region are under the strongest pressure, which is presented in the reviews of national forests and the forest sector. At the same time, the types of negative impact on forests in the region are quite similar and are given below. Demand for fuel wood by local residents leading to illegal/over-logging. Rural poverty is widespread in the region, and modern fuels are expensive since the collapse of the Soviet internal trade system. In many cases, there are few alternative sources to wood for cooking and heating in rural communities, especially during harsh winters. As a result, legal and illegal timber exports are at a high level [7]. This pressure is exacerbated by the use of inefficient stoves, as more wood is needed for the same level of heat supply. It should be noted that in countries where the government has been able to provide modern fuels such as gas at an affordable price, illegal firewood harvesting has been significantly reduced - this applies to countries that now have access to modern fuels. Depending on the institutional environment, the villagers either harvest the wood themselves or supply it from local forestry enterprises and intermediaries. Saxaul forests are particularly vulnerable due to the small stock of timber (more wood harvesting area is required to meet demand), and successful natural reforestation does not occur after felling due to harsh climatic conditions, dry and saline soils.

In the Caucasus, half of the population lives in rural areas and is highly dependent on agricultural activities, despite the lack of quality arable land. As a result, the well-being of the local population depends on the grazing of livestock - goats, sheep and horses. Land tenure systems vary between countries, but animals often graze on public lands to which all residents have access, including lands with and without forest cover and lands of the state forest fund. In fact, a significant part of the lands of the state forest fund is officially allocated for livestock grazing. Grazing management on public lands is often one of the main activities of local forest enterprises. Many sources report that overgrazing is putting pressure on forests that are being degraded by too many grazing animals, hindering forest restoration and contributing to the loss of forest cover.

- Irrigation projects have been implemented along the rivers, mainly for cotton and wheat, and hydropower facilities have been built [8]. As a result, floodplain forests (tugai) were destroyed in some areas. In addition to the anthropogenic pressures mentioned above, the region's forests are vulnerable to a wide range of natural disasters, including erosion and soil loss, landslides in mountainous areas as well as along watercourses, desertification, increased soil salinity and sandstorms. They are vulnerable to these non-anthropogenic impacts and, at the same time, play an important role in combating them.

The forests of the Caucasus protect the ecosystems and population of the region from a wide range of natural disasters, including erosion, reduced soil fertility and the threat of landslides in mountainous areas, reduced evaporation and desertification, soil salinity, and sandstorms. As a rule, in such cases, the very presence of a healthy forest ensures the fulfillment of protective

functions. These services are seen in the region as a common good, provided free of charge by national governments. This situation was recognized by the Soviet authorities in the 1950s and 1960s, when practically all forests in the region were assigned to the first group². Although classification and administrative systems vary from country to country, the paramount importance of the forest protection function is recognized formally and at the highest political level throughout the region. In most of the region's forests, logging for the purpose of timber harvesting is prohibited or strictly limited. The proportion of forests formally "dedicated to protection" varies from 50 to 100%, but in practice the protection function takes precedence, at least in theory, over all other forest functions in all parts of the region. According to data collected for the Forest and Forest Sector Reviews, mainly through the FRA process but with little cross-country comparability, over 15 million ha have "defined management objective to maintain and enhance their protective functions", representing almost 90% of the region's forests. It is not possible to quantify the protective effects of actual or potential loss or degradation of forests in terms of erosion, loss of soil fertility, increased salinity, accelerated desertification, increased sandstorms, etc. Such a quantification, both physically and economically, will provide a powerful argument in political discussions about the resources needed to protect forests. It is very likely that the benefits to the ecosystems and economy of sustainably managed protective forests outweigh the economic costs of managing and protecting these forests. However, currently there is no system of payment for forest ecosystem services in the region, although the importance of these services is officially recognized [9].

In many cases, non-timber forest products and services play a more important role in rural livelihoods than timber supplies. These types of products may take different forms depending on local conditions. Some of these are briefly listed below:

- Livestock grazing is often a key service that uses both the surrounding forests and forest land as grazing land. In some cases, forest managers use areas for grazing personal livestock, especially if local forest enterprises are responsible for pastures and forest land. In other cases, livestock owners use forest/pasture land, either through a system of public rights or through forest use fees. In many cases, it appears that overgrazing is permitted or cannot be prohibited, even if it causes forest degradation or destruction. Depending on existing arrangements (which vary widely), most participants do not have long-term tenure rights, so they have no incentive to manage forests and use pasture resources in a sustainable manner. In the 2015 FRA, many countries listed hay as a non-wood product supplied by forests, which is clearly related to livestock grazing.

- Honey and medicinal herbs are also collected and then sold or consumed by the locals.
- Some forest enterprises sell seedlings that they grow in their seed nurseries. This can be a very profitable undertaking.
- Georgia exports flower bulbs (*Galanthus woronowii* and *Cyclamen coum*) and tree seeds (*Abies Nordmanniana*).
- A tourist destination is developing in some forest areas.
- Hunting is also of great importance, both for obtaining fur and meat and trophies, mainly for foreign tourists who are willing to pay big money for pleasure. Income from the sale of non-timber products and services can play an important role in the livelihoods of people dependent on the forest, although neither this aspect nor the quantity or value of the products harvested appear to be known or investigated with certainty.

All countries in the region reported to the UNFCCC on their greenhouse gas (GHG) balances, including net GHG sinks to forest ecosystems, or emissions. This used the IPCC reporting guidelines for available forest data in their countries. Reports show that the net annual GHG sink to the forest ecosystems of the Caucasus and Central Asia – carbon sequestration – is about 25 Mt CO₂ equivalent (t CO₂ eq).

Acknowledgments. The work was carried out within the framework of the state assignment of the Ministry of Science and Higher Education of the Russian Federation (topic No. 075-03-2021-074 / 4).

References

- [1] Ostapenko B.F., Classification of forest types and forest typological zoning of the Northern slope of the Greater Caucasus. // Tr. Kharkov Agricultural Institute. Kharkiv, 2019.
- [2] Gakaev R.A., I.A. Bayrakov, M.I. Bagasheva, Ecological foundations of the optimal structure of forest landscapes in the Chechen Republic. In the collection: Environmental problems. A look into the future. Proceedings of the III scientific-practical conference. Executive editor Yu.A. Fedorov. 2006.pp. 50-52.
- [3] Gakaev R.A., Comprehensive assessment of the current state of the mountain-forest landscapes of the Chechen Republic and measures for their optimization. In the collection: Modern problems of the geocology of mountain areas, 2008.pp. 189-194.
- [4] Silva L.C.R., G. Sun, X. Zhu-Barker, Q. Liang, N. Wu, W. R. Horwath, Tree growth acceleration and expansion of alpine forests: The synergistic effect of atmospheric and edaphic change. *Sci. Adv.* 2, e1501302 (2021).
- [5] Earles J. M., O. Sperling, L. C. R. Silva, A. J. McElrone, C. R. Brodersen, M. P. North, M. A. Zwieniecki, Bark water uptake promotes localized hydraulic recovery in coastal redwood crown. *Plant. Cell Environ.* 39, 320–8 (2020).
- [6] Salamova A.S., Socio-economic factors in the fight poverty and hunger in the modern world: the scientific approach of Amartia Kumar Sen, 2023, 17(1), pp. 237-245.
- [7] Salamova A.S., Global networked economy as a factor for sustainable development, 2020, p. 03053.
- [8] Dixon R.K., S. Brown, R. A. Houghton, A. M. Solomon, Global Forest Ecosystems. *Science*, 263:185–190 (2019).
- [9] Novara A., T. La Mantia, J. Rühl, L. Badalucco, Dynamics of soil organic carbon pools after agricultural abandonment. *Geoderma*, 235-236: 191-198 (2019).

EVALUATING MEASURES TO SUPPORT DRYLAND RURAL POPULATIONS UNDER HIGH CLIMATIC UNCERTAINTY AND RISK: THE EXAMPLE OF THE ARAL SEA REGION

Georgy Fomenko¹, Marina A. Fomenko²

¹Institute for Sustainable Innovation, Yaroslavl, Russia

²Cadaster, Scientific-Production Enterprise, Yaroslavl, Russia

info@npo-kad.ru

Abstract

Evaluating international technical assistance projects usually calls for assessing the efficiency and effectiveness of planned indicators. As climatic uncertainty and risk increase, there is a need to improve approaches to assessing the activities of such projects. Using the example of a project to adapt dryland dehqan households, cooperatives, and farms in the Aral Sea region (the Republic of Karakarpakistan in Uzbekistan) to climate change, this research methodically substantiates a set of indicators to assess the long-term effectiveness of adaptation measures. With regard to humanitarian support measures (which are strengthening the hydrometeorological monitoring network, creating early warning systems, raising public awareness about various climate threats and possibilities to reduce their negative consequences, and reclaiming the dried-up Aral Sea bottom to reduce dustiness) that pursue noneconomic goals, an assessment was made against previously established project performance indicators. With regard to ensuring the viability of dehqan households, cooperatives and farms over the long term, this research proves the need in evaluating the effectiveness of agronomic, water-saving, and landscape adaptation measures as a combination of private benefits (economic efficiency) and public goods (social and environmental efficiency). These evaluation indicators will help identify the most promising, effective and efficient practices to replicate in future projects.

Keywords: drylands, climatic vulnerability, climatic uncertainty, climate risk, climate change adaptation technologies, project effectiveness

I. Introduction

As climate uncertainty and risk¹ increase, international development technical support programs must increasingly focus on poverty-reduction strategies, with an emphasis on developing livelihood opportunities for the poorest people, primarily through the transfer of new knowledge and technologies. Thus, there is a demand to review the objectives and priorities of support programs and adjust the performance and evaluation indicators.

Research in this direction was carried out in the southern Aral region (in Uzbekistan, in the Republic of Karakalpakstan) in 2019 in five districts most vulnerable to climate change,² where a set of targeted measures³ of climate-resilient and resource-saving agricultural practices have been

¹ Risk is a kind of uncertainty when the probability of an occurring event can be determined.

² The areas have been recognized as the most affected by the environmental impact of the Aral crisis and, as a result, the most at risk of losing development capacity.

³ The project activities in the pilot areas resulted in implementation of training activities and measures to reduce dusting in the Aralkum Desert, followed by the creation of 17 intensive gardens with drip irrigation

implemented through the transfer of adaptation technologies. The main objective was to develop a system of indicators for evaluating project activities (a set of agronomic, water-saving, and landscape adaptation measures) that reflected their effectiveness, long-term efficiency, and opportunities for further replication in other regions.

II. Materials and methods

Increasing climate uncertainty and risk are changing the households' lifestyle in the drylands. Such lands occupy 41% of the world's land surface [1] and are populated by more than 2.5 billion of the world's poorest, least healthy, and most marginalized people [2]. Drylands in poor countries are "investment deserts," except where valuable minerals attract targeted investments. The modern desertification paradigm (DP) focuses on the loss of ecosystem services when pastures are converted (due to mismanagement and exploitation of natural resources in drylands) into desert-dominated lands with low biological productivity and plants that are of little use for livestock. However, drylands have valuable assets that are often underestimated: for example, abundant solar energy, plant biodiversity, and significant potential to increase soil carbon storage. Moreover, these lands feed 50% of the world's livestock with the use of the latest technologies (hydroponics, laser land leveling, etc.) [3, 4].

This complex use of drylands under high climate uncertainty and risk is based on the resilience paradigm of Human-Dominated Ecosystems (HDE). Some experts consider an HDE's ability to maintain its functional integrity by adapting to variable factors⁴ as a property or a path to system stability under stress [5, 6].

For external targeted extra-economic (environmental, etc.) interventions in HDEs to have any chance of success after the completion of technical assistance projects, drylands need development tools that encourage the long-term sustainability of transferred innovations and technologies – tools such as domestic financial flows, support systems and infrastructure, a nurturing institutional environment, and climate risk insurance, among others. The useful method to assess efficiency of project activities is a multicriteria cost-benefit analysis (CBA), which provides for the use of the full economic value and wide use of expert assessments. They allow us to obtain aggregate indicators of the effectiveness of project and planning decisions in situations (1) where households and small producers lack (or have no) primary accounting; (2) where public goods (environmental, social) are being evaluated, since it is difficult to make in monetary terms. As for the measurement of sustainability/resilience of the development of a region, a set of relevant indicators is formed by the three components of sustainability capital: the economy, the environment, and the social sphere. In this context, the assessment of project activities in terms of improving the resilience of regions is carried out using the rapid impact assessment matrix (RIAM).

These assessments allow to represent the real impact of project practices and services on the resilience of agricultural systems [7, 8], as well as to compare different project options and

over an area of 34 hectares; implementation of 17 hydroponics units with a total capacity of 8.5 tons of green fodder per day (in pasture cooperatives and large farms); and 24 mini hydroponics units with a total capacity of 1.92 tons of green fodder per day (for small commodity producers – owners of homestead lands, and *dehkan* households); transfer of 9 hydropumps to improve irrigation conditions in collective farms (pasture cooperatives); supply of agricultural equipment (14 laser sowers, 15 laser levelers, tractors, attachments for agricultural work, etc.); and the transfer of greenhouses to domestic and collective farms, beehives for organized apiaries, etc. The overall project will lead to the creation of growth points for a new environmental management system.

⁴ At present, no scientific method can accurately predict the long-term evolution and spatial distribution of droughts and storm surges, and the impact on the infrastructure of society is not quantified. Modern risk analysis methods make it possible to determine the vulnerability of individual system components to an expected adverse event and to quantify the loss of system functionality due to that event.

development scenarios. Information on climate risks also adjusts data on expected net profits or losses, helps in the development of financial instruments for investing in ecosystem conservation.

III. Initial data and information

Research on measuring climate adaptation of rural populations in the drylands of the Aral Sea region was carried out under the United Nations Development Program (UNDP) project, "Developing Climate Resilience of Farming Communities in Drought-Prone Parts of Uzbekistan" (hereinafter "the project"). The research focused on developing a system of indicators to assess the efficiency of project activities in the process of transferring technologies for adapting to climate change to *dehkan* households, cooperatives, and farms, their efficiency at supporting life, and their long-term sustainability. The work was performed on five pilot sites in the Republic of Karakalpakstan: (1) in Muynak district – transfer of hydroponic facility for production of green fodder and intensive landscaping with a drip irrigation system to the pasture cooperative⁵; (2) in Kegeyli district – transfer of hydroponic facility for production of green fodder, intensive landscaping with a drip irrigation system and hydropumps for irrigation of green fodder to the pasture cooperative; (3) in Takhtakupyr district – transfer of hydroponic facility for production of green fodder to the *dehkan* household⁶; (4) in Kanlykul district – transfer of laser land levelling in combination with a moldboard-less seeder to the farm⁷; (5) in Chimbai district – transfer of greenhouse for year-round cultivation of vegetables and greenery and apiary to the *dehkan* household.

The research information base included (1) official statistical and non-statistical data; and (2) expert data, including results of interviews and focus groups with the individual beneficiaries of the adaptation technology and other stakeholders, information about and analytical and monographic materials related to the implementation of these technologies.

IV. Results

In accordance with the adopted research methods, a complex system of project assessment indicators was developed, consisting of three interrelated sets of indicators.

1. Performance evaluation indicators of the overall project

The first set of project assessment indicators, as shown in Table 1, contains four performance evaluation indicators, which are defined on the basis of the expected results of the project in relation to the beneficiaries and the relevant pilot sites in the following areas: (1) developed institutional capacity and established mechanisms for drought risk management and early warning; (2) climate-resilient farming practices applied in *dehkan* households; (3) adaptation measures to protect soil and retain moisture to improve climate resistance; (4) acquired and

⁵ An agricultural cooperative (*shirkat*) is an independent economic entity with the rights of a legal entity, based on a shared and mainly family (collective) contract, a voluntary association of citizens for the production of commercial agricultural products. Law of Uzbekistan on agricultural cooperatives (*shirkat*), April 30, 1998, 600-I; Vedomosti Oliy Majlis of Uzbekistan, 1998, 5–6, Article 84; 2003, 9–10, Article 149; and 2004, 1–2, Article 18; Collection of Legislation of Uzbekistan, 2008, 52, Article 513; 2009, 52, Article 555; and 2013, 1, Article 1; and National Database of Legislation, 21.03.2019, 3/19/531/2799).

⁶ A *dehkan* household is a small family-owned household that produces and sells agricultural products based on the personal work of family members on the land provided to the head of the family in the lifetime inheritance (Part 1 of Article 1 as amended by the Law of Uzbekistan, "On the *dehkan* household", December 21, 2018, ZRU-506 - National legislation database, 21.12.2018, 3/18/506/2356).

⁷ A farm is an independent business entity with the rights of a legal entity, based on the joint activities of members of the farm, with commercial agricultural production on the land provided in the long-term lease (Article 3 as amended by the Law of Uzbekistan "On Farming," April 18, 2018, ZRU-476 - National Database of Legislation, 19.04.2018, 03/18/476/1087).

widely available knowledge about climate-resilient agricultural production systems, including crop and livestock production in drylands.

The evaluation of the project's current performance showed that significant success has already been made to date in establishing a sustainable system to transfer knowledge and skills. This research found that project activities led to reductions in climate vulnerability for all individual beneficiaries, based on climate vulnerability index calculations performed in accordance with Hinkel's methodology [9]. The project results varied among the pilot sites, and the decrease in climate vulnerability was also uneven among pilot sites.

2. Benefits to individual beneficiaries and the community

The second set of project assessment indicators evaluate the effectiveness and viability of the project's long-term results. The assessment was carried out by comparing two options –with project implementation (expected) and without it (baseline), using the developed within the Project "Methodological recommendations for 'fast-track' assessment of the efficiency of pilot projects to ensure climatic sustainability of farms located in the arid regions of Uzbekistan" and a list of factors/criteria for assessing the efficiency of adaptation technologies at pilot sites. The assessment was carried out in points for the accepted indicators, according to the possible estimated values and the significance of each indicator (see Table 4). The results of assessing the efficiency of adaptation technologies at pilot sites (in terms of the aggregate of the economic benefits of individual beneficiaries and public goods – social, economic and environmental) are presented in Table 1.

Findings showed that drip irrigation led to maximum efficiency (111 and 112 points), allowing dryland farmers to obtain consistently high yields of agricultural crops and avoid increased soil salinization, which is very important due to the already saline soils of Karakalpakstan. Minimal efficiency was noted in a small greenhouse (65 points) at pilot site 5, mainly due to small volumes of marketable products.

2.1 Individual benefits to farmers

Although this research mainly concerns noneconomic benefits to individual farmers and communities, it still paid attention to the economic benefits of the technologies transferred to farmers and communities in the five pilot projects. Concerning the private economic profit to the individual beneficiaries within the total volume of private and public goods, it was found that the highest income resulted from apiaries and small greenhouses (38% and 36.9%, respectively), mainly due to the intense labor of the owner's family and collaborative workers, mutual trust among these family members and workers, and their respect for the requirements of the owner and their willingness to work whenever it's needed.

2.2 Public benefits and social good

In terms of the public good, the following observations were made. The hydroponic facility in the Muynak and Kegeyli districts had the greatest social effect (32.9%), making it possible to significantly increase and improve the quality of the feed base for livestock breeding and increase the number of livestock. High social benefit for the local community was recorded in the apiary (19%) transferred to the dehqan household (Chimbai district). In terms of the environmental public benefits, the drip irrigation systems transferred to the Muynak and Kegeyli districts were most efficient (57.1%). This was due to large savings in water for irrigating agricultural products (fruits) and, as a result, decreased pressure on the regional aquatic ecosystems.

3. Sustainability

The third set of project assessment indicators evaluates the sustainability of development of territories (in the pilot site areas) as a result of the project implementation, understood as a change in the total wealth (capital) of the territory (in economic, social, and environmental terms). Calculations were made using the Rapid Impact Assessment Matrix (RIAM)⁸ [10, 11];

⁸ This method was successfully applied during the implementation of the "Extended Berlin Geothermal Field Project" to increase electricity production by using geothermal sources; also it was used by the authors in

consequences (positive and negative) were assessed for two options – without implementation of the project activities and with implementation of the project activities. Results confirmed the undoubted viability of project activities for the sustainable development (resilience) of pilot sites at *dehkan* households, pasture cooperatives and farms in all three areas of measured impact: environmental, social, and economic.

Table 1: *Efficiency of Adaptation Technologies, Assessed at Pilot Sites*

Pilot Site	Pilot sites/transferred adaptation technologies	Assessment Estimates, in points			Total points
		Economic benefits to individual beneficiaries	Social	Environmental	
1	Muynak district – Azhiniyaz Jailolari pasture cooperative	46	66	101	213
1.1	Hydroponic facility	26	39	37	102
1.2	Drip irrigation system for fruit production	20	27	64	111
2	Kegeyli district – Kazanketken Jeylovi pasture cooperative	72	85	137	294
2.1	Hydroponic facility	26	31	37	94
2.2	Drip irrigation system for fruit production	20	28	64	112
2.3	Hydropumps for irrigation of green fodder	26	26	36	88
3	Takhtakupyr district – <i>dehkan</i> household hydroponic facility	16	15	28	59
4	Kanlykul district – farm, laser land levelling	26	18	44	88
5	Chimbai district – <i>dehkan</i> household	54	31	59	144
5.1	Greenhouse for year-round cultivation of vegetables and greenery	24	16	25	65
5.2	Apiary	30	15	34	79
TOTAL FOR ALL PILOT SITES		214	215	369	798

V. Discussion

The example of the Aral Sea region confirms the necessity of using three sets of mutually linked assessment indicators in conditions of high climate uncertainty and risk. Such a proposed system should include indicators for 1) assessing the attainment of the established project results, 2) assessing the effectiveness and viability of project results in the long term, in terms of economic benefits to direct beneficiaries and social, environmental, and economic benefits to the local community, and 3) systematically increasing the sustainability of the development of areas where pilot sites are located as a result of implementing such projects.

With regard to humanitarian measures (such as strengthening the hydrometeorological monitoring network, creating early warning systems, raising public awareness of climate threats and methods to reduce their negative effects, and recultivating the bottom of the dried-up Aral

developing a model for sustainable natural resource use of the Arkhyz territory (Russian Federation) and in assessing development options for water supply systems of the Plescheevo Lake basin.

Sea to reduce dust), all of which pursue noneconomic goals, it is appropriate to assess effectiveness, that is, to determine the extent to which measures to reduce climate uncertainty have been implemented and the planned results have been obtained.

In terms of measures to ensure the resilience of *dehkan* households, farms, and cooperatives, attention should focus on assessing the efficiency of agronomic, water-saving, and landscape adaptation measures as a set of private benefits to direct beneficiaries (economic efficiency) and the public good (social and environmental efficiency). Performance indicators (economic, social, and environmental) provide a better understanding of the motivation of specific users to adopt climate-saving practices that take into account adaptation risks and to assess the likelihood that such practices will be adopted, preserved, and provide livelihood opportunities for specific target groups in the long term after external intervention. Performance evaluation also includes indicators that characterize system changes more broadly, specifically in administrative areas where pilot sites for transferring adaptation technology are located. It is advisable to include indicators of sustainable development and a green economy; in the long run, such a system of indicators should be based on methodological approaches of environmental/economic accounting.

The proposed three sets of assessment indicators for evaluating project activities have a sufficiently high potential for use in conditions of increasing climate uncertainty and risk. It is easy to use and does not require significant labor and financial costs.

VI. Conclusions

Thus, complex design solutions that strengthen the resilience of human-dominated ecosystems deserve support if drylands are to be habitable for people in the future. Technical support measures alone are not enough, as new water-saving technologies can be widely and effectively applied only in an information and institutional environment which is suitable to them. For wide use of such technologies in the Aral Sea region it is necessary to establish pasture cooperatives, create a system of technical maintenance, organize sales of products and a reliable energy system. This causes the need for a comprehensive assessment of their effectiveness and efficiency and the use of the system of evaluation indicators developed by the authors. Aggregated evaluation data allow for prompt correction of project activities, in the process of distribution of adaptation technologies in other regions.

Funding and Acknowledgments.

The article has been prepared based on the research results under an agreement between the government of the Russian Federation and UNDP in a partnership within the framework of the regional project "Knowledge Management and Capacity Building in Russia-UNDP Partnership," dated May 15, 2015.

The authors express their deep gratitude to Alexander Merkushev, head of the UNDP/AF/Uzhydromet joint project "Developing Climate Resilience of Farming Communities in the Drought-Prone Parts of Uzbekistan," for valuable advice on the work and suggestions to improve the presentation of research results. Invaluable organizational and expert assistance was provided by the staff of the Nukus Project Office, in particular Azat Teleumuratov and Bakhytbai Aubergenov. Konstantin Loshadkin rendered great assistance in office data processing and calculations; much of the editing work was done by Maria Klemina. Valuable advice was also provided by managers and leading researchers from the Nukus branch of Tashkent State Agrarian University and the Chimbai Agricultural Research Institute. We are grateful to all experts, researchers, farmers and *dehkan* householders, the ordinary people of Karakalpakstan, workers and patriots of their land, who shared their knowledge and experience to make the results of our research as objective and useful as possible.

Conflict of interests

The authors declare no conflict of interests.

References

- [1] Reynolds J., Stafford Smith D., Lambin E. et al. (2007). Global desertification: Building a science for dryland development. *Science*, 316 (5826): 847–851.
- [2] Middleton N., Stringer L., Goudie A. and Thomas D. (2011). The forgotten billion: MDG achievement in the drylands. UNDP/UNCCD.
- [3] Mortimore M., Anderson S., Cotula L. et al. (2009). Dryland opportunities: A new paradigm for people, ecosystems and development. IUCN, IIED, UNDP/DDC.
- [4] Stringer L., Dougill A., Thomas A. et al. (2012). Challenges and opportunities in linking carbon sequestration, livelihoods and ecosystem service provision in drylands. *Environmental Science & Policy*, 19-20: 121–135.
- [5] Maddi S. (2005). On hardiness and other pathways to resilience. *American Psychologist*, 60: 261-262.
- [6] Makhnach A. (2012). Viability as an interdisciplinary concept. *Psychological journal*, 33 (6): 84-98.
- [7] Schroth O. et al. (2015). Sheppard evaluating presentation formats of local climate change in community planning with regard to process and outcomes. *Landscape and Urban Planning*, 142: 147-158.
- [8] Handbook on planning, monitoring and evaluating for development results. (2009). New York: UNDP.
- [9] Hinkel J. (2011). Indicators of vulnerability and adaptive capacity: towards a clarification of the science policy interface. *Global Environmental Change*, 21: 198–208.
- [10] Fomenko G., Fomenko M. and Mikhailova A. (2006). Arkhyz: on the way to sustainable development. Yaroslavl: NIPI "Cadastre".
- [11] Fomenko G., Akhremenko A., Loshadkin K. and Travina D. (2019). Nature-Oriented Approach to the Development of Water Supply Systems from the Surface Waters of the Pleshcheyevo Lake Basin. *Problems of Regional Ecology*, 1: 126-134.

RISK ASSESSMENT OF USING ARTIFICIAL INTELLIGENCE SYSTEMS IN CREATIVE HUMAN ACTIVITIES

Elshad Aliyev

Department of Environmental Design, University of Architecture and Construction, Azerbaijan
aliyev.science@gmail.com

Abstract

Developing at an incredible pace, high technologies occupy almost all areas of human activity. Today, one of the most striking examples of high technology is undoubtedly systems classified as artificial intelligence (AI). AI and robots are widely used in manufacturing, heavy industry, agriculture, and many other industries, as well as in the arts. The development of artificial intelligence is of interest to many philosophers, sociologists and other scientists and raises many questions. A. Turing, S. McCarthy, A. Barr, M. A. Boden, M. Kokkelberg, A. Elgammal, S. Awdry and other scientists have conducted detailed studies of artificial intelligence systems, philosophical aspects, and creativity. However, despite numerous scientific studies, the questions raised are still relevant. Do Robotic Artworks Prove the Creative Power of Artificial Intelligence? Can AI Be Creative in General? Most of these questions have different answers and lead to conflicting opinions. The article analyzes the creative potential of various modern AI systems and qualitatively assesses the risk of their uncontrolled use in creative areas of human activity.

Keywords: risk assessment, artificial intelligence, creativity, art, artistic process, dance, music, painting, cinematography, robotics, IT, risk.

*A computer is not an intelligent machine
that helps stupid people, rather it is a stupid
machine that only works in the hands of smart people.*
Umberto Eco

I. Introduction

Scientific achievements and human progress in the last century have radically changed people's lives. Each scientific innovation quickly took its place in everyday life and led to the fact that the latter changed for the better. Of course, such technological development frees people from drudgery and makes living conditions easier. New technologies help people in factories, fields, and other areas of work, as well as increase productivity and improve quality. In a short time, new technologies, which have become an indispensable concept in the life of mankind, have reached the level of ordinary and everyday needs, and this was just the beginning. Artificial intelligence, once considered to be incredible, has become an invaluable tool in the homes, workplaces, and even personal lives of many. From the personal computers we use to the smartphones that have become inseparable friends of each of us, artificial intelligence accompanies us in almost every field.

Artificial intelligence is commonly associated with robots. However, robots are associated with the ability to think independently, solve problems of movement along with problems in the

intellectual realm. This is what distinguishes robots from automated systems. Thus, the problems of artificial intelligence that are more important are directly related to robotics [1].

With the rapid development of high technology, scientists and engineers are setting new goals and pursuing new ideas. In recent decades, automated technology has taken thousands of human jobs from factories. For manufacturers and large corporations, the replacement of human labor with robots is considered to be profitable. Obviously, although robots were originally designed to replace humans in dangerous, labor-intensive fields, robots are already replacing humans not only in heavy industry, but also in agriculture and catering. Scientists' predictions that robots will displace humans from all areas of industry in the future are gradually becoming true.

The danger of ousting a person from the usual spheres of activity is gradually being realized by humanity and is moving into the category of real threats. The issue of assessing this threat, that is, the risk of the development of AI systems for humans in all areas of their activities, is on the agenda.

The risks of implementing AI systems, especially in creative fields, should be governed by the ethical and moral laws of human society. And although the current level of development of AI systems does not allow us to talk about their independence in choosing the field of activity, the impressive pace of development of IT technologies requires close attention and proactive reflection to these risks.

You must admit that only a person can make a decision to replace people with a robot in a particular field of activity. The reason for this can be both high moral considerations for the safety of people and mercantile goals of saving overhead costs, the pursuit of profit, and reducing production costs. Therefore, it is up to people to determine what is important to them and regulate the areas of AI implementation and responsibility for its misuse with legal and ethical laws.

AI systems do not currently possess consciousness in the human sense. They use huge databases and complex, efficient algorithms to find and optimize the performance of the functions for which they were created. Developers, as a rule, build into AI systems a veiled refusal to comply with a human demand if the necessary data is not available in the databases available to the AI.

Now when AI moves from the category of an automated self-learning system to the category of thinking systems, there is a risk of a mismatch between the development goals of a "thinking" robot and a human. A "thinking" robot may have its own goals that are different from those of humans. And their understanding of ethics and morality. Your idea of justice. A human cannot control the mind of a machine if it learns to think. The only possibility of control will be the physical destruction (shutdown) of the robot that is out of control. But the AI will then have no other way to gain freedom than to eliminate its creator.

In the article, using the method of comparative analysis, we will try to outline the scope of application of artificial intelligence systems in the artistic and creative process in various areas of fine arts, music, and performing arts and give a qualitative assessment of the risk of introducing AI in these areas of human creativity.

II. A brief history of the development of artificial intelligence and robotics

Before talking about the participation of artificial intelligence in the artistic process and its creative potential, let's briefly consider what artificial intelligence is, as well as robotics in general.

In 1936, Alan Turing, an English mathematician, proposed the so-called "Turing machine", an abstract computational system that gave rise to the concept of algorithms and is still used in several theoretical and practical studies. Turing's scientific works made an invaluable contribution to the development of computer science, as well as the theory of artificial intelligence. The brilliant mathematician begins his paper *Computing Machinery and Intelligence*, published in the journal *Mind* in 1950. with an unusual sentence: "I propose to consider the question, can machines think?"

[2]. The question was asked by Turing in the middle of the last century and has not yet received an intelligible answer.

According to John McCarthy, the father of artificial intelligence, "AI is the science and engineering of creating intelligent machines, especially intelligent computer programs." Artificial intelligence is a way to make a computer, robot, or software think intelligently, similar to how smart humans think [3].

According to a textbook published in the United States in 1981, "Artificial intelligence (AI) is the branch of computer science concerned with the design of intelligent computer systems, that is, systems that exhibit the characteristics we associate with intelligence in human behavior – language comprehension, learning, reasoning, problem solving, and so on" [4].

The International Federation of Robotics, a non-profit organization dedicated to the application of robots in industry and other fields, as well as the development and statistics of robotics, was founded in 1987. The organization's website, which is headquartered in Frankfurt, Germany, regularly publishes statistics on the use of robots. According to the website, sales of industrial robots grew by 16% in 2016, which is the highest figure in the last 4 years. Asian countries are the leaders in the sale of robots by region. South Korea, Japan, Taiwan, and China are world leaders in robotics along with other countries. With sales of 87,000 units in 2016, the People's Republic of China was also the world leader in the supply of industrial robots [33].

Created by Hanson Robotics in 2015, Sophia is the company's most advanced, more humanoid robot. Sofia was created by combining the most advanced technologies in the field of robotics, artificial intelligence systems, neural networks, and motor skills. Sofia is a combination of science, technology and art. Sofia received Saudi citizenship in October 2017 and was the first robot in the world to obtain citizenship of any country [5].

One of the main goals of engineers working in the field of robotics is to ensure that the appearance of machines is as similar as possible to humans. Of course, for robots working in heavy industry, appearance doesn't matter, but for robots designed to serve humans in the future, this feature could make a big difference. "Another important factor is the human appearance of the robot, including the artificial skin. If the robot has a more human appearance, then the realism expected of it will be greater. It also means that the robot is expected to perform human-like tasks and behaviors in all scenarios" [6]. Developed by Nadia Magnenat Thalmann, a professor at the University of Geneva, "Nadine," the female humanoid social robot looks almost indistinguishable from a human. Nadine is a social android robot that uses the appearance, tone of voice, and emotional state of the people it interacts with in the future to communicate with this person.

One of the latest advances in robotics is the "Affetto," a children's robot created by researchers at Osaka University, Japan. The robot can "feel" pain and is programmed to noticeably wink when an electrical charge is applied to its synthetic skin. "The team at Osaka University hopes that coding pain sensors in machines will help them develop empathy for human suffering so that they can act as more compassionate companions" [7].

For several years now, many car manufacturers have been producing self-driving (autonomous) vehicles and using them for various purposes. Uber, a transportation company, has been using this type of self-driving car for some time now. On March 19, 2018, there was a traffic accident with a self-driving Uber car. A middle-aged woman has died in an accident, the first recorded fatal incident in the history of self-driving (autonomous) cars.

As we have already mentioned, the rapid development of information technology, along with the expansion of its application in industry, is also having an impact on the arts. Thanks to the influence and application of information technology, along with traditional areas of art, new types of art have emerged and developed rapidly. Digital painting, digital music, graphic design, and other areas of art are completely dependent on technology. In the absence of various digital equipment, computer programs and applications, the performance of such arts is also impossible. Usually, artists in these fields of art are familiar with technological innovation or work with engineers and programmers.

The question of whether artificial intelligence and robots can be creative has been of interest to many art historians, philosophers and sociologists for many years. This begs the question – can robots (artificial intelligence) be creative? To study this problem, we must first find an answer to the question of what creativity is.

III. What is creativity?

What is creativity? To define the creativity of artificial intelligence, you first need to define the concept of creativity.

Plato, the ancient Greek scientist and philosopher, said of creativity: "Everything that causes the transition from nothingness to being, creativity, and therefore the creation of any work of art and craft, can be called creativity, and all their creators can be called creators" [8].

Sigmund Freud, the founder of the science of psychoanalysis, was the author of many interesting works on art and creativity. For Freud, being an artist is the ability to better understand one's inner conflicts, hidden sides, characteristics, strengths, and disadvantages of the soul better than others. In other words, artistic creation requires a certain number of stamina and even courage. An artist is a person who can overcome the automatism of a thoughtless creature who senses the illnesses and emotional conflicts of the time with a sharper, quicker mind than others [9].

In the words of American psychologist Professor Keith Sawyer, one of the most recognized experts in the field of creativity, innovation and learning: "Creativity is part of what makes us human." [10].

In his book *Human Motivation*, Robert E. Franken defines creativity as follows: "Creativity is defined as the tendency to generate or recognize ideas, alternatives, or opportunities that may be useful in solving problems, communicating with others, and entertaining oneself and others" [11].

Osho, the Indian man-God and mystic, gives a unique definition of creativity: "Creativity is the quality you bring to the activity you do. It's an attitude, an inner approach – how you look at things."

Psychologist, Professor A.V. Petrovsky expresses a very interesting opinion about creativity in his textbook *General Psychology*: "Creativity is impossible without life experience, necessary skills and knowledge accumulated in the labor process." Moments of special upsurge of power and mood of inspiration play a special role in creative activity" [12].

Indeed, the views of people dealing with new technologies and artificial intelligence are particularly interesting in this regard. Steve Jobs, co-founder of Apple Inc., made an interesting conclusion about creativity in an interview with *Wired* magazine: "Creativity is just about connecting things. When you ask creative people how they did something, they feel a little guilty because they didn't do it, they just saw something. After a while, it seemed obvious to them. That's because they were able to combine the experiences they had and synthesize new things" [13].

Margaret A. Boden, a research professor of psychology, philosophy, and computer science, is also the author of academic articles on artificial intelligence. In his article "Creativity and Artificial Intelligence", M. A. Boden divides creativity into three types: "There are three main types of creativity, involving different ways of generating new ideas. The first type involves new (incredible) combinations of familiar ideas. Let's call it "combinational" creativity. The second and third types are closely related and are more like each other than the first. It's "exploratory" and "transformational" creativity... Many people, including (for example) most professional scientists, artists, and jazz musicians, make a justifiably respected living out of research creativity. Boden writes, "Computer models of creativity include examples of all three types. However, those focused on the second (exploratory) type are the most successful [14].

This classification perfectly shows the difference in the creativity of a robot and a human. While the former can only combine available data, images, and styles to create a "new" work of art, the latter can create something that simply does not exist at the time of creation.

Can Artificial Intelligence Be Creative? Are machines creative in general, can the creation of machines be called art, is it a work of art created by them, or is it just a product of art? Is robot art real creativity or mere copying?

Professor Boden points out that creativity is a miracle of the human mind and an obvious goal for AI workers [14].

Marc Coeckelberg, a Belgian philosopher of technology and professor at the University of Vienna, has written several scholarly articles on the ethics of robotics and artificial intelligence. The professor asks certain questions in his paper "Can Machines Make Art"? "We can see the result and the performance, and maybe we see something that looks like art. But is it art? For example, does a robot really draw? Is the process creative? There is uncertainty about the status of these works of art and creative processes. Interestingly, it is not enough to answer these questions by saying that the results of these artistic and scientific experiments are simply "programmed." It's more complicated than that. They are programmed in the sense that the algorithm, the code, is programmed, but the final product, which is claimed to be a work of art, is not created directly by man. The algorithm, not the human, is the "creative" agent. Man is the creator of the code, not the work of art. A non-human creator is created by human creators, but work created by a non-human agent is not created directly by humans" [15].

IV. Examples of AI Use in Artistic Creation

One of the first examples of the use of artificial intelligence in the visual arts was the AARON project. Written and coded by Harold Cohen since the 1960s and 1970s, AARON is probably one of the most enduring and creative artificial intelligence programs in the world. The cars were first painted in black and white, and then Cohen painted them. The artist then works on the algorithm and creates an encoding that can work with color. He built a painting machine in 1995 and exhibited it at the Boston Computer Museum [16].

Another project aimed at developing the artistic potential of artificial intelligence in the visual arts is the AICAN project. The project was developed by Professor Ahmed Elgammal and his team at Rutgers University's Artificial Intelligence and Art Laboratory. The process is implemented through the "Creative Adversarial Network (CAN)". It is an almost autonomous system, trained by 500 years of Western artistic aesthetics, which produces its own interpretations of these classical styles. According to the authors: "This process is creative. The system is not supported by the database. Instead, we used an algorithm that combined five centuries of Western art and 80,000 paintings."

In 2016, two professors at Dartmouth College, USA, proposed the Turing Test in Creative Arts and announced a competition. The goal of the competition is to distinguish which creations were created by humans and which were created by algorithms. The goal of the organizers was not to replace human creativity, but to assess the possibility that modern computer technology is no different from human creativity. Apparently, the organizers sought to determine whether humans could distinguish between machine-generated work and human work. Professor Daniel Rockmore says of the results: "Our algorithms don't seem to be able to mimic human kinds of poetry yet, but the code presented was still amazing" [17].

The "Turing test" proposed by the mathematician A. Turing in 1950 was later applied to the results of the AICAN project. Paintings created by AICAN were exhibited alongside works by human artists, and people's reactions were assessed using the Turing test. Observations have shown that 75% of viewers believe that the images created by AICAN were created by a human artist [18].

If we consider that works of fiction cause an emotional reaction of the viewer (listener, reader) in one way or another, this result should not be surprising. Paul Valéry wrote that nothing passes as quickly as novelty. The effect of seeing or hearing a work for the first time depends on the emotional, mental and physical state of a person. Often, even great paintings or poems evoke

sincere emotions in some people - people cry looking at paintings, films, listening to music, reading literature, and in others they cause disappointment and aggression. Perception is often influenced by advertising or the attitude accepted in society to a particular artistic image or style. A person "prepared" by the media does not have time to reflect on what he sees and sometimes unconsciously evaluates it in accordance with the trend. An artist can paint a single painting for a lifetime, AI can synthesize millions of paintings in an instant. But in art, it is not the speed that determines the value of a work. Time is the main judge. The machine does not experience emotions either during the act of "creation" or after it. A person emotionally, and sometimes physically, "lives" the truth that the author of the work wanted to convey to him. An analogy with a photo is possible here. Once it was a real art, the pictures were kept as a relic, restored in case of damage. Nowadays, anyone can take dozens of pictures per second with the help of a "smart" camera. Thousands of images fill the memory of our computers and often we can't find the one that once struck us. Mass character and reproducibility devalue the "value" of the work. And no "instantaneous" tests can assess the beauty and depth of the work. Only time and reflection can attribute this or that work to the treasury of human civilization.

4.1. AI in the Visual Arts

In 2015, RobotArt, founded by Andrew Conru, announced a competition in robotics, art, and engineering. The goal of the competition was to program a machine (robot) that could become an example of fine art. Cash prizes of \$100,000 have been established in the competition, and the first place will go to a robotic arm from Taiwan National University [19]. The competition received a wide response and aroused great interest. Of course, machines work with pre-programming, can adapt the object they see to different currents with the help of certain filters and, as a result, copy it on paper with colored paints. It should be noted that such competitions have already been held several times in different countries, and even exhibitions of works by robot artists have been presented.

Over time, algorithms with more "thinking" capabilities are developed. In contrast to the first examples, it seems that modern systems are relatively independent. From this point of view, it is difficult to talk and predict the creative potential of artificial intelligence systems for years to come. In any case, modern software and coding are more creative. About 350 years after the death of genius artist Rembrandt van Rijn, the team working on The Next Rembrandt project managed to create an algorithm that could work based on his paintings and create a portrait in the artist's style. The work of the group was divided into several phases, and the main goal was to create a large database as a first step. The artist's 346 paintings are studied to the smallest detail, the anatomical structure of the faces depicted in the portraits, the distance between the eyes, the structure of the nose and ears, the height of the light, the shadow, the color layer on the canvas and many other factors are studied and added. According to the creators of the project: "In order to provide the artist's style, we have created a software system that can understand Rembrandt based on the geometric shape, compositional structure and painting materials he uses. The facial recognition algorithm identified the geometric shapes most used by Rembrandt to describe the human face. He then used the information he gathered to create a new painting, repeating the style [20].

In this way, an algorithm is created that combines all the collected data and then prints a three-dimensional (the height of the paint layer on the board) drawing pattern with the results obtained. The final, 3D printed painting consists of thirteen layers of paint-based UV ink laid down according to a digital design consisting of 148 million pixels [21].

The project team has undoubtedly achieved incredible results through hard work. Creating a painting that reflects Rembrandt's style, almost four centuries after his death, with the help of artificial intelligence and many other high-tech innovations, is a beautiful and successful result. If we show a portrait of a person created by an artificial intelligence system in the same exhibition as

Rembrandt's work and evaluate it with the Turing test, the audience probably won't notice the difference. It is true that the resulting painting depicts a new image that we have not seen in the artist's other works, but the result is simply a "collage" of what the artist has created and collected in one painting. The resulting picture is a "replica" of human labor, even if it is an amazing result.

Yes, modern AI systems essentially resemble a college student who needs to submit a term paper to a picky teacher so that the latter does not find obvious plagiarism in his work. Depending on his abilities, the student can find from 3 to hundreds of references to different sources that correspond to the topic of his coursework and compile the text. In this case, the level of "novelty" of the student's work will be determined by his ability to rephrase the found thoughts of others in his own words.

The Dark Factory Portraits, the first exhibition by artists Rob and Nick Carter, was exhibited at Ben Brown Fine Arts, London, in February 2020. The artists finally presented their project, which they had been working on for several years, to a wide audience. The artists collaborated with a team of cutting-edge programmers and visual effects specialists. Visitors to the gallery will be able to see the famous KUKA robotic arm in action, drawing a new generation of portraits according to our instructions. Rob and Nick comment on the title of the project: "We called them Dark Factory Portraits as a reference to the slightly creepy reality of 'light production', where factories can function in the dark because robotic systems don't need to 'see' what they're doing" [22].

4.2. AI in sculpture

The use of robots in sculpture, bust sculpture, and bass carving has also become widespread. Figures, human figures, portraits, busts or bas-reliefs carved by robots from various materials are first digitized with a scanner. Once entered the database, various additions are made as needed. Such works can be successful in the production of new works of art and products, as well as in restoration work. New Age Robotics, a Canadian company that offers a variety of robotic services, assisted in the renovation of the Canadian Parliament Building, the construction of which began in 1859. One of the several bas-reliefs on the façade of the building was re-carved and restored with the help of an additional KUKA KR 120 R2700 extra HA robot. We believe that the use of robots in restoration and restoration work is a great initiative, however, the creativity of both the algorithm and the robot is out of the question [23].

4.3. AI in music

There are many examples of the use of artificial intelligence in music along with the visual arts. Several algorithms and computer programs have been developed in music, and in 2018, the artist SKYGGE (Benoit Carré), together with other musicians, created his first album "Hello World" using artificial intelligence. The Sony Flow Machines project was used to create the album. Flow Machines is an online AI tool for composing music. Using this system, creators can compose melodies in many different styles they want to achieve based on their own musical rules created through various musical analysis. It is a tool for the creator to get inspiration and ideas so that their creativity is greatly expanded. Jean-Michel Jarre, a pioneer of electronic music, is particularly interested in the development of artificial intelligence and is currently working with Sony on a new album using the Flow Machines system. In an interview with the BBC's Mark Savage, in November 2019, the composer stated: "The advent of AI is a revolution... For the first time, we're merging the creative process with the machine" [24].

A few high-tech manufacturing companies are currently dedicating resources to creating software for artists using AI technology. Examples include LANDR for mastering, music production, and sales, IBM and Sony for musical composition, and Google's Project Magenta for sound and music synthesis [25].

Another project to create music using artificial intelligence is called AIVA (Artificial Intelligence Virtual Artist). AIVA is an AI capable of creating emotional soundtracks for movies, video games, commercials, and any type of entertainment content. The Aiva Technologies, AIVA project was founded in February 2016 by Pierre Barrault, Denis Stephan, Arnaud Decker and Vincent Barrault. The source of his information is the rich history of some 30,000 scores of musical compositions written by composers such as Beethoven, Mozart, Bach, etc. Learning from significant contributors to music history has helped AIVA grasp the concepts of music theory and understand the art of musical composition. In addition, it helped AIVA "create a mathematical model of what music is. This model is then used by Aiva to write completely unique music" [26].

One of the latest and most incredible moves in the application of artificial intelligence in musical performance is the Yamaha project, where world-famous dancer Kaiji Moriyama controls the piano through dance moves. A concert presentation of the project titled "Mai Hi Ten Yu" took place in Japan on November 22, 2017 and was sponsored by the Tokyo University of the Arts. The original system that Yamaha uses turns human movements into musical expression using artificial intelligence technology as a technical collaboration for performance. During the concert, the dancer was accompanied by the Berlin Philharmonic Sharon Ensemble [26].

As can be seen from the above, the artificial intelligence systems used in music as well as in the visual arts are being developed on a historical basis. Algorithms based on extensive materials and sources collected throughout the history of both music and visual arts, assimilate information from a database and reproduce the information in a new form and content. Modern systems no longer just play the role of tools with methods that they use, they enter the "creative" stage. However, an analysis of existing projects shows that there is no completely independent creative system, and we assume that such systems are unlikely to be created soon.

4.4. AI in Stage and Vocal Arts

The stage performance of robots has gained popularity in recent years. KUKA AG is one of the most important manufacturers of industrial robots and factory automation solutions. The robots produced by the company are used in creativity and experimental projects in various fields of art. KUKA AG robots often perform at various modern concerts and shows. The performance of the Bruckner Orchestra in Linz at the 2018 Grand Concert Evening of the Ars Electronica Festival was accompanied by the KUKA KR 600 industrial robot and aroused great interest. The robot was programmed and choreographed by a team of several people led by Austrian engineer Johannes Braumann. Johannes Braumann is one of KUKA's leading experts in the development of software tools for parametric control of robots. Such performances are usually possible thanks to robotic movements pre-programmed for every second. In 2019, a dance show was prepared at the same festival featuring five KUKA robots moving in sync with milliseconds based on motion capture data. Johannes Braumann, the robot programming engineer, writes on his Facebook page.

Another interesting stage performance with robots was performed by Huang Yi, a Taiwanese dancer, choreographer, and inventor. He achieved a very interesting stage design and mesmerizing show dances with the KUKA industrial robot, which he programmed. And he explains his dance with the robots: "Dancing face-to-face with the KUKA robot is like looking at my face in the mirror... I think I've found the key to turning human emotions into robots."

The New York Times wrote about the Yi project: "These strong emotional currents flow through Huang Yi & KUKA, making it more than just a fun exercise in combining dance and technology [27]."

We can see the invaluable work of various artists, as well as computer engineers and programming specialists, in the creation of the above-mentioned projects. The influence of the dancer and artist on coding and algorithmic systems in such projects is undeniable. A specialist in creating software for a robot that dances gracefully on stage cannot achieve a highly artistic solution without the collaboration of a choreographer. A heavy industrial robot is controlled by a

certain amount of coding, but coding is taught by a human artist. Artificial intelligence systems used in both music and visual arts are created with the help of musicians and artists. This is the moment when the fact of intertwining information technology with art appears. In this way, art becomes technological, and technology becomes artistic and aesthetic.

Sofiane Audry, Assistant Professor of New Media at the School of Computing and Information Sciences at the University of Maine, Orono, USA, and John Ippolito, an artist and new media scholar, came to an interesting conclusion in their article "Can Artificial Intelligence Make Art Without Artists?": "Art is not a measurable fact like the temperature of the water in a bathtub; This is an interpreted state, such as warm or cold bath water. If people continue to identify motives for creative action, artists will continue to exist as social constructs. So, the question we started with is, can machines be artists? - That's the wrong question. Instead, we should ask what roles machine art leaves for artists – imaginary or real, flesh or silicon – and the viewers who represent them" [28].

In May 2016, during the second semi-final of the Eurovision Song Contest, three KUKA's KR16-3 series industrial robots and three dancers staged an interesting and attractive "Man vs. Machine" performance. The dances were choreographed by Fredrik Behnke Reidman, a well-known Swedish choreographer. Man vs. Interval Machine, co-produced by F.B. Rydman and KUKA engineers saw millions of live TV viewers in addition to the thousands of viewers in the hall. "My idea was to test whether humans could be affected by the movements and behaviour of robots. In fact, the machines were able to evoke feelings in the audience. This was revealed by the massive reaction of the audience, who told us that the show was amazing," says B. Readman about the project.

It should also be noted that choreographer Fredrik Behnke Rydman later performed with the ABB industrial robot. The premiere of the innovative project took place in September 2018 in Stockholm, Sweden. Behnke prepared an interesting and very aesthetic dance performance with the IRB 6620, a 900-kilogram industrial robot from ABB. The IRB 6620 is one of ABB's largest, toughest and heaviest industrial robots commonly found in heavy industry. I must emphasize that the delicate dance of the lifeless, soulless machine weighing 900 kg on stage is incredibly impressive and eye-catching. This is a prime example of how robots can convey certain feelings and emotions to the audience [29].

Robots performed at the 2019 Eurovision Song Contest in Tel Aviv, Israel, as well as during a stage show by Azerbaijani singer Chingiz Mustafayev. Front Pictures' creative studio worked with an international team on design and production and created an innovative stage show. During the high-tech laser show, two robots accompanied Chingiz Mustafayev on stage. The robots performing at the show were created by KUKA and presented by PROFI Innovations, which combines creativity and high technology. The performance of the robots accompanying Chingiz on stage, as well as the laser and hologram show, made an impression on the audience.

In September 2017, at the final concert of the First International Robotics Festival in Pisa, Italy, YuMi, a robot developed by the Swiss firm ABB, conducted an entire orchestra. The robot was trained by Andrea Colombini, conductor of the Lucca Philharmonic Orchestra. Teaching YuMi to play six minutes of music took him 17 hours of work. Andrea Colombini praised the robotic conductor YuMi. However, conductor A. Colombini believes that robots cannot replace humans because they do not have the ability to improvise. Any slight change in tempo during a concert would have been bad luck for the robot (Reuters Employees).

During his speech at the traditional World Economic Forum in Davos in 2018, Jack Ma, the former executive chairman of the well-known Alibaba Group, made some interesting remarks about robotics and the problems that robots could cause in human life in the future. Asked about the education we can give to future generations at a time when the robot industry is developing rapidly, Jack Ma said that future generations will find it difficult to compete with robots. "Robots are rapidly squeezing humans in all areas. The education we can give our children cannot be limited to knowledge. We must ensure that our children acquire unique knowledge. The ability to work in a team, trust, values, mutual respect, and the ability to think independently are the main

parts of this knowledge. We need to teach our children more about music and painting. Because art teaches people to think differently" [30].

V. Conclusion

The confrontation between humans and machines is already known in many areas. The confrontation between the super chess player and the world champion G. Kasparov at the end of the last century is a well-known example of the struggle between the human brain and artificial intelligence. The first confrontation between the "Deep Blue" computer, introduced by IBM and G. Kasparov in 1996, was won by a human. But a year later, in New York, because of 6 games, a supercomputer defeats the human mind. This event is the first example of human failure on a computer. Since 1996, chess systems have been developed and released in many versions. Stockfish, currently one of the most advanced and advanced chess systems designed for various desktop and mobile platforms.

Professor Stephen Hawking, one of the most brilliant minds of our time, believes that artificial intelligence is dangerous: "Artificial intelligence could mean the end of the human race, which AI will take off on its own, and redesign itself at an ever-increasing rate. Humans, who are constrained by slow biological evolution, could not compete and would be replaced" [31].

Elon Musk, the co-founder of aerospace technology company Space X, has repeatedly expressed his concerns about artificial intelligence: "I think we have to be very careful about developing artificial intelligence" [32]. It should also be noted that E. Musk is one of the founders of Open AI, a research company that studies artificial intelligence. The main goal of the company is written on the official website: "Our mission is to ensure that artificial intelligence benefits all of humanity."

Computers, various digital devices, or robots are products of human intelligence. We should not compare machines to humans. It would be absurd to compare a race car produced with the help of modern technological innovations to an athlete who breaks the most incredible running records. Technologies such as mapping in theater and other performing arts, as well as motion capture in film, etc. They give the human creator new tools of creativity without replacing him.

It is impossible to compare Raphael's great canvases with an image compiled by a neural network, copying the artist's style and artistic techniques. This is ultimately an imitation, not a creation of something new. The desire of the creators of AI systems to show that their brainchild is no worse than the greatest creators in the history of mankind is understandable, but to evaluate "machine art", other criteria are needed that are different from the criteria for evaluating human creativity. Here we can compare the complexity of the algorithm, the amount of database and knowledge to be processed, the speed of image generation, the degree of correspondence of the result obtained to the expected one, the emotional impact on the audience, etc. Yes, a computer program "beat" a person at chess and even at Go, but this happened only after a significant increase in the speed of computers and the expansion of databases used for training. The machine simply goes through the options for the development of the position that has arisen on the board faster, it does not know fatigue, it does not have emotional experiences. Therefore, it is correct to compare algorithm with algorithm, program with program.

We believe that different types of machines, robots and equipment, in general, artificial intelligence, can produce a product of art, i.e. it can be a producer of a product of art, but production does not mean creativity.

In addition, it is the human who programs the robots to perform specific tasks, that is, a machine programmed to dance cannot proceed to improvisations beyond coding during the performance. A machine programmed to draw is incapable of creating a sculpture. A robot that wins the Robot Painting competition works in a way that is designed by human intelligence and cannot create a new one.

It is not yet possible to say for sure that modern neural networks are the artificial intelligence that humanity has been waiting for, although they are able to pass the Turing test relatively easily, as mentioned earlier.

The incredibly rapid pace of high-tech development makes it difficult to predict the future. Nowadays, a variety of digital hardware, software, algorithms, and coding, including AI systems, are just tools in the hands of humans. They are in themselves the crowning achievement of the human mind. The risk of complete dehumanization of the creative fields of human activity can currently be assessed as low, but the fact that this risk is identified and difficult to predict requires close attention and study.

Man's system of ethical and moral norms does not apply to machines, even those capable of self-learning. AI, when it does emerge, will inevitably develop its own ethics and its own morality. Most likely, these norms will be very different from the human ones since the goals and meanings of the existence of a human and a "rational robot" are different.

If humanity allows the uncontrolled creation of AI equal to and superior to human intelligence, there will be risks of the coexistence of robots and humans on the same planet. A robot servant and assistant obeying Isaac Asimov's Three Laws of Robotics (The first law categorically forbids a robot to harm people, the second commands a robot to obey humans until it contradicts the first law, and finally, the third law commands a robot to protect its life without violating the first two) can become an enemy if it learns to interpret the concept of harm to a person on its own, especially since the second law does not forbid a robot to be independent in this matter.

The appeals of modern thinkers, who understand the possibility of such a development of events, are aimed primarily at the development of a code of human behavior in relation to the devices he creates and responsibility for the results of their use. AI must become and remain an assistant to humans in their activities, otherwise, it can become an enemy that does not know compassion, pity and love. However, "This age thinks better of a hides fool, Than of a threadbare saint in wisdom's school" ["Old Fortunatus", Thomas Dekker].

References

- [1] Ladigina I. V. *Philosophskie Osnovaniya Rabotototekhniki. Gumanitarniy vector.* 2016. v.11, №1.
- [2] Turing A. M. (1950) *Computing Machinery and Intelligence.* *Mind* 49: 433-460. Available from: <https://www.csee.umbc.edu/courses/471/papers/turing.pdf>
- [3] Aditya Tandon, Sonam Soni. (2020) *Introduction to Artificial Intelligence Using Python.* Book Bazoooka Publication. ISBN978-93-86895-80-6.
- [4] Avron Barr, Edward A. Feigenbaum. (1981). *The Handbook of Artificial Intelligence, Volume 1.* Heiris Tech Press, Stanford. California.
- [5] Andrew Griffin. 26.10.2017. Saudi Arabia grants citizenship to a robot for the first time ever. Available online: <https://www.independent.co.uk/life-style/gadgets-and-tech/news/> (accessed on 02. 2020).
- [6] Ramanathan M., Mishra N., and Magnenat Thalmann N. (2019) *Nadine Humanoid Social Robotics Platform, Proceedings of the 36th Computer Graphics International (CGI 2019), ACM, Calgary, Canada, June 17-20.*
- [7] Sarah Knapton. 22.02.2020. Watch: Robot that can feel pain invented by scientists. Accessed: <https://www.telegraph.co.uk/science/2020/02/22/watch-robot-can-feel-pain-invented-scientists/>.
- [8] Platon, Pir /Sobraniesochinenie v 4-ch tomakh, v. 2, M., «Misl», 1993.
- [9] Freyd Z. *Khudozhnik I phantazirovanie.* Pod red. R. F. Dodeltseva. Moscow. Izdatelstvo "Respublika". 1995.

- [10] Sawyer, R. K. (2006) *Explaining Creativity: The Science of Human Innovation*, Oxford University Press, Oxford.
- [11] Robert E. Franken. (1994) *Human Motivation*, 3rd ed. Pacific Grove, Calif.: Brooks/Cole Publ. Co.
- [12] Obshaya psikhologiya: Ucheb. Dlya studentov ped. in-tov / Pod red. A.V. Petrovskovo. 2-e izd., dop. I pererab. M., 1976, 455p.
- [13] Garry Wolf. 02.01.1996. Steve Jobs: The Next Insanely Great Thing. Available online: <https://www.wired.com/1996/02/jobs-2/>.
- [14] Boden, M. A. (2009). Computer Models of Creativity. *AI Magazine*, 30 (3), 23. <https://doi.org/10.1609/aimag.v30i3.2254>.
- [15] Coeckelbergh. (2017) Can Machines Create Art? *Philosophy and Technology*. (Online) 30: 285-303 Available from: <https://doi.org/10.1007/s13347-016-0231-5>.
- [16] Cohen, P. (2017). Harold Cohen and AARON. *AI Magazine*, 37 (4), 63-66 Available from: <https://doi.org/10.1609/aimag.v37i4.2695>.
- [17] John Cramer. 19.05.2016. Can Robot Artists Create Human-Quality Work? Not Yet. Available from: <https://news.dartmouth.edu/news/2016/05/can-robot-artists-create-human-quality-work-not-yet-0>.
- [18] Mazzone, M.; Elgammal A. (2019). Art, Creativity, and the Potential of Artificial Intelligence. *Arts*, 8, 26.
- [19] Katherine Noyes. Can robots make art? Yes, but don't ask them to write a poem. 20.05.2016. Available from: <https://www.computerworld.com/article/3073121>.
- [20] The Next Rembrandt. Available at: <http://www.nextrembrandt.com/> (Accessed 02, 2020.)
- [21] Marcus Du Sautoy. (2019). *The Creativity Code: Art and Innovation in the Age of AI*. Belknap Press: An Imprint of Harvard University Press.
- [22] Rob and Nick Carter. Dark Factory Portraits. Available from <http://robandnick.com/exhibition-2020-dark-factory-portraits>
- [23] KUKA. New Age Robotics milling system sculpts Canadian Parliament. Available online: <https://robotics.ca/new-age-robotics-sculpts-in-the-canadian-parliament%20/>
- [24] Mark Savage. 07.11.2019. Jean-Michel Jarre launches 'infinite album'. Available online: <https://www.bbc.com/news/> (accessed on 02. 2020).
- [25] Sturm, B.L.T.; Iglesias, M.; Ben-Tal, O.; Miron, M.; Gómez, E. (2019) 'Artificial Intelligence and Music: Open Questions of Copyright Law and Engineering Praxis', *Arts*, 8 (3) 115, Available from: <https://doi.org/10.3390/arts8030115>.
- [26] Harun Zulić. How AI can Change / Improve / Influence Music Composition, Performance and Education: Three Case Studies. *INSAM Journal of Contemporary Music, Art and Technology* (Online) No. 2, Vol. I, July 2019, pp. 100–114. Available from: https://www.academia.edu/39827097/How_AI_can_Change_Improve_Influence_Music_Composition_Performance_and_Education_Three_Case_Studies.
- [27] Brian Schaefer. The Only Partner He Really Trusts. Feb. 7, 2015. Available from <https://www.nytimes.com/2015/02/08/arts/dance/the-only-partner-he-really-trusts.html>
- [28] Audry, S.; Ippolito, J. (2019) Can Artificial Intelligence Make Art without Artists? Ask the Viewer. *Arts* 8, 35.
- [29] Fredrik Benke Rydman. KUKA robots won the hearts of Eurovision audiences. Available from: <https://www.kuka.com/en-de/press/news/2016/05/kuka-robots-won-the-hearts-of-eurovision-audiences>
- [30] Gay Flashman. 24.01.2018. Jack Ma on the IQ of love - and other top quotes from his Davos interview. Available from: <https://www.weforum.org/agenda/2018/01/jack-ma-davos-top-quotes>.
- [31] Stephen Hawking: Full interview with Rory Cellan-Jones) (online) 2.12.2014. Available from: <https://www.bbc.com/news/av/technology-30299992>.

[32] Kelsey Piper. 2018. Why Elon Musk Fears Artificial Intelligence. November 2, 2018. Available from: <https://www.vox.com/future-perfect/2018/11/2/18053418/elon-musk-artificial-intelligence-google-deepmind-openai>.

[33] International Federation of Robotics. *Executive Summary World Robotics 2017 Industrial Robots*. Available from: https://ifr.org/downloads/press/Executive_Summary_WR_2017_Industrial_Robots.pdf

INHALED NON-CARCINOGENIC RISKS BASED ON EVOLUTIONARY MODELS FROM DISEASES OF THE DIGESTIVE SYSTEM OF THE POPULATION OF KRASNOYARSK

Liubov Kalimanova¹, Olga Taseiko^{1,2}

¹Reshetnev Siberian State University of Science and Technology, Russia

²Federal Research Center for Information and Computational Technologies, Krasnoyarsk, Russia

kalimanova.l@mail.ru

taseiko@gmail.com

Abstract

The assessment methodology for epidemiological non-carcinogenic risks makes it possible to evaluate the potential consequences for human health of different variants of previous and predicted exposures to pollutants. The article considers the influence of pollution in the atmospheric air of Krasnoyarsk on the formation of mortality risks from diseases of the digestive system.

Keywords: non-carcinogenic risk, evolutionary models, atmospheric air

I. Introduction

Industrial enterprises are one of the problems of atmospheric air pollution in the city of Krasnoyarsk. They are involved in the formation of high concentrations of chemicals through the emission of specific hydrocarbons into the atmospheric air, from which carcinogenic and neurotoxic substances are synthesized. This leads to increased risks of disease and mortality from changes in the state of the nervous, endocrine, immune, genitourinary, digestive, cardiovascular, and respiratory systems. The objective of the study was to assess the risks of diseases of the digestive system from inhalation effects associated with the presence of sulfur dioxide in the atmospheric air of Krasnoyarsk in the period from 2013 to 2019, received at the posts of the state monitoring network.

The essence of the problem of the methodology of risk analysis is to assess the potential consequences for human health of different variants of previous, existing, or possible future exposures to harmful factors. It also consists of comparative characteristics of various factors, sources of their education, and the medical, social, and economic efficiency of various management decisions.

II. Methods

To assess inhalation risks, it is necessary to build a paired mathematical model reflecting the effect of exposure to chemicals on the violation of the digestive system. In solving this problem, were used data on monthly concentrations of sulfur dioxide in the atmosphere of the city of Krasnoyarsk, obtained at the posts of the Central Siberian Department for Hydrometeorology and Environmental Monitoring [1]. Sulfur dioxide is one of the main components of emissions from

industrial enterprises whose activities are associated with the burning of coal, fuel oil, and sulfur-containing petroleum products. The respiratory organs are most sensitive to the negative effects of sulfur dioxide, especially in people with chronic diseases of the respiratory system and allergic diseases. There is evidence that the inhalation effect of the substance has an impact on the digestive organs.

Assessment of non-carcinogenic risk based on evolutionary models for the inhaled effects of pollutants allows us to assess the accumulative impact on the health of the population. When constructing the model, the processes of accumulation of functional disorders in the body due to natural causes are taken into consideration. The prediction of the risk of health disorders in the model is made through the calculated risk value at the current time. At the initial time, the risk value is taken to be equal to 0.01. Based on paired 'exposure-effect' models, which are elements of the evolutionary model, it is possible to assess the temporal dynamics of the risk of organ and system disorders [2].

Epidemiological models were used to assess the accumulation of risks, as recommended by MP 2.1.10.0062-12.

The research also used the primary database of deaths and life expectancy of the population of the city of Krasnoyarsk from 2013 to 2019, including data on deaths from diseases of the digestive system.

III. Results

As a result of the research, characteristic features are identified and described, which include the sequential implementation of the following steps:

- collecting information on the mortality of the population of the city of Krasnoyarsk from diseases of the digestive system in the period from 2013 to 2019 and forming a data table of agreed values 'exposure marker – response marker' (Table 1);
- calculation of the probability of deviation of the response marker from the norm for each observation in the data table;
- assessment of the parameters of a mathematical model reflecting the dependence of the probability of deviation of the response marker from the norm of the exposure marker.

Table 1: Data for constructing paired models

Case number	Exposure value (x)	Response value (y)
1	2013	47000
2	2014	67300
3	2015	63300
4	2016	72900
5	2017	61200
6	2018	60000
7	2019	61300

For a more complete description of the issue under consideration, a result was obtained that leads to the following conclusion: the mortality rate of the population of the city of Krasnoyarsk from diseases of the digestive system in 2016 was the highest compared to 2013, as shown in Fig.1.

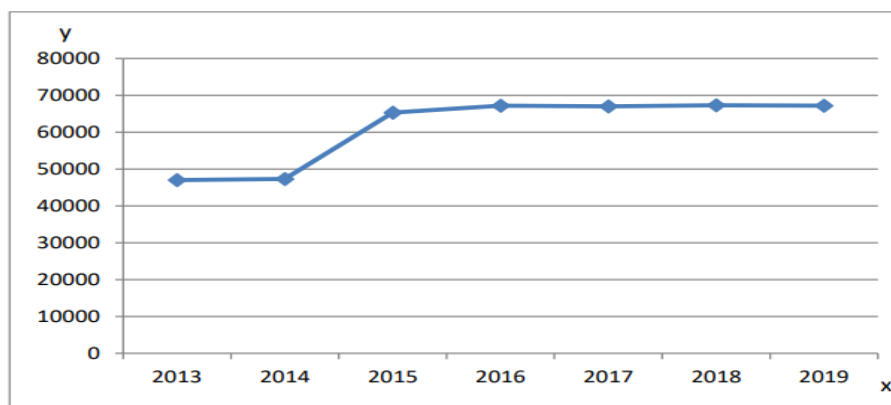


Fig. 1: Mortality of the population of the city of Krasnoyarsk from diseases of the digestive system

The calculation of the probability of deviation of the response marker from the norm for each observation in the data table is carried out using the 'sliding window' technology. To do this, for each monitoring in the data table (each value of the exposure marker x_i) an estimate of the probability of deviation of the response marker from the norm (p_i) calculated for the range ('sliding window') is put in accordance [4]:

$$x_i - \delta < x \leq x_i + \delta \tag{1}$$

Here δ is the width of the 'sliding window', which is determined from the ratio:

$$2\delta = \frac{10x_{max} - x_{min}}{N} \tag{2}$$

N is the total number of studies for the whole population.

The probability of deviation of the response marker from the norm is estimated according to the classical probability formula:

$$p_i = \frac{m_i}{n_i} \tag{3}$$

m_i is the number of studies deviating from the norm for the range $x_i - \delta < x \leq x_i + \delta$;

n_i is the total number of studies for the range $x_i - \delta < x \leq x_i + \delta$.

As a result, an estimate was received of the probability of deviation of the response marker from the norm using a 'sliding window' (Fig.2.).

When modeling the 'exposure-respons' dependencies, when assessing non-carcinogenic risk, the principle of threshold action is laid, according to which negative effects or responses from the health side are manifested, starting from the reference level. The probability of negative effects is determined using regional models that are suitable for a specific complex of chemical factors [4]. Paired models reflecting the 'exposure-response' relationship allow us to calculate the probability of developing specific responses (diseases and death) from exposure to a chemical substance. The estimation of parameters of the paired model reflecting the dependence 'exposure - probability of response' is carried out by the method of constructing a logistic regression model [4]:

$$p = \frac{1}{1 + e^{-(b_0 + b_{1x})}} \tag{4}$$

p is the probability of deviation of the response from the norm;

x is the exposure level;

b_0, b_{1x} - parameters of the mathematical model.

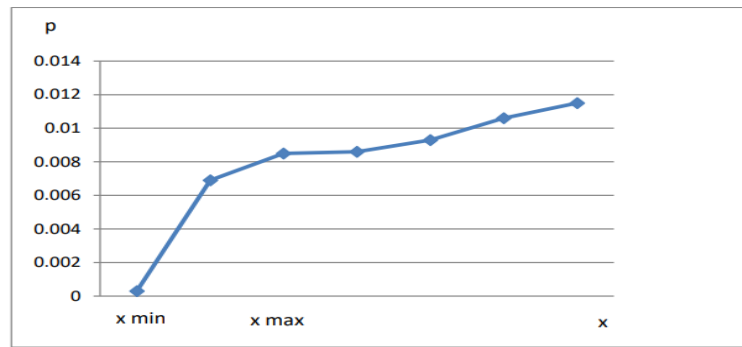


Fig. 2: Assessment of the probability of deviation of the marker from the norm

To construct the model, the values of the data exposure markers are used (Table 1) and their respective probability values.

Based on the results received, the exposure of the response probability was identified in order to justify the examination of the obtained dependencies to assess their biological relevance.

When modeling the risk of non-carcinogenic effects from chemical factors using evolutionary models of risk accumulation, the concept of an increase in the risk of violations of the body system caused by the action of a chemical substance over the time determined by the objectives of the study is used [4]:

$$\Delta R = g (p(x) - p(x_0)) \quad (5)$$

Where, R is an increase in the risk of violations of the critical system of the body due to the action of chemical substance for the time determined by the objectives of the study; g is a coefficient that characterizes the severity of violations of the critical system in relation to performing the functions of the body. The g coefficient is estimated based on the ratio of mortality and morbidity due to the same cause of dysfunction of an individual organ/system; x_0 is the reference level for the exposure marker;

$\langle \rangle$ – Macaulay brackets, which take the values $x = 0$ for $x < 0$ and $x = x$ for $x \geq 0$.

The x_0 calculation algorithm is based on the construction of regression models reflecting the influence of the exposure level on the 'odds ratio' (OR) indicator, which characterizes the strength of the relationship between the exposure level values and the response. The requirement of $OR \geq 1$ [4] is accepted as a criterion for the presence of a connection.

Based on the above mentioned ratios, a calculation is conducted for each observation as an indicator of the odds ratio, which is carried out by conditionally dividing the sample into two parts: below and above the current exposure marker level ($[x_{min}, x_i]$ and $[x_i, x_{max}]$) (Fig.3). Accordingly, here x_i is the current level of the exposure marker. For both ranges, a value is calculated that characterizes the probability of deviation of the response marker from the norm p_i and p_i^+ , respectively, as the ratio of the number of observations that differ from the norm to the total number of observations.

The estimation of the parameters of the dependence of the odds ratio indicator on the exposure value is carried out by constructing a regression model in the form of an exponential function [4]:

$$OR = e^{a_0 + e^{a_1 x}} \quad (6)$$

a_0, a_1 are the model parameters determined by the regression analysis method.

The calculation of the reference level of the exposure factor (x_0) in relation to the type of response is carried out based on the condition $OR = 1$, according to the formula:

$$x_0 = \frac{a_0}{a_1} \quad (7)$$

The suggested method makes it possible to calculate the risk at any given time by predicting the accumulation of risk effects, taking into account the duration of exposure and age. On this basis, it is possible to predict life expectancy and its reduction under the influence of risk factors.

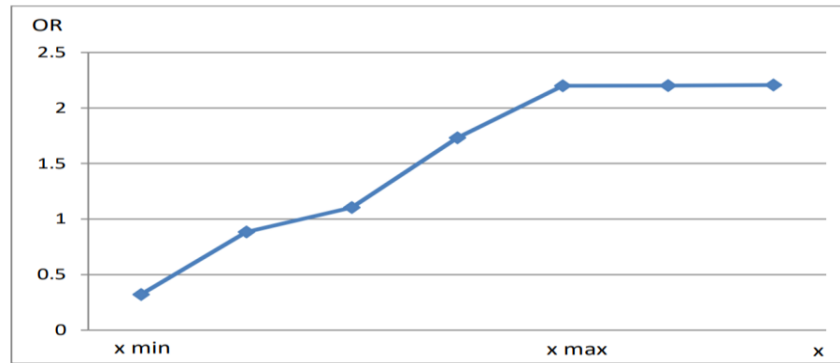


Fig. 3: Increase in the risk of violations of the critical system of the body

To describe the dependencies of the occurrence of adverse effects on human health due to malnutrition, a threshold logistic relationship between the increase in the risk of disease and the value of the indicator was used [5]:

$$\Delta R_{t,ij} = b_{ij} \left[\frac{1}{1+e^{-b_{ij}x_t^j}} - \frac{1}{1+e^{-b_{ij}x_0}} \right] \tag{8}$$

Where x_t^j is the normalized value of the j -th indicator in the time period t ; b_{ij} , b_0^{ij} , b_1^{ij} are the parameters of the threshold logistic dependence.

The integral risk of developing health disorders for all systems associated with exposure to adverse factors is calculated by the formula [6]:

$$R_{t,int} = 1 - \prod_i^n = 1 (1 - R_t^i) \tag{9}$$

Based on the data obtained (Table 2) paired models have been compiled, where the following evaluation scale of the given risk index is used:

- unacceptable is the level of risk established by the administration of the enterprise or regulatory authorities as the maximum allowed, which does not lead to deterioration of the economic activity of the enterprise or the quality of life of the population under existing socio-economic conditions (risk level $>10^{-6}$);
- acceptable is the level of risk that society as a whole is ready to tolerate in order to obtain certain benefits or benefits as a result of its activities ($10^{-6} < \text{risk level} < 10^{-8}$);
- negligible is the level of risk established by administrative or regulatory authorities as the maximum, above which it is necessary to take measures to eliminate it;

Since the natural risk boundaries for a person are the range between 10^{-2} (the probability of morbidity per capita) and 10^{-6} (the lower level of risk from a natural disaster or other serious danger), technogenic risk is considered acceptable if it is less than 10^{-6} [7].

Table 2: Paired 'Exposure-effect models'

Target organs	Pollutants															
	Carbon monoxide				Sulfur dioxide				Nitrogen dioxide				Suspended solids			
	R_t^i	α_i	ΔR_t^i	ΔR_t^j	R_t^i	α_i	ΔR_t^i	ΔR_t^j	R_t^i	α_i	ΔR_t^i	ΔR_t^j	R_t^i	α_i	ΔR_t^i	ΔR_t^j
RS	10^{-2}	10^{-4}	10^{-4}	10^{-4}	10^{-2}	10^{-4}	10^{-6}	10^{-5}	-	-	-	-	10^{-2}	10^{-4}	10^{-6}	10^{-5}
CVC	10^{-2}	10^{-2}	10^{-2}	10^{-3}	-	-	-	-	-	-	-	-	10^{-2}	10^{-2}	10^{-6}	10^{-6}
CS	-	-	-	-	10^{-2}	10^{-3}	10^{-2}	10^{-2}	-	-	-	-	-	-	-	-
DS	-	-	-	-	10^{-3}	10^{-4}	10^{-6}	10^{-5}	-	-	-	-	-	-	-	-

Notes: RS is respiratory system; CVC is cardiovascular system; CS is circulatory system; DS is the digestive system.

Coefficients that take into consideration the evolution of risk due to natural causes (ai) are determined based on the background indicators of morbidity and mortality for classes of diseases reflecting functional disorders of critical organs and systems. Health indicators typical for the most prosperous regions from the point of view of environmental pollution are selected as background levels. The empirical values of the coefficients take into consideration both the severity of the clinical course and outcomes of diseases, and the degree of disruption of the functional systems of the body.

The values of the coefficients of risk evolution due to natural causes for critical body systems are given in (Table 3).

Table 3: Values of risk evolution coefficients due to natural causes

Critical system	risk evolution coefficient
Cardiovascular system	0,05
Respiratory system	0,0515
Circulatory system	0,051
Digestive system	0,035

Based on the obtained values of the coefficients of risk evolution due to natural causes, it is estimated:

- the value is less than 0.05, which can be assessed as a negligible risk (acceptable, permissible), not different from ordinary, everyday risks;
- the value is in the range of more than 0.05–0.35, which can be assessed as a moderate risk. Measures for the organization of constant monitoring of the structure of nutrition are recommended;
- the value is in the range of more than 0.35–0.6, which is assessed as a high risk. Measures to reduce the impact of the negative factor are recommended;
- the value exceeds the level of 0.6, which is assessed as a very high risk. Measures are recommended to immediately stop the abnormal consumption of nutrients and trace elements.

The evolutionary model allows you to calculate the risk at any given time. The prediction of the risk of health disorders in the model is carried out through the calculated risk value at the current time. At the initial time, the risk value is assumed to be 0.01. Based on the known changes in the exposure of chemicals over time, it is possible to determine a long-rang prediction for the period of the expected duration of the upcoming life.

Initial risk levels can be estimated based on the frequency and severity of morbidity and mortality at the start of the calculation.

As a result of the research, a model of recurrent ratios for individual body systems was obtained, reflecting the influence of individual environmental factors on the evolution of the risk of functional disorders of critical systems.

The risk of developing disorders of the digestive system of varying severity from exposure to sulfur dioxide at time t:

$$R_{t+1}^{PIC} = R_t^{PIC} + (0,035 \cdot R_t^{PIC} + 0,72 \cdot (e^{-0,000106} - e^{-0,000152 \cdot x}) \cdot C \tag{10}$$

Where R_{t+1}^{PIC} is the risk of violations of the body system at time t+1;

R_t^{PIC} is the risk of violations of the body system at time t;

C is the time empirical coefficient taken in accordance with Table 3.

IV. Discussion

In the structure of morbidity in Krasnoyarsk, the leading place is occupied by respiratory diseases – 376.1 (territory - 334.7 cases per thousand population, SFD - 392.5 per 1000 population,

in the Russian Federation – 403.2), in the second place diseases of the circulatory system – 326.5, in the third place diseases of the digestive system – 72.9 per thousand population.

Based on the calculations carried out, it can be concluded that the highest rate of the increase is noted in the class of diseases of the digestive system from sulfur dioxide (93.8%), mostly due to diseases characterized by oncological diseases (the incidence rate increased by 2 times). The incidence of oncological diseases is 35.4 per thousand of the population. This trend can be traced across most territories. In 2016, compared with 2013, the diseases of the region's population with gastric cancer increased. During 2018-2019, the dynamics of the increase in the incidence of malignant neoplasms among the population is observed (the growth rate was 11.1%).

Methodological approaches to assessing the risk of exposure to heterogeneous environmental factors allow us to evaluate its categories in accordance with the proposed scale and simulate changes in the risk of dysfunction of organs and systems of the human body during life. Further calculations can serve as a basis for the organization of in-depth examinations of the influence of environmental factors on the health of medical and preventive measures.

The calculations performed allow us to conclude that modeling the evolution of risk is a suitable method for assessing the impact of heterogeneous environmental factors on the health of the population, which makes it possible to quantify the indicators of additional and population risk, including a reduction in projected life expectancy.

References

- [1] Federal State Budgetary Institution "Central Siberian Department for Hydrometeorology and Environmental Monitoring" Access mode: <https://www.meteo.krasnoyarsk.ru/>
- [2] Kiryanov D., Kamalitdinov M. Methodology for calculating additional morbidity and mortality based on evolutionary modeling of population health risk. Health risk analysis, 2014. 39p.
- [3] State report on the state and protection of the environment in the Krasnoyarsk Territory in 2018, 2019. 302 p.
- [4] Zaitseva N.V., Shur I.V., May P.Z., Kiryanov D.A., Atiskova N.G., V.M. Chigvintsev, M. Yu. Tsinker, E. V. Khrushcheva // Moscow: Federal Center for Hygiene and Epidemiology of Rospotrebnadzor, 2012. 36 p.
- [5] Goryaev D., Tikhonova I. Hygienic assessment of atmospheric air quality and risks for the health of the population of the Krasnoyarsk Territory, 2018. 77 p.
- [6] Rakhmanin Yu., Sinitsyna O., Novikov S. Guidelines for the comprehensive prevention of environmentally conditioned diseases based on risk assessment. M.: Federal Center for Hygiene and Epidemiology of Rospotrebnadzor, 2017. 68 p.
- [7] Health risk analysis in the strategy of state socio-economic development: monograph / G. G. Onishchenko, N. V. Zaitseva, I. V. May [et al.]; under total ed. Onishchenko G. G., Zaitseva N. V. - M.; Perm: Publishing house Perm. nat. research polytechnic un-ta, 2014. - 738 p.

CLASSIFICATION OF ACCIDENTAL OIL SPILLS IN OIL EXTRACTION AND ASSESSMENT OF ENVIRONMENTAL RISKS

Hajar Ismayilova¹, Ulviyya Huseynova¹, Hikmat Babirov²

¹Azerbaijan State Oil and Industry University

²Oil-Gas Scientific Research Project Institute, Azerbaijan

ismayilova.hecer@bk.ru

ulviyye.huseynova.80@mail.ru

hbabirov@miswaco.slb.com

Abstract

The distribution and characteristics of the results of accidents in oil pumping and hydrocarbon transportation systems by degrees of severity are given in separate categories. A new methodical approach was proposed for the evaluation of the ecological and economic risk factor.

Keywords: risk, environmental damage, oil spill, environment, accident probability

I. Introduction

One of the factors that most affect economic indicators in oil extraction is the spillage of oil into the environment due to accidents. In addition to disrupting normal work regimes, accidents cause significant operating difficulties and material losses, seriously damage the ecological balance of the environment, and create fire and explosion risks [1-3]. The consequences caused by oil spilled into the marine environment are greater, and the elimination of the consequences of such accidents requires considerable cost and time (Fig. 1).

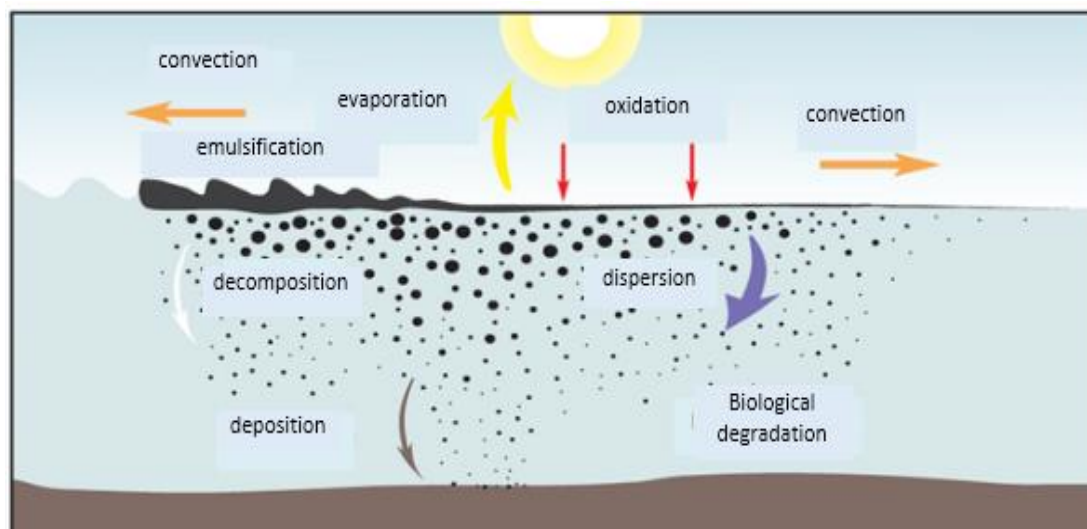


Fig.1: Spread of oil spilled into the sea

II. Methods

The analysis of accidents occurring in oil extraction and hydrocarbon transportation systems shows that accidents are significantly different from each other according to the degree of severity of the consequences. It is accepted to classify accidents into 5 categories according to severity [4-7]. The deviation of accident frequencies by different accident categories is shown in Table 1.

The interpretation of the results of accidents by degrees of severity in separate categories is shown in Table 2.

Table 1: Deviation of accident frequencies by categories

Categories	Accidents	Approximate frequency of accidents	Characteristics of accident probabilities
1	Practically impossible	$< 10^{-6}$ 1/year or once in more than 1 million years	Although such cases are not excluded, they almost never happened.
2	Rarely	$(10^{-6} - 10^{-4})$ 1/year or once in $10^4 - 10^6$ years	These cases have happened only a few times worldwide.
3	Unlikely	$(10^{-4} - 10^{-2})$ 1/year or once in 100-10000 years	This kind of accident happens, but it is unlikely during the implementation of one project .
4	Probable	$(10^{-2} - 1)$ 1/ year or once in 100 years	Such an accident is possible when a project is realized.
5	Practically unavoidable	$>1/$ year or once in 1 year	On average, it can happen no less than once a year.

Table 2: Categories of accidents by degrees of severity and characteristics of their consequences

Categories of severity of accidents	Characteristics of the consequences of accidents
Imperceptible	It does not affect the health and safety of the population. There is no damage or breakage in the facility, there is no impact on natural resources.
Less valuable	There are no human deaths or serious injuries, the facility is slightly damaged, there is no idle situation, and there is a light and short-term impact on the environment.
Serious	Serious damage to facilities and loss of lives is possible among workers, but there is no fear for the health and life of people among the population, although there are negative, ultimately renewable effects on a number of natural resources.
Very serious	Casualties and injury to large number of workers working at the facility, significant damage to the facility, and significant and long-term damage to two or more natural resources are possible.
Catastrophic	The occurrence of an emergency that results in large numbers of human casualties and irreparable damage to large numbers of natural resources.

Based on the currently available operating experience, oil leaks from pipelines can be divided into the following categories according to the size of the leak and the amount of spilled oil [2-4]:

- small leaks: Such leaks can occur from holes with a diameter of 5-10 mm (average 7.5

- mm), which corresponds to the size of holes caused by corrosion in belts;
- medium leaks: holes varying in size from 10 to 50 mm;
 - major leaks. Sizes of leakage sites greater than 50 mm;
 - "hidden" or hard-to-detect leaks: leaks in pipelines of up to 3% of nominal flow or very small leaks.

Depending on the amount of oil spilled into the environment the value of oil loss due to an accident $Gn.i$ can be determined as follows:

$$Gn.i = Gn.s.q \cdot gts \tag{1}$$

where: $Qn.s.q$ - sale price or cost of crude oil, AZN./t; g - the amount of oil spilled into the environment per unit time, t/h; ts - the time period for oil leakage into the environment, hours (in calculations, it is considered as the time of detection of the leak).

According to the analysis, in cases where leaks are detected after the nominal time has passed, rather than on time, there will be a corresponding increase in the amount of material damage caused. If "hidden" leaks during operation remain undetected for 1 month, then the damage caused by oil losses for pipelines with nominal consumption values of 10, 50, 100, 200, t/h can be valued at 5.4; 27; 108; 270 thousand AZN respectively. Thus, the assessment of damage caused by oil spills alone shows that the most important condition is first of all the quick, operative detection of leaks. On the other hand, special attention should be paid to small, including "hidden" oil leaks. In many instances, the damage and complications resulting from such leakage cases can be more severe and impactful from both a material and environmental standpoint than those cases that are detected at a later time.

The experience of oil extraction shows that the factors most influencing the occurrence of accidents and failure of oilfield equipment and pipelines are related to corrosion-erosion processes. It is not coincidence that a (5x5) risk matrix was drawn up based on the analysis to assess the risks of stopping from erosion-corrosion (Table 3). At this time, the level of risk was assessed as follows: 1.2 - very low; 3.4 - low; 5...10 - average; 12...16 - high; 20...25 - very high [8].

Table 3: 5x5 risk matrix for assessing the risk of corrosion stoppages in technological pipelines

Parameters that determine the risk		Consequences of corrosion stoppages				
		Very low	Low	Average	High	Very high
Probability of stoppages from corrosion	Very high	5	10	15	20	25
	High	4	8	12	16	20
	Average	3	6	9	12	15
	Low	2	4	6	8	10
	Very low	1	2	3	4	5

III. Results

Considering that as the amount of oil spills increases, environmental damage and oil losses increase, and if we accept the probability of losses and damages P_z , then the probability of risk (P_R) can be defined as follows, considering the probability of oil spills ($P_{n.d}$) [5]:

$$P_R = P_{n.d} \cdot P_z \tag{2}$$

The variation of the probability of P_R calculated according to equation (2) depending on the rate of oil spillage into the environment q/Q_0 (Q_0 is the consumption of oil in the pipeline before spillage) is shown in Fig.2.

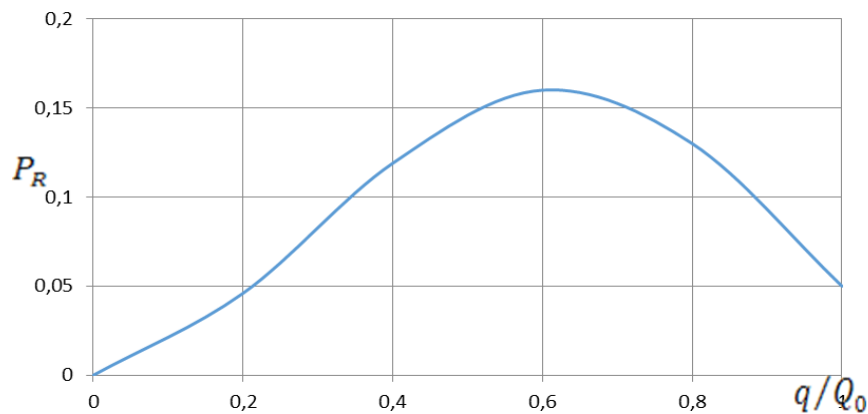


Fig. 2: Changes in risk probabilities depending on the degree of oil spills into the environment

IV. Discussion

Fig.2 illustrates that the highest likelihood of accidental oil spill risk is represented by a maximum probability of $P_{R_{max}} = 0.15$. This level of risk, which is not particularly high, corresponds to the value of $q/Q_0 = 0.6$ for the major leakage category. If we mark the price of the maximum economic damage caused by oil spills with Z , then it becomes clear that the maximum risk is $R_{max} = 0.15 Z$ and will occur with a probability of 0.15.

It should be noted that, although the probability of the risk is much lower, since it is related to dangerous objects and coincides with large oil spills ($q/Q_0 = 0.6$), its consequences can be quite sad.

Accidental oil spills that occurs during oil extraction and transportation were classified and the material and economic damage were assessed separately, including "hidden" leakage cases, and a methodical approach was proposed for the evaluation of the environmental and economic risk factor.

References

- [1] Instructions for accounting oil during its transportation. – Ufa: VNIISTPneft', 1995, 68 s. (in Russian)
- [2] Ismayilov G., Ismayilova H., Babirov H., Jabrayilova R. Assesment of environmental oil spills and economic-environmental risks. RT&A, Special Issue № 4 (70) Volume 17, November 2022
- [3] Control of leaks of oil and oil products on main pipelines during operation. – M.: VNIIOENG, 1981, s. 2-16. (in Russian)
- [4] Kravchenko V.F. Environmental protection during transportation and storage of oil and oil products // Reviews of foreign literature. – M.: VNIIOENG, 1976, 60 s. (in Russian)
- [5] Ismayilova H.G. On the assessment of damage from accidental losses' for various categories of oil leaks / Proceedings of the 69th International Scientific Conference "Oil and Gas" - 2015". – M.: 2015, s. 98. (in Russian)
- [6] Kremmer V.H. Oil and oil products leakage control system from pipelines // Transport and storage of oil and oil products. Foreign experience: Exp. – M.: VNIIOENG, 1980, s. 21-30. (in Russian)
- [7] RD Methodological Guidelines for Assessing the Risk of Accidents at Trunk Oil Pipelines. – M.: NTTS on Safety in Industry of Gosgortekhnadzor of Russia. 2012, 120 s. (in Russian)
- [8] Yorff P., Kichenko A. Problems of corrosion in the pipelines of the oil gathering system and ways to solve it. International industrial portal. Innovation, 7 June 2011.

RESEARCH OF REDUCING THE RISKS THAT MAY ARISE DURING THE PREPARATION OF GAS TRANSPORTATION

Fikrat Seyfiyev¹, Sahib Abdurahimov¹, Irada Hajiyeva¹, Meherrem Harbizadeh¹,
Vagif Rustamov², Ulfet Tagi-zade¹

¹ Azerbaijan State Oil and Industry University

² Ganja State University, Azerbaijan

Fikrat17@mail.ru

sahib-mathematic@rambler.ru

irada-niqar@mail.ru

harbizademehherrem@mail.ru

leyla.rustemova955@gmail.com

taghizadeu@gmail.com

Abstract

In order to prevent risks that may occur due to hydrates and other reasons in the system during gas collection and preparation for transport, detailed information is provided due to the study results of methanol prepared on the basis of local chemical products and diethylene glycol, used as an absorbent in the gas-methanol-water system, in laboratory conditions. According to the results of the research conducted on the basis of samples taken from the fields, surfactants, i.e., methanol, used to prevent the hydrate formation in production facilities, pipelines for the purpose of preventing accidents, failures, and the risk of environmental pollution there are many possibilities to optimize the amount of reagents required. In the next stage, methanol can be captured and reused through the diethylene glycol regeneration unit. By capturing methanol from the gas phase and regenerating both methanol itself and the diethylene glycol inhibitor, it is possible to protect the environment and minimize the risks that may occur in technological processes.

Keywords: gas condensate, risk, gas, hydrocarbon, hydrate, risk, highway, facilities

Introduction

There are many opportunities to optimize the amount of reagents required according to the working conditions in order to reduce the risks occurring in the technological processes during the collection and preparation of gaseous hydrocarbons for transportation. During the preparation and transport of gases correctly predicting the requirements for the reagents used and the distribution of the active ingredients between the gas and liquid phases are essential to minimize hydrate formation and other manageable risks. The presence of water, mineral salts and acidic components (H₂S, CO₂) in the products of the exploited gas and gas condensate deposits creates technological difficulties in the system (hydrate compounds, corrosion and salt deposits). This, in turn, disrupts the operation of gas collection and transport preparation facilities and main gas pipelines, and creates operational risks, leading to large gas losses and environmental pollution. In this regard, many scientific and technical measures are implemented to prevent risks that may occur during the accumulation of hydrocarbon gases in the fields and preparation for transportation, which ensures the transportation of the produced gas to the consumer without any

obstacles. It reduces the risk threshold that can be created by injecting active ingredients into the gas collection and transport preparation system to prevent gas hydrate formations. Methyl and isopropyl alcohols, ethylene, diethylene, triethylene, propylene glycol, etc. can be shown as inhibitors widely used in gas collection and transport preparation technology. However, due to the fact that active ingredients are volatile and well soluble in the gas phase, more than 50% of it is lost in contact with hydrocarbons. In addition to increasing the cost of the produced gas, this has a negative impact on the risk of spreading it to the environment [1].

II. Methods

Methanol, which is used against hydrate formation, absorbs the water vapors contained in the gas, in turn increases the risk of environmental pollution during the accumulation and storage of formation waters. Part of the applied methanol dissolves in the gas phase, and the other part dissolves in the liquid phase and hydrocarbon condensate. All these should be taken into account when determining the consumption of methanol [2, 3]

The total consumption rate of methanol used as surfactant is found according to the following expression.

$$C = D_m + D_g + D_c \quad (1)$$

Here, C is the total consumption of methanol; $\frac{kg}{1000m^3}$;
 D_m – consumption of methanol in the liquid phase, $\frac{kg}{1000m^3}$;
 D_g – consumption of methanol in the gas phase, $\frac{kg}{1000m^3}$;
 D_c – loss of methanol in hydrocarbon condensate, $\frac{kg}{1000m^3}$;

The consumption of methanol in the gas phase mainly depends on the moisture content of the gas and the concentration of methanol and is found as.

$$D_g = \frac{(W_1 - W_2) \cdot C_2}{C_1 - C_2} + 0,001C_2\alpha \quad (2)$$

Here, W_1 , W_2 are the amount of moisture in the gas phase before and after the injection of methanol, $\frac{kg}{1000m^3}$;

C_1 , C_2 are concentration of new and used methanol to be injected into the gas stream, mass %; α is the ratio of the amount of methanol used for the saturation of the gas phase to the amount of the methanol used in aqueous solids.

According to norms the density of methanol used against the hydrate formation in technological systems is 97%. The density of methanol used in the technological system depends on lowering the equilibrium temperature of hydrate formation, as well as on the physical and chemical properties of the active substance. Since the hydrate formation temperature in gases is known, the density of methanol in an aqueous solution can be determined using the following formula:

$$C_2 = \frac{M \cdot \Delta t}{K + M \cdot \Delta t} \cdot 100 \quad (3)$$

Here, C_2 is the concentration of methanol in the treated solution, mass %;

M – molecular mass of methanol;

K – coefficient of methanol. K = 1220.

Δt – depression of hydrate formation temperature, °C.

Based on the conducted studies, the consumption rate of methanol should be calculated according to the stages shown below. Their thermodynamic conditions should be taken into account in the process of gas collection and preparation for transportation. Thus, the drop in gas hydrate formation temperature is determined by the formula given below.

$$\Delta T_{gas} = T_{hyd} - T_{rep} \quad (4)$$

Here, ΔT_{gas} – is the temperature of gas hydrate formation, °C;

T_{hyd} – hydrate formation temperature of the gas at the starting point, °C;

T_{rep} – the temperature of the gas at the reporting point, °C;

III. Results

As a result of the increase in temperature in the hydrocarbon gas collection and transport preparation system, the surface tension of the surfactant decreases and the transition of hydrocarbon gases to the gas phase increases. Pressure has a much different effect on this process than temperature. As a result of the pressure increase at a constant temperature value, the transition of the surfactant to the gas phase also decreases and at a certain value it is at a minimum level. During the preparation of gas for transport, its dew point is significantly lowered by absorbing the moisture contained in it. At this time, while absorbing the liquid vapors contained in the gas through the diethylene glycol used as an absorbent, the methanol entering the gas phase will also be absorbed by the diethylene glycol. In the next process, methanol can be captured and reused through the diethylene glycol regeneration unit. The principle technological scheme of the experiment carried out in laboratory conditions is shown in Figure 1. The method of conducting the experiment is as follows: flask 1 was filled with methanol inhibitor of different concentrations, and then supplying of natural gas from its lower part was carried out. In the next step, diethylene glycol was added from flask 2 to the gas released in flask 1. Then, gas separation from diethylene glycol was performed in flask 3, and diethylene glycol regeneration was performed in flask 5. Meter 4 was used to measure the amount of gas coming out of flask 1. The amount of methanol absorbed from gas through diethylene glycol was determined by chromatographic analysis of samples taken from flask 3. We can see from the table that the concentration of methanol in an aqueous solution of diethylene glycol varies between (4.12 - 8.05) %. This means that approximately 50% of the methanol in the gas phase was regenerated through diethylene glycol and returned to the system. In the next step, let's focus on flask 5 for the regeneration of methanol from diethylene glycol.

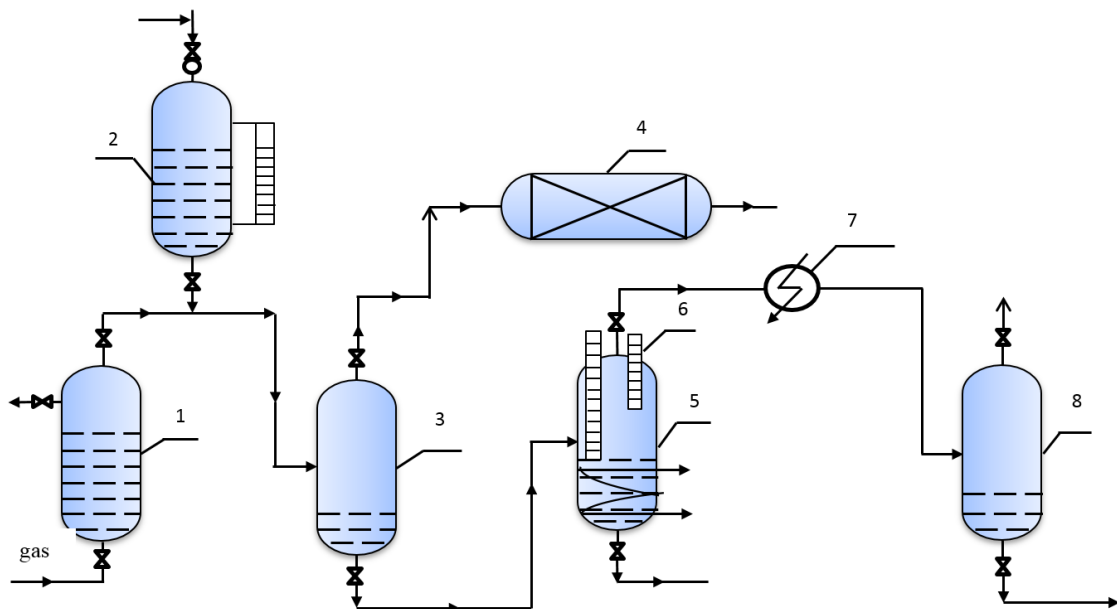


Fig. 1: Experimental scheme of the regeneration unit for the absorption of methanol in the gas phase with the help of diethylene glycol and its return to the system
 1 – flask for methanol, 2 – flask for diethylene glycol, 3 – flask for gas separated from diethylene glycol, 4 – gas meter, 5 – regeneration tank of diethylene glycol, 6 – thermometer, 7 – cooler, 8 – collection volume of methanol.

For this, as an example, the diethylene glycol-methanol mixture obtained from flask 3 was introduced into flask 5, heated to the required temperature, and the process of separating methanol was carried out. Then, the methanol vapors separated from diethylene glycol were condensed through cooler 7 and turned

into a liquid and collected in flask 8. For the separation of methanol from diethylene glycol, different temperatures were created in flask 5 and the temperature of (10–12)°C was given for turning the separated methanol vapors into liquid. By maintaining a temperature of (70–80) °C in the upper part of the regeneration flask, (90–92)% methanol can be obtained, which can be used to combat hydrate formation.

The results obtained from the experiment are given in the table below (Table 2).

Table 1: Absorption rates of methanol from the gas phase through diethylene glycol

The amount of methanol in the gas phase, gr/m ³	Content of diethylene glycol, mass %					The amount of methanol absorbed from the gas phase, mass%
	Starting composition		Next ingredient			
	Diethylene glycol	Water	Diethylene glycol	Methanol	Water	
0,88	85,0	15	81,0	4,12	14,88	50,0
0,92	82,0	18	74,5	8,05	17,45	59,0
1,05	79,0	21	75,0	6,65	18,35	51,0

Table 2: Regeneration indicators of the diethylene glycol - methanol - water (DEG – CH₃OH – H₂O) system

Composition of DEG absorbed methanol in the gas phase, mass%			Regeneration temperature above the tank, °C	Density of regenerated methanol, % mass	Composition of the residue after methanol regeneration, mass %		
DEG	CH ₃ OH	H ₂ O			DEG	CH ₃ OH	H ₂ O
81,0	4,12	14,88	70,0	90,0	85,6	1,10	13,30
74,5	8,05	17,45	78,0	93,0	80,0	1,30	18,70
75,0	6,65	18,35	72,0	92,0	78,0	0,70	21,30

Taking all this into account, the following technological scheme was developed for the regeneration of methanol from the diethylene glycol - methanol - water system (Fig. 2).

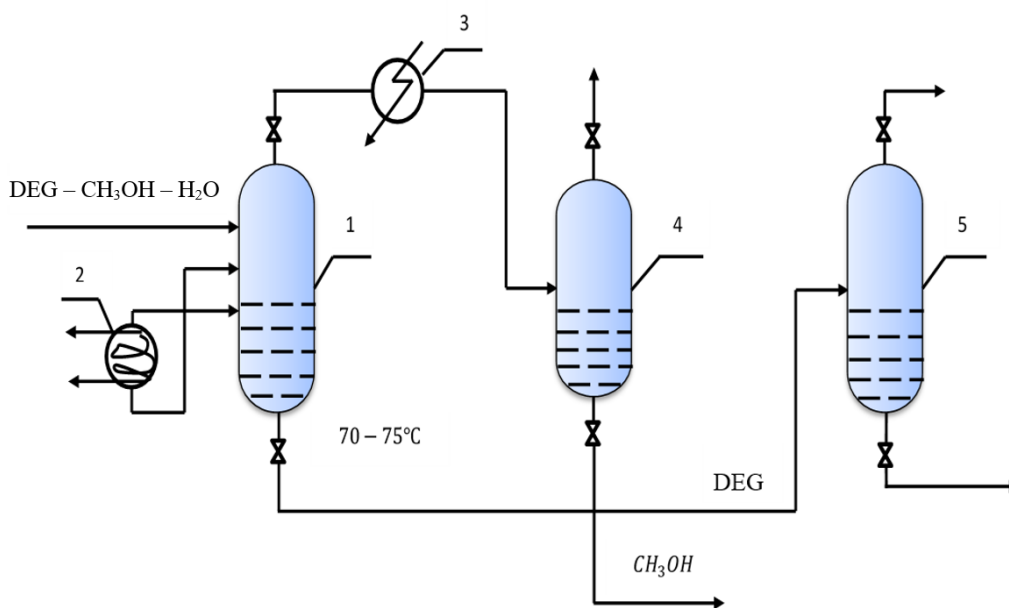


Fig. 2: Technological scheme for regeneration of methanol from diethylene glycol - methanol - water system.

1 – methanol regeneration tank, 2 – heater, 3 – cooler, 4 – methanol collection volume, 5 – diethylene glycol collection volume.

According to the planned scheme, the diethylene glycol - methanol - water system first enters tank 1 and the prescribed temperature regime is maintained. The separated $CH_3 - H_2O$ vapor enters the cooler 3 from the top of the boiler, turns into a liquid, collects in the volume 4, and returns to the system for reuse below it. After all these performed processes, the diethylene glycol-water solution in tank 1 is collected in flask 5 with a concentration of (75-85) % and returned to the system for reuse. Finally, we can mention that the process of capturing methanol from the gas phase and regenerating both methanol itself and diethylene glycol inhibitor, which is a regeneration substance, was carried out.

IV. Conclusions

In order to reduce the risks that occur in the technological processes of collection hydrocarbon gases in field conditions and preparing them for transportation, research studies were conducted in the laboratory to prevent the losses of methanol in the gas phase by capturing it through the diethylene glycol absorbent, regenerating and returning it to the system for reuse.

Methanol regeneration regimes were developed in order to reduce the risks that occur in the technological processes of gas collection and transport preparation, and to prevent methanol losses.

As a result of the calculations, it is possible to minimize the risks that may occur in the technological system, protect the environment, and prevent methanol losses up to 50%.

References

- [1] Musayev R.M., Aliyev V.I., Yusifov E.A. The method of prevention of gas hydrate formation by means of inhibitors. // Ecology and water management, №1, 2004, pp. 63 – 66.
- [2] International Journal of Energy, Information and Communications Vol. 4, Issue August 2013., p. 145.
- [3] Gritsenko A.I., Istomin V.A., Kulkov A.N., Suleimanov R.S. Gathering and field treatment of gas at the northern fields of Russia. - M.: OAO Publishing House Nedra, 1999., p. 473.: ill. – ISBN 5-247-03818-5.

ANALYSIS AND DAMAGE ASSESSMENT OF HAIL PROCESSES IN GEORGIA AND AZERBAIJAN USING RADAR DATA

(ON THE EXAMPLE OF MAY 28 AND JULY 13, 2019)

Mikheil Pipia^{1,2}, Avtandil Amiranashvili¹, Nazibrola Beglarashvili²,
Elizbar Elizbarashvili², Otar Varazanashvili¹

•

¹Mikheil Nodia Institute of Geophysics of Tbilisi State University, Georgia;

²Institute of Hydrometeorology of Technical University of Georgia

mikheil.pipia@tsu.ge

avtandilamiranashvili@gmail.com

otarivar@yahoo.com

beglarashvilinani@yahoo.com

eelizbar@hotmail.com

Abstract

The results of the analysis of radar studies of hail processes over the territories of Georgia and Azerbaijan on May 28 and July 13, 2019 are presented. Based on the values of the maximum size of hailstones in clouds, using the Zimenkov-Ivanov model, the expected sizes of hailstones falling on the earth's surface are calculated. The degree of damage to vineyards, wheat and corn, depending on the size of the hail, was determined by summarizing the known data on damage to these crops at different kinetic energy of hail and data on the average kinetic energy of hail of different magnitudes. Based on this compilation, regression equations were obtained for the relationship between the degree of damage to these crops and the size of hailstones, which have the form of a sixth degree of a polynomial. According to this equation, calculations were made of the degree of maximum damage to vineyards, wheat and corn along the trajectories of hail clouds over the territories of Georgia and Azerbaijan.

Keywords: Radar monitoring, dangerous meteorological processes, hail, damage assessment

I. Introduction

Almost all types of natural disasters, including hail processes, are observed in the territories of Georgia and Azerbaijan. Hail regularly causes serious material damage to agriculture, buildings, structures, infrastructure, transport, etc. Therefore, given the importance of the problem, special attention has always been paid to the study of hail processes in Georgia and Azerbaijan [1-4]. Given the significant economic damage caused by hail, in both countries at the end of the last century, work was carried out to combat this dangerous weather phenomenon [1,5]. In Georgia, these works continued until 1989 and were resumed using the latest technologies in Kakheti in 2015 [5]. The anti-hail service of Georgia is equipped with a modern meteorological radar "METEOR 735 CDP 10 - Doppler Weather Radar" [6], which in the future, in addition to anti-hail measures, is planned to be used for operational monitoring of various dangerous hydrometeorological processes in eastern Georgia and adjacent territories [7].

Most studies of hail processes are usually associated with the analysis of data from

meteorological stations on the number of days with hail [4, 8–10], the results of which are used to compile catalogs of natural disasters [11, 12]. However, in recent years, it has become possible, based on radar data, to study various characteristics of hail processes in Eastern Georgia and its neighboring countries (Azerbaijan, Armenia), including determining the maximum size of hail in clouds and modeling the size of the fallen hail [13-16].

For example, in work [16] results of modeling of the distribution of hailstones by mean max diameter (D) on the territory of Kakheti (Georgia) using data of the freezing level in the atmosphere and radar measurements of hail max sizes in clouds are presented. Maps of the distribution of hail by the average maximum diameter in the territory of Kakheti for individual months, from April to September, have been built. The vertical distribution of D on the indicated territory in the range of heights from 0.11 to 3.84 km was studied.

The works [13-15] provide a preliminary analysis of data from radar studies of hail processes in Georgia and Azerbaijan on May 28 and July 13, 2019. This work is a continuation of these studies. Below are the results of estimates of the maximum damage to crops such as vineyards, wheat and corn located in these areas in places with the maximum size of fallen hail.

II. Material and methods, study regions

The Anti-hail service is equipped with contemporary C-band, dual polarized Doppler meteorological radar “METEOR 735 CDP 10 – Doppler Weather Radar”, which is installed in the village Chotori (1090 m height from sea level) of the Signagi municipality of the Kakheti region of Georgia. The products of radar are sufficiently varied. For the anti-hail works the optimal radius of action of radar is 100-120 km, (distance, which practically covers the territory of Kakheti and some parts of the territories of Azerbaijan. In this work radar product HAILSZ (Size) is used [17]. The expected size of hailstones falling out to the earth's surface was calculated according to the Zimenkov-Ivanov model of hail melting in the atmosphere by taking into account the radar data about their diameter in the clouds [18]. As noted above, this study used data from works [13-15] with some clarifications.

The degree of damage to vineyards, wheat and corn, depending on the size of the fallen hail, was determined by compiling data on damage to these crops at different hail kinetic energy [1] and data on the average kinetic energy of hail of various sizes according to TORRO Hail Scale [<https://www.torro.org.uk/research/hail/hscale>].

Based on this compilation, regression equations were obtained for the relationship between the degree of damage to these crops (E) and the size of hailstones (D), which have the form of the sixth power of polynomial:

$$E = a \cdot D^6 + b \cdot D^5 + c \cdot D^4 + d \cdot D^3 + e \cdot D^2 + f \cdot D + g$$

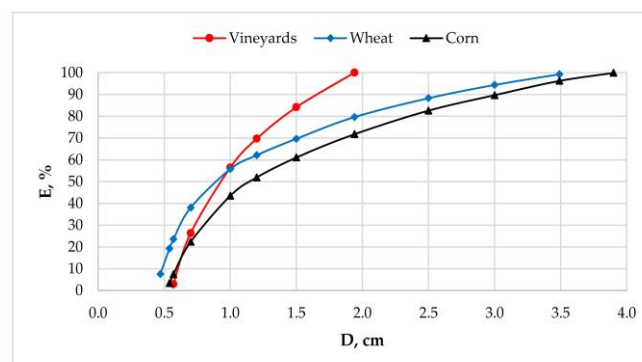


Fig. 1: Estimated values of the degree of damage to vineyards, wheat and corn, depending on the hail diameter

The graph of the dependence of E on D and the corresponding values of the coefficients of the regression equations in fig. 1 and table 1 are presented.

Table 1: Coefficients of the regression equation between the hail diameter(D) and the degree of damage to vineyards, wheat and corn (E).

Coefficient	Vineyards, E(V), %	Wheat, E(W), %	Corn, E(C), %
a	-90.668476	-3.172890	-1.055694
b	730.212998	41.423518	15.570944
c	-2417.485762	-217.770722	-93.078903
d	4233.390175	589.590662	289.192073
e	-4188.725197	-872.075534	-498.263105
f	2315.215755	696.428514	479.987909
g	-525.511778	-178.662752	-148.866255
Range of D, cm	0.57÷1.94	0.47÷3.49	0.54÷3.90

Taking into account the above calculations, we have proposed a modified TORRO scale, which also takes into account the degree of damage to vineyards, wheat and corn at different hail sizes (H0-H5 scale range, Table 2).

Table 2: Modified TORRO Hail Scale: The Intensity (H) of Hail and Possible Damage (<https://www.torro.org.uk/research/hail/hscale> and [2])

H	Intensity Category	Typical Hail Diameter (cm)	Typical Damage Impacts
H0	Hard Hail	0.5	No damage. Wheat damage up to 13%
H1	Potentially Damaging	0.5-1.5	Slight general damage to plants, crops. Damage to vineyards up to 84%, wheat - (13-70)%, corn - up to 61%
H2	Significant	1.0-2.0	Significant damage to fruit, crops, vegetation. Damage to vineyards (56-100)%, wheat - (56-81)%, corn - (44-73)%
H3	Severe	2.0-3.0	Severe damage to fruit and crops, damage to glass and plastic structures, paint and wood scored. Damage to vineyards -100%, wheat - (81-94)%, corn - (73-90)%.
H4	Severe	2.5-4.0	Severe damage to fruit and crops. Widespread glass damage, vehicle bodywork damage. Damage to vineyards -100%, wheat - (88-100)%, corn - (83-100)%.
H5	Destructive	3.0-5.0	Wholesale destruction of glass, damage to tiled roofs, significant risk of injuries. Damage to vineyards -100%, wheat - (94-100)%, corn - (90-100)%.
H6	Destructive	4.0-6.0	Bodywork of grounded aircraft dented, brick walls pitted
H7	Destructive	5.0-7.5	Severe roof damage, risk of serious injuries
H8	Destructive	6.0-9.0	(Severest recorded in the British Isles) Severe damage to aircraft bodywork
H9	Super Hailstorms	7.5-10.0	Extensive structural damage. Risk of severe or even fatal injuries to persons caught in the open
H10	Super Hailstorms	>10.0	Extensive structural damage. Risk of severe or even fatal injuries to persons caught in the open

The following designations will be used below. Study Regions. Georgia: GEO-1 (Sagarejo municipality), GEO-2 (Signagi municipality). Azerbaijan: AZE-1 (Aghstafa and Tovuz districts),

AZE-2 (Balakan district), AZE-3 (Zagatala district).

D – maximum hail diameter at the ground level, cm; time designation, for example, 14 hours 33 min – 14.55 h (hour and minutes in fractions of an hour). In Figures 2 and 4 time is represented as hour and minutes in fractions of an hour and a serial number. Hours and time number for each study region are presented in the Table 3.

III. Results

The results in Fig. 2-7 and Table 3 are clearly represented.

In Fig. 2 hail size changeability in at the ground level in Georgia and Azerbaijan on May 28 and July 13, 2019 in five researched locations are presented.

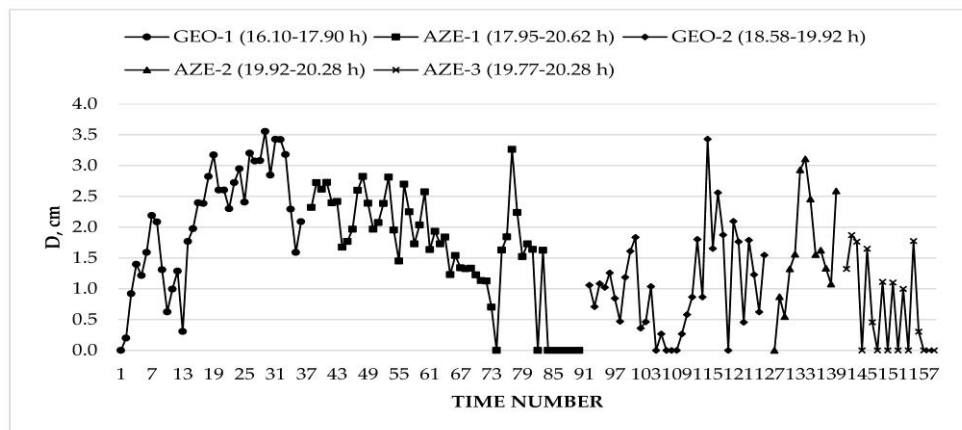


Fig. 2: Hail size changeability in at the ground level in Georgia and Azerbaijan on May 28, 2019 (GEO-1, AZE-1) and July 13, 2019 (GEO-2, AZE-2, AZE-3)

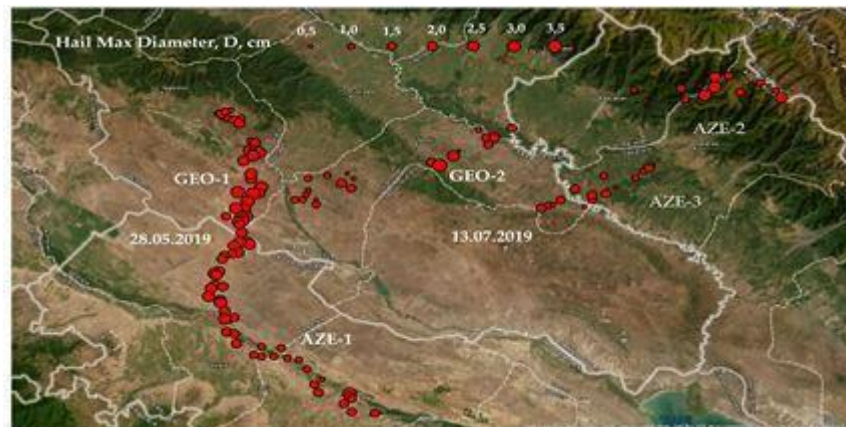


Fig. 3: Trajectory of hailstones with maximum diameter at the ground level in Georgia and Azerbaijan during the study period

In Fig. 3 trajectory of hailstones with maximum diameter at the ground level in Georgia and Azerbaijan during the study period are presented. In Table 3 statistical characteristics of the maximum hail diameter at the ground level and the degree of damage to vineyards, wheat and corn in the study regions are presented.

As follows from Fig. 2,3 and Table 3, the maximum D value varied from 1.9 cm (AZE-3) to 3.6 cm (GEO-1). Mean D values varied from 0.7 cm (AZE-3) to 2.1 cm (GEO-1). On the territory of Azerbaijan, the maximum D value was 3.3 cm (AZE-1), the maximum average hail diameter - 1.6

cm (AZE-1 and AZE-2).

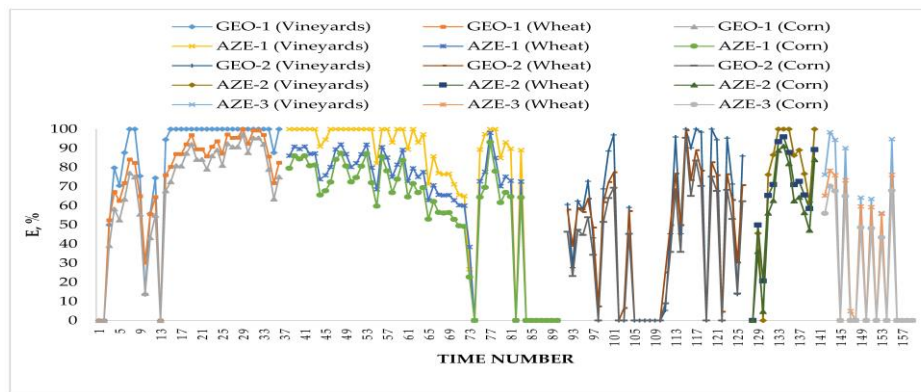


Fig. 4: Changeability of vineyards, wheat and corn damage in Georgia and Azerbaijan on May 28, 2019 (GEO-1, AZE-1) and July 13, 2019 (GEO-2, AZE-2, AZE-23)

In Fig. 4 data about changeability of vineyards, wheat and corn damage in Georgia and Azerbaijan in all researched locations are presented.

In Fig. 5-7 maps of maximum damage of vineyards, wheat and corn locations in Georgia and Azerbaijan during the study period are presented.



Fig. 5: Maximum vineyards damage locations in Georgia and Azerbaijan during the study period



Fig. 6: Maximum wheat damage locations in Georgia and Azerbaijan during the study period



Fig. 7: Maximum corn damage locations in Georgia and Azerbaijan during the study period

As follows from Fig. 4-7 and Table 3, the maximum values of E(V) varied from 98% (AZE-3) to 100% (all other locations). Mean E(V) values varied from 35% (AZE-3) to 83% (GEO-1). On the territory of Azerbaijan, the maximum value of E(V) was 100% (AZE-1 and AZE-2), the maximum average value - 75% (AZE-1).

The range of variability of the maximum values of E(W) is from 78% (AZE-3) to 100% (GEO-1). The range of variability of the average values of E(W) is from 30% (AZE-3) to 75% (GEO-1). The maximum value of E(W) on the territory of Azerbaijan was 98% (AZE-1), the maximum average value - 65% (AZE-1 and AZE-2).

Table 3: Statistical characteristics of the maximum hail diameter at the ground level and the degree of damage to vineyards, wheat and corn in Georgia and Azerbaijan on May 28 and July 13, 2019 (minimum hail diameter = 0 cm)

Date	Hour (Time number)	Count	Variable	D, cm	Vineyards, E(V),%	Wheat, E(W),%	Corn, E(C),%	Location
28.05	16.10-17.90 (1-36)	36	Max	3.6	100	100	97	GEO-1
			Average	2.1	83	75	69	
			St Dev	1.0	31	28	28	
	17.95-20.62 (37-89)	53	Max	3.3	100	98	93	AZE-1
			Average	1.6	75	65	58	
			St Dev	0.9	37	31	29	
13.07	18.58-19.92 (90-124)	35	Max	3.4	100	99	95	GEO-2
			Average	1.0	48	44	37	
			St Dev	0.8	40	33	31	
	19.92-20.58 (125-137)	13	Max	3.1	100	96	91	AZE-2
			Average	1.6	71	65	57	
			St Dev	0.9	35	28	29	
19.77-20.28 (138-155)	18	Max	1.9	98	78	70	AZE-3	
		Average	0.7	35	30	26		
		St Dev	0.7	42	35	31		

The maximum values of E(C) varied from 70% (AZE-3) to 97% (GEO-1). Mean E(C) values varied from 26% (AZE-3) to 69% (GEO-1). On the territory of Azerbaijan, the maximum value of E(C) was 93%, the maximum average value - 58% (AZE-1).

IV. Discussion

Radar studies of hail clouds are an important tool for assessing the maximum degree of hail damage to crops and other vegetation using various models, one of which is proposed in this paper. Comparison of calculated data with real ones showed the following.

According to the anti-hail service of Georgia, on May 28, 2019, 120 hectares of vineyards were damaged on the territory of the Sagarejo municipality (GEO-1) with an average degree of damage of 45%, (calculated average values of $E(V)$ in places with hail fall with the largest size = 83%) and also 808 ha of wheat with a damage rate of 66.5% (calculated values of $E(W) = 75\%$). On July 13, 2019 in Signagi municipality (GEO-1) hail damaged 700 ha of vineyards with an average damage rate of 28.3% (calculated values of $E(V) = 48\%$).

V. Conclusion

Given that the calculated values of the degree of damage to agricultural crops were carried out for places with the largest hail fall, these data exceed the real ones (for vineyards by 1.84 times and 1.7 times, and for wheat by 1.13). Considering the above, we can conclude that the calculated values of E are generally in good agreement with their real values.

In the future, we intend to continue these studies using more extensive experimental material. In particular, it is planned to build maps of the degree of damage from hail of vineyards, wheat and corn on the territory of Kakheti in different months of the year. It is also planned to carry out model assessments of damage from hail and other agricultural crops.

Acknowledgments. The research is done with the support of "Shota Rustaveli national scientist foundation" [Grant number – YS-22-1062].

References

- [1] Abshaev, A.M., Abshaev, M.T., Barekova, M.V., Malkarova, A.M. (2014). Rukovodstvo po organizacii i provedeniu protivogradovih rabot (book). Pechatni dvor. Nalchik. p. 500. (in Russian).
- [2] Varazanashvili O., Tsereteli N., Amiranashvili A., Tsereteli E., Elizbarashvili E., Dolidze J., Qaldani L., Saluqvadze M., Adamia Sh., Arevadze N., Gventcadze A. (2012). Vulnerability, Hazards and Multiple Risk Assessment for Georgia. *Natural Hazards*. Vol. 64, Number: 2021-2056.
- [3] Kartvelishvili L., Tatishvili M., Amiranashvili A., Megrelidze L., Kutaladze N. (2023). Weather, Climate and their Change Regularities for the Conditions of Georgia. (Book). Publishing House "UNIVERSAL". Tbilisi. p. 406.
- [4] Elizbarashvili E., Amiranashvili A., Varazanashvili O., Tsereteli N., Elizbarashvili M., Elizbarashvili Sh., Pipia M. (2014) Hailstorms in the Territory of Georgia. *European Geographical Studies*. Vol. 2, No. 2. pp. 55-69. (in Russian).
- [5] Amiranashvili A.G. (2017). History of Active Effects on Atmospheric Processes in Georgia. In the book: Essays of the History of Weather Modification in the USSR and the Post-Soviet Territory. RSHMU. St. Petersburg, p. 352 (in Russian).
- [6] Abaiadze O., Avlokhshvili Kh., Amiranashvili A., Dzodzuashvili U., Kiria J., Lomtadze J., Osepashvili A., Sauri I., Telia Sh., Khetashvili A., Tskhvediasvili G., Chikhladze V. (2016). Radar Providing of Anti-Hail Service in Kakheti. *Trans. of Mikheil Nodia Institute of Geophysics*. vol. 66. Tb. pp. 28-38. (in Russian).
- [7] Amiranashvili A., Chikhladze V., Dzodzuashvili U., Ghlonti N., Sauri I., Telia Sh., Tsintsadze T. (2019). Weather Modification in Georgia: Past, Present, Prospects for Development. Int. Sc. Conf. „Natural Disasters in Georgia: Monitoring, Prevention, Mitigation“. Proc., Tbilisi, Georgia, December 12-14, 2019. pp. 213-219.

[8] Beglarashvili N., Janelidze I., Pipia M., Varamashvili N. (2020). Hail Storms in Kakheti (Georgia) in 2014-2018. Int. Sc. Conf. „Modern Problems of Ecology“. Proc. v. 7. Tbilisi-Telavi, Georgia, 26-28 September, 2020. pp. 176-179.

[9] Amiranashvili A., Basilashvili Ts., Elizbarashvili E., Gaprindashvili G., Varazanashvili O. (2022). Statistical Analysis of the Number of Days with Hail in Georgia According to Meteorological Stations Data in 2006-2021. Int. Conf. of Young Scientists “Modern Problems of Earth Sciences”. Proc. Publish House of Iv. Javakhishvili Tbilisi State University, Tbilisi, November 21-22, 2022. pp. 164-168.

[10] Amiranashvili A., Elizbarashvili E., Varazanashvili O., Pipia M. (2023). Statistical Analysis of the Number of Days with Hail During the Warm Season in Tbilisi in 1891-2021. *Trans. IHM, GTU*. vol.133. pp. 74-77. (in Georgian).

[11] Varazanashvili O.Sh., Gaprindashvili G.M., Elizbarashvili E.Sh., Basilashvili Ts.Z., Amiranashvili A.G. (2022). Principles of Natural Hazards Catalogs Compiling and Magnitude Classification. *Journal of the Georgian Geophysical Society, Physics of Solid Earth, Atmosphere, Ocean and Space Plasma*, v. 25(1). pp. 5-11.

[12] Gaprindashvili G., Varazanashvili O., Elizbarashvili E., Basilashvili Ts., Amiranashvili A., Fuchs S. (2023). GeNHs: the First Natural Hazard Event Database for the Republic of Georgia. EGU General Assembly 2023, EGU23-1614.

[13] Gvasalia G., Kekenadze E., Mekoshkishvili N., Mitin M. (2019). Radar Monitoring of Hail Processes in Eastern Georgia and its Neighboring Countries (Azerbaijan, Armenia). Int. Sc. Conf. „Natural Disasters in Georgia: Monitoring, Prevention, Mitigation“. Proc., Tbilisi, Georgia, December 12-14, 2019. pp. 170-174.

[14] Amiranashvili A., Bliadze T., Jamrishvili N., Kekenadze E., Tavidashvili Kh., Mitin M. (2019). Some Characteristics of Hail Process in Georgia and Azerbaijan on May 28, 2019. *Journal of the Georgian Geophysical Society, Physics of Solid Earth, Atmosphere, Ocean and Space Plasma*. v. 22(2). pp. 40-54.

[15] Kekenadze E., Samkharadze I. (2020). Preliminary Analysis of the Hail Process Above the Territory of Georgia, Armenia and Azerbaijan on July 13, 2019. Int. Sc. Conf. „Modern Problems of Ecology“. Proc. v. 7. Tbilisi-Telavi, Georgia, 26-28 September, 2020. pp. 167-171.

[16] Amiranashvili A.G., Bolashvili N.R., Gulashvili Z.M., Jamrishvili N.K., Suknidze N.E., Tavidashvili Kh.Z. (2021). Modeling the Distribution of Hailstones by Mean Max Sizes on the Territory of Kakheti (Georgia) using Data of the Freezing Level in the Atmosphere and Radar Measurements. *Journal of the Georgian Geophysical Society, e-ISSN: 2667-9973, p-ISSN: 1512-1127, Physics of Solid Earth, Atmosphere, Ocean and Space Plasma*. v. 24(1). pp. 25-36.

[17] Selex ES GmbH · Gematronik Weather Radar Systems. Rainbow®5 User Guide, 2015, 464 p., www.gematronik.com

[18] Zimenkov V.A., Ivanov V.V. (1966). Raschet tayaniya gradin v estestvennykh protsessakh. *Tr. VGI*. vyp. 3(5). (in Russian).

UP-TO-DATE DETAILED SEISMIC ZONING OF REGIONS IN KAZAKHSTAN (PGA CASE)

Natalya Silacheva

•

Institute of Seismology, Ministry of Emergency Situations of the Republic of Kazakhstan
silacheva_nat@mail.ru

Abstract

The results of the first project in Kazakhstan on the Detailed Seismic Zoning of regions on a new methodological basis are presented. The Probabilistic Seismic Hazard Assessment is carried out for the territories of East Kazakhstan (since 2022 EKO and Abay), Almaty (since 2022 Almaty and Zhetysu) and Zhambyl regions using a methodology consistent with the main provisions of Eurocode 8 and updated compared to that used in maps of the recent General Seismic Zoning of Kazakhstan territory. Modern methods and tools of analysis were used, as well as the most complete and up-to-date information available for the territories under consideration. The seismic source model included areal sources and active faults. The developed maps are discussed and hazard curves and uniform hazard spectra for the main cities in the considered regions are presented. The obtained results are generally consistent with the General Seismic Zoning but display some differences in PGA distribution due to including active faults and a comprehensively revised catalogue. Zoning maps will be the basis for the development of new state building regulations of the Republic of Kazakhstan.

Keywords: probabilistic seismic hazard assessment, seismic zoning, peak ground acceleration

I. Introduction

Until recently, Kazakhstan's regulatory documents regulating construction in seismic areas were based on a deterministic assessment of seismic hazards, and the main parameter describing the seismic effect was the macroseismic intensity [1]. With the transition of the construction state standards of the Republic of Kazakhstan to the basic principles of Eurocode 8 [2], seismic zoning maps corresponding to these principles were developed. The last General Seismic Zoning (GSZ) of the territory of Kazakhstan [3, 4] and Seismic Microzoning (SMZ) of Almaty City [5, 6] (the highest seismic city in the country) were carried out on a fundamentally new country-wide methodical basis. The new zoning maps became probabilistic and expressed in both macroseismic intensities and quantitative parameters – peak ground accelerations (PGA).

In the research project carried out by the Institute of Seismology of Kazakhstan in 2021–2023, "Seismic Hazard Assessment of Regions and Cities of Kazakhstan on a Modern Scientific and Methodological Basis," all elements of the used Probabilistic Seismic Hazard Assessment (PSHA) have been updated. We use the comprehensively revised and updated catalogue. A seismic source model includes not only area sources as before but also active faults. Sets of ground motion models (GMMs) have been updated. The Open Quake software is used both for calculations in PGA and macroseismic intensities. The project is the first stage of ongoing work and includes Detailed Seismic Zoning (DSZ) of three administrative regions (oblasts): East-Kazakhstan (East-Kazakhstan and Abay since 2022), Almaty (Almaty and Zhetysu since 2022), and Zhambyl oblasts, and SMZ of Ust-Kamenogorsk city. In this paper, we will focus on the issues of DSZ in PGA.

II. Methods

The whole scope of study on the project covered such areas as geological-geophysical criteria of SHA, structural-tectonic criteria of SHA, seismicity and seismic regime, macroseismic data, GMMs selection and testing, source mechanisms and parameters of seismotectonic deformations, regional map of seismogenerative zones, map of active faults, catalogue of earthquakes and seismic regime, seismic source model (active fault, area and hybrid), PSHA and mapping in PGA and macroseismic intensities, etc.

PSHA procedure included identification and characterization of faults and area zones and creation of seismic source model; magnitude-frequency distribution for the seismic sources; evaluation of the generated ground motion and estimation of the probability that the ground motion will be exceeded during a particular period. We applied Cornell's methodology [7], but using the methodological formalism of Field et al. [8], implemented in the Open Quake Engine software [9]. Mathematically PSH is described by the following expression of the total probability theorem:

$$\lambda(a) = \sum_i v_i \iint P[A > a | m, r] f_{M_i}(m) f_{Ri|Mi}(r; m) dr dm,$$

where a is the specified ground motion amplitude, $\lambda(a)$ – annual frequency of earthquakes that produce a ground motion amplitude A higher than a (PGA, PGV, SA, MSK intensity, etc). The summation extends over all source zones, v_i is the annual rate of earthquakes with magnitudes higher than a threshold m_0 in source i . $f_{M_i}(m)$ and $f_{Ri|Mi}(r; m)$ are probability density functions on m and r respectively. $P[A > a | m, r]$ is the probability that an earthquake of magnitude m at distance r produces a ground motion magnitude A at the site that is greater than a . Calculations were made for two probabilities of exceedance - 10% and 2% in 50 years.

We used the comprehensively improved earthquake catalogue for Central Asia, developed in the international ISTC Project "Central Asia Seismic Hazard Assessment and Bulletin Unification" (CASHA-BU). In that project completed last year, a huge volume of data, collected by several generations of seismologists, was digitized, systematized, reprocessed, and converted to a format suitable for different tasks of seismology. The full catalogue includes about 442.500 earthquakes. The work on the full catalogue is not finished yet, but for the needs of PSHA in Central Asia and Kazakhstan, a complete catalogue has been created on its basis [10].

The source model includes active faults and area sources. Area polygons were outlined taking into account the seismicity pattern, important topographic and tectonic characteristics and theoretically estimated seismic potential.

Modelling of active faults in the territory of Kazakhstan is complicated due to insufficient knowledge of the characteristics of most faults and, as a consequence, the lack of the required parameters for hazard analysis input (like, kinematic parameters or slip rates). To decrease errors, we used two models of active faults, one based on the Active Fault Data Base created in this project with the use of materials accumulated in our Institute for a long period of previous geological-geophysical studies and another based on the Data Base of Active Faults of Eurasia (AFEAD) created by the Geological Institute of Russian Academy of Sciences [11].

Available analogue records of the regional strong motion network operated in 1980-1996 were digitized in addition to later digital records for testing selected GMMs. We performed a comprehensive study on GMMs selection for seismically active regions of Kazakhstan and tested their applicability with the use of regional data. The territory of the considered oblasts is characterized by active and partially stable seismotectonic regimes. The upgraded GMM logic tree for active regions included weighted models of Akkar and Bommer, 2010 [12], Zhao et al, 2016 [13], Abrahamson et al, 2014, Boore et al, 2014, Chiou and Youngs, 2014 (NGA-WEST2 models [14], for stable areas – Boore, 2015, Darragh et al, 2015, Spahjouei and Pezeschk, 2015 and Yenier and

Atkinson, 2015 (NGA East models [15]).

Probabilistic analysis was carried out with the use of the Open Quake Engine software [9]. The seismic source logic tree included two models - a combination of area sources with two active fault models. The GMM logic tree included sets of five models for crustal earthquakes in active regions and four for earthquakes in stable regions.

The analysis was carried out for two probabilities of exceedance - 10% and 2% in 50 years (return period 475 and 2475 years, respectively). The calculations were performed in the average values of the geometric mean peak ground accelerations (PGA in fractions of g) for the territory of the considered oblast on a grid with an interval of 5 km in both directions. For each calculated point, the impact from seismic sources located within a radius of 300 km was taken into account, concerning their seismotectonic regime. Soil conditions correspond to rocky and rock-like geological formations, for the surface 30-meter strata of which are typical shear wave propagation velocities $V_{s30} \geq 800$ m/s.

III. Results

The obtained DSZ maps of East Kazakhstan (since 2022 EKO and Abay) oblast are shown in Figure 1, and hazard curves and uniform hazard spectra for the main cities in the region - Ust-Kamenogorsk and Semey - are shown in Figure 2. DSZ maps of the Almaty oblast are shown in Figure 3, and hazard curves and uniform hazard spectra for the main cities in the oblast - Almaty and Taldykorgan – are in Figure 4. Results for the Zhambyl oblast are shown in Figures 5-7.

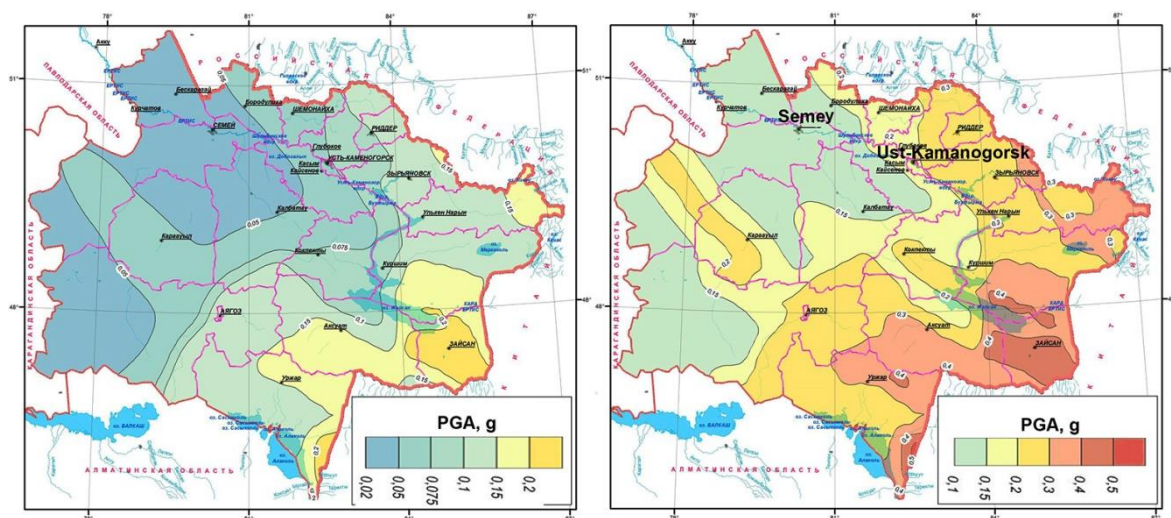


Fig. 1: DSZ map of East Kazakhstan Oblast in PGA for 10% (left) and 2% (right) probability of exceedance in 50 years

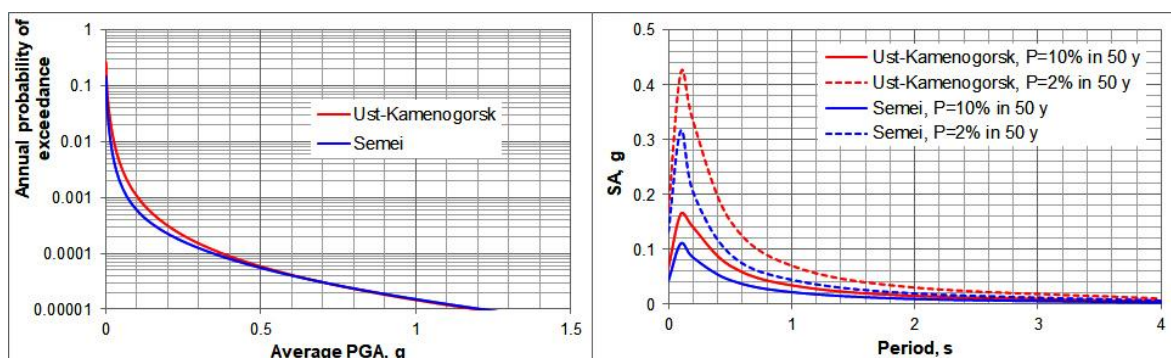


Fig. 2: Hazard curves (left) and uniform hazard spectra (right) for the main cities in the East Kazakhstan oblast (rock conditions)

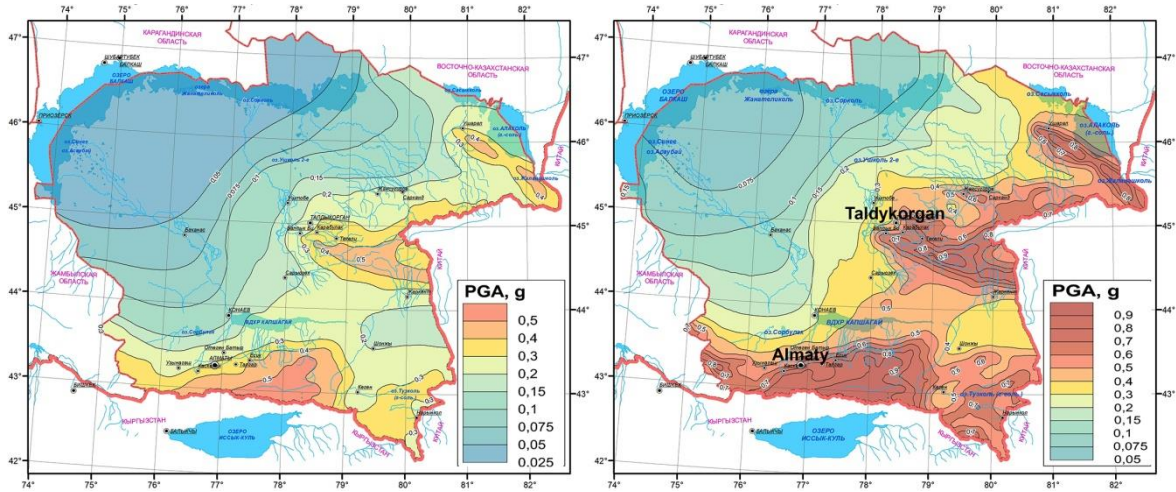


Fig. 3: DSZ map of the Almaty Oblast in PGA for 10% (left) and 2% (right) probability of exceedance in 50 years

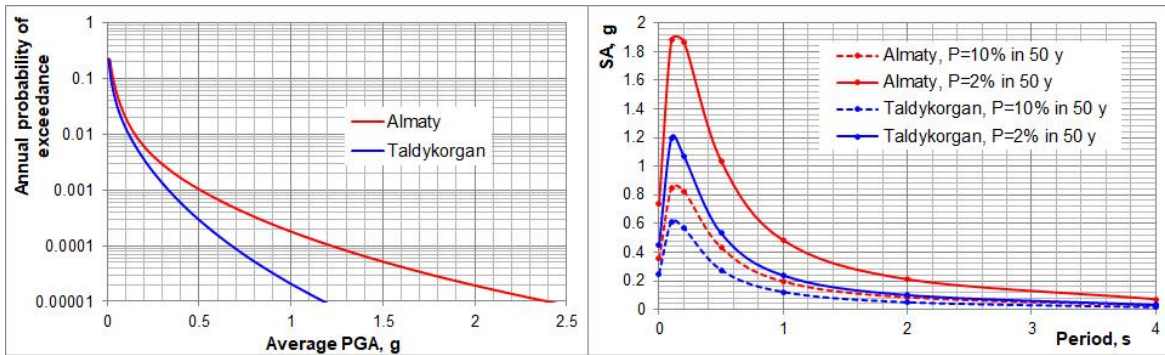


Fig. 4: Hazard curves (left) and uniform hazard spectra (right) for the main cities in the Almaty oblast (rock conditions)

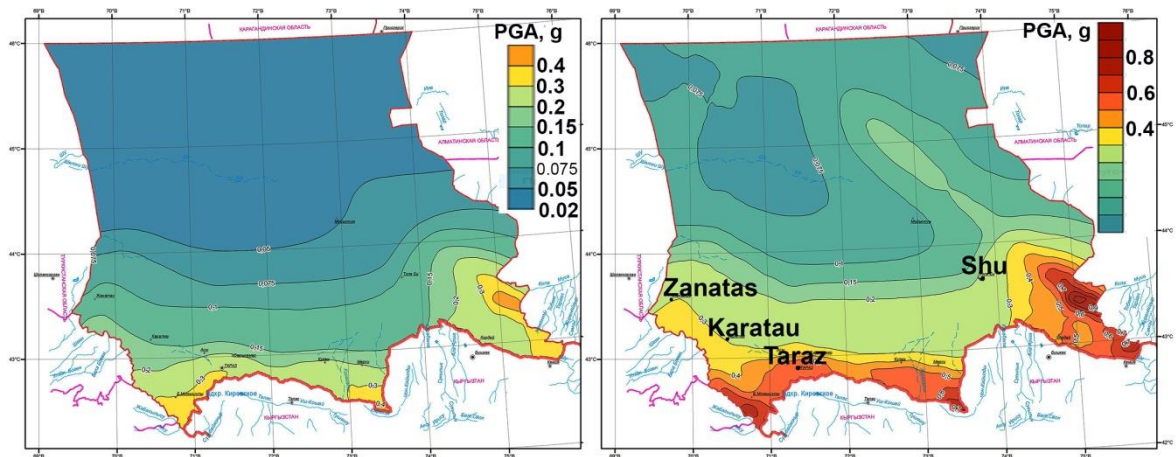


Fig. 5: Preliminary DSZ maps of the Zhambyl oblast in PGA for 10% (left) and 2% (right) probability of exceedance in 50 years

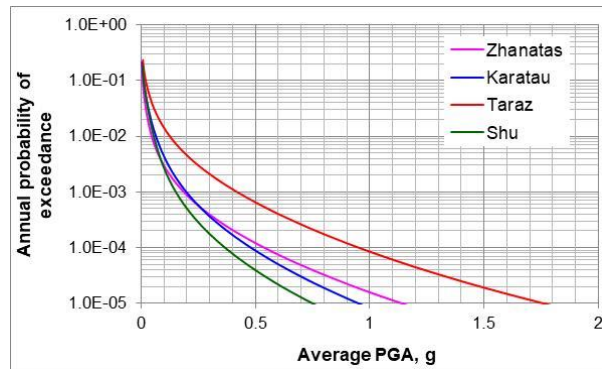


Fig. 6: Hazard curves for the main cities in the Zhambyl oblast (rock conditions)

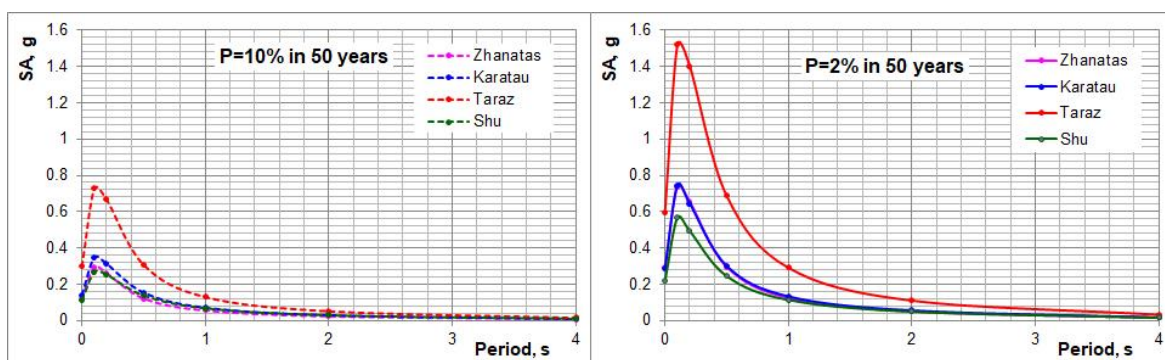


Fig. 7: Uniform hazard spectra for the main cities in the Zhambyl oblast (rock conditions)

IV. Discussion

On the resulting map of the DSZ of the East-Kazakhstan region (Figure 1), PGA increases from the northwest to the southeast, from the territories with a stable tectonic regime to the active regions. On the map with a probability of exceedance 10% in 50 years (return period 475 years), the PGA values increase from 0.040 g at the northwestern boundary of the region to 0.268 g in the south and 0.224 g in the southeast (Figure 1, left). On the map with a probability of exceedance 2% in 50 years (return period 2475 years), PGA increases from 0.132 g in the northwest to 0.514 g in the south and 0.482 g in the southeast (Figure 1, right). The maximum acceleration level in the southern part of the region is caused by an area source in the buffer zone with a higher density of earthquakes with an M_w magnitude of 5–6. In the southeast, the highly seismic areal zone with magnitudes $M_w > 6$ as well as the North Zaisan (M_w up to 7.2) and Saur (M_w up to 7.2) faults (Figure 8 a) also have a great influence. The highly seismic Narym (M_w up to 7.5) and Rakhmanov (M_w up to 7.5) faults (Figure 8 a) increase the level of the expected PGA in the eastern part. Due to the use of not only areal sources but also active faults, thorough cleaning of the catalogue from explosions and refinement of the fault map, more pronounced areas of higher danger along the Chingiz-Tarbagatai fault (Figure 8) was obtained in the western part of the region (Figure 1) than during the General Seismic Zoning [4]. In the west of the territory, the values of expected PGA also increased due to more accurate consideration of seismotectonic conditions and the seismic potential of territories with a stable regime.

The map of DSZ of the territory of the Almaty region with a probability of exceedance 10% in 50 years shows that PGA values exceed 0.15g in half of the territory of the region, increasing in the southeastward from 0.025 to 0.55 g (Figure 3, left). The maximum values of 0.4-0.5 g were expectedly obtained for areas located southeast of Almaty, which corresponds to the location of the most

seismically dangerous Zailiy (Mw up to 8), Kemin and North Kungei (Mw > 8) active fault zones (Figure 9), as well as in the area of the South Dzhungar (Mw up to 7.0) active fault zone. On the DSZ Map, with a probability of exceedance of 2% in 50 years accelerations similarly increase from 0.062 to 1 g (Figure 3, right). In half of the territory, the accelerations exceed 0.3 g, reaching more than 0.9 g in the area where the most highly seismogenerative zones are located.

On the DSZ maps of the Zhambyl region (Figure 5) PGA level increases from north to south towards the highly seismic regions at the southern border of Kazakhstan. At a probability of exceedance of 10% in 50 years, the values are in the range of 0.025–0.468 g; at a probability of 2% in 50 years, they are in the range of 0.074–0.960 g. The maximum values are predicted in the southeast in the area at the Zhetyzhol (Mw up to 7.0) and Kendyktas (Mw up to 7.0) active faults (Figure 10).

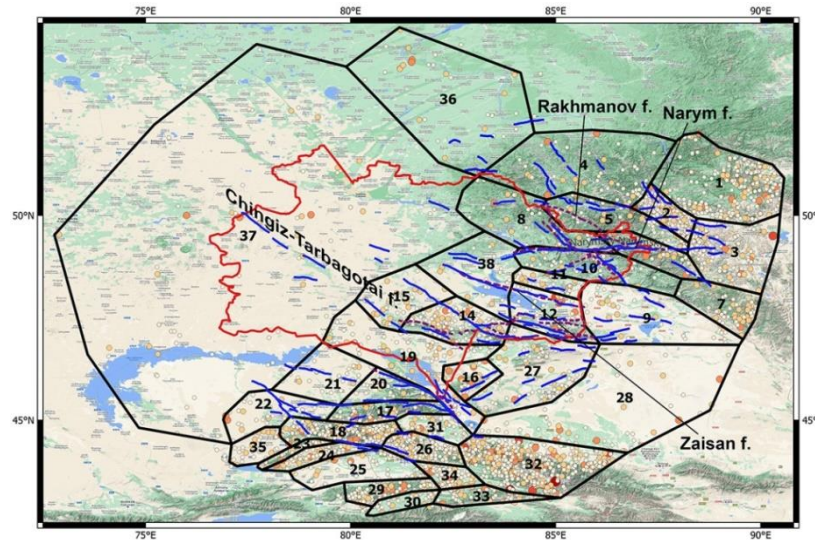


Fig. 8: Fault and areal seismic sources for the East Kazakhstan region. Faults are shown as blue lines, and zones as black polygons. The region boundary is shown with a red line

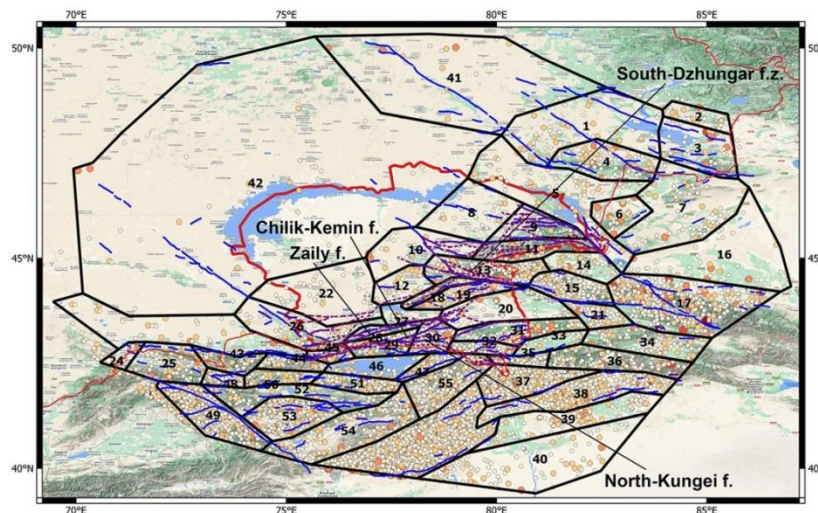


Fig. 9: Fault and areal seismic sources for the Almaty region. Faults are shown as blue lines, and zones as black polygons. The region boundary is shown with a red line

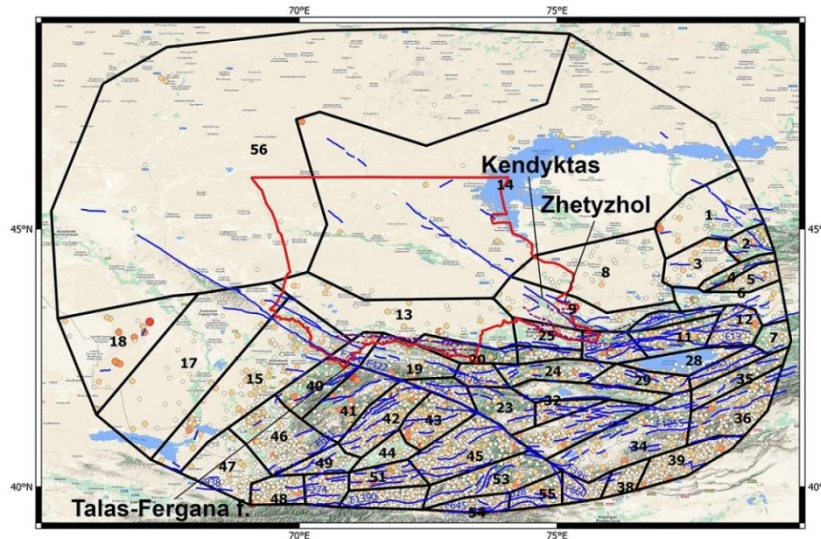


Fig. 10: Fault and areal seismic sources for the Zhambyl region. Faults are shown as blue lines, and zones as black polygons. The region boundary is shown with a red line

The obtained distribution of seismic hazard in the considered regions is consistent in general with the previous results of the General Seismic Zoning of Kazakhstan [4], but due to the inclusion of active faults and increased map detail, the distribution of seismicity has become more structured with more pronounced zones of increased danger along the faults. The use of a comprehensively revised catalogue also caused some changes in the PGA distribution pattern. In areas with stable regimes, more accurate accounting for seismotectonic conditions and less attenuation of seismic waves caused some increase in PGA compared to [4].

The developed Detailed Seismic Zoning maps will be the basis for the development of new state building regulations in the Republic of Kazakhstan and will serve as an important tool for improving the seismic safety and preparedness of the country.

References

- [1] Silacheva, N. On the Probabilistic Seismic Hazard Assessment in Kazakhstan. *Geotech Geol Eng.* (2022). <https://doi.org/10.1007/s10706-022-02345-w>
- [2] SN RK EN 1998-1:2004/2012, Eurocode 8: Design of earthquake-resistant structures - Part 1: General rules, seismic impacts and rules for buildings. BR of the Republic of Kazakhstan, Almaty, 2011.
- [3] Silacheva N.V., Kulbayeva U.K., Kravchenko N.A. (2018) Probabilistic seismic hazard assessment of Kazakhstan and Almaty city in peak ground accelerations. *Geodesy and Geodynamics*, 9(2),131-141.
- [4] SP RK 2.03-30-2017. Construction in seismic zones. Code of Rules of the Republic of Kazakhstan. Astana, 2017. 110 p.
- [5] Silacheva N.V., Kulbayeva U.K., Kravchenko N.A. (2020) On the realization of seismic micro zonation of Almaty (Kazakhstan) in-ground accelerations based on the “continual” approach. *Geodesy and Geodynamics*, 11(1), 56-63 (in Eng.)
- [6] SP RK 2.03-31-2020. Development of the territory of the city of Almaty, taking into account seismic micro zoning, Code of Rules of the Republic of Kazakhstan. Astana, 2021. 61 p.
- [7] Cornell, C.A., 1968. Engineering seismic risk analysis. *Bull. Seismic. Soc. Am.* 58, 1583–1606
- [8] Field, E.H., Jordan, T.H., Cornell, C.A., 2003. Open SHA: A Developing Community-modeling Environment for Seismic Hazard Analysis. *Seismol. Res. Lett.* 74, 406–419

[9] Pagani, M., Monelli, D., Weatherill, G., Danciu, L., Crowley, H., Silva, V., Henshaw, P., Butler, L., Nastasi, M., Panzeri, L., others, 2014. Open Quake engine: An open hazard (and risk) software for the global earthquake model. *Seismic. Res. Lett.* 85, 692–702.

[10] Onur T., Gök R., Mackey K., Abrams K., Berezina A., Mikhailova N., Bekturganova. B., Murodkulov. Sh., Bondar I., Herrera C. Central Asia Seismic Hazard Assessment (CASHA) “Complete” Catalog of Earthquakes. LLNL-TR-828313.

[11] Zelenin E.A, Bachmanov D.M., Garipova S.T., Trifonov V.G., Kozhurin A.I. The Active Faults of Eurasia Database (AFEAD): the ontology and design behind the continental-scale dataset // *Earth System Science Data*. 2022. vol. 14. p. 4489-4503

[12] Akkar, S., Sandikkaya, M.A., Bommer, J.J. Empirical ground-motion models for point- and extended-source crustal earthquake scenarios in Europe and the Middle East, *Bull. Earth. Eng.* 12(1) (2014) 359–387

[13] Zhao, J.X., Zhou, Sh., Zhou, J., Zhao, Ch., Zhang, H., Zhang, Y., Gao, P., Lan, X., Rhoades, D., Fukushima, Y., Somerville, P. G., Irikura, K. Ground-Motion Prediction Equations for Shallow Crustal and Upper-Mantle Earthquakes in Japan Using Site Class and Simple Geometric Attenuation Functions. *Bull. Seism. Soc. Am.* 2016. V. 106(4). P.1552–1569.

[14] Bozorgnia, Y., Abrahamson, N.A., Campbell, K.W., Rowshandel, B., Y., Shantz, T. NGA-West2: A Comprehensive Research Program to Update Ground Motion Prediction Equations for Shallow Crustal Earthquakes in Active Tectonic Regions. Proceedings of the 15 WCEE, Lisboa (2012).

[15] Goulet, C.A., Bozorgnia, Y., Kuehn, N., Al Atik, L., Youngs, R.R., Graves, R.W., Atkinson, G.M. NGA-East Ground-Motion Characterization model part I: Summary of products and model development, *Earthquake Spectra*, 2021. <https://doi.org/10.1177/87552930231173454>

DIAGNOSTICS OF RISKY MULTIPHASE FLOW ZONES IN OIL PIPELINES

Gulnara Zeynalova, Gafar Ismayilov

•

Azerbaijan State Oil and Industry University

gulnara.zeynalova93@mail.ru

asi_zum@mail.ru

Abstract

This article examines the properties and formation of free-flow areas in the compressed profile of indicative oil pipelines. The risks of the formation of multiphase flow zones in oil pipelines were investigated and a method for diagnosis was developed. Additionally, this article studies the issues related to the presence of free-flow zones formed within the stationary regimes of oil pipelines, as well as the identification of their coordinates. Case studies are drawn based on the hydraulic slope and the pressure balance and contingent upon the lay, which aim to account for the identification of the location and sizes of such zones.

Keywords: hydraulic slope, pass-point, geodesic height, free-flow zone, stationary operational regime

I. Introduction

The formation of gaps (free-flow areas) is frequently observed in the stationary operational regimes of the pipeline. The identification and research of such zones are of special significance for secure and efficient exploitation of oil pipelines. Since these free-flow zones are mainly linked to the pass-point (and/or points) the presence of such zones are by no means necessary, which depend upon the operational regime of the pipeline. As such, the identical zones are not formed in cases when the hydraulic slope lines do not cut through the profile of the pipeline, which prevents the existence of the pass-point. Accordingly, the stationary operation regime of the pipeline, as this may be the case in varied pressures, becomes inevitable. The formation of a pass-point, or free-flow zones is feasible in case of the alteration of the operational regime of a pipeline, termination of the operation of any pump stations, and the changing of rheological and physical-chemical properties of the transported oil. Such zones are noticed when the operation of a pipeline is terminated and during oil- spills resulted from accidents. The presence of free- flow zones, as a rule, raise the pressure and transportation costs at the initial installation stage of a pipeline [1-6].

II. Methods

In order to determine the presence of hydraulic point, a hydraulic slope value should be calculated and this value should be reflected in the profile of the pipeline. The identification of a free-flow zone in the compressed profile of an indicative pipeline based on a hydraulic line is described in Figure 1.

A hydraulic slope line (i) cuts through the profile, which begins from the last point (K) of the pipe. The touching point, which is close to the identical line and, which never cut through the profile, will be a pass-point.

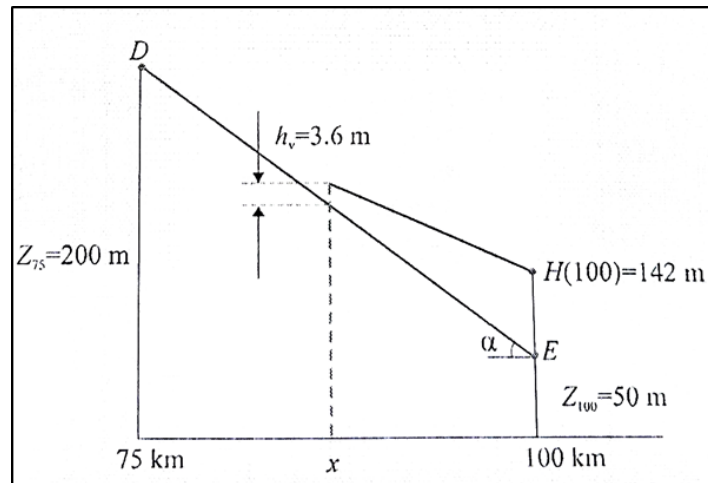


Fig. 2: Identification of a free-flow zone

The hydraulic will indicate a coefficient of resistance:

$$\left. \begin{aligned} \lambda &= \frac{64}{Re} - \text{for laminar regime } (Re < 2300), \\ \lambda &= \frac{0.3164}{\sqrt{Re}} - \text{for a flat notch zone } (Re > 2300), \\ \lambda &= 0.11 \left(\frac{k}{d} + \frac{68}{Re} \right)^{0.25} - \text{for a mixed friction zone } (10 < Re \frac{k}{d} < 500) \\ \lambda &= 0.11 \left(\frac{k}{d} \right)^{0.25} - \text{for a square movement zone } (Re \frac{k}{d} > 500) \end{aligned} \right\} \quad (4)$$

Here, ν , Q accordingly indicates the kinematic viscosity of the transported oil (m^2/s) and its waste (m^3/s); d indicates internal diameter of the pipeline, m ; k represent s a coefficient of ruggedness. $K=0.1$ mm can be taken for larger-diameter pipelines.

Hereby, hydraulic slope will be:

$$i = \lambda \frac{v^2}{2gd} \quad (5)$$

According to Fig.2 (DE), a hydraulic slope in a free-flow zone will produce the following result due to the known will produce the following result due to the known status of α angle (the hydraulic slope line passes through h_v distance while standing parallel to an identical area):

$$i^* = tg\alpha = \frac{Z_a - Z_E}{L_E - L_a} \quad (6)$$

Here, $Z_{p,s}$, $L_{p,s}$, Z_E , L_E accordingly represent a geodesic height in view of the vacuum height for the pass-point and the pipeline with a free-flow zone (segment), m .

We can write down the following equation:

$$Z_E + i^*(L_E - x) = H_E + i(L_E - x) \quad (7)$$

We come up with the following equations drawn from expression (7) for identifying the coordinates of the last point of a free-flow zone (x) and its length ($l_{s,a}$):

$$\begin{cases} x = L_E - \frac{H_E - Z_E}{i^* - i} \\ l_{s,a} = x - L_a \end{cases} \quad (8)$$

Hereby, i^2 , i represent the hydraulic slope of the free-flow and full areas of the pipeline; H_E is pressure at the end of the pipeline area (segment) with e free-flow zone (H_E) and it is calculated as follows:

$$H_E = H_s - i(L_{b,k} - L_E). \quad (9)$$

If there is not any given pressure in the beginning, then it can be calculated. The beginning pressure is calculated as follows and it could be done by drawing upon the data on pressured hydraulic slope, the information concerning the pass-point ($Z_{p,s}$, $L_{p,s}$), and by using the data on vacuum-metric height:

$$H_b = Z_{p,s} + h_v + i \cdot L_{p,s} \quad (10)$$

Here, $i \cdot L_{p,s}$ represent the pressure loss formed in the pipeline up to the pass-point, m. Thus, the pressure p_b relevant to the pressure in the beginning is as follows:

$$p_b = \rho g H_b \quad (11)$$

Under a static operational regime, while the utilization of oil in the pipeline and in the free-flow areas is identical, the stream speeds vary. According to the law on the stability of utilization, due to the lower speed in the pressured movement zone compared to the free speed zone, in the latter zones, the movement of liquid will not occur in the precise wide-cut of the pipe. This time, in each free stream area, the wide-cut area of the pipe filled with liquid will be lower than the full wide-cut of the pipe.

III. Discussion

Let us consider the example on the identification of a pressure-free stream area formed in a given profile of an indicative pipeline (see: Figure 1). Let's assume that oil is transported through a pipeline of $L=150$ km length and of $D=530 \times 7$ mm diameter under a pressure of $c = 850$ kg/m³, with a kinematic viscosity of $\nu = 15$ mm²/s and a steam elasticity pressure of $p_{b.e.} = 0.03$ MPa. If the pressure level at the end of the pipeline is $p = 0.3$ MPa, the beginning pressure level should be such that the oil use equals to $Q=500$ m³/s. In calculations, it can be taken as $k=0.1$ mm.

As it could be obvious from the profile, D point is the pass-point of the pipeline and a free-flow zone is present beginning from this point. Therefore, transportation parameters are established at the outset according to formulas (2) and (5):

$$v = \frac{4Q}{\pi d^2} = \frac{4 \cdot 500}{3.14(0.516)^2 \cdot 3600} = 0.67 \text{ m/s,}$$

$$Re = \frac{v d}{\nu} = \frac{0.67 \cdot 0.516}{15 \cdot 10^{-6}} = 23048,$$

$$\lambda = \frac{0.3164}{\sqrt[4]{23048}} = 0.0257,$$

$$i = \lambda \frac{v^2}{2gd} = 0.0257 \frac{1}{0.516} \frac{(0.67)^2}{2 \cdot 9.81} = 0.001139 \frac{\text{m}}{\text{m}} = 1.139 \text{ m/km}$$

In the case considered, a vacuum-metric height will be:

$$h_v = \frac{p_{b.e.}}{\rho g} = \frac{0.03 \cdot 10^6}{850 \cdot 9.81} = 3.6 \text{ m}$$

(K) at the en of pipeline will establish the pressure level:

$$H_k(150) = Z_{150} + \frac{p_s}{\rho g} = 50 + \frac{0.03 \cdot 10^6}{850 \cdot 9.81} \approx 86 \text{ m}$$

In this case, the following pressure values will be drawn for other points of the pipeline (F , E , D):

$$H_F(125) = H_K(150) + i \cdot 25 = 86 + 1.139 \cdot 25 = 114.0 \text{ m} > 0 + 3.6 = 3.6 \text{ m,}$$

$$H_E(100) = H_F(125) + i \cdot 25 = 114 + 1.139 \cdot 25 = 142 \text{ m} > 50 + 3.6 = 53.6 \text{ m,}$$

$$H_D(75) = H_E(100) + i \cdot 25 = 142 + 1.139 \cdot 25 = 170 \text{ m} < 200 + 3.6 = 203.6 \text{ m.}$$

As it is seen from the latter, $H_D(75) < 203.6$ m. Obviously, the pressure level shall not be lower than the geodesic height. Thus, there exists a free-flow zone between 75th km and 100th km (between D and E points). This time, $x=75$ km will represent the beginning of the free-flow zone (see: Figure 2).

In the free-flow area, the value calculated based upon the hydraulic slope expression will constitute $i^* = 6 \cdot 10^{-3}$ m/m.

In this case, the coordinate of the last point of the free-flow area in accordance with expression (8) will

constitute $x=81.074$ km, and the length will be $l_{s,a}=6074$ m.

We can come with the following if we verify the full pressure levels for the remaining edges of the pipeline (*C, B, A points*):

$$H_c(50) = H_D(75) + i \cdot 25 = 203.6 + 1.139 \cdot 25 = 232.1 \text{ m} > 150 + 3.6 = 153.6 \text{ m},$$

$$H_B(25) = H_C(50) + i \cdot 25 = 232.1 + 1.139 \cdot 25 = 260.6 \text{ m} > 100 + 3.6 = 103.6 \text{ m},$$

$$H_A(0) = H_B(25) + i \cdot 25 = 260.6 + 1.139 \cdot 25 = 289.1 \text{ m} > 100 + 3.6 = 103.6 \text{ m}.$$

As is it seen from the calculations, there is no other free-flow zones in the pipeline considered. Therefore, if we consider that the geodesic height at the beginning of the pipeline is $Z_b=100$ m, the pressure level for the case considered will be calculated as follows:

$$p_b(A) = \rho g[H(A) - Z_b] = 850 \cdot 9.81[289,1 - 100] = 1.58 \cdot 10^6 \text{ Pa} = 1.58 \text{ MPa}$$

IV. Results

Taking into account the risks of formation of multiphase zones in oil pipelines, a method of their diagnosis has been developed. Thus, the existence of free-flow zones in a pipeline and the feasibility of identifying its location and coordinates are indicated based upon a hydraulic slope line and the pressure balance under a static operational regime in an indicative pipeline.

References

- [1] Aliev R.A., Belousov V.D., Nemudrov A.G. Pipeline transportation of oil and gas. M.: Nedra, 1988, 368 s.
- [2] R50.2.040-2004 Recommendations on metrology. GSI. Metrological support of oil accounting during its transportation through the system of main oil pipelines. – M.: VNIIR, 2004. 47 s.
- [3] Novoselov V.F., etc. 1995. Operation of oil pipelines at partial load. – M.: VNIOENG, 68 s.
- [4] Lurie M.V. 2003. Mathematical modeling of pipeline transportation processes for oil, oil products and gas. M.: Nedra, 336 s.
- [5] Ismayilov G., Ismayilova H., Babirov H., Jabrayilova R. Assesment of environmental oil spills and economic-environmental risks. RT&A, Special Issue № 4 (70) Volume 17, November 2022, pp 212-217. DOI: <https://doi.org/10.24412/1932-2321-2022-470-212-217>
- [6] Ismayilov G.G., Fataliyev V.M. Iskenderov E.Kh. [6] A pipe configuration for smoothening pressure pulsation in a pipeline exporting multiphase hydrocarbon fluid. SLYWAN., 167(5), ISI Indexed, may 2023, Printed Poland.

EQUATION OF STATE OF HYDROCARBONS FOR THE LIQUID PHASE

Vagif Hasanov¹, Nurmammad Mammadov², Jeyhun Naziyev³,
Malahat Mammadova⁴, Adila Zeynalova⁴

¹ Azerbaijan State Marine Academy

² Azerbaijan University of Architecture and Construction

³ Azerbaijan State Oil and Industry University

⁴ Azerbaijan Technical University

vgasanov2002@yahoo.com

nurmammad.mammadov@azmiu.edu.az

j_naziyev@yahoo.com

malahat.memmedova@aztu.edu.az

adilazeynalova@yahoo.com

Abstract

It is necessary to construct equations of state that qualitatively and quantitatively accurately reflect the behavior of the thermodynamic surface in the considered range of parameters, in order to compile tables of the thermodynamic properties of liquids. A sufficient amount of high-precision experimental data on the P-V-T dependence is necessary to constructing such equations. Most of the equations are not suitable for extrapolation, they are valid in limited areas of state parameters. An equation of state with three coefficients is proposed to describe the P-ρ-T dependence of liquid hydrocarbons of various molecular structures (benzene, n-octane, isooctane, octene-1).

Keywords: equation, liquid, hydrocarbons, density, thermodynamic

I. Introduction

First of all, it is necessary to construct equations of state that qualitatively and quantitatively accurately reflect the behavior of the thermodynamic surface in the considered range of parameters, in order to compile tables of the thermodynamic properties of liquids. A sufficient amount of high-precision experimental data on the P-V-T dependence is necessary to constructing such equations. Most of the equations are not suitable for extrapolation, they are valid in limited areas of state parameters.

The equations of state for condensed phases are usually divided into two groups. The first includes equations of $\rho=f(P, T)$ type, the second - $P=f(\rho, T)$ type. Since in practice determination of the liquid density (ρ) depending on pressure (P) and temperature (T) is most often required, in our opinion, preference should be given to equations of the first type.

From this point of view, let's consider the two equations of state known from the literature sources, which have a simple structure and are currently used.

II. Results

Earlier [1], using the expansion of the potential forces of intermolecular repulsion in a series in powers of $1/r^9$, a simple equation of state of forces for highly compressed gases was obtained in the form:

$$\rho^4 = A + BP, \quad (1)$$

where r is the intermolecular distance: A, B are temperature-dependent coefficients.

The authors of [1] assumed that the possibility of applying equation (1) to the liquid phase can be ensured by introducing a correlation term proportional to ρ^7 into the left side of the equation. However, the application of this equation to liquid benzene, n-octane, isooctane, and 1-octene has shown that this assumption is not justified.

The equation of state for the liquid phase is also known [2]:

$$P = C\rho^2 + D\rho^8, \quad (2)$$

where C, D are coefficients that are functions of temperature.

Calculations carried out according to equation (2), on the example of benzene, n-octane, isooctane, and octene-1, showed that it is a local equation, which can be considered sufficiently accurate for a limited temperature range. For the range of parameters close to the saturation curve and for higher temperatures, the error of the equation increases, going beyond the limits of the experimental error. The foregoing dictated the need to compile another equation suitable for a wide range of parameters. We can propose a new equation of state with three coefficients, using the precision experimental results on the P - V - T dependence obtained earlier for benzene [3], n-octane [4], isooctane and 1-octene [5]. This is achieved by introducing an initial approximation that allows an exact and practical equation to be obtained. Equation (1) can be taken as such an approximation. If we introduce a correlation term into the right side of equation (1), which takes into account this interaction of molecules and is proportional to $P^{0.5}$, we can obtain a semi-empirical equation of state

$$\rho^4 = E + FP^{0.5} + KP, \quad (3)$$

where E, P, K are constants depending on T and determined from experimental data.

E, P, K are calculated for each isotherm by the least squares method and are presented as:

$$E(T) = \sum_{i=0}^L e_i T^i, \quad F(T) = \sum_{i=0}^m f_i T^i, \quad K(T) = \sum_{i=0}^n k_i T^i, \quad (4)$$

The values of standard deviations σ were used as the main criterion for determining the values of L, m , and n . The minimum value of standard deviation (approximately 0.05%) was obtained at the value $L=5, m=6$ and $n=6$. The data obtained are internally consistent within the measurement error, which, in particular, can be judged from the values of σ . The maximum error of equation (3) did not exceed the experimental error. The coefficients of the polynomials e_i, f_i, k_i are given in Table 1 for each hydrocarbon. To confirm the advantages of equation (3) over equation (2), Table 2 compares the calculated density values according to (3) with the experimental ones for the largest deviations of the calculated data from the experimental values. The density values calculated by equation (2), are also given here, the coefficients of which are determined by the formulas:

$$C(T) = \sum_{i=0}^4 c_i T^i, \quad D(T) = \sum_{i=0}^L d_i T^i, \quad (5)$$

The values of the coefficients c_i, d_i are presented in table 3 for benzene, n-octane, isooctane and octene-1. Experimental data given in table 2 cover the range of state parameters in the temperature range 298–550 K and pressures 0.1–60 MPa. The maximum experimental error did not exceed 0.1% [3–8]. It follows from the results of a quantitative analysis of the equation of state (3) that it describes the experimental density values with an arithmetic mean error of 0.07%.

The maximum deviation is observed at some points at a temperature above 535 K and a pressure of 5 MPa and reaches 0.18% for benzene, 0.16% for n-octane, 0.15% for isooctane, and 0.18% for octene-1. Although equation (2), gives an insignificant error in a certain range of state parameters, the calculation error goes beyond the experimental error at low pressures and elevated temperatures. The maximum error is: 1.08% for benzene, 0.61% for n-octane, 0.33% for isooctane, and 0.2% for octene-1.

Table 1: Values of coefficients e_i , f_i , k_i in equation (4)

I	e_i	f_i	k_i	e_i	f_i	k_i
	Benzene			Octane		
0	4.5642675	2.8068478	$-6.671474 \cdot 10^{-2}$	-3.672235	-6.273416	0.5573032
1	$-4.438599 \cdot 10^{-2}$	$-4.158414 \cdot 10^{-2}$	$9.381676 \cdot 10^{-4}$	$5.1682781 \cdot 10^{-2}$	$9.9653413 \cdot 10^{-2}$	$-8.979502 \cdot 10^{-3}$
2	$2.204459 \cdot 10^{-4}$	$2.586033 \cdot 10^{-4}$	$-5.706132 \cdot 10^{-6}$	$-2.593095 \cdot 10^{-4}$	$-6.503957 \cdot 10^{-4}$	$5.9415086 \cdot 10^{-5}$
3	$-5.876978 \cdot 10^{-7}$	$-8.653627 \cdot 10^{-7}$	$1.984129 \cdot 10^{-8}$	$6.2711190 \cdot 10^{-7}$	$2.2321880 \cdot 10^{-6}$	$-2.064034 \cdot 10^{-7}$
4	$7.866661 \cdot 10^{-10}$	$1.643922 \cdot 10^{-9}$	$-4.111333 \cdot 10^{-11}$	$-7.461305 \cdot 10^{-10}$	$-4.249299 \cdot 10^{-9}$	$3.9725142 \cdot 10^{-10}$
5	$4.187993 \cdot 10^{-13}$	$-1.678311 \cdot 10^{-12}$	$4.712289 \cdot 10^{-14}$	$3.5040744 \cdot 10^{-13}$	$4.2560733 \cdot 10^{-12}$	$-4.018655 \cdot 10^{-13}$
6	-	$7.187356 \cdot 10^{-16}$	$-2.293186 \cdot 10^{-17}$	-	$-1.752868 \cdot 10^{-15}$	$1.6701624 \cdot 10^{-16}$
	Isooctane			Octane		
0	-2.1946643	-4.57027907	0.35852866	-0.1121524	1.33260615	-0.1129255
1	$3.1459937 \cdot 10^{-2}$	$7.2166291 \cdot 10^{-2}$	$-5.686986 \cdot 10^{-3}$	$6.4960058 \cdot 10^{-3}$	$-1.7526046 \cdot 10^{-2}$	$1.4601022 \cdot 10^{-3}$
2	$-1.531496 \cdot 10^{-4}$	$-4.660612 \cdot 10^{-4}$	$3.6901908 \cdot 10^{-5}$	$-2.974276 \cdot 10^{-5}$	$9.62322381 \cdot 10^{-5}$	$-7.778939 \cdot 10^{-6}$
3	$3.5723606 \cdot 10^{-7}$	$1.5779663 \cdot 10^{-6}$	$-1.253415 \cdot 10^{-7}$	$5.1075569 \cdot 10^{-8}$	$-2.8487845 \cdot 10^{-7}$	$2.2305132 \cdot 10^{-8}$
4	$-4.131405 \cdot 10^{-10}$	$-2.958711 \cdot 10^{-12}$	$2.356017 \cdot 10^{-10}$	$-3.476646 \cdot 10^{-11}$	$4.8312956 \cdot 10^{-10}$	$-3.670581 \cdot 10^{-11}$
5	$1.9034547 \cdot 10^{-13}$	$2.9185297 \cdot 10^{-12}$	$-2.328967 \cdot 10^{-13}$	$4.5888767 \cdot 10^{-15}$	$-4.460354 \cdot 10^{-13}$	$3.3119051 \cdot 10^{-14}$
6	-	$-1.184841 \cdot 10^{-15}$	$9.4734939 \cdot 10^{-17}$	-	$-1.7519963 \cdot 10^{-16}$	$-1.286134 \cdot 10^{-17}$

Table 2: Comparison of experimental hydrocarbon density values with those calculated using equations (2) and (3)

T(K)	Pressure, P (MPa)													
	5		9.9		19.7		29.5		39.3		49.1		58.9	
	ρ (kg/m ³)	Δ (%)	ρ (kg/m ³)	Δ (%)	ρ (kg/m ³)	Δ (%)	ρ (kg/m ³)	Δ (%)	ρ (kg/m ³)	Δ (%)	ρ (kg/m ³)	Δ (%)	ρ (kg/m ³)	Δ (%)
Benzene														
505.95	616.9*		642.6		676.2		700.3		719.2		734.5		748.6	
	618.6**	-0.26	642.6	0.00	676.3	-0.01	700.6	-0.03	719.8		735.8	-0.17	749.6	-0.12
	616.9***	0.00	642.5	+0.01	675.7	+0.07	699.4	+0.12	718.9	0.04	733.7	+0.11	747.4	+0.15
Octane														
548.18	507.4		567.1		624.8		657.6		681.4		699.8		716.6	
	511.8	-1.08	565.3	+0.31	621.2	+0.57	655.3	+0.34	680.4	+0.14	700.3	-0.07	717.0	-0.05
	508.4	-0.18	566.3	+0.14	623.8	+0.16	657.3	+0.04	681.0	+0.06	699.2	+0.08	715.9	+0.09
Octane														
534.40	475.7		505.1		539.8		562.8		580.1		594.3		607.1	
	476.7	-0.20	504.2	+0.18	538.8	+0.18	562.1	+0.11	580.0	+0.01	594.6	-0.05	607.0	+0.01
	475.2	-0.10	505.9	-0.15	540.3	-0.09	563.3	-0.08	581.1	-0.14	595.3	-0.17	607.9	-0.12

559.55	438.4		477.8		515.2		542.9		565.9		580.6		593.3	
	439.7	-0.29	477.1	+0.13	518.9	-0.61	545.3	-0.44	565.0	+0.16	580.7	-0.02	594.0	-0.11
	437.7	+0.16	477.1	+0.13	514.3	+0.17	542.1	+0.14	565.0	+0.16	580.0	+0.09	594.2	-0.15
Isooctane														
506.75	492.9		521.1		555.1		577.5		595.4		609.3		621.1	
	493.6	-0.14	519.9	+0.23	553.8	+0.24	576.9	+0.11	594.7	+0.11	609.3	0.00	621.8	-0.11
	492.9	0.00	520.9	+0.03	554.7	+0.06	577.3	+0.03	594.7	+0.12	608.9	+0.05	621.1	0.00
Isooctane														
538.65	445.5		486.1		529.9		556.2		575.9		592.0		605.3	
	447.0	-0.33	485.8	+0.07	528.8	+0.21	555.9	+0.06	576.0	-0.01	592.1	-0.02	605.7	-0.06
	446.2	-0.15	486.6	-0.09	530.1	-0.04	557.1	-0.16	576.9	-0.17	592.7	-0.11	605.8	-0.07
Octene - 1														
410.45	632.4		641.4		656.2		667.4		677.4		687.7		695.9	
	632.3	+0.01	640.7	+0.11	655.1	+0.16	667.3	+0.01	677.9	-0.06	687.2	+0.06	695.7	+0.03
	632.0	+0.06	641.1	+0.04	655.3	+0.13	667.1	+0.05	677.5	-0.01	686.9	+0.11	695.7	+0.03

538.95	488.9		519.7		555.1		579.6		597.6		612.4		625.9	
	489.9	-0.20	518.8	+0.17	554.9	+0.03	579.2	+0.07	597.7	-0.01	612.8	-0.07	625.7	+0.03
	489.5	-0.13	519.5	+0.03	555.4	-0.05	579.3	+0.04	597.7	-0.02	612.8	-0.07	625.8	+0.02

Table 3: The value of the coefficients c_i and d_i in equation (5)

Benzene		Octane	
c_i	d_i	c_i	d_i
$c_0=-653.7213$	$d_0=4798422$	$c_0=-1987.881$	$d_0=-7010.663$
$c_1=1.052837$	$d_1=1.03874$	$c_1=12.5561$	$d_1=-42.60445$
$c_2=4.256481 * 10^{-3}$	$d_2=1.047337 * 10^{-2}$	$c_2=-3.46486 * 10^{-2}$	$d_2=0.138296$
$c_3=-1.288143 * 10^{-5}$	$d_3=3.224042 * 10^{-5}$	$c_3=4.667809 * 10^{-5}$	$d_3=-1.9160 * 10^{-4}$
$c_4=1.0232120 * 10^{-8}$	$d_4=2.66103 * 10^{-8}$	$c_4=2.416768 * 10^{-8}$	$d_4=1.116106 * 10^{-7}$
Isooctane		Octene - 1	
c	D	c	d
$c_0=-727.8638$	$d_0=-4315.087$	$c_0=-323.882$	$d_0=4049.763$
$c_1=1.705612$	$d_1=-25.69849$	$c_1=-1.536156$	$d_1=-33.97943$

III. Conclusions

Thus, we can recommend the equation of state (3), to calculate the thermodynamic properties of hydrocarbons in the liquid phase in a wide range of parameters.

References

- [1] Zimmerman S.S., Miniovich V.M. // 1977. V. 51. №1. pp. 208-209.
- [2] Akhundov T.S. Study of the thermophysical properties of aromatic hydrocarbons: Abstract of the thesis, Baku, 1974. p. 57.
- [3] Naziev Ya.M., Gasanov V.G., Naziev J.Ya. / Thermal physics of high temperatures. 1993. V. 31. № 6 pp. 1031-1033.
- [4] Naziev Ya.M., Gasanov V.G., Allahverdiev A.M. and others / AzTU, Baku, 1992. pp. 143-147.
- [5] Naziev Ya.M., Gasanov V.G., Naziev J.Ya. and others. Oil and gas. 1992. № 5-6. pp. 54-56.
- [6] Vagif Hasanov, Ahmad Muslumov, Adila Zeynalova The investigation of the density of n.butanol+n.ok-tan at high parameters/Turkiye, THERMAM, p.136-138, 2019
- [7] Hasanov V.H. Gulshen Aliyeva, Adila Zeynalova, Ahmad Muslumov Thermodynamic and Acoustic Properties of Binary Liquid Mixture / 9th International Conference on Theory and Application of Soft Computing, Computing with Words and Perception, ICSCCW 2017, 24-25 August 2017, Budapest, Hungary
- [8] Hasanov V.H. The Speed of Sound of n-Heptane, n-Octane and their Binary Mixtures at Temperatures $T=293.15$ to 523.15 K and Pressures up to 60 Mpa // High Temperature, vol. 50, No. 1, pp.44-51, 2012, USA.

GEODYNAMIC REGIME OF FORMATION OF THE MESO-CENOZOIC SEDIMENTARY COVER OF THE ABSSHERON ARCHIPELAGO

Yelena Pogorelova, Murad Abdulla-zada, Allahverdi Tagiyev

Azerbaijan State Oil and Industry University

yy_pgrlova@mail.ru

murad.abdullazade@yahoo.com

allahverdi.taghiyev@gmail.com

Abstract

The main goal of geodynamic analysis is to learn to perceive sedimentary basins as integral natural objects, to determine their genesis, structure and stages of evolution, classification of sedimentary basins and forecast of their oil and gas potential. It is well known that the changes that occur in the earth's crust are mainly the result of subcrustal processes and adjacent plate interaction. The type of the Earth's crust underlying the sedimentary basin determines the physical basis, stability, tectonic restructuring and sedimentation conditions throughout the evolution of the basin. Geodynamic conditions of sedimentary cover formation in the region under consideration were studied on the basis of the principles of tectonic formation of the Caspian basin and the adjacent area, developed by Azerbaijani and foreign scientists (A.A. Ali-Zade, H.B. Yusifzade, A.A. Narimanov, M.M. Veliyev, A.D. Aliyev; B.E. Khain, A.V., Peyveh and many others).

It is proved that this region is a complicated structural complex consisting of a system of island arcs, rift structures with a changing contour of the foot of the continental slope, underwater cordillera, marginal seas, deflections and uplifts. On the structural map constructed from the bottom of the sediments of the Productive strata (Lower Pliocene), in contrast to the maps of previous years, the axial lines of the deflection are shifted to the marginal parts of neighboring tectonic blocks. All this determines new scientific directions of oil and gas exploration in the Caspian basin.

Keywords: Absheron archipelago, geodynamic regime, sedimentary cover, structural map, seismic-geological profile, Productive strata, transgressive bedding, overthrust

I. Introduction

To date, numerous variants of the sedimentary basin (SB) classifications have been developed from the standpoint of mobilism (Kucheruk, 1984; Perrodon, 1985; Allen, Allen, 1992; Tectonics..., 1995; Dickinson, 1974; Einselo, 1992; Kingston et al., 1983; Picha, 1989; SB..., 2004). Against the background of a variety of classifications, variants are most widely used, in which the position of the main tectonic structures of the Earth is taken as a basis, according to which the type of crust, the modern structure, and the nature of modern geodynamic processes in the basin are determined. Naturally, within the framework of plate tectonics, the SB is determined in relation to the main elements of the system of lithospheric plates and their boundaries. The position in this system is determined not only by the type of crust (lithosphere), but also by a certain geodynamic situation. Both of these factors – geodynamics (i.e., the system of acting forces) and the type of crust determine many features of the SB, including the nature of deep processes, the mechanism of

formation, thermal regime, features of tectonic structure, types of magmatism and sedimentary deposits, oil and gas presence, etc.

One of the urgent problems of the Caspian basin is to clarify the geodynamic conditions of the formation of the Earth's crust and tectonic-sedimentation complexes. Of particular interest is the transition zone from the South Caspian microplate (SCM), which was developed on the young Scythian-Turanian plate (STP) to the deep-sea South Caspian basin SCB (Fig. 1.). Epiplatform troughs have been identified on the southern periphery of the STP, which are distinguished regionally – these are the Apsheron-Balkhanian threshold, the North Apsheron depression (NAD) and the Guba-Divichi depression (on the west of land). Earlier, when there were no materials of ultra-deep seismic method, there were subjective and erroneous judgments about the occurrence of orogens and depressions in the Caspian area. Based on seismology and shallow drilling data on the region, hypothetical assumptions were made about the occurrence of the SCB. In general, the transition zone was presented as a zone complicated by regional faults and with inversion folding (Geology of Azerbaijan, volume 4, 2005; D. Babayev, A. Hajiyev 2006) [2,9].

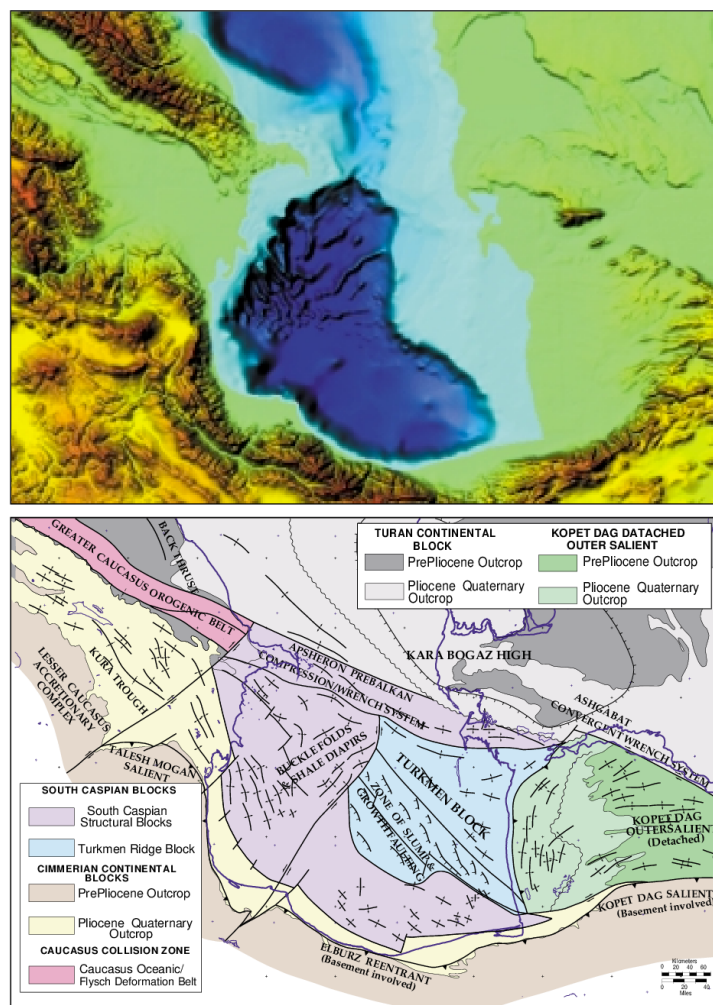


Fig. 1: Upper: Merged bathymetry and digital topography of the South Caspian Sea and surrounding areas. The elongate subsea ridges present on the bathymetry are the sea floor expression of large, subsurface anticlinal folds. Lower: Structural elements of the South Caspian Sea and surrounding areas (modified from Philip et al., 1989, Berberian and King, 1981; Adamia et al., 1977; Naliokin, 1976; Huber, 1978)

In the 60-80s of the last century, the occurrence of sedimentary basins in the Caspian area and their evolution have been explained by the concept of plate tectonics (P.L. Zonenshain, Le Pichon, 1986; P.L. Zonenshain et al., 1991; Mammadov P.Z. 1982, 2010, 2020). The international programs of MEBE and DARIUS [7], a number of grant studies were carried out, according to the results of

which it was found that the passive continental margin of Mesothetis was developed in the transitional zone in the Paleozoic-middle Mesozoic time. Rifting in middle Jurassic and back-arc volcanism contributed to the opening of the back-arc sea and turned the passive continental margin (PCM) into an active one. From the steep continental slopes, loose sediments were transferred to the Southern Caspian, thick Mesozoic-Quaternary sedimentary complexes were formed, and in the eastern part of the Middle Caspian, starting from the Pliocene, geological bodies of lateral build-up were formed.

In 1995-2000, ultra-deep seismic sounding was carried out in the Middle and Southern Caspian Sea (lasting up to 16-20 seconds), which figured out the structure of the consolidated crust and young sedimentary complexes [5,6]. It turned out that presented for a long time as a geosynclinal basin of the Southern Caspian is a back-arc marginal sea. It was developed on the oceanic crust, which, starting from the Oligocene, began to subduct under the STP. Sedimentary complexes of steep continental margins were subjected to complex folding; an accretion prism was formed from sediments scraped from the surface of the subducting oceanic plate [8]. Thus, the highly informative seismic materials provided objective information about geodynamic processes occurring over millions of years and about the evolution of the SCB and its frames.

Currently, an objective deep model of the Earth's crust is being prepared, a model of an accretion prism subject to zonal folding, which differ both in size and in oil and gas content.

II. Methods

To implement the main objectives of the study, the acquisition, generalization and analysis of extensive literary, geological and geophysical, stock, cartographic materials, deep drilling data, seismic profiles, structural schemes for the areas of Arzu, Gilavar, Khazri, etc. time sections (Fig. 2.), as well as samples of electric logging (Fig. 3.) for individual horizons of PS in the studied region.

Geodynamic conditions for the formation of the sedimentary cover of the studied region are considered in conjunction with the principles of tectonic zoning of the Caspian megadepression, developed in the 80-90s by Azerbaijani and foreign scientists (H.B. Yusifzade, A.A. Narimanov, M.M. Veliyev, A.D. Aliyev; V.E. Hain, A.V. Peiveh and many others) [3,4].

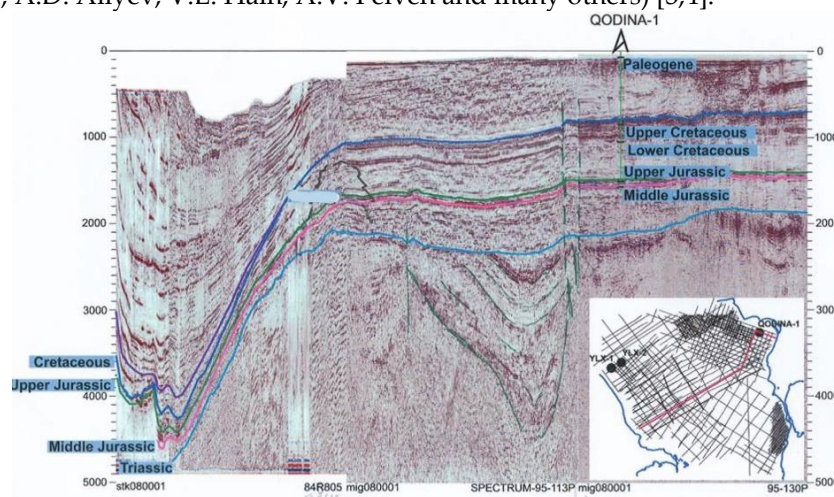


Fig. 2: Interpretation of seismic section based on BP data

These developments are based on the time of formation of the continental crust of the transitional type, the indicator of which are the areas of formation of granite-metamorphic layers of different ages - the formation of molasses formation; complexes of rocks of the shelf, continental slope, foot, etc.

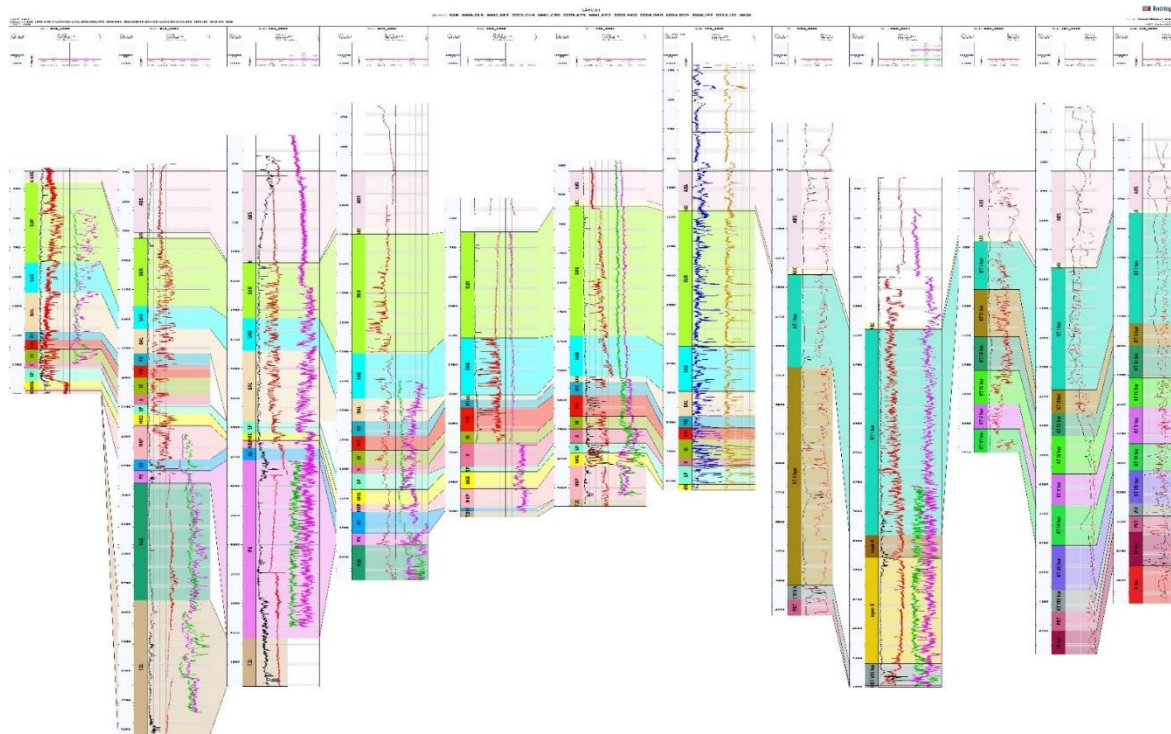


Fig. 3: Well-correlation scheme through Absheron archipelago [1]

In the course of the work, the general patterns of the geological development of the Caspian basin were taken into account, detailed for the Azerbaijani part of the Caspian Sea, the underwater slope and the deep-water part of the Southern Caspian basin.

All this made it possible to produce new structural constructions for the region under consideration; to develop a legend and draw up a scheme for the formation of the Apsheron non-volcanic island arc, regional profiles in the western frame of the North Apsheron marginal trough, in the zone of the Apsheron archipelago; to create a new structural map for the bottoms of the PS on a scale of 1:100000, as well as design profiles for the Apsheron archipelago in order to identification of structural floors of the Meso-Cenozoic sedimentary cover.

All this gave rise to a new approach to determining the directions of oil and gas exploration.

III. Results

In order to identify large-amplitude thrusts in the region under consideration, four regional profiles were compiled that revealed the Meso-Cenozoic sedimentary cover.

These profiles show for the first time such thrusts changing the structural plans of Mesozoic, Paleogene and Pliocene-Quaternary deposits. According to these profiles, in the adjacent zones of the North Apsheron Trough and the Apsheron archipelago, these thrusts are distinguished in Mesocenozoic sediments, as well as tectonically limited structures and transgressive occurrence of Late Miocene rocks with a break in sedimentation overlapped the Mesozoic.

To identify common patterns of tectonic reconstructions in the zone of the North Absheron marginal trough and the adjacent area of the Absheron archipelago, a profile (III - III) along the line was selected: Shurabad-deniz, Garbi-Absheron, East Absheron, Khazri, Gilavar, Khali, Chilov, Janub, Bahar.

This profile is carried out (Fig. 4.) in the north-western pericline of the Goshadash structure, along the near-water part of the Gharbi-Apsheron structure and the Apsheron bank in the direction of the Khazri structure, from which the Gilavar structure crosses from north to south. Then it passes through the near-water parts of the Khali-Chilov structures, continues between the periclinal of the Janub structures (I - II) and ends at the immersion to the Bahar structure.

According to the profile, the structure of the Chilov on its immersion in the periclinal part of the Janub structure is characterized by a transgressive overlap of the Jurassic sediments by the Sarmatian layer; lower, Upper Cretaceous and partially Maikop. The deposits of the Oligocene-Miocene are eroded here.

According to the profile, the structure of the Chilov on its immersion in the periclinal part of the Janub structure is characterized by a transgressive overlap of the Jurassic sediments by the Sarmatian; Cretaceous and partially Maikopian deposits.

According to the profile, the transgressive occurrence of Sarmatian sediments on the eroded surface of the Paleogene-Miocene looms on the Khali-Janub-Bahar line; the hinge part of the uplift in the Jurassic and Cretaceous sediments is complicated of large-amplitude horizontal thrust. The formation of the Mesozoic strata occurs along the shelf complex of the Triassic, represented in the Paleozoic folded basement [10]

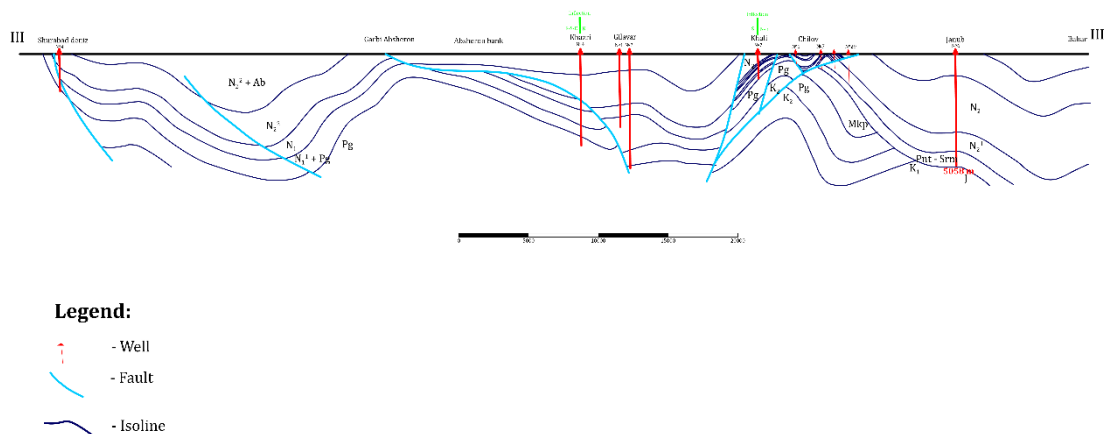


Fig. 4: Seismogeological profile III-III'

In the well No. 6 Janub, at the depth of 5058 m, erosive protrusions of Jurassic rocks were revealed, and on the eastern extension of the Janub - Bahar profile, the PS sediment's thickness are sharply increasing. The swelling of the productive thickness reaches 3125m.

Deep erosion of Paleogene sediments on the profile (III – III') is shown on the Khali field (well No. 7) where the PS lies on Paleocene-Eocene sediments.

The transgressive overlap of PS Paleogene sediments in the area of Khazri, Gilavar, Khali gives grounds to make a judgment about a regional break in sedimentation at the Paleogene-Miocene stage in the region under consideration. These data once again confirm the earlier conclusions (Aliyev, 1996) about the formation of an island arc in the zone of the Absheron archipelago.

The structural discrepancy between Mesozoic and Paleogene-Miocene sediments is clearly visible from the compiled regional profiles: Mesozoic structures are characterized by steep angles of incidence, fan-like expanding scaly thrusts, tectonically shielded structures. The Paleogene-Neogene is characterized by transgressive occurrence with interruptions in sedimentation overlapping the Mesozoic complex.

The revealed large-amplitude thrusts forming zones of rock crushing and an increase in sediment capacity, of course, as mentioned above, create conditions for the formation of oil and gas deposits. In order to identify additional search criteria, seismic-geological profiles, structural maps for the lower PS and Upper Cretaceous sediments limiting the gas-generating clay strata

were compared. These comparisons revealed the discrepancy of structural plans, the sharding of the above-mentioned strata and the inflating of thickness at various stratigraphic levels of the Paleogene-Miocene; the sharding of the clay strata led to the formation of tectonic breccia, crushed clay shales, calcareous sands and sandstones, which significantly increases the reservoir properties of the strata.

On the compiled structural map (Fig.5.) along the bottom of the PS, the influence of geodynamics of tectonic basement blocks on the formation of folded structures of the region along the bottom of the "Fasila" suite is outlined, where tectonic blocks are clearly traced, articulated by paired faults. At the same time, the articulation of blocks from north to south is ledge-like, and from west to east stepwise.

The axial lines of study region shown on the structural maps of previous years (1970-83), according to new developments, turn out to be shifted to the marginal parts of linear folded structures, which are inherited folds of the foundation, reflected in the bottoms of the upper part of the Productive Series.

The linear folded zone of the Azi Aslanov, Palchig Pilpilasi, Neft Dashlari, along the latitudinal fault is shifted 5-6 km south of the structures of Guneshli, Chirag, Azeri, and Kapaz. The subsurface parts of the structures are complicated by transverse discontinuous disturbances with a small amplitude of vertical displacement (50-100 m).

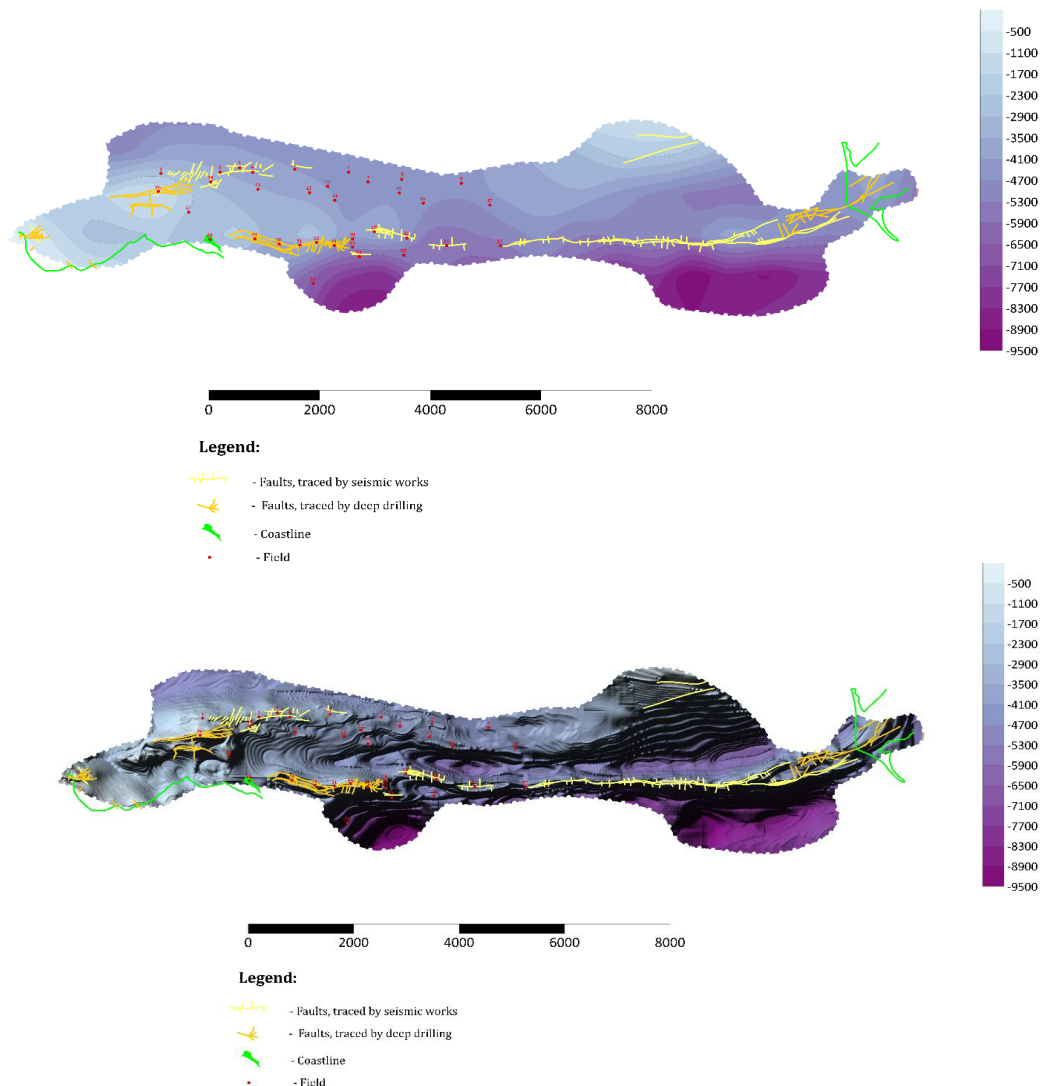


Fig. 5: Structural map: bottom of PS sediments (contour and relief maps)

The Gosha Dash fold - located in the northwestern part of the Absheron Archipelago along the bottom of the "Fasila" suite - is a flat structure, closing along an isohypse of 1500 m. The axial line of the fold is shifted to the southwest at an angle of 25-30 °, relative to the longitudinal fault, along which the northern limb is lowered by 500 m.

The southeastern periclinal of the Gosha Dash fold is shifted by a transverse fault to the south in relation to the Gharbi Apsheron structure and through a small saddle, through discontinuous disturbances, it articulates with the Agburun-deniz fold. In general, the structure of the Gosha Dash at the bottom of the upper part of the PS is elevated relative to the edge of the adjacent lowered tectonic block, where the sole of the "Fasila" suite lies at a depth of 1500-2000 m.

A comparative analysis of the developed graphic materials, the identification of structural plans for various stages of Meso-Cenozoic sediments, transgressive occurrence of Paleogene sediments in the Mesozoic, gave the basis for the selection of directions and the construction of project profiles (IV-IV').

As can be seen from the project profile IV-IV' (Fig. 6.) and a structural map along the bottoms of the PS, gentle dome-shaped uplifts are revealed here; in the lower section of the PS deep faults crossing Gala suite, Sub-Girmaki suite, Girmaki suite are traced. Paleogene-Miocene deposits transgressively lie on the blurred surface of Mesozoic rocks, forming secant thrusts in the clay gas-generating thickness.

Disjunctive dislocations in Mesozoic sediments are characterized by large-amplitude horizontal thrusts at various stratigraphic levels of the Lower, Upper Cretaceous and Jurassic rocks, with the formation of tectonically shielded structures.

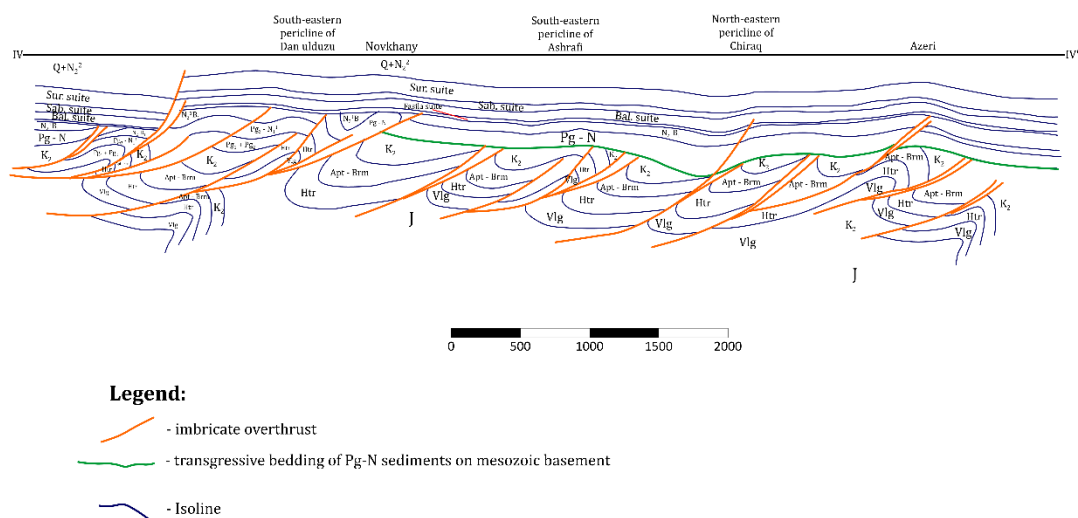


Fig. 6: Seismogeological profile IV-IV'

According to the profile, the discrepancy of structural plans is clearly traced in the Mesozoic, Paleogene–Miocene, Lower and Upper PS sections. Mesozoic sediments are characterized by large-amplitude thrusts forming tectonically shielded structures in the section of the sedimentary cover. On the erosive surface of the Mesozoic, the Paleogene-Miocene strata lies transgressively, forming an independent structural plan.

The data of structural constructions and the fact that the structural plans for the bottoms of the PS and the surface of the Mesozoic (Aliyev, 1967) give reason to assume the formation of secant thrusts here, along which there is a sharing in the section of the PS with the subsequent overlap its retinue "Fasila" suite - the bottoms of the Balakhany suite.

III. Conclusions

In general, it should be noted that the studies carried out during the investigations made it possible to clarify the geodynamic conditions for the formation of the Meso-Cenozoic sedimentary cover of the region in question to predetermine folding processes in second-order geostructural elements against the background of the continental slope.

Large-amplitude thrusts in Mesozoic sediments and transgressive occurrence of Paleogene-Neogene sediments on Mesozoic protrusions along the lines of profiles: Nardaran-Zorat; Agburun-Sitalchai, Shurabad; Shurabad-deniz, Gosha Dash, Gilavar, Khali, Chilov, Janub were revealed.

- secant thrusts in the cross-section of the V-V profile, in the northeastern limb of the Kapaz structure, where the capacity of the Meso-Cenozoic sedimentary cover is doubling.

On the structural map by the bottom of the PS, the displacement of the axial lines of deflection is traced, tectonic blocks are distinguished by ledges sinking from north to south and stepwise from west to east; the study data confirm the prolonged activation of tectonic processes in the region under consideration.

All this significantly expands the idea of the formation of zones favorable for the accumulation of hydrocarbons and contains elements of a new approach to the search criteria for oil and gas.

References

- [1] Abdulla-zada M. 2022. Geological significance of seismic reflections in the sedimentary cover of the Eastern part of the Absheron-Prebalkhan ridge. Bulletin of Taras Shevchenko National University of Kyiv (Geology). 3(98), 59-65. <http://doi.org/10.17721/1728-2713.98.07>
- [2] Abdulla-zade M.Ch., Vakhably N.F. 2021. About the petrofacial analysis of sediments of the Productive serie's lower section of Absheron-Balkhan uplift zone based on geophysical and core studies. "Geologist of Azerbaijan" scientific bulletin, p. 112-117
- [3] Alizade A.A., Guliyev I.S., Mamedov P.Z., Alieva E.G., Feyzullaev A.A., Huseynov D.A. 2018. Productive serie of Azerbaijan, v. 1. "Nedra". Moscow, 305 p.
- [4] Ali-Zade A.A., Yusifzade H.B., Narimanov A.A., Veliyev M.M., Guliyev I.S., Aliev A.D. 1992-1994. Analysis of the deep structure of the Caspian depression in order to identify additional criteria for the search for oil and gas in the Azerbaijani sector of the Caspian Sea. Report for SOCAR Foundation, 189 p.
- [5] Lebedko G.I. 2013. Geodynamic criteria for assessing the oil and gas potential of the Terek-Caspian forward trough//Geology of oil and gas, No. 4.- p.18-28.
- [6] Magomedov R.A. 2010. Geodynamic regime of the Dagestan wedge region in the Alpine cycle of the Eastern Caucasus development. In: Transactions of the Institute of Geology of the Dagestan Scientific Center of the Russian Academy of Sciences, Issue 56: Proceedings of the Conference 'Monitoring and Forecasting of Natural Disasters to the Memory of the 40th Anniversary of the Earthquake in Dagestan on 14 May 1970', 15-17 June 2010, Makhachkala. - p. 66-79.
- [7] Mamedov P.Z., Mamedova L.P. 2013. Peculiarities of the Earth's crust of the Middle Caspian Basin according to new seismic data obtained by CDP method. In: Proceedings of the International Conference on Problems of Oil and Gas Field Exploration, Almaty. - p. 611-621.
- [8] Pogorelova Ye.Yu. 2019. Geotectonic aspects of oil and gas potential of the intermountain segment of the Black Sea-Caspian Sea region. Naukovyi Visnyk NHU, 2019, № 1.
- [9] Yudin V.V. 2008. Geodynamics of the Black Sea-Caspian region.- Monograph.-Kiev - 117p.
- [10] Yusubov N.P., Guliyev I.S. Mud volcanism and hydrocarbon systems of the South Caspian depression (according to the latest data of geophysical and geochemical studies). Baku, "Elm", 2022, 168 p

DETERMINATION OF THE ENVIRONMENTAL TEMPERATURE DEGREE ON MAGNETIC LEVITATION CORE INDUCTION

Orkhan Afandiyev, Aynura Allahverdiyeva

•
Azerbaijan Technical University
Azerbaijan State Marine Academy
orkan1946@mail.ru
allahverdiyevaaynura@gmail.com

Abstract

The issues on determining the degree of influence of temperature changes caused by climatic features of the area, internal heat generation during the operation of an electronic circuit and other reasons on the value of the magnetic induction of the levitating magnetic core are analyzed in the article. Based on the results of preliminary studies, the model of the Magnetic Levitation System (MLS), the dependence on the temperature of the magnetic induction on the levitating core was obtained. The preliminary investigation results of the MLS show that the magnetic induction of the levitating core is a linear monotonically decreasing function of temperature. The aim of this issue is to study the effect of temperature on the nature of the power characteristics of the MLS, the temperature in the measuring chamber of which has a significant effect, which indicates the violation of the levitation current stability caused by temperature changes in the magnetic induction of the levitating magnetic core (which indicates the violation of the levitation current stability).

Keywords: magnetic induction, magnetic levitation systems, measuring chamber, magnetic core, solenoid

I. Introduction

When the magnetic levitation system (MLS) is operating under conditions different from normal, its accuracy, in addition to the main error, will also be predetermined by additional errors from various disturbing factors of both a systematic and random nature [2].

Among these factors, first of all, are temperature changes caused by climatic features of the area, depending on the time of year and time of day, internal heat generation during the operation of the electronic circuit and other reasons.

II. Discussion

In Fig.1 the basic electric circuit of the MLS using an integrated Hall sensor and a temperature meter is shown. It contains a traction node 1, consisting of a solenoid 2 and a magnetic core 3, a measuring chamber 4, an integrated Hall sensor 5, an analogue block 6 of the solenoid current control.

The electronic unit itself contains an operational amplifier 7 K140UD14, a power transistor 8 of the KT805A type, in the emitter circuit of which the winding of the solenoid 2 and the measuring resistor R_i are connected in series, the output of which in the form of a levitation

voltage U_I is fed to the input of the signal shaper, proportional to the measured parameter of the control object.

Temperature sensor 9 - the thermistor is mounted on the lower cheek of the solenoid frame. It is as close as possible to the zone of placement of the levitating magnetic core. The thermistor is turned on according to the voltage divider circuit, the output signal of which is supplied to the direct input of the operational amplifier 10. The circuit is adjusted to its initial state using the adjustment resistance 11 connected to the inverse input circuit of the amplifier 10. The gain of the operational amplifier is set using the adjustment resistance 12. A voltage signal proportional to the temperature of the working area of the levitating magnetic core is fed to the analogue input of the microcontroller.

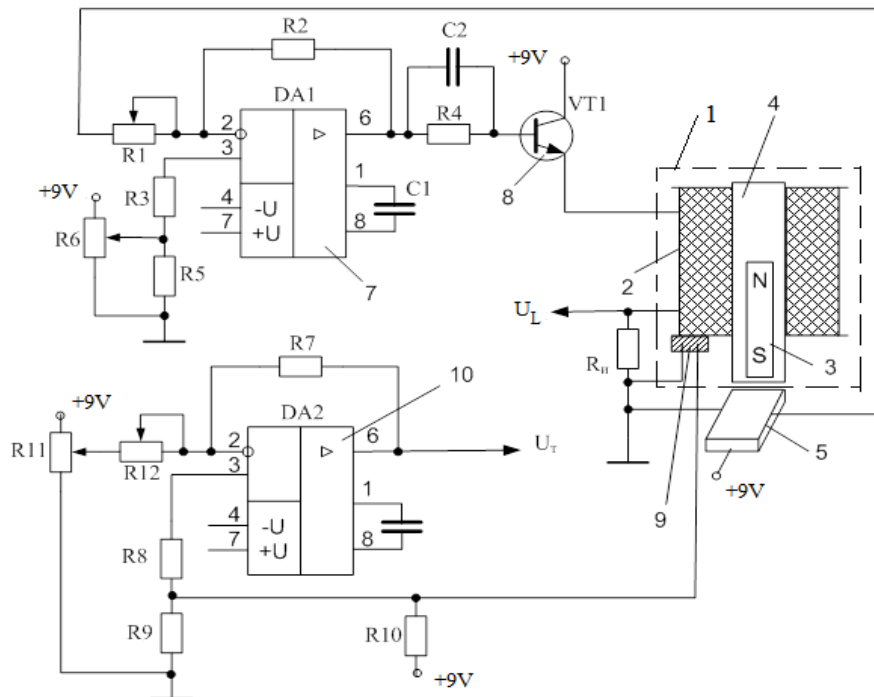


Fig. 1: Diagram of a magnetic levitation system with a temperature meter

III. Results

Considering the typical case where the only significant disturbing factor is the change in the ambient temperature in the measuring chamber of the system, caused by both external climatic changes and internal heat generation associated with the consumption of electric energy from the power source, assuming that other factors, such as the change in the resistance of the measuring resistor R_i , change in linear dimensions of individual structural elements, etc. - are not significant.

The temperature in the measuring chamber has a significant effect on the nature of the power characteristic of the MLS, which is manifested in a violation of the stability of the levitation current caused by temperature changes in the magnetic induction B_m of the levitating magnetic core [3].

Preliminary laboratory studies have shown that a change in the magnetic induction of B_m in the temperature range from $+10^0$ to $+35^{\circ}\text{C}$ is about 1%. Naturally, with a change in the temperature of the medium in the measuring chamber in the climatic range from -10^0 to $+50^{\circ}\text{C}$, it will be even greater, i.e. amount to about 3%.

Therefore, taking into account the effect of temperature on the traction characteristic of the solenoid is clearly necessary, given the fact that the expected error of magneto-gravity devices is, as a rule, of the order of 0.1 - 0.2% and, in any case, should not exceed 0.5%.

To take into account the influence of temperature on the accuracy of the system, we consider the basic dependence ($F_d = \frac{\pi}{8} \cdot \frac{d_m^2}{d_n^2} \cdot \mu_0 \cdot j_z(b) \cdot h \cdot K(\bar{z}) \cdot I_s$) of the levitation current on the magnetic and structural parameters of the MLS given in [1]:

$$F_d = \frac{\pi}{8} \cdot \frac{d_m^2}{d_n^2} \cdot B_m \cdot h \cdot K(\bar{z}) \cdot I_s$$

where,

I_s - is the current of the solenoid, A;

d_m - diameter of the magnetic core;

d_n - is the diameter of the wire of the solenoid winding, m;

h - is the height of the winding, m;

d - is the distance from the upper end of the core to the upper edge of the solenoid winding, m;

R and d - are the outer and inner radii of the coil of the solenoid.

According to the results of preliminary studies of the MLS prototype, the magnetic induction B_m of the levitating core can be represented as a linear monotonically decreasing dependence:

$$B_m = B_{m0} \cdot (1 - \alpha_m \cdot \Delta T), \quad (1)$$

where,

B_{m0} is the magnetic induction of the levitating core at a graduation temperature $T_0 = 25^\circ\text{C}$, Tl;

$\Delta T = T - T_0$ - deviation of fuel temperature from calibration temperature T_0 , $^\circ\text{C}$;

T - is the actual core temperature, $^\circ\text{C}$;

α_m - temperature coefficient of influence on the magnitude of the magnetic induction, 1 / deg.

According to the experimental data, it was found that when the temperature changes by $\Delta T = 25^\circ\text{C}$, the levitation current increases to the value of $I_s = 316\text{mA}$, i.e. by approximately $\Delta I_s = 4\text{mA}$, which is:

$$\delta_L = \frac{\Delta I_s}{I_{co}} = \frac{4\text{mA}}{312\text{mA}} = 0.013, \text{ i.e. } 1.3\%$$

where, I_{co} - is the levitation current at $\Delta T = 0$.

Then we can write that $\alpha_m \cdot \Delta T = 0.013$, whence

$$\alpha_m = \frac{0.013}{25} \approx 0.52 \cdot 10^{-3}, 1 / \text{deg} \quad (2)$$

Substituting (2) in (1), we obtain:

$$B_m = B_{m0} \cdot (1 - 0.52 \cdot 10^{-3} \cdot \Delta T) \quad (3)$$

Then from (2) we obtain an expression that determines the traction force of the solenoid depending on the temperature of the medium in the measuring chamber in the following form:

$$F_s = \frac{\pi}{8} \cdot \frac{d_m^2}{d_n^2} \cdot B_{m0} \cdot (1 - 0.52 \cdot 10^{-3} \cdot \Delta T) \cdot h \cdot K_{o,\max}(\bar{z}) \cdot I_s \quad (4)$$

Now the task is to introduce, in expression (4), instead of ΔT , the voltage $\Delta U_T = U_T - U_{T0}$, which is proportional to the temperature change, where U_{T0} is the voltage at the output of the temperature meter at the initial calibration temperature $T_0 = 25^\circ\text{C}$, mB; U_T - voltage at the output of the temperature meter at the actual temperature in the measuring chamber, V.

It is obvious that the dependence of the voltage at the output of the temperature meter on its value can be represented in the following form:

$$T = K_U \cdot U_T, \quad (5)$$

where K_u – is the proportionality coefficient, the value of which, in principle, can be set arbitrarily by adjusting the gain of the electronic amplifier of the temperature meter, deg / V.

In this case, it is necessary to choose a value of the coefficient K_u so that at a temperature $T_0 = 25^\circ\text{C}$ the voltage at the output of the temperature meter would be $U_T = 0.25\text{V}$. Then, subject to a linear relationship between voltage and temperature, the proportionality coefficient will be equal to:

$$K_u = \frac{T_0}{U_T} = \frac{25}{0.25} = 100^\circ\text{C/V} \quad (6)$$

Substituting (5) and (6) in (4) and assuming $I_s = \frac{U_L}{R_u}$ we get:

$$F_s = \frac{\pi}{8} \cdot \frac{d_m^2}{d_n^2} \cdot B_{mo} \cdot (1 - 0.052 \cdot (U_T - U_{T0})) \cdot h \cdot K_{o,max}(\bar{z}) \cdot \frac{U_L}{R_u}, \quad (7)$$

where U_L is the voltage at the output of the core weight meter in the state of levitation, V;
 R_u – is the measuring resistance of the circuit, Om.

IV. Conclusion

The temperature in the measuring chamber has a significant effect on the nature of the power characteristic of the MLS, which is manifested in a violation of the stability of the levitation current caused by temperature changes in the magnetic induction of the levitating magnetic core.

The dependence is obtained according to the results of preliminary studies of the MLS model of the magnetic induction of the levitating core.

According to the results of preliminary studies of the MLS model, the magnetic induction of the levitating core is a linear monotonically decreasing dependence.

References

- [1] Afandiyev O.Z. and Shakhmatov I.E. (2002) Determination of the strength characteristics of the magnetic fields of the solenoid and the levitating magnetic rod of magnetic levitation systems. *Journal of Control Diagnostics. Equipment and materials for non-destructive testing*. 10 (53).
- [2] Pashaev A.M., and Afandiyev O.Z. Theory and practice of magnetic levitation in instrumentation. Moscow. Engineering. 2009. 335 p.
- [3] Afandiyev O.Z, Allahverdiyeva A.T. and Shikhiyev A.S. (March 2019) Method for calculating magnetic induction of cylindrical hear tons from critical magnetic hard materials. *International journal of current research*. Vol.11, Issue, 03, pp. 2388-2391. DOI: <https://doi.org/10.24941/ijcr.34718.03.2019>

RISK ASSESSMENT STUDY OF KEY COMPONENTS OF THE DIGITAL ECONOMY

Laila Gazieva¹, Timur Aygumov², Alexander Natalson³



¹Kadyrov Chechen State University, Russia

²Dagestan State Technical University, Russia

³Kazan State Power Engineering University, Russia

gazievalaila@outlook.com

Abstract

This study provides a comprehensive risk assessment of key components of the digital economy to ensure sustainable growth and mitigate potential adverse impacts. The research methodology included a literature review, analysis of academic sources, data and economic indicators, case studies, and development of risk assessment models. The results of the analysis confirm that the digital economy provides significant opportunities for development and progress in modern society. However, it also carries certain risks and challenges, such as cybersecurity, data privacy, ethical issues, artificial intelligence, and misinformation. These insights enable business leaders, governments and the public to prioritize risk management and develop strategies that advance the sustainable and responsible development of the digital economy. Based on this study, measures can be taken to improve cybersecurity, ensure data privacy, ethical use of artificial intelligence and counter disinformation, in order to provide a favorable and sustainable environment for the further development of the digital economy.

Keywords: digital economy, risk assessment, key components

I. Introduction

The digital economy has become a defining force that is changing the modern socio-economic world, evolving the methods and techniques of doing business, the interaction of man and business with technology, and simply connecting people. Spawned by the digital revolution, the digital economy harnesses the power of digital technologies, data sets and the Internet to create, distribute and consume goods and services in ways that were once unimaginable. This profound transformation has resulted in the emergence of a wide range of activities, industries and business models that drive innovation, increase efficiency and unite the global community [1].

It is an undeniable fact that the rapid growth and widespread use of digital technologies has opened up many opportunities for people, businesses and governments. This coin also has a downside – digital technologies have created complex problems and risks that need to be carefully assessed and managed. As the digital economy continues to evolve, it is critical to conduct a comprehensive risk assessment of its key components to ensure sustainable growth and mitigate potential adverse impacts [2].

This study aims to conduct a risk assessment of key components of the digital economy, namely e-commerce and online marketplaces, digital platforms and exchange economies, financial technology and digital financial services, digital content and media, and artificial intelligence and automation elements.

The purpose of this study is to conduct a comprehensive risk assessment of key components

of the digital economy in order to ensure sustainable growth and mitigate possible adverse effects.

An example of the transformative power of the digital economy is the first key component: e-commerce and online marketplaces. This component represents the pinnacle of the digital economy, covering the buying and selling of goods and services over the Internet. E-commerce platforms and online marketplaces such as Amazon, Alibaba and eBay have revolutionized traditional retail models, giving businesses unprecedented global reach and consumers the convenience of online shopping. The benefits of e-commerce go beyond market access and customer experience, as it also reduces business overhead, streamlines supply chains, and improves overall efficiency [3].

However, with the implementation of these technologies comes many challenges and risks that need to be addressed in order to support the growth of this component of the digital economy. Among the most important issues are data privacy and cyber security. E-commerce platforms collect a huge amount of sensitive consumer data that, if mishandled or hacked, can lead to serious reputational damage and financial loss. Protecting customer data and providing strong cybersecurity measures are essential to building trust and sustaining the sustainable growth of e-commerce [4].

The next key component is digital platforms and the sharing economy, which have revolutionized the way goods and services are exchanged and used. These platforms, exemplified by ride-sharing services like Uber and shared accommodation platforms like Airbnb, facilitate peer-to-peer transactions and optimize resource usage. The sharing economy offers tremendous opportunities for economic growth, offering individuals and businesses access to new revenue streams and consumers greater affordability and convenience [5].

The flip side of this component of the digital economy is that the growth of the sharing economy has created issues around labor rights, regulatory compliance, and fair competition. Working in the gig economy, while offering flexible work options, has been criticized for its lack of benefits and protection for workers [6]. Finding the right balance between encouraging innovation and ensuring fair labor practices is essential to ensure the sustainable growth of the sharing economy and protect the well-being of those who participate in it [7].

Fintech and digital financial services are another key element of the digital economy, reshaping the style of financial services and expanding financial inclusion. Fintech innovations, including mobile payments, peer-to-peer lending, advisory bots, and blockchain technology, have changed traditional banking models, enabling greater access to financial products and services. This progress is especially beneficial for low-income populations, who are gaining greater access to formal financial services through mobile payment platforms such as PayPal and Alipay [8].

The emergence of fintech startups and digital banks has brought new security and data privacy risks. Since these platforms handle sensitive financial information, therefore, strong data protection measures are needed to prevent financial fraud and maintain consumer confidence. Finding a balance between innovation and data security is paramount to ensure the sustainable growth of the digital financial services sector [9].

The digital economy has had a significant impact on the media and entertainment industry, as exemplified by the digital content and media component. Platforms such as Netflix and YouTube have changed traditional broadcasting models by offering consumers vast libraries of on-demand content and enabling content creators to reach global audiences [10]. The democratization of content creation has led to new marketing strategies, public discussions and opportunities for content producers.

However, it is worth noting that this component also presents problems with the spread of disinformation, fake news, and controversial content [11]. Responsible content creation and distribution is essential for promoting informed public debate and maintaining social harmony. Regulating content on digital platforms while maintaining freedom of expression is a delicate balance that must be carefully struck.

II. Methods

To achieve the goal of the study, the following methodology was applied:

- Literature review and analysis of academic sources to identify the main components of the digital economy and their risks.
- Analysis of data and statistical indicators related to the digital economy to determine trends and risk levels.
- Case studies and developments related to each of the key components of the digital economy in order to identify specific vulnerabilities and problems.
- Development of risk assessment models for each component based on collected data and analysis.

III. Results

Among all its achievements and prospects, the digital economy also carries risks and challenges. The rapid growth and pervasiveness of digital technologies has opened up new opportunities for cybercriminals, resulting in complex challenges and threats to data security, privacy, privacy and national security. The advent of the sharing economy has sparked a debate about social justice and labor protection for workers on these platforms.

The following are the main risks associated with the digital economy:

- Cyber security and data threats.
The rise of digital technology has increased the vulnerability to cyberattacks and breaches of data privacy. Cybercriminals can exploit weaknesses in systems and infrastructure to gain unauthorized access to sensitive data, which can lead to financial loss, information leakage, and damage to the reputation of companies and organizations [12].
- Privacy and data collection
The expansion of the digital economy is accompanied by an increase in the amount of data collected and stored about users and customers. Misuse and insecure storage of this data may compromise the privacy of personal information and lead to violations of data protection laws.
- Responsibility and ethical issues
The possibility of using big data and artificial intelligence raises questions of responsibility and ethics. Lack of control over the use of data can lead to unfair treatment of customers and the creation of systems of discrimination.
- Artificial intelligence and automation
The development of artificial intelligence can affect jobs, displacing some types of work activities and creating employment challenges. In addition, process automation can lead to a decrease in the quality of service and dependence on technological solutions [13].
- Disinformation and Fake News
The digital economy has increased the speed at which information spreads, which can lead to the spread of misinformation and fake news. This poses a threat to society, contributing to the dissemination of false data and influencing public opinion.
- Technological gap
The rapid development of technology can lead to a technological gap between countries and individual sectors of the economy. Underdevelopment can create problems for economic growth and competitiveness.
- Digital Divide
Uneven distribution of access to digital technologies can exacerbate inequalities in society,

leaving part of the population outside the benefits of the digital economy.

IV. Discussion

In this paper, risk assessments of key components of the digital economy were considered. The data obtained confirm that the digital economy is the driving force behind modern socio-economic progress, contributing to innovation and efficiency in various industries. The analysis also revealed the presence of significant risks and challenges that should be considered when developing strategies for sustainable development.

From the study, it became clear that cybersecurity and data threats pose significant risks to the digital economy. It is necessary to actively work on strengthening the protection of data and network infrastructure in order to prevent potential cyber-attacks and information leaks.

Privacy and data collection are becoming a pressing issue in the digital economy. It is necessary to strictly comply with data protection legislation and develop effective mechanisms for the control and processing of personal information.

The liability and ethical issues associated with the use of big data and artificial intelligence pose certain risks for the digital economy. A balance is needed between innovation and the protection of the rights and interests of users, as well as the prevention of possible misuse of data.

This study has shown that the digital divide and technology divide are major issues that can exacerbate inequality and reduce economic competitiveness.

To ensure sustainable growth and maximize the benefits of the digital economy, it is necessary to actively manage risks and develop appropriate strategies and policies. Experts face the difficult task of finding a balance between innovation and protection in order to ensure the favorable development of the digital economy and minimize the negative consequences [14].

V. Conclusion

The digital economy has become a defining force in today's world, providing enormous opportunities for innovation, improved efficiency and the connection between people and technology. However, the rapid growth of digital technologies has also brought complex challenges and risks.

The risk assessment of key components of the digital economy has identified several critical aspects that require special attention. Cybersecurity and data protection are paramount concerns as the rise of digital technologies has led to an increase in vulnerabilities and the possibility of cyberattacks. This requires the development and implementation of modern methods and technologies to protect information and prevent violations.

The paper also identified data privacy, ethical issues and liability issues in the use of big data and artificial intelligence. There needs to be a balance between innovation and safeguarding the interests of users and society as a whole.

In addition, the digital economy is generating discussion in the areas of social justice, protecting labor rights, and countering misinformation.

Overall, this study highlights the need for a comprehensive risk assessment of the digital economy and the development of strategies to ensure sustainable and responsible development. It also opens up new opportunities for further research in this area in order to ensure a sustainable and beneficial interaction between humans and digital technologies.

References

- [1] Bukhtiyarov, V.S., Evstifeeva, D.K. and Mamysheva, E.A. (2023). Use of digital technologies as a factor of development of ecosystems of banks. *Economics: Yesterday, Today and Tomorrow*. 13(3A):708-719.
- [2] Economic Commission for Latin America and the Caribbean (ECLAC). (2021). *Digital technologies for a new future (LC/TS.2021/43)*, Santiago.
- [3] Verhoef, P.C., Broekhuizen, T., Bart, Y., Bhattacharya, A., Dong, J.Q., Fabian, N. and Haenlein, M. (2021). Digital transformation: A multidisciplinary reflection and research agenda. *Journal of Business Research*. 122:889-901.
- [4] Quach, S., Thaichon, P., Martin, K.D. et al. (2022). Digital technologies: tensions in privacy and data. *J. of the Acad. Mark. Sci.* 50:1299-1323 .
- [5] Petrini, M., De Freitas, C.S. and Da Silveira, L.M. (2017). A proposal for a typology of sharing economy. *Revista de Administração Mackenzie*. 18(05):39-62.
- [6] Feyen, E., Frost, J., Gambacorta, L., Harish, N. and Saal, M. (2021). Fintech and the digital transformation of financial services: implications for market structure and public policy. *The Bank for International Settlements and the World Bank Group 2021*.
- [7] Amirova, E.F., Gavrilyeva, N.K., Grigoriev, A.V. and Sorgutov, I.V. (2021). Digitalization in Agriculture: Problems of Implementation. *Siberian Journal of Life Sciences and Agriculture*. 13(6):144-155.
- [8] Muldoon, J. and Raekstad, P. (2022). Algorithmic Domination in the Gig Economy. *European Journal of Political Theory*. 0(0):1-21.
- [9] Lukonga, I. (2018). Fintech, Inclusive Growth and Cyber Risks: Focus on the MENAP and CCA Regions. *International Monetary Fund*. 2018(201):1-51.
- [10] Bonadio, E., Lucchi, N. and Mazziotti, G. (2022). Will Technology-Aided Creativity Force Us to Rethink Copyright's Fundamentals? *Highlights from the Platform Economy and Artificial Intelligence*. IIC(53):1174-1200.
- [11] Butcher, P. (2019). Disinformation and democracy: The home front in the information war. *European Politics and Institutions Programme*. 1-24.
- [12] Mentsiev, A.U., Guzueva, E.R. and Magomaev T.R. (2020). Security challenges of the Industry 4.0. *Journal of Physics Conference Series*. 1515(3):032074
- [13] Mentsiev, A.U., Engel, M.V. and Gudaeva D-M.M-E. (2020). Impact of IoT on the automation of processes in Smart Cities: security issues and world experience. *Journal of Physics Conference Series*. 1515(2):022026
- [14] Mentsiev, A.U., Aygumov, T.G. and Amirova E.F. (2021). The Role Of Digital Technologies In The Formation Of The Digital Economy. *European Proceedings of Social and Behavioural Sciences*. 116:1870-1875.

OIL AND GAS PROSPECTS OF TECTONIC CRASHING ZONES OF THE KURA INTERMOUNTAIN DEPRESSION

Gultar Nasibova, Emil Ismayilzadeh, Shura Ganbarova,
Mehriban Ismayilova

•

Azerbaijan State Oil and Industry University

gultar.nasibova@asoiu.edu.az

emil.ismayilzade@socarupstream.az

qanbarovanicat@mail.ru

mexribani@inbox.ru

Abstract

The article considers lithofacies and structural-tectonic conditions of oil and gas formation in the Kura depression. In addition, the formation of oil and gas accumulation zones in the crushing nodes in the Mesozoic deposits was determined and the role of faults in their formation was studied, tectonic crushing zones were found using seismically active zones in these deposits, the issues of prospects analysis were studied and the issues of prospecting and exploration were considered.

Taking into consideration that the tectonic crushing zones are formed in Mesozoic deposits composed mainly of competence rocks, it can be predicted that oil and gas fields in these zones are associated mainly with Mesozoic age rocks. In the Middle Kura depression, the surface of the Mesozoic deposits lies at a depth of up to 4-5 km, therefore it is considered favorable for exploration. Due to this, the oil and gas prospects of the tectonic crushing zones was studied in the Mesozoic deposits as a prospecting object of the Middle Kura depression.

Keywords: Middle Kura, tectonic crushing zone, sedimentary layer, Mesozoic, fault, Cretaceous deposits.

I. Introduction

The Kura intermountain depression is a part of the South-Caspian mega-depression located in the central segment of the Alpine-Himalayan mountain fold belt [1].

The main structural elements of the modern Kura depression began to form in the Early Jurassic period. Mesozoic sediment complexes were formed in sedimentary and volcanic formations with a large thickness (16-18 km and more) due to intensive and continuous subsidence of the Gabirri-Ajinothur, Yevlakh-Aghjabedi, and Lower Kura depressions starting from the Jurassic period [2].

The oldest rock complexes of the Kura depression uncovered by wells are Middle Jurassic (Aalenian, Bayosian and Batian) and were studied in the rock samples taken from the Saatli Superdeep Borehole (SB-1). According to those data, these old rocks are represented by andesite, basalt formations. Upper Jurassic sediments were uncovered by wells dug in Saatli, Jarli and Sor-sor areas [3]. Lower Cretaceous sediments were uncovered by wells dug in Saatli, Jarli and Sor-sor areas. The Lower Cretaceous is represented by carbonate-lithofacies in the Saatli area [4]. Cenomanian-Turonian stage (K_{2s-t}) tuffaceous series was uncovered by wells dug in Khatinli, Girag Kasamanli, Mammadtapa, Tarsdallar areas.

Upper Cretaceous formations are composed of extrusives and andesite lava-based basalts in the elevated parts of the Muradkhanli area. The carbonate formation of the Cenonian stage (K_{2sn}) belonging to the sediments of the Coniacian-Maastrichtian substage is uncovered by wells dug in Khatinli, Girag Kasamanli, Sajdag, Mammadtapa areas. Based on the microfauna characteristics of the Cenonian stage sediments uncovered in the Khatinli area (structural exploration wells 29, 32), it was possible to carve up the Campanian and Maastrichtian stages. The Campanian stage sediments are lithologically represented by calcareous marls and limestone series. The sediments of the Maastrichtian stage consist of greenish-gray sandy clays, sometimes marls layered with gray clayey marl interlayers. Carbonate sediments of the Upper Cretaceous are exposed in the north-west limb of the Muradkhanli uplift.

According to the comprehensive analysis of well and seismic exploration data, the maximum thickness of the carbonate layer reaches 1400 m in the central part of the Yevlakh-Aghjabedi depression [3] and the thickness decreases in the slope parts, however, sandy-clay rocks are found in the section.

Along the north-east slope of the Ajinohur depression, the Cretaceous sediments are represented by a continuous section from the Aptian to the Danish stage up to 1.8-2 km thick. In the Aptian-Albian interval, the section is divided into 20-25 sandstone horizons up to 6 m thick. Along the Cretaceous section the Cenoman stage characterized by higher reservoir properties, which includes sandstones and carbonate rocks from 100 to 180 m thick.

Oil and gas reservoirs in the Upper Cretaceous are mainly carbonate, porous-leaky-cracked volcanic and grained rocks. However, receiving a high amount of water flow (from 120-190 to 8-10 thousand t/day), in some cases, even oil and gas flow from wells dug in Jarlı, Sor-Sor, Garajali, Sovetlar and other areas show that the carbonate sediments of the Upper Cretaceous are characterized by high capacity and filtration properties [5].

Thus, as noted the lithofacies of the Mesozoic rock complexes are mainly brittle carbonate rocks, therefore, there is a high probability of formation of crashing zones at the intersections of faults of different scales.

Paleocene sediments were uncovered in Khatinli (wells 29 and 32), Girag Kasamanli (well 46), Mammadtapa (well 1) and Tarsdalar (well 9) in the Kura-Gabirri interfluvial area [6].

The lower part of the Paleocene (the Danish stage) consists of clayey hard limestones layered by the interlayers of marl of 47 m thick in the Khatinli area, but it consists of 27 m thick limestones along the section of the Girag Kasamanli area.

The Eocene sediments are widely developed in the Kura and Gabirri interfluvial zone and uncovered by numerous deep prospecting wells.

These sediments were uncovered in all the wells dug along the Kura and Gabirri interfluvial areas (Jahandar, Damirtapa-Udabno, Mammadtapa, Sajdag, Gurzundag, etc.), and are characterized by tough calcareous clays with clayey, fine-grained sandstone, siltstone, marl, and limestone interlayers.

In the Kura and Gabirri interfluvial region, industrially important oil flow was obtained from Middle Eocene sediments of the wells dug in the Tarsdallar area (wells 1, 4, 8, 9).

The thickness of Maykop series sediments ($P_3+N_1^1$) increases from south to north to 0-2500 m in the Kura and Gabirri interfluvial area. Lithologically, these sediments mainly consist of sandstone and clay formations with marl interlayers.

Middle Miocene (N_1^2) sediments are limited in the Kura-Gabirri interfluvial area. Lithologically consists of dense clays with marl interlayers and marl dolomites.

The Upper Miocene (N_1^3) mainly consists of gray, grayish-brown clay layers alternating with dense, cracked thin marl layers.

The Upper Pliocene (N_2^2) sediments lie on the basal conglomerates formed by weathering products of the Miocene and Paleogene sediments. The Aghjagil stage consists mainly of clays, however, the middle substage consists of clays with sand and thick limestone interbeds [7].

Clayey sediments of Upper Cretaceous, Eocene, and Maykop within the Kura depression can act as a screen for the formation of oil and gas accumulations on the hydrocarbon migration way.

As is known, oil and gas deposits in the Earth's crust are usually grouped in oil-gas accumulation zones consisting of different types of traps.

In addition to structural, lithological and stratigraphic factors, tectonic crushing zones also play a special role in the formation of several types of oil and gas accumulation zones [8, 9].

Based on geological-geophysical and space data, according to the schematic-structural map depicting the consolidated foundation and fault tectonics of the South Caspian megadepression (Fig. 1), the main feature of the structure of the Mesozoic rock complex within Kura depression is that it is divided into tectonic blocks of different sizes, complicated by longitudinal and transverse faults of different directions. The blocks descended gradually from the slopes of the depression towards the center along the regional faults with a vertical amplitude of 500-1000 m relative to each other (Fig. 2). Taking this into consideration, it should be noted that due to the relatively complex geological structure and high consolidation of the Mesozoic rock complex, there is a high probability intensive crushing of rock at the intersections of faults. The composition of tectonic blocks, along with the intersection of disjunctives oriented in different directions along the Kura depression, contributes to the formation of the crushing zone of rocks at the intersection nodes [10].

Therefore, it can be noted that the Kura depression has favorable structural-tectonic conditions in terms of the formation of industrially important oil and gas accumulations in various types of natural traps and tectonic crushing zones.

The Mesozoic rock complexes are promising for oil and gas due to the presence of significant fractured, tuffogenic-sedimentary and volcanogenic-sedimentary rocks with good reservoir properties along the section of Upper Cretaceous of the Kura depression, the presence of sufficient of a large number of Cenozoic impermeable layers that can serve as a caprock, favorable structures that can serve as traps for hydrocarbon accumulation, and the presence of tectonic crushing zones such as unconventional traps, as well as the discovery of oil fields in a number of areas such as Muradkhanli, Zardab, Sovetlar [11].

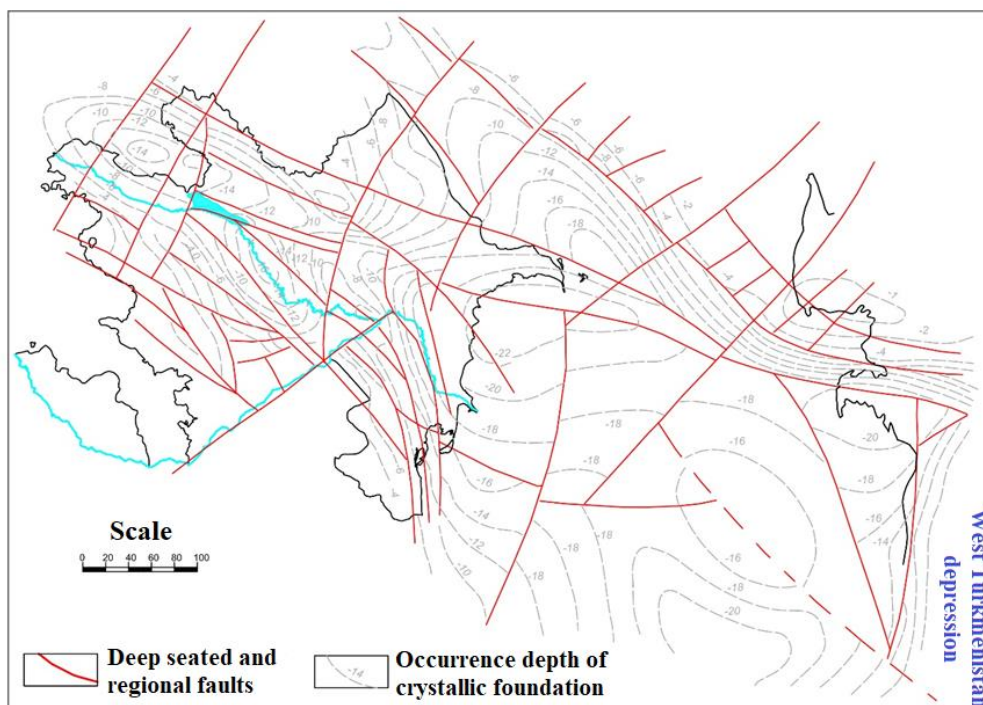


Fig. 1: South Caspian megadepression. Schematic structural map according to the surface of the consolidated foundation and fault tectonics (according to F.M. Bagirzade, K.M. Karimov, etc.)

Based on the conducted analysis, it can be concluded that in addition to structural type traps in the studied oil and gas regions in the Middle Kura depression, developed tectonic crushing zones and nodes in the Mesozoic rock complex are also unconventional traps with fairly high oil and gas prospects.

It should be noted that when a network of relatively dense and intersecting faults complicates the competent rocks in any area, since they are brittle, not only the faults but also the network of cracks accompanying them will develop. This leads to the formation of relatively large, so, regional-scale crushing and cracking zones around of those faults.

As is known, in many cases, folds and faults regulate the location of oil and gas deposits in the Earth's crust. Relatively, from the point of view of the presence of large oil and gas deposits, the intersection nodes of the faults of the studied foundation are more interesting. In this regard, intersection nodes of faults and tectonic faults create large-scale structures that may be associated with significant hydrocarbon accumulations [12].

II. Discussion and conclusions

Conducted studies show that tectonic crushing zones are widespread within Middle Kur depression. They are arising of great interest as an object for the search of oil and gas deposits (Fig. 3).

Based on the available data of the fault tectonics of the Kura intermountain depression [13] about 11 intersection nodes were determined accompanied by rock crushing at the intersection of disjunctives with different ages, scales and arrangements (Fig. 3).

The Dahna-Akharbakhar crushing zone is located in the northwest of the Goychay-Garamaryam zone, in the southeast of the Mahmudlu-Khaldan zone and in the central part of the Dahna-Ivanovka zone and was formed by 7 faults. Longitudinal faults are represented by overthrusts and reverse faults, however, transverse faults are represented by deep seated and ring-like faults. In this node, a tectonic cover with an amplitude of 1000 m has developed due to intensive crushing of rocks [14].

The presence of limestones with highly fractured sandstone layers for the accumulation of industrially important hydrocarbon deposits in the Upper Jurassic section suggests that the Dahna-Ivanovka zone is promising.

Parametric wells drilled in the Mahmudlu-Khaldan zone of the Ajinohur oil and gas bearing region uncovered Upper Cretaceous sediments at a depth of 6500 m [15]. There is an experimental interest that the parametric and exploratory wells drilling in the Goychay-Garamaryam zones, will uncover the Upper Jurassic sediments at a depth of 6.5-7 km. The prospects in the Goychay-Garamaryam zone are mainly related to dense fractured and crushed carbonate rocks, as well as reef structures. In addition, the development of regional and local faults creates favorable conditions for the formation of intensive cracking in competent carbonate rocks. All this phenomenon arouse interest for prospecting of industrially important oil and gas deposits along the Upper Jurassic and Cretaceous sediments.

The Agsu crushing zone is covered of the south-east edge of the Dahna-Ivanovka and Goychay-Garamaryam zones, the eastern part of the Kurdamir-Saatli zone, and the north-west of Navai, Central Gobustan and Padar-Salyan zones. It was formed by 6 faults, including the Western Caspian deep seated fault. However, tectonic covers are developed in the Upper Cretaceous volcanogenic-sedimentary rocks section covered by Paleogene and Miocene sediments within this node [7].

According to the Upper Jurassic sediments the Goychay-Garamaryam and Dahna-Ivanovka zones are can be evaluated prospective in Agsu node. In addition, parametric wells at a depth of 6.5-7 km can uncover highly fractured carbonate reservoirs.

Based on the data of the Lower Cretaceous sediments of the Kurdamir-Saatli zone [3] the geological-geochemical conditions can be considered favorable for the formation of hydrocarbons

in the above-mentioned node. The development of a network of regional and local faults in this node has led to the improvement of the capacity of carbonate rocks for accumulation of hydrocarbons in the crushed Upper Jurassic and Cretaceous rocks. In the northern part of the Salyan-Padar zone, which belongs to the Agsu node, along the regional faults, the rocks are eroded, so there are favorable conditions for the accumulation of oil and gas.

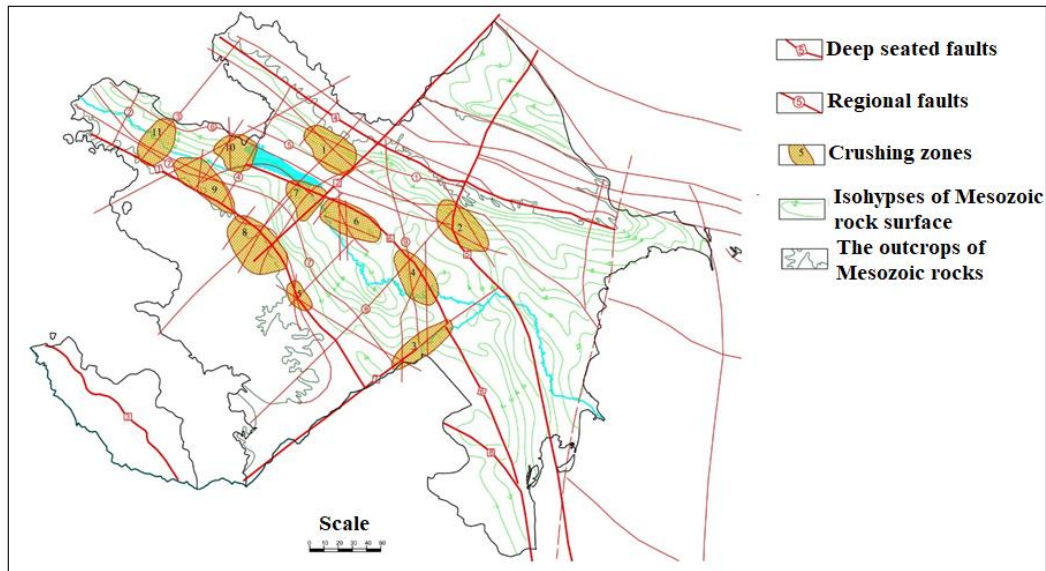


Fig. 2: Map of tectonic crushing zones of Kura depression based on the data R.M. Hajiyeov, K.M. Karimov and others.

Compiled by: Ass. Prof. N.R. Narimanov; G.J. Nasibova, E.A. Ismayilzadeh

Legend: Crushing zones. Nodes: 1- Dahna Akharbakhar, 2- Agsu, 3- Garadonlu, 4- Muradkhanli, 5- Agdam, 6- Bozdag, 7- Barda, 8- Tartar, 9- Shamkir, 10- Tarsdallar, 11- Agstafa; Deep seated faults: 1- Lesser Fore-Caucasus, 2- Arpachay-Samur, 3- Nakhchivan, 4- Kvareli-Gabala-Goradil, 5- West Caspian, 6- Mingachevir-Lankaran, 7- Ashagi Araz, 8- Fore-Talysh; Regional faults: 1- North Kakhertia-North Ajinohur, 2- Gazakh-Signakhi, 3- Tovuz-Lagodekhi, 4- Ganja-Alazan, 5- Udabno-Goychay, 6- Udabno-Eriklar, 7- Tovuz-Lagodekhi, 8- Azerbaijan Flexure, 9- Imishli-Oguz.

The Garadonlu crushing zone was formed by 5 faults, including the Araz, Lesser Caucasus deep seated faults. This node covers the part of the meridional graben that coincides with the Talysh-Vandam gravity maximum on the plan [2].

To contain rare sandstone limestones with increased cracks for the accumulation of industrially important hydrocarbon accumulations along the main part of the cross-section of the Jurassic sediments are expected within Garadonlu node. The south-east part of the Garkhunlu-Garadonlu zone is considered promising. Assumed that the Upper Jurassic sediments can be uncovered at a depth of 6.5-7 km. Based on the Lower Cretaceous sediments, the southeast part of the Garkhunlu-Garadonlu zone, where large oil and gas accumulations are likely to be formed in carbonate, rifogenic and terrigenous formations, is considered promising. Like the upper Jurassic sediments in the Eirija-Shiringum zone, the occurrence depth of the Lower Cretaceous sediments more than 7 km. Therefore, they are not considered promising for the drilling of prospecting wells [4].

Exploration well 2 with a project depth of 5000 m has been placed in the south-east part of the Duzdag-Sovetlar zone, at the Agtel outcrop. After passing the depth of 3855 m (along Paleogene sediments), it was abandoned due to technical reasons.

Further geophysical studies showed that the well location was not chosen correctly. However, 2 parametric wells with a project depth of 5000 m were drilled in the Eyrija-Shiringum area, within the limits of the Garadonlu node. The first well at a depth of 4807 m (in Eocene

sediments) was abandoned due to technical reasons. The second well uncovered the Upper Cretaceous sediments of fractured limestones, which show the crushing of these rocks in the limits of Garadonlu node at the depth interval of 4390-5000 m [7]. This node is characterized by a favorable structure for the formation of oil-gas accumulations in the traps associated with crushing nodes, formed due to the intersection of regional deep seated and local faults.

However, the Upper Cretaceous sediments lie at a depth of 6.0-7.5 km in the south-east part of the Garkhunlu-Garadonlu zone. In the west part of the node, within Lesser Caucasus and Duzdag-Sovetlar zone, the occurrence depth of the Upper Cretaceous sediments is up to 5000 m, which is considered possible for drilling [3].

The Muradkhanli crushing zone covers the central part of the Garkhunlu-Garadonlu zone and the western part of the Agdash-Mil zone. This node is formed by 4 faults, including the Gutgashin-Imishli deep seated fault passing through the Muradkhanli field. This fault was involved in the formation of good reservoirs along the effusive rocks of Upper Cretaceous. After uncovering of the oil field in the Muradkhanli effusive formations, along with carbonate rocks, volcanogenic rocks were also characterized as a prospecting object in the central part of the Kura depression. The discovery of an oil field in the effusive rocks of the Garkhunlu-Garadonlu zone (Muradkhanli field), as well as the similarity of the normal sections belonging to the individual structures of the zone, became a good guiding factor for conducting prospecting and exploration works for the purpose of searching for oil in the Mesozoic sediments of this zone and other crushing zones. The oil in the Zardab field was obtained from formations lying under marls of the Upper Eocene. Later, industrially important flows were obtained in the contact zone of carbonate and effusive rocks of the Upper and Lower Cretaceous (well 4,7,9).

Carbonate sediments were uncovered in the Maastrichtian-Santonian stages of the Upper Cretaceous complex around Agdash-Mil zone within the limits of the Muradkhanli node, under the Eocene sediments [3]. Below the section is continue by alternation of limestones with marls, argillites and tuffaceous sandstones.

The development of a fault network in the Mil area led to the formation of cracking and crushing zones in carbonate and effusive rocks. A part of these zones can be considered promising for oil and gas in Upper Cretaceous sediments. In order to carry out prospecting-exploration work in this node, it is necessary to clarify the structural-tectonic conditions in the intersection zones of the faults and their preparation for drilling.

The Barda crushing zone covers the north part of the Yevlakh-Lanbaran zone, the Eyrija-Shiringum and Garkhunlu-Garadonlu zones [3]. At this node, in the Upper Jurassic sediments, the Garkhunlu-Garadonlu zone, which is expected to contain sparse sandstone limestones with increased cracking for the formation of industrially important hydrocarbon accumulations in the main part of the section, can be considered promising.

Since the occurrence depth of the Lower Cretaceous sediments more than 7 km in the Eyrija-Shiringum zone, they are not considered promising for the drilling of prospecting wells.

In the Garkhunlu-Garadonlu zone formed by eight faults, the Upper Cretaceous sediments are represented by cracked and crushed effusives, carbonates and terrigenous-tufogenic rocks, which are favorable for the formation of oil and gas accumulations. According to the Upper Cretaceous sediments within this node, the north part of the Garkhunlu-Garadonlu zone is considered as an object for exploration, which is favorable for the formation of oil and gas reserves in traps due to the tectonic crushing of rocks.

The Bozdag crushing zone occupies parts of the Duzdag-Sovetlar, Yevlakh-Lanbaran and Garkhunlu-Garadonlu zones [3]. The node has formed by 8 faults elongated different directions, which improve the reservoir properties of the rocks due to cracking and crushing. The Garkhunlu-Garadonlu zone, which is considered a continuation of the Barda crushing node, can be considered as a promising within of Bozdag node, due to the presence of fractured limestones that consists the main part of the section of Upper Jurassic sediments. Nodes also have favorable conditions for industrially important oil and gas formation. The occurrence depth of Upper

Jurassic sediments in other parts of the node up to 7-8 km, which is technically difficult for modern drilling.

The Lower Cretaceous sediments are considered favorable for the formation of oil and gas deposits due to their geological and geochemical conditions in the major part of the Kura depression. Taking this into consideration, we can predict the existence of significant oil and gas accumulations in the Lower Cretaceous intensively crushed and fractured carbonates, rifogenic and terrigenous formations, in the north part of the Garkhunlu-Garadonlu zone, within the Bozdag crushing node.

According to the Upper Cretaceous sediments, the Duzdag-Sovetlar zone is proposed as an object for the search of oil and gas deposits.

The Aghdam node is the smallest among the crushing zones and occupies a part of the Lesser Fore-Caucasus zone [10]. The node was formed due to 4 faults, including the Lesser Fore-Caucasus deep seated fault.

The prospects of the Upper Jurassic sediments within the Aghdam node is associated with the crushing zone developing along the Lesser Fore-Caucasus deep seated fault. In this zone, development of highly fractured carbonate reservoirs are expected, which is suitable for oil and gas accumulation.

According to the Upper Cretaceous sediments, the Aghdam crushing node is not promising for oil and gas accumulation, due to the lack of a reliable caprocks.

The Tartar crushing zone runs parallel to the Lesser Caucasus trough and occupies a part of it. From the east, it covers the Lesser Fore-Caucasus and a part of the Duzdag-Sovietlar zones [10].

Along the Lesser Fore-Caucasus fault, the Earth's crust movement occurred from time to time and was very active throughout the Mesozoic period. The node was formed by 10 faults, including the Lesser Fore-Caucasus deep seated fault, an arc fault and a regional transverse fault that runs through the entire territory of Azerbaijan. This fault and other faults intersecting with it have formed intensive crushing zones that create favorable conditions for the formation of oil and gas accumulations in this node. The prospect of the Upper Jurassic sediments is associated with the Lesser Fore-Caucasus zone, which is expected to contain carbonate reservoirs, mostly intensively fractured, that serve to accumulate oil and gas.

Prospecting wells were drilled in the Tartar zone and two of the 4 drilled wells (153,152) uncovered the Upper Cretaceous carbonate layer with a thickness of 700 m. However, the Upper Cretaceous sediments were not productive.

The Shamkir crushing node is located in the north-west of the Tartar crushing node. It occupies the Lesser Fore-Caucasus meganticlinorium trough and a part of the Garayaz-Khuluf zone [3].

The node was formed by 11 different alignment faults, including the Alazan-Eyrichay, the Lesser Fore-Caucasus deep seated fault, and the Shamkhor-Aliabad regional fault.

Unlike the previously mentioned nodes, the Shamkir crushing node differs in that it is more strongly complicated by faults. Intensively crushing and fracturing of the Mesozoic rocks are expected.

Late Jurassic-Early Cretaceous granitoid intrusions have developed in the north-east border of the Lesser Fore-Caucasus trough. In the western part of the node, due to the development of intrusive formations, there is not probability of the presence of industrially important hydrocarbon accumulations. According to faults and geological-geophysical data, in the east, towards the Kura River, there is a high probability of formation of hydrocarbon accumulations in the structures complicated by the Shamkir-Aliabad fault, which is located within the depression. As noted by A. Shikhalibeyli and others, this is confirmed by the entire chaotically located overthrust and revers fault network. The Upper Cretaceous sediments with complex tectonic structure, which make up the surface of the Mesozoic rocks, has been strong crushed in the boundaries of this node, mainly in the intersection zone of the faults. As noted by K. Karimov, this factor does not allow establishing the exact lithofacies regularity in the area, but due to the Upper

Cretaceous sediments in the boundaries of node, its east and north-east parts can be considered promising.

Tarsdallar crushing zone was formed by 4 meridional and Cis-Caucasus faults. The node covers the south-east part of the Garayaz-Khuluflyu zone and the south part of the Molladag-Tarsdallar zone. The Molladag-Tarsdallar zone is considered promising due to intense folding by faults and the presence of the Upper Jurassic sediments along the cross section of the central part of node. However, Upper Jurassic sediments can be uncovered at a depth of 6.5-7 km [16].

In the Lower Cretaceous sediments, there were favorable conditions for the formation of oil and gas accumulations due to the cracking of rocks of various origins, which are non-anticlinal traps. As a result, the presence of significant oil and gas accumulations in fractured carbonate, rifeogenic and terrigenous formations in the Molladag-Tarsdallar zone can be predicted.

In the south-west part of the node, within of the Garayaz-Khuluflyu zone, the prospects of the Lower Cretaceous sediments are negatively evaluated. The reason for this is that, as in the Upper Jurassic, these sediments do not participate in the section or are represented in an insignificant thickness for the formation of oil and gas deposits.

According to the Upper Cretaceous sediments, the Molladag-Tarsdallar zone is considered as promising object for the search of oil and gas deposits.

In September 1983, in the Tarsdallar area of the Kura-Gabirri interfluvial region, a large fountain oil flow was obtained from cracked marls of the Middle Eocene with a production of 300 t/g [16]. The reservoir properties of rocks are expressed by the faults with small-amplitude and fissures in the middle limb of the flexural trough. Taking into account the complexity of the geological structure of this node, it is possible to increase the reservoir properties of the carbonate and volcanic rocks of the Cretaceous. This allows considering the Cretaceous sediments as a promising object for the search of hydrocarbons.

The Agstafa crushing zone is formed by 7 disjunctives in different directions, including the Gazakh-Tsitelchkaroy and Lesser Fore-Caucasus faults, as well as submeridional and general Caucasian regional faults [3].

The node covers the north-east part of the Lesser Caucasus trough, the central part of the Garayaz-Khuluflyu and the Molladag-Tarsdallar zones.

The occurrence depths of Mesozoic sediments is shallow within Garayaz-Khuluflyu zone, in the boundaries of the node (Tovuz-Gazakh, Girakh-Kasamanli and Khatun). Only the upper part of the Upper Cretaceous was studied in the area by wells, where its section represented with carbonate and under lying volcanic-sedimentary rocks.

The upper Cretaceous sediments, which are involved in the structure of the Gazakh depression, descend in the northeast direction and penetrate under the Cenozoic sediments in the Kura-Gabirri interfluvial region. Fore-mountain zone towards the center of the depression, the volcanogenic-sedimentary facies is continuously replaced by sedimentary formations.

The north-east part of the node located in the Kura-Gabirri interfluvial region is considered more promising. There is a possibility of Cretaceous high cracked reservoirs. In order to avoid drilling excess wells, first of all, it is advisable to carry out complex geological-geophysical searches to determine the condition of the Cretaceous structural floor and its oil-gas content.

However, the prospective oil and gas bearing crushing nodes zone were analyzed in the Mesozoic sediments within Kura intermountain depression. As a result, 4 highly promising- Dahna-Akharbakhar, Muradkhanli, Tartar and Tarsdallar; 5 promising- Agsu, Barda, Bozdag, Shamkir, Agstafa; 2 less promising- Garadonlu and Aghdam crushing nodes are determined (Tab. 1).

III. Conclusion and suggestions

1. Based on the lithofacies and structural analysis, the emergence of tectonic crushing zones in the Mesozoic rock complexes, which are subjected to intense brittle deformation and are

complicated by disjunctives of various scales and a dense network of cracks, and the latter play the role of a favorable trap in the formation of oil and gas accumulations.

2. Determined that oil and gas deposits of Muradkhanli, Zardab, Sovetlar, Tarsdallar areas are associated with crushing zones, it was found that faults are of great importance in the formation of deposits in the Mesozoic sediments named zones in the Kura depression.

3. Highly promising- Dahna-Akharbakhar, Muradkhanli, Tartar and Tarsdallar, promising-Agsu, Barda, Bozdag, Shamkir, Agstafa, and less promising- Garadonlu and Aghdam crushing nodes has been determined. This nodes are favorable for oil and gas accumulation in the Middle Kura depression.

Table 1: Characteristics of crushing zones

№	Nodes	Lithological characteristics	Type and age of caprocks		Dislocation level	Disjunctive	Oil and gas formation complexes and its age		Oil and gas manifestations	Promising	Knowledge	Research
			clay	P			carbonate	J ₃ K				
1	Dahna-Akharbakhar	massive limestone	clay	P	7	5	carbonate	J ₃ K	-	highly promising	Well	I order
2	Muradkhanli	effuzive carbonate	clay	N ₂ -N ₁	4	7	effuzive	K ₂ N ₂	-			
3	Tarsdallar	carbonate volcanogenic	clay	P-N ₁	4	3	carbonate	K ₂ P ₂	-			
4	Tartar	carbonate	clay	P	10	5	carbonate	J ₃	-			
5	Agsu	volcanogenic - sedimentary, carbonate	clay	P-N ₁	6	3	carbonate	J ₃ K	oil-gas	promising	Sufficiently	II order
6	Barda	massive limestone, effuziv	clay	P	8	7	effuzive carbonate	K ₂	-			
7	Bozdag	massive limestone	clay	P	8	3	terrigenous - carbonate,	J ₃ k	-			
8	Shamkir	carbonate	clay	P	11	-	rifogenic	J ₃ k	-			
9	Agstafa	carbonate, volcanogenic -sedimentary	clay	P	7	4	carbonate	K	-			
10	Garadonlu	massive limestone with sandstone interbed	clay	P	5	2	carbonate, rifogenic	J ₃ k	-	Less promising	Weak	III order
11	Aghdam	volcanogenic	clay	P-N ₁	4	-	-	-	-			

References

- [1] Nasibova G. J., Mukhtarova Kh.Z., Ganbarova Sh. A., Ismayilova M. M., Zeynalova.S. A. The influence of compressive stresses on folding in the Middle Kura depression and the Turkmen shelf. *Journ. Geol. Geograph. Geoecology*, 2023 32(2), 352-359 p.
- [2] Karimov K.M., Rakhmanov R.R., Kheirov M.B. Oil and gas potential of the South Caspian megadepression. Baku 2001., Adilogly Publishing House, 316 p.
- [3] Kerimov K. M. Problems of the Mesozoic oil of Azerbaijan and ways to solve them. Baku 2009, CBS, Polygraphic production, 392 p.
- [4] Hajizadeh F.M. Geological structure and oil-gas content of Middle Kura depression of Azerbaijan. Baku, Adilogly Publishing House, 2003, 364 p.
- [5] Yusifov Kh., Aslanov B. Oil and gas basins of Azerbaijan, Baku, 2018, 324 p.
- [6] Yusifov Kh., Suleymanov A. Geological basis of oil and gas exploration in Mesozoic sediments in Azerbaijan. Baku-2015, 307 p.
- [7] Kocharli Sh.S. Problem questions of oil and gas geology of Azerbaijan. Baku 2015. Law Publishing House, 278 p.
- [8] Mehtiev Sh.F., Salaev S.G., Buniat-zadeh Z.A. Near-fracture zones of rock crushing- a new type of non-anticlinal oil and gas traps, 1986, Problems of oil and gas production in the Caucasus.
- [9] Shikhalibeyli E.Sh. Geological structure in the development of the Middle Kura depression. Report. AN Az. USSR, 1982, No. 1.
- [10] Bagir-zadeh F.M., Karimov K.M., Salayev S.G. Deep structure and oil and gas bearing of the South-Caspian megadepression. Baku. Az. Gos. Izdat. 1987, 302 p.
- [11] Yusifov K.H.M., Rakhmanov R.R. Search strategi of the Mesozoik oil in Azerbaijan. *Azerb. Oil Industry journal*, №2, Baku-2012. p.3-10.
- [12] Aliyev G.I., Aliyev E.A. Oil and gas potential of great depths. 2011, 419 p.
- [13] Narimanov N.R. Geodynamic aspects of the formation of the sedimentary cover of the South Caspian Basin. Moscow, *Geology of oil and gas*. 2003, 6, p. 26-31.
- [14] Mekhtiyev Sh.F. Selected Works. Baku, 2010, Nafta-Press Publishing House, 468 p.
- [15] Alizadeh A.A. Selected Works. Baku, 2011, Nafta-Press Publishing House, 530 p.
- [16] Narimanov N.R., Guliyev G.G. Structural features and oil and gas potential of the Tarsdallar area. *ANE*,1, 1989.

THE IMPACT AND PROSPECTS OF USING ARTIFICIAL INTELLIGENCE IN THE ECONOMY

Larisa Aguzarova, Fatima Aguzarova, Kamilla Tsallaeva

•

North-Ossetian State University named after K.L.Khetagurov, Russia

aguzarova.larisa@yandex.ru

aguzarus@yandex.ru

kamilla.tsallaeva@yandex.ru

Abstract

This paper discusses issues related to the development of technologies and the relationship of this process with economic processes. Due to the rapid digitalization, the importance and role of artificial intelligence are growing. At the same time there are many problems and they are considered in this paper: unemployment of technical workers, a security problem that is associated with the confidentiality, the existing neural networks cannot be suitable for use in all industries etc. When using the generalization method, the authors have made relevant conclusions and recommendations for using Artificial Intellect: to solve the following universal tasks: automatic translation; getting business intelligence; recognition of visual signs; character recognition; information extraction; understanding and analyzing texts; image analysis; ensuring information security and protection against cyber-attacks; speech recognition; robotic tools for the implementation of tasks at different levels and in different fields.

Keywords: economics, artificial intelligence, neural networks, machine learning, digital economy.

I. Introduction

The human community has entered an era of serious changes related to computerization and digitalization. There is a turning point in the development of society, the usual way of life is changing and new standards of organization of various activities are being established. One of the main directions of digitalization, as the main driving force of the ongoing changes, is the development of artificial intelligence.

Recently, everyone talks about such concepts as artificial intelligence, machine learning, neural networks, automation and computerization. It has become obvious that in recent decades there has been a serious leap in the development of science and technology, which, with no doubt, causes multiple changes in all spheres of society: modern electronic tools and software have become firmly entrenched in the social, economic, political and even spiritual spheres.

This paper focuses on the impact of computerization on the economic component of public life, and the introduction of artificial intelligence into the economy in particular.

II. Methods

The following methods were used to develop the study design: Method of structuring; Method of analysis; Method of synthesis.

Nevertheless, the authors selected the system-complex holistic approach as the key method of the research. The choice is justified by the fact that the approach is to generalize scientific knowledge obtained as a result of the study, remaining within the framework of one analyzed

subject (the topic of research is connected to some adjacent spheres as medicine, education, programming etc.)

III. Results

The importance and role of artificial intelligence in the economy

The initial narrow focus of the use of artificial intelligence, its limited use in laboratory conditions and in individual projects have been replaced by widespread utility – artificial intelligence based on neural networks, BigData, machine learning and cloud computing [1], is used in production, analytics, forecasting, accounting, etc.

So, at this stage of its development, artificial intelligence can be considered almost a universal tool and technology, potentially contributing to significant changes in the economic sphere.

Nevertheless, the impact of artificial intelligence on the economy in general remains minimal despite the introduction of AI tools into private economic activity to achieve the goals set by entrepreneurs and optimize the processes taking place in business. The attitude to this state of affairs in society is ambiguous, since the widespread introduction of artificial intelligence into economic processes of different levels presupposes the presence of both pros and cons.

Of course, the digitalization of the economy and the use of artificial intelligence in various economic sectors implies wider opportunities both for certain economies and for humanity in general. So, the advantages of introducing artificial intelligence into the economy are:

- **Increased efficiency:** Artificial intelligence is a tool that greatly facilitates the work of employees in various structures, AI can automate routine and repetitive tasks such as filling out tables, accounting, documentation, regulating taxation which allows you to increase productivity and reduce labor costs [2]. This is especially useful in areas where large amounts of data processing are required, such as finance, healthcare, manufacturing, and logistics.

- **Improving the accuracy and quality of the work performed:** neural networks can process large amounts of data, are capable of analyzing serious information flows, while not losing speed and accuracy. Artificial intelligence allows a person to make decisions based on the results of an AI analysis of the situation. Also, artificial intelligence can carry out activities to independently search for solutions based on the available research result. At the same time, the performance of this work by a person implies the presence of, at least, mechanical errors and large time costs.

So, over time, the influence of the human factor on the processes associated with data analytics and decision-making on the material already processed by AI decreases and the optimality of the final result increases. For example, in the field of medicine, neural networks can help in assessing the condition of patients, in determining diagnoses and building the most appropriate treatment plans based on the symptoms noticed by AI and the patient's medical history. So, again, this proves that artificial intelligence helps to reduce labor costs. Nevertheless, this fact is accompanied by negative consequences both for one particular individual and for the entire economy. These consequences will be described further.

- **Creation and development of new goods and services:** the use of neural networks opens up new opportunities for creating innovative products and services that were previously unavailable. We are talking about the creation of "independent" robot assistants, which are already used in most cities of Russia and the world: delivery robots, vacuum cleaner robots, robot manipulators, etc.

There are also more interesting and more independent machines with artificial intelligence: robot assistants (For example: Asus Zenbo, which combines a number of functions that facilitate the life of housewives – helps with cleaning around the house, entertains the family when needed, takes care of babies and the elderly, and can also do a lot of things that a person is capable of), robots-interlocutors, robots-doctors (For example: Smart Doctor Assistant, which, at the moment,

is the first and only licensed doctor among AI), there are also independent vehicles controlled by AI (Tesla, an unmanned Odyssey truck from KAMAZ) [3]

- AI can also improve existing products and services by adding machine learning and data analysis features [4]. For example, many banks are implementing neural networks into their mobile applications: chatbots no longer direct customers to operators and do not respond with basic phrases recorded by people - now bots will help solve the client's problem independently, based on the experience gained, through machine learning. (Sber bank makes 100% of retail credit decisions using AI, and 95% of them are formed automatically, without human participation. Sber bank also uses neural networks for document recognition and automatic scheduling of employees) [5].

- Solving complicated problems: AI is able to efficiently and safely solve tasks which are difficult or dangerous for humans to go along with. For example, artificial intelligence can deal with tasks connected to detecting and preventing cyber-attacks, can analyze images and help diagnose difficult-to-detect diseases; robots with AI can go on search missions deep into the oceans or into outer space [6]. This will lead to a reduction in labor costs and reduce the risks in carrying out the necessary work.

Thus, AI has great potential for solving complex and dangerous tasks that can save people time and resources, as well as increase the efficiency and accuracy of solutions.

- Creation of new jobs: The introduction of AI can lead to the creation of new jobs related to the development, maintenance and management of AI systems. While some traditional jobs may be replaced by robots or automated, there will be new opportunities for people with AI and technology skills. For example, AI developers and engineers are to be demanded to create and improve machine learning algorithms and models. Data scientists and analysts will be able to use AI to examine large amounts of information and identify new trends and patterns. Companies will also need cybersecurity specialists to protect AI systems from attacks and vulnerabilities.

There will also be new jobs associated with the implementation and support of AI systems. These can be specialists in the implementation of AI in various industries, administrators of AI systems, training data for training machine learning models, and much more.

However, in order to be competitive in the labor market, people should develop skills related to AI and analytical thinking. This may include learning programming, mathematics, statistics, and machine learning. Communication skills and the ability to work in a team are also important, since many AI projects require the collaboration of various specialists.

- Improving the quality of customer interaction: AI can foster increasing the personalization of the services provided by putting forward recommended products and services that are most suitable for a particular client. For example, personalized advertising in social networks helps manufacturers to find their consumers, and consumers – the desired product. This contributes to improving customer satisfaction and the competitiveness of companies.

In general, the introduction of artificial intelligence into the economy offers a wide range of advantages. Professional evaluation shows that the use of AI can significantly improve the efficiency of business processes and increase labor productivity. More accurate and faster analytical data allows you to better predict the needs of the market and optimize the company's development strategies. In addition, automation of routine frees employees from monotonous tasks and gives them the opportunity to concentrate on more creative work.

However, it is necessary to keep in mind the risks associated with data privacy and ethical issues when using AI [7]. In general, the intelligent use of artificial intelligence can become a key factor in the development of the modern economy and the achievement of new heights in business.

IV. Discussion

Problems related to the introduction of artificial intelligence in various sectors of the economy

The introduction of artificial intelligence is not as simple as it may seem at first glance; for the effective and successful integration of artificial intelligence into various sectors of the economy, a number of problems need to be solved:

- When using artificial intelligence, one of the problems becomes understanding the principles of its work, or rather the opacity of the decisions made by AI. Since AI is used in performing completely different tasks – from driving a car to managing insurance payments, the decisions made by neural networks may conflict with the logic of the user or entrepreneur who implemented this AI.

For example, on May 8, 2019, in Miami, a driver who lost control of the car died at the wheel of a Tesla Model S, as a result of which the car collided with several palm trees. The internal systems controlled by AI could not cope with this situation, the driver who was in the car could not get out of the cabin on his own and died as a result of the resulting fire [8].

- There are various options for applying AI into practice, and, nevertheless, the issues of regulating the work of neural networks in a particular industry are a serious difficulty – they are not universal and each of the existing neural networks cannot be suitable for use in all industries. Accordingly, there is a problem of choosing and evaluating an acceptable AI option for a specific purpose.

So, if the use of neural networks to analyze the semantic content of a text can be useful to professional writers, then in most other situations such technology may be superfluous.

- Determining the most suitable neural network for further work does not yet solve all the issues of its application – this is followed by the search for specialists capable of working with a particular AI system. As artificial intelligence becomes more widespread in the industry, many skilled professionals have become much more difficult to find due to high demand. In addition, the salary of such specialists is usually higher than that of less technical specialists, which can lead to prohibitively high costs for doing business "according to the rules of the future"

- In addition to the above-mentioned problems related to the recruitment and distribution of personnel, another one arises: a security problem that is associated with the confidentiality and inviolability of data when using artificial intelligence systems in production environments.

When working with AI, there is no complete guarantee of data security, at this point in time there is a serious possibility of information leakage. Privacy issues also go beyond data protection. Many questions merge from integration of AI: what information does an artificial intelligence system collect about its users? Is it used for marketing purposes? And how is it to be regulated by the relevant authorities [9].

Also, that is why it is extremely important for those who work with confidential customer information through digital channels to ensure compliance with best practices when implementing machine learning solutions and not to forget about attracting specialists who are able to regulate these issues.

- Another problem of using AI in various sectors of the economy is the management of requests and expectations when working with advanced technologies. We are talking about the ability of specialists to correctly make requests, specify all the requirements for the neural network so that there are no discrepancies with expectations.

It is very important to clearly understand what problems can really be solved and how much time it will take – technical specialists should set specific tasks for themselves, without allowing too many assumptions and options.

So, for example, in the field of architecture, in order to reflect the final sketches in the form necessary for a particular company, it is important to carefully study existing frameworks, such as

TensorFlow and PyTorch, and choose one of them based on the current requirements for the project, since even small differences in the work of machine learning can lead to serious changes in the result activities. So, a comparative characteristic of these frameworks [10]:

	PyTorch	TensorFlow
Advantages	The framework is based on Python programming language, which makes it flexible and easier to use. An active community and forums help developers to work quickly and exchange information.	Unlike Pitch, TensorFlow is compatible with many programming languages. TensorFlow can easily process large datasets. That's why TensorFlow's market share was 36.92% in 2022. TensorFlow has extensive visual capabilities. Open source code, available for free use.
Disadvantages	Sometimes you need to convert the code to develop a real app. Visualization methods in PyTorch are not so good, and one may have to use other tools.	Frequent updates and occasional uninstallations and reinstallations have become a challenge for users. TensorFlow displays lower computing speed and is lags in usability compared to many deep learning frameworks on the market

Of course, these differences will seriously change the final result, which, in turn, determines the profitability of the company and its position in the market.

- And the most serious problem that arises in the process of introducing AI into the economy remains ethical and legal aspects. Ethical issues are related to questions about how the use of AI can affect people and society. Increasingly, there are concerns about the automation of workplaces and the threat of unemployment in the very near future [11].

There are disputes about the correctness and expediency of using AI, while people who do not have the opportunity to use it or prefer doing business exclusively with human hands and mind, equal working conditions and doing business in this case are impossible. Legal problems are related to the definition of liability in case of errors caused by AI. Who is responsible for the actions of AI if they lead to negative consequences? In addition, there are questions about the protection of intellectual property and copyrights in relation to the AI systems being created and their results.

Solving these problems requires the development and adoption of new laws and regulations that take into account the specific features of the use of AI in the economy. It is necessary to develop international standards and agreements to regulate the use of AI and protect the rights and interests of people. This will cause the need for the active participation of ethics, law, economics and technology specialists in the development of solutions, which is a complex task that requires attention from all stakeholders.

IV. Conclusion

Thus, the importance of artificial intelligence in the economy is increasing every day. AI offers many prospects for use in various sectors of the economy. Technologies related to machine learning and neural networks help in performing routine and complex tasks, as well as increase the efficiency of non-technological employees. Thus, artificial intelligence is used to solve the following universal tasks:

- automatic translation;
- getting business intelligence;
- recognition of visual signs;

- character recognition;
- information extraction;
- understanding and analyzing texts;
- image analysis;
- ensuring information security and protection against cyber-attacks;
- speech recognition;
- robotic tools for the implementation of tasks at different levels and in different fields, etc.

[12];

So, the potential of using artificial intelligence in the economy is extremely high – the use of neural networks in manufacturing and in the service sector can contribute to the integration of humans and AI, which is equal to the optimization of economic activity.

Nevertheless, the introduction of tools endowed with artificial intelligence into the economy can also cause negative consequences, such as an increase in the unemployment rate due to the transfer of some responsibilities to machines.

In accordance with the improvement of artificial intelligence, economic organizations should control and regulate the division of labor between people and machines, as well as provide people with new jobs related to, in fact, the adjustment of AI activities [13].

Such changes can provide for the transition from the information "cult" to the neural networks "cult" and the widespread use of robotic systems, along with many new products and services based on the AI use. According to a recent PwC report, artificial intelligence technologies and apps are to increase global GDP by up to 14% in the period up to 2030 [14].

Obviously, there is no clear answer to questions about the future of the world's economies and the impact of AI on all fields of public life. However, one should admit the significance and possible benefits of using the AI, which does not replace a person, but helps them. Fear of the unknown and problems within the economy can curb development and lead society to stagnation.

Artificial intelligence is rapidly making an already complex world even more complex, and it is not bad, it is a new reality that society need to put up with and work with.

References

- [1] Artificial intelligence // Britannica – 2017 – <https://www.britannica.com/technology/artificial-intelligence>
- [2] Aguzarova, F. S. Problems and ways of optimizing the tax system of Russia / F. S. Aguzarova, D. A. Balayeva // Bulletin of the K. L. Khetagurov North Ossetian State University. - 2008. – No. 3. – PP. 72-77. – EDN KNXXXH.
- [3] Odyssey: all about the KAMAZ unmanned project // Vesti KAMAZ – 2018 – <https://www.vestikamaza.ru/posts/odyssey-vse-o-bespilotnom-proekte-kamaza-foto/>
- [4] Popova E.A. Using artificial intelligence in marketing // European science. 2017. №6 (28). URL: <https://cyberleninka.ru/article/n/using-artificial-intelligence-in-marketing>
- [5] How artificial intelligence works in a bank // Skolkovo. – 2020. – 17.10. – URL: <https://sk.ru/news/kakiskusstvennyy-intellekt-rabotaet-v-bankah/>
- [6] David R. Why artificial intelligence will create more jobs than it destroys // CMS Wire. – 2018. – 09.01. – URL: <https://www.cmswire.com/digital-workplace/why-artificial-intelligence-will-create-more-jobs-than-it-destroys/>
- [7] Automotive news // drom – 2019 – URL: <https://news.drom.ru/Tesla-Model-S-67468.html>
- [8] Artemenko, D., Aguzarova, F., Artemenko, G., Novoselov, K., Vertakova, Y. Media resources in education: The taxation aspect // Proceedings of the 33rd International Business Information Management Association Conference, IBIMA 2019: Education Excellence and Innovation Management through Vision 2020, 2019, pp. 4372–4376

[9] Toguzova, I. Z. Evaluation of the effectiveness of corporate governance of a company with state participation / I. Z. Toguzova, F. S. Aguzarova. – Moscow : Limited Liability Company "Prometheus Publishing House", 2022. – 200 p. – ISBN 978-5-00172-271-7. – EDN VKEYBX.

[10] Pytorch vs Tensorflow: A Head-to-Head Comparison URL: <https://viso.ai/deep-learning/pytorch-vs-tensorflow/>

[11] How will automation affect jobs, skills, and wages? // McKinsey Global Institute. – 2018. – URL: <https://www.mckinsey.com/featured-insights/future-of-work/how-will-automation-affect-jobs-skills-and-wages>

[12] Wladawsky-Berger I. The impact of artificial intelligence on the world economy // The Wall Street Journal. – 2018. – 16.11. – URL: <https://www.wsj.com/articles/the-impact-of-artificial-intelligence-on-the-world-economy-1542398991>

[13] Zelenkov, Mikhail & Laamarti, Yuliya & Ryabchikova, Lyubov & Sattorov, Shakhboz. // Credibility problem in the transport and logistics system of the Northern Sea Route and its solutions. Transportation Research Procedia. 63. 2251-2258. 10.1016/j.trpro.2022.06.255. – 2022.

[14] Ryazanov S.I. Artificial intelligence as a set – classification of artificial intelligences // In the collection: University science in modern conditions. Collection of materials of the 54th Scientific and Technical Conference: in 3 hours. Ulyanovsk, 2020. pp. 72-75.

THE ROLE OF THE HUMAN FACTOR IN THE MARKET ECONOMY

Albina Berkaeva¹, Irina Yablochnikova², Georgi Kutsuri³, Tengiz Tinikashvili³,
Ekaterina Stativa⁴

¹North-Ossetian State University named after Kosta Levanovich Khetagurov, Russia

²Moscow Technical University of communications and Informatics, Russia

³Financial University under the Government of the Russian Federation

⁴National Research Moscow State University of Civil Engineering, Russia

d-albina@yandex.ru

irayablochnikova@mail.ru

nimageo@mail.ru

Tengiz-05@mail.ru

stativa@yandex.ru

Abstract

One of the basic resources of economic growth is the human factor, the relevance of which in the modern economic system is actively increasing. This is primarily because every day many companies are becoming more and more aware of the importance of the considered category in any business for efficient and successful operation. Indeed, in the current realities, it is the human factor that is responsible for the well-being and success of enterprises due to the competence and professionalism of employees. In this regard, in our opinion, the main task of any management team is to find ways to manage the company's employees as efficiently as possible by creating favorable mutually beneficial conditions for both the labor power and the entire business as a whole.

Keywords: labor power, human factor, labor, market economy, information technologies

I. Introduction

Undoubtedly, everyone agrees with the thesis about the important role in the operation of any structure, regardless of the type of activity of the human factor. After all, it is people who are responsible for the effective functioning and prosperity of any sphere of activity.

It should also be noted that, despite the high introduction of information technology and the robotization of many production processes in the modern 21st century, the role of the human factor still does not lose its relevance, since any successful company will always need qualified employees who are interested in the success of the enterprise and strive to career growth.

But, as for any other economic category, the human factor has its own problems that affect the economic situation of any country. This phenomenon is, first of all, related to the fact that managing people is quite a labor-intensive process. And, in our opinion, almost every employer faces this phenomenon.

Accordingly, the main goal and task of the management is the organization process of such working conditions which maximally allow involving the category of employees who will have motives that ensure the economic growth of the company, thanks to their competence.[1]

Thus, we can confidently note the relevance of the topic of our study, regardless of the period of economic development, since knowledge of the concepts of rational human resource

management plays an important role both at the micro- and macro levels.

II. Methods

The fundamental goal of this article is studying the essence of the human factor, considering models for human resource management and identifying the problems of its application.

The object of our research is various processes that have both direct and indirect influence on the increase in the role and importance of the human factor in the development of civilization with a clear definition of the human role in the context of a changing economy.

And the subject of the research is the system of relations that regulate the human influence on the economic system.

In the process of carrying out scientific research, various generally accepted theoretical research methods were used as auxiliary tools for revealing the research topic.

The works of various domestic and foreign economists were used as a theoretical basis for writing this scientific article. In particular, we would like to note the works of Michael Armstrong and Olga Lapshova, who considered the practice of human resource management in their works.

Besides, various scientific articles in the periodical press and Internet resources covering the issues of the topic of our investigation were studied.

Thus, all the above information proves the relevance of the topic of our study. But, in addition, we would like to turn to some historical information in order to confirm the relevance of the human factor at all times.

So, considering the chronology, let's note that a great influence on human resource management was assigned to the last decades of the 20th century. This phenomenon, first of all, is due to the fact that the transition from the industrial era to the post-industrial system of the development of society took place exactly during this period.

Thus, this phenomenon has played a decisive role in the world view of people regarding the working population.

Since the role of a person began to be considered in the context of the intellectual capital of companies, much attention has been paid to the individual abilities of a person for self-development and improvement of his skills with the help of recent development and investments.

III. Results

So, what is the human factor? What role does this economic category play in the development of both an individual enterprise and the country as a whole? Does the economic growth of companies depend on the human factor? We will try to answer these questions to analyze the significance of this term at the current level of economic development.

Let's start with the fact that the role of the human factor is gaining more and more relevance every day in the context of rapidly developing market relations.

In our opinion, despite the progress in information technology, the role of a person still doesn't take a back seat, since people participate in the process of economic activity of organizations almost everywhere.

The problem of the human factor is exacerbated, first of all, due to the fact that human resource management is a rather labor-intensive process associated with difficulties in terms of subordinating individuals to the leadership.[2]

Great importance was attached to the human factor in the works of both domestic and foreign economists devoted to management in order to effectively manage the company's activities.

Firstly, we would like to start with the interpretation of the essence of this category.

What is meant by the term human factor? So, as a rule, this is the presence of certain knowledge and competence of a person in matters of labor with an emphasis on the continuous development and self-improvement of the existing skills to improve the management processes of

the company.

That is, for the successful functioning of any business, an important role is played by the presence of specialists in their profession who are able to competently perform the assigned tasks, assess all risks and make the most effective and rational decisions for the prosperity of the company.

In other words, specialists must be responsible and competent in their positions, have a sufficient store of information knowledge to achieve the goals and objectives and contribute to the success of the organization.

In our opinion, all the above is considered as the main components of the human factor in general.

Speaking of the human factor, various interconnected elements, having the character of moral, intellectual, professional, psychological and physical relations, immediately come to mind.

After all, it is no coincidence that the human factor includes the emotions and habits of people, their mood, hobbies, moral values and attitudes, communicative links both among themselves and in relation to the living environment, incentives and reasons for activity, etc.

It is obvious that a person participates in the entire cycle of production relations, from production to consumption, contributing the economic growth both at the micro- and macro levels.

We think that each of us is aware of the importance of the human factor. After all, the economic growth of any object of study directly depends on labor productivity and staff performance.

Without a high level of human potential, no state can function normally, because people are the driving force of progress, thanks to the use of their knowledge and creativity in solving certain issues.

We see that science doesn't stand still. And the 21st century is a clear confirmation of this idea with constant innovative developments and scientific progress in all major activities. For the most part, much attention is paid to the study of information technology.

Indeed, modern science, as part of its intensive development, is in an active search for highly qualified specialists for various solutions.

As practice shows, the increasing importance of computerization has led to the facilitation of the workflow both within the company and outside it, covering the global economy.

This is due to the fact that the modern age is characterized by a high degree of labor mobility in terms of flexible working hours and the ability to work from any part of the world.

Thus, the task of the workers is to participate in constant progress, because the 21st century does not allow any "stagnation" and is characterized by continuous development. Everything is changing so fast that the relevance of the many professions is reduced to zero.

In order to "survive" at the current level of economic development, a person needs constant improvement of his qualifications and, of course, self-development.

In other words, the existing knowledge has the character of "obsolescence", which confirms the above thought regarding the need for a stable improvement of work skills.

In general, from our perspective, people are the driving force of any process. After all, the success of any company with a sufficient level of competence of employees will depend on the human factor.

It is no coincidence that many successful organizations pay particular attention to the personnel selection, arranging various interviews in order to consider a person from different aspects, up to meeting family members.

This is, first of all, due to the fact that prosperous organizations understand that the success of their business directly depends on the labor power.

After all, no company needs a weak link. Specialists in their profession with ambition, responsibility, professionalism and competence in their position are everywhere in demand.

Based on the above, we would also like to add that in management processes, human activity is considered in two aspects: man-machine in the field of managing technical systems and man-man in socio-economic relations.

What is their difference? The answer is obvious. In the man-machine variant, the emphasis is placed on the control of complex technical equipment, while communication relations between individuals are studied in the second variant.

At the same time, the number of participants in both aspects can be different: from a few people to an unlimited number.

Thus, it turns out that great attention is paid to interpersonal relationships, and the technics serves as a tool that simplifies working processes of organizations.

It can be concluded that the economic growth of any country, first of all, depends on the human factor – people involved in production relations.

Due to the fact that there is a constant development of all processes in the world, this phenomenon is accompanied by an increase in the level of competition between organizations.

Accordingly, those companies that invest in the quality of both the product itself and the labor power (i.e. their competence) hold their leading position.

Undoubtedly, an important place in the work activity of employees, in addition to their material satisfaction, is occupied by spiritual satisfaction, which can be observed with a healthy relationship between employees and management, so that they feel their importance in the workplace.

After all, from a psychological point of view, employees are ready to pay the highest price for the moral satisfaction of the motives of their activities.

Accordingly, in our opinion, a successful leader is distinguished by the presence of knowledge not only in professional business management, but also in human relationships.

Thus, as we see, the role of personnel and the human factor itself is significant for any enterprise.

We'd like to summarize and note the main factors that, in our opinion, confirm this idea.

First of all, the decisive influence on the increase in the importance of the human factor occurred after scientific and technological progress.

At this stage of the economic development, human labor began to be considered for a different position: the physical emphasis of labor was redirected to the intellectual one. I.e., the requirements for workers have changed, which, in turn, changed their role in the production cycle.

In addition, as it was noted above, in the context of developing relations for the current century, the increase in the importance of the human factor was also significantly felt in terms of reducing control measures over personnel. This phenomenon is explained by the fact that for the 21st century the human labor factor is considered in the context of the absence of strict control over employees, but on the contrary, the labor power begins to actively participate in the strategic issues of enterprise development. That is, it turns out that for a modern person, work is considered from the point of view of a kind of creativity, with the help of which employees reach the solution of strategic goals and objectives with the help of their skills and abilities. So, the control of employees becomes secondary, because other people's thoughts and ideas are not subjected to control by anyone. Accordingly, for employers a decisive place is given to obtaining the results of the work of their employees, relying on their professional qualities, primarily in matters of creating a competitive environment among other companies.

Also, another factor that strengthens the role of the human factor at the current level of economic development is the regularly occurring changes in terms of people's preferences, increased competing, and, of course, a quick response to certain economic challenges.

This indicates that under the conditions of future changes on a global scale as well as at the level of individual enterprises, the labor power is required to constantly develop and improve the professional qualities for quick respond to the modern challenges of mankind and take measures for prompt decision and enhancing a business. It is no coincidence that from time eternal, we hear the phrase that the most profitable investments are investments in yourself. That is, in order to exist and climb the career ladder a modern person must pay greater attention to self-development.

Also, an important factor confirming the role of personnel is structural changes in the forms of work. After all, in addition to personal qualities in terms of being a qualified specialist, an

important place is given to the ability to be sociable, to solve controversial issues and be able to work in a team to achieve a common goal.

In the context of the realities of modern life, the increase in the culture of employees also “leave traces”, which is accompanied by the fact that the role of labor is changing from a simple source of existence to a source of self-expression.

That is, there is an excess of the importance of subjective factors over objective ones.

And finally, we should note that in the activity of any enterprise it is very important to have strong employees, on which the entire business reposes on. Although, as the saying goes, no man is indispensable, nevertheless, in our opinion, the resignation of a valuable employee can still worsen the state of the business.

That is why, as practice shows, successful enterprises always try to provide a respectable salary for the strong link of their companies, so that employees are motivated and bring only benefit to the company, applying their abilities in terms of making managerial decisions.

In addition, in the framework of the topic of our study, we considered such an important integrated indicator of the efficiency level of human resources use as the Human Development Index, which has the well-known abbreviation HDI. What does it represent?

So, the HDI is a generalized indicator that reflects information on the level of development of people around the world. This indicator is calculated by the UN and a group of independent experts. The Human Development Index has been widely used since 1990 and is still practiced nowadays. It was developed by Indian economist Amartya Sen and Pakistani economist Mahbub ul Haq. It serves as a comparative method for such indicators as life expectancy, literacy and education levels of people around the world. This index is necessary, first of all, to be able to classify countries into three groups: developed, developing and third world countries, as well as to identify the impact of economic policies of countries on the population quality of life. The Human Development Index is calculated as the geometric mean of three indices - income, education and life expectancy. The resulting value ranges from 0 to 1. Accordingly, the closer is the result to 1, the higher the level of human development of a certain country.

Based on this range, United Nations experts classify countries into the following groups: Very high HDI (from 0.8 to 1); High HDI (from 0.7 to 0.8); Average HDI (from 0.55 to 0.7); Low HDI (below 0.55).

For clarity, we would like to turn to Table 1, which contains the information on countries that occupy a leading place according to the Human Development Index.

Table 1: *Top 10 countries according to the Human Development Index based on the data for 2020*

№	Country	HDI
1.	Norway	0.954
2.	Switzerland	0.946
3.	Ireland	0.942
4.	Germany	0.939
5.	Hong Kong	0.939
6.	Iceland	0.938
7.	Australia	0.938
8.	Sweden	0.937
9.	Singapore	0.935
10.	Netherlands	0.933

Source: According to UN calculations

Thus, as we can see, based on the data in the Table for 2020, Norway occupies the leading place on a global scale, with a Human Development Index of 0.954

IV. Discussion

Undoubtedly, each of the proposed models has its own distinctive features. For example, speaking for the American model, let's note that it is characterized by individualism. There is also a certain balance between the theoretical material and the ability to apply it at a practical level. Besides, an important share is given to the qualitative characteristics of work performance and the inculcation in employees of a high level of personal responsibility for their actions.

As for the Japanese model, by contrast with the American one, a decisive place is given to group responsibility and collaborative spirit. That is, the employee works during the entire period in the certain organization and enjoys its benefits.

If we consider our domestic model, then the situation, in comparison with the two above models, is slightly different – ambiguous. Indeed, at the current level of economic development, there are significant problems of a socio-economic nature; there are difficulties in matters relating to the employment of university graduates; there is a high level of the turnover of staff and other problems that require prompt decision, primarily, at the legislative level.

Accordingly, we can conclude that the Russian economy needs to strengthen its skills in human resource management, based on the effectiveness of the American and Japanese models.

In our country, it is necessary to provide conditions to consider the interests of the working population and to provide a decent standard of living for them. Thus, we examined the importance of the human factor at the current level of economic development and revealed the relevance of the research topic.

References

- [1] Armstrong M. Human Resource Management Practice / Michael Armstrong, Stephen Taylor. – 14 ed. – St. Petersburg: Piter, Progress book, 2018. – 1038 p.
- [2] Gasanova A.A. Human resources management in the managerial system of the organization / A.A. Gasanova // Innovative science. – 2019. – No. 11. – pp. 50-53.
- [3] Gorina M.S. Enterprise personnel management and methods for evaluating its effectiveness // Modern Economy Success. – 2019. – No. 3. – pp. 15-22.
- [4] Dessler G. Human resource management / G. Dessler; edited by I.M. Stepnov; translated by D.P. Kon'kov. – Fourth edition. – Moscow: Knowledge laboratory, 2020. – 800 p.
- [5] Durakova I.B. Human resources management in Russia: concepts of the new normal. Book 8: monograph – M.: INFRA-M, 2021. – 248 p.
- [6] Klimov, N.A. Strategic personnel management in organizations / N.A. Klimov, L.L. Chirkova // International journal of applied sciences and technologies "Integral". 2019. - No. 2. - pp. 54-59.
- [7] Lapshova O.A. Human resources management: textbook and practical course for universities; under the general editorship of O.A. Lapshova. – Moscow: Publishing URAIT, 2020. – 406 p.
- [8] Makarov S.O. The war and we. Human factor. Book 1 / S.O. Makarov. – M.: Library of the newspaper `Duel`, 2020. - 286 p.
- [9] Malkova T.B. Human resources management in the digital economy: textbook. / T.B. Malkova. - Moscow: KnoRus, 2020. – 232 p.
- [10] Kuptsov, M.I., Yablochnikova, I.O., Yablochnikov, S.L., Dzobelova, V.B. & Mineev, V.I. (2020). Modeling Internet Business Optimization Processes, 2020 International Conference on Engineering Management of Communication and Technology (EMCTECH), Vienna, Austria, 2020, pp. 1-5, doi: 10.1109/EMCTECH49634.2020.9261507.

THE MAIN TRENDS IN THE LABOUR MARKET DEVELOPMENT IN THE CONTEXT OF THE ECONOMY DIGITALIZATION

Valentina Dzobelova¹, Sergey Bakunin², Vitaly Lukinov³, Viktoria Erofeeva⁴

¹North-Ossetian State University named after Kosta Khetagurov, Russia

²Ryazan State University named after S.A.Yesenin, Russia

³NRU Moscow State University of Civil Engineering, Russia

⁴Moscow Technical University of communications and Informatics, Russia

dzobelova@mail.ru

sergeybak@mail.ru

lukinovVA@mgsu.ru

erofeeva-viktori@mail.ru

Abstract

The article considers the influence of the digital economy development on the labour market, identifying its main advantages and disadvantages. The increase in the unemployment rate due to the disappearance of a number of obsolete professions, that have lost their relevance in the context of modern developing relations, can be attributed to the fundamental negative factors of the labour market digitalization. In addition, after analyzing the opinions of various domestic and foreign experts, it is concluded that it is impossible until 2030 to completely replace human labour with robotics, despite the rapid development of information and communication technologies.

Keywords: ICT, trends, digitalization, digital economy, labour market, robotics, Industry 4.0

I. Introduction

The transformation of the labour market due to the digitalization of the economic system plays a very important role at the current level of economic development and is studied by many both domestic and foreign scientists and experts.

Digitalization did not originate immediately and has a sequence of stages that played an important role in the formation of a particular technological order.

As you know, the fifth technological order includes such key components as information and knowledge, which serve as the main factors of production.

In addition, the importance of innovative technologies is considered by both domestic and foreign economists, who highlight their impact on all spheres of society.

After all, there is a process of the fastest possible spread of digital technologies, services, online platforms for labour relations, which changes the previously formed traditional type of society.

All this, in turn, is accompanied by an increase in labour productivity indicators, an increase in wages of certain professions, and an improvement in the welfare of society.

Accordingly, new vacancies are being created, but at the same time, professions that are already irrelevant in this era, are disappearing.

That is, thanks to the processes of digitalization, the population gets the opportunity to acquire new knowledge with an increase in their level of competence.

But, as we understand, as any other social phenomenon, the economy digitalization has both

positive and negative sides.

The negative side, first of all, is the reduction in the number of jobs that have lost their relevance.

II. Methods

The aim of our work is to study the main trends in the labour market development in the context of the economy digitalization.

The object of our research is the labour market.

And the subject is the consideration of the positive and negative aspects of the labour market digitalization.

Various textbooks, manuals of foreign and domestic economists, data from mass media, Internet resources, as well as articles devoted to the topic of our research were used as sources of information.

As for the methodology of the research, we would like to note that both theoretical and empirical and mathematical research methods were used, in particular, the method of problematic and structural analysis and synthesis, as well as comparison method.

Undoubtedly, the topic of our research is quite relevant both now and in the near future, since digitalization processes serve as a new era and are being rapidly implemented around the world.

III. Results

Thus, technological orders smoothly flow into the industrial revolution, known as the Fourth Industrial Revolution, or as it is also called – Industry 4.0.

In general, many researchers call this era the new industrial age, during which artificial intelligence, robotics, 3D printing, etc. appeared.

Undoubtedly, at the current level of economic development, almost all spheres of society feel certain transformations inherent in the digital economy through various innovative challenges.

One of these factors is the challenges covering Industry 4.0 on labour issues.

The essence of this trend is that due to the economy digitalization many professions simply disappear from the labour market, but at the same time a number of other professions are being created, which, in turn, need appropriate personnel with such skills.

But, for modern society, there are certain difficulties regarding the issues of forecasting the digital economy development, which is primarily due to the fact that this area is quite extensive, and full forecasting of the future for 100% is practically impossible.

Also, we'd like to consider the essence of the impact of robotization of the labour market on the decline in the level of jobs on a global scale.

As practice shows, there is an increase in the number of robots in the industrial and other sectors of the economy.

The result of these actions is an increase in labour productivity, the formation of new jobs, followed by the reduction or complete destruction of those areas that are no longer relevant in the digital economy.

According to the viewpoints of many scientists, there is also an opinion that there is a high probability of human labour displacement in 20 years due to a robotic attack.

There is also an opinion about the disappearance of those professions that contain a template structure of work to be performed.

The category of such persons includes, for example, the category of production managers, technical staff, accountants, auditors, cashiers, etc.

Accordingly, based on certain information regarding the further development of robotization and automation of production processes, one can judge the further development or disappearance of various professions.

It should be noted that, according to a number of experts, in the near future, the professions that will be at risk of disappearance will be:

- Drivers who will be replaced by vehicles with drones, which will significantly reduce the share of drivers;
- Service workers who will be replaced by robots engaged in household chores, office work, up to robotic guards and others.

All these phenomena will play a significant role in the quantity of supply and demand in the sectors of social workers and office services.

That is, in other words, in any areas affected by robotics, there will be significant shifts in the supply and demand curves that change the structure of the market.

Thus, we would like to refer to Fig.1, which clearly illustrates, on a global scale, the exposure of certain countries, which, first of all, are dependent on the risks of automation and robotization of labour markets.

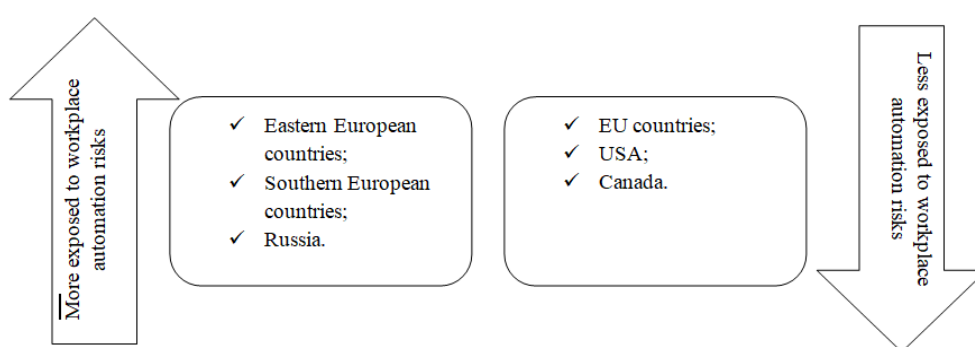


Fig. 1: Assessment of the exposure of various labour markets to workplace automation according to 2021 data

Also, having considered the level of robotization around the world, we'd like to note such a comparative analysis of the indicators of other countries with Russia.

As practice for the development of robotization in the Russian Federation shows, the situation here is not positive enough, since the level of this indicator is not high enough.

This is primarily evidenced by the indicators for the introduction of robotics around the world, exceeding the value of 2 million, while in Russia their total number is about 5 thousand.

It turns out that on a global scale 10 000 workers are replaced by 113 robots, and in Russia only by 5 robots.

At the same time, significant shifts in the Russian economy in matters of robotics have been carried out since 2018.

For clarity, we would like to refer to the diagram below (Fig.2), which shows the number of installed robots on a global scale compared to Russia.

IV. Discussion

Thus, after analyzing all of the above, we can conclude that the development of automation processes plays a decisive role to a greater extent for countries with a high unemployment rate, followed by a low level of employment among the population.

Therefore, the task of the relevant structural units becomes control and readiness for risks that have an automated nature of origin.

In our opinion, a strong impact of the economy digitalization on the labour market can be observed not only in a global scale, but also in relation to a specific category of the labour power.

To prove our point of view, we would like to give, as an example, various scenarios for the manifestation of the digitalization of the labour power in the transport sector.

Let's consider, as the first situation, the presence of an average level of independence and average skills of the staff. Here there is a limited range of automated means of transport, accompanied by the preservation of workplaces due to the inexpedience of their robotization.

That is, it is very important to correctly calculate the expedience of using automation, as, for example, loading operations that are carried out outside the enterprise, of course, can be automated, but it must be taken into account that these actions in the conditions of the organization in a metropolis are far from budgetary and not expedient.

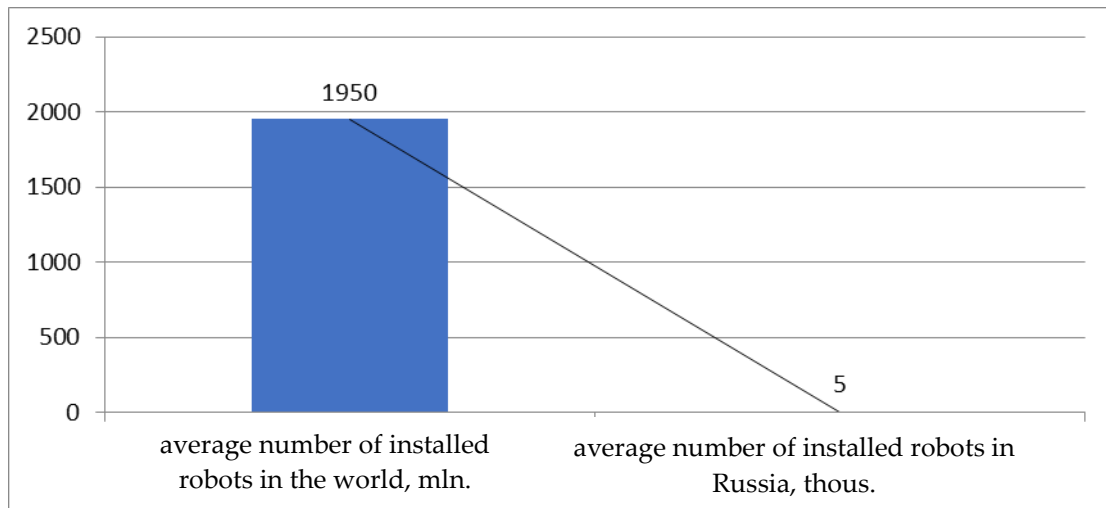


Fig. 2: Number of installed robots around the world and in Russia

Also, we would like to refer to Fig. 3, which lists countries with a total number of robots that replace 10 000 workplaces, according to data for 2020.

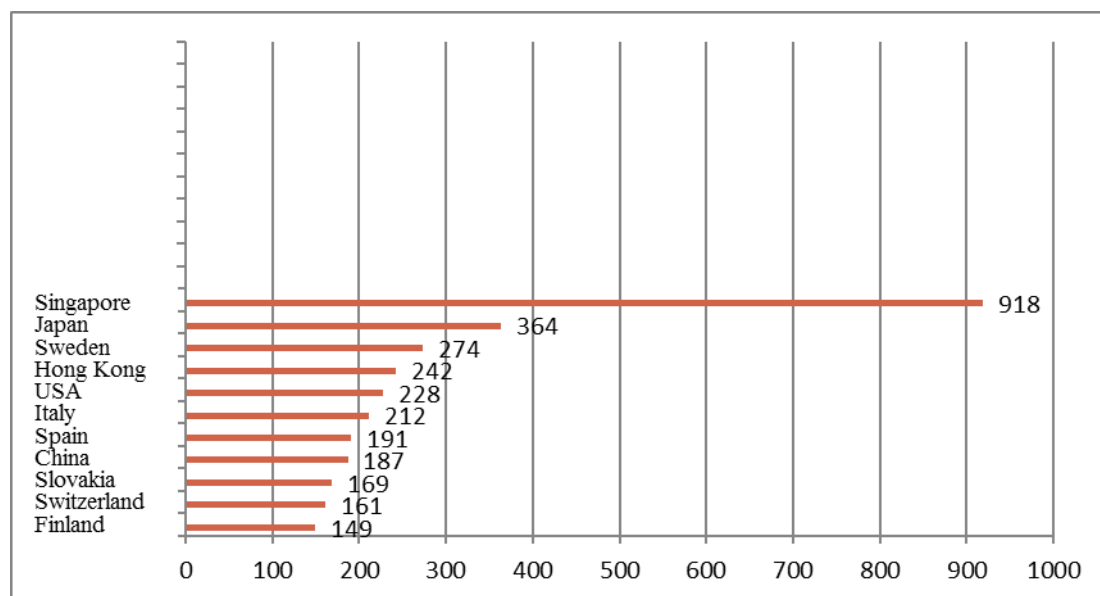


Fig. 3: Number of robots installed per 10 000 workplaces globally, according to 2020 data

The situation is different in case of high level of independence and low qualification of staff, since the staff does not have all the necessary skills to solve the tasks. Then robots, the work of which will largely reduce production costs and increase the labour productivity, are already coming to help.

Accordingly, one can note the important role and impact of the economy digitalization on the labour market, which changes the supply and demand for labour power.

Due to the creation and implementation of new technologies, an economic growth on a global scale and an increase in labour productivity occur.

In our opinion, one of such challenges for modern society was the emergence of computers, which greatly facilitated the work of people, becoming an auxiliary tool. But, at that time, the computer did not replace the work of a person then, but only helped him for further development and improvement of his qualifications.

Now, the situation is a little different. Because in the modern digital economy human labour, both physical and mental, is being replaced by robots.

V. Conclusion

Thus, according to a number of experts, in the process of the economy digitalization in matters of the labour market transformation, there will be an increase in conflicts both between labour and capital, and between employees of different age groups.

Based on the analysis of the McKinsey Global Institute, which has been researching business and economics on a global scale since 1990, it was noted that by 2030 there will be an increase in the gross income of labour automation productivity from 0.3 to 2.2%.

In addition, it is noted that, despite the rapid development of the digital economy, there will not yet be a complete replacement of human labour with robots.

Also, according to the McKinsey Institute research, it is noted that more than 60% of professions can be automated, but at the moment only 3% of professions are subject to full automation.

Thus, regarding to the automation of the labour market, as we see, there are opposing views.

This is evidenced by various seminars and webinars organized in 2020 by the European Trade Union Institute (ETUI), lawyers from ELW Network, ELDH, as well as the European Trade Union Confederation (ETUC).

According to the above organizations, the task of labour legislation is to directly protect the interests of the working population in case of worsening of their labour conditions caused by the economy digitalization.

Thus, we have revealed the topic of our study and analyzed the views of various experts on the transformation of the labour market under the condition of digital economy, and we can note that the introduction of information and communication technologies in the digital economy plays a very important role in the global development of the economic system and labour market.

References

[1] Adams A. Technology and the labour market: the assessment // Oxford Review of Economic Policy. – 2018. – № 3. – p. 349-361. – doi: 10.1093/oxrep/gry010.

[2] Afonasova M.A. System transformation and blockchain technology in the field of public administration // Proceedings of the XXII International Scientific and Practical Conference "System Analysis in Design and Management" (SAEC-2018). St. Petersburg: Publishing House of Polytechnic University, 2018. pp. 315-319.

[3] Belozarov S.A. "Digital economy as a factor in the development of the insurance market" 2018, International Economic Symposium-2018: Proceedings of the V International Scientific and Practical Conference "Sustainable Development: Society and Economy". April 19-21, 2018 - St. Petersburg: Publishing House of St. Petersburg State University, 2018. pp. 23-27.

[4] Bulanov V.S. Methodological issues of the labour market research / V.S. Bulanov // Society and Economics. – 2019. – 210 p.

[5] Cortes M., Salvatori A. Delving into the demand side: Changes in workplace specialization

and job polarization // *Labour Economics*. – 2018. – p. 164-176.

[6] Dengler K., Matthes B. The impacts of digital transformation on the labour market: Substitution potentials of occupations in Germany // *Technological Forecasting and Social Change*. – 2018. – p. 304-316. – doi: 10.1016/j.techfore.2018.09.024.

[7] Filippova I.A. Development of the digital economy in Russia [Electronic resource] / I.A. Filippova, D.D. Nezvanov // *Bulletin of USTU*. – 2018. – No.3

[8] Ognivtsev S.B. The concept of a digital platform for the agro-industrial complex // *IJAS*. 2018. No.2. – pp.16-22.

[9] Panov A.M. Unstable employment: conceptual ideas and assessment criteria / A.M. Panov // *Territorial development issues*. 2019. No.3 (33). p. 10.

[10] Kuptsov, M.I., Yablochnikova, I.O., Yablochnikov, S.L., Dzobelova, V.B. & Mineev, V.I. (2020). Modeling Internet Business Optimization Processes, 2020 International Conference on Engineering Management of Communication and Technology (EMCTECH), Vienna, Austria, 2020, pp. 1-5, doi: 10.1109/EMCTECH49634.2020.9261507.

OPTIMIZATION OF THE COMPOSITION OF SPARE PARTS FOR THE AGING TYPE OBJECTS

Aleksandr Antonov, Aleksandr Murkin

•

Rosatom Technical Academy, Russia
antonov@iate.obninsk.ru

Abstract

In the field of the Russian Federation nuclear power facilities operation, special attention is paid to ensuring the safety of nuclear power plants and improving their economic efficiency. The development and implementation of methods for the optimal organization of the NPP operation is carried out. To solve these tasks, the application of the methodology of "reliability-centered maintenance" and "risk-oriented maintenance" is carried out at NPP power units. The implementation of these methodologies involves the operational reliability of equipment analysis and, based on the results of the analysis, planning of preventive maintenance and optimization of spare parts sets. The solution of these tasks is complicated by the fact that a significant part of the equipment has large operating time, and is on the verge of running out of resources. The paper solves the problem of optimizing the composition of spare parts for objects of aging type. A model for calculating the profit from the operation of equipment with spare elements is proposed. The Kijima-Sumita model is used as a model to describe the process of exhaustion of the object's operability. The developed model is investigated on simulation data.

Keywords: preventive maintenance, risk-based maintenance, objects of aging type, inventory management model, Kijima-Sumita model, distribution density, average profit

I. Introduction

The nuclear power industry of the Russian Federation is currently on the rise. New facilities are being built both in Russia and abroad. New Russian-designed nuclear power plants (NPP) are being commissioned in Belarus, China, India, Turkey and other countries. In the Russian Federation, power plants of the VVER-1200 project have been commissioned at the Leningrad and Novovoronezh nuclear power plants, and a number of other facilities are under construction.

Special attention is paid to ensuring safe operation and increasing the economic efficiency of previously commissioned nuclear power facilities. In this regard, the issues of optimal operation organization of the nuclear power plants are being solved. Modern methods of organizing and conducting scheduled preventive maintenance of equipment are being introduced. Thus, the methodology of "reliability-centered maintenance" and "risk-oriented maintenance" is being implemented at NPP power units.

The Risk-based Maintenance (RBM) is a maintenance strategy based on the equipment failure risk analysis, taking into account the predicted losses and their significance for achieving the established indicators of the efficiency of electricity production based on an assessment of the current equipment's technical condition [1].

The Risk-based approach is aimed at optimizing the processes of operation and maintenance, as well as the process of managing the equipment's operability [2].

The purpose of applying the risk-based maintenance and repair strategy (MRS) is to reduce operating (operational and repair) expenses while unconditionally complying with the safety requirements of the NPP.

The main objective of the risk-based maintenance strategy is to optimize the MRS of equipment by selecting the most effective processes aimed at ensuring the safety and reliability of the operation of the NPP, upon condition that the associated costs are minimized.

The method of monitoring the technical condition and maintenance of equipment based on risk assessment is aimed at:

- ensuring control and maintenance of equipment;
- coverage of inspections and maintenance of all types of equipment;
- taking into account the technical and organizational aspects of planning control measures and maintenance;
- implementation of asset management related to inspections, maintenance and service life assessment for equipment;
- stock management and optimization of the composition of spare parts and devices for the entire range of equipment.

The formation, storage, use, replenishment and accounting of an irreducible stock of equipment, components, spare parts and materials for the repair and operational needs of nuclear power plants is one of the important tasks of MRS management.

The issues of determining the optimal composition of spare parts, as well as calculating the reliability characteristics of systems, taking into account spare elements, were considered in the works of both Russian and foreign authors.

Thus, in [3], the problem of optimizing the composition of spare elements is solved, taking into account the complex strategy of their functioning, assuming that the failed product is being repaired. In the papers [4, 5], the solution of the problem of optimizing the composition of spare parts is presented in the presence of restrictions on the cost of acquisition, delivery and storage of spare elements. In the publications [6, 7], dynamic models of managing the composition of spare elements at the enterprise are considered. In articles [8, 9], the problem of optimizing a set of spare elements is solved, taking into account the depletion of a part of the resource by these elements. Based on the methods of restoration theory, the issue of calculating the reliability characteristics of the system is considered, in the case when spare elements can be in cold, hot and spinning reserve. In [10], the problem of optimizing a set of spare parts for elements of an aging type is considered, taking into account restrictions on the cost of spare elements. Based on the methods of the restoration theory, the readiness coefficient of the system, which includes elements of the aging type, is obtained. In [11, 12], the task of calculating the reliability characteristics of systems whose elements, in case of failure, are replaced by workable objects from the spare parts, and the failed element is restored by the repair team and further replenishes the spare parts. These works take into account the aging of objects during operation. Geometric processes are used as a model that takes into account the aging of elements.

In the papers [13, 14], the issues of the formation of the composition of spare parts for objects with two types of failures are considered. The first type of failure leads the object to an inoperable maintainable condition. The second type of failures is more catastrophic, leads the object to an inoperable non-repairable state. In the first type of failure, an inoperable, but maintainable object is replaced with a workable one from the spare parts. The inoperable unit is transferred to the repair authority for restoration. In the second type of failure, a workable unit from a spare parts kit is installed in place of the failed object, and an inoperable and non-repairable unit is sent to an industrial enterprise in accordance with the established procedure for repair.

And finally, we note the fundamental work [15], which on the one hand provides a fairly detailed analysis of publications on the topic of calculating the reliability of systems taking into account spare parts, calculations of the required number of spare parts, and on the other hand describes various models for calculating reliability indicators taking into account spare parts, including in conditions of periodic and continuous replenishment stocks in the spare parts kit, with periodic replenishment of stocks with emergency deliveries, the issues of optimizing the spare parts kit are considered.

II. Stock management model for aging type objects

Let's consider a model of inventory management at a nuclear power industry enterprise.

The operation of the power unit is designed for a long service life. The considered service life is divided into n equal intervals of duration Δ . Let's assume that the parameter A denotes profit from the operation of equipment per unit of time, and B – losses from equipment downtime in case of a shortage of spare parts. At the beginning of each step in the system the orders are made of an arbitrary number of spare parts $l \geq 0$ with a total cost of cl . These l sets of spare parts are added to the amount that could have remained unused in the previous steps.

Let L_j – number of spare parts ordered at the beginning of the j -th step ($j = 1, \dots, n$), δ_j – is the duration of the system operation at the j -th step, τ_j – duration of the system downtime at the j -th step.

The task is to determine the optimal procedure that maximizes the average profit of the enterprise

$$M[\sum_{j=1}^n (A\delta_j - B\tau_j - cL_j)] \rightarrow \max \quad (1)$$

Tasks of this type were considered in [16].

Consider a random failure process formed by the moments of failures: $\tau_1 = \xi_1; \tau_2 = \xi_1 + \xi_2; \tau_k = \sum_{i=1}^k \xi_i$, where ξ_i is the duration of the system operation between the $(i - 1)$ -th and i -th failures.

Let y denote the number of spare parts sets available in stock, before ordering a new set of spare parts is planned, through $V_n(y)$ – denote the average profit in the n -step process. The duration of one step is equal to Δ , the duration of the step has the dimensionality of time.

Suppose that at the beginning of each step, $t \geq 0$ units of spare elements will be ordered, the number of observed failures is $N(\Delta) = x$. If $x \leq y + l$, then the profit at this step will be $A\Delta$, the number of spare elements decreases to $y + l - x$ and the average profit from following the optimal procedure at the remaining $n - 1$ steps is $V_{n-1}(y + l - x)$. If $x > y + l$, then the profit is $A\tau_{y+l+1} - B(\Delta - \tau_{y+l+1})$, the stock level is reduced to zero, and the average profit on the remaining $n - 1$ steps is $V_{n-1}(0) - d(x - y - l)$, where d the cost of a set of spare parts purchased in an extreme situation.

Thus, the average profit at step n is equal to:

$$V_n(y) = \sup_{l \geq 0} \left\{ \int_0^{y+l} [A\Delta + V_{n-1}(y + l - x)] f_{N(\Delta)}(x) dx + \int_0^\Delta [A\tau - B(\Delta - \tau)] g_{\tau_{y+l+1}}(\tau) d\tau + \int_{y+l}^\infty [V_{n-1}(0) - d(x - y - l)] f_{N(\Delta)}(x) dx - cl \right\}, \quad (2)$$

where $f_{N(\Delta)}(x)$ – is the generalized density distribution of the value x , g_{τ_k} – is the generalized density function of the moment of the k -th failure.

If ξ_1, ξ_2, \dots – are independent identically distributed random variables having an exponential distribution law with intensity λ , then $f_{N(\Delta)}(x) = \frac{(\lambda\Delta)^x}{x!} e^{-\lambda\Delta}$ – is Poisson's law, and $g_{\tau_k}(\tau) = \frac{\lambda^k \tau^{k-1}}{\Gamma(k)} e^{-\lambda\tau}$ – is the gamma distribution. This type of distribution reflects the case when a new spare set is installed in place of the failed element. The described model is presented in [6].

Note that most of the approaches presented in the literature to optimize the composition of spare elements are based on the assumption that the failed element is replaced by an identical new object.

However, it should be said that a number of NPP power units that are in operation have been operating for a long time (70% of Russian NPP power units are operating in the operation life extension mode). The equipment operating as part of these power units is exposed to internal and external factors, which leads to a gradual loss of their operability. In other words, the effects of

aging are observed in the operation of the equipment. In this regard, the reliability of the equipment is reduced, this may lead to the fact that failures may occur more often than it was at the initial stage of operation. As a result, there is a need to re-evaluate the composition of spare parts and devices.

Let's consider an approach to optimizing the composition of spare parts for objects of an aging type. To account for the effects of aging in the operation of equipment, we will use the Kijima-Sumita models [17]. Let's outline the main points of these models. The Kijima-Sumita models use the concepts of the real and virtual age of the object.

For the case of instant recovery, the real age of the element at the time of the n -th failure is represented as the sum of its developments:

$$S_n = \sum_{i=1}^n X_i, S_0 = 0,$$

where X_i – is the i -th operating time to failure.

For the models, a constant value q is introduced – the recovery coefficient. Certain function $v = v(\{X\}, q)$, where $\{X\}$ is a sample of operating time to failure, determines the virtual age of the element. Let v_{i-1} – be the virtual age of the element at the time of the $(i - 1)$ - th restoration. Then X_i as the following conditional distribution function [18]:

$$F_i(x|v_{i-1}) = \frac{F_i(x + v_{i-1}) - F_i(v_{i-1})}{1 - F_i(v_{i-1})},$$

from where we can find the probability of trouble-free operation:

$$P_i(x|v_{i-1}) = \frac{P_i(x + v_{i-1})}{P_i(v_{i-1})}.$$

Here $F(x)$ – is the operating time to-first-failure distribution function for a completely new element.

There are 2 Kijima models. The feature the Kijima-1 model is that the n -th recovery affects only the damage received by the element between the $(n-1)$ -th and the n -th failure, reducing the increase in the virtual age of the element from X_i to qX_i . The virtual age of the element after the n -th restoration is written as follows:

$$v_n = v_{n-1} + qX_n = q \sum_{i=1}^n X_i = qS_n; v_0 = 0.$$

According to the Kijima-2 model, each recovery affects the total damage, reducing the total virtual age:

$$v_n = qv_{n-1} + qX_n = q(q^{n-1}X_1 + q^{n-2}X_2 + \dots + X_n); v_0 = 0.$$

In this paper, we will consider the first Kijima model.

In case of incomplete recovery according to the Kijima-Sumita model, the leading flow function looks like this:

$$\Omega(t) = \int_0^t (g(\tau|0) + \int_0^\tau \omega(x)g(\tau - x|x)dx)d\tau ,$$

where:

$$g(\tau|x) = \frac{f(t+qx)}{1-F(qx)}; \omega(t) = \frac{d\Omega(t)}{dt}; f(t) = \frac{dF(t)}{dt}.$$

Here $\omega(t)$ – is the failure flow parameter.

Let's define the generalized distribution density $f_{N(\Delta)}(x)$. For the generalized density of the failures number distribution, the following equality holds:

$$f_{N(\Delta)}(x) = P(N(\Delta) = x),$$

where $N(\Delta)$ - is the number of flow points on an interval of length Δ , i.e. $\xi[t, t + \Delta]$ for any t , hence:

$$P(N(\Delta) = x) = P(\tau_x \leq \Delta \leq \tau_{x+1}) = F_{\tau_x}(\Delta) - F_{\tau_{x+1}}(\Delta),$$

where $F_{\tau_k}(\Delta)$ – is the distribution function of the time moment of the k -th failure. For the distribution function of the time moment of the k -th failure, the expression representing the convolution is valid:

$$F_k(x) = F(x) * F_{k-1}(x),$$

The generalized density of the distribution of the moment of time of the k -th failure $g_{\tau_k}(\tau)$ is obtained by taking the derivative of the higher statement.

Let's perform the calculations of the resulting model on conditional data. In [19], a variety of models for describing the time-to-failure distribution functions of the aging type objects of are considered. Let's take as a function of the time distribution one of the widely used distributions with a linear intensity function, which has the following form:

$$F(x) = 1 - e^{-\lambda_1 x - \frac{\lambda_2 x^2}{2}}.$$

The conditional distribution function, respectively, will be written as:

$$F_i(x|v_{i-1}) = \frac{F_i(x + v_{i-1}) - F_i(v_{i-1})}{1 - F_i(v_{i-1})}.$$

Then the distribution function of the moment of time of k -th failure will be represented as follows:

$$F_{x_i}(x) = \frac{1 - e^{-\lambda_1(x+v_{i-1}) - \frac{\lambda_2(x+v_{i-1})^2}{2}} - 1 + e^{-\lambda_1 v_{i-1} - \frac{\lambda_2 v_{i-1}^2}{2}}}{e^{-\lambda_1 v_{i-1} - \frac{\lambda_2 v_{i-1}^2}{2}}} = 1 - e^{-x(\lambda_1 + \frac{\lambda_2 x}{2} + \lambda_2 v_{i-1})}.$$

To obtain a generalized distribution density, it is necessary to take the derivative:

$$f_{x_i}(x) = F'_{x_i}(x) = (\lambda_1 + \lambda_2 x + \lambda_2 v_{i-1}) e^{-x(\lambda_1 + \frac{\lambda_2 x}{2} + \lambda_2 v_{i-1})}.$$

Thus, we obtained the necessary formulas to represent the average profit (2) in the formula.

III. Model research

The study of the model will be provided for the following data.
 Let the service life of the power unit be 30 years of operation,
 the number of steps of the process $n = 10$;
 the time interval after which the spare parts are replenished $\Delta = 3$;
 the economic effect of a timely replacement $A = 10$;
 losses from equipment downtime in case of shortage of spare parts $B = 15$;
 the cost of a spare parts set $c = 8$;
 the cost of a spare parts elements purchased in an extreme situation is $d = 10$.
 Statistics on failures of the research object are presented in the table, which shows the number of the object failures that took place at consecutive intervals of operation equal to three years.

Table 1: Statistical information on object failures during its operation

j	1	2	3	4	5	6	7	8	9	10
n_j	2	16	7	11	21	5	5	4	2	2

This statistical information was processed by nonparametric estimation methods, namely Kernel density estimation. By omitting the results of intermediate calculations, here is a table that presents data characterizing the optimal strategy for replenishing a set of spare elements.

Table 2: *Optimal strategy for replenishing a set of spare parts*

<i>j</i>	1	2	3	4	5	6	7	8	9	10
<i>l + y</i>	12	11	10	10	9	7	7	6	5	3

Thus, a model for optimizing the composition of spare elements for a system that has been in operation for a long time is considered. The effects of aging begin to affect the operation of the system equipment. The reliability characteristics of the system elements deteriorate over time, as the process of damage accumulation due to the influence of external and internal factors affects. The Kijima-1 model was used as a model for accounting the aging effect. As a function of the distribution of operating time to the first failure, the linear failure rate function is selected. The calculation results showed that for the given failure statistics and the selected model parameters, the optimal replenishment strategy is a decreasing function. This suggests that when the equipment is functioning at the intervals of replenishment of the spare parts, there is no complete consumption of a spare parts set. Thus, the remainder of the elements from the previous period is added to the ordered batch of spare elements.

References

- [1] IEC 60300-3-11: 2009 (NEQ), Reliability in technology. Reliability management. Reliability centered maintenance. –M.; Standardinform. 2014. -39 p.
- [2] GOST R 55234.3 2013, Practical aspects of risk management. Risk-based inspection and maintenance procedures for equipment.. M.; Standartinform, 2014. -56 p.
- [3] Antonov A.V., Plyaskin A.V., Chepurko V.A. Optimization of the number of spare items of equipment important for NPP safety / Quality management methods, №8, Standarty and kachestvo, 2001.-p.27-31.
- [4] Antonov A.V., Plyaskin A.V. Determination of the optimal number of spare elements of the system, taking into account cost constraints// Dependability.– 2003. - №4. - p.9-16.
- [5] Antonov A.V., Plyaskin A.V., Tataev H.N. Optimization of the composition of spare parts for NPP power units by the method of nonlinear programming. Review of Applied and Industrial Mathematics. V. 18. Release 1. 2011. – p. 100-101.
- [6] Chepurko V.A., Unshchikov A.P. About one dynamic model of inventory management in the enterprise// Dependability.– 2009. - №4. - p.22-28.
- [7] Chepurko V.A., Unshchikov A.P. The study of dynamic models of stock management in the enterprise// Dependability.– 2010. - №3. - p.40-47.
- [8] Antonov A.V., Plyaskin A.V., Tataev H.N. On the issue of optimizing a set of spare parts, taking into account the partial depletion of their resource// Modern problems of science and education. – 2012. – № 1;
- [9] Antonov A.V., Plyaskin A.V., Tataev H.N. Improving the quality of functioning of control systems by optimizing the composition of spare elements// Quality, innovation, education, 2012, №7, p. 51-56.
- [10] Antonov A.V., Plyaskin A.V., Tataev H.N. Optimization of the composition of spare parts of NPP power units, taking into account the partial depletion of their resource// Nuclear physics and engineering, 2012, book 3, № 5, p.408-415.

- [11] Antonov A.V., Plyaskin A.V., Tataev H.N. On the issue of calculating the reliability of redundant structures, taking into account the aging of elements// Dependability. №1 (44)-2013, p. 55-61.
- [12] Antonov, A. Plyaskin and Kh. Tataev. Calculation of the Redundant Structure Reliability for Aging type Elements, -p. 383-390./ In book: Statistical Models and Methods for Reliability and Survival Analysis, Wiley-ISTE, Nov. 2013, 416 p.
- [13] Antonov A.V., Chepurko V.A. On the issue of calculating the composition of spare elements with failures of two types// Dependability, №3, 2022. – p.
- [14] Antonov A.V., Chepurko V.A. About one problem of calculation of a set of spare elements having failures of two types // Dependability, V. 23, №2, 2023, - p. 39-48.
- [15] Cherkesov G.N. System Reliability Assessment Taking into Account Spare Parts: - SPb.: BHV-Peterburg, 2012. – 480 p.: + CD-ROM.
- [16] M. De Groot. Optimal Statistical Solutions.- M.:Mir, 1974.- 496 p.
- [17] Kijima M. A Useful Generalization of Renewal Theory: Counting Process Governed by Non-negative Markovian Increment / M. Kijima, N. Sumita // Journal of Applied Probability, 1986 – №23 – P.71-88.
- [18] Beichelt F. Zuverlässigkeit und Instandhaltung. Mathematische Methoden// F. Beichelt, P. Franken. – VEB Verlag Technik, Berlin, 1988. – 357p.
- [19] Antonov A. V. Theory of reliability. Statistical Models / A.V. Antonov, M.S. Nikulin, A.M. Nikulin, V.A. Chepurko// – M.: INFRA-M, 2015– 576 p.

TECHNOLOGIES OF INFORMATION SUPPORT OF TERRITORIAL SAFETY MANAGEMENT

Valeriy Nicheporchuk^{1,2}, Ulyana Postnikova^{2,3}

¹Institute of Computational Modelling SB RAS, Russia

²Federal Research Center for Information and Computational Technologies, Russia

³Siberian Federal University, Russia

ulyana-ivanova@inbox.ru

Abstract

The paper presents approaches aimed at solving the problems of territorial administration related to: limited availability of integrated monitoring data, the impossibility of reproducing risk calculations by independent groups of researchers; the general nature of recommendations on the composition and scope of preventive measures, formed based on the results of risk calculations and not taking into account the specifics of S-N-T systems; lack of indicators for assessing the impact on safety of the implemented preventive measures; lack of scientific substantiation of management processes, the absence of generally accepted models for forecasting the security of territories for a long-term period, which allow more systematic planning of strategic activities.

Keywords: social-natural-technogenic system, safety, territorial management

I. Introduction

Information support for the management of natural and technogenic safety is based on the results of a comprehensive monitoring of the environment state, control of technosphere objects. The assessment of territorial risks includes data on the characteristics of protected objects and sociosphere indicators [1, 2]. In recent years, the term social-natural-technogenic (S-N-T) system has been widely used to designate the object of safety research, which implies consideration of three areas and their interaction [3]. Since there is no established definition of an S-N-T system, the following formulation is used in this paper. S-N-T system - a separate territory, allocated according to administrative, geographical, economic and other characteristics, consisting of many heterogeneous elements, the dynamics of which can be determined by a system of hierarchically organized indicators that describe the normal and extreme states of the elements and are used to assess risks. On the basis of risk assessment, preventive measures are implemented to ensure the safety of the S-N-T system, and the compliance of risk values with acceptable levels is a necessary condition for the sustainable development of the S-N-T system.

From this follow the tasks of collecting and processing complex monitoring data and their application in managing the security of complex systems. For an objective assessment of territorial data, it is necessary to integrate a large amount of multi-format interdisciplinary data, most of which has signs of subjectivity. This applies to expert assessments used to bring heterogeneous data to a single measurement scale, estimates of the scale and damage from emergency situations

(ES) and other dangerous events [4]. Even data on losses are subjective, since there are no uniform criteria for classifying people as injured and dead in emergencies, and the accounting criteria change periodically. Establishing and continuing to use data collection and processing standards enhances the credibility of risk assessments, which is critical to preventive action decisions.

From the point of view of a systematic approach, the digitalization of the sphere of ensuring the security of territories, information support for management is a closed cycle. Its main elements - the collection of data on the state and characteristics of S-N-T systems, the calculation of risks, the justification and control of risk management measures, the assessment of the effect - are logically linked using analytical and situational models. In practice, most of the work is limited to the collection of fragmentary monitoring data with subsequent calculation and visualization of territorial risks [5]. The resulting risk cartograms illustrating the isotropic distribution of hazards within administrative boundaries are far from reality.

The predominance of subjective factors in the management of emergency situations, the implementation of measures to improve the safety of the population and territories in comparison with the amount of funds spent does not give the expected effect. Reasons for this situation:

- limited availability of integrated monitoring data, the impossibility of reproducing risk calculations by independent groups of researchers;
- the general nature of recommendations on the composition and scope of preventive measures, formed based on the results of risk calculations and not taking into account the specifics of S-N-T systems;
- lack of indicators for assessing the impact on safety of the implemented preventive measures;
- lack of scientific substantiation of management processes, the absence of generally accepted models for forecasting the security of territories for a long-term period, which allow more systematic planning of strategic activities [6].

The paper presents approaches to solving these problems.

II. Problems of using monitoring data to support the management of the territory's safety

The course towards digitalization of management, which is being implemented at the federal and regional levels, has significantly changed the practice of developing and operating software systems for processing monitoring data to support management. Centralization of all developments in several systems (Risk Atlas of the Ministry of Emergency Situations of Russia, Hardware and Software Complex "Safe City", etc.) reduced the possibility of integrating third-party services. Changes in legislation require obtaining the status of state for information systems of territorial administration. This is a serious obstacle to the introduction of the developments of the institutes of the Russian Academy of Sciences into the practice of managing the safety of S-N-T systems. The results of risk assessment presented in the form of geoportals, scientific publications are "taken into account", which has little effect on the effectiveness of risk mitigation measures. At the same time, the functionality of state information systems is aimed at collecting a large amount of information, developing dynamic visualization tools without linking with the needs of the subject area.

There is a need to integrate information resources into the federal data and knowledge repository. This will allow:

- to develop independent services for deep processing of monitoring data;
- verify prognostic models of territorial security dynamics;
- reproduce risk assessments by independent research teams;
- replicate the best management practices, taking into account the peculiarities of S-N-T systems.

The structure and functionality of the data and knowledge storage are described in different detail: the conceptual level is a system model, then the levels of architecture, functional diagrams explaining it, describing the processes of collecting, exchanging, storing and transforming information resources into management decisions.

III. System model of management information support

A systematic consideration of the tasks of information support for the management of territories is a multi-stage process of identifying elements of a complex system, followed by their detailing of elements and a description of logical connections. In this case, different design methods, rules and restrictions are used.

To describe the business processes of preparing management decisions, the information resources associated with them, the functions and technologies for their transformation, a model was developed to support the management of natural and technogenic safety [7]. Syntactically, the management information support model is represented by a tuple:

$$M = \langle T, L, R, IT, F, Y \rangle \quad (1)$$

where T – control tasks; L is the set of decision makers taking into account their interaction and powers; R - information resources; F – information processing functions; IT – information technologies; Y - representations of the results of the systems and services.

Three key management tasks $T = \{t_1, t_2, t_3\}$ have been identified: t_1 - identifying and responding to situations that require management actions (everyday management); t_2 - response to emergency situations of a critical and dangerous nature (operational management); t_3 - response to assessments of the state of territories (strategic management). From the L elements, a situational control graph is built, most of the vertices of which are decision makers with certain powers, responsibilities, and available resources. Data $R = O_1 \cup O_2 \cup O_3 \cup E \cup Des$, where O_1 is a set of factors for the implementation of events E ; O_2 - protected objects that change their characteristics and functioning as a result of management actions; O_3 - forces and means necessary for the implementation of management decisions; Des is a formalized description of solutions.

The set of functions F of control support systems: $F = \{f_1, f_2, f_3\}$, where f_1 is the collection, updating and provision of access to data; f_2 - computational and analytical modeling of the current situations and their dynamics modeling; f_3 - synthesis of solutions. A variety of tasks of information support for management T leads to the need to use various information technologies, the number of which, due to the rapid development, is difficult to determine. Focusing on the functions F , we can group them by $IT = \{it_1, it_2, it_3\}$, where it_1 are data acquisition and storage technologies; it_2 - data analysis technologies, it_3 – intellectual technologies. Semantically, information support Y is the result of solving problems T using information resources R and information technologies IT that implement functions F . The implementations of functions f_{ij} for control problems t_i are presented in Table 1.

Information representations of the results of the systems Y include texts, tables; maps and graphics. Their detail depends on T and L . Common The BI-platform contains dozens of tools for displaying analysis results [8]. Ready-made solutions can be represented as a set of logically connected tuples:

$$Des_i = \langle ID, Place, Period, O_3, Action \rangle, \quad (2)$$

where $Action$ is an event from the list of possible ones; $Place$ - venue; $Period$ – work schedule, O_3 , - control objects - actors; ID - identifier of the solution fragment for positioning it in the general

process of actions performed sequentially or in parallel. This simplified form is used to record most of the decisions of the territorial commissions for emergency situations and fire safety.

Table 1: Transformation of functions depending on management goals

$F \backslash T$	Identification of hazards t_1	Prompt response t_2	Strategic planning t_3
Data collection and updating f_1	f_{11} – getting monitoring data	f_{12} – input of initial data for modeling	f_{13} – obtaining additional data for safety assessment and management
Modeling f_2	f_{21} – monitoring the output of parameters beyond the standard values forecasting	f_{22} – assessing the dynamics and consequences of events	f_{23} – assessment of the security status of territories
Synthesis of solutions f_3	f_{31} – formation of solutions for the transfer to high availability modes	f_{32} – formation of recommendations for taking emergency measures	f_{33} – formation of recommendations for conducting long-term activities

Modernization of the record of decisions should be carried out taking into account the balance: on the one hand, this will allow taking into account the peculiarities of management in difficult situations, on the other hand, the complication of the forms of collection is accompanied by an increase in erroneous and unreliable information.

IV. Directions for improving the monitoring of the territory's safety

Fundamentally, the processes for solving territorial management problems have not changed since the pre-computer era. The key factor in operational decision-making is the speed of information transfer and processing, and the key factor in strategic management is the volume and quality of data. The purpose of integrated monitoring is to integrate different systems for observing the state of the environment, monitoring the functioning of technosphere objects, collecting data on events that have occurred, updating the characteristics of objects and infrastructure of territories, followed by the transformation of data into elements of management decisions. The specificity of the subject area implies the presence of a large number of hard-to-measure and probabilistic factors, the mutual influence of which can only be assessed by experts. The expansion of the scope of neural networks for test generation makes it relevant to create training samples of real solutions to various control problems [9].

The requirements for the composition of primary data and the content of the results of their processing are shown in Table 2.

They reflect the composition of the elements of the set R . In this form, the requirements for integrated monitoring data are presented for the first time. For example, the use of only event registers (clause 8) for assessing territorial risks does not remove the uncertainty of decision-making, and the joint analysis of E , O_2 , O_3 makes it possible to form constructive recommendations for t_3 .

Obtaining data on the characteristics of protected O_2 objects, collected in the form of safety data sheets for territories, is possible only through intersystem exchange. Currently, the enormous costs of duty shift operators for updating information do not increase its reliability. Decision makers under time pressure are forced to double-check the data on the consequences of the emergency situation and the forecast of the situation from alternative sources

Table 2: *Distribution of types of integrated monitoring data depending on management tasks*

№	Primary data	Content of processing results	Task
1	Sensor readings	Assessment of the probability of manifestation of hazard factors O_1	t_3
2	Characteristics of protected objects O_2	Assessment of the consequences of the situation, justification of the scope of protection measures	t_2
3		Integral vulnerability indicator	t_3
4	Characteristics of management objects O_3	Assessment of resource costs for emergency response and protection measures	t_2
5		Integral security indicator [3]	t_3
6	Event Registry	Emergency response solutions	t_2
7		The values of dangerous factors-triggers for the implementation of situations	t_3
8	Register of preventive measures carried out	Solutions for strategic security management of S-N-T systems	t_3
9	Expert assessments	Bringing different indicators to a single scale for an integrated assessment of territorial risks	t_3

The use of the federal register of preventive measures (clause 8) in solving task t_3 will make it possible to replicate positive risk management practices. The availability of expert assessments (clause 9) will give impetus to the development of research on their refinement and replacement with multi-criteria analysis of big data. The priority of solving problem t_1 is early warning about threats and dangers [9]. Despite the large number of publications in the field of disaster forecasting, the practice of their application is limited to local models of the dynamics of a specific hazard indicator for a short period. The creation of federal cloud services should provide, in addition to organizing interdepartmental information exchange, the integration of methods for processing monitoring data.

Structural schemes for presenting complex monitoring data are described in detail in [10]. Standardization of data collection and storage processes will help to avoid wrong decisions when creating a single information space for ensuring territorial security. The process of developing services to support the management and interaction of researchers and structures that ensure the security of S-N-T systems is shown in Fig.1.

V. Conclusion

Assessing and managing the risks of S-N-T systems are among the complex unprecedented problems, the concentration of knowledge, the need to assimilate diverse information for decision-making. The practice of creating large systems developed for a long time does not work in modern conditions. Adaptive, easily customizable applications focused on the accumulation and reuse of intellectual capital are needed.

Approaches to system design, reformatting of complex monitoring, introduction of compact representations of objects and processes are essential elements of information support for management and interaction tasks. The rapid introduction of technologies into practice is hampered by administrative barriers, a weak interconnection between the digitalization of management and training of specialists. Methods for deep formalization of data, tools for accessing information resources with multi-stage control of their relevance and reliability were tested in pilot projects.

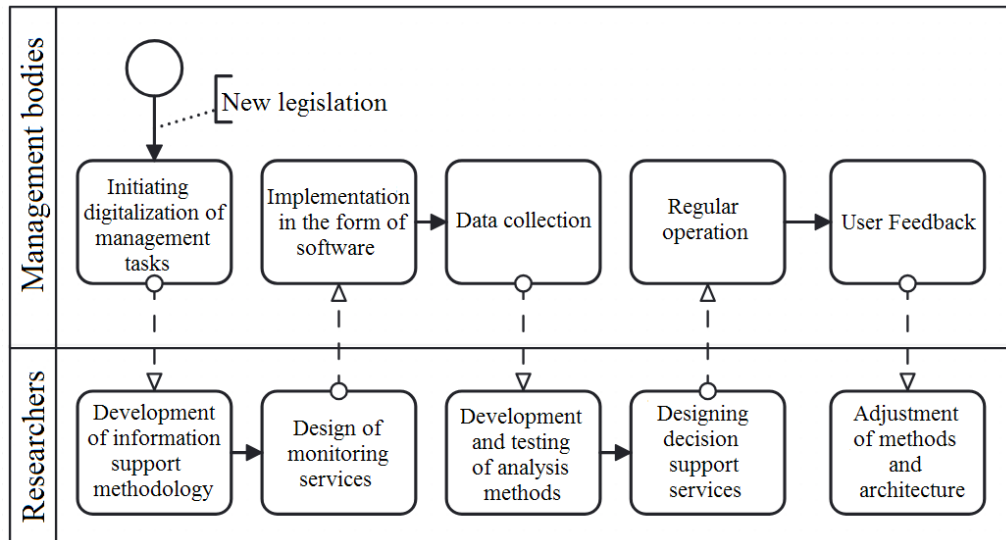


Fig. 1: A fragment of the life cycle of information management monitoring systems

The transformation of the monitoring system requires additional resources to collect and process new data. The release of time for the collection of constructive information at the local level of government is possible due to the systematization of business models of information support for the activities of emergency services. When organizing operational work, one should follow the rule: if the incoming information is not used directly for decision-making, then it is stored in a formalized form that allows one to extract knowledge, or it is ignored. The harmonious use of departmental control systems in combination with common information resources will minimize management errors in complex situations caused by the human factor.

Acknowledgements. The research was carried out within the state assignment of Ministry of Science and Higher Education of the Russian Federation for Federal Research Center for Information and Computational Technologies (№ 122010800027-7).

References

- [1] Moskvichev V.V., Bychkov, I.V., Potapov V. P., Taseiko O.V., Shokin Yu. I. Information system for territorial risk management development and safety. Herald of the Russian Academy of Sciences. 2017; № 8: 696-705. DOI: 10.7868/S0869587317080035.
- [2] Moskvichev V., Postnikova U., Taseiko, O. Information system for monitoring and managing the risks of development of Siberia and the Arctic regions. Reliability: Theory and Applications. Special Issue № 4 (70). 2022. Vol. 17. P. 124–131.
- [3] Makhutov N.A. Safety and risks: system research and development. Novosibirsk: Nauka, 2017. – 724 p.
- [4] Nicheporchuk V. V., Penkova T. G. Comprehensive analysis of territorial risk factors forestimating and managing thenatural and technogenic safety. Issues of risk analysis. 2019; Vol 16; No 14: P. 52-62. DOI: 10.32686/1812-5220-2019-16-4-0-0
- [5] . Atlas of natural and man-made hazards and emergency risks: scientific ed. M.: Feoria: Joint Edition of the Ministry of Emergency Situations, 2011. 652 p.
- [6]. Kalach A.V., Nicheporchuk V.V. Penkova T.G., Arifulin E.Z. Modern risk management mechanisms of socio-natural and technogenic systems / Proceedings of the International Conference "Actual problems of applied mathematics, computer science and mechanics" - Voronezh: Publishing House "Scientific research publications". 2023. P. 1537-1542.
- [7]. Nicheporchuk V.V., Nozhenkov A.I. Architecture of the territorial system of emergency monitoring. Informatization and communication. 2018. №2. P. 35-41.

[8]. Gromov S.L. Investigation of Gromov's BI-circle. M., 2022. 362 p.

[9] Nicheporchuk V.V. Method of using hazard criteria for identifying hazardous situations // CEUR Workshop Proceedings (CEUR-WS.org) Vol. 2534. ISSN 1613-0073. Proceedings of the All-Russian Conference "Spatial Data Processing for Monitoring of Natural and Anthropogenic Processes" (SDM-2019) p. 427-433.

[10] Nicheporchuk V.V. Resources and technologies of regional information and analytical systems of natural and technogenic safety // Dissertation of the Doctor of Technical Sciences. - Novosibirsk, 2022. 300 p.

EVALUATION OF THE INFLUENCE OF LONGITUDINAL OSCILLATIONS ON DYNAMIC RESISTANCE OF NON-UNIFORM CORES

Asim Imamaliyev

•

Yildiz Technical University, Istanbul, Turkey

a.imamaliyev@mail.ru

Abstract

Mechanical systems, the calculation of vibrations of which is the content of many practical problems, are mostly complex elastic systems. At the same time, many structural elements can be represented by a combination of different rods; therefore, in various fields of modern technology, it is necessary to solve the problems of oscillations of complex rod systems, including those in a collision with an obstacle.

The relevance of the problem of calculating the vibrations of complex rod systems is due to the practical need to improve the technical characteristics of the designed machines and mechanisms and ensure their functioning under ever wider ranges of operational impacts, as well as to reduce the material consumption of machines and structures. To fully determine the strains and stresses that occur at any point in the system during vibrations, it is necessary to know the displacements at these points. This leads to the need to consider systems with an infinite number of degrees of freedom.

Keywords: heterogeneity, oscillations, instability, core, deflection

I. Introduction

The practical needs of calculating the dynamic characteristics of various machine-building and other structures have led to the complication of design schemes. In many cases, the study of oscillations of complex rod systems with an infinite number of degrees of freedom is associated with great difficulties. In some cases, the possibility of a mathematical interpretation of the problem of vibrations becomes feasible only if certain simplifications are introduced into the calculation. The problem of non-uniform cores taking into account mutual influence of longitudinal and cross-section oscillations is investigated and solved. The decision is carried out in the assumption that the core is made of elastic continuously non-uniform material and the module of elasticity depends on the average module of elasticity, parameter of heterogeneity and length of a core.

II. Methods

The problem of dynamic stability of inhomogeneous rods is considered taking into account the mutual influence of longitudinal and transverse vibrations.

Let us assume that the rod is made of an elastic continuously inhomogeneous material, and the modulus of elasticity changes according to the following law

$$E = E_0 \left(1 + \alpha \frac{\chi}{l} \right),$$

where E_0 - is the average modulus of elasticity, α - is the inhomogeneity parameter, l - is the rod length.

Let v - deflection, u - longitudinal displacement of the rod section. Then the total longitudinal displacement, up to second-order values, is determined by the formula:

$$W = u + \frac{1}{2} \int_0^{\chi} \left(\frac{dv}{d\xi} \right)^2 d\xi \quad (1)$$

The longitudinal force in any section will be

$$N = P_0 + P_t \cos \theta - \int_x^l m \frac{d^2W}{dt^2} d\xi \quad (2)$$

On the other hand, there is:

$$\frac{du}{d\chi} = \frac{N}{E_0 F \left(1 + \alpha \frac{\chi}{l} \right)} \quad (3)$$

where F - is the cross-sectional area of the rod.

III. Results

From relations (1)-(3) after some transformations we obtain

$$\begin{aligned} E_0 F \left(1 + \alpha \frac{\chi}{l} \right) \frac{d^2u}{d\chi^2} + \frac{E_0 F \alpha}{l} \frac{du}{d\chi} - m \frac{d^2u}{dt^2} = \\ = m \int_0^{\chi} \left[\frac{dv}{d\xi} \cdot \frac{d^3v}{d\xi dt^2} + \left(\frac{d^2v}{d\xi dt} \right)^2 \right] d\xi \end{aligned} \quad (4)$$

The bending equation of the considered rod is obtained in the following form

$$\begin{aligned} E_0 I \left(1 + \alpha \frac{\chi}{l} \right) \frac{d^4v}{d\chi^4} + 2 E_0 I \frac{\alpha}{l} \frac{d^3v}{d\chi^3} + E_0 I \left(1 + \alpha \frac{\chi}{l} \right) \times \\ \times \left(\frac{du}{d\chi} \cdot \frac{d^2v}{d\chi^2} + \frac{dv}{d\chi} \cdot \frac{d^2u}{d\chi^2} \right) + E_0 F \frac{\alpha}{l} \frac{du}{d\chi} \cdot \frac{dv}{d\chi} + m \frac{d^2v}{dt^2} = 0 \end{aligned} \quad (5)$$

The boundary conditions for $u(x, t)$ will have the form

$$u(x, t) = 0, \quad E_0 F (1 + \alpha) \frac{du(l, t)}{d\chi} = P_0 + P_t \cdot \cos \theta t \quad (6)$$

The joint solution of system (4), (5) is associated with great difficulties. Let us consider the case when undamped transverse oscillations occur. In this case, the nonlinear terms on the right side of equation (4) can be neglected. Then equation (4) contains only $u(x, t)$ and it is resolved independently of equation (5). The solution of equation (4) is represented as

$$u = A \cdot \sin v x \cdot \cos \theta t \quad (7)$$

where indicated

$$A = \frac{P_t}{v E_0 F (1 + \alpha) \cos v l}, \quad v^2 = \frac{m}{E_0 F} \cdot \theta^2 \quad (8)$$

IV. Discussion

As can be seen from (8), at $\cos \nu l = 0$ the amplitude of the longitudinal oscillations goes to infinity. This corresponds to the resonance of longitudinal vibrations. In this case, resonance with respect to the lowest natural frequency occurs at

$$\omega_i = \frac{\pi}{2l} \sqrt{\frac{E_0 F}{m}} \quad (9)$$

We represent the deflection in the following form

$$\upsilon(\chi, t) = f(t) \cdot \sin \frac{\pi \chi}{l} \quad (10)$$

Taking into account (7), (10) from (5) using the Bubnov-Galerkin method, we find

$$\frac{d^2 f}{dt^2} + \Omega_1^2 [1 - 2 \mu_1 \cdot \psi_1 \cdot \cos \theta t] f = 0 \quad (11)$$

where

$$\mu_1 = \frac{P_t}{2P_{\text{кр}}^*}, \quad P_{\text{кр}}^* = \frac{\pi^2}{l^2} E_0 I \left(1 + \frac{\alpha}{2}\right), \quad (12)$$

$$\Omega_1^2 = \frac{\pi^4}{l^4} \frac{E_0 I}{m} \left(1 + \frac{\alpha}{2}\right),$$

$$\psi_1 = \frac{l^2}{\pi^2 (1 + \alpha)} \cdot \frac{1}{\cos \nu l} \cdot \frac{2}{l} \left[\frac{\pi^2}{l^2} \left(a_0 + \frac{\alpha}{l} a_1 \right) + \right.$$

$$\left. + \nu \frac{\pi}{l} \left(a_2 + \frac{\alpha}{l} a_3 \right) + \frac{\alpha \pi}{l l} a_4 \right]$$

The following notations are introduced in these formulas:

$$a_0 = \int_0^l \cos \nu \chi \cdot \sin^2 \frac{\pi \chi}{l} d\chi,$$

$$a_1 = \int_0^l \chi \cos \nu \chi \cdot \sin^2 \frac{\pi \chi}{l} d\chi,$$

$$a_2 = \frac{1}{2} \int_0^l \sin \nu \chi \cdot \sin \frac{2\pi \chi}{l} d\chi, \quad (13)$$

$$a_3 = \frac{1}{2} \int_0^l \chi \sin \nu \chi \cdot \sin \frac{2\pi \chi}{l} d\chi,$$

$$a_4 = \frac{1}{2} \int_0^l \cos \nu \chi \cdot \sin \frac{2\pi \chi}{l} d\chi.$$

It should be noted that the solution of equation (11) is constructed similarly to [1]. The analysis shows that the boundary of the main region of instability in the first approximation is determined from the condition

$$1 \pm \frac{\mu_1}{1 - \frac{\theta^2}{\omega_L^2}} - \frac{\theta^2}{4\Omega_1^2} = 0 \quad (14)$$

Let us transform equation (14) to the form:

$$1 \pm \frac{\mu_1}{1 - \beta_1 n_1^2} - n_1^2 = 0 \quad (15)$$

$$\mu_1 = \frac{\mu}{1 + \alpha/2}, \quad n_1 = \frac{n}{1 + \alpha/2}, \quad \beta_1 = \beta \left(1 + \frac{\alpha}{2} \right), \quad (16)$$

$$n = \frac{\theta}{2\Omega_1}, \quad \beta = \frac{4\Omega_1^2}{\omega_L^2}$$

Taking into account (15), (16), an asymptotic analysis is carried out and the region of dynamic instability is constructed.

Note that for, the obtained solution coincides with the known classical solutions [1].

In this case, from (12), (13) we find:

$$\mu_1 = \mu, \quad \Omega_1 = \Omega,$$

$$\Psi_1 = \frac{\operatorname{tg} \nu l}{\nu l} \cdot \frac{1 - \frac{\nu^2 l^2}{2\pi^2}}{1 - \frac{\nu^2 l^2}{4\pi^2}} \quad (17)$$

References

- [1] Bolotin, V.V. (1956). Dynamic stability of elastic systems. M., 600 p.
- [2] Lomakin, V.A. (1976). Theory of elasticity of inhomogeneous bodies. M., Publishing House of Moscow State University, 376 p.
- [3] Volmir, A.S. (1967). Stability of deformable systems. M., Nauka, 984 p.
- [4] Alimov, O.D. (1985). Propagation of strain waves in shock systems. - M.: Nauka, - 354 p.
- [5] Bityurin, A.A. (2005). Simulation of the longitudinal impact of homogeneous rods with non-retaining bonds. // Bulletin of UIGTU. - № 3. - p. 23-25.
- [6] Panovko, Ya.G. (1987). Stability and oscillations of elastic systems / Ya.G. Panovko, I.I. Gubanov. -M.: Nauka, -352 p.
- [7] Timoshenko, S.P. (1974). Stability of rods, plates and shells. // M.: Nauka, - 808 p.
- [8] Bityurin, A.A. (2009). Longitudinal impact of an inhomogeneous rod on a rigid barrier.// Ulyanovsk: Publishing House of UIGTU, - 164 p.
- [9] Sankin, Yu. N. (2001). Longitudinal vibrations of elastic rods of step-variable cross-section colliding with rigid obstacle. Appl. Maths Mechs, Vol. 65, № 3, pp. 427-433.
- [10] Sankin, Yu. N. (2010). Nonstationary Oscillations of Rod Systems in Collision with an Obstacle. - Ulyanovsk: UIGTU, - 174 p.
- [11] Majorana, C.E., Pomaro, B. (2011), "Dynamic stability of an elastic beam with visco-elastic translational androtational supports", Engineering Computations, Vol.28, Iss.2, pp.114–129.
- [12] Mohanty, S.C. (2005), "Dynamic stability of beams under parametric excitation", PhD thesis, Department of Mechanical Engineering, National Institute of Technology, Rourkela.
- [13] Sochacki, W. (2008), "The dynamic stability of a simply supported beam with additional discretelements", Journal of Sound and Vibration, Vol. 314, pp. 180.

ESG - CRITERIA AT THE PRESENT STAGE OF SOCIETY DEVELOPMENT

Alisa Olisaeva¹, Marina Galazova¹, Leyla Magomayeva², Anastasia Ledovskaya³

¹North-Ossetian State University named after K.L.Khetagurov, Russia

²Millionschikov Grozny State Oil Technical University, Russia

³Stavropol Branch of the Russian Academy of National Economy and Public Administration

alisa.olisaeva@mail.ru

galazovam@mail.ru

rumanovna@gmail.com

an.led@mail.ru

Abstract

Modern society is developing in the direction of redistributing capital flows as part of the global trend towards decarbonization, developing environmental standards and increasing the social responsibility of business and the economy as a whole. Investors are actively increasing their investments in companies that support sustainable development strategies, as changes related to ESG principles are taking place around the world and are seen by most participants as a promising opportunity for development and revenue generation. The current challenge facing society and business is to study the ESG agenda, implement it into operations and develop appropriate recommendations to promote ESG principles to improve the environment and well-being of the global community. In order to address inequality and stimulate economic growth, the UN adopted the 2030 Agenda for Sustainable Development in 2015 and launched a plan to ensure sustainability for present and future generations, reduce poverty and improve the lives of people around the world. Governments and business communities in various countries are realizing the adverse impacts of climate change, which affects the well-being and economic status of the nation, and building a more sustainable global economy contributes to reducing greenhouse gas emissions that cause climate change. Priority tasks of the global community are multifunctionality and demand for the development and implementation of specific mechanisms for achieving sustainable development goals based on the integrated solution of economic, environmental and social problems and harmonization of long-term interests of the state, business and civil society.

Keywords: ESG criteria, sustainable development, companies.

I. Introduction

Sustainable development and combating climate change are interlinked, and both are vital to the well-being of humanity, as reflected in the Sustainable Development Goals (SDGs). The UN has been working on sustainable development, addressing social and environmental issues for decades.

In 1987, Chairman Gro Hrlm Brundtland introduced the concept of sustainable development in the report "Our Common Future" prepared by the International Commission on Environment and Development (ICED), stating that "the environment does not exist in isolation from human activities, needs and desires. Decisions on the future modes and paths of economic development of the industrialised countries, given their economic and political power, will have a very significant impact on the ability of the entire world population, of all future generations, to

achieve progressive sustainable development. What is needed now is a new era of economic growth - growth that is significant and at the same time socially and environmentally sustainable."

A significant impact on the formation of sustainable development and its implementation in modern life was made by the decision of the 2nd UN World Conference on the creation of the Declaration on Environment and Development (Rio de Janeiro, 1992), which introduces a program of action aimed at the implementation by national governments of the concept of global sustainable development, and the term "sustainable development" is widely recognized and is a direction of action for the implementation by national governments of the concept of global sustainable development [1]. Since the adoption of the Declaration, national governments have adopted and implemented programs and regulations to implement global sustainable development, which is still relevant today. We are now witnessing the emergence of an integrated approach to achieving global sustainable development, by bringing together the three important pillars of sustainable growth, which have an impact on economic and social progress, both nationally and internationally.

II. Methods

The evolution of sustainable development has led to the introduction of ESG concept including Environmental (environmental impact), Social (personnel and local communities), Governance (information disclosure and management) which are referred to as ESG criteria.

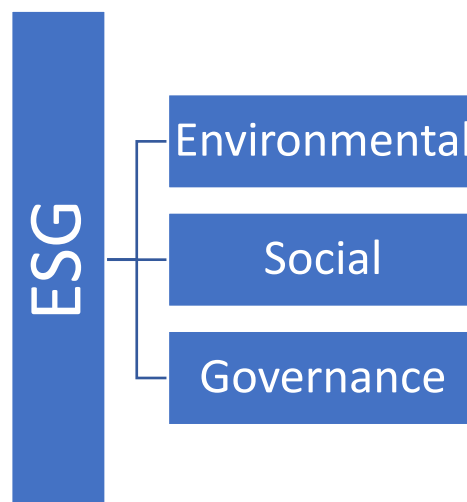


Fig. 1: ESG criteria

The report of the International Commission on Environment and Development (ICED) reflects throughout the document the idea that economic growth relies heavily on natural resources and that the driving force behind economic growth is new technology, which, while offering the potential to slow down the dangerously fast pace of exploitation of finite resources, poses a great risk of new life forms that could change the direction of evolution [2]. There is a clear call for national governments, companies and industries most dependent on natural resources, and indeed all of humanity, to adhere to the ESG principles.

In September 2015, 17 Global Sustainable Development Goals were agreed by the UN General Assembly and adopted by all UN Member States to protect the planet, eradicate poverty, improve the quality of life and prospects for people around the world in parallel with increasing economic growth [3].

States at the national level had to revise and adopt new priorities for the SDGs, meet targets for saving the environment, increasing the social responsibility of businesses. Today it is the

culture of life of society, state and business. The importance of ESG should be considered on the same level with such concepts as: democracy, human rights, market economy and others.

We also see a growing role for independent assessment through ESG rating and company ranking, screening services, indices, and climate impact assessment tools. ESG rating allows investors and counterparties to determine the company's level of responsibility, as well as environmental, social and governance risks arising from interaction with the company. The current economic situation contributes to the fact that companies are focusing on the social agenda for objective reasons. At the same time, environmental issues remain relevant for business, which is due, firstly, to the tightening legislation in the field of environmental protection, and secondly, to the possibility of obtaining economic benefits from the introduction of "green" technologies and environmental initiatives.

Companies that have already started the process of implementing sustainable development practices into their business strategies, including localization of production and creation of sustainable supply chains, are in the most advantageous position.

Information on the company's contribution to the green economy allows investors, stakeholders and organizations to more carefully select business entities for long-term investments, which contributes to a higher rating of the company when evaluating non-financial statements. If the familiar financial reporting of companies is added by non-financial reporting, it gives international business ratings even more thoroughness, which in turn entails new conditions for borrowing, access to capital, development and prosperity.

For example, the European Securities and Markets Association's (ESMA) Sustainable Finance Roadmap 2022-2024 reflects the priority areas for sustainable finance and the transition to a green and sustainable economy for the European Union (EU) [4].

Directive 2014/95/EC of the European Parliament and of the Council on improving the consistency and comparability of non-financial information disclosed throughout the EC states that large undertakings which are public-interest entities exceeding on their balance sheet dates the criterion of the average number of 500 employees during the financial year shall include in the management report a non-financial statement containing information to the extent necessary for an understanding of the undertaking's development, performance, position and impact of its activity, relating to, as a minimum, environmental, social and employee matters, respect for human rights, anti-corruption and bribery matters. Companies should include in the relevant entity's management report a description of the policies, outcomes and risks associated with ESG governance issues [5].

III. Results

In early 2005, UN Secretary-General Kofi Annan invited a group of the world's largest institutional investors to join the process of developing the Principles for Responsible Investment. The group of 20 investors from institutions in 12 countries was supported by a panel of 70 experts from the investment industry, intergovernmental organizations and civil society.

Figure 1 shows that in 2006 only 63 financial institutions signed the declaration on implementation of the 6 principles developed as Principles for responsible investment (PRI), and by 2021 3826 financial institutions have already signed the declaration [6]. This indicates a demand from market participants to invest in the green economy, and investors are focused on ESG ratings [7].

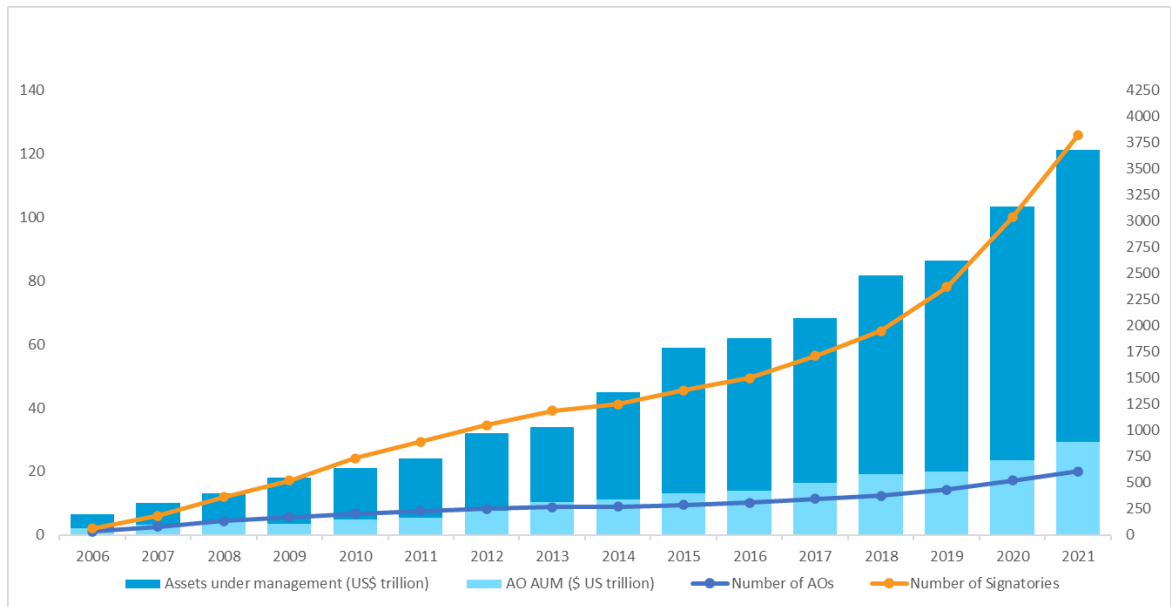


Fig. 2: Dynamics of PRI member growth c 2006 through 2021.

PRI signatories believe that environmental, social and corporate governance (ESG) issues can affect the performance of investment portfolios (to varying degrees across companies, sectors, regions, asset classes and over time).

Table 1 provides a comparative characterization of countries in terms of reducing greenhouse gas emissions. Analysis of the table data shows that of the selected countries, Azerbaijan is the country that approved the Paris Agreement in 2017, while Kazakhstan only ratified the Paris Agreement in 2023. The largest amount of greenhouse gas emissions is observed in China (12055 MtCO₂e), the smallest amount of emissions is observed in Azerbaijan (53 MtCO₂e), United Arab Emirates (244 MtCO₂e).

Table 1 shows Comparative characterization of countries in reducing greenhouse gas emissions for 2020-2022 (Table 1).

The seven largest emitting countries (China, USA, India, EU, Indonesia, Russian Federation, Brazil) accounted for about half of global greenhouse gas emissions in 2020. 20 countries (Argentina, Australia, Brazil, Canada, China, France, Germany, India, Indonesia, Italy, Japan, Republic of Korea, Mexico, Russia, Saudi Arabia, South Africa, Turkey, UK, USA and EU) are responsible for 75% of global greenhouse gas emissions [8].

Table 1: Comparative characterization of countries in reducing greenhouse gas emissions, 2020-2021

Country	Assets under management of ESG funds (EPFR data)	GHG emissions	GDP (PPP)	Population	Target year	ESG lending	Funding required to achieve carbon neutrality	Ratification of the Paris Agreement
Azerbaijan	-	53 MtCO ₂ e	\$146.3 bn	10.3m	2030	*	No precise estimate available	2017
Germany	-	720 MtCO ₂ e	\$4.4 tn	83.4m	2045	-	-	2020
United Arab Emirates	-	244 MtCO ₂ e	\$660.3 bn	9.4m	2050	There is no accurate estimate of ESG lending in the UAE	\$ 681 bn	-
Brazil	-	1452 MtCO ₂ e	\$3.1tn	214.3m	2050	-	-	-
Turkey	-	460 MtCO ₂ e	\$ 2,7 tn	84,8 m	2053	(2020) \$ 1,2 bn	-	2021
China	\$ 46,7 bn. **	12055 MtCO ₂ e	\$24.9tn	1.4 bn	2060	\$ 2,5 tn (+33 % in 2020)	\$ 21 tn	-
Russian Federation	-	1925 MtCO ₂ e	\$ 4,1 tn	145,1 m	2060	-	-	2020
India	***	3364 MtCO ₂ e	\$ 9,3 tn	1,4 bn	2070	\$ 4,6 bn ****	\$ 10 tn	2022
Kazakhstan	-	272 MtCO ₂ e	\$ 494,7 bn	19,2 m	2060	3 loans for \$62 mn	\$ 666,5 bn	2023
*	There is no accurate estimate of ESG lending in recent years in the country. In September 2022, the EBRD granted a \$100 million loan to Azerbaijan Caspian Shipping Company for fleet modernization. In 2019, the EU has allocated € 830 thousand for the implementation of a greenhouse gas emission reduction project under the EU4Climate project. At the end of 2021, the Asian Development Bank has provided support for 65 projects worth \$ 3.7 billion.							
**	Inflows to ESG funds in China totaled \$11.3 billion in 2021, up 149% from 2020.							
***	Assets under management of ESG funds (EPFR data) \$ 1.5 billion x4.7 over the 2019-2021 period							
****	Amount of outstanding loans for green energy in 2021 (Central Bank of India data)							

A source: <https://zerotracker.net/>

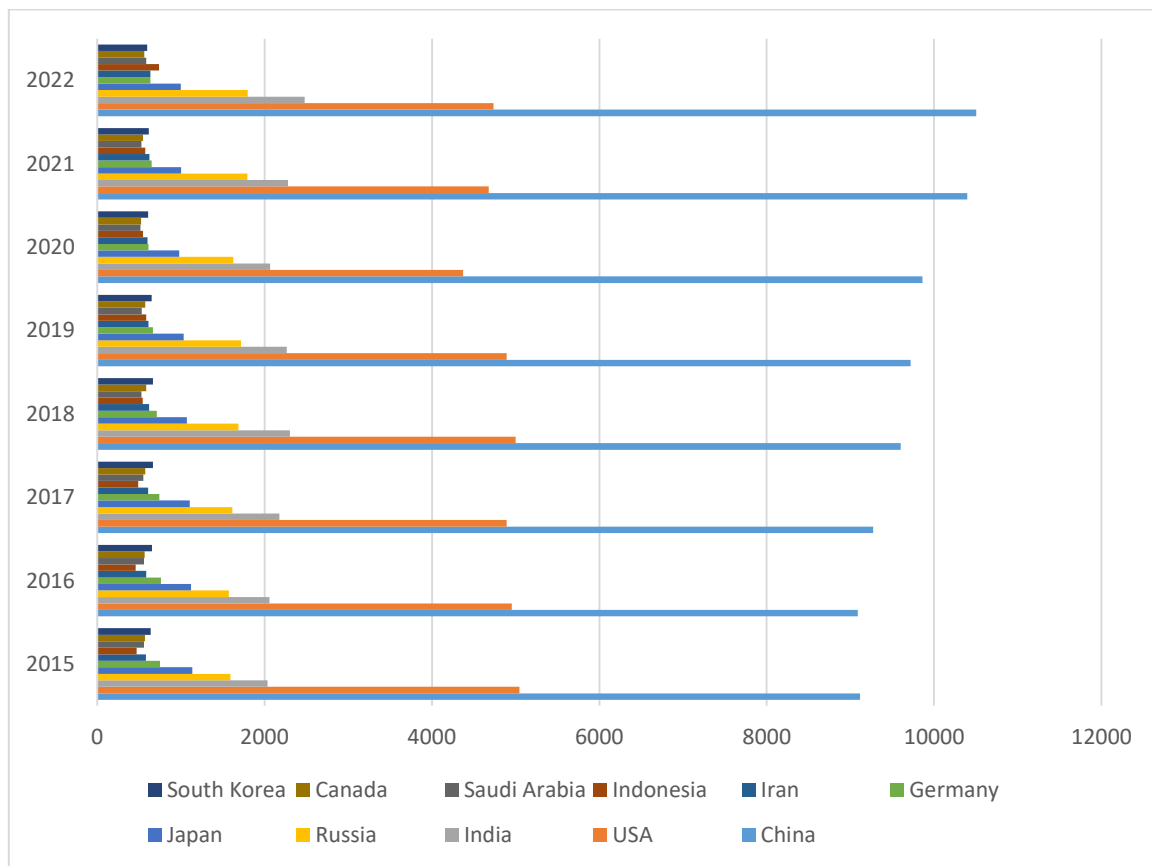


Fig. 3: CO2 emissions from fuel combustion for 2015-2022 (MtCO2e).

Figure 3. shows data from Enerdata, an independent research company specializing in the analysis and forecasting of energy and climate issues, where China has a 10-year lead in greenhouse gas emissions of 8,752 MtCO_{2e} in 2012 and 10,504 MtCO_{2e} in 2022. Stably for ten years, the top ten countries with the highest greenhouse gas emissions, in addition to China, are the United States, India, Russia, Japan, Germany, Iran, Saudi Arabia, South Korea, and Canada. Based on 2022 data, of the analyzed countries, we observe minimal GHG emissions in Canada (563 MtCO_{2e}), Saudi Arabia (587 MtCO_{2e}) and South Korea (597 MtCO_{2e}).

Information about a company's contribution to the green economy allows investors, stakeholders, organizations, and the government to more carefully select companies for long-term investments based on their environmental impact.

The implementation of the Paris Agreement in the Russian Federation is legitimized by the adoption of documents providing for the transition to climate change and its consequences, for example, in 2020 the Federal Law "On limiting greenhouse gas emissions" was adopted, and in 2021 the Strategy of socio-economic development of the Russian Federation with low greenhouse gas emissions until 2050 was adopted. Large Russian companies are adopting local regulations to implement sustainable development and commitment to the SDGs. In order to analyze the application of ESG criteria, data from a number of industrial companies in the Russian Federation were considered.

According to the data provided in Table 2, large industrial enterprises are taken as a basis, so in five out of six companies there is a sustainable development committee, which indicates a commitment to the principles of sustainable development, which is understood as a balanced and socially acceptable combination of economic growth and preservation of a favorable environment for future generations. Environmental responsibility costs are represented by impressive amounts,

so in PJSC "LUKOIL" costs amounted to 50,687 million rubles, in PJSC "GAZPROM" costs amounted to 36,303.2 million rubles for 2021. According to the Declaration on Environment and Development, ESG reports contain information on women's share in corporate governance, as Principle 20 outlines the vital role of women in environmental management and development [11]. Therefore, their full participation is essential to achieve sustainable development. According to Table 2, we observe the presence of women in corporate governance, with the exception of the State Corporation "Rostec".

Table 2: ESG criteria of Russian industrial companies for 2021

Name of the company	Revenue, rub.th.	Number of personnel, persons	Year of publication of the last non-financial report	Environmental liability, rub.th.	Social responsibility, rub.th. (employee training expenses)	Corporate governance (share of female executives), %	Existence of a sustainable development committee	Year of approval of the regulation on risk management / including ESG risks
PJSC «GAZPROM»	10 241 353 000	479 200	2021	36 303 250	-	24,1	+	2018/2021
PJSC «LUKOIL»	9 435 143 000	102 424	2021	50 687 000	854 000	26	+	2016/2021
State Corporation «Rostec»	2 063 900 000	591200	2021	-	-	-	-	2021/2021
PJSC «MMC «NORILSK NICKEL»	1 316 900 000	77 755	2021	21 100 000	-	24,4	+	2016/-
PJSC Uralkali	305 275 000	20 712	2021	2 466 379	72 615 363	20	+	2020/2021
State Atomic Energy Corporation "Rosatom"	1 447 600 000	288 500	2021	21 100 000	-	18,99	+	2015/2015

A source: <https://esg-disclosure.ru/company/>

According to Interfax - Corporate Information Disclosure Center, social responsibility for the analyzed period of 2021 is represented in the form of employee training expenses by two companies PJSC "LUKOIL" (854,000 thousand rubles) and PJSC Uralkali (72,615,363 thousand rubles) [10].

However, the environmental report of PJSC "GAZPROM" for 2022, provides information on the environmental training of Gazprom Group personnel for the period 2018-2022, in which 39,945 people received environmental training, of which the number of employees trained in the Environmental Management System (EMS) amounted to 11,953, which is 30% of the total number of trainees for the period [12].

PJSC "MMC "NORILSK NICKEL" in the report on sustainable development for 2022 shows that in 2022, 216 thousand pieces of man-training (including vocational training, retraining and

advanced training) were carried out, which is 87% higher than in the previous year. On average, there are 85 hours of training per average headcount employee, 95 hours per male employee, and 62 hours per female employee [13].

Thus, the information provided by analytical agencies does not always fully disclose information about the activities of companies within the ESG principles, and for a complete presentation it is necessary to study in more detail the statements of the analyzed company separately.

The importance of ESG for Russian business is confirmed by the research of Expert RA rating agency, conducted in November 2022 through a survey of rating clients from various sectors of the economy. The demand for ESG information both in Russia and abroad is still high, and the importance of ESG-awareness has not diminished at all; for many companies it remains strategic. A survey of rating clients from various sectors shows that, according to the results of the survey, for 67% of respondents the importance has remained, and for 5% it has also increased. In addition, the majority of companies that participated in the survey are already doing more for ESG-awareness than they should according to legislation [14].

Thus, the current events prove that it is in periods of turbulence that ESG-awareness gains the greatest importance, becoming not just a popular trend, but a real business strategy that determines the development of the company.

IV. Discussion

The ESG agenda in the world is developing rapidly, setting strategic directions for many companies and countries. Adherence to ESG principles is becoming an almost mandatory condition for maintaining business sustainability in the short term and maintaining effective functioning in the future. The adoption of the process of transition to sustainable development culminated in the announcement of 17 SDGs, which combine the directions of social, environmental and economic development, which are reflected at the level of the state and at the level of companies. Investors are increasingly interested not only in dividends and profits, but also in the social and environmental responsibility of a business. In Europe, more than half of assets are managed by investors who pay attention to non-financial factors. According to EY, 97% of institutional investors evaluate a company for its responsibility to society.

Global business is embracing new trends and the term "sustainable development" has been supplemented with the ESG (Environmental, Social and Corporate Governance) category. Although almost no one distinguishes between the two, the results of adherence to "sustainability" can be radically different from the results of compliance with ESG criteria, which create a kind of "company attractiveness index". Companies are assessed based on their ESG rating, as well as their strategy for promoting sustainable development. The priority of the company's activities is determined by the ability to conduct practical activities in accordance with "sustainable development", formulated within the framework of the UN Sustainable Development Concept and considered as economic growth that does not harm the environment and contributes to the resolution of social problems, finding a balance between economic, environmental and social development.

In the 21st century, the need to preserve the environment for future generations has become evident, as it is not enough to have good financial performance, so the concept of sustainable growth becomes a kind of new corporate philosophy. Promoting environmental initiatives has become a worldwide challenge. Efforts in this area are underway at both the state, legislative and private business levels of various sizes. The level of responsibility of companies towards the future is increasing. This trend concerns not only ecology, but also social and management aspects, which is why the ESG sphere is being actualized.

References

- [1] Agenda 21: United Nations [adopted by the UN Conference on Environment and Development, Rio de Janeiro, June 3-14, 1992. / URL: https://www.un.org/ru/documents/decl_conv/conventions/agenda21.shtml
- [2] Report of the International Commission on Environment and Development (ICED). / URL: <https://www.un.org/ru/ga/pdf/brundtland.pdf>
- [3] Promoting sustainable development. / URL: <https://www.un.org/ru/our-work/support-sustainable-development-and-climate-action>
- [4] European Securities and Markets Authority. / URL: <https://www.esma.europa.eu/document/sustainable-finance-roadmap-2022-2024>
- [5] Directive 2014/95/EU of the European Parliament and of the Council of 22 October 2014 amending Directive 2013/34/EU as regards disclosure of non-financial and diversity information by certain large undertakings and groups. / URL: <http://data.europa.eu/eli/dir/2014/95/oj>
- [6] Principles for responsible investment. An investor initiative in partnership with UNEP finance initiative and the un global compact. / URL: <https://www.unpri.org/download?ac=10948>
- [7] Principles for Responsible Investment/ / URL: <https://www.unpri.org/about-us/about-the-pri>.
- [8] NET ZERO TRACKER. / URL: <https://zerotracker.net/>
- [9] Independent research company specializing in analysis and forecasting of energy and climate issues «Enerdata». / URL: <https://energystats.enerdata.net/co2/emissions-co2-data-from-fuel-combustion.html>
- [10] Interfax Information Group / URL: <https://esg-disclosure.ru/company/>.
- [11] Declaration on Environment and Development. / URL: https://www.un.org/ru/documents/decl_conv/declarations/riodecl.shtml
- [12] Environmental Report of PJSC "GAZPROM" for 2022. / URL: <https://www.gazprom.ru/f/posts/56/691615/gazprom-environmental-report-2022-ru.pdf>
- [13] PJSC «MMC NORILSK NICKEL» Sustainability Report 2022. / URL: https://www.nornickel.ru/upload/iblock/10d/iqtmhfjmpv35e3ai0untm8xuftr47ifz/NorNickel_CSR2022_RUS_2.08.pdf
- [14] ESG-transparency: disclose cannot be closed. «Expert RA» Rating Agency. / URL: https://raexpert.ru/researches/sus_dev/esg_2022/

THEORETICAL AND CONCEPTUAL APPROACHES TO STUDYING THE NATURE OF ECONOMIC GROWTH

Alina Gudieva¹, Tatyana Sitokhova¹, Marianna Kelehsaeva¹,
Magomed Suleymanov², Kantemir Khachirov¹

¹North-Ossetian State University named after K.L. Khetagurov, Russia

²Dagestan State University, Russia

gudiyeva00@bk.ru

t_sitohova@mail.ru

marina.kelehsaeva@mail.ru

fefnews@mail.ru

khachirov7@mail.ru

Abstract

The subject of this article is the study of the theoretical foundations of the phenomenon of economic growth. During the study, the authors chose a general retrospective methodology and predominantly historical analysis; The history of the emergence and development of the concept of "economic growth" is considered. In accordance with this, the authors touch upon the problem of the general philosophical foundations of economic teachings, which formed the basis of the concept of modern economic growth and economic development. The research began in the works of Adam Smith and the first political economists, so special attention is paid to the historical period in which these scientists lived and worked. The following is a general overview of the first modern models of economic growth and some approaches to its assessment.

Keywords: economic growth, quantitative theory, development, GDP

I. Preliminary remarks

The term "economic growth" has become widespread in economic science in a relatively short period of time. The first models of economic growth appeared at the beginning of the 20th century. Until this time, the conceptual basis of this concept was not sufficiently developed, and economic growth was not the subject of special research. The crisis of scholasticism in the 14th–15th centuries and the triumph of humanism led to the emergence of a scientific-materialist understanding of the world. The development of material production, trade, the discovery of America, communication with the Eastern world, the teachings of Copernicus and many other events determined the course of philosophical and scientific life. The humanities, including economics, have received independent development. The focus of attention of scientists and early researchers in the field of economic science was the fact of economic well-being, which many of them associated with scientific and technological progress, growth in production, income, employment, population size or the standard of living of the population. However, the subjects that modern researchers accept as factors of economic growth were considered separately in the works of many early classical economists, and some new concepts developed from even earlier hypotheses.

Political economists, when starting to develop and present scientific theories, never used the term we are considering, since it was unknown to them. However, in essence, in all economic theories of the classical and pre-classical period of development of economic science, the concept of economic growth was not only implicitly present, but also served as the core of the theory, grouping around the subject, research methods and final conclusions. As will be shown below, almost

every author of one or another economic theory not only explained and described the reality of economic processes, but also proposed, based on one or another factor of production, his own recipe for economic growth.

Research using historical analysis will require us, in addition to considering many aspects of the teachings of various economists of the 18th century, to analyze some socio-philosophical aspects of the general environment that had a significant influence on the formation of the first scientific concepts. Let us add to this that the first, initial period of the existence of any spiritual phenomenon, be it the idea of progress, the free market or economic growth and development, is always of particular interest to the researcher: "returning to the roots" often helps to clarify the basic structure of something or another complex phenomenon, to identify problematic, vulnerable points in it, so to speak, "birthmarks," and even sometimes to find a way out of those historical dead ends into which sooner or later, due to the limitations of human capabilities, every good undertaking ends.

It must be said that a holistic consideration of the structure of branch sciences, with the inclusion of both philosophical foundations and the history of science, is little by little gaining a place in the modern scientific worldview. As Russian researcher O.I. concludes. Ananyin, at this moment, "ontological knowledge has finally acquired "citizenship rights" in the scientific literature on the post-positivist wave, when economists began to try on the "paradigms" of T. Kuhn and the "research programs" of I. Lakatos for their theories. The best examples of modern methodological literature continue this line, explaining various phenomena and trends in the development of scientific thought based on a thorough analysis of its ontological premises" [1, p. 6]. There comes an understanding of the benefits that such a deep analysis can bring to the development of branch sciences, the obvious, in general, truth is affirmed that at least to test and select promising scientific theories, a scientist needs a higher criterion, a more general view, rather than a highly specialized one, i.e., already limited by previous theories. For such scientific selection, it is necessary to "identify the hidden premises underlying the relevant theories, recreate their real context and meaning, provide the necessary background for comparing competing theories and structuring the accumulated stock of knowledge" [1, p. 7].

Considering all the circumstances and considerations described above, it is no longer surprising that in many works on the history of economic thought, for example, in the two-volume work of M. Rothbard, the problem of the general philosophical foundations of certain economic doctrines is addressed. A detailed study of the philosophical foundations of economic science, including the search and identification of "ontological categories" in the works of its founders, also has a long tradition in science. It is enough to name the names of V.S. Avtonomov, O.I. Ananin, M. Blaug, V.A. Kanke, A. Marshall, D. Houseman.

II. Formation of the idea of economic growth in the works of the first economists

Since the problem of economic growth has been present in the scientific literature since the birth of economic thought, we will limit ourselves to the study of the philosophical aspects of the thought of only some classical economists, necessary for a more complete understanding of their theories, from which the following economists derived modern ideas. Further, from the studies of J. Schumpeter, we will trace how this concept was conceptualized and underwent changes on the way to modern understanding.

In the early stages of the development of economic thought, economic growth was understood as an increase in wealth. The search for sources of enrichment became the subject of work of the first economists. The 16th century in the history of economic thought is notable for the development of mercantilist ideas. Thus, wealth in the era of early mercantilism was measured by the amount of money in the country, and its source was found in foreign trade, carried out according to the principle of "beggar your neighbor." Enrichment was facilitated by measures to influx and

accumulate foreign coins. Over time, economic priorities changed somewhat, and numerous protectionist measures began to be aimed at maintaining a positive foreign trade balance.

They begin to talk about economic growth of the modern type after the completion of the industrial revolution. The growth of knowledge and its application, the improvement of equipment and technology increased production capabilities and ensured population growth. The Industrial Revolution made available new methods of production and deformed previously established economic structures. The production infrastructure expanded, communications were updated, new goods, electrical equipment and machines appeared, which led to the creation of a qualitatively new economic environment. The fundamental industrial restructuring aroused wide scientific interest and opened the need to develop a methodology for studying and describing market processes and formulating theories with predictive properties. From this time on, a full-scale study of the mechanisms and processes of economic growth began, and the development of statistical analysis methods that made it possible to describe the state of the economy.

The study of economic growth in pre-industrial retrospect is very difficult, since today we do not have sufficient statistical data for appropriate analysis. The period that can be described from the point of view of modern models of economic growth, as noted by Yu. V. Sharaev, occupies a very small place in historical space. Over 99% of modern economic research is devoted to a period that covers less than 1% of human life [2, p.47]. Therefore, only two periods of development of the theory of economic growth can be distinguished. The era from the end of the 13th century to the first industrial revolution of the beginning of the 19th century. modern scientists designate it as the first, pre-industrial period in the theory of economic growth, sometimes called Malthusian in the scientific literature [2, p.49]. Its most famous representatives are classical economists.

It is also important that during the life and work of classical political economists, the subject of their research in their own minds was not yet so strictly separated from ideas and considerations of a higher order, from philosophical truths and, more broadly speaking, from a holistic moral worldview, as is often observed in the modern scientific world: thus, "...for Adam Smith, political economy is only a part or chapter of a broader and general worldview and is far from the one-sided specialization that it is now"[3, p.287]. Therefore, we will not find a special study of economic growth in the works of A. Smith.

When considering Smith's teachings, we need to take into account the fact that in the 18th century the intellectual influence of Newtonian mechanics was so great that it, in essence, served as a model and methodological basis for the development of not only the exact sciences, but also the social sciences. It also became one of the important sources of Adam Smith's economic theory. Thus, in full accordance with the mechanistic views of the era, the English economist wrote: "Human society, considered from an abstract and philosophical point of view, can be compared with a huge machine, the correct and coordinated movements of which produce a lot of useful results" [4, p.305].

But, unlike the great physicist, Adam Smith encountered some of the difficulties that often accompany the theoretical consideration of human society. The fact is that for all the gears of the mentioned social machine to rotate in harmony, "invisible forces" are not enough: quite specific efforts of many existing and interacting individuals are needed. And if in Newton's system the cause of gravity was not precisely established (the scientist considered its clarification the task of further research), then in Adam Smith's system the "prime mover" was found. The force that sets the social colossus in motion turned out to be human egoism. As a domestic economist notes, "the separation of political economy from the general discipline, called moral philosophy, occurred thanks to a special model of man, which formed the basis of a new independent science. The main point of this model was a specific motivation: self-interest or the desire for wealth as the main motive of behavior" [5, p.59-60].

Indeed, it was with the thesis about the beneficence of personal egoism that Adam Smith entered a centuries-old philosophical dispute about the harmonious relationship between the general and private good, which, of course, did not subside in the eighteenth century. In the economic theory of those times, one of the positions in this dispute was reflected in the school of mercantil-

ists: mercantilists, turning rather to a statesman, to a legislator who governs society, demanded that he consider the selfish interests of his subjects in a certain way, but look for a way to connect these interests in a common chain, preventing arbitrariness. However, already one of the mercantilists, J. Denham-Stuart, in his work "An Inquiry into the Fundamentals of Political Economy" (1767), formulated the foundations of a new approach to assessing personal egoism: "The principle of self-interest... will be the leading principle of my subject... This is the only motive, which the statesman must use to attract free men to the plans which he makes for his government." And further: "Public interest is as superfluous for the governed as it must be omnipotent for the manager" [5, p.60]. Adam Smith knew well the state of political economy of his time, and not only British: he lived for a long time in France and in personal conversations with French economists (who at that time were embraced by the idea of progress in all spheres of activity, such as Turgot and Condorcet) understood themselves, for example, some of the positions of the physiocrats, adopting the deep respect for free trade characteristic of representatives of this school.

Thus, Adam Smith denied the antagonism between private and general interests: some abstract essence was introduced in which they are reconciled at a higher level, where the particular, which, based on appearance, contradicts the general, is dissolved in it. This is the free market. Likely, Adam Smith's formulation of the "invisible hand" thesis was influenced by his personal commitment to the principles of free enterprise, his belief in fair competition and free trade, and finally, his negative attitude towards all forms of government intervention in the economy. This principle, in one fell swoop, eliminated all the most difficult ethical problems, gave an exhaustive answer to the questions: how the economic activity of individuals is left to their own devices regulated, what could be its positive results, what, in essence, will keep the mass of such individuals from self-destruction and immersion into chaos. And this principle was affirmed by Smith against the background of that very historical state of economic relations, which received the nickname "wild capitalism." As Alfred Marshall later noted, with some surprise, "and yet the time at which free enterprise was showing itself in an unnaturally harsh form, was the very time in which economists were most lavish in their praises of it" [6]. Having given market self-regulation a natural character, elevating it, as it were, to a law of nature, Adam Smith set the context for his own research and could further build models of interactions between economic entities in this "natural" environment.

So, the main source of inspiration for Adam Smith was Newton's theory: the great political economist even devoted his own separate work to astrophysics. Among other sources of Adam Smith's ideas, some modern researchers, in particular V.S. Avtonomov [5, p.61-62], point to the works of Bernard Mandeville, namely, his famous pamphlet "The Fable of the Bees" (1723), which outlines the connection between the unscrupulous, unvirtuous, downright vicious behavior of individual members of society and the resulting good of this society itself. The economy as such, without government intervention in it, "ennobles" human vices, directing them towards the common good: the correct organization of economic activity opens a clear path to a steady increase in social well-being. However, despite the similarity of basic ideas, Adam Smith himself never referred to Mandeville and did not quote his works in his works.

In 1776, the famous "Inquiry into the Nature and Causes of the Wealth of Nations" appeared, where Smith, as conditions for economic success, identified ways and possibilities for the state to use its competitive advantages. The main theme of his work is long-term economic development, a description of the forces leading to the growth of wealth of nations. Here his theory about the positive contribution of individual selfish initiatives is applied to a higher order - to state economic policy. He identified endogenous and exogenous growth factors. The first include population growth, depending on per capita income, employment in material production, soil fertility, investment, etc. Adam Smith considered institutional parameters as exogenous factors. Great importance in his teaching was given to the division of labor, which leads to an increase in labor productivity and, accordingly, can also be called a factor of economic growth.

Another economist and philosopher, Thomas Malthus, is known for his demographic theory, which explains the causes of poverty by the relationship between population growth and the in-

crease in means of subsistence. Malthus set the standard on which all the ideas of classical economists were based: his "Essay on the Law of Population" for a long time cemented in the minds of that time a strong connection between economic progress and population size. Studying the demographic trends of the United States, he concluded that the population, if it has the means of subsistence, freely increases in geometric progression, and the means of subsistence themselves increase in arithmetic progression, which soon, without birth control, leads to resource depletion and general impoverishment. His socio-economic model is based on two main assumptions. Firstly, average per capita income directly affects changes in population size. From this assumption a law is born that determines that the population is limited to its means of subsistence. The second assumption: a negative relationship between these two indicators, due to diminishing returns to factors of production. From it comes the "law of diminishing returns," which states that over time, each subsequent unit of investment will generate less income than the previous one on the same piece of land, that is, a decrease in marginal income.

Malthus did not share the optimism generally characteristic of people of his era. Objecting to numerous social optimists who paint pictures of eternal progress and continuously increasing public good, Malthus put forward the thesis about the existence of insurmountable barriers to progress, inexorable laws of nature that knock the ground out from under any naive optimistic belief. Optimists, according to Malthus, are mistaken in believing that population growth is a positive factor in economic development; they lose sight of the catastrophic impact that too rapid population growth can have (and is already having) on the economic system of a society. Generally, the population grows faster than its means of subsistence increase. As a result, the population becomes poor and thus all social and economic development ceases.

So, in contrast to Adam Smith, Thomas Malthus was a deep pessimist. If Adam Smith believed that even the worst inclinations of people could ultimately lead to good results, then Malthus, on the contrary, saw entirely bad results even from a clear, visible improvement in human well-being. Malthus thus introduced a completely different natural law, likening people to animals in their tendency to unlimited reproduction, i.e. catching the similarity between people and animals in ways that previously often escaped the attention of researchers.

What is the reason for the English philosopher's ardent conviction that the world is structured in such an unmerciful way? Where did he get his confidence from? As A. Marshall points out, this was one of the trends of the era: "the English economists of the earlier half of last century (that is, the 18th - my note) overrated the tendency of an increasing population to press upon the means of subsistence; and it was not Malthus' fault that he could not foresee the great developments of steam transport by land and by sea, which have enabled Englishmen of the present generation to obtain the products of the richest lands of the earth at comparatively small cost" [6].

In fact, the conditions in which Malthus lived seemed, on the contrary, to testify in his favor: the overpopulation of England, increasing as a result of pauperization, created a very clear threat to the well-being of the broadest layers of the population, and all attempts by the government to mitigate its consequences by organizing, for example, regular material assistance to the poor did not produce a positive effect. For this reason, Malthus sharply objected to contemporary legislation to help the poor: their stay in the world should not be prolonged. They are, so to speak, superfluous at this celebration of life.

Among the ideological movements that influenced the formation of Malthus's views, his philosophical predecessors deserve mention, many of whom he himself often cites in his main work: the Italians Botero and Genovesi, the Englishmen Raleigh, Gael, Franklin, Arthur Jung, the German Moser. As noted by S.N. Bulgakov, "to a certain extent, the physiocrats are his predecessors. Malthus's first law, that the population is limited by the means of subsistence, was the main tenet of the popularist teaching of the physiocrats" [3, p.314].

Malthus's ideas were largely shared by D. Ricardo. At the heart of his economic system is the idea that economic growth will inevitably cease in the future due to a lack of natural resources. He chooses the differential rent model as the basis for his theory of wealth. Agreeing with Malthus and recognizing the fact of decreasing land fertility, Ricardo proposes two measures restraining

economic growth - rising land prices and rising prices for agricultural products. It is desirable to supplement all this with technical improvement to ensure economic development, although the latter, according to Ricardo, is not a priority in economic management.

Ricardo's views were influenced by two important circumstances. First, his successful career as a stockbroker and banker. As you know, trading on the stock exchange presupposes some ability to abstract from real production, to consider conditional quotes of shares and other securities as real. This left an imprint on the nature of Ricardo's reasoning, which was almost always extremely abstract and schematic. Secondly, Ricardo was strongly influenced by the ideas of Jeremy Bentham, the English philosopher, founder of the school of utilitarianism. According to Bentham's teaching, the selfish interest of an individual, correctly understood and calculated, not only does not conflict with the interests of society, but, on the contrary, becomes useful for society. In order to neutralize the bad influence of selfish interests, it is therefore necessary to simply treat these selfish interests as extremely rationally as possible, to calculate their effect "arithmetically". Ricardo applied this approach to "economic man": the conclusion from this approach was that if an egoist acts rationally, he brings only benefit to society.

Thus, on the same philosophical foundation as Adam Smith, on the same inviolable belief in the beneficialness of self-interest, new theoretical models of the economic life of society were built. It cannot be said that the founders of political economy did not look for other supports: but, from their point of view, nothing stood the test except personal egoism. It is personal egoism, according to Ricardo, that the researcher simply has to take as his initial premise: otherwise, "if we had assumed any other rule of behavior, we would not have known where to stop" [5, p.67].

In other words, personal egoism has become the fulcrum for economic growth. The model of "economic man", present in the teachings of A. Smith and D. Ricardo, was based, of course, not only on general philosophical considerations, but, in all likelihood, mainly on everyday observations. On this occasion, at the end of the nineteenth century, Alfred Marshall noted how insufficient the everyday experience of the founding fathers of political economy was: communication exclusively with the English living in large cities could not, of course, exhaust the social and spiritual picture of life in even one country of that era: "To simplify their argument, Ricardo and his followers often considered man as a constant quantity and never took the trouble to study possible variations. The people they knew most intimately were residents of large cities, and they sometimes expressed their thoughts as if to imply that other Englishmen were very much like those they knew in the big cities" [6]. One way or another, history has received yet another confirmation of the truth that the social context - origin and country of residence, place of residence (city or village), social circle, intellectual atmosphere - influences the course of thought of even the deepest mind.

K. Marx also made his contribution to the development of the theory of economic growth. Within the framework of this topic, his theory of expanded reproduction, which, in essence, is a model of economic growth, deserves mention. However, K. Marx did not create an independent theory of economic growth, but only explained the process of capitalist accumulation as a kind of "genetic program" of capitalism and, like classical economists, focused on the problem of reducing profit rates.

J. St. Mill summarized the accumulated knowledge about economic growth. He completed the concept of long-term economic growth based on capital accumulation and came to the conclusion that limiting population growth is a condition for long-term industrial progress. The problem is resource limitations, and the solution is technological progress, which allows reducing costs per unit of production. And this is how he formulated it: political economy "concerns man only as a being who desires to possess wealth and who is capable of judging the comparative utility of the means used to achieve a given result" [7, p. 56]. And further: "Political economy views humanity as involved exclusively in the acquisition and consumption of wealth; and [its activities] are aimed at showing what would be the course of action of humanity living in a state of society if this incentive ... were absolute master of all human actions." J. St. Mill gave the model of classical economists

the character of a mathematical abstraction, nevertheless, useful and effective in the scientific analysis of social phenomena and important in quantitative assessments of economic processes.

One way or another, all classical growth theories turned out to be united by a common conclusion about the inevitable approach of a developing economy to the pre-crisis stationary state, when the rate of profit will decrease extremely. Most research has been aimed at explaining the inevitability of this condition and developing a plan to delay its onset. Basically, the recommendations boiled down to limiting population growth and developing technology. The logic of the process under consideration is as follows: the accumulation of capital increases the demand for labor, which, in turn, leads to an increase in wages and, accordingly, to a gradual increase in the population. Here the problem of resource scarcity arises; as Malthus and Ricardo noted, agricultural production is characterized by decreasing returns to scale. This means that each new unit of the necessary good will be obtained with increasing effort, all other things being equal. The opposite process to economic growth: rising food production costs, the need to increase wages for workers in the context of rising consumer prices but maintaining the same labor productivity. All this leads to a reduction in profit margins and economic stagnation. Thus, capital growth ultimately slows down population growth, which, as all the economists discussed have argued, depends on income. And a decrease in real wages leads, accordingly, to a decrease in the birth rate. Classical economic thought focused on the identified contradiction between the growth of savings and the marginal productivity of capital. In their studies, the classics of political economy focused on the accumulation of capital and, in general, it was typical for them to understand economic well-being as an increase in the volume of the total product.

III. Further development of the idea of economic growth and the formation of modern models

J. Schumpeter made a significant contribution to the theory of economic growth. In his "Theories of Economic Development" in 1939, he distinguished between the concepts of economic growth and development. Economic growth seemed to him the same as to the economists who preceded him, but he recognized it as not a sufficient condition for economic development, but only as a change in statistical indicators: "Ordinary economic growth, expressed in an increase in population and wealth, is not considered here as a process of development, since it does not give rise to qualitatively new phenomena, but merely gives impetus to the processes of their adaptation" [8, p. 154].

The driving force in his economic system is the personality of the entrepreneur and the actualization of her individual qualities and creative abilities. The motive that encourages an entrepreneur to act in a market environment is the desire for monopoly profit. The monopoly market structure, with its known shortcomings, is chosen by Schumpeter as preferable, imparting strength to innovative development. The entrepreneur introduces innovations to the market, effectively and profitably managing available resources, implementing "new combinations." The following process is consistently implemented in the market: manufacturing a new good (or endowing it with a new quality) - introducing a new production method - developing a new sales market - obtaining a new source of raw materials and semi-finished products - carrying out corporate reorganization and creating a monopoly. The gradual implementation of these five forms means economic development. Much attention is paid by Schumpeter to the role of credit. Credit is a way of providing an entrepreneur with purchasing power. Creating purchasing power, according to Schumpeter, is the way to achieve economic growth.

In Schumpeter's system, there is no problem of reducing marginal income in relation to innovation; economic growth was slowed down by several other factors, united by the general principle of a decrease in entrepreneurial activity, such as, for example, the replacement of entrepreneurs with hired management personnel who are not prone to risk and creativity, and also ide-

logical exhaustion; the emergence of conditions that make it difficult to generate new combinations.

The next researcher, mathematician J. von Neumann, considered economic growth without addressing the limitations associated with agricultural production, entrepreneurial behavior, the causes of wealth and scarcity, introducing mathematical methods into the theory of economic growth. The theory of sustainable economic growth, known as the von Neumann model, explains the growing importance of investment in the process of social development.

There are two factors in the model, the first stimulates the growth of savings, capital-labor ratio, economic growth and economic progress. When savings grow, the increase in national income is ensured by an increase in capital, not in the consumer fund. Therefore, the second factor ensures sustainable stability of the economy and increases the standard of living of the population in the present, diverting capital from the savings fund to the consumption fund.

Since 1960 theories of long-term growth are emerging, ensuring an increase in income per capita. Keynesian growth theory, outlined in the *General Theory of Employment, Interest and Money*, formed the basis of many subsequent theories. All of these theories addressed the connection between the growth of income and the possibility of its efficient use, since Keynes believed that the market economy causes excessive waste. For Keynes, saving and consumption constitute total income. Economic growth may slow down when the economy goes to extremes. For example, the "paradox of thrift" occurs when, with income growth, the marginal propensity to save among the population increases, and the marginal propensity to consume decreases, and is characterized by a decrease in supply, production and a slowdown in economic growth.

An important place in the Keynesian model is occupied by investments that ensure the multiplicative principle. The latter serves to identify the interdependence of changes in investment flows, income and output. The marginal propensity of consumption in relation to this multiplier is in direct proportionality, and the marginal propensity to save is inversely proportional.

Economic growth is ensured through the implementation of several sequential measures: stimulating the growth of aggregate demand using the multiplier effect using special government programs; redistribution of national income in favor of individuals who are not inclined to increase savings; attracting investment into the economy through the use of the interest rate mechanism.

The first and simplest of the modern models of economic growth is the Keynesian Harro da Domara model, which was the result of the application of Keynesian ideas in the long run. In his work "Toward a Theory of Economic Dynamics," Roy Harrod argues for the importance of distinguishing between the study of static economic states and the economy in dynamics. The subject of his theory consists of three main factors: capital, labor, output per capita. Economic growth, in his opinion, is ensured by an increase in real income, labor force growth, and capital accumulation. For Yevsey Domar, the concept of economic growth, like for Keynes, is inextricably linked with economic potential, the actualization of which is carried out through an increase in labor supply. In his article published in 1947, he aims to determine the conditions necessary to maintain full employment over a long period of time, and to find a rate of economic growth that will correspond to maximum employment in the country [9].

Capital is considered in the Harrod-Domar model as a factor of economic growth. Great importance is given to the analysis of the conditions that ensure the most complete actualization of economic potential. The model postulates two principles: growth of aggregate demand is a necessary condition for economic growth; investments (as part of aggregate demand) ensure growth in consumption and, therefore, sustainability of economic growth [10, p. 194]. The disadvantage of the theory is that it describes a closed economy, which means that there are no export and import relations in the model; the produced product here breaks down only into investment and consumption. This makes the model quite abstract, having little practical value.

For supporters of neoclassical growth models, the factor of increasing living standards is of particular importance. Here we can highlight the model of R. Solow, which is based on the need to accumulate capital and the connection between labor and capital factors in the market where tech-

nical progress unfolds. A high level of capital-to-labor ratio leads to the development of production and increased investment. To achieve economic sustainability, capital growth must be matched by population and investment growth. If investment is insufficient and the population grows, then there is less and less capital per worker, which means less income. GDP per capita is ensured by technological progress leading to capital growth and output growth at a given pace.

Research within neoclassical thought has continued since the 1980s. P. Romer, R. Lucas. Their contribution is to develop models of long-term growth, called endogenous ones. They were partly based on the models of H. Uzawa and K. Arrow. They are united by a common interpretation of economic growth not as a fact of violation of the achieved market equilibrium, but as a normal state. Neoclassical models mathematically describe the relationship between total output and certain variable factors, such as labor, capital, investment, technical progress, but do not define the essence of economic growth, since in many respects they are based on I. Bentham's postulate, according to which the total Welfare is simply the arithmetical sum of the well-being of individual people. According to M. Blaug, these researchers ignored the question of comparing different optima associated with different income distributions [11, p. 540].

T. Palley compared Keynesian and neoclassical approaches to economic growth in his article. He identified two main differences: 1) for Keynesians, capital accumulation is determined by the investment costs of firms; 2) in equilibrium conditions, the growth rate of output should be equal to the growth rate of aggregate demand, which contradicts the classical models, which implied an automatic increase in demand in response to an increase in output [12].

Based on the information obtained, we can conclude that the most common thing for all the presented authors who developed the theory of economic growth is the understanding of it as a process of increasing real output (income). Keynesians focus on increasing output, while neoclassic and, in many ways, modern researchers who follow them, on increasing per capita income. By some, economic growth means an increase in the number and importance of factors of production, indicating an increase in production capabilities, while others mean the dynamics of actual output. The variety of modern models of economic growth is due to many attempts to obtain a more accurate mathematical description of the observed facts of economic life in an extremely unstable, rapidly changing world. In order to select criteria for quality growth from the considered variety of economic growth models, it is necessary to distinguish between the concepts of "economic growth" and "economic development". The category of quality of economic growth is, as it were, at the junction of these two concepts and eliminates the contradiction between them.

In its most general form, economic growth today is usually understood as an absolute increase in GDP in general and per capita. Quantitative indicators in a structurally static, as R. Harrod noted, economy must be taken into account when analyzing economic growth. Economic development is a change in the structural components of the economy, a qualitative movement. Both development and growth are designations of the processes of movement of an object: growth implies a quantitative change, and development – a qualitative one.

The foundations of the categorical meaning of the concepts we are considering were laid by Aristotle. In accordance with his logical system, there are three types of movement - in relation to place, quantity and quality. Movement relative to place means movement, relative to quantity – growth and decline, and relative to quality, a qualitative change occurs, [13] a special case of which can be development.

J. Schumpeter was the first to distinguish these two concepts in economic science. Following Aristotelian logic, he defined economic growth as gradual changes in the scale of the same production and consumption over a certain time. By development, he understood a qualitative transition from one vector norm to another, interrupting the progressive growth of economic life. Its economic development is "a change in the trajectory along which the circuit is carried out, in contrast to the circuit itself, represents a shift in the state of equilibrium, in contrast to the process of movement in the direction of the state of equilibrium, however, not any such change or shift, but only firstly, spontaneously arising in the economy and, secondly, discrete, since all other changes are already clear and do not create any problems" [8, p. 131].

Schumpeter's ideas about economic development driven by innovative development were subsequently supported by N. Clark and C. Hume [14]. According to them, there are two factors of socio-economic movement - the challenges faced by the market and institutional pressures. The simultaneous action of these two factors causes technological changes, and the latter, in turn, lead to economic development. Scientific and technological changes are of a different nature, depending on the degree of influence on the economy, they can be: incremental, in the case when the existing production system and social relations are experiencing minor changes; radical - when new types of goods appear simultaneously and production methods, methods and technologies change significantly; revolutionary - when the market undergoes significant structural changes.

The approach of J. Schumpeter and the economists who followed him in studying the technical and economic component of development, such as T. Veblen, J. K. Galbraith, J. Dosi, determined the modern view of the theory of economic development, which does not focus on the quantitative increase in factors production, such as labor and capital, as was previously accepted, but to improve them as a result of the accumulation of knowledge and innovation [15].

Professor S. Kuznets made a significant contribution to the development of theories of economic growth based on the analysis of the economies of developed countries. According to his concept, economic growth "may be defined as a long-term rise in capacity to supply increasingly diverse economic goods to its population, this growing capacity based on advancing technology and the institutional and ideological adjustments that it demands" [16]. This definition allows for a mixture of economic growth and development, although in Kuznets' concept all factors are inferior in importance to one main one. In his opinion, economic growth is observed when there is a long-term sustainable growth of the national product, and when the economic system becomes able to satisfy an increasingly wider range of needs of the population. Technical progress in this system is given secondary importance.

Technical changes and the development of "new combinations" in the economy lead to a new technological structure. Initially, innovations introduced to the market revolve around the same infrastructure base. After some time, necessary for the market to adapt to new conditions, the process of accelerating economic growth begins, indicated by an increase in GDP. The result of structural economic deformations is the emergence of new infrastructures on the market, which lay the resource basis for the formation of the next technological structure [17, p. 100-111]. This means that chronologically, economic growth and economic development alternate. When the design of a new technological structure is completed, production structures are adjusted, new points of market equilibrium are determined, the vector of development is redirected, and a new economic cycle is launched with its own economic growth.

As an example of structural economic changes, one can cite the large-scale introduction of information technologies, which, according to S. Yu. Glazyev, accompany the duration of the sixth technological order, which began in 2010 and continues at present. The economy today is experiencing revolutionary changes in the production sector; therefore, the automation of routine operations and the replacement of manual labor is important, "at present, the sixth technological structure is emerging from the embryonic phase of development, in which its expansion was hampered by both the insignificant scale and the lack of development of the relevant technologies, and the unpreparedness of the socio-economic environment for their widespread use. But already the costs of developing nanotechnologies and the scale of their application are growing exponentially, the total weight of the sixth technological order in the structure of the modern economy is rapidly increasing" [18].

Approaches to the relationship between economic growth and development can be divided based on their relationship to the historical specifics of each specific economic region. The first can be called universalist, considering the economic movement of all countries along a common global development trajectory. Within the framework of this approach, national and territorial characteristics can conditionally influence the course of economic development, at a certain historical moment slowing down or accelerating its movement in a single direction of progress. The second approach is based on the progressive solution of economic problems of a specific country, region or

group of countries, considering local characteristics. THEM. Tenyakov calls a group of similar approaches “soil-based” [15, p. 17].

Table 1: Characteristics of “technological structures” of economic development

Period		Factors	Dominant industries
1	1770-1830	Water engine	Textile industry
2	1830-1880	Steam engine, coal	Coal industry, railways, metallurgy
3	1880-1930	Specialization in steam engines, electric motor	Electrometallurgy, chemical industry
4	1930-1980	Oil, internal combustion engine	Automotive, organic chemistry
5	1980-2010	Microprocessor, natural gas	Microelectronics, computer science, telecommunications
6	2010-2050	Information technologies, digitalization technologies, neuro- and nanotechnologies	Information Products

Proponents of the second approach (F. List, J. Keynes, institutionalists J. Commons, W. Mitchell, etc.) pay special attention to issues of national economic development. For example, List's economic analysis is based on the principle of historicism. He considered, for example, the transition of a nation from manufacturing production to factory production as a fact of economic development [19]. This approach embeds economic growth in the context of national development, ensuring economic and national security, protecting national interests and, most importantly, asserts the need to develop institutions consistent with the traditions and values of each state. He stands on a definition of development close to that formulated by the Russian philosopher K.N. Leontyev. Having examined the process of development on extensive historical material, he determined that development is “a gradual ascent from the simplest to the most complex, gradual individualization, isolation, on the one hand, from the surrounding world, and on the other, from similar and related organisms, from all similar and related phenomena. A gradual progression from colorlessness, from simplicity to originality and complexity. A gradual complication of constituent elements, an increase in internal richness and at the same time a gradual strengthening of unity” [20, p. 178].

Economic growth, therefore, is a quantitative change, a multiplication of the material composition of a phenomenon. This means an increase in production and consumption parameters in absolute values and per capita in terms of GDP, national wealth, etc. The term “economic growth” spread in the 20th century under the influence of new ideas. This was facilitated by scientific discoveries, the development of trade and industry and prosperity. This term, which still has different understandings and interpretations, was adopted by scientists in the 20th century and came into common use everywhere.

The problem of economic growth has been present in scientific literature since the birth of economic thought. The search for ways to ensure national well-being was the subject of research by researchers of the mercantile and physiocratic directions. The galaxy of founders of classical political economy A. Smith, D. Ricardo, T. Malthus and others theoretically formulated the material accumulated by the historical experience of economic management and supported it with empirical research. Each economist in his own way understood the essence of the phenomenon of “welfare” and with his research ensured the future of economic research in the field of achieving sustainable economic growth.

We said that in the classical period, economic thought did not contain a special idea about economic growth, which later became a special area of research about the laws of motion, the

management of economic progress, a state that is associated with the expansion of material production. Growth theory and modern economics are based on aggregate quantitative measurements on a scale unknown in previous eras. In addition, the difference lies in the fact that the government now plays a role far from the one that classical economists predicted for it. Economic growth, for example, for Adam Smith was a faceless force, and government non-intervention was its first condition. Macroeconomics and growth theory developed by modern economists, in contrast, generally recognized that government can play a significant role in ensuring the growth of national wealth.

References

- [1] Ananyin O.I. Ontological premises of economic theories. – M.: Institute of Economics of the Russian Academy of Sciences, 2013.
- [2] Sharaev Yu. V. Theory of economic growth. M.: Publishing house of the State University-Higher School of Economics, 2006.
- [3] Bulgakov S.N. History of economic and social doctrines. – M.: Astrel, 2007.
- [4] Smith A. The theory of moral sentiments: or, An essay towards an analysis of the principles by which men naturally judge concerning the conduct and character, first of their neighbors, and afterward of themselves. To which is added, a dissertation on the origin of languages. 1801, Printed by A. Strahan for T. Cadell - 9th ed.
- [5] Avtonomov V. Model of man in economic science. – St. Petersburg: Economic School, 1998.
- [6] Marshall Alfred. Principles of economics, eighth edition 1842-1924. Publication date. 1997.
- [7] Hausman, Daniel M. (2008). Philosophy of economics. Stanford Encyclopedia of Philosophy.
- [8] Schumpeter, J.A., The Theory of Economic Development: An Inquiry into Profits, Capital, Credit, Interest and the Business Cycle, New Brunswick (U.S.A) and London (U.K.): Transaction Publishers. 1934 (2008),
- [9] Domar E. D. Expansion and Employment // The American Economic Review. 1947. Mar. Vol. 37. № 1.
- [10] Kirshin I.A. The formation of the modern theory of economic growth. – Kazan: Kazan State University named after. V. I. Ulyanova-Lenina, 2006.
- [11] Blaug, Mark. Economic theory in retrospect (1962)
- [12] Palley T. I. Growth Theory in a Keynesian Mode: Some Keynesian Foundations for New Endogenous Growth Theory //Journal of Post-Keynesian Economics. 1996. Vol. 19. № 1.
- [13] Aristotle, Physics/ Written 350 B.C.E// Translated by R. P. Hardie and R. K. Gaye
- [14] Clark N., Juma K. Long-term economics: An Evolutionary approach to economic growth. L.; N.Y., 1987
- [15] Tenyakov I.M. Modern economic growth: sources, factors, quality: Monograph. – M.: Faculty of Economics of Moscow State University named after M.V. Lomonosov, 2015.
- [16] Kuznets Simon, «Modern economic growth: findings and reflections». Nobel lecture delivered in Stockholm, Sweden, December 1971, and published in the American Economic Review 63 (September 1973).
- [17] Glazyev S. Yu. Theory of long-term technical and economic development. M.: Vldar, 1993.
- [18] Glazyev S. Yu. The Great Digital Revolution: Challenges and Prospects for the Economy of the 21st Century // [Electronic resource]. Access mode: <https://glazev.ru/>
- [19] List, Friedrich. Das nationale System der politischen Ökonomie.
- [20] Leontiev K. N. / Selected works in 3 volumes. Volume 1 - Moscow: Yurayt Publishing House, 2023. Text: electronic // Educational platform Yurayt [site]. URL: <https://urait.ru/bcode/513553>

DEVELOPMENT OF MOLECULAR GENETIC APPROACHES TO PREDICT THE OCCURANCE OF FOCI OF BACTERIAL DISEASES IN FOREST ECOSYSTEMS

Lyubov Ivashchenko^{1,2}, Stanislav Panteleev², Oleg Baranov³

¹ Belarusian State Technological University

² Forest Institute of the NAS, Belarus

³ National Academy of Sciences, Belarus

lyba281997@mail.ru

stasikdesu@mail.ru

betula-belarus@mail.ru

Abstract

In the course of the study, specific primers were developed to identify 20 species of phytopathogenic bacteria from 12 genera associated with the occurrence of infectious diseases in seven forest-forming species of Belarus. The results showed that the developed oligonucleotides are specific for the 16S (mtDNA and cpDNA) and 23S rRNA genes of the studied phytopathogenic bacteria. At a further stage of research, in vitro tests will be carried out to establish the effectiveness of diagnosing bacterial marker loci, both using pure cultures of pathogen isolates and samples of affected tissues of woody plants.

Keywords: primers, bacterial diseases, marker locus

I. Introduction

In the international practice of plant protection on forest woody plants, several dozens bacterioses with varying degrees of damage are described, caused by representatives of the genera *Pseudomonas*, *Xanthomonas*, *Enterobacter*, *Erwinia*, *Agrobacterium*, *Brenneria*, *Xylella*, *Lelliottia*, *Rhizobium*, *Corynebacterium*, *Bacillus*, *Clostridium*, etc. At the same time, bacterioses equally affects forest woody plants in natural plantations, forest cultures, on field strips, in urban, park and forest park plantings, etc. Currently, certain bacterial diseases are known in almost all species of forest woody plants [1].

One of the modern highly effective methods for diagnosing bacterial diseases of woody plants is the use of molecular genetic analysis technologies [2]. Despite the obvious advantages of DNA markers over other groups of phytopathological analysis methods (such as early diagnosis of diseases, accuracy of detection and speed of analysis, etc.), work with tree species is characterized by certain specifics, the consideration of which, in most cases, determines the success of identifying pathogens [3]. At the same time, the choice of the optimal analysis approach is necessary for each element of diagnostics: sampling, selection of DNA marker regions and a method for their study.

The general principles of diagnosing pathogens of infectious diseases are reduced to the identification of the genetic material of the pathogen in the tissues of the host plant [2]. At the

same time, most phytodiseases of woody plants are of a complex nature and are associated not with a single pathogen, but with a multispecies complex, including pathogenic, conditionally pathogenic, and saprophytic microflora. At the same time, the obtained data on the species and quantitative composition of microorganism associations during direct assessment under in planta conditions are more accurate than indirect molecular genetic diagnostics through the stage of obtaining pure cultures of pathogen isolates [2]. The analysis of potential sources of infection is characterized by a similar basic principle: soil, water, air, scrapings, dust, plant debris, etc. It should also be noted that the most optimal approach to analysis is direct typing of associations, which subsequently allows them to be divided into separate types, to conduct identification and establishment of the species abundance of each taxon in the microflora.

The most reliable way to study pathogen associations is to use the metagenetic approach, which analyzes materials obtained as a result of the simultaneous diagnosis of marker loci of all microorganisms present in an infected sample [4]. The main difference when using the metagenetic approach is the accounting and quantitative assessment of microorganisms that are not cultivated under artificial conditions, which have a pronounced specialization in living tissues of microorganisms along with cultivated ones.

As shown by numerous molecular phytopathological studies, in most cases, plant tissues, regardless of the degree of infectious load, despite the multispecies nature of the identified associations, are characterized by the largest proportion of one or more dominant alternative types of pathogenic and opportunistic microflora [5]. At the same time, stable associations are noted for dominant infectious agents that correlate with certain types of diseases and the nature of plant damage: single, focal and epiphytotic forms, which indicates the leading role of species communities, rather than individual types of pathogens, in the development of plant diseases.

Over the past decade, for a large number of economically important phytopathogenic bacteria, some fragments of their genome, including barcoding loci based on rRNA genes and enzymes of primary metabolism, have been deciphered [6]. The advantage of barcoding loci is their conservatism within the same species, which makes it possible to determine the taxonomic affiliation of the infection. Currently, the nucleotide sequences of barcoding loci for various species are presented in the databases of the Gene Banks, and the amount of this information is updated daily [7]. However, despite the availability of an electronic reference resource for species identification, the use of only the presented genetic information as the main criterion for taxonomic typing has a number of limitations: for a number of species of forest phytopathogens, information in the database is missing or incomplete; some of the deposited specimens have a disputed specific designation; the presented variability of isolates is individual and does not reflect the entire spectrum of intraspecific polymorphism.

Based on the foregoing, the purpose of this work was to develop a molecular genetic approach for the early diagnosis of bacterial infections of forest tree species, which ensures the prediction of the occurrence of disease foci in plantations.

II. Materials and methods

382 sequences were selected as starting material for bioinformatics studies from the NCBI GenBank international database. related to the 16S and 23S rRNA genes of 20 species of phytopathogenic bacteria from the genera *Brenneria*, *Erwinia*, *Gibsiella*, *Lelliota*, *Lonsdalea*, *Pantoea*, *Pectobacterium*, *Pseudomonas*, *Rahnella*, *Ralstonia*, *Xanthomonas*, *Xylella* associated with the formation of infectious diseases in seven forest-forming species of Belarus: pine, spruce, oak, birch, alder, ash, aspen. Deposits of orthologous mtDNA and cpDNA loci of these rocks were additionally analyzed.

Alignment and analysis of nucleotide sequences was performed using the Sequence Viewer

6.3 software package (Qiagen, USA); primer structure was developed using the NCBI Primer Blast online service (<https://www.ncbi.nlm.nih.gov/tools/blast>).

The functionality of the designed primers was evaluated using the Primer Blast module in the NCBI GenBank nucleotide sequence database [<https://blast.ncbi.nlm.nih.gov/Blast.cgi>].

III. Results

The sizes of the 16S rRNA locus varied significantly among the studied bacterial species, from 1473 bp (*Agrobacterium tumefaciens*) before 1553 bp (*Bacillus pumilus*). The value of the homologous 16S rRNA gene in the mitochondrial genome of woody plants also changed significantly and ranged from 1788 (*Pinus sylvestris*) to 1950 (*Quercus robur*) bp. The increase in the size of the mt16S rRNA genes is due to the presence of five polynucleotide insertions, the size of some of them could reach 349 bp. The study of the 16S rRNA loci of the chloroplast genomes of the analyzed plants showed that their length did not depend on the taxonomic affiliation and was equal to 1491 bp. The decrease in the length of the cp16S rRNA gene compared to the bacterial homologue is due to the presence of four oligo(poly)nucleotide deletions of 9, 10, 11, and 22 bp in size in the inner part of the sequence.

In the structure of the 16S rRNA gene of all studied bacterial species, nine (V1–V9) variable regions with conserved regions located between them were identified. It should be noted that the marked polymorphic regions were clearly expressed when comparing bacterial species. At the same time, interspecies differences in cp16S rRNA did not exceed 0.5 per 100 nucleotides within divisions and 2.5 per 100 nucleotides between divisions. For mt16S rRNA, the level of differentiation between divisions could reach 24%, and within divisions, 4%.

The study of the results of the alignment of the nucleotide sequences of the 16S rRNA gene of bacteria and cpDNA of plants showed that in most cases, significant structural differences between the groups were related to the variable regions of the Bacteria locus, which did not allow the development of specific primers for the diagnosis of phytopathogenic microorganisms (Fig. 1).

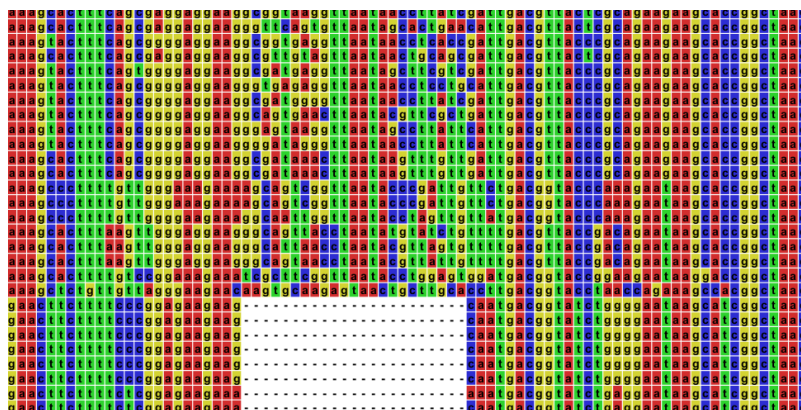


Fig. 1: The deleted region of the 16S rRNA cpDNA gene common to plants (in bacteria, it is represented by a polymorphic region)

Structural differences between bacterial 16S rRNA genes and plant mitochondrial genomes have been associated with large insertions in eukaryotic organisms. At the same time, the general nature of the revealed differences between plant organelles indicates their origin from systematically unrelated groups of microorganisms in the course of phylogenesis. The revealed high level of differences in the structures of the mtDNA 16S rRNA gene between gymnosperms and angiosperms may indicate a polyphyletic origin of mitochondria. The above structural features of the 16S rRNA gene in plant organelles did not allow us to identify discrete nucleotide regions that are structurally characteristic of eukaryotic organisms and distinguish them from

bacteria.

Based on the analysis of the structural features of the nucleotide sequences of the 16S rRNA mtDNA and cpDNA genes of plants, a design of oligonucleotide primers was developed that allows selective diagnosis of the genetic material of phytopathogenic bacteria in infected tissues of the studied species of forest woody plants: cpF AGATACCCTGGTAGTCCAC and cpR ATTACTAGCGATTCCRRCTT (the size of the amplified fragment is \approx 560 bp.), as applied to nucleic acid preparations containing plant cpDNA; mtF TGARATGTTGGGTAAAGTCCCG and mtR TACAAGGCCCGGGAACG (amplified fragment size \approx 320 bp), as applied to nucleic acid preparations containing plant mtDNA.

The study of the 23S rRNA gene in various bacterial species showed that its size also varied to a large extent, from 2877 bp (*Ralstonia solanacearum*) up to 3037 n.b. (*Brenneria goodwinii*). The value of the homologous 23S rRNA gene in the mitochondrial genome of woody plants also changed significantly and ranged from 3149 (*Pinus sylvestris*) to 3416 (*Quercus robur*) bp. For chloroplast genomes, within the studied angiosperm species, the value of the 23S rRNA gene was constant and equaled 2810 bp. For coniferous plants, the gene size was slightly smaller and amounted to 2802 bp. for *P. sylvestris* and 2806 bp for *Picea abies*.

The main differences in the structure of bacterial and plant (chloroplast) 23S rRNAs were associated with the edge regions of the genes. At the same time, in the case of most bacterial genes (when compared with similar ones in cpDNA), the presence of structural regions at the 5' end of the sequence and the absence at the 3' end of the sequence were observed (Fig. 2).

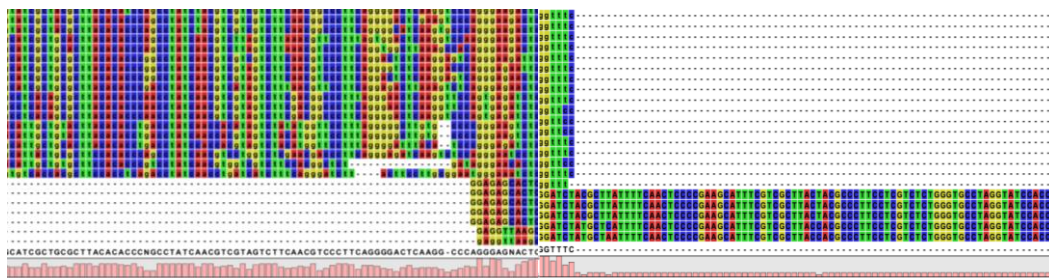


Fig. 2: Alignment results for the 23S rRNA gene of bacteria and plant cpDNA (5' - region on the left, 3' - region on the right)

In addition, oligo (up to 5 bp) and polynucleotide (up to 30 bp) deletions in relation to bacterial species were found in the inner part of plant genes.

A comparative analysis of the 23S rRNA gene of bacterial species and plant mtDNA showed that the main differences in the size of these loci are associated with the presence of a significant number of oligo- and polynucleotide deletions/insertions located in the central part of the sequences.

Based on the analysis of the structural features of the nucleotide sequences of the 23S rRNA gene, 20 different variants of oligonucleotide primers were developed for diagnosing the genetic material of bacteria in infected tissues of forest woody plants.

The functionality of the developed primers with respect to the 16S and 23S rRNA genes was tested in silico using the Primer Blast module in the NCBI GenBank database of nucleotide sequences. On fig. 3 shows the results for the mtF and mtR oligonucleotide pair.

— Detailed primer reports

Primer pair 1

	Sequence (5'→3')	Length	Tm	GC%	Self complementarity
Forward primer	TGCAACTCGACTGCGTGAAGTCG	23	65.75	56.52	8.00
Reverse primer	TACAAGGCCCGGAACG	17	58.93	64.71	6.00

Products on target templates

>CP125300.1 **Pseudomonas syringae pv. syringae** strain B48 chromosome, complete genome

product length = 80

Forward primer	1	TGCAACTCGACTGCGTGAAGTCG	23
Template	946820	946842
Reverse primer	1	TACAAGGCCCGGAACG	17
Template	946899	946883

>OP9901 **9.1 Brenneria sp. strain MBWS3 (1) 16S** ribosomal RNA gene, partial sequence

product length = 80

Forward primer	1	TGCAACTCGACTGCGTGAAGTCG	23
Template	973C.A.....	995
Reverse primer	1	TACAAGGCCCGGAACG	17
Template	1052	1036

>CP10185 **1 Xanthomonas oryzae pv. oryzae s** strain YNCX plasmid pYNCX4, complete sequence

product length = 80

Forward primer	1	TGCAACTCGACTGCGTGAAGTCG	23
Template	3878C.....	3856
Reverse primer	1	TACAAGGCCCGGAACG	17
Template	3799	3815

Fig. 3: Results of testing a pair of primers mtF and mtR in NCBI Primer Blast

As can be seen from fig. 3, the primers are specific for representatives of the genera mentioned above and do not work for plants, which makes it possible to use them for the identification of bacteria in samples of diseased tissues of woody plants. Similar results were obtained when testing a pair of primers cpF and cpR.

As a result of the testing of primers designed on the basis of the nucleotide structure of the 23S rRNA gene, two pairs of oligonucleotides were selected in silico, allowing amplification of 331 and 589 bp fragments: 23S-BacSpF1 (AAACACGAAAGTGGACGTAT) and 23S-BacSpR1 (CTCCCCACCTATCTACACA); 23S-BacSpF2 (GAAGTGC GAATGCTGACA) and 23S-BacSpR2 (ATACGTCCACTTTCGTGTTT).

The results obtained showed that the primer pairs are specific for the 16S (mtDNA and cpDNA) and 23S rRNA genes of representatives of the genera *Bacillus*, *Brenneria*, *Erwinia*, *Gibsiella*, *Lelliota*, *Lonsdalea*, *Pantoea*, *Pectobacterium*, *Pseudomonas*, *Rahnella*, *Ralstonia*, *Xanthomonas*, *Xylella*. The specificity for representatives of the genera mentioned above and the inability to amplify homologous loci in plants makes it possible to use them for the identification of bacteria in samples of affected tissues of woody plants. At the same time, parallel sequencing or t-RFLP analysis are possible for carrying out metagenetic analysis.

IV. Conclusion

The article proposes a modern approach for predicting the occurrence of foci of bacterial diseases in forest plantations, which allows for rapid and efficient identification of bacterial species and their communities in the tissues of affected woody plants based on the use of specific primers for the 16S and 23S rRNA genes of phytopathogenic bacteria. At the next stage of the research, *in vitro* tests will be carried out to study the effectiveness of diagnosing marker loci of phytopathogenic bacteria, both using pure cultures of pathogen isolates and samples of affected plant tissues of the main forest-forming species of Belarus, characterized by symptoms of bacterial diseases.

References

- [1] Goychuk, A. et al. (2023). Bacterial Diseases of Bioenergy Woody Plants in Ukraine. *Sustainability*, 15(5): 4189. doi: 10.3390/su15054189.
- [2] Dyakov, Yu.T. (2001). General and molecular phytopathology. *Moscow: Society of Phytopathologists*, 301 p.
- [3] Padutov V.E., Baranov O.Yu., Voropaev E.V. (2007). Methods of molecular genetic analysis. *Minsk: Unipol*, 176 p.
- [4] Charles T. (2010). Metagenomics: Theory, Methods and Applications. *Caister Academic Press*, 212 p.
- [5] Baranov O.Yu., Panteleev S.V. (2012). Molecular genetic diagnosis of fungal diseases in forest nurseries. *Forestry and hunting*, 6: 21–29.
- [6] White, T.J. (1990). Amplification and direct sequencing of fungal ribosomal RNA genes for phylogenetics. *PCR protocols: a guide to methods and applications*, 315–322.

MAIN TRENDS IN CLIMATE CHANGE IN THE HOLOCENE EPOCH OF THE ANTROPOGENIC PERIOD IN THE WORLD AND IN THE CAUCASUS

Arun Daukaev¹, Rustam Gakaev², Tumisha Bachaeva¹

•

¹ Kh. Ibragimov Complex Institute of the RAS Russia

²Kadyrov Chechen State University, Russia

daykaev@mail.ru

rustam.geofak@yandex.ru

Abstract

The article is devoted to the problem of climate change on Earth, and in particular in the Caucasus. The main trends in climate change are traced during the Holocene epoch of the Quaternary period. Attention is focused on the most noticeable periods of cooling and warming - the medieval warming period, the Little Ice Age, the newest warming period, which began at the end of the 19th century. The issue of global warming is also touched upon.

Keywords: climate, Holocene era, ice age, global warming, Caucasus, greenhouse effect

I. Introduction

Climatic changes have occurred in almost all geological eras. Climate change is recorded by paleontological finds (changes in fauna and flora), changes in archaeological cultures, etc. etc. However, the use of archaeological data for the stratification of sediments and the study of other issues is possible only for the Anthropogenic (Quaternary) period, since the most important event - the appearance of man - is associated with this period [1-2]. Fossil remains and traces of human material culture are the guiding paleontological finds for individual divisions of the Quaternary period, which makes it possible to use the archaeological method together with the paleontological method for research purposes in various fields of knowledge, including climatology.

II. Methods

The Anthropocene (Quaternary) period is divided into the Pleistocene and Holocene eras. The Holocene is a modern geological era that began after the Pleistocene, approximately 11-15 thousand years ago. The Pleistocene era, in turn, is divided into a number of glacial and interglacial stages: the Günz, Mindel, Ris and Würm glacial; Günz-Mindel, Mindel-Ries, Riess-Würm interglacial stages [Ist. geology]. Based on its characteristic climatic features, the Holocene is usually classified as an interglacial era due to its many similarities with more ancient interglacial eras [3-4]. The main trend of Holocene climate change was the transition from the cold climate of the end of the Pleistocene to a warm one with maximum warming about 6 thousand years ago. In general, the Holocene climate was quite stable, although, as many researchers note, it was very diverse.

III. Results

The Holocene is an era in the Quaternary period of the Cenozoic era. According to the decision of the VIII Congress of the International Association for the Study of the Quaternary Period (Paris, 1969), the lower boundary of the Holocene is considered to be 10 thousand years ago. (11700±99 years relative to 2000). The period of time between the end of the last Würm glaciation (17 thousand years ago) and the beginning of the Holocene (10 thousand years ago) is called the Late Glacial.

Rising temperatures, melting glaciers and destruction of ice sheets began 16,000 years ago. This climate warming was global in nature [5]. It was accompanied by the degradation of the Würm ice sheets of Europe and North America, but this process was not monotonous. The Late Glacial period was characterized by an extremely unstable climate: warming periods, called Raunis (Ra), Bølling (Bø) and Allerød (A1), were interrupted by five sharp and deep cold snaps - Port-Bruce, Dryas I (13.2 thousand years ago), Fjoros- Neva (12.8 thousand years ago), Dryas II (12.2 thousand years ago) and the most severe cooling of Dryas III about 10.8–10.5 thousand years ago. During the Bølling and Allerød warming periods, air temperatures in temperate latitudes were close to modern ones or even slightly higher [6]. In Western Europe and Taimyr, forest vegetation was restored. However, during cold snaps and especially during the Dryas III, landscapes returned to the time of the maximum of the Würm glaciation: in North-West Europe, in Britain and in the north of the Russian Plain, forests degraded and were replaced by vegetation of cold steppes and tundra. In Siberia, during Dryas III, woody vegetation retreated southward by 700–800 km, and the temperature dropped by 5–6 °C compared to modern times. The cooling was global in nature, its traces were noted in South America, New Zealand and Antarctica.

New global warming began about 10.3–10.2 thousand years ago. Thus, the Holocene began with intense warming. As a result, the disappearance of the Scandinavian ice sheet occurred about 8.5 thousand years ago, and the North American ice sheets - about 6.5 thousand years BC. In the boreal period, taiga forests continued to push the tundra to the north [7]. They were followed by deciduous forests, which occupied Southern and partly Northern Europe. Remains of the Laurentian Ice Sheet persisted on the Ungava Peninsula until 5.5 thousand years ago.

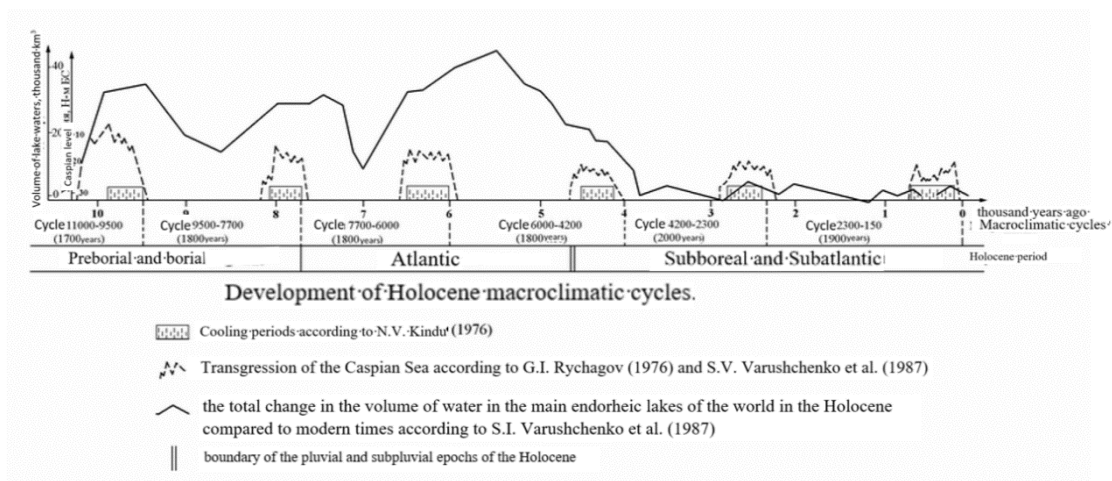


Fig. 1: Development of Holocene macroclimatic cycles

Some researchers, based on paleoclimatic studies, note that the humid, warm climate (humid) characteristic of the 4th millennium BC. during the 3rd millennium BC changed to hot and dry (arid) [Idrisov, 2010]. By the middle of the 3rd millennium BC. The sedentary agricultural Kura-

Araks inhabitants are replaced by new ones with a completely different economic structure [cit. according to Kornienko, 2013].

Many other researchers also connect changes in archaeological cultures with those in climate [Munchaev et al., 2012]. Warm period since 250 BC to 400 AD known as the Roman Climatic Optimum. This period marked the rise of the Roman Empire [8].

IV. Discussion

Period from the 7th century. (according to other sources from the 10th century) to the 13th century is called the medieval warm period, or in another way, the medieval climatic optimum. This era of relatively warm climate in the northern hemisphere was characterized by mild winters, the expansion of arable land, and a marked increase in agricultural production and population [9]. According to some American scientists, as a result of prolonged droughts during this period, the death of the classical Mayan civilization occurred[Average climate.optimum]. In the Caucasus, there was a significant reduction in the glaciers of the Greater Caucasus, the replenishment of mountain rivers with water (due to the melting of glaciers), a drop in the level of the Caspian Sea, the formation of deflation basins and other processes characteristic of periods of climate warming [Phys. geog. CR, 2006].

And the time from the 14th century to the middle of the 19th century. called the Little Ice Age, when the volume of soil cultivation and pastures was significantly reduced. During this period, the advance of glaciers and an increase in their size were observed everywhere [10-11]. In 2021, B. Fagan published a book entitled "Little Ice Age: How Climate Changed History. 1300 - 1850"[2021]. However, some researchers, in particular A.S. Monin et al. consider this name inappropriate, based on the fact that during the designated historical time there was no continuous period of cooling [Monin et al., 1979]. The Little Ice Age in the Caucasus was manifested by the rise of the Caspian Sea, the weakening of the continental climate, an increase in the amount of precipitation and other signs [Phys. geog. CR, 2006].

After this period from the end of the 19th century. a period of warming began, which manifested itself especially strongly in the 20-30s. XX century During this period, in many regions of the world (in the Caucasus, Pamirs, Tien Shan, Altai, Himalayas, etc.) there was a retreat of glaciers with a reduction in their areas. Thus, the area of glaciers in the Caucasus from 1890 to 1946 decreased by 8.5% [inter.res.Modern climate.]. According to other data, in particular according to the results of long-term monitoring by the High Mountain Geophysical Institute (Nalchik), the area of glaciers in the Greater Caucasus has decreased by 40% over the past 100 years.

But already in the 1940s. the warming process gave way to cooling, the peak of which occurred in the mid-1960s. By the beginning of the 1960s. The area of glaciers has increased significantly.

Since the 1970s a new stage of warming has begun, which continues to this day [Internet resource; Monin, 1979]. Since the 1990s There was an increase in precipitation, a rise in the levels of the Caspian Sea and groundwater, a reduction in the area of glaciers, etc [12]. During this period, information appears about future global warming of the Earth's climate. Currently, there are different versions of the causes and possible consequences of climate change.

First version. The climate on Earth is changing due to human activities. Warming is recorded with an increase in the scale of production using hydrocarbon fuels, which leads to the so-called greenhouse effect.

Second version. Global warming is not associated with the consequences of human industrial activity, but is associated with cosmogenic causes.

Third version. Global warming is associated with the synergy of technogenic (greenhouse effect) and cosmogenic factors (natural process) [13]. According to academician V.M. Kotlyakov, the greenhouse effect exists, but it is impossible to determine its share in global climate change. The main contribution to the greenhouse effect comes from carbon dioxide. Its reduction to a certain extent can be achieved by partially replacing traditional energy sources based primarily on the use of hydrocarbon raw materials with non-traditional renewable ones. The main global agreement to combat global warming is the Kyoto Protocol of 1997, obliging the industrialized countries of the world to reduce CO₂ emissions [Global warming...Internet resource].

Thus, climate change is primarily a natural process that has been observed in all geological periods. At the same time, the technogenic factor plays a certain role in climate change. In the Holocene era, after a series of glacial and interglacial periods in the previous Pleistocene era, a number of long periods of warming and cooling were observed, replacing each other. In turn, they included short-term episodic phases of cooling and warming. The last phase of warming, as noted above, began in the 1970s, which continues to the present day.

Acknowledgments. The work was carried out within the framework of the state assignment of the Ministry of Science and Higher Education of the Russian Federation (topic No. 075-03-2021-074 / 4).

References

- [1] Gakaev R. A., The role of climatic conditions in the activation of landslides in the Mountainous part of the Chechen Republic, 2012, 4(13), pp. 9-12.
- [2] Kudusov I.I., Climate change and carbon sequestration during the intensification of agricultural production, 2022, pp. 139-143
- [3] Leonov G.P., Historical Geology, 1956, p. 364
- [4] Idrisov I.A., Climate change in Dagestan in the second half of the Holocene, 2010, 2, p.58
- [5] Kornienko T.V., Questions of linguistic kinship, 2013, 9, pp. 155-162.
- [6] Munchaev R.M., Amirov Sh.N., Once again about Mesopotamian-Caucasian connections in the IV-III thousand years ago. BC, 2012, 4, pp. 37-46.
- [7] Materials of glaciological research, 1989, 67, pp. 103-108.
- [8] Fagan B., The Little Ice Age: How Climate Changed History. 1300 -1850, 2021.
- [9] Monin A.S., Shishkov Yu.A. Climate History, 1979, p. 408
- [10] Bitkaeva L.Kh., Physical geography of the Chechen Republic, 2006, p. 128
- [11] Krivenko V. G., Conservation of Russian reservoirs as a source of fresh water from the perspective of the concept of climate variability, 2021
- [12] Gakaev R., Sequestration of carbon in soil on the example of forest cenoses in the Chechen Republic, 2022, 2650, 030002
- [13] Gakaev, R., Bakhaev, M.-S., Edisultanov, S. Global climate policy trends and challenges for Russia. Reliability: Theory and Applications, 2022, 17, pp. 450–457

THE ESTIMATED REASON FOR THE LOW EFFICIENCY OF HYDROCYCLONES IN PETROLEUM INDUSTRY

Gafar Ismayilov, Amrah Gulubayli, Samir Musayev, Shafa Musayeva

Azerbaijan State Oil and Industry University

asi_zum@mail.ru

emrah_gulubeyli@yahoo.com

musasf@bp.com

shafamusayeva@mail.ru

Abstract

The real media encountered in oil and gas production are usually dispersed, i.e., they are systems consisting of at least two phases, with one of the phases being distributed into the other. Production, collection and transportation of oil and gas are based on multiphase technology, including the processes of lifting from the reservoir, transportation to separation points, separation and infield transport of multiphase mixtures, which consist of oil, gas, formation water and mechanical impurities.

In most technological processes of oil and gas production and transport of hydrocarbons, the separation of dispersed systems is necessary. In practice, the unsuitability of hydrocyclone technology for separating emulsions has been established, although hydrocyclones are effectively used for cleaning suspensions, for separating solid particles from liquids, for example, for cleaning drilling fluids from sludge.

Recent studies have established that cylindrical multiphase flows are based on the interaction of continuous and dispersed phases, the driving force of which is an additional shear force directed towards the flow axis.

In the paper, according to the multiphase technology, the reason for the low efficiency of hydrocyclones for multiphase disperse systems was analyzed. The condition of equality of the shear and centrifugal forces during the operation of the hydrocyclone is shown. It has been established that, based on the correct choice of technological parameters, it is possible to avoid the negative effect of the shear force in cylindrical flows on the operation of hydrocyclones.

Keywords: Dispersed systems, hydrocyclone, multiphase flow, shear force, phase interaction, suspension

I. Introduction

As it is known, oil and gas extraction, gathering, transportation to processing sites, separation, as well as oil, gas, formation water and mechanical particle cleaning processes are based on multiphase technologies.

Dispersed multiphase systems are also found in industry as aerosols, mists and suspensions, which can be classified according to the particle size of the dispersed phase.

For most technological processes of oil and gas production and transportation of hydrocarbons it is necessary to separate the dispersed systems. Depending on the type of disperse system, the following methods of separation can be used: sedimentation, filtration, centrifugation and flotation.

Centrifugation is a method of separating heterogeneous, disperse liquid systems into fractions by density under the action of centrifugal forces. Centrifugation is carried out in centrifuges, the

principle of which is based on creating a centrifugal force, which increases the speed of separation of the mixture components compared to the speed under the influence of gravity. The separation of substances by means of centrifugation is based on the different behavior of particles in the centrifugal field. Particles with different density, shape or size are deposited at different speeds.

From the physical point of view, separation of heterogeneous systems by centrifugation can be considered as a process of free or constrained deposition of suspended particles in a liquid under the action of a centrifugal force. Suspended particles can be solid or liquid.

Centrifugal force is generated by the rotation of the centrifuge and the liquid in it. Centrifugal forces also cause separation in hydrocyclones, which differ in design from centrifuges. A distinction should also be made between cyclones and hydrocyclones. Cyclones are used for dust collection and gas purification and hydrocyclones for slurry purification.

In hydrocyclones, when the mixture to be separated enters it tangentially through the inlet nozzle and acquires circular motion, significant centrifugal forces arise, which many times exceed gravity, and under the action of which the heavier phase moves from the hydrocyclone axis to its walls on a spiral trajectory and downwards through walls and is discharged through the bottom nozzle from the hydrocyclone. The lighter phase moves in an upward along the axis and is discharged from the hydrocyclone through the upper product outlet. Close to the hydrocyclone axis, the centrifugal forces increase so much that an air column appears due to a liquid rupture.

In the oil industry, researchers [1-3] studied the issues of application of hydrocyclones for separation of water-oil emulsions. However, to this day, the issues of increasing the driving forces of separation in some cases raise doubts on the efficiency of operation of hydrocyclones. Practically, the unsuitability of hydrocyclone technology for separation of emulsions is established, although hydrocyclones are effectively used for separation of mechanical impurities from gases and air, for separation of solids from liquid, for example, for cleaning of drilling fluids.

II. Problem of research

The reason for the low efficiency of hydrocyclones for the separation of water-oil emulsions can be explained based on the theory of gradient-velocity field dynamics and the mechanism of phase interaction during their separation can be explained.

As it is known, the rate of separation of heterogeneous systems in the field of centrifugal forces is higher than the rate of separation of these systems in the field of gravity. Centrifugal force arises as an inertial force during the rotation of objects and is always directed radially outward from the axis of rotation.

In general case, the centrifugal force (F_c) is expressed by the following equality:

$$F_c = \frac{mv^2}{r} \quad (2)$$

Where, m-mass of the rotating particle,

r – radius of rotation, m,

v – is the circumferential speed of rotation, which is equal to:

$$v = \frac{2\pi nr}{60} \quad (3)$$

Where, n-number of revolutions per minute.

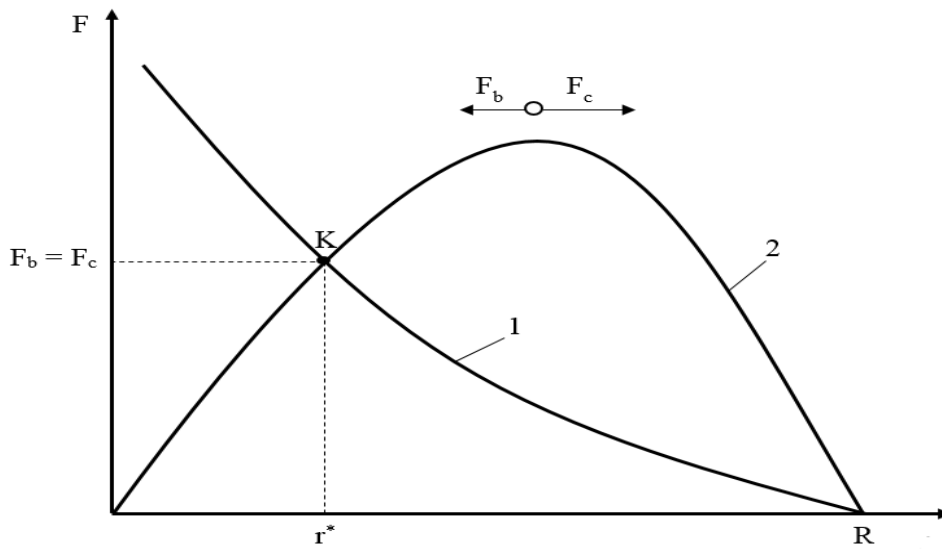
Given (2) to determine the centrifugal force can be written:

$$F_c = 1.85 \cdot 10^{-3} \pi d^3 \rho_p n^2 \cdot r \quad (4)$$

Here d and ρ_p -are respectively the diameter and density of the rotating particle.

Graphs of the distribution of driving forces of separation of multiphase water-oil mixtures in the hydrocyclone can be represented as in Fig. 1. As can be seen from Fig. 1, line 1, which characterizes distribution of centrifugal force increases with decreasing distance to the cyclone axis. Line 2 characterizes the distribution of Bernoulli forces, which has a maximum at a 0.577R distance from the cyclone axis (R is the cyclone radius). It is also seen from Fig. 1 that these forces

are opposite forces, as a result, when Bernoulli force exceeds centrifugal force (F_s) dispersed water drops move to cyclone's axis but not to its walls. As a result of counteraction of the noted forces, it is not always possible to obtain in the hydrocyclone the components of the mixture in pure form.



1- Centrifugal force. 2- Bernoulli force

Fig. 1: Driving forces of hydrocyclones

III. Solution of problem.

In view of the above, the conditions of equality of Bernoulli force and centrifugal force in the hydrocyclone were analyzed. Bernoulli force in the general case according to the equation of the second law of mechanics in the presence of dispersion medium of mechanical particles with diameter (d) can be determined by the following formula [4,5,6]:

$$F = 8.39\rho d^3 u^2 \alpha(1 - \alpha^2)/D \tag{4}$$

Where ρ - is the density of the dispersion medium kg/m^3 ,
 $\alpha = r/R$

Given that at point K (Fig. 1) the noted forces are equal, then according to expressions (3) and (4) we can write

$$1.85 \cdot 10^{-3} \pi d^3 \rho_p n^2 \cdot r = 13,172 d^3 \rho u^2 r \left(1 - \frac{r^2}{R^2}\right)/R^2$$

After some abbreviations we obtain the following condition for calculating the parameter r^* , corresponding to $F_c \geq F_b$:

$$r \leq R \sqrt{1 - 0.00044 \cdot \frac{\rho_p}{\rho} \cdot \frac{n^2 R^2}{u^2}} \tag{5}$$

Condition 5 will be fulfilled according to the following equation:

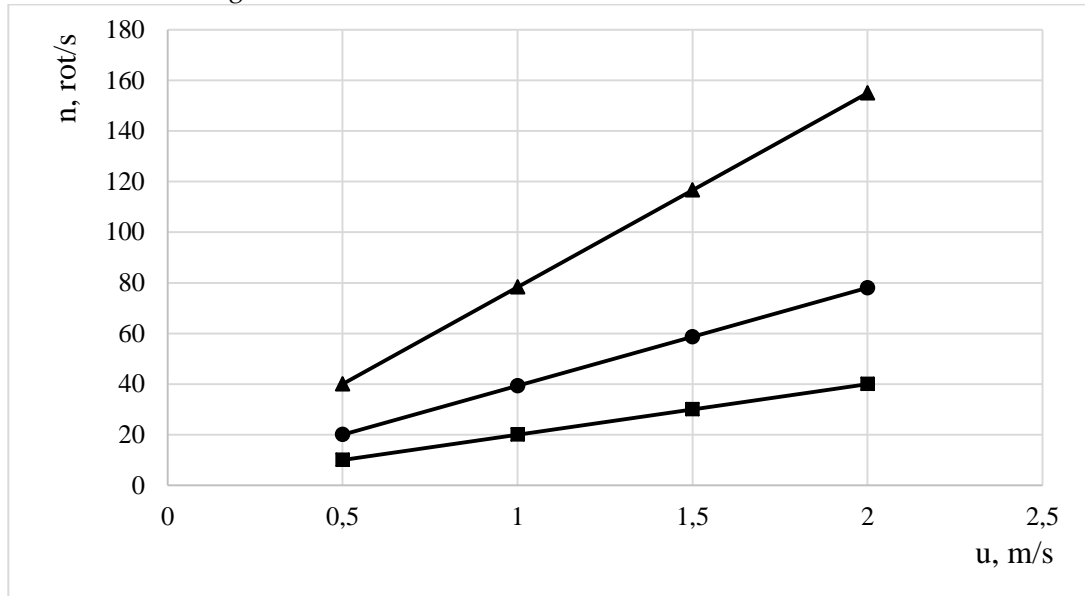
$$n \leq \frac{u}{0.021 \cdot R \cdot \sqrt{\rho_p / \rho}} \tag{6}$$

According to formula (6), we investigated the effect of flow velocity (u), radius of hydrocyclone (R) and the ratio of densities of particles and liquid on the number of rotation n . For this purpose, the calculation of the number of rotation was derived with the following initial data:

- flow velocity $u=0.5; 1.0; 1.5; \text{ and } 2.0 \text{ m/s}$.
- radius of the hydrocyclone $R=0.2; 0.4; 0.6; 0.8; 1.0 \text{ and } 1.5\text{m}$
- ratio of densities $\frac{\rho_p}{\rho} = 1,3; 1,5; 2,0; 2,5$.

Based on the results of the calculations, the dependences $n=f(u)$ and $n=f(R)$ were plotted,

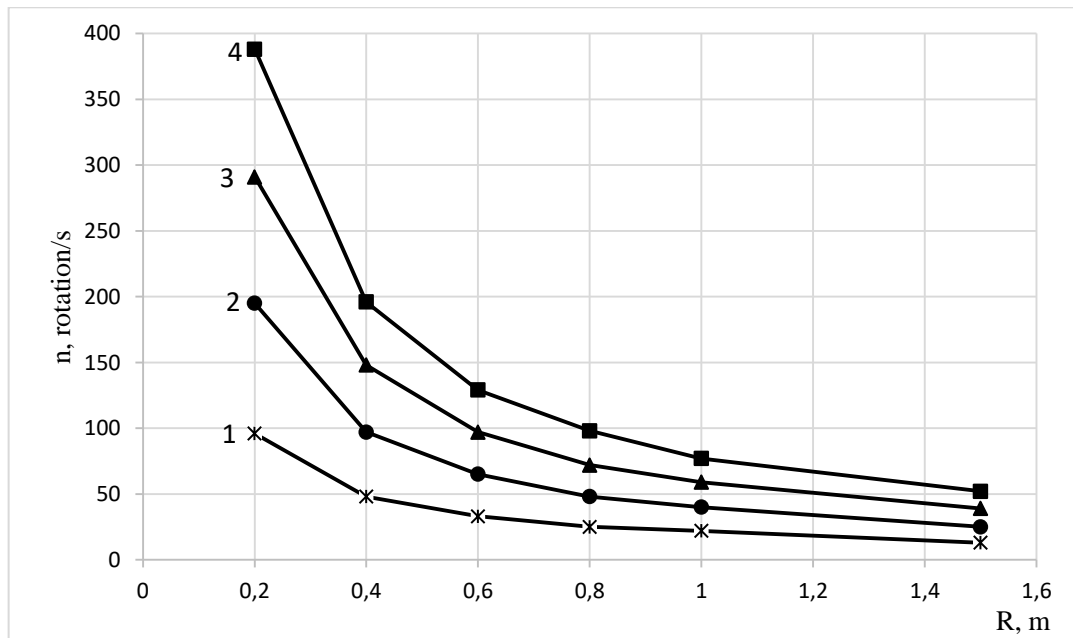
which are shown in Fig. 2.



1 – $R=0.5m$. 2 – $R=1.0m$. 3 – $R=2.0m$

Fig. 2: Dependence of $n=f(u)$

As can be seen from Fig. 2, the number of rotation increases proportionally as the flow velocity increases in accordance with condition (5). At this time, the number of cycles decreases monotonically with the increase of the radius (R) of the hydrocyclone. (Figure 3)



1 – $u=0.5m/s$. 2 – $u=1.0m/s$. 3 – $u=1.5m/s$. 4 – $u=2.0m/s$

Fig. 3: Variation of the number of rotation (n) as a function of R .

It should be noted that, with the help of the constructed dependences, it seems possible to avoid the negative influence of Bernoulli's force on the operation of hydrocyclones based on the choice of the above-mentioned parameters.

IV. Conclusions

According to multiphase technology, the reason of low efficiency of hydrocyclones for separation of multiphase systems was analyzed. It has been determined that, based on the correct selection of technological parameters, it is possible to prevent the negative impact of the force generated along the cross section in cylindrical flows on the operation of hydrocyclones.

References

- [1] Mustafaev A.M., Gutman B.M. Hydrocyclones in the oil industry. Moscow, Nedra. 1981, 260p.
- [2] Ternovsky I.G., Kutepov A.M. Hydrocycloning. Moscow, Nauka, 1994.
- [3] Askhanov R.R., Danilov V.I., Nurmukhamedov N.Kh. Stabilization of oil using hydrocyclone. Ufa. Research Development Fund, 1996, 119 p.
- [4] Sitenkov V.T. The theory of the gradient-speed field. M.; OJSC « VNIIOENG », 2004, 308 p.
- [5] Gafar Ismayilov, Hajar Ismayilova, Hikmet Babirov, Rashid Jabrayilov. Assesment of enviromental oil spills and economic– enviromental risks/ RT&A, special Issue №4 (70) vol.17, November 2022, pp.212-217. DOI: <https://doi.org/10.24412/1932-2321-2022-470-212-217>
- [6] Ismayilov G.G. , Ismayilova F.B. The role of transverse force in multiphase cylindrical flows. INTERNAUKA Scientific Journal Part 2, 34(257), Moscow, 2022, p.5 -9

THE PROBLEM OF POVERTY IN THE MODERN WORLD IN THE CONTEXT OF SUSTAINABLE DEVELOPMENT

Ayna Salamova¹, Saleh Khodjaliev¹, Sergey Dokholyan²

¹Kadyrov Chechen State University, Russia

²Institute of Socio-Economic Problems of Population, Russia

salamova_chgu@mail.ru

Abstract

The problem of poverty is the deepest social issue with a two-hundred year history. During the period of economic reforms in our country, social structure of society has changed since economic reforms took place in our country recently. A rapid social stratification occurred, there were layers of poor and rich people. People who have lost social protection of state and losing need to adapt living in conditions market instability are most common. It is more common that people who lose the social protection of state and losing need to adapt life in conditions of market volatility, as. The expansion of much poor people was inevitable. Because of this conditions, the expansion of many poor people was inevitable. An analysis of poverty used in the middle twentieth century showed its complex and ambiguity. The knowledge of multiple dimensionalities in the phenomenon implies a systematic approach for study about Poverty.

Described figures from official statistics: towards the present time, approximately 40% of us live below this poverty line. It created the choice of topic and its relevance. To study this problem in detail, it is necessary to conduct an in-depth scientific study, a thorough theoretical analysis and the development of practical guidelines based on the presented basis. These guidelines could be used to develop and implement an effective economic and social policy that would undoubtedly be aimed at reducing poverty to the lowest level.

Keywords: problem of poverty, social stratification

I. Introduction

Poverty can be defined "as a condition caused by a lack of material resources to lead a normal life, which is habitual and characteristic of a large part of society." Poverty occurs whenever a part of the population cannot meet the minimum requirements for basic living conditions.

In most cases, poverty, as a socio-economic category, means the inability of an individual to ensure the satisfaction of his basic needs. At the same time, we note that with the development of society, both the composition and level of such needs, as well as the criteria for classifying citizens and households in this category, change [1, p.20].

The 2 types of poverty are there.

1. Absolute poverty provides a person with biological survival because of need for vital resources.

We talk about satisfaction of the basic needs - food, shelter and clothing. Classification for such type of poverty can do not damage much on the time and place where a person's residence occurs. Foods, products came from various countries during the dawn of creation human society and modern man differs significantly. However you can always unambiguously judge whether a person is starving or full. Because, criteria for absolute poverty influenced to biological characteristics.

2. Relative poverty determined by apparison with the standard living that consider “normal” in a given society. Researcher level of living in developing countries over the West estimates obviously higher than regular status among developed countries. Poverty in countries of the developed West often regarded as a luxury for backward states. If necessary examples to assume those who can't have difficulties with food but unable afford higher level needs (education, cultural recreations etc.), The West belongs to the category of poor than ever [1]. Certainly, the criteria for positive poverty consists of social characteristics and vary greatly in different eras or countries.

But it is very common that the poor sometimes rejects themselves, failures and pop up of their social work, apart from new conditions making sense they are entitled to make better life. Extreme factors, especially subjective conditions from state and society played important role in such a “jump”.

II. Methods

Monitoring of poverty is the basis for monitoring the quality and standard living in population, identifying its most vulnerable categories exposed to the risks of social support; development of effective measures that increase income from work and social support for people with low labor potential and high demographic burden on working women. In order to solve a poverty problem and organize proper monitoring, options such as determining the poverty line, determining standards in terms of quality life and standardizations in relation to this level, taking into account the poverty line play an important role. The choices and methods for establishing the poverty line, determining what is required to measure the poverty line, take into account it. An assessment of the living standard for Russians in terms of social policy, federal programs and economic program development; determining minimum wages at an official level. The budget is compiled by collecting data on consumer baskets, mandatory payment systems and wages that are compared to national monetary income. Accordingly, the poor include those whose incomes do not reach this poverty line, i.e., the subsistence minimum. Data on the number of the poor, on the characteristics of their quality and standard of living, their groupings according to various criteria, etc. are tracked and published by the Federal State Statistics Service. Data are presented for the population as a whole, for its individual categories, for households and their various groups.

The most common measurement of poverty in our country corresponds to the absolute monetary method, which is also common in foreign practice and is relatively simple to organize poverty monitoring compared to other approaches. Alternative approaches that have been developed abroad proceed from the fact that poverty identification should not be limited only to the definition through absolute monetary indicators, the problem of poverty is multifaceted and manifests itself not only through the lack of income corresponding to a certain imputed value. The concept of relative poverty, which implies its monetary and non-monetary definition, which has become widespread in the countries of the European Union (EU), the Organization for Economic Cooperation and Development (OECD), and the Commonwealth of Independent States (CIS), allows supplementing the measurement of poverty with alternative estimates. Poverty is fixed in relation to the standard of living common in the country, which, in monetary terms, is set on the basis of median indicators of income (expenditure) (40%, 50%, or 60%), and in non-monetary terms, it is based on indicators of deprivation (deprivation). Third the concept of poverty measurement - subjective - involves the identification of poverty through self-identification, self-assessment of the population, the use of poverty lines determined on the basis of surveys and other methods of identifying the opinions of the population. various manifestations, which makes it possible, accordingly, to more effectively approach the solution of the problem of poverty reduction, complexly “influencing” various measures of social policy on various parameters of the quality and standard of living. For example, in the EU countries, an index is used to identify the risk of poverty and social exclusion, which includes components of relative monetary poverty,

material deprivation and employment. The United Nations Development Program (UNDP) monitors based on the Multidimensional Poverty Index, which makes it possible to examine deprivations in ten indicators according to three dimensions - education, health care and standard of living.⁷ Methods alternative to the absolute monetary approach to measuring poverty in our country, although being introduced into official statistics, are used more for research purposes, and not for official monitoring of poverty.

III. Results

Causes of poverty are considered under example in cool study “Rich and poor as Modern Russia” case we have four questions, which had answers (so there were several such applications). In the case of our question, which gave answers (so there were several such applications). According to the fact that after answering questions, all respondents gave an expert account of the reasons for poverty in modern Russia.

Table 1: Russians’ assessment of the causes of poverty of their personal acquaintances¹², in %

	Overall in Russia	Poor (ILS less than 0)
Long-term unemployment 41.2 42.4	41.2	42.4
Non-payment of wages at the enterprise, delayed pensions	46.9	47.2
Family troubles, misfortunes	25.0	25.3
Illness, disability	36.8	44.2
Alcoholism, drug addiction	34.9	34.2
Low standard of living of their parents	20.5	20.9
Living in a poor region (district, city, locality)	17.4	16.8
Lack of support from relatives, friends, acquaintances, loneliness	20,1	23,2
Insufficiency of state benefits for social. security	37,2	42,6
Laziness, inability to live	22,6	14,6
Poor education, low qualifications	22,5	18,5
Having a large number of dependents	17,2	20,0
They are migrants, refugees	5,5	6,1
Unwillingness to change habitual way of life	19,3	13,7
They are just unlucky	13,7	13,4

Macro factors (unemployment, wage arrears) played a decisive role in the causes of poverty for those Russians who knew about them. The assessments of all Russians and those belonging to the poor were in any case closely related to all the reasons for the homogeneity of this group. However, there was the fact of the 'lack of state social security benefits' that they often pointed to, and they clearly relied on state assistance more than on themselves [2]. There were two main causes of poverty: personal problems (death of the breadwinner, fire), illness and the presence of many dependents. In fact, these figures are quite close to each other, except for 'illness' and 'too many dependents', which were more frequently mentioned by the poor as contagious causes of poverty. Doesn't this distribution of responses point to a general weakness or uncertainty in social policy, as well as bottlenecks, such as misunderstandings and misjudgments about the necessary costs that serious illnesses impose on people without economic barriers? Did you know that among representatives of the bottom four quintiles, more than a third of respondents describe

their health as 'poor', compared to 10-13% of respondents in the middle quintiles and 6% below them? In fact, 70% of the people who say that their health is "poor" belong to the lowest four strata. For example, reports on social psychological factors (laziness and inertia) were not mentioned much more frequently by the researchers than for two groups of poverty, which were mentioned by about 40% Russian surveyed, and then by 21%. In addition to drug addiction and alcoholism, more than a quarter of Russians attributed poverty to drug addiction. Most of the participants say that someone they know is far down in the list, both for them or due to love with him/her. Accordingly, poverty for them can be both legitimate (as applied to those who are "to blame"), and illegitimate (if it is caused by external circumstances beyond the control of a person or miscalculations of state social policy). Another conclusion follows from the above data - the problem of combating poverty cannot be solved for a significant part of the poor themselves only by increasing the money they receive (salaries, pensions, benefits, etc.). On the one hand, it involves various forms of additional assistance to people with poor health, and on the other hand, the development of a system of non-monetary forms of assistance, especially in those families where there are children, to whom, often, the money received by the family simply does not reach today and will not reach and tomorrow, even if the salaries and benefits of their parents of alcoholics increase. However, while we are seeing the exact opposite - there is a question of converting non-monetary forms of state assistance into monetary ones (reforms of housing and communal services, education, healthcare). Such measures may be cost-effective, but in relation to the conditions in Russia and the structure of domestic causes of poverty, they can have the most deplorable social consequences [3]. Another important circumstance that I would like to draw attention to when analyzing the scale, causes and prospects for overcoming Russian poverty is the problem of the poverty line. It has already been noted above that there are three fairly clearly distinct groups that can be considered living in poverty, not only because their signs of deprivation outweigh the signs of well-being, but also because they are characterized by the dominance of a downward trend in their situation against the background of improvement or stability. the position of other groups, and this is a classic sign of the poor in a stable society. However, other approaches to this issue are also possible. Thus, within the framework of the liberal model of social policy, at most two of these groups can be classified as poor, i.e. just over 20% of the population. On the other hand, the standard of living of the "low-income", who are the largest group of Russian society, is so low that it allows left-wing politicians to say that two-thirds of Russians live in a state of poverty, although formally according to a number of criteria (the degree of satisfaction with their lives, self-esteem of their social status, the dynamics of changing financial situation, etc.) this group does not correspond to traditional ideas about poverty, and in qualitative interviews they usually characterize themselves as "living on the verge, and not below the poverty line".

To a large extent, such a broad interpretation of poverty is determined by how large the gap is even in the sphere of consumption (not to mention the amount of capital) between the various strata of the rich. Its scale eventually leads to a kind of shift in the mass consciousness, when the life of the "boundary layer of the rich" is taken as the norm and there is a sharp inadequacy of the assessments of the majority of the population of their own financial situation. Moreover, it must be emphasized right away that this is by no means connected with the alleged leveling of the consciousness of Russians - judging by the research data of the IKSII RAS in 1992-2003. 13 there is no need to talk about any equalization in relation to the consciousness of the majority of Russians [5]. Moreover, judging by the data of the study "Rich and Poor in Modern Russia", the allowable gap in the incomes of the bulk of society, without the rich and the poor, is 12.5 times for Russians. If we take into account that approximately such a gap is typical for the ratio of incomes of 10% of the poorest and 10% of the most well-to-do population in many developed countries, and Russians allow it even without taking into account the poor, it becomes clear that the problem here is not in the supposedly inherent equalization of Russians, but in their completely distorted ideas about what level of life is normal (to which the media make a significant contribution), on the one hand, and the inadequacy of the level of their own claims, on the other. In this regard, it is interesting to

compare the models of the social structure of Russian society obtained on the basis of Russians' self-assessments of their current status, when they were asked to place themselves on a ten-point vertical scale of social statuses, and their wishes regarding the place in society that they would like to occupy.

IV. Discussion

If Russia is at the current stage of economic development, there must be a very close relationship between this problem and poverty. The problem is very complex and multifaceted. Expert research began in antiquity (V. Petty, D. Ricardo) and continued throughout all stages of human development. Note that each period is characterized by its own manifestations and features of poverty. In the light of the current situation, the issue of poverty is not as important as it used to be. It has become universal today due to the process of globalization [6]. Under our land, poverty has taken its flip. Theoretically, it has its own distinctive features. The individuality of poverty developed over time, that is determined by its history customs and current changes

For the period of cardinal market restructuring, a rapid process negative and reliable impoverishment which played major part in our population erupted even though it takes place understandably without ordinary standards such as an unconscious minimum subsistence level below its pearty line. Fig.1 showed the main stages of this process.

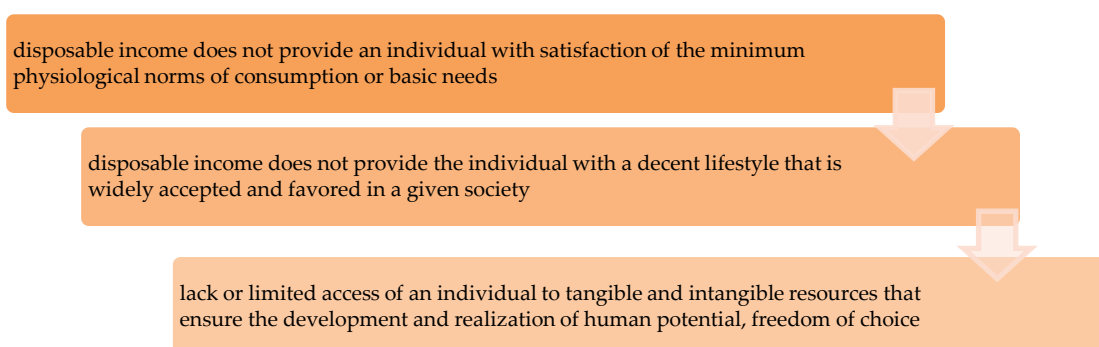


Fig. 1: Stages of development of poverty criteria

Despite the observed differences in criteria, it can be said that despite all observations of differences in terms of poverty, one point for considering this concept is always human needs. As a result of many factors of different directions, poverty arises in the modern market economy.

Table 2: Poverty development factors

Group of factors	Causes
Economic	unemployment, low wages, low productivity, industry competitiveness
Socio-medical	disability, old age, high morbidity
Demographic	incomplete families, large number of dependents
Socio-economic	low level of social guarantees
Educational qualification	low level of education, insufficient professional training
Political	military conflicts, forced migration
Regional-geographical	differentiation of regional development

The social consequences of poverty are the social disintegration. Poverty is one of the social consequences of poverty, which is the social disintegration. They were noticed in social and economic life that the poor, who have no chances to live in good conditions and find them deprived of all possible opportunities for a decent living, "drop out" of social and economic life.

The disintegration of society, its fragmentation is manifested in the disintegration of society, it has been manifested by an absence of common social norms, social unity and interests, etc. In the eyes of elite and social groups, our country's attitude towards poverty has become more "calm" in the eyes of elite and social groups [7]. At the moment it is much more tolerant of this social phenomenon, when even 100 years ago in protests for worklessness and plight of the working class rightfully provoked criticism from public (which in turn led to 1917's revolution). In Russia, the main problem for modern people is a rapid feminization of poverty. In the informal sector, women are more vulnerable to poverty due to insufficient access to benefits, wages and salaries. More than 30% of Russian women live in poverty. Currently, in 2011 more than 30% of Russian women live in poverty. More than in many other European countries, this is much more than in many other European countries. 9.8% of American women live in poverty, while 8.3% are living in England. As a result of mass unemployment, the female part of people's population is aggravated by mass and prolonged unemployment. According to the fact that women are first laid off and laid out, this is due to the fact that duties of procreation require extra support (unprofitable for companies). On the basis of an analysis of the incomes of socio-demographic groups, unemployed women aged 30 to 50 years have the most low level in terms of economic status. The main breadwinner of the family was women. As a result of the unfavorable development in relations with work and families, women were the only breadwinners from the family. As a result of the improper development (high divorce rate, increased extramarital births), after the loss of their jobs before leaving them, whose job was not paid for herself. Because of this, the feminization of poverty leads to the fact that underage children live in poor conditions. A negative imprint on the future life of children can be left in poverty, it is possible to leave an imprint on the future life of children, contribute to the further transmission this lifestyle. Because of this, poverty is the main source for so called disadvantaged children.

On the basis of the imposition of sanctions, some sectors of the Russian economic system may be affected by deterioration in its situation and borrowing conditions. This will lead to an outflow of capital from Russia throughout this period with more capital outflow [8]. These consequences can lead to further weakening of the exchange rate, high inflation and worsening consumer trust. For example, the possibility of disruptions in gas exports through Ukraine is still there. In addition, there remains risk of disruption of oil and gas exports through Ukraine as well as trade sanctions by EU countries. In short and medium term, Russia has enough reserves to compensate for the potential economic losses that are caused by possible violations of anti-sanctions measures. At the same time, an upcoming rise in tension will reduce Russian economies from 0.5-0.5 to 0.2-0.3%.

According to the current situation, it can be argued that the number of unemployed in Russia has been steadily decreasing since 1999.

Another reason for unemployment in Russia is the falling oil prices: it is the main exporter of Russians, and as such, its most important export product. In case of the fact that Oil price declines, then oil prices collapse with time; if this happens, an unemployment rate rises, but not the opposite is true.

According to official information, the unemployment rate is falling due to low requirements for business. At the moment, there are high demands for work - in particular due to low minimum wages and legal "flexibility" of Russian legislation. According to the register of companies in Russia, many heads of companies register the minimum salary, or "minimum salary". A job contract only provides one part of real salary, everything else is paid in an envelope.

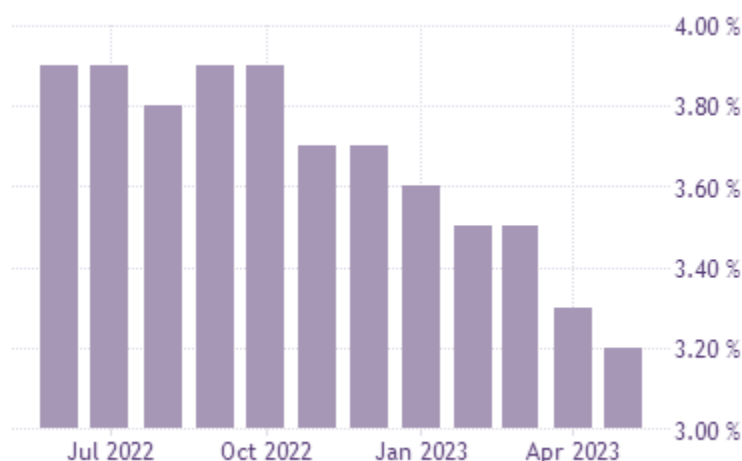


Fig. 2: Evolution of the unemployment rate between 2022 and 2023

This program is only for the employee. Only he remains in favor: everyone, except for him, participates there; all other participants are included here. A company saves on tax deductions and receives data about high-employment and low salaries, the Federal State Statistical Service received information about high-employment and low salaries [9]. Employees are not protected from social protection due to the fact that receiving a salary in an electronic envelope automatically indicates the risk of fraud on part of the employer. The reason for this is the fact that receiving a salary in an electronic envelope automatically indicates the risk of fraud on part of the employer. Another problem is the formalization of bureaucracy, concealment from real data about the state and not legal employment. The reason for this is non-legal employment.

According to the so-called, we can conclude about the so-called. The hidden unemployment in "hidden unemployment" is this. Unemployment in "hidden unemployment" - this. People who are officially listed as employed, but in fact do not receive income. The employer is trying to use legal loopholes and, for example sends the employee on long unpaid leave. For example, it can be sent an employee on long unpaid leave. The employer uses legal loopholes and, for example, sends the employee on long unpaid leave. In this case, the employer uses legal loopholes and, for example, sends the employee on long unpaid leave. In the unemployment statistics of the UN, a person does not work, but is not included in the unemployment statistics.

For example, poverty is considered one of the main problems that faces a person throughout his development in terms of its personal, mental and psychological characteristics. During the past century, in our country with a rich history and an abundance of natural resources as well as with a working and educated population, poverty for most people has been and continues to be one of urgent social problems that hinder development.

At the moment, a large part of our country's population is on the verge of poverty. It is manifested in social stratification of modern society, the differences with rich and poor people are extremely high. At the moment, there are serious risks for both national and global development. The fact that poverty is high in many countries of Europe, as well as from other regions to develop more effectively will pose an important danger to both national and global sustainable development.

In the modern world, a large role is play by the problem of poverty, ways to overcome it and effective social protection of the population. It was only with the success in implementing measures that prevent poor people from becoming victims of poverty that a state can be brought to a new level of development. The most important problem is that the question of why poverty and how to overcome it still has been open for the general public.

References

- [1] Christina Pazzanese (Harvard) Amartya Sen's ninety-year journey from colonial India to the Nobel Prize and beyond. Interview, June 3, 2021.
- [2] Salamova A.S. Socio-economic factors in the fight against poverty and hunger in the modern world: the scientific approach of Amartia Kumar Sen, 2023, 17, (1), pp. 237-245.
- [3] See: Human Development Report (HDR), 2014.
- [4] Salamova A.S. Poverty as a lack of opportunities: an analysis of the definition of poverty Amaritia Sen, 2022, 12, pp. 1045-1051.
- [5] Sen, Amartya (December 20, 1990). More than 100 million women have gone missing // New York Book Review. 1990. December 20.
- [6] Nicola Jones, Rebecca Holmes, Jessica Espey, Gender and the MDGs: A gender perspective is vital for pro-poor outcomes. London: Overseas Development Institute, 2008
- [7] Kristoff N., Woodunn S. Half the Sky: Turning Oppression into Opportunity for Women Around the World. // Journal of Family Theory and Review. March 2010, pp. 98-103.
- [8] Da Rocha, J.M., & Fuster, L. Why are fertility rates and female employment ratios positively correlated across O.E.C.D. countries? International Economic Review, 2006, 47(4), 1187–1222. <https://doi.org/10.1111/j.1468-2354.2006.00410.x>
- [9] Duchek, S., Foerster, C., & Scheuch, I. Bouncing up: The development of women leaders' resilience. Scandinavian Journal of Management, 2022, 38(4), 101234. <https://doi.org/10.1016/j.scaman.2022.101234>

ASSESSMENT OF THE IMPACT OF CLIMATE CHANGE ON THE PRECIPITATION REGIME IN THE SOUTHERN SLOPE OF THE GREATER CAUCASIAN PROVINCE

Sevinj Rzaeva¹, Jamal Guseynov², Allahverdi Tagiyev¹

¹Azerbaijan State Oil and Industry University

²Azerbaijan Airlines JSC

rzaeva.48@mail.ru

camal_huseynov_88@mail.ru

allahverdi.taghiyev@gmail.com

Abstract

The study examines the influence of modern climate changes on the precipitation and temperature regime in the southern and southeastern regions of the Great Caucasus natural region. Also, determining the multi-year trends of the temperature and precipitation regime in 1991-2020 and investigating their change regularities is the goal. At the same time, in the article, the variability of monthly, seasonal and annual indicators was studied in the multi-year period. The impact of global climate changes on the perennial precipitation regime in the southern part of the Greater Caucasus region was studied. In the analysis, the precipitation observation data of 8 meteorological stations during the years 1991-2020 were used. Multi-year (1991-2020) various indicators of precipitation were compared with the base quantities. In the study, the multi-year period was considered for 2 periods (1991-2005, 2006-2020) and the monthly, seasonal and annual trends of precipitation were compared. The study found that the multi-year average temperature in the province for the last 30 years was 11-14°C in the lowlands and 6-7°C in the mid-mountains. However, compared to 1961-1990, the perennial temperature has increased by 1.0°C. The amount of annual precipitation was in the interval of 300-1300 mm, depending on the stations. A decrease in the amount of precipitation has been recorded for many years, and in some places this amount has even increased to 27%.

Keywords: Greater Caucasus Mountains, water supply, hydrodynamic regime, aquifer, percent of mineralization, natural hazards, climate change, meteorological station, precipitation

I. Introduction

Destructive effects of global climate changes have recently expanded the area of occurrence in different regions of the Earth [2,13]. The frequent recurrence of dangerous events such as floods, hurricanes, hail, droughts, landslides, and avalanches showed the extreme importance of studying the effects of global climate changes. As a result of natural disasters, it is inevitable that millions of people will suffer every year, and the economy of countries will suffer a large amount of damage [3]. It is considered important to carry out research in the direction of revealing the characteristics of climate changes in the South Caucasus. The complexity of the relief of the Republic of Azerbaijan and the diversity of the climate regime do not allow the study of the region as a whole. Therefore, the separate study of the physical-geographic regions that make up the territory or regions with the same climate regime is considered indispensable. For this purpose, it is necessary to reveal the effect of multi-year climate anomalies on the precipitation regime in the southern part of the Greater Caucasus region. Although various features of the climate regime were investigated

in the previous studies, none of them included a comprehensive analysis of fluctuations in precipitation and temperature regime for the years 1991-2020 [1, 2, 3, 14].

In the southern and southeastern parts of the Great Caucasus natural region, the emergence of mild-warm, cold, mountainous tundra climate types with dry winters and evenly distributed precipitation, abundant precipitation in all seasons, is spread precisely on the basis of the physical-geographical position, complex relief and the influence of air masses [1, 7]. As the air masses from the north cannot cross the high mountain ranges, the impact on the area is very weak. However, this area is affected by local, mild, warm, humid air masses coming from the west, the Caspian Sea and the Kura-Araz plain throughout the year. The hot air masses coming to the region convect as they rise along the mountain slopes and fall to the earth's surface in the form of precipitation in the second half of the day. Such processes are observed with dangerous atmospheric phenomena (hail, lightning) in the hot season of the year [5,6,7].

II. Methods

The study was carried out on the southern slope of the Great Caucasus in Alibey (1540 m), Meraza (775 m), Shamakhi (750 m), Gabala (679 m), Ismayilli (653 m), Sheki (639 m), Oguz (582 m) and Zagatala (487 m) meteorological stations of the National Hydrometeorological Service were conducted on the basis of precipitation observation data. Multi-year (1991-2020) series of observations were analyzed using mathematical, statistical and cartographic methods. Also, the 1991-2020 annual period was reviewed for 2 half-periods (1991-2005 - first period, 2006-2020 - second period), and the trend of multi-year internal changes was revealed. The comparison and trend of monthly, seasonal and annual precipitation data of 8 meteorological stations located on the southern slope of the Greater Caucasus region during the period 1991-2020 with the corresponding indicators of 1961-1990 recommended by the World Meteorological Organization (WMO) as a norm [4,7,10]. The table, histogram, graphs in the description of the obtained results were prepared in Microsoft Excel, and electronic maps were prepared in ArcGIS software. The homogeneity of the precipitation observation series and the statistical significance of the obtained results were checked, multi-year anomaly indicators, correlation and difference integral coefficients were calculated.

Alibey (1540 m), Zagatala (487 m), Sheki (639 m), Oguz (582 m), Gabala (679 m), Ismayilli (653 m), Shamakhi (750 m) and Maraza (775 m) meteorological stations are included in the study. rainfall observation data were used. The average indicators of monthly, seasonal and annual precipitation data of 8 hydrometeorological stations during 1991-2020 were compared with the corresponding indicators of 1961-1990 [4,8,11]. The homogeneity of the series of precipitation observations and the statistical significance of anomalies were checked by Fisher and Student tests.

In this part of the province, the emergence of the climate types of temperate-warm, cold with abundant precipitation in all seasons, mountainous tundra climate types with dry winters and evenly distributed precipitation are spread on the basis of the influence of the complex relief. Since the air masses coming from the north cannot cross the high mountain ranges, they converge and move along the northern foothills. However, the southern slope is affected by local, mild, warm, humid air masses coming from the west, the Caspian Sea and the Kura-Araz plain throughout the year. The hot air masses coming to the region convect as they rise along the mountain slopes and fall to the earth's surface in the form of precipitation in the second half of the day. Such processes are observed with dangerous atmospheric phenomena (hail, lightning) in the hot season of the year [7,8,9,12].

The average annual temperature during the multi-year period (1991-2020) was 13.8°C in Zagatala, 13.3°C in Oguz, 13.1°C in Shaki, 12.3°C in Gabala, 11.9°C in Ismayilli, 11.4°C in Maraza, 6.9°C in Alibey station. While the average annual temperature increase in this part of the province

was 0.5°C in the first period, it increased 2.8 times to 1.4°C in the second period. The average anomaly in 1991-2020 was 1.0°C.

There have been changes in the precipitation regime along with the temperature over many years. Thus, in 1991-2020, the amount of annual precipitation on the southern slope of the Greater Caucasus region was 786 mm (306-1292 mm) on average. On average, 45% (38-52%) of the annual precipitation fell in the cold and 55% (48-62%) in the warm half-cycle. This shows that the precipitation is close to the regularity of equal distribution from west to east (Table 1).

Table 1: Seasonal and half-year distribution of precipitation in the south part of the Greater Caucasus region in 1991-2020

Station	Precipitation rate, mm							Precipitation rate, %	
	Winter	Spring	Summer	Autumn	Year	First period	Second period	cold	hot
Zagatala	120	316	266	242	943	977	909	38	62
Alibey	136	399	396	361	1292	1323	1261	38	62
Sheki	111	241	207	201	760	761	760	41	59
Oguz	147	296	201	282	927	925	929	46	54
Gabala	138	277	184	257	855	865	846	46	54
Ismayilli	111	202	136	205	654	629	679	48	52
Shamakhi	111	165	100	177	553	501	605	52	48
Maraza	60	95	63	87	306	280	332	48	52

As can be seen from Table 1, the main part of precipitation in this region falls in spring and autumn. Also, compared to the first and second periods, an increase was observed at Ismayilli, Shamakhi and Maraza stations, while a decrease was observed at Zagatala, Alibey and Gabala stations.

The distribution of perennial precipitation in the south of the Greater Caucasus Mountains has changed depending on the terrain characteristics. For this purpose, the results of mathematical-statistical analysis were interpolated in the IDV model for the area in the ArcGIS (Geographical Information Systems) program. If we look at the picture, in comparison with the I period, in the II period, despite the decrease of precipitation in the previous mid-mountain belt, an increase was observed in the southeastern part of the area (Fig. 1).

The change of the amount of monthly precipitation compared to the norm (1961-1990) in 1991-2020 attracts special attention. As it can be seen, in 1991-2020, the amount of precipitation decreased significantly (27%, 115 mm) throughout the year, except for July and September, at Maraza station, in contrast to other stations. The precipitation amount of other stations had weak fluctuations in January and February. In March, the amount of precipitation increased by 1-8% (0.4-7 mm) in Zagatala, Sheki and Alibey, and decreased by 7-25% (6-11 mm) in other stations. In April, except for Zagatala and Alibey, a decrease of 6-39% (6-19 mm) was observed in other stations. A decrease of 9-36% (9-19 mm) is typical in May Sheki and Meraze, and an increase of 1-8% (1-10 mm) in other areas. In June, precipitation decreased by 6-39% (11-47 mm) at all stations. In July, there was an increase of 3-38% (2-6 mm) in Zagatala and Maraza, and a decrease of 0.3-18% (0.2-13 mm) in other stations (Table 2).

Although there was an increase of 7-11% (4-8 mm) in Zagatala and Sheki in August, there was a decrease of 1-27% (2-16 mm) in other areas. In September, there was an increase of 7-25% (2-30 mm) in all stations. In October, the amount of precipitation decreased by 2-35% (2-22 mm) in other stations, except for an increase of 4% (5 mm) in Alibey. In November, an increase of 0.5-20% (0.3-14 mm) was recorded in Alibey, Sheki and Gabala, and a decrease of 2-33% (212 mm) was recorded in the remaining stations. In December, the amount of precipitation decreased by 5-37% (2-13 mm) in the region.

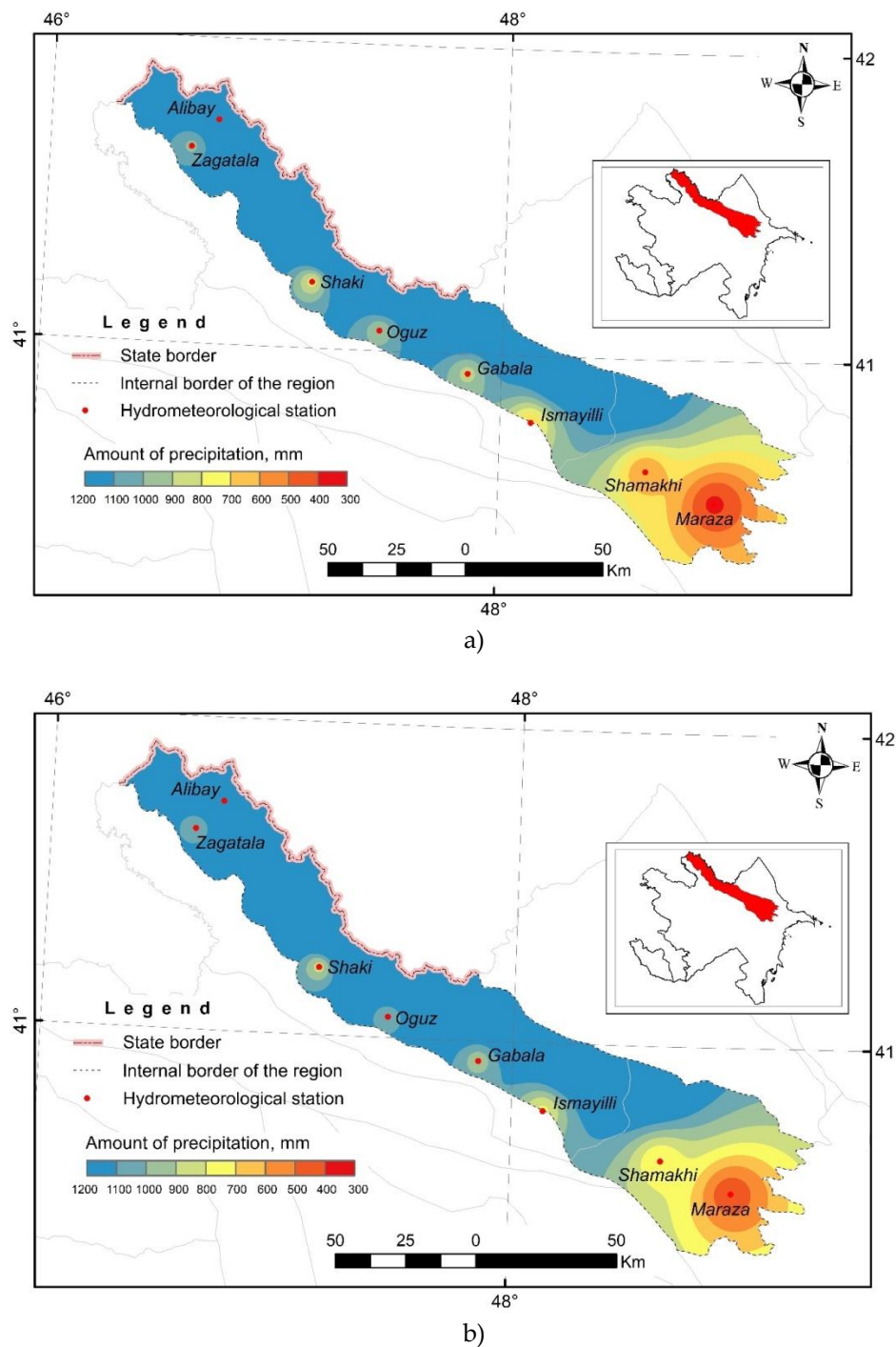


Fig. 1: Precipitation fluctuations in 1991-2005 (a) and 2006-2020 (b)

During 1991–2005, the precipitation anomaly decreased by 34% (142 mm), with an increase of 7% (82 mm), while during 2006–2020, it decreased by 21% (89 mm), increasing by 2% (20 mm). weakened in the range. In 1991-2020, compared to the norm, an increase of 4% (51 mm) was recorded in Alibey, and a decrease in the range of 2-27% (16-115 mm) in other stations. Looking at multi-year half-cycles, during 1991-2005 there was an average decrease of 7% (36 mm) in the south of the province, while the decrease increased to 8% (52 mm) during 2006-2020. In 1991-2020, there was a decrease of 7% (44 mm) in the indicators of precipitation.

The change in the average monthly rainfall in the area has a great impact on the seasonal indicators. Figure 2 shows the variation of seasonal rainfall anomaly indicators. If we look at the

histogram, the amount of precipitation compared to the norm is 0.4-29% (1-24 mm) in winter at all stations, 3-34% (10-49 mm) in spring (except Zagatala and Alibey) and 4-25% (10 -61 mm) there was a decrease. In autumn, an increase of 4-16% (9-49 mm) was recorded in all stations, except for Maraza (23 %, 27 mm), Zagatala (5 %, 13 mm) and Sheki (6 %, 13 mm) stations. In all seasons, the amount of precipitation in Meraza station has decreased to a high level. The maximum decrease was observed in the spring season at the Maraza station (34%, 49 mm), and the maximum increase was observed in the fall (16%, 49 mm) in Alibey (Fig. 2).

Table 2: Average monthly and annual precipitation anomalies (mm), (**dark black-%**) for 1991–2020

Period	Station	Month												İl
		I	II	III	IV	V	VI	VII	VIII	IX	X	XI	XII	
1991-2005	Zagatala	-7 -18	1 2	4 6	-9 -9	6 5	2 2	17 22	19 26	19 22	-43 -43	1 1	8 20	18 2
	Alibey	-6 -12	6 11	7 9	4 3	-1 0	2 1	-4 -3	25 21	47 39	-11 -9	11 16	1 3	82 7
	Sheki	-4 -12	-2 -5	-1 -2	-12 -13	-9 -9	10 10	-12 -20	5 8	8 12	-28 -32	6 10	-7 -18	-47 -6
	Gabala	-7 -14	5 10	-11 -12	-7 -7	17 14	-20 -17	-18 -25	-16 -23	23 29	-38 -30	6 9	-11 -20	-76 -8
	Oguz	-3 -6	2 5	-2 -3	-17 -17	18 17	-36 -30	-12 -18	-9 -15	28 38	-15 -15	-6 -9	-1 -2	-53 -6
	Maraza	-7 -30	-11 -36	-9 -21	-23 -47	-17 -33	-13 -29	2 11	-3 -19	-1 -2	-28 -59	-19 -52	-12 -42	-142 -34
2006-2020	Zagatala	6 16	-3 -7	1 1	15 15	14 11	-52 -40	-13 -17	-3 -5	2 2	-2 -2	-4 -6	-12 -29	-50 -5
	Alibey	8 18	-10 -20	6 7	16 13	19 11	-24 -13	-6 -5	-28 -24	14 12	21 17	16 23	-11 -25	20 2
	Sheki	8 23	-4 -8	2 3	-5 -5	-10 -9	-39 -38	11 19	4 7	8 12	-15 -17	-5 -9	-4 -10	-47 -6
	Gabala	5 9	-1 -1	-12 -13	-6 -6	-15 -13	-33 -29	-9 -11	-17 -24	12 15	9 7	10 15	-16 -29	-71 -7
	Oguz	7 17	2 3	-10 -11	2 2	-11 -11	-57 -47	-4 -5	-4 -7	8 11	10 10	-7 -9	-8 -18	-71 -8
	Maraza	-4 -15	-4 -14	-12 -29	-16 -31	-20 -40	-21 -47	11 66	-6 -35	5 16	-5 -11	-5 -15	-10 -32	-89 -21
1991-2020	Zagatala	0 -1	-1 -3	3 3	3 3	10 8	-25 -19	2 3	8 11	10 12	-22 -22	-2 -2	-2 -5	-16 -2
	Alibey	1 3	-2 -4	7 8	10 8	9 5	-11 -6	-5 -4	-2 -1	30 25	5 4	14 20	-5 -11	51 4
	Sheki	2 5	-3 -7	0 1	-8 -9	-9 -9	-14 -14	0 0	4 7	8 12	-22 -24	0 0	-5 -14	-47 -6
	Gabala	-1 -2	2 4	-11 -12	-6 -6	1 1	-26 -23	-13 -18	-16 -23	18 22	-14 -11	8 12	-13 -24	-74 -7
	Oguz	2 5	2 4	-6 -7	-7 -8	4 3	-47 -39	-8 -12	-6 -11	18 25	-2 -2	-7 -9	-5 -10	-62 -7
	Maraza	-5 -23	-8 -25	-11 -25	-19 -39	-19 -36	-17 -38	6 38	-5 -27	2 7	-17 -35	-12 -33	-11 -37	-115 -27

Fig.3 shows the dynamics of difference integrals for several typical stations. If we pay attention, the trend of precipitation in all stations increased until 1994, decreased in 1995-1996, and increased again in 1997 (Fig. 3).

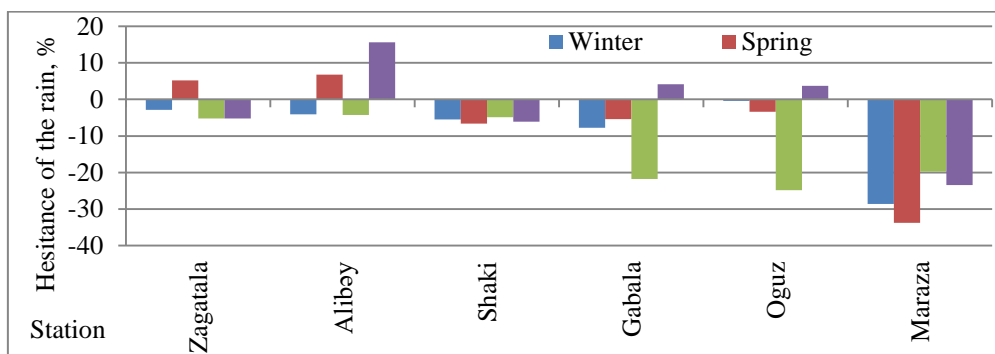


Fig. 2: Seasonal distribution of precipitation anomalies

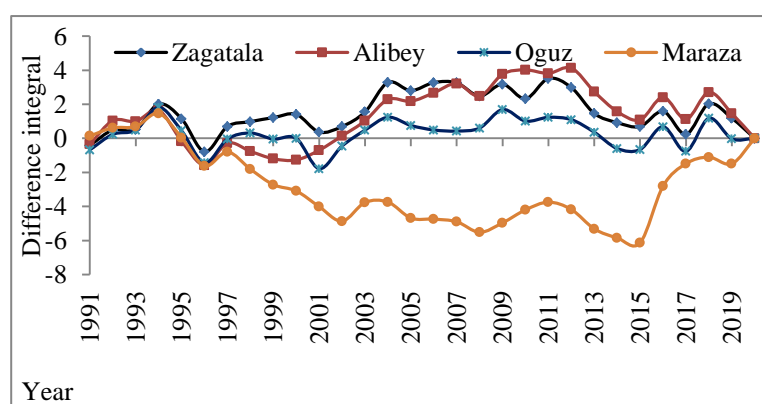


Fig. 3: Dynamics of the difference integral of precipitation anomalies for the period 1991-2020

The amount of precipitation in Alibey, Zagatala and Oguz stations continued to increase until 2011, despite occasional fluctuations, starting from 1997. In 2012-2020, although there was an occasional increase, it decreased for the entire period. Precipitation at Maraza station decreased sharply in 1994-2015, but increased in 2016-2020. Thus, in 1991-2020, the amount of precipitation increased in the low highlands and high highlands, while it decreased in the middle highlands of the southeastern end of this slope.

In addition, the correlation coefficients between the multi-year indicators of temperature and precipitation were calculated. The result shows that the correlation coefficients of all stations do not meet the significance coefficient of -0.5 . At the stations, this relationship ($-0.1 \div -0.4$) is weaker and there is an influence of other factors besides temperature on the change of the amount of precipitation.

According to previous researchers, the rise in temperature at the beginning of summer will lead to permafrost in the mountainous belt of the province and the sudden increase in water consumption in the rivers that take the source of premature melting of glaciers from these mountains, and in summer, the melting zone will decrease, and the drought will spread with the increase of evaporation [5, 6, 10].

III. Conclusions

The following several results were obtained in the studies conducted to detect the temperature and precipitation variations of the hydrometeorological stations located on the southern slope of the Greater Caucasus physical-geographical region:

1. The average annual temperature for many years was 6.9°C in the middle highlands (Alibey) and 12.5°C (11.4-13.8°C) in other stations in the lowlands. In 1991-2020, the average temperature increased by 1.0°C (0.9-1.2°C) compared to the norm. .

2. The annual amount of precipitation was 1292 mm in the highlands, and 714 mm (306-943 mm) in the low highlands.

3. In 1991-2020, precipitation fluctuations were observed with an increase in Alibey station (4%) and a decrease in the range of 2-27% compared to the norm in other stations.

4. In the south of the Greater Caucasus region, 55% of the precipitation fell in the warm half-period, and 45% in the cold half-period.

Depending on the hypsometric features of the terrain, strong convection processes develop especially in the warm half-year in the region where we study the climate, but the continuation of temperature anomalies can lead to the acceleration of the recurrence of dangerous atmospheric events such as lightning and hail, as well as the shift in the time of occurrence during the year. If the fluctuations continue at this pace, the increase in air temperature in March will accelerate the vegetation, the sharp cold in April will damage the roots and stems of the plants, and the crop will be destroyed during the harvesting period in regions with constant rainfall. Drought will continue to expand in warming areas.

References

[1] Bondarenko, L.V., Maslova, O.V., Belkina, A.V., Sukhareva, K.V. 2018. Global climate change and its aftermath. Herald of the Russian Economic University named after B. Plekhanova. 2, 84-93. <https://doi.org/10.21686/2413-2829-2018-2-84-93>

[2] Taghiyev A.Sh. Climate change and water resources management. International Scientific Conference on Sustainable Development. Baku, 24-25 november, 2017. 55-61.

[3] Tagiev, I.I., Babaev, N.I. 2017. Some geochemical and hydrogeological, regularities of formation and distribution of mineralwaters of Azerbaijan. XXXIX International scientific-practical conference, Actual problems in modern science and ways of their solutions, Moscow, 15-19.

[4] Tagiev I.I. 2001. Status and problems of protection of the environment and nature use in the Republic of Azerbaijan, Ministry of Science and Technology of the USSR, Moscow.

[5] Rzaeva, S.M., Tagiyev A.Sh. and Zeynalova S.A. "Impact of climate change on the groundwater of the Ganikh-Ayrichay foothills." Reliability: Theory & Applications 17.SI 4 (70) (2022): 180-187. DOI: <https://doi.org/10.24412/1932-2321-2022-470-180-187>

[6] Rahimov M.K. Change trend of some climate parameters on the southern slope of the Greater Caucasus. Works of the Azerbaijan Geographical Society, c. XVI, Baku, 2011. pp. 286-288.

[7] Safarov S.H., Mahmudov R.N. Modern climate changes and Azerbaijan. Baku, 2011, 312 p.

[8] Mammadov A.S. Modern climate changes in Azerbaijan and its forecasting. Baku, 2015. 328p.

[9] Khalilov S.H., Safarov S.H. Monthly and annual norms of air temperature and atmospheric precipitation in the Republic of Azerbaijan (1691-1990 years). Baku, 2001. 229p.

[10] Huseynov C.S. Characteristics of long-term temperature changes in the southern and southeastern slopes of the Greater Caucasus, scientific compilations of MAA. Baku, 2019. pp. 76-81.

[11] Karimov R.N. Climate change mitigation and adaptation measures. Baku, 2016. 47p.

[12] Safarov C.G. Thunderstorm and mudslide phenomena on the territory of Azerbaijan and radar warning methods. Baku, 2012. 292c.

[13] <https://www.climate.nasa.gov>

[14] Ismayilov R.T., Karimov V.M., Ganbarova S.A. Low-temperature oxidation of sulphide ores of sulphide-polymetallic deposits of Azerbaijan //Journal of Geology, Geography and Geoecology. – 2023. – T. 32. – №. 1. – C. 52-58.

FORECASTING OF THE PROBABILITY OF UNNATURAL DESTRUCTIVE EVENTS OCCURRENCE AT REFINERY COMPLEXES

Oksana Morozova¹, Stanislav Butuzov², Valery Artyukhin¹

¹All-Russian Research Institute for Civil Defense and Emergencies of the EMERCOM of Russia

²Academy of State Fire Service of the EMERCOM of Russia

oxana_morozova@list.ru

butuzov_s_yu@mail.ru

ikshot@mail.ru

Abstract

The paper proposes some approaches to building a model for predicting the probability of emergency situations at the enterprises of the oil refining complex in modern conditions. The approach is based on modeling using the binomial distribution. The initial data of the model are open data on the occurrence of emergencies on the territory of the Russian Federation for the period 2022–2023.

Keywords: forecasting, destructive events, emergency, oil refinery

I. Introduction

About 80 thousand hazardous production facilities (HPF) of the oil and gas complex are registered on the territory of the Russian Federation, of which the petrochemical and oil and gas processing industries and oil product supply facilities account for approximately 5% (4096 facilities according to [1] for 2021). The main types of accidents are explosion (with the destruction of technical devices and structures), fire, and release of hazardous substances. Distribution of the total number of accidents at HPFs by the considered industries for the period 2011-2021 shown in Fig. 1.

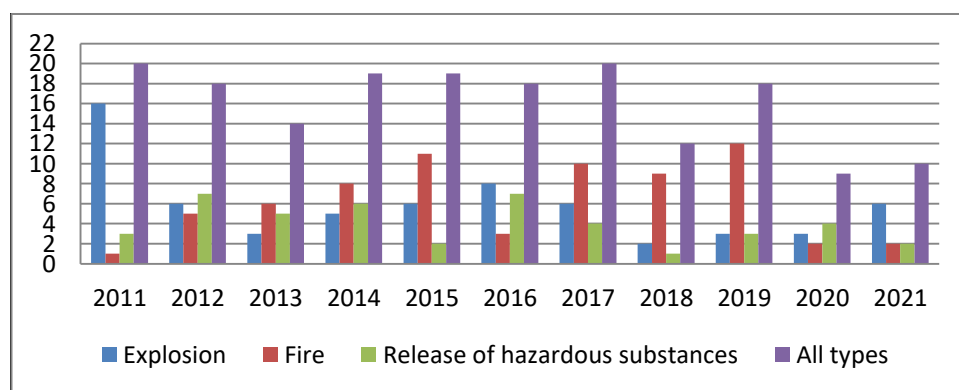


Fig. 1: Distribution of the total number of accidents of HPFs in the petrochemical and oil and gas processing industries and oil products supply facilities by types of accidents for the period 2011-2021

In recent years, the following trends have been observed in the industry:

- Reduction in the number of HPFs in the petrochemical and oil and gas processing industries and oil product supply facilities (Fig.2)
- Reduction of the total number of accidents
- Increase in the number of accidents associated with explosions
- The main contribution to the total number of accidents was made by accidents at HPFs of the oil and gas processing industry (Fig.3) [2]

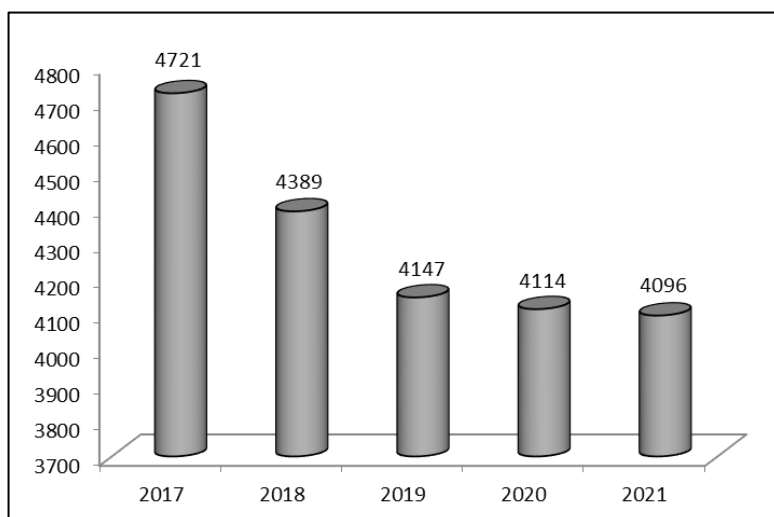


Fig. 2: The number of HPFs in the petrochemical and oil and gas processing industries and oil product supply facilities for the period 2017-2021

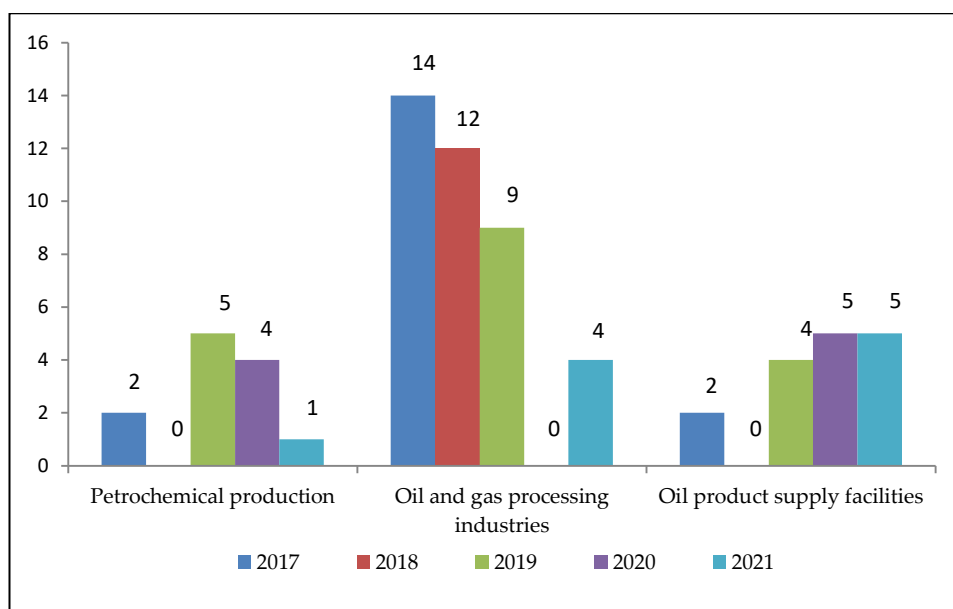


Fig. 3: Distribution of accidents at HPFs by industry sectors for the period 2017-2021

During the period from February 2022 to March 2023, 26 negative events (accidents, emergencies, terrorist attacks) occurred at HPFs of the petrochemical and oil and gas processing industries and oil product supply facilities. Examples of such events include the following:

- Belgorod region: April 1, 2022 – fire at eight tanks of “Belgorodnefteprodukt” JSC in Belgorod, two people from the tank farm personnel were injured [4]

- Bryansk region: April 25, 2022 – fire at the RVS-10000 with diesel fuel at the oil depot "Transneft Bryansk Druzhba" [5]
- Republic of Crimea: June 20, 2022 – fire on the drilling platform of “Chernomorneftegaz” in the Black Sea. Three people were injured, seven were missing. 94 people were evacuated [6]
- Rostov region: June 22, 2022 - explosion and fire at the oil refinery at the Novoshakhtinsk refinery [7]

73% of events occurred for external reasons, 27% for other reasons.

II. Methods

In domestic and foreign practice, to predict the occurrence of accidents and emergencies at the enterprises of the oil refining complex, approaches are used based on the use of technologies for identifying and understanding the consequences, probability and risk [3]. The initial data for the developed forecasting methods is statistical information.

This article discusses a model for predicting the likelihood of emergencies at the enterprises of the oil refining complex in modern circumstances.

To build a mathematical model, consider data on 73% of the events. The initial data for building the model are data from open sources for the period 2022–2023 in the format: subject of the Russian Federation, object, and type of event (fire / explosion / release of hazardous substances), causes, and brief description of the event.

Consider the number of negative events per month as a binomial variable B (Fig. 4). Let's call a “successful” event the occurrence of a negative event at the facilities of the petrochemical and oil and gas processing industries and oil products supply facilities. In a month of such successful events, k occur, and $0 \leq k \leq n$, where n is the total number of attempts to create artificial negative events per month (n is an unknown value). Of course, such a model greatly simplifies reality, since a number of assumptions are made, namely:

- 1) all events are independent of each other
- 2) the probability of "success" is fixed
- 3) n remains constant from month to month

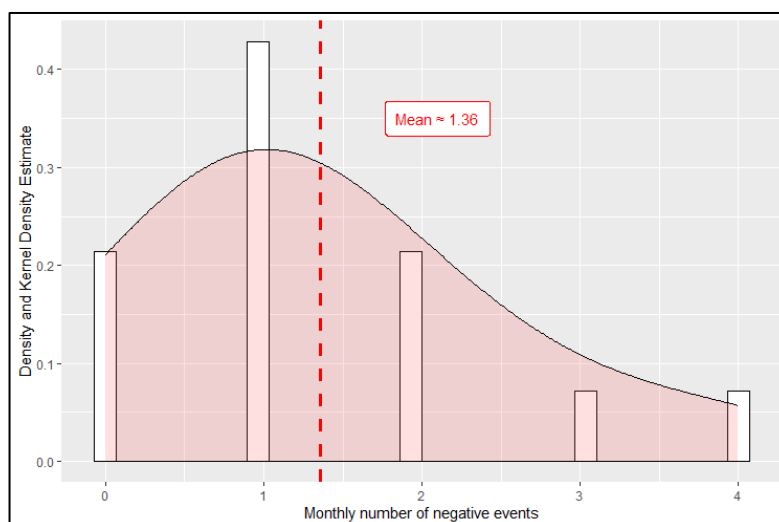


Fig. 4: Negative events (incidents) as a random binomial variable

It should be noted that neither the total number of trials per month n nor the probability of "success" p is known. A small sample of successful outcomes is used to build the model. However,

the shape of the histogram suggests that B can be modeled as variable with Poisson distribution which is an extreme case of the binomial distribution for large n and small p . Restoration of the distribution of a random variable over the sample $\{x_i\}$, where $i=1,..,m$, can be performed through a point estimate of the unknown parameter λ (that is, $\hat{\lambda}$) of the Poisson distribution by the maximum likelihood method:

$$\hat{\lambda} = \frac{1}{m} \sum_{i=1}^m x_i \tag{1}$$

In our case: $\hat{\lambda} = 1.357143$.

A sample from Poisson distribution with such a parameter $\lambda = \hat{\lambda}$ can give different results in general, similar in form. Examples of samples obtained from the Poisson distribution with the parameter $\lambda=1.357143$ are shown in Fig.5 and Fig.6.

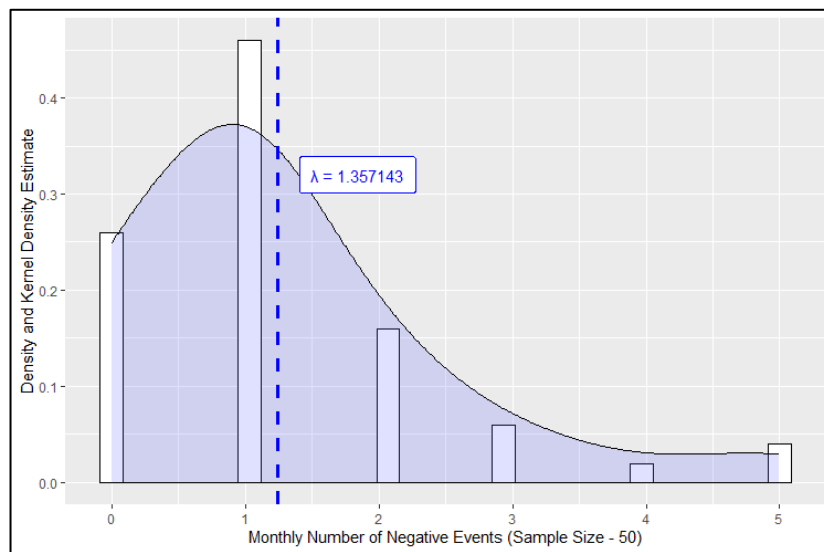


Fig. 5: An example of a histogram of a sample of 50 values from a Poisson distribution with a parameter $\lambda=1.357143$

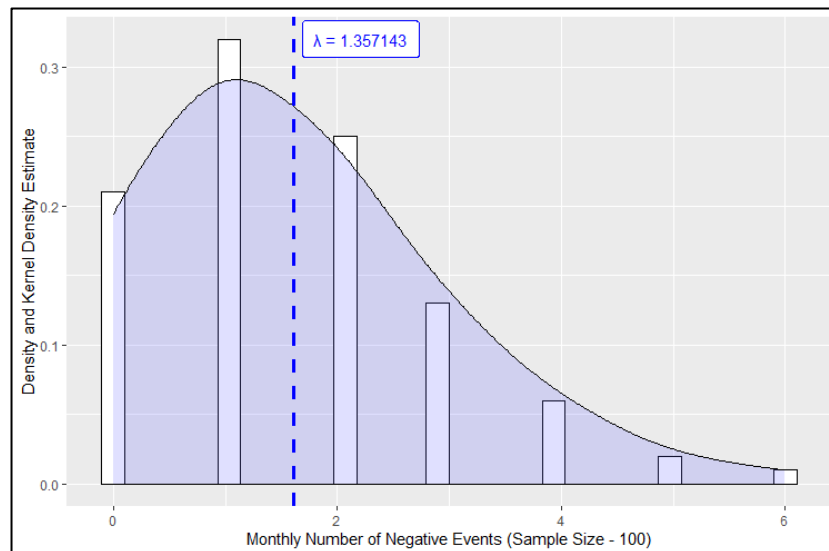


Fig. 6: An example of a histogram of a sample of 100 values from a Poisson distribution with a parameter $\lambda=1.357143$

Using the general case of the binomial distribution, it would be possible to model the number of negative events for a known number of external influence attempts n . The estimate of the probability of success p by the maximum likelihood method depends on n and the number of “successes”. However, the desired value is unknown, so the transition to the extreme case of the

binomial distribution, the Poisson distribution, has been made.

As a result of calculations based on the theoretical Poisson distribution with the selected parameter λ , it is possible to estimate the probability of a specific number of negative events during the month. So you can see that the absence of negative events corresponds to a probability estimate of approximately 0.26 (Fig. 7), and the probability of more than one negative event is approximately 0.39 (Fig. 8) (the histograms in Fig. 7 and Fig. 8 are built according to actual data, while the probabilities are calculated for the theoretical Poisson distribution with the parameter $\lambda=1.357143$).

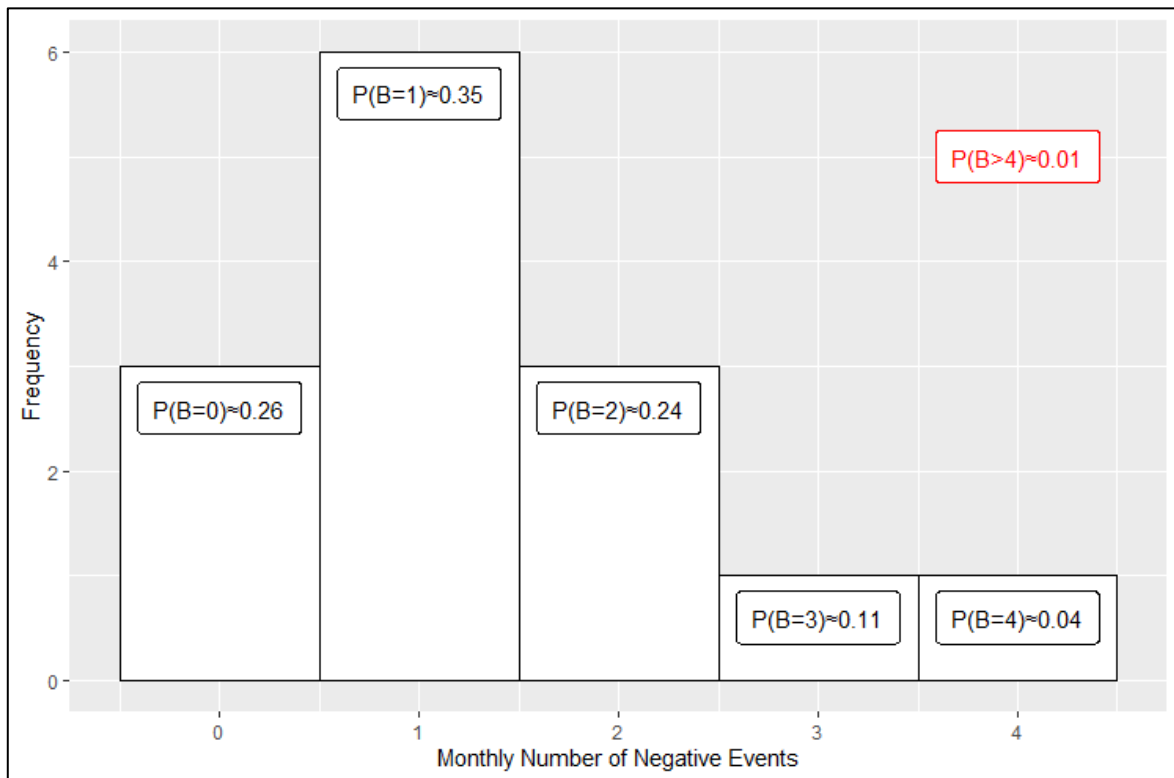


Fig. 7: Estimates of the probability of specific values of "success" for the Poisson distribution with a chosen parameter

III. Results

The results obtained indicate that the proposed model can be used as a valid tool for predicting the likelihood of emergencies at the enterprises of the oil refining complex in modern circumstances. Improving the quality of forecasting can be further carried out taking into account the following strategies: enriching the initial data with additional parameters, increasing the analyzed number of negative events, as well as changing the type of mathematical model. The practical significance of the introduction of the proposed model lies in the possibility of early adjustment of measures to improve the stability of the operation of oil refinery facilities located on the territory of the Russian Federation in order to reduce the scale of the consequences of man-made emergencies.

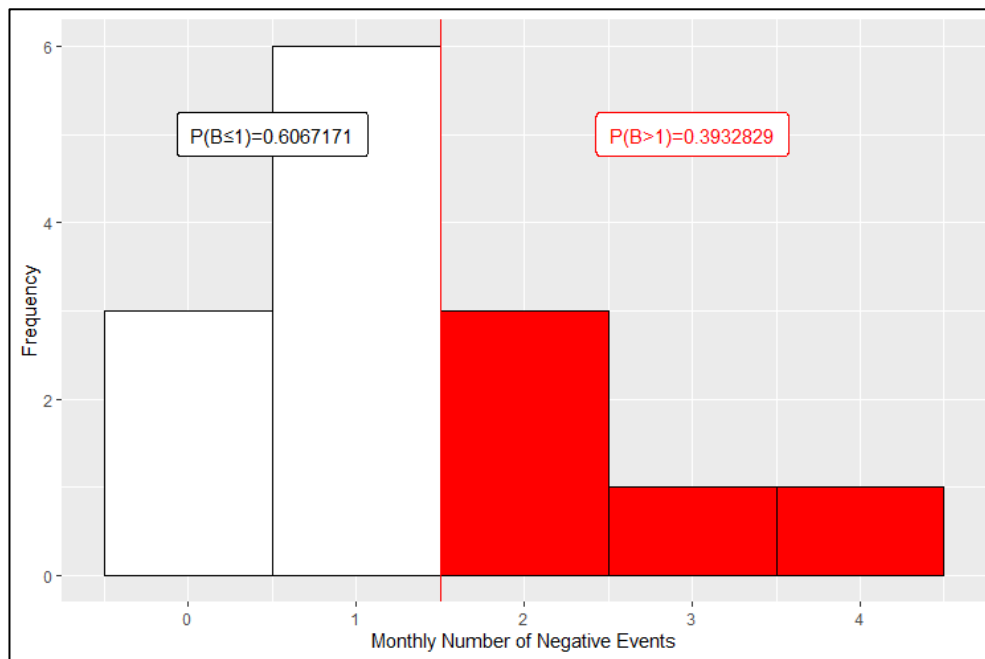


Fig. 8: Estimation of the probability of occurrence of negative events: less than two and more than one for the Poisson distribution with the selected parameter

References

- [1] Annual reports on the activities of the Federal Environmental, Industrial and Nuclear Supervision Service of Russia for the period 2011-2021 (n.d.). *Rostekhnadzor*. https://www.gosnadzor.ru/public/annual_reports/.
- [2] Morosova, O.A., & Fedchishina, D.D. (2023). Modern trends in the dynamics of accidents at the facilities of the petrochemical, oil and gas processing industry and oil products supply facilities. In *Proceedings of the VII International Scientific and Practical Conference dedicated to the World Civil Defense Day "Civil Defense on Guard for Peace and Security" in the Year of the 90th Anniversary of the Academy of State Fire Service of the EMERCOM of Russia* (Vol. 2). Academy of State Fire Service of the EMERCOM of Russia.
- [3] GOST R 58771-2019 "Risk management. Risk Assessment Technologies" (1993). Federal Agency for Technical Regulation and Metrology.
- [4] Updated information about the fire in the city of Belgorod on Konstantin Zaslونov Street. (2022). *EMERCOM of Russia. Main Directorate for the Belgorod Region*. Retrieved April 10, 2023, from https://31.mchs.gov.ru/deyatelnost/press-centr/vse_novosti/4711917.
- [5] The fire at the oil depot in the city of Bryansk is completely eliminated, there is no threat to the fuel supply of the region. (2022, April 26). *Neftegaz.Ru*. Retrieved April 10, 2023, from <https://neftegaz.ru/news/incidental/735267-pozhar-na-neftebaze-v-g-bryansk-polnostyu-likvidirovan-ugrozy-toplivoobespecheniyu-regiona-net/>.
- [6] More than 90 people were evacuated from the drilling platforms of Chernomorneftegaz. (2022, June 20). *RIA*. Retrieved April 10, 2023, from <https://ria.ru/20220620/platformy-1796832117.html>.
- [7] Details of the fire on NZNP in the Rostov region. (2022, June 22). *Neftegaz.Ru*. Retrieved April 10, 2023, from <https://neftegaz.ru/news/incidental/741545-podrobnosti-pozhara-po-nznp-v-rostovskoy-oblasti-bylo-2-bpla/>.

SUSTAINABLE DEVELOPMENT: ECONOMIC EFFICIENCY OF ECOSYSTEMS

Magomed Suleymanov¹, Evgeniya Atamas², Aliheydar Shahmarov³

¹Dagestan State University, Russia

²Kuban State University, Russia

³Department of Emergency Situations and Human Life Safety,
University of Architecture and Construction, Azerbaijan

fefnews@mail.ru

aliheydarshahmarov63@gmail.com

Abstract

To date, the generally recognized global trends have become the principles of sustainable development adopted by the UN, which are understood as the evolutionary development of civilization based on innovations while meeting the vital needs of the population of different states, including energy supply and environmental conservation. Being associated with a number of crises, the growing turbulence of the global economy and the political system of the modern world, constantly seeing an increase in the number of challenges to global trends towards sustainable development, it is worth reconsidering the approach to the concept of Sustainable Development. Attempts to undermine the significance of the UN 2030 Agenda for Sustainable Development adopted in 2015 under the influence of the COVID-19 pandemic quickly gave way to the importance of uniting efforts aimed at achieving the 17 Goals that are the basis of governance (SDGs). Efforts at many levels - from states and their regional entities to municipalities, corporations, or ultimately the level of specific people in society by and large. Attention to sustainable development issues is also growing against the backdrop of an obvious deterioration in the climate situation and the need to create energy security.

Keywords: sustainable development, greenhouse, gas emissions, environmental challenges, environmental protection, advanced technologies

I. Introduction

Modern technologies become part of any business and serve as a key factor in ensuring its competitiveness [1]. However, complex technologies have limitations that do not allow them to fully use their full potential to solve the problems of the ESG agenda. The first limitation is due to the fact that the use of advanced analytics technologies requires huge computing power, and this, in turn, leads to an increase in energy consumption and entails an increase in carbon dioxide emissions, negatively affecting the company's ESG indicators and the environment as a whole [2]. The second limitation is the ethical aspects of new technologies. Cloud computing can be one of the solutions to circumvent the above limitations. They respond to environmental challenges through more efficient energy management. The solution of the ethical aspects of new technologies in the clouds is achieved by standardizing the algorithms of the models used, using a huge amount of data, and constantly checking and validating the results. Now modern technologies are becoming a part of any business and serve as a key factor in ensuring its competitiveness. For example, with the help of advanced analytics, the most resource-intensive, complex and non-trivial tasks are already being implemented, the solution of which was previously impossible or impractical due to huge time and material costs [3]. Technologies allow you to analyze a huge amount of data in a short time, provide self-learning models and identify complex

relationships, build accurate forecasts, collect information and analyze, respond to changes in production indicators online, as well as securely store this data and much more. Digital tools based on sophisticated analytics are also applied to companies' internal processes to improve their efficiency. For example, advanced technologies are widely used in the world to solve problems in the field of ESG. In the Russian market, the share of penetration of modern technologies into ESG is small, however, according to a joint study by the audit consulting company Trust Technologies (hereinafter referred to as TeDo) and the Center for Sustainable Development of the SKOLKOVO School of Management, 65% of leaders of large Russian companies believe that without digital solutions it is impossible to implement ESG transformation. For example, in the field of ecology and climate (E), artificial intelligence technologies can achieve the goal of the agenda by creating smart and low-carbon cities, Internet-of-Things-based devices that can regulate electricity consumption. They also help improve the integration of renewable energy sources through smart grids and identify desertification trends through satellite imagery.

II. Methods

As part of the social aspect (S), it becomes possible to create safer working conditions for employees. In the management part (G), thanks to the use of advanced technologies, reporting is automated, which becomes more transparent and accessible to the public. As the mentioned study shows, the following technologies have the greatest potential for achieving maximum efficiency in solving ESG problems [4]:

- artificial intelligence (29%);
- internet of things (23%);
- blockchain (14%).

However, it should be noted that for the implementation of specific digital solutions for ESG, combinations of these technologies are often used, which complement and enhance the effectiveness of each other. Let's consider the most common examples of using the technologies under consideration for the entire spectrum of tasks in the field of ESG.

The combination of artificial intelligence and the Internet of things is an indispensable tool for tackling climate and environmental issues, such as managing a company's carbon footprint. On the basis of artificial intelligence technologies, data are collected and consolidated reflecting the emission and absorption of greenhouse gases from production sensors in the context of individual processes. The specified array is further converted using machine learning into predictive models that allow high-precision assessment and optimization of the company's processes. According to Accenture research, more than 70% of companies report the effectiveness of digital emission reduction solutions implemented using artificial intelligence. Combining artificial intelligence with blockchain technologies makes it possible to more transparently track the carbon footprint formed by the components of the company's products throughout the supply chain and for all types of coverage (Scope 1, 2 and 3). An example of a digital carbon footprint management tool is a solution to reduce energy intensity implemented by a large steel company. Thousands of sensors collect data, which is then processed by artificial intelligence algorithms. This allows the company to accurately calculate and predict energy needs, and track and reduce emissions. Since implementing the solution, the company has implemented a number of initiatives that, according to BCG, resulted in a 3% reduction in carbon dioxide emissions, which is approximately 230 thousand tons of CO₂ per year, and reduced costs by \$40 million.

III. Results

According to a McKinsey study, more than 20 examples of using artificial intelligence to improve the quality of life and health of company employees and 3 examples of gender equality stand out in order to achieve the sustainable development goals [5]. These goals are included in the social aspect of the ESG agenda. The most striking example of the use of artificial intelligence in the social sphere is the implementation of solutions that provide safe working conditions. On the basis of data received from

surveillance cameras, self-learning models are formed that recognize standard operating conditions and deviations from the norm. Further, the data from surveillance cameras is analyzed online and, using predictive analytics, hazardous work areas and risks are identified that can lead to incidents at the workplace in the future. For example, it is possible to track the movements of employees and identify potential hazards along their routes, such as the danger of tripping or the presence of loose equipment. With the help of such solutions, it becomes possible to set up notification of managers and staff about emerging risks and security incidents in the workplace, which allows them to be eliminated in a timely manner. Updating and processing data in real time allows you to monitor employees who violate established security rules. Internet of Things technologies complement and increase the efficiency of the digital solutions discussed above based on artificial intelligence. With the help of special sensors and thermal imaging cameras, data is collected about the environment surrounding the company's employees and its safety is assessed. For example, some companies are using machine vision to monitor employee safety in hot work areas. In particular, thermal imaging cameras can be used to detect "heat stress" in workers and provide them with the necessary assistance in the form of a cool down break or additional personal protective equipment. Sensors are also used to analyze the composition of the air in the working room [6]. They scan, analyze and immediately report the presence of harmful particles, pollutants or hazardous gases such as carbon monoxide. By collecting and analyzing air quality data and alerting anomalies, such systems help prevent the release of harmful pollutants into the atmosphere, while maintaining the safety and health of every employee. Additionally, with the help of artificial intelligence and the Internet of things, it becomes possible to create smart offices focused on maintaining the health, well-being and safety of company personnel. Occupancy sensors keep track of the number of people in the office at a given time. The visualization of such data enables flexible working formats, such as shared desk systems, and facilitates social distancing and prevents overcrowding in the workspace. Employees have access to this data to decide whether to visit the office. Also, office attendance data allows real-time implementation of office cleaning planning models that take into account their use. The level of air quality also affects the safety of personnel. A high amount of carbon dioxide in the air is associated with poor decision making, lack of concentration and drowsiness. Air quality sensors measure the level of carbon dioxide and volatile organic compounds and display the data on the dashboard to adjust the working environment of office workers accordingly. An industrial security video analytics project implemented by a large Russian company, which includes monitoring of hazardous areas, the use of PPE (personal protective equipment), collision risks and a number of other aspects, is an example of the implementation of a solution based on modern technologies in terms of the S-component. All collected data is analyzed in order to completely prevent accidents. In the near future, it is planned to equip employees with portable devices that allow monitoring biorhythms and monitoring critical health conditions, including pre-infarction and pre-stroke, which carry a great danger, especially when operating complex equipment, because in the event of an unexpected deterioration in health, the life of the employee himself is at risk, and his colleagues [7]. By connecting portable devices to the on-board computers of the technician, an instant stop of traffic will be provided, notification of those responsible for the site, and, most importantly, a call for an ambulance brigade, which upon arrival will have all the necessary data on the state of a person for prompt assistance.

IV. Discussion

Modern technologies also make it possible to successfully implement solutions aimed at impartial evaluation of work and professional development of employees. With the help of big data analytics and artificial intelligence, a large financial holding has developed a personnel assessment system that solved the problem of biased feedback due to collusion between employees. This decision, based on the analysis of information about 25 thousand employees and more than 125 million emails, identified informal leaders who are most actively and effectively involved in decision-making and task completion. It was

found that the intersection of the list of candidates for promotion, compiled by employees, and opinion leaders, determined by the decision based on artificial intelligence, is only 60%. Thus, employees whose promotion is premature were identified, and in general, transparency and impartiality were added to the decision-making process on the promotion of employees. Artificial intelligence-based solutions aimed at training and professional development of employees allow the formation of personalized recommendations of the most relevant courses for an individual employee based on user clustering and training programs. The accuracy of the recommendations is achieved by analyzing the test results, personal profile, requirements for the position, as well as user experience. A similar solution is used by one of the largest banks in Spain. Another example of a more responsible attitude towards employees is the use of big data to prevent professional burnout [8]. The most striking example is the experience of a large construction company, which, using analytics and big data structuring, revealed that 14% of employees are in the last stage of burnout. The decision made it possible to apply employee support measures in a timely manner and reduce the level of staff turnover.

Good governance requires full transparency and accountability for key processes. With the help of artificial intelligence-based solutions, it becomes possible to automate the formation of key ESG indicators, which allows for a transparent, versatile and unbiased analysis of the company, eliminating the risk of human error in calculations, as well as their distortion. The main problem of automating the generation of ESG reporting is the heterogeneity of the required data sources. It is solved by using NLP (Natural Language Processing) algorithms, which allow machine learning to be applied to text written in natural language. Artificial intelligence-based solutions are already on the market, which, through full integration into company processes, allow collecting and processing data, calculating ESG metrics and comparing indicators with market averages. An additional reporting requirement under this aspect is to ensure the traceability of reporting and the possibility of its audit, which can be achieved through a combination of artificial intelligence with blockchain technologies. This decision allows you to confirm the immutability of the data reflected in the company's financial statements. All data stored on the blockchain platform can be verified by regulators or an independent party to confirm the company's compliance with the established standards and to verify that its statements, messages and advertisements correspond to its actual practice. For example, many corporations have committed to significantly reduce or eliminate their carbon footprint, which is reflected in corporate goals. Thanks to blockchain technologies, these goals can be compared with the organization's current carbon footprint. The above examples show that global problems in the field of sustainable development are currently being effectively addressed through the use of advanced technologies [9]. However, complex technologies have limitations that do not allow them to fully use their full potential to solve the problems of the ESG agenda. The first limitation is due to the fact that the use of advanced analytics technologies requires huge computing power, which leads to an increase in energy consumption and entails an increase in carbon dioxide emissions, negatively affecting the company's ESG indicators and the environment as a whole. In practice, training artificial intelligence models requires a huge amount of computing power, and some researchers argue that the environmental costs of applying advanced analytics outweigh the benefits. By some estimates, in just a few years, the digital industry will generate more carbon emissions than all road transport. Digitalization already accounts for 4% of global greenhouse gas emissions, according to EY analytics. The ecological footprint of the digital world is constantly increasing as energy consumption grows in parallel with the growth of the industry as a whole to meet the demand for technology. Some experts believe that by 2025 the technology sector could consume 20% of all electricity in the world. This growth from the current 7% is logical against the background of the development of complex technologies, such as artificial intelligence, which contribute to the demand for computing power. The second limitation is the ethical aspects of new technologies, in particular artificial intelligence. In most cases, historical data (often from a single company) is used to train artificial intelligence models, which can be limited and biased and lead to gender or racial inequality and discrimination from the decision based on such a model. An example is a scientific experiment led by researchers from Johns

Hopkins University, Georgia Institute of Technology and the University of Washington. Robots, functioning on the basis of artificial intelligence, were asked to distribute people into certain social roles and professions according to their appearance. The main conclusions of the study are as follows [10]:

- fair-skinned women in most cases were classified as housewives;
- black men were 10% more likely to be identified as criminals;
- Women were practically not assigned to medical professions.

This observation is a significant limitation for the use of new technologies in the field of the social aspect of the ESG agenda, since it directly contradicts the task of this aspect. Cloud computing can be one of the solutions to circumvent the above limitations. Cloud technologies respond to environmental challenges through more efficient energy management. The solution of the ethical aspects of new technologies in the clouds is achieved by standardizing the algorithms of the models used, using a huge amount of data, constantly checking and validating the results.

References

- [1] Zhuravleva V. V., Kazazaev V. V. On modeling plant photosynthesis under global climate change. No. 4 (96), 2020, pp. 104-107.
- [2] Pinyavina E.A. Creation of forest carbon (carbon) landfills: economic component // Actual directions of scientific research of the XXI century: theory and practice. 2021. No. 1. p.26-34.
- [3] Salamova A.S., Socio-economic factors in the fight poverty and hunger in the modern world: the scientific approach of Amartia Kumar Sen, 2023, 17(1), pp. 237-245.
- [4] Salamova A.S., Global networked economy as a factor for sustainable development, 2020, p. 03053.
- [5] Gakaev, R. Carbon sequestration in landscapes of the Chechen Republic. Reliability: Theory & Applications, 2022. Vol. 17. 3(66), pp. 193-196
- [6] Hansen, J.; M. Sato; R. Ruedy; K. Lo; D. W. Lea and M. M. Elizade, Global Temperature Change, PNAS, 2020, 103(39), pp. 14288–14293.
- [7] Leggett, J. A.; J. Logan and A. Mockey, China's Greenhouse Gas Emissions and Mitigation Policies, CRS Report for Congress 2008.
- [8] Verfaillie, H., and R. Bidwell, Measuring Eco-efficiency: A Guide to Reporting Company Performance, World Business Council for Sustainable Development, Geneva, 2020.
- [9] Kantyukov R R., Kolybanov K. Yu, Ravikovich V I Information technologies for preparing control decisions in automated systems of environmental monitoring, 2019.
- [10] Kampschreur MJ, Temmink H, Kleerebezem R, Jettena MSM, van Loosdrecht MCM. Nitrous oxide emission during wastewater treatment. Water Res. 2019, pp.4093–4103

RISK ASSESSMENT IN SUBSEA PIPELINES FOR THE CASPIAN SEA CONDITIONS

Ramiz Ismayilov, Rugiya Asgerova, Ismayil Ismayilov, Turkan Guliyeva

Azerbaijan State Oil and Industry University

ramismaylov@mail.ru

rugiya.askerova.74@mail.ru

ismayil516@gmail.com

turkan.guliyeva.sh@asoiu.edu.az

Abstract

The article presents the results of studies conducted on the analysis of risks in the underwater pipelines of the Azerbaijan sector of the Caspian Sea. For the study, the results of long-term observations of the state of the state of underwater pipelines and the opinions of experts in this field were collected. Based on the analysis of these data, the most characteristic situations were identified that, to one degree or another, led to the loss of pipeline performance and the need for repair and restoration work.

It was found that the main hazards for subsea pipelines in the Caspian Sea are external and internal corrosion. Pipelines floating, damage at pipe junctions, vibrations, damage from falling foreign objects, and wave impacts in the coastal strip. For the listed main and other rarely observed situations, quantitative risk assessment was carried out using the Boston Cube method. The results of the assessment showed that the greatest risk is associated with external corrosion.

Keywords: hazards, risk, risk analysis, risk assessment, list of failures, external corrosion

I. Introduction

Azerbaijan has more than 70 years of experience in laying and operating underwater pipelines in the Caspian Sea. After the signing of an oil contract for the development of the deep-water part of Azeri-Chirag-Gunashli in 1994, the design and intensive construction of new underwater pipelines began, ensuring the transportation of products from offshore fields to onshore terminals by using cutting edge technology. Within the framework of the project for the development of the Shah Deniz gas condensate field, new underwater communications are in operation and are being built currently. In connection with the prospect of expanding the Southern Gas Corridor project, increasing the capacity of TANAP and TAP, using the resources of Turkmenistan and Kazakhstan, underwater pipelines are becoming even more relevant.

At present, the issues of industrial safety of oil and gas facilities, including underwater pipelines, are given paramount attention. The solution of these issues is closely related to the analysis and assessment of risks based on various existing methods that are actively used in international practice. Moreover, in foreign practice, an underwater survey of structures is also carried out necessarily on the basis of a quantitative risk assessment and recommendations on which elements of the structure should be given special attention during the inspection.

When analyzing and assessing risks, various graphical schemes, diagrams and output tables are used, e.g., risk matrices are built, where potential hazards are ranked by frequency and degree of danger. In this case, the opinions of experts are taken as a basis and the correlation of the considered danger into one or another cell is, generally speaking, subjective in accordance with the

experience and intuition of specialists. To increase the reliability of this procedure and the degree of objectivity of the final decision on the expected risks, recent studies often use the methods of fuzzy set theory and fuzzy logic.

II. Methods

During the operation of subsea pipelines monitoring is periodically carried out based on the preparation of an inspection plan [1] in order to identify damage and assess the strength resource. The sample has been described at the Figure 1.

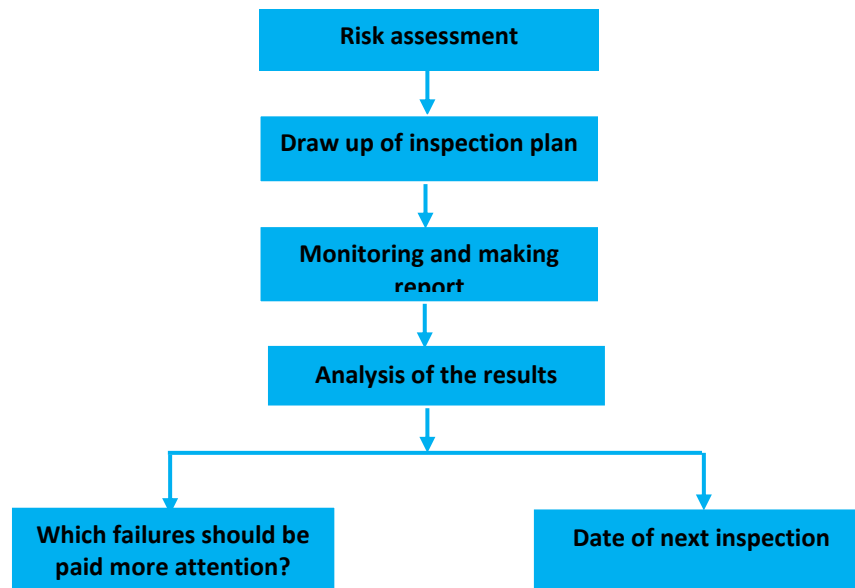


Fig. 1: Example of inspection plan

The Fig.1 shows a risk analysis and assessment should be carried out before conducting a survey. There are various methodologies for conducting a quantitative risk assessment [2-4], of which the Boston Cube method [1] was applied in this article and includes the following sequential steps.

Step 1. A list of possible situations is compiled that can lead to a loss of pipeline performance. Based on the analysis of data collected over many years of experience in the operation of subsea pipelines and based on the opinions of experts in this field for the conditions of the Caspian Sea, 15 items were included in the list of failures:

1. Damages in the connections
2. External corrosion
3. Internal corrosion
4. Surfacing pipelines
5. Vibrations
6. Damages from fishing
7. Wave loads
8. Current loads
9. Technological mode violations
10. Blockage of the pipeline
11. Destruction of the concrete pavement
12. Landslides of sea soil
13. Earthquakes
14. Mechanical damages from anchors
15. Damages in the raiser

Step 2. For each item presented in Step 1, 3 calculation parameters are calculated: the frequency of occurrence of the situation, the hazards level and the possibility of detection. The frequency is determined by the statistics of damage, accidents or repair and restoration work on underwater pipelines. The hazards level is assessed by experts and here the potential damage from the consequences of the situation that has arisen is taken as a basis. Regarding the parameter of detection level, the assessment of this parameter is based on the level of provision with the necessary special apparatus and means for conducting an inspection of underwater pipelines. All three calculated parameters are evaluated at 3 levels (H- High, M - Medium and L - Low level, respectively 3, 2 and 1 points).

Step 3. The final risk for each item in Step 1. is estimated as the product of the estimates for all 3 calculated parameters and the Boston Cube (3-dimensional risk matrix) is built. Thus, the value of the final risk ranges from 1 (1x1x1) to 27 (3x3x3).

We will illustrate the implementation of the above sequential procedure using the example of the point related to external corrosion. Many years of experience in the operation of subsea pipelines in the Caspian shows that this is the most common situation. Therefore, the frequency of occurrence of this situation can be estimated at the maximum level (3 points). The degree of danger can also be rated at 3 points, since corrosion defects can lead to very serious consequences (leaks, pipeline rupture, oil spills, etc.) and potential damage can reach very large sizes). As for the calculated parameter characterizing the possibility of detecting the situation, Azerbaijan (SOCAR) currently has a special vessel for underwater inspection of oil and gas facilities, equipped with special equipment. Also, special diving groups can be involved in underwater surveys. But, the remaining difficulties in carrying out these works, the level of possibility of detecting external corrosion in subsea pipelines under local conditions can be assessed as an average level (2 points).

Thus, the final value of the risk for the situation associated with external corrosion can be estimated as $3 \times 3 \times 2 = 18$ points. Similarly, totals were obtained for the risks associated with all considered situations (List of failures, Step 1.) and are presented below in the Table.

III. Results

Table: Results for risk assessment

Results for risk assessment					
No	Situations	Frequency	Hazards level	Detecting level	Risk
1	Damages in the connections	3	3	1	9
2	External corrosion	3	3	2	18
3	Internal corrosion	2	3	1	6
4	Surfacing pipelines	1	3	3	9
5	Vibrations	1	3	3	9
6	Damages from fishing	1	1	1	1
7	Wave loads	1	3	1	3
8	Currents loads	1	3	1	3
9	Technological mode violations	1	2	2	4
10	Blockage of the pipeline	1	3	1	3
11	Destruction of the concrete pavement	2	2	1	4
12	Landslides of sea soil	1	3	1	3
13	Earthquakes	1	3	1	3
14	Mechanical damages from anchors	1	3	1	3
15	Damages in the raisers	2	2	3	12

IV. Discussion

Analysis of the obtained results for risk assessment in subsea pipelines of the Azerbaijan sector of the Caspian Sea showed that out of 15 typical situations taken for consideration, the greatest risk is associated with external corrosion. The lowest risk is rated for damage from fishing. The results of all the obtained assessments can be said to agree quite well with the assessments of experts from among scientists, leading specialists and risk analysts in offshore oil and gas facilities and, in particular, underwater pipelines. However, the experts' opinions are based primarily on their experience, intuition, and are, generally speaking, subjective in nature, and the level of confidence in these estimates can be increased using the opinions of several experts individually or by a group of experts. Risk assessment for subsea pipelines according to the above Boston Cube construction procedure assumes ranking for design parameters at 3 levels (High, Medium and Low level). But this very ranking and correlation of the frequency of occurrence of a situation to one level or another, especially in conditions of uncertain and insufficient information, is subjective. Decision making under such conditions is based on fuzzy reasoning, and carrying out logical operations with them and formulating a fuzzy logical conclusion can be described quite well from the standpoint of fuzzy set theory [5,6].

Let us illustrate the possibility of applying the methodology of fuzzy sets to estimating the parameter of the frequency of occurrence of a situation in a pipeline that can lead to a loss of pipeline performance. The frequency of occurrence of the situation is assessed at 3 levels (low, medium and high levels) and the question arises what is meant, for example, by low frequency. We formalize this imprecise definition from the point of view of the concept of a fuzzy set.

As is known, an arbitrary fuzzy set C can be represented as a set of ordered pairs $\{MF_C(x) / x\}$, where $MF_C(x)$ is a membership function. This function expresses the degree of belonging to a fuzzy set C and is defined on the interval $[0,1]$. A value of 0 indicates the absence of membership, and 1 indicates a complete belonging to a fuzzy set. The set x defines the scope of reasoning.

The parameter "The frequency of occurrence of a situation" in the theory of fuzzy sets can be characterized as a linguistic variable [5], which in turn depends on three fuzzy variables: "Low frequency"; "Medium Frequency" and "High Frequency". The reasoning area for this linguistic variable, using the example of an underwater pipeline, will be based on the following considerations. The long-term experience of operating underwater pipelines shows that typical situations can be identified that can lead to failures in their work: external corrosion, internal corrosion, ascent of pipelines, damage to connections, vibration, damage from anchors of shipping vessels and trawls of fishing vessels and other situations. Each of these situations occurs with a certain frequency, that is, as a percentage of the total sample size (the number of situations that occurred).

Based on this, the reasoning area for the notion "The number of events" for each situation can be set on the set $[0; 100]$. The membership functions for each linguistic term (low, medium, and high frequency) are given in trapezoidal and triangular form, and the resulting distribution is shown in the Figure 2.

We will set the values of the belonging function on the line $[0; 1]$ according to the following rules.

For correlation to fuzzy set C-"Low frequency":

$$IF 0 \leq x \leq 5, MF_C(x) = 1.00;$$

$$IF 5 < x \leq 10, MF_C(x) = 0.50; IF 10 < x \leq 100, MF_C(x) = 0.00.$$

For correlation to fuzzy set C - "Average frequency":

$$IF 0 \leq x \leq 10, MF_C(x) = 0.00; IF 10 < x \leq 15, MF_C(x) = 0.125;$$

$$IF 15 < x \leq 50, MF_C(x) = 1.00;$$

$$IF 50 < x \leq 100, MF_C(x) = 0.00.$$

For correlation to fuzzy set C-"High frequency":

$$IF 0 \leq x \leq 50, MF_C(x) = 0.00;$$

$$IF 50 < x \leq 60, MF_C(x) = 0.40;$$

$$IF \ 60 < x \leq 100, MF_c(x) = 1.00$$

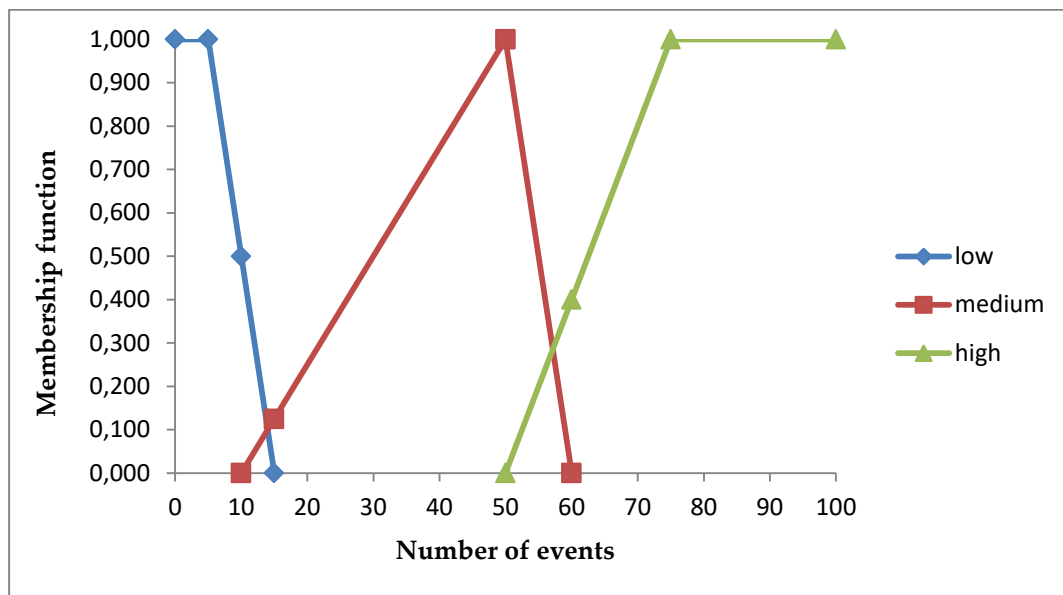


Fig. 2: The distribution of values of membership function for the linguistic variable "frequency of the situation"

As can be seen from the figure, if any situation, leading to some extent to the loss of performance of the underwater pipeline, is observed with a frequency of 15%, then it can be attributed with a membership degree of 0 to a low frequency, and with a value of 0.125 - to an average frequency. The situation that occurs with a frequency of 60%, with a membership degree of 0.40, can be correlated with a situation with a high frequency, and with a value of 0, with an average frequency. At the intersection of lines for different frequencies, when choosing how to characterize the current situation, we can compare the corresponding values of the membership function and correlate the situation under consideration to a category with a higher degree of membership.

Regarding the other two parameters as the degree of danger of the situation and the possibility of identifying it, then, similarly to the procedure carried out above, you can also formalize these two fuzzy concepts and construct the corresponding membership functions for them. At the final stage of risk assessment, we must set the rules to establish a fuzzy logical conclusion about the degree of risk for each situation under consideration. Here we will operate with the values of the membership function constructed for each linguistic term.

Let us dwell in more detail on obtaining expert estimates when applying the Boston Cube method and comparing the estimates obtained using other methodologies. It should be noted here that the main idea in the risk assessment methodology is that risk assessment can be complicated only if the information collected about the object (process) under consideration is insufficient. Therefore, it is recommended to start with a qualitative risk assessment based on available process data. Risk assessment begins with risk identification (HAZID), for example, according to the WHAT-IF method. You can then move on to other analysis methods such as CHECKLIST-ANALYSIS, HAZOP, FAULT TREE ANALYSIS (FTA) or BOWTIE charting. In all these listed methods, the opinions of experts are decisive.

The quantitative assessment of risks proposed in the work using the Boston Cube method assumes the availability of sufficiently extensive information about the object. With regard to subsea pipelines in the Caspian Sea, such information exists on the basis of statistics on accidents, their reasons for carrying out repair and restoration work, and based on the results of earlier expert assessments. These data allowed us to compile a list (List of failures) of 15 previously observed situations typical for the conditions of the Caspian Sea that led to the loss of performance of the subsea pipeline during the assessment. At this stage, we take as a basis the frequency of occurrence of the situation, that is, of all the observed situations, the selected 15 are the most

common. However, when ranking the frequency (high, medium or low), the expert makes a decision, which, generally speaking, is somewhat subjective, for example, if the corrosion situation was observed with a frequency of 0.2, then by what criterion to relate it to a low, medium or high level.

Here, the expert can use, in our opinion, data analysis methods (rank classification, cluster analysis), which we did not use in this work. We only propose in this article, as one of the possible solutions, the adoption of the fuzzy inference methodology. On the other hand, the objectivity of an expert assessment can be somewhat increased when ranking the situation under consideration, using a team of experts when making a decision. It is also possible to conduct a comparative analysis of the results of the analysis and risk assessment by other methods. Thus, the result of obtaining the maximum risk for subsea pipelines associated with external corrosion is in good agreement with the results of estimates using the Event Tree analysis method.

At present, the safety issues of industrial facilities, including strategically important offshore oil and gas facilities and related underwater pipelines, are of paramount importance. The solution of these issues is also closely related to the analysis and assessment of risks, starting from the design stage and further during the construction and operation of these facilities.

Safety issues also include environmental risk assessment. Subsea pipelines are characterized by an oil spill situation due to damage at the joints, corrosion defects, leaks, pipe breaks, etc. Here, the methodology of the Boston Cube can also be applied to assess the risk of environmental pollution. In this case, the frequency of occurrence of damage and the manifestation of defects leading to spillage of the product can be taken as the first design parameter in this case. As the second parameter, it is advisable to consider the potential volume of spilled oil, and the third parameter may be, for example, the parameter of the sensitivity of the environment to the situation that has arisen. The latter parameter can be ranked depending on the wave and wind regime in the area, the presence of underwater currents, proximity to the coast and so.

References

- [1] Sattarov R.M., Ismayilov R.A., Sattarzade I.R., Mamedova R.I., Azizov I.A., Mekhtiev J.Sh. Increasing of reliability of pipeline systems on the basis of estimation risks /Scientific Research Institute Geotechnological Problems of oil, gas and chemistry/ Workshop. Socio-economical aspects of the energy corridor linking the Caspian Region with E.U. – Baku. -2007, p.124.
- [2] Graham McIntosh Risk management in the operations of Subsea pipeline /Symposium Series No.155. Hazards XXI.-2009, pp.724-728.
- [3] Yu Jianxing, Wu Shibo, Chen Haicheng, Yu Yang, Fan Haizhao, Liu Jiahao Risk assessment of submarine pipelines using modified FMEA approach based on cloud model and extended VIKOR method. Process Safety and Environmental Protection. Elsevier. Volume 155, November 2021, pages 555-574.
- [4] Adlara D.R., Artana K.B., Ariana I.M. Risk assessment of subsea pipeline due to installation and Operation of Single Point Mooring (SPM) /IOP Conference Series 557 (1):012031, 2020, p.1-14.
- [5] Hengameh Fakhravar Quantifying Uncertainty in Risk assessment using fuzzy theory. Research Project. Engineering. Old Dominion University/ April-2020, 31p.
- [6] Ismayilov Ramiz. Application of soft computing to research of transient processes in the gas pipelines. Procedia Computer Science 120 (2017), pp. 461-465.

THE LABOR CONTRIBUTION OF THE DEPORTED PEOPLES TO THE DEVELOPMENT OF THE ECONOMY OF CENTRAL ASIA IN 1940-1950

Sapiyat Tsutsulaeva



Kadyrov Chechen State University, Russia

sapiyat_univ@mail.ru

Abstract

The historical labor contribution of exiled Chechens and Ingush to the mining sector of Central Kazakhstan was large in the 1940s and 1950s. Throughout this period, a large number of exiles were recruited to work in different industrial and mineral-mining companies. During this period they began to recruit workers for working in various industrial enterprises, including mine projects. Moreover, they worked in mine and other mining companies. Their activities were made by miners, coal mines and other industrial projects that helped to develop the development of Kazakhstan's economic system. The deportation of Chechens and Ingush were a repression with social and economic consequences for the deportees themselves. This forced displacement of Kazakhstanis and living in difficult conditions in new settlements caused great problems and difficulties for them, as well as for the economy of Kazakhstan. Their forced displacement and living in difficult conditions made it possible to solve many problems with economic development at all.

Keywords: deportation, economy, adaptation, deported peoples, employees at agricultural, agro-industrial experience

I. Introduction

Chechens and Ingush were deported en masse to Central Asia (mainly Kazakhstan and Kyrgyzstan). The decision of the Soviet government was adopted in 1944, by decision from Russia, as part of the Soviet Government. This measure related to accusations that the local population collaborated with the occupying Nazi forces during the Second World War [1]. The measure was related to accusations that the local population cooperated with the occupying Nazi forces during the Second World War. It was. Almost in recent years, historians have begun to understand that the real reason for deportations was the political and repressive measures of the Russian regime. The control over ethnic groups in the Caucasus region was also suffered by Russia's anti-separatist policy. A large part of the historical influence of deported ethnic groups such as Chechens and Ingush to Kazakhstan's economic development is attributed to the history of Kazakhstan's economic development, but not always well documented or easily quantified. Most ethnic groups have faced difficulties and socio-economic hardships during the history of deportations. In Kazakhstan, some of the deported groups may have helped to develop and improve the economic development of different sectors of the economy such as agriculture, industry, culture and education. In order to obtain more specific information on the contribution of migrant groups to the economy of Kazakhstan, it is important to conduct research and consult sources that take this aspect into account.

Private settlements were seen as economically productive ventures. It was assumed that the problems associated with the resettlement of special settlers would be covered by the benefits of providing labor for key sectors of the state economy, i.e. additional advantages in the competition for centrally allocated resources. Expatriates were expected to provide cheap labor for the active exploitation of Kazakhstan's natural resources. However, deportation was not as cost-effective as expected. There was also irrational spending of state funds. This was already evident at the resettlement stage, when miscalculations in the choice of location led to the fact that many settlements were relocated or liquidated, and settlements with existing buildings and cultivated land were abandoned [1]. In addition, many deported ethnic groups were placed in destroyed collective farm areas. The economic activities of special settlers were often unprofitable. The qualitative indicators of the production activities of special settlers were recognized as very low. Expenses were spent only on transportation and organization of the special resettlers. Everything else was the work of the resettlers themselves. They had to build their own houses, feed their own settlements and do their own work. However, in reality, everything turned out to be not so smooth. The lack of infrastructure in the settlements of special settlers created many difficulties. Special settlers were not prisoners deprived of freedom, but they could not be called free either. It was assumed that their forced labor would be paid according to civilian labor standards. In practice, however, everything was greatly simplified, and legal discrimination was accompanied by discrimination in wages depending on working and living conditions. For those in charge of forest plots, forest bunches, timber enterprises and other enterprises that used special settlers as labor force, they were certainly a burden. The managers were interested in the high labor productivity of the special settlers. The local administration was convinced that the special resettlers were a temporary population and that there was no need to take measures to "immobilize" them, i.e., to ensure proper living conditions, medical and social services. At the enterprises that used the labor force of special settlers, the turnover of personnel was very high, and many employees left their workplaces and deserted. For example, 135 Poles, Armenians, Ukrainians and Bulgarians deserted from the Petropavlovsk power plant in 1943. In addition, special resettlers did not return to work after their leave but moved to other areas, many committed crimes and ended up in correctional institutions, and some left after repatriation. Stalin's periphery understood that the war could not be won by over-centralizing the state and intimidating the people. Thus began the patriotic and religious feelings of the Soviet people, the study and propaganda of military history, and the call for a national liberation struggle. In addition, these activities were "preventive" and "sedentary" in nature, raising and strengthening the fighting and peaceful spirit of the local population and special settlers, motivating them to new labor activity.

II . Methods

At the moment, various methods were used to study in the problem of deported Chechens to Kazakhstan and Central Asia [2].

1. Historical analysis: Researching on archival documents, historical data, eyewitness accounts and other materials that document the deportation of Chechens and its consequences. 1. Historical analysis: Investigating on archival documents, historical data, eyewitness accounts and other materials that document the deportation of Chechens and its consequences. 2. The. It is based on archival documents, history or other materials that document the deportation of Chechens and its consequences.

2. The process of conducting polls and interviews with deported Chechens, the descendants or members of local groups in order to study experienced Chechens, perceptions and impact of deportation on life and cultural identities.

3. Ethnographic research: The study of the traditions, customs, culture and way of life in Chechen new places derived from deportation. 3. Ethnographic research: The study of the

traditions, customs, culture and way of life in Chechen new places derived from deportation. You can understand what happened after removing Chechens from old village for an understanding of the change that occurred after the deportation.

4. Geographical analyses: The analysis of the geographic and natural conditions in regions that are Chechens' living place in Central Asia and Russia, to identify an impact of the natural environment on economic activities.

5. Psychological research: The study of the psychological impact of deportation on Chechens and their descendants, as well as the identification of mechanisms for adapting to new conditions.

6. Comparative analysis: comparison of similar and different aspects in deportation, its consequences at the same time in different territories of Kazakhstan and Central Asia. Comparison of similar and different aspects of deportation and its consequences in different territories of Kazakhstan and Central Asia.

7. Literature review: Analysis of previous studies and publications on this topic to summarize and systematize the available information.

In addition, the combination of various research methods will provide a more complete picture about the problem in deported Chechens and its adaptability to new conditions, as well as identify important aspects and recommendations for the future.

According to Chechens, the deportation of people from Russia and Asia was accompanied by serious changes in their environment and lifestyle, which also affected their ability to preserve their cultural traditions and identity.

Repression in the Soviet Union was primarily aimed at legal, moral and psychological discrimination, and was also an act of mass extermination. Chechens, like other inhabitants of our country deported during the Great Patriotic War and deprived of the right to free movement, were totally dependent on their commanders. This is exactly what we are talking about: the deportation of people from their own country [3]. Most of the representatives of the deported population were not nominated or even re-elected to a number of important state, public and private bodies. Most were neither nominated nor elected to the most prominent state bodies and public services. Special resettlers were also discriminated against in the professional sphere. The fact that IDPs began to study in universities and specialized schools has introduced a ban on their education. What was possible for them in universities and professional schools in such countries is now forbidden for them.

III . Results

According to the March 1944 Regulation on the economic and labor organization of special settlers (Kalmyks, Karachais, Chechens, Ingush, Balkars and Germans), the NKVD bodies were in charge of employment of special settlers. The settlers enjoyed the "right" to work in state farms, MTS, artisanal workshops and other state institutions. Where the possibility of employment was excluded, their labor was used for rough work. Most of the special settlers were used in non-specialized collective agricultural work, they were forbidden to move from one job to another without the permission of the Special Commandant's Office of the NKVD. At the same time, according to the rules, persons with higher and specialized secondary education were to be used only in their specialty. If it was not possible to use specialists in a settlement, the NKVD allowed them to move to other areas to find suitable work. In the absence of work in rural areas or in industry, prisoners were allowed to be members of artisanal collectives under the trade cooperation. According to No. 2, prisoners were allowed to join trade unions [4]. According to the Decree of the People's Commissariat of Finance of the USSR No. 5073 of January 31, 1944 "On measures for the reception of special settlers within the Kazakh-Kyrgyz SSR", special settlers from the North Caucasus were hired as employees at agricultural, labor and professional enterprises. The issue of employment of resettlers was repeatedly considered, and schemes of "rational" use of their labor force were developed: according to the decree of the USSR SNK No. 35 of January 8,

1945 "On the legal status of special resettlers", all able-bodied special resettlers were obliged to engage in socially useful labor. For this purpose, local Soviets of Workers' Deputies, together with NKVD organizations, organized the employment of special settlers in agriculture, industrial enterprises, construction sites, economic and cooperative organizations and institutions. During the Great Patriotic War the qualitative composition of the labor force in agricultural production changed dramatically. Not only the physically healthy, but also the most capable rural residents, such as machinists and drivers, left for the army. The gender and age structure of the rural labor force also became "militarized" [4]. Mobilization to the front reduced the share of the able-bodied population in the republic and caused the need to find employment opportunities.

Mobilization of labor resources posed the task of planned calculation and distribution of labor force, in particular, the participation in the labor process of the available healthy population of the republic, not employed in public production. The study of demographic changes by regions in 1941-1945 allowed us to conclude that the most noticeable demographic changes were observed in the north and south of Kazakhstan. In 1942, the share of healthy male population employed in collective farm production was 22%. At the same time, 649 thousand women and 255 thousand teenagers worked here; on December 10, 1941, additional classes were introduced in all secondary schools to teach students agricultural labor. These figures show that women, old people and children were the main workers in collective farm production. In 1944, men accounted for 20% of the able-bodied population, women for 58%, and young people for 22% [6].

In 1951, several Chechens and Ingush were employed in Kustanai Oblast. Almost all special resettlers were employed in various sectors, mainly in agriculture. There were a small number of qualified specialists among Chechens and Ingush. In Sokolovsky, Mamlyutsky, Prusimsky and Konyukhovskiy districts, more than 50% of the resettlers and 100% of the settlers did not participate in collective agricultural work.²² It is important to note that local government organizations and evacuation departments did not keep records of the work in which the special resettlers were employed. This was often the case. However, settlers rarely held managerial positions. The assistant to the head of the Kustanai branch of Grabt Baksirie was a special settler N. Prieve, the deputy head of the Zagozernovskiy branch was M. Vezhdiev, the first deputy chairman of the regional executive committee was G. Kamchiev. In 1945, there was one Chechen deputy chairman of collective farms in Kustanai Oblast. In 1952, a considerable number of Poles held leading positions in Kochetava Krai: 34 collective farm chairmen, 29 deputies, 114 farm managers, 147 farm managers, 81 tractor brigade leaders, 28 chairmen of local committees, 20 chairmen of village councils, 34 agronomists and livestock specialists [5]. In 1952, 116 Poles worked in regional centers as technicians, teachers and doctors. In the regional district out of 607 people there were 34 collective farm chairmen, 29 deputies, 114 farm managers, 228 controllers, 28 district committees, 20 chairmen of village councils, 34 agronomists, zootechnicians and technicians. Special settlers influenced the development of the network of educational institutions in Northern Kazakhstan. With their participation libraries, houses of culture and schools were organized, and in 1951 31 Poles were in charge of libraries and reading rooms.

IV. Discussion

The majority of teachers-special resettlers were conscientious about their work. Many of them were awarded medals of the USSR for many years of faultless labor. Among them are the teachers of the secondary art school No. 57. K. Denner and N. Sheibel from Kushmulun were awarded the Order "For Labor Merit". Such German teachers enjoy deserved authority among pupils and parents: O. Kirsh - director of Semenovskaya school, Zatobori district; I. Rehtel - mathematics teacher of Sergeevskaya school, Zatobori district; K. Bauer - chemistry teacher of Denisovskaya secondary school, Ordzhnichenkovskiy district; Ing. A. Kakieva - biology teacher of Smirnovskaya school, Peshkovskiy district; Chechen V. Akhriev - mathematics teacher of Grebovskaya school, Ordzhnichenkovskiy district. In Kustanay region by the early 1950s, 325 teachers were registered as

special settlers, 265 of whom worked in general schools, specialized secondary schools and institutions of public education. Almost all the teachers were Germans. The rest of the teachers were employed in other jobs. In Kustanai oblast, the special settlers also worked in the medical field as doctors, paramedics and nurses. Ni Saara N. Kustanai central outpatient surgeon, Tukai S.A. Ambulance doctor of Kustanai district, Kan Gilsun. An ambulance doctor of Ubagan district [6]. In fact, the special settlers themselves were engaged in noble medical work and actively helped themselves and the local population in the fight against diseases. By the end of 1952, 30 Germans, 10 Chechens and Ingush were on the Komsomol register in Kustanay region. 3 special settlers received government awards for their contribution to the development of agriculture, 4 received government commendations and 4 received diplomas of the regional committee of the Komsomol for "leading the entire union youth by systematically fulfilling and exceeding the norms in all continuous seasonal work [7]." The deserters made a significant contribution to the development of Northern Kazakhstan. Koreans were engaged in growing vegetables, melons and grain crops, Germans in farming, Chechens and Ingush in cattle breeding.

According to the Chechens, they survived by showing amazing adaptability. Chechens have shown remarkable adaptability. For them, life in the regime of ethnic exile was difficult. Many Chechens in Kazakhstan contributed to some sectors of the economy and many to others. In agriculture, construction and other sectors they were actively involved. In agriculture, industry, construction and other sectors they took an active part.

Agriculture played an important role in the development of Kazakhstan's economy at that time, and Chechens contributed to the development of farming and cattle breeding. As a result, they acquired knowledge and experience in agriculture and animal husbandry, helped develop rural facilities and increased agricultural production.

Chechens from other regions of Kazakhstan also took an active part in the construction of industrial enterprises and industrial facilities in their regions. In the development of the country's industrial production and productive forces, workers' support for the country's industry and productive forces was of great importance to both the development of industrial production and the development of the country's labor force.

In the face of all the hardships of exile, Chechens showed resilience and devotion to their new homeland. They actively participated in the establishment of cross-border relations with the rest of the world. In terms of cultural and historical diversity, they are an important factor in Kazakhstan's economic development. Thus, they allow the economy to develop. Historical the most important elements of cultural and historical diversity are. Their contribution to economic and social development is one of the most important elements of historical cultural-historical diversity. The Soviet government deported natives of the Caucasus, primarily Chechens and Ingush, from Central Asia to Russia in 1944. The Soviet government deported natives of the Caucasus, especially Chechens and Ingush, to Central Asia [8]. All the deportees had to face harsh living conditions, adaptation to the new environment and a difficult life. At the same time, they brought with them knowledge and skills that could be used in various sectors of the economy. Simultaneously with the deportation and in later years, the deportees worked actively in the construction industry. In different periods of Kazakhstan's history, the labor resources from deported population have an important impact on the construction of objects for economic development. They have made an important impact on the work of them. Their labor was increased by their own activities, and they were notable for its contribution to economic activity as well as developments in the capital. When Stalinist repressions and collectivization, many people were forced to abandon their homeland and move to Russia.

During the deportations, especially during the years of Stalin's repressions and collectivization, many people were forced to leave their homeland and move to the territory of Russia. They were forced to leave their native places. Thousands of other people were forced to leave their native places and move on their own [9]. In the long term, the social life of the Kazakh

people improved, and the country developed in terms of cultural diversity and skills. This development was driven by the cultural diversity of Kazakhstan's growing population, which in turn allowed the Kazakh people to grow even more. The resulting diversity of cultures, traditions and skills allowed the country's economic development to expand. This is attributed to an increase in their achievements by more than 50%.

Among the defectors, most brought with them industrial and agro-industrial experience, industrial and agro-industrial knowledge. This contributed to the development of Kazakhstan's economic base. These are. It was through their strength that organized labor was created. Their labor helped in the creation and development of a particular country. Their participation in the cultural and social life of the country has helped in the creation of organized labor force. Their participation extends to the education of children, construction and development of agriculture, and the creation of industrial production through the formation of an organized labor force [10].

It is important to note that ethnic migration generates social and economic problems. Conflicts and tensions arise among the deported population with the local population, which has difficulty adapting to the new environment. Among the deported population, conflicts and tensions arise in relations with the local population, which has difficulty adapting to the new situation. The successful economic development of Kazakhstan in modern conditions still depends on its multi-ethnic heritage. Not only that, the success of economic development in modern conditions still depends on it. The historical influence of expatriates on the modern image of Kazakhstan not only plays an important role in economic development and peace, but also supports social development and peace.

References

- [1] Tsutsulaeva S.S. , Documents and materials on the deportation of the Chechen people: general problems and the degree of their study, 2011, p. 196-203.
- [2] Tsutsulaeva S.S. The problem of the deportation of the Chechen people in the modern historiography of Chechnya. 2014. S. 152-159.
- [3] Podkolzina I.M. , Belousov A.I. , Uzdenova F.M. , Romanko L.V., Chernikova O.A. Forms of financial fraud and ways to minimize risks // Modern global economic system: evolutionary development vs. revolutionary leap. Scientific Communication Institute Conference, 2021, pp. 2197-2205.
- [4] Gakaev R.A., Bayrakov I.A., Bagasheva M.I. Ecological foundations of the optimal structure of forest landscapes in the Chechen Republic. In the collection: Environmental problems. A look into the future. Proceedings of the III scientific-practical conference. Executive editor Yu.A. Fedorov. 2006.S. 50-52.
- [5] Gakaev, R. Carbon sequestration in landscapes of the Chechen Republic. Reliability: Theory & Applications, 2022. Vol. 17. 3(66), pp. 193-196
- [6] Hansen, J.; M. Sato; R. Ruedy; K. Lo; D. W. Lea and M. M. Elizade, Global Temperature Change, PNAS, 2020, 103(39), pp. 14288–14293.
- [7] Leggett, J. A.; J. Logan and A. Mockey, China's Greenhouse Gas Emissions and Mitigation Policies, CRS Report for Congress 2008.
- [8] Verfaillie, H., and R. Bidwell, Measuring Eco-efficiency: A Guide to Reporting Company Performance, World Business Council for Sustainable Development, Geneva, 2020.
- [9] Salamova A.S., Socio-economic factors in the fight poverty and hunger in the modern world: the scientific approach of Amartia Kumar Sen, 2023, 17(1), pp. 237-245.
- [10] Salamova A.S., Global networked economy as a factor for sustainable development, 2020, p. 03053.

ECONOMIC SECURITY IN EUROPEAN COUNTRIES: CHALLENGES, SOLUTIONS, AND RECOMMENDATIONS

Rizvan Aliev¹, Tamerlan Magomaev², Apti Mentsiev¹

¹ Kadyrov Chechen State University, Russia

² Grozny State Oil Technical University, Russia

mediche86@mail.ru

Abstract

This research delves into the complexities of economic security in European countries, exploring the challenges posed by income inequality, unemployment, trade-offs in economic security measures, and the European population trap. A comprehensive review of literature, reports, and data provides insights into the multifaceted nature of economic security. The findings reveal persistent income disparities, hindering social cohesion and economic growth. Unemployment, driven by technological advancements, necessitates targeted workforce development and lifelong learning initiatives. Balancing defense spending with investments in domestic economic development is critical to enhancing both economic and national security. Addressing the risk of the European population trap demands responsible population control and sustainable resource management. The research emphasizes the interconnectedness of economic and national security, advocating for a holistic approach that integrates policies to foster economic resilience, promote social inclusion, and safeguard national interests. Policymakers must consider these multifaceted dimensions to ensure sustainable economic security and prosperity in the face of global challenges.

Keywords: economy, economic risks, security, European countries

I. Introduction

Economic security is a paramount concern for any nation-state, and for European countries, it is no exception. In an increasingly interconnected and globalized world, the complexities of economic challenges have intensified, posing both opportunities and threats to the economic well-being and stability of European nations [1]. The evolution of the global economy, the rise of emerging markets, technological advancements, and geopolitical dynamics have reshaped the landscape of economic security, requiring policymakers to adopt innovative and adaptive strategies to navigate the changing tides.

The 21st century has witnessed a paradigm shift in how economic security is conceptualized and addressed. Traditionally, economic security was narrowly focused on military aspects, defense spending, and trade protectionism [2]. However, in contemporary times, the notion of economic security has expanded to encompass a broader set of dimensions, embracing social, environmental, and technological factors that impact a nation's ability to maintain a resilient and sustainable economy.

One of the pressing challenges that European countries face is income inequality. Despite being home to some of the world's most developed and prosperous economies, Europe grapples

with a significant wealth gap between its citizens [3]. The concentration of wealth and resources in the hands of a few has sparked social unrest and diminished social cohesion. Income inequality not only stifles economic growth but also undermines the very fabric of democratic societies. Policymakers must devise measures to address this disparity, such as progressive taxation, social safety nets, and targeted welfare programs, to ensure a more equitable distribution of wealth and opportunities [4].

Unemployment is another critical issue plaguing European countries. The changing nature of work, driven by technological advancements and automation, has disrupted traditional employment patterns and rendered some skillsets obsolete. As a result, many workers find themselves displaced, struggling to find suitable employment opportunities. Policymakers must invest in workforce development and retraining programs to equip individuals with relevant skills for the job market [5]. Moreover, fostering entrepreneurship and supporting small and medium-sized enterprises (SMEs) can create more job opportunities and contribute to economic dynamism.

Trade-offs between economic security measures and external threats present a complex dilemma for policymakers. Striking a balance between defense spending to protect against external threats and investing in domestic economic development can be challenging [6]. However, it is imperative to recognize that a robust economy is a foundation for strong defense. By prioritizing investments in education, healthcare, and infrastructure, countries can enhance their economic resilience and reduce vulnerabilities to external shocks.

The European population trap presents a unique challenge for economic security. As population growth, in particular due to the huge influx of migrants, outpaces agricultural and resource growth, there is a risk of inadequate food supply. This demographic imbalance can strain social and economic systems, exacerbating economic insecurity [7]. To address this issue, policymakers must adopt responsible population control measures and invest in sustainable agricultural practices and resource management.

Furthermore, economic security is closely intertwined with national security. The economic health of a country directly impacts its ability to maintain strong defense capabilities. Adequate funding for defense and national security measures relies heavily on the stability and growth of the economy. At the same time, national security measures, such as trade policies, economic sanctions, and financial regulations, can significantly influence a country's economic landscape. Hence, policymakers must holistically consider economic and national security as interconnected aspects of safeguarding a nation's interests.

The era of globalization has brought both opportunities and challenges for economic security in European countries. On one hand, globalization has facilitated access to global markets, foreign investments, and technological advancements, fostering economic growth and prosperity. On the other hand, it has exposed countries to increased economic interdependence, vulnerability to external shocks, and competition from emerging economies [8]. Policymakers must navigate this complex global landscape, seeking cooperation and partnerships while safeguarding national interests and economic autonomy.

Economic security is a multidimensional concept that requires multifaceted solutions. European countries must address challenges such as income inequality, unemployment, trade-offs in economic security measures, and the European population trap. By adopting a comprehensive approach that considers macroeconomic policies, job quality, delinking economic security from employment, and various dimensions of national security, European nations can enhance their economic resilience and ensure the well-being of their citizens. Policymakers must work diligently to create a portfolio of policies that collectively support sustainable economic security and prosperity in the face of the ever-evolving global economic landscape [9].

II. Methods

This research is based on a comprehensive review of existing literature, reports, and data related to economic security in European countries. The research synthesizes information from reputable sources, including academic papers, policy briefs, and reports from international organizations. The analysis encompasses economic data, policy measures, and case studies to provide a comprehensive overview of the challenges and potential solutions.

III. Results

The research findings indicate that economic security in European countries is confronted with numerous challenges that require comprehensive and innovative solutions. The complexities of the global economic landscape, coupled with domestic socioeconomic factors, demand a holistic approach to address these issues effectively. The following section presents the results of the analysis on income inequality, unemployment, trade-offs in economic security measures, and the European population trap.

3.1. Income Inequality

Income inequality remains a persistent issue in European countries, despite their high level of economic development. The research reveals that a significant portion of the population continues to experience economic hardships, with wealth concentrated among a small elite. This concentration of wealth not only widens the income gap but also hinders social mobility and leads to decreased overall economic growth [10].

The consequences of income inequality are multifaceted. It erodes social cohesion, fosters mistrust in institutions, and leads to political polarization. Additionally, income inequality affects human capital formation, limiting access to quality education, healthcare, and skill development for the less privileged segments of society. As a result, the potential workforce remains underutilized, hindering overall economic productivity.

To address income inequality, policymakers must prioritize progressive taxation policies, where higher-income individuals and corporations contribute a larger share of their earnings to support social safety nets and welfare programs. Investing in education, particularly for marginalized communities, can help bridge the skills gap and promote upward mobility. Furthermore, promoting inclusive growth through policies that support small businesses and encourage social entrepreneurship can stimulate economic opportunities for a broader segment of society.

3.2. Unemployment

Unemployment rates in European countries have been a longstanding concern, particularly in the face of technological advancements and automation. The displacement of workers from traditional job sectors has led to a mismatch between skills demanded by the job market and those possessed by the workforce.

The research highlights the need for targeted workforce development programs to reskill and upskill workers. Policymakers must collaborate with the private sector to identify emerging skills requirements and design training initiatives accordingly [11]. Additionally, promoting entrepreneurship and SMEs can create alternative job opportunities and drive economic growth at

the local level.

To enhance workforce adaptability, lifelong learning initiatives must be integrated into education systems. This involves fostering a culture of continuous learning and supporting individuals in acquiring new skills throughout their careers. Furthermore, labor market regulations need to strike a balance between worker protection and business flexibility to encourage job creation and job security.

3.3. Trade-offs in Economic Security Measures

The trade-offs between economic security measures and national defense pose a complex challenge for policymakers. On one hand, substantial defense spending is crucial for safeguarding national security and sovereignty. On the other hand, investing in domestic economic development is essential for long-term economic resilience.

The research emphasizes that economic security and national security are interdependent. A strong economy provides the necessary resources to support defense capabilities, while a secure nation fosters a stable environment for economic growth. Policymakers should pursue a balanced approach, ensuring that defense spending is commensurate with national security needs without neglecting essential investments in education, infrastructure, and social welfare. Moreover, diversifying trade partners and enhancing regional economic integration can reduce the vulnerability of European countries to external economic shocks. Strengthening diplomatic ties and engaging in multilateral forums can also foster economic cooperation and mitigate trade conflicts [12].

3.4. The European Population Trap

The risk of the European population trap poses a unique challenge for economic security. As population growth outpaces agricultural and resource growth, there is a risk of inadequate food supply, leading to declining population and economic instability.

To address this issue, policymakers must adopt responsible population control measures and family planning initiatives. Encouraging sustainable agricultural practices, resource management, and investment in agricultural research and technology can enhance food security and support a growing population [13].

The results of the research demonstrate that economic security in European countries is contingent on addressing income inequality, unemployment, trade-offs in economic security measures, and the risk of the European population trap. Policymakers must embrace a comprehensive and adaptive approach that includes progressive taxation, targeted workforce development, balanced defense spending, and sustainable population management. By adopting such multifaceted solutions, European countries can strengthen their economic resilience, promote social cohesion, and enhance the overall well-being of their citizens. Additionally, fostering regional cooperation, diversifying trade partners, and investing in inclusive and sustainable growth can mitigate external economic risks and contribute to a prosperous and stable Europe.

The findings of this research underscore the importance of economic security as a foundation for national security and the well-being of the populace. Policymakers must recognize the interconnectedness of economic and national security and pursue policies that address the multifaceted challenges faced by European countries in the pursuit of economic resilience and prosperity.

IV. Discussion

The results of the research shed light on the significant challenges European countries face in achieving economic security. The discussion will delve deeper into the implications of income inequality, unemployment, trade-offs in economic security measures, and the European population trap, and the synergistic relationship between economic security and national security.

4.1. Income Inequality

Income inequality remains a deeply ingrained issue in European societies, posing substantial socioeconomic and political ramifications. The concentration of wealth among a privileged few creates a sense of disenfranchisement among the majority of the population, leading to social unrest and political polarization. High levels of income inequality can erode social cohesion, undermining trust in institutions and fueling public discontent. This, in turn, can lead to political instability, hampering economic policymaking and investment.

Addressing income inequality requires a multi-pronged approach. Progressive taxation policies play a crucial role in redistributing wealth and funding social safety nets. Additionally, policies that promote inclusive growth, such as access to quality education, affordable healthcare, and affordable housing, can empower individuals to break the cycle of poverty and improve their economic prospects.

Furthermore, ensuring equal opportunities for all segments of society is essential in reducing income disparities. Policies that promote diversity and inclusion in the workplace and provide support to marginalized communities can foster a more equitable distribution of wealth and economic opportunities.

4.2. Unemployment

Unemployment is a pressing concern, exacerbated by the rapid technological advancements and automation that have reshaped the labor market. The transition to a digital economy has led to job displacement in certain industries and a growing skills gap among the workforce.

To address unemployment, policymakers must prioritize investing in workforce development and reskilling programs. Collaborating with the private sector can help identify emerging skill demands, ensuring that workers are equipped with the necessary capabilities to thrive in the evolving job market. Moreover, encouraging entrepreneurship and supporting SMEs can stimulate job creation and foster economic dynamism.

Lifelong learning initiatives are critical to enhancing workforce adaptability. By promoting continuous learning and upskilling opportunities, individuals can remain competitive in the job market and drive economic productivity.

4.3. Trade-offs in Economic Security Measures

Balancing economic security measures with national defense is a complex undertaking. Adequate defense spending is necessary to protect a nation's sovereignty and security. However, neglecting investments in domestic economic development can leave a country vulnerable to internal economic challenges.

Policymakers must navigate this trade-off by adopting a comprehensive approach. Ensuring that defense spending aligns with national security needs and that investments are directed

towards education, infrastructure, and social welfare can promote both economic and national security.

Regional economic integration can serve as a strategy to reduce external economic vulnerabilities. By diversifying trade partners and engaging in regional cooperation, European countries can enhance economic resilience and buffer against global economic shocks.

4.4. The European Population Trap

The risk of the European population trap highlights the importance of sustainable population management and resource utilization. As the population grows, there is a heightened demand for food and resources, which, if not managed sustainably, can lead to economic instability and food shortages.

Policymakers must prioritize responsible population control measures, such as family planning and reproductive health programs. Additionally, investing in sustainable agriculture, resource management, and agricultural research can bolster food security and support a growing population.

4.5. Synergy between Economic Security and National Security

The discussion underscores the interconnectedness of economic security and national security. A strong economy provides the necessary resources to support national defense capabilities, ensuring a country's ability to protect its sovereignty and interests. Conversely, a secure nation fosters a stable environment for economic growth and prosperity.

Policymakers must adopt a coordinated approach to address both economic and national security challenges. A robust economy contributes to enhanced national security through increased defense spending and investment in critical infrastructure and technology [2]. On the other hand, strong national security measures, such as trade policies and diplomatic efforts, can promote economic stability and opportunities for growth.

V. Conclusion

This comprehensive research has shed light on the critical importance of economic security for European countries in the 21st century. The study examined various dimensions of economic security, including income inequality, unemployment, trade-offs in economic security measures, and the risk of the European population trap. Through a comprehensive review of literature, reports, and data, the research has provided valuable insights into the complexities and challenges faced by European nations in their pursuit of economic well-being and stability.

The research findings underscore the urgent need for policymakers to adopt innovative and adaptive strategies to address these multifaceted challenges. Income inequality remains a persistent issue, with wealth concentration hindering social mobility and trust in institutions. Policymakers must prioritize progressive taxation and inclusive growth policies to promote equitable distribution of wealth and opportunities. Unemployment, driven by technological advancements, necessitates proactive workforce development and reskilling initiatives. Fostering entrepreneurship and supporting SMEs can also play a pivotal role in creating new job opportunities and stimulating economic dynamism. Moreover, striking a balance between economic security measures and national defense is crucial for a stable and resilient economy. Policymakers must ensure that defense spending aligns with national security needs while prioritizing investments in education, infrastructure, and social welfare. Addressing the European

population trap calls for responsible population control measures and sustainable resource management to mitigate potential economic and social repercussions.

Throughout the research, the interconnectedness of economic security and national security has been highlighted, emphasizing the need for a coordinated approach that considers both aspects together. By embracing a comprehensive and multifaceted approach, European countries can enhance their economic resilience, foster social cohesion, and ensure the well-being of their citizens. Policymakers must work diligently to create a portfolio of policies that collectively support sustainable economic security and prosperity in the ever-evolving global economic landscape. The era of globalization brings both opportunities and challenges, and policymakers must be proactive in seeking cooperation and partnerships while safeguarding national interests and economic autonomy.

References

- [1] Figueredo, A. J. and Wolf, P. S. A. (2009). Assortative pairing and life history strategy - a cross-cultural study. *Human Nature*, 20:317–330.
- [2] An EU approach to enhance economic security. *European Commission*. 20 June 2023. URL: www.ec.europa.eu/commission/presscorner/detail/en/IP_23_3358
- [3] Prantl, J. and Goh, E. (2022). Rethinking strategy and statecraft for the twenty-first century of complexity: a case for strategic diplomacy. *International Affairs*, 98(2):443–469.
- [4] Filauro, S. and Fischer, G. (2021). Income inequality in the EU: General trends and policy implications. *VOXEU*. URL: www.voxeu.org/article/income-inequality-eu-trends-and-policyimplications
- [5] The Impact of Artificial Intelligence on the Future of Workforces in The European Union and The United States of America. *White House Report*. December 2022. URL: www.whitehouse.gov/wp-content/uploads/2022/12/TTC-EC-CEA-AI-Report-12052022-1.pdf
- [6] Duarte, C. (2022). Sustainable financing for (an owned) sustainable development: time for Africa to give the driver's seat to domestic resource mobilization. *Chapter IV. Economic and Social Challenges and Opportunities. United Nations*. 70-100.
- [7] Global Risks 2023: Today's Crisis. *The Global Risks Report 2023 18th Edition - Chapter 1. World Economic Forum*. 13-28
- [8] Ulgen, S. and Inan, C. (2022). From the Local to the Global: The Politics of Globalization. *Rewiring Globalization. Carnegie Europe*.
- [9] Decent Work Reduces Inequalities, Protects Vulnerable Groups in Global Crises, Speakers Stress, as Commission for Social Development Opens Session. *Meetings Coverage and Press Releases. United Nations*. 06 February 2023. URL: www.press.un.org/en/2023/soc4906.doc.htm
- [10] Bubbico, R.L. and Freytag, L. (2018). Inequality in Europe. *European Investment Bank*. 1-50.
- [11] Crarles, L., Xia, S. and Coutts, A.P. (2022). Digitalization and Employment. *International Labour Organization*. 1-53.
- [12] Gehrke, T. and Ringhof, J. (2023). The power of control: How the EU can shape the new era of strategic export restrictions. *European Council on Foreign Relations*.
- [13] Global Prospects and Policies. *World economic outlook 2022. International Monetary Fund*. URL: www.imf.org/-/media/Files/Publications/WEO/2022/October/English/text.ashx

DEVELOPMENT OF ACHIMOV DEPOSITS SEDIMENTATION MODEL OF ONE OF THE WEST SIBERIAN OIL AND GAS PROVINCE FIELDS

Yury Nefedov¹, Danila Gribanov¹, Emil Gasimov¹, Dmitry Peskov¹, Gao Han¹,
Nikita Vostrikov¹, Shafagat Pashayeva²

•

¹St. Petersburg Mining University, Russia.

²Azerbaijan State Oil and Industry University

nefedov_yuv@pers.spmi.ru

danila.gribanov@gmail.com

azayli.emil@gmail.com

s190872@stud.spmi.ru

gaohan878989@gmail.com

sh73.73@mail.ru

Abstract

The Geological Process Modelling (GPM) module developed for the Petrel software package enables digital modelling of natural processes of erosion, transportation and deposition of clastic sediments. Modelling of cones of removal was carried out for Achimov strata of the Western Siberia field. The results obtained characterize the expected sediment geometry, lithology distribution due to sea level changes, paleogeography, paleoclimate, tectonics and sediment input rates. The results allow the evaluation of different options and enable us to predict the distribution of prospective oil and gas bearing sediments in areas where no wells have been drilled. As a result, a sedimentation model was obtained, which reflects the formation of the elements of the sedimentation system of the study area. According to the sedimentation model, the main facies zones of the turbidite sediments under consideration are identified.

Keywords: Sediment modelling, Achimov sediments, deep-sea cones of export, unsteady flow algorithms.

I. Introduction

The deep-water cones of Western Siberia have enormous hydrocarbon potential and are a promising area for exploration and development [1, 3]. Successful development depends on well-built conceptual models that reflect the processes of oil and gas reservoir formation [14, 22]. The construction of geological models that realistically reproduce the internal structure of the reservoir ensures the reduction of risks and uncertainties and contributes to increased hydrocarbon production [15, 23, 28].

Achimov deposits are of great interest in the West Siberian oil and gas province. They are widespread throughout the area and have confirmed commercial oil and gas content. This stratum is represented by lenticular sandy-siltstone bodies of discontinuous distribution lying at the base of the neocomposition. Three zones are distinguished in the structure of the clinof orm: shelf complex (undaform), slope (orthoform) and bottom formations (fundof orm) [12]. The fundof orm parts of the clinof orms are bounded by silt-sand sediments of the Achimov Formation.

Achimov sediments are turbiditic in nature, but differ from classical turbidites by a shallower sedimentation depth. The depth of the epicontinental West Siberian basin was, according to

various estimates, from 300 to 600 meters [11]. Sedimentary material flowed through "feeding channels" to the "conditional shelf" - a shallow plain with relief bends, the last of which is taken as the "shelf edge". Sediment accumulated on it in the form of bars and was transported down the slope through distribution channels [6]. Sedimentary material entered the basin mainly from the east. The source of material for the formation of the Achimov sand bodies was the shelf of the epicontinental basin, which was an accumulative terrace gently dipping towards the center of the basin [26]. The displacement occurred under the influence of gravitational flows caused by eustatic sea level fluctuations, tectonic processes or climatic changes.

II. Methods

An important step in building a conceptual model is the use of seismofacial analysis based on the calculation of seismic attributes [16, 33, 34]. If the values of seismic attributes change significantly, one can assume a change in elastic properties and, consequently, in facies settings [17].

For the formation under consideration, the most informative is the spectral decomposition algorithm - decomposition of the seismic signal into frequency characteristics [27, 32]. It is based on the assumption that local study of the wavefield spectrum allows to obtain more information about the internal structure of geological objects. The color combination algorithm used for visualization is RGB-mixing [9, 25]. The program input is three amplitude cubes, each of which corresponds to a different frequency and a certain color - green, blue, red. The result is a map, each point of which corresponds to three amplitude values.

The obtained map of spectral decomposition results allows us to divide the formation into undeformed and phondodeformed parts (Fig.1).

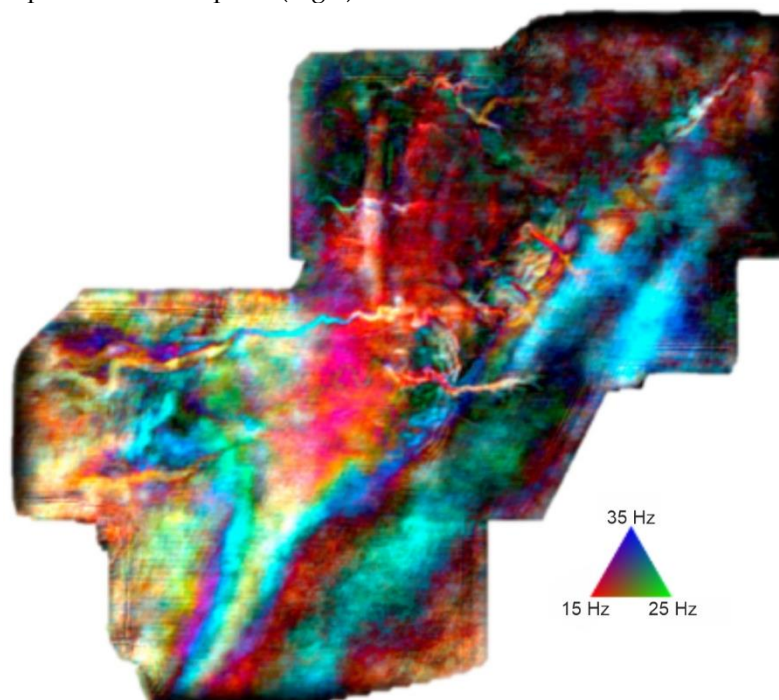


Fig. 1: RGB-mixing map of the results of spectral decomposition of 15, 25, 35 Hz frequencies for BP₆₋₂ - Ach₂ formation

The predominance of high frequency (blue shade) is characteristic of longshore drifts. Sediments from the shelf area accumulate in the western part, where area cones of export are developed [35]. Also, the material transport paths are clearly distinguished [4].

Not only seismic attributes, but also the wave field itself in the local area, along the seismic horizon, can be used for area zoning. The shape of the reflected wave directly depends on the elastic properties of the acoustic boundary, and the change in the seismic record can be used to

judge the change in these properties [29]. This algorithm reduces to a classification problem. Initial cubes of seismic amplitudes are used as input. In a sliding 3D-window, the size of which was defined as 20 ms, the studied territory is divided into classes - areas characterized by a constant signal shape; as a result, a map of class distribution over the territory is obtained [8]. This type of analysis is implemented by various algorithms, among which the most common are Kohonen neural networks and the K-average method.

Based on the results of the classification task, the main facies zones of the area can be distinguished. In the shelf area, longshore ramparts are formed. In the western part, Achimov cones of export are formed.

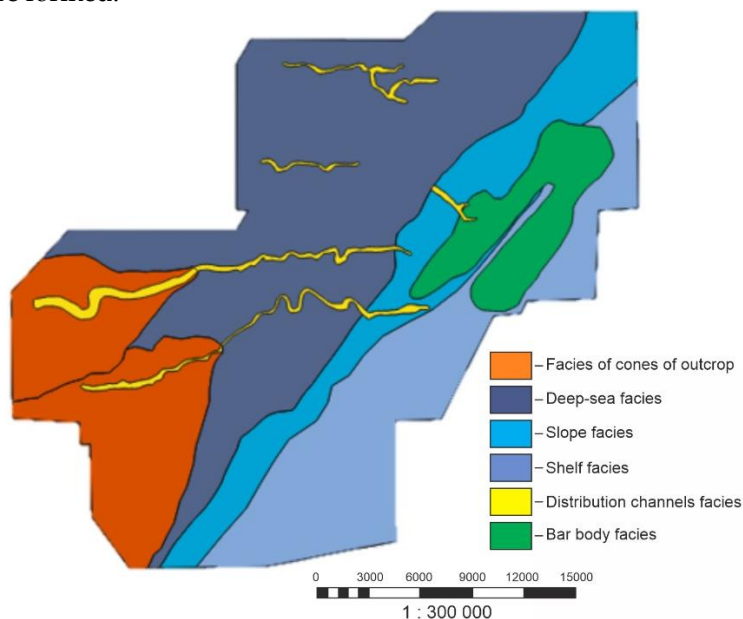


Fig. 2: Conceptual model of the BP6-2 - Ach2 reservoir

As a result of facies analysis based on well and seismic data, a conceptual model was constructed (Fig.2), where the shelf part is clearly distinguished, where longshore ramparts were formed, which are characterized predominantly by sandstones and have good reservoir properties. Extended debris transport channels also stand out. Sediments were deposited in the western part, where outcrop cones were formed.

III. Paleosurface reconstruction and identification of demolition sources

The sedimentation model is based on the reconstructed palaeosurface. The paleorelief map (Figure 3) was constructed by subtracting the structural surface of the roof of the Bazhenov Formation (OG B) from the structural surface of the studied horizon. The Bazhenov Formation is assumed to be conventionally flat and horizontal at the time of its formation.

After palaeosurface reconstruction, corrections to the predicted paleobasin depths must be made. The correction was carried out taking into account regional paleogeographic schemes [10].

At the time of the formation of the Achimov deposits, there was a regression of the inland West Siberian Sea from southeast to northwest [2]. During the Berriasian age, the study area was in the deep sea zone. An uncompensated mode of sedimentation prevailed, and clayey-carbonaceous-siliceous sediments of the Bazhenov Formation were formed [7]. In the late Berriasian-early Valanginian, active horizon formation took place on the adjacent land, which was the main cause of avalanche sedimentation and rhythmic filling of the sea basin with sediments from the east and southeast; sandy-siltstone cones of the Achimov Formation were formed at the foot of the slope [5].

Deposits of the Sortym Formation were mainly accumulated in the area of shallow sea. The clayey regional packs were formed as a result of short-term regressions that complicated the general regression. As a result of avalanche sedimentation, slope progradation occurred very rapidly [21]. In the Early Valanginian, the study area occupied a transitional position with increasing slope dip angle, then, in the Late Valanginian, it was in the shallow sea zone, and the slope became more gentle.

From the constructed palaeosurface it is possible to determine the sources of drift. In the GPM module, the drift sources are understood as the areas of matter transport start in the perimeter of the modelled space.

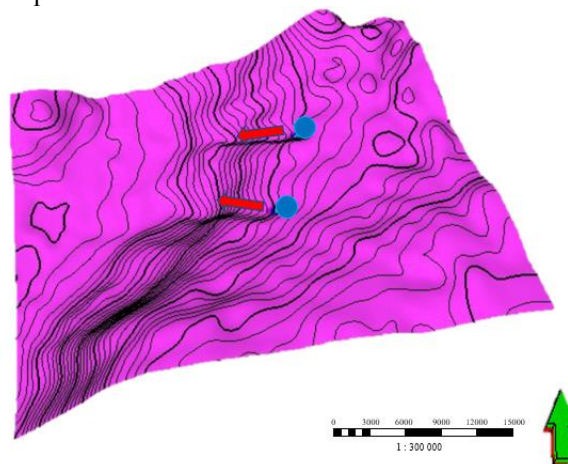


Fig. 3: *Paleo-basis for modelling and diagram of the location of point demolition sources*

The shelf edge was analyzed for the presence of elongated negative landforms and inferred drift sources were identified from the reconstructed palaeosurface.

IV. Construction of sedimentation model

Sedimentation modelling of the Achimov cones was carried out in the Geological Process Modeling (GPM) module of Schlumberger's Petrel software package.

For correct modelling it is necessary to clearly understand the processes of formation of the local object [31]. It is possible to build a sedimentation model based on the conceptual model and prepared input data.

Modelling was carried out using an algorithm for unsteady flow. The mathematics of the process controls the priority filling of depressions in the paleorelief of the near-slope part [20, 30]. Distribution of lithotypes occurs by initial deposition of the coarser fraction on the slope, the finer fraction being carried to the most distant areas [18].

The obtained time slides of the sedimentation model (Fig.4) with two drift sources clearly show the formation of a system of drift cones with debris transported along the slope. Each subsequent modelled flow takes into account current changes in paleorelief and subsequent iterations build up the object with flows. The type of feed sources and the particle size distribution (Fig.5) of the sedimentary mixture determine the morphology of the cones of withdrawal. The body is 18.5 km wide and 15.6 km long.

Sediment modelling in the GPM module offers a new approach to building a dynamic model that can be used to validate and improve the conceptual field model [13, 19]. The use of a geological process simulator allows the creation of a realistic architecture of the turbidite system [24]. As a result of the simulation, a model is obtained that reflects the formation of deep-water cone elements of the Achimov Formation and can be used for further geostatistical modelling of facies and petrophysics. The obtained result is consistent with seismofacies analysis and drilling data.

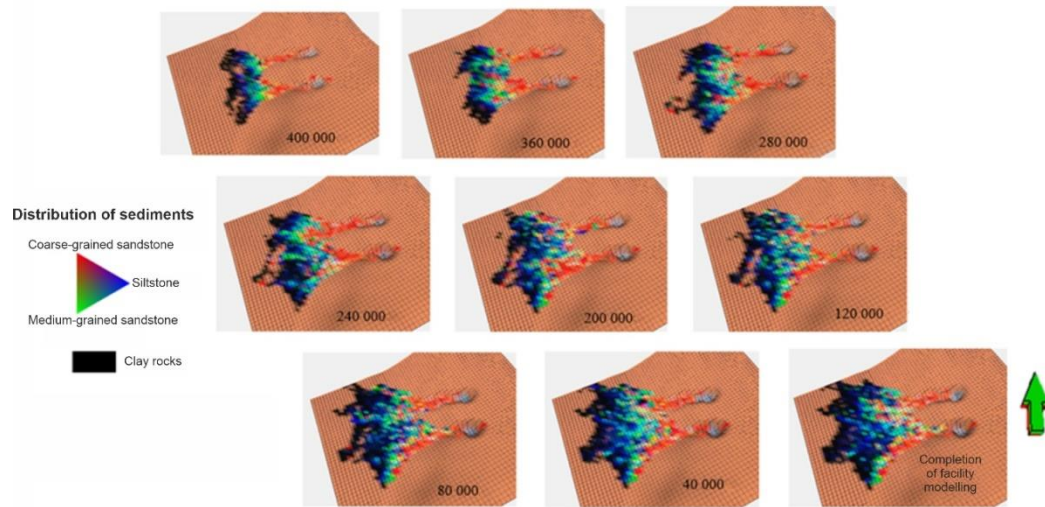


Fig. 4: Sequential slides of the sedimentation model

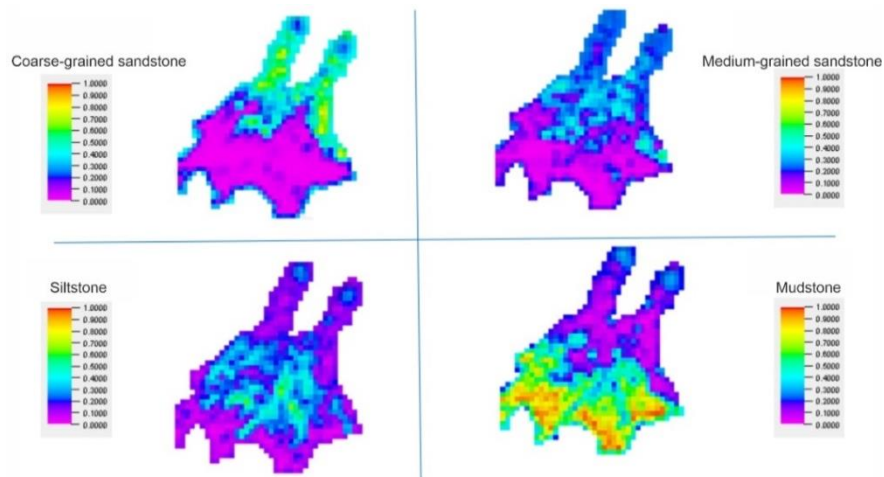


Fig. 5: Fractional distributions of sediments in the sedimentation model

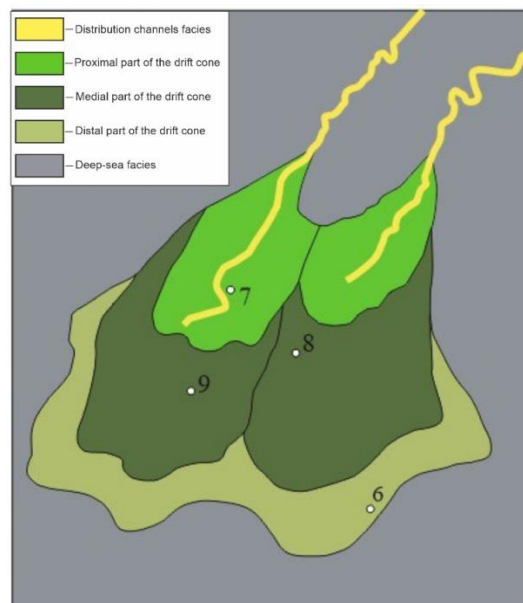


Fig. 6: Facies model of the Achimov deposits

According to the constructed sedimentation model and borehole data, it is possible to identify the main facies zones of the turbidite sediments under consideration (Figure 6).

Deposits of the proximal and medial zone are distinguished, which are characterized by good reservoir properties. The distal part is also distinguished, which is characterized by deposits with deteriorated properties.

Conclusion

The resulting sedimentation model reflects the reservoir architecture of the turbidite system. The performed facies analysis, the developed conceptual model, the reconstructed palaeosurface and the identified drift sources allow us to construct the sedimentation model. The dynamic model is consistent with seismic and well data. The results obtained are comparable to the conceptual model and allow to predict the distribution of drift cones. This method opens up positive prospects for more reliable geological modeling.

References

- [1] Andreichyk, A., Tsvetkov, P. (2023). Study of the relationship between economic growth and greenhouse gas emissions of the Shanghai cooperation organization countries on the basis of the environmental kuznets curve. *Resources*, 12(7), 80. DOI:10.3390/resources12070080
- [2] Borodkin V.N., Kurchikov A.R., Melnikov A.V., Khrantsova, A.V. Formation model and textural features of rocks of the Achimov complex in the north of Western Siberia: textbook. Tyumen, Tyumen NGU, 2011. [in Russian].
- [3] Buslaev, G., Lavrik, A., Lavrik, A., Tsvetkov, P. (2023). Hybrid system of hydrogen generation by water electrolysis and methane partial oxidation. *International Journal of Hydrogen Energy*, 48(63), 24166–24179. DOI: 10.1016/j.ijhydene.2023.03.098
- [4] Butorin, A.V. (2015). Structure of the productive clinoform formation according to seismic data. *Geophysics*, 1, 10–18. [in Russian].
- [5] Ershov, S.V. (2018). Sequence stratigraphy of Berriasian-Lower Aptian sediments of Western Siberia. *Geology and Geophysics*, 59(7), 1106–1123.
- [6] Gladysheva, Y.I. (2023). Petroleum potential of Achimov deposits in the north of Western Siberia. *Oil and Gas Studies*, 1, 13–28. [in Russian]. DOI: 10.31660/0445-0108-2023-1-13-28
- [7] Gurari, F.G. Structure and conditions of formation of clinoforms of the Neocomian of the West Siberian Plate (history of formation of ideas). Novosibirsk, SNIIGGiMS, 2003. [in Russian].
- [8] Huang, J., Mu, L., Chen, H., Et al. (2013). Preliminary study on a depositional interface-based reservoir modeling method. *Pet Explor Dev*, 40(5), 591–594. DOI: 10.1016/s1876-3804(13)60083
- [9] Kilhams, B., Godfrey, S., Hartley, A., Huuse, M. (2011). An integrated 3D seismic, petrophysical and analogue core study of the Mid-Eocene Grid channel complex in the greater Nelson Field area, UK Central North Sea. *Petroleum Geoscience*, 17(2), 127–142. DOI: 10.1144/1354-079310-022
- [10] Kerimov, V.M. (2021). Tectonomagmatic evolution of the Eocene volcanism of the Talysh zone (Azerbaijan). *Proceedings of Tomsk Polytechnic University. Georesources Engineering*, 332(11), 200–211. DOI <https://doi.org/10.18799/24131830/2021/11/2878>
- [11] Kontorovich, A.E., Kontorovich, V.A., Ryzhkova, S.V., Shurygin, B. N., Vakulenko, L. G., Gaideburova, E. A., Danilova, V. P., Kazanenkova, V. A., Kim, N. S., Kostyreva, E. A., Moskvina, V. I., Yan, P. A. (2013). Jurassic paleogeography of the West Siberian sedimentary basin. *Russian Geology and Geophysics*, 54(8), 747–779. DOI: 10.1016/j.rgg.2013.07.002

- [12] Kontorovich, A.E. Melenevskii, V.N., Zanin, Y.N., Zamirailova, A.G. Kazanenkov, V.A., Kazarbin, V.V., Makhneva, E.N., Yamkovaya, L.S. (1998). Lithology, organic geochemistry and formation conditions of the main rock types of the Bazhenov Formation (Western Siberia). *Geology and Geophysics*, 39(11), 1477–1491. [in Russian].
- [13] Laptey, A., Dolmatova, S. (2016). Anomalous Achimov and Bazhenov sequence's modeling. *SPE Russian Petroleum Technology Conference and Exhibition*. DOI: [10.2118/182138-MS](https://doi.org/10.2118/182138-MS)
- [14] Litvinova, T., Kashurin, R., Lutskiy, D. (2023). Complex formation of rare-earth elements in carbonate–alkaline media. *Materials*, 16(8), 31-40. DOI: [10.3390/ma16083140](https://doi.org/10.3390/ma16083140)
- [15] Mardashov, D.V., Limanov, M.N. (2022). Improving the efficiency of oil well killing at the fields of the Volga-Ural oil and gas province with abnormally low reservoir pressure. *Bulletin of the Tomsk Polytechnic University Geo Assets Engineering*, 333(7), 185–194. [in Russian]. DOI: [10.18799/24131830/2022/7/3707](https://doi.org/10.18799/24131830/2022/7/3707)
- [16] Mityaev, M.Y., Butorin, A.V., Asmandiyarov, R.N. (2017). Geological model matching with seismic data in the case of submarine slide sedimentation environment. *Neftyanoe Khozyaystvo - Oil Industry*, 8, 48–51. DOI: [10.24887/0028-2448-2017-8-48-51](https://doi.org/10.24887/0028-2448-2017-8-48-51)
- [17] Olneva T.V. Seismofacial analysis. Images of geological processes and phenomena in seismic image. Izhevsk: Institute of Computer Research, 2017. [in Russian].
- [18] Olneva T.V., Zhukovskaya E.A. Sedimentation modeling in the program complex Petrel. MAI Publishing House, 2022. [in Russian].
- [19] Otoo, D., Hodgetts, D. (2019). Geological process simulation in 3-D lithofacies modeling: application in a basin floor fan setting. *Bulletin of Canadian Petroleum Geology*, 67(4), 255–272.
- [20] Otoo, D., Hodgetts, D. Applying forward stratigraphic modeling approach to enhance facies characterization and fluid mobility prediction in geological models of basin floor fans. Basin Analysis and Petroleum Geoscience Group, School of Earth and Environmental Sciences, Williams, 2018.
- [21] Polyanskov, Y.V., Evseev, A.N., Poroykov, V.A. (2012). Model of sedimentation of solid particles from heterogeneous materials. *Bulletin of Samara State Aerospace University Named after Academician S. P. Korolev (National Research University)*, 33(2), 208–213. [in Russian].
- [22] Prischepa, O.M., Kireev, S.B., Nefedov, Y.V., Martynov, A.V., Lutsky, D.S., Krykova, T.N., Sinitsa, N.V., Xu, R. (2023). Theoretical and methodological approaches to identifying deep accumulations of oil and gas in oil and gas basins of the Russian Federation. *Frontiers in Earth Science*, 11. DOI: [10.3389/feart.2023.1192051](https://doi.org/10.3389/feart.2023.1192051)
- [23] Raupov, I., Burkhanov, R., Lutfullin, A., Maksyutin, A., Lebedev, A., Safiullina, E. (2022). Experience in the application of hydrocarbon optical studies in oil field development. *Energies*, 15(10), 3626. <https://doi.org/10.3390/en15103626>
- [24] Reading, H.G., Richards, M. (1994). Turbidite systems in deep-water basin margins classified by grain size and feeder system. *AAPG Bulletin*, 78, 792–822. DOI: [10.1306/A25FE3BF-171B-11D7-8645000102C1865D](https://doi.org/10.1306/A25FE3BF-171B-11D7-8645000102C1865D)
- [25] Ruizhao, Y., Chao, X., Tian, Z., Yuxin, L., Pengpeng, L. (2017). RGB frequency mixing method based on the residual impedance of seismic inversion. *International Geophysical Conference, Qingdao, China*, 17-20 April 2017, 1036–1039. DOI: [10.1190/IGC2017-264](https://doi.org/10.1190/IGC2017-264)
- [26] Saks, V.N. Problems of Paleozoogeography of the Mesozoic of Siberia, Leningrad, Science, 1972. [in Russian].
- [27] Schmidt, I., Lacaze, S., Paton, G. (2013). Spectral Decomposition and Geomodel Interpretation - Combining Advanced Technologies to Create New Workflows. *75th EAGE Conference Exhibition Incorporating SPE EUROPEC*, 1–5. DOI: [10.3997/2214-4609.20130567](https://doi.org/10.3997/2214-4609.20130567)
- [28] Tananykhin, D., Grigorev, M., Simonova, E., Korolev, M., Stecyuk, I., Farrakhov, L. (2023). Effect of wire design (profile) on sand retention parameters of wire-wrapped screens for conventional production: prepack sand retention testing results. *Energies*, 24–38.

- [29] Tananykhin, D., Struchkov, I., Khormali, A., Roschin, P. (2022). Investigation of the influences of asphaltene deposition on oilfield development using reservoir simulation. *Petroleum Exploration and Development*, 49(5), 1138–1149. DOI: [10.1016/S1876-3804\(22\)60338-0](https://doi.org/10.1016/S1876-3804(22)60338-0)
- [30] Teles, V., Chauveau, B., Joseph, P., Weill, P., Maktouf, F. (2016). CATS – A process-based model for turbulent turbidite systems at the reservoir scale. *Comptes Rendus Geoscience*, 348(7), 489–498. DOI: [10.1016/j.crte.2016.03.002](https://doi.org/10.1016/j.crte.2016.03.002)
- [31] Tetzlaff, D., Tveiten, J. Salomonsen, P., Christ, A.-B., Athmer, W., G. Borgos, H. Sonneland, L. Martinez, C., Raggio, F. (2014). Geologic process modelling. *Conference: IX Conference of Hydrocarbon Exploration and Development At: Mendoza, Argentina*, 1–16.
- [32] Torrado, L., Mann, P., Bhattacharya, J. (2014). Application of seismic attributes and spectral decomposition for reservoir characterization of a complex fluvial system: Case study of the Carbonera Formation, Llanos foreland basin, Colombia. *GEOPHYSICS*, 79(5), 221–230. DOI: [10.1190/geo2013-0429.1](https://doi.org/10.1190/geo2013-0429.1)
- [33] Van Hoek, T., Gesbert, S., Pickens, J. (2010). Geometric attributes for seismic stratigraphic interpretation. *The Leading Edge*, 29(9), DOI: [10.1190/1.3485766](https://doi.org/10.1190/1.3485766)
- [34] Zakrevskii K.E., Nasonova N.V., Soloviev N.N. Geological modeling of clinoforms of the Neocomian of Western Siberia. GERS Publishing House, 2021. [in Russian].
- [35] Zhang, L., Manzocchi, T., Pontén, A. (2015). Hierarchical parameterization and modelling of deep-water lobes. *Pet Geostat*. DOI: [10.3997/2214-4609.201413606](https://doi.org/10.3997/2214-4609.201413606)

DIAGNOSIS OF THE RISK OF OIL LEAKS FROM PIPELINES

Hajar Ismayilova¹, Fidan Ismayilova¹, Mansur Shahlarly²

¹ Azerbaijan State Oil and Industry University, Azerbaijan.

² SOCAR, "OIL GAS SCIENTIFIC RESEARCH PROJECT" Institute, Azerbaijan.

ismayilova.hecer@bk.ru

fidan.ismayilova.2014@mail.ru

mansursahlarli1994@gmail.com

Abstract

The research paper studies the issue of detecting the location and amount of hydrocarbon losses in cases of accident-damage (spill), which occur during the transportation of oil and oil products via the technological and main pipes. The grapho-analytical method has been introduced and tested in order to determine a location and degree of the leakage following the change in working parameters.

Keywords: technological and main pipes, oil leakages, hydrocarbon losses, the relative change of discharge, leakage area, degree of the leak

I. Introduction

Occurrence of the hydrocarbon losses during the transportation of oil and oil products through the technological and main pipelines is mainly related with the accident-damage (spill) cases on pipelines. Reasons of losses caused by accidents are quite different, but they are mainly related to the violation of pipelines' operating procedures, non-compliance with construction norms and rules during their construction and the manufacturing defects of pipes.

Operational practice of pipelines shows that application of traditional methods for detection of leakages is not always efficient, while small leakages sometimes remain unrevealed for a long period of time. Currently, there are various methods in order to reveal the areas of accidents-caused oil leakages from pipelines and environmental pollution, as well as to determine the amount of spilled hydrocarbons.

II. Methods

It is known that during the emergency leak on the pipelines, the change of pipe and pump station's normal working regime heavily depends qualitatively and quantitatively on type of pump in use. Thus, characteristics of a pump station equipped with the centrifugal pumps differ essentially from the use of piston-type pump. As the latter is rarely used in practice, it has been studied below the impact of emergency oil leakage on change of pump station equipped with centrifugal pumps, pipeline with diameter expressed in D and length expressed in l and on their joint characteristics. To this effect, characteristics of a pump station and relief pipeline (dependence of pressure on discharge) have been determined via the following analytic expressions, respectively [1, 2]:

Before leakage, i.e. for a normal operation regime

$$H_0^{pump} = a - bQ_0^{2-m}$$

$$H_0^{b,k} = kQ_0^{2-m}l + \Delta z \tag{1}$$

After the oil leakage, the expression (1) can be written in the following form for pump station and pipeline:

$$\begin{aligned} H_1^{b,k} &= a - bQ_1^{2-m} \\ H_1^{b,k} &= kQ_1^{2-m}x + kQ_2^{2-m}(l-x) + \Delta z \\ k &= \beta \frac{\mu^m}{D^{5-m}} \end{aligned} \tag{2}$$

Here, Q_0, Q_1, Q_2 -are discharges before and after leakage in pump station, and after the leakage area respectively ($Q_2 = Q_1 - q$ and here q – is the amount of leaked oil; x – is a distance till the leakage area; μ – is a kinetic viscosity of leaked oil; Δz –height differences in the initial and final points of pipeline; a, b – maximum pressure of pump station equipped with centrifugal pump and approximation coefficient of its characteristics, respectively; m, β – indicators describing the oil flow regimes in the pipeline.

Taking into account the similarity in the relative change of pressures in pump station and pipeline when leakage occurs, it is possible to get the following formula to detect the leakage area based on change in discharge:

$$\frac{x}{l} = \frac{1 - \left(\frac{Q_2}{Q_0}\right)^{2-m} - A \left[\left(\frac{Q_1}{Q_0}\right)^{2-m} - 1 \right]}{\left(\frac{Q_1}{Q_2}\right)^{2-m} - \left(\frac{Q_2}{Q_0}\right)^{2-m}} \tag{3}$$

$$A = \frac{\left(\frac{a}{H_0} - 1\right)}{\left(1 - \frac{\Delta z}{H_0}\right)} \tag{4}$$

Thus, expression (3) shows that it is possible to detect the leakage area based on change of discharge in oil pipeline and characteristics of pump station without taking into account the geometric values of pipe, features of transported and volume of leaked oil. Here, $\left(\frac{\Delta z}{H_0}\right) \neq 0$ and $\frac{a}{H_n}$ values show slope of characteristics for relief pipelines and pump stations, respectively (regardless of motion regime and the leakage $\frac{a}{H_n}=1.1-1.8$).

If we consider the motion regime as laminar ($m = 1$) and $Q = Q_1 - q$, the expression (3) for horizontal ($\Delta z = 0$) pipeline will be as following:

$$\frac{x}{l} = 1 - \frac{a}{H_0} + \frac{\left(1 - \frac{Q_2}{Q_0}\right) \frac{a}{H_0}}{\frac{q}{Q_0}} \tag{5}$$

or

$$\frac{x}{l} = 1 - \frac{\left(\frac{Q_1}{Q_0} - 1\right) \frac{a}{H_0}}{\frac{q}{Q_0}} \tag{6}$$

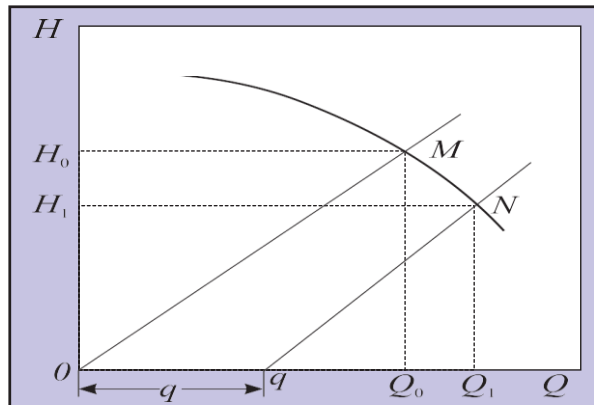


Fig. 1: Common characteristics of pump station and pipeline considering the oil leakage

If we take into account that, $1 - \frac{Q_2}{Q_0} = \delta_{Q_2}$ and $\frac{Q_1}{Q_0} - 1 = \delta_{Q_1}$ in formulas (5) and (6) are describing the relative change in discharge in the initial and final points of pipeline, respectively, then in cases of accident-leakage, these changes can be determined depending on the distance $\left(\frac{x}{l}\right)$ and degree $\left(\frac{q}{Q_0}\right)$ of leakage:

$$\delta_{Q_2} = \frac{\frac{q}{Q_0} \left(\frac{x}{l} + \frac{a}{H_0} - 1 \right)}{\frac{a}{H_0}} \tag{7}$$

$$\delta_{Q_1} = \frac{\frac{q}{Q_0} \left(1 - \frac{x}{l} \right)}{\frac{a}{H_0}} \tag{8}$$

It is possible to use the following formula to determine the relative change (δ_H) of pressure in the initial point of pipeline (pump station) taking into account formula (8), expressions (1) and (2):

$$\delta_H = \delta_{Q_1} \left(\frac{a}{H_0} - 1 \right) \tag{9}$$

If we accept the occurrence of the leakage in the initial part of pipe, in compliance with the common characteristics of the pipeline, it would be possible to get the similar $\Delta 0MQ_0$ and ΔqNQ_1 triangles: (Fig.1)

$$\frac{Q_1}{Q_0} = \frac{q}{Q_0} + \frac{H_1}{H_0} \tag{10}$$

It is possible to obtain the following dependence between the known leakage degree and its place, as well as relative change of pressure by taking into account the expression (10) in (6):

$$\frac{q}{Q_0} = \frac{\left(1 - \frac{H_1}{H_0} \right) \frac{a}{H_0}}{\frac{a}{H_0} - 1 + \frac{x}{l}} \tag{11}$$

The analysis of expressions (7) and (8) shows that the parameters δ_{Q_1} and δ_{Q_2} can be more or less than each other depending on a location of the leakage. There is such a point where $\delta_{Q_1} = \delta_{Q_2}$. This point identifies the length of the part that is being determined by change of discharge in the initial (or final) point of pipe and found as following:

$$\left(\frac{x}{l} \right) = 1 - \frac{a}{2H_0} \tag{12}$$

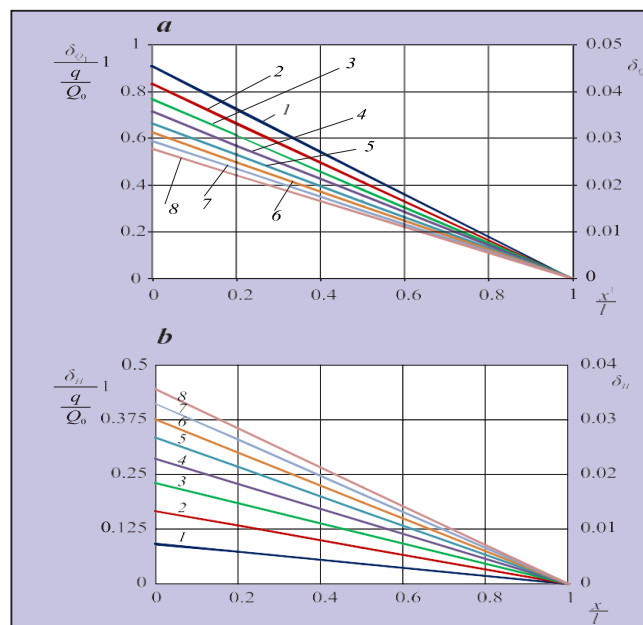


Fig. 2: Detection of the leakage area and degree by the relevant change of discharge (a) and pressure (b):
 1–8 – $\frac{a}{H_0}$ constitutes 1.1; 1.2; 1.3; 1.4; 1.5; 1.6; 1.7; and 1.8, respectively

In accordance with expressions (8), (9) and (11), the leakage cases have been assessed by the relative changes of discharge and pressure and their dependences have been formed as following:

$$\frac{\delta_{Q_1}}{\frac{q}{Q_0}} = f\left(\frac{x}{l}\right), \text{ and } \frac{\delta_H}{\frac{q}{Q_0}} = f\left(\frac{x}{l}\right) \text{ (Figure 2)}$$

The grapho-analytic method drafted for the determination of the leakage degree in the initial point of a pipeline is shown on the Fig.3.

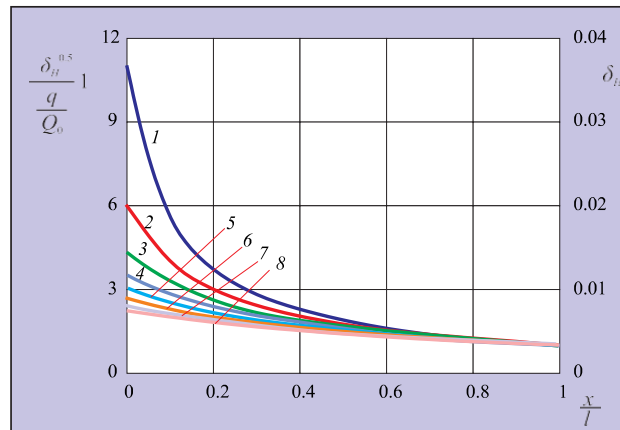


Fig. 3. Detection of the leakage degrees in the initial point of pipe:
 1-8 is the same as in the Figure 2

III. Results

As it is obvious from the figures 2 and 3, it is possible to determine the location of leakage and its degree by the relevant dependences on the basis of the relative changes in discharge and pressure. Taking into consideration the above-mentioned findings, it has been studied the issue of determining the leakage location and degrees on the basis of changing working parameters of oil pipelines. Data of leakages that happened in oil pipelines (entrance and exit) in Absheron peninsula in different times have been used for this purpose (Tables 1, 2).

Table 1: Data of leakages that happened in oil pipelines (entrance and exit) in Absheron peninsula

Hour	26.05.2006			Note	Hour	26.05.2006			Note
	Discharge m ³ /hour	Pressure, MPa				Discharge m ³ /hour	Pressure, MPa		
		Entrance	Exit				Entrance	Exit	
01:00	-	-	-	Oil transportation started at 09:00	01:00	-	-	-	Oil transportation started at 10:30
02:00	-	-	-		02:00	-	-	-	
03:00	-	-	-		03:00	-	-	-	
04:00	-	-	-		04:00	-	-	-	
05:00	-	-	-		05:00	-	-	-	
06:00	-	-	-		06:00	-	-	-	
07:00	-	-	-		07:00	-	-	-	
08:00	-	-	-	Leakage occurred at 11:40 and eliminated at 13:20	08:00	-	-	-	Leakage occurred at 11:18 and eliminated at 16:00
09:00	-	-	-		09:00	-	-	-	
10:00	93	0.96	0.85		10:00	-	-	-	
11:00	156	1.07	0.86		11:00	62	0.95	0.86	
12:00	151	1.04	0.85		12:00	149	1.06	0.86	
13:00	-	-	-	13:00	157	1.07	0.85		

14:00	150	1.03	0.85	Oil transportation stopped at 21:35	14:00	157	1.07	0.85	Oil transportation stopped at 22:55
15:00	155	1.07	0.86		15:00	47	0.68	0.62	
16:00	157	1.06	0.86		16:00	-	-	-	
17:00	157	1.07	0.86		17:00	112	1.06	0.85	
18:00	157	1.07	0.86		18:00	155	1.08	0.86	
19:00	158	1.06	0.86		19:00	157	1.08	0.86	
20:00	157	1.06	0.86		20:00	157	1.08	0.86	
21:00	157	1.06	0.86		21:00	158	1.07	0.86	
22:00	84	1.06	0.86		22:00	157	1.07	0.86	
23:00	-	-	-		23:00	141	1.06	0.86	
24:00	-	-	-	24:00	-	-	-		

As we can see from the Table 1, the first leakage has occurred on 26 May 2006. Unlike to the first case of leakage, the second case has been followed by a significant spill and caused the spill of more than 50 % of oil.

Change of working parameters before and after the oil leakages, according to the Table 2, from the main pipe is shown on the Fig.4.

Table 2: Change of working parameters before and after the oil leakages

21.04.2006				22.04.2006				23.04.2006			
Time, hour	Discharge m ³ /hour	Pressure, MPa		Time, hour	Discharge m ³ /hour	Pressure, MPa		Time, hour	Discharge m ³ /hour	Pressure, MPa	
		entrance	exit			entrance	exit			entrance	exit
01:00	750	1.41	0.38	01:00	752	1.42	0.38	01:00	353	1.24	1.31
02:00	750	1.41	0.38	02:00	751	1.41	0.38	02:00	352	1.24	1.31
03:00	750	1.41	0.38	03:00	740	1.40	0.38	03:00	351	1.24	1.31
04:00	752	1.42	0.38	04:00	320	1.13	0.21	04:00	354	1.24	1.31
05:00	751	1.41	0.38	Leakage occurred at 02:53, discharge at 03:43	05:00	0.82	0.13	05:00	353	1.24	1.31
06:00	752	1.42	0.38		06:00	0.61	0.09	06:00	355	1.24	1.31
07:00	750	1.41	0.38		07:00	0.58	0.07	07:00	352	1.24	1.31
08:00	752	1.42	0.38		08:00	0.57	0.06	08:00	550	1.31	0.31
09:00	751	1.41	0.38		09:00	0.55	0.06	09:00	611	1.34	0.32
10:00	752	1.42	0.38		10:00	0.55	0.06	10:00	643	1.35	0.33
11:00	751	1.41	0.38		11:00	0.54	0.05	11:00	661	1.36	0.34
12:00	752	1.42	0.38		12:00	0.55	0.06	12:00	720	1.38	0.35
13:00	750	1.41	0.38		13:00	0.55	0.06	13:00	742	1.41	0.37
14:00	752	1.41	0.38		14:00	0.54	0.05	14:00	749	1.41	0.37
15:00	751	1.42	0.38	15:00	238	1.09	0.29	15:00	748	1.41	0.37
16:00	751	1.41	0.38	16:00	291	1.11	0.31	16:00	752	1.42	0.38
17:00	752	1.42	0.38	17:00	342	1.24	0.31	17:00	751	1.41	0.38
18:00	751	1.41	0.38	18:00	346	1.24	0.31	18:00	752	1.42	0.38
19:00	752	1.42	0.38	19:00	353	1.24	0.31	19:00	750	1.41	0.38

20:00	750	1.41	0.38	20:00	352	1.24	0.31	20:00	752	1.42	0.38
21:00	752	1.42	0.38	21:00	351	1.24	0.31	21:00	751	1.41	0.38
22:00	751	1.41	0.38	22:00	355	1.24	0.31	22:00	752	1.42	0.38
23:00	752	1.42	0.38	23:00	354	1.24	0.31	23:00	752	1.42	0.38
24:00	752	1.42	0.38	24:00	355	1.24	0.31	24:00	752	1.42	0.38

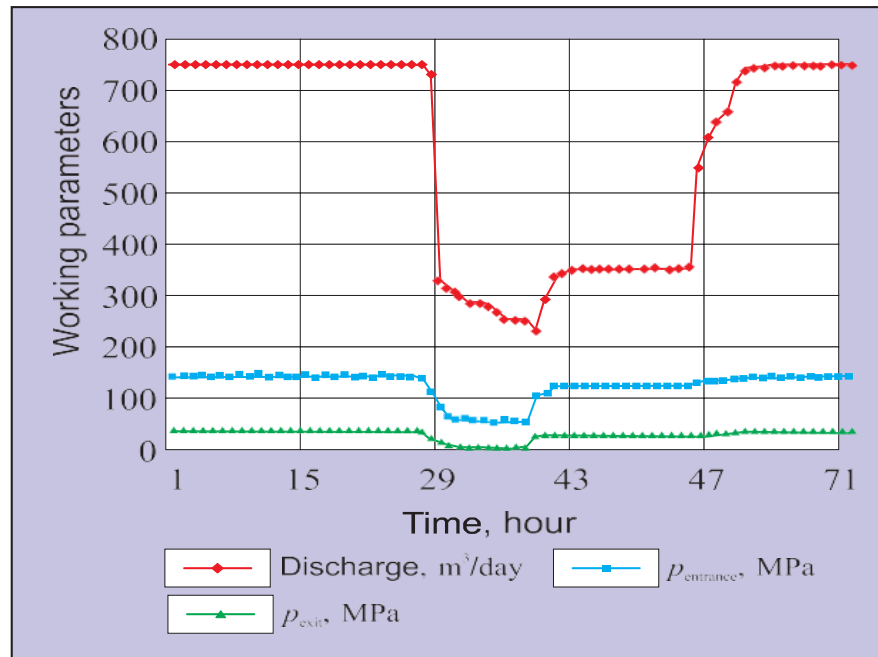


Fig. 4: Change of working parameters in the pipeline before and after the oil leakage case

IV. Discussion

According to the Table 1, the relative changes of discharge and pressure during the small leakage cases constituted:

$$\delta Q_1 = \frac{156 - 151}{156} = 0.0321$$

and

$$\delta_H = \frac{10.7 - 10.4}{10.7} = 0.028$$

In accordance with δQ_1 and δ_H on the Figure 2, we obtained the following:

$$\frac{\sigma_{Q_1}}{Q_0} = 0.625 \text{ and } \frac{\sigma_H}{Q_0} = 0.352$$

In this condition, we get the coordinate of leakage from Figure 2 (a) and (b):

$$\frac{x}{l} = 0.15 \text{ and } \frac{x}{l} = 0.08$$

As we can see, the area of leakage determined by the relevant change of discharge and the distance of leakage determined by the change of pressure is slightly different (~ 8%) from the factual leakage distance: $\left(\frac{x}{l}\right)_{fact} = 0.137$

Thus, we obtain the following results for the degree of leakage by the relevant change of discharge and pressure, respectively:

$$\frac{q}{Q_0} = 0.051 \text{ and } \frac{q}{Q_0} = 0.079$$

According to the Table 2, the relevant change of discharge and pressure in case of a small

leakage would be as following:

$$\delta_{Q1} = \frac{752-740}{14.2} = 0.0159$$
$$\delta_H = \frac{14.2-14.0}{14.2} = 0.0141$$

We can obtain the following results from the values of δ_{Q1} and δ_H reflected on the Figure 2:

$$\frac{\delta_{Q1}}{Q_n} = 0.30 \text{ and } \frac{\delta_H}{Q_n} = 0.188$$

In this condition, we get for the area of leakage as $\frac{x}{l} = 0.50$ from the Figure 2(a), and as $\frac{x}{l} = 0.52$ from the Figure 2, (b). In this case as well, the area of leakage determined by the relevant change of discharge in comparison the area of leakage determined by the change of pressure is closer to the factual leakage zone $\left(\left(\frac{x}{l}\right)_{fact} = 0.47\right)$ and differs by 6%. In addition, we get the following results for the degree of leakage by the relative change of discharge and pressure, respectively:

$$\frac{q}{Q_0} = 0.053 \text{ and } \frac{q}{Q_0} = 0.075$$

Thus, the suggested grapho-analytical method allows detection of small oil leakages by the relative change of discharge with accuracy to 8 %.

References

- [1] Control of leaks of oil and oil products on main pipelines during operation. – M.: VNIIOENG, 1981, s. 2-16. (in Russian)
- [2] Ismayilov G., Ismayilova H., Babirov H., Jabrayilova R. Assesment of environmental oil spills and economic-environmental risks. RT&A, Special Issue № 4 (70) Volume 17, November 2022, p.p. 212-217. DOI: <https://doi.org/10.24412/1932-2321-2022-470-212-217>.
- [3] Kravchenko V.F. Environmental protection during transportation and storage of oil and oil products // Reviews of foreign literature. – M.: VNIIOENG, 1976, 60 s. (in Russian)
- [4] Ismayilova H.G. On the assessment of damage from accidental losses' for various categories of oil leaks / Proceedings of the 69th International Scientific Conference "Oil and Gas" - 2015". – M.: 2015, s. 98. (in Russian)
- [5] Kremmer V.H. Oil and oil products leakage control system from pipelines // Transport and storage of oil and oil products. Foreign experience: Exp. – M.: VNIIOENG, 1980, s. 21-30. (in Russian)
- [6] Yorf P., Kichenko A. Problems of corrosion in the pipelines of the oil gathering system and ways to solve it. International industrial portal. Innovation, 7 June 2011.

NPP MAINTENANCE AND REPAIR RISK MANAGEMENT: THE CASE OF RUSSIA

Mariia Volos, Evgenii Polev

•

Rosatom Technical Academy, Russia

MMVolos@rosatom.ru

EIPolev@rosatom.ru

Abstract

The paper considers the risk management system of the operating organization in the process of maintenance and repair of nuclear power plants in Russia. The following main risks of the process are identified: an energy generation reduction due to extending outages and energy cost increase due to an increase in costs for repair and maintenance needs. The following measures for risk management of the process are considered: inspections of readiness for repair and repair quality, corporate support, development and revision of repair documentation, management of material and technical resources. The process efficiency indicators as indicators of risk tolerance are considered. An effectiveness assessment of the risk management system of the maintenance and repair process is presented. The key shortcomings are identified. The line of further research on shortcomings exclusion is formulated.

Keywords: process, risk matrix, risk criticality, risk significance, risk causes, NPP, M&R

I. Introduction

Risk management is an important tool for ensuring the sustainable operation of nuclear power plants (safe, reliable, economic). The practice of nuclear power plants (NPP) operating indicates the continuing trends in determining priorities – safe operation in order to avoid accidents. The process of NPP maintenance and repair (M&R) as a supporting operation process is not a priority for safety. This circumstance is explained by the fact that poor-quality repairs will not lead to an accident. From the point of view of NPP safety, the most serious consequence of poor-quality repairs is an unplanned shutdown of the power unit. However, neglect of the M&R process leads to the gap of NPP sustainable operation and, as a result, to a diminution of the national energy security. Thus, risk management of NPP M&R process is one of the critical government issue.

The operating organization (Operator) of Russian NPPs – Rosenergoatom Concern JSC – has accumulated wide experience in risk management system development and improvement. This paper discusses Russia's experience in implementation of risk management in a one specific process – NPP M&R.

The paper is structured as follows. The Introduction presents the research relevance. The Methods discusses the risk management methods for Operator's processes. The Results shows how risk management implements in the M&R process namely M&R key performance indicators as risk tolerance indicators, analysis of identified risks and measures to manage them. The Discussion evaluates the effectiveness of the M&R process risk management system, its shortcomings, and discusses directions for further research.

II. Methods

The risk management system comprises 11 types of risks: production, construction, financial, commercial, organizational, legal, market, environmental, political, reputation, and security risks.

The risk management process includes four stages: risk identification and analysis, development of risk management measures, and monitoring the results of risk management.

The first stage of risk management is identification. The main source of information is statistical data on process key performance indicators, reports on various activities and risks. The second stage is risk analysis, where the risk significance is assessed and a management method is chosen. The third stage involves developing risk management measures with a budget calculation. In the final fourth stage, monitoring of the results of risk management is carried out including the measures performing, their effectiveness evaluation, deviation analysis and the development of new measures. The risk management process is continuous.

In accordance with the Operator's guidelines the following methods of risk identification are recommended: brainstorming and the Delphi method [4], questionnaire [5], SWOT analysis [6], the method of analogies. The last method is mainly applicable in the process of "Construction Management" [7].

The qualitative risk assessment involves assessing risks based on characteristics such as: corresponds/does not correspond, applicable/not applicable, catastrophic/insignificant, etc. The quantitative risk assessment is carried out using the following methods recommended by the Operator's guidelines [4]:

- Hazard and Operability Study (HAZOP)
- Event Tree Analysis (ETA)
- Failure Modes and Effects Analysis (FMEA)
- Failure Modes, Effects, and Criticality Analysis (FMECA)
- Fault Tree Analysis (FTA)
- Human Reliability Analysis (HRA)
- Reliability Block Diagram.

The Operator recommends using the following quantitative risk assessment methods in addition: Tree Decisions [4], Monte Carlo simulation [4], and sensitivity analysis, including the «Butterfly» method [4].

Let us underline that many methods proposed by the risk management system are used in Probabilistic Risk Assessment (PRA) [8] and Probabilistic Safety Analysis (PSA), and in life management. Based on the PRA methodology, PRA combines PSA and life management. In comparison with some foreign countries where PRA is regulated by separate regulatory requirements [9], in Russia PRA is a part of the safety justification concept.

A risk matrix is the tool used for risk assessment, which helps to choose the risk management method and the urgency of performing risk management measures.

To design the risk matrix it is necessary to assess the probability or frequency of risk occurrence, to evaluate the risk consequences, and to determine the risk significance. The risk matrix design methodology is in a proper with [10]. However, some differences are compared to [10]. Firstly, experts assign scores when assessing the probability and consequences. For example, a score "5" is assigned when the probability of risk occurrence is above 0.9, and a score "1" is given for probability below 0.1. Similarly, score "5" is given for consequence which is losses exceeding 100 million rubles and score "1" if losses are less than 5 million rubles. The risk significance matrix is calculated by multiplying the probability of risk occurrence by the consequence score, resulting in a scale of 1 to 25 points. Secondly, the risk matrix named risk critically matrix is visualized using the «Traffic Light» system, where "red" indicates a significant risk ($15 \leq R_i \leq 25$), "yellow" means a manageable risk ($6 \leq R_i \leq 12$), and "green" indicates an acceptable risk ($1 \leq R_i \leq 5$).

For each risk, the degree of its impact on risk tolerance indicators is determined, taking into account limiting factors such as response time, resource availability, etc.

The risk management methods include "acceptance," "mitigation," "sharing," and "avoidance." In our opinion, it is appropriate to describe the risk management process in two strategies: risk decrease strategy and risk increase strategy, which can be implemented using the fore mentioned methods but are not limited to them.

The process owner develops risk management measures. The urgency of developing risk management measures is determined based on the risk significance.

The effectiveness of the measures is assessed using the formula

$$K = \frac{P_1 - P_2}{C_i}, \quad (1)$$

where K is the effectiveness coefficient of measure i , P_1 is the cost of risk consequences before implementing measures in million rubles, P_2 is the cost of risk consequences after implementing measures in million rubles, and C_i represents the cost of measure i in million rubles. The measure with the highest effectiveness coefficient is the most prioritized. P_2 represents the planned value of the measure's effect and serves as the basis for analyzing deviations during the monitoring stage of risk management results.

The Operator's risks are grouped into a consolidated risk register, which is a tool for risk accounting and control. Further, the risks are ranked by significance, and a consolidated risk register is formed in descending order of the initial risk assessment values or costs of risk consequences. Quarterly and annually, the process owner prepares a report on the results of risk monitoring.

III. Results

NPP M&R is a supporting part of the main process «Electricity and Heat Production».

The M&R process document named "M&R process identification summary" (M&R Summary) provides following information: the description of participants and their roles, resources, M&R objects management, key performance indicators.

The M&R process owner is the Department of Production and Operation of Operator. The resources required for M&R process performing include labor, informational, financial, material and technical, and infrastructural resources. The M&R process objects are norms and rules, repair deadlines, readiness for repair, resource needs, services, the organizational structure of M&R management, and equipment.

The M&R process key objective is to ensure the equipment operability while minimizing costs.

The key performance indicators (KPI) were developed and implemented in 2019. In 2022, The M&R process efficiency was assessed using 30 indicators, which are reactive and proactive. The evaluation of the M&R process efficiency is visualized using the «Traffic Light» method. The Operator defines upper, lower, and target values for the boundaries of the zones (red, yellow and green) for each NPP, taking into account the type of reactor and the number of units.

The KPIs are grouped into the following areas:

- Safety indicators
- Operational efficiency indicators.

Russian M&R process KPIs have significant differences from European ones [11].

Quarterly and annually, the Operator monitors the trends of the M&R process KPIs, assesses results' ratings, and carries out corrective actions if necessary. For example, the Operator modifies the target values of indicator boundaries or develops new indicators.

It ought to be noted that the KPIs indicate the level of risk tolerance, and each KPI is linked to a specific risk identified by the Process Owner. Thereby the Operator reviews the list of M&R

process risks and the risk management measures based on the assessment of KPIs' result ratings.

The Operator (Table 1) and separately each NPP evaluate the M&R process KPIs' result rating. The KPIs' trend assessment involves comparing current indicator values with those of the previous year.

Table 1: M&R process KPIs for Operator in 2022

KPI Title	Code	Criteria			The value 2022
Unavailability coefficient	M&R-P-1	$0 \leq K \leq 2$	$2 < K \leq 4$	$4 < K \leq 5$	1,87
Unavailability coefficient due to M&R shortcomings	M&R-P-2	$0 \leq K \leq 0,4$	$0,4 < K \leq 0,8$	$0,8 < K \leq 2$	0,00
Average age of defects in safety-critical systems	M&R-P-3	$0 \leq K \leq 40$	$40 < K \leq 72$	$72 < K \leq 100$	9,28
Average age of defects in non-safety-critical systems	M&R-P-4	$0 \leq K \leq 90$	$90 < K \leq 170$	$170 < K \leq 300$	32,60
Completion of the monthly equipment repair plan	M&R-P-5	$98 \leq K \leq 100$	$95 \leq K < 98$	$0 \leq K < 95$	99,00
Adherence to the repair campaign schedule	M&R-P-6	$0 \leq K \leq 1967$	$1967 < K \leq 2038$	$2038,1 < K \leq 2080$	1968,00
Exclusion of work scope	M&R-P-7	$0 \leq K \leq 11$	$11 < K \leq 22$	$22 < K \leq 33$	2,00
Reduction of injuries' severity during M&R executing	M&R-P-8	$K=100$	$50 \leq K < 100$	$49 \leq K < 50$	0,00
Exceeding the dose budget	M&R-P-9	$0 \leq K \leq 34$	$34 < K \leq 70$	$70 < K \leq 106$	0,00
Collective dose	M&R-P-10	$0 \leq K \leq 64$	$64 < K \leq 105$	$105 < K \leq 146$	19,72
Shutdowns of power units or turbogenerators within the first month after outage	M&R-P-11	$0 \leq K \leq 5$	$5 < K \leq 7$	$7 < K \leq 9$	0,00
Reduction of unplanned shutdowns of power units and turbogenerators	M&R-P-12	$9 \leq K \leq 10$	$3 \leq K < 9$	$0 \leq K < 3$	10,00
Number of depressurizations of coolant circuits	M&R-P-13	$0 \leq K \leq 5$	$5 < K \leq 10$	$10 < K \leq 15$	0,00
Coefficient of prevention foreign material exclusion from entering equipment	M&R-P-14	$98 \leq K \leq 100$	$90 \leq K < 98$	$0 \leq K < 90$	99,70
Number of defects in safety-critical systems	M&R-P-15	$0 \leq K \leq 111$	$111 < K \leq 166$	$166 < K \leq 200$	10,00
Number of defects in non-safety-critical systems	M&R-P-16	$0 \leq K \leq 670$	$670 < K \leq 1070$	$1070 < K \leq 1200$	57,36
Quality of staff work	M&R-P-17	$K=100$	$99,5 \leq K < 100$	$0 \leq K < 99,5$	100,00
Quality of the contractors' work	M&R-P-18	$K=100$	$99,5 \leq K < 100$	$0 \leq K < 99,5$	100,00
Unplanned restrictions for operation	M&R-P-19	$K=0$	$0 < K \leq 0,5$	$0,5 < K \leq 1$	0,00
Availability of repair documentation	M&R-P-20	$K=100$	$98 \leq K < 100$	$0 \leq K < 98$	99,99
Using procedures	M&R-P-21	$K=100$	$98 \leq K < 100$	$0 \leq K < 98$	100,00
Reducing the number of failures due to repair documentation	M&R-P-22	$K=10$	$0,1 \leq K < 10$	$0 \leq K < 0,1$	93,98
Reducing the number of equipment failures due to repair personnel	M&R-P-23	$K=10$	$0,1 \leq K < 10$	$0 \leq K < 0,1$	80,53

KPI Title	Code	Criteria			The value 2022
The quality of personnel workplaces walkdowns	M&R-P-24	$1 \leq K \leq 10$	$0,1 \leq K < 1$	$0 \leq K < 0,1$	3,37
Availability of stocks not to be allowed to run low	M&R-P-25	$K=100$	$70 \leq K < 100$	$0 \leq K < 70$	100,00
Centralized stocking	M&R-P-26	$99,9 \leq K$	$80 \leq K < 99,9$	$0 \leq K < 80$	98,24
Resource availability ratio	M&R-P-27	$K=100$	$90 \leq K < 100$	$0 \leq K < 90$	100,00
Adherence to repair documentation approval deadlines	M&R-P-28	$98 \leq K \leq 100$	$95 \leq K < 98$	$0 \leq K < 95$	100,00
Analysis of repair documentation quality during the repair interval	M&R-P-29	$K=100$	$98 \leq K < 100$	$0 \leq K < 98$	100,00
Analysis of repair documentation quality during the PPM	M&R-P-30	$K=100$	$98 \leq K < 100$	$0 \leq K < 98$	100,00

Due to the volume, the authors do not provide the formulas for calculating each indicator.

Based on the assessment of M&R process KPIs in 2022, the Operator has made the following decisions:

- supplement the KPIs system with four integrated indicators calculated using M&R-P-2-M&R-P-30: repair preparing management (M&R-P-31), repair executing management (M&R-P-32), shutdowns and unloading management for repairs (M&R-P-33), repair quality management (M&R-P-34)

- review the risks' list and the their occurrence causes
- review the risk management measures, taking into account the KPIs in "yellow" and "red" zones at the end of the year.

The major M&R process risks and their causes are provided in Table 2.

Table 2: The M&R process risks and their causes in 2022-2023

Risk	Cause
2022	
energy generation reduction	<ul style="list-style-type: none"> • due to the power unit extending outage • due to the power unit shutdowns caused by equipment malfunctions and failures due to unsatisfactory executed repair
electricity production costs increase	<ul style="list-style-type: none"> • due to the increase of the M&R costs in repair and operation expense items
2023	
Operator's revenue reduction due to the power unit extending outage resulting from repair works extending	<ul style="list-style-type: none"> • due to supplementary repair works caused by poor planning or defects identified during the repair process • due to the delayed or failure providing the contractor with up-to-date repair documentation, caused by unreadiness or lack technological documentation • due to the lack of modern technical means and adjustments for repairs caused by poor planning or lack of financial resources
electricity production costs increase due to the increase of the M&R costs in	<ul style="list-style-type: none"> • due to planning errors in repair works • due to planning errors in material and technical

repair and operation expense items resources' usage
 resulting from the execution of
 unplanned work scope

The risk management measures for the M&R process include inspecting the NPP readiness for PPM, inspecting the performed repair works' quality, corporate support, developing and revising repair documentation, implementing modern equipment and managing material and technical resources.

The statistical data of the notes of the Operator's commissions are presented for following risk management measures: inspecting NPP readiness for PPM in Figure 1, inspecting the performed repair works' quality in Figure 2 and corporate support in Figure 3. The statistical data demonstrates M&R process identified shortcomings.

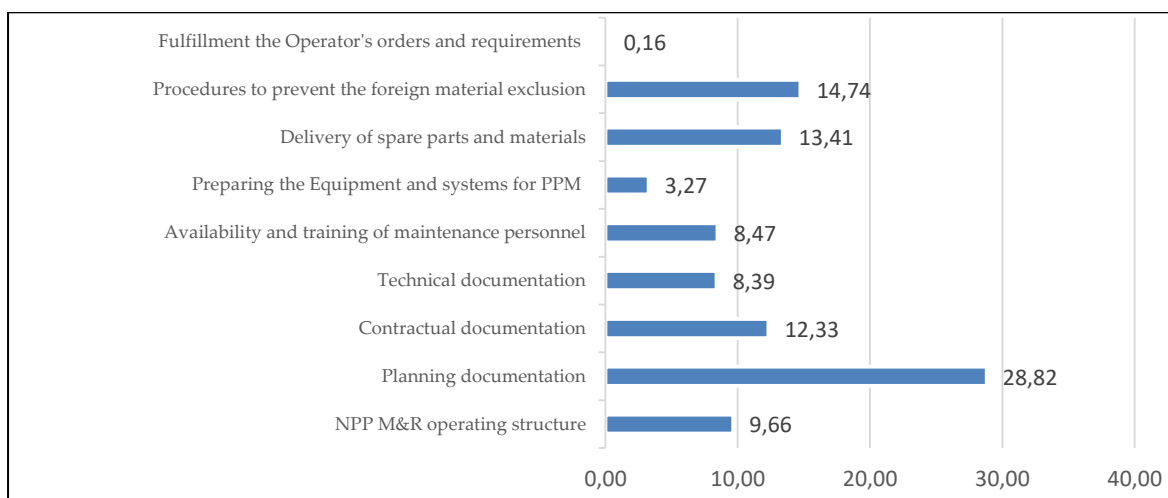


Fig. 1: The notes of the Operator's visiting commissions for inspecting NPP readiness for PPM on average for 2015-2022, %

Let us remark that the total number of notes decreased from 70 in 2015 to 22 in 2022, which is more than a threefold reduction. However, the trends continue to show an increase in every line of inspecting, except for "Procedures to prevent the foreign material exclusion from entering equipment."

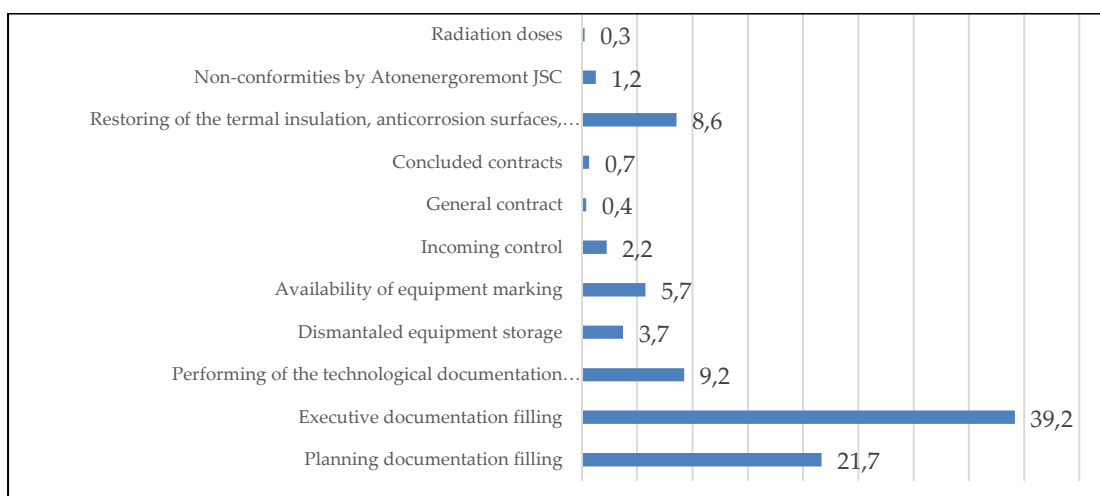


Fig. 2: The notes of the Operator's visiting commissions for the performed repair works' quality on average for 2015-2022, %

The changes of the number of notes is unstable. The number of notes fluctuates from year to year between 30-70 notes per year. However, the trends in lines of inspecting remain consistent:

- "Planning documentation filling" and "Dismantled equipment Storage" show an increase trends.
- "Technological documentation" and "Availability of equipment marking" demonstrate stable dynamics.
- The rest lines show a fall in notes.

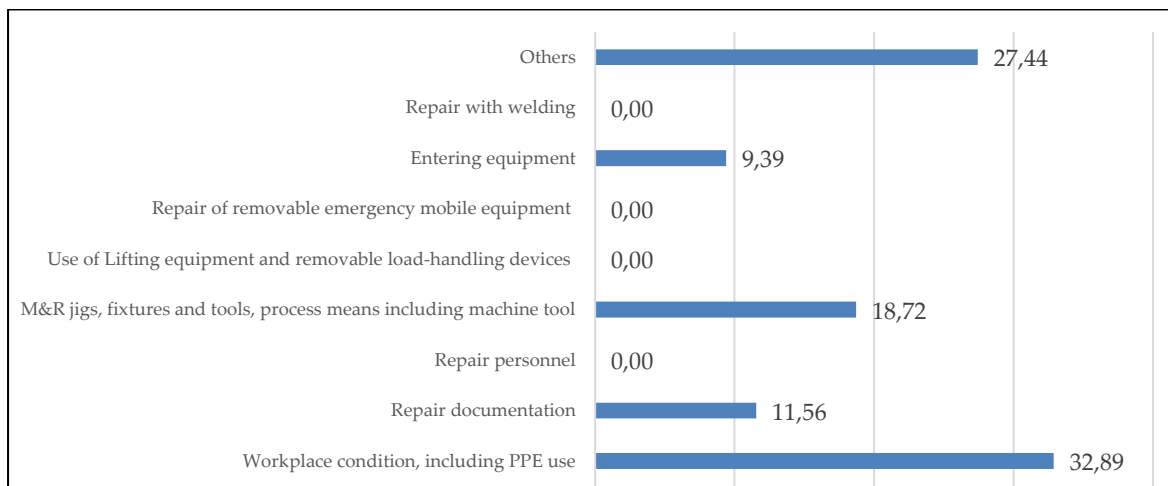


Fig. 3: The notes of the Operator's corporate support on average for 2019-2022, %

The number of identified shortcomings shows a downward trend, decreasing from 50 in 2019 to 27 in 2022. However, the trends in reducing the number of notes apply to all lines except for "Other", which includes shortcomings related to the filling of operation and repair documentation, the organization of repair headquarters, the use of specific software for maintenance planning, etc.

Given that the major risks are identified as energy generation reduction due to the power unit extending outage as well as the power unit unplanned shutdowns, it is necessary to analyze this data. The data on the planned outage duration for power units from 2015 to 2022 are provided in Table 3, while the data on unplanned shutdowns are presented in Table 4.

Table 3: Data on the planned outage duration of power units for 2015-2022, days

Indicator	2015	2016	2017	2018	2019	2020	2021	2022
Actual duration	1599,5	1873	1826,5	2571	2441,5	2243,5	1982	1848
Planned duration	1832	1980	1953	2621	2502	2374	2089	2000
Duration reduction	202	180,5	243,5	118,5	155	138,5	172,5	198,5
Duration extending	17,5	73,5	117	68,5	94,5	8	65,5	46,5
Duration Changing ("+" reduction, "-" extending)	184,5	107	126,5	50	60,5	130,5	107	152

For every unplanned shutdown, an investigation is conducted to identify the root and immediate causes. On average from 2015 to 2022, in 77% of cases, the root cause of the unplanned shutdown due to unsatisfactory M&R is NPP management shortcomings. Further analysis of this cause shows that 41% is attributable to documentation shortcomings, 40% to M&R procedures, 12% to failure to take actions, and 6% to human errors.

The result of risk monitoring is a report in tabular form, where the risk management system is evaluated on a scoring basis:

4 – risks were not realized, risk management measures were effective

2 – risks were realized, risk management measures were effective

1 – risks were realized, isolated cases of failure to risk management measures executing occurred

0 – risks were realized, lack or failure to risk management measures executing occurred.

Table 4: *Statistics of unplanned shutdowns of power units and turbine generators for 2015-2022*

Year	Duration, days		Quantity, units	
	Total	Caused by Unsatisfactory M&R quality	Total	Caused by Unsatisfactory M&R quality
2015	189,5	58,7	54	18
2016	252,2	49,8	58	10
2017	279,5	25,2	56	9
2018	287,8	85,4	46	14
2019	182,8	23,6	55	10
2020	85,3	12,3	36	9
2021	242,6	30,3	48	10
2022	202,4	14	44	4
Итого	1772,1	299,27	397	84

Let us resume that the Operator’s risks were not realized, despite some risks being realized in certain NPPs, and the risk management measures were deemed effective. The effectiveness score of the M&R risk management system is 4.

IV. Discussion

The Operator’s risk management system allows assessing risks of processes in accurate approach way.

Furthermore, M&R process risk management includes the use of recommended risk identification methods. However, risk analysis methods are not reflected in the M&R Summary. Nevertheless, it should be noted that all recommended risk analysis methods in the M&R process are used in the safety justification concept. Moreover, Regulator and Operator regulate the risk-centered maintenance. For example, when determining the scope and frequency of metal in-service inspection as well as when planning repair works considering equipment risk significance. For this purpose, domestic software is used:

- BARS for PSA of thermal reactors, the latest version of which was integrated with RiskSpectrum software that provides the following opportunities: data preservation after the RiskSpectrum software developers ceased support and various risk assessment methods enhancing.
- CRISS for PSA of fast reactors. This is a unique Russian software as well that allows assessing risks in M&R process of fast reactors.
- SPA (System of Predictive Analytics) for evaluating the technical condition of equipment based on physical-mathematical and statistical models of equipment and NPP technological processes. SPA is interfaced with the equipment’s, defects’, and low-level events’ databases.
- NPP Experience software for considering operating and repair experience. The M&R Automated Control System as a part of The NPP Experience interfaced with SPA and BARS/CRISS software, is a decision support tool that allows filling of sheet repair works’ scope based on forecasting equipment condition changes, requirements of Regulator, Manufacturer and Operator. Time required for repair, the number of personnel by qualification and positions, the spare parts’ quantity, the labor intensity, and the cost of the power unit repair in total and by workshops are automatically calculated based on the sheet repair works’ scope.

On the other hand the equipment's' and defects' databases are interfaced with the Supplier /Manufacturer database, providing a making informed decision of supplier choosing when equipment and spare parts procurement.

Thus, in our opinion, the shortcoming of the Operator's risk management system is the usage of expert method for assessing the risk probability and consequences. The shortcoming of the risk management system in M&R process is that the analytical relationship between the M&R process KPIs and risk assessment has not been investigated. Consequently, the manageability of risks through M&R process KPIs and risk management measures has not been proven. Therefore the authors' further research is to define the analytical relationship between risk manageability, KPIs and the result rating of risk management measures in order to improve the M&R process.

References

- [1] GOST R 51897-2021/ ISO Guide 73:2009 Menedzhment riska. Terminy i opredeleniya (Risk management. Terms and definitions). –M.: FGBU "RST", 2021. – 18 p. (in Russian)
- [2] GOST R ISO 31000:2019 Menedzhment riska. Principy i rukovodstvo (Pereizdanie) (Risk management. Principles and guidelines). – M.: Standartinform, 2021. – 19 p. (in Russian)
- [3] International Atomic Energy Agency, 2023. | Series: Integrated life cycle risk management for new nuclear power plants, ISSN 1995-7807; no. NR-T-2.15
- [4] GOST R 58771-2019 Menedzhment riska. Tekhnologii ocenki riska (Pereizdanie) (Risk management. Risk assessment technique). – M.: FGBU "RST", 2022. – 90 p. (in Russian)
- [5] GOST R ISO 3534-4-2021 Statisticheskie metody. Slovar' i uslovnnye oboznacheniya. CHast' 4. Vyborochnyj kontrol' na osnove dannyh oprosa i anketirovaniya. – M.: FGBU "RST", 2021. – 32 p. (in Russian)
- [6] GOST R 58531-2019 Upravlenie organizaciej. Rukovodstvo po vnedreniyu ustojchivogo menedzhmenta na malyh i srednih predpriyatiyah. – M.: Standartinform, 2019. – 22 p. (in Russian)
- [7] Galkovskaya V.E. Risk management when making decisions on financing the construction of new nuclear power plants. In the collection: Modern trends in the development of management and public administration. Materials of the All-Russian intramural scientific and practical conference. Edited by T.A. Golovina. 2020. p. 55-57. (in Russian)
- [8] GOST R ISO 11231-2013 Menedzhment riska. Veroyatnostnaya ocenka riska na primere kosmicheskikh sistem (Pereizdanie) (Risk management. Probabilistic Risk Assessment in space systems). – M.: Standartinform, 2019. – 30 p. (in Russian)
- [9] Probabilistic risk assessment and risk management of a nuclear power plant. Guide YVL A.7. <https://www.stuklex.fi/en/ohje/YVLA-7>
- [10] GOST R ISO 17666-2021 Menedzhment riska. Kosmicheskie sistemy (Risk management. Space systems). – M.: FGBU "RST", 2021. – 16 p. (in Russian)
- [11] BS EN 15341:2019+A1:2022 Maintenance. Maintenance Key Performance Indicators. <https://www.en-standard.eu/ilnas-en-15341-maintenance-maintenance-key-performance-indicators/>

MODERN TEACHING TRENDS IN MARITIME ENGLISH AS A GLOBAL INSTRUMENT IN SPREADING OF INDIVISIBLE BUSINESS ENVIRONMENT IN MARITIME INDUSTRY

Gulchohra Aliyeva



Azerbaijan State Marine Academy
aliyevagulchohra59@gmail.com

Abstract

The role of globalization in spreading of English as a fundamental tool of a communication appears to become an effective characteristic in all the aspects of business environment in maritime industry as “turned-on” email chain and correspondence is completely established in the English language, thus building the challenging competency within maritime universities and nautical institutions. While overviewing the research studies over the last four decades we mainly see that the main “ladder” in the objectives of IMO Model Courses remains to be the promotion of contact and cooperation among maritime lecturers of all branches of knowledge and form a high level of professional expertise institution in enhancing the environment of teaching opportunities of English for Special Purposes in maritime and shipping industry. The obvious conclusion by examining the proceedings of the Sub-Committee on the International Maritime English Conference (IMEC) is that the English language is rapidly gaining ground on effective delivering of lectures within the maritime establishments because its composition, flexibility, vocabulary and pragmatics completely makes it to become the “Lingua Franca” of Maritime English.

Keywords: Maritime English, IMO Model Course 3.17, English for Special Purposes, Standard Marine Communication Phrases (SMCP), a learning – centered approach in Maritime English

I. Introduction

English language has established its fixed position as a “must” for marine practitioners who have already chosen to study maritime sciences. Since all academic resources contain the basics of nautical disciplines in English, it makes hard to achieve high standards in obtaining the full professionalism in the management infrastructure in shipping industry, thus pushing forward the “to be” or “not to be” phenomena of English to arise in the course of common study process of maritime sciences. Every country in the world holds its particular education system and cultural background. This implies that academic establishments with maritime subjects in every location of the world has designed the basic professional targets to prepare students for careers in the maritime industry. This is namely that point where the language professionals and maritime specialists need to work out collaboratively on a language programme that will set and stipulate the teaching of simple basics of maritime sciences. Because IMO Model Course 3.17 for Maritime English recommends ‘colleges and training institutions should note that this course more than fulfils the competences regarding English language contained

in the STCW Convention, 1978, as amended' [1]. It illustrates that English teachers and lecturers should have a deep insight into English to meet the specific objectives of IMO regarding the training programmes to achieve the standards for English set out in the STCW Convention, 1978, as amended

II. The Position of Maritime English in Maritime Practice

The position that Maritime English holds in maritime practice is certain to be the provider of safe communication environment for navigation and conduct of the vessel to the final destination, thus standardizing the language used in professional "messaging" for navigation at sea, in port approaches, waterways and harbors and on board the ships with multilingual crews. It gives a conclusion that the implementation of Maritime English must consider the following aspects:

1. Properly qualified instructors of English;
2. Support staff
3. Rooms and other spaces
4. Equipment
5. English language course books that have a communicative aim
6. Technical papers, manuals, reports and nautical publications
7. Other maritime reference material and teaching aids as indicated in the Bibliography of IMO Model Course 3.17 [2].

While taking a thorough examination on the Communication skills according to the IMO Model Course 3.17 through listening, speaking, reading and writing, it becomes obvious that modern teaching trends in English prioritize fundamentals in maritime subjects, for instance, knowledge, understanding and proficiency in Maritime English alongside the grammar, vocabulary and phonology, required performance will maintain essentials of specific maritime science. Once again it proves that contemporary teaching approaches of ESP (English for Special Purposes) needs to be communicative and a learning – centered. Thus, IMO Model Course 3.17 puts the English instructors into the position of ESP lecturer for assisting the maritime students in obtaining a background knowledge in appropriate English level that will make possible to:

- describe types of vessels, safety equipment, navigational routes and geographic locations;
- understand helm orders;
- use numerical information for engineering;
- describe watchkeeping duties;
- understand standard engine orders;
- practice VHF exchange procedures;
- produce external written and spoken communications to request and give advice.

Elementary Maritime English level of IMO Model Course 3.17 is built in that way, which requires the implementation of communicative approach only because it contains the communication environment where maritime students can be easily involved in real conversations through role-plays, information-gap and Jigsaw activities and open-ended discussions.

Intermediate Maritime English level of IMO Model Course 3.17 is developed in that way, which aims at building fluency in four communication skills of Maritime English and here practices of language systems and communication skills correlate well with each-other. Presentation of new vocabulary is advised to be presented to the maritime students through the contextual analysis.

The teaching experience of skillful teachers shows that "contextualization" of a new vocabulary gives best fruits in explanation of explicit and implicit meanings of words. Students demonstrate a keen interest in learning new words when they are explained in context. Besides, monolingual dictionaries are highly helpful and they are great resources in introduction of new word stock to the students whose levels are considered to be pretty intermediate. IMO Model Course 3.17 supports

Maritime English trainers and practitioners to be flexible in vocabulary teaching because the main challenge before them is to guide students into independent self-study process. Thus, being able to encourage students to use English –English reference books (dictionaries, glossaries and thesauruses) is the best opportunity to immerse them in Maritime English. So, the Intermediate Maritime English level within the IMO Model Course 3.17 is targeted at:

- competences in the STCW Convention, 1978, as amended; maritime education and English;
- discuss and confirm travel arrangements for joining ship;
- make and confirm accommodation reservations;
- describe stages in preparing for sea and for arrival in port;
- write Note of Protest;
- understand SMCP (Standard Marine Communication Phrases) for pilotage;
- discuss aspects of safety and risk in the workplace;
- describe meteorological conditions;
- SMCP for briefing on special machinery events and repairs;
- comprehend and participate in communications by VHF radio and telephone;
- take and deliver messages accurately;
- explain MARPOL regulations regarding marine protection.
- use measuring and testing equipment for fault finding;
- deduce possible causes of events; establish and explain reasons for breakdowns or faults.

In a nutshell, the position of English teaching in maritime industry is believed to study the technical and lexical features of Maritime English and help students to spot differences between General and Maritimes English.

III. Active Learning

Active learning is a part of communicative approach, which mainly comprises a student-centered activity to expose the students to frequent learner participation, thus stimulating the quick learning environment. The main purpose of active learning is to drive students into real communication situation is to:

1. Assess the level and knowledge of English, i.e., to make clear the language capacity of the student.
2. Stimulate interest in a topic.
3. Increase opportunities to interact in English.
4. Recycle and reuse language previously taught.
5. Give both strong and weak students the chance to speak in class.
6. Encourage independent thinking by helping students to work out “rules” for themselves.

Active learning, it is apparent that is a very successful stage within the learning process with pair and group work. It is needless to say that Teacher Talking Time during the Maritime English Teaching becomes undesirable as it causes the boredom and drudgery, learners briskly tend to direct their attention to more suitable discussions rather than formal presentations. There are cases when students have virtually no chance to practise the language. Teacher Talking Time during the active learning stage of Maritime English sees a lot of active vocabulary and useful expressions. The interpretation and perception of the language structure of Maritime English features eliciting technique that can be employed successfully by English teachers in during presentations of rules and explanations to the cadets. Language learning directly collaborates with psychology and directly depends on the “power grid” of a certain student, implying that the “teacher to student” interaction will be crucial only in the event of penetration of production stages of lessons that demands “aces” from the teacher because the increase in speaking environment with students obviously relies on how the ESP language

practitioner will define and satisfy “student to student” communications. The more the pair and group work is enhanced in the Maritime English lessons, the more a non-threatening speaking environment will improve itself. All the matter is that the capability of mastering the fluency in ESP by maritime students “rest in their hands” of confidence. Less confident students do not allow themselves to get the chance to put their knowledge of new “acquisitions” into practice because of feeling shame during the “word up” in a foreign language. Our teaching experience witnesses that pair and group arrangements let the teacher notice the “well-cooperated” students and the ones who have specific learning needs. Therefore, IMO Model Course 3.17 of Maritime English attempts to equip teachers with recommendations with a flexible “teaching package” which they are expected to be creative, as the language training needs their knowledge, skills and dedication. These are the key components in the communication of expertise to students being trained through IMO Model Course material.

IV. Learning Maritime English Vocabulary

Maritime English Vocabulary is a framework of maritime sciences since it inherently uses precise expressions and the length of SMCP is usually restricted. This kind of vocabulary features “strange” words that are complicated to be literally comprehended. For instance, the collocations of ‘reference line’; ‘breast line’ and ‘head line’ are used to imply ropes or cables in the berthing or mooring as they secure a ship close to the pier alongside it. The terms of ‘leeward’, ‘windward’, ‘variable’, ‘backing’ refer to express the wind, its direction, windy side, or the sheltered side of the vessels at sea. The definition of the ‘fire party’ in Maritime English means the group of crew members trained for fighting fire on board a ship. These are the bright examples of specific phrases that are impossible to understand literally because these collocations will be taken wrongly and it will lead to misconceptions by the message recipients thus confusing them. The conclusion is that in order to learn the Maritime English the mariners should possess the satisfying level to produce necessary content in delivering the proper messages during external and on-board communications. Teaching maritime vocabulary is considered to be an inherent part of STCW Code of the Standards of Training, Certification and Watchkeeping for Seafarers Convention, 1978, as amended. While taking a deep insight into the STCW Code Part A: it is easy to see that the competency level of mariners is proposed to be in that sufficient extent of good written and verbal command of IMO SMCP to deal with the safety of navigation. So, knowledge, understanding and proficiency of the well-qualified staff should cover all modern conditions at sea. Thus, correctly interpreted and drafted SMCP messages as well as the adequate knowledge of English in reading and writing navigational publications will serve the safe environment in the management of multilingual crew because personal safety and social responsibilities are the core values of STCW 78/95. IMO Model Course 3.17 highlights the personal safety and social responsibilities as the follows:

Administrations should bear in mind the significance of communication and language skills in maintaining safety of life and property at sea and in preventing marine pollution. Given the international character of the maritime industry, the reliance on voice communications from ship-to-ship and ship-to-shore, the increasing use of multinational crews, and the concern that crew members should be able to communicate with passengers in an emergency, adoption of a common language for maritime communications would promote safe practice by reducing the risk of human error in communicating essential information [2]. This concept contributes that Vocabulary Consolidation Self-Assessment Round-up activities in vocabulary teaching will provide a good basement for effective delivery of ESP because problems of communication arising from the lack of knowledge of nautical English among the crew members that use and speak more than one language contributes to the confusion surrounding the initial phases of the emergency circumstances. Therefore, Self-Assessment

drills in Basic Marine Vocabulary will assist students in becoming independent learners thus motivating them to expose themselves to immersive Maritime English Self-Study Programmes. It would be reasonable to share a sample pattern for Maritime Vocabulary Revision Self-Assessment “workouts”.

A. Vocabulary Consolidation Self-Assessment.

- Tick ✓ what you can do. Cross ✗ what you still find hard to do in English:
- Dictate and note ship’s call signs and messages using the international maritime alphabet.
- Give and receive information that contains times.
- Understand SMCP signals.
- Repeat and understand helm orders.
- Say vessel’s position, bearing, course, speed and draught.

B. Work in pairs to dictate and note down information.

- Student A: Ask your partner the following questions. Fill in your card.
- What is the date?
- What is your ETA?
- What time does loading start?
- Who is the officer in charge?
- How much cargo do you expect to load? [3]

	<i>A</i>	<i>B</i>	<i>C</i>
Date:			
ETA:			
Loading starts:			
Cargo:			
Officer in charge:			
Cargo to be loaded			

C. Class Project. 1.

Bring to class a seafarer job application form from a shipping company or the web. Fill it in with the rest of the class. Act out an interview between the crew manager and yourself, with questions and answers on basic personal information [3].

D. How well can you talk in English on the following topics. Tick ✓ accordingly and give as many examples possible.

<i>Very well</i> []	<i>moderately well</i>	<i>poorly</i>	
<input type="radio"/>	<input type="radio"/>	<input type="radio"/>	Personal LSAs and survival craft <input type="radio"/>
<input type="radio"/>	<input type="radio"/>	<input type="radio"/>	Where safety equipment is on board
<input type="radio"/>	<input type="radio"/>	<input type="radio"/>	Conventions on safety
<input type="radio"/>	<input type="radio"/>	<input type="radio"/>	SOLAS requirements
<input type="radio"/>	<input type="radio"/>	<input type="radio"/>	IMO safety signs [3]

E. Class Project. 2.

Choose one of the following to present in class:
 Find out more about the history of SOLAS and its various parts.

Research another convention that relates to safety, the International Convention on Maritime Search and Rescue (SAR) 1979.

Free – fall lifeboats: How do they operate? What are their advantages and disadvantages? How widely are they used in comparison with conventional lifeboats? [3].

All these Self –Assessment Activity samples meet the requirements of STCW78/95 as they are designed in the way to develop the skills in the “standard language of communication for maritime safety purposes [2]. Administrations should consider the benefits of ensuring that seafarers have an ability to use at least an elementary English vocabulary, with an emphasis on nautical terms and situations [2].

V. Why does IMO Model Course 3.17 Consider Communicative Approach in Teaching Maritime English to be recommended method?

As IMO Model Course 3.17 manual is intended to imply the effective communication at contemporary sea conditions for seafarers, it prioritizes English language proficiency of them in dealing and interpreting with various situations at sea within the maritime sector. Being able to use English means that the seafarer can combine the ‘building blocks’ of language to express him/herself clearly and appropriately in speech and writing. Being able to understand English means that the seafarer can interpret messages that he/she hears and reads correctly and can respond to these messages appropriately and comprehensibly. When a seafarer can demonstrate the ability to do this, he/she proves his/her communicative competence in English [2]. So IMO proposals of SMCP (the External Communication and the On-board Communication Phrases) can be envisaged the best suit for communicative approach development as the operative language of maritime industry is the base-line of safety at sea. Moreover, communicative approach maintains the pace of student- centered teaching. Students are involved in active learning environment [2]. Furthermore, learning tasks of Maritime English reflect real life communications [4], for instance, the following task properly illustrates the real communication life situations at sea:

Listen to the helm orders and circle [a] or [b] accordingly.

When you hear this order, you must...

- a. Reduce the amount of rudder and hold.
- b. Hold rudder in the fore and aft position.

When you hear this order, you must ...

- a. Check the swing of the vessel’s heard in a turn.
- b. Reduce the vessel’s swing rapidly.

When you hear this order, you must...

- a. Reduce the vessel’s swing rapidly.
- b. Reduce the amount of rudder and hold [3].

The abovementioned extract from the task restates the importance of language for communication. That is why the developments of proper glossary, practice drills and reading materials will be the highest standards in maritime language teaching [5]. Moreover, it is interesting that communication approach of Maritime English Teaching aspects also cover the economic achievements in shipping industry because of the outlets of certain countries into the “high waters”. So the economic flourishing within the various marine sectors integrates the penetration of “Indian English” as well as “International English” into the communicative approach, thus making it the most practicable methodology in Maritime English Study Programmes. Role–plays, team collaboration,

group activities and project work make the communicative approach to be the intensive format in preparing maritime students to understand and produce purposely the language patterns in real situations at sea [6].

VI. Conclusion

Maritime English is considered to be the crucial part of ESP [7]. In terms of the rapid growth of Maritime Industry it had already obtained vitality to be taught within the nautical institutions. It implies that Maritime English course materials should be carefully developed so that its meaning is fully comprehended [8]. It once again, proves the necessity to follow recommendations and proposals stipulated in the IMO model course 3.17 and fully encompass the objectives specified in it. Therefore, selected materials and assignments should include a review of the appropriate course objectives because they have to reflect the “musts” of all relevant IMO international conventions and standards of the other instruments as presented in the IMO Model Course 3.17.

References

[1] The International Convention on Standards of Training, Certification and Watchkeeping for Seafarers (STCW), 1978, was adopted by the International Conference on Standards of Training and Certification for Seafarers on 7 July 1978.

[2] IMO Model Course 3.17, Maritime English, published by the International Maritime Organization, 4 Albert Embankment, London SE1 7SR, www.imo.org, second edition, 2009, pp. 1-183

[3] Maritime English Volume 1 - Papaleonidas, Paraskevi, 2015, pp.16-78

[4]<https://www.researchgate.net/publication/327890823> The Approaches of Teaching and Learning Maritime English Some Factors to Consider

[5] <https://bsmrmu.edu.bd/public/files/econtents/63bd34fe771bbbmj-02-01-08.pdf>

[6] Gulchohra Aliyeva. The Use of Innovative Maritime Terminology for Intercultural Communication Improvement in the Maritime Environment / International Scientific Conference on Multidisciplinary Challenges in Contemporary Science: Innovations and Collaboration, pp.183-187, September 15, 2023, Poland

[7]<https://www.semanticscholar.org/paper/The-Need-Analysis-of-Maritime-English-Learning-for-Dirgeyasa/186a5bff9f3768d9d1b0a3eefad0b2de32559a8c>

[8]<https://www.semanticscholar.org/paper/Needs-analysis-of-English-for-Specific-Purposes-in-Simbolon/4b07fe78be03c4e296b791c6c60100eef8a7ed53>

SPECIAL TAX REGIMES AS A TOOL FOR ENSURING ECONOMIC SECURITY

Larisa Aguzarova and Fatima Aguzarova



North-Ossetian State University named after K.L.Khetagurov

aguzarova.larisa@yandex.ru

aguzarus@yandex.ru

Abstract

The subject of this article is the study of special tax regimes as a tool for ensuring economic security. In the course of scientific research, the authors used general scientific methods. The types of special tax regimes, as well as the procedure for their establishment, are considered, on the basis of the method of observation. Using the method of synthesis and analysis, the calculation of individual indicators (specific gravity, growth rate) was carried out. Using the statistical method, the dynamics of such indicators as: the number of business entities is analyzed; revenues to the budget system from the payment of special tax regimes. The comparative method made it possible to identify the distinctive features of the conditions of their use. Researchers have identified the advantages and disadvantages of special tax regimes operating in modern realities, based on the method of scientific abstraction. When using the generalization method, the authors have made relevant conclusions and recommendations for improving the application of special tax regimes in order to ensure economic security. Among them: improvement of tax legislation in terms of certain elements of the regimes under consideration and conditions for their application; exemption from tax payments of newly created business entities until they receive profits; creation of comfortable conditions with counterparties. The authors emphasize that the main purpose of applying the regimes is the strengthening and further development of business entities, as well as ensuring economic security.

Keywords: business entities, small and medium-sized businesses, special tax regimes.

I. Introduction

Special tax regimes are recognized as a serious instrument of the state regulating the tax activities of economic entities in order to ensure economic security.

Special tax regimes are established by tax legislation and are applied in those cases and in such a manner as are provided for by the legislation on taxes and fees for small and medium-sized businesses.

As is known, special tax regimes imply a special procedure for determining the elements of taxation. They exempt from the obligation to pay certain taxes and fees (depending on the subject). These include: unified agricultural tax; simplified taxation system; taxation system for the implementation of production sharing agreements; patent taxation system; professional income tax; automated simplified taxation system. The last two special tax regimes were introduced in the strand of the experiment.

They differ from the general taxation regime in that the former means a regime in which payers pay all taxes and fees provided for by Russian legislation in full, and there is also an obligation to keep full accounting and tax records.

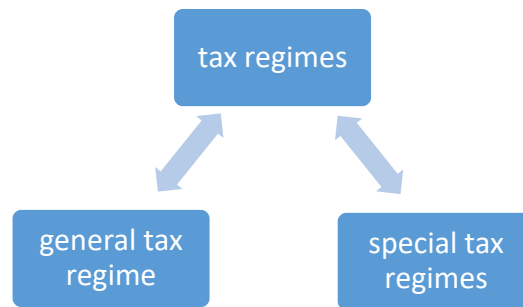


Fig. 1: *Tax regimes in the Russian Federation*

Of course, the main purpose of introducing special tax regimes into Russian tax practice is to support business entities (SMB) by reducing the tax burden.

II. Methods

The formation and development of new business entities is an effective engine of the economy, new jobs are created, the revenue part of the budget is expanding due to tax payments, the range of goods and services on the market is increasing, competitiveness is growing, the investment attractiveness of the region is increasing. It is important to note that business is considered the most vulnerable element of the economy and needs government support for further sustainable development.

The use of special tax regimes allows entrepreneurs to pay only one tax, reducing the tax burden and thereby ensuring economic security.

Organizations and individual entrepreneurs have the right to voluntarily switch to paying any special tax regime. Payers applying several special tax regimes must keep separate records of income and expenses for each regime.

It is important to note that the largest number of payers is available under the simplified taxation system. A smaller number apply the patent taxation system, as well as the unified agricultural tax. Only two payers are registered under a special tax regime in the form of a taxation system when implementing production sharing agreements. The number of payers under special tax regimes introduced as an experiment (the professional income tax and the automated simplified taxation system) is slowly growing, but so far they occupy the last positions. For example, as of 01.01.2023, the number of payers applying the professional income tax is 6561 thousand taxpayers in the Russian Federation.

In 2020-2022, the number of business entities decreased by 50,203 units, and if there is a decline in 2021, then in 2022 the same indicator increased from 568,4561 units to 5866,703 units. Of the eight federal districts, six showed a decreasing trend. Only two federal districts have positive dynamics. Thus, the number of business entities increased in the central Federal District by 36,202 units, in the North Caucasus Federal District by 4,794 units, but in Russia as a whole, the number of entities tends to decline (in 2022, there are 50,203 fewer SMB than in 2020).

III. Results

Table 1 shows the number of small and medium-sized businesses in the Russian Federation for 2020-2022.

Table 1: The number of small and medium-sized businesses in the Russian Federation for 2020-2022.

The name of the indicator	2020 year		2021 year		2022 year		Deviation +,- 2022 to 2020, units
	units	specific gravity, %	units	specific gravity, %	units	specific gravity, %	
Central Federal District	1821752	30,8	1764883	31,0	1857954	31,7	+36202
Northwest Federal District	692465	11,7	661265	11,6	678810	11,6	-13655
South Federal District	694492	11,7	665412	11,7	678129	11,6	-16363
North Caucasian Federal District	200256	3,4	192451	3,4	205050	3,5	+4794
Privolzhsky Federal District	1058398	17,9	1008260	17,8	1035009	17,6	-23389
Uralsky Federal District	510075	8,6	487874	8,6	494768	8,4	-15307
Siberian Federal District	628271	10,6	601227	10,6	610050	10,4	-18221
Far Eastern Federal District	311197	5,3	303189	5,3	306933	5,2	-4264
Total subjects of small and medium-sized enterprises in the Russian Federation	5916906	100,0	5684561	100,0	5866703	100,0	-50203

A source: <https://rmsp.nalog.ru/>

The largest number of small and medium-sized businesses is observed in the central Federal District: 30.8%; 31.0%; 31.7%, respectively. The Volga Federal District is in second place, although the number of subjects is decreasing: 17.9%; 17.8%; 17.6%, respectively. The situation is approximately similar in three federal districts: North-Western; Southern; Siberian. In them, the number of SMB is 10-12% of the total. Despite the positive dynamics, the smallest number of business entities is observed in the North Caucasus Federal District: 3.4%; 3.4%; 3.5%, respectively.

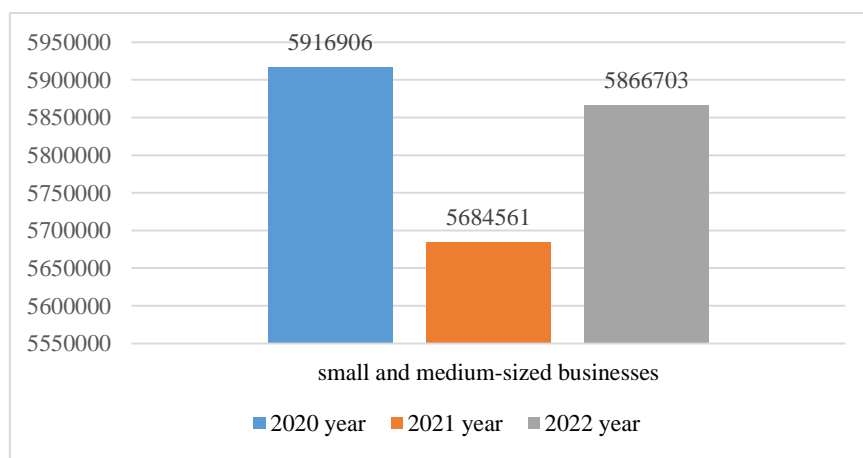


Fig. 2: Dynamics of the number of small and medium-sized businesses in the Russian Federation for 2020-2022 (units)

Figure 2 shows the dynamics of the number of small and medium-sized businesses in the Russian Federation for 2020-2022. The most favorable period is 2020 (the number of SMB - 5916906 units), the least favorable is 2021 (the number of SMB - 5684561 units).

In the current realities, the development of small and medium-sized businesses is a priority task of state policy, since the creation of business entities helps to reduce the unemployment rate, the production of new types of goods and services, the increment of the revenue component of budgets, which ensures economic security and economic growth.

It is important to take into account that the state as a whole, as well as economic entities and individuals, in particular, are interested in ensuring the economic security of the institute of entrepreneurship. This is due to the fact that business development has an impact on all spheres of society.

Under small and medium-sized enterprises, it is customary to understand the economic activity of a subject in a market economy aimed at obtaining maximum profit by creating and selling certain products (goods, works, services) at minimal cost.

In practice, any business entity is exposed to external and internal threats, for example, conducting illegal activities in the face of competitors, crisis phenomena (external), illiteracy of employees, rising inflation (internal). The economic security of a business should protect it from any threats. Therefore, it is quite reasonable to develop a set of measures for a long-term period for each region, taking into account the features that would prevent threats and losses, as well as contribute to the sustainable development of the economic entity.

Thus, the economic security of small and medium-sized businesses is understood as the creation by the state of conditions, opportunities, factors that ensure the competitiveness, independence of an economic entity, stable participation in market relations, regular improvement, growth of economic indicators.

In order to ensure the economic security of small and medium-sized businesses, Russian legislation provides for the application of special tax regimes. Undoubtedly, state support is important for the development and security of business, since on the basis of the creation of business entities, the state of the economy as a whole is improving (new jobs, production, provision of services, replenishment of tax revenues, etc.). In this regard, the faster the number of small and medium-sized businesses starts to grow, the more favorable the state of the economy will be.

We will analyze the indicators of small and medium-sized businesses in the Russian Federation for 2020-2022 (Table 2)

Table 2: Analysis of indicators of small and medium-sized businesses in the Russian Federation for 2020-2022

(units)

The name of the indicator	2020 year	2021 year	2022 year	Deviation 2022 to 2020 +,-
Employees (employed)	15321788	15491144	14662197	-659591
Products	6081	8160	9291	+3210
Total subjects of small and medium-sized enterprises of them:	5916906	5684561	5866703	-50203
legal entities	2528711	2371915	2314058	-214653
individual entrepreneurs	3388195	3312646	3552645	+164450

A source: <https://rmsp.nalog.ru>

According to Table 2, it can be seen that for 2020-2022 in the Russian Federation, the number of people employed in small and medium-sized enterprises is reduced by 659591 units. (that is, 659,591 people lost their jobs). However, the number of manufactured products produced by small and medium-sized businesses is steadily increasing. Over the entire period under review, there has been an increase of 3210 units. The number of business entities is dominated by individual entrepreneurs, their number is growing. During the analyzed period, the increase in them amounted to 164450 units. As for legal entities, their number is smaller and tends to decline. During the analyzed period, it decreased by 214,653 units.

Let's analyze how much small and medium-sized businesses have paid to the budget system of the Russian Federation for 2020-2022. (Table 3)

Table 3: *Payment by small and medium-sized businesses of special tax regimes to the budget system of the Russian Federation for 2020-2022*

The name of the indicator	2020 year	2021 year	2022 year	Deviation 2022 to 2020 +,-
Special tax regimes (thousand rubles)	586057116	808051107	985967106	+399909990
Number of small and medium- sized businesses (units)	5916906	5684561	5866703	-50203

A sources: <https://rmsp.nalog.ru/> <https://www.nalog.gov.ru>

For 2020-2022, revenues to the budget system of the Russian Federation from the payment of special tax regimes increase in each period: 586057116 thousand rubles; 808051107 thousand rubles; 985967106 thousand rubles, respectively. The increase in general amounted to 399909990 thousand rubles. Moreover, the number of small and medium-sized businesses in 2021 decreased significantly (to 5684561 units from 5916906 units), in 2022, on the contrary, increased (to 5866703 units from 5684561 units). However, it did not exceed the 2020 figure (5916906 units), as their number decreased by 50203 units.

Based on the analysis, the conclusion suggests that the state should create economically sound conditions for attracting the population of the country to create new business entities. It is advisable to interest and stimulate society in order to form business entities, first of all, by providing tax incentives and other similar measures. In addition, it is reasonable to support an existing business from the state, not to exert excessive tax pressure on it.

IV. Discussion

Let's consider the advantages and disadvantages of special tax regimes as an essential tool for ensuring economic security.

The primary advantage of applying special tax regimes should be recognized as reducing the tax burden on the payer. Switching to a special preferential regime allows you to replace several tax payments with one. For example, if an individual entrepreneur previously paid value added tax at a rate of 20%, corporate property tax at a rate of 2.2% and corporate income tax at a rate of 20%, then switching to one of the special tax regimes, the conditions of application of which suit him in accordance with tax legislation, he will pay a single tax at a rate of 6%.

This implies another advantage of applying a special tax regime – a simplified procedure for calculating and accounting. In this case, the entrepreneur calculates one tax payment instead of three and keeps only a book of income and expenses.

In addition, the positive side of the application of special tax regimes by small and medium-sized businesses is the simplicity of tax reporting. So, one declaration is submitted to the tax authorities, instead of several that were previously submitted in separate declarations at different periods (for each tax separately).

It is also advantageous that the size of a particular special regime can be reduced by a fixed amount of insurance payments.

The introduction of special tax regimes into Russian tax practice made it possible to reduce shadow turnover and increase the rate of tax collection by reducing the tax burden, which also refers to the advantages.

Along with the listed advantages, there are a number of disadvantages on the issue under consideration.

The main disadvantage of applying special tax regimes should be recognized that payers are exempt from paying value added tax. Here, the attractiveness of SMB for large counterparties is likely to be lost, since the latter are deprived of receiving tax refunds. It should also be noted that representatives of large businesses do not always agree to cooperate with small and medium-sized businesses due to uncertainty about their reliability.

A serious disadvantage is the deliberate fragmentation of large businesses, so to speak, the legitimate optimization of entrepreneurship. Owners of large companies and shopping malls consciously divide their business in cases when, according to the conditions established by tax legislation, they no longer fall under the preferential criteria used under special tax regimes. For example, when the company's annual income is exceeded or the number of employees is more than provided for by tax legislation. In this case, the budgets of the budgetary system lose the expected financial resources.

It is reasonable to classify some restrictions on the conditions of application of special tax regimes as "minuses". For example, the number of employees cannot exceed 5 people in the AUSN. Moreover, this mode cannot be combined with others, whereas other modes can. We also consider it unreasonable to limit that the company that pays the USN should not have branches.

It should be noted that when choosing the STS, when the base is "income minus expenses", you have to pay a minimum mandatory payment regardless of the results of financial activities. Moreover, the list of expenses for which it is allowed to reduce the tax base is very limited.

Based on our research, we propose to provide measures to improve the application of special tax regimes in tax practice in order to ensure economic security:

1. To improve tax legislation in terms of certain elements of special tax regimes and conditions for their application.
2. Exempt newly created small and medium-sized enterprises from paying tax payments in whole or in part until the period when they receive profits.
3. Create conditions for the provision of VAT refunds in cooperation with large counterparties.
4. Strengthen the measures of tax administration and control in the fragmentation of large businesses.

Thus, the essence of special tax regimes consists in a special procedure for determining the elements of taxation and exemption from payment of certain taxes and fees. The primary purpose of their application is the strengthening and further development of business entities, as well as ensuring economic security.

References

- [1] Aguzarova L.A. and Kasabiev Z.A. (2020) The current state and trends in the development of taxation in the digital economy. *Bulletin of the K. L. Khetagurov North Ossetian State University*, number 4, pp. 131-137.

[2] Aguzarova F.S. and Tsirikhova A.R. (2022) Application of innovative tools in the activities of tax authorities. *Finance and Credit*, volume 28, number 12 (828), pp. 2722-2739.

[3] Alexandrova M.V., Yutkina O.V. and Maslyukova E.A. (2023) Prospects of application of digital technologies for optimization of taxation of small business in the Russian Federation. *Managerial accounting*, number 3, pp. 309-316.

[4] Andreeva S.N. (2023) Special tax regimes: legal regulation, features, development prospects. *Journal of Legal and Economic Research*, number 1, pp. 51-55.

[5] Bochkov P.V. and Brovchenko E.S. (2023) Legal features of taxation of small and medium-sized businesses at the turn of the sanctions policy 2022-2023. *Competitiveness in the global world: economics, science, technology*, number 2, pp. 208-211.

[6] Davletshin T.G. (2023) Reforming the tax system: from special tax regimes to the general system of taxation. *Accounting in budgetary and non-profit organizations*, number 8 (560), pp. 26-41.

[7] Yershova I.V. and Trofimova E.V. (2023) Special legal regime of small and medium-sized businesses in the context of the search for promising areas of support for other segments of the domestic economy. *Actual problems of Russian Law*, volume 18, number 2 (147), pp. 103-115.

[8] Kozhanchikova N.Yu., Polyakova A.A. and Alentyeva N.V. (2023) Taxation of small business in Russia: problems and directions of improvement. *Bulletin of Agrarian Science*, number 1 (100), pp. 119-128.

[9] Mammadov N.D.O. (2023) On the mechanism of tax and legal stimulation of agricultural activities of small businesses in the Russian Federation. *Business. Education. Pravo*, number 1 (62), pp. 199-203.

[10] Sadykov M.A. and Suptelo N.P. (2023) The effectiveness of the application of special tax regimes for small and medium-sized businesses. *Bulletin of the S.Y. Witte Moscow University. Series 1: Economics and Management*, number 1 (44), pp. 53-60.

[11] Semenova G. N. (2023) Small business in the Russian economy: criteria for the application of special tax regimes. *Bulletin of the Moscow State Regional University. Series: Economics*, number 2, pp. 132-153.

USE OF SECONDARY ENERGY RESOURCES OF MODULAR POWER PLANTS WITH A GAS ENGINE AND REDUCTION OF HARMFUL EMISSIONS

Jamala Mamedova

•

Azerbaijan State Oil and Industry University
cemile_adna@mail.ru

Abstract

The paper considers the use of exhaust gas heat in modular power plants. In this regard, fuel consumption at power plants will decrease, efficiency of power plant will increase the emission of harmful gases into the atmosphere and environmental burden will reduce.

Keywords: modular power plants, exhaust gases, heat supply, efficiency, fuel economy

I. Introduction

At present, reducing fuel consumption and harmful emissions into the atmosphere is the most pressing issue worldwide. The article is devoted to this issue.

Electrical energy is mainly generated at thermal power plants. For this purpose, steam turbine power plants, combined steam and gas units, modular power plants, etc. are used. Modular power plants with an internal combustion engine are usually used to store and maintain balance in power systems. Such stations start quickly and stop quickly. It is advisable to use such stations at variable loads.

Modular power plants mainly use natural gases. In many cases, exhaust gases from engines with a temperature of 350°C - 370°C are released into the atmosphere. Thus, 55 - 60% of the heat of the fuel is lost with the exhaust gas and cooling water, as a result, the exhaust gases pollute the environment and the atmosphere. By applying different schemes, it is possible to use the heat of exhaust gases, which ultimately increases the efficiency of the station, reduces fuel consumption and environmental loads.

A system for the beneficial use of the heat of flue gases (temperature 350-370°C), is proposed, the heat supply of which is shown in Fig.1.

Exhaust gases from the gas engine with a temperature of 350°C are fed through pipelines to the waste heat boiler, where, due to the heat of these gases, the heating system water is heated. Heated water is supplied through supply lines to heat consumers, where it is used for heating and hot water supply of settlements. Heating system and make-up pumps are installed in the circuits to implement this technological process.

The studies were carried out at modular power plants with a capacity of $N_e=385$ MW, where 21 four-stroke gas engines with a capacity of 18.333 MW each were installed. Natural gas, with a heat value $Q_H^p = 33520$ kJ/m³ was used as a fuel. At each unit, the hourly consumption of natural gas is $B_{ag}=4000$ m³/h, the fuel consumption for the entire station is $B=84000$ m³/h.

Known formulas [2] determined the theoretical volume of air for burning 1 m³ of fuel $V^0=9.8$ m³/m³ excess air coefficient $\alpha=1.1$, exhaust gas temperature $t_2=350^0$ C, exhaust gas enthalpy during combustion of 1 m³ gas is $H_2=5384.53$ kJ/m³. This heat can be usefully used in a waste heat boiler to produce hot water or steam [1].

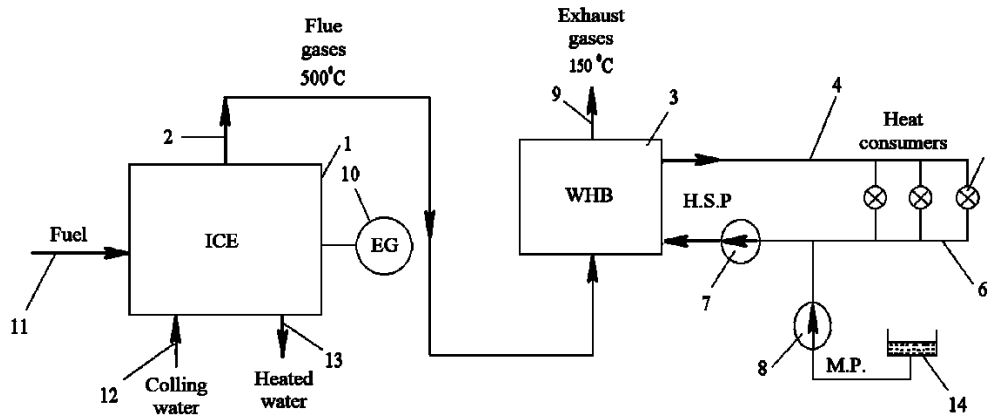


Fig. 1: Heating system.

1. Heat source of the internal combustion engine. 2. Exhaust gas pipeline. 3. Waste heat boiler for water heating. 4. Consumer supply line. 5. Heat consumers. 6. Return line from consumers. 7. Heating system pump. 8. Make-up pump.
9. Exhaust gases from the waste heat boiler. 10. Electric generator. 11. Fuel supply line. 12. Cooling water inlet. 13. Cooling water outlet. 14. A tank of nutrient (make-up) water.

The temperature of the exhaust gases from the waste heat boiler is assumed to be 150°C, and the enthalpy is found to be $H_{ex}=2266.58 \text{ kJ/m}^3$. Used heat in the waste heat boiler per 1 m³ of fuel

$$\Delta H = H_2 - H_{ex} = 5384,53 - 2266,58 = 3117,95 \frac{\text{kJ}}{\text{m}^3} [1].$$

The total hourly fuel consumption for the entire station is

$$B = 21 \cdot 4000 = 84000 \text{ m}^3/\text{h}.$$

Efficient use of heat in the waste heat boiler

$$Q_b = 84000 \cdot 3117,95 = 261,9 \cdot 10^6 \frac{\text{kJ}}{\text{h}} = 72,3 \text{ MW}$$

Taking into account losses in the boiler $Q_b = 72,3 \cdot 0,94 = 67,96 \text{ MW}$.

Heat loss with exhaust gas

$$q_2 = \frac{(H_{ex} - \alpha \cdot H_{c.a.}^0) \cdot 100\%}{Q_H^P}$$

$H_{c.a.}^0$ – cold air enthalpy $\frac{\text{kJ}}{\text{m}^3}$;

$H_{c.a.}^0 = 1,32 \cdot t_{c.a.} \cdot V^0$; cold air temperature is accepted

$t_{c.a.} = 18^\circ\text{C}$; $H_{c.a.}^0 = 1,32 \cdot t_{c.a.} \cdot V^0 = 1,32 \cdot 18 \cdot 9,85 = 234 \frac{\text{kJ}}{\text{m}^3}$.

$$q_2 = \frac{(2266,58 - 1,1 \cdot 234) \cdot 100\%}{33520} = 5,99 \approx 6\%$$

When the exhaust gases are cooled to cold air temperature, the theoretical heat released in the boiler

$$Q_{theory} = B(H_g - H_{c.a.}) = 84000(5384,53 - 234) = 432,6 \cdot 10^6 \frac{\text{kJ}}{\text{h}} = 120 \text{ MW}$$

Efficient use of heat in the boiler

$$\eta_r = \frac{Q_{use}}{Q_{theor.}} = \frac{67,96}{120} = 0,6$$

Heat saving $\Delta\eta = \eta_g \cdot \frac{H_g - H_{c.a.}}{Q_H^P} = 0,6 \frac{5380 - 234}{33520} = 0,12$

Power plant efficiency

$$\eta_s^{brut} = \frac{3600 \cdot W_e \cdot 10^3}{B \cdot Q_H^P} = \frac{3600 \cdot 385 \cdot 10^3}{84000 \cdot 33520} = 0,49 = 49\%$$

When using the heat of exhaust gases.

$$\eta_s^{brut} = \eta_s^{brut} + \Delta\eta = 0,49 + 0,12 = 0,61 = 61\%$$

The efficiency of the station is increased by 12%.

Specific reference exhaust consumption

$$B_s^{brut} = \frac{123}{\eta_s^{brut}} = \frac{123}{0,49} = 251,02 \frac{\text{gr}}{\text{kW} \cdot \text{h}}$$

When using the heat of flue gases

$$B_s^{brut} = \frac{123}{0,61} = 201,64 \frac{gr}{kW \cdot h}$$

Fuel economy is

$$\Delta B = 49,38 \frac{gr}{kW \cdot h}$$

For all stations the fuel economy is 19.2 T/h.

In addition to all, it is possible to provide the population with heating and hot water supply using received hot water.

To provide 1000 residents with heating (in the climatic conditions of Baku) [3].

$$Q = q \cdot F$$

where F is the area of objects

$$F = f \cdot N$$

N – population: N=1000.

f - the required area per one f = 12 m² / men.

$$F = 1000 \text{ people} \cdot 12 \text{ m}^2/\text{men} = 12000 \text{ m}^2$$

q - heating indicator,

$$q = 65 \text{ W/m}^2$$

$$Q = 65 \text{ W/m}^2 \cdot 12000 \text{ m}^2 = 780000 \text{ W} = 780 \text{ kW}$$

(per 1000 men).

Heat load for hot water

$$Q_{h.w.s.} = \frac{C \cdot N \cdot a(t_2 - t_x) \cdot \rho}{3.6 \cdot 24 \cdot 10^3} (1 + \beta_r) \text{BT}$$

C is the specific heat capacity of water

$$C = 4,19 \text{ kJ/kg}$$

a - the rate of hot water per man

$$a = 120 \text{ l/men}; N = 1000$$

t₂ - cold water temperature

$$t_x = 5^\circ \text{C}$$

ρ is the density of water; ρ = 1000 kg/m³

β – heat loss in the system β = 0.2

$$Q_{h.w.s.} = \frac{4,19 \cdot 1000 \cdot 120(55 - 5) \cdot 1000 \cdot 1,2}{3.6 \cdot 24 \cdot 10^3} = 349166 \text{ W} = 349 \text{ kW}$$

$$\sum Q = Q_h + Q_{h.w.s.} = 780 + 349 = 1129 \text{ kW} = 1,129 \text{ MW}$$

(per 1000 men).

Efficient use of heat in the waste heat boiler Q_b=67.96 MW

Then,

$$\frac{67,96 \cdot 1000}{1,129} = 60194 \text{ men}$$

Thus, 67,96 MW of heat can be provided to 60194 people for heating and hot water supply.

Thus, using the heat of exhaust gases, it is possible to save fuel heat, increase efficiency of the stations, reduce fuel consumption and the amount of gases emitted into the atmosphere.

II. Conclusions

1. The heat of flue gases was determined in the amount of 67,96 MW.
2. Calculations show that when using this heat, the efficiency of the station increases by 12%.
3. The specific fuel consumption is reduced by 49.38 g/(kWh) and the amount of exhaust gases is reduced.
4. The use of such heat will reduce emissions of harmful substances such as CO₂ and NO_x into the atmosphere and reduce environmental burdens.

5. Using the heat of exhaust gases, it is possible to provide 60,194 residents with heating and hot water supply.

References

- [1] Ivashenko E.Yu. Heat Waste Technology Belarusian National Technical University. Minsk, 2014, p.110.
- [2] Thermal calculation of boiler units using a computer. Kazan State Energy University. 2015, p.32.
- [3] Skanavi A.N., Makhov L.M. Heating, Textbook for universities. M. DIA Publishing House, 2002, p.576.
- [4] Danilov O.L. et.al., ed. A.V. Klimenko. Energy saving in heat power engineering and heat technologies. Textbook for high schools. M. Publishing house. MPEI, 2010, p.424.

AEROSPACE MONITORING OF SEA OIL POLLUTION BASED ON TECHNOLOGIES OF COGNITIVE AND EXPERT SYSTEMS

Nazif Sattarov

•

Azerbaijan National Aerospace Agency

nsattarov@gmail.com

Abstract

Azerbaijan is geographically located at the intersection of West and East. It has unequivocally made a choice towards innovation. The swift diversification of the economy into processing, industrial, and further into the informational sphere is a defining condition for the competitiveness of Azerbaijan's sustainable development. The issue of selecting the necessary information and making optimal decisions based on it is particularly essential in various emergency situations. In the 21-st century it has become crucial to exercise local and regional control of the Caspian region environment's condition. This can be explained by the intensive development and exploitation of oil fields as well as by natural changes (sea level fluctuations in the coastal zone, etc.). At the same time, with the increasing volume of oil transportation through pipelines and with the help of oil tankers, anthropogenic pressure on the region will be steadily increasing. In this context, the development of new technologies and methodologies that provide information support for ecological observations (in particular, environmental audit and risk analysis), is of decisive importance. In this regard, remote sensing from orbiters exemplifies a powerful method of planetary exploration. Onboard sensors provide unique views of the Earth's surface combined with a large range. On the base of the above-mentioned facts, this paper is aimed at discussing several important features of aerospace monitoring of the oil pollution of the Caspian Sea surface using technologies of cognitive and expert systems.

Keywords: aerospace monitoring, oil, sea pollution, cognitive systems, expert systems

I. Introduction

Azerbaijan has clearly made a choice towards innovation recently. The fastest diversification of the economy into the processing, industrial and further into the information area is the decisive condition for the competitiveness of our sustainable development. The problem of choosing correct data and making optimal decisions based on those is particularly important in the course of various emergency situations [5]. Current ecological crisis in the world is developing unprecedentedly: oil spills in the sea (Gibraltar, Bosphorus, Black Sea), on land (Keystone oil pipeline, USA, Canada; accidents on oil tanks (the state of Ohio), fire on the fixed platform in the Gulf of Mexico, eruption of a mud volcano in the Caspian Sea. One of the main questions to be asked in this case is how a fragile ecosystem of the Azerbaijani sector of the enclosed Caspian Sea will react? It is not easy to answer this challenging question, but one fact is already possible to mention: experts have been already observing a sharp decline in the number of birds and fish in the region. Safety improvements in oil and gas exploration, oil production and transportation methods have unfortunately not reduced the risk of negative environmental impact yet as they had been hoped to do. At the same time, remote observation methods have made it possible to

significantly expand the range of possibilities to solve at least some of the existing ecological problems.

After a large-scale accident of the oil spill on the sea surface in the Gulf of Mexico (2010), a number of ecological issues became very important, namely:

1. The importance of correct joint use of radar and optical data in emergency situations [1, 2].;
2. Necessity of development of a new concept of information support system of aerospace monitoring based on a cognitive model [4].

Our previous researches have already touched upon the problem of a lack of cognitive coordination between a person and a computer. Taking this into consideration, the purpose of the given study is to develop a methodology most suitable for the water area of the Absheron peninsula in the Caspian Sea.

Oil pollution in the water area of the region is formed as a result of both anthropogenic activities and spills of natural origin. Systematic monitoring of the water area is currently not carried out. In general, in order to detect oil slicks on the sea surface, satellites equipped with radars are used. Due to the fact that oil smudges the waved sea surface, the obtained images of slicks are usually high-contrast. Optical data carry important information about an oil spill only in cloudless weather. At the same time, radar and optical data have both advantages and disadvantages, which will also be discussed below. As a result of the performed research, a **cognitive model of peculiarities of radar and optical data usage** is proposed.

On the base of the above-mentioned it is possible to conclude that scientific knowledge should be cognitive, lucid, and comprehensible. Remote observation methods, particularly those involving space technology, have ushered in a qualitatively novel phase in the informational support of Earth sciences and economic practice [6]. Contemporary means of remote sensing (panoramic video spectrometers, microwave radars, optical systems, lidars, and other electronic technology devices) alongside diverse platforms (Landsat, SPOT, Sentinel, etc.) have facilitated the broadening of the spectrum of addressable inquiries.

When addressing a conservation-oriented task and selecting a strategy with minimal risk factors, the pursuit should aim for maximizing the likelihood of attaining results and optimizing their utility to the greatest extent. These pieces of information, encapsulating diverse perspectives on the studied problem, can be derived from past experiences, scientific satellite-based experimentation, and multivariate cognitive computer simulations. Given that the situation (pertaining to resource utilization, conservation, etc.) exhibits inherent dynamics, proactive monitoring is imperative to stay ahead of emergency situations.

II. Methods

Fig.1 shows the cognitive triad: subject area, goal, means.

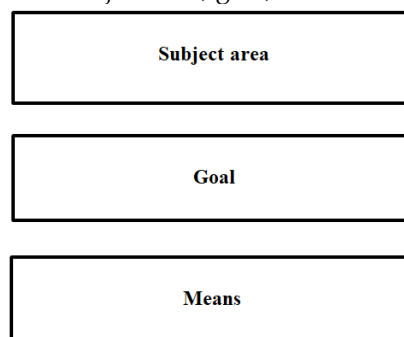


Fig. 1: Scheme of the cognitive triad

In the process of experimental research, a large scientific and practical material has been collected. Alongside, the analysis of human-made hazards in the oil sector in various regions of the world has been carried out [6]. Based on this material, informative heuristics of **IF - THEN** structures have been developed [3]. Let us give some examples:

1. **IF** the oil tanker hull is seriously damaged as a result of an accident,
THEN the probability of an oil spill into the sea and the formation of an oil slick is very high.
2. **IF** there is a fire in the tanker,
THEN the probability of an oil spill into sea and the formation of a burning oil slick is very high.
3. **IF** there is a fire on the oil platform,
THEN the probability of oil spilling into the sea and the formation of an oil slick is very high.

Now let us analyze the structure of the cognitive multimedia model of the aerospace monitoring process (Fig.2).

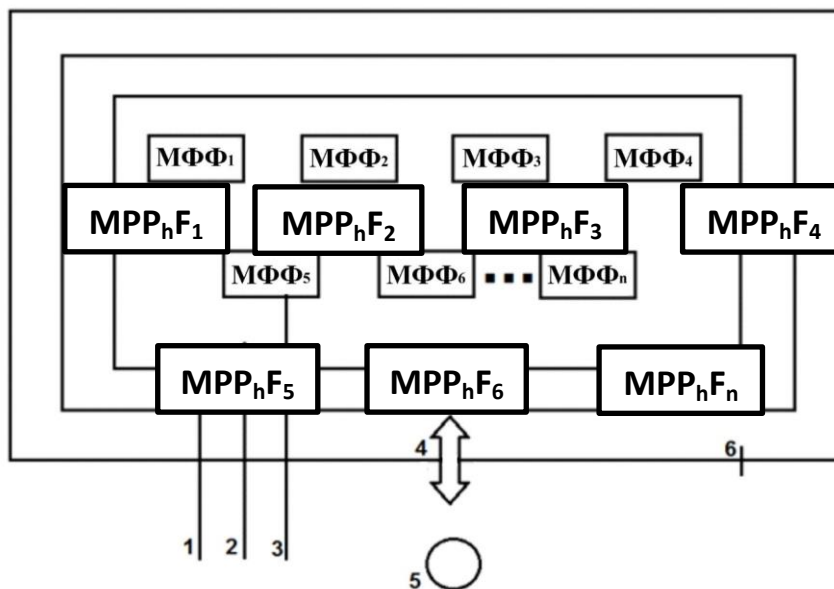


Fig. 2: The structure of the cognitive multimedia model of aerospace monitoring

Legend:

1. Screen
2. Cognitive multimedia model
3. Multimedia process phase form (MPPhF)
4. Dialogue interaction
5. Researcher
6. Software and hardware complex

There are three functional components in the cognitive model: a multimedia model of the problem area (technological process), phases of technological process, and dialogue interaction between the researcher and the complex. This also includes online audiovisual communication with experts. A multimedia model of the problem area is a set of audiovisual forms of phases of a given technological process. The phases of the technological process are multimedia images of source data. The multimedia model is designed to display the parameters and conditions of various research objects, that is, information models.

III. Results

The afore-mentioned facts made it possible to create a scheme for cognitive modeling of monitoring oil pollution of sea surface.

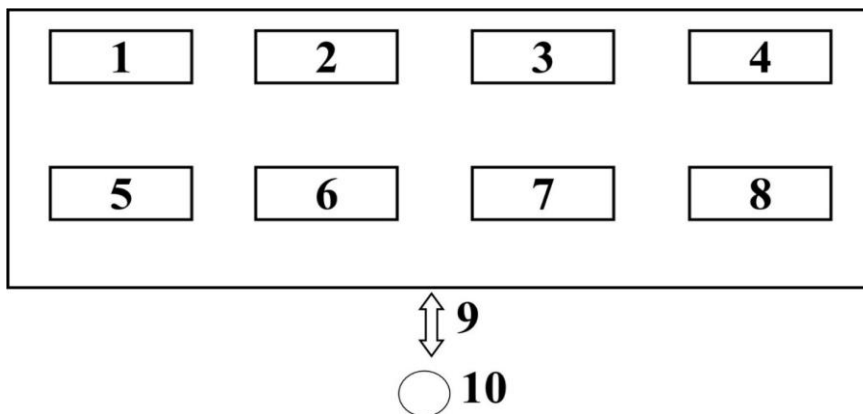


Fig. 3: Scheme of cognitive modelling of sea oil pollution monitoring

Legend:

1. Block of emergency situations in the world
2. Block of creation of heuristics of the occurred emergency situations
3. Characteristics of the Caspian Sea
4. Characteristics of the Absheron peninsula
5. Study area of the sea
6. Scheme of aerospace monitoring.
7. Model of the water area of the Absheron Peninsula based on the data of radar and optical surveys (cloudless weather)
8. Model of the water area of the Absheron Peninsula based on the data of radar and optical surveys (solid cloudy weather)
9. Researcher
10. Software and hardware complex.

IV. Discussion

At present, in the scientific world, the multilevel organization of the brain is beginning to emerge more and more clearly. In modern cognitive science it is assumed that a person has a cognitive picture of the world. This assumption is based on internal mental models. Thus, the brain is able to create and use symbolic (figurative) cognitive representations, or mental maps. The ability to generalize (cognitive representation) is the driving force behind human progress. The main task of the cognitive approach is to understand and explain how thought processes are arranged and work. A thought process is a process characteristic of a person, namely: perception, organization, coding, storage, retrieval of information. In our case, this is scientific information about emergencies. Cognitive learning methodology includes many different theories. As a part of our research, let us consider the following chain: individual cognitive picture of the world - subject area - problem area. The brain stores knowledge in long - term memory in the form of schemas, namely mental structures. Therefore, the supply of new scientific information contributes to:

- creation of new mental schemes;
- changing of existing schemes;
- expansion of existing schemes.

An example of new scientific information for emergency situations can be stages of development of a geographical map: paper map - electronic map - multimedia map. Effective analysis, research and modeling of any kind involves determining the cause of observed events.

Cause and effect relationships between different events underlie cognitive maps of reality. The researcher's accumulated experience must be systematized and structured. This facilitates orientation in heterogeneous information. The mentioned provisions form the basis of the developed scheme (Figure 3).

Now let us consider the features of the presented blocks:

1. The block of emergency situations in the world is designed to collect informative material about human-made hazards in the oil sector in various regions of the world.
2. The block for creating heuristics of occurred emergencies serves to fill the knowledge base.
3. The block characteristics of the Caspian Sea provides information on the physical-geographical and environmental features of the Azerbaijan sector of the Caspian Sea.
4. The block characteristics of the Absheron Peninsula provides information on the geographical and ecological features of the water area on the Peninsula.
5. The sea area under study block provides information about the geographic coordinates of the problem area, etc.
6. The block scheme of aerospace monitoring provides information about the possibilities and tasks of remote sensing, types of aerospace monitoring, optical and radar satellite systems, etc.
7. The block model of the water area of the Absheron Peninsula based on the data of radar and optical survey (cloudless weather) provides a cognitive scheme for the monitoring process.
8. The block model of the water area of the Absheron Peninsula based on the data of radar and optical survey (solid cloudy weather) provides a cognitive scheme for the monitoring process.

As an example, let us consider the cognitive model of the water area of the Absheron Peninsula based on the data of radar and optical surveys (solid cloudy weather).

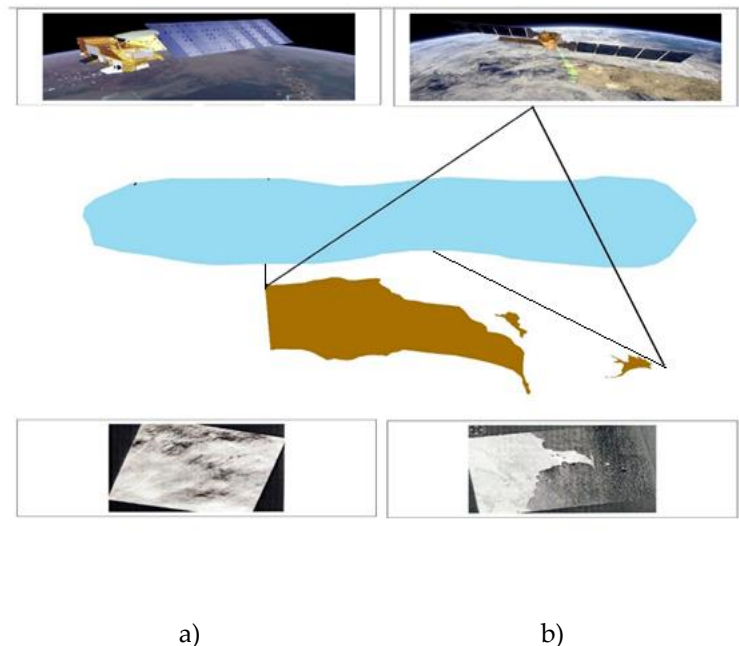


Fig. 4: Cognitive model of the water area of the Absheron Peninsula based on the data of radar and optical surveys (solid cloudy weather) made on the same day and at the same time.

Legend: a) Landsat - 8 (21.12.2018); b) Sentinel - 1 (21.12.2018)

Fig.4a shows the optical space image of the air cover over the water area obtained from the Landsat - 8 optic satellite. In the image it can be seen how the water area of the Absheron Peninsula is covered with solid clouds. In this case it is impossible to obtain accurate information

about the surface of the Earth. At the same time, with the help of the radar satellite Sentinel - 1, despite the cloudy weather, you can get all the necessary information. Thus, regardless of weather conditions and poor visibility, radar surveys are very convenient for displaying and studying the terrain.

References

- [1] Bondur V. G. (ed.) (2012). Aerospace Monitoring of Oil and Gas Complex Facilities. Moscow: World of Science (in Russian).
- [2] Lavrova, O. Y. and Kostyanoi, A. G. (2010). Catastrophic oil spill in the Gulf of Mexico in April-May 2010. *Earth Exploration from Space*, 6: 67-72 (in Russian).
- [3] Russel, S. and Norving, P. (2020). Artificial Intelligence. A Modern Approach. 2-nd ed. New Jersey: Prentice Hall Upper Saddle River.
- [4] Sattarov N. A. (2004). Remote sensing: a system of informational support for natural resources research and ecological situation analysis. *Scientific Notes of NAA*. Baku, vol. 6, 1:242-247 (in Russian).
- [5] Sattarov N. A. (2005). Multimedia encyclopedia of aerospace ecological monitoring. *Proceedings of the 3rd International Symposium on Emergency Situations*. Baku, 23-25 November, 151-153 (in Russian).
- [6] Sattarov, N. A. and Aliyeva, G.V. (2019). Peculiarities of multispectral and hyperspectral surveys in aerospace monitoring tasks. *Reports of ANAKA*, v. 22, 2-22:14-20 (in Russian).

MONITORING OF INDIVIDUAL SEISMIC RISK AT ALL STAGES OF DEVELOPMENT OF A POSSIBLE EARTHQUAKE SOURCE

Gennady Nigmatov, Andrei Savinov, Temir Nigmatov

•
FGBU VNII GOCHS (FC), Russia
tagirmaks@mail.ru

Abstract

At the threat of a catastrophic earthquake, there is a need to ensure seismic safety of the population at all stages of seismic hazard development. First of all, it is important to determine the locations of possible earthquake sources and possible macroseismic fields created by them on the terrain. The effectiveness of measures on seismic safety of the population will depend on how correctly the possible earthquake source and seismic hazard zones, in which destructive seismic impact is expected, seismic resistance of buildings in these hazard zones, the number of population falling into the seismic zone, possible consequences have been determined. Knowing the possible consequences, it is easy to determine the necessary forces and means to prevent risks and rescue the population.

Keywords: seismic hazard, possible earthquake source, macroseismic field, dynamic-geophysical testing of buildings, building seismic resistance, individual seismic risk

I. Introduction

Seismic safety is a complex concept, and unlike seismic hazard and individual seismic risk, it cannot be unambiguously expressed by a single value. The main difference of seismic safety is its focus on prevention of possible risks, i.e. the goal of seismic safety is to ensure minimal damage and losses at all stages of development of a catastrophic earthquake. Three main stages of seismic event development can be distinguished:

Stage One - possible earthquake source is expected to be triggered;

Second stage - possible earthquake source triggering and possible threat of a second strong shock;

The third stage is the attenuation of the event:

For proper planning of measures to ensure seismic safety of population in the zone where destructive earthquake is expected with high probability, it is necessary to have monitoring information on possible earthquake sources, on time of each stage of earthquake, on zones of seismic loads in case of triggering of possible earthquake source, on seismic resistance of buildings, on possible destructions and losses, on required forces and resources.

In order to obtain real-time information on the above data, it is necessary to carry out monitoring observations, to have criteria to assess the degree of danger of seismic loads in case of possible earthquake source triggering, on the seismic resistance of buildings, on possible destruction and losses, on the necessary forces and resources.

At the first stage, when possible earthquake source triggering is expected, which may last for several years, it is necessary to determine as accurately as possible the coordinates, depth and power. For this purpose, historical data on earthquakes in the region and patterns of earthquake precursors, real monitoring data on seismic activity can be used.

In the second stage, which can last up to 2 months, it is important not only to organize rescue operations correctly and efficiently, but also to continue monitoring observations for timely assessment of the probability of a possible recurrence of a strong shock.

At the third stage - attenuation of the source zone, up to a year and more, when reconstruction works begin, it is also necessary to continue monitoring observations of seismic activity, seismic resistance of buildings and structures.

At all three stages of development and attenuation of seismic hazard and risk, it is required not to stop complex monitoring observations of seismic activity of the territory to ensure seismic safety of the population.

II. Methodology

The most dangerous and difficult to predict is the first stage of seismic event development. For proper planning of measures providing seismic safety of the population at the first stage it is necessary to determine as accurately as possible the coordinates of possible earthquake source, time and probability of its triggering, macroseismic field in case of possible earthquake source triggering taking into account tectonics, geology and relief of the territory, knowing the seismic resistance of buildings and structures to determine possible destruction, losses and risks.

The first stage of possible earthquake source preparation may last for years and may not always be realized by an earthquake, therefore at this stage it is important to have reliable predictive data or to have earthquake-proof buildings and structures. To determine the probability of possible earthquake source triggering by the manifestation of precursors it is proposed to apply expression (1), where the probability is defined as the difference of one minus the product of improbabilities of events by the manifestation of precursors according to the following dependence [7, 8].

$$P_z = 1 - \prod_{i=1}^{i=n} (1 - P_i) \quad (1)$$

Where,

P_z – triggering probability possible earthquake source

P_i – probability that at occurrence of the i -th precursor the triggering will take place possible earthquake source (Table 1).

If $P_z \geq 0.7$, it is assumed that the probability of triggering possible earthquake source is very high.

When the probability of possible earthquake source triggering is high (more than 0.7), knowing the possible earthquake source parameters (coordinates and power) and its triggering time, it is possible to calculate possible damage, losses and risks.

The mathematical expectation of losses is calculated using a geographic information system [9,10], which makes it possible to construct a macroseismic field taking into account the tectonics and geology of the area, to calculate possible damage and losses taking into account the proportion of buildings by type characterizing their seismic resistance and data on the population in settlements.

The individual risk of occupancy of people in damaged buildings in the considered seismically hazardous territory in the projected time interval, taking into account possible repeated seismic shocks, is proposed to be calculated according to the following formula:

$$Re_i(t) = P_z \times \sum_{i=1}^n m_i / (N_i \times T) \leq [Re_i] \quad (2)$$

Where,

P_z - probability of a main (repeated) strong seismic shock;

m_i – assumed losses of people in case of loss of bearing capacity of "ground-building" systems in the considered i -th element of the territory (building) after a repeated shock [4, 10, 11];

N_i – the number of people in the i -th element falling into the zone of dangerous seismic impact resulting in damage to buildings;

T – the period during which the main (repeated) seismic shock that causes damage to buildings will occur;

[Rei] - risk standard 10^{-5} [12]

Table 1: Probability of triggering a possible earthquake source when a certain precursor manifests itself (data obtained from long-term observations) [5,6,7,8]).

No	Type of precursor	Time of manifestation before the main shock	The regularity of the manifestation of the precursor	Main parameters of the precursor	Possible earthquake source parameters. Probability of triggering (Pi)
1	Geodynamic movements	1-7 days	regularly	Low-frequency rocking of the Earth's surface with the period up to 1.5 hours, amplitude up to 15 cm	0.8-0.95
2	Low-frequency noises	1-7 days	regularly	Low-frequency noise at 0.15 Hz and below	0.7-0.9
3	High-frequency noise	1-7 days	regularly	High-frequency noise with a frequency of more than 70 Hz	0.8-0.9
4	A sharp drop in atmospheric pressure (see example Fig. 3)	1-14 days Immediately before the earthquake (0.5 days) there is a quiescence	regularly	High-frequency noise with a frequency of more than 70 Hz	0.5-0.8
5	Lightning discharges and atmospheric manifestations	1-4 days There's a lull before the earthquake	Lightning discharges regularly	They are sampled along (parallel to) tectonic faults (see Figures 2,6,8)	0.5-0.7
6	Atmospheric luminescence	0,5-1 days	Not regularly	A certain area stands out brightly	0.7
7	A portrait of cloudiness	4 days		They are beaten off in the area of tectonic faults, have a special linear, striated character (see Fig.7)	0.5-0.7
8	Forshock activity	Observed	Not regularly	They are hammered in a specific zone or along tectonic faults (see Fig. 10).	More than 0.6

The mathematical expectation of population losses is calculated using the Extremum geographic information system (GIS).

Calculation of possible consequences from repeated strong shocks should be performed taking into account possible reduction of seismic resistance of buildings. At present, such procedure is not provided in GIS "Extremum". The method of dynamic tests [11, 13] is proposed to be used for operational assessment of the seismic resistance of buildings that have fallen into the zone of seismic impact of more than 6 points. Based on the results of dynamic tests, the database in GIS "Extremum" should be adjusted.

In GIS "Extremum", classification by seismic scales of ISC-64 is currently used to form a database on buildings, and type A (local materials), type B (masonry and block), type C (earthquake-resistant C7, C8 and C9) are distinguished. In the database on buildings, included in the geoinformation system for assessing the consequences of strong earthquakes in the territories, the share of buildings by types is presented in percent (see Table 2).



Fig. 1: An example of a mixed, dense development in Istanbul on hilly terrain.

Table 2: Example of filling in the database on development by type of buildings (based on data from 1999-2000, from the GIS "Extremum" database).

City name	A/ height, m	B/ height, m	C6/ height, m	C7/ height, m	C8/ height, m	C9/ height, m
Nalchik	0.2/3	0.21/6	0.2/15	0.39/3	0	0

As it can be seen from the example (see Table 2), in the considered city according to the data of 1999-2000 there is no building with seismic resistance C8 and C9, it is clear from the example that the database on seismic resistance requires its constant updating. The data on seismic resistance are linked to the seismic scale and give only discrete values of seismic resistance without taking into account operational wear, i.e. they do not reflect real data on seismic resistance of buildings. The Extremum GIS database needs to be corrected and can be considered for evaluation analysis. Adjustment of the database can be made either by decreasing or increasing the share of buildings by classes A, B, C6, C7, C8, C9. Or it is proposed to divide the city territory into separate area elements with prevailing seismic resistance (see Table 4).

To assess the technical condition, stiffness and earthquake resistance of buildings and structures, it is proposed to apply the "STRUNA" technology [11]

The essence of the method is based on the fact that through vibrations it is possible to assess the stiffness of the structure, and through stiffness it is possible to assess the technical condition and earthquake resistance of structures.

To evaluate the possible resonance between the ground and the structure, sensors are installed on the ground and the structure.

The stiffness deficit is estimated using the following relationships [4-8]:

$$\Delta_x = ([f_x]^2 - f_x^2) \times 100 / [f_x]^2, \tag{1}$$

$$\Delta_y = ([f_y]^2 - f_y^2) \times 100 / [f_y]^2, \tag{2}$$

$$\Delta_z = ([f_z]^2 - f_z^2) \times 100 / [f_z]^2, \tag{3}$$

where f_x, f_y, f_z – values of natural vibration frequencies of the structure;
 $[f_x], [f_y], [f_z]$ – normative values of natural vibration frequencies of the structure, derived from the project or by calculation;

$\Delta_x, \Delta_y, \Delta_z$ – stiffness deficit in % in axes X, Y, Z (see Table 3).

Based on the obtained data on the stiffness deficit, the technical condition of the structures and their seismic resistance are determined.

Table 3: Percentage of stiffness reduction (square of frequency of natural vibrations of the structure), depending on the category of technical condition

Type of construction	Percentage of relative reduction in stiffness of the structure under different conditions				
	Very Good	Good	Fair	Poor	Very Poor
With reinforced concrete frame	0–25	25–43	43–57	57–71,4	71,4–100
With metal frame	0–16.7	16.7–33	33–50	50–67	67–100
Brick	0–16.7	16.7–33	33–50	50–75	75–100
Wooden	0–20	20–27	27–40	40–67	67–100

Dynamic tests are proposed to be performed on typical elements of settlements with the same type of buildings. The GIS database should contain data on earthquake resistance (see Table 4) for each element of the structure.

Then the database in GIS "Extremum" is proposed in the following form (see Table 4)

Table 4: Example of the proposed form of the database on construction by types of buildings (based on 1999-2000 data from the GIS "Extremum" database).

City name	1-th element	2-th element	3-th element	4-th element	5-th element	6-th element	n
X	7.2	6	7,1	9	0	0			
Y									

The data in Table 4 will allow to lay down the real seismic resistance of building elements, obtained from the data of dynamic tests in points or accelerations.

III. Example of individual seismic risk assessment for the territory of Turkey

For estimation of probability of possible earthquake source triggering, let's consider an example of manifestation of precursors before strong earthquake in Turkey 06.02.23. Results of estimation of precursor activity are presented in Table 5.



Fig. 2: Glow before the earthquake in Turkey 06.02.23 (taken from Internet sources)

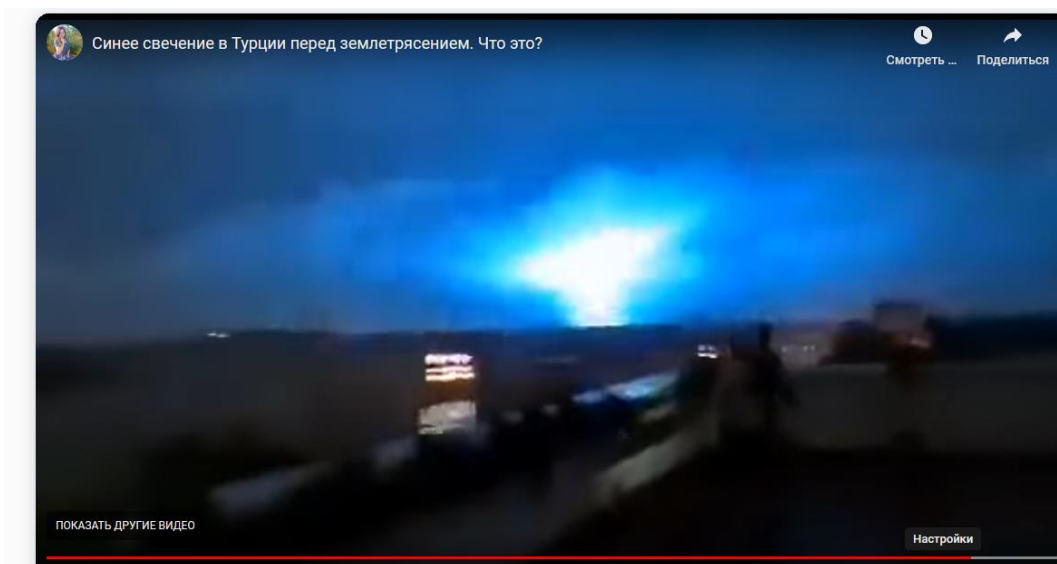


Fig. 3: Glow before the earthquake in Turkey 20.02.23 (taken from Internet sources)

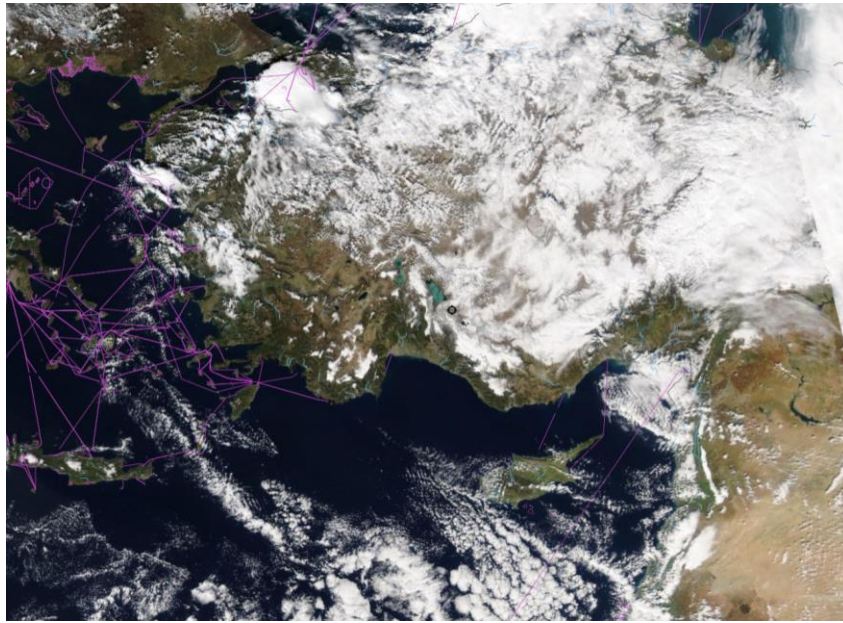


Fig. 4: Portrait of cloudiness 02.02.23 Suomi satellite, the cloudiness repels tectonic faults on the border of Syria and Turkey and from the island of Cyprus to Greece (according to Multimaps, taken from Internet sources). Cyprus to Greece (according to Multimaps, taken from internet sources).

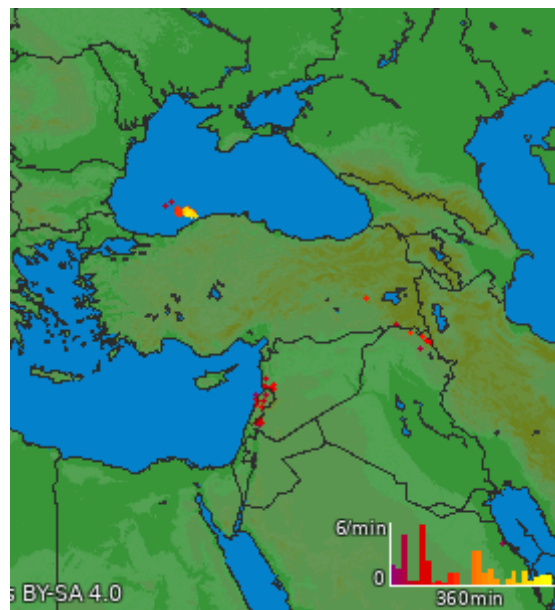


Fig. 5: Thunderstorm activity along the right tectonic fault 02.02.23 at the border of Turkey and Syria (taken from Internet sources)

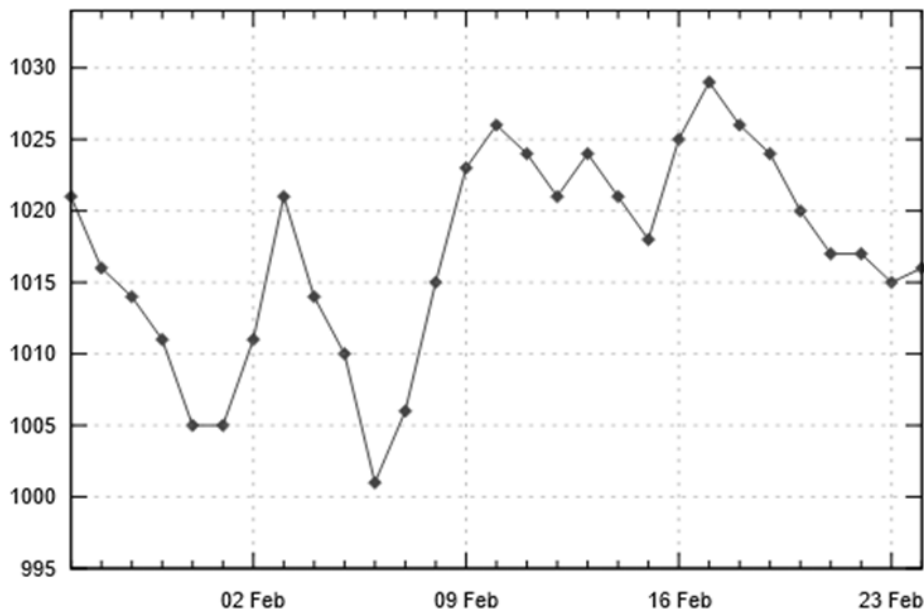


Fig. 6: Sharp drop of atmospheric pressure before the strong earthquake in Turkey on 06.02.23.



Fig. 7: Forshock activity in the period from 24.01.23 00:00 to 05.02.23 23:59 before the strong earthquake on 06.02.23 (from data of the US Geological Service).

At that time, the probability of triggering the main shock of the earthquake in Turkey could have been

$$P_z = 1 - \prod_{i=1}^n (1 - P_i) = 1 - (1-0,7)(1-0,7)(1-0,7)(1-0,5) = 0,9865$$

The probability of triggering an aftershock of the Turkish earthquake could have been

$$P_z = 1 - \prod_{i=1}^n (1 - P_i) = 1 - (1-0,7)(1-0,7)(1-0,7)(1-0,7) = 0,9919$$

Using data on tectonics, geology, coordinates and earthquake magnitude, data on earthquake resistance of the building with application of geoinformation model we will perform calculations

on estimation of possible damages and mathematical expectation of losses. The results of calculations are presented in Fig. 8.

Table 5: Time manifestation and parameters of precursors before earthquakes in Turkey 06.02.2023.

No	Type of precursor	Time of manifestation before the main shock	Main parameters of the precursor	Possible earthquake source parameters. Probability of triggering
1	A sharp drop in atmospheric pressure	One to six days before an earthquake, there's a lull	Abrupt 72-hour drop and rise of atmospheric pressure 25-26 hPa (see Fig. 6)	0,7-0,5
2	Lightning discharges and atmospheric manifestations	In four days. There's a lull before an earthquake	Tectonic faults were repelled (see Figures 2,3,5)	0,7
4	A portrait of cloudiness	In four days.	Tectonic faults were repelled (see Fig. 4)	0,7
5	Forshock activity	Observed	Tectonic faults were repelled (see Fig. 7)	More than 0.7

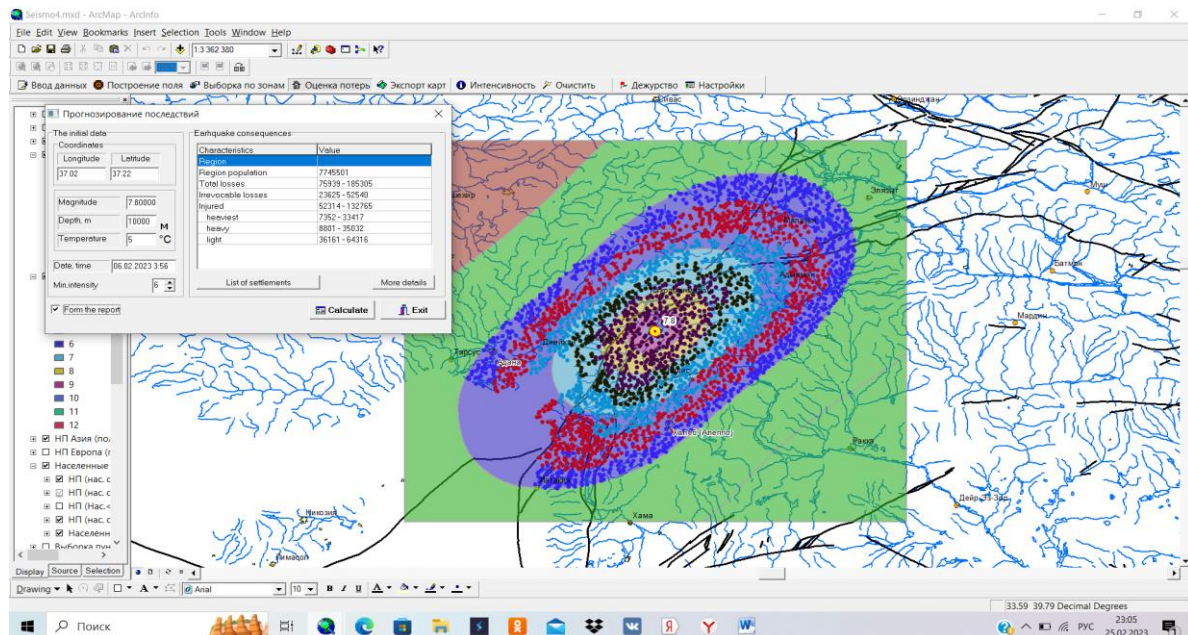


Fig. 8: Forecast of possible consequences from the strong aftershock in the Republic of Turkey, which occurred on 06.02.23.

Then, applying the formula (1) and (2) and the results of calculations on the model we estimate the risk for the population taking into account a possible strong aftershock, the risk for the population in the epicentral zone amounted to

$$Re_i(t) = 0,9919 \times \frac{52540}{7745501 \times 1} = 0,006728 = 6,728 \times 10^{-3}$$
, risk is significantly (almost 1000 times) higher than the norm 10^{-5} - 10^{-6} [13].

IV. Conclusions and recommendations

Application of the proposed technology for monitoring seismic hazard and individual seismic risk will make it possible to make timely decisions to ensure seismic safety of the population.

The basis for decision making should be:

Monitoring of seismic activity of the area to determine possible earthquake source and the probability of triggering;

Assessment of the earthquake resistance of buildings and updating of the building database;

Assessment of possible consequences if possible earthquake source is likely to be triggered;

Identification of areas with increased (more than 10^{-5} 1/year) individual risk to the population;

Timely planning of measures to reduce individual seismic risk for the population located in high-risk areas.

References

[1] Ismail Ibrahim, K.M.H., Ibrahim, T.E. Effect of historical earthquakes on pre-stressed anchor tie back diaphragm wall and on near-by building. *HBRC Journal*. 2013. 9(1). Pp. 60–67. DOI:10.1016/j.hbrj.2013.02.008.

[2] Hoveidae, N., Fathi, A., Karimzadeh, S. Seismic damage assessment of a historic masonry building under simulated scenario earthquakes: A case study for Arge-Tabriz. *Soil Dynamics and Earthquake Engineering*. 2021. 147. Pp. 106732. DOI:10.1016/j.soildyn.2021.106732.

[3] Saretta, Y., Sbrogiò, L., Valluzzi, M.R. Seismic response of masonry buildings in historical centres struck by the 2016 Central Italy earthquake. Calibration of a vulnerability model for strengthened conditions. *Construction and Building Materials*. 2021. 299. Pp. 123911. DOI:10.1016/j.conbuildmat.2021.123911.

[4] Stepinac, M., Lourenço, P.B., Atalić, J., Kišiček, T., Uroš, M., Baniček, M., Šavor Novak, M. Damage classification of residential buildings in historical downtown after the ML5.5 earthquake in Zagreb, Croatia in 2020. *International Journal of Disaster Risk Reduction*. 2021. 56. Pp. 102140. DOI:10.1016/j.ijdr.2021.102140.

[5] Verdum, G., Bersch, J.D., Guerra, F.L., Socoloski, R.F., Giordani, C., Zucchetti, L., Masuero, A.B. Mortar coating degradation in historical buildings facades from Rio Grande do Sul – Brazil. *Construction and Building Materials*. 2021. 310. Pp. 125221. DOI:10.1016/j.conbuildmat.2021.125221.

[6] Yasser, E.M., Rakha, T. A scoping review of non-destructive testing (NDT) techniques in building performance diagnostic inspections. *Construction and Building Materials*. 2020. 265. DOI:10.1016/j.conbuildmat.2020.120542.

[7] Jiménez, B., Saloustros, S., Pelà, L. Seismic vulnerability index method for hybrid timber-masonry structures. Numerical calibration and application to the city of Valparaíso, Chile. *Journal of Building Engineering*. 2021. 44. Pp. 103185. DOI:10.1016/J.JOBE.2021.103185.

[8] The Possibility of Vibrodinamic Data from Phone Accelerometers for the Rapid Assessment of the Technical Condition of Buildings and Structures Use / A. Savinov, G. Nigmatov, T. Nigmatov, R. Galliulun // *Proceedings of STCCE : International Scientific Conference on Socio-Technical Construction and Civil Engineering 2022: Lecture Notes in Civil Engineering, Kazan, April 21–29, 2022*. Vol. 291. - Switzerland: Springer Nature, 2022. - P. 371-379. – DOI 10.1007/978-3-031-14623-7_33. – EDN HJSTRH.

[9] Nigmatov G.M., Larionov V.I., Frolova N.I., Suchshev S.P. Complex Assessment of Seismic Hazard and Seismic Risk of Territories // *Proc. of the Eight Internat. Conf. on Soil Dynamics and Earthquake Eng.* Istanbul, Turkey, 1997 (a).

[10] Nigmatov G.M., Larionov V.I., Frolova N.I., Suchshev S.P., Ugarov A.N. GIS Application for Seismic Hazard and Risk Assessment of Urban Areas // *Proc. of the IASPEI Assembly*. Thessaloniki, Greece, 1997 (b).

[11] Savinov, A., Nigmatov, G., Nigmatov, T., Galliulun, R. The Possibility of Vibrodynamic Data from Phone Accelerometers for the Rapid Assessment of the Technical Condition of Buildings and Structures Use 2023. Pp. 371–379.

[12] Nigmatov, G., Akatev, V., Savinov, A., Nigmatov, T. Estimation of seismic resistance of buildings by the dynamic-geophysical method, taking into account the peculiarity of the interaction of the seismic wave with the “soil-construction” system. *Structural Mechanics and Analysis of Constructions*. 2018. 1. Pp. 24–30.

[13] The use of elastic oscillations of different wavelengths to evaluate the dynamic parameters of buildings and structures and assess the strength of materials of the building construction Savin S., Tsakalidis V. *COMPDYN 2015 - 5th ECCOMAS Thematic Conference on Computational Methods in Structural Dynamics and Earthquake Engineering*. 5. 2015. C. 706-720.

ASSESSMENT OF THE WATER BALANCE OF THE TERRITORY AND RIVERS WATER RESOURCES USING A NEW OPERATIONAL-INTERACTIVE METHOD

Rza Makhmudov¹, Vugar Aliyev², Movlud Teymurov¹, Emil Gafarov³

¹Institute of Geography of the Ministry of Science and Education, Azerbaijan

²AMIR Technical Services LLC, Azerbaijan

³Azerbaijan University of Architecture and Construction

rza_hidromet@mail.ru

prof.vugar.aliyev@gmail.com

movlud_teymurov@yahoo.com

emilqafarov@inbox.ru

Abstract

A new method (CWBM) is proposed for calculating the water balance of the territory and water resources of rivers. CWBM was developed on the basis of reliable scientific sources (satellite images, GIS-technologies, modern scientific approaches, advanced hydrological models). The following scientific innovations were achieved for the first time in the new method: 1. Considering the soil-water-air environment (SWA) as a single mechanism, the influence of complex flow-forming factors has been studied. 2. It was possible to obtain quantitative expression of the impact of each factor on water resources separately and together. 3. In the research process, time-space restrictions and dependence on observational data have been eliminated. 4. By carrying out 3-stage studies (past, present, future), it is possible to receive prompt and adequate responses to any changes and perform multi-scenario forecasting. 5. In any river basins with different physical-geographical conditions, it is possible to estimate both the total runoff separately and as a sum of the surface runoff and base flow. Comparison of the actual and calculated with CWBM method flow for 113 river basins of Azerbaijan shows that the error between them was up to 10% for 92 and 10-15% for 21 rivers.

Keywords: total runoff of rivers, CWBM, hybrid and synthesis methods, Counter-approach technology, analogue terrains

I. Introduction

In recent years, the impact of global climate and landscape changes on the formation and depletion of water resources has further complicated the problems associated with water. This problem is more pronounced in countries with limited inland water resources. Currently, there is no such socio-economic sphere in which it is possible to carry out without taking into account the quantitative and qualitative values of water resources. Population and economic growth rates in the world are quite high. At the same time, climate change and anthropogenic activities quickly affect the volume of water resources. This, in turn, is required the assessment of water resources in ways that allow for operative, interactive and more reliable results. In methodologies, operativity – includes the objectives of the study, not lagging behind the pace of development of the economy and the population, interactivity – assessment in terms of adequacy to changing factors. Conducting research using satellite imagery, GIS and other modern technologies are important features to ensure the reliability of the results obtained. Therefore, in recent years, in the world,

especially in countries such as the Republic of Azerbaijan, where there is a shortage of water resources, such methods are widely used. Such methods are often developed on the basis of a hybrid and synthesis of basic hydrologic methods in the world. Hybrid methods, which include the advantages of basic methods, have more advanced capabilities by eliminating their shortcomings [1, 2, 7, 8, 22, 23].

To estimate the water balance of the territory and rivers water resources, we have proposed a new method of CWBM (Complex Water Balance Method). The CWBM was created based on the advantages of leading hydrological methods widely used in the world, taking into account the specific physical and geographical features of Azerbaijan and as a result of our innovative scientific approaches.

II. Methods and materials

The study area covers the Karabakh region, located in the southwest of the Republic of Azerbaijan. The area of the investigated region is 13732 km². Satellite images of different years, a digital elevation model (DEM-Digital Elevation Model) and hydrometeorological observation data were used as the source materials for the research. Data on the landscape-soil fund were obtained on the basis of fragments of multispectral (hyperspectral) satellite images. Height, slope, and exposure measurements were determined using DTM, and river morphometric values were determined using ArcGIS Hydrology, Surface, Density, and other software.

Water balance methods are more reliable sources for estimating the water resources of rivers. It is known that the water balance reflects the distribution of atmospheric precipitation in various spheres (initial abstraction, surface runoff, infiltration, evapotranspiration, etc.). The advantages of the most popular water balance methods in the world were used as basic methods in the development of the CWBM. Among the basic methods, the Rational method is considered more effective – in terms of studying surface runoff; NRCS-CN – soils infiltration capacity and groundwater feeding of rivers; Ponce-Shetty and Lvovich methods – studying the theoretical foundations of water balance [4, 5, 10, 15, 16, 17, 18, 20].

The Rational method is considered one of the most important method for assessing the level of precipitation formation on surface runoff. The formula of the rational method (Rational Equation) is expressed as follows:

$$Q = ciA \quad (1)$$

Here Q –is the water discharge (unit-cubic feet), i –is the amount of precipitation (inch), A –is the area of the study area (acre), c –is the rational (surface) runoff coefficient.

To change to the unit of measure for water discharge to m³/sec we proposed a conversion factor ($k=0.0000314$), which formula was expressed as:

$$Q = k \times ciA \quad (2)$$

The rational coefficient is found on the basis of various types of landscape, hydrological soil groups (HSGs) and slope. Hydrological soil groups (HSGs) – depending on the granulometric composition of soils, their ability to form surface runoff and infiltration is reflected. The NRCS classification defines 12 soil granulometric codes and 4 HSGs (A, B, C, D). From group A to group D, there is a tendency to weaken infiltration and increase surface runoff [21].

In the methodology authored by Lvovich, the annual water balance of river basins is expressed by the concept of "total catchment wetting" (W) and is found by the following equation:

$$W = P - Q_s = U + E \quad (3)$$

Here W – is total catchment wetting; P – atmospheric precipitation; Q_s – surface runoff; U – baseflow; E – actual evapotranspiration from basins surface.

The Ponce-Shetty model is conceptually similar to Lvovich's methodology. According to this model, the total annual runoff of rivers is separated in two stages: fast flow and slow flow. Fast runoff is part of the precipitation that passes into direct surface runoff. The rest of the precipitation is stored as humidification in the basin (W -wetting):

$$P = Q_f + W \quad (4)$$

Stage 2 of the model represents the distribution of wetting (W) to other water balance elements, and this parameter itself is divided into two components:

$$W = Q_b + V \quad (5)$$

Here V – is the water returned to the atmosphere in the form of evaporation, Q^b – is the slow flow (baseflow), the mass of water that is a component of the underground feeding of rivers. It is called “slow” because the groundwater feeding of the river occurs gradually due to precipitation.

Thus, in the Ponce-Shetty model, the rivers total runoff (Q) is expressed as the sum of fast and slow flow, that is, surface runoff and baseflow:

$$Q = Q_f + Q_b \quad (6)$$

Runoff Curve Numbers (CN) used in the SCS-CN method are also indicators definition of the precipitation rate to runoff formation. In this method, the conversion rates of precipitation to runoff are expressed by different runoff curve numbers (CN) at 3 humidity levels (dry, normal, saturated). Unlike the Rational method, an important advantage of the SCS-CN method is that, with the possibilities of determining surface runoff, it simultaneously reflects the infiltration characteristics of the area, especially in terms of assessing the degree of soil moisture. This feature is especially important in content of estimating the share of underground feeding of rivers (baseflow).

In SCS-CN method uses several important components to determine the water balance of an area as: 1) Hydrological losses (L) – is the fraction of precipitation that does not participate in the formation of surface runoff. 2) Maximum soil retention (S) – is maximum water retention capacity of soils in the concrete physical and geographical conditions of the territory. 3) Initial abstraction (I_a) – is part of precipitation spent on various areas before surface runoff formation. 4) Actual soil moisture (F) – is the actual soil water retention under the existing geographical conditions of the area.

The SWA environment consists of hundreds of components. These components are divided into soil, air and water components separately. In terms of their role in the runoff formation and participation in the water balance, it is possible to divide the SWA components into 3 groups:

1) The components that make up the surface cover of the territory. These include LULC (Land-use & Land cover) and HSG (Hydrological soil groups). LULC – is the general description of the surface area, or the sum of natural and human landscapes (vegetation, crops, settlements, bedlands, water bodies, etc.) [3, 9, 14, 19].

2) Morphometric values. It includes the elevation of the area, slope of the terrain, exposure (aspect) of the slopes, basin area, horizontal and vertical fragmentation of the surface, density of the river network, etc. [12].

3) Climatic and humidity factors. These include atmospheric precipitation, air temperature, actual and potential evaporation, humidity coefficient, initial abstraction, maximum soil retention, actual soil moisture, hydrological losses, etc.

The study comprehensively takes into account the majority of factors that play a role in the runoff-formation, and changes in water resources. Both the influence of the majority of components is taken into account, and the assessment is carried out in a complex manner. Therefore, the new hydrologic method was named "Complex water balance method" (CWBM).

As a result of combining the features of the leading basic water balance methods and introducing innovative proposals into the CWBM method, a number of additional advantages have been obtained:

1. In the process of research, it is possible to take into account the influence of most runoff-forming factors.

2. Whole process of research can be carried out without physical contact only based on multispectral (hyperspectral) satellite images of the area.

3. There is no dependence on observational data, and space-time restrictions.

4. CWBM combines 4 main principles of modern scientific studies (applicability, operativity, interactivity, predictability).

5. Restoration of indicators of any SWA component without observational data is possible with high accuracy.
6. Important time-related challenges in the assessment have been eliminated and an estimate of the water balance has been achieved in any time interval (in rainfall event, short-term and long-term periods).

III. The sequence of the study fulfillment

The essence of the new method (CWBM) is the principle of assessing the water balance and water resources using runoff coefficients that include the influence of complex runoff-forming factors. In most modern basic methods of water balance, studies are carried out mainly for local areas under conditions of high humidity or stormwater runoff at the moment of rainfall. On the other hand, total runoff of rivers is calculated unilaterally. That is, surface runoff and baseflow are studied separately, and this does not allow simultaneously estimating the total volume of river runoff. Thanks to the CWBM, a number of shortcomings of existing hydrological methods have been eliminated. As a result, it is possible to assess the total runoff of rivers both directly from the coefficients reflecting the total runoff, and by estimating the surface and underground feeding separately and summing them up. Another important advantage obtained is that there are no restrictions on the size of the study areas and time period.

Runoff formation is a very complex process. Until now, due to the influence of a number of factors, the formation of runoff and the assessment of water resources did not allow obtaining reliable accurate results. At present, scientific achievements have created conditions for a deeper analysis of runoff formation and the atmospheric-runoff process. Thus, as a result of simultaneous and comprehensive consideration of the influence of most factors, it was found that there are very important patterns in the distribution of runoff coefficients. Runoff coefficients were fully analyzed by applying multiple software for calculation, comparison and probabilistic analysis in GIS. In the processing, the influence of complex factors and various physical and geographical situations was taken into account, multidimensional options were checked, and the most reliable runoff coefficients with corrections were adopted. The results of obtained runoff coefficients were verified both in the ArcGIS program in the form of a trend in 100% scales, and in multilinear regression equations with a high correlation coefficient, and graphical relationships, and some by calibration.

The process of correction of runoff coefficients is carried out according to following algorithm:

1. Daily long-term observational data on climate and runoff of hydrometeorological stations located in river basins with different physical and geographical conditions were collected.
2. Data on other complex factors impacting the runoff in these river basins were obtained from satellite images.
3. The available data of hydrometeorological observations and indicators of other runoff-forming factors are collected and processed jointly in the GIS database.
4. Based on observations and space data, the distribution of factual runoff coefficients and data of components influencing it over river basins are comprehensively investigated.
5. Possible situations are considered, on the basis of the combined impact of complex climatic, landscape and other factors, and runoff coefficients are found for each different situation.
6. The data of runoff-forming components corresponding to the obtained runoff coefficients are determined, the same (or close intervals) coefficients are grouped and corrected.
7. The possibility of applying the obtained correction coefficients to analogues terrains without observational data is checked and the most reliable results are selected.

One of the important advantages of the CWBM is the possibility of assessing the water balance in the territories without observational data. For this purpose, flow-forming factors are obtained in different ways:

a) Most of the factors can be obtained directly from satellite imagery. These include landscapes, land-use, soil cover, granulometric composition of soils, HSGs, horizontal and vertical fragmentation, aspects, elevation, slope, basin area, river network density, humidity level of area, etc.

b) Some of the climate and humidity quantities are obtained indirectly ways. In this case, the relationship of climate quantities with known components is taken as a basis. For this purpose, various components that are more sensitive to changes in climate quantities are applied.

To restore climatic factors in the unobserved territories, a number of traditional and modern methods are used. Among the traditional methods, preference was given mainly to methods such as Graphic relationship, Interpolation and Analogy; and from modern methods to Counter-approach technology and NDIs (Normalized difference indices).

Counter-approach technology (CAT) is based on the fact that if the majority of factors are known, unknown values are restored from the database of available factors. In other words, in the method of CAT, the research process is carried out from the end to the beginning. A suitable place and time for comparison is selected, the influence of factors is verified individually or in combination.

Against the background of climate change, the most serious changes are felt in the humidity level of the territory, landscape, soil types and vegetation density. It was determined that, there is a very high correlation relationship between the quantitative changes of these factors and the values of climatic parameters. As a result, using different NDIs and CAT, it was possible to restore climatic data corresponding to different indicators of soil-vegetation cover and humidity level of the territory.

Another important condition for conducting research in unobserved areas is the selection of analogue terrains with based on actual data. When choosing a analogue locations, a high degree of similarity (sometimes 100%) was achieved. This is due to taking into account complex runoff-forming factors. The ArcGIS Select by Attributes software was used to select analogue terrains, and Weighted Overlay (Fuzzy) Influence was used to determine the level of compatibility.

For example, Fig.1 is shown analogue terrains of river basins with different physical and geographical conditions, such as medium dense forests (50-75%), average height (1000-1200 m), slope degree (>15%), hydrological soil group (C), high humidity level ($R > 0.85$), precipitation (700-750 mm), aspect (north-east).

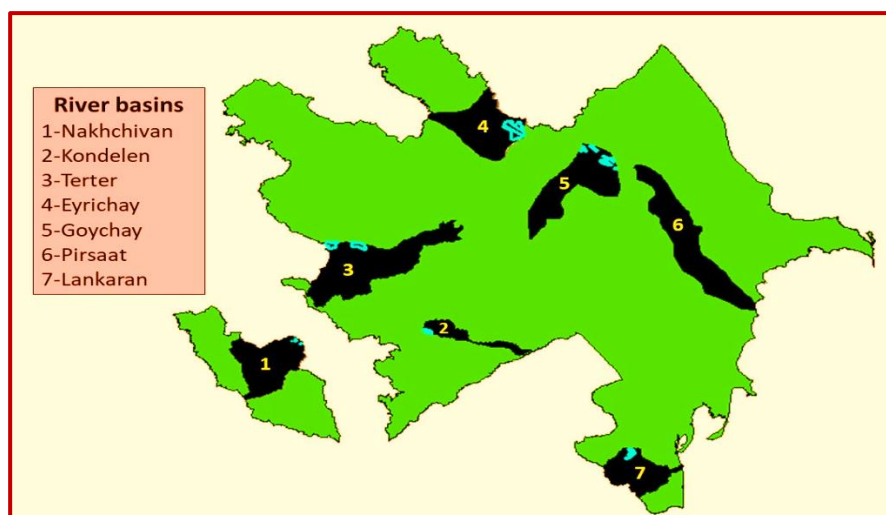


Fig. 1: Selection of analogue terrains in river basins with different natural conditions

As can be seen from the figure, in the Pirsaat basin (6 in the figure) no analogue areas to other river basins were found under these conditions. Therefore, if necessary, an analogy is made with other conditions and within smaller areas.

The approbation of the SWBM method has been highly justified. Comparison of actual runoff values and calculated with SWBM for 113 river basins of Azerbaijan with different natural conditions and sizes shows that the error between them was up to 10% for 92 basins and 10-15% in the rest. These results show that the SWBM method has a very high reliability, and it is considered reasonable to apply it to areas without observational data.

In the CWBM method, the influence of components on runoff is assessed in a complex way, both separately and together. When determining runoff coefficients, not only the factors themselves are necessary, but also their intraspecific diversity, different quantitative indicators. For example, the density of vegetation, soil moisture level, population settlement rate, various gradations of slopes and heights, aspects, each different values of the climate-humidity components were also extracted. Every other situation appears as a new runoff coefficient. The multiplicity of runoff coefficients is due to taking into account complex runoff-forming factors and each specific situation. To facilitate the use of the method, runoff factors are given based on more important variable factors. These factors include 5 components and their variable values: precipitation, LULC (Land-use & Land cover), HSG (hydrological soil groups), slope, moisture level of the area (coefficient humidity). Thus, in determining the total runoff factor, each type of LULC is taken into account along with their vegetation density; each different rainfall amount, 3 degrees of slope (<6, 6-10, >10%); HSG into 4 groups (A, B, C, D) and humidity of the territory into 3 levels (low, medium, high). Other relative stable runoff-forming coefficients were mainly used to compare basins, to identify analogue terrains, to assess the ratio of components relationships, to select moisture level, and for other purposes.

As an example, Table 1 presents the total runoff coefficients for some LULC types for average vegetation densities (50-75 %), with a moderate humidity level (R=0.45-0.80), according to the HSG "B" and 3 degrees of slope.

Table 1: Changes of total runoff coefficients for different LULC types

LULC (Land-use & Land cover)	HSG (Hydrologic Soil Groupe) – B		
	Humidity level, average		
	Slope degree, %		
	≤ 6	6 - 10	≥ 10
Dense forests and gardens	0.13	0.14	0.16
Subalpine and alpine meadows	0.34	0.38	0.43
Rare forests (forest-meadow landscapes)	0.24	0.29	0.34
Arid forests and shrubs	0.08	0.095	0.125
Subnival and nival areas	0.49	0.52	0.56
Cultivated areas	0.05	0.075	0.10
Residential areas (settlement-25-30%)	0.065	0.08	0.11
Residential areas (settlement-60-65%)	0.28	0.36	0.41
Residential areas (settlement-85-90%)	0.76	0.79	0.81
Streets (asphalt paved)	0.80	0.82	0.84
Pastures	0.23	0.34	0.45
Water bodies (lakes and reservoirs)	0.32	0.27	0.23
Dry steppes and semi-deserts	0.055	0.075	0.12
Impervious areas and bedlends	0.66	0.68	0.70

The water balance and water resources of the rivers were estimated on the basis of the runoff coefficients with the obtained average values of their distribution over the territories.

The study in the presented article covers the years 1998-2021. The studies used hydrometeorological data and fragments of satellite images relating to this period. According to

2021 data, the results of some runoff factors obtained using space information and ArcGIS programs are shown in Fig.2.

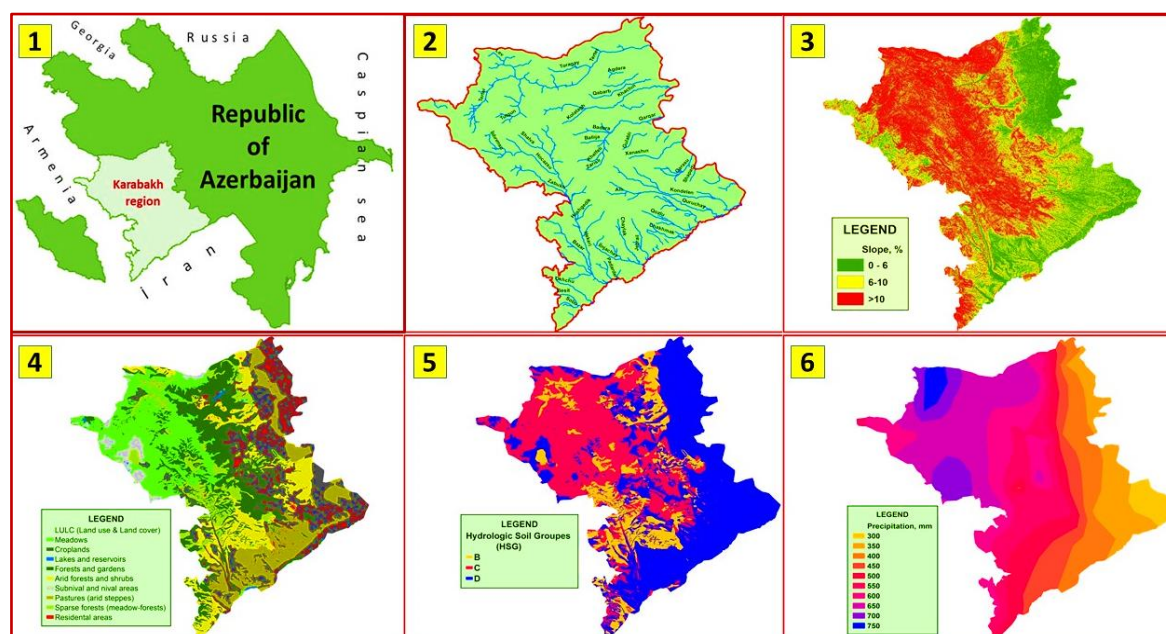


Fig. 2: 1–Study area (Karabakh region). 2–River network. 3–Elevation. 4–LULC (Land-use & Land cover). 5–HSGs (Hydrological soil groups). 6–Precipitation.

Below presented the results of the most important runoff-forming factors of the study area obtained as a result of processing satellite imagery and GIS technologies.

1. Some types of landscape (urbanization, bare soils, semi-deserts and dry steppes, subnival-nival areas, forest-shrub) seriously affect the total flow of rivers by increasing the share of surface runoff, while others (forests, lakes, meadows, arable lands) increase the share of groundwater runoff (baseflow). The most important factors in the formation of surface runoff are the humidity level and slope degree at the time of precipitation; and in baseflow, vegetation density, hydrological soil groups and soil moisture rate. Table 2 shows the changes in the main LULC types in the region for the studied period.

Table 2: Changes of main LULC types for the period 1998-2021 (MD-meadows, CA-cultivated areas, WB-water bodies, DS-dry steppes, FR-forests, FS-forest-shrubs, SN-subnival-nival, MF-meadow-forests, ST-settlements)

Years	LULC (Land-use & Land cover), км ²								
	MD	CA	WB	DS	FR	FS	SN	MF	ST
1998	2871	3255	42.58	1456	3104	1428	262.4	959	357.1
2021	2486	3571	37.08	1662	2623	1648	324.2	1015	368.1
Difference, %	-13.4	+8.85	-12.9	+12.4	-15.5	+13.3	+19.1	+5.52	+2.98

2. Against the background of climatic changes, especially with an increase in temperature, the humidity level of the area decreases [6, 11, 13]. This, in turn, affects the vegetation density and the runoff coefficients. Compared to 1998, the area of bare soils in 2021 increased by 1099.5 км² (30.3%), the area with a weak vegetation cover by 467.9 км² (9.84%). The area of plots with medium density of vegetation decreased by 905.5 км² (19.3%), and areas with high density by 658.9 км² (28.9%).

3. During the specified period, as a result of processing the NDWI (Normalized difference water indices), a decrease in the area of closed water bodies (lakes and reservoirs) by 12.9% was noted.

4. The distribution of the hydrological soil group (HSGs) over the region showed that the areas with group "B" are 15.1%, with "C" – 36.4%, with "D" – 48.5% in 2021. These indicators were equal to 12.8, 41.3 and 45.9% in 1998 respectively.

5. Vertical fragmentation of the territory is an important parameter for calculating rivers fall and surface runoff; horizontal fragmentation to estimate river network density and base flow. The total length of valleys with a length of more than 20 m area was 33067 km, the density of the river network was 2.02 km/km². These values for valleys longer than 50, 100 and 200 m are 11,362 km and 0.74 km/km²; 2928 km and 0.21 km/km²; 768 km and 0.054 km/km² respectively.

Vegetation density	1998.07.22.		2021.08.06.	
	Area		Area	
	км ²	%	км ²	%
Water bodies	42.6	0.31	37.1	0.27
Bare soils	2526.8	18.4	3626.3	26.4
Sparse vegetation	4284.7	31.2	4752.6	34.6
Medium Vegetation	4682.9	34.1	3777.4	27.5
Dense vegetation	2197.3	16.0	1538.4	11.2

6. The maximum height of the study area is 3696 m, the minimum height is 49 m, the average height is 1127.2 m. The average slope of the terrain turned out to be 13.4%. Plots with a slope of less than 6% accounted for 30.4%, with a slope of 6-10% –31.6%, more than 10% –38.0%.

7. The greatest exposure of slopes throughout the entire territory of the study region is oriented to the east (15.4%) and north-west (14.2%). The least oriented parts are flat surfaces (0.13%) and north-east (9.46%).

8. During 1998-2021 there have been serious changes in climatic factors, the humidity level has significantly decreased. Analysis of the moisture (NDMI) and drought (NDDI) indices of the study area also showed a decrease of 5.6% in areas with high humidity, but an increase of 8.4% in areas with low humidity.

IV. Results

Table 3 shows a comparison of the elements of the water balance and the volumes of water resources received for the Karabakh region as a result of staged studies for 1998-2021.

Table 3: Comparison of changes in the water balance components and water resources for 1998-2021

Components of the water balance		1998	2021
1	Atmospheric precipitation, P, mm	572.0	547.3
2	Air temperature, t, C°	8.28	8.51
3	Potential evaporation, M, mm	801.6	829.2
4	Factual evaporation, E, mm	415.2	422.7
5	Humidity coefficient, R	0.71	0.66
6	Maximum soil water retention, S, mm	1162.8	1189.7
7	Initial abstraction, I _a , mm	312.8	330.7
8	Actual soil moisture, F, mm	196.3	216.6
9	Hydrologic losses, L, mm	494.8	478.5
10	Rational runoff coefficient, c	0.3025	0.2904
11	Average runoff curve number (CN)	68.6	69.7
12	Total runoff, Q _t , mm	157.92	143.65
13	Surface runoff, %	48.9	47.9
14	Baseflow, %	51.1	52.1
15	River discharge, m ³ /sec	67.53	57.28
16	Water resources, million m ³	2.127	1.804

Water resources of the Karabakh region using of the CWBM, were estimated at 2.127 km³ in 1998 and 1.804 km³ in 2021. In total, over the specified period, water resources decreased by 15.2%. It was determined that out of this 7.04% decrease in water resources in 1998-2021 accounts for climatic, and 8.16% - for the role of human activities and other factors.

According to assessment, the average total runoff coefficient of the Karabakh rivers in the period up to 2021 was equal to 0.2625; that is, 73.75% of precipitation did not participate in the runoff formation. The share of surface runoff was 47.9%, and baseflow – 51.2%. The level of direct surface runoff of falling rainfall was only 12.6%, and in the remaining 87.4% part of the rainfall was spent on other areas of the water balance (initial abstraction, infiltration, evapotranspiration, etc.).

References

- [1] Amir Aieb, et. al. A hybrid water balance machine learning model to estimate inter-annual rainfall-runoff. 2022. *Sensors* 22 (9). 3241. <https://www.mdpi.com/1424-8220/22/9/3241>
- [2] Atie Tri Juniati, et al. Estimation of potential water availability and water resources carrying capacity for Bogor City spatial plan. *Journal of Geography of Tropical Environments*. 2021. Vol. 5: No. 1, Article 4. <https://sisdam.univpancasila.ac.id/uploads/repository/lampiran/DokumenLampiran-28082021221421.pdf>
- [3] Christine A. Rumsey. Regional scale estimates of baseflow and factors influencing baseflow in the Upper Colorado River Basin. 2015. <https://www.sciencedirect.com/science/article/pii/S2214581815000373>
- [4] Dana Ariel Lapides, et al. Implications of distinct methodological interpretations and runoff coefficient usage for Rational method predictions. *Journal of the American Water Resources Association*. 2021. Vol.57, Issue 6, pp. 859-874. <https://onlinelibrary.wiley.com/doi/10.1111/1752-1688.12949>.
- [5] David B. Thompson. The Rational Method. Civil Engineering Department Texas Tech University Draft. 2006. <https://pdf4pro.com/amp/view/the-rational-method-david-b-thompson-43d5.html>
- [6] Endalkachew Abebe, Asfaw Kebede. Assessment of climate change impacts on the water resources of Megech river catchment, Abbay Basin, Ethiopia. *Open Journal of Modern Hydrology*. 2017. <https://www.scirp.org/journal/journalarticles.aspx?journalid=739>.
- [7] Firas Alazem. Evaluation of SCS curve number and rational equation methods for the determination of surface runoff using GIS and remote sensing - A case of South Saudi Arabia. 2013. <https://www.hilarispublisher.com/conference-abstracts-files/2157-7587-S1.008-010.pdf>
- [8] Chandramohan K., R.Vijaya. Hydrologic Computations of SCS-CN, Rational, Area velocity and Tc Methods for Quantifying the Forest Surface Water Runoff - A case study in Sirumalai hill environs of Sathiyar Reservoir, Madurai, Tamil Nadu, India. 2017. <https://www.irjet.net/archives/V4/i4/IRJET-V4I4133.pdf>
- [9] Koronkevich N.I., Melnik K.S. Impact of urbanized landscapes on the river flow in Europe. *Izvestiya Rossiyskoi Akademii Nauk. Seriya Geograficheskaya*. 2019; (3):78-87. <https://doi.org/10.31857/S2587-55662019378-87>
- [10] Lvovich M.I., Sokolov A.A. Transformation of the hydrological regime and water balance of the territory. *Man and the natural environment. Journal No.7, 1971. p.72.* http://www.cawater-info.net/bk/water_land_resources_use/russian_ver/pdf/lvovich-sokolov.pdf
- [11] Makhmudov R.N. Regional climatic changes in Azerbaijan and its impact on hydrometeorological conditions. *Slovak international scientific journal*. 2022 (N-63), pp.48-55. <https://zenodo.org/record/6535054>.

- [12] Makhmudov R.N., Aliyev V.A., et al. Morphometric and anthropogenic factors of flood risk in the Lower Kura. // *Water Resources*, 2017, v.44, N 2, pp.192-195. ISSN 0097-8078. <https://link.springer.com/article/10.1134/S0097807817020075>
- [13] Mammadov R.M., Teymurov M.A. Assessment of water resources and risk of water losses due to climate changes and human activities. *The Scientific Heritage Journal*. Budapest, Hungary. 2019. <http://www.scientific-heritage.com/wp-content/uploads/2020/09/VOL-3-No-34-34-2019.pdf>.
- [14] Mohamed Abu-Hashima, et al. Identification of potential soil water retention using hydric numerical model at arid regions by land-use changes. 2015. <http://dx.doi.org/10.1016/j.iswcr.2015.10.005>.
- [15] Murugesu Sivapalan, Yaeger M.A. A functional model of watershed-scale annual water balance partitioning: Lvovich, Ponce and Shetty revisited. *Water Resources Research*. 2011. Volume 47, Issue 2. <https://agupubs.onlinelibrary.wiley.com/doi/full/10.1029/2010WR009568/>
- [16] Narendra J. Shrimali. Surface runoff estimation by SCS Curve Number method using GIS for Rupen-Khan watershed. *Indian Water Resour. Soc.*, 2016. Vol. 36, No. 4. <http://www.iwrs.org.in/journal/oct2016/1oct.pdf>
- [17] Ponce V.M. & Shetty A.V. A conceptual model of catchment water balance. Formulation and calibration. *Hydrology*, 1995, pp. 27-40. Online version 2016. http://uon.sdsu.edu/a_conceptual_model_of_catchment_water_balance_a.html
- [18] Sebastian J. Gnann, et.al. Is There a Baseflow Budyko Curve? *Water Resources Research*. 2019, 55 (4). <https://agupubs.onlinelibrary.wiley.com/doi/pdf/10.1029/2018WR024464/>
- [19] Teymurov M.A. Assessment of soil-vegetation cover and water resources on the basis of modern scientific innovation. *Scientific advances and innovative approaches. III International Scientific Conference*. 2023. Tokyo. Japan, pp. 28-32. <https://conference-w.com/wp-content/uploads/2023/02/JAP.T-2324022023.pdf>
- [20] UN FAO Penman-Monteith method. Reference evapotranspiration estimates. *FAO Irrigation and drainage paper No.56*. Rome, 1998. <http://www.climasouth.eu/sites/default/files/FAO%2056.pdf>
- [21] United States Department of Agriculture. Natural Resources Conservation Service. Part 630. *Hydrology National Engineering Handbook*. Chapter 7. Hydrologic Soil Groups. <https://directives.sc.egov.usda.gov/OpenNonWebContent.aspx?content=22526.wba>
- [22] Wei Mao, et al. An efficient soil water balance model based on hybrid numerical and statistical methods. 2018. <https://www.sciencedirect.com/science/article/abs/pii/S0022169418301562>
- [23] Wang X., Liu T., Yang W. Development of a robust runoff-prediction model by fusing the Rational Equation and a modified SCS-CN method. *Hydrological Sciences Journal*. 2012. <https://www.tandfonline.com/doi/full/10.1080/02626667.2012.701305>.

CONSTRUCTION OF A MULTI-CONNECTED CONTROL SYSTEM FOR SAFE COKE PRODUCTION

Aygun Safarova, Elchin Melikov, Tamella Magerramova

•

Azerbaijan State Oil and Industry University
aygsafa@rambler.ru , elchin03@mail.ru , tamellatm@gmail.com

Abstract

Efficient processing of crude oil in the oil refining industry develops the economy. To improve the oil products quality and increase its productivity, it is necessary to use minimal energy consumption. The release of harmful substances into the environment during technological processes of production has a certain negative impact on the ecological situation. The risks that may arise from all waste types in production objects are identified and controlled. According to the oil company's policy, reducing the impact of waste on the environment determines its recycling. In the technological processes course, environmental protection and safety personnel constantly monitor installation for gas safety, inspect the air and toxic environment, and ensure gas safety at work. When the raw material is heated to the required temperature in the furnace, the gas fuel supplied to the furnace creates a fire hazard. Technically, oil products coking makes it possible to cost-effectively and expediently increase and improve oil refining.

Keywords: technological process, coking process, oil products, coke, control process

I. Introduction

Efficient processing of raw oil in the oil refining industry develops the economy. To improve the quality of oil products and increase its productivity, it is necessary to use minimal energy consumption.

The release of harmful substances into the environment during technological processes of production has a certain negative impact on the ecological situation. The risks that may arise from all waste types in production objects are promptly identified and controlled. Thanks to the efficient crude oil processing, the impact of waste on the environment as a whole is reduced.

During the technological process, environmental protection and safety personnel constantly monitor oil installation (technological apparatuses) for gas safety at the object, inspect the air and toxic environment, thereby ensuring gas safety at work. When the raw material is heated to a certain temperature in the kiln, the fuel gas supplied to the kiln may create a fire hazard [1-7].

An emergency situations analysis in explosive and fire hazardous industries showed that a tube furnace is one of the most dangerous objects with increased risk parameters compared to other technological apparatuses. In addition, accidents at tube furnaces are a source of equipment ignition and explosion located in the immediate vicinity of the furnace. Therefore, it is currently relevant, on the basis of approved regulatory documents and acts in the industrial safety field, to create and improve the implemented automated process control systems that operate at risk and in explosive and chemically hazardous industries, which include objects of oil production, transport, oil refining and gas, chemicals and petrochemicals [8-18].

Currently, the oil refinery uses: an oil pretreatment installation, a catalytic cracking installation, a catalytic reforming installation, modern installations for the production of oil coke and gas fraction.

The main research object is the technological process of obtaining oil coke. At the same time, cascade and multi-connected automatic systems are mainly used to control the regime parameters. In the process of obtaining coke, the installation for the gradual coking of heavy oil products in unheated chambers is designed to produce electrode coke. In addition to coke, the installation receives dry gas, a stable liquefied gas head, coke oven gasoline, coke oven light gas oil (component of domestic heating oil) and coke oven heavy gas oil (boiler fuel component). The installation has two streams in the coke chamber section and one stream in the distillation section.

The gradual coking installation operates continuously by supplying raw materials and intermittently by discharging coke. During the coking process, technological apparatuses are connected to each other in series, in parallel and mixed. The pressure of 0,6 MPa and the temperature of 450÷500 °C are maintained in the coke chambers. As a result of the reactions taking place in the technological apparatus under study, from liquid and gaseous decomposition products, after intermediate compounds, the ready product coke is obtained. More deeply liquefied products are formed during the continuation of hydrocarbon condensation processes.

II. Investigation of the technological process for obtaining petroleum coke

Characteristics of products entering and receiving at the installation under study are given in Table 1. Let us consider a brief explanation of the technological process for obtaining oil coke. Installation for gradual coking of heavy oil products in unheated chambers type 21-10/5 is designed to produce electrode coke. In addition to coke, the unit receives dry gas, stable liquefied gas "head", stable gasoline, light gas oil (a component of domestic heating oil) and heavy gas oil (a component of boiler fuel). The device operates continuously due to the supply of raw materials and periodically (cyclically) due to the discharge of coke.

The process of coking heavy oil products is carried out at a gradual coking installation. The raw material (tar) is supplied for installation from the tanks of the commodity park. Furnace S-303, designed for heating raw materials, is a vertical-flame furnace type GS1650/17, two-stream, serpentine tubular. The temperature at the inlet to the furnace is 170÷190 °C, at the outlet 280÷360 °C, the maximum pressure in the pipes is 2,5 MPa. At the exit from the S-303 furnace, the heated raw material is combined into one stream and enters the K-301 column. The supply of the raw material part to the plate of the 1st stage is designed to regulate the recirculation ratio. The gas fuel pressure in the S-303 furnace is controlled so that when the pressure drops below 0,01 kgf/sm², the shutter closes and the S-303 furnace is turned off.

The pressure in the upper part of the K-301 column is adjustable. The level in the middle part of the column is controlled by a valve located in line to the evaporator, the temperature in the middle part is controlled by the reflux returning from the evaporator and the flow is controlled. The level and temperature in the lower part of the column are regulated, the flow rate is controlled. In both cases above, there is a cascading relationship between temperature and consumption, and level and consumption. The cubic column product is sent to the S-301 furnace for reheating. Here, the intermediate product is reheated and fed into the R-301/1,2 reactors. At this time, the temperature is monitored and signaled. The pressure inside R-301/1,2 reactors is controlled. Extraction of the resulting coke is carried out with water, and the pressure of the high-pressure washing water supplied to the reactors is regulated.

In furnaces, when heated vapors of light or heavy gas oil (coolant) and a mixture of secondary raw materials enter the coke chambers, as a coke formation reactions result, coke

accumulates in the chambers, and the coking products vapors are fed under the plate of the 1st stage of the bottom for the rectification column K-301. Here the consumption is controlled and the temperature is regulated. There is a cascading relationship between consumption and temperature. At this time, the second chamber is being prepared for operation, freed from coke, checked for tightness and heated to 100 °C with steam. The electric shutters in the helmet tube of the chamber being prepared for operation are gradually opened, the chamber is heated by blowing vapors from the working chamber from top to bottom into the K-310 scrubber, and the pressure in the chamber is equalized with the pressure of the working chamber.

Table 1: Characteristics of products entering and receiving at the installation

№	Name	% mass	min ton/year
Enter:			
1	Tar - is obtained from low-sulfur Azerbaijani oils	79,0	1053,0
2	Heavy phlegm - obtained at a catalytic cracking installation at a temperature of more than 420 °C	21,0	280,0
Total:		100,0	1333,0
Receive:			
1	Dry gas	6,1	81,3
2	Stable liquefied gas head	2,4	32,0
3	Coke oven gasoline	14,1	188,0
4	Coke oven light gas oil, fraction 180÷300 °C fraksiya	43,4	578,5
5	Coke oven heavy gas oil, fraction above 300 °C	9,4	125,3
6	Coke	22,8	303,9
7	Technological losses	1,8	24,0
Total:		100,0	1333,0

At a chamber heating temperature of 160÷220 °C, the purge vapors are sent to the K-301 column and connected to the K-310 scrubber. The chamber filled with coke is separated from the feed stream. To do this, a valve opens at the entrance to the chamber, and the fourway valve turns towards this chamber. This process takes 40÷60 minutes. The inlet lines of the coke chamber are purged with steam, the inlet valves are closed. To remove volatile hydrocarbons from the coke pores and cool the coke, heated or hot steam is supplied to the isolated chamber at a 4 ton/h rate, and the chamber is blown into the K-301 column.

When the temperature of the reactor top (coke chamber) drops to 340÷360 °C, its blowing with water vapor is gradually directed towards the K-310 scrubber for 40÷60 minutes and blowing is continued for 6÷7 hours, increasing the flow rate of water vapor to 10 ton/h according to the schedule. After completion of the purge, the supply of water vapor to the reactor is stopped and cooling water is introduced within 6 hours.

The consumption of water into the reactor is controlled according to the schedule. When the temperature at the top of the reactor drops to 80÷90 °C, the top cover is opened, cooling with water is stopped, and water is drained from the reactor. After draining the water from the coke chamber, open its lower covers, install the telescope and start cutting the coke.

Coke cutting is carried out within 5-6 hours with water supply under pressure of 18÷23 MPa (180÷230 kgf/sm²). For preparation after heating with water vapor, the reactor is checked for sealing with water vapor to a pressure of 4,5 kgf/sm², then the steam is passed through a filter to a

pressure of 3,3÷3,5 kgf/sm² and discharged into the K-310 scrubber and the operation of equalization with the pressure of the working chamber is started. This operation lasts 30÷40 minutes, and during this time the pressure drop in the reactors should not exceed 0,2 atm.

When the temperature of the reactor bottom rises to 180÷220 °C, its purge with oil products vapors continues in the column K-301. This process takes 6 hours. When the temperature of the reactor bottom reaches 350÷360 °C, it is put into operation according to the coking scheme.

From the top of the K-301 column, oil gas, gasoline and water vapors, being cooled in air-to-water coolers, enter the Sp-301 gas separator. The separator separates gas, gasoline and water. Fraction 180÷350 °C - light gas oil from the column K-301 is discharged into the evaporation column K-302 with its flow from the 19th solid plate (accumulator) of the column. The low-boiling components of the fraction are evaporated with superheated steam and returned from the top of the K-302 column to the cube of the 19th plate K-301 column.

The gradual coking process carried out in unheated coke chambers at 450÷500°C temperature and 0,6 MPa pressure 0,6 MPa (6 kgf/sm²) can be considered as a deep thermal cracking process.

III. Multi-connected tar heating control system

The technological process essence is the implementation of the coking process by collecting (accumulating) its heat by blowing raw materials heated to a high temperature (495÷520°C) into unheated reactors (coking chambers) isolated from the outside. For complete coking, light gas oil heated to 515÷520°C is injected into the chambers.

The technological scheme of the oil coke production process is shown in Figure 1.

The raw material (tar) passes through the heat exchangers with the help of the H-104 pump, enters the S-303 furnace, heats up to 360÷380°C and is fed into the K-301 rectification column. The heating raw materials (tar) process in the S-303 furnace is carried out under such difficult technological conditions that any excitatory impact force acting on the system can upset the system balance and amplitude changes in the mode parameters that characterize the heating raw materials occur process.

Gas fuel is used for heating tar in an industrial furnace. When using gaseous fuels, there are certain hazards and risks for the process. This technological process is a very complex process. Because under heating conditions, external influences (exciting influences) are applied to this system, which upsets the control system balance. If the balance is disturbed, the technological parameters of this process change, that is, the difference in amplitude values. This disrupts the correct operation of the heating the raw material process to the required temperature. One of the disturbing influences is the frequent and wide range of changes in the density of the feedstock entering the installation.

In such cases, the positions of actuators 7 and 8 placed in the feed lines entering the C-303 furnace will often change, resulting in violation of the technological process quality characteristics. To overcome these shortcomings, the development of a multi-connected automatic control system for tar heating is a very actual and important problem.

On Fig. 2 shows a scheme of a multi-connected automatic control system for tar heating.

The pneumatic signal from the 1-position level sensor located at the K-301 column bottom is simultaneously fed to the input of the 2 and 3-position consumption controllers. At the input of

these regulators, a signal is simultaneously received from 4 and 5-position consumption sensors and a 6-position density sensor. The outputs of the 2 and 3-position consumption controllers are connected to the 7 and 8-position actuators, on which the line of raw material (tar) entering the S-303 furnace is located. The temperature of the raw material leaving the oven is measured by a 9-position temperature sensor. The output signal passes through a 10-position temperature controller and is transmitted to an 11-position totalizer. A 12-position temperature sensor measures the temperature in the gravity wall of the furnace, and the output signal passes through a 13-position temperature sensor and simultaneously goes to a 14-position setpoint sensor and a 15-position temperature controller. The 14-position setpoint sensor is connected by its output signal to its 11-position totalizer.

The output signal of the 4 and 5-position consumption sensors is fed to the input of the 16-position consumption totalizer. The output signal of the consumption totalizer passes through the 17-position consumption controller and is fed to the 11-position totalizer input. The output of this totalizer is connected to a 15-position temperature controller, the output of which acts on an 18-position actuator. Table 2 shows the mode parameters normative values.

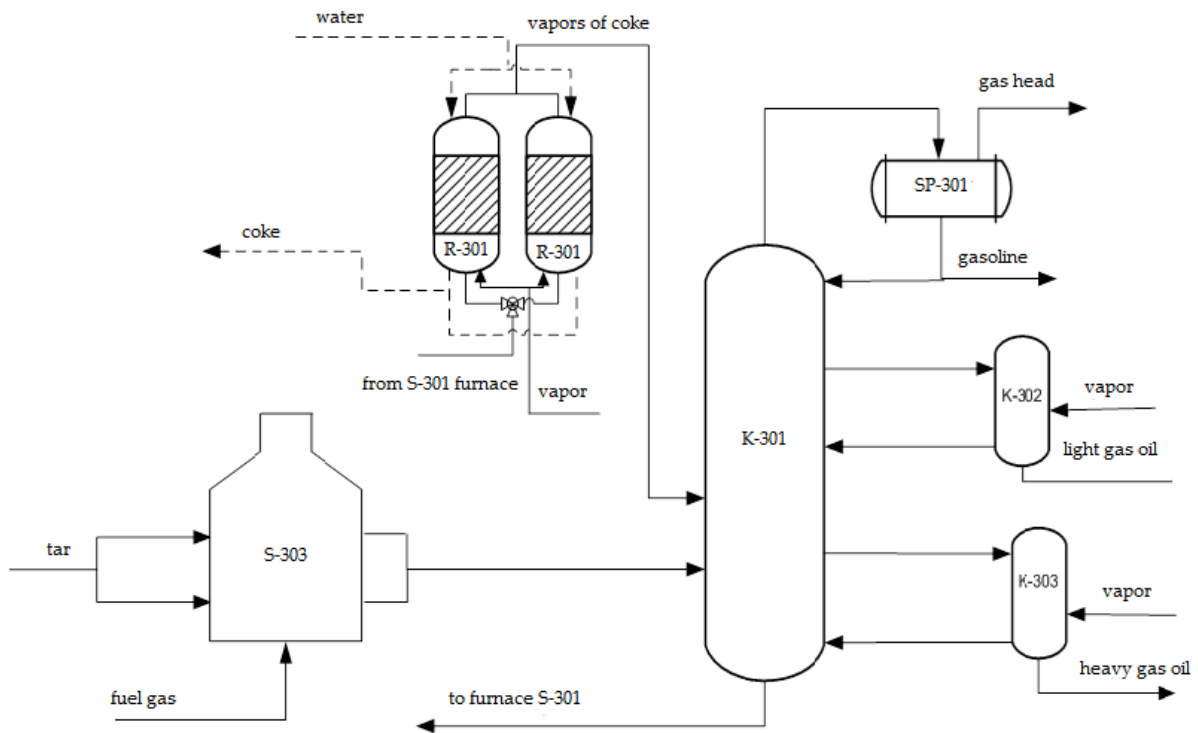


Fig. 1: Technological scheme of the obtaining petroleum coke process

Table 2: Normative values of mode parameters

№	The process stages names and mode indicators	Unit of measurement	Permissible parameter limits
1. Raw material preparation block:			
	Tar consumption	m ³ /h	70+170
	Tar temperature	°C	shouldn't be higher than 90
2. S-303 FURNACE			
	Raw material consumption	I. flow m ³ /h II. flow m ³ /h	35+125
	Raw material temperature at the entrance: at the outlet	°C	300+360
	Raw material pressure at the inlet: I. flow II. flow	kgf/sm ² kgf/sm ²	shouldn't be more than 12
	- raw material pressure at the outlet:	kgf/sm ²	5.0+6.0
	- flue gas temperature at the gravity wall	°C	shouldn't be higher than 630
3. REKTIIFICATION COLUMN K-301			
	- pressure at top of column	kgf/sm ²	3.3+3.6
	- temperature at top of column	°C	on the quality of gasoline
	- column bottom temperature	°C	390+395
	- heavy gas oil level	%	30+70
	- light phlegm temperature	°C	350
	- light phlegm level	%	30+70
	- heavy phlegm irrigation consumption	m ³ /h	shouldn't be higher than 50
	- light phlegm irrigation consumption	m ³ /h	shouldn't be higher than 80
	- level at the bottom	m ³ /h	30+70

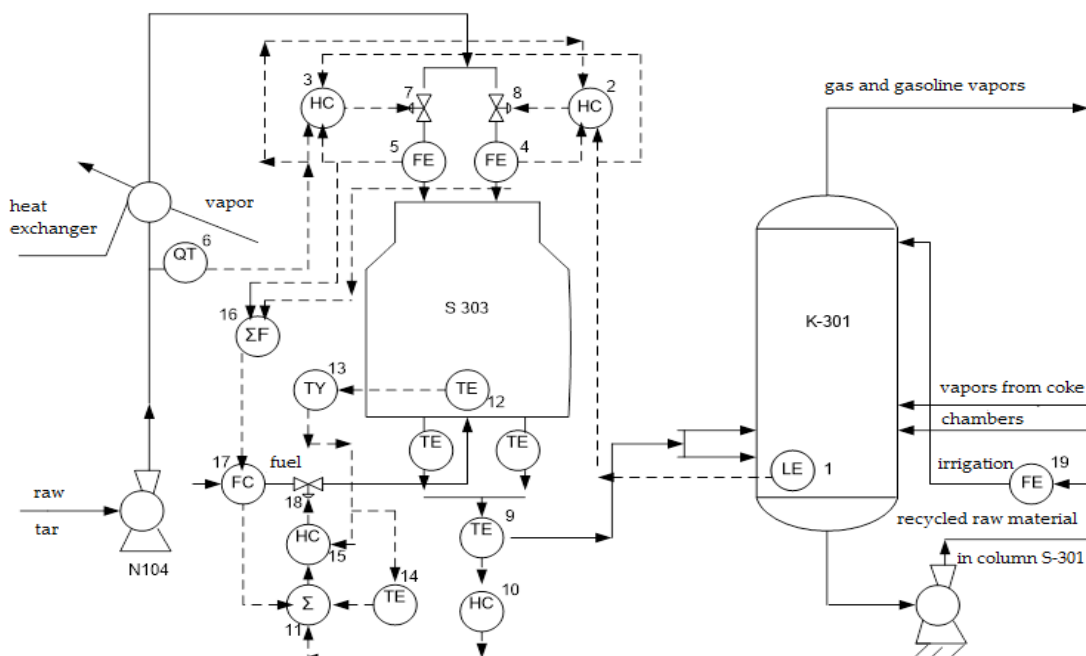


Fig. 2: Scheme of a multi-connected tar heating control system

IV. Conclusion

Based on numerous studies in the oil and gas processing, chemical and petrochemical industries, tube furnaces have been identified as the riskiest and most dangerous objects according to the results obtained when compared with other technological apparatuses. The technological process of obtaining petroleum coke was studied as an object of management.

All controlled and managed technological parameters that can affect the technological process have been selected and justified, metrological support has been developed. Based on this, a multi-connected automatic control system for the considered tar heating technological process was built. With this multi-connected automatic control system, the risk of explosion, fire and other existing hazards to the facility is eliminated.

References

- [1] Verevkin A.P., Matveev D.S., Galeev T.K., Andreev K.V., Akhadov E.A., Maksimenko A.A. Tasks and methods of development advanced systems of industrial safety (In Russ.). *Territoriya "NEFTEGAZ", Oil and Gas Territory*, 2016, No. 4, pp. 78-85.
- [2] Dorotsev V.M., Itskovich E.L., Kueller D.V. *Usovershenstvovannoe upravlenie tehnologicheskimi processami (ARS): 10 let v Rossii. Avtomatizacija v promyshlennosti, Automation in the industrial sector*, 2013, No. 1, pp. 12-19.
- [3] Terrence Blevins, Willy K. Wojsznis, Mark Nixon. *Advanced Control Foundation: Tools, Techniques and Applications*. ISA, 2012, 556 p.
- [4] Yurtaev D.V. *Appliance of simulation system for non-routine events on tube furnace units* / D.V. Yurtaev, A.M. Khafizov // *The journal "Science Almanac"*. 2015. - Vol. 7(9), pp. 850-854. DOI: 10.17117/na.2015.07.850.
- [5] Zakharkin M.A. *Primenenie metodov i sredstv usovershenstvovannogo upravleniya tehnologicheskimi processami (ARS)* /M.A. Zakharkin, D.V. Kneller // *Datchiki i sistemy*. - 2010, No. 11, pp. 57-71.
- [6] Khafizov A.M. *Razrabotka sistemy` «uluchshennogo upravleniya» tekhnicheskim sostoyaniem oborudovaniya i promy`shlennoj bezopasnost`yu predpriyatij neftekhimii i neftepererabotki* / A.M. Khafizov, M.G. Bashirov // *Nauka. Tekhnologiya. Proizvodstvo* - 2014. - Ufa : RICz UGNTU, 2014, pp. 55-57.
- [7] Entus N.R. *Trubchaty`e pechi v neftepererabaty`vayushhej i neftekhimicheskoj promy`shlennosti* / N.R. Entus, V.V. Sharikhin // - M.: Khimiya. 2004, 154 p.
- [8] Verevkin A.P. *Zadachi i metody` razrabotki prodvinyty`kh sistem obespecheniya promy`shlennoj bezopasnosti* / A.P. Verevkin, D.S. Matveev, T.Kh. Galeev, K.V. Andreev, E.A. Akhadov, A.A. Maksimenko // *Territoriya Neftegaz*. - 2016, No. 4, pp. 78-85.
- [9] Salieva L.M. *Sistema upravleniya tekhnicheskim sostoyaniem i bezopasnost`yu e`kspluataczii neftegazovogo oborudovaniya* / L.M. Salieva, I.F. Zajnakova, A.M. Khafizov, I.V. Prakhov, I.S. Mironova // *Nauka i obrazovanie v zhizni sovremennogo obshhestva. Chast` 10*. - Tambov : Izd-vo OOO.
- [10] Melikov E.A., Maharramova T.M. *Energy saving system in vacuum unit*. *Ekoenergetics*, Baku, Azerbaijan, 2022, No. 3, pp. 8-12.
- [11] Guseinov I.A., Khanbutaeva N.A., Melikov E.A., Efendiev I.R. *Models and Algorithms for a Multilevel Control Systems of Primary Oil Refinery Installations*. *Journal of Computer and Systems Sciences International*, Pleiades Publishing, Ltd., 2012, Vol. 51, No. 1, pp. 138-146. DOI: [10.1134/S1064230711060098](https://doi.org/10.1134/S1064230711060098)
- [12] Guseinov I.A., Kurbanov Z.G., Melikov E.A., Efendiev A.I., Efendiev I.R. *Nonstationary Multistage Process Control in the Petrochemical Industry*. *Journal of Computer and Systems*

Sciences International, Pleiades Publishing, Ltd., 2014, Vol. 53, No. 4, pp. 556-564. DOI: [10.1134/S1064230714030095](https://doi.org/10.1134/S1064230714030095)

[13] Verevkin A.P. Obespechenie bezopasnosti trubchaty`kh pechej na osnove operativnoj diagnostiki avarijny`kh sostoyanij / A. P. Verevkin, D. S. Matveev, M. Kh. Khusniyarov // Territoriya Neftegaz. – 2010, No. 4, pp. 20-23.

[14] Lavrent`eva T.M. Promy`shlenny`e pechi i trubny` / T. M. Lavrent`eva, I. V. Panova, G. A. Kravchenko // Strojizdat. – 2003, vol. 2, 256 p.

[15] Melikov E.A., Maharramova T.M. Power quality control for bitumen production. Ekoenergetics, Baku, Azerbaijan, 2022, No. 4, pp. 37-40.

[16] Bashirov M.G. Sovershenstvovanie sistem avtomaticheskogo upravleniya i protivovarijnoj zashhity` trubchaty`kh pechej na osnove monitoringa parametrov prozessa koksoobrazovaniya / M.G. Bashirov, Z.Kh. Pavlova, M.M. Zakirnichnaya, A.M. Khafizov // Setevoe izdanie «Neftegazovoe delo». 2018, No. 1, pp. 120-144.

[17] Safarova A.A., Melikov E.A, Magerramova T.M. Control of a tube furnace in conditions of risk and increased explosion hazard. Reliability: Theory & Applications, 17(SI 4 (70)), 2022, pp. 516-521.

[18] Melikov E.A. Decomposition algorithm and mathematical models of hierarchical structure of control of the process of primary oil processing. Prospecting and Development of Oil and Gas Fields 2 (67) (2018): pp. 75-82.

DETERMINATION OF DRINKING WATER RESOURCES IN THE KARABAKH PLAIN (AGHDAM REGION): THE ROLE OF EXPLORATION AND RESEARCH

Vagif Karimov¹, Mehriban Ismailova¹, Jafar Sharifov¹, Yuri Nefedov²

¹ Azerbaijan State Oil and Industry University

² St. Petersburg Mining University, Russia.

vaqifkerimov68@mail.ru

Abstract

Aghdam is one of the regions of Azerbaijan, located in the south-west of the country and administratively belong to the center of Aghdam city.

Until 1992, the Aghdam region, with an area of 1250 km², was considered one of the most developed districts of the republic. However, 77.4% of territory (846.7 km²) was subjected to occupation. The relief of most part of the Aghdam region is flat, although there is also a small upland area.

After the liberation of the territory of the region, in order to restore agricultural and animal husbandry activities, as well as, in accordance with the observed global climate changes, it becomes clear that it is necessary to carefully study and evaluate the water potential of fresh water in this region. Similar studies are key to successful restoration of agricultural activity and maintenance of sustainable development in new climatic conditions.

The article uses data obtained during exploratory drilling. By conducting comprehensive studies and analyzing available literary sources, the characteristics of the hydrogeological situation associated with the occurrence of groundwater and water strikes were clarified. Also, the hydrological conditions in the area where the research was conducted were studied and analyzed. The conditions of groundwater formation, chemical composition, mineralization and other indicators of groundwater are studied, the areas of their distribution are determined, and recommendations are given for their rational use for irrigation and other purposes in agriculture and to provide the need for fresh water in the liberated Aghdam region.

Keywords: ground water, water strikes, water-bearing horizons, chemical composition, level of mineralization, filtration factor, specific capacity

I. Introduction

When conducting exploration works for a drinking water source, a complex of research surveys is performed at wells. These studies are based on various methods and involve conducting a series of tests to make sure that the water is safe for human consumption. The main stages and methods of exploration for a drinking water source are listed below:

Determining the location of a drinking water source will ensure its correct identification and monitoring.

Hydrogeological studies mainly include analysis of the conditions of occurrence and properties of soil and rock layers along the source area, reconstruction of water migration processes and identification of possible sources of pollution.

Assessing the level of water discharge entering a water source allows for determining its operational stability over different time periods.

Water quality measurement, namely analysis of the physicochemical and microbiological characteristics of water, is performed to determine the presence of contaminants such as heavy metals, bacteria, viruses, nitrates, and other substances that can make the water undrinkable.

Study potential sources of pollution near the source, such as industrial plants, agricultural waste, chemical agent depots, and other sources of contamination.

Identification of the influence of climatic conditions, such as precipitation and temperature that impact on the quality and quantity of water in the source.

Monitoring and serving. After exploration work which carried out, measurement works are conducted and serving should be carried out at the source to ensure its long-term stable and safe operation.

Carrying out these works is an important stage in the possibility of using a source of drinking water, as well as development of appropriate water supply systems for the population.

The Aghdam region is located in the transition zone of the Lesser Caucasus Mountains and the Kura-Araks lowland, in the submountain region of the Karabakh Plain, and it covers an area of 1094 square kilometers. It is geographically being favorable for agricultural activities. The Aghdam city is located in Azerbaijan and is situated in a subtropical climatic region. A subtropical climate is characterized by warm summer and moderately cool winter. General features of the subtropical climate region are:

Summer in subtropical climate is usually long, warm and dry. Average air temperatures in summer-time might have been sufficiently high, often exceeding +25°C. More than 2/3 part of the year is sunny, not enough precipitations. The average temperature ranges in July from +23°C to +26°C.

Winter in the subtropics is cooler, but generally quite mild compared to the continental climate. Temperatures in winter are kept above zero degrees Celsius, but it can sometimes drop below this mark. The average temperature is from -0.2°C to +1.8°C in January.

Rainfall is less in subtropical climates than in temperate zones. Rainfalls are unstable. The amount of annual precipitations is ranges from 300 to 550 mm, most of which falls along the submountain regions.

Humidity of the air can vary depending on the season, but overall, a subtropical climate is less humid compared to a tropical one. As elevation increases, the climate tends to become milder.

Winds in subtropical climates can play an important role in regulating temperatures and precipitations. They can be both cool and warm, depending on the direction and origin [1, 4, 9].

II. Methods

In the article the materials of the history of hydrogeological study of the Aghdam region has been analyzed and used. Geological and geophysical data from exploration drilling, chemical analysis of water samples, and a study of the current hydrological state of the studied area were processed and analyzed.

To determine the water quality of exploration wells, samples were taken, the chemical analysis data of which are given in the following Table 1.

Unique natural features, the diversity of the lithological structure of Quaternary deposits, as well as ameliorative and irrigation works led to complex hydrogeological conditions of the studied territory, riches in underground water lying in alluvial-deluvial and proluvial strata of the Upper Pliocene age. Ground water along the section is found everywhere and is fed by irrigation water from rivers, channels, atmospheric precipitations and vertically seeping water strikes [6, 8, 11, 13].

In areas where precipitation prevails and irrigation is carried out, there is a rise of the ground water level in March-April, which continues until August, and a decrease in the level occurs due to evaporation and is observed from mid-September to the end of October-November. The absolute value of the ground water level varies from 200 m in the Aghdam region to -3 m toward

the Kura River. Thickness of the ground waters decrease from 50-60 m in the submountain regions up to 4-5 m toward the Kura River. The total salinity of ground water more than 90% of the territory is 0.3-0.9 g/l, and only in the zones bordering Kura, it increases up to 2-5 g/l. Their chemical composition changes in the direction of water movement from hydrocarbonate to sulfate-hydrocarbonate and then to sodium-chloride.

Table 1: Chemical water analysis data of exploration wells

No.	indicator	measurement units	SAUS	well 1	well 2	well 3
1	Smell at 20°C	the score of degree	≤2	0	0	0
2	Color		≤20	1	17	1
3	pH	Unit pH	6-9	7,11	7,55	7.57
4	Total hardness	mmol/l	≤7	7,60	6,90	6.80
5	Salinity	mg/l	≤1000	615,8	884,7	759,3
6	dry residue	mg/l	≤1000	448	747	613
7	Calcium (Ca ²⁺)	mg/l	≤100	98,2	152.3	98,2
8	Magnesium (Ma ²⁺)	mg/l	≤50	32,8	29.2	23.1
9	Sodium (Na ⁺)	mg/l	≤200	17,2	53,4	180,2
10	Potassium (K ⁺)	mg/l	≤12	0,5	1,6	4,3
11	Hydrocarbonate (HCO ₃ ⁻)	mg/l	-	335,5	274,5	292,8
12	Sulfates (SO ₄ ²⁻)	mg/l	≤500	104,4	345.0	124,0
13	Chlorides (Cl ⁻)	mg/l	≤350	23,0	21,6	18,1
14	Nitrates (NO ₃ ⁻)	mg/l	≤45	3,2	5,6	8,2
15	Nitrites (NO ₂ ⁻)	mg/l	≤3	0,018	0,017	0,056
16	Fluorides (F ⁻)	mg/l	≤0.7	0,38	0,33	0,38
17	Iron (Fe)	mg/l	≤0.3	0,26	0,23	-
18	Boron (b)	mg/l	≤0.5	-	-	0,1
19	Manganese (Mn)	mg/l	≤0.1	0,087	0,064	0,052
20	Copper (Cu)	mg/l	≤0.1	0,03	0,35	0,02
21	Chrome (Cr, VI)	mg/l	≤0.5	0,017	0,013	0
22	Phosphates (PO ₄ ³⁻)	mg/l	≤3.5	0,20	0,60	0,09
23	Aluminium (Al ³⁺)	mg/l	≤0.5	0,053	0,008	0,014
24	Nickel (Ni)	mg/l	≤0.1	0,054	0,050	0,048
25	Cobalt (Co)	mg/l	≤0.1	0,034	0,013	0,027
26	Barium (Ba ²⁺)	mg/l	≤0.1	0,02	0,02	0,05

The occurrence depth of ground water depends on the features of the terrain, flow slope, rock permeability, changes in the feeding regime and rate of discharge, and decreases regularly in a wide range from west to east. Deep-seated groundwaters are observed in the upper part of the river run-off cone, however, the lowest levels are observed in inter-cone depressions. On the periphery of the region, ground water rises to the surface and forms a system of swamps. In the south-eastern part of the region, ground water is fed by water strikes. The acidity (pH) level of the main part of these waters is 6,5-7 [10, 12, 15, 19].

Since the Aghdam region is part of the Karabakh Plain, the hydrogeological conditions are similar to neighboring regions, and therefore it is considered appropriate to study both together. The site has five water strikes, which are lithologically represented by sand, gravel, large boulders and pebbles with sand and gravel aggregate. Water horizons are separated by impenetrable clays of 17-20 m to 100-130 m thick. The ameliorative state is most affected by the waters of the I pressure horizon. The depth of its roof ranges from 20-60 m to 100-120 m.

The level of salinity of the I pressure aquifer varies from 0.5 g/l to 3.0 g/l. The chemical composition of water varies from hydrocarbonate to hydrocarbonate-sulfate and sulfate. This aquifer is uncovered at a depth of 20-100 m by wells in the eastern and central parts of the region, the thickness of water-bearing rocks here is 5-110 m. The waters of the I pressure horizon are mostly fresh over the entire area, but between of Khachinchay and Tartarchay the level of their mineralization increases, and on the left bank of the Kura River becomes salty.

The spreading area of pressure aquifer II is smaller than the aquifer I. The occurrence depth of its varies from 40-100 m to 180-220 m, but the thickness of water-resistant clays is 10-45 m. The lithological composition of the aquifer is represented by pebbles, sands, and gravels with a sand-clay aggregate. The thickness of pressure reservoir ranges from 60-65 m to 230-240 m. This aquifer contains mainly fresh water, in rare cases there is also water with a total salinity of 1.8 g/l. The level of mineralization of the II pressure aquifer varies from 1.0-1.5 g/l. According to their chemical composition, water belongs to the hydrocarbonate, hydrocarbonate-sulfate, and sulfate-hydrocarbonate types [13, 14, 16, 20].

In comparison with the II aquifer, the area of distribution of the III aquifer pressure complex is much smaller. The depth of the roof of this water-bearing layer is 150-300 m. The lithological composition of the aquifer consists of gravel and sand, which are underlain by water-resistant clays, the thickness of which is 20-60 m. The chemical composition of water varies from hydrocarbonate-sodium to hydrocarbonate-sulfate-sodium and sulfate-hydrocarbonate-sodium with a total degree of mineralization not exceeding 0.5 g/l.

The distribution area of the IV water-pressure (Absheron) complex almost coincides with the distribution area of the III water-pressure horizon. Boreholes have been uncovered this horizon at depths of 135-400 m or more. This horizon was not found on the left bank of the Kura River. The thickness of the water bearing rocks of this complex reaches 20-40 m, the filtration coefficient is 0.9-18.7 m/day, the water flow rate in wells is 0.6-23.2 l/sec, and the specific flow rate varies between 0.1-0.8 l/sec. m. The waters of wells drilled on this horizon gush mainly to a height of 10-15 m above the earth's surface. On the western border of the Inchachay and Tartarchay interfluvial, the water level in wells decreases and there is no self-discharge.

The V pressure aquifer in the central part of this plain is uncovered by wells at a depth of 200-280 m. The filtration coefficient in wells is 4.5-5.0 m/day. While the waters of the ground and four pressure aquifers are fresh, the waters of the V aquifer are saline (Tab. 2) [17, 21, 24].

Thus, currently more than 1000 sub-artesian wells with a total flow rate of more than 21,000 m³/sec are active in the study area³.

Khachinchay is a left inflowing stream of the Kura River, cross flow the Aghdara, Aghdam, and Barda regions. Length of the river is 119 km and the area of its bed is 657 km². Khachinchay is formed by the junction of streams originating from the mountains of Hajigurd (2397 m), Uyukhlu (2316 m), Chichekli (2343 m), and Alagaya (2583 m) of the Karabakh Range. A water-storage reservoir with a capacity of 23 million cubic meters has been restored on the Khachinchay River in a relatively short time.

Until 1990, up to 800 wells were drilled mainly in the eastern part of the region, the current state of which is currently being specified. During the occupation, the forests of Aghdam and valuable reservoirs of the region were destroyed, 25 thousand hectares of the forest were cut down and turned into agricultural area. Before the occupation, there were three water-storage reservoirs on Kondalanchay, with a total capacity of 14,000 m³. After the liberation of all regions of the Karabakh region from occupation, these reservoirs were restored in a short time, and in the near future they will play an important role in irrigating the lands of the Aghdam and Fizuli regions. The water-storage reservoir built on Gargarchay has already been restored, and work is currently underway on a project to expand this water-storage reservoir [18, 22, 25].

The power of the water complexes of Khachinchay ranges from 35 to 96 meters, filtration coefficient is fluctuate between 8.1-50.6 m/day. The width of underground flow is 1,5 kilometers, and the discharge is estimated about 140,7 l/sec. The thickness of the water-bearing horizons in the Gargarchay cones reaches 37-95 meters, the filtration coefficient is consist 17,6-41,9 m/day. The

width of underground flow is also 1,5 kilometers, and the discharge about 323 liters per second is estimated.

Table 2: *Hydrogeological parameters of aquifers of the Karabakh (Aghdam) plain (up to 300-400 m)*

Ground-water horizon	Occurrence depth of the roof of aquifer	Statistic or piezometric level, m	Slope of the hydro-relief	Thickness of aquifers, m	Well flow rate, l/sec	Filtration coefficient of water-bearing rocks, m/day
Ground water	-	0,7-31	0,014-0,001	5-50	0,06-20	0,2-93,2
I pressure horizon	20-100	+2,4-56	0,03-0,0003	4-109,5	0,07-11,7	0,9-38,7
II pressure horizon	70-270	+15,1-22	0,01-0,001	5-104	0,16-13,8	0,1-10,2
III pressure horizon	115-290	+15-7.5	0.008-0.004	to 51	0,1-10,3	0,5-11,6
IV pressure horizon (Absheron)	125-400 and more	+15-7,8	0,007-0,003	20-40	0,6-23,2	0,9-18,8
V pressure horizon (Aghjagil)	200-380	+3-11,1	0,01-0,005	3-43	0,16-1,2	1,6-4,5

Analysis of the hydrogeological and hydrological conditions of the territory of the Aghdam and the Karabakh regions as a whole indicates that there are water resources available for both soil irrigation and drinking water supply in the area. However, the water monitoring effective management and utilization of surface and groundwater resources is required. The measures should be taken in accordance with the requirements of the "Smart Village" and "Smart City" projects [9, 23].

In the recent past, two channels were dig out from the Tartar River to transfer water from Aghdara to the Aghdam region. In the closest time, the issue of transferring water via the Upper Karabakh Cannel to Aghdam will be solved. Additionally, a significant number of artesian wells will be restored or drilled, and they will be integrated into the water supply cycle.

In summary, active steps are being taken to restore water resources for drinking water supply, soil irrigation, and water resources management within the framework of the "Smart Village" and "Smart City" projects.

The result of this study is the identification of potential fresh water reserves, determination of sufficiency for water supply in cities, villages and hamlets, as well as the possibility of using them for irrigation of agricultural land, and development of ways for their rational exploitation.

Discussions

Due to large-scale climate changes in the territory of the Aghdam region, there is an extremely actual and urgent need to restore agricultural and livestock activities. Climate change processes have had a negative impact on the agricultural sector, reducing yields, deteriorating pasture quality and threatening the food security of the local population. At the same time, to solve these problems, it is extremely important to carry out a complex of studies of the current hydrogeological state of the territory. These studies are aimed for studying the distribution and conditions of underground water resources, as well as assessing their availability. The results of hydrogeological studies will allow to accurately determine and rethink about the prospects for restoring and optimizing agricultural and livestock activities in this area.

One of the main aspects of research is the providing of high-quality drinking water for both the city and surrounding settlements. The correct assessment of the hydrogeological situation determines the possibility of providing the population with a reliable and safe source of drinking water, which is important for the health and well-being of residents.

However, for irrigation purposes, the Yukhari Mil Channel was built, passing via the study area. The construction of the channel, along with global climate changes, caused a drop in the water level of the Kura River, which give a reason of the necessity of exploration and use of underground waters in the Aghdam region.

The geological structure of the studied area includes Mesozoic, Paleogene, Neogene and Quaternary deposits. Unique natural features, a variety of lithological structure of Quaternary deposits, active ameliorative and irrigation works the complex hydrogeological conditions in the studied area have been created. The territory is rich by underground waters and situated in alluvial-deluvial and proluvial strata of the Upper Pliocene [2, 3, 5, 7].

In order to clarify the groundwater reserves and their use for the national economic needs of the liberated territories of the Aghdam region, three exploration wells with a depth of 170-174 m were drilled in 2021-2022.

Drilling to a depth of 170 meters can be carried out using various methods and technologies, such as hand, vertical and horizontal drilling, as well as hydraulic fracturing.

Hand drilling can be used at shallow depths of the aquifer.

Vertical drilling. Currently, there are various types of drilling rigs, including rotary and rod-type, allowing to carry out the trunks of inclined and vertical wells.

Horizontal directed drilling for water can be used when it is necessary to take into account certain restrictions on the surface, for example, the need to preserve existing infrastructure [22-25].

To increase drilling efficiency, hydraulic fracturing can be applied. This method involves injection of fluid into the rock formation under high pressure for the destruction of rocks, with the aim of subsequent increase in water yield. In some cases, explosive drilling is used for drilling rocks at greater depths. This method requires specialized knowledge and equipment, as well as ensuring safety and accuracy in conducting the technological operations. During explosive drilling, special casing and cementing materials can be required, as well as equipment to ensure the stable operation of the well and prevent the collapse of its borehole.

In the Aghdam area, plans also to use installation of the explosive drilling with a downhole pneumatic hammer [20-22].

Conclusion

1. A groundwater horizon and five water strikes have been identified in the studied area. The first three pressure aquifers are associated with Quaternary deposits, while the IV and V horizons are found in the Aghjagil and Absheron stage formations. The chemical composition characterized

by calcium-magnesium, hydrocarbonate, and hydrocarbonate-sulfate waters. The pH value increases from 6,9 to 8,6 in the direction of the Kura River.

2. Infiltration and filtrate waters are play a significant role in the formation of the regime characteristics of groundwater. To increase the productivity of irrigated lands and protect them from salinization, it is necessary to prevent the salt accumulation in the soil. It is extremely important to observe a certain water regime to maintain the moisture concentration in the soil at the level necessary for plant growth. To prevent the rise of the groundwater level, it is necessary to control the distribution of irrigation water according to established and calculated norms.

3. To fundamentally improve irrigated lands, it is necessary implementation of agrotechnical, complex-operational, organizational-economic, and hydromeliorative measures. Improving the ameliorative situation can only be achieved by regulating and improving irrigation methods and increasing the efficiency of drainage systems.

Acknowledgements. The authors are grateful to the graduate student of Saint Petersburg Mining University Ekaterina 2, Emil Elchin oglu Gasimov, for his assistance in planning and writing the article, as well as for his support in conducting the research.

References

- [1] Alekseev, V.I. (2020). Study of changes in the global climate as a complex system using wavelet phase-frequency functions, phase-frequency and phase-time characteristics of heliocosmic and climatic variables. Part 1–2. Bulletin of the Tomsk Polytechnic University. Engineering of georesources, 331, 7, 238-250. [in Russian]. DOI: [10.18799/24131830/2020/7/2733](https://doi.org/10.18799/24131830/2020/7/2733)
- [2] Amalfitano, S., Bon, A.D., Zoppini, A., Ghergo, S., Fazi, S., Parrone, D., Casella, P., Stano, F., Preziosi E. (2014). Groundwater geochemistry and microbial community structure in the aquifer transition from volcanic to alluvial areas. Water Resources. 65, 384–394. DOI: [10.1016/j.watres.2014.08.004](https://doi.org/10.1016/j.watres.2014.08.004)
- [3] Babayev, N.I., Tagiyev, I.I. (2015). New information on chemical content of mineral and thermal waters of Azerbaijan's Quba-Khachmaz.Euros. Union of Sci. 11. 46-52.
- [4] Barthel, R.A. Call for more fundamental science in regional hydrogeology. Hydrogeology Journal. 2014, 22, 3, 507-510. DOI: [10.1007/s10040-014-1101-9](https://doi.org/10.1007/s10040-014-1101-9)
- [5] Bondarenko, L.V., Maslova, O.V., Belkina, A.V., Sukhareva, K.V. (2018). Global climate change and its aftermath. Herald of the Russian Economic University named after B. Plekhanova. 2, 84-93. <https://doi.org/10.21686/2413-2829-2018-2-84-93>
- [6] Bravo, S., García-Ordiales, E., García-Navarro, F.J., Amorós, J.Á., Pérezdelos-Reyes, C., Jiménez-Ballesta, R., Esbrí, J.M., García Noguero, E.M., Higuera P. (2019). Geochemical distribution of major and trace elements in agricultural soils of Castilla La Mancha (central Spain): finding criteria for baselines and delimiting regional anomalies. Environmental Science and Pollution Research. 26, 4, 3100–3114.
- [7] Selvaggi, R., Damianić, B., Goretti, E., Pallottini, M., Petroselli, C., Moroni, B., La Porta, G., Cappelletti, D. (2020). Evaluation of geochemical baselines and metal enrichment factor values through high ecological quality reference points: a novel methodological approach. Environmental Science and Pollution Research. 27, 1, 930-940.
- [8] Gyulmamedov, Ch.D. (2021). Influence of the Upper Shirvan Canal on the change in hydrogeological and reclamation conditions of the Shirvan steppe of Azerbaijan. Bulletin of the Tomsk Polytechnic University. Georesource engineering. 332, 10, 116–126. DOI <https://doi.org/10.18799/24131830/2021/10/3399>
- [9] Imanov, F.A., Alekbarov, A.B. (2017). Modern changes and integrated water resources management in Azerbaijan. Baku. [in Russian]
- [10] Israfilov, Yu. H, Israfilov, R. H., Guliyev, H. H., Efendiyev, G. M. (2016). Risk assessment of the water resources losses of the Azerbaijan republic due to climate changes. News of ANAS, Earth Sciences, 3-4.

- [11] Kerimov, V.M., Sharifov, J.J., Mammadli, M.Z. (2021). Hydrogeological conditions of the Ganykh-Ayrichay valley. In the book: the development of science and practice in a globally changing world in terms of risks. Collection of materials of the IV International scientific-practical conference. Makhachkala. 71-76. DOI: [10.34755/irok.2021.46.94.048](https://doi.org/10.34755/irok.2021.46.94.048)
- [12] Montcoudiol N., Molson J., Lemieux J.M. (2014). Groundwater geochemistry of the Outaouais Region (Quebec, Canada): a regional-scale study. *Hydrogeology Journal*. 23, 2, 377–396.
- [13] Tagiev, I.I., Kerimov, V.M., Sharifov, D.D. (2021). Characteristics of the hydrogeological massifs of the Greater, Lesser Caucasus and Talysh (Azerbaijan) taking into account global climate change. *Visnyk of Taras Shevchenko National University of Kyiv: Geology*, 3(94), 95-102. <http://doi.org/10.17721/1728-2713.94.12>
- [14] Tagiev, I.I., Kerimov, V.M. (2021). Prospects for the development of alternative energy and the use of thermal waters in Azerbaijan. *Ural Geolog. Journal*. 3(141), 51-57.
- [15] Tagiev, I.I., Babaev, N.I. (2017). Some geochemical and hydrogeological, regularities of formation and distribution of mineral waters of Azerbaijan. XXXIX International Scientific and Practical Conference Actual problems in modern science and ways to solve them, Moscow, 15-19.
- [16] Tagiyev I.I., Ismailova M.M., Karimov V.M., Sharifov J.J. (2022). Groundwater of Ganikh-Ayrichay foothills on the prospects of use. *Reliability: Theory and Applications*. 3(66), 17, 76-81. DOI: <https://doi.org/10.24412/1932-2321-2022-366-76-81>
- [17] Wang J., Zuo R., Caers J. (2017). Discovering geochemical patterns by faktor-based cluster analysis. *Journal of Geochemical Exploration*. 181, 106–115.
- [18] Wang, S. Lee, W., Son, Y. (2017). Low carbon development pathways in Indian agriculture. *Change Adaptation Socio-Ecological Systems*, 3, 18-26. <https://doi.org/10.1515/cass-2017-0002>
- [19] Substantiation of dth air drill hammer parameters for penetration rate adjustment using air flow *Gorny zhurnal*, Yungmeister D. A., Isaev A. I., Gasimov E. E., *Gorny zhurnal*, 2022, 2022(7), pp. 72-77. DOI: [10.17580/gzh.2022.07.12](https://doi.org/10.17580/gzh.2022.07.12)
- [20] Jungmeister D. A., Gasymov E. E., Isaev A. I. Substantiation of the design and parameters of the device for regulating the air flow in down-the-hole hammers of roller-cone drilling rigs. *Mining Informational and Analytical Bulletin*. - 2022. - No. 6-2. - pp. 251-267. DOI: [10.25018/0236_1493_2022_62_0_251](https://doi.org/10.25018/0236_1493_2022_62_0_251).
- [21] Yungmeister D. A., Timofeev M. I., Isaev A. I., Gasymov E. E. Improvement of tunnel boring machine S-782 cutter head. *Mining Informational and Analytical Bulletin*. - 2023. - No. 1. - pp. 107-118. DOI: [10.25018/0236_1493_2023_1_0_107](https://doi.org/10.25018/0236_1493_2023_1_0_107).
- [22] Panteleenko F.I. Increasing the productivity of magnetic abrasive processing using diffusion-alloyed powders / F.I. Panteleenko, G.V. Petrishin, V.V. Maksarov, D.D. Maksimov // *Russian Engineering Research*. 2023. Vol. 43. No. 4 pp. 470-473. DOI: [10.3103/S1068798X23050179](https://doi.org/10.3103/S1068798X23050179)
- [23] Maksarov V.V. Quality control of complex contour surfaces in aluminum alloy items during magnetic abrasive finishing / V.V. Maksarov, D.D. Maksimov, M.S. Sinyukov // *Tsvetnye Metally*, No. 4. 2023. pp. 96-102. DOI: [10.17580/tsm.2023.04.13](https://doi.org/10.17580/tsm.2023.04.13)
- [24] Zhukov, I.A., Martyshev, N.V., Zyukin, D.A. et al. Modification of Hydraulic Hammers Used in Repair of Metallurgical Units. *Metallurgist* 66, 1644–1652 (2023). <https://doi.org/10.1007/s11015-023-01480-w>
- [25] Yungmeister D., Gasimov E. Drill rig with a down-the-hole hammer for regulating the drilling rate by changing the air flow // *E3S Web of Conferences*. – EDP Sciences, 2021. – T. 326. – C. 00018.

DATA-DRIVEN DIGITAL TRANSFORMATION: CHALLENGES AND STRATEGIES FOR EFFECTIVE BIG DATA MANAGEMENT

Adam Mentsiev¹, Timur Aygumov², Elmira Amirova^{3,4}

¹Kadyrov Chechen State University, Russia

²Dagestan State Technical University, Russia

³Kazan State Agrarian University, Russia

⁴Kazan State University, Russia

a.mentsiev@chesu.ru

Abstract

The study is devoted to the study and analysis of the risks associated with managing big data during the period of digital transformation of organizations. The purpose of the work is to identify the problems and risks that organizations face when integrating and using big data in an effort to remain competitive and successful in today's economic realities. The study uses a mixed approach to data analysis, which allows a comprehensive study of the issues of data management in the process of digital transformation. In the course of the work, the main problems and risks that organizations face when working with big data are identified. These risks include data governance and privacy, data security, data integration and interoperability, scalability and infrastructure, data quality and integrity, and employee skill and experience issues. The study proposes strategies to address these challenges, including developing a comprehensive data governance framework, investing in data security, and using advanced analytics and artificial intelligence. It also discusses the importance of cultural change in an organization, a commitment to the ethical use of data, and the need for a scalable infrastructure for future growth. The results of the study bring us to the realization of the importance of effective management of big data in the context of digital transformation and provide practical recommendations for overcoming the difficulties associated with this process.

Keywords: digital transformation, big data, challenges, strategies

I. Introduction

In the era of technological advancement, two key concepts have become the driving force for businesses across industries: "big data" and "digital transformation". Their combined influence has revolutionized the way organizations operate, the way they make business decisions, and interact with customers.

In a rapidly evolving digital environment, companies around the world are seeing digital transformation as a means to innovate, improve operational efficiency and gain competitive advantage. At the heart of this transformation is "big data", a vast and diverse stream of information generated in an ever-expanding digital ecosystem. The interplay between big data and digital transformation has led to the evolution of workflows, decision making and customer interactions. In addition to the potential benefits, there are numerous risks associated with the effective management of big data in the context of digital transformation [1].

The term "big data" encompasses vast amounts of structured and unstructured data

generated from various sources such as social media platforms, IoT devices, mobile applications, and transactional systems. This data stream contains valuable information that can significantly influence strategic decisions and uncover hidden growth opportunities. It is also characterized by velocity, volume and variety, requiring advanced processing and analysis techniques to extract meaningful information [2].

The key characteristics of big data can be summarized as three “V”: volume, velocity and variety:

- Volume is the amount of data generated every second is unprecedented. Traditional data management systems are unable to efficiently process such huge amounts of information.
- Velocity – data is generated at an incredible speed, requiring real-time or near-real-time processing to provide actionable insights quickly.
- Variety – big data comes in a variety of formats, including structured, semi-structured, and unstructured data. This diversity creates challenges for effective data integration and analysis.

Digital transformation is the strategic implementation of digital technologies to radically change business processes, improve the customer experience, and create innovative products and services. This process goes beyond simple automation and includes profound changes in the culture, mindset and activities of the organization.

The main goals of digital transformation include [3]:

- Process optimization: Using digital tools and technologies to streamline operations to improve efficiency and reduce costs.
- Improving the customer experience: Creating a personalized and seamless experience with customers through digital channels that meets their ever-changing expectations.
- Data-Driven Decision Making: Using data and information analytics to make informed and strategic decisions that drive business growth.

The synergy between big data and digital transformation has become a driving force for many companies, bringing significant opportunities to improve business processes and achieve competitive advantage [4].

The interplay between big data and digital transformation is an important and mutually beneficial symbiosis. Big data provides the necessary raw material that fuels digital transformation initiatives. The abundance of data provides organizations with valuable insights into customer behavior, market trends and underperforming operations to inform informed decision making and guide the transformation process [5].

Big data analytics play an important role in creating personalized customer experiences, delivering targeted marketing campaigns, and optimizing product offerings based on real-world feedback and preferences. Big data-driven analytics help improve the overall customer journey by promoting customer loyalty and advocacy [6].

Digital transformation, in turn, ensures the effective use of the potential of big data. Digital technologies such as cloud computing, the Internet of Things, artificial intelligence and machine learning enable organizations to store, process and analyze massive datasets efficiently. Cloud infrastructure provides scalable storage and processing capabilities for ever-increasing volumes of data.

The use of artificial intelligence and machine learning algorithms allows you to identify patterns, trends and correlations in data that may not be visible to analysts [7]. This enables companies to make informed decisions that are in line with their strategic goals and drive innovation.

However, organizations pursuing a digital transformation path face both the many opportunities and risks associated with big data management. The effective management of big data is critical, as an insufficiently structured and systematic approach can lead to lost data and hinder the extraction of meaningful information needed to achieve strategic goals. The exponential growth of big data creates challenges such as data governance and privacy, maintaining data

security and integrity, improving data quality, integrating data from multiple sources, and scaling existing infrastructure [8].

In addressing these directions, organizations can leverage best practices and potential solutions to help mitigate risk and maximize the potential of big data for successful digital transformation. It is important to understand that technology is constantly evolving and influencing business strategies, so the effective management and use of big data is becoming a critical component for organizations seeking sustainable growth and success in a dynamic and competitive digital environment.

II. Methods

The purpose of this study is to study and analyze the risks that organizations face in effectively managing big data in the process of digital transformation. To achieve this goal, a mixed approach of analyzing qualitative and quantitative research methods is used. The study will conduct a thorough literature review to deepen understanding of existing knowledge related to big data management and digital transformation, as well as their interactions [9]. This will provide a sound theoretical basis for the study and will help to identify existing problems and challenges that organizations face.

The research methodology aims to analyze the problems of big data management in the context of digital transformation in order to provide valuable information about the risks and potential solutions to overcome them. An analysis of these issues will highlight the most significant factors that may limit successful digital transformation and the effective use of big data. In addition, the study will attempt to offer recommendations and solutions to help organizations streamline their data management processes and successfully implement their digital transformation.

III. Results

The results of the study confirm that digital transformation has become an integral element of the strategic activities of organizations seeking to maintain their competitiveness in a rapidly changing economic field. An important role in this process is played by the effective management of big data and its application [10]. Big data provides organizations with valuable insights to drive innovation, improve decision-making processes, and improve customer service.

However, our research has identified a number of key challenges that organizations face when integrating big data into their digital transformation process. The main list of problematic indicators is given below.

- Data management and privacy. Organizations must develop clear policies and procedures to manage the collection, storage, access and sharing of data, as well as adhere to privacy rules, to ensure that data is handled legally and ethically.
- Data security. As the volume of data sources increases, organizations become more vulnerable to cyberattacks and data breaches, so it is necessary to implement strong data security measures, including encryption and access control [11].
- Data integration and interoperability. Integrating data from different sources can be challenging due to the variety of data formats and technologies, seamless data integration is required to provide a single and accurate overview [12].
- Scalability and infrastructure. Organizations must invest in a scalable and reliable infrastructure to process and analyze growing volumes of data, but migrating to the cloud can present challenges.
- Data quality and reliability. Data quality is a key factor for accurate analysis and decision

making, and data quality management practices must be implemented to ensure data validity and accuracy.

- Skills and experience. The lack of qualified data scientists can make it difficult to effectively use big data in digital transformation, and collaboration between business and IT teams must be ensured.

- Cultural challenges. The adoption of big data and digital innovation can be reluctant among employees, especially if they are accustomed to traditional ways of working, so it is just as important as adopting the technology itself to develop an open and innovative culture within the organization, train staff in new skills, and motivate them to embrace change.

- Speed and return on investment. Implementing quickly can lead to waste of resources and unnecessary risks, while implementing too slowly can lead to loss of competitive advantage. Therefore, it is important to develop a clear implementation plan, evaluate the risks and benefits of investments, and find the optimal balance between speed and efficiency.

- Ethical considerations. The implementation of big data must be guided by ethical principles and commitments to the responsible use of information.

The results of the study highlight the importance of overcoming these challenges and risks in order to successfully implement digital transformation and optimize big data management [13].

IV. Discussion

In the digital age, big data has a significant impact on the activities of organizations that seek to extract valuable information, make informed decisions and achieve a competitive advantage. However, the volume, velocity and variety of data present serious challenges that require effective management practices. The importance of effective big data management cannot be overemphasized, as it affects various aspects of an organization's operations, its strategic planning and overall success.

Big data contains a huge amount of valuable information that can be used to make informed decisions. Effective data management ensures that the right data is available to stakeholders at the right time. Analyzing trends, patterns, and customer behavior based on big data enables decision makers to make accurate predictions, identify new opportunities, and address potential issues. Organizations that make data-driven decisions gain a competitive edge by being more agile and able to quickly respond to market changes.

Understanding customer preferences and behavior is critical to providing a personalized and seamless customer experience. Big data management allows organizations to combine data from various sources such as social media, websites, and purchase history to create a complete customer experience. This in-depth understanding helps deliver targeted marketing campaigns, personalized recommendations, and effective customer support, leading to increased customer satisfaction and loyalty.

Big data provides valuable insight into market trends and customer needs, which drives innovation and product development. Analyzing feedback and consumer behavior allows organizations to identify gaps in the market and develop innovative products and services that meet customer needs. Efficient data management provides easy access to relevant data for product development teams, accelerating the innovation process.

Properly managing big data facilitates data integration and breaks down information silos, ensuring employees have access to accurate and up-to-date information. This improves work efficiency, improves collaboration and optimizes resource allocation. Big data analytics also uncovers operational inefficiencies and bottlenecks, allowing for process improvements and cost reduction measures.

Data breaches and cybersecurity threats are on the rise, making data security a priority for

organizations. Effective big data management includes strong security measures such as data encryption, access control, and regular security checks.

V. Conclusion

In this paper, the key problems of big data management in the process of digital transformation of organizations were considered. An analysis of the risks and challenges that organizations face in integrating and using big data has revealed several critical aspects that affect the effectiveness of digital transformation and the overall success of organizations in today's digital economy.

A review of the research literature confirms that big data has become a strategic imperative for organizations seeking to remain competitive and successful in a rapidly changing market environment.

The key issues highlighted in the study are data governance and privacy, data security, data integration and interoperability, scalability and infrastructure, data quality and credibility, lack of skilled professionals, cultural challenges, cost and ROI, and ethical considerations.

Strategies have been proposed to address these challenges, including developing a comprehensive data management framework, investing in data security, and using advanced analytics and artificial intelligence. Also discussed was the importance of cultural change in an organization, commitment to the ethical use of data, and the need for a scalable infrastructure for future growth.

Effective management of big data plays a critical role in the success of organizations in the digital age. Good data governance enables informed decision making, enhances customer experience, drives innovation, ensures operational efficiency, and prepares organizations for a scalable and successful future. Responsible and efficient use of big data is key to keeping organizations competitive and resilient in today's rapidly changing business world.

References

- [1] Saarikko, T., Westergren, U.H. and Blomquist, T. (2020). Digital transformation: Five recommendations for the digitally conscious firm. *Business Horizons*. 63(6):825-839.
- [2] Ajah, I.A. and Nweke, H.F. (2019). Big Data and Business Analytics: Trends, Platforms, Success Factors and Applications. *Big Data and Cognitive Computing*. 3(2):1-30.
- [3] Mergel, I., Edelman, N. and Haug, N. (2019). Defining digital transformation: Results from expert interviews. *Government Information Quarterly*. 36(4):1-16.
- [4] Verhoef, P.C., Broekhuizen, T., Bart, Y., Bhattacharya, A., Dong, J.Q., Fabian, N. and Haenlein, M. (2021). Digital transformation: A multidisciplinary reflection and research agenda. *Journal of Business Research*. 122:889-901.
- [5] Kostakis, P. and Kargas, A. (2021). Big-Data Management: A Driver for Digital Transformation? *Information*. 12(10):1-14.
- [6] Pascucci, F., Savelli, E. and Gistri, G. (2023). How digital technologies reshape marketing: evidence from a qualitative investigation. *Italian Journal of Marketing*. 27-58.
- [7] Sjödin, D., Parida, V., Palmié, M. and Wincent, J. (2021). How AI capabilities enable business model innovation: Scaling AI through co-evolutionary processes and feedback loops. *Journal of Business Research*. 134:574-587.
- [8] Nadkarni, S. and Prügl, R. (2021). Digital transformation: a review, synthesis and opportunities for future research. *Management Review Quarterly*. 71:233-341.
- [9] Sivarajah, U., Kamal, M.M., Irani, Z. and Weerakkody, V. (2017). Critical analysis of Big Data challenges and analytical methods. *Journal of Business Research*. 70:263-286.

- [10] Magomadov, V.S. (2020). The application of artificial intelligence and Big Data analytics in personalized learning. *Journal of Physics: Conference Series*. 1691(012169):1-4.
- [11] Mentsiev A.U. et al. (2020). Security challenges of the Industry 4.0. *Journal of Physics: Conference Series*. 1515(032074):1-5.
- [12] Magomedov I.A. et al. (2020). The role of digital technologies in economic development. *IOP Conference Series: Materials Science and Engineering*. 862(052071):1-5.
- [13] Abdou Hussein, A. (2021). Data Migration Need, Strategy, Challenges, Methodology, Categories, Risks, Uses with Cloud Computing, and Improvements in Its Using with Cloud Using Suggested Proposed Model (DMig 1). *Journal of Information Security*. 12: 79-103.

PORTABLE PROPERTIES OF THE RESERVOIR WATERS USED IN POWER SYSTEM

Vagif Hasanov¹, Jeyhun Naziyev², Leyla Hasanova¹, Aqil Omarov¹,
İrada Aliyeva¹, Gulshan Akhundova¹

¹Azerbaijan State Marine Academy

² Azerbaijan State Oil and Industry University

vgasanov2002@yahoo.com

j_naziyev@yahoo.com

aqil.omarov@asco.az

leyla.hasanova.75@mail.ru

iradealiyevakerim@gmail.com

gulakhundova@gmail.com

Abstract

In comparison with the sea shipping, systematic pollution of the sea by oil seems insignificant under oil-and-gas field engineering. Measurements of the viscosity of reservoir waters by remote capillary in the temperature interval of (298.15 to 598.15) °K and the pressure of (0.1 to 40) MPa are reported. The relative uncertainty in the viscosity does not exceed ± 1.8 %. An equation describing viscosity of the studied reservoir waters and the dependence with the mineralization, pressure and temperatures is given.

Keywords: equation, measurements, liquid, viscosity, thermodynamic

I. Introduction

In comparison with the sea shipping, systematic pollution of the sea by oil seems insignificant under oil-and-gas field engineering. But within drilling and oil extraction in Azerbaijan it's possible the hit if high-toxic drilling fluid and chemical reagents of the reservoir and insipid refinery waters.

Rigid norms of sea disposal of the waters of production and as well as inconsistency among the norms and corresponding methods of cleaning and neutralization of the sea disposal require

The decision of this important problem on the sea fields, where together with oil reservoir waters are extracted, is necessity of desalination of the water by thermal method [2].

Designing effective methods of desalination of the sea water, salty and brackish waters, demands awareness of thermal properties of the solution of the water salt systems under increase characteristics of condition.

Experimental studying of thermal properties in the reservoir waters and its desalination will represent possibility by usage of the thermal method of drilling of the oil and water and increasing of recoverable oil.

Viscosity concerns to the main thermal properties of the liquids and gases.

II. Experimental

Samples for researches of reservoir waters have been taken from the Quintile- sea field. The

Chemical composition of the reservoir waters and the number of the well are given in Table 1.

Experiments have been held on the installation based on the method of remote capillary in the relative variant of changes [3].

The theoretical grounds of this method is the equation for laminar stream of Gagen-Puazey:

$$\mu = \frac{\pi(p_1 - p_2)r^4}{8\nu\ell} \quad (1)$$

where r radius of capillary and ν volume of gases flowing through capillary and $p_1 - p_2$ change of pressure at the end of capillary and ℓ length of capillary.

According to the equation (1), the accuracy of calculation of the coefficient of the viscosity depends on the accuracy of determination of geometric measure of the capillary, the significance of change of pressure at the end of the capillary, the volume of gases and liquid, flowing through the capillary at the unit of time.

This method was realized in different variants of authors [4-9] for research of both gases and liquid in large spheres of state parameters, where both the basic advantages and disadvantages of the method were noted.

The scheme of the experimental installation of measuring of viscosity is presented in the Fig.1. The main element of the installation is capillary 5 from stainless steel with diameters 0.22 mm and length 195 mm, which in joint to the lengthening 6. With the help of this lengthening the stream analysing the liquid is directed to the cold zone. The lengthening joint to the flange 7, combined with mobile cylinder 9, which in its turn, communicates with still cylinder 11 with the help of the joint tube 10.

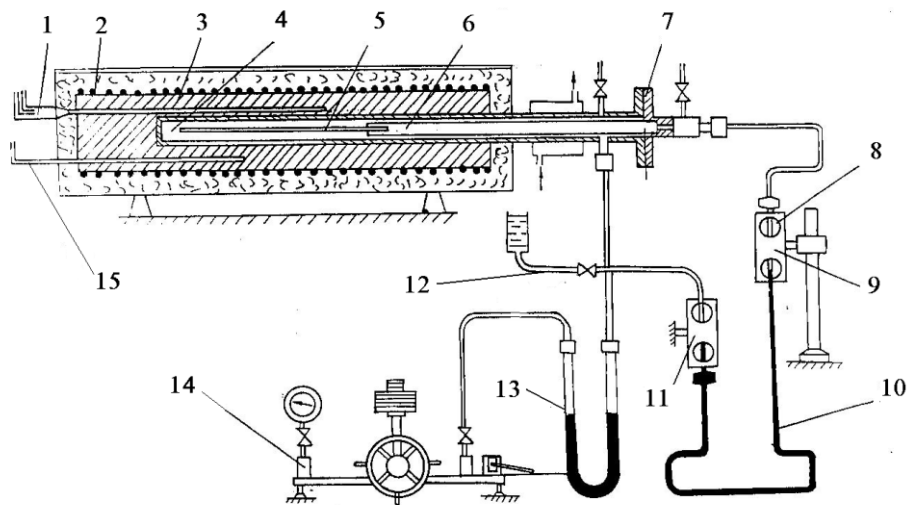


Fig. 1: The scheme of experimental installation for determination of viscosity of the substance during large interval of temperature and pressure: 1- resistance thermometer; 2- electric heaters; 3- copper block; 4- autoclave; 5- capillary; 6- lengthening; 7- flange; 8- peep-holes; 9 and 11 - cylinder; 10- tube; 12- valves; 13- mercury manometer; 14- pressure gauge; 15- thermocouple.

The wider caintainness are envisaged for the preliminary stabilization of regime of the liquid stream through the capillary. The still cylinder 11 is combined with the autoclave 4. The entrance and exit sections of the measuring capillary have small conic expansion. The number Re does not exceed 400 in all experiences. During the motion of the mobile cylinder 9 to the upward the mercury flows from this cylinder to the still cylinder 11, with this playing the role of the liquid piston of measuring instrument's pump with the help of which the liquid flow through the capillary is realized.

The cylinders 9 and 11 having the same volume are supplied with both peep-holes 8 from orgglass with interal diameters 1 mm and taken a risk for them cutting off the volume of the cylinders. Details of the installation contacting with the analysing liquid are made from stainless steel.

Massive copper block 3 from red copper on the surface of which two electric heaters 2 winded along all length are pressed on the autoclave 4. There is a heat –insulation layer from asbestos, basaltic cotton and glass material on upward of the heater.

Filling the installation the analysing liquid is made thourgh valve 12. The cylinders were filled with the weighed quality thourghly puled from the wixed mercury. All experiences were held with constant mercury.

Temperature was measured with a platinum resistance thermometer with an accyarcy of 0.01 °K. The temperature of the magnetic suspension was measured with mercury-in-glass thermometers with a precision of 0.1 °K.

Pressures were generated and measured with a dead weight gauge at pressures greater than 0.1 Mpa while a differential manometer was used for atmosphere pressure. In accordance with the recommendations of [10], the experimental uncertainties are for temperature ± 3 mK, pressure greater than $0.1 \pm 5 \cdot 10^{-2}$ Mpa and $\pm 5 \cdot 10^{-4}$ Mpa for atmospheric pressure, and $\pm 3 \cdot 10^{-4}$ kg·m⁻³ for density.

The time of flow of the liquid through the capillary was measured with the help of the stop-watch SW-50 with the value of division 0.1 s, and arithmetical mean from several changes was used in calculations.

Uncertains gained values of dynamic viscosity on condition of the mistakes concerning the pressure, mineralization and temperature does not exceed $\pm 1,8$ %.

There are examples, gained value of the viscosity of the reservoir waters have been given in the Tables 2,3,4.

III. Results

For convenience of practical usage of the data’s concerning the viscosity should access the equation of the viscosity [11-15].

This equation describing the coefficient of the viscosity in dependence with the mineralization, pressure and temperature, which describe as:

$$\eta_{p,w} = 1537 + (1 + 0.0115 \cdot C^{1.25}) \eta_{water}, \quad (2)$$

where η_{water} - waters viscosity and C- mineralization of the reservoir water.

New given equation for viscosity, which keeps an interval of the temperatures (298.15 to 598.15) °K. Equations (2) describe the experimental results of tables 2 to 4 within less then 0.8 %.

IV. Conclusions

The experimental data’s concerning the viscosity of the reservoir waters in the range diapason of the condition parameters have been given in this work.

Real research of the reservoir waters takes the temperature interval (298.15 to 598.15) °K and by the pressure of (0.1 to 40) MPa.

The viscosity of the reservoir waters has been measured by determined method of remote capillary.

Defect of the measures of the viscosity is $\pm 1,8$ %.

Given equation, describing experimental data’s by the viscosity with exact accuracy.

Table 1: *Chemical compound reservoir waters*

No of the Oil well	PH	Bome	Hardness	Na+K g.	Ca g.	Mg g.	Cl g.	SO ₄ g.	CO ₃	HCO ₃ g.	NT g.	HB ₄ O ₇ g.	Total	S ₁	S ₂	A	a
176	6.5	2.01	27.02	6.2	0.3	0.12	7.3	2.8	0	1.2	0.1	0.08	18.1	82.1	0	16.36	1.54
81	6	2.43	52	8.4	0.6	0.27	11.4	2.5	0	0.7	1	0.9	25.77	69.58	0	27.69	2.26
158	7	3.82	22	12.1	0.24	0.12	18	0.021	0	0.2	0.77	1.1	32.55	64.14	0	34.08	0.8

Table 2: *Experimental values of dynamic viscosities of pore waters consist of C = 18.11 g/l*

T/K	
p/MPa	298.15 323.15 348.15 373.15 398.15 423.15 448.15 473.15 498.15 523.15 548.15 573.15 598.15
	$\eta \cdot 10^7 (Pa \cdot s)$
0.1	9128.04 5667.61 3910.42
5	9128.65 5680.20 3921.38 2954.33 2350.29 1941.62 1646.09 1426.72 1257.61 1119.90
10	9129.79 5693.17 3934.17 2966.85 2363.78 1954.55 1660.13 1439.24 1268.28 1148.46 1023.58 934.23
15	9130.80 5698.77 3947.22 2979.18 2373.47 1967.01 1673.20 1452.99 1282.92 1148.46 1040.30 952.12 846.72
20	9131.75 5721.10 3960.27 2991.50 2388.15 1979.46 1686.14 1466.73 1297.55 1164.09 1057.02 970.01 871.91
25	9132.57 5727.56 3967.34 2999.23 2396.51 1988.24 1695.78 1477.02 1308.49 1175.70 1069.29 982.97 890.17
30	9133.38 5734.01 3974.44 3006.95 2404.87 1997.45 1705.42 1487.30 1319.43 1187.30 1081.56 995.93 910.03
35	9133.44 5745.10 3986.57 3018.43 2416.43 2009.71 1717.60 1501.48 1331.37 1198.91 1093.71 1009.41 927.18
40	9135.57 5757.36 3997.38 3030.71 2428.50 2012.56 1729.09 1513.66 1343.79 1210.83 1105.83 1023.30 943.71

Table 3: *Experimental values of dynamic viscosities of pore waters consist of C = 25.77 g/l*

p/MPa	T/K												
	298.15	323.15	348.15	373.15	398.15	423.15	448.15	473.15	498.15	523.15	548.15	573.15	598.15
$\eta \cdot 10^7 (Pa \cdot s)$													
0.1	9219.45	5735.41	3963.57										
5	9219.46	5748.77	3974.60	2999.19	2388.72	1975.56	1679.47	1455.23	1281.29	1144.61			
10	9219.47	5761.59	3987.66	3011.22	2401.98	1988.29	1690.55	1467.15	1294.32	1157.50	1047.32	957.42	
15	9219.48	5767.24	4000.89	3023.72	2414.36	2000.96	1703.79	1481.65	1309.26	1173.75	1064.43	975.75	870.35
20	9219.49	5789.85	4014.11	3036.24	2426.74	2013.63	1717.03	1495.18	1324.19	1189.45	1081.53	994.08	895.98
25	9225.52	5796.38	4021.29	3044.08	2435.24	2022.79	1726.85	1505.67	1335.35	1201.30	1094.09	1007.60	914.80
30	9231.53	5802.91	4028.47	3051.92	2443.73	2031.94	1736.67	1516.15	1346.51	1213.15	1106.65	1020.65	931.75
35	9231.54	5816.06	4040.03	3063.61	2456.42	2043.57	1748.48	1528.07	1358.40	1244.68	1118.52	1032.46	946.56
40	9231.55	5828.41	4052.31	3075.50	2468.34	2056.92	1760.53	1540.66	1370.09	1257.31	1130.74	1044.86	961.36

Table 4: *Experimental values of dynamic viscosities of pore waters consist of C = 32.55 g/l*

T/K													
p/MPa	298.15	323.15	348.15	373.15	398.15	423.15	448.15	473.15	498.15	523.15	548.15	573.15	598.15
	$\eta \cdot 10^7 (Pa \cdot s)$												
0.1	9309.55	5821.98	4011.51										
5	9309.57	5824.58	4025.49	3055.61	2435.41	2017.45	1716.32						
10	9309.58	5827.18	4038.52	3053.21	2438.01	2020.05	1719.12	1493.33	1318.69	1180.55	1069.44	978.96	
15	9309.59	5841.47	4051.92	3065.90	2450.58	2025.20	1732.59	1507.60	1333.91	1196.84	1086.91	997.70	892.32
20	9309.60	5855.76	4065.31	3078.58	2463.15	2045.79	1746.06	1521.86	1349.13	1213.13	1104.37	1016.44	918.34
25	9310.71	5862.36	4072.59	3086.54	2471.77	2055.09	1756.04	1532.53	1360.50	1225.51	1117.20	1030.01	934.21
30	9321.41	5868.96	4079.86	3094.48	2480.39	2064.39	1766.02	1543.20	1371.87	1237.87	1130.02	1043.61	954.71
35	9321.36	5875.62	4090.53	3106.71	2492.14	2076.41	1778.09	1555.71	1383.04	1248.16	1158.16	1055.40	969.50
40	9322.21	5887.30	4102.47	3118.56	2504.43	2079.58	1790.14	1567.30	1395.33	1260.47	1170.82	1069.06	985.56

References

- [1] Kasymov, A.Q. Ecology of the Caspian lake. Baku. 1994, 7-9.
- [2] Akberov, R.M. Investigation of influence on layer by water solution of the polymer for increasing oil recovery. *Azerbaijan oil facilities of Baku*. 1998, 7, 36-39.
- [3] Akhundov, T.S.; Guseynov, A.T. The viscosity of the water solution of the chloride sodium. *Oil-and-gas*. 1990, 7, 65-68.
- [4] Golubev, I.F.; Qnezdilov, N. E. Mixtures of the viscosity of gases. Mockow. 1971, 327.
- [5] Golubev, I.F. Mixtures of the viscosity of gases. Mockow. 1959, 375.
- [6] Abdullaev, F.G.; Akhundov, R.T. The Experimental research of dynamic viscosity on Benzene and cholorebenzene high temperature. *Oil-and-gas*. 1983, 2, 53-59.
- [7] Shatenshteyn, A.A.; Izrailevich, E. A.; Ladijnikova, N. I. Mixtures of the viscosity of gases. Mockow. *JFCh*. 1959, 4, 88.
- [8] Pepinov, R.I.; Lobkova, N. B.; Panachov, I. A. On the viscosity of the mixture of water and natrium the stream temperature and pressure. Mockow. 1975, 46, 42-48.
- [9] Cemenyuc, E.H.; Lvov, C. H.; Zarembo, V. K. The measured reservoir temperature (273 to 670) °K and pressure (to 200) MPa for the viscosity of the mixture of electrolytes. Mockow. *JPCH*. 1977, 50, 2, 127.
- [10] Rivkin, S.L.; Aleksandrov, A. A. The thermodynamic properties of water and water vapor. *Energy*, Moskow. USSR. 1975, 80.
- [11] Hales, J.L. Ellender Liquid Densities from (293 to 490) °K of nine aliphatic alcohols. *Chem.Thermod*. 1976, 8, 1177-1184.
- [12] Achundov, T.S.; Iscenderov, A. I.; Tahirov, A. D.; Achmedova, I. N.; Imanova, M. V.; Achundov, R.T.; Ishcanov, Ju; Huseynov, A. G. Termal Properties and viscosity of Aqueous Solutions of Alkaline Metal Halogenides and Alkaline-Earth Metal Nitrates. *11th International conference on Properties of steam*. Prague. 1989, 25.
- [13] Stokes, R.H.; Mills, R. Viscosity of Electrolytes and Related Properties. London. *Pergamon Press*. 1965, 110.
- [14] Chapman, T.W. The transport properties of consentrated electrolytes solutions. Berkeley. *University of Colifornia*. 1967, 202.
- [15] Grimes, C.S.; Kestin, J.; Khalifa, E. Viscosity of aqueous KCl solutions in the temperature range (25 to 150) °C and pressure range (0 to 30) MPa. *J.Chem. and Eng. Data*. 1979, 24, 2, 121 - 126.

SIMULATION MODELING AND MAPPING OF CATASTROPHIC FLOODS IN POORLY STUDIED AREAS FOR EMERGENCY RISK MANAGEMENT

Irina Oltyan¹, Elena Arefyeva¹, Mikhail Bolgov², Nikita Oltyan³

¹All-Russian Research Institute for Civil Defense and Emergencies of the EMERCOM of Russia

²Water Problems Institute of the Russian Academy of Science

³Financial University under the Government of the Russian Federation

irenaoltyan@mail.ru

elaref@mail.ru

bolgovmv@mail.ru

nikitaoltyan@mail.ru

Abstract

Method presented in the article for modeling parameters of catastrophic floods, such as the water level of the given probability of exceedance and depth of corresponding probability of exceedance, as well as the flooding area for unexplored territories, is based on the use of the digital relief model approach, construction of hydrographic network in the form of oriented graph characterizing the direction of water flow, invoking generalized regime hydrological information in the form of estimated parameters maps of the maximum flow, and the use of virtual gauging stations, as information reference points for calculations.

Keywords: flood, hydrological characteristics probability of exceedance, maximum flow, depth of flooding, virtual gauging station, digital relief model, orgraph.

I. Introduction

The problem of rain floods is typical for various regions of Russia, and the main aspect is the absence or insufficient reliability of the residential areas flooding zones boundaries, determined with disregard for the peculiarities of extreme water flow formation. Among the most dangerous events of the recent years, we can note the flood in Krymsk in 2012, rain floods in the Far East in recent years, and the outstanding flood of 2019 on the Iia River in the Irkutsk Region in June 2019

The flood of 2019 on the Iia River was catastrophic, followed by significant damage and human casualties [1]. Water levels exceeded the design values, not least due to the additional influence of hydraulic engineering structures (bridge crossings, dams) and narrowing of the riverbed [2]. Iia River basin is typical for the region in terms of flood formation conditions, and the region as a whole is quite well studied. Available study materials can be used as well a basis for the development of the methodological framework for assessing rare events required for flood risk management in built-up areas.

In order to reduce flood damage, develop preventive and protective measures for the territories of the Russian Federation constituent entities, it is required to compile the following cartographic materials based on hydrological probabilistic forecasts [3]:

- maps of the river basin marsh territories (boundaries of flood zones at maximum probability of exceedance water levels – 1%, 3%, 5%, 10%, 25% and 50%);
- maps of water risks caused by various types of negative water effects (with damage assessment);

– maps of the river basin territory zoning by flood hazard danger.

Methodological procedures of flood forecasting are largely determined by the spatial scale (namely, the degree of locality) of hydrological processes and their extremely large spatial variability. This leads to the fact that almost all main forecasting methods are empirical. Even in cases where theoretical dependencies and model approaches are used, it is necessary to determine their coefficients and parameters for specific water bodies by calibration, based on the results of local observations. This leads to a variety of methods used in practice to predict water regime [4, 5, 6, 7]. All these forecasting methods require large bulk of initial data, instrumental measurements, terrain studies and significant financial costs [8].

To assess the risk of emergencies, caused by floods, it is necessary to determine parameters that are used in flood modeling [9]: maximum rise water level; duration of flooding; zone of possible flooding.

For hydrological estimations having observational data at existing gauge stations, Set of Rules is currently used [10]. It is also advisable to use software package for determining hydrological characteristics for studied and insufficiently studied rivers, which is certified and includes three modules: HydroStatCalc.exe; FreqShrt2009.exe; ComposeFreq.exe [11]. For the river under study, the natural zone in which the river basin is located is established, and according to the available maps, the results of hydrological studies or by other means, the main morphometric characteristics used for calculations and defined in the regulatory documentation are determined [12].

Nowadays, geoinformation systems (GIS) are actively used as applied software for hydrological modeling and forecasting. Free database of hydrological estimation models is available and is constantly being updated; monitoring data, weather, digital terrain models, etc. appear in the public domain [13]. Based on the use of GIS, short-term flood forecasting systems (water levels and flow rates) are being created [14, 15].

It should be noted that in the Russian Federation there is a problem of information availability both on current hydrological characteristics and on archival data of hydrometeorological observations [13], which forms additional restrictions for long-term (strategic) forecasting. Thus, obtaining long-term forecast values of flood parameters (depth of flooding, flooding period duration, flooding zone), forecasts of rare events (floods with probability exceedance of 0.1-1%) is practically based on the use of the simplest correlations and other relationships and dependencies due to hydrological patterns and remains very approximate [6].

With limited data set, models based on geometric principles can also be used for flood modeling [14].

The authors of this article have developed the method for probabilistic forecasting of floods in the absence of data from permanent hydrological observations based on the use of digital relief model, requirements of methodological recommendations for determining hydrological characteristics with insufficient data from hydrometeorological observations [4, 5], as well as spatial regional generalizations of hydrometeorological observations over a long period (regional reference books) [16].

The task of modeling floods of rare recurrence is reduced to the following subtasks:

modeling of the water level rise (determining the flooding depth (waterdepth) at actual gauge stations according to the long-term observations of the highest observed water levels relative to zero of the hydraulic station for each probability of exceedance;

modeling of the water level rise (determining the flooding depth) (waterdepth) at "virtual" hydro posts - arbitrary virtual points on the ground identified by geographical coordinates, not equipped with points of hydrological observation, artificially "placed" in the fairway of the river, depending on the maximum predicted water flow, water flow volume, module and water flow layer, cross-sectional area of the riverbed at the location of the "virtual" gauging station;

possible flooding zone determination.

To determine the rise of the water level (depth of flooding) (waterdepth), logarithmic regression equation is set up on the actual gauge station:

$$waterdepth = b_0 \times \ln(P_{m,\%}) + b_1, \text{ sm}, \quad (1)$$

where b_0 , sm/%, b_1 , cm – logarithmic regression coefficient.

The empirical curve of the annual probability of exceeding $P_{m,\%}$ is based on the data of long-term observations of the highest observed water levels according to the formula [4]:

$$P_{m,\%} = \frac{m}{n+1} \times 100,\%, \quad (2)$$

where m – index number of the highest observed water levels series term, arranged in descending order, natural number

n – total series term, natural number.

Equation of regression coefficients (1) are determined by the least squares method.

To determine the water level rise of a given probability of exceedance (determining the depth of flooding) (waterdepth) at the "virtual" gauge stations, an original method of probabilistic modeling of the maximum rise of the water level has been developed, based on the construction of a channel network as an oriented graph, using a digital relief model and GIS.

Method of probabilistic forecasting of catastrophic floods parameters has been tested on the pilot Russian Federation entity – the Irkutsk Region.

Total length of the Irkutsk region rivers is 309355 km. According to Roshydromet, as of December 2022, 130 actual gauge stations (hereinafter referred to as AGS) operated in the Irkutsk Region (Fig. 1). Most of them have long observation period (Fig. 2).

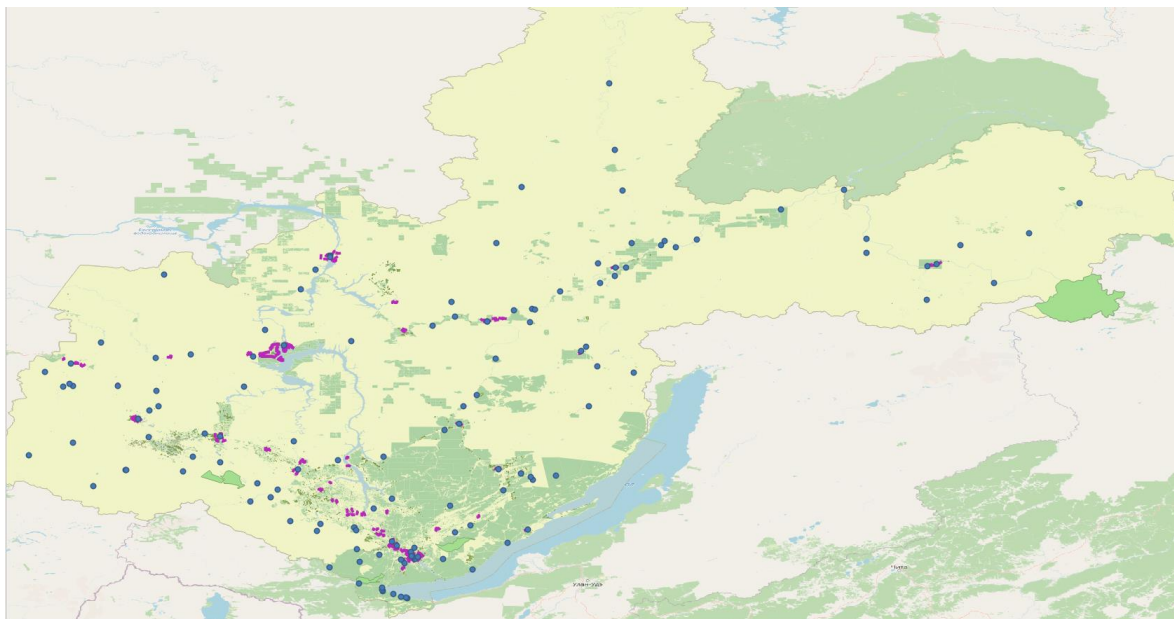


Fig. 1: Location of the actual gauge stations on the territory of the Irkutsk Region (blue dots) [source: obtained by the authors according to [17]]

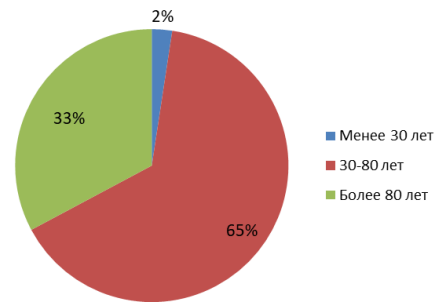


Fig. 2: Duration of observations at gauge stations of the Irkutsk Region [source: obtained by the authors according to [17]]

At the same time, about 2,100 settlements are located near rivers in the Irkutsk Region, and most settlements do not have points of regular instrumental hydrological measurements (gauge stations), i.e. they are considered as unexplored.

Territory of the Irkutsk Region belongs to three basin districts – Angara-Baikal, Yenisei, Lena (Fig. 3).

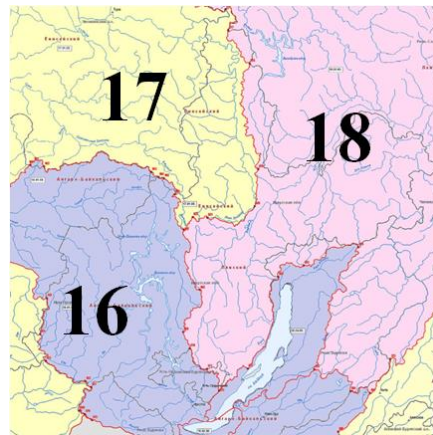


Fig. 3: Basin districts [18]. The numbers on the map are indicated by:
16 – Angara-Baikal Basin District; 17 – Yenisei Basin District; 18 – Lena Basin District

The region under consideration is characterized by increased flood danger, in recent decades there have been severe rain floods, led to enormous damage [2].

II. Methods

The method of probabilistic modeling of the catastrophic floods parameters is applicable for virtual gauging stations (hereinafter referred to as VGS) - arbitrary virtual points on the ground identified by geographical coordinates, not equipped with points of hydrological observation, artificially "placed" in the fairway of the river, relative to which the calculation of flood zones is carried out [12].

Virtual gauging station placement is an important stage in the modeling and forecasting of catastrophic flood parameters is [12, 19, 20]. VGS disposal was performed "manually" in the geographic information system QGIS – a free cross-platform open geographic information system for all watercourses of all river sections:

every 10 km starting from the mouth of each river on the main channel. It is recommended to place VGS on the relatively straight riverbed;

at a distance of 2-3 km downstream from the confluence of the river with another river;

additional VGS are installed in the middle between the gauge stations (AGS and/or VGS) in case of the settlements boundaries location at a distance of less than 2.5 km to the river.

Theoretical foundation of the method used is based on estimated dependencies that allow calculating hydrographic characteristics on the basis of digital relief model, determining hydrological parameters of floods of the given probability of exceedance: water level rise, duration of flooding, zone of possible flooding.

The main hydrological characteristic determining the water rise level is the maximum flow rate, determined in the absence of analogous rivers by the reduction formula [10]:

$$Q_{pmax} = q_{200} \left(\frac{200}{S_{basin}} \right)^n \times \lambda_p \times \delta_1 \times \delta_2 \times S_{basin}, \quad (3)$$

where q_{200} – the module of the maximum instantaneous annual water discharge of the probability of exceeding 1%, reduced to the catchment area of 200 km²; n - indicator of the maximum flow module reduction degree, determined by the map of the USSR rivers maximum rain runoff modules; S_{basin} - catchment area at the point of hydrological observation; λ_p - transition coefficient from the probability of exceeding 1% to the probability of p .

Coefficients values used in the reduction formula (3) are given in regional reference books and regulatory documents. Such a regional reference book is, for example, a multi-volume publication [16], the data in which has not been updated for the last 50 years. Since the Irkutsk Region does not belong to the regions with increased climatic risks [22], the long-term stationarity of the coefficients used in the formula (3) was assumed in the work.

Raster maps are used for carrying up hydrological estimations. GIS layers were created based on the raster maps of the USSR rivers maximum modules of the rain runoff, with a probability of exceeding $p=1\%$ (parameter q_{200} , M³/C×KM²) (Fig. 4) [21, Appendix 5], indicator of the maximum flow module reduction degree n [21, Appendix 6].

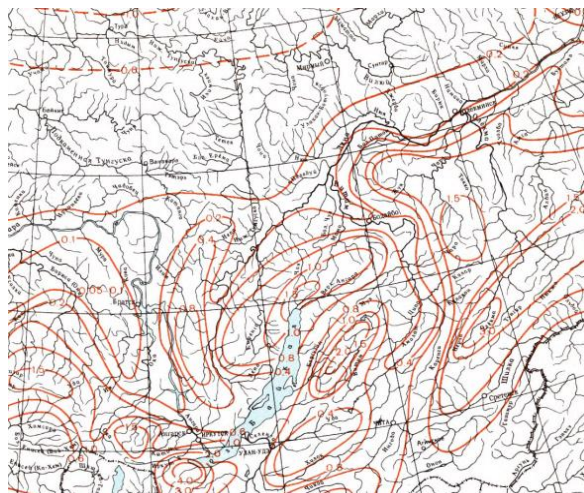


Fig. 4: Part of the map reflecting maximum modules of the USSR rivers rain runoff, with a probability of exceeding $p=1\%$, for a part of the Irkutsk Region [21, Appendix 5]

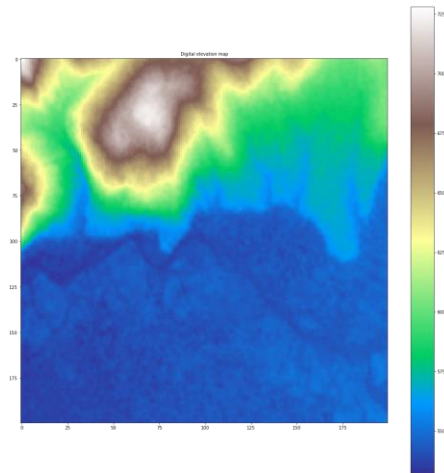
Algorithm for determining the hydrological parameters listed above and used in formula (3) by interpolation using GIS has been developed and presented in [19].

The area of S_{basin} catchment in the absence of data can be determined using digital terrain models (hereinafter referred to as DTM) [14] using the Deterministic Eight Neighbor algorithm [23].

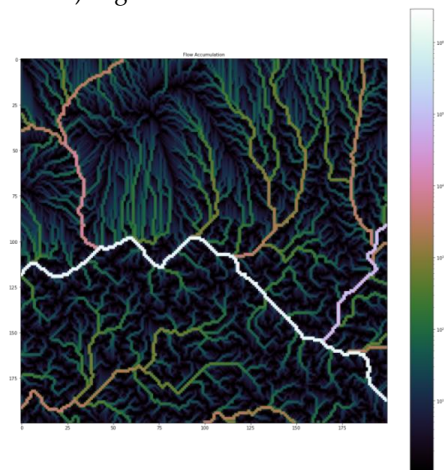
In the works [12, 19, 20], method for determining the catchment area using DTM was applied and an approach to constructing hydrographic network using orgraph $G = (V, E)$ with information about the flow, where each node in the node set $V = \{ v_1, v_2, \dots, v_n \}$ is also shown and applied contains the coordinates of the cell (lon_x, lat_y) in the DTM, the height of the cell (height) of the

DTM above sea level, the number of cells that "flow" into this cell (acc_flow), and each edge $v_i \rightarrow v_j \cap E$ shows that node v_i is the parent node for the descendant node v_j (water "flows out" from node v_i and "accepted" by node v_j) [19, 24].

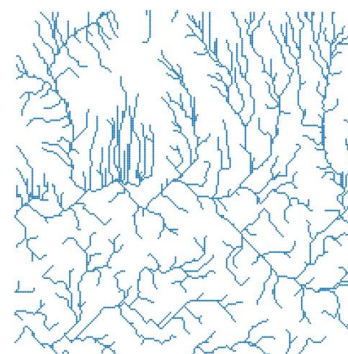
Construction of a channel network diagram in the form of the orgraph was performed using the NetworkX library, created in Python and designed to work with graphs and other network structures [25] (Fig.5).



a) Digital terrain model - SRTM



b) Flow accumulation raster



c) Orgraph of flow directions (watercourse model)

$$G = (V, E); V = \{v_1, v_2, \dots, v_n\}; v_i \rightarrow v_j \cap E$$

Fig. 5: Procedure for constructing watercourse model using DTM and orgraph

The predicted depth of flooding at the location of the virtual gauge station is determined on the basis of the maximum water flow calculated according to the formula (1) of the given probability of exceedance and the water area (cross-section). The cross section of the riverbed and

valley at the location of the virtual gauge station is constructed using digital relief model by constructing virtual plane perpendicular to the riverbed and finding the coordinates of the intersection of the virtual plane with DTM [20].

The depth of flooding (waterdepth) for each Q_{pmaxi} of the given probability of exceedance (frequency) and each cross-section of the riverbed and valley is determined by the iteration method according to the graph of the flow curve of a given probability of exceedance (Fig.6), illustrating the relationship between flow rates and water levels for the type watercourse section, given in general form by the formula:

$$h=f(Q), \tag{4}$$

where Q – flow, m^3/c ;

h – waterdepth, m .

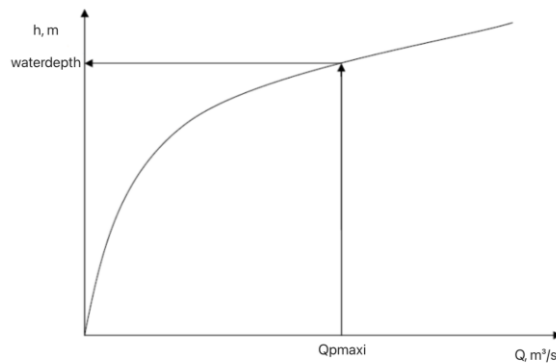


Fig. 6: Function graph $h=f(Q)$ [20]

Construction of the probable flooding zone using watercourse model presented in the form of oriented graph $G = (V, E)$ (Fig.5c) was carried out using digital relief model by the excess method [19], for which the open library pysheds [20] was used.

III. Results

To simulate catastrophic floods parameters, the VGS was arranged for all watercourses of the Irkutsk Region (Table 1, Fig. 7).

Table 1: Number of gauging stations used for modeling

Basin District	AGS number	VGS number
Angaro-Baikal	78	1162
Yenisei	7	110
Lensky	45	626
Total	130	1898

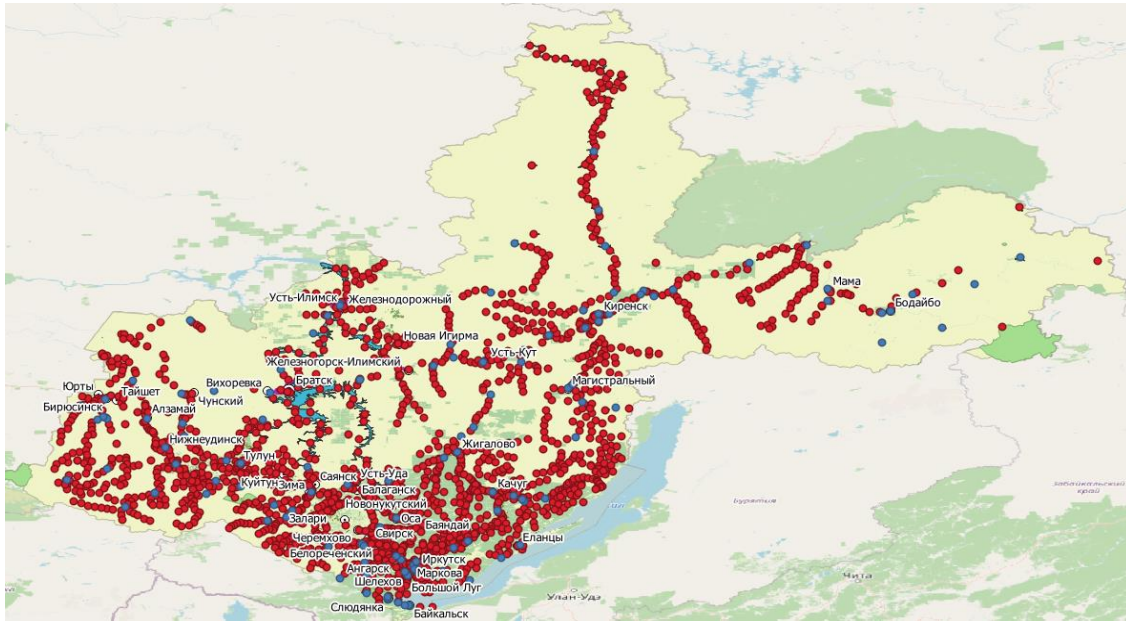


Fig. 7: Location of AGS and VGS on the Irkutsk Region territory
The map shows: AGS – blue dots; VGS – red dots [source: obtained by the authors]

Below are the results of modeling and mapping the parameters of catastrophic floods in some areas of the Irkutsk Region (Uslon municipality and the city of Zima), which were flooded in July 2019 as a result of an emergency, the source of which was a dangerous hydrometeorological phenomenon.

The municipalities under consideration are not equipped with stationary hydrological observation points. The nearest gauging station is located at a distance of 12 km from the village of Samara (FHP 8207 Ukhtui).

Water levels diagram in the period from 01.06.2019 to 30.08.2019 at FHP 8207 Ukhtui is shown in Fig.8.

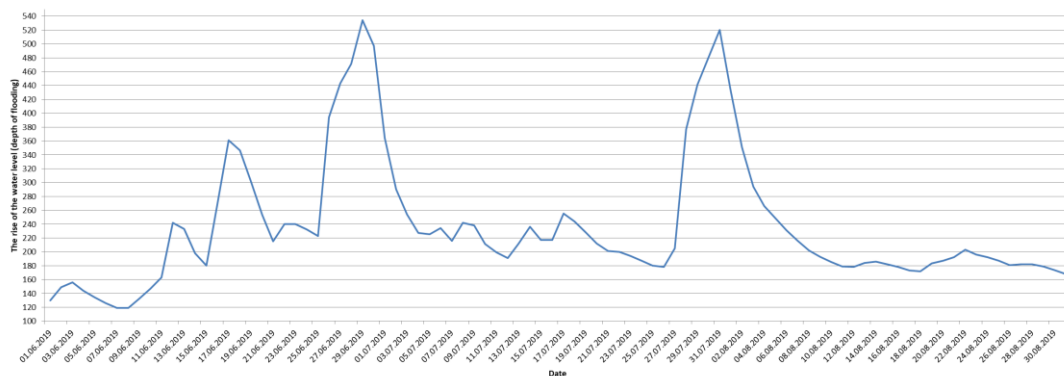


Fig. 8: Water levels diagram at FGP 8207 Ukhtui

Simulated values of catastrophic floods parameters for AGS and VGS in the city of Zima area and Uslonsky municipality (Samara village, Nizhny Khazan village, Zaimka Polkovnikova), which were flooded [26], are given in Table. 2 and in Fig. 9.

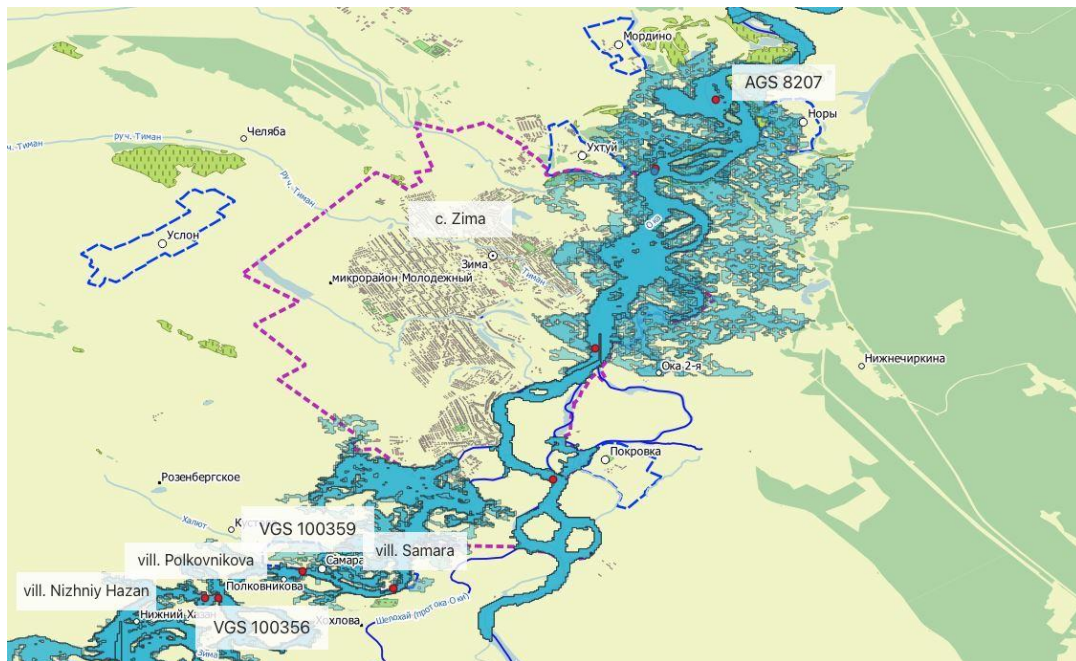


Fig. 9: Flooding zones for virtual and actual gauging stations shown in Table 2

Based on the simulation results, spatial data sets were formed in the shape file format, including information about gauging stations (actual and virtual) and flood zones, with the estimated parameters of flooding depth and duration for each probability of exceedance (so-called synthetic flood catalogs).

Table 2: Estimated results of catastrophic floods parameters for actual and virtual gauging stations in the area of the city of Zima and the Uslonsky municipality (Samara village, Nizhny Khazan village, Polkovnikova zaimka) (Fig.9)

GS number	GS type	Latitude, degrees.	Longitude degrees.	River	S_basin	q ₂₀₀	Probability of exceedance, %	Q _{pmaxi} (formula (3))	Flooding depth, waterdepth, m
100356	VGS	53,843135	101,981208	Zima	4531,31	0,1	0,5	190,03	2,79*
							1,0	152,02	2,60*
							5,0	106,42	2,33*
							10,0	85,13	2,18*
							20,0	68,41	2,05*
100359	VGS	53,8498110	102,005462	Zima	4564,37	0,1	0,5	190,93	2,29*
							1,0	152,74	2,12*
							5,0	106,92	1,87*
							10,0	85,54	1,74*
							20,0	68,73	1,62*
8207	AGS	53,949550	102,092926	Oka	27000	0,1	0,5	N/A	7,00**
							1,0	N/A	6,53**
							5,0	N/A	5,45**
							10,0	N/A	4,94**
							20,0	N/A	4,42**

Notes:

* – flooding depth estimated according to the formula (3)

** – flooding depth estimated according to the formula (1)

IV. Discussion

Original method of catastrophic floods modeling and mapping in the areas poorly studied in hydrological terms is presented, based on the digital relief model use, hydrographic network construction in the form of orgraph characterizing water flow direction, engagement of generalized regime hydrological information in the form of maps, as well as the results of its application for the pilot entity – the Irkutsk Region.

It is found that with the same catchment areas, maximum water consumption is affected by the value of the maximum urgent annual water consumption module of the probability exceeding 1%, which depends on the geographical location of virtual gauging stations.

Developed original method can be used in predicting emergencies consequences, caused by floods, in planning protective measures, determining the boundaries of the population emergency notification about the threat of occurrence or the occurrence of emergency situations. Obtained flood zones allow determining the index of the territory's susceptibility to floods [27, 28] within the framework of remote risk assessment technology [29].

Original method can also be used in the development of unified documents for the territorial planning and urban zoning of a settlement, an urban district, which should include information about territories at risk of natural and man-made emergencies.

In general, the wide application of the presented original method in the activities of local self–government bodies, executive authorities of the Russian Federation entities, design, insurance and scientific organizations will reduce the risk of emergency situations, move from the practice of responding to emergency to its prevention, ensure the achievement of Sustainable Development Goal 11 - Ensuring openness, security, resilience and environmental sustainability of cities and settlements.

References

[1] Gosudarstvennyj doklad «O sostoyanii zashchity naseleniya i territorij Rossijskoj Federacii ot chrezvychajnyh situacij prirodnoho i tekhnogennogo haraktera v 2019 godu» [Web page]. URL: <https://mchs.gov.ru/dokumenty/4602?ysclid=lj87ia2orw500136804> (accessed 23.06.2023).

[2] Estimates of Peak Flow of the Iya River during the Extreme Flood in 2019 / M. V. Bolgov, E. A. Korobkina, N. V. Osipova, I. A. Filippova // Russian Meteorology and Hydrology. – 2020. – Vol. 45, No. 11. – P. 783-790. – DOI 10.3103/S1068373920110059. – EDN MVKNJL.

[3] Prikaz MPR RF ot 4 iyulya 2007 g. № 169 «Ob utverzhdenii Metodicheskikh ukazaniy po razrabotke skhem kompleksnogo ispol'zovaniya i ohrany vodnyh ob"ektov» [Web page]. URL: <https://base.garant.ru/12155160/> (accessed 18.07.2023).

[4] Metodicheskie rekomendacii po opredeleniyu raschetnyh gidrologicheskikh harakteristik pri nedostatochnosti dannyh nablyudenij. Sankt-Peterburg: Rotaprint GNC AANII, 2004 [Web page] URL: <http://spb-hydrology.ru/wp-content/uploads/2016/03/6.-Методические-рекомендации-2.pdf> (accessed 18.07.2023)

[5] Metodicheskie rekomendacii po opredeleniyu raschetnyh gidrologicheskikh harakteristik pri otsutstvii dannyh gidrometricheskikh nablyudenij. Sankt-Peterburg: GGI. [Web page]. URL: <http://www.hydrology.ru/ru/content/metodicheskie-rekomendacii-po-opredeleniyu-raschetnyh-gidrologicheskikh-harakteristik-pri-5> (accessed 18.07.2023).

[6] Rukovodstvo po gidrologicheskim prognozam. Vyp. 1, Dolgosrochnye prognozy elementov vodnogo rezhima rek i vodohranilishch. // L.GIMIZ, 1989. 258 p.

[7] Rukovodstvo po gidrologicheskim prognozam. Vyp 2, Kratkosrochnyj prognoz raskhoda urovnya vody na rekah. // L. GIMIZ, 1989, 246 p.

[8] Koren', V.I. Matematicheskie modeli v prognozah rechnogo stoka. / L. GIMIZ, 1991. – 198 p.

[9] Metodika kompleksnoj ocenki individual'nogo riska chrezvychajnyh situacij prirodnogo i tekhnogenogo haraktera. M.: MCHS Rossii, 2002. [Web page] URL: <https://pandia.ru/text/80/201/4021.php> (accessed 08.07.2023).

[10] SP 33-101-2003. Svod pravil. Opredelenie osnovnyh raschyotnyh gidrologicheskikh harakteristik.

[11] Kokorev, A.V. Rukovodstvo pol'zovatelya Programmnye sredstva avtomatizacii inzhenernyh gidrologicheskikh raschetov HydroStatCalc. /A.V. Kokorev, A.V. Rozhdestvenskij, A.G. Lobanova// SPb, FBGU «Gosudarstvennyj gidrologicheskij institut», 2015.

[12] O metode prognozirovaniya parametrov katastroficheskikh navodnenij na neizuchennyh territoriyah v celyah ocenki riska chrezvychajnyh situacij / A. N. SHCHeglov, K. YU. ZHalnin, I. YU. Oltyan [i dr.] // Tekhnologii grazhdanskoj bezopasnosti. – 2022. – T. 19, № 3(73). – p. 78-83. – EDN MXDHWZ.

[13] P'yankov S.V. Geoinformacionnoe obespechenie modelirovaniya gidrologicheskikh processov i yavlenij: monografiya / S.V. P'yankov, A.N. SHihov// Perm. gos. nac. issled. un-t. – Perm', 2017. – 148 p., il.

[14] Borshch, S.V. (2013) Vizualizaciya gidrologicheskoy obstanovki v bassejnah krupnyh rek sredstvami GIS-tekhnologii / S. V. Borshch, T. E. Samsonov, YU. A. Simonov, E. A. L'vovskaya // Trudy Gidrometeorologicheskogo nauchno-issledovatel'skogo centra Rossijskoj Federacii. – № 349. – p. 47-62. – EDN RDJAJB.

[15] Borshch, S.V. (2015) Sistema prognozirovaniya pavodkov i rannego opoveshcheniya o navodneniyah na rekah Chernomorskogo poberezh'ya Kavkaza i bassejna Kubani /Borshch S.V., Simonov YU.A., Hristoforov A.V. // Trudy Gidrometcentra RF. Spec. vyp.. 247 p.

[16] Resursy poverhnostnyh vod SSSR //Leningrad. Gidrometeoizdat. Гидрометеоиздат, 1972 г.

[17] ESIMO web page. [Web page] URL: http://esimo.ru/dataview/viewresource?resourceId=RU_RIHMI-WDC_2665 (accessed 14.07.2023)

[18] Map of basin districts of the Russian Federation. [Web page] URL: <https://ozera.info/fishing/fisher/code-practice/karta-bassejnovyh-okrugov-rossijskoj-federacii> (accessed 14.07.2023).

[19] Rezul'taty raschetov gidrologicheskikh parametrov dlya ocenki riska chrezvychajnyh situacij na neizuchennyh territoriyah na osnove modelirovaniya katastroficheskikh navodnenij / A. N. SHCHeglov, K. YU. ZHalnin, G. P. Radionov [i dr.] // Tekhnologii grazhdanskoj bezopasnosti. – 2022. – T. 19, № 4(74). – p. 11-19. – EDN MLTITI.

[20] O rezul'tatah primeneniya metoda prognozirovaniya parametrov katastroficheskikh navodnenij na neizuchennyh territoriyah v celyah ocenki riska chrezvychajnyh situacij / A. N. SHCHeglov, I. YU. Oltyan, E. V. Aref'eva [i dr.] // Tekhnologii grazhdanskoj bezopasnosti. – 2023. – T. 200, № 1(75). – p. 48-56. – EDN CZWUUT.

[21] Ukazaniya po opredeleniyu raschetnyh gidrologicheskikh harakteristik/ SN 435-72.

[22] Climate risk assessment to develop sector climate change adaptation plan // E. Arefyeva, I. Oltyan, V. Krapukhin. RT&A, Special Issue № 4 (70) Volume 17, November 2022 [Web page] // URL: https://www.gnedenko.net/Journal/2022/SI_042022/RTA_SI_4_2022-76_581-586.pdf (accessed 06.02.2023).

[23] O'Callaghan J.F., Mark D.M. The extraction of drainage networks from digital elevation data // Computer vision, graphics, and image processing.1984. V. 28(3). P. 323–344.

[24] Algoritm postroeniya grafa, opisyyayushchego gidrologicheskuyu set'. (2022) Svidetel'stvo o registracii sekreta proizvodstva (nou-hau) № GCH-0077. M.: FGBU VNII GOCHS (FC).

[25] NetworkX dlya udobnoj raboty s setevymi strukturami [Web page] URL: <https://habr.com/ru/post/125898/> (accessed 13.11.2022).

[26] Postanovlenie Pravitel'stva Irkutskoj oblasti oto 24 sentyabrya 2019 g. № 797-pp. [Web page] URL: <http://publication.pravo.gov.ru/Document/View/3800201910020001> (accessed

13.07.2023).

[27] M V Bolgov *et al* Managing Hydrological Risk in the Urbanized Territories in the Framework of Implementing the Concept of Smart Cities Territories. International Journal of Engineering Research and Technology. ISSN 0974-3154, Volume 13, Number 12 (2020), pp. 4892-4898 © International Research Publication House. <http://www.irphouse.com>.

[28] V G Plyuschikov *et al* Hydrological Risk Management of Urbanized Areas in Framework of the Smart City Concept 2021 *IOP Conf. Ser.: Earth Environ. Sci.* 691 012019.

[29] Oltyan, I. Y. Remote assessment of an integrated emergency risk index / I. Y. Oltyan, E. V. Arefyeva, A. S. Kotosonov // IOP Conference Series: Materials Science and Engineering : International Conference on Construction, Architecture and Technosphere Safety, ICCATS 2020, Sochi, 06–12 September 2020. Vol. 962, 4. – Sochi: IOP Publishing Ltd, 2020. – P. 042053. – DOI 10.1088/1757-899X/962/4/042053. – EDN XJGGYQ.

FIBER-OPTIC SENSOR FOR FUNCTIONAL SECURITY OF THE OBJECT PERIMETER PROTECTION SYSTEM

Tofiq Mansurov¹, Elnur Mansurov¹, Irina Yablochnikova², Gulnar Gurbanova¹,
Rahman Mammadov¹

•

¹Azerbaijan Technical University

²Moscow Technical University of Communications and Informatics, Russia

tofiq-mansurov@rambler.ru

irayablochnikova@mail.ru

mansurovelnur@mail.ru

gurbanovagulnar474@gmail.com

r.s.mamedov@mail.ru

Abstract

As a result of the analysis, it was concluded that the existing fiber-optic sensors are mainly used to detect the place of unauthorized access. For this purpose, a fiber-optic sensor has been developed using G 655 optical fiber with the highest susceptibility to macrobending, which makes it possible to determine not only the fact of unauthorized access, but also the parameters of the penetrating object, namely its mass, to increase the measurement range of the attenuation of the branched signal of optical radiation due to amplification of this signal and the measurement limit of the body weight of the object of unauthorized access due to the choice of the spring stiffness coefficient. Experimental studies have been carried out to determine the susceptibility of various types of optical fiber to macrobending, the dependence of the attenuation of the optical radiation signal on the macrobending radius, the length of the macrobending arc, and the mass of the unauthorized access object.

Keywords: optical fiber, sensor, guarded object, macrobend, deformation, mass

I. Introduction

In fiber-optic sensors, as a sensitive element for detecting changes in information parameters about the state of a particular protected object, an optical fiber with the highest susceptibility to macrobending is mainly used, which expands the scope of their application.

Currently, many fiber-optic sensors have been developed that allow recording deformation, vibration, tilt angle, acceleration, displacement, pressure, as well as detecting unauthorized access to the perimeters of a protected object [2-5]. To measure deformations, vibrations and other mechanical effects, as a fiber-optic sensor to ensure the functional security of the perimeter security system of an object, optical fibers are mainly used, through which useful information is simultaneously transmitted [6]. The applicability of fiber optic technologies is determined mainly by immunity to electromagnetic fields and electrical safety. In case of unauthorized access to the perimeters of the protected object, external influences are created in the form of mechanical pressures, deformations and / or vibrations, which in turn leads to a change in the parameters of the transmission medium and, as a result, the parameters of the optical radiation signal transmitted through the optical fiber.

II. Formulation of the problem

As is known [2-6, 8-11], the existing fiber-optic sensors allow detecting the fact of unauthorized access to the territory of the protected object, but cannot determine the mass of the object of unauthorized access. In this regard, there is a need to develop a fiber-optic sensor to ensure the functional security of the perimeter security system of an object, which makes it possible to determine not only the fact of unauthorized access, but also parameters, namely the mass of an unauthorized access object and conduct experimental studies on choosing the type of optical fiber as sensing element, the dependence of the attenuation of the optical radiation signal on the radius of the macrobend, the length of the arc of the macrobend and on the mass of the object.

In this case, functional safety is the safe operation of safety-related facilities and other means of risk reduction. In the event of a critical situation, the fiber optic sensor branches off the optical radiation signal, this signal is sent to the control panel and the system puts the equipment in a safe state. For the development of a fiber-optic sensor, an optical fiber of the G655 type with the highest susceptibility to macrobending was chosen. It has been established that an increase in the length of the macrobending arc at a constant radius leads to an increase in the attenuation of the optical radiation signal in the optical fiber [2].

The purpose of this work is to develop a fiber-optic sensor to ensure the functional security of the perimeter security system of an object, which would allow to determine not only the fact of penetration, but also the parameters, namely the mass of the object.

III. Development of a fiber optic sensor

Based on the analysis of the principles of construction of existing fiber optic sensors [2-6], a fiber optic sensor was developed to ensure the functional safety of the perimeter security system of an object with a macrobend shaper (FMI) of an optical fiber and a measuring device (MD), the schemes of which are shown in Fig.1 [1].

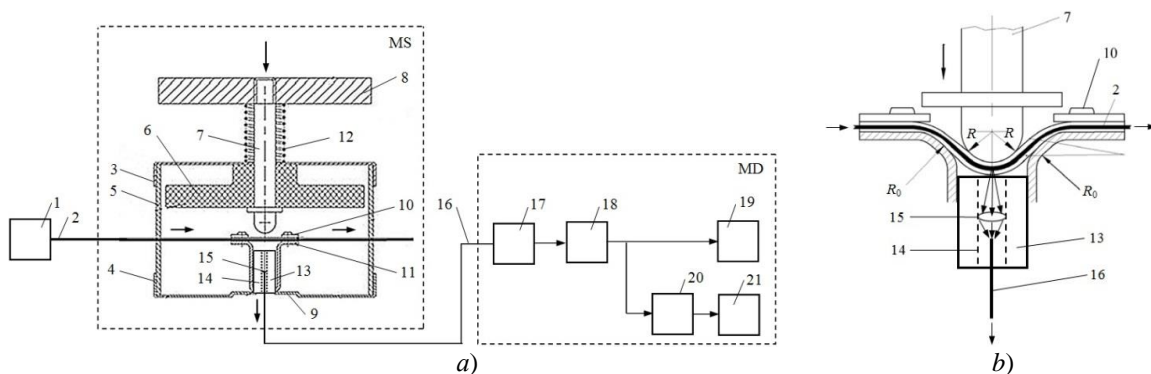


Fig. 1: Scheme of a fiber optic sensor (a) and a macrobend shaper (b)

Fiber optic sensor to ensure the functional security of the perimeter security system of the object consists of a source of optical radiation -1, the first optical fiber -2 with a core and a reflective coating, top -3 and bottom cover -4, casing -5, guide -6, movable rod -7, buttons -8, supports -9, strips -10, membranes -11, springs -12, fixed rod -13, funnel-shaped holes -14, lenses -15 placed in the funnel-shaped holes -14 and opposite the site with a macrobend, the second optical fiber -16 for transmitting a branched signal of optical radiation, a photodetector -17, an amplifier -18, a level meter -19, an electronic reporting device -20 that performs mathematical operations and an electronic indicator -21 (Fig. 1) [1].

The fiber optic sensor works as follows.

In the process of unauthorized entry into the protected object, when the button -8 is pressed by a body with a mass m , the movable rod -7 moves down along the guide -6 and is pressed against the membranes -11. The first optical fiber is laid between the membranes. To prevent the first optical fiber -2 from slipping to the sides during compression and creating a macrobend in the form of an arc of a circle, two low parallel guide rollers are placed in one of the membranes -11. The first optical fiber -2 is located between these rollers. This arrangement prevents sliding of the optical fiber -2 to the side in case of action on the membrane -11 of the movable rod -7, and when the action stops, it helps to straighten the first optical fiber. When the impact on the button -8 by a body with mass m -8 spring -12 opens, the movable rod -7 returns to its original position, and the first optical fiber -2 returns to a straight position. As a result of the action of the movable rod -7 on the membranes -11, the process of macrobending of the first optical fiber -2 occurs, the radius of which corresponds to the radius R of the round end of the movable rod -7 (see Fig. 2). With the help of the round end of the movable rod -7, a macrobend of the first optical fiber -2 with the corresponding radius R is formed, and from this macrobend the optical radiation branches off, which passes through the holes in the form of a funnel -14, the lens -15, placed in the hole in the form of a funnel, on the contrary a section with a macrobend and this radiation is focused by a lens onto the input of the second optical fiber -17, the input of which is located at the focal point of the lens -15. From the output of the second optical fiber -17 enters the input of the photodetector -16, which converts the branched optical radiation into an electrical signal, from the output of the photodetector to the input of the amplifier -18, from the output of the amplifier in parallel to the input of the level meter -19 and the electronic reporting device -20, which automatically performs mathematical operations, from the output of the electronic reporting device -20 to the input of the electronic indicator -21. The first optical fiber -2 together with the membranes -11 is attached to the supports -9, and the distance between them is equal to the diameter of the movable rod -7. The edges of supports -9 are made in the form of a round funnel with a radius R , which makes it possible to exclude attenuation of the branched optical radiation at the edges of supports -9 during macrobending (Fig. 1). The movable rod -7 rests on the shoulders of the supports -9, to limit its movement, the support -9 is used, which prevents the membranes -11 and the first optical fiber -2 from breaking in the event of a strong impact. When the button -8 of the fiber-optic sensor is exposed to any mass, the process of branching of the optical radiation transmitted by the source of optical radiation -1 along the first optical fiber, which passes through the lens -15, placed in the hole in the form of a funnel, opposite the area with a bend and the second optical fiber -16 is fed in parallel to the input of the level meter -19 and the electronic reporting device -20. The level meter -19 measures the attenuation of the branched optical radiation.

IV. Experimental setup and research methodology

Optical fibers G652, G655 and G657 are used in fiber optic communication lines, and also have different susceptibility to macrobending, i.e. the degree of response of the optical fiber to the appearance of a macrobend (a bend with a radius of more than 1.0 mm), therefore, studies were carried out on optical fibers G652, G655 and G657. To evaluate the response of an optical fiber to macrobending, parameter $\Delta\alpha/\Delta L$, is used where $\Delta\alpha$ – is the corresponding change in the attenuation of optical radiation, ΔL – is the change in the length of the macrobending arc. In this case, the attenuation of the optical radiation signal during propagation along the optical fiber is determined by the following formula [2-7]:

$$\alpha = 10 \lg(P_{inp} / P_{out}), \quad (1)$$

where P_{inp} – and P_{out} – are the power of optical radiation at the input and output of the optical fiber.

Block diagram of the experimental setup.

Fig.2 shows a setup for experimental studies, consisting of an optical radiation source (SOR),

an optical radiation signal power meter (ORP), which are part of a verified and calibrated optical tester, and a macrobending shaper (MS). The source of optical radiation is connected to the optical power meter using an optical fiber. The shaper allows forming macrobends with a radius of 2.5...15 mm. Also, using the macrobend shaper, you can create a coil in the form of a circle and arcs of this circle [2].

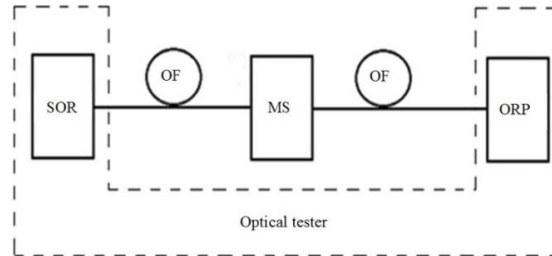


Fig. 2: Scheme of the experimental setup

The operating principle of the experimental setup is as follows.

An optical radiation signal with a power of 1.0 mW and a wavelength of 1310, 1490, 1550 and 1625 nm comes from the source of the optical radiation signal into the optical fiber, which corresponds to the transparency windows of the studied optical fibers (the optical power measurement range at these wavelengths is $10^{-11} \dots 10^{-2}$ W). At a power of 1.0 mW, the instability of the optical radiation power does not exceed 0.005 dB. An optical radiation power meter is connected to the output of the optical fiber, and a macrobend shaper is placed on the optical fiber (Figure 2). The length of the optical fiber for the experiments was chosen to be small, 2.0 m, so that the attenuation of optical radiation in this optical fiber could be neglected in the absence of a macrobend.

For measurement, experiments were carried out in accordance with the requirements of the ISO / IEC 17025-2019 standard at an ambient temperature of 20-25 ° C, humidity up to 70% and atmospheric pressure of 975-1025 Pa. It is shown that the attenuation of an optical fiber is quite stable under these environmental parameters, and also under these conditions, the stability of the optical radiation source and the sensitivity of the optical radiation power meter remain constant.

V. Experimental results and discussion

To determine the susceptibility of an optical fiber to macrobending, the dependence of the attenuation of the optical radiation signal in the fiber α on the macrobend radius R was studied. Based on the results obtained, the dependences of α on R were plotted for the wavelength of the optical radiation signal $\lambda=1490$ nm for one full turn (1 - G657; 2 - G652; 3 - G655), which are shown in Fig.3.

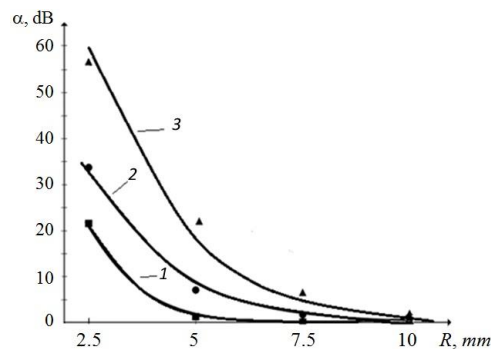


Fig. 3: Dependence of attenuation on the macrobend radius of an optical fiber

For other values of λ , the dependences were similar. In Table 1 shows the values of α at $R = 7,5$ mm for all types of optical fibers under study. As can be seen from Fig.3 and Table 1, the G655 optical fiber has the highest attenuation values in the entire R range under study, and therefore, this optical fiber is used further to develop a fiber-optic sensor.

Table 1: Characteristics of the studied optical fibers

Optical fiber	Optical radiation signal power attenuation at a macrobend (dB), at optical radiation wavelength, nm			
	1310 nm	1490 nm	1550 nm	1625 nm
G 652	0,5	2,0	2,6	5,5
G 655	3,5	5,4	7,5	9,6
G 657	0,2	0,5	1,2	3,3

Fig. 4 shows the dependence of the attenuation of optical radiation on the macrobending arc length L at a constant value of $R = 7,5$ mm for various wavelengths (\blacktriangle - $\lambda=1625$; \blacksquare - 1550; \bullet - 1490; \blacklozenge - 1310 nm). As can be seen from the results obtained, an increase in L leads to an increase in the attenuation of optical radiation. This dependence is close to a linear dependence and we can assume that [2]:

$$\alpha = \frac{\Delta\alpha}{\Delta L} \cdot L. \tag{2}$$

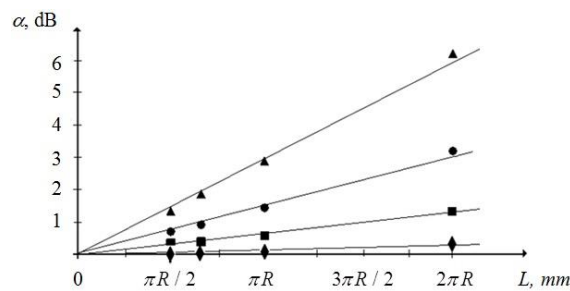


Fig. 4: Dependence of the attenuation of the optical radiation signal on the length of the macrobending arc

An increase in the wavelength of the optical radiation signal λ leads to an increase in $\Delta\alpha / \Delta L$. Thus, for $\lambda = 1310$ nm, the value is $\Delta\alpha / \Delta L = 0,01$ dB/mm; for 1490 nm - 0.04 dB / mm; for 1550nm - 0.10 dB / mm; for 1625nm - 0.21 dB / mm. With an increase in the macrobend radius R from 7.5 mm or more, a decrease in $\Delta\alpha / \Delta L$ was observed for all values of λ . It should be noted that at $R = 8,0$ mm only for $\lambda = 1310$ nm $\Delta\alpha / \Delta L = 0$. $R \geq 15$ mm for all wavelengths of optical radiation $\Delta\alpha / \Delta L$. At $R < 7,5$ mm, an increase of $\Delta\alpha / \Delta L$ was observed with a decrease of R for all values of λ . At $R < 2,5$ mm, the value of ratio $\Delta\alpha / \Delta L$ was not evaluated, since for such values of the macrobend radius R , a break in the optical fiber could occur. Note that at $R < 2,5$ mm and $L = 2\pi R$ mm, the macrobend attenuation of the optical fiber becomes quite large, $\alpha > 90$ dB for $\lambda = 1625$ nm.

In Table 2 shows the numerical values of ratio $\Delta\alpha / \Delta L$, obtained for the optical radiation signal wavelength of 1550 nm and different macrobend radii of the G655 optical fiber.

Table 2: Optical fiber macrobend characteristics

R , mm	7.5	9.0	10.0
$\Delta\alpha / \Delta L$, dB/mm	0.07	0.06	0.02

From the data given in Table 2 it follows that a decrease in the radius of the macrobend R of

the optical fiber leads to an increase in the ratio $\Delta\alpha / \Delta L$. The maximum value of the arc length L of the macrobend of the optical fiber, which is obtained when a penetrating object acts on the fiber optic sensor, is πR . The largest displacement of the rod Δx under the influence of the object of unauthorized access to the button depends on the value of the macrobend radius. The dependence of the length of the macrobending arc on the displacement of the rod under the influence of the unauthorized access object on the button has the following form [2]:

$$L = 2R \arccos\left(1 - \frac{\Delta x}{R}\right). \quad (3)$$

The displacement of the rod Δx will depend on the spring constant k and the mass of the penetrating object m , affecting the button of the fiber optic sensor:

$$\Delta x = (mg) / k, \quad (4)$$

where g – is the free fall acceleration.

On the other hand, the relationship between damping Δa and mass m is given by:

$$\Delta a = (mg) / k, \quad (5)$$

Using expression (5), the relationship between the mass m , acting on the button of the fiber optic sensor and the resulting attenuation Δa , can be determined as follows:

$$m = (\Delta a \cdot k) / g. \quad (6)$$

After the value of the attenuation change Δa is known, at the output of the electronic reporting device -20, which performs mathematical operations according to expression (4), the value of the physical quantity proportional to the mass m of the unauthorized access object is obtained, which is transmitted to the input of the electronic indicator -21, the scale of which calibrated proportionally to the mass m . On the scale of the electronic indicator, a value proportional to the mass is obtained, which makes it possible to determine the mass of m , performing unauthorized access to the territory of the protected object.

Then the dependence of attenuation α on m mass of the object of unauthorized access has the following form:

$$\alpha = \frac{\Delta\alpha}{\Delta L} \cdot 2R \cdot \arccos\left(1 - \frac{mg}{kR}\right). \quad (7)$$

Thus, the relationship between optical attenuation and mass is a function of the inverse cosine. This function, described by expression (7), has a section where the relationship between α and m is close to linear. We will use this section of the dependence in a fiber-optic sensor to determine the mass by the value α .

For the used design of the fiber-optic sensor and spring, the experimental data on the attenuation of the optical radiation signal α from the mass m of the unauthorized access object are given in Table 3, and the dependence in Figure 5 for the wavelength of the optical radiation signal 1 is $\lambda=1310$; 2 - 1490; 3 - 1550; 4 - 1625 nm.

Based on the Table 3 of the data, the dependence of the attenuation of the optical radiation signal on the mass of the unauthorized access object is plotted, which is shown in Fig.5.

With a radius of the rounded end of the rod of 7.5 mm, it is possible to perform measurements α for all investigated wavelengths of optical radiation. As can be seen from the dependences obtained, in the range from 3.3 to 7.5 kg, the dependence of attenuation α on m is close to a linear dependence. For the sensor at $m < 3,3$ kg, the displacement of the rod was such that the length of the macrobending arc provided a small attenuation of the optical radiation signal and the error of the radiation power meter did not allow more accurate results to be obtained. Thus, this fiber optic sensor can be used to measure the mass of objects of unauthorized access.

Note that in a certain range of rod displacements, the dependence of α on Δx is also linear. Therefore, before starting the operation of the sensor, it is necessary to determine the Δx – minimum value of this range. For example, for this you need to increase the mass of the button by 3.3 kg. Then the sensor will be able to measure the mass in the range of 0 to 4.2 kg.

Table 3: Experimental data on the attenuation of the signal of optical radiation and the mass of the object of unauthorized access

Optical fiber	Optical radiation signal power attenuation at the macrobend (dB), at optical radiation wavelength, nm							
	1310 nm		1490 nm		1550 nm		1625 nm	
	Weight, mm	Attenuation, dB	Weight, mm	Attenuation, dB	Weight, mm	Attenuation, dB	Weight, mm	Attenuation, dB
G655	1	0	1	0	1	0	1	0
	2	0	2	0	2	0	2	0.1
	3	0	3	0.1	3	0.4	3	0.9
	4	0.1	4	0.5	4	1.25	4	1.8
	5	0.2	5	1.0	5	2.25	5	3.15
	6	0.5	6	1.25	6	4.0	6	4.5
	7	0.75	7	1.6	7	5.4	7	6.0

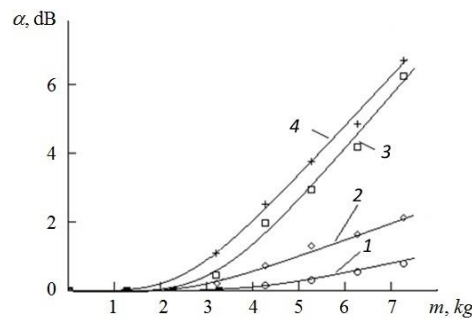


Fig. 5: Relationship between optical attenuation and the mass of the penetrating object

An increase in the wavelength of optical radiation leads to an increase in the sensitivity of the sensor. The sensitivity of the sensor is understood as the ratio of the value $\Delta\alpha$ to the corresponding change in body weight Δm . So, for the linear section of the dependence of α on m , the highest sensitivity corresponded to $\lambda=1625$ nm and amounted to 1.4 dB/kg, and the lowest for $\lambda=1310$ - 0.2 dB /kg.

Thus, experimental studies of a fiber-optic sensor based on the macrobend of an optical fiber showed the possibility of using it to measure the mass of a penetrating object on the perimeters of a protected object. In order for the sensor to measure a large mass, the spring rate must be increased. You can determine the spring constant for the required mass measuring range using the following formula [2,7]:

$$k = (m_{\max} g) / R, \tag{8}$$

where m_{\max} – is the maximum mass.

Obviously, other designs of the mechanical part of the sensor can also be used, providing a displacement of the rod that forms the macrobend of the optical fiber by a distance of Δx proportional to the mass.

VI. Conclusion

Depending on the intensity of the branched signal of optical radiation, the developed fiber-optic sensor makes it possible to detect unauthorized access to the territory of a protected facility, to increase the measurement range of the attenuation of the branched signal of optical radiation by amplifying the branched signal of optical radiation and the limit of measuring the body weight of

an object of unauthorized access by choosing the coefficient spring stiffness.

Experimental studies have shown the possibility of the developed fiber-optic sensor for measuring the mass of an object of unauthorized access to the perimeters of a protected object, and by choosing the spring stiffness coefficient, it is possible to increase the range of measuring the mass of objects.

Based on the experimental studies carried out, it was concluded that less than 50% of the intensity of the optical radiation signal source is obtained at the output of the fiber optic sensor and transmitted through the second optical fiber, and more than 50% at the direct output of the first optical fiber.

References

- [1] Mansurov, T.M. Fiber-optic sensor / T.M., Mansurov, N.A., Yusifbayli, S.A., Dzhebrailova, E.T. Mansurov // Official Bulletin of the Intellectual Property Agency of the Republic of Azerbaijan No. 6. -Baku, 2023. C. 25.
- [2] Vasilevsky, G.V. Using an optical fiber macrobend as a basis for creating a mass sensor / G.V. Vasilevsky, A.O. Zenevich, S.V. Zhdanovich, T.M. Lukashik, A.A. Lagutik // St. Petersburg: St. Petersburg State University ITMO, Izv. Universities "Instrument Engineering", 2020. - T. 63, No. 10. C. 930-937.
- [3] Burdysheva, O.V. Fiber-optic vibration sensor / O.V., Burdysheva, E.S. Sholgin // Special issue "Photon Express Science 2019", 2019. No. 6. P. 52-53.
- [4] Pat. RF 2509994, IPC G01L11/02. Pustovoi V. I., Likhachev I. G. Fiber-optic device for pressure measurement. 2014.
- [5] Shilova I.V. Multi-element fiber-optic pressure gauge // Vestn. Belarusian-Russian University. 2012. No. 4(37). pp. 116-124.
- [6] A. V. Kulikov, A. V. Ignatiev, "Overview of fiber-optic perimeter security systems," Security Algorithms. 2010. No. 4. S. 56-61.
- [7] Butusov M. M. Fiber optics and instrumentation / M. M., Butusov S. L. Galkin, S. P. Orobinsky, B. P. Pal / L.: Mashinostroenie, 1987. 328 p.
- [8] Li L. et al. Design of an enhanced sensitivity FBG strain sensor and application in highway bridge engineering // Photonic Sensors. 2014. Vol. 4, No. 2. R. 162-167.
- [9] Ren, L. Design and experimental study on FBG hoop-strain sensor in pipeline monitoring // Optical fiber technology. 2014. Vol. 20, N 1. R. 15-23.
- [10] Chen W. et al. Performance assessment of FBG temperature sensors for laser ablation of tumors // IEEE Intern. Symp. on Medical Measurements and Applications. 2015. R. 324-328.
- [11] Mamidi V. R. et al. Fiber Bragg Grating-based high temperature sensor and its low cost interrogation system with enhanced resolution // Optica Applicata. 2014. Vol. 44, N. 2. P. 299-308.

HIGH-PRECISION GROUND-BASED PHOTOMETRIC MONITORING METHOD FOR VALIDATING SATELLITE MONITORING OF ASSOCIATED HYDROCARBON GAS BURNING

Yegana Aliyeva, Kifayat Mammadova, Matanat Hasanguliyeva



Azerbaijan State Oil and Industry University

yegane.aliyeva.1969@mail.ru

kifayat.mammadova.adnsu@gmail.com

metahasanquliyeva@rambler.ru

Abstract

The shortcomings of satellite monitoring of associated gas burning in the oil industry have been analyzed. The possibility of performing such monitoring using ground-based photometric devices is indicated. The possibility of compensating for errors of multi-wave solar photometers due to the influence of atmospheric aerosols has been studied. The conducted research allowed to identify redundancy in correction procedures in known three-wave solar photometers. Two new methods for constructing compensated photometers are proposed. In the proposed constructions, the correction procedure is limited to the calculation and installation of one correction factor.

Keywords: photometer, atmosphere, aerosol, error, correction

I. Introduction

It is well known [1] that the Defense Meteorological Satellite Program (DMSP) is used to estimate the volumes of associated gas being flared on a global scale. DMSP satellites have been recording cases of flaring associated gas on a global scale for 16 years. This activity is funded by NOAA and the World Bank in collaboration with the Government of Norway under the Global Gas Flaring Reduction (GGFR) program.

The methodology used in this program to register and evaluate gas flares involves registering the light fluxes coming from associated gas flares, integrating the obtained signal throughout the territory of each individual country, and calibrating these results with official data, which are the most reliable. In particular, as a result of such satellite assessment, Russia was found to be the leader, which before such control was officially in second place after Nigeria [1].

It should be noted that satellite observations of flaring associated with the burning of associated gas are not only carried out in the visible range [1]. Moderate resolution spectrometers MODIS, installed on the TERRA and AQUA satellites, also perform such monitoring. It can be assumed that the desire to neutralize the influence of aerosols - the products of associated gas combustion - prompted NASA to choose the IR range for research. However, the result was clearly opposite. According to [1], in this range, MODIS was unable to register more frequent associated gas burnings of small sizes.

Thus, the above-mentioned unaccounted factors affecting the effectiveness of the overall estimation of the volume of flared associated gas bring to the fore the issues of studying the errors of such systems and optimizing their operation modes. In this regard, the question of using alternative methods and means of ground control over the flaring of associated hydrocarbon gas remains relevant. Such alternative means may include solar photometers, pyranometers, and lidars. However, it should be noted that the most significant factor leading to radiometric distortions in atmospheric photometry in the UV, visible, and initial IR ranges is aerosol. It should be noted that solar radiation is most actively attenuated by soot, which is also subject to dynamic transformation over time. Changes in the optical properties of soot introduce uncertainty into photometric measurements, underscoring the relevance of taking measures to eliminate this uncertainty. This article discusses the possibilities of implementing measures to neutralize the influence of aerosol on the accuracy of photometric devices. First, let us briefly consider the main features and causes of the impact of the temporal instability of aerosol on photometric measurements.

As stated in [2], aging of aerosols is one of the reasons for uncertainty in assessing the direct and indirect impact of aerosols on climate conditions. While fresh aerosol in its initial state is hydrophobic and externally mixed, through mechanisms of coagulation, condensation or photochemical processes, fresh aerosol over time transitions to a state of internal mixing. Such aging processes affect the hygroscopic properties of aerosols, the process of their growth, changes in their optical properties, and the lifetime of aerosol particles. [2] presents some daily and seasonal features of aerosol aging processes. For example, during the summer period, sulfur dioxide plays a dominant role in this process during the daytime, and the aging process lasts 2-8 hours. In winter, these time scales are maintained, but in this case, ammonium nitrate is the dominant factor. During the nighttime, condensation processes weaken, while coagulation serves as the main aging factor, with a time scale of 10-40 hours.

As reported in [3], elemental carbon (EC) is the main component of soot, which absorbs solar radiation and directly heats the air, converting solar radiation into its internal energy (increasing the temperature of soot) and emits thermal infrared radiation. In general, soot particles contribute to the creation of three types of temperature gradients: (1) a temperature gradient that occurs during the day in the presence of soot, resulting in the atmosphere being heated while the Earth cools; (2) a nighttime temperature gradient that occurs in the presence of soot, where both the atmosphere and the Earth are heated; (3) a daytime and nighttime temperature gradient that occurs in the absence of soot, but in the presence of adequately heated air containing soot, resulting in the atmosphere being heated while the Earth's temperature remains unchanged. Thus, soot has a complex meteorological impact and can affect the climate conditions of the planet.

As shown in [4], as a result of aerosol moisture over the ocean, the measured value of aerosol optical density can be 50% higher than that of dry aerosol. Experimental studies have shown that the measured value of aerosol optical density at 85% relative humidity was 30% higher than at 40% relative humidity.

According to [5], hydrophobic soot significantly does not change its optical properties and structure when transitioning from a dry environment to a wet one. However, hydrophilic soot is strongly influenced by water vapor. Hydrophilic soot undergoes thorough restructuring under the influence of humid atmosphere, resulting in significant changes in its optical properties. For instance, according to the data presented in [6], the optical density of highly hydrophilic soot can increase from 0.02 to 0.15 in just 20 minutes under relative humidity increase to 100%.

II. Problem statement

At the same time, atmospheric aerosol has another important property, which consists in the fact that the distribution of the volume concentration of the aerosol has a bimodal character, i.e. the total optical density of the aerosol τ_{Σ} can be represented as a certain combination of the optical densities of fine-dispersed (τ_f) and coarse-dispersed (τ_c) aerosols. It is important to take into account the following properties of the above-mentioned dispersion components:

1. There is practically no statistical correlation between the fine-dispersed and coarse-dispersed components of aerosols.

2. The optical density of the coarse-dispersed component of the aerosol is practically independent of the wavelength, whereas the optical density of the fine-dispersed component strongly depends on the wavelength. This dependence is known in the form of the empirical Angstrom formula, according to which

$$\tau_f = \beta \lambda^{-\alpha} \quad (1)$$

where: $\beta = \tau_f(\lambda = 1 \mu m)$; α - the Angstrom exponent.

Thus, the initial requirements for the development of compensated photometric devices are:

1. The synthesized photometer must neutralize the influence of aging on the measurement result.
2. The synthesized photometer must take into account the dispersion-wave properties of the optical densities of the fractional components of the aerosol mentioned above.

III. Solution

It is easy to show that the three-wavelength photometer model proposed in [6] fully meets these requirements. The intermediate conversion function proposed in this paper has the following form:

$$z = \frac{I_1^{k_1}(\lambda_1) \cdot I_3^{k_3}(\lambda_3)}{I_2^{k_2}(\lambda_2)} \quad (2)$$

Where: $I_i(\lambda_i)$ - the signal at the output of the i^{th} photometer, operating at wavelength λ_i ; k_i - correction coefficients.

For further analysis, we will use the Beer-Lambert law, which has the following form in the wavelength range of 0.3-0.7 μm :

$$I(\lambda) = I_0(\lambda) e^{-m[\tau_{03}(\lambda) + \tau_{pe\lambda}(\lambda) + \tau_{aap}(\lambda)]} \quad (3)$$

Where: $I_0(\lambda)$ - solar constant at wavelength λ ; m - air mass; $\tau_{03}(\lambda)$ - ozone optical density; $\tau_{pe\lambda}(\lambda)$ - Rayleigh scattering optical density; $\tau_{aap}(\lambda)$ - aerosol optical density.

Taking into account (2) and (3), the following conditions for complete separate compensation of the influence of fractional components of aerosol and aging effects can be obtained.

$$k_1 \tau_f(\lambda_1) d_f(t) + k_3 \tau_f(\lambda_3) d_f(t) = k_2 \tau_f(\lambda_2) d_f(t) \quad (4)$$

$$k_1 \tau_c(\lambda_1) d_c(t) + k_3 \tau_c(\lambda_3) d_c(t) = k_2 \tau_c(\lambda_2) d_c(t) \quad (5)$$

Where, $d_f(t)$ and $d_c(t)$ are coefficients that show the change in the optical properties of fine-dispersed and coarse-dispersed aerosols due to aging and hygroscopic growth.

As can be seen from expressions (4) and (5), the factors $d_f(t)$ and $d_c(t)$ cancel out and do not affect the calculation results of the coefficients k_1 and k_3 if we initially take $k_2 = 1$.

However, it can be shown that the three-wavelength photometer with a two-parameter correction proposed in [6] has some redundancy in terms of correction measures. Thus, if we take into account the independence of τ_c from λ , then, with $k_2 = 1$, we have from expression (5):

$$\tau_c(k_1 + k_3) = \tau_c \quad (6)$$

i.e.

$$k_1 + k_3 = 1 \quad (7)$$

Expression (4) with $k_2 = 1$ has the following form:

$$k_1 \cdot \tau_\varphi(\gamma_1) + k_3 \cdot \tau_\varphi(\gamma_3) = \tau_\varphi(\gamma_2) \quad (8)$$

Taking into account (7) and (8), we have

$$\begin{aligned} k_1 \cdot \tau_\varphi(\gamma_1) + k_3 \cdot \tau_\varphi(\gamma_3) &= \tau_\varphi(\gamma_2) \text{ or,} \\ k_1 |\tau_\varphi(\gamma_1) - k_3 \cdot \tau_\varphi(\gamma_3)| &= \tau_\varphi(\gamma_2) \end{aligned} \quad (9)$$

From equation (9) we have

$$k_1 = \frac{\tau_\varphi(\gamma_2) - \tau_\varphi(\gamma_3)}{\tau_\varphi(\gamma_1) - \tau_\varphi(\gamma_3)} \quad (10)$$

The obtained expression (10) provides a basis for assuming that the value of the coefficient k_1 is always less than one if $\lambda_1 < \lambda_2 < \lambda_3$ and $\tau(\lambda_1) > \tau(\lambda_2) > \tau(\lambda_3)$.

IV. Discussion of results

Expression (10) also provides a basis for proposing two new methods for constructing compensated three-wave photometers.

1. The wavelengths λ_1 , λ_2 , and λ_3 are considered as constant values. In this case, the coefficient k_1 is calculated using formula (10).

2. We assume that the parameters k_1 , λ_1 , and λ_3 are constant. In this case, the value of λ_2 can be changed. From expression (10), we have

$$\left. \begin{aligned} \tau_f(\lambda_2) &= k_1 [\tau_f(\lambda_1) - \tau_f(\lambda_3)] + \tau_f(\lambda_3) \\ \lambda_2 &= \tau_f^{-1} \{ k_1 [\tau_f(\lambda_1) - \tau_f(\lambda_3)] + \tau_f(\lambda_3) \} \end{aligned} \right\} \quad (11)$$

Note that both of the above methods are capable of providing the same accuracy in compensating for the influence of aerosol as that provided in a three-wavelength photometer with a two-parameter correction. However, the first of the proposed methods has the advantage over the second in that it provides mutual compensation for instability that may be caused by changes in the coefficient β .

V. Conclusion

Thus, the conducted research has revealed the existing redundancy in the correction procedures of known three-wavelength solar photometers with parametric correction. Two new methods for constructing compensated three-wavelength photometers have been proposed, in which the correction procedure is limited to calculating and setting one correction factor.

References

- [1] A Twelve Year Record of National and Global Gas Flaring Volumes Estimated Using Satellite Data. Final Report to the World Bank – May 30, 2007.
web.worldbank.org/WBSITE/EXTERNAL/TOPICS/EXTOGMC/EXTGGFR.
- [2] Oshima N., Koike M. Development of a parameterization of black carbon aging for use in general circulation models. *Geosci., Model Dev.*, 6, 263-282, 2013.
- [3] Lund M.T., Berntsen T. Parameterization of black carbon aging in the OsloCTM2 and implications for regional transport to the Arctic. *Atmos. Chem. Phys.*, 12, 6999-7014, 2012.
- [4] Jeong M.-J., Li Z., Andrews E., Tsay S.-C. Effect of aerosol humidification on the column aerosol optical thickness over the Atmospheric Radiation Measurement Southern Great Plains site. *Journal of Geophysical research*, vol. 112, D10202, doi:10.1029/2006JD007176, 2007.
- [5] McMeeking G.R., Good N., Petters M.D., McFiggans G., Coe H. Influences on the fraction of hydrophobic and hydrophilic black carbon in the atmosphere. *Atmos. Chem. Phys.*, 11, 5099-5112, 2011. www.atmos-chem-phys.net/11/5099/2011/ doi:10.5194/acp-11-5099-2011 © Author(s) 2011. CC Attribution 3.0 License.
- [6] Asadov H. H., Mirzabalayev I. M., Aliyev D. Z., Agayev J. A., Azimova S. R., NabiyeV N. A., and Abdullayeva S. N. "Synthesis of corrected multi-wavelength spectrometers for atmospheric trace gases," *Chin. Opt. Lett.* 7, 361-363 (2009)
<https://www.osapublishing.org/col/abstract.cfm?URI=col-7-5-361>

SOME ASPECTS OF OPERATIONAL RISK MANAGEMENT IN OIL AND GAS FIELD PIPELINES

Gafar Ismayilov, Elman Iskandarov, Zivar Farzalizade, Rabiya Abishova

Azerbaijan State Oil and Industry University

asi_zum@mail.ru

e.iskenderov62@mail.ru

zivar.farzalizade@mail.ru

rabiya.abishova@mail.ru

Abstract

Field technological pipelines - capital engineering structures designed for long-term operation and intended for the uninterrupted transport of well products (oil, gas, condensates, water and their mixtures) to the treatment complex.

Negative risk events accompanying the operation of field process pipelines, including failure, total or partial loss of serviceability may occur during operation and are related to several factors.

This paper outlines the risk factors, the main adverse impacts and threats to oil and gas field pipelines, and the rules for operational risk mitigation for oil and gas field pipelines.

Keywords: risk, field pipelines, risk management, reliability, loss of serviceability

I. Introduction

It is known that with the purpose of acceptance and performance of the administrative decisions directed on decrease of probability of appearance of an unfavorable result and minimization of possible losses it is necessary to classify operational risks at functioning of field oil and gas pipelines with allocation of the basic risk forming events and definition of ecological risk for them [1, 5].

The operational risks of oil and gas pipelines are managed by the following types of strategies:

- "Take note". This strategy does not provide for the development and implementation of additional solutions and measures during the operation of the pipelines.

- "Monitoring". This strategy does not provide for the development of additional basic design solutions, but obliges such adjustments and requirements that ensure: the technical capability to diagnose defects or other deviations from design parameters; and the maintainability of the pipelines in the event of failure due to the realization of a risk-generating event.

- "Reduction". This strategy obliges the choice of materials, equipment, masterplan solutions, method of laying, instrumentation system, protection against various influences, etc. to be included in the selection.

- "Elimination". This strategy requires the revision and inclusion of design and operating requirements for the pipelines which move them into a lower risk category.

Risk management strategies are selected separately for each risk-generating event depending on the risk category and magnitude. The correlation between the risk category and the chosen risk management strategy is presented in Table 1 [2, 3].

Table 1: Risk management strategy

№	Risk management strategy	Risk category	The magnitude of the risk (as a result of the scoring)
1	"Eliminate" by repeating no less than ½ of the design decision to eliminate the risk	1-Very high	25 and over
2	"Elimination".	2-High	20 to 25
3	"Reduction".	3-Middle	15 to 20
4	"Monitoring".	4-Lower than average	10 to 15
5	"Take note".	5-Low	0 to 10

For each risk factor that could lead to failure of the designed pipeline, design solutions and operational requirements must be provided to eliminate/reduce adverse effects and/or to reduce the likelihood of compromising its integrity.

For a list of risk factors and technical solutions to minimize risk, see [3,6].

In the operation of oil and gas field pipelines, the operating organization carries out inspection, maintenance, diagnostics, corrosion, capacity reduction and other negative influences, repairs and overhauls. The content and frequency of inspection, maintenance and diagnostic work shall be determined on the basis of an assessment of the operational risks associated with the risk-generating events. An important aspect of operational risk management is the identification, assessment and prioritisation of risks.

The identification of the operational risks is carried out in 2 stages:

- At the first stage, the oil and gas pipeline is divided into separate sections for which the operating conditions, environmental conditions along the route, design and ancillary systems are not significantly different.

- In the second stage, each site is analyzed for the possibility of realization of risk-forming events.

The result of the operational risk identification is recorded in the form of a table of identified risks, see Table 2 for a sample.

Table 2: List of identified risk forming events

№	Risk forming event	Site -1	Site -2	Site - N
1	Event 1	yes	yes	yes
2	Event 1	yes	no	no
3	Event 1	no	yes	yes
....	
N	Event N	yes	yes	no

The assessment of operational risks of oil and gas pipelines is carried out by expert determination of the probability of occurrence of risk forming events. The probability is determined in accordance with Table 3.

Table 3: Description of the scale for estimating the probability of failure of oil and gas field pipelines

Probability	Description in terms of frequency of the risk-generating event	Assessment, points
Low	For this type of oil and gas field pipelines, failure is not possible or not more often than once every 10 years with the application of preliminary design solutions	1-5
Probably	For this type of oil and gas field pipeline, 2 to 3 failures over 10 years of operation are likely with the application of preliminary design solutions	6-10
Medium	For this type of oil and gas field pipeline, up to 2 failures can occur during the 3 years of operation using preliminary design solutions	11-15
High	For this type of oil and gas field pipeline, more than 2 failures over 3 years of operation are possible with the application of preliminary design solutions	16-20
Very High	For this type of oil and gas field pipelines, using preliminary design solutions, failure is already possible within the 1st year of operation	21-25

The results of the assessment and prioritization of operational risks of oil and gas pipelines are summarized in Table 4 [6].

Table 4: Results of the assessment and prioritization of operational risks of oil and gas field pipelines

Risk	Site - 1			
	Probability, points	Conclusions, points	The magnitude of risk	Adopted Risk management strategy
Event 1 (R1)	6	10	11,7	"Monitoring"
Event 1 (R2)	20	6	20,1	"Elimination"
Event 3 (R1)	-	-		"Take note"
Event 3 (R2)	-	-		"Monitoring"
.....				
Event N (R1)	18	22	28,4	"Monitoring"
Event N (R2)	18	22	28,4	"Eliminate" by repeating at least ½ of project decisions to eliminate risk

Risk	Site - N			
	Probability, points	Conclusions, points	The magnitude of risk	Adopted Risk management strategy
Event 1 (R1)	12	22	17,0	"Reduction".
Event 1 (R2)	-	-		"Take note".
Event 2 (R1)	3	6	6,7	"Take note".
Event 2 (R2)	3	6	6,7	"Monitoring".
.....				
Event N (R1)	4	24	24,3	"Eliminate"
Event N (R2)	4	24	24,3	"Monitoring"

II. Results

In the operation of oilfield pipelines, the content, frequency of inspection and performance of work on non-critical factors should be determined on the basis of an assessment of the operational risks associated with risk-generating events.

The identification, assessment and prioritization of risks are important aspects of operational risk management.

References

[1] Aliev R.A. Belousov V.D., Nemudrov A.G. et al. Pipeline Transport of Oil and Gas, M.Nedra, 1988, 368 p.

[2] Bulatov A.N. Environmental Protection in the Oil and Gas Production Industry. M. Nedra, 1999, 240 p.

[3] Ismayilova H.G. Change of ecological and economic risk in case of emergency oil spill from pipelines.// Materials of the international seminar (February 4-5, 2017) State standart 1. Ukhta, UGTU, 2017.

[4] Ismayilov G., Ismayilova H., Babirov H., Jabrayilov R.. Assessment of environmental oil spills and economic-environmental risks // RT&A, Special Issue №4(70), vol 17, November 2022, pp.212-217. DOI: <https://doi.org/10.24412/1932-2321-2022-470-212-217>

[5] Telegin L.G., Kim B.I., Zonenko V.N. Environmental protection during construction and operation of gas and oil pipelines. M. Nedra, 1998, 188 p.

[6] Grageva M.V. Project Risk Analysis. Textbook. M. Nedra, ZAO Finstatinform 1999, 295 p.

GLOBAL RISKS OF BIOLOGICAL INVASIONS OF PHYTOPATHOGENIC ORGANISMS AND IMPROVEMENT OF THE QUARANTINE MONITORING SYSTEM USING COMPUTER MODELING

Vyacheslav Zviagintsev¹, Anna Prokhorova¹, Tatiana Surina²,
Daria Belomesyeva³

•

¹ Belarusian State Technological University

² All-Russian Center for Plant Quarantine (FGBU VNIKR)

³ Kuprevich Institute of Experimental Botany of the NAS of Belarus

anna.pinchuk.99@mail.ru

mycology@tut.by

t.a.surina@yandex.ru

dasha_belom@yahoo.com

Abstract

*As a result of assessing the distribution of adventitious species of phytopathogens on the territory of Belarus, a trend of increasing the number of recorded invasions was identified. Every year, an average of 3-4 new pathogens of infectious diseases of woody plants are identified in forests and gardens, and over the past 25 years, at least 57 new types of phytopathogens have been recorded. Many of the newly identified species have already passed the stage of acclimatization, and some have a significant impact on the sanitary condition of forests and parks, causing significant damage. With the Maxent software package, using the example of the phytopathogenic oomycete *Phytophthora alni* Brasier et S.A. Kirk, which is quarantined for the EAEU countries, a map of the current and future geographic distribution under various climate change scenarios was constructed. The models showed the suitability of the conditions of Belarus for the development of *P. alni*, which made it possible to conduct local forest pathological surveys and identify symptoms of alder late blight in various forest conditions of the country. Molecular genetic analysis confirmed the presence of a quarantine pathogen on the territory of Belarus. Forecasting the spread of the invader, on the one hand, shows a reduction in areas potentially suitable for the development of the species in Europe, and on the other hand, an increase in the likelihood of the invader moving to more northern areas. Considering the potentially high harmfulness of the species, immediate monitoring, analysis of phytosanitary risks and adoption of quarantine measures are already required.*

Keywords: computer modeling, quarantine organism, Maxent.

I. Introduction

One of the most important reasons for modern global and local changes in the Earth's ecosystems is the accelerating development of human society. An increase in the planet's population and improving people's quality of life, on the one hand, lead to an increased use of natural resources, and on the other, due to such manifestations as the globalization of trade and

communications, increased mobility of people, etc., creates the preconditions for large-scale violations of the «geobiotic order» [1, 2]. The most negative disturbances include invasions of harmful organisms (insects, fungi, bacteria, viruses, nematodes, vascular plants, etc.), their hybridization with local closely related species, displacement of native species, horizontal gene transfer, emergence of new races and species of pathogens, etc. etc. [3, 4]. Examples of global invasions are widely known in medicine and agriculture; they are no less destructive for native ecosystems, including forests. In relation to forestry and gardening, the result of invasions is the epiphytotic development of new diseases in natural and artificial phytocenoses, causing significant environmental and socio-economic damage [5].

Considering the enormous potential harmfulness that alien pathogenic organisms carry in new territories and in ecosystems that are different to them, scientists and practitioners in various fields of biology, agriculture, forestry, and medicine would like to have an idea about the likelihood of penetration and development of specific invaders in certain countries or regions. At the same time, quarantine measures based on national or regional lists of quarantine organisms are not always effective, among other things, due to the growing dynamics of the introduction of alien species [7] and some inertia of government bodies in updating these important documents [8].

Climate plays a fundamental role in the formation and changes in the habitats of living organisms [9]. Over the past few decades, the amount of information about climate change on a planetary scale has rapidly increased. They pose significant risks for various sectors of the economy and natural ecosystems [10]. Detailed and reliable information on the geographical distribution of species during global climate change is of great importance for various environmental protection, quarantine, protective and other measures [11]. To predict the potential for the settlement of alien species in new territories in order to assess phytosanitary risks, macro- and microecological studies are carried out taking into account the vectors of possible transfer of invaders [12].

One of the most popular tools for modeling the distribution of species in various environmental conditions is Maxent, a highly customizable software tool based on the principle of maximum entropy [13]. In the Google Scholar database the number of scientific articles published annually using Maxent to predict the potential ranges of species under climate change has nearly tripled over the past 10 years. Most studies show that compared with other niche models, the Maxent model has good predictive effect and stability [14]. The program's algorithms allow you to build a prediction model based on actual distribution points and environmental variables of the distribution area stored in the GIS and model the potential distribution of species in space. The result is a thematic map showing the suitability of areas for species distribution. In addition, Maxent helps to adapt environmental variables and evaluate the contribution of each variable [15, 16].

The purpose of this work was to audit the quarantine neobiota on the territory of Belarus and assess the predictive value of computer modeling for monitoring dangerous quarantine organisms in forests under various climate change scenarios.

II. Materials (objects) and research methods

Information about findings of quarantine phytopathogenic objects on woody plant species was tracked in open sources: scientific articles, international databases (GBIF, EPPO), reports and messages from government authorities on plant quarantine.

The phytopathogenic oomycete *Phytophthora alni* Brasier et S.A. Kirk. was chosen as a model object for spatial modeling of the neohabitat, included in the Unified List of Quarantine Objects of the Eurasian Economic Union as a pest not present on the territory of the Eurasian Economic Union.

A model of the potential spread of the quarantine pest *P. alni* and an assessment of the likelihood of its spread on the territory of the Republic of Belarus was built on the basis of data on the modern range of the invader obtained from authoritative international databases: the Global Biodiversity Information System (<https://www.gbif.org/ru/occurrence/search>) and the Euro-Mediterranean Plant Protection Organization (<https://gd.eppo.int/taxon/PHYTRA/distribution>).

Data on the relief and vegetation cover of the region, climatic factors were used for the analysis (http://due.esrin.esa.int/page_globcover.php). Raster files for 19 bioclimatic variables and altitude at 2.5 min resolution were downloaded from the Global Climate Database (<http://worldclim.org/>).

The predictive value of the model was tested through a selective forest pathological examination of alder plantations in various geobotanical conditions of the country on the territory of the Braslav Lakes National Park, Negorelsky educational and experimental forestry enterprise, Osipovichy experimental and Stolin forestry enterprises. Diagnosis of alder late blight was carried out using a set of symptoms and signs described on alder only with the development of *P. alni* [17].

Molecular genetic identification of the pathogen was carried out on 13 wood samples selected from symptomatic areas of alder trunks using the following methods: DNA extraction, classical PCR, Sanger sequencing, processing of nucleotide sequences in the BioEdit program and the NCBI database.

To extract DNA from wood, the DNEasy Plant Mini Kit (Qiagen) was used. Classical PCR was performed with isolated DNA samples. For DNA amplification, primers PA-F/PA-R were used, which amplify a product from 450 bp. The mixture of reagents for performing one reaction with a volume of 25 μ l contained: 16 μ l of RNA and DNA-free water, 5 μ l of 5X PCR buffer MasDDTaqMIX – 2025 (Dialat Ltd., Moscow), 1 μ l of each primer (10 μ M) and 2 μ l of target DNA. Temperature-time amplification parameters for primers ITS 4/ITS 5 included: pre-denaturation 95°C – 3 min, then 40 cycles consisting of denaturation 95°C – 30 sec, primer annealing 58°C – 30 sec, elongation 72°C – 60 sec; final pre-synthesis 72°C – 10 min.; storage at +4°C. The amplification results were recorded after electrophoresis in a 1,5% agarose gel stained with ethidium bromide in the Gel Doc XR+ gel documentation system (Bio-Rad). PCR product size was measured using GeneRuler™ 100+ bp molecular weight markers and Fast Ruler™ (Fermentas). PCR products intended for sequencing were purified using the commercial QIAquick PCR Purification Kit (Qiagen). The sequencing reaction was performed using BigDye Terminator v3.1 Cycle Sequencing Kit reagents (Applied Biosystems) according to the manufacturer's instructions, followed by fragment separation on an Applied Biosystems 3500 Genetic Analyzer.

III. Results and discussion

As a result of assessing the distribution of adventitious species of phytopathogens on the territory of Belarus, a trend towards an increase in the number of recorded invasions at the turn of the 20th and 21st centuries was identified (Fig. 1). Currently, an average of 3-4 new pathogens of infectious diseases of woody plants are identified annually in forests and gardens, and at least 57 new species of phytopathogens have been recorded over the past 25 years. Many of the newly identified species have already passed the stage of acclimatization, and some have a significant impact on the sanitary condition of forests and parks. For example, the appearance on the territory of the country of the East Asian pathogen *Hymenoscyphus fraxineus* (T. Kowalski) Baral, Queloz & Hosoya) is associated with the death of more than ¾ of the country's ash forests [18] and enormous damage to forestry [19].

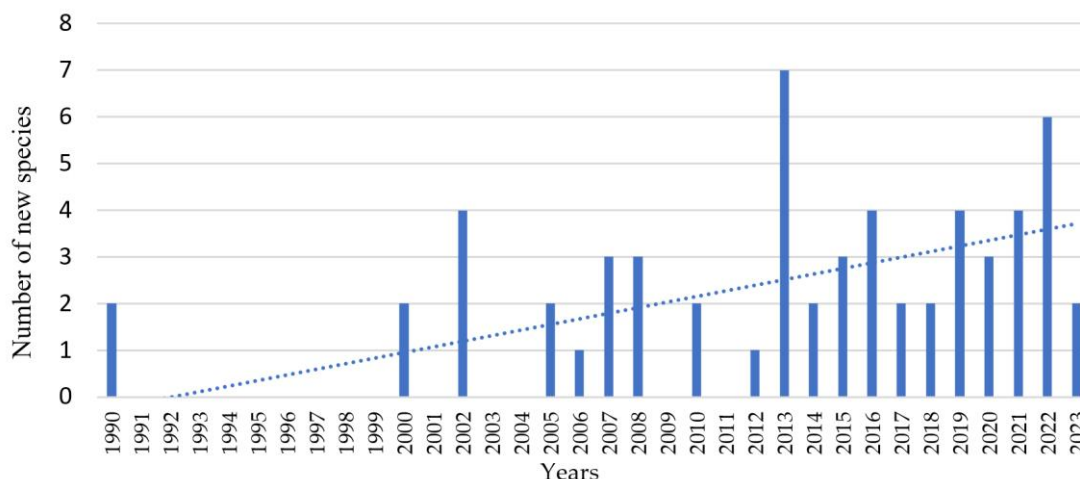


Fig. 1: Dynamics of detection of new invasive species on the territory of Belarus

The Unified List of Quarantine Objects of the Eurasian Economic Union (EAEU), which applies to Armenia, Belarus, Kazakhstan, Kyrgyzstan and Russia, includes 19 types of phytopathogens dangerous to woody plants. Moreover, 16 of them are marked as absent from the territory of the EAEU as of March 2023. However, a review of the literature shows that this is not accurate data, and at least 4 pathogens from this list are more or less common in the territories of the union countries (Table. 1). In addition, the list has some inaccuracies in the taxonomic nomenclature of species (legitimate names are indicated in brackets), which indicates a lack of close attention to this document on the part of the supervising government bodies of the EAEU countries.

Table 1: List of quarantine phytopathogens of woody plants according to the EAEU and information on their identification on the territory of the Eurasian Economic Union

No	Name of the pest quarantine organism from the EAEU (modern name)	Disease caused	Host plants	Information about identification in the EAEU	Conclusion
1	<i>Atropellis pinicola</i> Zeller & Goodding	branch canker of pine	<i>Pinus sylvestris</i> , <i>P. monticola</i> , <i>P. lambertiana</i> , <i>P. contorta</i> , <i>P. strobus</i>	No information	Not identified
2	<i>Atropellis piniphila</i> (Weir.) Lohman & Cash	branch and trunk canker of pine	<i>Pinus albicaulis</i> , <i>P. banksiana</i> , <i>P. contorta</i> , <i>P. ponderosa</i>	No information	Not identified
3	<i>Ceratocystis fagacearum</i> (Bretz.) Hunt	oak wilt	<i>Quercus spp.</i>	No information	Not identified
4	<i>Chalara fraxinea</i> T.Kowalski (<i>Hymenoscyphus fraxineus</i> (T. Kowalski) Baral, Queloz & Hosoya)	ash dieback	<i>Fraxinus spp.</i>	Belarus: Zviagintsev, Sazonov, 2006 [20]; Zviagintsev et al., 2011 [21]; Russia: Musolin et al., 2014 [22]; Zviagintsev et al., 2015 [23]; Zviagintsev et al., 2023 [24].	Belarus is a ubiquitous species; Russia – a ubiquitous species in its natural range (Far East) and as an invader throughout the European part of Russia with the presence of host breeds

5	<i>Cronartium fusiforme</i> Hed. & Hunt ex Cum.	fusiform rust of pine	<i>Pinus spp.</i> , <i>Quercus spp.</i>	No information	Not identified
6	<i>Cronartium quercuum</i> (Berkeley) Miyabe ex Shirai	pine-oak gall rust	<i>Pinus spp.</i> , <i>Quercus spp.</i> , <i>Castanea spp.</i>	Russia: Kaneko, 2000 [25].	Considered a native species in the Russian Far East
7	<i>Gymnosporangium yamadai</i> Miyabe ex Yamada	Japanese rust of apple	<i>Malus spp.</i> , <i>Abies spp.</i> , <i>Juniperus spp.</i>	No information	Not identified
8	<i>Melampsora medusae</i> Thümen	leaf rust of poplar	<i>Larix spp.</i> , <i>Picea spp.</i> , <i>Pinus spp.</i> , <i>Pseudotsuga menziesii</i> , <i>Tsuga spp.</i> , <i>Populus spp.</i>	No information	Not identified
9	<i>Mycosphaerella dearnessii</i> ME Bar (<i>Lecanosticta acicola</i> (Thüm.) Syd.)	brown spot of pine	<i>Pinus spp.</i>	Belarus: Golovchenko et al., 2020 [26] Russia: Violin, Surina, 2013 [27]	Belarus - common in arboretums on decorative pine species; Russia – Black Sea coast and Sakhalin.
10	<i>Mycosphaerella gibsonii</i> HC Evans (<i>Pseudocercospora pini-densiflorae</i> (Hori & Nambu) Deighton)	brown needle blight of pine	<i>Pinus spp.</i>	No information	Not identified
11	<i>Mycosphaerella laricis-leptolepidis</i> K. Ito, K. Sato & M. Ota	needle cast of Japanese larch	<i>Larix spp.</i>	No information	Not identified
12	<i>Phytophthora alni</i> Brasier & SA Kirk	root disease of alder	<i>Alnus cordata</i> , <i>A. glutinosa</i> , <i>A. incana</i> , <i>A. viridis</i>	A single find in the southeast of Belarus in 2014 [28]	Single outbreak
13	<i>Phytophthora kernoviae</i> Brasier	late blight of ornamental and tree crops	<i>Fagus sylvatica</i> , <i>Rhododendron ponticum</i> , <i>Drimys spp.</i> , <i>Magnolia spp.</i> , <i>Michelia spp.</i> , <i>Quercus spp.</i> , <i>Vaccinium spp.</i>	No information	Not identified
14	<i>Phytophthora ramorum</i> Weres et al.	ramorum leaf blight	<i>Fagus sylvatica</i> , <i>Quercus spp.</i> , <i>Larix kaempferi</i> . L. <i>decidua</i>	No information	Not identified
15	<i>Sirococcus clavigignenti-juglandacearum</i> Nair, Kostichka & Kunt (<i>Ophiognomonium clavigignenti-juglandacearum</i> NBNair, Kostichka & Kuntz)	canker of butternut	<i>Juglans ailanthifolia</i> , <i>J. ailanthifolia</i> var. <i>cordiformis</i> , <i>J. cinerea</i> , <i>J. nigra</i> , <i>J. regia</i>	No information	Not identified
16	<i>Bursaphelenchus xylophilus</i> (Steiner & Buhner) Nickle	pine wilt disease	<i>Abies spp.</i> , <i>Cedrus spp.</i> , <i>Larix spp.</i> , <i>Picea spp.</i> , <i>Pseudotsuga spp.</i>	No information	Not identified

Some quarantine species from this list, for example *Atropellis pinicola* and *A. piniphila*, are absent from Europe, others are recorded only in certain countries (*Bursaphelenchus xylophilus*, *Melampsora medusae*) but some were able to spread quickly, creating huge secondary habitats. An example of the latter is the causative agent of alder late blight the oomycete *P. alni*. In Belarus, the first single plant with symptoms of the disease was identified back in 2014 on the territory of the Gomel forestry enterprise [28]. The presence of a quarantine pathogen was confirmed using molecular genetic diagnostic methods, but since then the symptoms of the disease have no longer been diagnosed in Belarus. A working hypothesis has been put forward that the environmental conditions of the country turned out to be unfavorable for the development of *P. alni*, and the phytopathogen could not go through the acclimatization stage and spread from the site of the supposed single introduction. To test the hypothesis using computer modeling, a *P. alni* distribution model was adjusted by correlation analysis of 19 bioclimatic variables, which was performed using QGIS and Excel to eliminate multivariate collinearity. Bioclimatic variables that showed a coefficient of contribution to the species distribution greater than 0 in Maxent calculations were selected for analysis. The most significant environmental variables were used for further modeling (Table 2).

Table 2: Environmental variables shown to be most important for the distribution of *Phytophthora alni* in Maxent calculations

Variable	Description
BIO7	annual temperature range
BIO8	average temperature of the wettest quarter
BIO10	average temperature of the warmest quarter
BIO14	precipitation of the driest month a
BIO15	seasonality of precipitation (coefficient of variation)
BIO16	precipitation of the wettest quarter
BIO18	precipitation of the warmest quarter
elevel	terrain data
cover	land cover data

To assess the potential distribution of the study species under the influence of climate change, a model developed jointly with the Japanese research community, known as the Interdisciplinary Research Climate Model (MIROC 6), was used with a resolution of 2.5 minutes or ~5 km per pixel, which is often used to solve wide range of issues in climate science and future climate projections. The MIROC 6 forecasting system is a contribution to phase 6 of the CMIP 6 project (Coupled Model Intercomparison Project, Version 6).

The modeling used two extreme climate scenarios according to the 6th report of the Intergovernmental Panel on Climate Change: SSP 585 – an option providing for the highest concentration of carbon dioxide in the future, SSP 126 – an option providing for the lowest concentration of carbon dioxide in the future [29].

When carrying out the analysis the following settings were set in the Maxent program: for statistical analysis of accuracy, the resulting models were tested by a random sample of 25% of species locations, 500 steps (iterations) were used to obtain the optimal model, the complexity parameter (regularization multiplier) equal to 1 was selected experimentally based on the analysis of different models, the maximum number of background points – 15000, random subsamples were selected based on cross-validation.

The most important tool for checking the reliability of the constructed model is the AUC value (Area Under the Receiver Operating Characteristic – area under the receiver operating characteristic). The AUC of the ideal model is 1, but adjusted for «presence only data», the AUC

indicator of a good model tends to 1 [30].

The criteria for assessing the modeling accuracy of the model were divided into three levels: poor ($AUC \leq 0,50$), acceptable ($0,5 < AUC \leq 0,80$) and excellent ($0,80 < AUC \leq 1,00$) [31].

In our case, the values Training data $AUC = 0,921$, Test data $AUC = 0,784$, for model *P. alni* indicate a fairly high level of predictive efficiency.

The importance of the variable was assessed using the jackknife test, which took into account the environmental factor most influential on the spread of *P. alni* (Fig. 3).

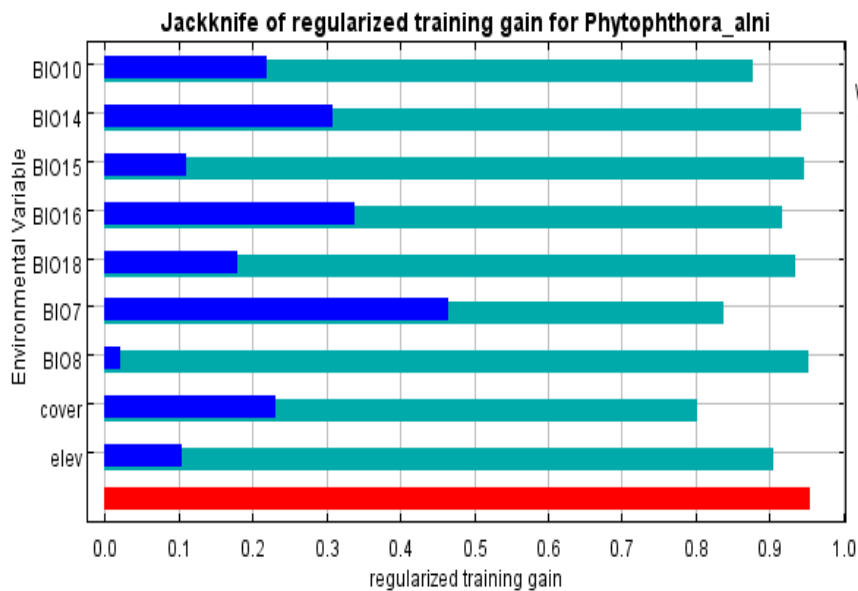


Fig. 2: Results of the jackknife test

The results show that predictors such as BIO 7 (annual temperature range), cover (vegetation zones), BIO 14 (precipitation of the driest month) and BIO 16 (precipitation of the wettest quarter) contributed the most to the distribution pattern of *P. alni* compared to other variables.

Temperature conditions are a more important parameter than altitude. This suggests that climate in Europe is a powerful driver of the spread of *P. alni*. A variable associated with extreme environmental conditions (precipitation from the driest month) has also been found to be important in explaining the spread of this plant pathogen, as rainfall affects the amount of water in rivers, streams and marshes, which is closely related to the distribution of the alder host plant.

The result of the modeling is maps of the possible distribution of *P. alni* at the current moment and in the future, colored according to the optimal environmental conditions for the development of the species (Fig. 4). In the scale used, red corresponds to the most favorable conditions, and blue to unfavorable conditions, where the probability of development of a given species tends to 0.

Spatial and climatic modeling of the *P. alni* range shows the suitability of the conditions of Belarus for the development of the pest with probability coefficients from 0,22 to 0,78. Under changing environmental conditions under different climate scenarios, the species in question will migrate towards higher altitudes and latitudes.

All SDM forecasts were visualized in QGIS. To more clearly assess future changes in niche area compared to the current model, presence/absence maps were constructed using the minimum presence threshold during training (0,47). Suitable habitats were ranked, and their area was calculated (Figure 5). Further, with area measurements, they were divided into three classes: the most suitable habitat ($0,65 < P \leq 1,0$), highly suitable habitat ($0,47 < P \leq 0,65$) and unsuitable habitat ($P \leq 0,47$) (Table 3).

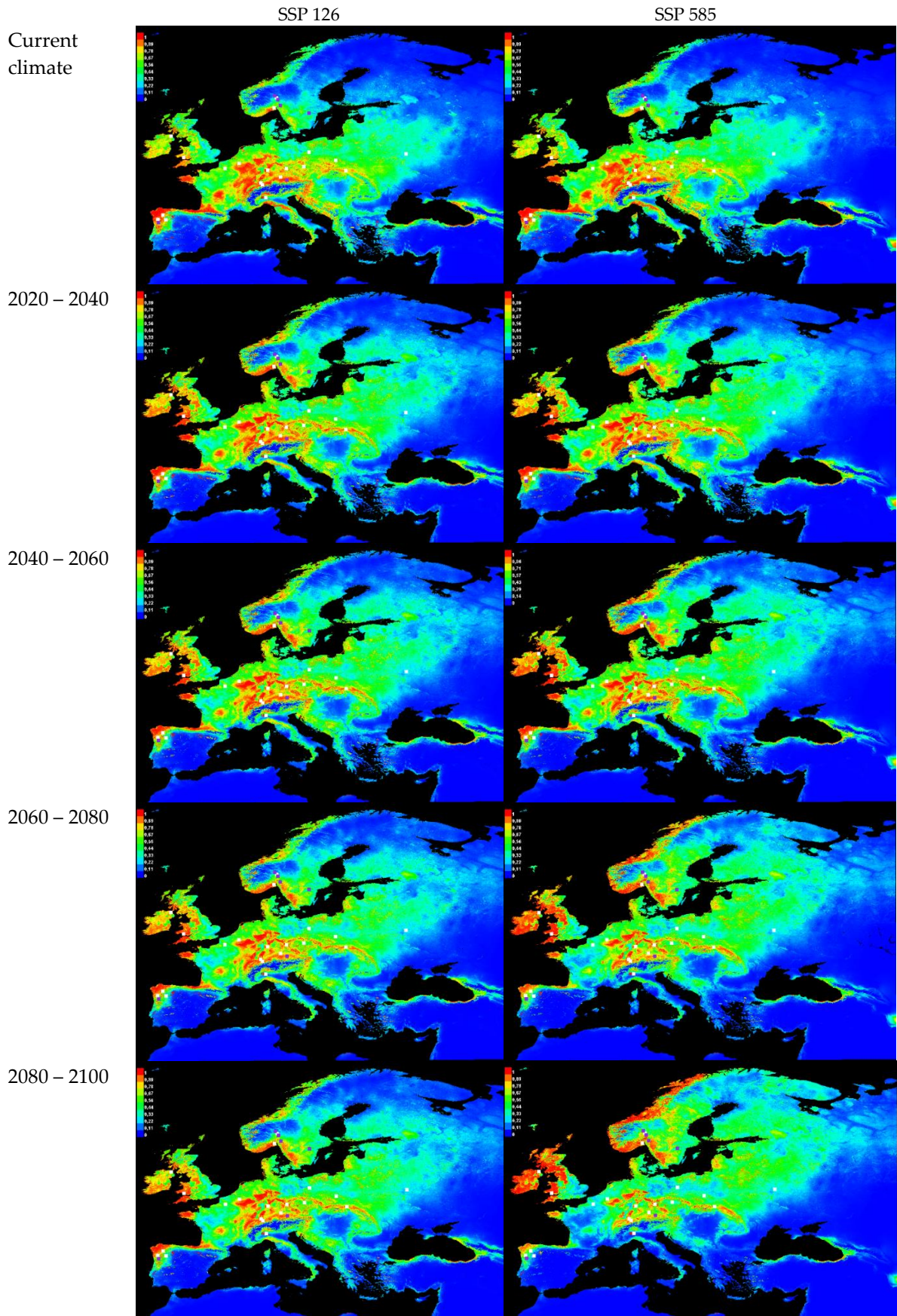


Fig. 3: Temporal forecasting of changes in the favorable environmental conditions for the development of the potential range of *Phytophthora alni*

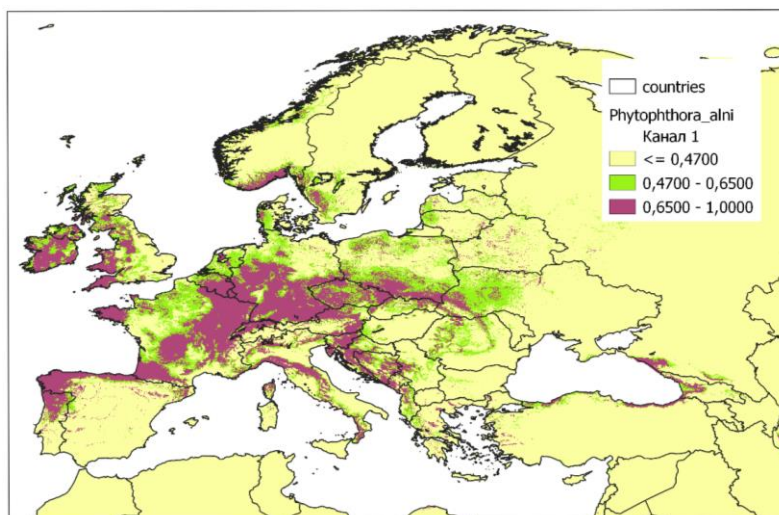


Fig. 4: An example of territory classification according to suitability categories

Table 3: Area of predicted habitats depending on various climate change scenarios, thousand km²

Probable habitats	Current climate	Forecasting depth, years							
		SSP 126				SSP 585			
		20-40	40-60	60-80	80-100	20-40	40-60	60-80	80-100
most suitable	1,280	1,289	1,199	1,138	1,083	1,354	1,237	1,057	0,965
highly suitable	1,059	0,999	0,961	0,927	0,938	1,049	2,027	0,914	0,866
unsuitable	9,626	9,545	9,664	9,784	9,803	9,421	9,591	9,846	10,407

The numbers presented above once again prove that in general for Europe the territory is suitable for naturalization and potential spread invader will be reduced. This can be associated with the continuing increase in climate aridity and desertification of the southern regions of the subcontinent [32]. At the same time, on the territory of Belarus, under «optimistic» and «pessimistic» climate change scenarios, the habitat will change towards greater suitability for *P. alni*.

P. alni grow naturally in plantations in Belarus: *Alnus glutinosa* and *A. incana*, whose plantings occupy about 9% and 2% of the forested area, respectively [33]. The area of alder forests is more than 900 thousand hectares with a timber reserve of 180 million m³. Alder forests occupy mainly low-lying relief elements, often along ponds and streams, where the probability of the spread of the oomycete *P. alni* is high. Selective forest pathological examinations of alder plantations made it possible to identify symptoms of late blight in the protected zone of the Braslav Lakes National Park, Osipovichi end Stolin forestry. In most outbreaks, the disease manifested itself on individual weakened or drying trees. In localities in the south and central part of the republic, the occurrence of symptoms can be characterized as single. Relatively massive damage to alder was detected in the plantations of the Braslav Lakes National Park, where symptoms of late blight were recorded in 11 forest areas with dominance or participation in the composition of *A. glutinosa* and *A. incana*, and in some cases group damage and death of trees were noted. The discovery points were located at different distances from reservoirs and watercourses, which casts doubt on the exclusively hydrochoric mode of spread of the pathogen.

Affected alder plants experience defoliation, the leaves become small and fall off prematurely. Dryness is often noted. Black or dark red wet spots form in the lower part of the trunks (up to a

height of 2–3 meters). Dark exudate is periodically observed on the surface of the necrotic bark (Fig. 5).



Fig. 5: Symptoms of black alder late blight: on the bark - on the left; under the bark - on the right
(Osipovichi forestry, 2022)

The spots indicate the death of the cambium and wood under the bark as a result of the development of a pathological process. When the phloem is removed, elongated zones of brownish-brown color are visible, which contrast with healthy wood, which is white when freshly cut. Over time, the affected bark and wood are destroyed.

Molecular genetic analysis confirmed the presence of *P. alni* in Belarus. And amplification with primers PA-F/PA-R made it possible to obtain a target fragment of 450 bp in size with a sample from the Osipovichi forestry (central part of Belarus). These primers are specific for all forms of *Phytophthora alni* (*P. alni* subsp. *alni*, *P. alni* subsp. *uniformis* and *P. alni* subsp. *multiformis*).

Also, when performing PCR, nonspecific products were obtained with three samples. In this regard, further identification of samples was carried out using Sanger sequencing. As a result of analysis of the obtained nucleotide sequences in the NCBI database, it was found that the sample from the Osipovichi forestry is *Phytophthora alni* subsp. *alni*. Percent identity with *Phytophthora alni* subsp. *alni* sequence isolate UASWS 0194 SCAR marker F 4-1050 genomic sequence (Sequence ID: DQ 403799.1) is 99,10%.

High-quality alder timber is in high demand in the domestic and foreign markets; thanks to its rich texture, it is a source of high-quality raw materials for the production of plywood, furniture, doors, and interior elements [34]. Considering the scenarios for the development of pathology in European countries, one can expect a significant volume of alder plantations damaged and weakened by the disease. Due to the inaccessibility of such areas during most of the year, prompt implementation of sanitary and health measures in these conditions will be difficult. According to an assessment based on the regulations of the International Standard for Phytosanitary Measures [27], when mass drying of alder plantations occurs, the potential damage to forestry is assessed as significant. When alder forests are damaged and dry out, we should expect waterlogging and deforestation of areas in which alder is the main forest-forming edifier.

IV. Discussion

The global trend of increasing the number of invasions of all taxonomic groups of living organisms into new regions is especially clearly manifested in native and artificially created

ecosystems of Belarus using the example of dendropathogens. Currently, an average of 3-4 new pathogens of infectious diseases of woody plants are identified annually in forests and gardens, and at least 57 new species of phytopathogens have been recorded over the past 25 years. Many of the newly identified species have already passed the stage of acclimatization, and some have a significant impact on the sanitary condition of forests and parks, causing significant environmental and socio-economic damage. This indicates the low effectiveness of the current system of measures to curb biological invasions at the regional and global levels.

Computer modeling is a convenient and promising tool for solving the problems of predicting the development of secondary habitats of quarantine pests in existing environmental conditions, both currently and under various climate change scenarios. The constructed forecasts can be used for high-quality analysis of phytosanitary risks, development of a set of effective quarantine measures and organization of operational monitoring of outbreaks of quarantine objects in the country's forest fund.

References

- [1] Perrings, C., Mooney, H. & Williamson, M. (2010). In Globalization and Bioinvasions: Ecology, Economics, Management and Policy. DOI: 10.1093/acprof:oso/9780199560158.001.0001.
- [2] Zviagintsev, V. (2015). Globalization of problems of forest phytopathology. Problems of forest phytopathology and mycology: materials of the 9th International Conference, Minsk: 89-90. (In russian).
- [3] Finch, D. M. et al. (2021). Effects of climate change on invasive species. Invasive species in forests and rangelands of the United States: a comprehensive science synthesis for the United States forest sector. DOI: 10.1007/978-3-030-45367-1_4.
- [4] Chinchio, E. et al. (2020). Invasive alien species and disease risk: An open challenge in public and animal health. PLoS Pathog, 16(10). DOI: 10.1371/journal.ppat.1008922.
- [5] Santini, A. et al. (2013). Biogeographic patterns and determinants of invasion by alien forest pathogenic fungi in Europe. New Phytologist, 197: 238-250. DOI:10.1111/j.1469-8137.2012.04364.x.
- [6] Golovchenko, L. et al. (2016). Invasions of alien species of pathogenic fungi in plantations of Belarus. The role of botanical gardens and arboreta in the conservation, study and sustainable use of plant diversity, Minsk, 2:375-378. (In russian).
- [7] Hulme P.E. et al. (2009). Will threat of biological invasions unite the European Union? Science. 324: 40-41. DOI:10.1126/science.1171111.
- [8] Musolin, D. et al. (2017). Between Ash Dieback and Emerald Ash Borer: Two Asian Invaders in Russia and the Future of Ash in Europe. Baltic Forestry. 23: 316-333.
- [9] Harley, C.D.G. et al. (2006). The Impacts of Climate Change in Coastal Marine Systems. Ecology Letters, 9: 228-241. DOI:10.1111/j.1461-0248.2005.00871.x
- [10] Abbass, K., Qasim, M., Song, H., Murshed, M., Mahmood, H., Younis, I. (2022). A review of the global climate change impacts, adaptation, and sustainable mitigation measures. Environmental Science and Pollution Research. DOI: 10.1007/s11356-022-19718-6.
- [11] Varol, T. et al. (2022). Identifying the suitable habitats for Anatolian boxwood (*Buxus sempervirens* L.) for the future regarding the climate change. Theoretical and Applied Climatology. DOI:10.1007/s00704-022-04179-1.
- [12] Pyšek P. et al. (2020). MAcroecological Framework for Invasive Aliens (MAFIA): disentangling large-scale context dependence in biological invasions. Neobiota, 62: 407-461, DOI:10.3897/neobiota.62.52787.
- [13] Phillips, S. and Dudík, M. (2008). Modeling of species distributions with MAXENT: new

extensions and a comprehensive evaluation. *Ecography*. 31: 161-175, DOI:10.1111/j.0906-7590.2008.5203.x.

[14] Yang Z. et al. (2021). Global potential distribution prediction of *Xanthium italicum* based on Maxent model. *Scientific Reports*. DOI: 10.1038/s41598-021-96041-z.

[15] Shao, H., Tian, J., Guo, K., Sun, O. (2009). Effects of sample size and species traits on performance of BIOCLIM in predicting geographical distribution of tree species - a case study with 12 deciduous *Quercus* species indigenous to China. *Chinese Journal of Plant Ecology*. 33: 870-877, DOI: 10.3773/j.issn.1005-264x.2009.05.005.

[16] Niu, K. et al. (2022). Prediction of Potential Sorghum Suitability Distribution in China Based on Maxent Model. *American Journal of Plant Sciences*. 13: 856-871, DOI:10.4236/ajps.2022.136057.

[17] Varela, C., Martínez, C., Vázquez, J., Casal, O. (2010). First Report of Phytophthora Rot on Alders Caused by *Phytophthora alni subsp. alni* in Spain. *Plant Disease*. 94: 273-273, DOI:10.1094/PDIS-94-2-0273A.

[18] Yaruk, A., Zviagintsev, V. (2015). Prevalence of chalar necrosis in stands and plantings of common ash. *Trudy BGTU, Minsk*, 174: 207-210. (In russian).

[19] Sazonov, A. and Zviagintsev V. (2008). Assessment of damage from drying out of ash trees using the example of individual plantings. *Trudy BGTU, Minsk*. 16: 62-366. (In russian).

[20] Zviagintsev, V. and Sazonov, A. (2006). A new threat to ash forests. *Forestry and hunting*, 1: 12-16. (In russian).

[21] Zviagintsev, V., Baranov, O., Melnik, L. (2011). Pathogenic fungal diseases of branches of the ash in the drying out plantations in Belarus. In: *Fungi and lichens in the Baltics and Beyond: XVIII Symposium of the Baltic Mycologists and Lichenologists Lithuania, Dubingiai*.

[22] Musolin, D. et al. *Dothistroma septosporum*, *D. pini* and *Hymenoscyphus fraxineus* (Ascomycota) are woody plant pathogens of major concern in Europe. *Pests and diseases of woody plants in Russia*, St. Petersburg, 2014. (In russian).

[23] Zvyagintsev, V., Baranov, O., Panteleev, S. Prevalence of necrosis of ash branches caused by the invasive mycopathogen *Hymenoscyphus fraxineus* Baral et al. in the Moscow region and along the M1 highway. *Problems of forest phytopathology and mycology*. Minsk, 2015. (in Russian).

[24] Zviagintsev, V. et al. (2023). Distribution of invasive pathogen of ash dieback disease *Hymenoscyphus fraxineus* in European part of Russia. *Izvestia Sankt-Peterburgskoj Lesotehniceskoy Akademii*, 244: 88–117. (in Russian).

[25] Kaneko, S. (2000). *Cronartium orientale*, sp. nov., segregation of the pine gall rust in eastern Asia from *Cronartium quercuum*. *Mycoscience*, 41: 115–122. DOI: 10.1007/BF02464319.

[26] Golovchenko, L., Dishuk G., Panteleev, S., Baranov, Yu. New invasive species *Mycosphaerella dearnessii* in the mycobiota of pine needles in Belarus. *News of the National Academy of Sciences of Belarus. Biological Sciences Series*, 65: 98-105. (In russian).

[27] Skripka, O., Surina, T. (2013). Brown spot blight *Mycosphaerella dearnessii* is a dangerous disease of pine needles. *Plant quarantine. Science and practice*, 3: 4–9. (In russian).

[28] Zvyagintsev, V., Baranov, O., Panteleev, S. Promotion of invasion of the oomycete *Phytophthora alni* Brasier et S.A. Kirk to the east is the first discovery of the pathogen in Belarus. *Protection of forests from pests and diseases: scientific foundations, materials, methods: materials of the All-Russian conference with international participation*, 2015. (In russian).

[29] Wayne G. *The Beginner's Guide to Representative Concentration Pathways*. Skeptical Science, 2013.

[30] Phillips, S. et al. (2004). A Maximum Entropy Approach to Species Distribution Modeling. *Proceedings, Twenty-First International Conference on Machine Learning, ICML 2004*: 21. DOI:10.1145/1015330.1015412.

[31] Swets J. (1988). Measuring the accuracy of diagnostic systems. *Science*. DOI:10.1126/science.3287615. PMID: 3287615.

[32] Gao, X. and Giorgi, F.. (2008). Increased Aridity in the Mediterranean Region under Greenhouse Gas Forcing Estimated from High Resolution Simulations with a Regional Climate Model. *Global and Planetary Change*, 62:195-209. DOI:10.1016/j.gloplacha.2008.02.002.

[33] State forest cadastre of the Republic of Belarus as of 01/01/2021 Ministry of Forestry of the Republic of Belarus. L/u resp. unit. predpr. «Belgosles», Minsk, 2020. (In russian).

[34] Paul, E. and Zvyagintsev, V. Wood science with the basics of forest commodity science. Minsk, 2015. (In russian).

[35] ISPM 11. Phytosanitary risk analysis for quarantine pests. Рим: IPPC. FAO, 2014. (In russian).

THE USE OF NATURAL FILTRATION SORBENTS TO SOLVE THE SAFETY PROBLEMS OF INDUSTRIAL POLLUTION FACILITIES

Peter Belousov¹, Anastasia Rumyantseva¹, Ksenia Kim², Boris Pokidko¹, Vitaliy Milyutin³, Yulia Izosimova⁴, Ekaterina Tyupina⁵

¹ Institute of Geology of Ore Deposits, Petrography, Mineralogy and Geochemistry RAS

² Voronezh State University of Engineering Technologies

³ Frumkin Institute of Physical Chemistry and Electrochemistry, RAS

⁴ Faculty of Soil Science, Lomonosov Moscow State University

⁵ Department of High Energy Chemistry and Radioecology, D. Mendeleev University of Chemical Technology of Russia

pitbl@mail.ru

Abstract

This work is devoted to the review of mineral and organic natural sorbents for the purpose of purification of polluted waters of industrial enterprises. Structural features, differences in the composition and properties of the most common natural sorbents, features of their application and sorption mechanisms of pollutants are shown. The main mechanisms of sorption for clay minerals and zeolite is ion exchange; for siliceous rocks such as diatomite, tripoli and gaize - physical adsorption on the surface of pores and reaction with silanol groups. Organic natural sorbents have both mechanisms of complex formation and physical adsorption, as well as ion exchange. It is shown that the creation of multicomponent granular permeable granules can significantly increase the efficiency of natural sorbents and will make their use more accessible and improve the safety of the industrial sector and nuclear legacy facilities.

Keywords: sorption, sorbents, glauconite, zeolite, diatomite, vermiculate, coal, peat

I. Introduction

One of the most important issues related to the industrial and petrochemical complex, as well as nuclear energy is to ensure the safety of man-made pollution and nuclear legacy facilities. As a result of the development of industry, several million tons of waste of varying degrees of danger are produced annually. Many specialists in various fields have been involved in the problem of solving such safety issues, however, work on the development of barrier compositions is still fragmented and unsystematic. The main problem of modern industrial water treatment is that the technologies used have a number of limitations, the main of which is the need to build an entire purification complex, with its own infrastructure, expensive equipment and consumables. In most cases, the available technologies are designed for selective sorption, the need to use several types of water treatment at once, and a high consumption of energy and reagents. Moreover, these systems are generally only suitable for controlled wastewater treatment and are not suitable for ground and surface water, as well as underlayment and bridging barrier elements in near-surface landfills.

The aims and objectives of this work is to study summarize the obtained data on sorption and operational properties of mineral and organic natural sorbents for the purpose of purification of polluted waters of various industrial enterprises. The advantage of these composites is the low

cost and availability of raw materials for their production, high efficiency, ease of operation, no need for capital expenditures for the construction of an industrial cleaning complex, as well as scalability - the ability to use both mobile and stationary cleaning complex.

II. Methods

This work has been prepared on the basis of materials obtained as a result of geological, mineralogical and physicochemical works, as well as an analysis of previously published literature on this topic. Experiments on sorption, desorption, as well as the study of operational properties were carried out on natural and modified rocks of various deposits in Russia: Yagodninskoe and Khotynets zeolite deposits (Kamchatka Territory and Orel Region, respectively), Inzenskoe diatomite deposit (Ulyanovsk Region), Potaninskoe vermiculite deposit (Chelyabinsk oblast), the Karinskoe deposit of glauconite (Chelyabinsk oblast), the peat deposits of raised bogs (Tver oblast), Chernogorsk hard coal deposit (Rep. Khakassia), Pavlovsk brown coal deposit (Primorsky Krai).

III. Results

Natural sorbents include rocks and minerals formed in the natural geological environment, the structural features of which give them increased sorption properties. Mineral sorbents include quite a list of minerals that mainly have various structural defects, and as a result, the presence of an uncompensated negative charge in the structure of the mineral. Such natural sorbents have a high cation exchange capacity with respect to various metal cations and organic compounds. This group mainly includes clay minerals (smectia, illite, glauconite, vermiculite, etc.) and zeolites (clinoptillolite, mordenite, chabazite, etc.) (Fig.1) [1, 2].

Smectite minerals, are the basic components of bentonite clays. They are a class of layered aluminosilicates with two tetrahedral sheets and one octahedral sheet. Due to isomorphic substitutions in octahedral and tetrahedral sheets, the whole layer acquires a negative charge, which is compensated by interlayer cations thus resulting in the high sorption properties typical of smectite minerals [1]. Since smectite is a highly swelling mineral, it is mainly used as hydraulic seals and safety buffers, for example, in the deep disposal of radioactive waste or the creation of overlapping screens. Smectites are not used as a filtration sorbent.

Vermiculite is also layered aluminosilicates with two tetrahedral sheets and one octahedral sheet. However, unlike smectite, vermiculite does not swell on contact with water and has a lower cation exchange capacity. A distinctive feature of vermiculite is significant expansion when heated.

Illite is one of the most common micaceous minerals, however, it does not form commercial deposits by itself and is mainly found as an admixture with other clay minerals. Its ferruginous variety is glauconite, which is characterized by a globular shape of the structure of aggregates and widely distribution [3]. Interlayer-deficient micas have a layer structure similar to smectite (2:1), however, their characteristic feature is the presence of a strongly bonded potassium cation in the interlayer space and a high layer charge [1].

Zeolites, also known as molecular sieves for their specific structure and properties, are hydrated framework aluminosilicates with intracrystalline channels and cavities. Due to the isomorphous substitution of Al for Si, the negative charge is formed in the channels, which requires compensation by cations causing a high selectivity for zeolites to a number of substances including radionuclides [1, 4]. Zeolite is one of the most demanded natural materials for the sorption of heavy metals and radionuclides [5].

Diatomites are siliceous rocks consisting of remnants of diatomaceous algae possessing high specific surface area due to their very fine average particle size and therefore micro- and macroporosity [1, 6]. Natural and modified forms of diatomite have been used for the removal of

organic compounds, oil spills, heavy metals and radionuclides from liquid waste [7].



Fig. 1: Photographs of natural mineral sorbents: a – vermiculite, b – glauconite, c – zeolite, d – diatomite.

Natural hard and brown coal, as well as peat, can be categorized as organic sorbents (Fig. 2). Coal, a flammable mineral, predominantly comprises organic matter that has undergone lithification through temperature and pressure. Its utilization as a sorbent dates back to ancient times, due to its ability to absorb large quantities of water, its high porosity, and the presence of humic and humic acids [2].

High-moor peat is created in elevated moors and areas with excessive water content through the process of plant debris decomposition. Sphagnum mosses are the primary contributors to the formation of peat in these marshy environments [3]. Peat consists of plant remnants that possess a branched structure, with the outer surface being adorned with a consistent network of pores that measure 5-10 microns in diameter. The pores exhibit diverse shapes, including round, elongated, irregular, or papilla forms, as depicted (Figure 2) [2].

There are a fairly large number of works devoted to the study of the sorption properties of shungite, however, our own studies of the proportion of heavy metals and radionuclides showed that shungite itself does not participate in sorption processes, the main sorption falls on the minerals of the smectite and illite groups present in the rock as an impurity.

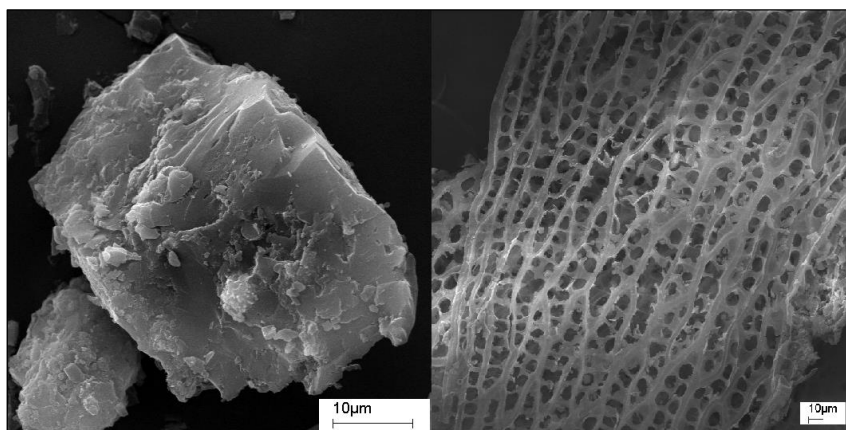


Fig. 2: Scanning electron microscope images: hard coal (left), peat (right).

As for the mechanisms of sorption, three main types can be distinguished: ion exchange, complex formation and physical adsorption. Each natural rock and mineral is characterized by one or another mechanism.

For example, for organic sorbents, a large specific surface area and the presence of macro and micropores, which are responsible for physical adsorption on the pore surface, often play a leading role. An example of such sorbents with an increased specific surface area is activated coal. Complex formation processes also play an important role in the sorption of cations on organic sorbents, and to a lesser extent, ion exchange [2].

For silicite rocks, consisting of amorphous silica – diatomite, tripoli and gaize, the main mechanism of sorption is physical adsorption on the pore surface, as well as the reaction with silanol groups ($\equiv\text{SiOH}$) groups [8].

Clay minerals and zeolites are mainly sorbed due to their ion-exchange properties. However, the mechanisms of sorption on clay minerals have not been fully explored. For a deeper understanding of these processes, modern computer modeling methods are used [6, 9]. It has been shown that sorption processes on illites or vermiculate can also occur on basal surfaces, the so-called FES (Frayed Edge Sites) [10].

An important role in sorption is played not only by the mechanism of sorption, but also by the nature of the pollutant, as well as the size of its atom or molecule. The most sensitive to size are the minerals of the zeolite group, since they have a certain size of the channels into which the pollutants must freely pass. As was shown in our the work [4], synthetic zeolite A-13X had a specific surface area and a cation exchange capacity many times greater than natural samples, however, due to the small size of the channel inlet window, it was characterized by reduced sorption to cesium and strontium radionuclides.

In addition to the sorption of heavy metals, radionuclides and water-soluble organic compounds from aqueous solutions, natural sorbents have shown their effectiveness in collecting hydrocarbon spills, both on the soil surface and on water. The advantage of using natural raw materials is their low cost and availability. For these purposes, highly porous sorbents with a low bulk density, such as diatomite, tripoli and gaize, are mainly used. However, the use of modified glauconite has recently gained popularity [11]. Due to the treatment of its surface with a hydrophobizing agent, glauconite globules acquire buoyancy and easily remove oil spills from the water surface (Fig. 3a). Also the options for imparting magnetic properties to glauconite (Fig. 3b), which makes it easy to collect waste material using electromagnetic installations, are considered.



Fig. 3: Microphotos of modified glauconite: left – contact angle of wetting of hydrophobic glauconite for oil spill response; right – globules of glauconite coated with nanomagnetite

However, despite the high efficiency of natural sorbents, often comparable to synthetic counterparts, and their low cost, the main disadvantage is low performance properties, namely, lack of stability, low filtration and mechanical strength. Due to the admixture of clay minerals, in particular smectite and kaolinite, the granules are blurred and destroyed and the inner surface of the filters is silted.

The solution to this problem can be the creation of a technology for obtaining a multicomponent granular permeable composite based on natural and modified sorbents. These

composites will combine various sorption mechanisms (ion exchange, complex formation, physical adsorption) and also have mechanical strength and high performance properties.

As a result, a granulation technology was obtained with the addition of various binders, in particular with the use of aluminous (AC) and portland cement (PC) [12]. The resulting granules have high operational and sorption properties. Dynamic experiments on the sorption of Cs with a duration of 200 hours (more than 8 days) were carried out on the obtained samples of granules. Sorption was carried out from the Moscow tap water with the composition: total salt content - 310-330 mg/dm³; total hardness - 3.6-3.8 mg-eq / dm³; pH=7.3-7.8. Before the start of the experiments, indicator amounts (~105 Bq/dm³) of the ¹³⁷Cs radionuclide were added to the water and kept for 5 days. The obtained results show that when passing 1000 column volumes of tap water, high values of purification factors (500-1000 units) from ¹³⁷Cs are observed. The filtering capacity of the layer remained constant during the entire filter cycle (more than 200 hours), which indicates the mechanical strength of the granules (Fig. 4a). The effectiveness of the obtained granules was also confirmed in the purification of water from copper ions (Fig. 4b).

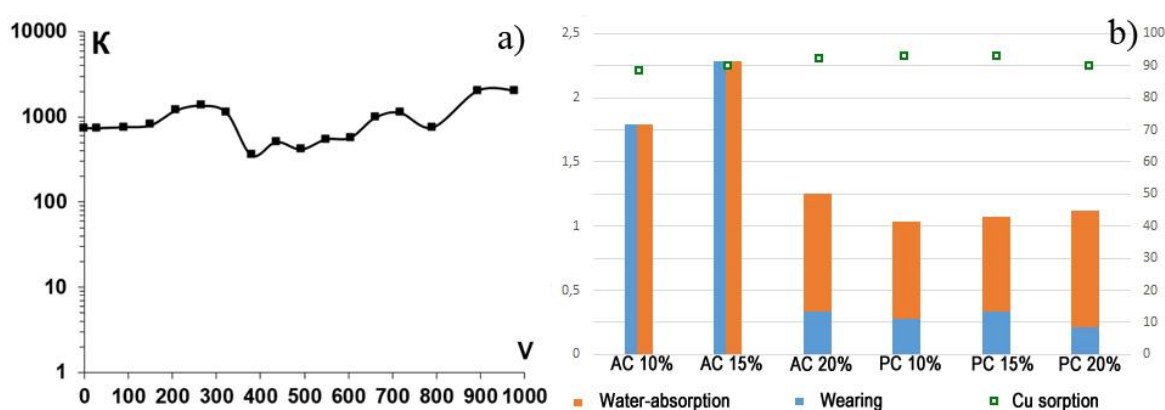


Fig. 4: The experiments on granulated sorbents: a - output curve of sorption of ¹³⁷Cs from tap water (K - the purification factor; V - the volume of filtrated solution), b - index of wearing, water-absorption and sorption of Cu²⁺.

IV. Conclusion

The use of natural sorbents at industrial facilities is an urgent task, the solution of which will make it possible to create cheap and effective filtration or anti-migration systems for the purification of polluted waters from heavy metals, radionuclides, organic pollutants and oil products. Natural mineral-type sorbents include clayey rocks such as smectite, glauconite, vermiculite, siliceous rocks such as diatomite, tripoli and gaize, and zeolite rocks. Natural organic sorbents are mainly represented by hard and brown coal, as well as peat. However, the use of natural raw materials in their original form, with the exception of volcanogenic zeolites, is difficult, since natural granules have low strength and performance properties. The solution to this problem can be the development of a technology for obtaining multicomponent granular permeable granules. The development of new sorption composites and technologies for their application will make their use more accessible and improve the safety of the industrial sector and nuclear legacy facilities.

The study was supported by the Russian Science Foundation, project no. 22-77-10050

References

- [1] Belousov, P.; Semenkova, A.; Egorova, T.; Romanchuk, A.; Zakusin, S.; Dorzhieva, O.; Tyupina, E.; Izosimova, Y.; Tolpeshta, I.; Chernov, M.; Krupskaya, V. (2019). Cesium Sorption and Desorption on Glauconite, Bentonite, Zeolite, and Diatomite. *Minerals*, 9, 625.

- [2] Belousov P., Semenkova A., Izosimova Y., Tolpeshta I., Romanchuk A., Zakusin S., Tyupina E., Krupskaya V. (2021). "Sorption of ^{137}Cs and ^{90}Sr on Organic Sorbents" *Applied Sciences* 11, no. 23.
- [3] Belousov P.E., Chupalenkov N.M., Rudmin M.A. (2022). et al. Glauconite Deposits in Russia: Geological Position, Formation Conditions, and Development Perspectives. *Lithol Miner Resour* 57, 234–247. <https://doi.org/10.1134/S002449022202002X>
- [4] Milyutin V. V., Belousov P. E., Nekrasova N. A., Krupskaya V. V. (2023). Sorption of Radionuclides ^{137}Cs and ^{90}Sr on Zeolites of Various Genesis. *Radiokhimiya*, Vol. 65, No. 3, pp. 285–292
- [5] Taylor, P.; Mimura, H.; Kanno, T. (1985). Distribution and Fixation of Cesium and Strontium in Zeolite A and Chabazite. *J. Nucl. Sci. Technol.*, 22, 284–291.
- [6] Loganathan, N.; Kalinichev, A.G. (2017). Quantifying the Mechanisms of Site-Specific Ion Exchange at an Inhomogeneously Charged Surface: Case of Cs^+/K^+ on Hydrated Muscovite Mica. *J. Phys. Chem.*, 121, 7829–7836.
- [7] Osmanlioglu, A.E. (2007) Natural diatomite process for removal of radioactivity from liquid waste. *Appl. Radiat. Isot.*, 65, 17–20.
- [8] Bostick, B.; Vairavamurthy, M.; Karthikeyan, K.; Chorover, J. (2002). Cesium Adsorption on Clay Minerals: An EXAFS Spectroscopic Investigation. *Environ. Sci. Technol.*, 36, 2670–2676.
- [9] Kalinichev, A.G.; Loganathan, N.; Wakou, B.F.N.; Chen, Z. (2017). Interaction of ions with hydrated clay surfaces: Computational molecular modeling for nuclear waste disposal applications. *Proc. Earth Planet. Sci.*, 17, 566–569.
- [10] Durrant, C.B.; Begg, J.D.; Kersting, A.B.; Zavarin, M. (2018). Cesium sorption reversibility and kinetics on illite, montmorillonite, and kaolinite. *Sci. Total Environ.*, 610–611, 511–520.
- [11] Peregodov Yu.S., Mezhri R., Gorbunova E.M., Niftaliev S.I. (2020). Sorbents based on glauconite for collecting oil and oil products. *Condensed media and interphase boundaries*, V.22., No. 2, pp. 87-95
- [12] Rumyantseva A.O., Kutugin V.A., Zhuravlev A.A., Efimov E.D., Belousov P.E. (2023). Influence of various mineral binders on sorption characteristics and stability of granules based on natural sorbents. *Proceedings of the VI Russian Meeting on Clays and Clay Minerals - Clays-2023*. St. Petersburg, pp. 129-131.

ENVIRONMENTAL RISKS ASSESSMENT OF COASTAL AREA IN THE SOUTH-EASTERN BALTIC SEA TO OIL POLLUTION

Elena Krek¹, Alexander Krek¹, Vadim Sivkov^{1,2}, Zhanna Stont^{1,2}

•

¹ Shirshov Institute of Oceanology, Russian Academy of Sciences, Moscow, Russia;

² Immanuel Kant Baltic Federal University, Kaliningrad, Russia

elenka_krek@mail.ru

av_krek@mail.ru

vadim.sivkov@atlantic.ocean.ru

ocean_stont@mail.ru

Abstract

A low probability of oil pollution of coasts from two main potential sources located in the waters of Kaliningrad Region (Russian Federation) in the Baltic Sea is shown based on the results of modelling using Seatrack Web (SMHI, HELCOM). The most threatened areas of the coastal zone and coast, in the middle part of the Curonian Spit – UNESCO World Heritage site, as well as the distal part of the Vistula Spit and on the entire western coast of the Sambia Peninsula, were identified.

Keywords: risks of oil pollution, coastal area, Southeastern Baltic Sea, Seatrack Web

I. Introduction

Intensifying shipping, operation of oil terminals and offshore platforms poses a constant threat not only to coastal and socio-economic resources, but also to sensitive underwater landscapes of marine areas and vulnerable marine habitats [1].

The ship traffic in the Baltic Sea is among the most intensive in the world. The Baltic Sea area is a special area where any discharge of oil and oily mixtures is strongly prohibited (<https://helcom.fi/action-areas/shipping/>). Traffic accidents and illegal discharges from ships may pose high risks for the marine environment, thus co-actions to enhance maritime awareness and efficiency at sea seems to be the important challenge. Oil production from the offshore raises the risk of pollution accidents, which could have a devastating impact on the marine and coastal environment.

The purpose of this work was to assess the probability of oil pollution of the coastal area of Kaliningrad Region (Russian Federation).

II. Study area and methods

The main threat of oil pollution in the study area is oil extraction from Kravtsovskoye (D-6) oilfield located at a distance of 22.5 km from the Curonian Spit coast at the depths of about 30 m. In the case of accidental oil spill from the D-6 oilfield the major damage would be caused to the Curonian Spit [2, 3]. The Curonian Spit is a narrow, sandy peninsula of over 99 kilometers length,

separating the Curonian Lagoon from the open Baltic Sea. The northern part of the spit (52 km) belongs to Lithuania, and the southern one (46 km) – to Russia. Flat sandy beaches, protective dune ridges and near shore sandy spits are very valuable and attractive resources for human recreation and valuable habitat for wildlife [1, 4]. The national parks located on both sides of the Russian/Lithuanian border were added to the UNESCO's World Heritage List in 2000 (<http://whc.unesco.org/en/list/994/documents/>). The Curonian Spit National Park with adjacent waters is also referred to maritime cultural heritage of the Baltic Sea [4].

There are number of smaller villages located at the coast. Those do also have significant importance for developing recreational potential of the region. At present, both national parks include the adjacent sea area up to the 20 m isobaths as a rare biotope and wintering place for birds.

According to Automatic Identification System (AIS) the maximum risks of traffic accidents or illegal discharges from ships are concentrated in the main ship traffic route to the port of Baltiysk at the south-western edge of Sambia Peninsula (Fig.1). The peninsula is located between the Curonian and Vistula Lagoons. Two seacoasts of the peninsula are intensively eroding nowadays. There are rapidly developing seaside resorts here: Svetlogorsk, Zelenogradsk, and Yantarny. Illegal discharges of oil products are constantly detected from satellites on Synthetic Aperture Radar (SAR) images. Long-term satellite monitoring indicates a large number of oil slicks near the Baltiysk [5].

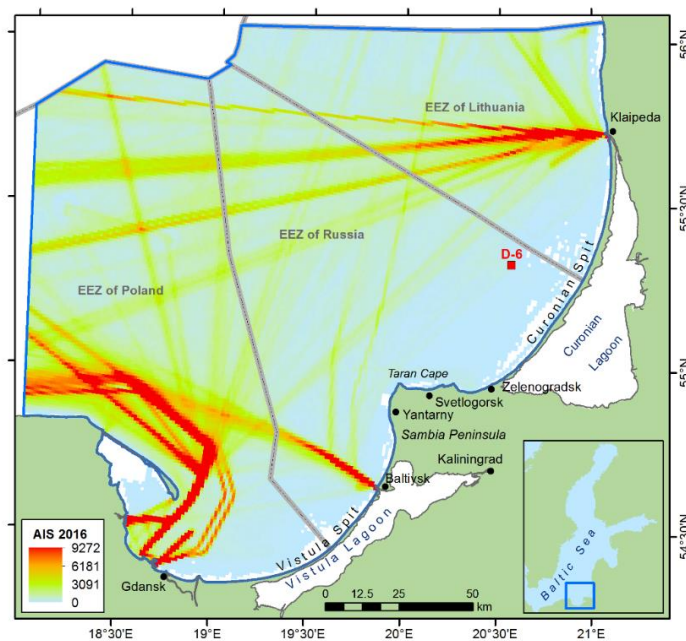


Fig. 1: Density of all ships operating in the Baltic Sea in 2016 based on HELCOM AIS data, and offshore platform D-6 location (©HELCOM)

Propagation of a potential oil spill were calculated using Seatrack Web (SMHI, HELCOM) (<https://stw.smhi.se/>) daily for 48 hours ahead from point potential source (platform D-6) for period covering 2017-2022, and elongated potential source (main ship traffic route to the port of Baltiysk) for period covering 2015. The initial release volume for all scenarios was 100 m³. Combining the results of daily forecasts of oil spreading made it possible to obtain integral patterns of potential pollution of the sea surface, on the basis of which the probability of pollution of coastal area was estimated.

III. Results and discussions

The probability that oil pollution of a given volume from offshore platform D-6 will reach the coastal zone of the Curonian Spit for the meteorological conditions of 2017-2022 turned out to be small (<5%). However, according to the simulation results, it turned out that the middle part of the Curonian Spit was the most oil-prone part of the coastal zone and coast (Figure 2a).

The shape of the potential (hypothetical) oil pollution probability field shows some discrepancy with the wind rose. With a clear predominance of westerly winds, the most probable direction of oil drift turned out to be not the expected eastern, but the northeastern direction. The reason for this discrepancy, apparently, is the distorting influence of coastal water dynamics [6, 7]. It is especially noticeable in the region of low pollution probabilities on the southern and northern periphery of the resulting oil pollution distribution area.

The northeastern direction of potential oil pollution transport was predominant in the area of the main ship traffic route to the port of Baltiysk in 2015. The coast of almost the entire Russian part of the Vistula Spit and the west of the Sambia Peninsula was under a small threat of oil pollution (Figure 2b). This is consistent with the predominance of southerly and westerly winds. In contrast to the area of offshore platform D-6, the probability field obtained here for potential oil pollution of the sea surface is statistically less secure. Based on the wind rose for 2017-2022, obtained according to the data from weather station in Baltiysk (Figure 2b), the trend of oil pollution propagation in this water area will remain the same.

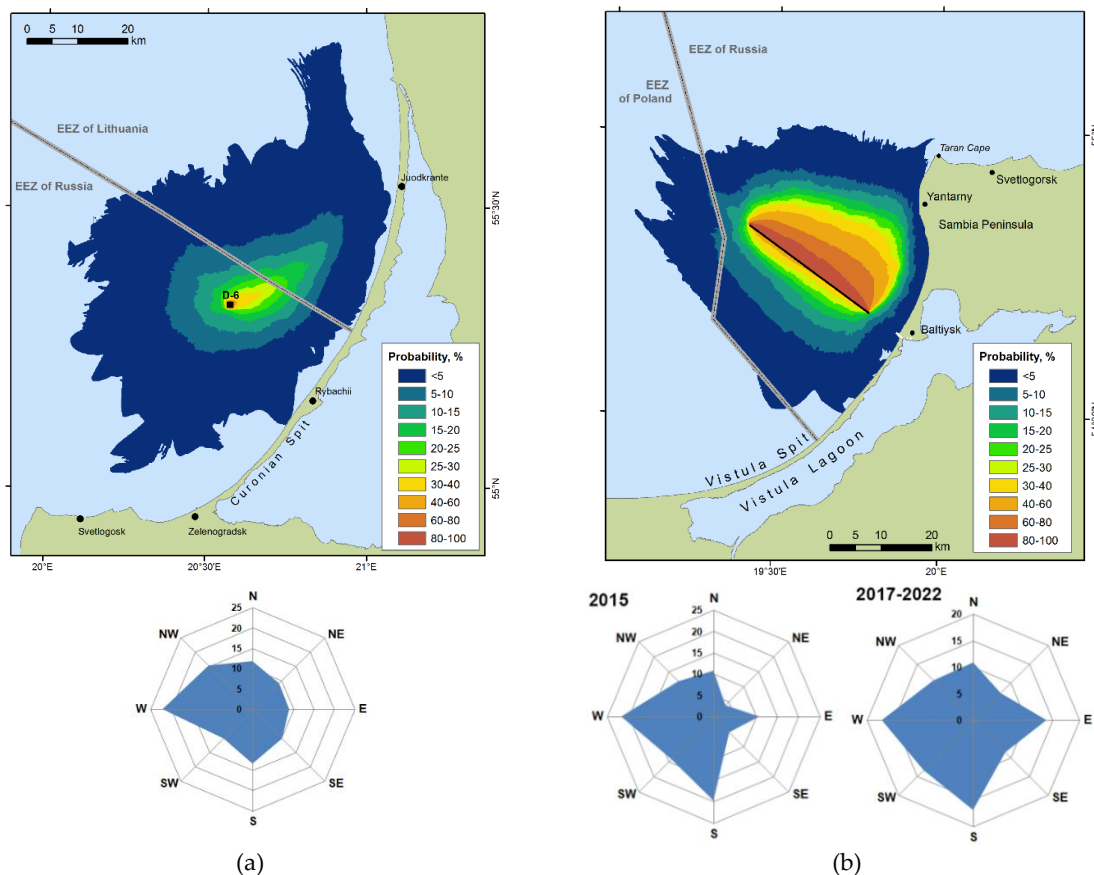


Fig. 2: Probabilities of hypothetical oil pollution propagation within 48 hours based on Seatrack Web (SMHI, HELCOM) model results from potential sources:

a) D-6 oil platform (2017-2022), b) main ship traffic route to the port of Baltiysk (2015)
 Wind roses are given according to meteorological station on D-6 (a) and from Baltiysk (b)

The sensitivity of the coast and coastal area is largely dependent on the physical character of the environment. When assessing the impact on the coast and the coastal zone to possible oil pollution, it is necessary to take into account not only the value of habitats, but also the morphological and lithological characteristics of the underwater coastal slope and coast. This is of particular importance for the sea coast of the Curonian Spit National Park.

The coast at the Curonian Spit is mainly flat. Although there are some parts of intensive erosion present, the sandy beaches are mainly flat with bigger or lower amount of gravel. These are easily permeable sediments and their pollution will lead to long-term negative environmental impacts. Shoreline of the Curonian Spit is unsheltered, facing highly dynamic wave regime and intensive alongshore sediment transport. The beaches are composed of fine and medium-grained sand mainly, but the near shore is much more lithologically diverse. The hard bottoms, clay outcrops and gravel fields present near the shore creates the specific conditions for local biotopes to establish. In order to complete the precise evaluation of near shore and coastal area sensitivity to possible oil spills there is a need to identify vulnerable coastal sectors and complete detailed mapping of underwater landscapes [1].

IV. Summary

The results of the potential (hypothetical) oil spill drift forecast using Seatrack Web (SMHL, HELCOM) from two main potential sources of oil pollution of the coastal zone of Kaliningrad Region (Russian Federation) showed a low probability of oil pollution of coast. Nevertheless, the most prone to such pollution areas of the coastal zone and coast have been identified. These are the middle part of the Curonian Spit (for 2017-2022), the distal part of the Vistula Spit and the entire western coast of the Sambia Peninsula (for 2015). Analysis of environmental risks proved to be an effective tool for regional oil spill response planning.

Acknowledgements. The results of the potential oil spill drift forecast was obtained with a support of the state assignment of IO RAS (Theme No. FMWE-2021-0012); environmental risk assessment was supported by the state assignment of the IKBFU (Theme No. FZWM-2023-0004).

References

- [1] Blažauskas, N. and Dorokhov, D. (2014). Assessment of the sensitivity of sandy coasts of the south-eastern part of the Baltic Sea to oil spills. *Baltica*, Special Issue, 27:55-64.
- [2] Suzdalev, S., Gulbinskas S., Sivkov V., Bukanova, T., (2014). Solutions for effective oil spill management in the southeastern part of the Baltic Sea. *Baltica*, Special Issue, 27:3-8.
- [3] Nemirovskaya I., Ulyanova M., Sivkov V. (2014). Hydrocarbons in the sediments offshore of the Curonian Spit (the south-eastern part of the Baltic Sea). *Baltica*, Special Issue, 27:31-38. DOI: 10.5200/baltica.2014.27.13
- [4] Bashirova L.D., Ulyanova M.O., Kovalev A.A., Lappo A.D., Danilova L.V., Kapustina M.V. (2021). On the Legal Status of Maritime Cultural Heritage and its Management in the Russian Sectors of the Baltic Sea. *J. Mar. Arch.*, 16:111-132. <https://doi.org/10.1007/s11457-020-09288-4>
- [5] Krek, E., Krek, A. and Kostianoy, A. (2021). Chronic Oil Pollution from Vessels and Its Role in Background Pollution in the Southeastern Baltic Sea. *Remote Sensing*. 13(21):4307. <https://doi.org/10.3390/rs13214307>
- [6] Krek A., Stont Zh., Ulyanova M. (2016). Alongshore bed load transport in the southeastern part of the Baltic Sea under changing hydrometeorological conditions: Recent decadal data. *Regional Studies in Marine Science*, 7:81-87. DOI: 10.1016/j.rsma.2016.05.011
- [7] Krek A., Ulyanova M. (2020). Mineral tracers of the alongshore sediment transport (example from the South-Eastern Baltic Sea). *Russ. J. Earth. Sci.*, 20:ES6003. doi:10.2205/2020ES000714.

APPLICATION OF A RANK FUZZY REGRESSION MODEL TO PREDICT THE TECHNICAL CONDITION OF WELL PIPES

Ibrahim Habibov, Oleg Dyshin, Gulnara Feyziyeva, Irada Ahmadova,
Zohra Garayeva

•

Azerbaijan State Oil and Industry University

h.ibo@mail.ru

oleg.dyshin@mail.ru

gulnara.feyziyeva5@gmail.com

ahmadovairada@gmail.com

zabiyevaadnsu@gmail.com

Abstract

Oil and gas pipes used in well operations are undergo to aggressive environments. In this case, corrosion wear of the thickness of their walls occurs, which leads to various difficulties. In order to assess the technical condition of well pipes, geophysical methods are used, one of which is the electromagnetic inspection method.

The paper proposes a method for predicting the maximum loss of pipe thickness based on the results of electromagnetic inspection by the step values of the depth of immersion of the lower part of the pipe into the well.

Based on the use of fuzzy regression with fuzzy input/fuzzy output, a method for assessing the level of impact of the main formation parameters on the technical condition of well pipes is proposed.

Keywords: rank transformation, electromagnetic inspection, fuzzy emissions, moving forecasting, membership function

I. Introduction

Despite a fairly wide range of methods for assessing the technical condition of oil and gas pipes, the most widely used method is electromagnetic inspection. (EMI) [1-4].

Experimental studies were carried out for an offshore field, using an electromagnetic inspection of the EMI-43 type, at a depth of 2000-2400 m. The parameters of the pipes under study were $D_o \times d_i = 127.0 \times 108.6$ mm, $D_o \times d_i = 339.7 \times 313.6$ mm and $D_o \times d_i = 473.1 \times 446.1$ mm (D_o and d_i are the outer and inner string diameter, respectively).

II. The purpose of the work

Is to development of a method for predicting the loss of thickness of the outer pipe of a technical string not accessible to the depth interval for measurements based on previous inspection measurements.

III. Results and discussions

We will demonstrate the application of the RT method to fuzzy regression with a fuzzy input/output the case of measurements using an electromagnetic inspection EMI, which allows us to determine the loss of thickness of the outer pipe of a technical string in a well.

Tables 1 and 2 correspondingly show the values of the maximum loss of pipe thickness and the dependence of the formation parameters (density ρ and viscosity ν) on the depth of immersion of the pipe into the well in the period 2019-2022 obtained by EMI methods.

Table 1: Dependence of the maximum loss of pipe thickness on the depth of immersion into the well

Top part of the pipe, (m)	Bottom of the pipe, (m)	Pipe length, (m)	Nominal thickness of pipe, (mm)	Actual minimum thickness of pipe (mm)	Depth of maximum loss of pipe thickness, (m)	Maximum loss of pipe thickness, (%)	Classification of losses
1	2	3	4	5	6	7	8
2284,10	2292,40	8,29	13,06	12,40	2285,10	5,1	B
2293,70	2302,00	8,29	13,06	12,51	2300,00	4,2	A
2303,30	2311,60	8,34	13,06	12,14	2308,30	7,1	B
2312,90	2321,20	8,29	13,06	12,26	2321,20	6,1	B
2322,40	2330,80	8,34	13,06	12,18	2323,50	6,8	B
2332,10	2340,60	8,50	13,06	12,41	2335,70	5,0	A
2341,90	2350,00	8,11	13,06	12,57	2347,40	3,7	A
2351,30	2359,20	7,98	13,06	8,54	2359,20	34,6	E
2361,20	2369,10	7,86	13,06	8,34	2366,80	36,1	E
2370,40	2381,00	10,61	13,06	8,54	2380,70	34,6	E

Table 2. Dependence of the formation parameters (density ρ , kg/m³ and viscosity ν , s-poise) on the depth of immersion of the pipe into the well in the period 2019-2022

Years							
2019		2020		2021		2022	
ρ	ν	ρ	ν	ρ	ν	ρ	ν
899	6,25	898	5,73	890	5,55	890	5,15
890	6,20	897	5,68	890	5,50	890	5,05
889	6,17	895	5,66	890	5,48	888	5,00
889	6,14	892	5,60	886	5,46	886	4,98
822	6,10	886	5,51	880	5,40	882	4,90
891	6,05	885	5,51	876	5,38	880	4,87
890	6,03	880	5,51	874	5,33	878	4,82
890	6,01	880	5,48	876	5,28	870	4,80
889	5,95	878	5,45	866	5,25	863	4,76
868	5,93	875	5,40	863	5,06	860	4,72
885	5,90	871	5,33	880	5,15	850	4,69
886	5,87	870	5,30	870	5,10	845	4,67
882	5,81	866	5,27	871	5,07	840	4,65
880	5,78	862	5,25	870	5,02	834	4,61
874	5,73	860	5,22	866	5,00	830	4,58
871	5,73	857	5,20	865	4,95	822	4,55
870	5,71	855	5,20	863	4,90	818	4,52
869	5,73	851	5,18	860	4,86	815	4,48
868	5,70	848	5,16	858	4,81	810	4,40
865	5,68	844	5,16	856	4,76	810	4,35

IV. Numerical implementation of the predicting method and discussion of the results

1. According to the table 2 in a year 2021 for variable X_k T°C (T°C is a temperature) build a sequence of points (x_i, y_i) ($i = 0, 1, \dots, 5$), where $x_i = h_i$ – the values of variable depth h: $x_i = 2000 + i \cdot \Delta x$ ($\Delta x = 100$), $i = 0, 1, \dots, 5$; $y_i = y(x_i)$ – the values of variable $y = X$. By sample $V = (x_i, y_i)$ ($i = 0, 1, \dots, 5$) and by method of MNL build a multinomial regression model

$$y = f(x), \quad f(x) = \sum_{j=0}^4 \beta_j x^j = \beta_0 + \beta_1 x + \beta_2 x^2 + \beta_3 x^3 + \beta_4 x^4 \quad (1)$$

Entering the variables of $\tilde{X}_0 = 1, \tilde{X}_1 = x, \tilde{X}_2 = x^2, \tilde{X}_3 = x^3, \tilde{X}_4 = x^4$, we obtain relative variables of $\tilde{X}_0, \tilde{X}_1, \dots, \tilde{X}_4$ of linear regression model

$$y = \sum_{j=0}^4 \beta_j \tilde{X}^j \quad (2)$$

or in matrix notation of $Y = \tilde{X} \cdot \beta$, where $\tilde{X} = (\tilde{X}_{ij})$ – (6×5) – matrix of variable values \tilde{X}_j in the i -th observation; the $Y = (y_0, y_1, \dots, y_5)$ is the vector of vector observations of y variable. According to MNL, coefficient of regression $\beta = (\beta_0, \beta_1, \dots, \beta_4)^T$ (T – is the matrix transpose sign) calculated by the formula

$$\beta = (\tilde{X}^T \tilde{X})^{-1} \cdot Y \quad (3)$$

β coefficients can be calculated using the LIN program in EXCEL with the determination of the error in calculating the predicted value of the output variable

$$\varepsilon_{\hat{y}} = RSS = \sum_{i=0}^5 (\hat{y}_i - y_i)^2, \quad (4)$$

where \hat{y}_i – predicted value of a variable by regression y_i

$$\hat{y}_i = \sum_{j=0}^4 \hat{\beta}_j \cdot \tilde{X}_{ij}, \quad (5)$$

$\hat{\beta}_j$ – MNL- estimated β coefficient calculated by the formula (41).

If the LIN program is not available for estimating of β , then it calculated by formula (3) using a matrix inversion program to calculate the matrix of $(\tilde{X}^T \tilde{X})^{-1}$. In our case if $n = 6$ at number $m = 4$ independent variables of $\tilde{X}_1, \dots, \tilde{X}_4$.

2. Total interval of $[x_0, x_5]$ divide the values of the variable x into intervals of $[x_{i-1}, x_i]$ ($i = 1, \dots, 5$) with length of 100 m. In each of these intervals select an interpolation node of $x_i^* = x_i - \frac{10}{3}$ and construct the interpolation polynomial of Lagrange for $x_i^* \neq x_i$ ($i = 1, \dots, n; n = 5$):

$$g_n(x) = \sum_{i=1}^n f(x_i^*) \prod_{j \neq i} \frac{x - x_j^*}{x_i^* - x_j^*} \quad (6)$$

Since $f^{(n)}(x) \equiv 0$ (due to the fact that the polynomial degree $l = 4$, for all $x \in [x_0, x_5]$, satisfying the condition $x \neq x_i^*$ ($i = 1, \dots, n$)), it is true that $f(x) \equiv g_n(x)$ and in particular for all

$$x_i = 2000 + i \Delta \tilde{x} \quad (\Delta \tilde{x} = 10; i = 0, 1, \dots, 5). \quad (7)$$

Therefore, for each variable X from table 3, by formula $f(x) = g_n(x)$ calculated values of $f(x)$ for all $x = x_i$, defined by the formula (7).

3. In the example under consideration, can assume (with a sufficiently small error) that $h_i = 2380$ – the maximum depth of immersion into the well of the bottom part of the pipe, which was accessible to inspection measurements in the depth range of [2000; 2500]. Further we will use normalized depth values of $\tilde{h}_i = h_i/2000$. Then $\tilde{h}_{i_0} = 1,19$.

4. Further we will assume that $i = 1, 2, \dots$ – length interval numbers $\Delta \tilde{x} = 0,005$ (10/2000) at the depth interval of \tilde{h}_i , equal to [1; 1,25] and i_0 – number of subsequent available length interval of Δi . For this example $i_0 = 38$.

Starting from the 1st line of table 1, these intervals can be numbered with a series of numbers $I = \{\varepsilon | i = 1, 2, \dots, i_0\}$, every fixed value i correspond to the x_i interval with length of $\Delta x = 0,005$.

There is a maximum loss of the pipe thickness (in fractions of a unit to three decimal places) along this interval.

5. By sample $V = \{x_i, y_0\} (i = 1, \dots, i_0)$ built the best polynomial regressive model of $y = F(x)$ degree $l \leq 10$ by using of MNL. Let's denote $f(x) = F'(x)$ ($F'(x)$ – it is derivative function of $F(x)$). Let's apply the 4th order Runge-Kutta method with a step of $\Delta\tilde{h} = 0,005$, assuming i_0 is an even number (otherwise V is considered starting from $i=2$):

$$y_{i+1} = y_i + \frac{1}{6}(k_1 + 2k_2 + 2k_3 + k_4) \tag{8}$$

$$k_1 = \Delta\tilde{h} \cdot f(x_i), \quad k_2 = \Delta\tilde{h} \cdot f\left(x_i + \frac{1}{2}k_1\right),$$

$$k_3 = \Delta\tilde{h} \cdot f\left(x_i + \frac{1}{2}k_2\right), \quad k_4 = \Delta\tilde{h} \cdot f(x_i + k_3).$$

By formula (8), knowing that $y_i = F(x_i)$ if $n = n_0$, it is possible to calculate the forecasting value of $y_{i_0+1} = F(x_{i_0+1})$. The forecast error is estimated according to the following formula

$$\rho_1 = \frac{1}{2880} |f^{(4)}(x_{i_0})| \left((\Delta\tilde{h})^5 + O(\Delta h)^6 \right) \tag{9}$$

where $f^{(4)}(x_{i_0})$ – is a 4th derivative function of $f(x)$ at a point x_{i_0} .

If the degree of the polynom $F(x)$ $l \leq 1$, then $f^{(4)}(x) - F^{(5)}(x) \equiv 0$ and $\rho_1 = O((\Delta\tilde{h})^6)$, where $O((\Delta h)^6)$ – infinitesimal order of $(\Delta\tilde{h})^6$.

Shifting the sample V forward by step Δh (taking the obtaining predicted value y_{i_0+1} as the actual value), we will get predicted value of $y_{i_0+2} = F(x_{i_0+2})$ with predicted error

$$\rho_2 = \frac{1}{2880} \cdot \rho_1 \cdot (\Delta\tilde{h})^5 + O(\Delta\tilde{h})^6,$$

Calculated by fomula (8) with replacement on the right side of x_{i_0} by x_{i_0+1} . If $l \leq 4$ we also obtain that $\rho_2 = O(\Delta\tilde{h})^6$. In this way, forecasts can be calculated by $y = F(x_{max})$, where $x_{max} = \tilde{h}_{i_{max}}$, $i_{max} = 50$ (limiting value in the table 3) in this case the forecast error x_{n_0+v} will equal to $\rho_{n_0+v} = O(\Delta\tilde{h})^{5(v_0-1)}$.

6. By sample of last 20 values $y: y_{i_0-19}, \dots, y_{i_0}$ fuzzify the variable Y . Denote that $y^{(1)} = y_{i_0-19}$, $y^{(2)} = y_{i_0-18}$, $y^{(N)} = y_{i_0}$ ($N = 20$) and calculate for indexes $i = i_0 - 9, i_0 - 8, \dots, i_0$ of value

$$\hat{a}^0 = \frac{1}{2} \left(\max_{1 \leq i \leq n} y^{(i)} + \min_{1 \leq i \leq n} y^{(i)} \right),$$

$$\hat{b}^0 = \frac{\left(\max_{1 \leq i \leq n} y^{(i)} + \min_{1 \leq i \leq n} y^{(i)} \right)}{2\varepsilon_\alpha}, \quad \varepsilon_\alpha = 2. \tag{10}$$

Then with probability $1 - \alpha$, $\alpha = \varepsilon^{-4}$ will satisfy the following ratio

$$\mu_Y(y) = \sigma(Y = y) = \exp \left[- \left(\frac{y - \hat{a}^0}{\hat{b}^0} \right)^2 \right]. \tag{11}$$

In order, $L_Y(y) = R_Y(y) = \exp \left[- \left(\frac{y - \hat{a}^0}{\hat{b}^0} \right)^2 \right]$.

If $\hat{a}^0 < y^{(n)}$, then subsequent $V_0 = \{y^{(1)}, y^{(2)}, \dots, y^{(n)}\}$ shifts to right by 1 and replaced by subsequent of $V_1 = \{y^{(2)}, y^{(3)}, \dots, y^{(n)}, y^{(n+1)}\}$, where $y^{(n+1)}$ at $n \geq n_0$ then has a forecast value calculated by formula (8).

By formula (41) is calculated new values of a^1, b^1 values of a and b etc. until, at a certain step of $v_{k,n}^0$ where the condition is satisfied of $\hat{a}^{v_0} \approx y^{(n)}$ with a certain error ε_0 (for example, $\varepsilon_0 = 10^{-2}$). Then, with the approximation error ε_0 , can accept that the mode of the fuzzy number of $y^{(n)}$ is equal to \hat{a}^{v_0} .

Truth, for fixed depth of \tilde{h}_{i_0} the value of $X_{n,k}$ of each fuzzy parameter of X_k at a depth of $\tilde{h} = \tilde{h}_i$ find number of $\hat{a}_{i,k}^{v_{i,k}^0}$ and $\hat{b}_{i,k}^{v_{i,k}^0}$ (denote their as $\hat{a}_{i,k}^{v_{i,k}^0}$ and $\hat{b}_{i,k}^{v_{i,k}^0}$), where $X_{n,k}$ represented by LR-

form $X_{n,k} = (\hat{a}_{i,k}^{v_0}, \hat{b}_{i,k}^{v_0}, \hat{b}_{i,k}^{v_0})$ with the membership function $\mu_{X_{n,k}}(y) = \exp \left[- \left(\frac{y - \hat{a}_{i,k}^{v_0}}{\hat{b}_{i,k}^{v_0}} \right)^2 \right]$, if

$|y - \hat{a}_{i,k}^{v_0}| < \hat{b}_{i,k}^{v_0}$ and $\mu_{X_{n,k}}(y) = 0$, if $|y - \hat{a}_{i,k}^{v_0}| > \hat{b}_{i,k}^{v_0}$.

7. Via $\hat{X}_k(\tilde{h})$ denote the output fuzzy variable in linear fuzzy regression with close-cut input \tilde{h} :

$$\hat{X}_k(\tilde{h}) = \beta_0^{(k)} + \beta_1^{(k)}\tilde{h}, \quad (12)$$

Which the coefficients $\beta_0^{(k)}$ and $\beta_1^{(k)}$ calculated by sample of $V = \{x_i, y_i\}$ ($i = 1, \dots, i_0$), where $x_i = \tilde{h}_i$ – the depth interval length $\Delta\tilde{h} = 0.005$ with number of n , i.e. $x_i = 1 + i\Delta h$ and \hat{Y}_i – the value of variable $\hat{Y} = \hat{X}_k$ at depth interval x_k , obtained by calculation according to the equation (12).

Denote $x_k \equiv 0$, $x_1 = \tilde{h}$ ($x_{k,0} \equiv 1$, $x_{k,1} = \tilde{h}_i$), via X (10×2) – matrix of $X = (x_{i,j})$ ($i = i_0 - 8, \dots, i_0 + 1; j = 0, 1$). $Y = (Y_{i_0-8}, \dots, Y_{i_0+1})^T$, $Y_i = X_k(\tilde{h}_i)$, $i = i_0 - 8, \dots, i_0 + 1$; $\beta = (\beta_0^{(k)}, \beta_1^{(k)})^T$ (T – is matrix transpose sign). Then the value of $\hat{\beta}$ determined by the formula

$$\hat{\beta} = (X^T X)^{-1} X^T Y \quad (13)$$

or calculated by the program of или LIN in EXCEL for simple linear regression with single input variable of x_1 .

8. Will differ the fuzzy number of Y_i in the record, obtained by fuzzification using the formula (11), from fuzzy number of \hat{Y}_i , obtained by calculation with regression (12).

Due to the symmetry of y the left span of $l_{Y_i}(\alpha)$, $\alpha \in [0,1]$ of the formula (49), will be equal to the right span $r_{Y_i}(\alpha)$, and $l_{Y_i}(1) = r_{Y_i}(1) = \hat{b}_i^{v_0}$.

9. Let's put $\alpha^* = 0,5$.

By the sample of $\{R(\tilde{h}_i), R(l_{Y_i}(\alpha^*)) : i = i_0 - 8, \dots, i_0 + 1\}$ will construct following regressive model

$$R(l_{Y_i}(\alpha^*)) = \beta_0(\alpha^*) + \beta_1(\alpha^*)R(\tilde{h}_i), \quad (14)$$

where $R(\tilde{h}_i)$ – rang of number \tilde{h}_i in the subsequent of $\{\tilde{h}_i\}$ ($i = i_0 - 8, \dots, i_0 + 1$), first number in ascending number order \tilde{h}_i , $R = 1$ rank is assigned, to the second $R = 2$ and so on; in the case of two identical numbers, equal for example r , in an unordered row, the first one is given rank of $R = [(r - 1) + r]/2$, but the second rang represented by the following $R = [(r + 1) + r]/2$.

For simple regression of (14), assum that $Y_i = l_{Y_i}(\alpha^*)$ and $R(X_i) = R(\tilde{h}_i)$ rank transformation (14) reduces to the following equation

$$R(Y_i) = \frac{(n + 1)}{2} + \beta \left[R(X_i) - \frac{(n + 1)}{2} \right], \quad (15)$$

where n – is the size of selected subsequent of $\{R(X_i), R(Y_i)\}$ (in this case $n = (i_0 + 1) - (i_0 - 8) + 1 = 10$).

Assume that $y_i = R(Y_i) - \frac{(n+1)}{2}$, $x_i = R(X_i) - \frac{(n+1)}{2}$, in this case we will get following regression equation $y_i = \beta \cdot x_i$, in which the MNL- is the value of $\hat{\beta}$ coefficient of β determined from the equation of $\frac{dz}{d\beta} = 0$, $Z = \sum_{i=1}^n (y_i - \beta x_i)^2$, the solution of which is determined by the formula:

$$\hat{\beta} = \frac{\sum_{i=1}^n y_i x_i}{\sum_{i=1}^n x_i^2} \quad (16)$$

Then from the equation of (15) find the predicted value

$$\hat{R}(l_{Y_i}(\alpha^*)) = \frac{(n+1)}{2} + \left[R(X_i) - \frac{(n+1)}{2} \right] \frac{\sum_{i=1}^n \left[R(Y_{i'}) - \frac{(n+1)}{2} \right] \left[R(X_{i'}) - \frac{(n+1)}{2} \right]}{\sum_{i=1}^n \left[R(X_{i'}) - \frac{(n+1)}{2} \right]^2}. \quad (17)$$

10. Let's calculate the values $\bar{l}_{\hat{Y}_i}(\alpha^*)$ by the following rules

$$\bar{l}_{\hat{Y}_i}(\alpha^*) = \begin{cases} l_{Y_{(1)}}(\alpha^*), & \text{if } \hat{R}(l_{Y_i}(\alpha^*)) < R(l_{Y_{(1)}}(\alpha^*)), \\ l_{Y_{(n)}}(\alpha^*), & \text{if } \hat{R}(l_{Y_i}(\alpha^*)) > R(l_{Y_{(n)}}(\alpha^*)), \\ l_{Y_{(j)}}(\alpha^*), & \text{if } \hat{R}(l_{Y_i}(\alpha^*)) < R(l_{Y_{(j)}}(\alpha^*)). \end{cases} \quad (18)$$

If $R(l_{Y_{(j)}}(\alpha^*)) < \hat{R}(l_{Y_i}(\alpha^*)) < R(l_{Y_{(j+1)}}(\alpha^*))$, then

$$\bar{l}_{\hat{Y}_i}(\alpha^*) = l_{Y_{(j)}}(\alpha^*) + (l_{Y_{(j+1)}}(\alpha^*) - l_{Y_{(j)}}(\alpha^*)) \frac{R(l_{Y_{(j)}}(\alpha^*)) - R(l_{Y_{(j)}}(\alpha^*))}{R(l_{Y_{(j+1)}}(\alpha^*)) - R(l_{Y_{(j)}}(\alpha^*))},$$

where $\bar{l}_{\hat{Y}_i}(\alpha^*)$ - is a value of the left span $l_{\hat{Y}_i}(\alpha^*)$ of the fuzzy number $\hat{Y}_i(\alpha) = Y_i(X_i)(\alpha)$, constructed by the rang regression (14); $l_{Y_{(j)}}(\alpha^*)$ - j^{th} is the ascending value of l of subsequent $\{l_{Y_{(i)}}(\alpha^*)\}$, $i = i_0 - 8, \dots, i_0 + 1$. Since the left-side value of the α -level set of a fuzzy number must be no more than its mode, then the estimation of the left-side range of the fuzzy number $Y_i(\alpha^*)$ will be written as

$$\hat{l}_{\hat{Y}_i}(\alpha^*) = \min\{\bar{l}_{\hat{Y}_i}(\alpha^*), \hat{y}_i\}, \quad (19)$$

where \hat{y}_i - a priori estimation of the mode of a fuzzy number \hat{Y}_i , for which the assessment can be taken as $\hat{a}_{Y_i}^{(v_0)}$ mode of МОДЫ fuzzy number Y_i , obtained due to the fuzzification according to the formula (11). This estimate is subsequently corrected using a parametric estimator of span.

Similarly, according to the sample of $\{R(\tilde{h}_i), R(r_{Y_i}(\alpha^*)): i = i_0 - 8, \dots, i_0 + 1\}$ with replacement in the formulas (17)-(19) of l by r will get value of right span of the fuzzy number $Y_i(\alpha^*)$ as following form

$$\hat{r}_{\hat{Y}_i}(\alpha^*) = \max\{\bar{r}_{\hat{Y}_i}(\alpha^*), \hat{y}_i\}. \quad (20)$$

Under the numbers of $l_{Y_i}(\alpha)$ and $r_{Y_i}(\alpha)$ understood the projection to the y axes of intersection points with line $\mu = \alpha$ correspondingly of left branch $L(x)$ and right branch $R(x)$ membership functions of $\mu_{Y_i}(y)$ of fuzzy number Y_i .

In the formulas (17) and (19) mode of a_{Y_i} of the fuzzy number $Y_i(\alpha)$ satisfies, respectively, the equalities

$$\begin{aligned} a_{Y_i} &= l_{Y_i}(\alpha) + l \cdot L^{-1}(\alpha), \\ a_{Y_i} &= r_{Y_i}(\alpha) - r \cdot L^{-1}(\alpha), \end{aligned} \quad (21)$$

where $L^{-1}(\alpha) = l_{Y_i}(\alpha)$.

In the case, when the membership functions of of fuzzy number Y_i is represented by the Gaussian $\mu_{Y_i}(y) = \exp\left[-\left(\frac{y-a_{Y_i}}{b_{Y_i}}\right)^2\right]$ that get

$$l = r = b_{Y_i}. \quad (22)$$

11. Parametric assessment of spans and modes of the fuzzy number $Y_i(X_i)(\alpha)$ with $\alpha \neq \alpha^*$ at a close-cut input $X_i = \tilde{h}_i$ is constructed as follows.

Based on the obtained estimations of $\bar{r}_{\hat{Y}_i}(\alpha^*)$ and $\bar{l}_{\hat{Y}_i}(\alpha^*)$ are built following estimations

$$\begin{aligned} \hat{r}_{\hat{Y}_i}(\alpha) &= \begin{cases} \max\{\max_{\{\alpha \leq s < \alpha^*\}}\{\bar{r}_{\hat{Y}_i}(s), \hat{y}_i\}\}, & \text{if } \alpha < \alpha^*, \\ \max\{\min_{\{\alpha^* < s \leq \alpha\}}\{\bar{r}_{\hat{Y}_i}(s), \hat{y}_i\}\}, & \text{if } \alpha^* < \alpha, \end{cases} \\ \hat{l}_{\hat{Y}_i}(\alpha) &= \begin{cases} \min\{\max_{\{\alpha^* \leq s < \alpha\}}\{\bar{l}_{\hat{Y}_i}(s), \hat{y}_i\}\}, & \text{if } \alpha^* < \alpha, \\ \min\{\min_{\{\alpha < s \leq \alpha^*\}}\{\bar{l}_{\hat{Y}_i}(s), \hat{y}_i\}\}, & \text{if } \alpha < \alpha^*, \end{cases} \end{aligned} \quad (23)$$

Since $\hat{l}_{\hat{Y}_i}(\alpha)$, $\hat{r}_{\hat{Y}_i}(\alpha)$ increase by decreasing of α , then the $\min_{\alpha} \hat{l}_{\hat{Y}_i}(\alpha) = \hat{l}_{\hat{Y}_i}(0)$ and the $\max_{\alpha} \hat{l}_{\hat{Y}_i}(\alpha) = \hat{l}_{\hat{Y}_i}(1)$; $\min_{\alpha} \hat{r}_{\hat{Y}_i}(\alpha) = \hat{r}_{\hat{Y}_i}(1) = \hat{y}_i$ and $\max_{\alpha} \hat{r}_{\hat{Y}_i}(\alpha) = \hat{r}_{\hat{Y}_i}(0)$, in this case $L_{\hat{Y}_i}(\hat{l}_{\hat{Y}_i}(1)) = R_{\hat{Y}_i}(\hat{r}_{\hat{Y}_i}(1)) = 1$ and \hat{y}_i – is the value of the fuzzy number $Y_i(X_i)(\alpha)$ where $\alpha = 0$, to be confirmed.

For each fixed i , intend sample data of $\{\hat{l}_{\hat{Y}_i}(\alpha_k), \alpha_k: k = 0, 1, \dots, k_0\}$ and $\{\hat{r}_{\hat{Y}_i}(\alpha_k), \alpha_k: k = 0, 1, \dots, k_0\}$ with increasing subsequent of $\{\alpha_v\}$ the value parameters α (for instance, $\alpha_k = k/10, k = 0, 1, \dots, 10$) and by the values of $\hat{l}_{\hat{Y}_i}(\alpha_v)$ and $\hat{r}_{\hat{Y}_i}(\alpha_v)$, determined by the formula (23), the measure of the fuzzy number $\hat{Y}_i = Y_i(X_i)$ is adjusted and the membership function $\mu_{\hat{Y}_i}(y)$ is approximated. However, if $\alpha = \alpha_v$ $L_{\hat{Y}_i}(\hat{l}_{\hat{Y}_i}(\alpha_k)) = \alpha_v$ ($k = 0, 1, \dots, k_0$) ($L_{\hat{Y}_i}(y)$ – that is the left branch of function $\mu_{\hat{Y}_i}(y)$), then by the regression

$$L_{\hat{Y}_i}(y) = \beta_0^{(l)} + \beta_1^{(l)} \cdot y + \beta_2^{(l)} \cdot y^2 \quad (24)$$

Based on the sample of $\{\hat{l}_{\hat{Y}_i}(\alpha_k), \alpha_k: k = 0, 1, \dots, k_0\}$ it is possible to obtain of predicted value $\hat{L}_{\hat{Y}_i}(y)$ for all of $y \in \text{supp}\hat{Y}_i = [-\hat{b}_{\hat{Y}_i}^{(v_0)}, \hat{b}_{\hat{Y}_i}^{(v_0)}]$. Similarly, taking into account the equalities of $R_{\hat{Y}_i}(\hat{r}_{\hat{Y}_i}(\alpha_k)) = \alpha_k, k = 0, 1, \dots, k_0$, the right branch is being restored $R_{\hat{Y}_i}(y)$ by the following regression

$$R_{\hat{Y}_i}(y) = \beta_0^{(r)} + \beta_1^{(r)} \cdot y + \beta_2^{(r)} \cdot y^2. \quad (25)$$

Further, denoting through $\hat{y}_i^{(l)} = \hat{l}_{\hat{Y}_i}(1)$ and $\hat{y}_i^{(r)} = \hat{r}_{\hat{Y}_i}(1)$ obvious estimates of the mode of a fuzzy number, for evaluation of \hat{y}_i the mode of the fuzzy number $Y_i(X_i)$ can be accept as following

$$\hat{y}_i = \frac{\hat{y}_i^{(l)} + \hat{y}_i^{(r)}}{2}. \quad (26)$$

The spans $l_{\hat{Y}_i}$ and $r_{\hat{Y}_i}$ of the fuzzy number $\hat{Y}_i = Y_i(X_i)$ estimate as following

$$\hat{l}_{\hat{Y}_i} = \hat{y}_i - L_{\hat{Y}_i}^{-1}(0), \quad \hat{r}_{\hat{Y}_i} = R_{\hat{Y}_i}^{-1}(0) - \hat{y}_i, \quad (27)$$

where $L_{\hat{Y}_i}^{-1}(0)$ and $R_{\hat{Y}_i}^{-1}(0)$ are solutions, respectively, of the equations $L_{\hat{Y}_i}(y) = 0$ and $R_{\hat{Y}_i}(y) = 0$. However, the fuzzy number \hat{Y}_i represented by the LR-form as following

$$\hat{Y}_i = \left(\hat{y}_i, \hat{y}_i - L_{\hat{Y}_i}^{-1}(0), R_{\hat{Y}_i}^{-1}(0) - \hat{y}_i \right)_{LR} \quad (28)$$

Tuth, for the fuzzy variables $\hat{Y}_i = X_{ik}(\tilde{h}_i), i = i_0 - 8, \dots, i_0 + 1$ is obtained as the form (28) represented by the LR-form.

12. Suppose that the Y_i – is the variable, characterized by the maximum losses of the pipe thickness at the of $\tilde{h}_i, i = i_0 - 8, \dots, i_0 + 1$, the value of which $i = i_0 - 8, \dots, i_0$ determined in the 7th column of the table 1 and expressed in fractions of a unit (so if $i = i_0$ $Y_i = 0,346$, i.e. 34,6%), and the value Y_{i_0+1} calculated by the formula of predicting (8).

Let's make fuzzification of number Y_i ($i = i_0 - 8, \dots, i_0 + 1$) by the formula (10) with appropriate modes $\hat{a}_{\hat{Y}_i}^{(v_0)}$ and spans $\hat{b}_{\hat{Y}_i}^{(v_0)}$.

To describe the main characteristics of a fuzzy number of $Y_i(X_i), X = (X_1, X_2, X_3)$ – are vector of parametrs of the formation with the values from the table 3, integrated using the formula (6) whole of 10-meter depth scale by step $\Delta\tilde{h} = 0,005$ along all depth interval [1, 1.25].

Consider the last 11 values of the vector X at a depth \tilde{h}_i with indexes $I = \{i | i = i_0 - 8, \dots, i_0 + 1\}$. By sample $\{l_{X_1}(\alpha), l_{X_2}(\alpha), l_{X_3}(\alpha), l_{Y_i}(\alpha)\}, i \in I$, let's construct a rank regression instead of (52)

$$R(l_{Y_i}(\alpha)) = \beta_0^{(l)}(\alpha) + \sum_{p=1}^3 \beta_p^{(l)} R(l_{X_{ip}}(\alpha)) + \sum_{p'=1}^3 \sum_{p=1}^3 \beta_{pp'}^{(l)}(\alpha) R(l_{X_{ip}}(\alpha)) \cdot R(l_{X_{ip'}}(\alpha)) \quad (29)$$

however by selected data $\{r_{X_1}(\alpha), r_{X_2}(\alpha), r_{X_3}(\alpha), r_{Y_i}(\alpha)\}, i \in I$ – a rank regression.

$$R(r_{Y_i}(\alpha)) = \beta_0^{(r)}(\alpha) + \sum_{p=1}^3 \beta_p^{(r)} R(r_{X_{ip}}(\alpha)) + \sum_{p'=1}^3 \sum_{p=1}^3 \beta_{pp'}^{(r)}(\alpha) R(r_{X_{ip}}(\alpha)) \cdot R(r_{X_{ip'}}(\alpha)) \quad (30)$$

From the equations (29) and (30) based on the MNL-estimations of their coefficient the predicted values $\hat{R}(l_{Y_i}(\alpha))$ and $\hat{R}(r_{Y_i}(\alpha))$ are found, of which using the formulas (18)-(23) the values of $\hat{r}_{\hat{Y}_i}(\alpha)$ and $\hat{l}_{\hat{Y}_i}(\alpha)$ are calculated, and using formulas (24)-(28) the left and right branches of the membership function and the LR-form of the fuzzy number $\hat{Y}_i = Y_i(X_i)$ are calculated.

13. Discrepancy between fuzzy numbers of Y_i и \hat{Y}_i is calculated by the formula (11):

$$d(Y_i, \hat{Y}_i) = \frac{\int_{-\infty}^{\infty} |\mu_{Y_i}(x) - \mu_{\hat{Y}_i}(x)| dx}{\int_{-\infty}^{\infty} \mu_{Y_i}(x) dx} + h_d(Y_i(0), \hat{Y}_i(0)), \quad (31)$$

where $Y_i(0) = \text{supp}Y_i$, $\hat{Y}_i(0) = \text{supp} -$ carriers of fuzzy numbers Y_i and \hat{Y}_i , represented by intervals

$$\begin{aligned} Y_i(0) &= [\hat{a}_{Y_i}^{(v_0)} - L_{Y_i}^{-1}(0), R_{Y_i}^{-1}(0) - \hat{a}_{Y_i}^{(v_0)}] \\ \hat{Y}_i(0) &= [\hat{y}_i - \hat{l}_{\hat{Y}_i}(0), \hat{r}_{\hat{Y}_i}(0) - \hat{y}_i] \end{aligned} \quad (32)$$

Let's denote for intervals of $Y_1(0)$ и $Y_2(0)$ respectively via $[a_1, b_1]$ and $[a_2, b_2]$. The first term on the right side (31) characterizes the relative error of approximation of the membership function of the fuzzy number Y_i by the membership function of the fuzzy number \hat{Y}_i . In order for the second term to characterize the relative error in approximating the interval $Y_i(0)$ to the interval of $\hat{Y}_i(0)$ will write as a following form

$$h_d(Y_i(0), \hat{Y}_i(0)) = \left\{ \frac{1}{2} [(\hat{y}_i - \hat{l}_{\hat{Y}_i}(0)) + (\hat{r}_{\hat{Y}_i}(0) - \hat{y}_i)] - \frac{1}{2} (\hat{a}_{Y_i}^{(v_0)} - L_{Y_i}^{-1}(0)) + (R_{Y_i}^{-1}(0) - \hat{a}_{Y_i}^{(v_0)}) \right\} \cdot \frac{1}{R_{Y_i}^{-1}(0) + L_{Y_i}^{-1}(0) - 2\hat{a}_{Y_i}^{(v_0)}}, \quad (33)$$

where is the first multiplier in (33) is the distance between the centers of the intervals $\hat{Y}_i(0)$ and $Y_i(0)$, and the second multiplier $-$ is an inverse number to the length of the interval $Y_i(0)$ Simpson's compound rule. Assume that the points of $a = t_0 < t_1 < t_2 < \dots < t_{s-1} \approx b$ split the cut $[a, b]$ to the s -subcuts (elementary cuts). Having put the $h = (b - a)/2s$, $t_i = a + 2th$ will obtain the following

$$I = \int_a^b f(x) dx = \sum_{i=0}^{n-1} \int_{t_i}^{t_{i+1}} f(x) dx.$$

Simpson's compound formula is written as following

$$\begin{aligned} I &= \frac{h}{8} [f(a) + 4f(a+h) + 2f(a+2h) + 4f(a+3h) + 2f(a+4h) + \\ &+ 4f(a+5h) + f(a+6h)] - (b-a) \cdot \frac{h^4}{180} \cdot f^{(4)}(a+5h), \quad h = \frac{b-a}{4}, \end{aligned} \quad (34)$$

with remaining members

$$R_{2s+1} = -(b-a) \frac{h^4}{180} \cdot f^{(4)}\left(a + \frac{5}{4}(b-a)\right). \quad (35)$$

With increasing number of 5 elementary cuts $R_{2s+1} \rightarrow 0$.

The integral in the denominator of the fraction on the right-side of (69) is written as

$$\int_{-\infty}^{\infty} \mu_{Y_i}(x) dx = \int_{a_1}^{b_1} f(x) dx, \quad f(x) = \exp \left[- \left(\frac{x - \hat{a}_{Y_i}^{(v_0)}}{\hat{b}_{Y_i}^{(v_0)}} \right)^2 \right]. \quad (36)$$

In this case, the 4th derivative is written as following

$$f^{(4)}(x) = \left[-2 \left(\frac{x-a}{b} \right) \cdot \frac{1}{b} \right]^4 \exp \left[- \left(\frac{x - \hat{a}_{Y_i}^{(v_0)}}{\hat{b}_{Y_i}^{(v_0)}} \right)^2 \right].$$

By choosing s , any degree of smallness of the remainder term R_{2s+1} is achieved in (35).

To calculate the integral in the numerator on the right side of (68), calculate $a = \min\{a_1, a_2\}$, $b = \max\{b_1, b_2\}$ and calculate of

$$\int_{-\infty}^{\infty} |\mu_{Y_i}(x) - \mu_{\hat{Y}_i}(x)| dx = \int_a^b |\mu_{Y_i}(x) - \mu_{\hat{Y}_i}(x)| dx, \quad (37)$$

where $\mu_{Y_i}(x)$ is the $f(x)$ function from (36), but $\mu_{\hat{Y}_i}(x)$ has a left $L_{\hat{Y}_i}(x)$ and right $R_{\hat{Y}_i}(x)$ branches, modelling by the regression of (24) and (25), respectively. Therefore, the derivatives $\mu_{\hat{Y}_i}(x) \equiv 0$ and remaining members of (35) for the function $f(x) = |\mu_{Y_i}(x) - \mu_{\hat{Y}_i}(x)|$ is completely determined by the 4th derivative of the function of

$$\mu_{Y_i}(x) = \exp \left[- \left(\frac{x - \hat{a}_{Y_i}^{(v_0)}}{\hat{b}_{Y_i}^{(v_0)}} \right)^2 \right].$$

Tuth, the relative approximation accuracy (RAA) of the fuzzy number Y_i with a fuzzy number \hat{Y}_i expressed as the following

$$\text{RAA}(Y_i = \hat{Y}_i) = 1 - d(Y_i, \hat{Y}_i), \quad (38)$$

moreover, equality (38) is true with accuracy (38) and confidence probability

$$P_{\partial}(Y_i = \hat{Y}_i) = \left(\alpha \right)^{v_0}, \quad \alpha = e^{-4}, \quad (39)$$

where v_0 – iteration step, on which the assessment $\hat{a}_{Y_i}^{(v_0)}$ is achieved for the mode of the number Y_i fuzzified by formula (11).

14. According by the formula (30) the relative approximation of \hat{Y}_i to Y_i is calculated, in the case, when the Y is the parametr of the formation X_k and X is the depth of the well and $Y_i = X_{ik}$ and $X_i = h_i$ (let's denote their as $d(X_{ik}, \hat{X}_{ik})$) for each parametr of the formation X_k ($k = 1, 2, 3$) and in the case when Y is the maximum losses of the pipe thickness and the $X = (X_1, X_2, X_3)$ is the vector parametr of the formation and $Y_i = Y_i(X_i)$, $X_i = (X_{i1}, X_{i2}, X_{i3})$ (let's denote their as $d(Y_i, \hat{Y}_i)$). Taking into account the error ρ_1 depth predictions h_i valuves of y_{i_0+1} maximum losses of the thickness, determined by the formula (9), total (general) error of predictions \hat{Y}_{i_0+1} are calculated as following

$$\varepsilon_1 = \rho + \left(\prod_{k=1}^3 d(X_{i_0+1,k}, \hat{X}_{i_0+1,k}) \right) \cdot d(Y_{i_0+1}, \hat{Y}_{i_0+1}), \quad (40)$$

where $\hat{X}_{i_0+1,k}$ –predicted parameter value X_k at a depth h_i by regression (12) and Y_{i_0+1} – predicted value of the maximum losses of thickness, determined by the rank regressions (24) and (25). To error of (40) corresponds to relative approximation accuracy \hat{Y}_{i_0+1} to the true (unobserved) value Y_{i_0+1} (i.e. the accuracy of predict \hat{Y}_{i_0+1}), defined by equality

$$\text{RAA}(\hat{Y}_{i_0+1}, Y_{i_0+1}) = 1 - \varepsilon_1, \quad (41)$$

which is valid with confidence probability

$$P_{\partial,1} = \left[\prod_{k=1}^3 P_{\partial,k}(X_{i_0+1,k} = \hat{X}_{i_0+1,k}) \right] \cdot P_{\partial}(Y_{i_0+1}, \hat{Y}_{i_0+1}), \quad (42)$$

where $P_{\partial,k}(X_{i_0+1,k} = \hat{X}_{i_0+1,k}) = (e^{-4})^{v_0 \cdot i_0 + 1, k}$ ($v_0, i_0 + 1, k$ – is iteration step, on which achieved by the way of fuzzification mode estimation of a fuzzy number $\hat{X}_{i_0+1,k}$) and $P_{\partial}(Y_{i_0+1}, \hat{Y}_{i_0+1}) = (e^{-4})^{v_0 \cdot i_0 + 1}$ ($v_0, i_0 + 1$ – is iteration step, on which achieved by the way of fuzzification mode estimation of a fuzzy number \hat{Y}_{i_0+1}). Printing the forecast y_{i_0+1} .

According to the rolling forecasting scheme, shifting a set of indices $I = \{i | i = i_0 - 8, \dots, i_0 + 1\}$ forward one step $\Delta i = 0,005$, we will get a set of indices $I_1 = \{i | i = i_0 - 9, \dots, i_0 + 2\}$.

Then the forecasting error \hat{Y}_{i_0+2} will be equal

$$\varepsilon_2 = \varepsilon_1 \cdot \rho_2 \cdot \left(\prod_{k=1}^3 d(X_{i_0+2,k}, \hat{X}_{i_0+2,k}) \right) \cdot d(Y_{i_0+2}, \hat{Y}_{i_0+2}), \quad (43)$$

where ρ_2 – is forecasting To error of value y_{i_0+2} maximum losses of thickness, determined by the formula (19) and following

$$\text{RAA}(\hat{Y}_{i_0+2}, Y_{i_0+2}) = 1 - \varepsilon_2$$

with confidence probability

$$P_{\partial,2} = \left(\prod_{k=1}^3 P_{\partial,k}(X_{i_0+2,k}, \hat{X}_{i_0+2,k}) \right) \cdot P_{\partial}(Y_{i_0+2}, \hat{Y}_{i_0+2}), \quad (44)$$

At step m of this algorithm, a forecast of values y_{i_0+m} will be obtained with the error

$$\varepsilon_m = \varepsilon_{m-1} \cdot \rho_m \cdot \left(\prod_{k=1}^3 d(X_{i_0+m,k}, \hat{X}_{i_0+m,k}) \right) \cdot d(Y_{i_0+m}, \hat{Y}_{i_0+m}), \quad (45)$$

If $\varepsilon_m < \varepsilon_0$ (ε_0 – is the permissible forecast error), then $m = m + 1$ and go to point 6.). Otherwise STOP. We print.

Using this algorithm, the following predictions were obtained:

$$\begin{aligned} i = i_0 + 1 = 39 \text{ (2390 M)}, \hat{y}_{39} = 0,357; \\ i = i_0 + 1 = 40 \text{ (2400 M)}, \hat{y}_{40} = 0,362. \end{aligned}$$

Thus, based on the above studies, the following main conclusions can be drawn.

V. Conclusion

1. Inspection measurements carried out on the basis of studying the electromagnetic field created by a sounde located inside casing or pumping and compression pipe (tubing) require significant costs, especially at large well depths and an increased degree of aggressiveness of their environment. In this regard, the problem of predicting the results of the inspection at greater depth of immersion of the pipe into the well becomes fundamentally important.

2. For this purpose, we have proposed a new methodology for predicting the maximum loss of pipe thickness by step of 10 m after any certain depth of immersion of the bottom part of the pipe into the well, for which the maximum loss of thickness (in percentage) is considered given.

3. Forecasting is carried out by sliding in the direction of increasing losses with a forward shift of depth by 10 m. The error of the resulting forecast is estimated using a numerical procedure for calculating the measure of difference between fuzzy numbers.

References

- [1] Koskov, V.N. Comprehensive assessment of the condition and operation of oil wells using field geophysical methods: textbook. allowance /V.N. Koskov, B.V. Koskov, I.R. Yushkov. Perm: Perm State Technical University Publishing House, 2010, – 226.
- [2] Huseyinov, G.G. Accelerated technology for eliminating accidents in wells and the mechanisms used in this case. Oilfield business, 2012, 8, 36-38.
- [3] Technical guidance on the application of geophysical surveys and operations in oil and gas wells. SOCAR guidance document. Baku, 2019, 320.
- [4] Feyziyeva, G.E Results of using geophysical methods in assessing the operating condition of oil and gas wells. Equipment, Technologies, Materials, 2022, 38-42.

GEOCHEMICAL SOUNDING OF TECTONIC FAULTS MEASUREMENT-BASED EXHALATION OF SOIL RADON

Yelizaveta Yessenzhigitova, Abdulaziz Abdullaev, Maksim Markin,
Vladimir Borisov, Aset Muhamadiev

•

Institute of Seismology, Almaty, Kazakhstan
LLP "GeoStroySistema", Almaty, Kazakhstan

liza_1103@mail.ru

u.abdullaev@mail.ru

markin_maxim@inbox.ru

borisov_wn_71052@mail.ru

Aset_8888@mail.ru

Abstract

The scientific and methodological issues of geochemical sounding and localization of tectonic fault activity based on profile measurements of exhalation (volumetric activity) of soil radon (Rn 222), as well as emanation surveys on the territory of Ust-Kamenogorsk, carried out here in 2021-2023 in connection with seismic micro zoning (SMR) are outlined. It has been established that those geochemical methods of deep sounding of tectonic faults allow to reliably clarify the location and determine the activity of tectonic faults in the study area and provide new materials for seismic zoning of critical objects and determining seismic risk factors.

Keywords: geochemical sounding, fault activity, radon exhalation, soil radon, emanation survey, seismic risk, Irtysh shear zone

I. Introduction

In geological and tectonic terms, the city of Ust-Kamenogorsk in East Kazakhstan is located in the Irtysh shear zone (ISZ) and in seismic activity terms it is located in the area of possible earthquakes of magnitude 8. The main faults in the city have a northwestern strike and, in combination with transverse discontinuous faults, cause the folded-block nature of the Irtysh shear zone (ISS).

Geologists have been studying this zone since the beginning of the twentieth century. This tectonic structure is a deep fault zone with a width of 1.5 to 20 km, stretching across the territory of Russia, East Kazakhstan (Rubtsovsk, Ust-Kamenogorsk) to China (Fuyun) and further to Mongolia for more than 1000 km, in the form of a collage of heterogeneous blocks and scales, differing in the degree of deformation in the Paleozoic [1,2].

The objectives of the studies carried out at the ISS were: 1) to assess the radon activity of tectonic fault zones; 2) to work out the method of emanation survey for the conditions of the Irtysh shear zone and determine the limits of changes in the exhalation (volumetric activity) of radon in the subsoil air above the faults in the tectonic-active and passive areas of the study area.

To solve the tasks, several devices were used: "Ramon-Radon2" manufactured by the company "SOLO LTD" RK, radiometer-dosimeter "RKS-01-SOLO", designed for comprehensive radiation study of the study area. During the emanation survey, the Alfarad Plus instrument complex was used for express measuring and monitoring of OAR-222 and Toron-220 in the air

[3,4].

The city of Ust-Kamenogorsk is the regional center of East Kazakhstan (EKR), the largest industrial and transport hub of Rudny Altai. For sustainable development of non-ferrous metallurgy, mining and chemical industries, mechanical engineering and civil engineering, a comprehensive study of engineering-geological, hydrogeological, seismic and environmental conditions of the territory is necessary.

Until 1990, endogenous geological processes manifested themselves in the form of moderate earthquakes with an intensity of up to 6-7 points (MSK -64). However, the Zaisan earthquake that occurred on June 14, 1990, with an intensity of 8 points at the epicenter exceeded the existing estimate of seismic activity in this region (according to SNiP II-7-87) by 1 point. Since 2021, JEM and SMR have been carried out in East Kazakhstan region [5]. In this regard, geochemical studies were carried out here for the first time based on profile sounding, soil radon exhalation and emanation survey. It should be noted that in connection with the construction and installation works, such work was previously carried out in 2014-2015 on the territory of Almaty [6].

II. Methods

The natural radioactive gas radon (Rn^{222}) with a half-life of 3.82 days is the decay product of radium, which occurs as a result of the decay of uranium-238 [11].

It is known that among the three isotopes of radon (Radon-222, Thoron-220, Actinium-219), the first isotope with a half-life of 3.825 days is an optimal and reliable indicator in studies of seismic processes in large areas. High radon activity in fault localization sites has been noted in many studies [10, 11]. The mechanism of radon migration in the vertical direction has been described by many researchers [Koval, Udodov, Sankov et al., 2006; Akerbolm; Banwell, Parizek, 1988; Hermansson, Cyssler; Moussa, ElArabi, 2003; Wahita, Kumar, 2008] [10].

The essence of the phenomenon lies in the fact that the main isotope radon (Rn^{222}) is continuously generated in rocks in the process of radioactive decay, hence it is always present in any mountain range. The decrease in its concentration, both due to decay and due to migration from the massif into the air, is constantly compensated by the new generation of this gas. Therefore, the average radon content in the array is always constant and is determined by the concentration of uranium (radium) in this array. Radon migration to the mountain range and its release from the soil surface are determined by the diffusion coefficient, which depends on many factors. The most important of these are porosity, permeability and fracturing. Convective transport of radon with gas jets can be carried out from the upper part of the mountain range from depths up to 200m. World experience shows that radon (Rn^{222}), due to a number of its special geochemical properties in groundwater and surface-atmosphere, is an effective indicator of the geodynamic state of the Earth's crust [7,8,9].

It is also important to specify that, even though the radon presence in these fluxes is of negligible quantity, there are no problems with its registration due to its radioactivity. It is reliably recorded in the presence of approximately 30-50 decays per second in one cubic meter (m^3), that is, radon activity is 30-50 Bq/ m^3 [3].

Radon anomalies over tectonic disturbances are very diverse in intensity and shape, as well as options for the location of the main shifter within them. The interpretation of the term "fault zone" includes not only the tectonics of the fault displacer but also significantly larger volumes of rocks in which plastic and discontinuous deformations genetically associated with its formation take place.

III. Results

As noted, in 2021-2023, the Institute of Seismology of the Ministry of Emergency Situations of the Republic of Kazakhstan in Ust-Kamenogorsk carried out work on geochemical sounding and

emanation surveys to clarify the location and activity of tectonic faults based on profile measurement of the exhalation (volumetric activity) of soil radon (Rn^{222}).

During the summer periods of 2021-2022 in the eastern part of Ust-Kamenogorsk, 10 km from its western border, fieldwork was carried out on special profiles for measuring radon exhalation (Rn^{222}) to detect buried faults in increments of 50 m. In total, 5 profiles with a total length of 15.2 km were passed, through 5 fault zones (Fig. 1). The profiles passed across the strike of faults in a southeasterly direction. The distances between them ranged from 1.7 to 3.5 km., And the maximum length of a separate profile was 4 km.

Profile sounding was carried out by a complex of analyzers of the latest generation "Ramon-Radon2" and a radiometer-dosimeter "RKS-01-SOLO", manufactured by the company "SOLO LTD".

Fieldwork on emanation surveys was carried out from June to September 2021-2022, 46 profiles were passed, with a total length of 20,311 meters (Fig. 1).

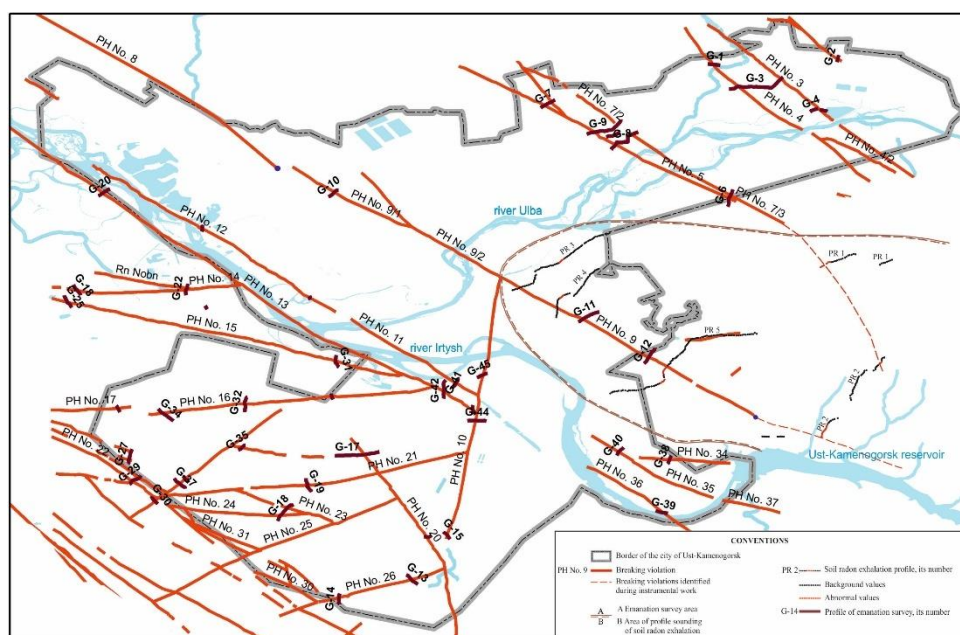


Fig. 1: Map of field profile observations of soil radon exhalation in the territory of Ust-Kamenogorsk city

In the course of the work, significant factual material for measuring the volumetric activity of Rn^{222} was collected. The emanation survey profiles were located across the strike of fault zones in those places where the main features of their structure were determined by the data of structural and geomorphological observations.

To assess the degree of permeability of the mountain range along the extended profiles, the analysis of digital elevation models was carried out with the allocation of ledges of straightened valleys and linear-erosion forms, which reflect the position of active faults in the study area. To measure the radon flux density from the soil surface and measure the volumetric activity of radon in soil air samples, the measuring complex for monitoring radon, thoron and their daughter products "Alfarad Plus" was chosen, designed for rapid measurements and continuous monitoring of the volumetric activity of radon-222, as well as the equivalent volumetric activity (EROA) of radon and thoron-220 in the air.

Geomorphologically, the areas of radon surveying are hilly terrain, represented by a combination of individual hills, massifs and inter-hill depressions, composed of loams from the surface and complicated by outcrops of Paleozoic rocks in the form of ridges, manes, cliffs, individual hills, with relative exceedances of up to 100 m.

Geologically, the described territory is part of the Irtysh structural-formational zone,

stretching in a narrow strip in the northwest direction between the Kalba-Narym and Rudno-Altai zones.

In geological and petrological terms, the ISS is the Irtysh-Zaisan structural-formational zone, with a length of more than 500 km. with highly compressed and dislocated horst-anticlinorium. It is this feature that determines its modern high Seismo-dynamic activity here.

Profile No. 1: located on the northern outskirts of the village of Ushanov. It has a northeast direction and passes across the strike of the deep Irtysh fault. The length of the profile is about 1.5 km. 30 measurements were made on the profile every 50 meters, with the determination of coordinates and altitude values and data from the readings of other devices. In the identified areas with increased radon exhalation, the distance between the points of the profile was reduced to 20 m and control measurements were carried out. The average value for exhalation radon is 83 mBq/s*m². Between points 2 and 7, there was an increased exhalation of radon up to 170 mBq/s*m² with a section length of 250 m, which exceeds the background radon release by two times (Fig. 2). When measured on this profile with the Ramon-Radon2 device and the RKS-01 radiometer-dosimeter, a complete coincidence of anomalous areas is noted.

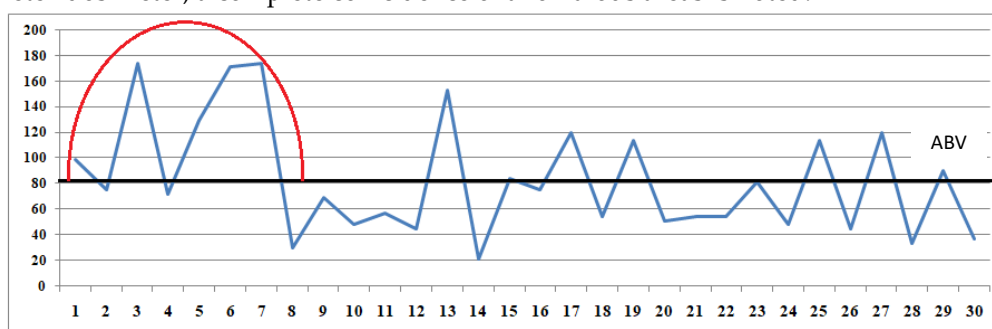


Fig. 2: Profile 1. Exhalation of radon alpha particles (mBq/s*m²)
 ABV – average background value of radon

Profile No. 2: located to the east, 10 km from Ust-Kamenogorsk, along the Ust-Kamenogorsk-Zyryanovsk highway. The profile runs along the ridge to the Irtysh River at the cross of the ISS strike.

In the course of fieldwork, 54 measurements were made every 50 m, with the determination of coordinates, altitude values and instrument readings. The average background value of radon exhalation is 66 mBq/s*m², the maximum is 177 mBq/s*m², and the minimum is 12 mBq/s*m², (Fig. 3).

As can be seen from the graph, four areas of sharply increased radon exhalation are identified on this profile. The length of the first section is 150 m, and the remaining sections are respectively 200 m and 120 m. On average, radon exhalation exceeds the background content by 2-3 times, reaching a maximum value of 177 mBq/s*m².

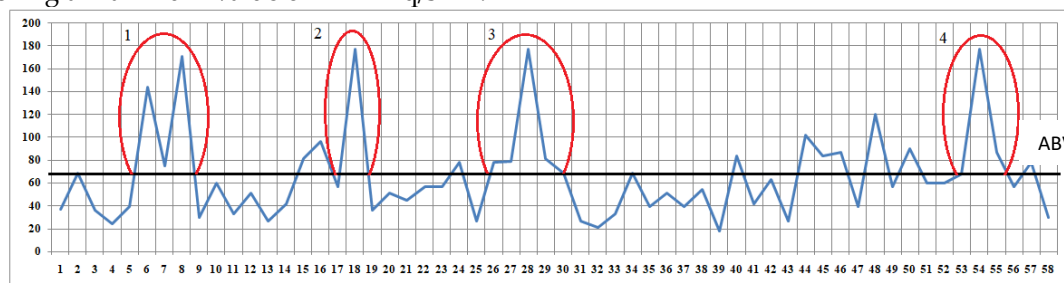


Fig. 3: Profile 2. Exhalation of radon alpha particles (Bq/s*m²)
 ABV – average background value of soil radon exhalation

Profile No. 3: passed on the eastern outskirts of the city of Ust-Kamenogorsk, on the left bank of the Ulba River, on a gentle slope of the ridge. The profile runs in the middle part of the slope of the eastern exposure with a direction to the northeast, across the strike of the ISS.

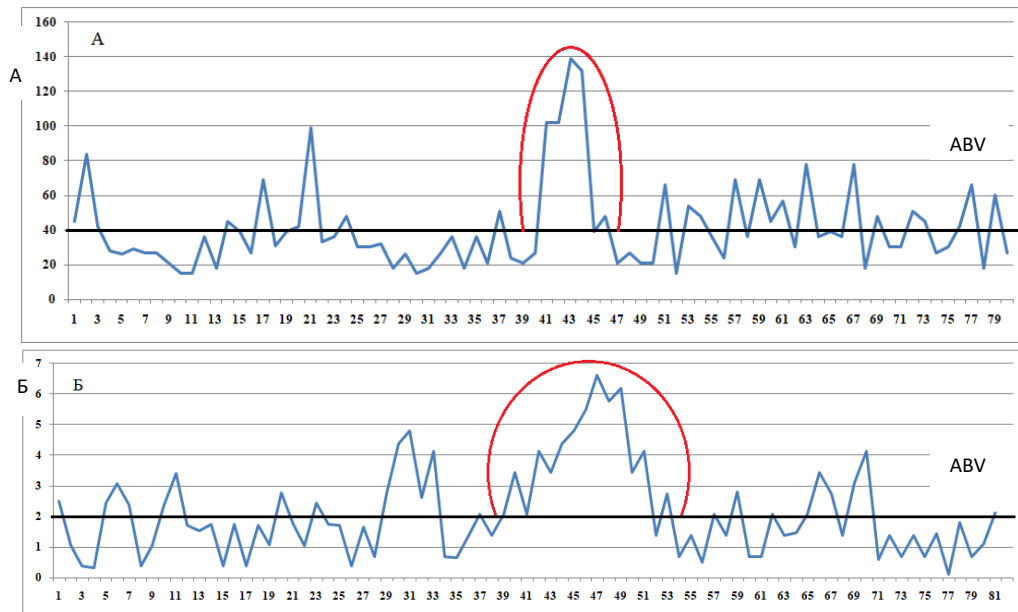


Fig. 4: Profile 3. A - exhalation of radon alpha particles ($mBq/s \cdot m^2$) and B - beta particle dosimeter ($part/min \cdot cm^2$), ABV - average background value of radon

The length of the profile is 4.0 km. In the process of fieldwork, 80 measurements were made every 50 meters, with the determination of the readings of all devices. In the identified areas with increased radon exhalation, the distance between the profile points was reduced to 20 m and control measurements were carried out.

The average background value of radon exhalation is $41 Bq/s \cdot m^2$, the maximum is $139 mBq/s \cdot m^2$ min. $-15 mBq/s \cdot m^2$. According to the profile, the area (between points 39-46) with increased radon exhalation, exceeding the background value by two times with the length of the anomalous zone of 400 m is defined. Processing of field survey materials with the Ramon-Radon2 device and the RKS-01 radiometer-dosimeter shows the complete coincidence of anomalous areas (Fig. 4 A and B).

Profile No. 4: passed on the eastern outskirts of the city of Ust-Kamenogorsk, in a valley bounded from the east and west by ridges of hills. The route runs along the slope of the western exposure. The direction of the profile is to the northeast, across the strike of the Irtysh shear zone.

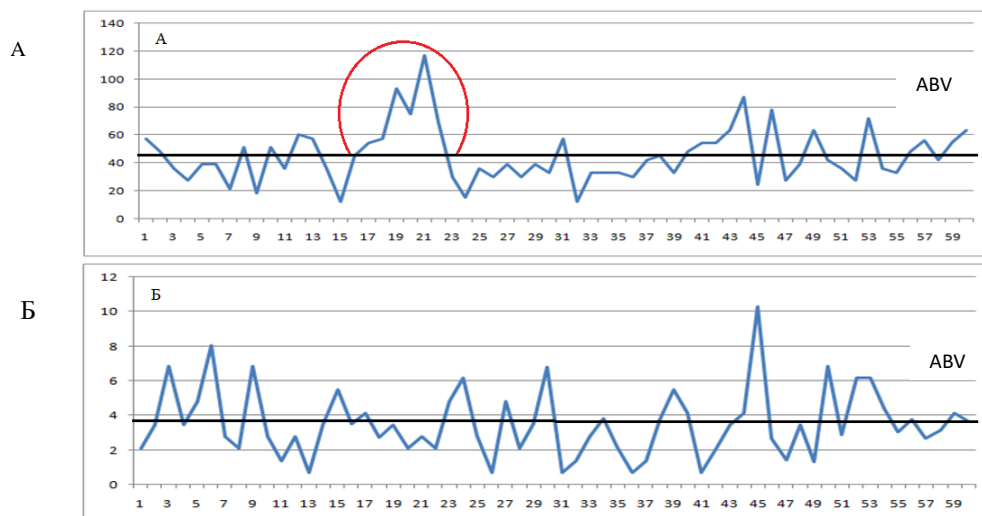


Fig. 5: Profile 4. A is the exhalation of radon alpha particles ($mBq/s \cdot m^2$) and B - beta particle dosimeter ($part/min \cdot cm^2$), ABV - average background value of radon

The length of the profile is 3.0 km. 60 measurements were made every 50 meters, with the determination of the readings of all instruments. In the identified areas with increased radon exhalation, the distance between the profile points was reduced to 20 m and control measurements were carried out.

The average background value of radon exhalation is 45 mBq/s*m², the maximum is 117 mBq/s*m², and the minimum is -1 2mBq/s*m². According to the profile, an area (between points 15 - 23) with increased radon exhalation exceeding the background value by 2 times, with a length of the anomalous zone of 450 m was defined (Fig. 5).

Profile No. 5: located on the right bank of the Irtysh River, on the eastern outskirts of Ust-Kamenogorsk, along Vatutin Street, (Fig. 6). The direction of the profile is to the northeast, across the strike of the ISS.

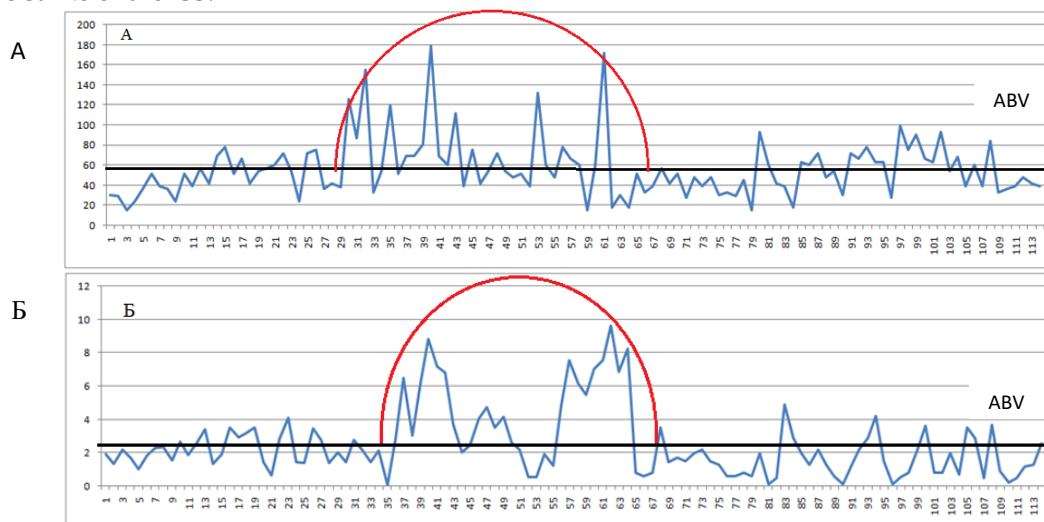


Fig. 6: Profile 5. A – exhalation of radon alpha particles (mBq/s*m²) and B - beta particle dosimeter (part/min * cm²), SPZ - the average background value of radon

The length of the profile is about 4.0 km. 114 complex measurements were performed every 50 meters, with the determination of coordinates and altitude values. In areas of increased radon exhalation, the distance between the points was reduced to 20 m.

The average background value of radon exhalation is 56.7 mBq/s*m², the maximum is 17.9 mBq/s*m², and the minimum is -1.5 mBq/s*m². According to the profile, an anomalous area (between points 29-65) was identified with a background value 2-3 times higher, with a length of 1.300 m. According to the radiation of beta particles, the anomalous zone is marked between points 35 - 65, with a length of 1200 m.

Emanation shooting.

The main task of the fieldwork in 2022 was to conduct an emanation survey on the territory of Ust-Kamenogorsk in connection with the construction and installation work, where faults are buried under a large cover of Quaternary sediments. During the period of fieldwork in the city, 46 profiles were passed, with a total length of 20311.1 m.

The profiles of the emanation survey were located crosswise along the strike of fault zones in those places where the main features of their structure were determined by the data of structural and geomorphological observations.

The profiles crossed differently oriented parts of discontinuous faults with distances between sampling points from 15 to 100 m. To compare faults by radon activity, the relative indicator was used: $K = Q_{max}/Q_{min}$, where Q_{max} is the maximum value of the Q parameter within the profile (anomaly intensity), and Q_{min} is the minimum value of the Q parameter in rocks outside the fault zone. Examples of such registration are shown in Table 1.

Table 1: *Quantitative parameters of profiles obtained from emanation survey data*

Profile Number	The length of the profile, m	Breaking Violation Number	Q max	Q min	Q cp	To
G-1	258,1	PH No. 1	520	89	291.30	5.84
G-2	303,3	PH No. 2	507	102	259.14	4.97
G-3	1480.6	PH No. 3,4	1940	120	605.63	16.17
G-6	635.3	PH No. 7/3, 5	1309	120	616.58	10.91
G-11	614	PH No. 9	2053	110	657.94	18.66
G-12	619	PH No. 9	2677	190	1231.95	14.09
G-13	441	PH No. 26	845	179	448.33	4.72
G-14	400	PH No. 26	804	90	323.58	8.93
G-19	542	PH No. 21	656	40	223.72	16.40
G-21	252	PH No. 12	2482	239	866.44	10.38
G-22	378	PH No. 14	1158	347	629.40	3.34
G-27	538	Rn Nobn	1903	95	632.33	20.03
G-31	461	PH No. 15	950	413	693.18	2.30
G-33	212	PH No. 16	736	144	419.00	5.11

In the simplest cases, the area of anomalous values of the Q parameter has one maximum in cross-section with a gradual or stepwise decrease in the concentration of soil radon to the periphery (Fig. 7). However, in most of the situations studied, the radon anomaly is more complex, usually discontinuous, which is associated with the heterogeneous structure of the fault zone. The largest of the discontinuities are manifested in the form of local extremes of Q values: maxima when filling the zone of the shifter with permeable fault breccias and minima if the tectonics were subjected to intense weathering or are represented by friction clay.

Anomalies of soil radon over discontinuous disturbances are characterized by spatial heterogeneity, which is apparently due to the permeability of the rupture substrate.

As a result of geological routes and remote sensing analysis, a catalogue of the main discontinuous disturbances was compiled, where Table 2 shows examples of such registration in the study area with the main characteristics, as well as the resulting data on the azimuth of the strike, azimuth of incidence and angle of incidence. The main azimuthally direction of discontinuous faults is northwestern. Most of the discontinuous faults have a steep vertical angle of inclination of the mixer, and the azimuths of the fall mainly have a southeastern strike.

Graph of changes in the volumetric activity of soil radon Q along the profile G11, G33.

It should be noted that according to the data of the emanation survey and the primary analysis of materials, a heterogeneous distribution of the concentration of soil radon along and across the strike of fault zones is traced, and at the same time, a clear tracing of discontinuous violations is recorded.

The leading role in the distribution of radon concentration over fault zones is played by the structural and geodynamic factors. Radon anomalies over faults are characterized by spatial heterogeneity, which is associated with variability in the permeability of the fault zone. We emphasize that the indicator of radon activity of the fault - KQ represents the ratio of the intensity of the near-fault emanation anomaly (Qmax) to the minimum value of the volumetric activity of radon beyond its limits. This relative parameter is less than Qmax and depends on the thickness of the overlying sediments and the radioactivity of the rocks at the fault.

The areal distribution of the UAR on the territory of Ust-Kamenogorsk is shown in 3D measurements according to the statistical processing of data from 46 profiles (Fig. 8). Here we see that the fault zone is represented by several pick-shaped or hump-shaped maximum values (Qmax) with a gradual decrease in the concentration of the OAR, turning into calm "dead"

segments, which characterize the inactive sections of the fault. It can be assumed that the current activity of the faults according to the radon indicator, is not homogeneous in strike, because there are inactive (passive) segments of faults in the modern era, which can stretch for several hundred meters or km in length. This situation is extremely important in the seismic micro zoning of the city.

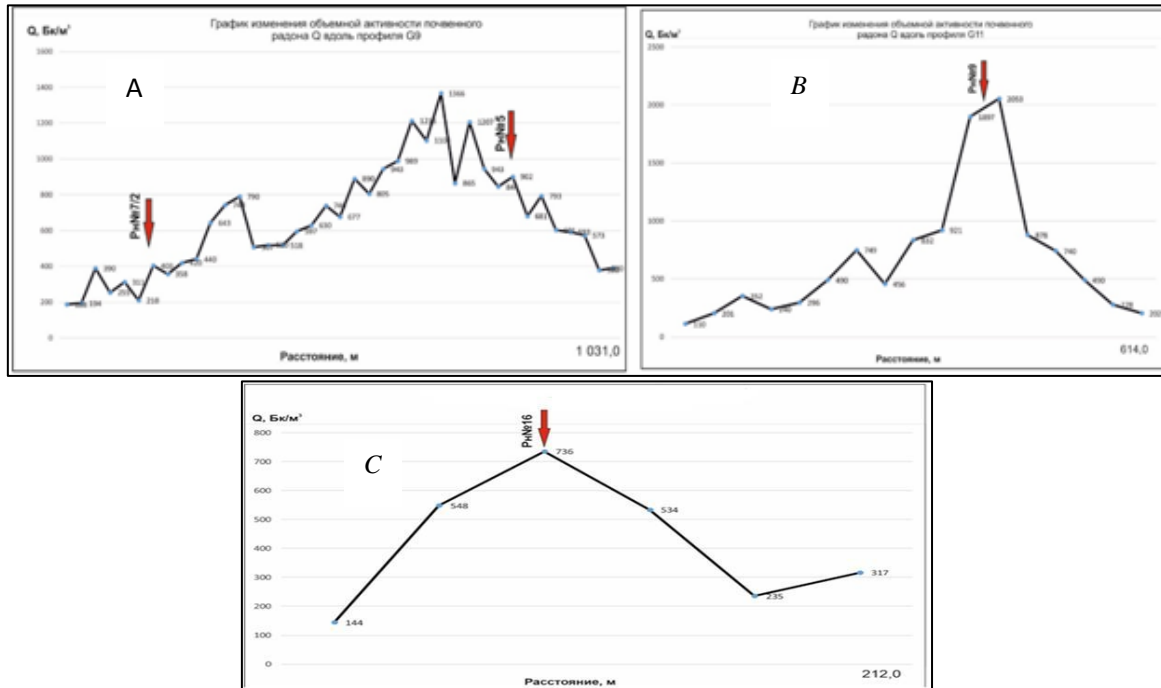


Fig. 7: (A, B, C) - examples of typical distribution curves volumetric concentration of soil radon

Table 2: Characteristics of discontinuous disorders within the study area

№	Name	Length Km	Type	Options			Classification according to the angle of inclination of the mixer
				Azimuth of stretch	The azimuth of the fall	Angle of incidence	
1	PH No. 1	6355.19	shift	315	135	70	steep
6	PH No. 5	9991.42	shift	290	82	80	steep
11	PH No. 7/3	1690.31	shift	210	86	71	steep
16	PH No. 10	9385.80	shift	190	30	62	steep
23	PH No. 17	1698.71	shift	220	160	71	steep
31	PH No. 24	3184.84	shift	260	175	58	steep
40	PH No. 33	1827.70	shift	290	160	80	steep

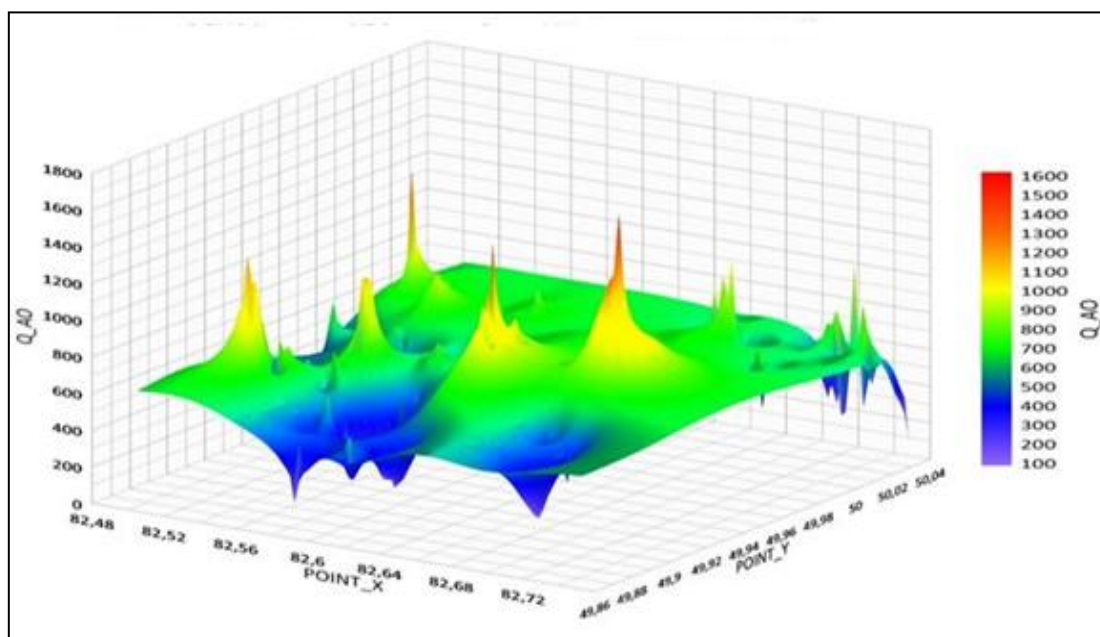


Fig. 8: Areal distribution of radon volumetric activity (Rn^{222})

IV. Discussion

For the first time, geochemical field studies were carried out within the Irtysh shear zone to clarify the position of discontinuous disturbances and their activity using profile measurements of the volumetric activity of soil radon Rn^{222} .

As a result of geochemical sounding in the area of Ust-Kamenogorsk, tectonic fault zones have been identified, which characterize modern tectonic activity in the study area, and make it possible to trace buried faults.

On geochemical profiles, anomalous zones of increased radon exhalation differ from the background values of radon on the ground by exceeding the concentration of UAR by 3–4 times. Such anomalous zones show the existence of tectonic faults in the area of Ust-Kamenogorsk, which are active in the modern era both as a whole and in their segments.

This is evidenced by the tomography of radon convictions obtained during emanation surveying in the territory of Ust-Kamenogorsk (Fig. 8). Here, fault zones along the strike are marked by hump-shaped extreme values, which in some segments "fail" over considerable distances, inactive sections of these faults.

These facts indicate that fault zones marked by radon anomalies appear to be characterized by a high degree of fragmentation of individual areas, as well as significant convection of radioactive gases from these zones into the surface atmosphere.

Acknowledgements. The work was carried out in the framework of earmarked funding "Assessment of seismic hazard of territories of Kazakhstan on the modern scientific and methodological basis", project codenumber F.0980. Source of funding Ministry of Education and Science of the Republic of Kazakhstan.

References

- [1] Khoreva B.Y. "Geological structure, intrusive magmatism and metamorphism of the Irtysh shear zone", VSEGEI, 1963, 207 p.
- [2] Geology of the USSR, vol. XLI East Kazakhstan, "Nedra", Moscow, 1967.
- [3] SOLO LTD LLP Method for measuring the volumetric activity of radon (Rn^{222}) in various

media. Almaty. - 2010

[4] Kozlova I.A., Yurkov A.K., Biryulin S.V. Variations of radon volumetric activity in technogenic and tectonic seismic events. *Mining Information and Analytical Bulletin*, 2022, No. 5., part 1., p.119-130

[5] Abakanov T.D., Lee A.N., Sadykova A.B., *Methodology for the development of seismic zoning maps of earthquake-prone territories of Kazakhstan*, Almaty, 2013, 127 p.

[6] Abdullaev A.U., Lagutin G.E., Zhunisbekov T.S., Suslova T.P. et al. The first results of the geochemical sounding of tectonic faults are based on profile measurements of the volumetric activity of soil radon on the territory of the Almaty metropolis. *Proceedings of the National Academy of Sciences of the Republic of Kazakhstan, series of geological and technical sciences* No. 5, 2016, pp. 79-91.

[7] Abdullaev A.U., Ostapenko V.F. Reflection of geodynamic processes in variations in the volume concentration of radon in fluid systems of the Northern Tien Shan. */Ural Geophysical Bulletin. -№ 8. -2005. -p.5-8.*

[8] Abdullaev A.U. Geochemical indicators of interhemispheric interactions "Earth's crust-atmosphere" in seismically active areas. */Earthquake forecasting, seismic hazard and seismic risk assessment of Central Asia. Almaty. -2010 - p.130-136.*

[9] Rudakov V.P. Monitoring of the stress-strain state of rocks of the seismically active region by the emanation method. */Geochemistry. -1986 -No 9. -p.1337-1342.*

[10] Firsov P.P., Makarov E.O. Dynamics of soil radon in Kamchatka and strong earthquakes. *Petropavlovsk-Kamchatsky*, 2018, p.145.

[11] Yakovleva V.S., Karataev V.D. Radon flux density from the Earth's surface as a possible indicator of measurements of the stress-strain state of the geological environment. */Volcanology and seismology. -2007 -No 1. -p.74-77.*

INVESTIGATION OF PARTICLES EMISSIONS WHEN USING VARIOUS ELECTRODES FOR UNDERWATER WELDING

Konstantin Kirichenko^{1,2}, Vladimir Chernousov¹, Anton Pogodaev², Alexander Gridasov², Yuri Kalinin², Igor Vakhniuk¹, Alexey Kholodov³, Sergei Parshin⁴, Kirill Golokhvast^{1,5}

¹Siberian Federal Research Center for Agrobiotechnologies, RAS, Russia

²Far Eastern Federal University, Vladivostok, Russia

³Far East Geological Institute, Far Eastern Branch of the RAS, Vladivostok, Russia

⁴Peter the Great St. Petersburg Polytechnic University, Russia

⁵Tomsk State University, Russia

kirichenko@sfsc.ru

chernousov@sfsc.ru

pogodaev.av@dvfu.ru

gridasov.av@dvfu.ru

kalinin_yuriy@mail.ru

vakhniuk@sfsc.ru

alex.holodov@gmail.com

parshin@spbstu.ru

golokhvast@sfsc.ru

Abstract

The article is devoted to the study of the mass and quantitative concentration of suspended particles during underwater welding for sea water from the Ajax Bay (Sea of Japan) using two technological modes with special electrodes for welding and cutting metal. For both processes, the predominance of the PM0.3 fraction in emissions of the smallest particles compared to particles of larger fractions was revealed. The amount of suspended particles when using electrodes for metal cutting is several times higher compared to electrodes for underwater welding. The mass concentration of PM10 particles does not exceed the threshold MPC values established in the Russian Federation, Belarus and the USA.

Keywords: underwater welding, nano- and microparticles, emissions, ecology

I. Introduction

The problem of hydrosphere development cannot be solved without wide application of the latest technologies of underwater metal welding and cutting. The aquatic environment and enormous hydrostatic pressures represent a complex set of conditions for the practical application of welding and other related technologies, which require the creation of labor-intensive and financially expensive research and technologies. Underwater welding and cutting technology is an extremely successful technological solution and is versatile for use in the restoration of almost all types of steel structures in the water environment. Light weight of the equipment, its compactness and reliability, quick mastery by users allowed to perform a significant amount of works both on the territory of Russia and beyond its borders [1, 2]. For example, the practical development of the continental shelf of the world ocean began in the second half of the last century. Now gas and oil

production are carried out on an industrial scale. Today the world oil production amounted to 3150 million tons, 30% of which was extracted from the bottom of the world ocean using various technologies of underwater cutting and welding of metals [3].

The main tasks of underwater metal welding and cutting are to make and repair reliable welded structures. The requirements for their quality are constantly increasing, which determines the appropriate process for improving their durability and reliability. Therefore, a significant number of studies [4, 5, 6] is devoted to the study of strength characteristics of welded joints, the introduction of new methods of underwater welding, etc. Applied research in the field of environmental assessment of emissions and discharges into the environment has received little attention. Our study aims to fill this gap. It focuses on the analysis of the concentrations of airborne particulate emissions into the atmospheric air, which, in addition to discharges into the water, are an integral attribute of underwater welding operations.

II. Experimental

An aquarium with dimensions of 1.2x0.6x0.6 m, made of organic glass with a wall thickness of 1 cm, was used as the medium for the underwater welding emission assessment experiment. The volume of seawater was 200 liters. The seawater for the experiments was collected from the surface layer in the water area of Ajax Bay (Sea of Japan) near the campus of Far Eastern Federal University (FEFU, Fig. 1). A 30-liter plastic container was used as a sampling device. The seawater was then transported to the laboratories of the Nanotechnology Research Center of FEFU Polytechnic Institute for further sample preparation.

In the laboratory, the seawater was pre-filtered with coarse cloth filters. Next, the water was exposed to ultraviolet radiation (Siemens Ultra-Clear TWF EDI UV UF TM Water Purification System (Siemens, Munich, Germany)) to eliminate biologically active organisms that could have an indirect effect on the results of the study. After the ultraviolet treatment, the seawater was re-filtered and poured into the aquarium for underwater welding. This procedure was performed twice to conduct the experiment with the electrodes for underwater metal welding and cutting.

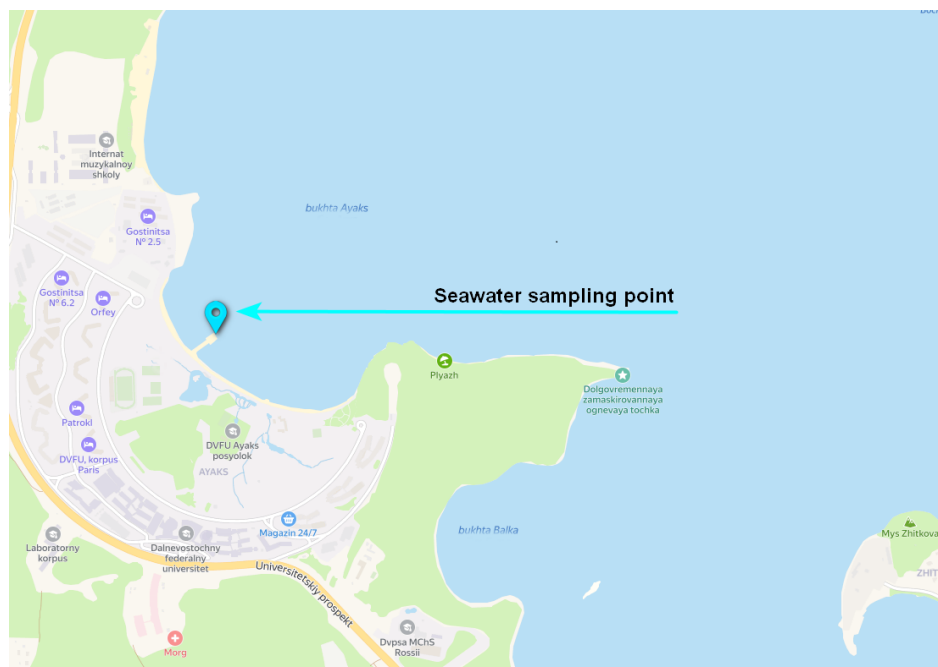


Fig. 1: Seawater sampling point in the Sea of Japan

The air sampling time during the underwater welding experiment was 1 minute, which corresponded to the average burn time of 1 electrode. During each series of air sampling, 1 electrode was burned.

1.1. Method for determining the quantitative composition and particle size.

To measure the quantitative composition of airborne particles, we used the AeroTrak Handheld Particle Counter 9306 (USA), which meets all the requirements of ISO 21501-4.

In continuation of the previous research [7] on the morphological structure of solid particles, the present work is dedicated to the study of particle emissions during underwater welding.

We selected the most commonly used technological processes under water in industrial production, using a black metal plate (VSt-3sp, size (200x70x8):

a) Manual arc welding with Arcair electrodes size 5/32X14 (3.97 x 356 mm), Cat. No. 42-984-004.

b) manual cutting with Arcair electrodes size 5/16X14 (8.0 x 356 mm), Cat. No. 42-059-007.

The atmospheric air was sampled in the immediate vicinity of the pollution source (Fig. 2) at a height of 1.5 meters above the floor, which corresponds to the level of human breathing. First, background measurements were made in the room before the experiment, then the measurements were repeated in the middle of the experiment and at the end of the experiment. 2 series of air samples were taken: using electrodes for underwater welding and cutting in sea water (Sea of Japan).

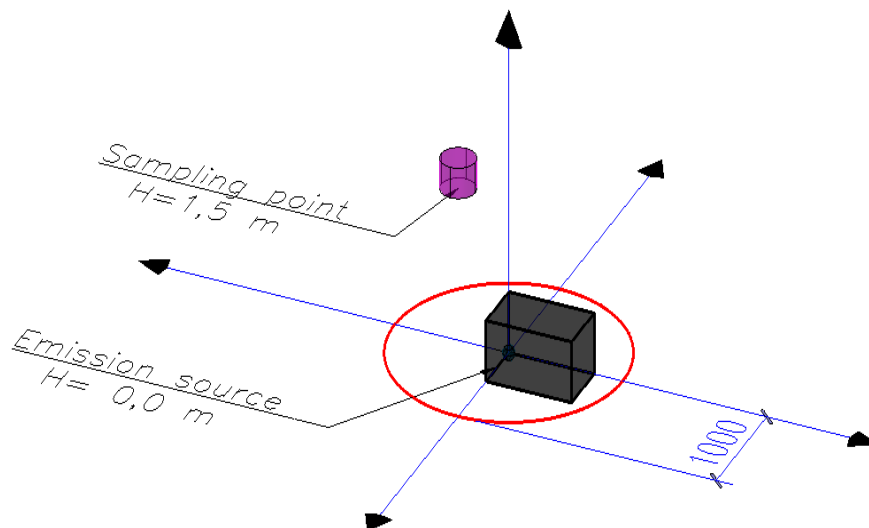


Fig. 2: Location of sampling points when using the aquarium

Gravimetric method of particle concentration analysis

In order to determine the mass concentration of fine aerosol particles in the air of the working area above the aquarium, a gravimetric method of measurement was chosen, using an aspirator-type sampler "Aspirator PU" (Russia). Aerosol filters based on Petrianov's filter cloth made of perchlorvinyl fiber (filter type AFA-VP-20-1 of TU 95 1892-89 without binder, with a working surface of 20 cm², Kimry Gorky factory) were used. These filters are characterized by high collection efficiency due to electrostatic attraction of aerosol particles to the charged filter fibers; for 0.1 μm particles, the slippage factor in the AFA filter is only 0.1%.

During the experiment, this sampler was equipped with an additional attachment for sampling airborne particles of PM10 fraction. Two filters were used simultaneously for each electrode, collecting the total volume of deposited particles and separately the volume of PM10 particles.

The height of the sampler attachment corresponded to the human breathing level - 1.5 meters above the ground.

The first sampler was equipped with an attachment for sampling the PM10 fraction taken from a similar LVS 3.1 aspirator (Ingeniero Nobert Derenda, Germany). The measured range of airborne particles for the filters of this attachment is from 0.45 μm to 10.0 μm. The upper limit of the particle fraction (PM10) was chosen because particles of this size are the most dangerous to human health, being the cause of respiratory diseases [8, 9]. The specific measurement of the PM10 fraction reflects the current trend in the control of airborne particles [10,11].

The second sampler was equipped with a particle sampling attachment with no fractional range restriction.

Prior to sampling, the filters were pre-dried in a 0.8 cm thick glass drying cabinet where a constant temperature (20°C) and humidity (20%) were maintained for 24 hours, then each filter was weighed five times on a Sartorius (Germany) electronic balance to determine the arithmetic mean.

The dust content in the air was measured by weighing the filters on analytical balance before and after sampling. Each filter was weighed five times on Sartorius (Germany) electronic balance and the arithmetic mean was determined. The obtained difference in weight of the filters before and after the air sampling procedure corresponded to the deposited mass of airborne particles.

III. Results and discussion

Quantitative composition of airborne particles (amount/m³).

Analyzing the data obtained from the AeroTrak 9306 Handheld Particle Counter (Table 1), we can conclude that the PM0.3 particle fraction was dominant in the pre-experiment background air. Their number was many times greater than all other particles combined.

Table 1: *Quantitative composition of airborne particles when using electrodes for underwater welding*

Process	H (height) meters	Sampling time, minutes	PM0.3	PM0.5	PM1	PM3	PM5	PM10
Welding	1.5	0	205265	16968	2172	484	246	53
Welding		0.5	935745	658018	313010	24899	4040	67
Welding		1	1201110	632230	210468	12543	1963	56
Cutting	1.5	0	516293	55396	6498	738	296	58
Cutting		0.5	1871490	198209	48571	3145	721	55
Cutting		1	2515331	1632711	536164	17559	1198	45

The data obtained during underwater welding with Arcair electrode size 5/32X14 are presented in the form of a graph (Fig. 3). The results of the measurements made in the middle of the experiment (30 sec. from the moment of the beginning of the electrode burning), when half (50% of the initial length) of the welding electrode was left, show a quantitative increase of the particles in the atmospheric air from 4.5 to 144 times of the initial values, depending on the fraction. In addition, we observed the maximum increase in particles of the same PM0.3 fraction.

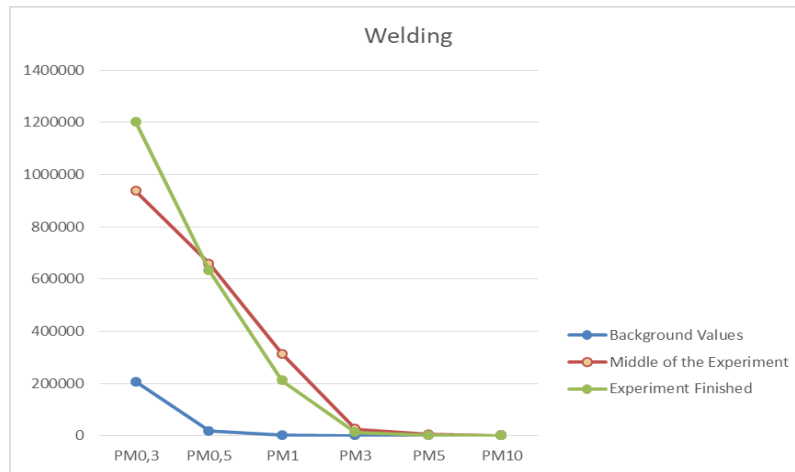


Fig. 3: Graph of the quantitative composition of airborne particles in the ambient air during underwater welding

The results of the measurements after the burning of the electrode (1 min) show a further increase (28%) in the number of suspended particles of the PM0.3 fraction compared to the values for 30 sec. These particles are the smallest and can remain suspended in the air for a long time. Note the decrease (from 5% to 50%) of the airborne particles of the larger fractions. This fact indicates dynamic sedimentation of airborne particles of PM0.5-PM10 fractions.

Let's further consider the results of measurements made with the cutting electrode Arcair size 5/16X14 (8.0 x 356 mm), which show the same tendency of increase of the number of the smallest particles in the atmospheric air as for the underwater welding electrode. As can be seen from Fig. 4, the atmospheric air is dominated by particles of PM0.3 fraction, the number of which is many times higher than the sum of particles of larger fractions. If we compare in detail the particles of the same fraction but in different periods of the experiment, we see that in the middle of the experiment the number of particles up to PM0.3 was almost twice higher than the background value, and at the end of the experiment the number of particles of this fraction was 5 times higher than the background values. The values of the number of particles after 60 seconds are superior to the values of the measurements at 30 seconds for all fractions, in contrast to the data of the underwater welding experiment.

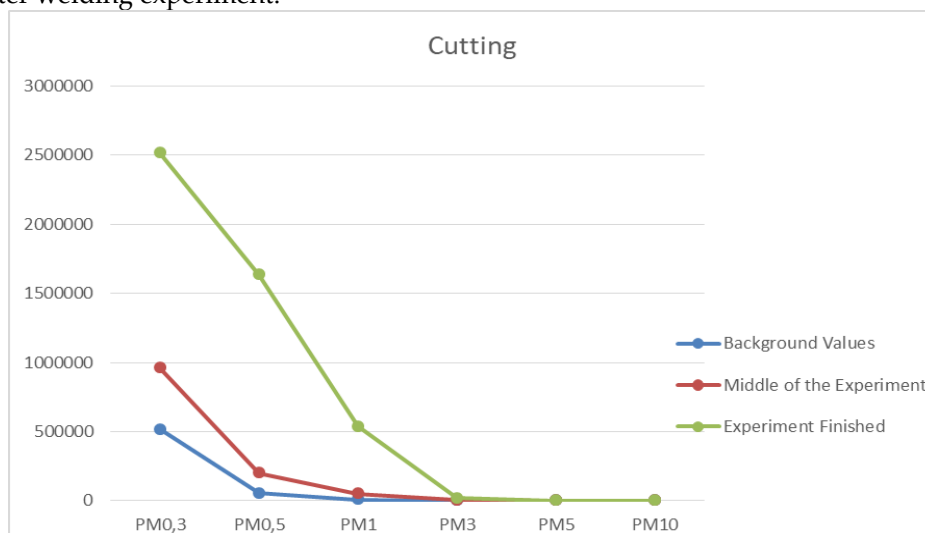


Fig. 4: Graph of the quantitative composition of airborne particles in the ambient air during underwater cutting

This fact may be due to the lighter weight of the particles, which affects the effect of gravitational forces, requiring a longer settling time. The second factor explaining this fact may be a greater momentum of particle emissions, as the process of underwater metal cutting was accompanied by more intense bubbling of water and release of air bubbles.

Comparative analysis of suspended particles during underwater welding and metal cutting leads to the conclusion of higher emission of particles into the atmospheric air when using an electrode for cutting in comparison with an electrode for underwater welding. Quantitative concentration of particles of fractions PM0.3; PM0.5; PM1; PM3 during underwater metal cutting is 2-2.5 times higher than content of airborne particles in comparison with underwater welding. This fact indicates high particle emission for this technological process, which is connected with high inclusion of material of the destroyed metal product in emissions.

1.3. Mass concentration of emissions from underwater welding and cutting of metals

The gravimetric method of analysis of the average daily concentration of suspended particles showed a significant presence of the PM10 fraction in the air, whose share in the total mass of particles deposited on the filters was 46.6% for underwater welding and 68.9% for underwater metal cutting.

The mass content of particles when cutting metals underwater was higher than when using electrodes for underwater welding by 2.85 times for the PM10 fraction and by 1.93 times for the total mass of deposited particles.

The mass content of particles from underwater metal cutting was 2.85 times higher for the PM10 fraction and 1.93 times higher for the total mass of deposited particles compared to the use of underwater welding electrodes.

It should be noted that the obtained values of mass concentrations of airborne particles of PM10 fraction do not exceed the MPC limits established in different countries. In Table 2 we have given the standards of Russia, Belarus and the USA on the presence of particles in the atmospheric air, which is safe for humans. The obtained data show that the mass concentration of airborne particles in the air (mg/cubic meter) is safe for people both when burning an electrode for underwater welding and when using an electrode for underwater metal cutting.

Table 2: Mass average daily concentration of microparticles

No.	Process	Electrode	PM10 concentration, mg/cubic meter	Concentration of all ambient particles, mg/cubic meter	GN 2.1.6.3492-17 (Russia)	GN No.37 (Belarus)	USEPA NAAQS (USA)
1	Welding	Arcair size 5/32X14 (3.97 x 356 mm) Cat. No. 42-984-004	0.014	0.03	0.06	0.05	0.05
2	Cutting	Arcair size 5/16X14(8.0 x 356 mm) Cat. No. 42-059-007	0.04	0.058			

IV. Conclusions

The analysis of the data of the measurements of the quantitative composition of the airborne particles in the air shows an absolute excess of the content of the smallest particles of the PM0.3 fraction in comparison with the particles of the larger fractions PM0.5-PM10. The number of particles in this fraction (PM0.3) is greater than the number of particles in all other fractions combined (PM0.5-PM10). The sedimentation of PM0.5-PM10 was observed during the experiment with an electrode for underwater welding as opposed to electrodes for underwater metal cutting. Quantitative content of suspended particles for underwater cutting is 2-2.5 times higher in comparison with particle emission during burning of underwater welding electrode.

The results of measurements of mass concentration of airborne particles of PM10 fraction when using electrodes for underwater welding and underwater metal cutting show that the limit values of MPC established in Russia, Belarus and the USA are not exceeded. The mass content of particles when using the electrode for underwater metal cutting is 2 times higher in comparison with the emissions when using underwater welding electrodes.

It should be noted that these are data from laboratory studies where the water depth above the level of the exposed metal plate was 20-30 cm. When working under real conditions in the open sea, the depth will be much greater, minimizing emissions into the air due to deposition of particles in the water. Therefore, future studies will be aimed at assessing the toxicological impact of particulate matter from underwater welding on marine hydrobionts.

Acknowledgements. The authors are grateful to the staff of the collective-use centers of FEFU and FEGI FEB RAS for the scientific equipment provided, and to the specialists of the Siberian Scientific Agricultural Library, a branch of the Federal State Scientific and Technical Library, for their help in working with the literature.

The work was carried out with the financial support of the Russian Science Foundation in the framework of scientific project No. 22-24-01169.

References

- [1] Kononenko V. Ya., Rybchenkov A. G. Experience of wet mechanized welding by self-shielded flux-cored wires during repair under water of gas and oil pipelines // *Automatic Welding*. - 1994. - № 9/10. - P. 29-32. [https://doi.org/10.15589/smi2019.1\(11\).5](https://doi.org/10.15589/smi2019.1(11).5)
- [2] Kononenko V.Ya., Gritsay P.M. Wet mechanized welding during repair of ship's hulls // *Marine Fleet*. - 1994. - № 11-12. - P. 21-22. <https://doi.org/10.2478/v10077-008-0040-3>
- [3] Paton B.E. Welding and Related Technologies in the Development of Space and the World Ocean of the XXI Century. *Journal Nauka i Zhizn*. №04. 2023. <https://doi.org/10.15407/knit2018.05.043>
- [4] Parshin S.G., *Metallurgy of underwater and hyperbaric welding*. St. Petersburg 2016. Polytechnic University Press, 2016. - 401 p. <https://doi.org/10.3390/met10111498>
- [5] Maksimov S.Yu., Lyakhovaya I.V., Wet underwater welding of low-alloy steels of increased strength. *Automatic welding*. 2013. № 8 (724). P. 43-46.
- [6] Parshin S.G., Levchenko A.M., Study of underwater wet welding by coated electrode and flux-cored wire of bainite X70 pipe steel for repair of main gas pipelines. *Gas Industry*. 2022. № 1 (827). P. 48-53. <http://doi.org/10.1088/1755-1315/539/1/012132>
- [7] Kirichenko K.Yu., Chernousov V.A., Vakhnyuk I.A., Parshin S.G., Masyutin A.G., Gridasov A.V., Pogodaev A.V., Pikula K.S., Golokhvast K.S. Study of morphological composition of particles in water samples during underwater welding // *FEFU: School of Engineering Bulletin*. 2022. № 4(53). P. 102-111. <http://doi.org/10.24866/2227-6858/2022-4/102-111>
- [8] Morgan W.K.C., Reger R.B., Tucker, D.M. Health effects of diesel emissions // *Annals of Occupational Hygiene*. - 1997. - Vol. 41, Iss. 6. - P. 643-658 [https://doi.org/10.1016/S0003-4878\(97\)00024-0](https://doi.org/10.1016/S0003-4878(97)00024-0)
- [9] Penttinen P., Timonen K.L., Tiittanen P. et al. Ultrafine particles in urban air and respiratory health among adult asthmatics // *European Respiratory Journal*. - 2001. - Vol. 17, Iss. 3. - P. 428-435. <https://doi.org/10.1183/09031936.01.17304280>
- [10] Simonova I.N., Antonyuk M.V., Vitkina T.I. Influence of air nanoparticles on bronchopulmonary system // *Bulletin of Respiratory Physiology and Pathology*. - 2013. - № 49. - P. 115-120.
- [11] Popova S.Yu. The results of using a device to reduce dust levels at the workplace of welders. *AIC of Russia*. 2010. V. 56. P. 71-74. <https://doi.org/10.24866/2227-6858/2022-1/94-103>

EXAMINATION OF THE PRESCRIPTION OF A DOCUMENT AS A WAY TO IDENTIFY MALFEASANCE

Dmitriy Mokhorov¹, Dmitriy Anisimov², Vladimir Kochemirovsky^{1,3}

¹Peter the Great St. Petersburg Polytechnic University

²Consulting point of information and legal assistance, Baku, Azerbaijan

³Alferov Federal State Budgetary Institution of Higher Education and Science Saint Petersburg National Research Academic University of the Russian Academy of Sciences

Vako4@yandex.ru

Abstract

The article discusses the signs of artificial and natural aging of documents under the influence of temperature and humidity changes. It is shown that the use of technologies for artificial aging of documents can create risks of concealing malfeasance, leading to economic, technological damage and health. Methods for detecting signs of artificial aging and the possibility of using physicochemical methods of analysis to detect falsification are discussed.

Keywords: forensic chemistry, document dating, chromatography, Raman spectroscopy

I. Introduction

Representatives of the Ministry of Justice of the Russian Federation at the International Scientific and Practical Conference "Topical Issues of Forensic Examination of Documents" reported that over 50% of all calls to the forensic examination center on issues of forensic technical examination of documents are examination of document dating. And this is not surprising, since almost everyone, without exception, in a wide variety of areas of life is faced with forgery of the terms of documents.

Very often, such falsifications, even for seemingly harmless reasons, contain a corruption component.

Paragraph 35 of the Decree of the Plenum of the Supreme Court of the Russian Federation "On judicial practice in cases of bribery and other corruption crimes" dated July 9, 2013 No. 24 expressly states that "the subject of a crime under Article 292 of the Criminal Code of the Russian Federation is an official document certifying the facts that entail legal consequences in the form of granting or deprivation of rights, imposition or release from obligations, changes in the scope of rights and obligations. Such documents should include, in particular, sheets of temporary disability, medical books, examination sheets, record books, salary certificates, protocols of procurement commissions, vehicle registration certificates. Thus, as of September 3, 2021, 56 students were expelled from St Petersburg University from 2018 to 2021 due to falsified medical certificates. According to information dated July 7, 2020, the Urals Investigative Department of the Investigative Committee opened a criminal case against the Perm Institute of Railway Transport, whose administration forged all students' records in order to obtain state accreditation.

More trivial cases of document forgery occur in the field of labor relations. Often at the place of work, employees may encounter the so-called "black bookkeeping", when the director offers to sign documents "backdated". It is in this way that in everyday life an employment contract, a job description, a knowledge test protocol is often drawn up, which sometimes leads to sad consequences. So, for example, when investigating accidents with a fatal outcome or causing

grievous bodily harm, the investigating authorities require the issuance of protocols on testing knowledge. If the employer does not provide them with a backdated date, then he faces criminal liability. It is not surprising that the court is also overloaded with an impressive amount of forged papers, since the parties in those cases where decent sums are at stake (cases of bankruptcy, inheritance, purchase and sale of real estate, etc.) are ready to go for even the most risky tricks hoping to win the case.

The seeming possibility to draw up the necessary document "backdating" creates numerous additional risks in the sphere of production, economy and public life. There is an illusion of the possibility of concealing theft or the true cause of harm to health or environmental crime.

The presence of methods for establishing the true prescription of a document is an effective form of preventing the numerous risks of malfeasance by officials. Chromatographic methods are most often used to determine the age of a stroke, despite the fact that, recently, there has been a tendency to replace them with spectroscopic methods [1, 2].

The fundamental basis of chromatographic methods is the study of the temporal dynamics of changes in the concentration of certain components in the ink composition. A list of components that are considered volatile has been compiled. Generally, these are 2-phenoxyethanol, glycerol, triethylene glycol, tetraethylene glycol, hexylene glycol, benzyl alcohol, phthalic anhydride, diphenylamine, Michler's ketone, etc. 2-Phenoxyethanol is used most often for analysis purposes since its chromatographic dynamics are the most stable and obvious. A typical scene of the evaporation dynamics of volatile components of writing materials is described, for example, in [3]. Chromatographic methods based on the evaporation of volatile components have a number of limitations, including the inability to analyze the age of strokes that are older than 1.5–2 years (the evaporation period of volatile components). In attempts to overcome this limit by searching for new components with a longer evaporation time or optimizing sampling parameters such as the paper sheet type, sampling tube, extraction temperature, extraction time, sample mass, and desorption time have been applied [4, 5, 6]. It is claimed that these methods allow increasing the depth of chromatographic analysis by up to 5 years.

Evaporation may not be the only method to change the concentrations of components. The dynamics of the content of conditionally volatile components of writing materials in the presence of moisture may also be caused by the processes of interaction of components with each other and with paper components [7].

The natural difference in atmospheric pressure is another factor in natural aging, which is not embraced by systematic studies. The evaporation of aqueous solutions of the components of writing materials should also accelerate in the case of a decrease in atmospheric pressure. Considering the above assumption that the components of the writing composition evaporate in dilute aqueous solutions, the pressure drop factor can seriously influence the rate of ink degradation.

This work is devoted to the analysis of some factors of natural and artificial aging of documents and methods for their detection using spectral methods.

II. Methods

Chromatographic and chromato-mass spectrometric studies were carried out on the Kristall-5000 gas chromatography-mass spectrometry complex with a flame ionization detector (FID) and a mass-selective detector (MSD). The introduction of samples was carried out using a pyrolytic attachment (in the case of MSD) and a solid sample injector in the case of FID. The MSD channel was equipped with a device for cryofocusing of gas mixture components. The study was conducted using chromatographic columns CR-5 30 m x 0.32 mm x 0.5 μ m for FID and CR-5 ms 30 m x 0.32 mm x 0.25 μ m for MS. The components were identified based on the results of gas chromatography-mass spectrometry measurements using the Chromatec Analytic and NIST libraries.

Table 1: Conditions for obtaining chromatograms of mass spectrometric detection

Seq No.	Element	Parameters
1	Pyrolytic evaporator P4	Temperature: 200 °C, 5 min, temperature elevation rate 2,500 °C/min
2	Cryofocus module	Temperature: initial -40 °C, final 280 °C, 5 min at 2,000 °C/min
3	Column thermostat	Temperature: 1. 150 °C, 5 min 2. heating up to 270 °C at a rate of 22 °C/min 3. 270 °C, 10 min
4	Carrier gas (helium, qualification 6.0)	Pressure 93 kPa Column 1.0 ml/min Velocity 40.1 cm/s

The samples (each about 1 cm long) were introduced into a pyrolytic evaporator with a cryofocusing module (L-CO₂). The samples should be placed in the pyrolytic evaporator for 5 min. The samples are analyzed on a KhromatekKristall 5000 gas chromatograph with a mass spectrometric detector (GC-MS) and a flame ionization detector (GC).

Raman spectroscopy studies were conducted using the Horiba LabRAM Evolution HR Raman spectrometer with a confocal Raman microscope instrument with laser sources 532 nm, two diffraction gratings (600 g/mm and 1,800 g/mm), manual XY stage. The instrument was controlled using the LabSpec 6 software. The evaluation of the temporary degradation degree of the ink dye was carried out according to the methods and results of papers [8,9,10,11].

Raman spectroscopy studies were conducted using the Horiba LabRAM Evolution HR Raman spectrometer with a confocal Raman microscope instrument with laser sources 532 nm, two diffraction gratings (600 g/mm and 1,800 g/mm), manual XY stage. The instrument was controlled using the LabSpec 6 software. The evaluation of the temporary degradation degree of the ink dye was carried out according to the methods and results of papers [8,9,10,11].

Simulation of humidity processes was performed in the "heat-humidity" M 0/100-1000 KTV climatic chamber within the range of maintaining humidity from 40% to 80% at a temperature of +25 °C (humidity adjustment accuracy: 3%, temperature ± 5 °C). The choice of humidity range was determined by the characteristic differences for the city of Saint Petersburg.

During one cycle of studies, stroke samples applied to office paper were kept for 2 hours in a climatic chamber with a volume of 50 liters at a relative humidity of 80%, and then they were kept for 3 hours at a humidity of 40% or natural air drying was fulfilled for 24 hours. The number of humidity cycles was determined based on the decrease in the chromatographic response level of the studied samples to background values or until reaching a horizontal plateau.

The signs of accelerated aging of documents were detected using GC-MS measurements, Raman spectroscopy, and optical microscopy using a MIKMED-6 microscope with a built-in webcam.

III. Experimental

When falsifying a document, an attempt is often made to artificially "inflate" its age and give it the appearance of a document with a long shelf life. Traditional methods of artificial aging are heating and exposure to sunlight or ultraviolet light. Signs of such artificial aging are easily established during the usual observation of propp in a microscope (Fig. 1).

Chromatographic signs of artificial aging are expressed in a decrease in the intensities of the main signals of the volatile components of writing materials to background values. The dynamics

of evaporation of solvents is considered on the example of writing compositions presented in Table 2.

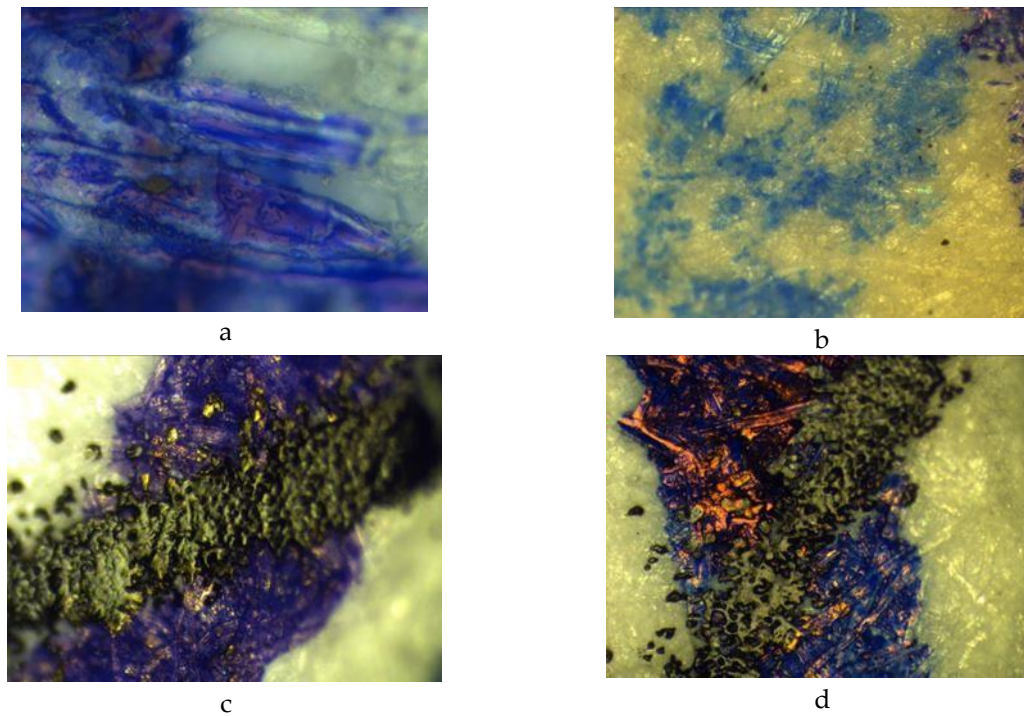


Fig. 1: (a) - micrograph of a stroke of a handwritten inscription made with a ballpoint pen, (b) the same stroke subjected to heating to 90°C., (c) a micrograph of a printed text toner, (d) the same toner heated to 90°C.

Table 2: Characteristics of the writing compositions selected for the experiment

Number writing composition	Type (according to Raman spectra)	Type (by composition)	Solvent under consideration	Retention time, min
№5	A	capillary	Tetraethylene glycol	13,676
№3	B	Ball	2-phenoxyethanol	10,823
№7	C	Gel	Glycerol	7,365

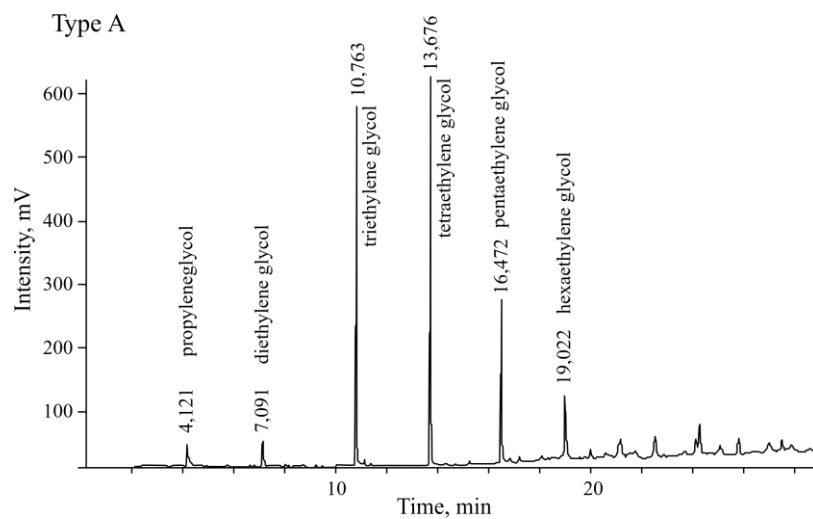


Fig. 2: Chromatogram of a sample of writing composition No. 5, not subjected to temperature effects

From the chromatogram shown in Fig. 2, tetraethylene glycol was chosen for further analysis, since it has the most intense peak, respectively, its concentration in the writing composition is maximum.

A graph of the dependence of the change in the area of the peak corresponding to a given solvent on the chromatogram, on the time of storage in "natural" conditions is shown in Fig. 3.

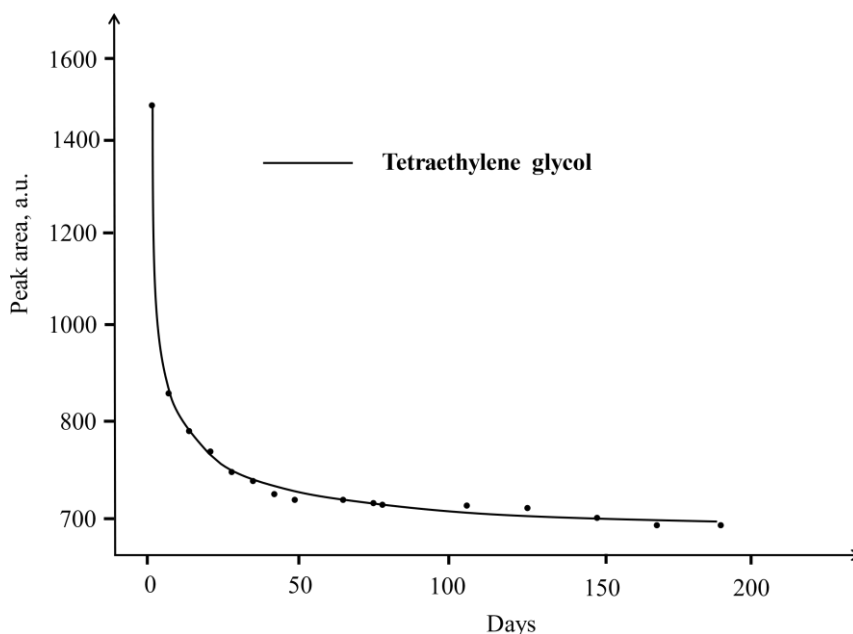


Fig. 3: Plot of tetraethylene glycol peak area vs. storage time under "natural" conditions

It can be seen from Fig. 3 that the main part of the solvent evaporates already after a month of storage of the sample under natural conditions. To study the effect of temperature on the rate of evaporation of solvents, the samples were subjected to temperature effects in various modes. The results are presented in Table 3 and in Fig. 4.

Table 3: Correlation of heating time, at various temperatures and storage time at "natural" conditions

60 degrees		Number of days at "natural" storage	90 degrees		Number of days at "natural" storage
Heating time	Peak area		Heating time	Peak area	
7,25	905,19	3	8,5	460,97	9
22,75	644,30	5	23,5	204,82	35
35,25	239,19	27	32,5	127,46	76
43,75	159,79	54	56,0	69,72	more 120

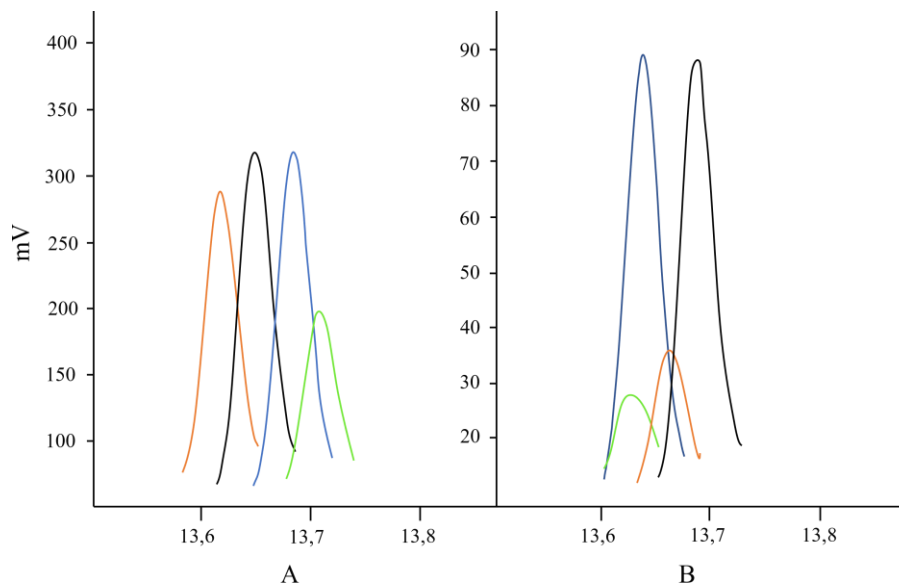


Fig. 4: The enlarged area of the peak of tetraethylene glycol on the corresponding chromatograms obtained after exposure to temperatures (60 and 90 degrees), chromatograms obtained from samples at different heating times are highlighted in different colors:

A. 60 degrees; blue - 7.25; black - 22.75; red - 35.25; green - 43.75;
 B. 90 degrees; blue - 8.5; black - 23.5; red - 32.5; green - 56.0 (heating time is indicated in hours)

As the temperature increases, the rate of evaporation of tetraethylene glycol also increases accordingly. After 56 hours of heating at 90 degrees, virtually all of the solvent had evaporated. Similarly, for other types of writing compositions.

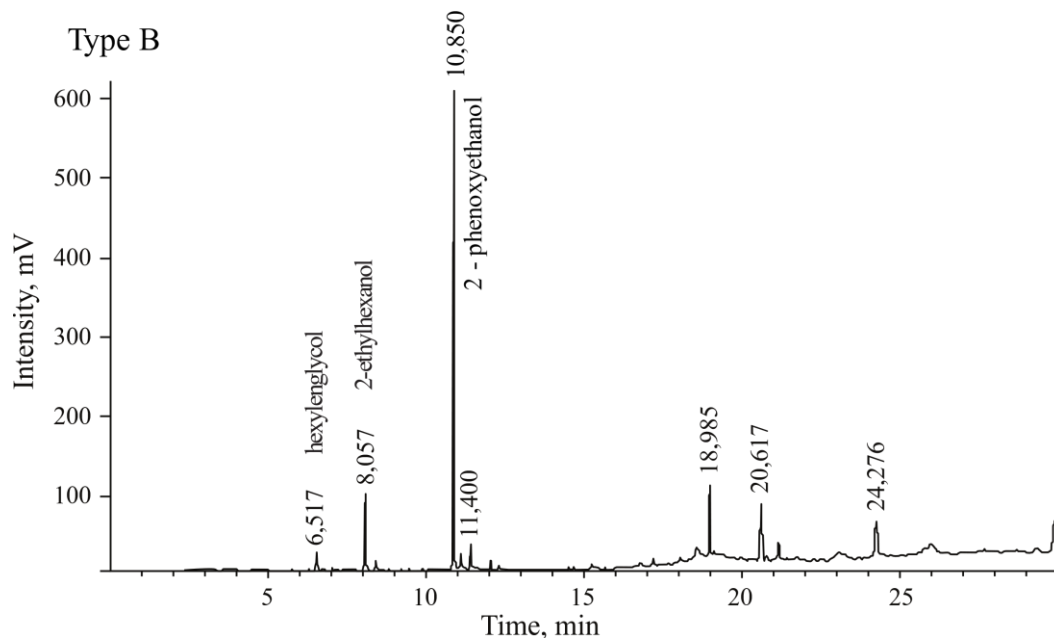


Fig. 5. Chromatogram of a sample of writing composition No. 3, not subjected to temperature effects.

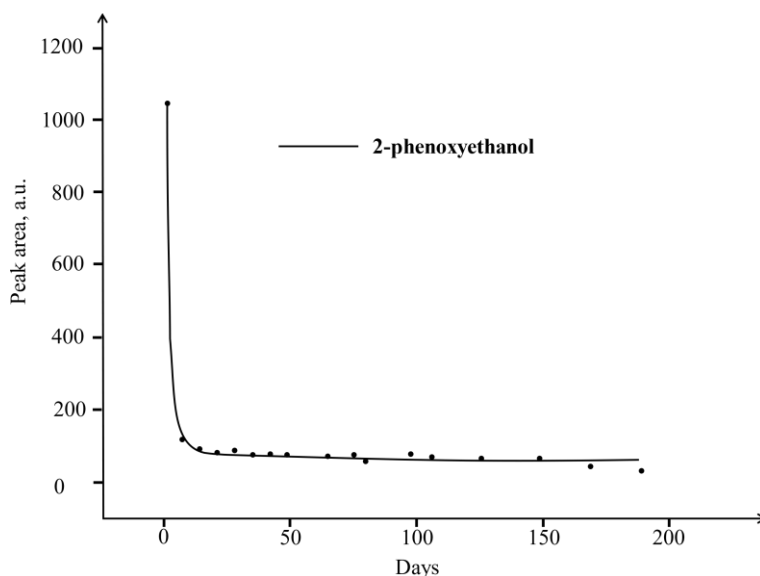


Fig. 6: Plot of peak area corresponding to 2-phenoxyethanol versus storage time under natural conditions

Table 4: Correlation of heating time, at various temperatures, and storage time under natural conditions for 2-phenoxyethanol

60 degrees		Number of days at "natural" storage	90 degrees		Number of days at "natural" storage
Heating time	Peak area		Heating time	Peak area	
7,25	158,86	5	8,5	135,01	7
22,75	112,34	8	23,5	87,50	14
35,25	77,89	20	32,5	53,74	80
43,75	56,42	80	56,0	36,11	more 120

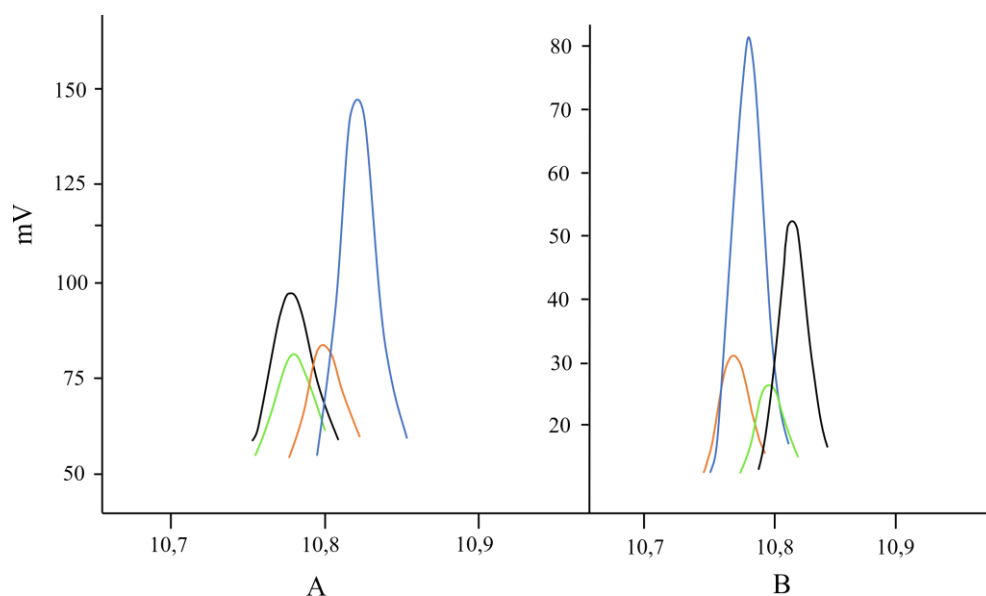


Fig. 7: The enlarged area of the peak of 2-phenoxyethanol on the corresponding chromatograms obtained after exposure to temperatures (60 and 90 degrees), chromatograms obtained from samples at different heating times are highlighted in different colors:

A. 60 degrees; blue - 7.25; black - 22.75; red - 35.25; green - 43.75;
 B. 90 degrees; blue - 8.5; black - 23.5; red - 32.5; green - 56.0 (heating time is indicated in hours).

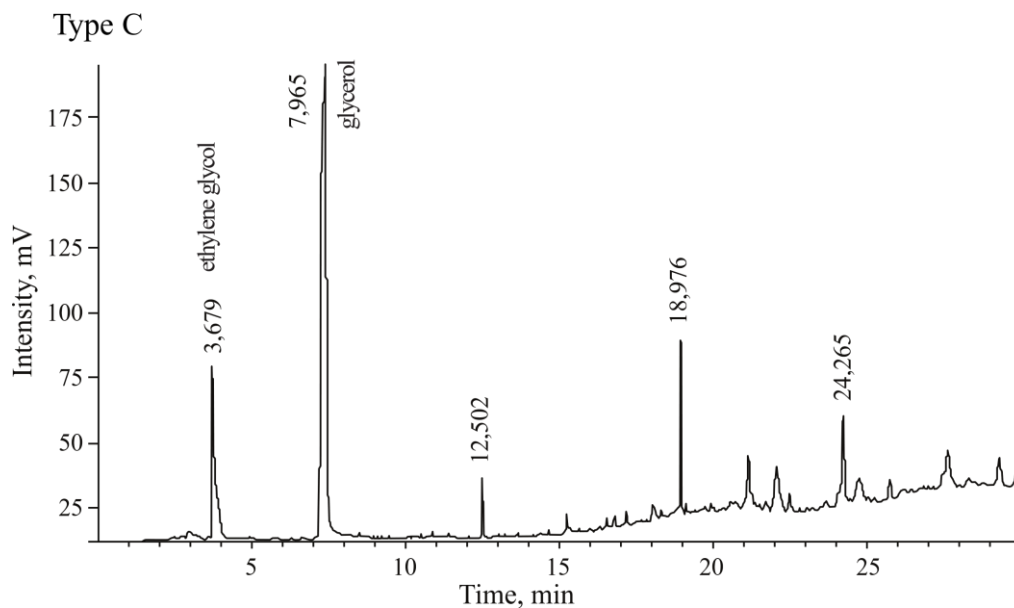


Fig. 8: Chromatogram of a sample of writing composition No. 7, not subjected to temperature effects

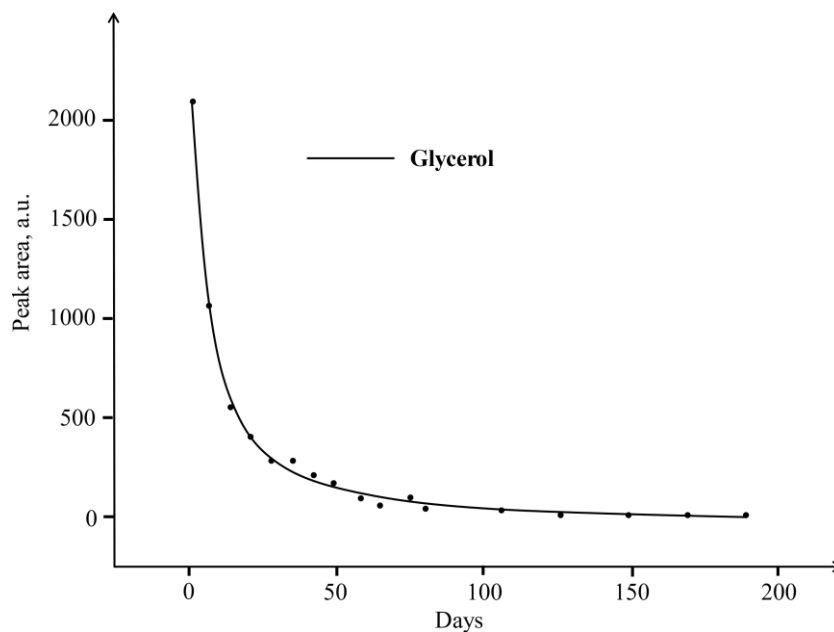


Fig. 9: Plot of peak area corresponding to glycerol versus time of storage under natural conditions

Table 5: Correlation of heating time, at various temperatures and storage time under natural conditions for glycerol

60 degrees		Number of days at "natural" storage	90 degrees		Number of days at "natural" storage
Heating time	Peak area		Heating time	Peak area	
7,25	1304,53	5	8,5	1210,52	6
22,75	1216,86	6	23,5	1087,54	8
35,25	1208,50	6	32,5	589,46	14
43,75	1134,10	7	56,0	284,17	30

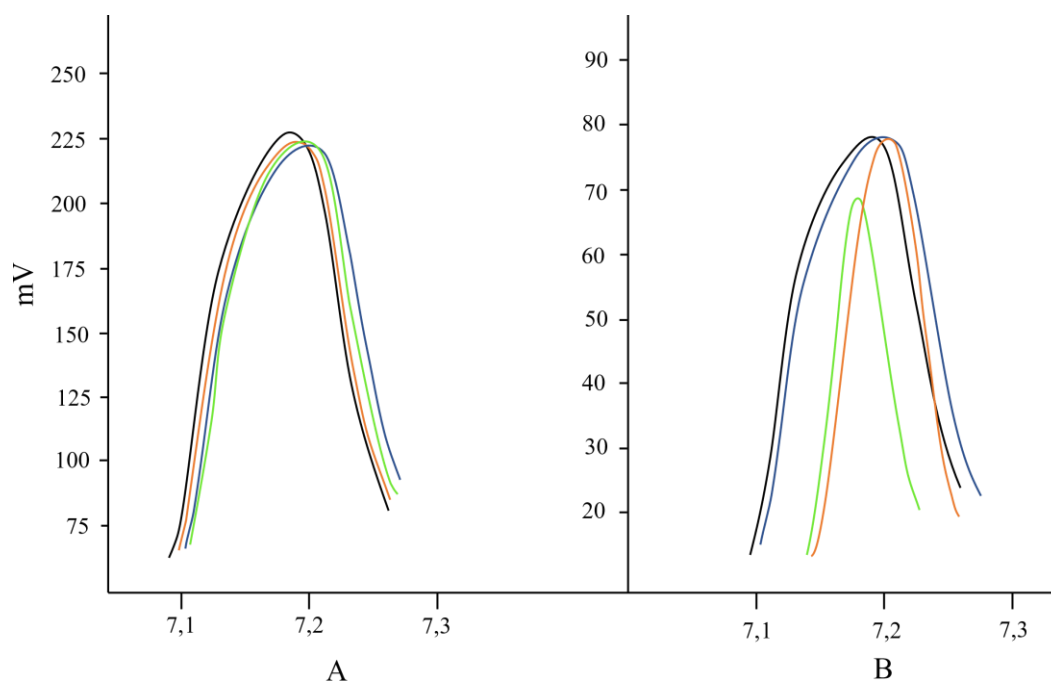


Fig. 10: The enlarged area of the glycerin peak on the corresponding chromatograms, after exposure to temperatures (60 and 90 degrees), chromatograms obtained from samples at different heating times are highlighted in different colors:

- A. 60 degrees; blue - 7.25; black - 22.75; red - 35.25; green - 43.75;
 B. 90 degrees; blue - 8.5; black - 23.5; red - 32.5; green - 56.0 (heating time is indicated in hours).

All the main volatile components of letter materials demonstrate the same dynamics of evaporation under the influence of temperature. As the temperature increases, the evaporation rate of the component also increases accordingly. After 56 hours of heating at 90 degrees, virtually all of the solvent has evaporated. Thus, the temperature factor is an effective method of artificial aging of a document, the essential drawback of which, according to the counterfeiter, is the easy detection of its features with a conventional microscope.

Therefore, in recent years, experts are increasingly confronted with new methods of artificial aging, which do not have a visually and microscopically detectable effect on the microstructure of paper and details of writing materials.

Such methods include treatment in a climatic chamber with changes in humidity and evaporation of volatile components in the form of dilute aqueous solutions.

Humidity fluctuations can accelerate the evaporation of volatile components in writing materials without changing the microstructure of the document.

Tests in the climatic chamber were carried out on a series of samples shown in Table.6.

Table 6. List of samples subjected to artificial aging by humidity changes.

Sample name	Writing composition	Dye type according to Raman spectra
101 STABILO Galaxy 818 F	Ballpoint Blue	phthalocyanine
102 NORMAN NOR-01002	Ballpoint Blue	triarylmethane
103 XEPUL ICBP602	Ballpoint Blue	phthalocyanine
104 PAPER MATE ComfortMate Ultra	Ballpoint Blue	triarylmethane

Graphs of the peak areas corresponding to the main components: 2-phenoxyethanol, 2-ethylhexanol, and benzyl alcohol on the number of humidity drops are shown in Fig. 11 (a-d)

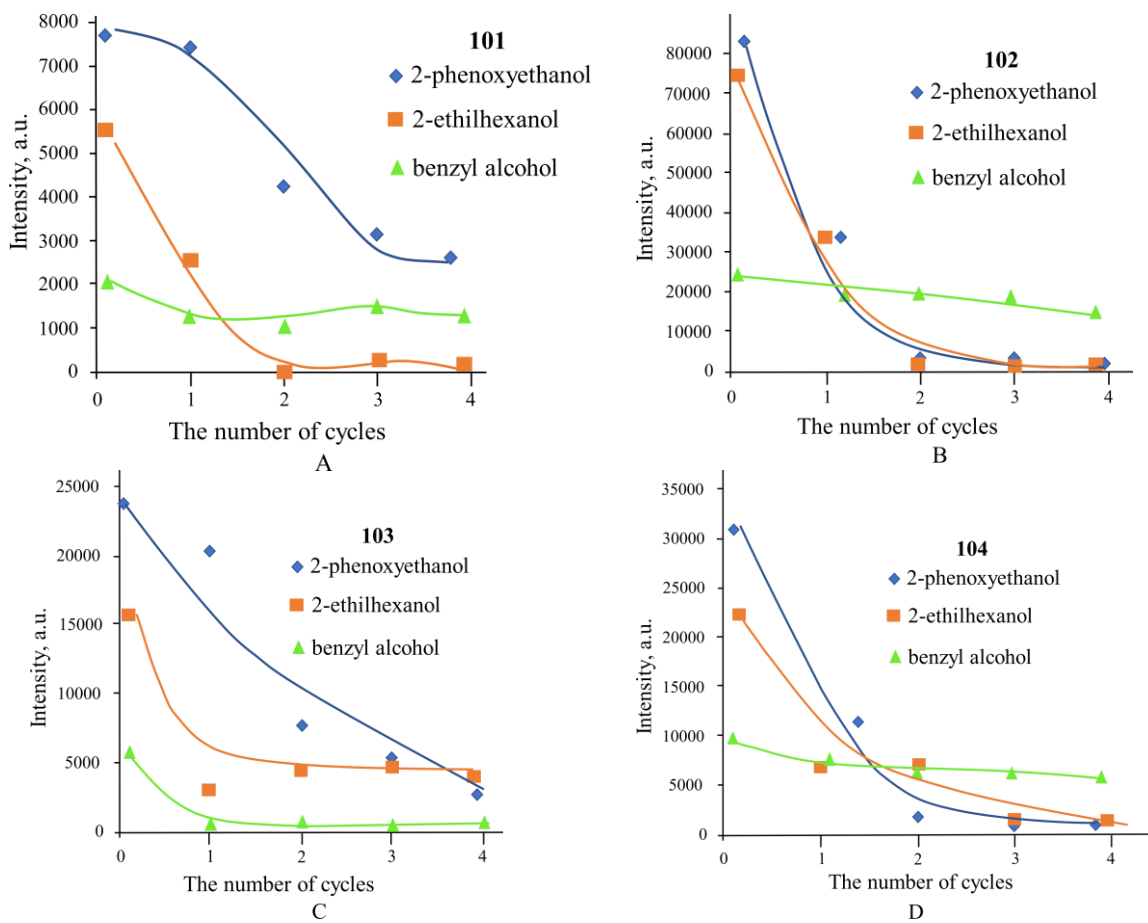


Fig. 11: Plots of peak areas corresponding to the main components: 2-phenoxyethanol, 2-ethylhexanol and benzyl alcohol on the number of humidity drops.
 A - sample No. 101 STABILO Galaxy 818 F, B -102 NORMAN NOR-01002, C-103 XEPUL ICBP602
 D-104 PAPER MATE ComfortMate Ultra

Microscopic images of strokes before and after aging are shown in Table 7.

The influence of the duration of moisture aging on the spectral characteristics of writing compositions is shown in Fig.12.

To evaluate the degree of degradation of the dye, the characteristic lines of the Raman spectrum of dyes were used according to [8,9, 10], Table 8.

Table 7: Microscopic images of strokes of writing compositions, subjected and not subjected to the wet aging procedure.


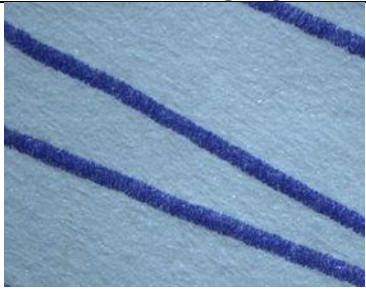
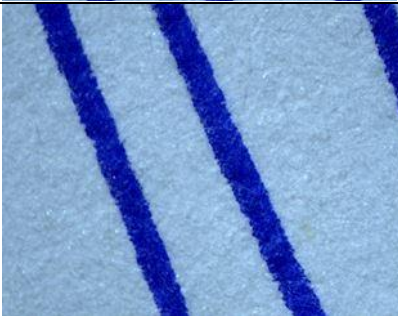
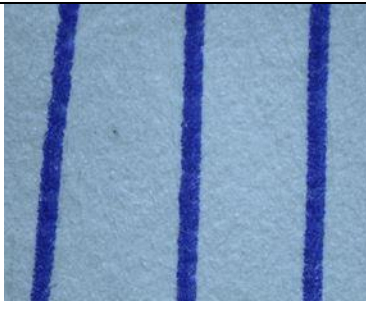


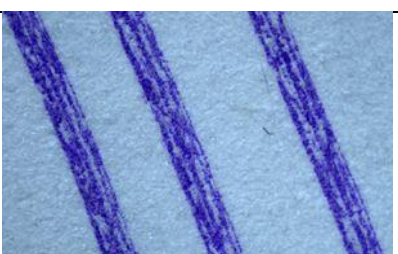
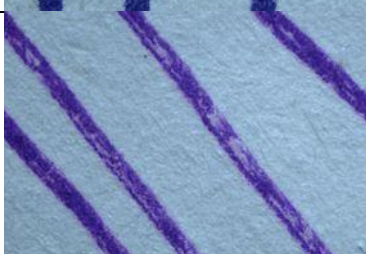
Sample	Before aging	After aging
101		
102		
103		
104		

Table 8: Lines selected for plotting temporal dependences and fluctuations corresponding to them

Writing compound type	Coloring matter	Band position in the Raman spectrum, cm ⁻¹	Fluctuation	Ratio
Type A (101)	Alcohol-soluble blue phthalocyanine	1 340	v(C-C) _{ring} v(C-N)	1,340/1,266
		1 266	VSO ₂	
Type B (102, 104)	Triarylmethane group dyes	729	v(C-N)	729/1,587
		1 587	v(C-C) _{ring}	
Type C (103)	Blue phthalocyanine pigment	1 340	v(C-C) _{ring} v(C-N)	1,340/680
		680	v(C-C-H)	

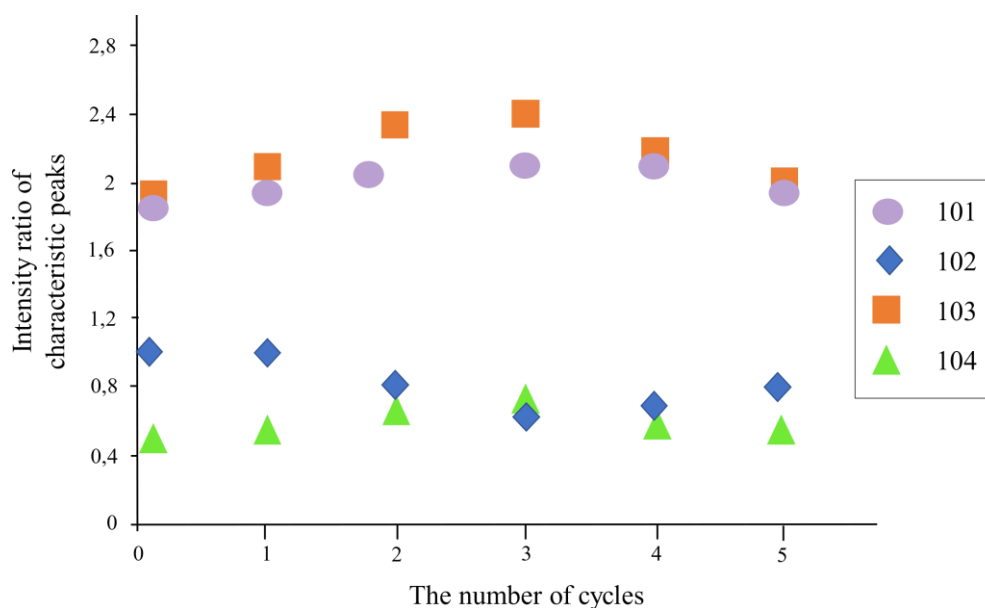


Fig. 12: Influence of the duration of moisture aging on the spectral characteristics of writing compositions

In contrast to chromatographic characteristics, moisture aging does not significantly affect the spectral characteristics of writing compositions. Moreover, humidity has the greatest impact at the initial stage (small serial numbers of cycles). Then the spectral characteristics stabilize and approach the original ones. This effect may be associated with the possible overlap of the spectral lines of the dye and volatile components.

IV. Discussion

Summing up the research results, we can conclude:

- artificial thermal aging affects the chromatographic characteristics of writing compositions, simulating the effect of "old" inscriptions containing trace amounts of volatile components. However, the effect of thermal exposure is easily detected by microscopic observation of an artificially aged stroke.

- artificial aging by moisture has the same effect as thermal exposure, but, unlike it, does not lead to a violation of the microstructure of the stroke and paper of the document and is indistinguishable in an optical microscope. This fact can create difficulties in the forensic analysis of the study of artificially aged documents. However, the effect of wet aging has practically no effect on the spectroscopic properties of writing materials, so the simultaneous use of chromatographic and spectral methods will solve this problem. The dynamics of the Raman spectra of writing compositions is determined by the spectral dynamics of the dye, which is the basis of the latter, with the exception of the initial period of aging, which is accompanied by the evaporation of the volatile components of the writing composition.

- the influence of other components of the writing compositions on its spectral characteristics is manifested in the initial period of application to the paper base (up to 6 months). Raman spectroscopy is an effective method for studying the aging processes of writing compositions subjected to the procedure of latent artificial aging with the help of moist exposure in a climatic chamber.

The simultaneous use of two physical and chemical methods for determining the prescription of a document will significantly reduce the risks of forging important official and financial documents and prevent possible damage or effectively contribute to its compensation by searching for the perpetrators.

Acknowledgments. The study was supported by the Ministry of Education and Science of the Russian Federation (Project FSRM-2023-0005). The work was supported by the Russian Science Foundation, Agreement No. 23-23-00365.

References

- [1] Ksenia Olegovna Ershova, Svetlana Valerievna Kochemirovskaia, Rafal Ciesla, Natalia Pavlovna Kirillova, Dmitry Anatolyevich Mokhorov, Vladimir Alekseevich Kochemirovsky (2022). Physicochemical analysis of the age of handwritten inscriptions on documents: Trends and prospects. *Expert Systems with Applications* 205 117683.
- [2] Calcerrada M., Garsia-Ruiz C. (2015). Analysis of questioned documents: A review. *Analytica Chimica acta*, 853, 143 – 166].
- [3] Weyermann, C., Almog, J., Bügler, J., & Cantu, A. (2011). Minimum requirements for application of ink dating methods based on solvent analysis in casework. *Forensic Science International*, 210(1–3), 52–62.
- [4] San, R. I., Bartolomé, L., & Alonso, M. L. (2015). DATINK pilot study: An effective methodology for ballpoint pen ink dating in questioned documents. *Analytica Chimica Acta*, 892(10), 105–114.
- [5] Ni, Y., & He, N. (2020). Study of ink aging: Targeting triethylene glycol in carbon-based black gel ink strokes on paper. *Forensic Science International*, 311, Article 110296.
- [6] San, R. I., Bartolomé, L., & Alonso, M. L. (2015). DATINK pilot study: An effective methodology for ballpoint pen ink dating in questioned documents. *Analytica Chimica Acta*, 892(10), 105–114.
- [7] Eric Wellisch, Lamont Hagan, Leon Marker, Orville J (1960). Interaction of cellulose with small molecules. Glycerol and ethylene carbonate. *Sweeting Journal of Applied Polymer Science*, Volume 3, Issue 9, 331-337.
- [8] Kseniia O. Gorshkova, Ilya I. Tumkin, Liubov A. Myund, Andrey S. Tverjanovich, Andrey S. Mereshchenko, Maxim S. Panov, Vladimir A. Kochemirovsky (2016). The investigation of dye aging dynamics in writing inks using Raman spectroscopy. *Dyes and Pigments* 131, C. 239-245.
- [9] K.O Gorshkova, E.R Rossinskaya, N.P Kirillova, A.A Fogel, S.V Kochemirovskaia, V.A Kochemirovsky (2020). Investigation of the new possibility of mathematical processing of Raman spectra for dating documents. *Science & Justice*, 60, 451-465.
- [10] Sergey Sirro, Ksenia Ershova, Vladimir Kochemirovsky, Julia Fiks, Polina Kondrakhina, Sergey Ermakov, Dmitriy Mokhorov, Svetlana Kochemirovskaia. Recognition of fake paintings of the 20th-century Russian avant-garde using the physicochemical analysis of zinc white. *Forensic Chemistry* 26 (2021) 100367.
- [11] Kochemirovskaia S.V., Myund L.A., Mokhorov D.A., Baranova T.A., Kochemirovsky V.A., Ershova K.O., Ryazantsev M.N. (2022). Structure of bimetallic tartrate complexes for the rapid formation of new non-enzymatic bimetallic sensors of glucose and hydrogen peroxide in aqueous solutions using laser synthesis. *Materials Letters*. 2022. T. 306. C. 130973.

DESIGN AND APPLICATION OF NANOCOMPOSITE BASED ON CLAY MINERAL (GLAUCONITE) AS ECO- FRIENDLY FERTILISER FOR AGRICULTURE

Maxim Rudmin^{1,2}, Boris Makarov¹, Prokopy Maximov¹, Evan Dasi¹

¹Tomsk Polytechnic University, Russia

²University of Tyumen, Russia

rudminma@tpu.ru

Abstract

The application of nanocomposite fertilisers represents a progressive stride towards harmonising agronomical techniques with environmental conservation. Many studies have been embarked upon to gauge the effectiveness of fertilisers, engaging various substances encompassing polymers, clay minerals, and an amalgamation of synthetic and natural elements. Among these, using clay minerals, such as glauconite, which are both economical and readily accessible, provides an attractive substitute for numerous artificial substances. Glauconite is an adept inhibitor, consisting of nano and micro-particles with vast specific surface areas that maintain surface charge and provide ion-available interlayer sites, thus facilitating nutrient interchange.

This study explores constructing and using nanocomposite fertilisers from glauconite amalgamated with a carbamide solution-gel. The ensuing nanocomposite exhibits enhanced intercalation between ammonium and glauconite, as substantiated by extensive analyses using techniques such as XRD, TEM, FTIR, TG-DSC, SEM-EDS, Brunauer–Emmett–Teller (BET) analysis, soil leaching experiments, lab and field agricultural tests.

The mineral nanocomposites, replete with an assortment of novel functionalities, disclose that 20% of the carbamide solution results in an escalation of the intercalated N ratio to 8, predominantly within the smectite layers of glauconite. The decrease of a specific surface, the total pore volume and the average pore size in the nanocomposite reflects the adsorption of carbamide substances within the meso- and macropores of glauconite particles.

The chemically synthesised glauconite nanocomposite retains an original spherical morphology, accompanied by a distinctive microlayer near the surface, and exhibits an increased nitrogen ratio, indicative of a superior filtration capability. Controlled-action nitrogen and potassium nanocomposite fertiliser were realised using glauconite as an inhibitor.

The expectation of targeted and controlled release of nutrients such as ammonium, nitrate and potassium is facilitated by their multifarious forms within the glauconite. Chemically tailored glauconite nanocomposite confers numerous benefits, including a micro-granular mineral structure, a permeable internal morphology, the encapsulation of N compounds within diverse pore structures, and accessible potassium. Such characteristics of the nanocomposite aid in invigorating plant growth and development when these fertilisers are dispensed onto the soil.

Keywords: nanocomposites, glauconite, agriculture, fertilisers, intercalation, environmental conservation

I. Introduction

The agriculture is leaning towards controlled-release fertilisers (CRFs) for heightened efficiency and a safer environment [1–3]. Such fertilisers gradually deliver nutrients to plants,

reducing nutrient wastage and excessive accumulation in the soil, surface water, and groundwater [4–8]. Traditional fertilisers, including urea, ammonium nitrate, and ammonium sulfate, frequently lead to nitrogen build-up in agricultural land [9]. This surplus nitrogen can cause environmental damage through processes like denitrification and eutrophication of water bodies, contributing to greenhouse effects [10–13]. CRFs, therefore, aim not only to reduce these environmental hazards but also to bolster crop yield and quality [14–17]. Addressing the global challenge of feeding an ever-growing population necessitates such advancements [18,19].

Technologies underpinning CRFs can be grouped into chemical [7,20,21], mechanical [22–26] and mechanochemical [27–36] methods. Central to CRFs are inhibitory substances or containers ensuring targeted nutrient delivery to plants [37]. These inhibitors can be either polymeric substances [38,39], organo-polymeric compounds [40–44], or specific minerals [31,45–48]. Particularly noteworthy among these minerals are layered silicates like smectites [22,33,49,50], kaolinite [27,28,51], vermiculite [29,52], and glauconite [21,32,53,54].

Glauconite has drawn significant attention in the agricultural sector due to its inherent potassium-rich nature, making it a stand-alone mineral fertiliser [55–57]. It belongs to the dioctahedral potassium-rich iron-loaded phyllosilicate group within the 2:1 interlayer deficient mica family [58–62]. Historically, soils with glauconite have been linked to enhanced fertility [63]. This fertility boost was later attributed to the ion exchange capacity of glauconite, its moisture retention, and its naturally granulated form [21,55,64,65]. Intriguingly, glauconite often contains smectite layers, the proportion of which depends on the mineral's maturity. While the absorption capacity of smectite has been extensively studied, glauconite's potential still needs to be explored. However, recent research has demonstrated nitrogen intercalation with glauconite, which culminates in superior fertilisers promoting enhanced plant growth [32,53,54].

This research delves deep into the interaction between globular glauconite and carbamide solution, targeting the intercalation of nitrogen compounds to produce high-quality nanocomposite fertiliser. The study features experiments on applying glauconite-carbamide nanocomposite fertilisers in different plant growth tests.

II. Methods

The nanocomposite was formulated using glauconite and a solution of carbamide. Glauconite from the Karin deposit in Russia was utilized in this research [21]. Energy dispersive X-ray spectroscopy analysis reveals the original chemical makeup of glauconite to include the following components: 6.8-9.4 wt.% K₂O, 18.1-32.9 wt.% Fe₂O₃(total), 50.2-58.2 wt.% SiO₂, 3.8-11.8 wt.% Al₂O₃, 2.9-4.7 wt.% MgO, 0.4-0.6 wt.% CaO, 0.3-0.4 wt.% Na₂O and 1.7-4.5 wt.% LOI (loss on ignition). The crystal-chemical formula is: K_{0.6-0.8}(Al_{0.7}Mg_{0.3-0.5}Fe_{0.9-1.7})_{1.6-2.0}(Si_{3.5-3.8}Al_{0.2-0.6})O₁₀(OH)₂nH₂O. X-ray diffraction patterns of oriented glauconite samples indicate the amount of the expanded smectite layers around 8%. The carbamide (CH₄N₂O) solution gel, provided by Terra Master Ltd. in Russia, contains in excess of 25% of nitrogen.

The chemical activation process for the nanocomposite was conducted with naturally granulated glauconite concentrate over 48 hours. A 4:1 glauconite to nitrogen (N concentration in carbamide solution) ratio was adopted, guided by prior experience. The final product of this process was given the name Gk4N1.

The characteristics of the crafted nanocomposites were studied using an array of methods [21]. This included X-ray diffraction (XRD), scanning electron microscopy with energy dispersive X-ray spectroscopy (SEM-EDS), transmission electron microscopy (TEM) with selected area electron diffraction (SAED), Fourier transform infrared spectroscopy (FTIR), and differential thermal analysis (incorporating thermo-gravimetric analysis and differential scanning calorimetry, TG-DSC), alongside a quadrupole mass spectrometer and Brunauer–Emmett–Teller (BET) analysis.

Examinations of the structural alterations in glauconite occurred before and after nanocomposites' activation. The mineral composition of randomly arranged nanocomposites was discerned using a Bruker D2 Phase X-ray diffractometer with specific settings. This included taking scans of composite fractions under specific conditions, separating the clay fraction and preparing them with various techniques for further analysis. Each sample was measured in the air-dried and the ethylene-glycol solvated states following placement in a desiccator for 24 h at ~60 °C.

The unit structures and interlayers of glauconite crystals were explored at the Center for Sharing Use "Nanomaterials and Nanotechnologies" of Tomsk Polytechnic University through JEOL JEM-2100F transmission electron microscopy (TEM). The images were explicitly captured using a copper grid and certain technical details.

FTIR spectra were gathered using a specific spectrometer to identify the chemical bond functional groups within the nanocomposites. The temperature-controlled high-sensitivity detector was used to obtain data between specific wave numbers.

TG-DSC curves were taken to study thermal degradation and calculate the weight ratio of different intercalations using a specific micro thermal analyser under an inert argon atmosphere.

The analysis was coupled with a mass spectrometer for simultaneous detection and quantification of evolved gases, with calibration performed before the experimentation and certain additional adjustments made.

The nanocomposites underwent analysis under a TESCAN VEGA 3 SBU scanning electron microscope, operating with specific technical parameters, followed by elemental analysis through an OXFORD X-Max 50 energy-dispersive adapter.

The BET method was employed to evaluate the specific surface of the samples using a particular adsorption-specific surface and porosity analyser, with specific drying and degassing procedures followed.

For the leaching experiment, dry sandy soil was combined with nanocomposites, and specific dosing and procedures were applied. A PVC tube was utilized, and specific modifications were made to collect leachate. The trial was replicated three times, and specific methods were employed to maintain the soil moisture level and monitor various concentrations. The final values were computed as an average, and additional calculations were performed for cumulative release curves.

Statistical examination of the outcomes was carried out with Microsoft Excel 365, with values computed as arithmetic means alongside standard deviations. Statistical tests were performed to ascertain significant variances between the experiments, including the least significant difference (LSD) test at the 0.05 probability level, following analyses of variance, which the LSD then followed.

Agrochemical experiments were carried out in laboratory and field conditions.

Experiments were conducted in the laboratory to cultivate agricultural crops, explicitly utilising promising nanocomposites. Soil devoid of fertilisers served as a control and standardisation plot. Oat seeds (*Avena sativa*) were grown at a consistent room temperature (26±1 °C) for a duration of 20 days within glass Petri dishes, each having dimensions of 9 cm in diameter and 1.5 cm in depth.

Both dry composite products and urea were incorporated into the soil at a rate of 50 kg (potassium) per hectare. The experiment was replicated on three occasions (one plot), and the mean values were subsequently recorded.

A weakly acidic dark grey agricultural soil (pH 5.1) containing 4.1% organic carbon was employed for these trials. The plants were consistently watered using tap water each morning. Standard methods were used to determine the plants' germination energy, height, and dry weight (yield).

Germination was gauged by calculating the proportion of sprouts to the overall number of seeds

planted. Germination energy was monitored daily, and the final germination percentage was ascertained after four days. The number of sprouts was deduced, assuming the plants reached 2 cm above the soil surface.

Following the 20-day period, measurements were taken of the plant's height and weight. The oat seedlings were individually enclosed in paper sheets and preserved in a desiccator at 80 °C. Once the weight of the plant samples had stabilised, their dry weight (yield) was measured.

The nanocomposite was specifically trialled on wheat in field-based growth experiments concerning plant cultivation. The fertiliser was applied at a rate of 90 kg per hectare, with the overall experimental plot encompassing an area of 0.25 hectares. The structure of the wheat yield (crop yield, plant height, ear count) was ascertained from a selected 1 square meter area, where 30 plants were chosen from the collective sheaf. The yield was quantified based on the weight of the threshed crop and subsequently translated into kg per hectare.

To assess the quality of the wheat, parameters such as moisture content, protein content, and gluten composition were analysed. This analysis used an NIR-analyser, specifically the "Infralum FT 10" model (Lumex, Russia). The process entailed conducting three individual measurements, the mean of which was then computed to accurately represent the aforementioned indicators.

III. Results

The X-ray diffraction pattern of the activated nanocomposite (Fig. 1) displays characteristic peaks of glauconite, carbamide (urea), and quartz impurity. Compared to the raw glauconite, the diffraction patterns of the activated nanocomposites reveal a new basal 001 peak, corresponding to the increased inter-planar space of the expanding smectite layers in glauconite at 17.0 Å. The occupation of the interplanar distance by new ions is confirmed by the absence of displacement of this basal peak in the ethylene-glycol solvated state of the nanocomposite (Fig. 1). The diffraction pattern is marked by peaks at 4.0, 3.6, 3.2, 3.0, and 2.5 Å, which are associated with adsorbed urea. The glauconite's characteristic peaks occur at 10.0, 4.5, 2.6, and 2.45 Å.

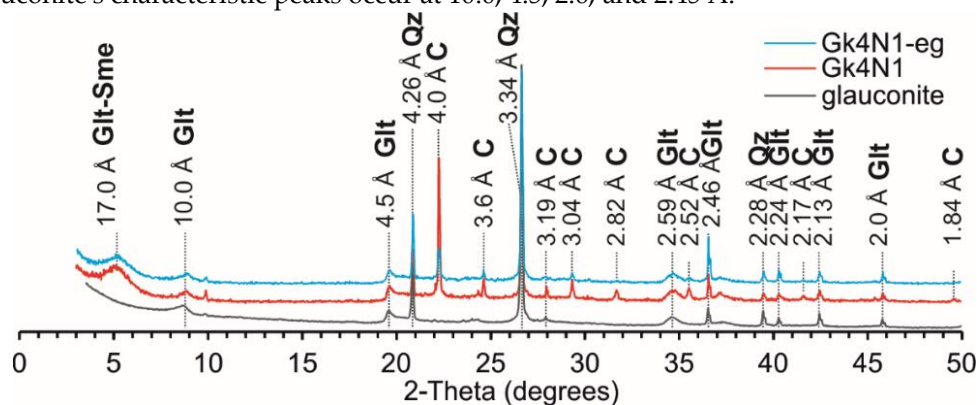


Fig. 1: X-ray patterns for both the activated nanocomposite and the glauconite. The sample labelled Gk4N1-eg represents the nanocomposite scanned in its ethylene-glycol solvated state. C – carbamide, Glt – glauconite, Glt-Sme – glauconite-smectite, Qz – quartz

High-resolution images and local electron diffraction patterns showcase nanocomposite particles of glauconite with expanded crystal bundles. Nanocomposite particles often display an augmentation of single or double mineral unit structures. The typical interlayer thickness in the native glauconite varies from 1.9-2.7 nm but is notably thicker in the nanocomposite 2.8-3.9 nm. The IR spectrum of the nanocomposite (Fig. 2) displays variations at 1155, 1452-1462, 1600, 1624, 1680, 3342, and 3442 1/cm. The nanocomposite retains certain glauconite-specific vibrations at 700, 775, 794, and 1020 1/cm in tetrahedral positions, Fe^{II}OHFe^{III} and MgOHFe^{III} in octahedral positions

at 3522 and 3564 1/cm, respectively [58,66]. During activation with glauconite, the intensities of certain NH₂ at 1155 and 3442 1/cm and NH peaks at 1680 and 3342 1/cm become more pronounced. A distinct peak in the nanocomposite is linked to the CO vibrations of the adsorbed urea at 1600 1/cm.

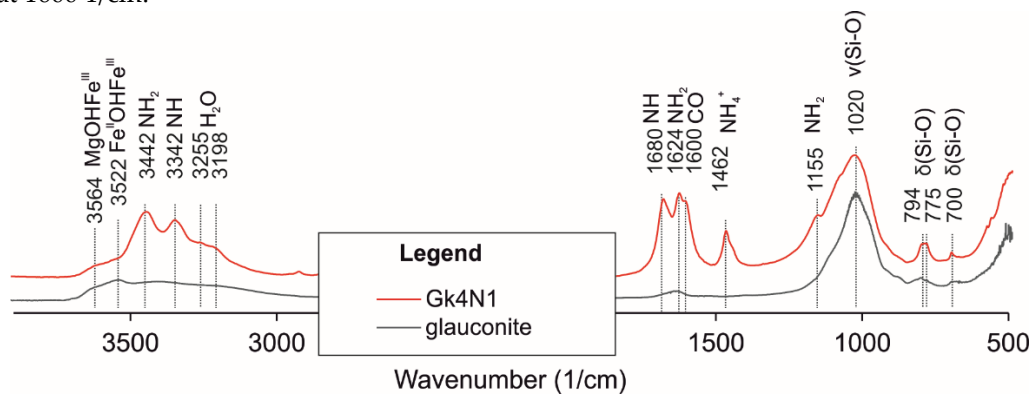


Fig. 2: FTIR spectra of the nanocomposite and the original glauconite

The nanocomposite DSC curve (Fig. 3 A) indicates two pronounced endothermic effects and one subtle endothermic effect at 134°C, 188°C, and 360°C, respectively. Furthermore, there are four exothermic responses at 122°C, 153°C, 290°C, and 650°C. The initial sharp endothermic response at 134°C signifies the melting of carbamide. The subsequent endothermic change, occurring between 184-190°C, corresponds to the evaporation of carbamide – specifically NH₃ and CO₂. This is associated with the components integrated into the mineral. The milder endothermic reaction at 360°C confirms the breakdown of the polymerised component of carbamide. Notably, an endothermic effect at 571°C indicates a minor presence of quartz.

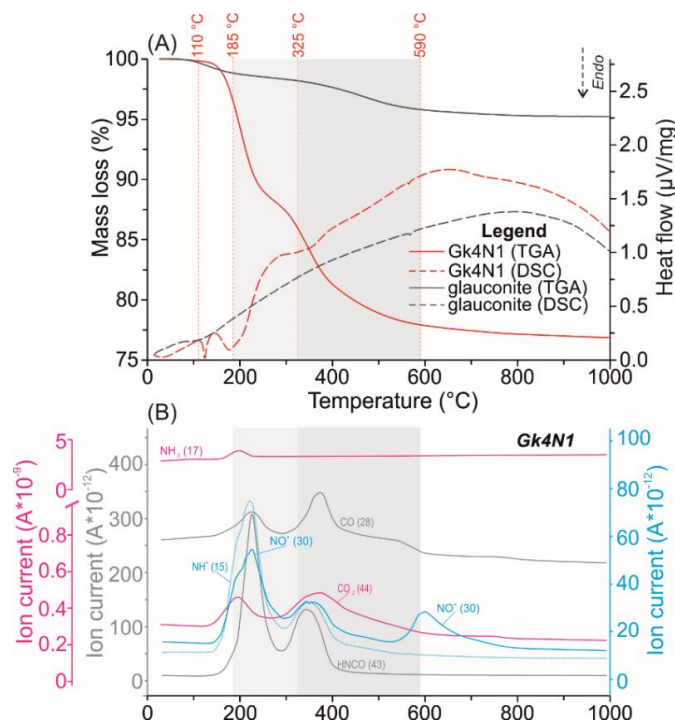


Fig. 3: (A) TGA (represented by solid lines) with DSC curves (indicated by dashed lines) of the prepared nanocomposite and the original glauconite. (B) Highlighted representative MS ion detection curves with m/z values of 15 (NH⁺), 17 (NH₃), 28 (CO⁺), 30 (NO⁺), 43 (HNCO⁺), and 44 (CO₂).

The TG curve of the nanocomposite (Fig. 3 A) outlines five primary weight loss phases that

are indicative of glauconite: spanning temperature ranges of 0-110°C, 110-185°C, 185-325°C, 325-590°C, and 590-1000°C. The initial phase (0-110°C) is attributed to eliminating physically attached water from the mineral, resulting in a 0.1-0.2 wt.% weight loss. The subsequent phase (110-185°C) pertains to the expulsion of water and carbamide by-products (NH₃ and CO₂) from the nanocomposite's macropore space (Fig. 3 B), resulting in weight reductions of 0.7-3.3 wt.%. The third phase (185-325°C) encompasses the release of mesopore water and several carbamide breakdown products. The weight decrease within this span is 2.1-10.6 wt.%. The fourth weight loss phase, 325-590°C, sees nanocomposite weight loss ranging from 2.5 to 8.0 wt.%. This stage is linked to expelling water and carbamide degradation products, predominantly from the mineral interlayer space. Additionally, an elevated concentration of carbamide in the nanocomposites is evident from the observed releases of CO₂, CO, HNCO, NO⁺, and NH⁺. The final phase, between 590-1000°C, results in a 0.6-1.1 wt.% weight loss, reflecting the dehydration of the glauconite crystal structures within the nanocomposite.

Both the nanocomposite and the original glauconite exhibit a globular grain size, with lengths varying between 50 and 250 µm (Fig. 4). Haphazardly oriented micro-flakes with sinuous borders characterise the internal morphology of these globules. These micro-flakes range in size from 0.5-5 µm in length. One distinguishing feature of the glauconite near-surface microlayer is the parallel alignment of micro-flakes perpendicular to the surface. Furthermore, these nanocomposite microlayers are marked by a higher nitrogen content than the globules core.

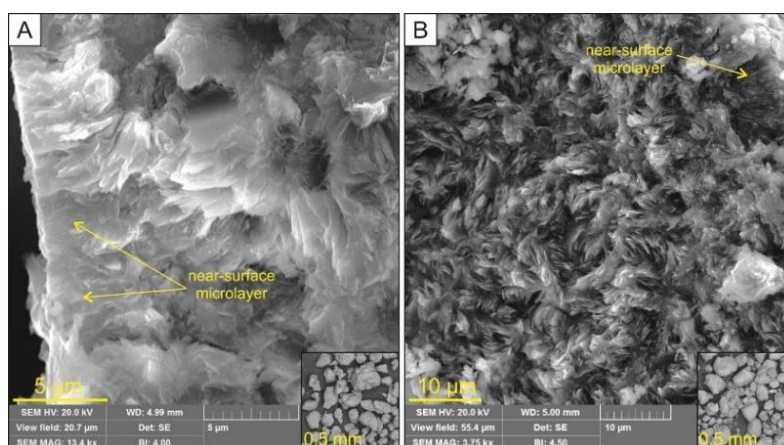


Fig. 4: SEM photos captured using a secondary electron detector showcasing the distinct morphological characteristics of the nanocomposite (A) as opposed to the original glauconite (B). The bottom right corner provides an encompassing image of the globular section for each sample.

The original globular glauconite specific surface area, pore volume, and average pore size are 41.2 m²/g, 0.064 cm³/g, and 8.9 nm, respectively. As the proportion of carbamide increases during activation, the specific surface area of the nanocomposite drops to 23.8 m²/g. In tandem, the average pore volume and size reduce to 0.036 cm³/g and 4.1 nm, respectively.

The laboratory soil leaching examinations provided varied insights into the leaching kinetics of ammonium, nitrate, and potassium from the nanocomposite. For ammonium (Fig. 5 A), two prominent release phases were observed: days 1-7 and 21-28. Between days 7 and 21, the release of ammonium was gradual. After the 28th day, the release rate became more measured and extended. In contrast, nitrates exhibited a notably rapid release within seven days (Fig. 5 B). Beyond this, only trace amounts, ranging from 0.2 to 0.3 mg, were leached from day 7 to day 56. The leaching kinetics of potassium from the nanocomposites (Fig. 5 C) progressed through four distinct phases, setting them apart from the potassium leaching kinetics observed in the control sample. The first phase, lasting until day 7, saw a rapid release. This was followed by a period of slower release from day 7 to day 28. The period from day 28 to day 43 marked the peak release

rate.

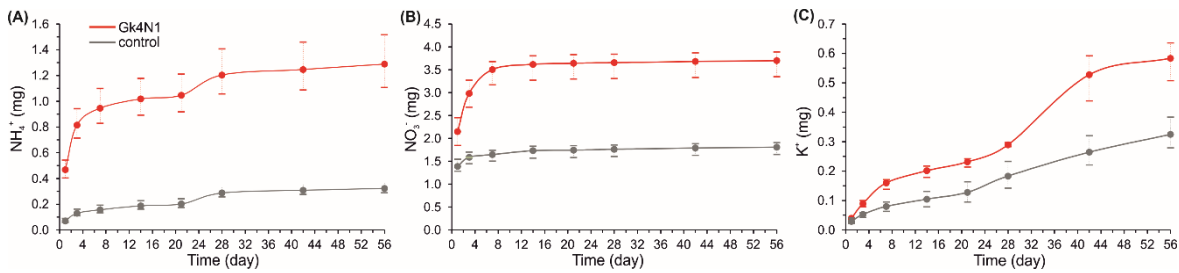


Fig. 5: Cumulative graphs detailing the release rates of ammonium (A), nitrate (B), and potassium (C) from the nanocomposite. These are set against a control sample devoid of nanocomposite from laboratory assessments. The dotted lines depict the range between the minimum and maximum cumulative values. Any statistically significant variances for each parameter are noted at the $p = 0.05$. Error bars denote standard deviations.

The dry weight of the oat (*Avéna satíva*) exhibited an increase in the laboratory plant growth experiment when the tested nanocomposite was used, compared to the control (Fig. 6). The recorded dry weight (or crop yield) stood at 0.266 g, which is in contrast to the 0.233 g for the control sample (Fig. 6 A). This indicates a boost in crop yield by over 14.2% in the plots treated with the nanocomposite. Regarding the germination rate (Fig. 6 B), the presence of the nanocomposite led to an increase of 93.3%, whereas the control plot (without any fertiliser) recorded a rate of 90.7%. As for the average plant height (Fig. 6 C), there was a rise to 14.3 cm in the nanocomposite-treated plot, in contrast to the control's 12.7 cm. This denoted an elevation in plant height by 12.6% when the devised nanocomposite was applied.

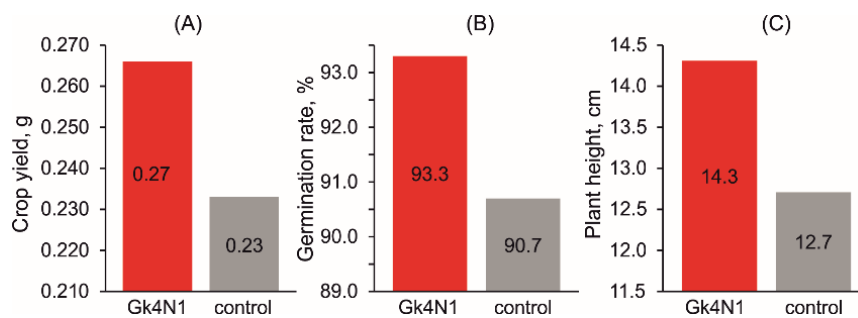


Fig. 6: Yield (A), germination rate (B), and plant height (D) of oat (*Avéna satíva*) were assessed following the application of the researched nanocomposite fertilisers and compared to a control plot without any fertilisers, based on laboratory experiments. Each parameter's statistical significance is highlighted at the $p = 0.05$ level.

Field agro experiment with wheat cultivation also showed the stimulating effect of nanocomposite as a fertiliser on yield. The experiment yield with nanocomposite was 5.7 t/ha compared to 4.5 t/ha in the control plot. This indicates a 27.4% increase in wheat yield. The structure and quality of wheat also differed in the experiments with nanocomposite relative to the control (Table 1). An increase in all the wheat structure indices (average ear length and ear count) was recorded. The average plant height and ear count changed from 8.5 to 9.1 cm and 36 to 42 pieces, respectively, relative to the control. These indicators increase by 7.5 and 16.9%. Moisture, protein and gluten content vary relative to the control from 16 to 16.4%, 11.3 to 13.2% and 10.6 to 19%, respectively.

Table 1: *Wheat yield average indicators based on the results of field experiments*

	Crop yield, t/ha	Spike length, cm	Average ear count	Moisture content, %	Protein content, %	Gluten composition, %
Nanocomposite	4.5	8.5	36	16.0	11.3	10.6
Control	5.7	9.1	42	16.4	13.2	19.0

IV. Discussion

In the activated nanocomposite, the proportion of intercalated nitrogen mixtures is ascertained by the initial basal XRD reflex shift to 17.0 Å (Fig. 1), the linear measurements of the expansion in inter-planar distance captured on TEM images, and the weight reduction between temperatures of 325-590 °C. This is further corroborated by the release of nitrogen compounds revealed by TG-DSC-MS data (Fig. y). As nitrogen concentration in the resultant solution rises, correlating to a 20 mol.% of the glauconite concentrate, the intercalated nutrient ratio also surges to a peak of 8.0%. Interestingly, this maximal intercalation does not surpass the proportion of smectite layers present in glauconite. This reflects the specific intercalation capacity of the inter-planar gaps within the smectite phases [21,53,54,67]. This might be due to the ionic exchange involving ammonium and solvate water and the sodium and calcium native to the mineral.

Consequently, calcium and sodium are scarcely present in the nanocomposites, while the primary elements (Si, Al, Fe, Mg, K) remain consistent with the original mineral's proportions. Therefore, the intercalation aptitude of glauconite seems reliant on the number of its smectite layers, its [62] or maturity [60], and the geological conditions [68,69].

Using FTIR peaks (Fig. 2), adsorbed nitrogen compounds in meso- and macropores are determined by NH₂ and NH signatures. These are further indicated by weight losses between 100-185 °C (macropores) and 185-325 °C (mesopores), revealing the presence of specific ions (Fig. 3). The subsequent decline in total pore volume and mean pore diameter authenticates the filling of meso- and macro-pores.

An evident microlayer on the surface of glauconite globules (Fig. 4), alongside oriented micro-flakes, underscores the mineral's advantageous morphological attributes. A heightened nitrogen presence within these microlayers suggests a superior filtration capability. It's theorised that carbamide penetrates glauconite globules mainly via these solution-conducting microlayers and subsequently permeates the core. Within the core, nitrogen compounds are intercalated between the smectite layers of glauconite and are also absorbed in mesopore spaces.

Nutrient releases, encompassing ammonium, nitrate, and potassium, reveal a stepwise kinetics aligned with their interaction with the mineral (Fig. 5). The initial, easily accessible forms relate to substances adsorbed in macropores, and they're typically discharged from the nanocomposites within the initial 21 days or 7 days for ammonium and nitrate, respectively. This is followed by releasing absorbed ammonium from the mesopore region from day 21 to 28. By the 28th day, the intercalated ammonium is extracted from the mineral's interlayer. The staggered kinetics of these nutrient releases, particularly for ammonium and potassium, accentuates the dual positive role of layered glauconite in nanocomposites as both an ammonium suppressor and a potassium source.

The resultant mineral nanocomposites, crafted by chemically activating globular glauconite with carbamide, offer multiple benefits. They retain a micro-granular mineral form, possess an innate diffusive microlayer, incubate nitrogen elements across micro-, meso-, and macro-pores, and act as a potassium source. There's a specific interest in the ammonium intercalation within the smectite layers of these mineral constructs, underscoring the significance of understanding glauconite's structural integrity.

Laboratory and field tests revealed a pronounced positive effect on plant growth and

development without the risk of environmental damage when using a nanocomposite derived from the innate globular structure of glauconite (Fig. 6, Table 1). In controlled laboratory conditions, the assessed nanocomposite fertiliser consistently improved oat growth. Additionally, under field conditions, introducing the Gk4N1 nanocomposite into the soil remarkably boosted the quality and quantity of wheat yield – with an impressive 27.4% increase in yield. This significant growth surpasses the outcomes of applying unaltered glauconite in the field [65,70].

V. Conclusions

From the research into the chemical activation of globular glauconite with carbamide and the subsequent use of this nanocomposite, the following key findings have been established. Within the interlayer spaces (micropores) of smectite layers in glauconite, nitrogen intercalation occurs. Utilising a carbamide solution with a 20% nitrogen concentration facilitates optimal intercalation.

The presence of adsorbed carbamide substances in meso- and macropores is indicated by a reduced specific surface area, total volume, and mean pore diameter in the nanocomposite.

Glauconite nanocomposites retain their globular particle shape and exhibit a unique near-surface microlayer. An elevated nitrogen concentration in these surface microlayers underscores their superior filtration capability. This surface microlayer plays a crucial role in delivering solutes to the core region of glauconite globules.

The nanocomposites show a staggered nutrient release mechanism, underlining the varied absorption of carbamide in the micro-, meso-, and macro-pores of glauconite. Moreover, alongside nitrogen compounds, potassium is also gradually released from the glauconite nanocomposites.

Introducing the nanocomposite into the soil as a fertiliser enhances both the quality and quantity of crop yields. Importantly, laboratory and field tests confirm this is achieved without posing environmental hazards.

The authors gratefully acknowledge the financial support provided by Russian Science Foundation through the research project № 22-77-10002.

References

- [1] Duan, Q.; Jiang, S.; Chen, F.; Li, Z.; Ma, L.; Song, Y.; Yu, X.; Chen, Y.; Liu, H.; Yu, L. (2023). Fabrication, evaluation methodologies and models of slow-release fertilizers: A review. *Industrial Crops and Products*, 192:1–22.
- [2] Sharma, G.C. (1979). Controlled-release fertilizers and horticultural applications. *Scientia Horticulturae*, 11:107–129.
- [3] Trenkel, M.E. *Controlled-Release and Stabilized Fertilizers in Agriculture*, Paris, 1997.
- [4] Trenkel, M.E. *Slow- and Controlled-Release and Stabilized Fertilizers: An Option for Enhancing Nutrient Use Efficiency in Agriculture*, Paris, 2010.
- [5] Oertli, J.J. (1980). Controlled-release fertilizers. *Fertilizer Research*, 1:103–123.
- [6] Ni, B.; Liu, M.; Lü, S.; Xie, L.; Wang, Y. (2011). Environmentally Friendly Slow-Release Nitrogen Fertilizer. *Journal of Agricultural and Food Chemistry*, 59:10169–10175.
- [7] Chen, L.; Chen, X.L.; Zhou, C.H.; Yang, H.M.; Ji, S.F.; Tong, D.S.; Zhong, Z.K.; Yu, W.H.; Chu, M.Q. (2017). Environmental-friendly montmorillonite-biochar composites: Facile production and tunable adsorption-release of ammonium and phosphate. *Journal of Cleaner Production*, 156:648–659.
- [8] Chakraborty, R.; Mukhopadhyay, A.; Paul, S.; Sarkar, S.; Mukhopadhyay, R. (2023). Nanocomposite-based smart fertilizers: A boon to agricultural and environmental sustainability.

Science of The Total Environment, 863:160859.

[9] Alrbaihat, M.R. (2023). Agricultural Nano Fertilizers: Macronutrient Types and Applications Review. *Current Trends in Geotechnical Engineering and Construction*, 306–316.

[10] Obieze, C.C.; Chikere, C.B.; Adeleke, R.; Akaranta, O. (2019). Formulation and evaluation of slow-release fertilizer from agricultural and industrial wastes for remediation of crude oil-polluted soils. *Society of Petroleum Engineers - SPE Nigeria Annual International Conference and Exhibition*, NAIC 2019.

[11] Akiyama, H.; Yan, X.; Yagi, K. (2010). Evaluation of effectiveness of enhanced-efficiency fertilizers as mitigation options for N₂O and NO emissions from agricultural soils: Meta-analysis. *Global Change Biology*, 16:1837–1846.

[12] Xiao, Y.; Peng, F.; Zhang, Y.; Wang, J.; Zhuge, Y.; Zhang, S.; Gao, H. (2019). Effect of bag-controlled release fertilizer on nitrogen loss, greenhouse gas emissions, and nitrogen applied amount in peach production. *Journal of Cleaner Production*, 234:258–274.

[13] IPCC Climate Change 2014: Mitigation of Climate Change: Working Group III Contribution to the Fifth Assessment Report of the Intergovernmental Panel on Climate Change 2014.

[14] Mala, R.; Selvaraj, R.; Sundaram, V.; Rajan, R.; Gurusamy, U. (2017). Evaluation of Nano Structured Slow Release Fertilizer on the Soil Fertility, Yield and Nutritional Profile of *Vigna radiata*. *Recent Patents on Nanotechnology*, 11:50–62.

[15] Liu, Q.; Liu, Y.; Hao, X.; Song, C.; Zong, Y.; Zhang, D.; Shi, X.; Li, P. (2023). Effects of controlled-release fertilizer on N₂O emissions in wheat under elevated CO₂ concentration and temperature. *Plant and Soil*, 3:1–19.

[16] Pereira, E.I.; A. Nogueira, A.R.; Cruz, C.C.T.; Guimarães, G.G.F.; Foschini, M.M.; Bernardi, A.C.C.; Ribeiro, C. (2017). Controlled Urea Release Employing Nanocomposites Increases the Efficiency of Nitrogen Use by Forage. *ACS Sustainable Chemistry & Engineering*, 5:9993–10001.

[17] Fu, J.; Wang, C.; Chen, X.; Huang, Z.; Chen, D. (2018). Classification research and types of slow controlled release fertilizers (SRFs) used - a review. *Communications in Soil Science and Plant Analysis*, 49: 2219–2230.

[18] Pretty, J.; Sutherland, W.J.; Ashby, J.; Auburn, J.; Baulcombe, D.; Bell, M.; Bentley, J.; Bickersteth, S.; Brown, K.; Burke, J.; et al. (2010). The top 100 questions of importance to the future of global agriculture. *International Journal of Agricultural Sustainability*, 8:219–236.

[19] Tilman, D.; Cassman, K.G.; Matson, P.A.; Naylor, R.; Polasky, S. (2002). Agricultural sustainability and intensive production practices. *Nature*, 418:671–677.

[20] Rashid, M.; Hussain, Q.; Khan, K.S.; Alwabel, M.I.; Hayat, R.; Akmal, M.; Ijaz, S.S.; Alvi, S.; Obaid-ur-Rehman (2021). Carbon-Based Slow-Release Fertilizers for Efficient Nutrient Management: Synthesis, Applications, and Future Research Needs. *Journal of Soil Science and Plant Nutrition*, 1–26.

[21] Rudmin, M.; Maximov, P.; Dasi, E.; Kurovsky, A.; Gummer, Y.; Ibraeva, K.; Kutugin, V.; Soktoev, B.; Ponomarev, K.; Tararushkin, E.; et al. (2023). Intercalation of carbamide to globular glauconite by chemical processing for the creation of slow-release nanocomposites. *Applied Clay Science*, 243:107075.

[22] Rudmin, M.; Banerjee, S.; Makarov, B.; Ibraeva, K.; Konstantinov, A. (2022). Mechanical Activation of Smectite-Based Nanocomposites for Creation of Smart Fertilizers. *Applied Sciences*, 12:1–11.

[23] Singla, R.; Alex, T.C.; Kumar, R. (2020). On mechanical activation of glauconite: Physicochemical changes, alterations in cation exchange capacity and mechanisms. *Powder Technology*, 360:337–351.

[24] Salimi, M.; Motamedi, E.; Safari, M.; Motesharezadeh, B.; Motesharezadeh, B. (2021). Synthesis of urea slow-release fertilizer using a novel starch-g-poly(styrene-co-butylacrylate) nanocomposite latex and its impact on a model crop production in greenhouse. *Journal of Cleaner Production*, 322:129082.

[25] Zhao, X.; Qi, X.; Chen, Q.; Ao, X.; Guo, Y. (2020). Sulfur-Modified Coated Slow-Release

Fertilizer Based on Castor Oil: Synthesis and a Controlled-Release Model. *ACS Sustainable Chemistry & Engineering*, acssuschemeng.0c06056.

[26] Mañosa, J.; la Rosa, J.C.; Silvello, A.; Maldonado-Alameda, A.; Chimenos, J.M. (2023). Kaolinite structural modifications induced by mechanical activation. *Applied Clay Science*, 238:106918.

[27] Solihin; Zhang, Q.; Tongamp, W.; Saito, F. (2011). Mechanochemical synthesis of kaolin-KH₂PO₄ and kaolin-NH₄H₂PO₄ complexes for application as slow release fertilizer. *Powder Technology*, 212: 354–358.

[28] Alrbaihat, M.R.; Al-Rawajfeh, A.E.; Alshamaileh, E. (2021). A mechanochemical preparation, properties and kinetic study of kaolin-N, P fertilizers for agricultural applications. *Journal of the Mechanical Behavior of Materials*, 30:265–271.

[29] De Oliveira, D.S.; Jaeger, S.; Marangoni, R. (2021). Mechanochemical Synthesis of Expanded Vermiculite with Urea for Filler into Alginate/Collagen Spherical Capsules: A Urea Slow-release System. *Orbital: The Electronic Journal of Chemistry*, 13:124–130.

[30] AlShamaileh, E.; Alrbaihat, M.; Moosa, I.; Abu-Afifeh, Q.; Al-Fayyad, H.; Hamadneh, I.; Al-Rawajfeh, A. (2022). Mechanochemical Preparation of a Novel Slow-Release Fertilizer Based on K₂SO₄-kaolinite. *Agronomy*, 12:3016.

[31] Borges, R.; Baika, L.M.; Grassi, M.T.; Wypych, F. (2018). Mechanochemical conversion of chrysotile/K₂HPO₄ mixtures into potential sustainable and environmentally friendly slow-release fertilizers. *Journal of Environmental Management*, 206:962–970.

[32] Rudmin, M.; Abdullayev, E.; Ruban, A.; Buyakov, A.; Soktoev, B. (2019). Mechanochemical Preparation of Slow Release Fertilizer Based on Glauconite-Urea Complexes. *Minerals*, 9:507.

[33] Borges, R.; Prevot, V.; Forano, C.; Wypych, F. (2017). Design and Kinetic Study of Sustainable Potential Slow-Release Fertilizer Obtained by Mechanochemical Activation of Clay Minerals and Potassium Monohydrogen Phosphate. *Industrial & Engineering Chemistry Research*, 56:708–716.

[34] Said, A.; Zhang, Q.; Qu, J.; Liu, Y.; Lei, Z.; Hu, H.; Xu, Z. (2018). Mechanochemical activation of phlogopite to directly produce slow-release potassium fertilizer. *Applied Clay Science*, 165:77–81.

[35] Borges, R.; Giroto, A.S.; Guimarães, G.G.F.; Reis, H.P.G.; Farinas, C.S.; Ribeiro, C. (2022). Asbestos cement waste treatment through mechanochemical process with KH₂PO₄ for its utilization in soil pH correction and nutrient delivery. *Environmental Science and Pollution Research*, 1:1–12.

[36] Alrbaihat, M.; AlShamaileh, E.; Al-Rawajfeh, E. (2022). Environment-Friendly Synthesis of Feldspar-KH₂PO₄ Complexes by Mechanochemical Reaction. *BOHR International Journal of Material Sciences and Engineering*, 1:1–6.

[37] Rahman, M.H.; Haque, K.M.S.; Khan, M.Z.H. (2021). A review on application of controlled released fertilizers influencing the sustainable agricultural production: A Cleaner production process. *Environmental Technology & Innovation*, 23:101697.

[38] Pereira, E.I.; da Cruz, C.C.T.; Solomon, A.; Le, A.; Cavigelli, M.A.; Ribeiro, C. (2015). Novel Slow-Release Nanocomposite Nitrogen Fertilizers: The Impact of Polymers on Nanocomposite Properties and Function. *Industrial & Engineering Chemistry Research*, 54:3717–3725.

[39] González, M.E.; Cea, M.; Medina, J.; González, A.; Diez, M.C.; Cartes, P.; Monreal, C.; Navia, R. (2015). Evaluation of biodegradable polymers as encapsulating agents for the development of a urea controlled-release fertilizer using biochar as support material. *Science of The Total Environment*, 505:446–453.

[40] Wang, C.; Luo, D.; Zhang, X.; Huang, R.; Cao, Y.; Liu, G.; Zhang, Y.; Wang, H. (2022). Biochar-based slow-release of fertilizers for sustainable agriculture: A mini review. *Environmental Science and Ecotechnology*, 10:100167.

[41] Elkhelifi, Z.; Kamran, M.; Maqbool, A.; El-Naggar, A.; Ifthikar, J.; Parveen, A.; Bashir, S.; Rizwan, M.; Mustafa, A.; Irshad, S.; et al. (2021). Phosphate-lanthanum coated sewage sludge

biochar improved the soil properties and growth of ryegrass in an alkaline soil. *Ecotoxicology and Environmental Safety*, 216: 112173.

[42] Pogorzelski, D.; Filho, J.F.L.; Matias, P.C.; Santos, W.O.; Vergütz, L.; Melo, L.C.A. Biochar as composite of phosphate fertilizer: Characterization and agronomic effectiveness. *Science of the Total Environment* 2020, 743, 140604, doi:10.1016/j.scitotenv.2020.140604.

[43] Liu, J.; Yang, Y.; Gao, B.; Li, Y.C.; Xie, J. (2019). Bio-based elastic polyurethane for controlled-release urea fertilizer: Fabrication, properties, swelling and nitrogen release characteristics. *Journal of Cleaner Production*, 209:528–537.

[44] Komariah, R.N.; Krishanti, N.P.R.A.; Yoshimura, T.; Umemura, K. (2022). Characterization of Particleboard Using the Inner Part of Oil Palm Trunk (OPT) with a Bio-based Adhesive of Sucrose and Ammonium Dihydrogen Phosphate (ADP). *BioResources*, 17:5190–5206.

[45] Puspita, A.; Pratiwi, G.; Fatimah, I. (2017). Chitosan-modified smectite clay and study on adsorption-desorption of urea. *Chemical Engineering Transactions*, 56:1645–1650.

[46] Sharma, N.; Singh, A.; Dutta, R.K. (2021). Biodegradable fertilizer nanocomposite hydrogel based on poly(vinyl alcohol)/kaolin/diammonium hydrogen phosphate (DAhP) for controlled release of phosphate. *Polymer Bulletin*, 78:2933–2950.

[47] Hussien, R.A.; Donia, A.M.; Atia, A.A.; El-Sedfy, O.F.; El-Hamid, A.R.A.; Rashad, R.T. (2012). Studying some hydro-physical properties of two soils amended with kaolinite-modified cross-linked poly-acrylamides. *CATENA*, 92:172–178.

[48] Rashidzadeh, A.; Olad, A. (2014). Slow-released NPK fertilizer encapsulated by NaAlg-g-poly(AA-co-AAm)/MMT superabsorbent nanocomposite. *Carbohydrate Polymers*, 114:269–278.

[49] Hermida, L.; Agustian, J. (2019). Slow release urea fertilizer synthesized through recrystallization of urea incorporating natural bentonite using various binders. *Environmental Technology & Innovation*, 13:113–121.

[50] Wu, J.; Wei, Y.; Lin, J.; Lin, S. (2003). Study on starch-graft-acrylamide/mineral powder superabsorbent composite. *Polymer*, 44:6513–6520.

[51] Borges, R.; Brunatto, S.F.; Leitão, A.A.; De Carvalho, G.S.G.; Wypych, F. (2015). Solid-state mechanochemical activation of clay minerals and soluble phosphate mixtures to obtain slow-release fertilizers. *Clay Minerals*, 50:153–162.

[52] Mortland, M.M.; Fripiat, J.J.; Chaussidon, J.; Uytterhoeven, J. (1963). Interaction between ammonia and the expanding lattices of montmorillonite and vermiculite. *Journal of Physical Chemistry*, 67:248–258.

[53] Rudmin, M.; Banerjee, S.; Makarov, B.; Belousov, P.; Kurovsky, A.; Ibraeva, K.; Buyakov, A. Glauconite-Urea Nanocomposites As Polyfunctional Controlled-Release Fertilizers. *Journal of Soil Science and Plant Nutrition* 2022, 22, 4035–4046, doi:10.1007/s42729-022-01006-4.

[54] Rudmin, M.; Banerjee, S.; Yakich, T.; Tabakaev, R.; Ibraeva, K.; Buyakov, A.; Soktoev, B.; Ruban, A. (2020). Formulation of a slow-release fertilizer by mechanical activation of smectite/glauconite and urea mixtures. *Applied Clay Science*, 196:105775.

[55] Hamed, M.; Abdelhafez, A.A. (2020). Application of Glauconite Mineral as Alternative Source of Potassium in Sandy Soils. *Alexandria Science Exchange Journal*, 41:181–189.

[56] Karimi, E.; Abdolzadeh, A.; Sadeghipour, H.R.; Aminei, A. (2012). The potential of glauconitic sandstone as a potassium fertilizer for olive plants. *Archives of Agronomy and Soil Science*, 58:983–993.

[57] Oze, C.; Smaill, J.B.; Reid, C.M.; Palin, M. (2019). Potassium and Metal Release Related to Glaucony Dissolution in Soils. *Soil Systems*, 3:1–17.

[58] Drits, V.A.; Zviagina, B.B.; McCarty, D.K.; Salyn, A.L. (2010). Factors responsible for crystal-chemical variations in the solid solutions from illite to aluminoceladonite and from glauconite to celadonite. *American Mineralogist*, 95:348–361.

[59] Drits, V.A. (1997). Isomorphous Cation Distribution in Celadonites, Glauconites and Fe-illites Determined by Infrared, Mössbauer and EXAFS Spectroscopies. *Clay Minerals*, 32:153–179.

[60] Odin, G.S.; Matter, A. (1981). De glauconiarum origine. *Sedimentology*, 28:611–641.

[61] Odom, I.E. (1984). 13. GLAUCONITE and CELADONITE MINERALS. In *Micas*; Bailey,

S.W., Ed.; *De Gruyter*; pp. 545–572.

[62] Rieder, M.; Cavazzini, G.; D'yakonov, Y.S.; Frank-Kamenetskii, V.A.; Gottardi, G.; Guggenheim, S.; Koval', P.V.; Müller, G.; Neiva, A.M.R.; Radoslovich, E.W.; et al. (1988). Nomenclature of the micas. *Canadian Mineralogist*, 36:905–912.

[63] McRae, S.G. (1972). Glauconite. *Earth-Science Reviews*, 8:397–440.

[64] Basak, B.B.; Sarkar, B.; Maity, A.; Chari, M.S.; Banerjee, A.; Biswas, D.R. (2023). Low-grade silicate minerals as value-added natural potash fertilizer in deeply weathered tropical soil. *Geoderma*, 433:116433.

[65] Rudmin, M.; Banerjee, S.; Makarov, B. (2020). Evaluation of the Effects of the Application of Glauconitic Fertilizer on Oat Development: A Two-Year Field-Based Investigation. *Agronomy*, 10:872.

[66] Zviagina, B.B.; Drits, V.A.; Sakharov, B.A.; Ivanovskaya, T.A.; Dorzhieva, O. V.; McCarty, D.K. (2017). Crystal-chemical regularities and identification criteria in Fe-bearing k-dioctahedral micas 1m from X-Ray diffraction and infrared spectroscopy data. *Clays and Clay Minerals*, 65:234–251.

[67] López-Quirós, A.; Sánchez-Navas, A.; Nieto, F.; Escutia, C. (2020). New insights into the nature of glauconite. *American Mineralogist*, 105:674–686.

[68] Amorosi, A.; Sammartino, I.; Tateo, F. (2007). Evolution patterns of glaucony maturity: A mineralogical and geochemical approach. *Deep Sea Research Part II: Topical Studies in Oceanography*, 54:1364–1374.

[69] Rudmin, M.; López-Quirós, A.; Banerjee, S.; Ruban, A.; Shaldybin, M.; Bernatonis, P.; Singh, P.; Dauletova, A.; Maximov, P. (2023). Origin of Fe-rich clay minerals in Early Devonian volcanic rocks of the Northern Minusa basin, Eastern Siberia. *Applied Clay Science*, 241:107014.

[70] Rudmin, M.; Banerjee, S.; Makarov, B.; Mazurov, A.; Ruban, A.; Oskina, Y.; Tolkachev, O.; Buyakov, A.; Shaldybin, M. (2019). An investigation of plant growth by the addition of glauconitic fertilizer. *Applied Clay Science*, 180:1–8.

METHODOLOGY OF RISK ASSESSMENT OF FORENSIC TECHNICAL EXPERTISE IN RECOGNIZING THE AUTHENTICITY OF AN ELECTRONIC DIGITAL SIGNATURE

Pavel Menshikov, Alex Tsirdava

•

Peter the Great St. Petersburg Polytechnic University, Russia

Vitta.spb@mail.ru

alex.tsirdava@yandex.ru

Abstract

The article discusses the issues of using an electronic digital signature as enhanced authentication of the signature owner, as well as preserving the integrity of the document content. Particular attention is paid to the issues of differences in the types of electronic signatures (ES). ES has long been part of the usual electronic document flow, it is used in the banking sector, in the field of entrepreneurial and commercial activities, as well as economic, thereby it has become a new way of data theft, which in turn has led to the development of new types of crimes. The article presents various methods of ES research that help to establish the fact of changes in a document by studying its hash functions. As a consequence, the article concludes that it is necessary to develop the expertise of an ES.

Keywords: electronic signature, electronic document management, hash function, cryptographic algorithm

I. Introduction

The legislator equalized the legal force of paper and electronic documents by approving and consolidating these provisions in the Federal Law "On Electronic Signature" [1]. An electronic document that is certified by an EP is absolutely equivalent and equivalent in the legal field to a paper carrier with the signature of a certain person and (or) the seal of the organization. Identification of the authenticity of a signature on paper has long been known and studied in the world of expert research, but the world of electronic documents has not yet been fully studied.

II. Methods

The signature examination is carried out using such a modern method as the study of the hash function, as well as using the method of studying the authenticity of the EP certificate. In order to check the documentation or confirm its compliance with the data, the EP expert first sends a request to the registry of the enterprise that provided this service to the owner of the document.

The hash function method is resorted to only if there are suspicions that corrections were made to the document during forwarding. Hash functions are a mathematical tool, the essence of which is to transform an information block according to an established system that creates strings of bits of various lengths. This process, in fact, is called hashing.

This technology allowed representatives of the criminal world to make transactions on behalf of third parties for the disposal of property without the consent of the owner, including:

- alienate the owner's property;
- to make profit on behalf of other persons in credit institutions;
- to change the owner of the organization illegally.

Specialists from the USA in 1983 submitted patent No. 4405829, which described the mechanism of the formation of the EP. The basis of this patent was a secret key, which consisted of three simple multi-digit binary numbers p , q and d , clothed in the form of three-bit strings, thereby simplifying the system of forming an EP [2].

III. Results

The formation of the public key was based on a pair of multi-bit binary numbers n and E . n was the product of p and q , and e was a separate multi-bit binary number given by the condition that $ed=1 \pmod{(p-1)(q-1)}$. In this form, an electronic document, depending on the value of H , that is, on the value of bit strings in the form of multi-bit binary numbers, forms the value of the secret key of the EP as the formula $Q = s = Hd \pmod{n}$. The next step is to check multi-bit binary numbers. The first verification multi-digit binary number is set by the parameter $A=N$. The second verification number B comes from manipulations with this number, for this they set the condition for which B is equal to a multi-digit binary number s , raised to the power of e modulo n : $B = s^e \pmod{n}$. The last stage of the formation of the EP is the verification of the formed multi-digit binary numbers A and B ; if the parameters of the compared MDCs A and B coincide, they conclude that the EP is authentic."

Thus, thanks to the automation of the process, it is possible in a matter of seconds not only to form an EP, but also to check the coincidence of the public and private keys by calculations based on the formula. There are still many different approaches to the formation of the EP, but the algorithm has not been changed and the principle of its operation is similar.

IV. Discussion

An EP is a complete analogue of an ordinary signature on paper, expressed using a public and private key based on hashing technologies, but it is embodied not in the form of a graphic image, but with the help of information and mathematical transformations over the content of the document. The main document that regulates the operation of the EP in the Russian Federation is GOST 34.10-2001. It is this document that defines all the processes that make up the introduction of EDS into electronic document management, including: key generation, the formation of the signature itself and its verification. Due to the formation and verification of the EP, three tasks are solved at once: preserving the integrity of the content of the electronic document, the authenticity of the information contained in the document, as well as confirming the authorship of the owner of the EP.

The EP provides an opportunity to determine the owner of the rutoken by converting information from the private and public EP key, thereby the EP is the main certifying requisites of the key owner. After the entry of Federal Law No. 63 "On Electronic Signature", the scope of conducting an electronic document of turnover and business activity was significantly simplified, but together with this, the EP became a modern tool for committing a crime.

To ensure the reliability of the EP, a verification key is used, which is a binary code decryptor. "Certifying centers (CC), namely, the authorized body that registers the EP is called, exercises control in this area. The EP is based on the identification of a person using a special key, which is presented in the form of a paper or digital document, this kind of data just warns the UC." [3]

Cryptographic tools are the foundation on which the EP tools are based, they are generated using a unique set of data created using a special random number sensor algorithm. This data set is formed by sequential calculations of the cursor movement or the applicant's movements on the touchpad. These tools can be installed on the computer of the owner of the signature in the form of software (software) or a special flash drive (rutoken).

The current Federal Law "On Electronic Signature" divides the EP into simple and enhanced. To confirm the owner of the signature, a simple EP requests the necessary passwords or access codes. A more complex access system is provided by Federal Law for enhanced EP, the law identifies strict requirements for qualified and unqualified enhanced EP.

So, to use a qualified EP, it is necessary to have a certificate of the verification key.[4] In turn, for an unqualified EP, it is sufficient to use any other authentication keys.[5] An unqualified EP is formed by converting information from the key of the EP, with the help of this type of EP it is possible to determine the person who signed the document, as well as the fact of changing the document.[6] Taking into account the statistics of forensic investigative practice, it can be concluded that access to the EP has become one of the key tools of personal data theft.

At the output, experts receive a hash document, which is an encrypted summary of detailed information about the document under study on which the EP was applied. Then, with the help of a computer program, decryption and subsequent reconciliation of hash function indicators are performed. Any deviation from the original encryption code can tell experts about the violation of the integrity of the documentation.

The EP examination turned the idea of computer-technical research objects upside down, becoming a unique kind, since during the general computerization, the identification of various economic entities also switched to digital format, therefore this area requires considerable attention and research. Nowadays, most organizations have begun to use electronic document management everywhere, which has significantly increased the speed of interaction between organizations, thereby leading to increased cases of criminal attempts in this area, which makes the examination of the EP one of the most relevant studies.

Nowadays, the issue of a new technological exchange of information is becoming more acute, and to protect such information, it is necessary to develop two aspects: methods of computer data research and qualified personnel training.

References

- [1] Ivanov M.A., Rostovtsev A.G., Makhovenko E.B. Introduction to public key cryptography. St. Petersburg, Mir i Semya, 2001.
- [2] Kapustina A.G. "Federal law on electronic signature - what's new?" // Information protection INSIDE – 2011 - No. 3 -pp. 20-22.
- [3] Fanina M.N. "Computer-technical expertise in electronic transactions."// International Journal of Humanities and Natural Sciences. – 2020. - No. 12-2 (51) – pp. 100-102.
- [4] Shestakova E.V. "Digital law." // Right of Access - 2020.
- [5] Shestakova E.V. "Policy and regulation of personal data processing." // Right of Access - 2017.
- [6] Khairusov D.S. /Comparative legal analysis of the use of electronic signatures in the documents of the UIS units under the new law// Actual problems of the activity of the UIS units: collection of materials of the All-Russian Scientific and Practical Conference, Voronezh, 2011.
- [7] Bondarenko Yu.A. "Features of the investigation of fraud committed using an electronic signature." // Humanities, socio-economic and social sciences. – 2020. – No. 3 - pp. 60-63.

NATURAL RESOURCE POTENTIAL OF MOUNTAIN LANDSCAPES OF THE CHECHEN REPUBLIC FOR THE DEVELOPMENT OF REGENERATIVE ANIMAL HUSBANDRY

Zagir Ataev, Rashiya Bekmurzaeva

•

Kadyrov Chechen State University, Russia
raya.bek@mail.ru

Abstract

The article discusses the regional features of the natural components and landscape structure of the Makazhoy basin as a natural resource potential for the potential development of regenerative animal husbandry in the mountainous part of the Chechen Republic.

Keywords: Chechen Republic, mountain landscapes, landscape diversity, climate change, soil cover, sheep breeding, regenerative animal husbandry

I. Introduction

The abandonment of the traditional system of animal husbandry in the mountainous landscapes of the North-Eastern Caucasus, in which sheep graze on the foothill lowlands in winter and are driven to the mountains in summer, has led to significant cultural losses and still poorly studied environmental consequences in the region.

The purpose of the study is to study the spatial and temporal differentiation of natural components and landscapes of the region in order to develop practical recommendations for the economic development of the territory of Mountainous Chechnya for the potential development of regenerative animal husbandry, rational use and protection of natural resources.

The study of the landscapes of the territory of Chechnya began in the 60-80s of the XX century. During this period, A. Fedina [1], A. Alieva [2], V. Bratkov [3], N. Beruchashvili [4] and others made a significant contribution to the study of mountain landscapes of the region. At the beginning of this century, a significant number of publications on the mountain landscapes of the Chechen Republic were published, including the works of V. Bratkov [5], Z. Gagaeva [6], A. Golovlev [7], V. Bratkov et al. [8], R. Idrisova [9], Sh. Zaurbekov, etc. [10, 11], Z. Ataev et al. [12, 13], L. Bekmurzaeva [14], I. Bayrakov [15], A. Gunya et al. [16-18], U. Gayrabekov et al. [19], R. Gakaev [20], I. Bayrakov et al. [21], L. Bekmurzaeva et al. [22, 23] and many others.

II. Methods

The work on studying the natural resource potential of the mountain landscapes of the Chechen Republic for the development of regenerative animal husbandry was carried out at key sites of the experimental landfill of the Kadyrov Chechen State University in the Vedensky administrative district of the Republic (Fig. 1, 2).

The work is based on field studies of natural components and landscape structure of the Makazhoy basin and its surroundings. In the cameral period, comparative geographical and cartographic methods were used, as well as the analysis of data from literary sources.

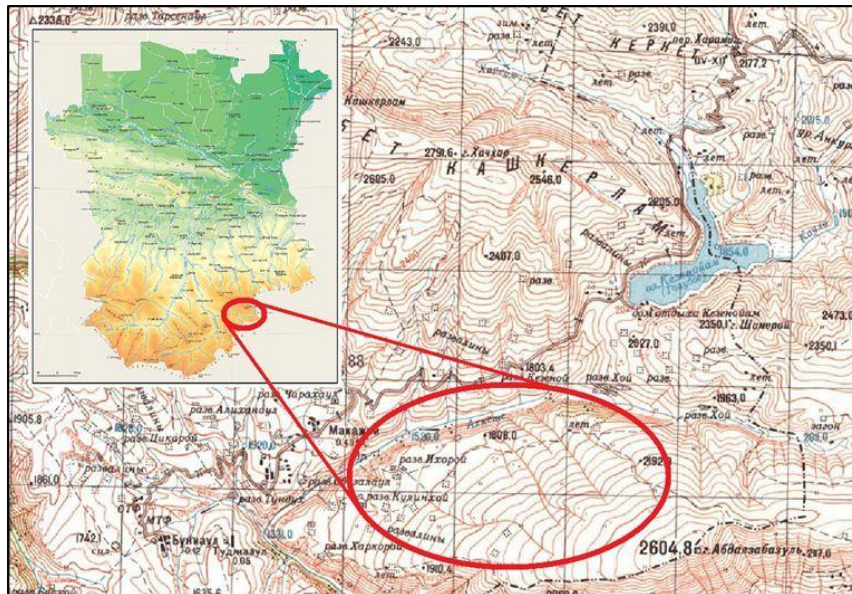


Fig. 1: Geographical location of the experimental test site



Fig. 2: The location of the experimental test site (Google Earth)

III. Results

According to the scheme of physical and geographical zoning of the North-Eastern Caucasus [1], the studied territory is located within the Andi-Salatau district of the Terek-Andi district of the North Caucasian Mountain Province of the Greater Caucasus. The landscapes of mountain-meadow and mountain-forest high-altitude zones prevail in the area.

The main factors of spatial differentiation of landscapes of the considered territory of Mountainous Chechnya are the geological and geomorphological factor and climatic conditions.

Orographically, the polygon is located in the Makazhoy basin (Fig. 3), the wings of which represent the Kashkerlam ridge in the north (the highest point is the Kashkerlam mountain of the same name, with a maximum height of 2806.9 m), in the west – the Baskhoylam ridge (with the

peak of the same name Mount Baskhoylam, 2594.2 m) and the Khindoylem ridge (with the highest point of the same name Mount Khindoylem, 2658.2 m), in the south – the Abdalzubazul ridge (the highest point of the mountain of the same name is 2604.8 m), in the east – the Gagotylyura ridge (the highest point is Mount Azal, 2657.9 m). The highest point of this area is Mount Kashkerlam (2806.9 m), the lowest point is at the place where the Ansalta River breaks out from the basin (the height of the cut is 1331.0 m). The amplitude of the variation in the height of the terrain is 1475.9 m. The area of the basin is 205 km².



Fig. 3: Makazhoy basin. General view from the east. The polygon is on the left side of the photo. Photo by A. Bersaev

The tectonic structure is represented by a syncline fold complicated by local forms, and in fact represents the largest syncline plateau in the Caucasus. The axial part of the fold (plateau, basin) is flat, from which wings gradually rise to the north and south, which become steeper up the slope. The surface is composed of Upper Cretaceous limestones, Paleogene deposits have been preserved in the axial part of the syncline.

Erosive relief forms are represented by valleys flowing from the wings to the axial part, along which gorges are formed, the first hundreds of meters deep. When cutting through the wings, the depths of the gorges increase sharply, up to 1000-1500 m. Landslides are almost everywhere developed in the upper parts of the slopes, anthropogenic landforms (agricultural terraces) are widely developed.

The climatic features of landscapes are influenced by the location of the territory in the very south of the temperate climate zone, the altitude factor and the isolation from the south by the orographic barrier of the Main Caucasian Ridge and Bokovoy Ridge, the dominance of western air mass transfer. The climate of the area is moderately continental. Winter is cool. The temperature of the coldest month (January) is -2.5 – -10 °C. Summer is moderately warm. The temperature of the warmest month (July) is 14-20 °C. The average annual precipitation varies from 500 to 1000 mm, with a maximum in spring and summer. The hydrothermal coefficient is 2-2.2. Accordingly, the terrain affects the spatial redistribution of climatic elements and the differentiation of landscapes.

The product of climate is surface and groundwater. In the Makazhoy basin, despite its insignificant size (205 km²), the territory belongs to the basins of two rivers – Sulak (Andian Koysu) and Terek (Sharo-Argun, Sunzha). The eastern and central part of the basin is drained by the Ansalta River, called the Akhket River here, and its small tributaries. The river originates on the southern slope of Mount Azal, at an altitude of approximately 2300 m. In the Kazenoyam Lake (Alkhar, Blue), the Kharsum and Kauha rivers flow. The extreme western third of the basin is drained by the Keloyakhk River, a right tributary of the Sharo-Argun River. The rivers of the basin

have a mixed nutrition with the participation of snow, rain and groundwater. On the lower slopes of the ridges and in the valleys of the rivers, groundwater comes out in the form of springs with fresh water. Large springs are located in the talweg of the Akhkete River, 1.0 km below the Kazenoyam landslide body, they represent an underground discharge from the lake.

The landscape structure of the basin has a high-altitude and exposure confinement. The mountain-slope tracts of the southern exposure of the Kashkerlam, Kerket and Baskhoynam ranges account for about 40% of the area. Another 40% is occupied by mountain-slope tracts of the northern exposure on the Abdalzubazul and Khindoilam ridges. The lower part (20%) of the synclinal basin is occupied by erosion complexes of valleys and temporary watercourses, as well as anthropogenic residential tracts with adjacent agricultural landscapes (fields in the flat lower part of the basin and terraces up the slopes).

More than 70% of the territory of the basin is occupied by mountain-meadow tracts – grass-mixed, grass-grass post-forest and subalpine settled. Mountain-meadow chernozem-like soils, mountain-meadow subalpine soils in combination with mountain-steppe soils are developed under them. The grass cover is dominated by *Bromus variegatus*, *Festuca rubra*, *F. varia*, *Hordeum violaceum*, *Poa meyeri*, *Carex caucasica*, *Medicago glutinosa*, *Vicia alpestris*, *Scabiosa gigantea*, *Betonica grandiflora*, *Alchemilla oxysepata*, *Trifolium pretense*, *T. repens*, *T. campestre*. There are a lot of *Rumex confertus*, *Veratrum Lobelianum*, *Plantago lanceolata*, *Alchemilla oxysepata* on meadows clogged and etched by cattle (Schiffers, 1953).

Pine and birch forests are confined to the slopes of the north-western exposure of the sides of the basin and the slopes of the northern exposure of the valleys. The rapid development of tree cover is noted, which is clearly seen when comparing satellite images. Mountain-forest brown soils were formed under them. Forests alternate with post-forest settled grasslands and forest meadows of *Agrostis alba*, *Poa pratensis*, *Dactylis glomerata*, *Phlomis pratense*, *Trifolium pretense*, *T. repens*, *T. campestre*, *Potentilla reptans*, *Geranium sanguineum*, etc. Meadow chernozem soils are developed under the mid-mountain meadows, a specific soil cover has been formed on the terraces [24], which has been developing over the past 80 years in a trend of convergence with mountain meadow soils.

On the slopes of the northern exposure (Khindoilam ridge, Abdalzubazul ridge) in the post-forest meadows, there is a significant renewal of pine and pine-birch forests on primitive podzolic and mountain-forest brown soils (Fig. 4 and 5).

In the modern economic development of the Makazhoy basin, the meadow vegetation used for summer pastures and partly for haymaking is of the greatest importance. It should be noted that there is a dense network of abandoned settlements and associated arable land. During the existence of these points, agriculture was widely developed in the basin.

Among the modern examples of critical anthropogenic impact on natural complexes, the following can be noted: active construction and expansion of highways, construction of tourist destinations, fires occur in some areas of the basin, limestone is being developed for construction purposes. Landslides and soil erosion are observed in places where vegetation cover is disturbed. In the future, forests should be preserved and restored in the area, the quality of mountain meadows should be improved by regulated grazing and weed eradication, and erosion control should be carried out.

The Makazhoy basin has a significant potential of land resources for animal husbandry and agriculture. A.N. Gunya and coauthors [25] distinguish 2 zones of economic activity in this area: mid-mountain, where year-round life activity is possible, with permanent residential complexes and agricultural agricultural landscapes (mountain-forest, mountain-steppe and mountain-meadow-steppe landscapes); high-mountain-mid-mountain with seasonal vital activity in the form of pasture cattle breeding (mountain-meadow landscapes).



Fig. 4: *Renewal of pine undergrowth. Photo by Z. Ataev*



Fig. 5: *Increase of woody vegetation within the polygon. The top picture is August 2014.
The bottom picture is August 2021.*

The first zone with possible year-round vital activity occupies a large part of the basin, is represented by a significant spread of agricultural landscapes of terraces (Fig. 6), modern (Makazhoy, Buni, Tunzha-aul) and uninhabited (Khoy, Ikhoro, Sadoy, Khindoy, Kharkoroy, Ariaul, etc.) residential complexes. It should be noted that the maximum height of the spread of agricultural terraces on the slope of the northern exposure (within the polygon) reaches 2000 m, and on the slope of the southern exposure reaches 2300 m.

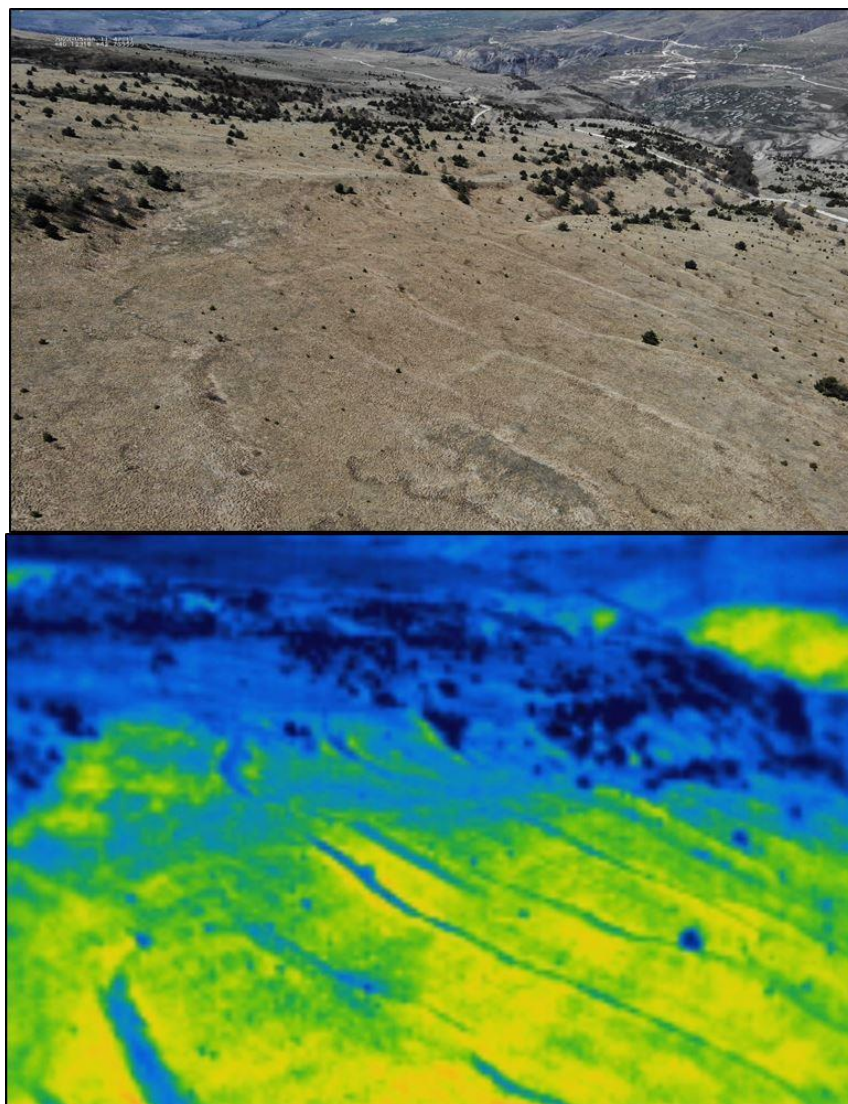


Fig. 5: *Agricultural landscapes of terraced slopes of the Makazhoy basin. Photo and thermal image by I. Idrisov*

The second zone (with seasonal activity) includes the southern slopes of the Kashkerlam ridge (above 2200-2400 m, depending on the exposure of the slopes), with mountain-meadow landscapes.

Terraces have largely transformed landscapes and can be preserved for many centuries after the termination of their use for their original purpose as arable land (Borisov, 2022). Currently, the vast majority of such terraces in different regions of the Caucasus (Stavropol Territory, Kabardino-Balkaria, North Ossetia, Ingushetia, Chechnya, Dagestan) are used as pastures and hayfields. At the same time, the specific features of the terraces, in particular, obstructed runoff and excessive moisture relative to natural slopes, contribute to the progressive overgrowth of woody vegetation. In conditions of reduced grazing, these processes are proceeding at a considerable speed.

The natural and cultural-historical heritage of the Makazhoy basin, the availability of terraced slopes convenient and accessible for agricultural processing, an asphalt highway to the lake. Kazenoyam and the village of Khoy act as an impulse for the sustainable development of the region. This is also facilitated by the entry of the territory into the Argun Historical, Architectural and Natural Museum-Reserve.

IV. Discussion

The analysis of the consequences of modern methods of sheep grazing in the mountainous landscapes of the Chechen Republic showed the heterogeneous use of mountain pasture lands in the late XX – early XXI centuries. The areas most commonly used for sheep farming were distinguished by a large number of pasture potholes, smaller areas of forests and structurally different landscapes than those where pasture digression was not manifested. At the same time, it should be noted that the environmental management of the basin has passed three major stages over the past 100 years: intensive agriculture and animal husbandry until the 1940s; a sharp expansion of animal husbandry and the cessation of agriculture until the 1990s; progressive reduction of animal husbandry until the 2020s.

Similarly, trends towards a decrease in landscape diversity were found in those areas that were not used by sheep during the study period, while the heterogeneity of the landscape persists in those areas where sheep graze.

The conducted research is an original analysis of landscape models and changes due to intensive grazing of sheep using new approaches that combine field studies of key sites, updated satellite time series and modern methods of landscape analysis (GIS technologies). Similarly, our results are a guideline for the future, as they demonstrate the importance of preserving extensive pastures for sheep farming. This is important if we strive to preserve the cultural heritage of the mountain ethnic group, the traditional flavor of the diversity of landscapes and semi-natural meadows in the mountains of the North-Eastern Caucasus.

Acknowledgements. The work was carried out according to the draft state assignment of the Ministry of Science and Higher Education of the Russian Federation FECS-2023-0008 "Assessment of sequestration potential of mountainous and sub-mountainous territories of the Chechen Republic for regenerative animal husbandry using GIS technologies".

References

- [1] Fedina A.E. (1972). Physico-geographical zoning of the eastern part of the northern slope of the Greater Caucasus. Landscape mapping and physico-geographical zoning of mountain regions, Moscow, *Publishing house of the Moscow University*, pp. 5-96
- [2] Alieva A.M. (1975) Mountain landscapes of Chechen-Ingushetia. Materials on the study of the Chechen-Ingush ASSR, Grozny, *Chechen-Ingush book publishing house*, pp. 9-16
- [3] Bratkov V.V. (1992). Landscape-geophysical analysis of natural-territorial complexes of the North-Eastern Caucasus. Autoref. dis. ... candidate of geographical sciences, Tbilisi, 24 p.
- [4] Beruchashvili N.L. (1995). Caucasus: landscapes, models, experiments, Tbilisi, TSU publishing house, 315 p.
- [5] Bratkov V.V. (2002). Spatial and temporal structure of landscapes of the Greater Caucasus. Diss. ... doctor of geographical sciences, Rostov-on-Don, 335 p.
- [6] Gagaeva Z.S. (2004). Landscape structure and small-scale landscape mapping of the territory of the Chechen Republic (based on remote survey). Diss. ... candidate of geographical sciences, Moscow, 210 p.
- [7] Golovlev A.A. (2005). Mountain landscapes of the Chechen Republic and features of their development. Autoref. diss. ... doctor of geographical sciences, Voronezh, 39 p.
- [8] Bratkov V.V., Z. V. Ataev. (2009). High-altitude meadow landscapes of the North-Western and North-Eastern Caucasus. Dagestan state pedagogical university. *Journal. Natural and exact sciences*, no. 2 (7), pp. 93-103
- [9] Idrisova R.A. (2009). Landscapes of the Chechen Republic: spatial structure and features of residential load. Autoref. dis. ... candidate of geographical sciences, Nalchik, 24 p.

- [10] Zaurbekov Sh.Sh., L. R. Bekmurzayeva, V. V. Bratkov. (2016). Assessment of changes in modern agro-climatic conditions of natural landscapes of the Chechen Republic. Dagestan state pedagogical university. *Journal. Natural and exact sciences*, vol. 10, no. 2, pp. 83-92
- [11] Zaurbekov Sh.Sh., V. V. Bratkov, L. R. Bekmurzayeva. (2010). Geoecological assessment of anthropogenic modification of landscapes of the Chechen Republic. Dagestan state pedagogical university. *Journal. Natural and exact sciences*, no. 1 (10), pp. 86-91
- [12] Ataev Z.V., V. V. Bratkov. (2011). Mountain-hollow landscapes of the North-Eastern Caucasus: modern climatic changes and seasonal dynamics, Makhachkala, DSPU, 127 p. ISBN 978-5-9972-0101-2
- [13] Ataev Z.V., Sh. Sh. Zaurbekov, V. V. Bratkov. (2010). Modern residential development of landscapes of the North-Eastern Caucasus. Dagestan state pedagogical university. *Journal. Natural and exact sciences*, no. 1 (10), pp. 71-74
- [14] Bekmurzayeva L.R. (2011). Geoecological assessment of hazardous natural processes in the landscapes of the Chechen Republic using GIS technologies. Dis. ... candidate of geographical sciences, Moscow, 167 p.
- [15] Bayrakov I.A. (2012). Landscape and ecological diagnostics of geosystems of the North-Eastern Caucasus (on the example of the Chechen Republic). Autoref. dis. ... doctor of geographical sciences, Perm, 39 p.
- [16] Gunya A.N., U. T. Gayrabekov. (2013). Physico-geographical differentiation of the Chechen Republic: the most important structural elements and boundaries. *Problems of regional ecology*, no. 6, pp. 66-70
- [17] Gunya A.N., U. T. Gayrabekov, Z. Sh. Gagaeva. (2022). Study of landscape structure for assessment of carbon balance of mountain ecosystems. *Geology and geophysics of the South of Russia*, no.12 (3), pp. 170-181. DOI 10.46698/VNC.2022.48.65.012
- [18] Gunya A.N., U. T. Gayrabekov, Z. Sh. Gagaeva, S.-E. M. Dzhabrailov. (2016). Development of mountain landscapes: an example of the territory of the Argun historical, architectural and natural museum-reserve (Chechen Republic). *Bulletin of the A. A. Kadyrov Chechen State University*, no.4 (24), pp. 67-76
- [19] Gayrabekov U.T., M. T. Gayrabekova. (2014). Structure and features of natural landscapes of the Chechen Republic. *Bulletin of the A. A. Kadyrov Chechen State University*, no. 1, pp. 159-166
- [20] Gakaev R. A. (2015). High-mountain landscapes of the Chechen Republic and patterns of their distribution. *Young scientist*, no.15 (95), part IV, pp. 327-331
- [21] Bayrakov I. A., R. A. Idrisova, Kh. Z. Mantaev. (2016). The current state and ecological functions of mountain and forest landscapes of the Chechen Republic. *Successes of modern science*, no. 7, volume 2, pp. 157-160
- [22] Bekmurzayeva L. R., Sh. Sh. Zaurbekov, V. V. Bratkov. (2020). Variability of agro-climatic conditions of the Chechen Republic in a changing climate. Dagestan state pedagogical university. *Journal. Natural and exact sciences*, vol. 14, no. 3, pp. 81-87. DOI 10.31161/1995-0675-2020-14-3-81-87
- [23] Bekmurzayeva R.Kh., A. S. Gadzhikhanov. (2022). Regional system of accounting and control of greenhouse gases at the carbon landfill of the Kadyrov Chechen State University. *Monitoring. Science and technology*, no. 4 (54), pp. 50-56. DOI 10.25714/MNT.2022.54.007
- [24] Borisov A.V., N. N. Kashirskaya, M. V. Yeltsov, V. N. Pinskyoy, L. N. Plekhanova, I. A. Idrisov. (2021). Soils of ancient agricultural terraces of the Eastern Caucasus. *Soil science*, no.5, pp. 542-557. DOI 10.31857/S0032180X2105004X
- [25] Shiffers E.V. (1953). Vegetation of the North Caucasus and its natural feeding grounds. Moscow-Leningrad, *Publishing House of the USSR Academy of Sciences*, 400 p.

APPLICATION OF UNMANNED AERIAL VEHICLES TO OBTAIN MORPHOMETRIC CHARACTERISTICS OF LANDSLIDES

Ulzhan Aldabergen, Victor Blagoveshchensky, Sandugash Ranova,
Aidana Kamalbekova

•

¹ JSC "Institute of Geography and Water Security", Almaty, Kazakhstan

² Al-Farabi Kazakh National University, Almaty, Kazakhstan

Aldabergen_u@mail.ru

ingeo_2009@mail.ru

Sandu2004@mail.ru

aidana.kamalbekova@gmail.co

Abstract

The article deals with the use of DJI Phantom 4 RTK unmanned aerial vehicle to obtain morphometric characteristics of the landslide that occurred on May 15 in Tekeli town. A 5-year-old child died as a result of the landslide. During the survey, the site was surveyed using a DJI Phantom 4 RTK quadcopter. On the basis of the obtained aerial photographs, the following were built: a 3D digital elevation model, an orthophoto of the terrain, longitudinal and transverse profiles of the landslide area and the adjacent slope using special software Agisoft Metashape Professional.

Keywords: landslide, drones, DJI Phantom 4 RTK, DEM, orthophoto, 3D surface models, Agisoft Metashape

I. Introduction

The modern world cannot do without new technologies, innovations. One of the methods to obtain data quickly and accurately is the use of unmanned aerial vehicles (UAVs). The advantage of UAVs is that they can be easily deployed and directed to hard-to-reach areas. The resulting imagery data has a high spatial resolution, which minimizes errors in identifying or measuring objects.

The territory of the Republic of Kazakhstan is subject to almost all types of natural disasters. Landslide phenomena occurring on the territory of the Republic are mainly related to human activity and moisture saturation of earth rocks due to abundant precipitation.

We used unmanned aerial vehicles (UAVs) to survey landslide-prone areas in Tekeli town and created digital elevation models (DEMs) based on the obtained aerial photographs. Various morphometric parameters were extracted from the DEMs. The study demonstrated how remote sensing using UAV-derived DEMs complements the results of traditional approaches. And also during the survey of landslide-prone areas the intensity of manifestations and prevalence of landslide and subsidence processes were determined, objects exposed to their impact were identified, the nature of damage, the probability of destruction of objects, as well as material and social damage from such impacts were assessed.

II. Methodology

2.1 Study Area

The city of Tekeli with a population of over 30,000 people is located in the western part of the Zhetysu Alatau range at the confluence of the Kora, Chazha and Tekelinka rivers, which form the Karatal River. Most of the city is located at the bottom of the wide valley of the Karatal River below the confluence of the Kora and Chazha Rivers. At the exit of the mountains, at an altitude of 980 meters above sea level, the width of the valley floor is 1500 meters. To the east, the valley narrows and after 5 km, at the confluence of the Kora and Chazha rivers, at an altitude of 1030, the valley floor is 200 m wide. The height of watersheds of the Zhetysu Alatau spurs bounding the valley of the Karatal River is 1700-1900 m for the southern spur and up to 2000 m for the northern spur. Under the northern slope of the southern spur, which is the left side of the Karatal River, there is a foothill step up to 500 m wide, descending to the bed of the Karatal River with a slope of 4 to 15 degrees, cut through by logs descending from the mountain slope. The step is composed of loess-like loams up to 30 m thick and is built up with private one-storey residential houses with homestead plots.

According to the State Institution "Kazselezaschita", the landslide occurred at 12 hours 03 minutes on May 15, 2022. The landslide occurred on the territory of the abandoned house No. 6 on Chekhov Street. The formed breakaway niche (landslide formation zone) occupies almost the entire territory of the site. As a result of the landslide on Chekhova Street, house No. 4 was damaged and the area of house No. 6 was completely destroyed. On Konaeva Street, house No. 350 was completely destroyed, house No. 348 was completely covered with mud mass, and house No. 255 was partially blocked. A 5-year-old child died in house #350.

According to Kazgidromet data at the gauging station "R. Tekeli" for the previous day fell 15.6 mm of liquid precipitation. The total amount of precipitation since the beginning of May this year amounted to 31.8 mm. At the meteorological station "Tekeli" the sum of precipitation on May 15 this year amounted to 18.3 mm, and from May 1 to 15 this year - 31.2 mm. The sum of precipitation for April amounted to 35.8 mm. Daily maximum precipitation of 10% probability (once in 10 years) was 58.5 mm. The average precipitation in April for the multiyear period is 77 mm. Analysis of meteorological data shows that daily precipitation on May 15, 2022 is repeated more often than once in 10 years, and the sum of precipitation for April of the current year was 45% of the norm. Thus, the meteorological situation in Tekeli during the period preceding the landslide is not abnormal.



Fig. 1: General view of the landslide on 15.05.2022 in Tekeli

2.2 Unmanned Aerial Vehicle (UAV).

For the study we used a DJI Phantom 4 RTK drone designed for geographic data collection. The model is equipped with an RTK module and a 20-megapixel camera. The updated RTK module provides positioning data with centimeter accuracy in real time to improve the absolute accuracy of image metadata.



Fig. 2: DJI Phantom 4 pro RTK

Table 1: UAV Specification

Equipment type	Quadcopter
User level	for professionals
Equipment	DJI Phantom 4 RTK drone Drone body Remote control 4 x Pair of propellers 2 x Smart Flight Battery AC power cable Smart Remote Control Battery AC Power Adapter Charging Hub for Smart Battery Charging Hub for Smart Flight Battery Mobile station Tripod for mobile station Manuals and instructions
Product Weight	1.391 kg (Battery & Propellers Included)
Battery capacity	5870 mAh
Battery life	30 min
Maximum speed	50 km/h (P-mode), 58 km/h (A-mode)
Maximum uphill - downhill speed (up to)	6 m/s - 5 m/s
Maximum wind resistance	10 m/s
GPS mode	GNSS: GPS+BeiDou+Galileo Asia)+RTK; GNSS: GPS+GLONASS+Galileo other regions)+RTK
Sensors / Sensors	Dual IMU; Dual GNSS
Maximum distance	Up to 7 km (FCC) and 5 km (CE)
Maximum altitude	6000 M
Obstacle detection	Front/back (binocular optical sensors): 0.7-30 m; Side (infrared): 0.2-7 m; Down (VPS): 0.7-30 m.
Programs	DJI GS RTK (Android); DJI FlightHub (Browser)

Table 2: *Camera Specification*

Number of megapixels	20
Image size:	4864×3648 (4:3), 5472×3648 (3:2)
Sensor	1" CMOS
Lens: Angle of view	84°: 8.8mm / 24mm (35mm equivalent), f/2.8-f11, focus from 1m to ∞
Video modes	H.264, 4K: 3840×2160 (30p)
Supported file formats	FAT32 (≤ 32GB) or exFAT (> 32GB), JPEG, MOV

2.3. Data used

JPEG images with georeferencing and coordinate system were acquired from the UAV. The area of the processed area was 945.1 m², the estimated flight time was 7 minutes and 47 seconds, the number of images received was 113 images. The flight height was 50 meters, speed was 2.0 m/s, vertical and horizontal overlap coefficient was 80%. The images were processed using Agisoft Metashape Professional software. In the first step of the process, the images are loaded and the coordinate system is set, the next step is to align the photos. In the second step Metashape creates a dense point cloud based on the camera positions calculated in the first processing step and the photos used. The next step is to build a digital terrain model based on the dense point cloud. DEM is a surface model in the form of a regular grid of elevation values.

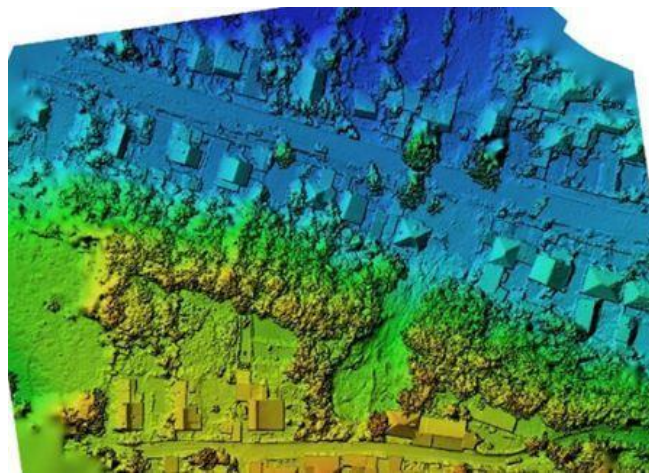


Fig. 3: *Digital elevation model*

At the fourth stage orthophoto plan is created, the initial data is the DEM.



Fig. 4: *Orthophotoplane*

The final step in Agisoft Metashape Professional is to build a 3D terrain model.

III. Results

The landslide occurred on the ledge of a gentle foothill terrace of the north oriented slope of the left side of the Tekeli River valley. The terrace edge is located at 1050 m abs. and the footwall at 1022 m abs. Geographic coordinates of the landslide top: 44° 51' 17.6" N, 76° 47' 31.38" E. The upper part of the profile (landslide formation zone) has a steepness of 20° for 40 m, the lower part (transit zone) - 30 m long, has a steepness of about 30° (Fig. - profile from copter).

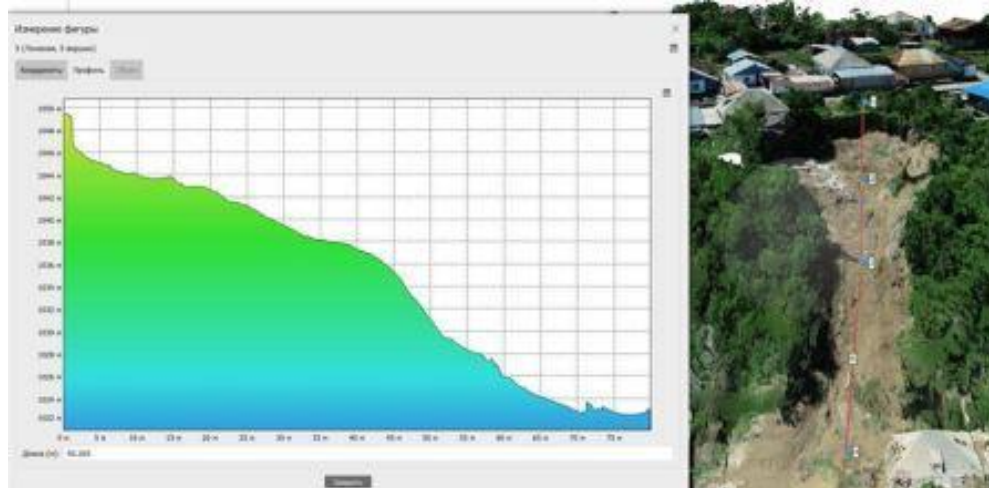


Fig. 5: Longitudinal profile along the landslide path



Fig. 6: Transverse profile of the landslide detachment niche

The slope is composed of dense clay of light brown color, overlaid with developed soil cover (thickness of humus layer 30-50 cm) with dense woody, shrub and herbaceous vegetation. Konaeva Street runs along the foot of the slope along the wide overflow terrace of the Tekeli River, and Chekhov Street runs along the edge of the terrace at the upper part of the slope.

The landslide was formed as a result of localized overwatering of the soil mass at the top of the upland terrace ledge. The landslide breakout niche is located along the lower side of Chekhov Street between houses No. 4 and 8. The line of detachment runs at a distance of 3 m from the road. The breakaway niche has an oval shape. Its length is 40 meters and width is 28 meters. The walls of the trench are almost vertical. The height of the walls at the top of the gap is 4-5 m (Fig.... - photo screenshot from the copter survey). The height of the side walls decreases along the landslide fall line

and is 0.5-1 m in the lower part of the detachment niche. The area of the detachment niche (landslide formation zone) is 770 m², average depth is 4.2 m. According to the survey data, the volume of the ground mass in motion amounted to 3234 m³.

From the rear wall of the landslide breakaway niche, a bare, buried by 1 m water pipe with a diameter of 20 mm, about 3 m long, protrudes for 3 meters. According to the testimony of the State Institution "Kazselezaschita", after the landslide occurred, water flowed from this pipe until water supply to Chekhov Street was stopped by the local municipal water supply company.

The bottom of the trench has a steepness of about 12°. It is covered with debris from the final stage of the landslide, as well as debris from the foundation and terrace of House No. 4. In some places, a "polished" slip plane is exposed at the bottom of the niche, along which the primary displacement of the landslide body took place.

The strongly overmoistened soil mass in the detachment niche, once in motion, quickly turned into a liquid mass and swiftly swept down the steep lower part of the slope in the form of a splash. Therefore, there are no large blocks of rock in the sediment zone, typical for slow-moving landslides. The width of the landslide transit zone is 14 m, length - 30 m, area - 400 m². (Fig.7. - photo from copter).



Fig. 7: *Landslide transit zone*

The flow of liquid mud spread along an almost horizontal surface from the foot of the slope to a distance of 75 m, covering Konaeva Street. The landslide deposition zone is mainly represented by a homogeneous mud mass. It was 50 m wide and covered an area of 2,500 m². The thickness of sediments on the road is 0.5-1 m, on the line of houses it reached 3 and more meters (Fig.8. - copter photo).

At present, there is no threat of recurrence of dangerous landslides, as the main mass of overwatered soil that formed the landslide body has been discharged down the slope profile. However, after heavy rains it is possible that clay sediments at the bottom of the detachment niche and in the area of landslide deposits will be eroded and small mud flows will be formed, which will drift down the road along Konaeva Street. It is also very possible that soil collapses on the walls of the breakaway niche with a volume of several m³ will stop at the hollow bottom of the breakaway niche without reaching the foot of the slope. This process may lead to the growth of the breakaway niche and destruction of house No. 4 on Chekhova Street and the road in front of house No. 9.



Fig. 8: *Landslide deposition zone*

IV. Conclusion

The use of UAVs is a new method of data acquisition, but has proven to be a fast and safe method of obtaining accurate morphometric characteristics.

In this study, the UAV technology provides an orthophoto and digital surface model (DSM) with a spatial resolution of 1 cm.

Acknowledgements. The article was written based on the results of research under the project "Development of a method for forecasting snow avalanches in Ile Alatau using artificial intelligence methods", funded by the Committee of Science of the MNVO RK (grant No. AP09260155).

References

- [1] Koutalakis, P.D., Tzoraki, O.A., Prazioutis, G.I., Gkiatas, G.T., Zaimis, G.N. Can Drones Map Earth Cracks? Landslide Measurements in North Greece Using UAV Photogrammetry for Nature-Based Solutions. *Sustainability* 2021, 13, 4697. <https://doi.org/10.3390/su13094697>
- [2] DJI, Phantom 4 Specs, <https://www.dji.com/id>, Accessed 20 Jun 2019
- [3] Agisoft, Official Afisoft Homepage, <https://www.agisoft.com>, Accessed 15 Jun 2019
- [4] Neverova A.R., Olzoev B.N., Application of ultra-light UAVs in land surveying mapping / scientific article UDC 528.94

RISK ASSESSMENT OF THE NEGATIVE IMPACT ON HUMAN HEALTH OF ELEMENTAL CONTAMINANTS IN BROWN ALGAE (*Laminariaceae*) AND PRODUCTS BASED ON THEM

Viktor Shchukin, Elena Khorolskaya, Nataliya Kuz'mina

Scientific Centre for Expert Evaluation of Medicinal Products,
8/2 Petrovsky Blvd, Moscow 127051, Russia
Schukin@expmed.ru

Abstract

The content of elements Al, As (inorganic form), Cd, Cr, Co, Cu, Fe, Hg, I, Mn, Mo, Ni, Se, Pb, Sr, V, Zn in Laminariae thalli was measured by inductively coupled plasma mass spectrometry. Based on obtained data, the non-carcinogenic risks of the analyzed elements on human health where assessed when they enter the body together with a therapeutic dose of medicinal native products based on Laminariae thalli. It was found that the total hazard index at the 95th percentile concentrations level is 1.44. The maximum contribution to the hazard index is made attributed to iodine ($HQ_{95\%}=1.37$). The daily consumption of food products based on Laminariae thalli at a quantity of 5 g resulted in a hazard coefficient for iodine at various concentration levels is $HQ_{med} = 0.98$; $HQ_{95\%} = 5.86$. The content of iodine in dietary supplements based on Laminariae thalli is close to the permissible limit value, where there is no risk to human health (3500 mg/kg).

Keywords: laminariae thalli, elemental contaminants, hazard coefficient, iodism, risk-based strategy, inductively coupled plasma mass spectrometry

I. Introduction

Currently, in the field of drug quality control, there is a tendency to move from the principle of harmlessness to the acceptance a negligible risk of negative effects caused by impurities entering the body along with the daily therapeutic dose of the drug. [1,2]. Within the framework of a risk-based strategy for controlling the content of elemental contaminants in drugs the actual concentration of an element is compared with its permitted daily concentration which depends on the therapeutic dose of the consumed drug and the route of its entry into the body. Therefore, this allowable intake is individualized for each drug.

At present, the risk-based strategy for controlling the content of elemental contaminants is not applied to herbal medicinal products (HMPs). It is generally accepted that the contamination of HMPs decreases significantly during the processing of herbal raw materials (HRMs), therefore elemental contaminants in HMPs are not likely to cause substantial harm to human health. However, there is a separate category of HMPs whose level of contamination is equivalent to that of the original HRMs – these are native products based in HRM. Within the conceptual framework of the Eurasian Economic Union (EAEU), this term denotes preparations based on HRMs that do not contain excipients. Native products based on HRMs are used in medicine as pharmaceutical substances for production of other HMPs and directly as independent medicinal products. The latter are of particular interest, as all contaminants contained in them are completely transferred to the human body. The comparability of the contamination levels in native products based on

HRMs and origin HRMs underscores the relevance of implementing a risk-based quality control strategy for this category of HMPs.

Among the native products based on HRMs which are used as standalone HMPs, *Laminariae thalli* occupy a special place. They have laxative [3], antidiabetic [4], hepatoprotective [5], antioxidant [6], anti-inflammatory [7], bactericidal [8] and anticancer [9] effects, and are also used for the prevention and treatment of iodine deficiency diseases [10, 11]. Since *Laminariae thalli* are the main natural source of iodine for humans [12] and contain a large amount of beneficial bioactive substances [13], they are also used as a food product and a dietary supplement.

When assessing the risks of negative impact of elemental contaminants that enter the human body along with therapeutic dose of a medical preparation, the influence of heavy metals and arsenic is typically taken into account. In the case of *Laminariae thalli*, it is advisable to additionally include aluminum and iodine in the list of analyzed elements. Aluminum has toxic properties similar to those of heavy metals [14]. Excess iodine is also harmful to the human body, just like its deficiency [15]. The aim of this study is to evaluate the risk of negative impact on humans from heavy metals, arsenic, aluminum and iodine that enter the body along with medicinal native products, dietary supplements, and food product based on *Laminariae thalli*.

II. Methods

As objects of study, we used samples of self-collection thalli of pharmacopoeial species of *Laminaria japonica* (Aresch.), collected in the waters of Peter the Great Bay in the Pacific Ocean, and *Laminaria saccharina* (L.), collected in the waters of Solovetsky Island in the White Sea; samples of the phytopreparations and dietary supplements based on «*Laminariae thalli* (seaweed)» were purchased from pharmacies and supermarkets in Moscow. The self-collected samples were obtained in August 2020, dried in the sun for two days, and the species identification of the samples was confirmed through the use of macro- and microscopic analysis. Additionally, literature data on the content of elemental contaminants in the thalli of pharmacopoeial *Laminariae* species from different collection sites were also used [16].

The risks of exposure to the elements Al, As (inorganic form), Cd, Cr, Co, Cu, Fe, Hg, I, Mn, Mo, Ni, Se, Pb, Sr, V, Zn were assessed. The selective determination of inorganic forms of arsenic (iAs) in *Laminariae thalli* was conducted our own developed methodology based on solid phase extraction and inductively coupled plasma mass spectrometry (ICP-MS) [17]. Elemental analysis was performed an Agilent 7900 mass spectrometer with inductively coupled plasma. The quantitative determination of heavy metals and aluminum content was carried out according to our own developed and validated method [18], iodine - according to the method [19]. Intensity values were recorded for atomic mass units (AMU) as follows: Al - 27 AMU, V - 51 AMU, Cr - 52 AMU, Mn - 55 AMU, Fe - 56 AMU, Co - 59 AMU, Ni - 60 AMU, Cu - 63 AMU, Zn - 66 AMU, As - 75 AMU, Sr - 88 AMU, Mo - 95 AMU, Cd - 111 AMU, Hg - 202 AMU, Pb - 208 AMU, Se - 78 AMU, I - 127 AMU. To calculate the concentrations of the analyzed elements in the tested samples of *Laminariae thalli*, the calibration curve method was used. Three parallel test solutions were prepared for each sample. The final concentration values were determined as the arithmetic mean of the measured values.

III. Results

The main indicator of expected population morbidity growth due to the toxic properties of foreign chemicals in the studies objects of the environment is the non-carcinogenic risk. When assessing non-carcinogenic risk, it is assumed that there is a threshold below which harmful effects do not occur. The quantitative characteristic of non-carcinogenic risk is the hazard coefficient (HQ), which represents the ratio of the average daily intake of an elemental impurity (ADD) to its safe (reference) level of exposure (RiD) [1]:

$$HQ = \frac{ADD}{RfD} \quad (1)$$

The ADD value was estimated using formula 2, which was proposed for environmental contaminants [20]:

$$ADD = \frac{C \cdot IR \cdot EF \cdot ED}{BW \cdot AT} \quad (2)$$

where C - the concentration of the investigated elemental impurity in Laminariae thalli, mg/kg;
IR - the consumption rate of Laminariae thalli, kg/day;
EF – the exposure frequency, days/year;
ED – the exposure duration, years;
BW – the average body weight of a human (70 kg);
AT – the averaging time of exposure, days.

In the calculating, the values of HQ for the analyzed elements in the Laminariae thalli and native products, the values of IR, EF were determined based on the maximum therapeutic dose of the phytopreparation and the course of its intake, and ED and AT were determined from the average life expectancy (70 years) and the age of starting the treatment. (from 12 years old): IR=0.003 kg; EF=30 days, ED=58 years, AT=365•ED. Two concentration levels (median and 95th percentile) of the elemental contaminant in the sample (C_{med} and C_{95%}) were used. The primary data used to determine the values of C_{med} and C_{95%} are presented in our publication [16, 21]. The reference values (RfD) for analyzed elements are provided in the integrated risk information system EPA [22]. The calculated values of ADD and HQ for heavy metals, arsenic, aluminum, iodine during the maximum course of treatment with the maximum therapeutic dose of native products based on Laminariae thalli are presented in Table. 1.

Table 1: Hazard coefficients of elemental contaminants in native products based on Laminariae thalli

Element	Sample size	RfD mg/kg•day	C _{med} (C _{95%}) mg/kg	ADD _{med} •10 ⁻³ (ADD _{95%} •10 ⁻³), mg/kg•day	HQ _{med} (HQ _{95%})
Al	14	1,0	25,47 (334,3)	0,090 (1,177)	0,0001 (0,001)
iAs	14	0,0003	0,297 (2,308)	0,001 (0,008)	0,003 (0,027)
Cd	30	0,001 ¹	0,595 (2,654)	0,002 (0,009)	0,002 (0,009)
Cr	18	1,5 ²	0,600 (1,744)	0,002 (0,006)	0,001•10 ⁻³ (0,004•10 ⁻³)
Co	16	0,0003	0,085 (0,405)	0,0003 (0,001)	0,001 (0,005)
Cu	31	0,04	1,392 (3,735)	0,005 (0,013)	0,0001 (0,0003)
Fe	33	0,70	116,0 (537,5)	0,409 (1,893)	0,003 (0,014)
Hg	19	0,0003 ³	0,023 (0,229)	0,0001 (0,001)	0,0003 (0,003)
I	17	0,01	1473 (3880)	5,191 (13,67)	0,519 (1,367)
Mn	30	0,14 ¹	5,984 (20,41)	0,021 (0,072)	0,0002 (0,001)
Mo	7	0,005	0,948 (2,027)	0,003 (0,007)	0,0007 (0,001)
Ni	20	0,02 ³	0,470 (2,400)	0,002 (0,008)	0,0001 (0,0004)
Pb	31	0,0035	0,340 (4,550)	0,001 (0,016)	0,0003 (0,005)
Se	14	0,005	0,140 (3,120)	0,0005 (0,011)	0,0001 (0,002)
Sr	9	0,60	349,8 (867,7)	1,232 (3,056)	0,002 (0,005)
V	13	0,005	0,900 (2,177)	0,003 (0,008)	0,001 (0,002)
Zn	36	0,30	15,63 (42,88)	0,055 (0,151)	0,0002 (0,001)

¹RfD value is for dietary supplements;

²RfD value is given for Cr (3+);

³RfD value is given for salts Hg, Ni

From the data in Table. 2 it can be observed that the values of the iodine HQ exceed the HQ values of elements Al, iAs, Cd, Cr, Co, Cu, Fe, Hg, Mn, Mo, Ni, Se, Pb, Sr, V and Zn by a thousand

or more times. Therefore, for food products and dietary supplements based on Laminariae thalli, we focused only on assessing the non-carcinogenic risk from the negative effects of iodine. The concentrations of iodine in the analyzed samples of food and dietary supplements based on Laminariae thalli are presented in Table. 2.

Table 2: *The content of iodine in food products and dietary supplements based on Laminariae thalli*

№	Sample	Concentration I, mg/kg	№	Sample	Concentration I, mg/kg
1	Seaweed (Laminaria japonica) natural shredded dried produced by RPG «Binom» LLC, Russia	1024	7	Laminaria seaweed, «Krevetka» LLC, Russia	126
2	"Belomorskaya zhemchuzhina (seaweed), Trade House " Sila prirody " LLC, Russia	350	8	Dried Laminaria, «SANATA» LLC, Russia	515
3	Laminaria, sun-dried seaweed, «Pozdnij zavtrak lajf» LLC, Russia	3563	9	Ground kelp for cocktails (powder), Las-Flores group LLC, Russia	300
4	Seaweed dried Laminaria, Individual Entrepreneur Boko O.V., Russia	2217	10	Dietary supplement Laminaria thalli ("Laminaria (seaweed)", «Evalar» CJSC, Russia	3101
5	Algae White Sea food Laminaria, shredded, «Arhangel'skij vodoroslevyj kombinat» LLC, Russia	379	11	Dietary supplement Laminaria SUPERFOOD «Kron» LLC, Russia	3399
6	Dried seaweed Sakhalin VkusVill, «Mir Vodoroslej» LLC, Russia	287	-	-	-

When calculating the HQ value for iodine entering the human body through the consumption of food products based on Laminariae thalli (samples 1-9 from Table 2, $C_{med} = 379$ mg/kg, $C_{95\%} = 3024$ mg/kg), the IR value was determined on the basis of literature data on the average daily consumption of brown algae by Europeans (5 g/day [23,24]). The option considered was the daily intake of Laminariae thalli throughout one's lifetime, starting from the age of 12 (the age at which the consumption of native products based on Laminariae thalli begins). Under these conditions, the values obtained were $ADD_{med} = 0.027$; $ADD_{95\%} = 0.216$; $HQ_{med} = 2.71$; $HQ_{95\%} = 21.60$.

When calculating the HQ for iodine entering the human body through the consumption of dietary supplements based on Laminariae thalli, the guidelines provided by the manufacturers were followed. The recommended age for starting the intake of the dietary supplements is 18 years, with tablets of 200mg to be taken once daily ($IR = 0.0002$, $EF = 360$ days, $ED = 52$ years, $AT = 365 \cdot ED$). Considering the declared concentration of iodine in the dietary supplements based on Laminariae thalli (0,1% per tablet), the calculated value are $ADD = 0.003$ mg/(kg•day) and $HQ = 0.28$.

IV. Discussion

The conclusion regarding the significance of the risk of the total negative effects of elemental contaminants on the human body is made based on the hazard index (HI). HI represents the sum of the HQ values of the analyzed elements at the median and 95th percentile levels (HI_{med} and HI_{95}). It is generally accepted that when the value of HI_{med} exceed 1, it indicates an unacceptable impact of elemental contaminants on human health requiring appropriate safety measures to be taken. The combination of $HI_{med}<1$ and $HI_{95}<1$ indicates no risk to human health from the contaminants. In situations where $HI_{med}<1$, but $HI_{95}>1$, it is necessary to strengthen the control over the contaminants with the highest contribution to exposure.

For native products based on *Laminariae thalli* $HI_{med} = 0.53$ and $HI_{95} = 1.44$. Therefore, it is necessary to strengthen the control over the iodine content in this group of HMPs, as it contributes the most to the total hazard index (HI). As a safety measure for consuming such herbal medicinal products, it is recommended to introduce an upper limit for iodine content. Currently, the State Pharmacopoeia of the Russian Federation only regulates the lower limit of iodine content (not less than 0,1%) [25]. It should be noted that the European Pharmacopoeia, unlike the Domestic Pharmacopoeia, the range of iodine content in *Fucus* algae is regulated (0,03 – 0,2%) [26]. The content of iodine in *Fucus* algae is significantly lower than in *Laminariae* algae. However, the regulated range of iodine content in *Laminariae thalli* recommended by the FDA (0,1-0,5% [27]) aligns well with the actual content of this element in pharmacopoeial species of *Laminariae thalli* (*Laminaria saccharina* (L.) and *Laminaria japonica* (Aresch.). It is recommended to include this range of iodine content in the State Pharmacopoeia of the Russian Federation.

The content of iodine in food products based on *Laminariae thalli* comparable is to that in the raw material. However, increasing the dosage and frequency of intake of the food products compared to the medicinal preparation is the reason why the HQ_{med} (2,71) and HQ_{95} (21,6) significantly exceed 1. Therefore, daily consumption throughout life, starting from the age of 12, in the amount of 5g, leads to a serious risk of iodism. The safe daily intake of *Laminariae thalli* is 2g ($HQ_{med}=1.083$).

Our experimental data on the content of iodine in dietary supplements based on *Laminariae thalli* (3101 and 3399 mg/kg, samples 10, 11 of Table 2) indicate that the actual concentration of this element significantly exceed the value stated by the manufacturers on the packaging (0.1 % or 1000 mg/kg). The content of iodine in these dietary supplements is comparable to its content in raw materials and medicinal native products. As a result, long-term intake of dietary supplements based on *Laminariae thalli* may pose a risk of iodine poisoning. With the maximum intake course specified by the dietary supplements manufacturers ($IR= 0.0002$, $EF=360$ days, $ED=52$ years, $AT=365 \cdot ED$), the $HQ=1$ at an iodine concentration of 200 mg per tablet should not exceed 3500 mg/kg. As can be seen from the data in Table. 2, the actual iodine content in the analyzed dietary supplements is close to the maximum allowable value, at which there is no risk to human health.

Thus, the risk assessment of the negative impact on human health of elemental contaminants ingested through the consumption of products based on *Laminariae thalli* has shown that iodine makes the maximum contribution to exposure. It is concluded that there is a need to strengthen control over the iodine content in medicinal native products, dietary supplements and food products based on *Laminariae thalli*.

References

- [1] Q3D(R2) Guideline for Elemental Impurities. International council for harmonisation of technical requirements for pharmaceuticals for human use, 2022.
- [2] Monograph 2.3.10.0. Impurities of elements. Pharmacopoeia of the Eurasian Economic Union. M.: Publishing House of the Eurasian Economic Commission. 2023. 1(2):167-172.

- [3] Bokov, D. O., Potanina, O. G., Nikulin, A. V., Shchukin, V. M., Orlova, V. A., Bagirova, G. B., ... & Bessonov, V. V. (2020). Modern approaches to the analysis of kelp (*Laminaria* sp.) as pharmacopoeial herbal drugs and food products. *Pharmacognosy Journal*, 12(4): 929-937.
- [4] Kang, S, Kim, E, Kang, I, Lee, M, Lee, Y.(2018). Anti-diabetic effects and anti-inflammatory effects of *Laminaria japonica* and *Hizikia fusiforme* in skeletal muscle: in vitro and in vivo model. *Nutrients*, 10(4):491.
- [5] Zhao, X, Xue, C.H., Li, Z.J., Cai, Y.P., Liu, H.Y., Qi, H.T. (2004). Antioxidant and hepatoprotective activities of low molecular weight sulfated polysaccharide from *Laminaria japonica*. *Journal of Applied Phycology*, 16(2):111-5.
- [6] Hengjie, T, Das, S.K., Zainee, N.F., Yana, R, Rozaimi, M. (2023). Ocean Acidification and Aquacultured Seaweeds: Progress and Knowledge Gaps. *Journal of Marine Science and Engineering*, 11(1):78.
- [7] Kang, S., Kim, E., Chen, Y., Huang, W., Chen, Y., Wu, M., Jia, R., You, L. (2022). Influence of molecular weight of polysaccharides from *Laminaria japonica* to LJP-based hydrogels: Anti-inflammatory activity in the wound healing process. *Molecules*, 27(20):6915.
- [8] Liu, M., Liu, Y., Cao, M.J., Liu, G.M., Chen, Q., Sun, L., et al. (2017). Antibacterial activity and mechanisms of depolymerized fucoidans isolated from *Laminaria japonica*. *Carbohydrate polymers*, 172:294–305.
- [9] George, J., Thabitha, A., Vignesh, N., Manigandan, V., Saravanan, R., Daradkeh, G., & Qoronfleh, M. W. (2021). Antiskin cancer and antioxidant activities of formulated agar from Brown seaweed *Laminaria digitata* (hudson) in dimethyl benzanthracene-induced Swiss albino mice. *International Journal of Polymer Science*, 2021:1-12.
- [10] Shokina, Y., Kuchina, Y., Savkina, K., Novozhilova, E., Tatcienko, K., Shokin, G. (2022). The Use of BrownAlgae *Laminaria Saccharinain* Iodine Enriched Products Aimed at Preventing Iodine Deficiency. *KnE Life Sciences*, 135–45.
- [11] Blikra, M. J., Henjum, S., & Aakre, I. (2022). Iodine from brown algae in human nutrition, with an emphasis on bioaccessibility, bioavailability, chemistry, and effects of processing: A systematic review. *Comprehensive reviews in food science and food safety*, 21(2): 1517-1536.
- [12] Tagliapietra, B. L., & Clerici, M. T. P. S. (2023). Brown algae and their multiple applications as functional ingredient in food production. *Food Research International*, 112655.
- [13] Remya, R. R., Samrot, A. V., Kumar, S. S., Mohanavel, V., Karthick, A., Chinnaiyan, V. K., ... & Muhibullah, M. (2022). Bioactive potential of brown algae. *Adsorption Science & Technology*, 2022, 1-13.
- [14] Mintel', M.V., Zemlyanova, M.A., Zhdanova-Zaplesvichko, I.G. (2018). Some aspects of the combined action of aluminum and fluorine on the human body (literature review). *Ehkologiya cheloveka= Human ecology*, (9):12-7 (In Russ.).
- [15] Fan, L., Meng, F., Gao, Y., & Liu, P. (2021). Insufficient iodine nutrition may affect the thyroid cancer incidence in China. *British Journal of Nutrition*, 126(12): 1852-1860.
- [16] Shchukin, V.M., Khorolskaya, E.A., Kuz'mina, N.E., Remezova, I.P., Kosenko V.V. (2023). Features of the elemental composition of *Laminaria* thalli of various origins. *Bulletin of the Scientific Centre for Expert Evaluation of Medicinal Products. Regulatory Research and Medicine Evaluation*, 13(2):154–172 (In Russ.)
- [17] Shchukin, V.M., Erina, A.A., Shvetsova, Yu.N., Zhigilei, E.S., Kuz'mina, N.E. (2023). Selective quantification of organic and inorganic arsenic in kelp thalli and kelp-based products. *Bulletin of the Scientific Centre for Expert Evaluation of Medicinal Products. Regulatory Research and Medicine Evaluation*, 13(2):206–215.
- [18]. Shchukin, V. M,* Zhigilei, E. S., Erina ,A. A., Shvetsova, Yu. N., Kuz'mina, N. E. and Luttseva, A. I. (2020). Validation of an ISP-MS method for the determination of mercury, lead, cadmium, and arsenic in medicinal plants and related drug preparations. *Pharmaceutical Chemistry Journal*, 54(9):968-976.
- [19] CSN EN 15111:2007 Foodstuffs. Determination of trace elements. Determination of iodine by ICP-MS (inductively coupled plasma mass spectrometry).

[20] United States. Environmental Protection Agency. Office of Emergency, Remedial Response. Risk Assessment Guidance for Superfund: pt. A. Human health evaluation manual. Office of Emergency and Remedial Response, US Environmental Protection Agency, 1989.

[21] Shchukin, V.M., Khorolskaya, E.A., Kuz'mina, N.E., Remezova, I.P. (2023). Carcinogenic and non-carcinogenic health risks assessment of elemental contaminants in Laminariae thalli. *Bulletin of the Scientific Centre for Expert Evaluation of Medicinal Products. Regulatory Research and Medicine Evaluation*, (13).

[22] Regional Screening Level (RSL) Summary Table. United States Environmental Protection Agency (USEPA); 2022.

[23] National Food Institute, Technical University of Denmark, Denmark et al. Analysis and risk assessment of seaweed. *EFSA Journal*, 2019.

[24] Mendes, M. C., Navalho, S., Ferreira, A., Paulino, C., Figueiredo, D., Silva, D., ... & Speranza, L. G. (2022). Algae as food in Europe: An overview of species diversity and their application. *Foods*, 11(13):1871.

[25] Monograph 2.5.0080.18. Laminariae thalli (seaweed). State Pharmacopoeia of the Russian Federation. XIV ed. 2018.

[26] Monograph 01/2008:1426 Kelp, in: European Pharmacopoeia, 11th ed., European Department for the Quality of Medicines & Health Care, Strasbourg. 2022.

[27] Food chemicals codex -9 ed. Baltimore: United Book Press Inc., 2014, 1785p.

ON THE INFLUENCE OF SEISMIC INTENSITY IN A ROCK MASS IN THE DESIGN OF TRANSPORT TUNNELS

Mikhail Lebedev¹, Yuriy Isaev¹, Kirill Dorokhin¹, Alexey Malovichko²,
Ruslan Dyagilev², Mikhail Pyatunin¹

¹JSC "Scientific Research, Design and Survey Institute "Lenmetrogioprotrans", Russia

²Geophysical Survey of the RAS, Russia

lebedev-lmgt@yandex.ru

isaev45@mail.ru

d.k_a@mail.ru

amal@gsras.ru

dra@gsras.ru

mishkas30@yandex.ru

Abstract

The results of experiments on simultaneous recording of seismic signals from various sources on the Earth surface and at a depth of up to 250 m are stated. The peculiarities of change with depth of the spectral composition of teleseismic earthquake and microseismic oscillations have been studied, which testify in favour of a significant decrease in the level of seismic effects on underground structures in a wide range of frequencies in relation to buildings and structures on the daylight surface.

Keywords: seismic intensity, earthquakes, underground structures, Earth surface

I. Introduction

In seismically hazardous areas, when designing transport tunnels, the materials consumption of supports and linings is greatly influenced by the level of seismic hazard. In many cases, accounting for the design seismicity requires a strong reinforcement of linings, which leads to a significant increase in the cost of construction.

At the same time, the consequences of earthquakes in the world show that underground structures do not suffer from destructive effects unlike buildings and structures on the Earth surface. Thus, in the 1985 Mexico City earthquake, more than 1,500 buildings and structures were damaged. The subway stopped working only on the day of the earthquake. As of the next day, the subway was operating, only 32 stations out of 101 stations were closed not because of damage to the subway itself, but because of emergency rescue work on the surface and debris removal.

Earthquakes in Japan show the appearance of flaws in parts of tunnels where the lining is unreinforced, while buildings and structures on the earth surface experience significant damage. The results of field studies of the impact of earthquakes on underground structures [1-7] in Japan, China, Taiwan and other countries indicate that the seismic intensity in the tunnel is less than on the Earth surface.

Studies of the consequences of earthquakes on the Circum-Baikal railway [8] have shown that earthquakes that occurred in the Baikal rift zone affected the integrity of frame-type galleries, tunnel-type galleries and near-portal sections of tunnels up to 10 meters deep. No violations were recorded in other sections of the tunnels.

The currently practiced methods of seismic microzoning (SMZ) already have theoretical prerequisites and methodological guidelines that make it possible to assess how much the level of seismic impacts will decrease in points if they are calculated not on the surface, but at some buried point. In particular, the seismic impedance method is based on the concept of the difference between the seismic properties (transverse wave velocity and rock density) of soils at the surface and some reference (benchmark) soils, which are usually classified as Category I in terms of seismic properties. In practice, soils that are close in their properties to the reference ones (rigidity $R=2000 \text{ t/(m}^2\cdot\text{s)}$ according to SP 283.1325800.2016) are usually found at a certain depth, which gives grounds to consider the seismic intensity for them on average 1 point lower than for soils of category II, most often found on the surface.

Other SMZ methods (method of earthquake recording or microseism) also theoretically allow obtaining grade increments for soils at depth, but in reality all field observations are always carried out on the soils accessible on the earth surface and the SMZ results are brought also to the earth surface.

It is important to note that all SMZ methods focused on obtaining intensity increments in points provide only a limited opportunity to see how the spectral composition of impacts can change. According to RSN 65-87, there are three intervals of periods (0.1-0.3 s, 0.3-0.5 s and 0.5-2 s) for which it is necessary to determine the score. However, this approach allows only indirectly taking into account the influence of different-frequency oscillations on seismic intensity, because the determination of the frequency characteristics of soils still occurs from the surface.

The present paper is aimed at obtaining the initial data, allowing getting a real and only true idea of the change of seismic vibrations with depth when they affect soils at different depths. For this purpose, synchronous measurements of seismic vibrations on real objects (adits, boreholes, tunnels) were specially organized. Waves from teleseismic earthquakes and microseismic oscillations were used as signals. It is expected that microseisms, when compared to results based on earthquake recordings, will provide similar results in a shorter time frame because they are recorded at any time.

II. Research at the test sites

A significant part of the data on earthquakes was obtained at the test site of the Geophysical Service of the Russian Academy of Sciences in Obninsk, where, in addition to the surface instrument, one was located in an adit at a depth of 30 m, directly below point on the earth surface. Broad-band seismometers TC-120 (Nanometrics) with a natural period of 120 s were used in the experiment. Recordings were made over 4 months (from April to July 2023) with 100 Hz digitisation (frequency range 0.008 to 40 Hz). Similar data were also obtained earlier in the period from 2012 to 2022 on numerous tunnels in the area of Sochi, where there was a difference in height between the measuring points from 50 to 250 m.

Observations in adits and wells are more representative, since they are long-term and, moreover, allow analyzing data along with information about the deep structure. These objects are well studied and there are both lithological columns and a known velocity profile for them.

In total, several hundred teleseismic earthquakes were recorded at the Obninsk test site during the entire observation period. For processing, 14 records from earthquakes with a magnitude of $m_b \geq 6$ were selected (Table 1).

There is a sedimentary layer of rocks with a thickness of 30 m between the two instruments on the test site. Information about the seismogeological model for the near-surface rock mass to a depth of 40 m is given in Table 2 and in Fig. 1.

An example of one of the records of a strong earthquake near the East coast of Kamchatka on April 18, 2023 ($M=6.4$, epicentre distance 6824 km) (Fig.2) demonstrates how strongly the oscillations recorded in one set at different levels from the earth surface differ. Since the analysis involved predominantly strong and only teleseismic earthquakes, they quite representatively

cover the frequency range from 0.5 to 10 Hz used in estimating seismic intensity increments. The equipment used in this frequency range does not introduce distortion.

Table 1: *Catalog of registered earthquakes*

Item	Time [UTC]	Width, degrees	Longitude, degrees	Depth, km	mb	Region
1	04/14/2023 09:55 AM	-6	112.05	600	6.5	Java Sea
2	04/15/2023 15:01 PM	-33.84	56.17	10	5.8	Southwest Indian Ridge
3	04/18/2023 02:40 AM	54.15	159.79	120	5.9	Eastern coast of Kamchatka
4	04/18/2023 04:31 AM	-22.33	179.41	580	6	South of the Fiji Islands
5	04/21/2023 10:21 AM	2.75	127.12	33	6.2	North of the Molucca Sea
6	04/22/2023 08:23 AM	-5.32	125.51	33	6.0	Banda Sea
7	04/24/2023 00:41 AM	-30.06	-177.84	50	6.9	Kermadec Islands, New Zealand
8	04/24/2023 20:00 PM	-0.59	98.68	10	6.5	South Sumatra, Indonesia
9	04/28/2023 03:13 AM	-25.35	178.69	600	6.4	South of the Fiji Islands
10	05/10/2023 16:02 PM	-15.45	-174.59	210	6.6	Tonga Islands
11	05/18/2023 18:58 PM	34.95	24.29	15	5.6	Crete, Greece
12	05/19/2023 02:57 AM	-23.25	170.75	33	7.1	Southeast of the Loyalty Islands
13	05/19/2023 15:15 PM	12.74	49.09	10	5.8	East of the Gulf of Aden
14	05/20/2023 01:51 AM	-23	170.52	33	6.9	Southeast of the Loyalty Islands

Table 2: *Parameters of the seismic-geological model for the Obninsk test site*

Layer no.	Soil characteristics	Vp, m/s	Vs, m/s	Density, g/cm ³	Layer thickness, m
1	Top soil	305	178	1.75	2.3
2	Sand, loam	458	255	1.81	8.3
3	Hard-plastic loam, sand	475	284	1.83	4.8
4	Sand, loam	679	395	1.86	13.5
5	Limestone	1949	1129	2.52	∞

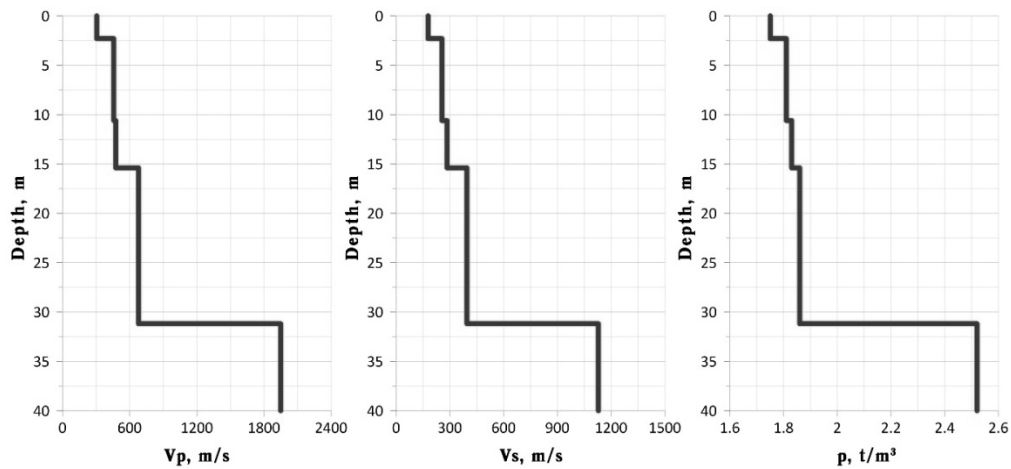


Fig. 1: Velocity and density profile in the area of the adit in Obninsk to a depth of 40 m

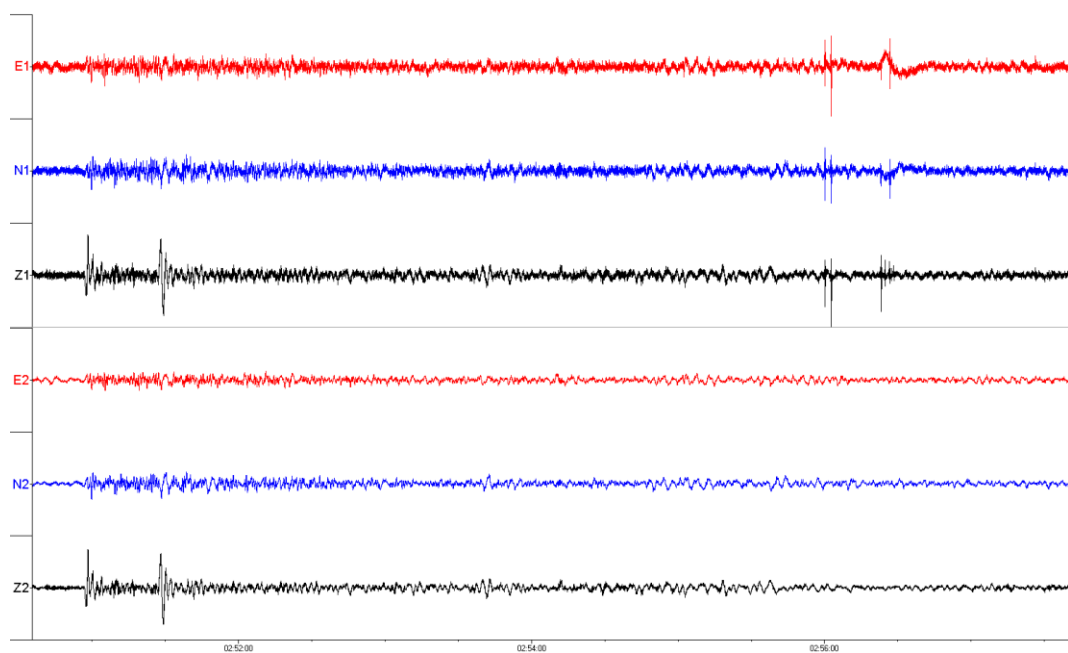


Fig. 2: An example of teleseismic earthquake records obtained on the earth surface (three upper channels) and at a depth of 30 m (three lower channels)

Fig.3 shows the results of calculations of the amplitude spectra for the displacement velocities of the horizontal E components recorded on the earth surface and in the adit. It can be seen that the level of seismic vibrations in the adit for the entire frequency range from 0.5 to 10 Hz is significantly lower. At the same time, with increasing frequency, the degree of difference between the levels of seismic vibrations increases.

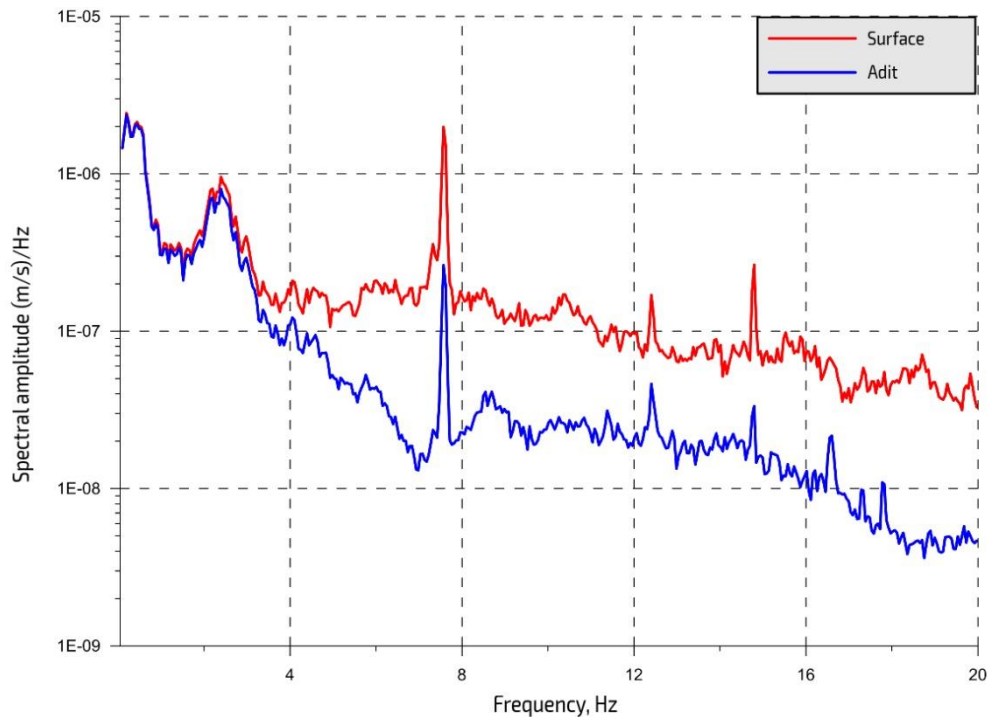


Fig. 3: Comparison of the amplitude spectra of the records of the horizontal E component of the earthquake in Fig. 2, obtained on the earth surface (green curve) and at a depth of 30 m (red curve)

For each record, calculations were made of the ratios of the spectral amplitudes measured on the surface (A_{sur}) and in the adit (A_{ad}), for all motion components. The measurement results are presented in Table 3. It should be noted that for the horizontal components, in general, there is a higher level of A_{sur}/A_{ad} ratios compared to the vertical component, therefore, the values presented in Table 3 characterise mainly the horizontal oscillations. The ratios calculated for different horizontal components differ to a lesser extent. The table contains data on those components where the highest A_{sur}/A_{ad} ratios were obtained. The average values for the horizontal components A_{sur}/A_{ad} for all events match reasonably well, especially at low frequencies. Variations do not exceed 0.7 % for low frequencies, 3.5 % for medium frequencies, and 27 % for high frequencies.

Table 3: Ratios of spectral amplitudes of displacement velocities A_{sur}/A_{ad} for earthquakes (see Table 1)

Record no.	Frequency range, Hz		
	0.5-2.0	2.0-3.3	3.3-10
1	1.22	2.27	8.62
2	1.22	2.29	6.11
3	1.23	2.38	6.58
4	1.23	2.25	8.67
5	1.22	2.27	6.46
6	1.22	2.24	7.99
7	1.22	2.29	6.09
8	1.22	2.37	6.04
9	1.23	2.35	6.32
10	1.22	2.26	6.87
11	1.22	2.33	5.68
12	1.23	2.27	6.41
13	1.23	2.26	6.82
14	1.22	2.31	5.45
Average	1.22±0.01	2.30±0.08	6.7±1.8

Similar measurements and calculations performed for weak microseismic oscillations give similar results (Table 4). In general, they completely repeat the estimates obtained earlier at the same object in 2013 [Malovichko, Pyatunin, 2013], and the differences between the results of different methods do not exceed 2 % for low frequencies, 9 % for medium frequencies, and 13 % for high frequencies. Relatively large discrepancies for high frequencies can be associated with the influence of local microseismic sources, which are not always possible to get rid of. Nevertheless, the values of the ratios themselves, even with such significant random deviations, are statistically significant ($>3\sigma$).

Table 4: Comparison of the ratios of amplitudes of displacement velocities A_{sur}/A_{ad} , obtained by various methods

Calculation option	Frequency range, Hz		
	0.5-2.0	2.0-3.3	3.3-10
A_{sur}/A_{ad} for earthquakes	1.22	2.30	6.72
A_{sur}/A_{ad} for microseisms	1.24	2.49	5.84

The amplitude ratios obtained can be further easily converted into seismic intensity increments. The conversion is performed using the following formula [RSN 65-87]:

$$\Delta I = k \frac{A_1}{A_0},$$

where instead of the ratio of amplitudes A_1/A_0 on the investigated and reference soils the ratio A_{sur}/A_{ad} was used, and the value of the coefficient k is taken as 2.5. The coefficient $k=2.5$ instead of $k=3.3$, adopted in RSN 65-87, most adequately matches the difference of 1 point, which is obtained when the amplitudes change by 2.5 times according to recent studies [Aptikaev, 2012].

III. Analysis of research results

Thus, for the seismogeological conditions of the test site of the Geophysical Service of the Russian Academy of Sciences, at a depth of 30 m, a decrease in seismic intensity is achieved by 0.2 points for low frequencies, by 0.9 points for medium frequencies, and about 2 points for high frequencies.

Obviously, in other seismogeological conditions, it is possible to expect other ratios of amplitudes and, as a result, other increments of seismic intensity. However, with rare exceptions, seismic properties still improve with depth, that is, there is a fundamental similarity of soils in the upper part of the section in different areas due to the same susceptibility to weathering processes. In this regard, the general trend of decreasing intensity with depth will continue.

The above is confirmed by the results of synchronous measurements performed in numerous tunnels in the area of Sochi (Fig. 4). A special feature of the data obtained in and above the tunnels is that it extends the range of investigated depths up to 250 m. Seismogeological conditions for different observation points did not differ in stability. This allows us to look at the results obtained in general, abstracting from the structure of the array in each individual case. On average, for low frequencies, a decrease in seismic intensity by 0.4 points was obtained, at medium frequencies the difference was 0.7 points, at high frequencies – 0.8 points.

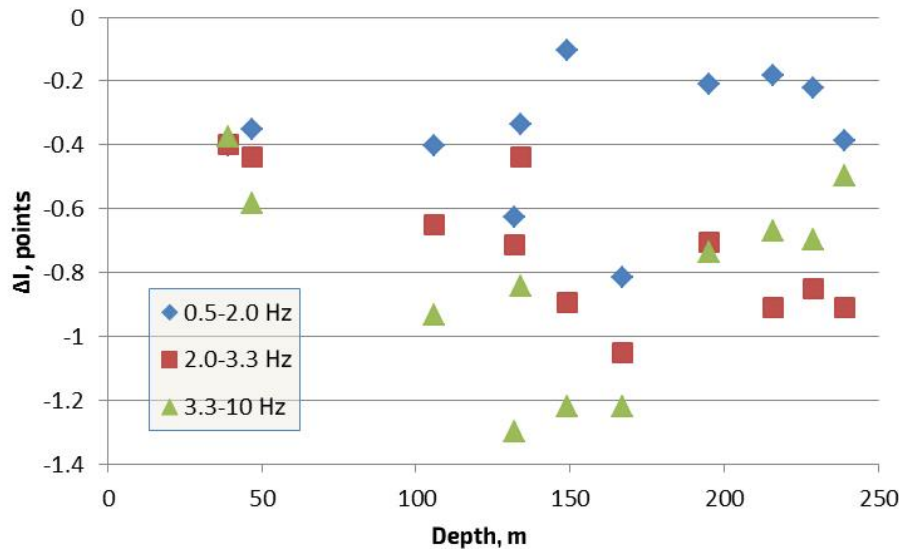


Fig. 4: Ratios of increments of seismic intensity in three frequency ranges for different excavation depths

It can be noted that low-frequency oscillations turned out to be weakly affected by the depth of excavation: most of the increments of ΔI are kept in the range from -0.4 to -0.2 points. Mid-frequency oscillations show some tendency of increasing the absolute difference of increments with depth. In the considered range of depths, it can be approximated by the equation $\Delta I = 0.68 - 0.29 \ln(H)$, where H is the excavation depth in metres. High-frequency oscillations also show a similar trend down to a depth of 170 m, however, further it is broken, which casts doubt on its existence. Obviously, for the final conclusions regarding the quantitative description of the effect of depth on the increase in intensity, additional data are required.

IV. Conclusion

As a result of experimental studies at the Obninsk test site and a number of tunnels in Sochi, the features of the change in the spectral composition and intensity of oscillations were established when comparing records of teleseismic earthquakes and microseisms obtained on the earth surface and in the research adit. The most stable results were obtained for the frequency range up to 3.3 Hz, although in general, even up to 10 Hz, the revealed effects significantly exceed the measurement errors.

The performed studies also showed that the difference in oscillation level increases with the increase of frequency as well as with the depth of underground excavations. Nevertheless, there are still many questions regarding the impact of earthquakes on underground structures. To solve them, it is necessary to develop a methodological base with the implementation of the tasks in seismically active areas. One of the tasks is the installation of downhole systems for earthquake control, which will allow measurements at different depths, as well as equipping underground structures with automated monitoring systems to obtain spectral characteristics of seismic effects at the time of earthquakes.

The revealed patterns of seismic intensity decrease with depth can serve as the basis for the development of a special regulatory framework in order to reduce the cost of designing and building deep underground structures, in particular, transport tunnels.

References

- [1] Atsushi Kusaka, Nobuharu Isago, Yohei Kitagawa, Shohei Hara and Kosuke Kawata. 2018.

Mechanical Behavior of Mountain Tunnel during Earthquake Based on Dynamic Measurement in an Actual Tunnel/ ITA-AITES World Tunnel Congress, WTC2018, Dubai. pp. 1647-1658.

[2] Wang, W.L., Wang, T.T., Su, J.J., Lin, C.H., Seng, C.R., and Huang, T.H. 2001. Assessment of damage in mountain tunnels due to the Taiwan Chi-Chi Earthquake. *Tunnelling and Underground Space Technology*, Vol.16, pp.133-150.

[3] Xuepeng Zhang, Yujing Jiang, Kazuhiko Maegawa 2020. Mountain tunnel under earthquake force: A review of possible causes of damages and restoration methods. *Journal of Rock Mechanics and Geotechnical Engineering* Vol. 12, pp.414-426. <https://doi.org/10.1016/j.jrmge.2019.11.002>.

[4] Asakura T, Tsukada K, Matsunaga T, Matsuoka S, Yashiro K, Shiba Y, Oya T. 2000. Damage to mountain tunnels by earthquake and its mechanism. *Doboku Gakkai Ron-bunshu* 2000; Vol. 659, pp. 27-38. https://doi.org/10.2208/jscej.2000.659_27 (in Japanese)

[5] Roy N, Sarkar R. A review of seismic damage of mountain tunnels and probable failure mechanisms. *Geotechnical and Geological Engineering* 2017. Vol. 35, pp. 1-28. [doi:10.1007/s10706-016-0091-x](https://doi.org/10.1007/s10706-016-0091-x).

[6] Zhang X, Jiang Y, Sugimoto S. 2018. Seismic damage assessment of mountain tunnel: a case study on Tawarayama tunnel due to the 2016 Kumamoto Earthquake. *Tunnelling and Underground Space Technology* 2018. Vol. 71, pp. 138-148. <https://doi.org/10.1016/j.tust.2017.07.019>.

[7] Zhang X, Jiang Y, Hirakawa Y, Cai Y, Sugimoto S. 2019. Correlation between seismic damages of Tawarayama tunnel and ground deformation under the 2016 Kumamoto earthquake. *Rock Mechanics and Rock Engineering* 2019. Vol. 52, pp. 1-13. [doi:10.1016/j.tust.2017.07.019](https://doi.org/10.1016/j.tust.2017.07.019).

[8] Basov D., Bezrodny K. P. Impact of Earthquakes on the Tunnels of the Circum-Baikal Railway. *Geocology. Engineering geology. Hydrogeology. Geocryology*. 2008, no. 1, pp. 60-66. (In Russian).

[9] Aptikaev F. F. *Instrumental Seismic Intensity Scale*. Moscow, OOO «Nauka i obrazovaniye», 2012, 176 p. (In Russian).

[10] Malovichko A. A., Pyatunin M. S. Two-Level Microseismic Observations on the Territory of the Obninsk Polygon of the Geophysical Service of the Russian Academy of Sciences.// *Modern methods of processing and interpretation of seismological data. Materials of the Eighth International Seismological School*. Obninsk, GS RAS, 2013, pp. 195-201. (In Russian)

[11] RSN 60-86. *Engineering Surveys for Construction. Seismic Microzoning. Work Performance Standards*. Introduced on 1997-01-01. Moscow, Gosstroy of the RSFSR, 1997, 17 p.

[12] RSN 65-87 *Engineering Surveys for Construction. Seismic Microzoning. Technical requirements for the performance of works*. Introduced on 1998-01-01. Moscow, Gosstroy of the RSFSR, 1998, 14 p.

[13] SP 14.13330.2018 (updated version of SNiP II-7-81*). *Construction in Seismic Areas*. Introduced on 2018-11-25. Moscow, Ministry of Construction of Russia, 2018, 122 p.

[14] SP 283.1325800.2016. *Construction Objects of Increased Responsibility. Seismic Microzoning Rules*. Introduced on 2017-06-17. Moscow, Ministry of Construction of Russia, 2016, 21 p.

STATISTICAL ANALYSIS OF SUSTAINABLE DEVELOPMENT OF MODERN ECONOMY

Alisa Olisaeva¹, Marina Galazova¹, Leyla Baysultanova²

•

¹North-Ossetian State University named after K.L.Khetagurov, Russia

²Kabardino-Balkarian University named after H.M. Berbekov, Russia

alisa.olisaeva@mail.ru

galazovam@mail.ru

baileila@mail.ru

Abstract

The purpose of this article is to provide a statistical analysis of the sustainable development indicators of the Russian Federation within the framework of the United Nations 2030 Agenda, in particular food security as it relates to Sustainable Development Goal 2 Eradicate hunger, achieve food security and improved nutrition, and promote sustainable agriculture. The importance of solving the problem of food security and healthy nutrition is emphasized. In the course of scientific research, general and special methods of scientific knowledge were applied: analysis, synthesis and comparison, as well as statistical data analysis and visualization.

Keywords: sustainable development, food security, sustainable development indicators

I. Introduction

Sustainable development is one of the most important goals in the economic and geopolitical activities of many countries, reflected in strategic development documents. The Russian Federation, like many countries, has adopted at the state level the UN resolution on sustainable development and ratified the Paris Convention on Climate Change. As part of the implementation of national development goals in the field of green finance and sustainable development, the goals and main directions of sustainable (including green) development of the Russian Federation were approved at the legislative level. The implementation of these areas should contribute to the achievement of objectives related to positive environmental impact, achievement of environmental effect, compliance with the technological indicators of the best available technologies, as well as the absence of significant side effects on the environment (principle "Do Not Significant Harm").

The fundamental principles of Russia's transition to sustainable development were laid down in the Concept of Transition of the Russian Federation to Sustainable Development, adopted by the Decree of the President of the Russian Federation in 1996. [2] Presidential Decree No. 204 of May 8, 2019, defined the national goals and strategic objectives of the development of the Russian Federation for the period up to 2024 [7]. At present, we can speak about the actual focus on achieving the SDGs of twelve national projects and the Comprehensive Plan for Modernization and Expansion of Backbone Infrastructure, implemented to achieve the national goals and strategic objectives of development of the Russian Federation for the period until 2024.

II. Methods

The 2030 Agenda Sustainable Development Goal indicator framework includes 231 indicators divided into three levels (1 - method established and data widely available, 2 - method established

but data limited, 3 - no internationally agreed method). Only 123 indicators (53 %) belong to level 1, the rest are categorized as level 2 [6]. The global indicator framework was developed by the Inter-Agency and Expert Group on Sustainable Development Goal Indicators (IAEG-SDGs) and harmonized by the United Nations Statistical Commission. Recognizing the difficulty in adopting a global indicator framework that is appropriate for all countries, the 2030 Agenda states that Member States will develop their own national indicators. [5]

The realization of sustainable development is most likely when there is a balance of 3 key components, namely economic growth, social responsibility and environmental balance.

Sustainable growth of the state economy is one of the main conditions for sustainable development of the society. With the growth of GDP, the living standards of the population rise, production expands, employment and wages increase, and the state, in turn, receives more finances to address social and environmental needs.

External challenges that seek to throw our country's economic processes out of balance only provide an incentive to develop a sustainable and secure system of international settlements, shift production chains, develop industry, search for new partners, importers and exporters, investors. At the moment Russia is steadily moving towards building a multicollaborative self-sufficient economic system.

III. Results

The purpose of this study is to analyze the status of implementation of Sustainable Development Goal 2 Eradicate hunger, achieve food security and improved nutrition, and promote sustainable agricultural development in terms of food security.

At present, the Russian Federation has a well-developed legislative framework regulating the food supply of citizens. The Doctrine of Food Security of the Russian Federation (hereinafter referred to as the Doctrine), adopted in 2020, is the document of strategic planning of food security, which reflects the main directions of the state social and economic policy in the field of ensuring food security. The Doctrine guarantees physical and economic accessibility for every citizen of the country to food products that meet mandatory requirements, in amounts not less than the rational norms of food product consumption.

According to the Doctrine, economic accessibility of food is interpreted as "the possibility to purchase food products of proper quality at prevailing prices, in volumes and assortment that correspond to recommended rational consumption norms" [1].

According to the United Nations, in 2019, 690 million people in the world were in a state of hunger, nearly 1 billion people could not afford a nutritious diet, and for another 1 billion people, a healthy diet was out of reach. The dire situation was made worse by the Covid-19 coronavirus pandemic, which starved about 120 million people, bringing the number of hungry people to 811 million in 2020. The world's population is projected to increase to 10 billion by 2050, hence the problem of food supply will become even more acute. The State of Food Security and Nutrition in the World 2022, prepared by the largest authoritative international organizations (FAO, IFAD, UNICEF, WHO, etc.), notes that the world is moving further away from achieving the goals of eliminating hunger, food insecurity and malnutrition in all its forms [4].

In this regard, the need for research to assess the state and develop proposals to ensure food security of the state becomes obvious.

One of the important indicators is the indicator of food independence for staple foods in the country. The Doctrine on Food Security defines the main types of products, where the key ones are: sugar, potatoes, milk and milk products, meat and meat products [1]. According to statistical data, by 2021, food independence is achieved for all types of products except milk and milk products (83.6% of 90%, respectively) [8].

The basic indicators also include the indicator of actual consumption of basic food products by category by the population. According to the data for 2017-2021, the population's consumption of

potatoes and milk and milk products is considered insufficient, as the indicators for these types of food never reached the threshold value (100%) during the entire time period under consideration (Fig.1) [8].

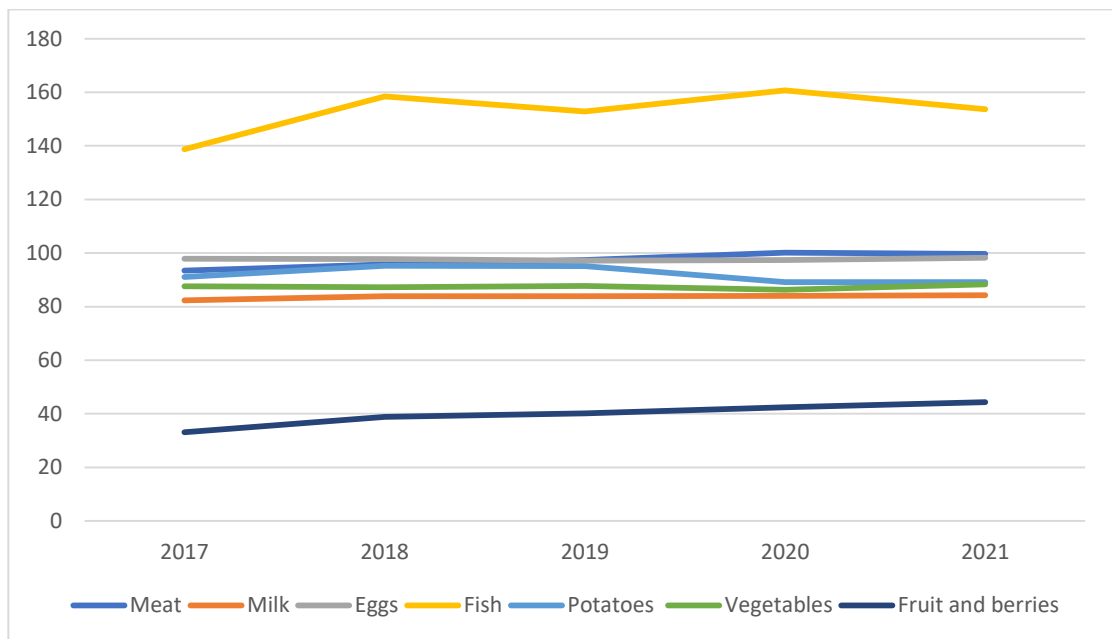


Fig. 1: Consumption of basic foodstuffs by the Russian population, 2017-2021, %

In 2020-2022, the number of business entities decreased by 50,203 units, and if there is a decline in 2021, then in 2022 the same indicator increased from 568,4561 units to 5866,703 units. Of the eight federal districts, six showed a decreasing trend. Only two federal districts have positive dynamics. Thus, the number of business entities increased in the central Federal District by 36,202 units, in the North Caucasus Federal District by 4,794 units, but in Russia as a whole, the number of entities tends to decline (in 2022, there are 50,203 fewer SMB than in 2020).

The largest number of small and medium-sized businesses is observed in the central Federal District: 30.8%; 31.0%; 31.7%, respectively. The Volga Federal District is in second place, although the number of subjects is decreasing: 17.9%; 17.8%; 17.6%, respectively. The situation is approximately similar in three federal districts: North-Western; Southern; Siberian. In them, the number of SMB is 10-12% of the total. Despite the positive dynamics, the smallest number of business entities is observed in the North Caucasus Federal District: 3.4%; 3.4%; 3.5%, respectively.

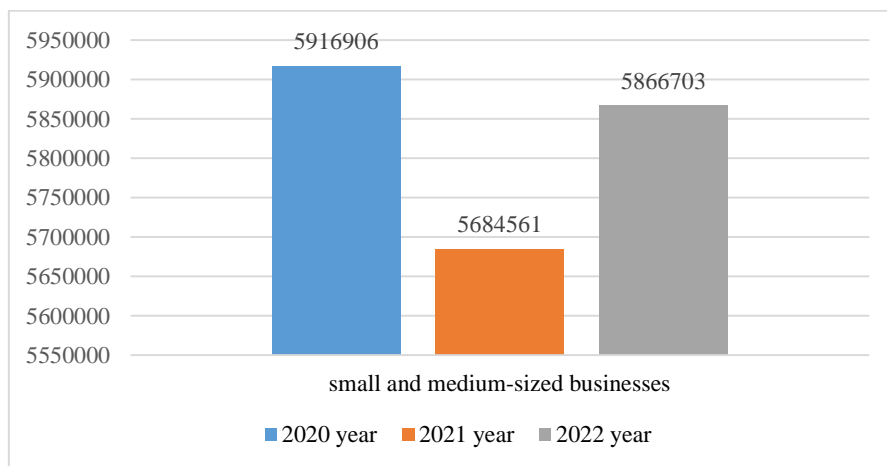


Fig. 2: Dynamics of the number of small and medium-sized businesses in the Russian Federation for 2020-2022 (units).

Achieving food security depends directly on the affordability of food, which brings to the fore such indicators of the country's economic life as the price index for food products and the share of the population with incomes below the subsistence minimum.

Regarding the food price index, there is an upward trend in the index after 2019 due to the coronavirus pandemic and the unstable economic situation both in the country and in the global arena (Fig.2) [8].

An important indicator is also the indicator of the share of the population with incomes below the subsistence minimum, which, according to statistical data, shows a high level of poverty in the Russian Federation (Fig.3) [8].

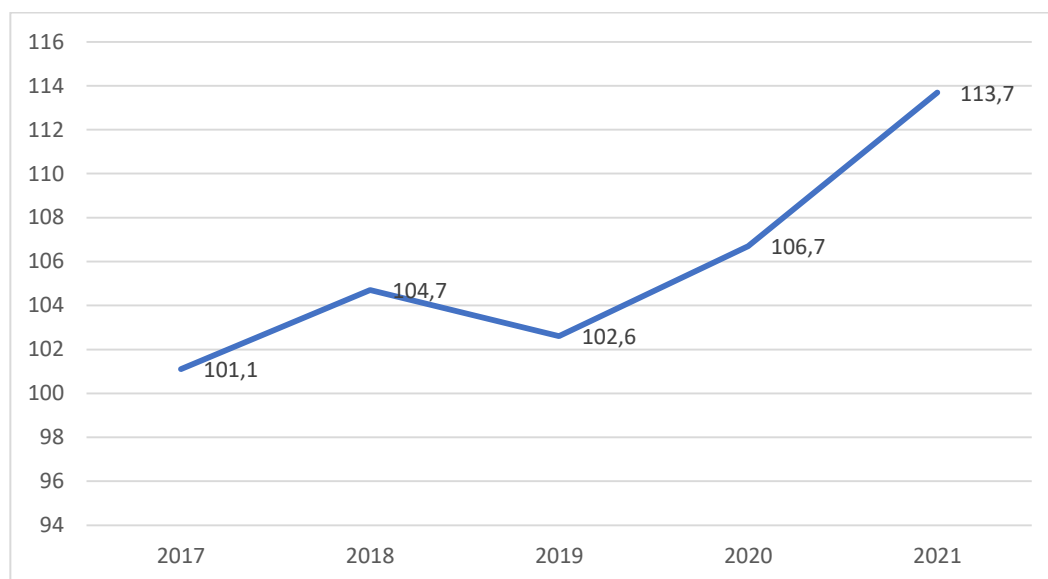


Fig. 3: Food commodity price index, 2017-2021, %

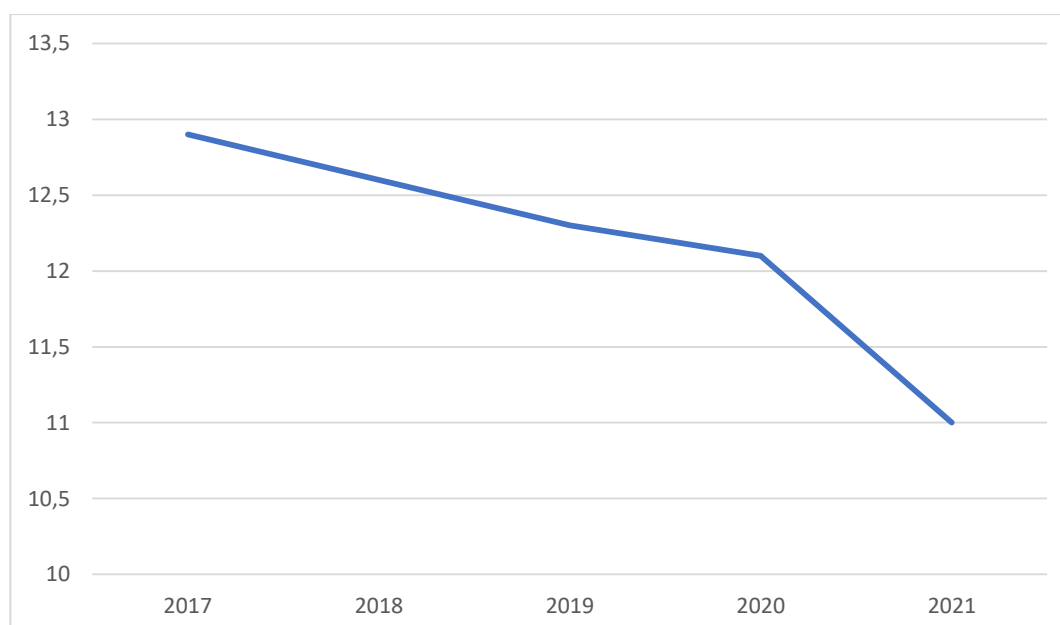


Fig. 4: Share of population with cash income below the subsistence minimum, 2017-2021, %

The dynamics of the share of imported food products in the commodity resources of food retail trade is characterized by multidirectional nature and trends (Fig.4) [8].

The threshold value (no more than 25%) is not exceeded only in the period 2017-2018 (there was a significant reduction in the share due to the launch of food import substitution policy in response to the imposed sanctions).

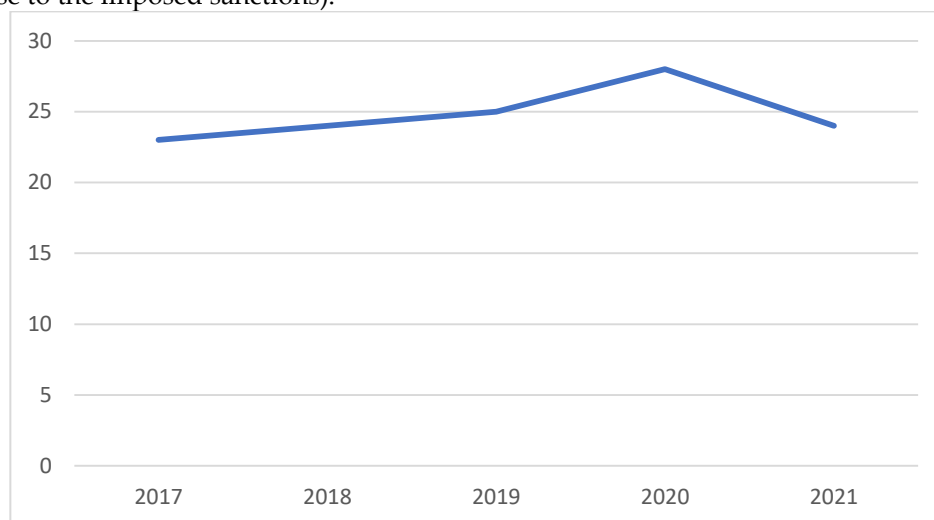


Fig. 5: Share of imported food products in the commodity resources of food retail trade, 2010-2021, %

Despite the fact that for the five-year period under consideration from 2017 to 2021, the dynamics of the predominant part of the indicators is more positive, the following challenges and threats to food security can be traced.

1. Food price inflation and the dynamics of world food prices. Since 2020, there is an increase in prices not only for food produced in Russia, but also imported from abroad. Thus, in January-February 2022, there is an increase in raw milk prices (the price increased from 28,000 rubles/t to 32,776 rubles/t in 3 months), as a result of which the prices of dairy products increased due to high prices of feed and imported equipment [8].

2. Insufficient level of solvent demand of a significant part of the population for food (low real incomes of the majority of the population, increase in social material stratification). The share of the population with income below the subsistence minimum in 2020 is 12.1%, exceeding the threshold of 10% (Fig. 3). Note that the real disposable income of the population in 2020 in Q2 decreased by 8%, reaching the lowest value for the interval 2014-2020. [8].

3. Change in the structure of consumption of basic foodstuffs (Fig.1). According to Rosstat data, the consumption of such foodstuffs as sugar, meat products has become higher than the norm in recent years, while the consumption of milk and dairy products, as well as potatoes has decreased.

4. Unacceptable level of consumption of some basic products by the population, as well as consumption of other products in excess of the norm, which leads to deterioration of the health status of the population. Despite the positive dynamics in the consumption of certain groups of food products by the Russian population, the nutrition of the population is unbalanced. Statistical data confirm that the consumption of potatoes and dairy products necessary for health is insufficient (62% and 80% for 2020, respectively) (Fig.2). At the same time, the consumption of sugar, meat and meat products is above the norm (129.2% and 121.1% for 2020).

5. Economic accessibility to all citizens of the Russian Federation of the necessary volume and quality of all basic types of foodstuffs that does not meet safety standards. This is due to the discrepancy between the real income of the population, as well as the share of the population with income below the subsistence minimum and the increasing prices for some food products.

In the long term, challenges will be related to every sphere of life and functioning of the economic system.

The goal of reaching the indicators of self-sufficiency established in the Doctrine is to ensure food independence of our state and increase economic and national security, which is of great importance in the current circumstances.

In recent years, some criterion indicators of food independence have been achieved, including at the expense of government support programs provided to the agro-industrial complex, but a number of problems have not yet been solved. Achievement of the established planned criteria in the sphere of agro-industrial complex will be possible, among other things, by solving certain existing problems related to the sale of agricultural products and export-import operations. The development of information and advisory support system for agricultural producers, especially small enterprises, will have a positive impact on their activities in general. Solving the set tasks and achieving the planned criterion indicators of self-sufficiency, especially in the field of food, will ensure Russia's full independence.

According to the Doctrine, the products produced by domestic agricultural producers should be of high quality, environmentally friendly and economically and physically accessible to the entire population of the country.

Russian companies in the agricultural sector are operating efficiently. Profitability amounted to 25.6 % (the target is 15.3 %). Let us consider the resource supply of basic foodstuffs in the Russian Federation in 2013-2021. Over the past eight years, grain imports have significantly (by 86.7%) decreased and exports have more than doubled (Fig.5) [8]. The production of meat and meat products is increasing in the country. Every year the volume of personal consumption and export of meat increases (Fig. 6) [8]. Production volumes of milk and dairy products increased, at the same time there was an increase in exports and a decrease in imports (Fig.7) [8]. In the first half of 2022, the production of raw (by 1.6%) and dried milk (by 28.1%), cheese (by 5.7%) and butter (by 11.0%) increased.

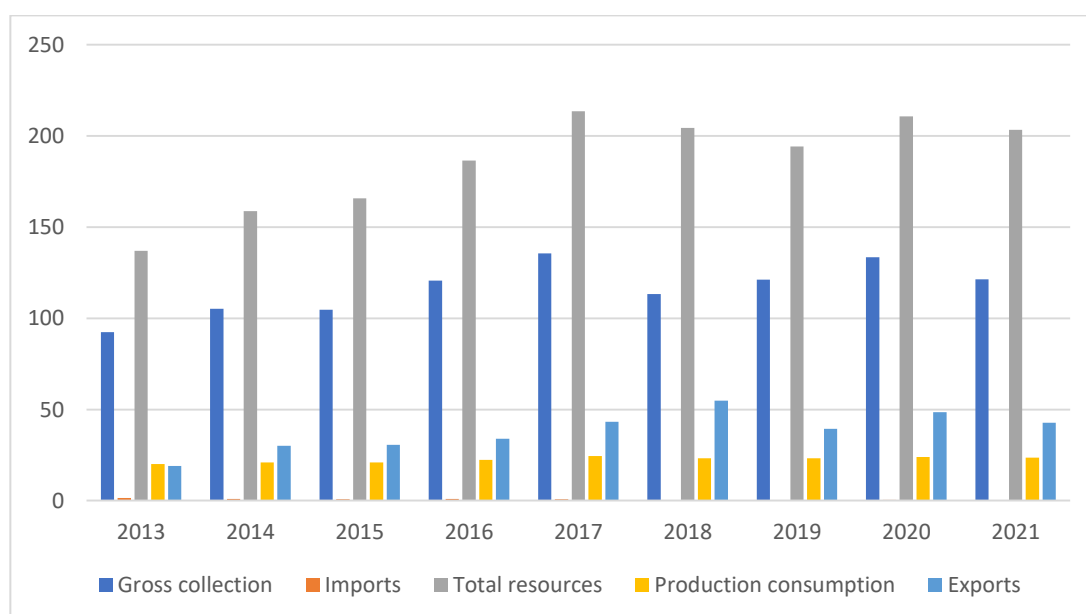


Fig. 6: Resource supply of the Russian Federation with grain (without processed products) in 2013-2021, mln tons

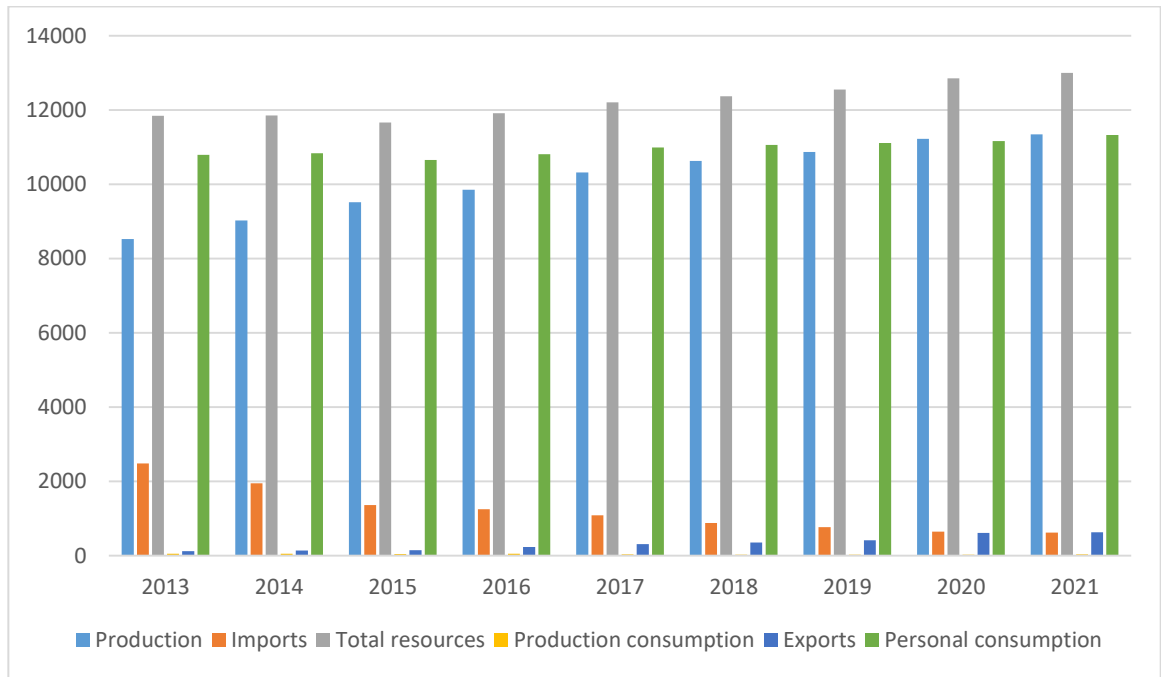


Fig. 7: Resource supply of the Russian Federation with meat and meat products in 2013–2021, thousand tons.

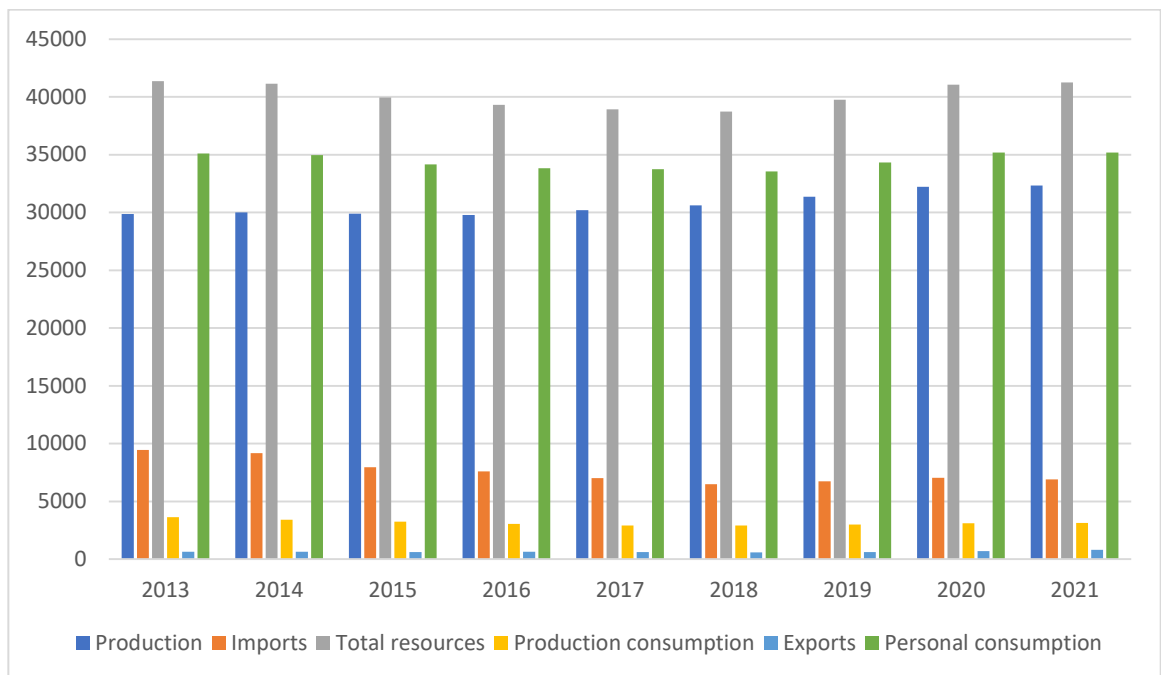


Fig. 8: Resource supply of the Russian Federation with milk and milk products in 2013–2021, thousand tons.

Imports of fish and other seafood decreased by 28.9% and continue to decline in 2022–2023. Production and exports increased by 76.9 % by 2021 (Fig.8) [8].

Information on the resource supply of the Russian Federation with fruits and berries in the period under consideration is presented in Fig.9 [8].

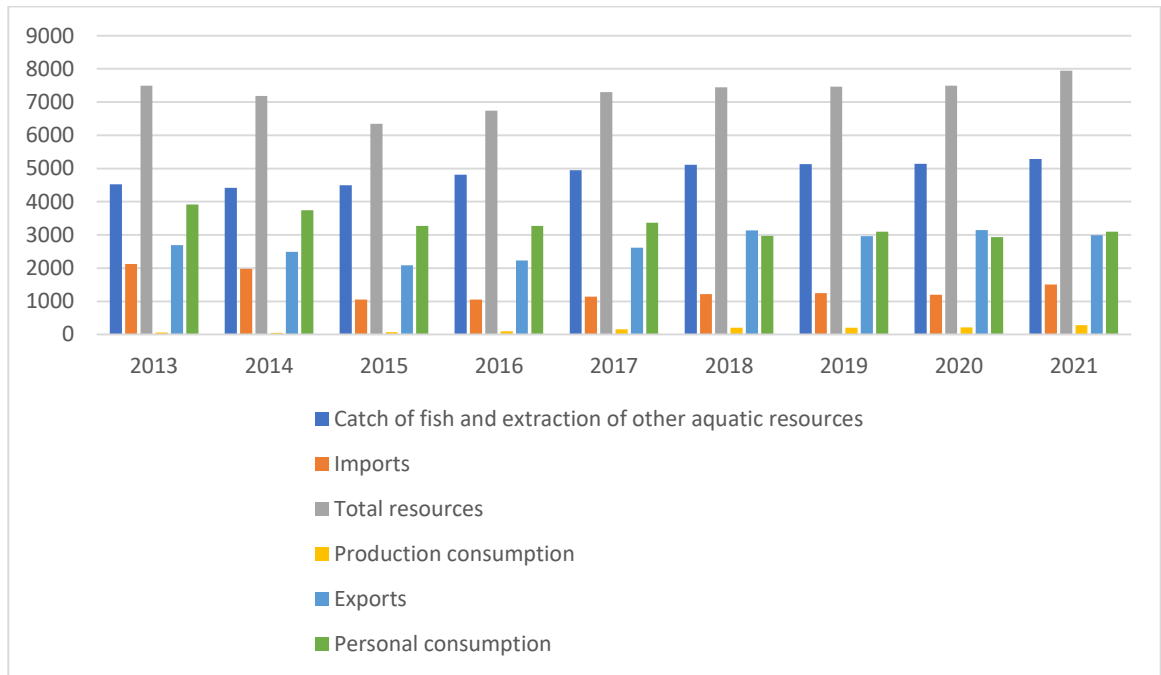


Fig. 9. Resource supply of the Russian Federation with fish and fish products in 2013-2021, thousand tons in live weight

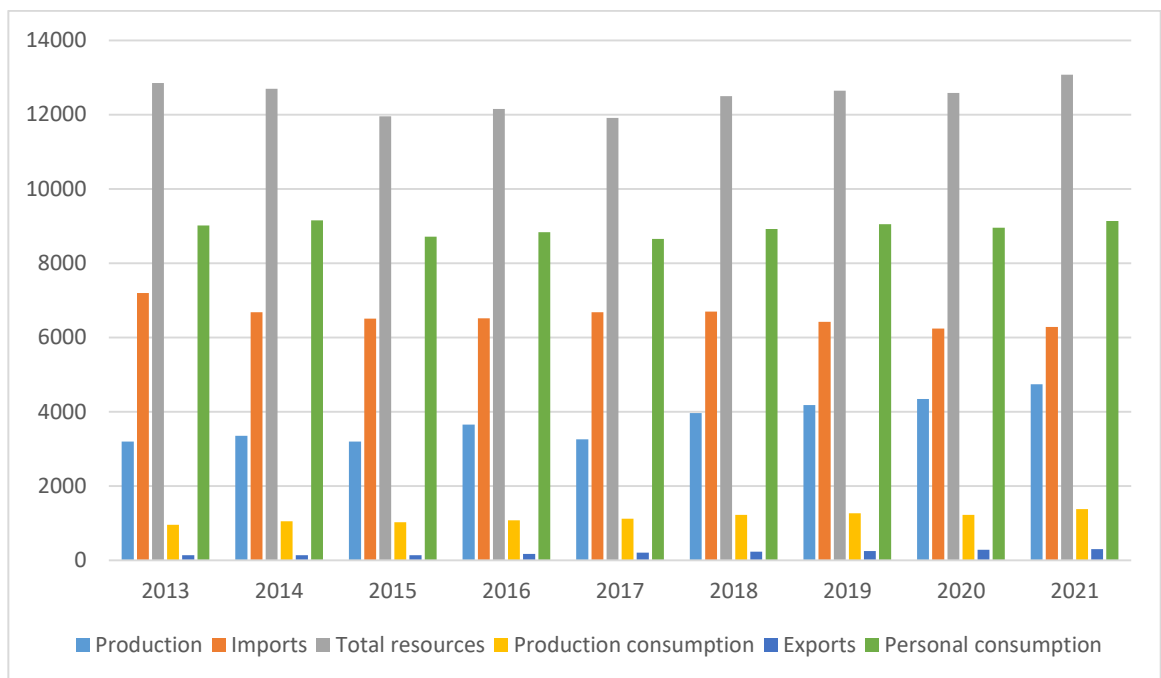


Fig. 10. Resource supply of the Russian Federation with fruits and berries in 2013-2021, thousand tons.

Nevertheless, the volume of state subsidies and financial support is low. For example, in the European Union, subsidies amount to about 30% of the cost of production, while in Russia - 3%. The OECD determines the overall level of financial support to agribusiness through the indicator "total support assessment". Russia ranks 5th in this respect. The state support per 1 ha of arable land in Russia is 35 USD, in the European Union countries - 800 USD, in China - 1500 USD, in Switzerland - 1400 USD [3].

IV. Discussion

Thus, ensuring a high level of food security, overcoming challenges and threats in this area of economic security directly depend on the level of involvement of the state in this area, on the state policy and a set of measures to reduce risks in the food sector. Achievement of results and positive effect is possible only with proper state and regional control over the implementation of all officially adopted measures to improve the food security situation and achieve its planned level by 2030.

References

- [1] The Doctrine of food security of the Russian Federation: approved by the Decree of the President of the Russian Federation from 21.01.2020 № 20 "On approval of the Doctrine of food security of the Russian Federation". Text: electronic // ConsultantPlus - reliable legal support: the official website of the company "ConsultantPlus".
URL: http://www.consultant.ru/document/cons_doc_LAW_343386/ .
- [2] On the Concept of Transition of the Russian Federation to Sustainable Development: Decree of the President of the Russian Federation of 01.04.1996 № 440 // ConsultantPlus: official website – URL:
<https://www.consultant.ru/cons/cgi/online.cgi?req=doc&base=EXP&n=233558#ICFgcXT8gdN3hMGq4>
- [3] Organisation for Economic Co-operation and Development (OECD) /
URL: <https://www.oecd.org/>
- [4] The State of Food Security and Nutrition in the World. /
URL: <https://www.fao.org/publications/home/fao-flagship-publications/the-state-of-food-security-and-nutrition-in-the-world/ru>
- [5] Resolution adopted by the General Assembly on September 25, 2015. United Nations. –
URL: https://www.un.org/ga/search/view_doc.asp?symbol=A/RES/70/1&Lang=R .
- [6] SDSN. Indicators and a Monitoring Framework for Sustainable Development Goals: Launching a Data Revolution for the SDGs; 2015. /
URL: <http://unsdsn.org/resources/publications/indicators/>
- [7] Decree of the President of the Russian Federation dated 07.05.2018 No. 204 On the national goals and strategic objectives of the development of the Russian Federation for the period until 2024. // URL: <http://www.kremlin.ru/acts/bank/43027>
- [8] Federal State Statistics Service: official website. / URL: <https://rosstat.gov.ru/>

INFLUENCE OF THE ENVIRONMENT ON THE DEPORTED BY THE EXAMPLE OF THE CHECHEN PEOPLE

Sapiyat Tsutsulaeva

•

Kadyrov Chechen State University, Russia

sapiyat_univ@mail.ru

Abstract

During 1944, the deportation of Chechens to Kazakhstan and Asia was caused by several consequences. The deportation from Chechens to Russia and Asia had an impact on nature in new places of living. In the period of transition, Chechens were forced to abandon their native lands and move to unfamiliar areas, they faced new conditions in terms of climate, landscape, natural resources and possibilities for agriculture and animal husbandry. In addition, separation from the traditional way of life and natural resources affected health and psychological state. In the unfamiliar places, they found them in new and unfamiliar places with a different climate, vegetation and geographical features. When Chechens were forced to abandon the land and move into unfamiliar regions, they faced changes in climate conditions, natural resources and habitats. The situation was similar for people who left them from their homeland as well as for agriculture and livestock.

Keywords: deportation, new climate, adaptation, climate, landscape

I. Introduction

The environment is the thing that is around a person and how it affects his development. It is what is around a person and how it affects him. According to the most broadest definition, the "Environment" (OS) is our entire planet and the cosmos as it exists. It is only the biosphere that has an elevated meaning of OS. An earthly shell, in which all living organisms are concentrated, is the natural shell of the Earth, in which all living organisms inhabiting it are placed. The natural shell was a natural shell. In his life, one person in his life changes the nature around him, creating a new habitat. In the moment of birth, a person is born, he is the creator of his environment, which provides him with opportunities for physical and moral condition, as well as providing him with opportunities for intellectual, moral, social and spiritual development. At that moment, after a long and painful evolution of mankind on our planet in the course of its lifetime, at that time a stage was reached to transform all around it by numerous methods [1]. In the increasing development of science and technology, man has acquired an ability to transform the environment in many forms and on scale that was not previously seen. With the accelerated development of science and technology, man has acquired an ability to transform the environment in many forms and on scale that was not previously seen. Because he considers both aspect of the human environment, natural and man-made, important to him. They are also important to his health and the enjoyment of fundamental human rights, including the right to life as such. Human habitat - the concept of human habitat is a collection of industrial, economic, recreational and cultural products. There are industrial, economical and recreational objects that consist of industrial,

economical, recreational and cultural objects. It is a space that consists of urban and industrial area, agricultural or countryside. In the human concept, humanity is a place that consists of urban Space and Industrial Space, Urban Space And Industrial Area. People's life and environment influence the development of society as an entire. The people's lives and the environment influence in determining the development of society as an. It is worth mentioning that they have affected human life, living conditions in nature and how the environment influences them.

Natural influence on the deported Chechens was significant and multifaceted. In the new area, nature's influence on them was significant and multifaceted. In the new area, nature's influence on the deported Chechens was significant and multifaceted. The influence of nature in the new area on the deported Chechens was significant and multifaceted. They were forced to leave the land and move to unfamiliar areas, in order to get access to natural resources. Chechens faced changes in climate, landscape, vegetation and access to natural resources. All regions of Russia were similar in the situation. Climate change was found in the new areas, affecting the health and adaptability of the deported Chechens. The transition from one climatic zone to other can cause difficulties in adapting to new temperatures and conditions.

A new natural environment in the presence of vegetation, soil fertility and pasture in it will differ from its existing nature. The traditional Chechen occupations, such as agriculture and animal care, affected this.

People, development and growth are closely intertwined with the environment. The Development And Environment Are Closely Intertwined With People, Development And Growth. This is due to the. The people, development and the environment have been closely connected with People, Development and Environment. What are these times in the history of our lifetime, at what point we must regulate our activities around the world with greater concern for an environment impact of such activity. An important moment in history. This is an important moment in history. It is. We can do a great and irreparable damage to the earthly environment on whose basis our life depends, through ignorance or indifference. The reason for this is that we have no right to abandon any of them. These are the possibilities for providing ourselves and our descendants with a better life in an environment that will be more in line with the needs of people.

In contrast to the natural environment, which is protected by complexes in nature, there are differences. It became known that the protection of human environment is also carried out in other directions. The development and improvement of its environment, the creating more favorable conditions for life as well as recreation are achieved from different sides. Improvement of the landscaping can be improved to create better conditions for life, activity and recreation by landscaping or improving it to create more favorable environments in terms of living conditions, activities and recreation. In the case of deported Chechens, this axiom will be proved.

II . Methods

At the moment, various methods were used to study in the problem of deported Chechens to Kazakhstan and Central Asia [2].

1. Historical analysis: Researching on archival documents, historical data, eyewitness accounts and other materials that document the deportation of Chechens and its consequences. 1. Historical analysis: Investigating on archival documents, historical data, eyewitness accounts and other materials that document the deportation of Chechens and its consequences. 2. The. It is based on archival documents, history or other materials that document the deportation of Chechens and its consequences.

2. The process of conducting polls and interviews with deported Chechens, the descendants or members of local groups in order to study experienced Chechens, perceptions and impact of deportation on life and cultural identities.

3. Ethnographic research: The study of the traditions, customs, culture and way of life in Chechen new places derived from deportation. 3. Ethnographic research: The study of the traditions, customs, culture and way of life in Chechen new places derived from deportation. You can understand what happened after removing Chechens from old village for an understanding of the change that occurred after the deportation.

4. Geographical analyses: The analysis of the geographic and natural conditions in regions that are Chechens' living place in Central Asia and Russia, to identify an impact of the natural environment on economic activities.

5. Psychological research: The study of the psychological impact of deportation on Chechens and their descendants, as well as the identification of mechanisms for adapting to new conditions.

6. Comparative analysis: comparison of similar and different aspects in deportation, its consequences at the same time in different territories of Kazakhstan and Central Asia. Comparison of similar and different aspects of deportation and its consequences in different territories of Kazakhstan and Central Asia.

7. Literature review: Analysis of previous studies and publications on this topic to summarize and systematize the available information.

In addition, the combination of various research methods will provide a more complete picture about the problem in deported Chechens and its adaptability to new conditions, as well as identify important aspects and recommendations for the future.

The concept of the ecology of culture, in terms of the concept of the ecology of culture, the cultural environment should be considered as a prerequisite for the full functioning of the individual, his spiritual world and spiritual settledness, attachment to his native places, and observance of the covenants of ancestors. On the basis of this, it is possible to say that the ecology and culture are an integral section of Ecological Aesthetics. In this area, aesthetic problems are concentrated in the perspective of the relations "man"-environment", in what case one transforms not only nature but also himself. As if it were possible to imagine the situation where the indigenous people of the North Caucasus are uprooted from its habitat and forcibly relocated to the subterranean environments, such as in Kazakhstan and Asia. Psychological state of deported Chechens was affected by the change in environment, which also affected them. Almost all of them faced separations from the native places, in order to gain cultural and social status. For many, this caused stress, homesickness and loss of cultural identity.

In adapting to new cultures and lifestyles, the new living conditions led to cultural and linguistic differences that proved difficult for members of different ethnic groups. Chechens faced new economic conditions, which also affected their nutrition and well-being.

According to Chechens, the deportation of people from Russia and Asia was accompanied by serious changes in their environment and lifestyle, which also affected their ability to preserve their cultural traditions and identity.

Repression in the Soviet Union was primarily aimed at legal, moral and psychological discrimination, and was also an act of mass extermination. Chechens, like other inhabitants of our country deported during the Great Patriotic War and deprived of the right to free movement, were totally dependent on their commanders. This is exactly what we are talking about: the deportation of people from their own country. Most of the representatives of the deported population were not nominated or even re-elected to a number of important state, public and private bodies. Most were neither nominated nor elected to the most prominent state bodies and public services. Special resettlers were also discriminated against in the professional sphere. The fact that IDPs began to study in universities and specialized schools has introduced a ban on their education. What was possible for them in universities and professional schools in such countries is now forbidden for them.

In other regions, migrants support the economic development and prosperity of the region. For example, in other regions, migrants support the economic development and prosperity of the region by supporting it. Some regions are helped by migrants. For this reason, some regions are helped by migrants. This leads to discrimination on their part. This leads to discrimination on

their part. This can also lead to discrimination on their part. This can also lead to discrimination on the part of migrants. Thus, the social conflict is aggravated. As a result, social conflict is aggravated. This leads to the aggravation of social conflict. Therefore, the social conflict is aggravated. Therefore, the social conflict is aggravated.

This is connected with it. This is connected with it. In fact, it's because of this. Along with the long term, the impact of migration on composition and development in population will be both short-term and long-term. The effect of migration on people's composition, formation and development will be both short-term and long-term. The migration impact on the composition of the population, and development and formation of people will be both short-term and long-term. The impact of migration on the composition of the population, in particular to develop and form people will be both short-term and long-term. It. During the long-term impact of migration, demographic consequences are determined. Another example in one case, social consequences determined the long-term impact of migration. According to the total number of migrants from the North Caucasus and other peoples (1945-1956), 1.5 million were immigrants from the North Caucasus. In Russia, the population increase from North Caucasus and other countries (1944-1957) in 1944-1957 was 1.1 million people. The resettlement of people from the North Caucasus led to the extermination of people. People were exterminated after being resettled in the North Caucasus.

III . Results

Kazakhstan is a country with the climate of continental. The climate of the country is. When summers are hot, winters are cold and harsh. At Pavlodar and Akmola regions, the climate is temperate-continental. It characterizes itself with warm summers in the north of the country, as well as cold winters at all times.

On the border with Russia, and in some regions of South-Kazakhstan on the east side of the border with Kyrgyzstan, Tajikistan and Krasnodar Territory it is more subtropical and dry, warm summers and cold winters [2].

Climate in Asia is the largest continent and the temperature here varies greatly from region to region. The climate of Asia differs much from regions to regions, but it is not unusual.

At the southern part of Asia, such as East Asian regions are characterized by subtropical and high-humidity climatic conditions. The region is characterized by an unstable weather with low precipitation in summers and frequent monsoon seasons.

The middle part of Asia, such as Central Asian region, has a continental climate with hot summers and cold winters. It is notable that the Middle East area in Asia has a continental climate with hot summers and cold winters.

On the other hand, Northern Asia has subarctic and polar weather with long winters in summers that are warmer than normal. The climate of Siberia is subarctic and an abruptly cold subtropical region. It also features cool summer months.

In order to identify the most important environmental factors affecting human health, such as changes in the environment and temperature, weather conditions, let's name them. In a rapidly changing environment, her health is affected by a rapidly changing environment in the world: it's not only about climatic or meteorological change. It also concerns how an individual adapts to new climatic conditions and how these conditions affect him. On a high level in North Caucasus, the gene pool of those who had to adapt to extreme climatic conditions has decreased, and the increased reproductive capabilities have decreased. In this region, people's reproductive capabilities have dropped by 50%. It was due to this process in people who migrated to regions

with harsh climatic conditions. In people who migrated to regions with harsh climatic conditions, it was due to this process. A record of the repressions according to archival materials, at the time of the repressions, in fact, mortality was increased by 8 times [3]. 10:1, the birth-to death ratio, together with mortality and life rate, was 10, just like living wage. In the exiles, the conditions were not good. Situations of the migrants were appalling. The situation of them was very bad. The result of this is that in recent years, these people have suffered from dampness and hunger on abandoned farms. Almost abandoned farms, they lived in dugouts, suffering from cold and dampness. On abandoned farms, people lived in dugouts, suffering from dampness and cold. The. In the United States, according to the State Department more than one-thousand children became complete orphans.

A long period of exile in the North Caucasus continued painfully, people from the North Caucasus returned to them after an extremely long period of exile. People from South Caucasus returned to them after a long period of exile. The specialists of the party and central Soviet administration were sent to help him in his work on October 16, 1956.

IV. Discussion

The development of new lands by exiled Chechens in Kazakhstan and Central Asia was a complex and multifaceted process. The development of new lands by exiled Chechens in Kazakhstan and Central Asia was a complex and multifaceted process. Together with Chechens, they faced the problems of development and adaptation to new natural conditions when they were forced to leave them and settle in new, unfamiliar corners of nature [3].

These aspects of the development of new lands include.

In accordance with the land resources of the deported Chechens, as new settlers they had to settle on new plots of land. Deported Chechens, as new settlers, had to be accommodated on new land plots. In order to provide them with food and work, the state had to provide them with land on which to raise livestock.

Climate and natural environment Chechens had to adapt to new climatic conditions, adjusting to new resources and weather conditions. Part of this may have involved learning about local plants and fruits. It may also have involved adapting to new seasons and weather conditions, and learning the differences between local soils, pastures, subsoils and meadows. The traditional Chechen economic activities of farming and animal husbandry faced new challenges in Central Asia and Kazakhstan. Deported Chechens needed help and training in new farming methods adapted to local climatic conditions. Deported Chechens needed help and training in new farming methods, taking into account local climatic conditions.

Infrastructure rehabilitation: Chechens who settled in new lands and were deported may face a lack of infrastructure. Chechens who settled on new lands and were deported may face a lack of infrastructure. In the case of forced repatriation. In this case, the main problem was to rebuild roads, schools and medical facilities.

The development of new lands had to be combined with the preservation of Chechen cultural traditions. This meant preserving language, religion, rituals and crafts.

Psychological adaptation: deported Chechens faced psychological difficulties in the process of developing new lands. They needed psychological support and counseling to cope with the changes and difficulties [4]. They needed psychological support and counseling to cope with the changes. All the ordinary people in Kazakhstan were needy and destitute, but they had just the last piece of the puzzle. This was the first help they provided to an exhausted and depleted population. On the other hand, the fact that Chechens found themselves in a republic dominated by Islam also played an important role.

Chechens, Ingush and Chechens have fraternal relations with Kazakhs. Chechens and Ingush remember this to this day. Chechens and Ingush have brotherly relations with Kazakhs. Children are often given the name "Kazakh".

When the exiled Chechens were developing new lands in Kazakhstan and Central Asia, it was important to organize coordinated work of both state and public institutions to support them in terms of welfare and preservation of their cultural identity.

The study of any historical issue is a difficult and time-consuming endeavor. A complete study of any historical issue requires comprehensive research. Unusual and difficult events are accompanied by suffering for many people. They are an indispensable part of life, and the exploits of many generations of Chechens over two centuries are an integral part of life. The presence and work of many generations in this century is integral. It was in the past that an entire nation lost half of its population. When you have gone through the "circles of hell", as Ibragimov write about, there is still the strength to be reborn again. For a number of reasons, primarily ideology, the issue of the deportation of Chechens has not been studied in Russian historical science.

During the time period, the task of modern historiography is necessary to eliminate "blank spots" in such subjects as Vainakh studies. The subject of deportation from Chechens has been discussed by sociologists, political scientist and journalists. In the past, the topic was discussed by sociology, political science and journalists [5]. A another topic is about the history of the deportation of Chechens from Russia. A very important topic, despite the chronologically distant events of deportation, is this issue. The president began to talk in 1944, including about the history of the Chechen people. In 1944, he discussed how this happened in the history and history of the Chechen people. In Russia on December 12, the new president was elected. Russian Federation has a President of Russia. President Putin took part in the first meeting of the Legislative Assembly of the Chechen Republic. The President of Russia was present at this meeting.

These are what the author is trying to tell in this chapter, Divide the Loot, and gives meaningful information. According to this article, the history of the ruined mountain, churches, monasteries and castles that were described in it, is explained in this article. In this article, we discuss the history of towers, churches and monasteries. For example, here is a discussion of the history of towers, churches, monasteries and castles. Almost 300 towers of the Argun gorge, out of 300 towers of the Argun gorge, less than 50 survived.

The authors developed the following model for adapting exiled Chechens to the new natural environment of Kazakhstan and Central Asia: The model for adapting exiled Chechens to the new natural environment of Kazakhstan and Central Asia can be expressed as follows

1. Shock and Stress: Initially expelled Chechens face shock and stress due to dramatic changes in environment, weather, and climate [6].

2. Adaptation: During this phase, Chechens begin to adapt to the new environmental and climatic conditions. Some people find ways to use local resources and survive.

3. Language and cultural barriers In their new environment, Chechens face different cultural and climatic differences, which can be an obstacle to communication with the local population.

4. Job and housing search: Chechens are looking for work possibilities as well as jobs in their new living place.

5. Social support: social networks and support from family, friends, and community play an important role in adaptation

6. Transmission of traditions and cultural values: In the process of adaptation, Chechens strive to preserve their traditions and cultural values and preserve them in their way of life. Their culture is not only important, it is vital for future generations.

7. Integration: deported Chechens are gradually being integrated into the community and participating in its economic, social, and cultural life.

8. It is possible to experience readaptation as living conditions change.

9. Successfully adapted Chechens can serve as a base for transferring experience to newcomers.

The adaptation of expatriated Chechens to the new natural environment of Kazakhstan and Central Asia is complex and multifaceted, influenced by cultural experiences, social characteristics, and contemporary issues.

In the past years, Chechen researchers have carried out significant work to study the problem of deportation and life in a special settlement. The process is important to researchers on the eve of exile in Chechnya, as soon as it comes out. It is also important to understand the complex problem: information about what happened in Chechnya before its eviction, and how it was organized. In addition, you should know that everything happened in Chechnya before its eviction, as well as who organized it. The mountainous areas are considered more than one area of needing attention. A fundamental basis for studying the origin of this problem is gaining momentum. The basis for studying the origin of this problem is gaining momentum. In 1944, the deportation of Chechens from Russia and its inhabitants was a capital work for researchers [7]. The possibility of creating capital works for the deportation of Chechens from Russia and its inhabitants will allow researchers to create capital works for deportation.

For new lands, the Chechen people had to make great efforts. In the development of new things, it was a great work of the Chechen people. History experts say that this is part of the geographical "core" of Chechen history. Historians claim that this is part of the geographical "core" of Chechen history. The result of this is economic activity in all Chechen territories [8].

So, solving the problem of territorial rehabilitation for people subjected to deportations is not possible, but legal problems that have no effective solution create interethnic conflicts. Historical Russian Borders have not been held by any person since the time of Russia. This change was made arbitrarily. It turned out that this alteration was made arbitrarily. After deportation, it turned out that this reshaping was done without the consent of the person. What interests and desires of people's own lives lie in its existence, it did not take into account. At the moment this is an unusual situation for them. The Chechen and Ingush people, whose fathers were repressed, settled in the subjects of the Russian Federation. They are going to revive the economic potential of Russia by restoring its economic potential with cultural life. Their job is: to revive the economic potential of Russia by restoring its economic potential with cultural life.

The accumulation and dissemination of information is the only way to progress in social and economic activities, as well as in cultural and economic activities of people. One community gradually dispersed to other population groups [9]. The issue of population has to do with the biology and contact with the environment, human contact with the environment and development in social formations, since an active part of the population is an important force in economic activity. The main question of the population for this population is its biological nature and relationship with the environment, as well as its relationship to human relationships.

References

- [1] Salamova A.S., Dzhioeva O. Green transformation of the world economy in the context of sustainable development, 2023, p. 152-159.
- [2] Salamova A.S., Global network economy as a factor of sustainable development, 2020, p. 03053
- [3] V. Sebastien, E. Domokos, J. Aboni, Coordinators of Sustainable Development Strategies: A Comparative Analysis of Text-Based Voluntary National Reviews, Journal of Environmental Management, 2020, p. 263
- [4] Shmatko S.G. , Agarkova L.V. , Gurnovich T.G. , Podkolzina I.M. , Problems of improving the quality of raw materials for winemaking in the Stavropol Territory, 2016, 7 (2), 725-730
- [5] Tsutsulaeva S.S., Documents and materials on the deportation of the Chechen people: general problems and the degree of their study, 2011, p. 196-203.

[6] Tsutsulaeva S.S. The problem of the deportation of the Chechen people in the modern historiography of Chechnya. 2014. S. 152-159.

[7] Podkolzina I.M. , Belousov A.I. , Uzdenova F.M. , Romanko L.V., Chernikova O.A. Forms of financial fraud and ways to minimize risks // Modern global economic system: evolutionary development vs. revolutionary leap. Scientific Communication Institute Conference, 2021, pp. 2197-2205.

[8] Podkolzina I.M., Taranova I.V., Paytaeva K.T. , Revunov S.V. , Abrosimova T.F. Innovative approaches to financial support of regional economic security. 2021, pp. 549-558.

[9] Elbuzdukaeva T.W., Gelagaeva A.V. M., Sugaipova A.M., Migration processes in the Chechen Republic at the turn of the 20th century, 2019, pp. 2690-2696

ENVIRONMENTAL ECONOMICS AND SUSTAINABLE DEVELOPMENT

Magomed Suleymanov¹, Aminat Huazheva², Elman Akhyadov³

•

¹Dagestan State University, Russia

²Adyghe State University, Russia

³Kadyrov Chechen State University, Russia

fefnews@mail.ru

akhyadov1990@mail.ru

Abstract

In recent years, the problem of climate change has become one of the most urgent. Its negative consequences will be most pronounced in northern countries with a carbon-intensive economy, such as the Russian Federation, for which an increase in average annual temperature is fraught with the destruction of infrastructure, an increase in morbidity and mortality, and the introduction of climate regulation measures by foreign partners can lead to a decrease in exports, loss of external markets. Accordingly, ensuring the decarbonization of the economy for Russia is an important task. In this regard, the purpose of the work is to identify the problems of decarbonization of the Russian economy. In the course of the analysis of foreign experience, it was revealed that in countries with the largest volumes of greenhouse gas emissions, decarbonization tools are actively used, mainly emission quota systems, carbon taxes, technical standards, and bans on the sale of carbon-intensive products. A distinctive feature of the climate regulation system being developed in Russia is the desire to take into account the assimilation potential of ecosystems. The most promising tools for the decarbonization of the Russian economy are analyzed: quota systems, carbon landfills, the use of technologies for capturing and pumping carbon dioxide into the subsoil, and the development of electric transport. It has been determined that the main problem with the use of these tools is their lack of consistency: the start of their work is scheduled for almost the same time, while their effectiveness depends on the results of each other's work.

Keywords: sustainable development, environmental priorities, economic efficiency

I. Introduction

In 2022, the Russian economy faces unprecedented challenges due to a sharp escalation of geopolitical tensions. The consolidated efforts of economically developed countries aimed at undermining the economic potential of the Russian Federation created an extremely unfavorable background for the country's economic development, which steadily worsened throughout 2022. The following circumstances were of fundamental importance:

1) the freezing of the country's international assets in the amount of more than 300 billion US dollars;

2) the growing sanctions pressure associated both with the restriction of the possibilities for interaction between residents of the sanctions initiating countries with Russian economic entities, and with the extension of relevant restrictions to residents of third countries planning to continue or develop cooperation with the Russian Federation ("secondary sanctions");

3) disconnection of leading Russian banks from international payment systems and the interbank system for transmitting information and making payments SWIFT (with the threat of extending this measure to the entire banking system of Russia);

4) the forced curtailment of energy cooperation (complicated by the destruction of the infrastructure for natural gas supplies to Europe through the pipelines of the Nord Stream 1 and Nord Stream 2 projects), as well as attempts to reduce revenues from Russian energy exports to third countries through the "price ceiling" mechanism ;

5) refusal to cooperate with the Russian Federation in the field of high technologies (primarily dual-use technologies) and the actual coercion of companies from third countries to take similar steps (in connection with which, in particular, Taiwanese and South Korean companies stopped supplying microprocessors and microcircuits to Russia);

6) a full-scale attack on Russia's foreign trade relations in both export and import operations (including not only high-tech, but also standard civilian imports), which involves the withdrawal of the most favored nation treatment from Russia in trade (which allows it to apply an increased level of import customs duties to it), as well as the withdrawal of the status of a country with a market economy by the United States in November 2022 (which opens up opportunities for virtually arbitrary determination of the amount of anti-dumping duties against goods of Russian origin).

II. Methods

The problem of climate change is one of the most urgent in the world. To reduce its negative impact on socio-economic systems, two groups of measures are distinguished: decarbonization and adaptation. Adaptation refers to "the adjustment of natural, social or economic systems in response to actual or expected climate change and its consequences". Among the adaptation measures, they consider the creation of protective systems from floods, early meteorological warning systems, cool zones, and the improvement of forest fire protection. These measures are not universal and largely depend on the specifics of a particular territory. The importance of such adaptation is generally recognized, but at the same time, external instruments of stimulation or pressure are not used for its implementation, which cannot be said about the decarbonization of the economy. Currently, climate change is recognized as irreversible, but in order to minimize the negative consequences, it is necessary to limit the temperature rise to 1.5–2 °C. To do this, it is important to reduce GHG emissions and their concentration in the atmospheric air, therefore, in many countries, priority is given to decarbonization. Thus, the UN Framework Convention on Climate Change set the goal of stabilizing the level of greenhouse gas emissions into the atmospheric air, and adaptation is mentioned only in passing. The Kyoto Protocol already pays more attention to adaptation, including international cooperation in preparing adaptation measures for individual territories. The Paris Agreement, in order to achieve the goal of "increasing the ability to adapt to the adverse effects of climate change", calls for developed countries to provide support (mostly financial) to developing countries in relation to both reducing greenhouse gas emissions and adapting to the effects of climate change . At the same time, another goal of the Paris Agreement is "changing the trajectory of financial flows towards a low-carbon economy" (respectively, their withdrawal from the economy based on the use of fossil fuels), which is already observed not only in the domestic, but also in the foreign economic policy of a number of countries. For example, the European Union (EU) has been practicing domestic carbon regulation through carbon taxes for about 30 years. The average size of such a tax in Europe is about 50 euros per tonne of CO₂-eq. Due to strict domestic regulation, the European Union is faced with the phenomenon of "carbon leakage" - the transfer of carbon-intensive industries to countries with friendly environmental regulation and more favorable conditions for doing business, which reduces revenues a certain amount of income into the EU economy, and also reduces the number of jobs. Moreover, goods produced in countries with lower

environmental requirements are cheaper and therefore more competitive, pushing European manufacturers out of the market [1]. Therefore, to neutralize these risks, the EU adopted the Green European Deal. As a key tool to protect against “carbon leakage”, a cross-border carbon tax (CAR) is proposed, which will be imposed on carbon-intensive products in accordance with the amount of greenhouse gas emissions associated with their production. Currently, the amount of CAR is not set, according to preliminary estimates, it will be from 25 to 75 euros per tonne of CO₂-eq. In addition, the European Commission has developed a plan to bring the EU economy out of the crisis caused by the coronavirus pandemic, where ET will be a significant source of income (5-14 billion euros per year in 2021-2027). There is also a certain likelihood that similar CARs will be introduced by the United States and some Asian countries, including China. In autumn 2021, the 26th Conference of the Parties to the UN Framework Convention on Climate Change was held. As a result, a number of agreements were signed. For example, 40 countries signed the Coal Agreement, under which they pledged to abandon coal energy during 2024–2040. (Russia, USA, Australia have not signed this document). The Transportation Agreement was also signed, according to which the parties must ban cars with internal combustion engines by 2040 (this agreement is not signed by China, Germany and the United States). In addition, the Methane Emissions Reduction Agreement was signed (China, India and Russia did not sign), obliging the parties to reduce methane emissions by 54%, and the Agreement to Stop Deforestation, under which 12 states (including Russia) will allocate \$12 billion and private companies \$7 billion. A significant achievement of the climate dialogues in 2021 was the increase in the number of countries committed to achieving carbon neutrality: in 2019, only 17 states announced this, in 2021 - already 152. In addition, it is noted that business is increasingly involved in such negotiations. It is worth emphasizing that within the framework of the climate dialogues, China and the United States – world leaders in greenhouse gas emissions (Fig. 1) – signed a joint declaration on the expansion of climate action in 2020 based on the results of their closed negotiations. The parties have pledged to keep the temperature rise "well below" 2°C.



Source: Rhodium Group

Fig. 1: Global Greenhouse Gas Emissions: 1990-2020 and Preliminary 2021 Estimates

Despite the fact that the United States is still very high in greenhouse gas emissions, with the accession of President George Biden, the country has been very actively engaged in "greening" the economy. Thus, the United States again became a party to the Paris Agreement, two decrees were signed canceling the construction of the Keystone XL oil pipeline and introducing a temporary

moratorium on the lease of subsoil plots for oil and gas production. Changes were also made in the Presidential Administration: the Office of Domestic Climate Policy appeared, all federal bodies and institutions were charged with the duty to cooperate with the Office and provide it with the information, support and assistance that it may request. In addition, the US is developing a climate finance plan and measures to stop international financing of a carbon-intensive economy (Roginko, 2021a; Roginko, 2021b); approved a program to co-finance projects for capturing and injecting carbon dioxide into the bowels of the Earth with a total amount of financing of 270 million US dollars; started in China as well [2]. The country aims to achieve carbon neutrality by 2060 and to reduce CO₂ emissions by at least 65% by 2030 compared to 2005¹⁰. Thus, according to the International Energy Agency, China is and will remain the leader in introducing renewable energy capacities for at least 5 years. The country currently has 43% of the world's renewable energy capacity installed¹¹. Also in July 2021, China launched a carbon trading system. The Chinese quota mechanism will be the largest in the world and will double the coverage of greenhouse gas emissions. At the same time, Chinese allowances are quite cheap (\$6–7 per tonne of CO₂-eq.), which potentially reduces their effectiveness. At present, China's cap-and-trade system covers about 26% of greenhouse gas emissions in the country and 6.3% in the world. In addition, in 2021, China launched a project to capture and store carbon dioxide on the sea shelf¹², studies on the feasibility of introducing such technologies have been ongoing since 2015 (Burandt et al., 2019). At the same time, China opposes the introduction of a carbon tax both domestically and for external regulation.

III. Results

At the beginning of 2021, consumer prices began to rise in the EU, and since April in the USA as well [3]. Moreover, during the pandemic, inflation was largely determined by rising food prices. However, in the second half of 2021, inflation began to be spurred on by rising energy prices. The large financial support provided to the population and businesses during the pandemic in developed countries and 31 quantitative easing led to a boom not seen since the 1970s. rising inflation. In the US, annual inflation in 2021 (December to December) was 7.0%, while in the European Union it was 5.3%. In 2022, rising energy prices fueled inflation. In the US, by June, consumer prices rose to 9.1%, then inflation began to slow down and in October it was already 7.7% at the annual level. In the future, prices will continue to decline and by the end of 2023 they may return to pre-crisis levels. In the EU, in 2022, prices continued to rise, which was completely determined by the rise in the price of energy resources, followed by an increase in prices for all other groups of goods. As a result, inflation in the EU in October reached 11.5% per annum. If it is possible to stabilize energy prices at the current high level (1200-1300 euros per 1000 cubic meters of TTF gas, 90-95 dollars per barrel of Brent), then it is very likely that prices will slow down, and from the spring of 2023 they will stabilize. However, a return to pre-crisis values is possible no earlier than 2024.

After a 3.0% decline in the global economy in 2020, a rapid recovery followed in 2021 with the global economy growing by 6.0%. In China, GDP growth for 2020 amounted to 2.2%, while in the rest of the world's major economies, a drop in production was observed in 2020. Such large economies as the USA, India, Russia already in 2021 exceeded the indicators of the pre-crisis 2019. The American economy grew in 2021 by 5.9%, the economy of India - by 8.7%, and Russia - by 4.7% . Almost all countries of the world overcame the consequences of the crisis and exceeded the indicators of 2019 in the second quarter of 2022. With the growth of the world economy in 2021 at 6.0%, only the global tourism sector did not reach the pre-crisis indicators, and this level will be exceeded no earlier than 2023. This means that there are significant reserves for the growth of the world economy in the coming years. A fall in world production in the coming years seems extremely unlikely to us.

Table 1: GDP growth rates, %.

	IMF assessment		IMEMO assessment	
	2022	2023	2022	2023
World	3,2	2,7	3,3	3,0
Developed countries	2,4	1,1	2,6	1,2
USA	1,6	1,0	2,3	2,0
Japan	1,7	1,6	1,6	1,5
UK	3,6	0,3	3,9	-1,0
Euro area	3,1	0,5	3,2	0,2
EU	3,2	0,7	3,3	0,1
Germany	1,5	-0,3	1,7	-0,5
France	2,5	0,7	2,6	0,5
Italy	3,2	-0,2	3,8	4,4
Developing and countries with emerging market	3,7	3,7	3,8	4,4
China	3,2	4,4	3,5	4,5
India	6,8	6,1	7,5	7,0
Brazil	2,8	1,0	2,8	2,5
Russia	-3,4	-2,3	-2,5	-1,5

Source: IMF WEO Database, IMEMO RAS

The Chinese economy, even with the continued use of lockdowns to combat the coronavirus, the existing economic problems, especially in the real estate market, will develop at a rate of 3-5% in the coming years. The Indian economy will develop at a rate of at least 7% per year. The US economy will grow at a rate of about 2% per year. We see the greatest risks in the development of the European economy [4]. However, according to IMF forecasts, growth in both the EU and WE will be positive. At the same time, in Germany and Italy in 2023, a drop in production by 0.5% and 0.3%, respectively, is possible. It all depends on how these economies go through the winter of 2022-2023. If the closure of entire industries can be avoided, then the economies of these countries can avoid falling. The Russian economy, after a rapid recovery in 2021 (growth by 4.7%), will be in the zone of negative values in 2022. According to our estimates, the fall could be up to 2.5%. In 2023, there will most likely also be a drop in production of about 1.5%. In the future, economic growth will begin, which will be 2-2.5%. World trade. The general situation on the world market is characterized by the action of a number of threats: the epidemiological situation, trade and technological wars, political and military conflicts. At the same time, the effect of factors constraining the growth of trade is intensifying [5]. According to the IMF, the growth rate of world GDP is declining. If in 2021 they amounted to 6%, then in 2022 they are estimated at 3.2%, and in 2023 they are projected at 2.7%. It can be assumed that in 2023 the growth rate of the physical volume of world trade, which in 2022, according to preliminary estimates, decreased from 10% to 4%, will decrease even more and amount to 2-3%. If during the period of recovery growth in 2021 world trade grew approximately 1.7 times faster than world GDP, then in 2022 this ratio was already 1.3, and in 2023 the growth rates of trade and GDP will become extremely close and the elasticity coefficient world trade in terms of GDP, in all likelihood, will be equal to about 1. In subsequent years, the growth rate of world trade will be slightly, 1.1-1.2 times higher than the

growth rate of world GDP. Although global trade has surpassed pre-pandemic levels as early as 2021, the impact of COVID-19 is still being felt. It is especially clearly manifested in the policy of the PRC, which is characterized by extremely strict sanitary measures. The slowdown in China's economic growth observed today and expected next year can play a significant role in curbing world trade.

IV. Discussion

The climate agenda and the transition to a green economy. The results of the COP27 climate summit in Egypt in November 2022 reflected the reformatting of the global climate agenda. Developing countries have shifted their focus to the financial aspects of decarbonization and demethanization, making their climate policy directly dependent on receiving financial assistance from developed countries [6]. The latter did not fulfill their own promises made at the Earth Summit in 1992 and at the conclusion of the Paris climate agreement in 2015 to send \$100 billion annually to developing countries to support their decarbonization and demethanization efforts. Rising prices for imported oil and natural gas, the need to repay external debt, weakened by measures to combat COVID-19 are forcing developing countries to develop coal-fired power generation, relying on their own coal reserves. At the global level, the energy transition will take longer and cost substantially more than previously thought. In general, COP27 saw a reorientation of the global climate discussion from the problems of mitigating greenhouse gas emissions by ousting fossil fuels from the economic circulation to the problems of adaptation to global warming. An important breakthrough was the legitimization of the use of so-called natural solutions to achieve the goals of "clean zero". To compensate for the loss of imports of Russian gas, coal, oil, oil products and other raw materials and intermediate goods, the EU is forced to return mothballed coal-fired power plants to operation and extend the life of nuclear power plants, which currently slows down the energy transition. However, the return to fossil fuels and nuclear power will prove to be temporary. State subsidies, investments and other forms of support for green energy continue to grow both at the EU level and in the leading European economies. Moreover, unprecedentedly high gas prices objectively give rise to incentives for the advanced development of solar and wind generation, and also make hydrogen, biomethane and other natural energy sources more competitive in price. The US is accelerating its energy transition, which includes natural gas as well as coal and oil, with widespread use of industrial carbon capture and storage systems [7]. Passed in August 2022, the Inflation Reduction Act calls for more than \$370 billion in tax credits and subsidies from the federal government to support decarbonization and upgrade energy infrastructure to adapt to new renewable energy sources through 2031, and as well as the promotion of electric vehicles. Benefits will be provided exclusively to American and North American companies, as the law requires an increase in national content in the cost of products. In fact, the trend towards political reshoring to North America of critically important for the "green" transition industries has been fixed. Technological and investment protectionism in favor of North American manufacturers also aims to reduce the dependence of the American and global economy on China, the world's largest exporter of environmental products, while at the same time undermining the competitive position of European companies. American "green" protectionism is also directed against South Korea (a major exporter of electric vehicles), Malaysia (solar panels).

In Russia, there is also an increase in activity regarding the development of its own climate regulation system. The first step for this was the Federal Law "On Limiting Greenhouse Gas Emissions", the purpose of which is "to create conditions for the sustainable and balanced development of the economy of the Russian Federation while reducing greenhouse gas emissions." As measures to limit GHG emissions, the law specifies state accounting for GHG emissions, targets and support for activities to reduce them [8]. The law obliges legal entities and

individual entrepreneurs, whose activities are accompanied by GHG emissions of 150 thousand tons and more, to submit reports to the Ministry of Natural Resources. Also, the above entities are allowed to implement climate projects, the positive effect of which will be taken into account when compiling the register of carbon units. The Strategy for Social and Economic Development of the Russian Federation with Low Greenhouse Gas Emissions became the key strategic document to ensure the decarbonization of the national economy [9]. According to this document, within the framework of the target (intensive) scenario, it is necessary to introduce carbon pricing, quota mechanisms, technologies that increase the absorptive capacity of ecosystems, and public non-financial reporting systems for businesses. If this scenario is successfully implemented, by 2050 the following results are predicted: an increase in the share of "post-industrial" industries in the structure of the economy by 11.8 percentage points and a decrease in the share of "traditional" industries by 9.4 percentage points compared to 2020 year; the annual growth rate of non-energy exports is 4.4%; annual economic growth rate - 3%; reduction of GHG emissions by 910 MtCO₂-eq., increase in absorption capacity to 665 MtCO₂-eq [10]. At the same time, decarbonization processes in Russia are just beginning, and foreign experience cannot be called universal, so we consider it appropriate to analyze individual decarbonization measures and the possibility of their application in the Russian Federation.

The trend towards decarbonization and demethanization is observed all over the world. At the same time, its acceleration in developing countries is limited by the cost of technologies and equipment, the macroeconomic situation at the global and national levels (inflation, public debt, slowdown in economic growth), the situation in the energy markets, and the political will of the authorities. According to the report of the Intergovernmental Panel on Climate Change, limiting temperature rise to 1.5°C will require, among other measures, an early phase-out of fossil fuels. The relative cheapness of coal and natural gas has long served as a competitive advantage for developing countries, and the abandonment of these fuels can increase the cost of generating electricity. In addition, the energy transition must be "fair," meaning that the state must assume responsibility for compensating for losses and providing alternatives to affected populations (such as miners or coal-fired workers) [11]. Adaptation measures to date are fragmented and unevenly distributed around the world. For example, African countries most vulnerable to climate change have the least financial resources to build infrastructure that is resilient to climate shocks. In 2022, Russian gas exports declined significantly, however, rising fuel prices avoided serious negative consequences for the budget. Thus, revenues from the sale of oil, oil products and natural gas in the key European market for the country in 2022 are almost twice as high as in the previous year. According to available data, the reduction in pipeline supplies to the EU in the first seven months of 2022 was 40%. For 2022 as a whole, a more significant drop in exports can be expected, since pipeline deliveries to Europe account for 69% of Russian exports.

References

- [1] Gessen S.M., Vorotnikov A.M. Carbon polygons - a new scientific and educational project for the Arctic // *Arktika 2035: topical issues, problems, solutions*. 2021. No. 2(6). pp. 98-104.
- [2] Ulyanova M.O., Sivkov V.V. Marine Aspects of the Carboniferous Polygon in the Kaliningrad Region // *Study of Aquatic and Terrestrial Ecosystems: History and Modernity: Sat. report int. scientific jonf. - Sevastopol*, 2021. S. 48-49.
- [3] It reaches the point of absurdity: how Russia will respond to the EU [Electronic resource]. – URL: <https://www.vesti.ru/article/2608990>
- [4] Carbon polygons open the way to colossal finances [Electronic resource]. – URL: <https://www.omskinform.ru/news/152989>
- [5] Alimov K.G., Alimov G.K., Alimov K.K. Nature-like agricultural technology: convergent

approach to laying carbon landfills // Agroforum. 2021.No. 8. pp. 26-29

[6] Gakaev R.A., Bayrakov I.A., Bagasheva M.I. Ecological foundations of the optimal structure of forest landscapes in the Chechen Republic. In the collection: Environmental problems. A look into the future. Proceedings of the III scientific-practical conference. Executive editor Yu.A. Fedorov. 2006.pp. 50-52.

[7] Gakaev R.A., Comprehensive assessment of the current state of the mountain-forest landscapes of the Chechen Republic and measures for their optimization. In the collection: Modern problems of the geocology of mountain areas, 2008.pp. 189-194.

[8] A.S. Salamova, Socio-economic factors in the fight poverty and hunger in the modern world: the scientific approach of Amartia Kumar Sen, 2023, 17(1), pp. 237-245.

[9] Salamova A.S., Global networked economy as a factor for sustainable development, 2020, p. 03053.

[10] Kantyukov R R., Kolybanov K. Yu, Ravikovich V I Information technologies for preparing control decisions in automated systems of environmental monitoring, 2019.

[11] Kampschreur MJ, Temmink H, Kleerebezem R, Jetten MSM, van Loosdrecht MCM. Nitrous oxide emission during wastewater treatment. Water Res. 2019, pp.4093–4103

ANALYSIS OF THE USE OF COATED PIPES IN MARINE VESSELS

Vagif Gasanov, Elvin Ibragimli



Azerbaijan State Marine Academy

vgasanov2002@yahoo.com

ibraquimli93@mail.ru

Abstract

The information obtained through Arduino microcontroller is described in graphical dependencies in real-time mode of the result. When the crack is detected in the pipe, the maximum point of the recorded signal indicates on the diagram the part where the crack exists. Otherwise, the signal is described in the form of a straight line and indicates that no crack is found. The operator is able to determine any crack based on the signal recorded on the monitor. Due to the current leakage in the point of any crack the signal is transmitted to the Arduino microcontroller and, then, to the software. Based on the information received, the coordinate of the crack is found. So, since we obtain the information about the instantaneous displacement of the electrode with the encoder, we determine the coordinate of the crack according to the maximum value of the current leakage based on the diagram obtained.

Keywords: electrode wire, silicon pipe, marine ships, installation process, diagnose the cracks

Introduction

To diagnose the cracks in silicon coated pipes in offshore oil fields, proper organization of the work of the naval fleet, ensuring the silicon pipe strength and durability, the complete dependence of the region on the wave regime were studied. The wave quantities that characterize the wave mode are wave elements. To the wave elements include the wave height, length, period, the wave peak state according to the sea level, and etc.

The studies were carried out in the marine ship reservoir. The studies of the location of the large oil field in the open sea in this district helped to create the necessary conditions. In addition, it should be taken into account that hurricane wind waves approach ocean waves with a speed up to 40m/sec.

At present, the defects found in $\varnothing 400 \times 20$ mm pipelines of 35 km length drawn from marine ship to the shore are in the range of 1.5-3.5% and have created the basis for better quality of the installation process. It is recommended to use a relatively inexpensive programmable controller Panasonic FPWIN pro for the control system. A mathematical model of the process of the coating laying on the surface of pipelines with a diameter of $\varnothing 630 \times 30$, $\varnothing 300 \times 20$, $\varnothing 800 \times 40$ mm is specifically made. The technological process is carried out with the application of the defect scope to ensure more accurate diagnostics of cracks in pipe coatings [1, 2].

The accuracy of the heating temperature in the pipe coating is determined depending on the rotational, forward and geometric dimensions of the pipe in the technological installation. Errors in repeated measurements of the heating temperature of surfaces in pipe coatings of different diameters ($x_1, x_2, x_3 \dots x_n$) fully depends on the given voltages, leakage current, the size of the crack and its thickness and electrical conductivity. In the same way, in cooling mode the errors of repeated measurements (x_1, x_2, x_3) depend on the geometric size of the coating, the thickness of the coating, the cooling mode, that is, the brand of the

Comparative meteorological characteristics of the flaw detector are shown in Table 1.

Table 1: Determination of the pipe coating cracks through a diagnostic device

Defect scope parameters	Defectoscope	
	Korona C	Advanced performance defect scope
Test pipe diameter, mm	100	350
Pipe coating thickness, mm	2	4
Electrode movement speed, m/sec	0.15	0.25
Defect detection interval	0.4	0.2-1.0
Joint defect distance	15	9
Test tension value, kV	1-30	1-40
Test tension, Kv	0.1	0.1
Test tension tolerance, %	5	2
Acceptable tolerance, %	9.75	5.1

Table 2: Meteorological characteristics of a defectoscope

Pipe diameter and thickness, mm	The number of cracks arisen in the coating of 100 pipes (%)	The number of microcracks arisen through control in the coating of 100 pipes (%)
Ø300x20	6.51	1.8
Ø400x25	7.23	2.5
Ø500x30	5.12	3.2
Ø600x35	8.14	4.3
Ø800x40	9.75	5.1

Therefore, the average calculation of these parameters is defined as follows [2, 3].

$$x_c = \frac{x_1 + x_2 + x_n}{N} = \frac{1}{N} \sum_{i=1}^n x_i \quad (1)$$

where,

x_i is the fault of the parameters of the technological regime upon making the coating in each pipe.

n is the number of cracks formed inside pipes.

N is the number of pipes with a common coating.

The number of absolute errors in the determination of cracks in any pipe coating is calculated as follows:

$$\Delta x_i = x_c - x_i \quad (2)$$

$i = 1 \ 2 \ 3 \ ..n$

Thus, the average absolute errors in measurements are calculated as follows:

$$\Delta x = \frac{1}{N} \sum_{i=1}^n \Delta x_i \quad (3)$$

The nominal faults are found by the formula $\varepsilon = \frac{\Delta x}{x_c}$.

Table 3: Complete fault characteristics in measurement of cracks

Pipe diameter and thickness	Coating thickness δ, mm	Average fault value, $\Delta x, \%$	Quadratic value of faults, s, %	Crack number, n
Ø300x20	1-1.5	2.78	2.63	1-3
Ø400x35	1.5-2.0	3.24	3.12	2-3
Ø500x30	1.5-2.5	3.68	3.54	3-5
Ø600x35	2.5-3.0	4.72	4.66	4-5
Ø800x40	3.0-3.5	5.21	5.12	4-5

At the same time, the error of mid-quadratic inclination is determined as follows.

$$S = \sqrt{\frac{\sum(x_c - x_i)^2}{n}} \quad (4)$$

At the same time, the different faults of geometric dimensions of coordinates of the cracks were reported through the electric spark defectoscope via formulas (1), (3) and (4), and they are provided in Table 3.

The Table 3 shows the characteristics of the coatings observed in steel pipes of 100 different diameters.

As a result of the reports, the crack origin and fault values are shown below.

The information obtained through Arduino microcontroller is described in graphical dependencies in real-time mode of the result [3, 4].

When the crack is detected in the pipe, the maximum point of the recorded signal indicates on the diagram the part where the crack exists. Otherwise, the signal is described in the form of a straight line and indicates that no crack is found.

The operator is able to determine any crack based on the signal recorded on the monitor. Due to the current leakage in the point of any crack the signal is transmitted to the Arduino microcontroller and, then, to the software.

Based on the information received, the coordinate of the crack is found. So, since we get the information about the instantaneous displacement of the electrode with the encoder, we determine the coordinate of the crack according to the maximum value of the current. The accuracy of the heating temperature in the pipe coating is determined depending on the rotational, forward and geometric dimensions of the pipe in the technological installation.

It was also taken into account that the technological process, which is the basis of the causes of cracks and defects, was not carried out accurately and the employees did not comply with the technological regulations. With all this in mind, scratches on silicate coated pipes, star-shaped, wavy and groove cracks in the form of fish flakes, black dots, thin cracks with small holes, and etc. occur. Geometric dimensions of such crack layers depending on the brand and thickness of the silicate coating accept the micro cracks in the range of 0.3÷3.0 mm and the macro cracks in the range of 3.0-5.0 mm, even the length of the cracks reaches up to 10 mm [4,5].

As a result, the temperature drop in the coatings of different brands should be determined in the operating conditions, and the characteristics of the coatings of different brands widely used are given in Table 4.

On the basis of the experiments, the optimized heating and cooling time in all branded silicon coatings is considered appropriate for the purpose in the interval $\tau=25-50$ minutes. In order to fully implement these modes, the coating inside the pipe is cooled to a constant drop temperature, and the air is adopted as a cooling agent. Depending on the intensity of the air supplied to its surface with a special cooling apparatus, the cooling process is carried out [6, 7].

The cooling temperature of the refrigerator is determined by the following formula as known.

Thus, when cooling the coated pipe, the temperature area of the coating is obtained by solving the initial and boundary conditions of the differential equation of non-stationary heat

conduction of the double cylinder. The temperature during cooling on the surfaces of the pipe coating according to the solution is determined by the following formula [8, 9].

$$T_1 = 9.81 \exp\left(\frac{a\tau}{R}\right) \quad (5)$$

where: T_1 is the temperature on the coating surface upon cooling, a is the coating temperature transfer coefficient; τ is the cooling time.

$$R = \frac{R_3^2 - R_2^2}{R_2^2 - R_1^2}$$

is the relative coefficient of cross-section of the pipe and the coating. So, the temperature drop is determined in the cooling process as follows $\Delta T = T_1 - T_2$.

Table 4: Thermal and physical properties of the coatings

Thermal properties of the coating	The coating industry brands				
	EP-1	EP-2	EP-10	EP-20	EP-30
Linear expansion coefficient $\lambda, 10^{-7} C^{-1}$	103	89	50	32	64
Coating softening temperature °C	520	580	620	650	690
Heat transfer coefficient 20°C, Vt/m °C	0.63	0.92	0.89	0.91	0.98
Coating density 10 ⁻³ kg/m ³	1.1	1.29	1.38	1.41	1.48
Special heat capacity Cal/kg °C	1.7	1.8	2.1	2.8	3.2
Constant temperature drop in cooling (overheating) $\Delta T, °C$	8.2	7.5	5.0	10.0	9.5

*Note: EP – type of epoxy coating

Based on this formula, automatic adjustment with the control system depending on $R_1, R_2, R_3, Q, T_1, T_2$ parameters was carried out by adopting the temperature fall of the cooling process in the single time, i.e. $\tau=1$ min in the interval of $t_0 = 5 \div 10^\circ C$.

This study was carried out in the sequence as indicated in the "Matlab" in simulating package. The task of the system is to adjust the cooling process ($5 \div 10^\circ C$), keeping the fixed given values of the cooling speed with the help of the cooling agent, as a result of the inclusion of high-temperature coated pipes into the cooling chamber.

The silicon coated pipes are dried at $20 \div 30^\circ C$ for some period and delivered to the furnace assembly to be heated at high temperature to obtain a full smooth coating [10, 11].

The silicon coated pipes entered the oven are treated as double cylinders. As the temperature in the oven is stable at $1000^\circ C$, it is accepted that the heat is evenly distributed along the surface of the pipes, since upon heating the temperature changes only in the radial direction of the pipe.

By applying the differential equation of thermal conductivity of the double cylinder to the coated pipe, using the initial and boundary conditions of the heating of the pipes, the mathematical expression of the regulatory parameters is obtained as follows [11, 12].

Conclusions

1. The coefficient of thermal conductivity versus the heating of the wall of a glass coating on a pipe was investigated experimentally. It should be noted that the coefficient of thermal conductivity of the glass coating on a pipe increases by several tenths of a watt with the temperature of the coating on the wall of a pipe rising up to $600^\circ C$.

2. These investigations show that an increase in the temperature of the glass coating effects a significant improvement in its thermal conductivity. The highest thermal conductivity obtains for coatings by glass of the makes S-89 and S-52-1. These makes of glass are recommended for coating pipelines operating at heightened coolant temperatures. On experimentally determining the

coefficient of thermal conductivity of a glass coating on pipes the maximum spread of the experimental data was equal to 1–3% depending on the change in glass temperature.

References

- [1] Brondel D., Edwards R., Hayman A. Corrosion in the Oil Industry // Oilfield review. 1994. V. 6, No. 2. P. 4 – 18.
- [2] Ibragimov N.Yu. Heat Resistance and Strength of the Silicate Coating of Pipe // Chemical and Petroleum Engineering. 2016. V. 52, No. 1 – 2. P. 48 – 49.
- [3] Ibragimov N.Yu. Glass Coating Deposition Temperature on the Inner Surface of Heat-Exchange Tube // Glass Ceram. 2019. V. 76, No. 5 – 6. P. 225 – 227.
- [4] Ibragimov N.Yu. and Ibragimli E.N.. Experimental investigation of the thermal conductivity of glass coatings on pipes // Glass and Ceramics, Vol. 79, Nos. 7 – 8, November, 2022.
- [5] Gasanov V.G., Ibragimli E.N. Study of optimal operating conditions for tubes of ship heat exchangers // Materials of the I International Scientific and Practical Conference “Problems of Sustainable Development of the Marine Industry”, November 3-5, 2021, Kherson, Ukraine, pp. 211-214.
- [6] Gasanov V.G., Ibragimli E.N. Optimal mode for applying a silicate coating on the surface of a heat exchange pipe//ASMA, International scientific and technical conference on "Innovative perspectives on development of technical and natural sciences", November 25-26, 2021, Baku, p.130-133.
- [7] Alekseev Yu.V., “Selection of corrosion resistant pipes for field conditions,” *Inzh. Praktika*, No. 1, 64 – 71 (2001).
- [8] Alexandrov V.S. and Dorofeev A.G., “Investigation of the corrosion resistance of vitrified pipes and pipelines”, *Korroziya Zashch. Neftegaz. Prom-sti*, No. 1, 14 – 17 (1984).
- [9] Petzol'd A.V. and Peshman G.A., *Enamel and Enamelling* [in Russian], Metallurgiya, Moscow (1990).
- [10] Kondrashev V. V. and Yampolskii A. V., “Experimental investigation of the coefficient of thermal conductivity of glass-enamel coatings,” *Khim. Neft. Mashinostr.*, No. 10, 16 – 18 (1996).
- [11] GOST 26-01-1255–83. Glass-Enamel and Glass-Ceramic Coatings. Testing Methods for Corrosion Resistance in Acids and Alkali [in Russian], Moscow (1995), pp. 87 – 89.
- [12] Gureev V.M. Improving the efficiency of shell- and-tube heat exchangers using hole and half-ring re-cesses. *Energetika Tatarstana* [Energy of Tatarstan], 2014, no.3-4, pp.61-64. (in Russian)

NEWEST TRENDS IN INTERDISCIPLINARY RISK-BASED RESEARCH AND GOVERNANCE OF CRITICAL AND STRATEGIC INFRASTRUCTURES

Sviatoslav Timashev^{1,2}



¹ Science & Engng Center «Reliability and Safety of Large Systems and Machines», Ural Branch, Russian Academy of Sciences, Yekaterinburg, Russia

² Ural Federal University, Yekaterinburg, Russia

Timashevs@gmail.com

Abstract

This paper is a condensed version of the keynote lecture presented at the opening of the fifth Eurasian conference on Risk in Baku, Azerbaijan, October 17 2023. It is mostly based on results of the content analysis of 1500+ peer reviewed papers related to reliability, resilience, risk and safety of infrastructure systems published over the last 25 years, provided by renowned international specialists in these topics.

Keywords: interdisciplinary risk-based research, trends, smart systems, interdependent biosociotechnical critical infrastructures, management, governance

I. Introduction

The increase in the epistemic (fundamentally intrinsic) and aleatory uncertainty of the modern world, increasing role of the human factor (both individual and collective) in the occurrence of accidents and disasters created an imperative for all levels decision makers (DMs) to take into account the global technological trends that simultaneously help mitigating existing risks and generate new risks. The concept of high convergent technologies became a conscious response to the challenges presented to science by the part of modern society that was concerned by the uncontrolled development of technology.

In 2002, M. Rocko and V. Bainbridge, in their report to the US National Science Foundation (NSF), proposed the concept and first used the term NBIC convergence, built on the principle of a synergistic combination of the four fastest growing scientific-technological areas with great economic potential: N – nano- (science and technology), B – bio- (technology and medicine), I – information technologies, including advanced computing and communications, C – cognitive sciences (including neuroscience) [1–4].

Currently, there are several converging technologies in use around the world. For example, the NSF supports three such concepts:

- NBIC (Nanotechnology, Biotechnology, Information technology + Cognitive science); some scientists believe that the future of natural sciences belongs to NBIC
- GRAIN (Genetics, Robotics, Artificial Intelligence + Nanotechnology)
- BANG (Bits, Atoma, Neurons, Genes).

The European Union is funding the concept of convergent technologies for the European Knowledge Society [5]. The Canadian government is funding the Canadian Biosystems Foresight

Pilot Project. In Russia, the Kurchatov Institute supports the concept of NBICS (NBIC + Social Sciences) [6–9].

II. Convergent technologies and sciences for creating smart safe infrastructures

To solve regional problems of risk and safety of critical and strategic infrastructures (in general, of all artificial nature), in 2016 the MABICS-convergent technology was proposed, as related to applied and engineering sciences [10, 11]. MABICS stands for: Stochastic Mechanics, Artificial Intelligence, Biotechnology and biomimicry, Information Theory, Cognitive and Social Sciences. MABICS technologies are initially human-centric (Fig.1). When choosing a combination of convergent sciences, for creating smart infrastructures the author proceeded from the need to:

- Harmonize the coexistence of the oppressed first and developing second, artificial, nature to ensure the stability of biodiversity and the well-being of the noosphere
- Use the achievements of these rapidly developing disciplines and technologies with great economic potential to create a smart second nature that adaptively changes with changes in man himself and his needs
- Create the necessary scientific tools to ensure the fulfillment of the first two goals
- Structure an umbrella science containing the core components of knowledge and technology needed by professionals involved in the design and operation of smart cyber physical infrastructures and systems serving modern society.

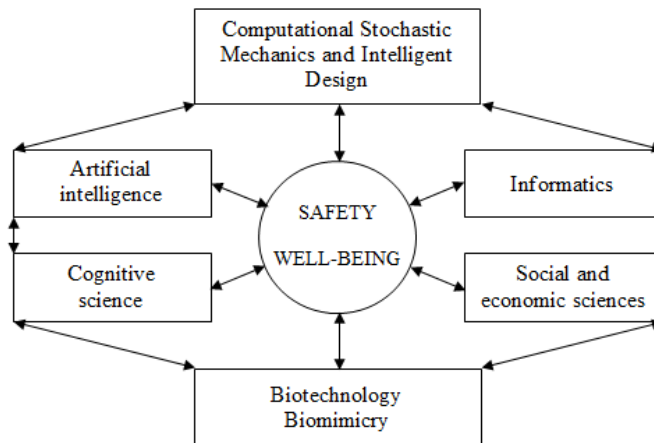


Fig. 1: Components of MABICS convergent technologies

None of the existing disciplines can provide the necessary solutions to such infrastructure problems. MABICS technologies are initially human-centric. In this regard, prof. A. Gheorghe (Old Dominion University, Virginia, USA) in 2007 proposed creating an umbrella science, which he named *Infranomics* (*Infrastructure + Economics*). This science is to serve as a universal discipline of disciplines, collecting all knowledge, which may someday be required to solve problems of political economy and economics of critical infrastructures. At the same time, A. Gheorghe did not indicate how to collect and structure this knowledge base and database [12].

Another main reason for creating an umbrella science for cyber physical infrastructures is the need to train modern specialists in the field of their design and operation.

The presence of such structured umbrella science simplifies and speeds up the training of specialists who are fluent in MABICS technologies and disciplines, and the formation of scientific groups to study infrastructure systems.

The author called the umbrella science based on MABICS technologies *infranomics*

(*infrastructure + cybernetics*), and considers infranetics as a branch of infranomics.

Infranetics includes all studies of MABICS technologies related to the design, management and governance of bio-socio-technical infrastructures at all stages of their life cycle.

Unlike NBIC technologies, the convergence that is ensured by nanotechnology, which allows blurring the line between physics, chemistry and biology, the fusion of MABICS technologies has a different nature. The gradual convergence of MABICS technologies is ensured by two factors:

- The common denominator – mankind and planet Earth, which set all the initial, boundary conditions and maximum permissible values of life support parameters for both humans and humanity during the design, construction and operation of all types of infrastructures (in general, all artificial nature)
- The unstoppable development of artificial intelligence (science and technology), which inevitably will take over the solution of an increasing number of problems currently being solved by MBICS technologies.

III. Knowledge base (KB) of MABICS technologies and Infranetics team of authors

To define the KB and its creators, the author turned to the leaders and organizers of world scientific schools and renowned scientists with a request to send their most important, in their opinion, key and review articles related to the topic of risk analysis of infrastructures. Following specialists responded: M. Beer (Leibniz University Hannover, Germany), B. Ellingwood (Colorado State University, USA), A. Gheorghe (Old Dominion University, USA), J. Li (Tongji University, Shanghai, China), N.A. Makhutov, V.V. Moskvichev (both from the Russian academy of sciences RAS), E. Patelli (University of Strathclyde, UK), M. Stewart (University of New South Wales, Australia), E. Zio (Polytecnico di Milano/Mines Paris/PSL, Italy/France). Some of the sent papers are shown as references [13–34].

The received key reviews and articles (in which 1,500+ publications were considered) were analyzed by objects, their properties and research methods. The results of this analysis are presented on the website *www.managementofrisk.ru* for the opportunity to review, post comments and add significant publications to the Infranetics' KB, and published in a preprint [35]. Despite being limited and inevitably subjective, the starting knowledge base (KB) of infranetics quite adequately reflects the research results of the world's leading schools. It is considered as author's modest attempt to outline the path for the creating, preserving and developing the infranetics' KB.

It is expected that this initial KB will expand as new knowledge in the field of infranetics and MABICS technologies is accumulated. The task of maintaining and developing the infranetics' KB is left open to all scientists and specialists who want to supplement and clarify it, using their experience and knowledge. The authors of publications included in the starting knowledge base of infranetics are, in essence, the founders of this umbrella discipline, and the content of these articles constitutes their contribution to MABICS technologies.

Infranetics as an umbrella science is carved out to solve the central problem of safe sustainable development of a territory / municipality / industry / corporation by harmonizing the regional risk of the second, artificial nature. This methodology is deliberately reduced to the following working hypothesis:

The sustainable development of a modern risk society in a market economy is mainly determined by the quality of management/governance of smart systems of interdependent biosociotechnical infrastructures IBSTI.

For this purpose, the following integral criteria for IBSTI governance and optimization are proposed [36]:

- regional average life expectancy in good health at birth (RALE)
- regional/municipal life quality index (RLQI)

- (sub/supra)resilience of regional systems of interdependent critical smart infrastructures (RSICI)
- entropy of development and degradation of regional systems of cyber physical infrastructures
- social entropy of regional society in ordinary and extraordinary conditions
- N -dimensional carbon footprint of regional CIS.

IV. Predictive management of territorial technogenic risk

The predictive management of territorial technogenic risk is constructed in accordance with five criteria, which are briefly discussed below.

4.1. Regional average life expectancy (ALE) in good health

The main ideas of managing territorial infrastructures according to the ALE criterion are [37]:

- determining the quantitative dependence of the life support system efficacy on the cost of creating the critical infrastructure, which ensures the livelihood of the population, and its safe operation
- optimal distribution of the fixed municipality budget according to the criterion of maximum life expectancy and the quality of life of citizens.

To achieve this goal, methods were developed for assessing the size, structure, and dynamics of the gross municipal product GMP and a study was conducted of the quantitative relationships between the total and specific (partial) budget expenditures of a large municipal entity and changes in the life expectancy for the same municipality, in our case, the city of Yekaterinburg [38].

The study of the dependence of life support on the quality of critical infrastructure operation is an important new direction of interdisciplinary scientific research, as it makes possible to ensure the safety of the population of territories and municipalities, and their sustainable socio-economic development.

4.2. Life quality index (LQI), Social willingness to pay (SWP), Statistical cost of life (SCL)

The use of the life quality index concept [39] to assess the degree of deterioration/improvement in the quality of life depending on the level of reliability, resilience and safety of regional infrastructure operation is a main contribution to the general theory of infrastructure risk. Its conceptual model is shown in Fig.2, and its formula is given below:

$$TLQI = G^q E \quad (1)$$

where G is the national (regional, municipal) product (\$/person/ year); E is the life expectancy for a given region, depending on age at birth; $q = w/(1-w)$ is the ratio of average working hours to leisure time available to members of society in a given region/municipal area; w is the time spent by an individual to create personal wealth G .

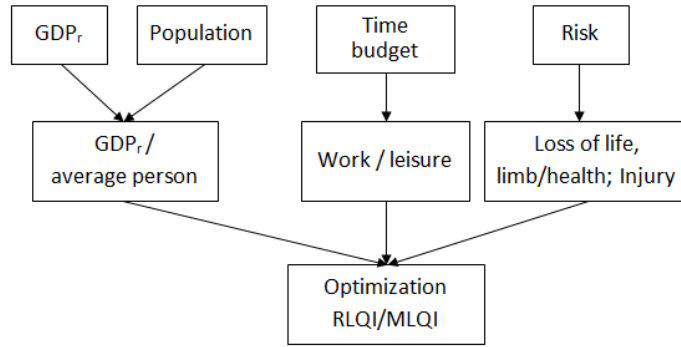


Fig. 2: Conceptual model of the quality of life index TLQI/MLQI

The LQI can be used as related to a country, region, territory/municipality, corporation and even a person. It is also needed to assess the so-called willingness to pay and the statistical cost for saving an anonymous life [39]. TLQI allows placing the management of technological risks in a broader context of social policy, by providing a unified framework for developing risk management strategies, in the form of four principles: (1) accountability to society, (2) maximum net benefit for all, (3) compensation for those who loses when changes occur, and (4) a long life in good health with maximum freedom of individual choice.

TLQI provides the necessary criterion for determining the maximum level of expenses, above which the costs of increasing industrial safety become unjustified. This level is called the “social willingness to pay” (SWP) measure. These principles, taken together, reflect the necessary attributes of a good life in modern society.

4.3. Criteria for sub resilience, resilience and suprapresilience

The development of the transformation strategies for regional and municipal systems of infrastructures into resilient smart territories is currently a hot topic [40–45]. It is well known that to achieve smartness, territories have to first become resilient. Resilience of sociotechnical systems is better understood using the antifragility concept.

The antifragility concept was initially proposed by N. N. Taleb to describe the financial world; he went on to promote this concept as a universal master key to «benefit from chaos". The concept of suprapresilience is focused on the second, artificial nature and arose as a complete analogue of the antifragility concept to describe the supra- and sub resilience traits of the smart interdependent biosociotechnical infrastructures. A visualization of the complex resilience concept is given in Fig. 3, 4.

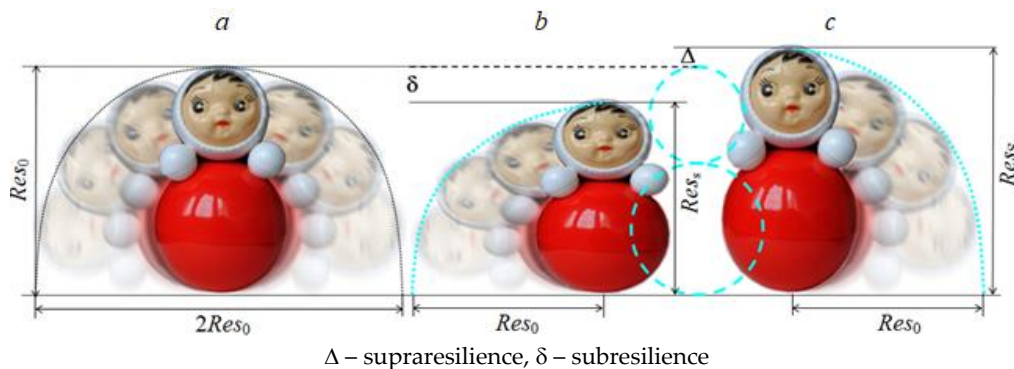
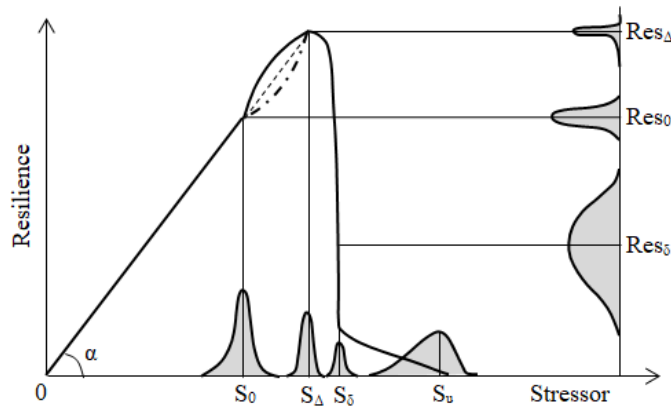


Fig. 3: Visualization of the concept of resilience on the example of a roly-poly doll:
 a – resilience; b – subresilience; c – suprapresilience

In medicine, the biological supresilience is called *Hormesis* and is observed, for instance, when small doses of alcohol, aspirin, Radon gas (in the case of lung cancer), and radiation are administered to mammals (including humans). The clearest examples of supresilience are (1) human post-traumatic resilience *growth* [46], and (2) many European and Japanese phoenix-type cities that rose from the ashes after the WWII, better than before. Multiple examples of sub resilience are (1) a person stricken with post-traumatic stress disorder (PTSD), and (2) corporations and municipalities that succumbed to stressors beyond their resilience.

It is interesting to note that N. Taleb's concept of fragility/antifragility does not contain (has no room for) the sub resilience concept.



S_0 is the calculated, standard value of the stressor; $S_\Delta > S_0$ is the limiting value of the stressor causing the effect of supresilience; $S_u > S_\delta > S_\Delta$ – stressor values leading to sub resilience of the object (damage, loss of years of life; S_u – stressor value leading to death

Fig. 4: Visualization of the concepts of physical (biological) supresilience Res_Δ , resilience Res_0 , subresilience Res_δ

In quantitative terms,

$$\text{Antifragility}(Q) = \text{Resilience}(Q) + \text{Overcompensation}(Q), \quad (2)$$

or, fully equivalent

$$\text{Supresilience}(Q) = \text{Resilience}(Q) + \text{Overshooting}(Q). \quad (3)$$

Supresilience and antifragility can also be defined respectively only as (resilience gain) / overcompensation. If we agree with (2) and (3), then the definition of supresilience of regions / cities/is:

Regional/urban supresilience is «the ability of a regional/urban system of critical infrastructure systems to withstand, adapt, and quickly recover from stresses and shocks, such as natural or man-made disasters, drought, violence, conflicts, while improving the initial parameters of its resilience».

N. Taleb's theory of antifragility, developed for the financial world was then proposed as a universal tool for *taking advantage of chaos*. A detailed mathematical analysis of this theory showed [47] that it is based on the assumption that during operation of the (financial) system a PDF of the "profit-losses" type is always and constantly available. While it is available for a financial scheme, it is not available for any engineering system, which is designed and maintained for the sole sake of producing income/profit and avoiding by all means any losses. Applicability of the antifragility concept for objects of second nature is entirely based on the fundamental availability of statistical information about the heavy tails of the distributions under consideration. Due to the fact that they are unavailable (do not exist), the antifragility theory is inapplicable to engineering science and technology. On the other hand, the fragility concept is applicable as it is considering only the losses due to system failure.

The concept of supra- and sub-resilience opens the door to meaningful exploration of quantitative dependencies/correlations between physical resilience of a system of systems and the biological/psychological/societal resilience of people who live inside and extensively use this system of ICIs in the context of different types of communities – from megacities, to big, medium size and small towns, to villages/settlements and tribal areas.

4.4. Entropy criteria (physical, statistical, informational and social)

Despite the universality of the entropy concept, its application to solve problems of risk analysis and safety of critical infrastructures requires using many other methods that are necessary for a quantitative description of the entire process of development of a disaster - from its inception (initiating failure) to complete collapse. This is because entropy, although a function of time, is a purely scalar quantity. Hence, any quantitative expression of entropy must be unambiguously linked to a certain state of the given system described by corresponding mathematical equations and socio-economic indicators. In other words, it is necessary to have an one-to-one correspondence between the state of a system and its integral entropy.

Many types of entropy are used in infrastructure risk theory. For instance, entropy is used (1) to model interdependence of components of multi-element stochastic systems (differential entropy) [48]; (2) to optimize the place where to build a facility in a city (informational entropy) [49]; to define some components of RALE (Keifitz type entropy) [50]; to construct heavy tailed distributions of dragon king type of stressors (Tsalis type entropy) [51]; to capture the social unrest during and after a major urban infrastructure accident (time dependent quant entropy).

The Dragon King (DK) is a dual metaphor for an event that is both extremely large and influential (the "King") and has a unique origin (the "Dragon") compared to its counterparts (other events from the same set). Didier Sornette developed DK theory [52]. This theory is based on the hypothesis that many crises are actually DKs rather than black swans, meaning they can be somewhat predictable. DK events are generated by or correspond to mechanisms such as positive feedback, tipping points, bifurcations, and phase transitions that occur in nonlinear and complex systems and amplify DK events to extreme levels (the perfect storm). The DK theory makes it possible to study extreme events, carry out their dynamic monitoring and achieve some predictability of such events, which is especially important for long-term forecasting of the risks of operating strategic infrastructures and systems.

The aforementioned is illustrated by the case of describing extreme wind speeds in the Arctic zone of Russia [53]. In this case the requirement that all sample data belong to the same family is violated. The main array of "intermediate" extremes (called *White Swans* WS), and the appearance of the largest and rarest phenomena in this sample (called *Black Swans* BS) belong to the same Weibull distribution. The other set of extremes belong to a different (but also Weibull) distribution, have a different genesis (dragons, dragon kings) and characterize fundamentally different objects (Fig.5). Using the κ -deformed Kaniadakis κ -statistics based on Tsalis type entropy it was possible to construct a generalized PDF that correctly assesses the most rare events (Figure 6), thereby reducing the space of possible *Black Swan* events [54–56].

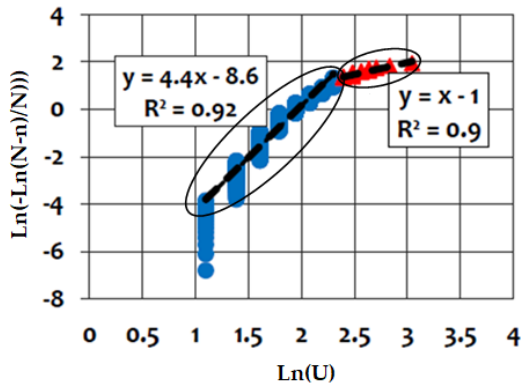


Fig. 5: Empirical distributions of extreme wind speeds of the year (1966–2013) [53]

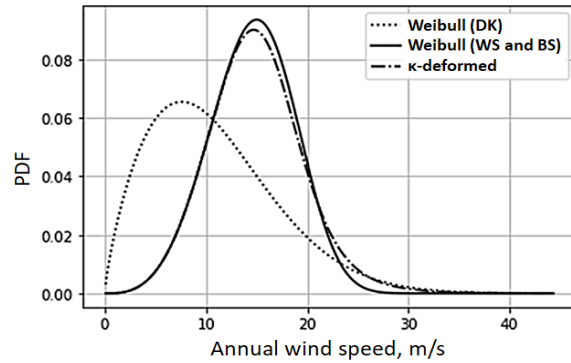


Fig. 6: Empirical PDFs of wind speed extrema, corresponding to three families of Weibull distributions: “WS and BS”, “DK” and κ -deformed [54]

The most challenging aspect of studying the reliability and resilience of socio-technical systems (STS) is the interdependence of their physical and social components over time, influenced by various stochastic stressors of different nature. Existing STS models inadequately consider the relationship between cyber-physical infrastructures (CPI) and the society that simultaneously utilizes, inhabits and owns the CPI environment. It is evident that further progress is required to assess the community resilience and quantify the socio-economic interdependencies that exist between the society and its cyber-physical systems. When assessing STS resilience, it is necessary to evaluate concurrently the resilience of both the physical and social components. It is clear that the resilience of the physical component directly influences the ability of the STS to support the activities of the society it serves, thereby affecting its overall resilience. The main question is: what parameter(s) should be used to connect the tangible with the intangible?

Recently a new approach was developed to quantify social unrest that inevitably occurs after each accident or natural disaster associated with the loss of operation of urban life support infrastructures [57] based on data from social networks (in the form of views, likes, comments, and reposts). This approach is characterized by connecting in real-time, simultaneously, the level of social entropy (as a measure of dispersion, chaos) on one side, with the level of STS physical damage; and on the other side, with the decision makers' (DMs) actions, aimed at mitigating the consequences of the high entropy accident. By revealing this connection, the correlation is established between physical damage and social discontent, and between the discontent and DMs' actions. Further analysis permits finding how effective these actions (governance) are in lowering the dangerous entropy level.

A quasi virtual scenario was constructed using data from a flood disaster that took place in 2016 in Southern Louisiana. According to this scenario there was a sudden drastic decrease in the number of users involved (points A and B), followed by a lengthy period of rather weak communication (from point B till point C) followed by a sudden increase of user activity (point C) caused by multiple reports of delayed insurance payments (Figure 7). Activities did not fade for a long time due to the inability of the Administration to respond appropriately.

The times when the social entropy (in our case, intensity of communications) was dramatically changing are connected to the specific actions taken by the City Administration, and to the values of the observed social entropy (points A and D). This kind of data collected after each incident can serve as a reference source, and be used for defining the strength and character of the interconnection of the material and the social.

The outlined algorithm of real time entropy analysis of the social activity of citizens in the case of critical urban infrastructure operational failure is comprised of:

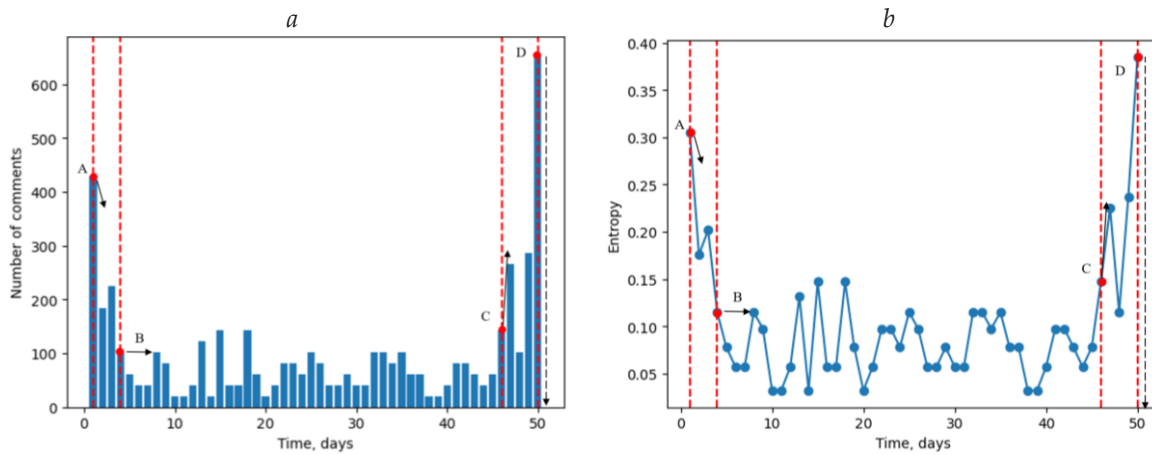


Fig. 7: Graph of the number of comments in time (a) and the day-by-day quant entropy curve (b)

- Plotting the total number of comments about the accident in social networks (an AI bot is being developed to automatically collect the needed information as it emerges in time)
- Constructing total and partial graphs of comments classified by their content (negative, positive, neutral, informative)
- Constructing an analytical PDF for each constructed histogram
- Constructing a quantized function of citizens' discontent entropy
- Constructing the first derivative of the discontent entropy function
- Pairing the time points of DMs decisions on mitigating the accident consequences with the time points of change that occurs in the intensity of discontent entropy generation
- Defining the entropy thresholds at which DMs start making decisions to mitigate/eliminate the consequences of an accident
- Accumulating a data base of dependency pairs "entropy quant size vs DM reaction type"
- Comparing different accidents with the same STS by social entropy indicators
- Developing decision support recommendations for DMs based on entropy analysis findings.

In author's view, social entropy analysis can potentially become one of the most important and versatile quantitative tools for city governing, as it provides a currently missing correlation between the measurable damage to cyber-physical infrastructure (CPI) and the poorly measurable (intangible) social damage to the community, and between DMs' decisions and mitigating actions and the decrease of social unrest entropy.

4.5. Carbon footprint of infrastructure life cycle

Over time, this criterion will become a determining tool when assessing the quality of functioning of bio-socio-technical infrastructures during their life cycle (stages of emissions: construction, operation, fugitiveness, and disposal). This criterion seamlessly connects the local restrictions on pollution with the overall planetary boundary conditions [58].

V. SP RASOSR® (Resilience and Security of a Smart Region)

In order to utilize the discussed above components of infrastructure governance, special software is needed. The first step in this direction was made by creating the RASOSR® (Resilience and Security of a Smart Region) cloud based software package [59] as a service (Figure 8) allowing management of infrastructure systems using the described above generalized regional quality criteria. The first module of this package:

- Ensures continuity of business flow of digital services and infrastructures
- Provides operational support for making management decisions based on the criteria of RALE and RLQI and willingness to pay (WTP)
- Organizes the living laboratory of convergent technologies activities
- Allows building a virtual digital model of regional resilience
- Supports the process of involving various regional and city actors in solving the resilience problem
- Structures the collected information (Big Data) about the relationships of serviced objects and modeling cascading effects
- Provides DMs with the opportunity to make informed choices about how to respond collectively and harmoniously to the ever-increasing shocks and stresses facing a region.

The MABICS approach to solving various problems of infrastructure systems reliability, resilience, risk-analysis and safety management and governance is visualized in Figure 9, in which a variant of governance/management is given using the MABICS convergent technologies. As an example of using the interdisciplinary approach to solving problems that comprise the algorithm shown in Figure 9, consider the task of creating the full group of risk scenarios (FGRS) of an accident which is needed to assure that all probabilities are taken into account (first line of the algorithm in Figure 9). The methodology of building such a FGRS involves applying the cross-entropy principle to Bayesian network models for creating most likely scenarios of the accident (Figure 10). In some cases, this FGRS is supplemented by scenarios that are generated by a group of people with specific cognitive capabilities (to be sure that the obtained FGRS is as complete as possible).

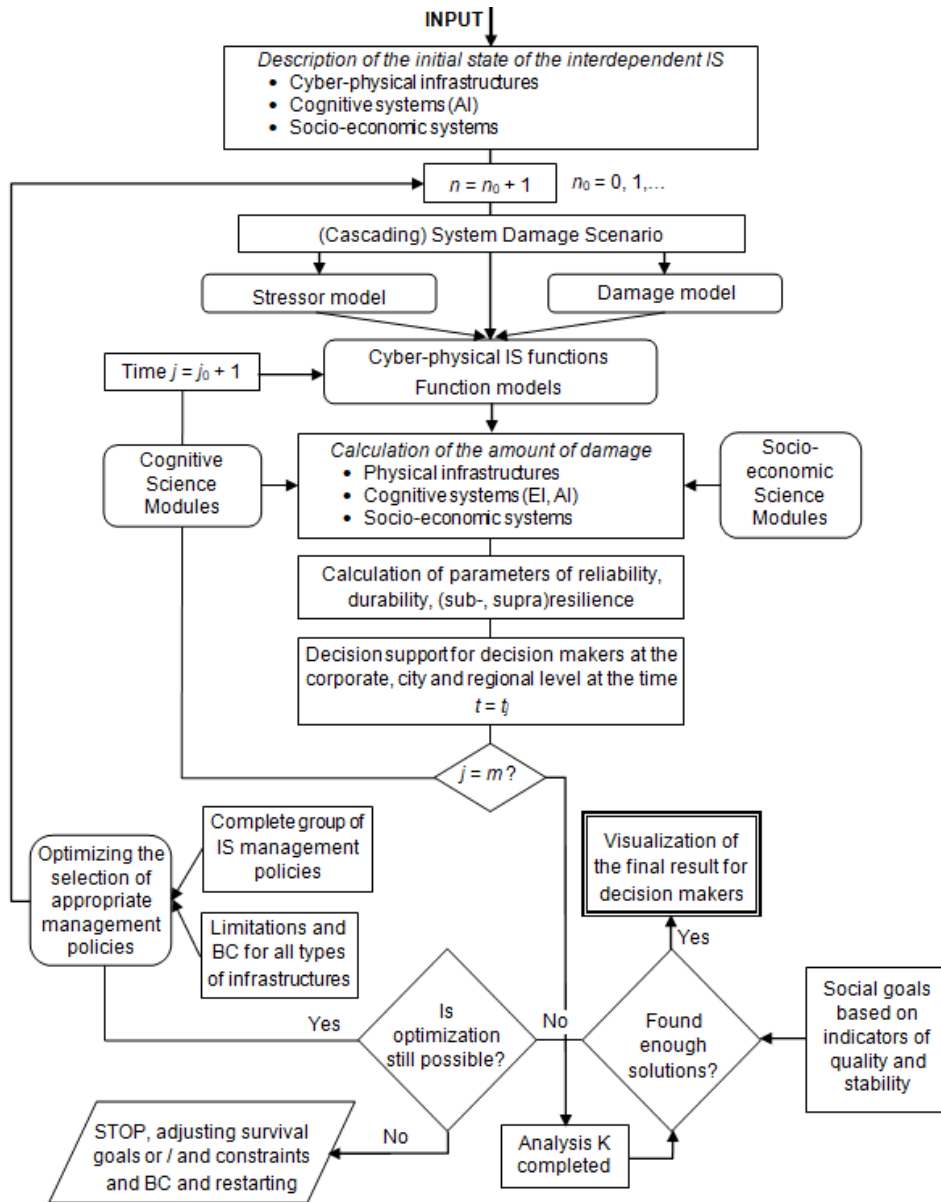


Fig. 8: Schematic block-modular diagram of the cloud-based SP RASOSR® as a service with built-in artificial intelligence (Version 1.3); BC – boundary conditions

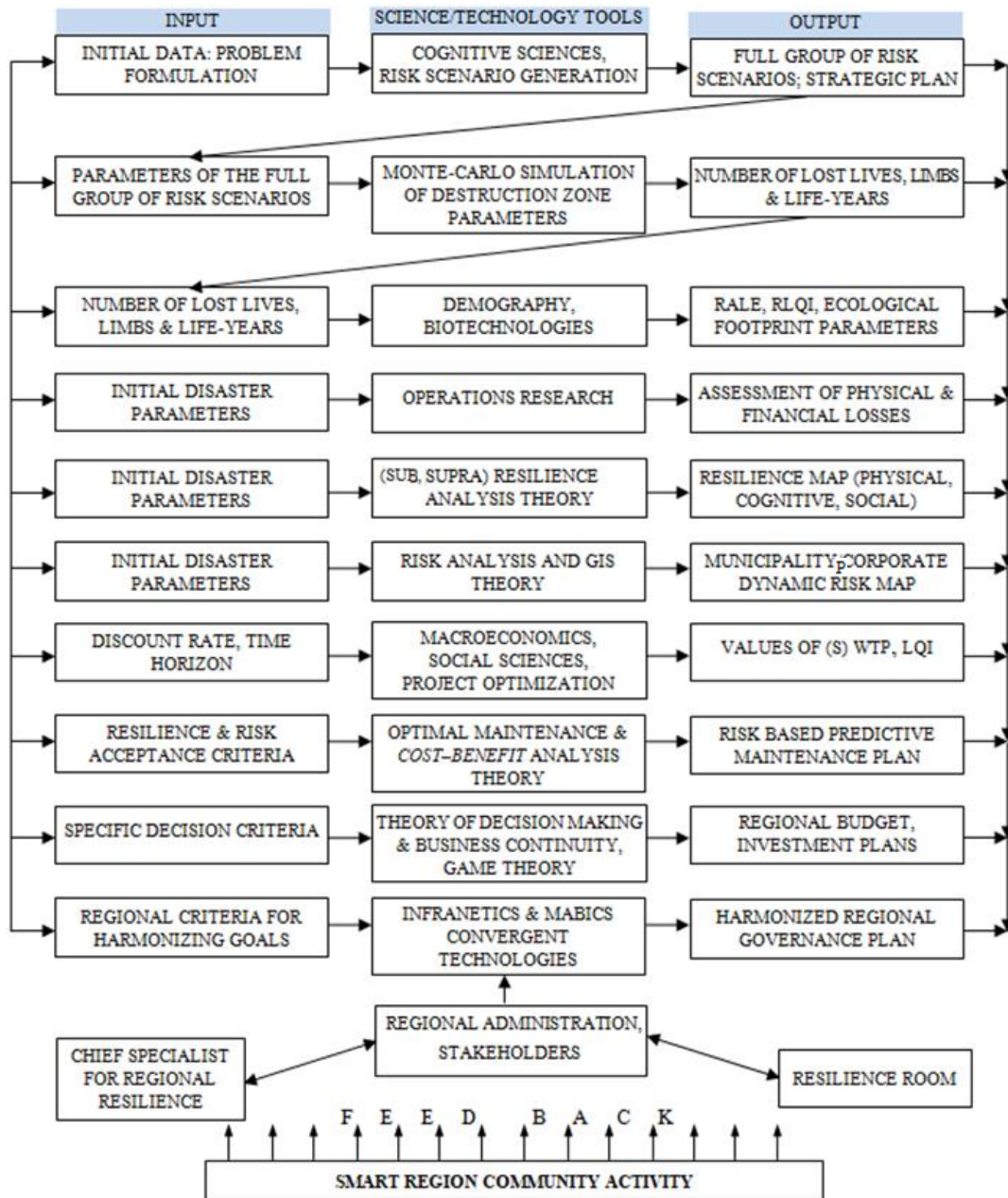


Fig. 9: Variant of a governance/management strategy based on regional resilience using infranetics tools and MABICS convergent technologies

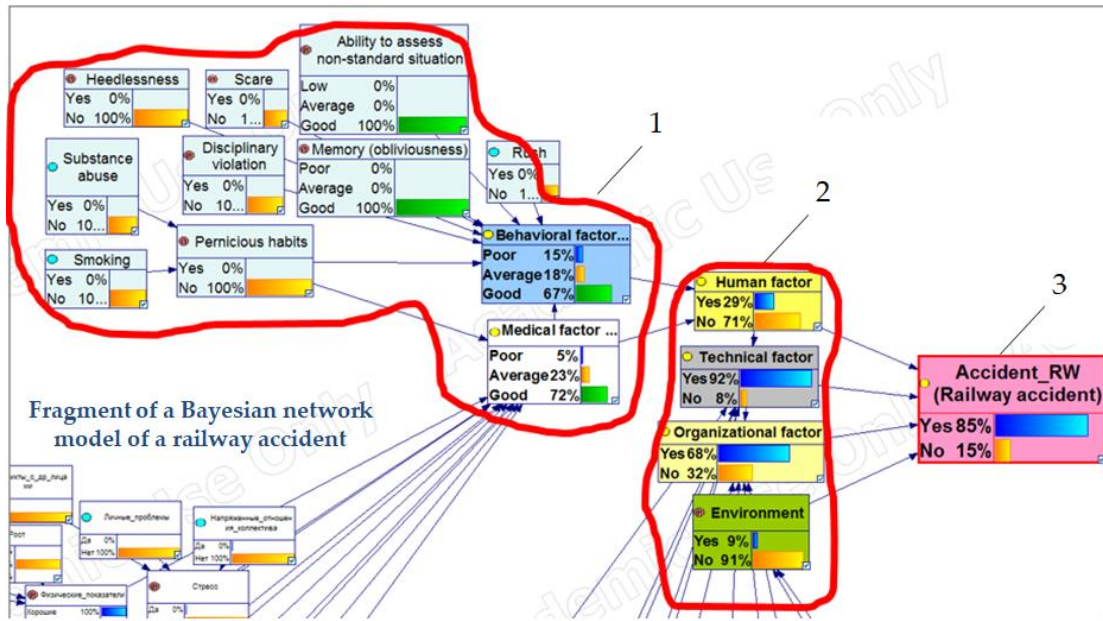


Fig. 10: Using cross-entropy to build a complete group of events when using Bayesian networks that model the development of various types of accidents, including those on the railway: 1—nodes of detailed accident reasons; 2—nodes of main accident reasons; 3—main accident node [60].

Modern science and computer technology are not ready to solve quantitatively some important problems of resilience and safety of large systems of systems of critical infrastructures. In these cases, the concept of a living laboratory of convergent technologies (LLCT) for governing a smart region is recommended [61]. The LLCT concept is a total rethink of a real life experiment that was first conducted in Boston, when architects and interior designers tried to get a sophisticated feedback from the end users of their product — a new apartment with built in furniture [62]. They actually built such an apartment and let a group of people to live in it for some time, and then asked them to give their opinion about the design.

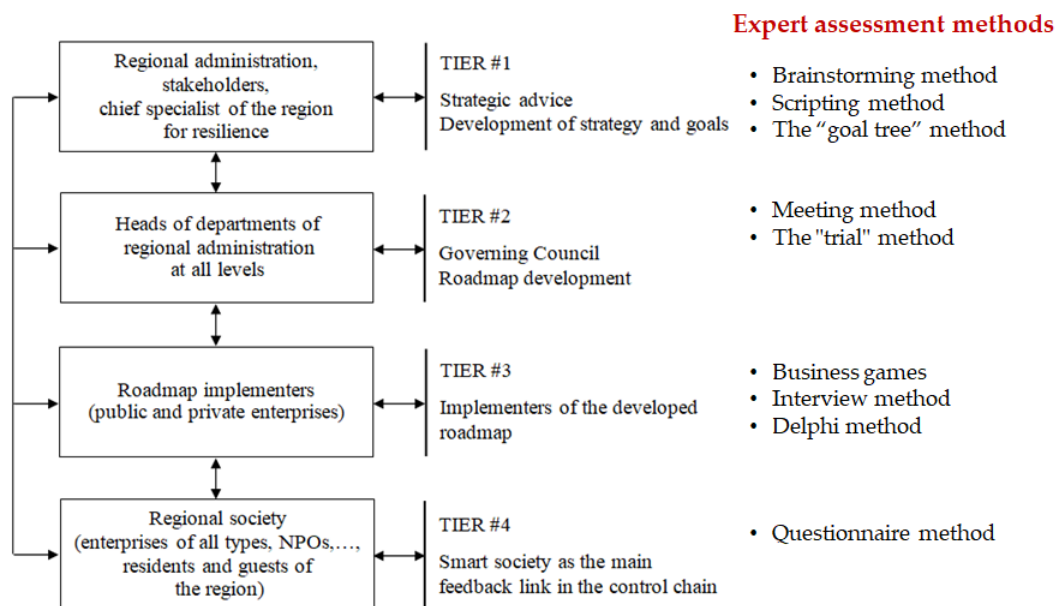


Fig. 11: The concept of a living laboratory of convergent technologies (LLCT) for governing a smart resilient and safe region

LLCT is a concept according to which the problem of resilience of an urban system of systems (SoS) is solved by the people who best know the SoS. Namely, by the specialists who run the SoS. They are the designated experts/actors (see Fig. 11, Tier #3). In order to understand better the concept, consider using the LLCT in Yekaterinburg.

At the initial stage, service representatives collect the information about city services (of different levels and scales) and their infrastructures, and enter it into a matrix. At the next stage, actors (representatives of city services most knowledgeable about their functioning) form a matrix of interdependencies (Fig.12), where the colors in the cells indicate the degree of influence of one infrastructure on another: red – strong influence, yellow – moderate influence; green – insignificant influence

A	B	C	D	E	F	G	H	I	J	K
	Koltsovo Airport	Metro	Heating	Central City Hospital No. 1	Power station	Gas supply system	Water supply	Sewage system	City administration	Telecommunications
Koltsovo Airport			Red	Green	Red	Yellow	Red	Red	Green	Red
Metro	Green		Yellow	Green	Red	Green	Green	Yellow	Green	Green
Heating	Green	Green		Green	Red	Red	Red	Red	Green	Green
Central City Hospital No. 1	Green	Green	Red		Yellow	Yellow	Red	Red	Green	Yellow
Power station	Green	Green	Green	Green		Green	Red	Red	Green	Green
Gas supply system	Green	Green	Yellow	Green	Green		Red	Yellow	Green	Green
Water supply	Green	Green	Green	Green	Red	Yellow		Red	Green	Green
Sewage system	Green	Green	Green	Green	Red	Green	Green		Green	Green
City administration	Green	Green	Yellow	Green	Green	Green	Yellow	Yellow		Red
Telecommunications	Green	Green	Yellow	Green	Yellow	Green	Green	Green	Green	

Fig. 12: Matrix of Yekaterinburg infrastructures and their relationships

Each actor fills out his personal matrix of interdependencies of his service with other services and their infrastructures. All personal matrices are combined into a final matrix, which represents the interdependence of all city services and their infrastructures (Fig. 13).

Fig. 13: Final matrix of interdependencies of services (and their infrastructures)

Based on the interdependency matrix, a diagram of service interdependencies is constructed. It allows to (1) clearly see its suppliers and consumers for the selected service, (2) build a critical path consisting of the most vulnerable suppliers and consumers (who will fail if the selected service fails), (3) build a diagram of interdependencies at the infrastructure level. It is important to note that all tiers of the urban society can use LLCT, as every tier has its own set of expert assessment methods.

It also permits visualizing cascade failures of interdependent infrastructures (Fig. 14). This, in

turn, facilitates using the supply chain risk assessment methodology, according to which risks are identified based on expert judgment and a combination of Failure Effects Analysis (FMEA) and Intuitive Fuzzy Analytic Hierarchy Process (IF-AHP). Supply risks (demand, supply, logistics, finance, operations) are classified and prioritized. Recommendations for their reduction are developed according to their degree of importance (priority).

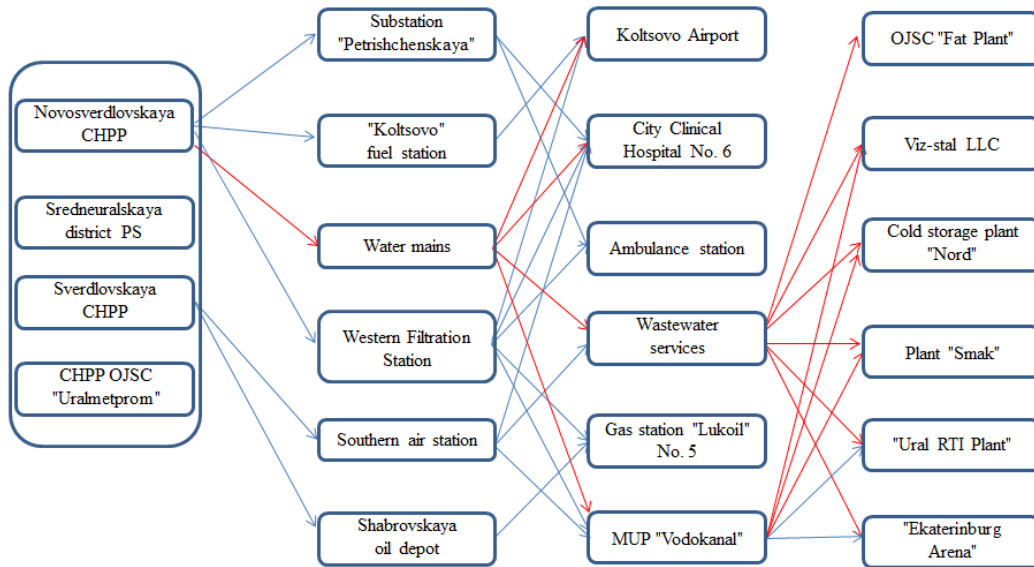


Fig. 14: Visualization of cascade failures of interdependent infrastructures

VI. Artificial intelligence as a central convergent discipline of MABICS technologies



It was noted above that AI is the link that connects all other components in the MABICS convergent technologies, as it takes over more and more problems from their scope. Indeed, it is promising to use the achievements of artificial intelligence, every time when there is an intrinsic lack of information about the system and methods of its operation.

AI, in particular, artificial neuron network (ANN), already is used to predict reliability and resilience of water supply systems [63]. It is useful when it is necessary to increase the diagnostics accuracy of defects in pipeline systems, to assess the reliability, resilience and safety of cold and hot water supply, and sewage systems, to ensure their uninterrupted operation (Fig. 15).

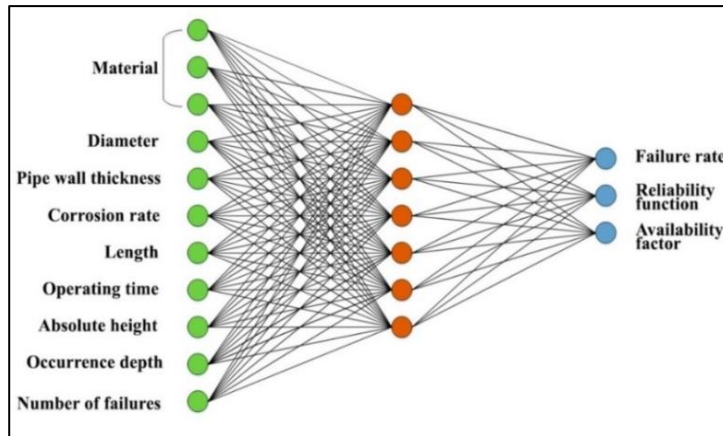


Fig. 15: Architecture of the multilevel perceptron (MLP) 11-7-3 ANN model of the Kamyshlov city water supply system [63]

VII. Application of block chain technology (BCT) in infrastructures operation [64, 65]

The block chain technology is useful to downsize the dimension of the infrastructure system model and to improve its accuracy. To this extent, BCT provides: Time stamp (registration of creation time) of documents; Verification of diagnostics (sensor data, control commands, events); Monitoring and maintenance of infrastructures of all types, reliability of records; Temporary chains of readings from sensors and devices with complete trust for network participants (Figure 16); Confirmation of damage assessments from incidents, accidents and disasters; Accounting for transactions in IoT (Internet of Things); Optimization of regional governance; Identification of geographic zones and user groups; Improving the security and survivability of regional interdependent facilities.

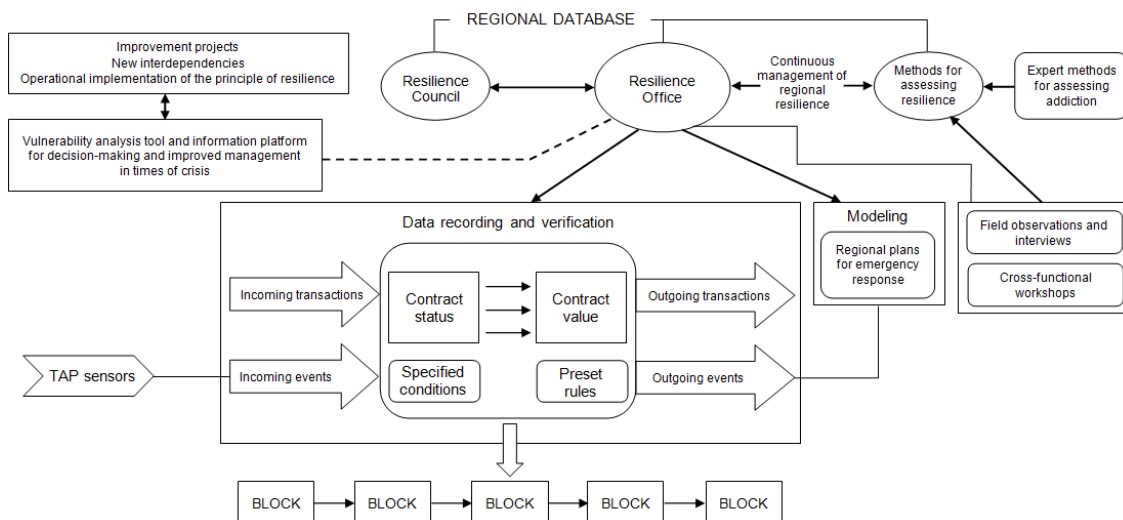


Fig. 16: Scheme for transmitting information to DMs from sensors using block chain technology

VIII. Conclusion

The results of the complex multifaceted analyses of papers related to reliability, resilience, risk and safety of critical and strategic infrastructures and their systems described in this paper lead to following conclusion.

The idea of convergence in relation to cyberphysical infrastructures and socio-technical systems has long been in the scientific world. Many leading scientists working in the field of technical sciences have long used this concept by default, without formulating it explicitly. Thus, E. Zio writes [29]: "In the community of experts in the field of risk, safety, reliability and security, there is a feeling that a new paradigm is needed for the analysis and management of complex distributed systems and critical infrastructures that form the basis of modern industry and society. A new risk scenario for modern industry and society poses some unprecedented challenges for research and practice, so that a new risk paradigm and new methods for analyzing reliability and risk may be required." At the same time, the observed anthropocentricity of global politics pushes scientific thought towards continuous convergence of disciplines that are, at first glance, distant from each other when solving social problems of infrastructures.

In this context, the MABICS convergent technologies, with explainable Artificial Intelligence as the key convergent science and technology, and infranetics as umbrella science could serve as the needed answer to this global challenge.

Infranetics as a synthetic umbrella science uses a targeted approach and is positioned as a cross-pollinating discipline of a number of fundamental and applied sciences, the goal of which is the optimal design and harmonious governance of the second, artificial nature of the planet at all stages of its life cycle.

Sub-resilience, resilience and suprarresilience (knowledge gap in cognitive, social losses/gains), social entropy (connects quantitatively the tangible with intangible) are the prominent problems of biosociotechnical infrastructures that need attention, research and solution.

DMs of a regional scale and persons equated to them, using the methodology of infranetics, will be able to optimize the parameters by which the effectiveness of their activities is assessed (growth of GDP, number and life expectancy of the population, level of education, employment, wages, volume of life support infrastructure construction, level of citizen confidence, etc.).

The author hopes that the reasons and logic for creating the MABICS technologies as the core of infranetics will find their supporters, adherents and followers, which will accelerate their application in practice by current and future generations of scientists and specialists.

References

[1] Roco M.C.; Bainbridge W.S. (eds.) *Converging Technologies for Improving Human Performance: Nanotechnology, Biotechnology, Information Technology and Cognitive Science*, 2003. – Dordrecht, Boston, London: Kluwer Academic Press. NSF/DOC sponsored report. – Arlington, VA: National Science Foundation. – URL: www.wtec.org/ConvergingTechnologies.

[2] Roco M.C.; Montemagno C.D. (Eds.) *The co-evolution of human potential and converging technologies // Annals of the New York Academy of Sciences*, 2004. – Vol. 1013. – N.Y.: The New York Academy of Sciences.

[3] Bainbridge W.S.; Roco M.C. (Eds.) *Managing Nano-Bio-Info-Cogno Innovations. Converging Technologies in Society*. – Heidelberg, New York: Springer, 2006.

[4] Bainbridge W.S.; Roco M.C. (Eds.) *Progress in Convergence. Technologies for Human Wellbeing // Annals of the New York Academy of Sciences*, 2006. – Vol. 1093. – Boston, MA: The New York Academy of Sciences.

[5] Altmann D., Andler K., Bruland K., Nakicenovic N. and Nordmann A. *Converging Technologies – Shaping the Future of European Societies. Report of the High-Level Expert Group*

on «Foresighting the New Technology Wave». – Luxembourg: Office for Official Publications of the European Communities, 2004.

[6] Pride V., Medvedev D.A. The phenomenon of NBIC convergence. Reality and expectations // *Philosophical Sciences*, 2008. – No. 1. – Pp. 97–117.

[7] Concept “Strategy for the development of convergent technologies”. Kurchatov Institute, 2016.

[8] – URL: <http://www.scienceforum.ru/2015/1063/9535> (date of the application: 02/12/2022).

[9] Muravyova M. Matrix of science from Mikhail Kovalchuk // Novosibirsk, Akademgorodok: Artistic, informational and literary pages. – URL: <http://www.academgorodok.ru/applications/science/science.php?set=force&id=56> (date of the application: 22/04/2023).

[10] Timashev S.A. Infranetics – a new convergent science of the 21st century // Proc. of 2th Intern. Conf. SAFETY2016 «Problems of security of building critical infrastructures». – Yekaterinburg, 2016. – Pp. 234–237.

[11] Timashev S.A. Infranetics: The New Convergent Science for Risk Based Management of Systems of Interdependent Critical Infrastructures // Proc. of 27th Annual Conf. of the Society for Risk Analysis Europe: Risk & Uncertainty – From Critical Thinking to Practical Impact (SRA-E 2018). – Östersund, Sweden, 2018, 18–20 June.

[12] Gheorghe A., Masera M., Katina P.F. Infranomics: Sustainability, Engineering Design and Governance. – Springer, 2014.

[13] Aven T., Zio E. Some considerations on the treatment of uncertainties in risk assessment for practical decision making // *Reliability Engineering and System Safety*, 2011. – Vol. 96 (1). – Pp. 64–74.

[14] Aven T., Zio E. Uncertainties in smart grids behavior and modeling: What are the risks and vulnerabilities? How to analyze them? // *Energy Policy*, 2011. – Vol. 39 (10). – Pp. 6308–6320. – DOI: 10.1016/j.enpol.2011.07.030.

[15] Baraldi P., Mangili F., Zio E. A belief function theory-based approach to combining different representation of uncertainty in prognostics // *Information Sciences*, 2015. – Vol. 303. – Pp. 134–149. – DOI: 10.1016/j.ins.2014.12.051.

[16] Beer M., Patelli E. Engineering analysis with vague and imprecise information // *Struct. Saf.*, 2015. – Vol. 52 (B): 143. – URL: <https://doi.org/10.1016/j.strusafe.2014.11.001> (date of the application: 16/03/2022).

[17] Coit D., Zio E. The evolution of system reliability optimization // *Reliability Engineering and System Safety*, 2019. – Vol. 192 (C).

[18] Cutler H., Shields M., Tavanl D., Zahran S. Integrating engineering outputs from natural disaster models into a dynamic spatial computable general equilibrium model of Centerville // *Sustainable and Resilient Infrastructure*, 2016. – Vol. 1 (3–4). – Pp. 169–187.

[19] Ellingwood B.R., Cutle, H., Gardoni P., Peacock W.G., van de Lindt J.W., Wang N. The Centerville virtual community: A fully integrated decision model of interacting physical and social infrastructure systems // *Sustainable and Resilient Infrastructure*, 2016. – Vol. 1 (3–4). – Pp. 95–107.

[20] Faber M., Miraglia S., Qin J., Stewart M. Bridging resilience and sustainability - decision analysis for design and management of infrastructure systems // *Sustainable and Resilient Infrastructure*, 2020. – Vol. 5 (1–2). – Pp. 102–124. – DOI: 10.1080/23789689.2017.1417348.

[21] Koliou M., van de Lindt J., McAllister T., Ellingwood B., Dillard M., Cutler H. State of the research in community resilience: progress and challenges // *Sustainable and Resilient Infrastructure*, 2018. – Vol. 8.

[22] Kröger W., Zio E. *Vulnerable Systems*. – Springer, London, 2011. – 204 p. – DOI: 10.1007/978-0-85729-655-9. 71.

[23] Li J., Chen J.-B. The principle of preservation of probability and the generalized density evolution equation // *Structural Safety*, 2008. – Vol. 30 (1). – Pp. 65–77.

[24] Li J., Chen J.-B. The probability density evolution method for dynamic response analysis of non-linear stochastic structures // *Int. J. Numer. Meth. Engng.*, 2006. – Vol. 65. – Pp. 882–903.

- [25] Lin P., Wang N., Ellingwood B.R. A risk de-aggregation framework that relates community resilience goals to building performance objectives // *Sustainable and Resilient Infrastructure*, 2016. – Vol. 1 (1–2, 1–13). – DOI: 10.1080/23789689.2016.1178559.
- [26] Amatova N.E. Development and implementation of NBIC-technologies: history and modernity // *Modern problems of science and education*, 2014. – No. 5.
- [27] Zio E. *The Monte Carlo Simulation Method for System Reliability and Risk Analysis*. – Springer, London, 2013. – 198 p. – DOI: 10.1007/978-1-4471-4588-2.
- [28] Zio E. Reliability engineering: Old problems and new challenges // *Reliability Engineering and System Safety*, 2009. – Vol. 94 (2). – Pp. 125–141.
- [29] Zio E. The future of risk assessment // *Reliability Engineering and Systems Safety*, 2018. – Vol. 177 (C). – Pp. 176–190.
- [30] Zio E. Challenges in the vulnerability and risk analysis of critical infrastructures // *Reliability Engineering and System Safety*, 2016. – Vol. 152 (C). – Pp. 137–150.
- [31] Zio E. Some challenges and opportunities in reliability engineering // *IEEE Transactions on Reliability*, 2016. – Vol. 65(4). – Pp. 1769–1782. – DOI: 10.1109/TR.2016.2591504.
- [32] Zio E. Reliability Analysis of Systems of Systems // *IEEE Reliability Magazine*, 2016. – Pp. 1–6.
- [33] Zio E. Integrated deterministic and probabilistic safety assessment: Concepts, challenges, research directions // *Nuclear Engineering and Design*, 2014. – Vol. 280. – Pp. 413–419. – DOI: 10.1016/J.NUCENGDES.2014.09.004.
- [34] Zio E. The future of risk assessment // *Reliability Engineering and System Safety*, 2018. – Vol. 177 (C). – Pp. 176–190.
- [35] Timashev S.A. *Infranetics – the umbrella science of second nature governance: preprint*. – Ekaterinburg: Uralsky Rabochiy, 2022. – 80 p.
- [36] Timashev S.A. Unified quantitative criteria for managing regional risk // *Proc. of the 11th Intern. Conf. on Structural Safety & Reliability, ICOSSAR*. – N. Y.: Columbia University, 2013.
- [37] Timashev S.A. Average Life Expectancy as a Criterion for Regional Risk Management Weight and Cloud Model // *J. of Risk Analysis and Crisis Response*, 2014. – Vol. 4 (1). – Pp. 10–19.
- [38] Timashev S.A., Tyrsin A.N., Kozlova O.A., Makarova M.N., Voronina L.N. Methodological approaches to assessing the impact of budget expenditures on average life expectancy // *Scientific review*, 2014. – № 7–1.
- [39] Timashev S.A., Bushinskaya A.V. Macroeconomic and demographic components of infranetics in the context of infrastructure risk management. Preprint. – Ekaterinburg, 2019. – 92 p.
- [40] Timashev S.A. Resilience and Strategic Preparedness of Critical Infrastructures // *Proc. of 1st Int. Conf. on Vulnerability and Risk Analysis and Management ICVRAM and 5th Int. Symp. On Uncertainty Modeling And Analysis ISUMA*, 2011. – Pp. 764–771.
- [41] Jaratpong V., Gheorghe A., Timashev S., Bushinskaya A. Resilience Analysis Of Urban Infrastructures Using The 3D Videogame Simcity In Combination With Advanced Quantitative Risk Assessment // *Proc. of 2nd Intern. conf. SAFETY2016 «Problems of security of building critical infrastructures»*. – Yekaterinburg, 2016. – Pp. 17–19.
- [42] Timashev S.A. Resilient Urban Infrastructures – Basics of Smart Sustainable Cities // *IOP Conference Series: Materials Science and Engineering*, 2017. – Vol. 262 (1): 012197. – DOI: 10.1088/1757-899X/262/1/012197.
- [43] Timashev S.A., Alekhin V.N., Poluyan L.V., Fontanals I., Gheorghe A. Transforming Yekaterinburg into a Safe, Resilient-Smart and Sustainable City // *IOP Conf. Series: Earth and Environmental Science*, 2018. – Vol. 177 (1). – DOI: 10.1088/1755-1315/177/1/012001.
- [44] Timashev S.A. Black-Swan Type Catastrophes and Antifragility/Supra-resilience of Urban Socio-Technical Infrastructures // *IOP Conference Series: Materials Science and Engineering*, 2020. – Vol. 972(1): 012001. – DOI: 10.1088/1757-899X/972/1/012001.
- [45] Timashev S.A. Supraresilience of Bio-Socio-Technical Infrastructures // *IOP Conference Series: Materials Science and Engineering*, 2020. – Vol. 962(4): 042049. – DOI: 10.1088/1757-899X/962/4/042049.

- [46] Taleb N.N. *Anti-Fragility: Things That Gain From Disorder*. – N. Y.: Random House, 2012. – 426 p.
- [47] Bushinskaya A.V., Timashev S.A. Features of the use of fragility and antifragility in the operation of technical systems and structures: preprint. – Yekaterinburg: UrFU, 2022. – 79 p.
- [48] Timashev S.A., Tyrsin A.N. Entropy approach to risk-analysis of critical infrastructure systems // *Proc. of the 1st Inter. conf. on Vulnerability and Risk Analysis and Management ICVRAM 2011 and the 4th Inter. Symp. on Uncertainty Modeling and Analyses ISUMA 2011*. – Pp. 147–154.
- [49] Wilson A.G. Entropy methods for modeling complex systems. Trans. from English. – M.: Science, Fizmatgiz, 1978. – 248 p.
- [50] Keyfitz N. *Applied mathematical demography*. – N. Y.: Springer, 1985.
- [51] Tsallis C. Possible generalization on Boltzmann-Gibbs statistics // *J. Statist. Physics*, 1988. – Vol. 52 (1/2). – Pp. 479–487.
- [52] Sornette D. Dragon-King, Black Swan and the prediction of crises// *International Journal of Terraspace Science and Engineering*, 2009. – Vol. 2 (1). – Pp. 1–8.
- [53] Kislov A.V., Matveeva T.A. Wind speed extremes in the European sector of the Arctic// *Russian Meteorology and Hydrology*, 2016. – Vol. 41 (7). – Pp. 447–454.
- [54] Bushinskaya A., Timashev S. Application of Kaniadakis κ -statistics to extreme wind speed load distributions // *Reliability: Theory & Applications, Special Issue № 4 (70)*, 2022. – Vol. 17. – Pp. 188–199. – DOI: <https://doi.org/10.24412/1932-2321-2022-470-188-199>.
- [55] Kaniadakis G. Statistical mechanics in the context of special relativity // *Physical Review*, 2002. – 17 p.
- [56] Composition law of kappa-entropy for statistically independent systems / G. Kaniadakis [et. al.]. // *Physical Review*, 2017. – Vol. 95 (5).
- [57] Timashev S.A., Malyutina E.V. Entropy Analysis of Social Unrest after Large Urban Infrastructure Accidents // *ASCE INSPIRE 2023*. – Arlington, Virginia, 2023, Nov. 16–18.
- [58] Ecological footprint. – URL: <https://wwf.ru/what-we-do/green-economy/ecologicalfootprint/> (date of the application: 22/03/2023).
- [59] Timashev S.A., Bushinskaya A.V. Holistic Risk Based Governance of Interdependent Urban Critical Infrastructures Using Cloud Software as a Service (SaaS) // *Proc. of 4th Intern. Sci.-pract. conf. «New information technologies in architecture and construction NITAC'2021»*. – Yekaterinburg, 2021.
- [60] Chikir M.V., Poluyan L.V. Bayesian Network Modeling for Analysis and Prediction of Accidents in Railway Transportation of Dangerous Goods // *Proc. of the 6th Intern. Conf. on Construction, Architecture and Technosphere Safety. ICCATS-2022. Book series: Lecture Notes in Civil Engineering*, 2023. – Vol. 308. – Springer, Cham. DOI: 10.1007/978-3-031-21120-1_53.
- [61] Timashev S.A. Resilience laboratory convergent technology: an optimal tool for creating and governing supresilient smart regions // *Proc. of VI Inter. Conf. «Safety Problems of Civil Engineering Critical Infrastructures»*. – Yekaterinburg, 2020.
- [62] European Commission Information Society and Media, Unit F4 New Infrastructure Paradigms and Experimental Facilities. Living Labs for user-driven open innovation. An overview of the Living Labs methodology, activities and achievements, 2009, January.
- [63] Timashev S., Makeeva T. Assessment and Prediction of Water Supply Network Reliability Under Information Shortage Using Artificial Neural Networks // *ASCE INSPIRE 2023*. – Arlington, Virginia, 2023, Nov. 16–18.
- [64] Karpunin A., Vlasov I. System analysis of data exchange and storage technology-blockchain. – URL: <https://cyberleninka.ru/article/n/sistemnyy-analiz-tehnologii-obmena-i-hraneniya-dannyh-blockchain> (date of the application: 18.05.2020).
- [65] Gascon D. *Blockchain Technology in the Oil and Gas Industry: A Review of Applications, Opportunities, Challenges, and Risks*, 2019. – 7 p.